GEOLOGICAL SURVEY OF CANADA
COMMISSION GÉOLOGIQUE DU CANADA

PAPER / ÉTUDE
91-1A

CURRENT RESEARCH, PART A
CORDILLERA AND PACIFIC MARGIN

RECHERCHES EN COURS, PARTIE A
CORDILLÈRE ET MARGE DU PACIFIQUE

NOTICE TO LIBRARIANS AND INDEXERS

The Geological Survey's Current Research series contains many reports comparable in scope and subject matter to those appearing in scientific journals and other serials. Most contributions to Current Research include an abstract and bibliographic citation. It is hoped that these will assist you in cataloguing and indexing these reports and that this will result in a still wider dissemination of the results of the Geological Survey's research activities.

AVIS AUX BIBLIOTHÉCAIRES ET PRÉPARATEURS D'INDEX

La série Recherches en cours de la Commission géologique paraît une fois par année ; elle contient plusieurs rapports dont la portée et la nature sont comparables à ceux qui paraissent dans les revues scientifiques et autres périodiques. La plupart des articles publiés dans Recherches en cours sont accompagnés d'un résumé et d'une bibliographie, ce qui vous permettra, on l'espée, de cataloguer et d'indexer ces rapports, d'où une meilleure diffusion des résultats de recherche de la Commission géologique.

GEOLOGICAL SURVEY OF CANADA
COMMISSION GÉOLOGIQUE DU CANADA

PAPER / ÉTUDE
91-1A

CURRENT RESEARCH, PART A
CORDILLERA AND PACIFIC MARGIN

RECHERCHES EN COURS, PARTIE A
CORDILLÈRE ET MARGE DU PACIFIQUE

1991

Available in Canada through

authorized bookstore agents and other bookstores

or by mail from

Canadian Government Publishing Centre
Supply and Services Canada
Ottawa, Canada K1A 0S9

and from

Geological Survey of Canada offices:

601 Booth Street
Ottawa, Canada K1A 0E8

3303-33rd Street N.W.,
Calgary, Alberta T2L 2A7

100 West Pender Street
Vancouver, B.C. V6B 1R8

A deposit copy of this publication is also available for reference in public libraries across Canada

Cat. No. M44-91/1A
ISBN 0-660-56281-2

Price subject to change without notice

Cover description

Looking northeast across Georgia Strait from Gabriola Island towards Entrance Island lighthouse and the Coast Mountains of the B.C. mainland. Foreground rocks are part of the Mayne Formation, Nanaimo Group, a submarine fan succession of sandstones and mudstones deposited in the Georgia Basin during the late Cretaceous. Photo by P.S. Mustard.

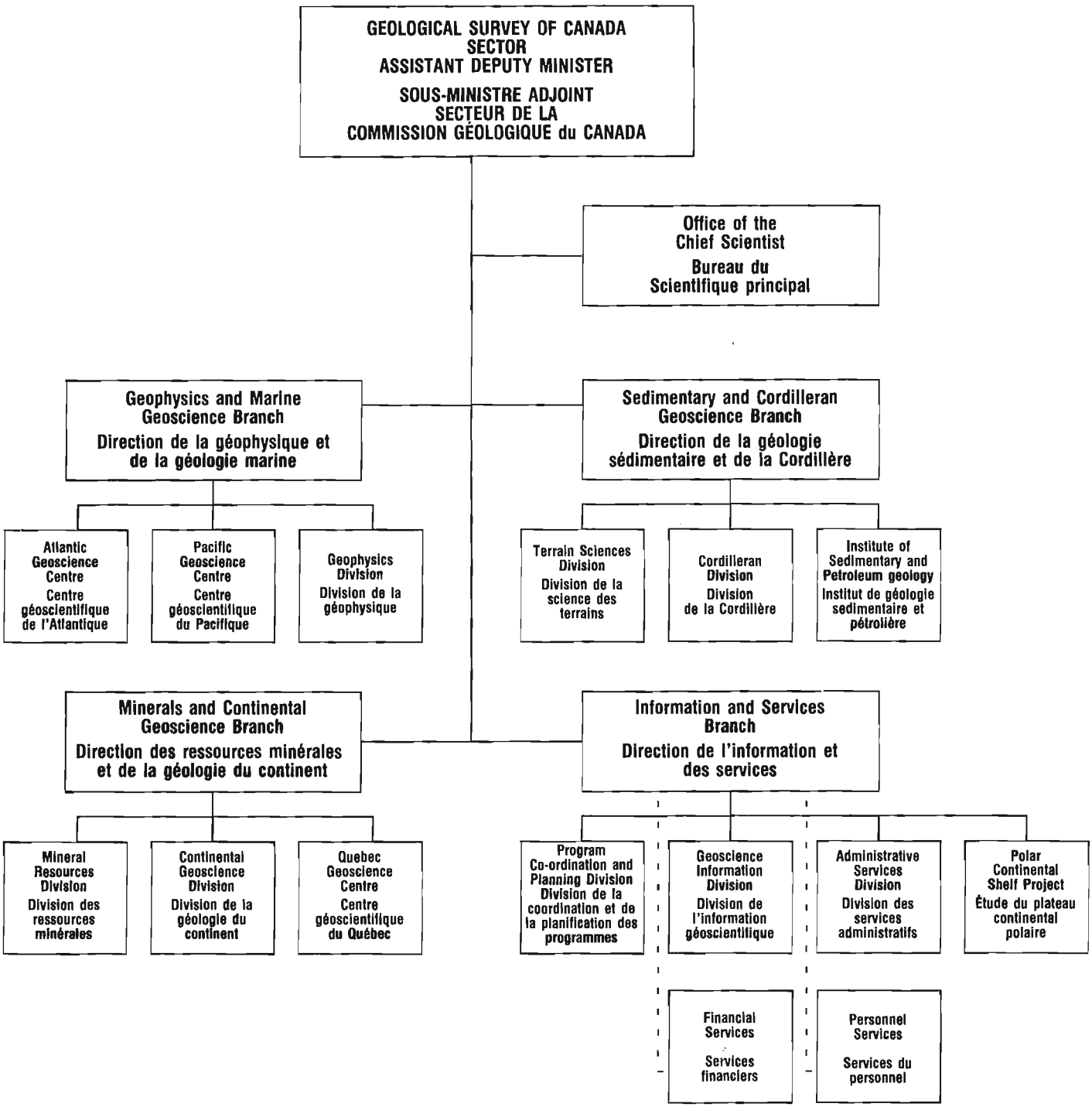
GEOLOGICAL SURVEY OF CANADA
SECTOR
ASSISTANT DEPUTY MINISTER
SOUS-MINISTRE ADJOINT
SECTEUR DE LA
COMMISSION GÉOLOGIQUE du CANADA
Office of the
Chief Scientist
Bureau du
Scientifique principal
Geophysics and Marine
Geoscience Branch
Direction de la géophysique et
de la géologie marine
Sedimentary and Cordilleran
Geoscience Branch
Direction de la géologie
sédimentaire et de la Cordillère
Atlantic
Geoscience
Centre
Centre
géoscientifique
de l'Atlantique
Pacific
Geoscience
Centre
Centre
géoscientifique
du Pacifique
Geophysics
Division
Division de la
géophysique
Terrain Sciences
Division
Division de la
science des
terrains
Cordilleran
Division
Division
de la Cordillère
Institute of
Sedimentary and
Petroleum geology
Institut de géologie
sédimentaire et
pétrolière
Minerals and Continental
Geoscience Branch
Direction des ressources minérales
et de la géologie du continent
Information and Services
Branch
Direction de l'information et
des services
Mineral
Resources
Division
Division des
ressources
minérales
Continental
Geoscience
Division
Division de la
géologie du
continent
Quebec
Geoscience
Centre
Centre
géoscientifique
du Québec
Program
Co-ordination and
Planning Division
Division de la
coordination et de
la planification des
programmes
Geoscience
Information
Division
Division de
l'information
géoscientifique
Administrative
Services
Division
Division des
services
administratifs
Polar
Continental
Shelf Project
Étude du plateau
continental
polaire
Financial
Services
Services
financiers
Personnel
Services
Services du
personnel

Separates

A limited number of separates of the papers that appear in this volume are available by direct request to the individual authors. The addresses of the Geological Survey of Canada offices follow:

601 Booth Street,
OTTAWA, Ontario
K1A 0E8
(FAX: 613-996-9990)

Institute of Sedimentary and Petroleum Geology,
3303-33rd Street N.W.,
CALGARY, Alberta
T2L 2A7
(FAX: 403-292-5377)

Cordilleran Division,
100 West Pender Street,
VANCOUVER, B.C.
V6B 1R8
(FAX: 604-666-1124)

Pacific Geoscience Centre
P.O. Box 6000,
9860 Saanich Road
SIDNEY, B.C.
V8L 4B2
(FAX: 604-356-6565)

Atlantic Geoscience Centre
Bedford Institute of Oceanography,
P.O. Box 1006
DARTMOUTH, N.S.
B2Y 4A2
(FAX: 902-426-2256)

Québec Geoscience Centre
2700, rue Einstein
C.P. 7500
Ste-Foy (Québec)
G1V 4C7
(FAX: 418-654-2615)

When no location accompanies an author's name in the title of a paper, the Ottawa address should be used.

Tirés à part

On peut obtenir un nombre limité de «tirés à part» des articles qui paraissent dans cette publication en s'adressant directement à chaque auteur. Les adresses des différents bureaux de la Commission géologique du Canada sont les suivantes :

601, rue Booth
OTTAWA (Ontario)
K1A 0E8
(facsimilé : 613-996-9990)

Institut de géologie sédimentaire et pétrolière
3303-33rd St. N.W.,
CALGARY (Alberta)
T2L 2A7
(facsimilé : 403-292-5377)

Division de la Cordillère
100 West Pender Street,
VANCOUVER (British Columbia)
V6B 1R8
(facsimilé : 604-666-1124)

Centre géoscientifique du Pacifique
P.O. Box 6000,
9860 Saanich Road
SIDNEY (British Columbia)
V8L 4B2
(facsimilé : 604-356-6565)

Centre géoscientifique de l'Atlantique
Institut océanographique Bedford
B.P. 1006
DARTMOUTH (Nova Scotia)
B2Y 4A2
(facsimilé : 902-426-2256)

Centre géoscientifique de Québec
2700, rue Einstein
C.P. 7500
Ste-Foy (Québec)
G1V 4C7
(facsimilé : 418-654-2615)

Lorsque l'adresse de l'auteur ne figure pas sous le titre d'un document, on doit alors utiliser l'adresse d'Ottawa.

CONTENTS

Quaternary stratigraphy and history of Quesnel and Cariboo river valleys, British Columbia: implications for placer gold exploration

John J. Clague
Terrain Sciences Division, Vancouver

Clague, J.J., Quaternary stratigraphy and history of Quesnel and Cariboo river valleys, British Colombia : implications for placer gold exploration ; in Current Research, Part A, Geological Survey of Canada, Paper 91-1A, p. 1-5, 1991.

Abstract

Thick unconsolidated sediments in Quesnel and Cariboo river valleys record late Quaternary events in central British Columbia. The succession consists of: till and recessional glaciolacustrine sediments deposited during the penultimate (Early Wisconsinan or older) glaciation; plant-bearing interstadial (Middle Wisconsinan) sediments; fluvial gravel and sand probably deposited at the beginning of the last (Late Wisconsinan) glaciation; Late Wisconsinan advance and recessional glaciolacustrine sediments; Late Wisconsinan till; and postglacial sediments, mainly alluvium and colluvium. Most of these units contain little or no placer gold and thus are low-priority exploration targets. Economic quantities of gold are most likely to be found along and directly above unconformities produced during Middle Wisconsinan and Holocene time as streams incised valley fills.

Résumé

D'épais sédiments non consolidés présents dans les vallées de la rivière Quesnel et de la rivière Cariboo témoignent d'événements survenus à la fin du Quaternaire dans le centre de la Colombie-Britannique. La succession se compose : de till et de sédiments glacio-lacustres de retrait déposés au cours de l'avant-dernière glaciation (Wisconsinien précoce ou avant); de sédiments interstadiaires contenant des végétaux (Wisconsinien moyen); de gravier et de sable fluviatiles probablement déposés au commencement de la dernière glaciation (Wisconsinien tardif); de sédiments glacio-lacustres déposés durant l'avancée et le retrait glaciaires au Wisconsinien tardif; de till du Wisconsinien tardif; et de sédiments post-glaciaires, principalement composés d'alluvions et de colluvions. La plupart de ces unités contiennent peu ou pas d'or alluvionnaire et sont donc des cibles d'exploration peu importantes. Des quantités exploitables d'or existent en toute probabilité le long et directement au-dessus de discordances apparues pendant le Wisconsinien moyen et l'Holocène, sous forme de remblai de vallées entaillées par des cours d'eau.

INTRODUCTION

The Cariboo mining district is the most productive placer gold region in British Columbia, having yielded over 70 000 kg of the metal since the first discoveries in the late 1850s (Johnston and Uglow, 1926; Boyle, 1979). Today, the area accounts for almost 30 % of the total annual placer gold output in the province (Eyles and Kocsis, 1988b). Although the richest placers are now largely exhausted, gold continues to be recovered from sediments that have been mined one or more times and from previously unexploited deposits.

One of the important placer areas in the Cariboo district is the Quesnel and Cariboo river basin (Fig. 1). Quesnel River flows west from the Cariboo Mountains across the easternmost Interior Plateau; its largest tributary is Cariboo River. Both valleys are deeply incised into the Interior Plateau and contain remnants of a complex Quaternary sediment fill deposited during at least two glaciations. The glaciers that covered this area during the Pleistocene flowed west from the Cariboo Mountains and, at times, coalesced over central British Columbia with easterly flowing ice derived from the Coast Mountains (Tipper, 1971a, b; Clague, 1987, 1988). Glaciation repeatedly disrupted interglacial stream courses, thus present valleys commonly diverge from buried valleys cut earlier during the Quaternary and during the Tertiary (Fig. 2). Numerous anomalies in the present drainage provide evidence for piracy and stream diversion induced by glacier growth and decay (Clague, 1989).

This report provides a short summary of the Quaternary stratigraphy of Quesnel and Cariboo valleys, based on an examination of over 50 river bluff and placer mine exposures in the area. Generalized stratigraphic and sedimentological logs of some of these sections are included in this report to facilitate discussion (Fig. 3). This work is an extension of stratigraphic and sedimentological studies conducted in Fraser River valley to the west and southwest (Clague, 1987, 1988; Eyles et al., 1987). The stratigraphic framework in the latter area is similar to that reported here, indicating that events of regional importance have controlled sedimentation and erosion throughout central British Columbia. The importance of these events in localizing placer gold deposits is discussed in this report, building on previous work by Eyles and Kocsis (1988a, 1989) and Clague (1989).

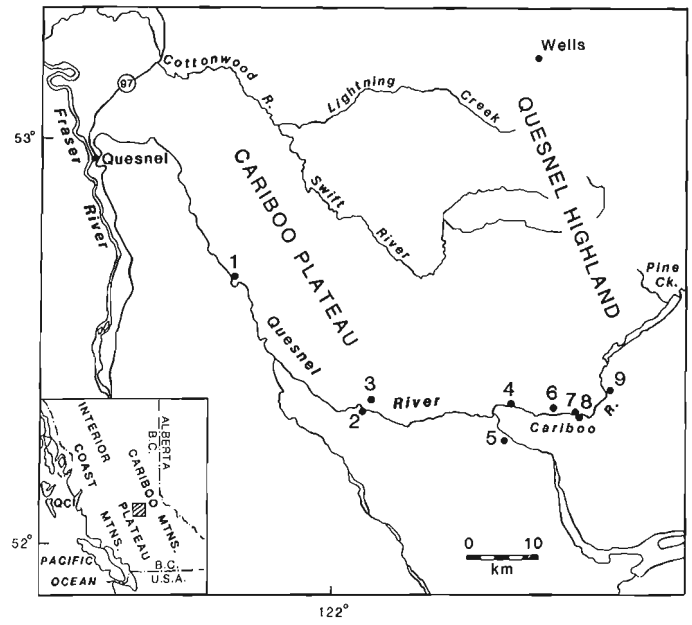

Figure 1. The study area showing locations of stratigraphic sections discussed in the report.

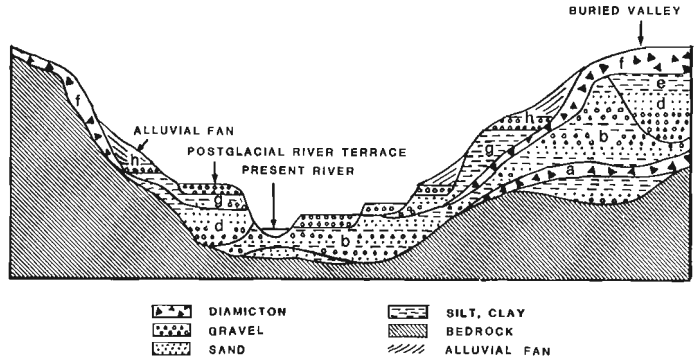

Figure 2. Diagrammatic cross-section of Quaternary succession in Quesnel and Cariboo valleys. Letters correspond to units discussed in the text.

QUATERNARY STRATIGRAPHY AND HISTORY

Quaternary deposits in Quesnel and Cariboo valleys consist mainly of thick stratified drift deposited during the Fraser Glaciation (Late Wisconsinan) and during the penultimate glaciation (Early Wisconsinan or older) (Fig. 3). Tills are present, but are subordinate to glaciolacustrine and glaciofluvial sediments. Older Quaternary and Tertiary sediments may be present in these valleys, but are either subordinate to Late Pleistocene deposits or occur below present base level and thus are not exposed.

Deposits of the penultimate glaciation consist mainly of massive and stratified silt, sand, gravel, and minor diamicton (unit b in Fig. 3) deposited in one or more ice-dammed lakes (see Eyles et al., 1987, for a description and discussion of correlative, although generally coarser, sediments in Fraser valley). This unit is characterized by large- and small-scale intertonguing of different lithologies. Syndepositional and postdepositional deformation structures, including folds, faults, and sedimentary dykes, record gravitational foundering and porewater expulsion caused by downslope movement of sediments and, perhaps, melting of adjacent stagnant glacier ice.

These sediments typically are tens of metres thick and occur as erosional remnants at many sites in the study area. They were deposited during a period of regional ice-sheet downwasting and stagnation at the end of the penultimate glaciation (Fig. 4A). There is little stratigraphic evidence for the maximum phase of this glaciation; basal till (unit a) has been identified at only one site in the area (section 5, Fig. 3).

An erosional unconformity marks the top of this glaciolacustrine unit (except at section 5) and records erosion and valley incision during the nonglacial interval (at least in part Middle Wisconsinan) that followed the penultimate

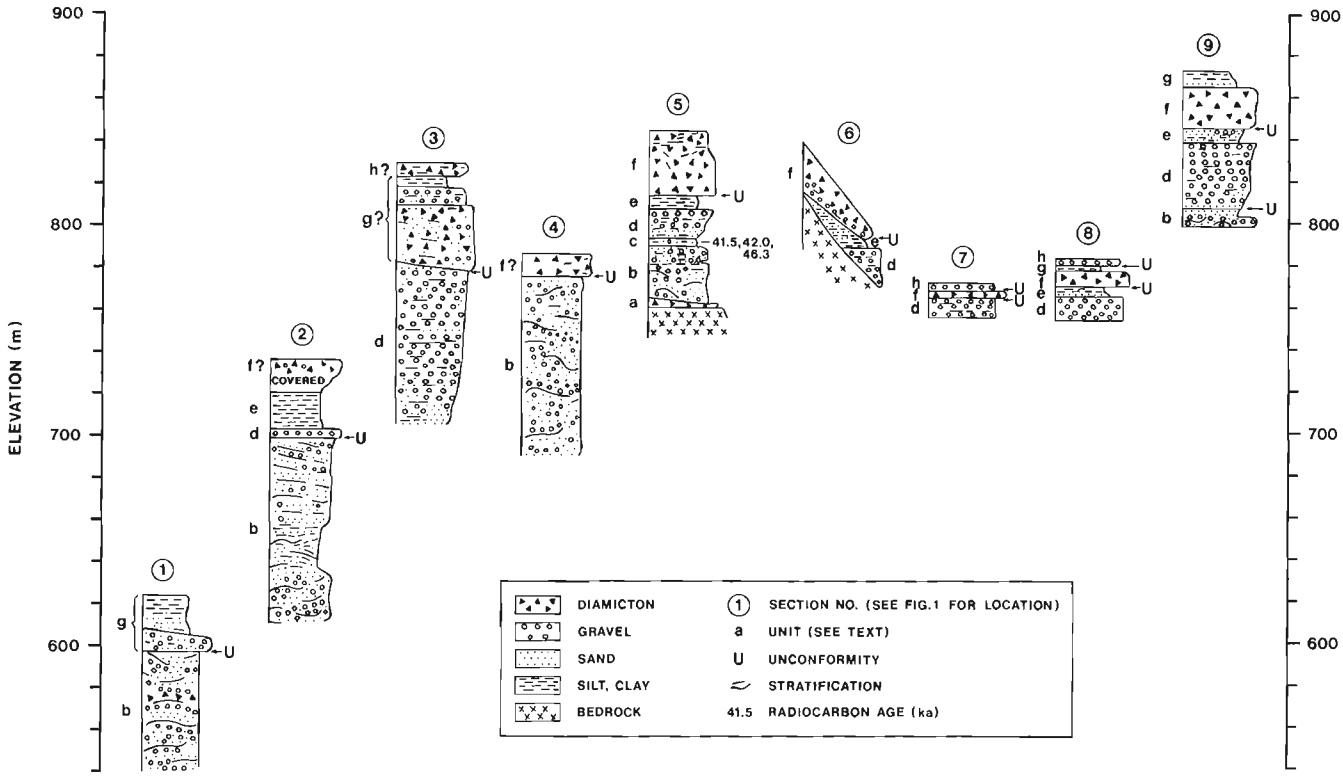

Figure 3. Stratigraphic sections. See Figure 1 for locations.

glaciation (Fig. 4B). The large amount of relief on this unconformity indicates that ancestral Quesnel and Cariboo valleys may have been as deeply incised during the Middle Wisconsinan as today.

Plant-bearing nonglacial sediments of Middle Wisconsinan age (unit c) have been found at only one site in the study area (section 5, Fig. 3; Clague et al., 1990). Even here, these sediments are thin and record only localized deposition adjacent to a rock slope. The restricted occurrence of such sediments indicates that the Middle Wisconsinan, like the present, was a period of denudation; significant sedimentation probably was limited to lakes and fans.

The unconformity developed on glaciolacustrine sediments of the penultimate glaciation is locally overlain by thick, horizontally stratified, clast-supported, fluvial gravel and sand (unit d). Stratification is dominantly parallel, but channel cut-and-fill structures are common in most exposures. Paleocurrent directions differ from site to site, possibly reflecting inputs of sediment into Quesnel and Cariboo valleys from tributaries such as Birrell and Seller creeks (sites 3 and 9, Fig. 1). This thick gravel-sand unit may have been deposited as a result of an increase in the supply of sediment caused by the expansion of glaciers into this area during the early part of the Fraser Glaciation (Fig. 4C).

In some sections (5 and 9 in Fig. 3), fluvial sediments are conformably overlain by horizontally stratified sand, silt, and mud (unit e) deposited in one or more lakes which are thought to have been dammed by advancing Late Wisconsinan glaciers (Fig. 4D).

At the Fraser Glaciation maximum, ice flowing west from the Cariboo Mountains deposited till (unit f) on the eroded sediment fills in Quesnel and Cariboo valleys (Fig. 4E).

Glaciolacustrine sediments (unit g) overlie Fraser Glaciation till and older Pleistocene deposits (sections 1, 3, 8, 9, Fig. 3). They include laminated and bedded sand, silt, and mud which are similar in character to Fraser advance glaciolacustrine sediments, and poorly sorted gravelly, sandy, and diamictic facies. This unit superficially resembles unit b, deposited at the end of the penultimate glaciation, but lacks the pervasive deformation and complex intertonguing of lithologies typical of the latter. It was deposited in an ice-dammed lake at the end of the Fraser Glaciation (Fig. 4F).

Soon after the late-glacial lake in Quesnel and Cariboo valleys disappeared, the present drainage became established. After a short period of fluvial (paraglacial) aggradation, streams dissected valley fills and produced terraces at successively lower levels (Fig. 4G). Relatively thin Holocene fluvial gravels overlie these terraces. These, together with colluvium produced mainly by mass wasting of till, constitute the youngest sediments in the Quaternary succession (unit h; sections 3, 7, and 8, Fig. 3).

In summary, there is stratigraphic evidence for two phases of ice-retreatal glaciolacustrine sedimentation, each followed by a lengthy period of denudation and valley incision. The earlier period of valley incision ended with the deposition of thick fluvial and lacustrine sediments, probably at the beginning of the Fraser Glaciation. The later period of incision began in the early Holocene and continues today.

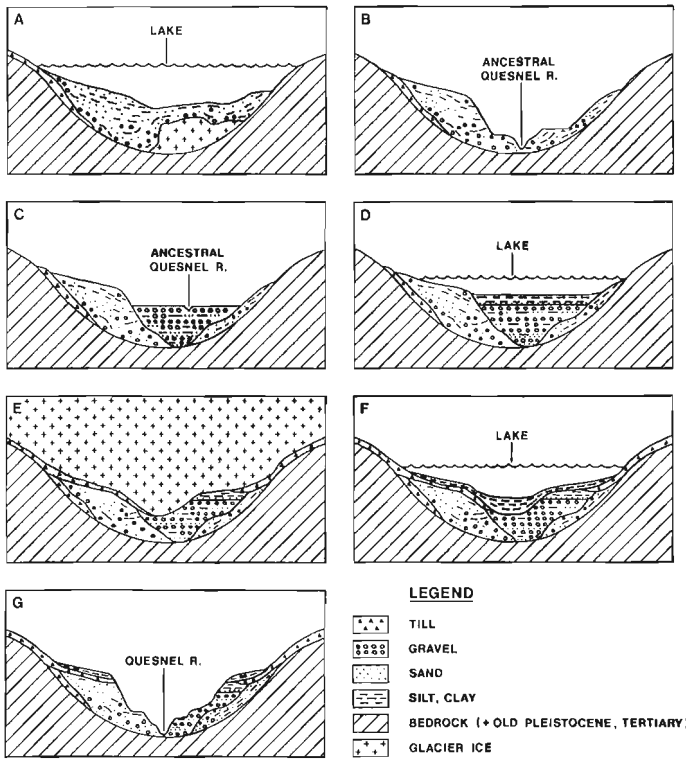

Figure 4. Generalized cross-sections showing sequential deposition and erosion of units forming the sediment fill in Quesnel and Cariboo valleys. A. Glaciolacustrine sedimentation at the end of the penultimate glaciation. B. Middle Wisconsinan valley incision. C. Fluvial aggradation. D. Glaciolacustrine sedimentation during the early part of the Fraser Glaciation. E. Deposition of Late Wisconsinan till. F. Glaciolacustrine sedimentation at the end of the Fraser Glaciation. G. Holocene valley incision.

PLACER GOLD IMPLICATIONS

The main source of placer gold in the Cariboo district is auriferous metasedimentary rocks of the Cariboo Group (Johnston and Uglow, 1926). Most of the gold was released from host rocks during a lengthy period of Tertiary weathering and denudation and was concentrated in Miocene and Pliocene colluvial and alluvial sediments by mechanical processes and chemical precipitation.

During the Quaternary, streams and glaciers removed most Tertiary auriferous sediments, but much of the gold was redeposited in younger sediments. Although glaciers, as a rule, are agents of dispersion, gold can be concentrated at the base of the ice by subglacial meltwater and by melt-out of large quantities of debris in the lee of subglacial obstructions (Eyles and Kocsis, 1989). Placer gold has been recovered from till in the study area, but grades typically are low.

Glaciolacustrine sediments, which dominate the stratified Quaternary fill in Quesnel and Cariboo valleys, contain only small amounts of fine gold. A few glaciolacustrine deltas have been mined in the past (e.g., Pine Creek, Fig. 1), but with little success. It thus can be concluded that the three glaciolacustrine units identified in the course of this study (units b, e, and g) are poor placer gold exploration targets.

The same can be said for the fluvial gravel-sand sequence (unit d) overlying the oldest glaciolacustrine unit. Channels within the fluvial sequence are likely to contain some gold, but average grades for the unit as a whole are low. In the past, expensive, unsuccessful attempts have been made to recover gold from this unit, for example at Birrell Creek (site 3, Fig. 1).

The best placer gold targets in the study area are the bedrock floors of former valleys, and nonglacial (fluvial) unconformities within the Quaternary succession. In the early years of mining in the Cariboo, large amounts of gold were recovered from rock-floored channels in relict valleys filled with Pleistocene sediments. Within the Quaternary succession, economic quantities of gold are most likely to be found along: (1) the unconformity separating glaciolacustrine sediments of the penultimate glaciation (unit b) from younger aggradational fluvial deposits (unit d); and (2) the unconformity separating Pleistocene sediments from Holocene terrace gravels (unit h). These unconformities are relict fluvially eroded surfaces; gold washed from Pleistocene deposits during periods of valley incision was concentrated on these surfaces and in immediately overlying sediments. Today, many placer operators in the study area recover gold from terrace gravels at and just above the Holocene unconformity. The Middle Wisconsinan unconformity is more difficult to explore and mine because it generally is covered by thick sediments containing little or no gold. Aside from the practical problem of exploiting pay zones beneath thick overburden, it may be difficult to trace the course of Middle Wisconsinan valley floors any distance from existing exposures.

The Middle Wisconsinan and Holocene unconformities have a much higher placer gold potential than the unconformity at the base of unit f, produced by glacial erosion during the Fraser Glaciation. In general, glacial unconformities are unlikely to contain significant gold and should be avoided during exploration.

SUMMARY

Quaternary sediments in Quesnel and Cariboo valleys are divisible into several lithostratigraphic units of regional significance. Much of the succession consists of glaciolacustrine sediments deposited at the end of the penultimate glaciation and at the beginning and end of the Fraser Glaciation. The two older glaciolacustrine units are locally separated by thick fluvial sediments which may be advance outwash of the Fraser Glaciation. A major unconformity marks the contact between the fluvial sediments and underlying penultimate glaciolacustrine deposits. This unconformity records erosion and valley incision during Middle Wisconsinan time. The area was covered by the Cordilleran Ice Sheet at the maximum of the Fraser Glaciation, and older sediment units were eroded by ice and locally mantled with till. A second period of erosion and valley incision, which is still continuing, commenced after the area was deglaciated and the present drainage became established.

Most Quaternary sediment units in Quesnel and Cariboo valleys contain little or no placer gold. Gold occurs in small amounts in some tills and in fluvial and deltaic gravels. The

best exploration targets, however, are the bedrock floors of relict buried valleys and nonglacial unconformities within the Quaternary succession.

REFERENCES

Boyle, R.W.
1979: The geochemistry of gold and its deposits (together with a chapter on geochemical prospecting for the element); Geological Survey of Canada, Bulletin 280, 584 p.

Clague, J.J.
1987: Quaternary stratigraphy and history, Williams Lake, British Columbia; Canadian Journal of Earth Sciences, v. 24, p. 147-158.
1988: Quaternary stratigraphy and history, Quesnel, British Columbia; Géographie physique et Quaternaire, v. 42, p. 279-288.
1989: Placer gold in the Cariboo district, British Columbia; in Current Research, Part E, Geological Survey of Canada, Paper 89-1E, p. 243-250.

Clague, J.J., Hebda, R.J., and Mathewes, R.W.
1990: Stratigraphy and paleoecology of Pleistocene interstadial sediments, central British Columbia; Quaternary Research, v. 34, p. 208-226.

Eyles, N. and Kocsis, S.P.
1988a: Gold placers in Pleistocene glacial deposits, Barkerville, British Columbia; Canadian Mining and Metallurgy Bulletin, v. 81, p. 71-79.
1988b: Placer gold mining in Pleistocene glacial sediments of the Cariboo district, British Columbia, Canada 1858-1988; Geoscience Canada, v. 15, p. 293-301.
1989: Sedimentological controls on gold in a late Pleistocene glacial placer deposit, Cariboo Mining District, British Columbia, Canada; Sedimentary Geology, v. 65, p. 45-68.

Eyles, N., Clark, B.M., and Clague, J.J.
1987: Coarse-grain sediment gravity flow facies in a large supraglacial lake; Sedimentology, v. 34, p. 193-216.

Johnston, W.A. and Uglow, W.L.
1926: Placer and vein gold deposits of Barkerville, Cariboo district, British Columbia; Geological Survey of Canada, Memoir 149, 246 p.

Tipper, H.W.
1971a: Glacial geomorphology and Pleistocene history of central British Columbia; Geological Survey of Canada, Bulletin 196, 89 p.
1971b: Multiple glaciation in central British Columbia; Canadian Journal of Earth Sciences, v. 8, p. 743-752.

Preliminary study of the Quaternary geology of the northern interior of British Columbia

Alain Plouffe
Terrain Sciences Division

Plouffe, A., Preliminary study of the Quaternary geology of the northern interior of British Columbia; in Current Research, Part A, Geological Survey of Canada, Paper 91-1A, p. 7-13, 1991.

Abstract

Preliminary interpretation of the Quaternary history of the central part of British Columbia includes the following events: (1) piedmont glaciers advanced to the east and southeast from the Skeena and Coast mountains; (2) a shift in ice flow direction occurred as these glaciers coalesced with ice from the Cariboo Mountains; and (3) deglaciation was marked by the formation of a glacial lake and the development of postglacial drainage.

Résumé

L'interprétation préliminaire de l'histoire du Quaternaire pour la partie centrale de la Colombie-Britannique comprend trois évènements: 1) l'avancée de glaciers de piémont vers l'est et le sud-est à partir de la chaîne Côtière et du chaînon Skeena; 2) un changement dans la direction de l'écoulement glaciaire dû à la coalition des glaciers de piémont avec la glace des monts Caribou; et 3) une déglaciation caractérisée par la formation d'un lac glaciaire et le développement d'un réseau de drainage post-glaciaire.

INTRODUCTION

Relatively little work has been done on the Quaternary geology of the northern interior of British Columbia compared to more southern regions of that province. The Geological Survey of Canada has undertaken a four year regional mapping project of the surficial materials of two 1:250 000 scale map areas (Fort Fraser and Mansen River, NTS 93 K and N, respectively; Fig. 1). The project was started during the summer of 1990 and will continue through three more field seasons. The objectives of the project are to map the surficial materials of this area and establish details of the glacial history. Other aspects of the study include investigations of till geochemistry, geological hazards in mountainous areas, distribution and origin of placer deposits, and environmental problems which involve Quaternary geology.

Most of the work during this first season was concentrated in the southern quarter of the area. The results of the preliminary study and a brief overview of future work are presented here.

PHYSIOGRAPHY AND DRAINAGE

The study area is entirely within the Interior System of the Canadian Cordillera and can be subdivided into three major parts as defined by Holland (1976) and Mathews (1986): the Interior Plateaus, the Omineca Mountains, and the Rocky Mountain Trench (Fig. 1). The boundaries between these divisions were drawn arbitrarily since they represent transitional zones (Holland, 1976; Mathews, 1986).

The Interior Plateaus subdivision includes the Nechako Lowland and Plateau which consist of flat to gently rolling country with elevation varying between 635 to 1515 m. Bedrock geology is characterized by deformed sedimentary, metasedimentary, volcanic, and igneous rocks of Permian to Cretaceous age, which are intruded by granite, granodiorite, and syenite of Jurassic age. These are overlain extensively by gently dipping Tertiary lava flows.

The Omineca Mountains, in the northern part of the study area, range from 1520 to over 1820 m elevation, with the highest summit at 2081 m (Mount Porter in the northeast). The topography consists of numerous peaks, cirques, and arêtes along with U-shaped valleys. Granitic rocks of the Omineca Intrusions form the core of these mountains (Armstrong, 1949).

The Rocky Mountain Trench intersects the northeastern tip of the study area. It is a prominent topographic feature which extends about 1400 km from the 49th Parallel to Liard River (Holland, 1976). The Rocky Mountain Trench is filled with a thick cover of unconsolidated glacial and nonglacial sediments; bedrock outcrops are rare.

Endako, Nechako, Stuart, Middle, and Tachie rivers, in the south and central part of the study area (Fig. 2), are part of the Fraser River system emptying into the Pacific

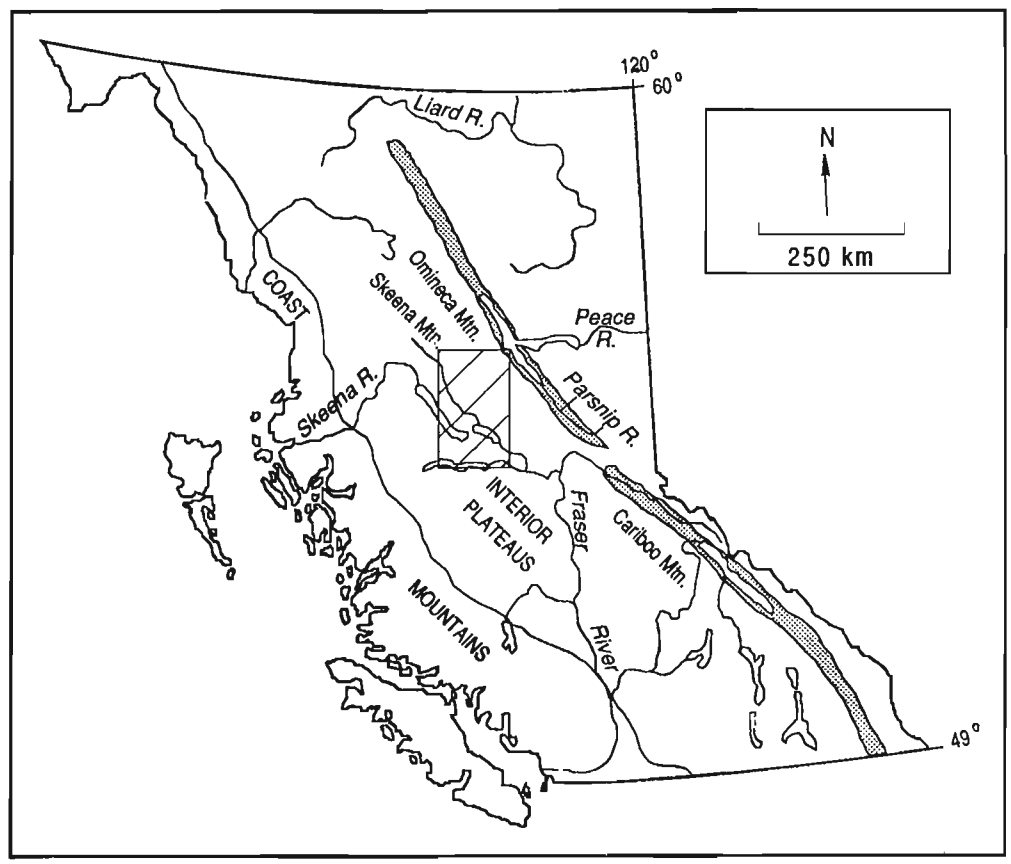

Figure 1. Location of study area (oblique pattern; see also Figure 2) with surrounding physiographic subdivisions. The Rocky Mountain Trench is shaded.

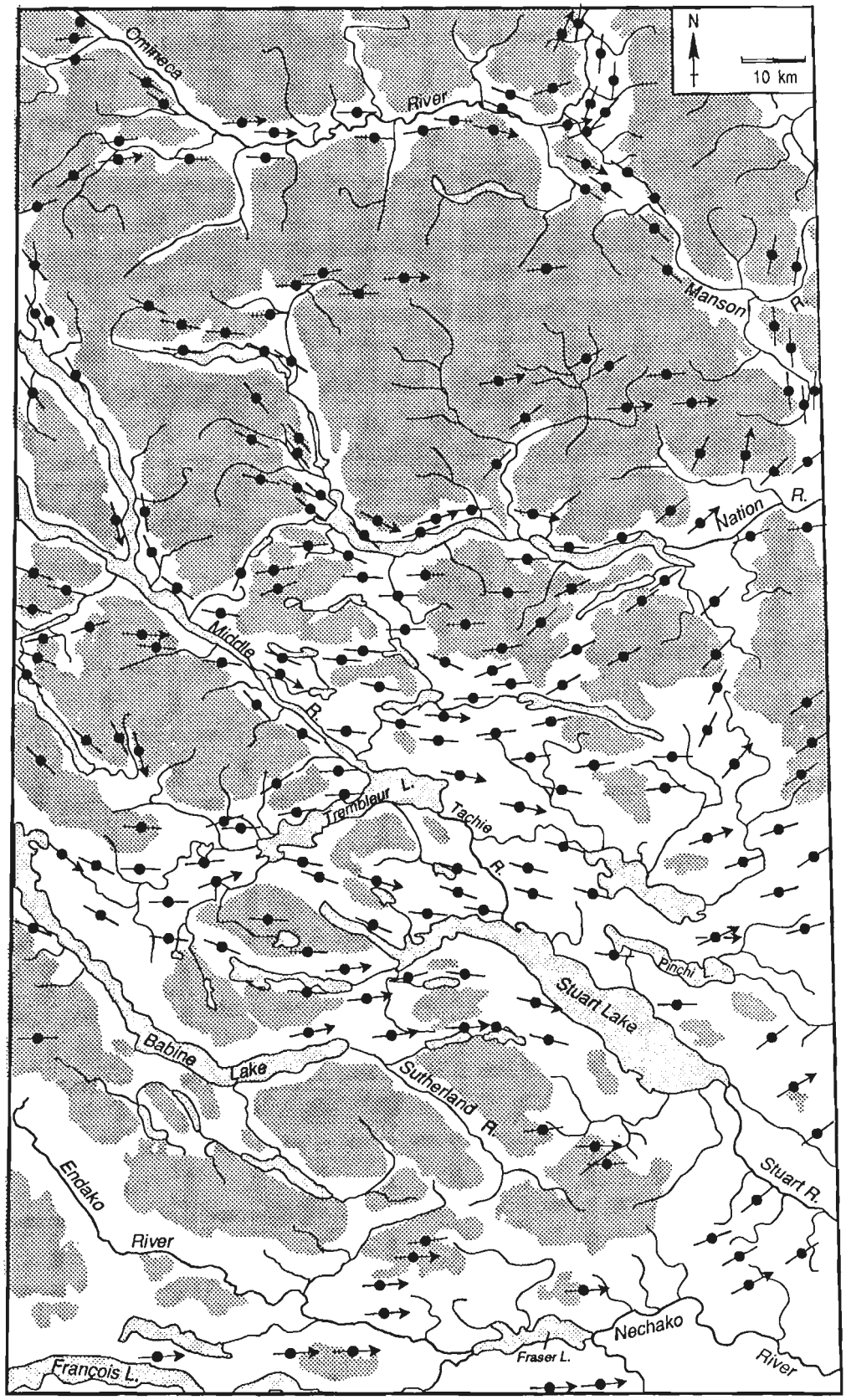

Figure 2. Pattern of ice flow direction as deduced from drumlins, glacial grooves, crag and tail, and striations. An arrow is used where the direction of ice movement is known. Terrain above 1000 m is shaded with dense stipple. Armstrong and Tipper (1948) published a similar map for this area.

Ocean; Sutherland River drains part of the Nechako Plateau to the Pacific Ocean through the Skeena River system to the west in the south-central part of the study area. Farther north, the Nation, Manson, and Omineca rivers are tributaries of the Peace River system which in turn flows to the Arctic Ocean via Mackenzie River.

Drainage anomalies

Stellako and Endako rivers present certain drainage anomalies which suggest glacially induced drainage diversion (Fig. 3). Between François Lake and the valley of Endako River, Stellako River flows in a narrow deep bedrock gorge. On the other hand, approximately 6 km south of Stellako riverhead, a gently sloping broad valley, occupied by Nithi River, extends eastward from François Lake. To the east, this valley is occupied by Smith Creek and joins Nechako River valley. At some time prior to the last glaciation, this valley probably served as the outlet for François Lake. The situation is similar for Nechako River draining Fraser Lake. From the mouth of Nautley River to east of Vanderhoof, Nechako River occupies a narrow valley. In contrast, east of Vanderhoof and just south of the confluence of Nautley and Nechako rivers, Nechako valley is much broader. Also, to the south of the study area, there is a broad buried channel that extends from Nechako River along Goldie and Stony creeks to just west of Vanderhoof. This old channel probably represents the course of the ancestral Nechako River. As is the case with Stellako River draining François Lake, the cause of the drainage disruption (whether it be ice or sediment damming, or isostatic rebound) is still unknown.

PREVIOUS STUDIES

Evidence of glaciation in the interior of British Columbia was first presented by Dawson (1878). His idea about the glaciation of the province evolved from a concept that the land subsided under 1520 m of water (Dawson, 1878, 1881) to a glacial ice theory in which he introduced the preliminary idea of the Cordilleran glacier (Dawson 1888, 1889). Armstrong and Tipper (1948) and Armstrong (1949) presented a clearer picture for the last glaciation of the northern interior in which ice was flowing east and northeast over the northern Nechako Plateau from a source in the Skeena Mountains. They also recognized the glacial lake basins of the Vanderhoof and Fort St. James areas. Some researchers proposed that during the last glaciation ice became thick enough to form a dome over interior British Columbia with radial surface flow from the centre (e.g. Dawson 1889, Kerr, 1934; Flint, 1971). Tipper (1971b) rejected the ice dome theory because airphoto interpretation of central British Colombia revealed that ice flow direction indicators did not suggest radial flow from a central accumulation zone; instead, he presented a model for the last glaciation in which piedmont glaciers flowed from accumulation zones in the Coast, Omineca, and Cariboo mountains and coalesced over the Interior Plateaus (Fig. 2), but with the ice never reaching an ice dome stage.

Harington et al. (1974) reported a radiocarbon date of 34 000 ± 690 BP on remains of a mammoth skeleton from just to the west of the study area. That date revealed the presence of sediments from the Olympia nonglacial interval, that is, the time period preceding the last glaciation (Clague, 1981).

GLACIAL LANDFORMS AND FEATURES

Different types of glacial landforms and features have been observed in the field and on air photographs. The most prominent ones are described below.

Glacial striations. Glacial striations are rare at least in the southern part of the study area because bedrock is covered by thick unconsolidated sediments over wide areas. Where bedrock is exposed, it is jointed and poorly indurated and striations are not well preserved. The few striations measured in the field were usually parallel to the larger streamlined features such as drumlins and glacial grooves observed on airphotos. Some striae, however, have a different orientation than these larger glacial landforms. This is particularly notable northeast of Pinchi Lake where east-west striations are crosscut by ENE-WSW striations in an area where glacial grooving has an east-northeast orientation (Fig. 2). This relationship is believed to indicate a shift in ice flow direction

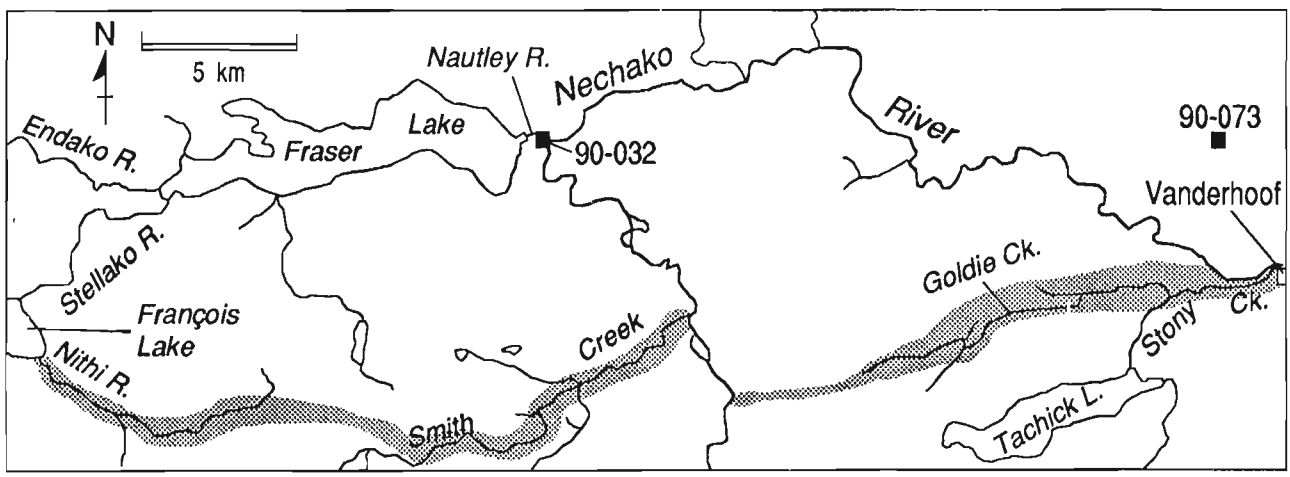

Figure 3. Location of buried channels (stipple pattern) between François Lake and Vanderhoof (along southern boundary of study area). Location of sections 90-032 and 90-073 is also shown.

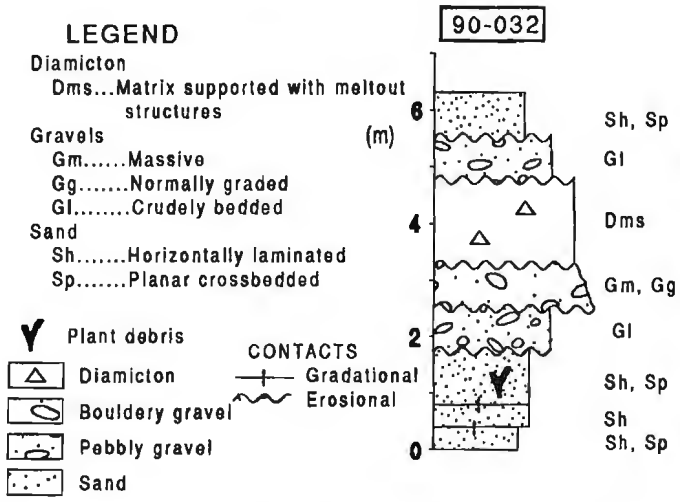

Figure 4. Lithostratigraphic column of Nautley River section (90-032).

as interacting piedmont glaciers flowing from the surrounding mountains coalesced. Ice from the Skeena and Coast mountains first flowed toward the east and later flow shifted to a more east-northeasterly direction when it coalesced with ice from the Cariboo Mountains. Future work on till geochemistry and lithologies might reveal more information on ice flow direction variation.

Drumlins and glacial grooves. For a thorough description of these glacial features which occur in the study area the reader is referred to the work of Armstrong and Tipper (1948, p. 287-293). The glacial grooves can be described as elongated depressions in between low drumlins. At several sites, grooves are occupied by small creeks. Drumlins, crag and tail, glacial striations, and glacial grooves were used to deduce the ice flow patterns depicted in Figure 2.

Meltwater channels. Abandoned meltwater channels occur throughout the area. They vary in size from a few metres to hundreds of metres wide and reach lengths of several kilometres. More work will have to be done to classify them but on a preliminary basis, some can be described as lateral overflow channels, that is, formed by meltwater flowing along the ice margin. They are encountered on hillsides and are commonly oriented perpendicular or at an angle to the slope, which indicates that they were carved while the meltwater was flowing against a temporary physical support —ice. Certain channels do not have a constant orientation and are believed to represent the shape of stagnant bodies of ice at a late stage during deglaciation of the area. Other channels oriented perpendicular to ice flow direction probably show the shape of the ice front during recession.

Eskers. Two major categories of eskers are present in the area : single ridge eskers and esker complexes. This classification has been reported previously by Armstrong and Tipper (1948) and by Tipper (1971a, b). The esker complexes are a series of anastomosing ridges which can reach a few kilometres in width. Most eskers do not parallel ice flow direction and usually occur near valley bottoms, and thus are believed to have formed when the ice was stagnant.

Figure 5. Thinning upwards of silt layers in glaciolacustrine varves south of Fraser Lake.

SURFICIAL SEDIMENTS

Apart from the work of Harington et al. (1974) in the Babine Lake area west of the study area, no other radiocarbon dates are available for the study area. Consequently, the surficial sediments will be described here in three broad classes: pre-Fraser sediments (deposits older than the last glaciation), Fraser sediments (deposits of the last glaciation), and post-glacial sediments.

Pre-Fraser sediments

Sediments deposited prior to the Fraser Glaciation have been observed only at the Nautley River section (Fig. 3 and 4). At that site, compacted and glacially tectonized alluvial sediments are overlain by 1.5 m of till. Plant debris has been found in the alluvial sediments, and pollen and paleoclimate studies are presently in progress. Future work at this site will include collection of plant fragments for radiocarbon dating, and analysis of glacigenic deformation structures. In other studies, such structures have been found useful in determining ice flow directions (see for example Broster and Clague (1987)).

Fraser sediments

At station 90-073, 8 km north of Vanderhoof (Fig. 3), horizontally stratified and deformed sand and gravel overlain by till have been interpreted as glacial outwash sediments deposited during the advance phase of the Fraser Glaciation; they indicate free drainage conditions during the growth of the glacier. In the study area, the most areally abundant sediment is Fraser till. Except for a few localities, it has a clayey texture. This clayey till is the result of ice which was largely flowing over clayey unconsolidated sediments during the Fraser Glaciation. Apart from the outwash gravel described above, other fluvioglacial sediments have been observed in the area. They include eskers, esker complexes, and probably other types of supraglacial, englacial, and subglacial sand and gravel deposited by running meltwater.

Valleys of the Endako and Stuart rivers, and some terrain below approximately 725 m, are characterized by a cover

of laminated glaciolacustrine silt and clay which reaches thicknesses of 30 m in drill holes at the west end of Fraser Lake in what appears to be a buried valley. Nevertheless, the thickness of glaciolacustrine sediments is generally not great enough to obliterate the underlying morphology. The laminations consist of silt and clay couplets with several coarsening and fining upward cycles within the silt layers. At sections along Stuart River and south of Fraser Lake, the silt layers thin (Fig. 5) and fine upwards over the exposures. These trends within a sequence are thought to represent the retreat of an ice front with a concomitant decrease of the sediment influx to the glacial lake or the increasing predominance of progressively distal glaciolacustrine sedimentation. The silt and clay layering possesses characteristics similar to the annual rhythmites described by Smith and Ashley (1985) and consequently is thought to represent varves.

Postglacial sediments

Postglacial sediments include fluvial sand and gravel, organic deposits developed in poorly drained areas, colluvium formed through the reworking of various types of glacial and probably nonglacial sediments, and lacustrine silt and clay at the eastern end of Stuart Lake.

PRELIMINARY QUATERNARY HISTORY INTERPRETATION

The only indications of sedimentary environment prior to the Fraser Glaciation come from the subtill alluvial sediments at the Nautley River section which indicate a period of fluvial aggradation. At the onset of Fraser Glaciation, piedmont glaciers advanced toward the east and southeast from the Coast and Skeena mountains as indicated by the orientation of drumlins, glacial grooves, and striations (Fig. 2). During this advance phase, it is believed that the drainage was free and that outwash gravel was deposited in front of the glacier. As the ice from the Skeena and Coast mountains coalesced with ice from the Cariboo Mountains, ice flow shifted in the southeastern sector of the study area and perhaps elsewhere as indicated by crosscutting striations to the northeast of Pinchi Lake. Flow to the east shifted to a more east-northeasterly direction.

During ice retreat, Endako and Nechako rivers were blocked and their valleys and all connecting ground below approximately 725 to 760 m were flooded. According to Clague (1981) and Tipper (1971a, b), this glacial lake, along with others in the central Interior Plateaus, were ponded behind ice retreating south in Fraser Valley. Based on the highest occurrences of glaciolacustrine sediments, the glacial lake in Endako and Nechako valleys probably reached 725 to 760 m elevation. The lake level might have been controlled by an outlet through Summit Lake about 90 km west of the study area. The water divide, at the source of Endako River, at 719 m, is not likely to have played a major role since ice in the Coast Mountains was probably blocking the valley during most of the existence of the lake. Also abundant evidence of ice stagnation (meandering eskers and ice contact stratified drift) is preserved in the valley of Burns Lake near the headwaters of Endako River; this stagnant ice could have blocked the overflow to the west.

The glacial lake drained upon destruction of the dam. Water levels in most lakes dropped to an elevation slightly higher than present day lake levels. This is evidenced by delta surfaces slightly above lake level in Fraser, Stuart, and Burns lakes along with fluvial gravel terraces graded to about the same elevation along Nechako and Endako rivers. Also, lacustrine sediments at the eastern end of Stuart Lake, 18 m above the lake level, were probably deposited during this period of higher water levels. The nature of the dams which caused these higher base levels is still unknown. The high lake levels possibly represent a period of stabilization prior to downcutting of lake outlets which accompanied a general lowering of base levels associated with development of postglacial drainage and entrenchment.

SUMMARY

During the last glaciation, Fraser Glaciation, piedmont glaciers originating from the Skeena and Coast mountains invaded the area from the northwest and west and later coalesced with ice from the Cariboo Mountains. During this glacial event, ice flowed towards the east and northeast sculpting the land and forming drumlins, crag and tail, and glacial grooves. Deglaciation was marked by drainage blockage of Nechako and Endako rivers and the formation of a glacial lake. Deltas, alluvial terraces, and lacustrine sediments are all evidence that, after the existence of the glacial lake, the base level was at a higher level than today for a certain period of time. This last event was followed by lowering of base level.

ACKNOWLEDGMENTS

R.J. Fulton and L.E. Jackson, Jr. reviewed and improved the original version of the manuscript. The author was capably assisted in the field by Trish McKay. G. Labrash from Vanderhoof is thanked for his expert canoeing services.

REFERENCES

Armstrong, J.E.
1949: Fort St. James map-area Cassiar and Coast District, British Columbia; Geological Survey of Canada, Memoir 252, 204 p.

Armstrong, J.E. and Tipper, H.W.
1948: Glaciation in north central British Columbia; American Journal of Science, v. 246, p.283-310.

Broster, B.E. and Clague, J.J.
1987: Advance and retreat glacigenic deformation at Williams Lake, British Columbia; Canadian Journal of Earth Sciences, v. 24, p. 1421-1430.

Clague, J.J.
1981: Late Quaternary geology and geochronology of British Columbia, Part 2 : Summary and discussion of radiocarbon-dated Quaternary history; Geological Survey of Canada, Paper 80-35, 40 p.

Dawson, G.M.
1878: On the superficial geology of British Columbia; Quarterly Journal of the Geological Society of London, v. 34, p. 89-123.
1881: Additional observations on the superficial geology of British Columbia and adjacent regions; Quarterly Journal of the Geological Society of London, v. 37, p. 272-285.
1888: Recent observations on the glaciation of British Columbia and adjacent regions; Geological Magazine, New Series, v. 5, p. 347-350.
1889: Glaciation of high points in the southern interior of British Columbia; Geological Magazine, New Series, v. 6, p. 350-352.

Flint, R.F.
1971: Glacial and Pleistocene Geology; J. Wiley and Sons, New-York.
Kerr, F.A.
1934: Glaciation in northern British Columbia; Transaction of the Royal Society of Canada, v. 28, sec. IV, p. 17-32.
Harington, C.R., Tipper, H.W., and Mott, R.J.
1974: Mammoth from Babine Lake, British Columbia; Canadian Journal of Earth Sciences, v. 11, p. 285-303.
Holland, S.S.
1976: Landforms of British Columbia, a physiographic outline; British Columbia Department of Mines and Petroleum Resources, Bulletin 48, 138 p.
Mathews, W.H.
1986: Physiography of the Canadian Cordillera; Geological Survey of Canada, Map 1701A, scale 1:5 000 000.
Smith, N.D. and Ashley, G.M.
1985: Proglacial lacustrine environment; in G.M. Ashley, J. Shaw, and N.D. Smith (ed.); Glacial sedimentary environments, Society of Economic Paleontologists and Mineralogists, Short course No. 16, p. 135-215.
Tipper, H.W.
1971a: Multiple glaciation in central British Columbia; Canadian Journal of Earth Sciences, v. 8, p. 743-752.
1971b: Glacial geomorphology and Pleistocene history of central British Columbia; Geological Survey of Canada, Bulletin 196, 89 p.

Holocene sea level change, south-coastal British Columbia

John J. Clague, S. Lichti-Federovich[1], J.-P. Guilbault[2], and R.W. Mathewes[3]
Terrain Sciences Division, Vancouver

Clague, J.J., Lichti-Federovich, S., Guilbault, J.-P., and Mathewes, R.W., Holocene sea level change, south-coastal British Columbia; in Current Research, Part A, Geological Survey of Canada, Paper 91-1A, p. 15-21, 1991.

Abstract

Stratigraphic and paleoecological studies of late Holocene organic and mineral sediments at Burns Bog on the Fraser River delta near Vancouver indicate that the sea was about 3 m below its present level relative to the land 4000-4500 radiocarbon years ago. Uninterrupted deposition of terrestrial peat at this site over the last 4000 years further suggests that the sea has not fluctuated more than 2 m from its present position during this time. Although the data do not deny that large earthquakes have occurred in the Vancouver area, there is no evidence for coseismic subsidence or uplift on the scale that might be expected during great thrust earthquakes.

Résumé

Les études stratigraphiques et paléoécologiques des sédiments organiques et minéraux datant de la fin de l'Holocène, à Burns Bog dans le delta du Fraser près de Vancouver, indiquent que la mer se situait à environ 3 m au-dessous de son niveau actuel il y a 4 000 à 4 500 ans, selon les datations établies à l'aide du carbone radioactif. Le dépôt ininterrompu de tourbe terrestre à cet endroit, depuis 4 000 ans, semble aussi indiquer que le niveau de la mer n'a pas fluctué de plus de 2 m par rapport à sa position actuelle, pendant cet intervalle de temps. Bien que les données ne permettent pas d'infirmer que d'importants séismes aient eu lieu dans la région de Vancouver, rien ne prouve qu'il se soit produit des épisodes de subsidence ou de soulèvement cosismiques de l'envergure prévue lorsqu'ont lieu de grands séismes accompagnés de chevauchements.

[1] Terrain Sciences Division, Ottawa, Ontario K1A 0E8
[2] BRAQ-Stratigraphie, 10545 Meilleur, Montréal, Québec H3L 3K4
[3] Department of Biological Sciences and Institute for Quaternary Research, Simon Fraser University, Burnaby, B.C. V5A 1S6

INTRODUCTION

The Geological Survey of Canada (GSC) is conducting studies aimed at determining the character and extent of recent and contemporary crustal deformation in the western Canadian Cordillera. These studies may provide information on the frequency and magnitude of large earthquakes in this region during the Holocene, which in turn can be used to assess the likelihood of comparable earthquakes in the future.

A major component of the GSC's west coast neotectonics program (Clague, 1989) involves the reconstruction of Holocene sea level change. The sea surface provides a datum for determining vertical crustal movements. Regional uplift and subsidence during large earthquakes are manifested by sudden shifts in the level of the land relative to the sea. These shifts commonly are recorded by raised beaches and related littoral landforms in uplifted areas and by submerged marshes and soils in areas of subsidence.

The pattern and chronology of relative sea level movements are being documented at several places along the British Columbia coast in an attempt to determine what factors have controlled these movements and whether or not large earthquakes have occurred in this region in the recent past. This is done through airphoto interpretation, stratigraphic and sedimentological logging of natural and artificial exposures and cores, paleoecological analysis, and radiocarbon dating of organic material (Clague, 1989; Clague and Bobrowsky, 1990).

In this report, we attempt to demonstrate the value and power of microfossil and plant macrofossil analyses in reconstructing relative sea level change. Pollen, plant macrofossils, diatoms, foraminifera, and arcellacea can provide precise information on former sea level positions. Changes in the relative abundance of key taxa in sediment sequences, in some cases, may indicate changes in sea level in the past. To demonstrate these points and to provide information on late Holocene sea level change in coastal southwestern British Columbia, we present here preliminary results from Burns Bog, a large domed peat bog located near present sea level on the Fraser River delta near Vancouver (Fig. 1; Hebda, 1977; Clague and Luternauer, 1982).

METHODS

Samples from part of a piston core (Fig. 2) collected from Burns Bog were analyzed for pollen, plant macrofossils, diatoms, foraminifera, and arcellacea using standard methods. Palynomorph subsamples first were treated with hot 6 % KOH to disperse sediments and remove humic acids, then screened at 250 μm to remove coarse debris, and finally treated with

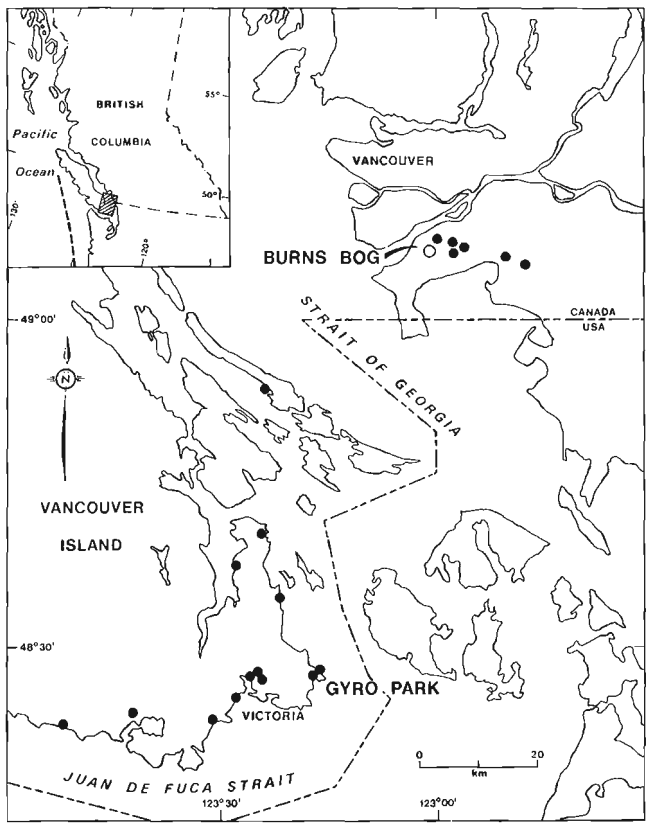

Figure 1. Location map showing sites that have been studied in detail since 1988. This report focuses on work done in 1989 and 1990 at Burns Bog, just south of Vancouver. The open circle shows the location of the core reported in this paper. The dashed line on the inset indicates the approximate boundary between the America and Juan de Fuca plates (Cascadia subduction zone).

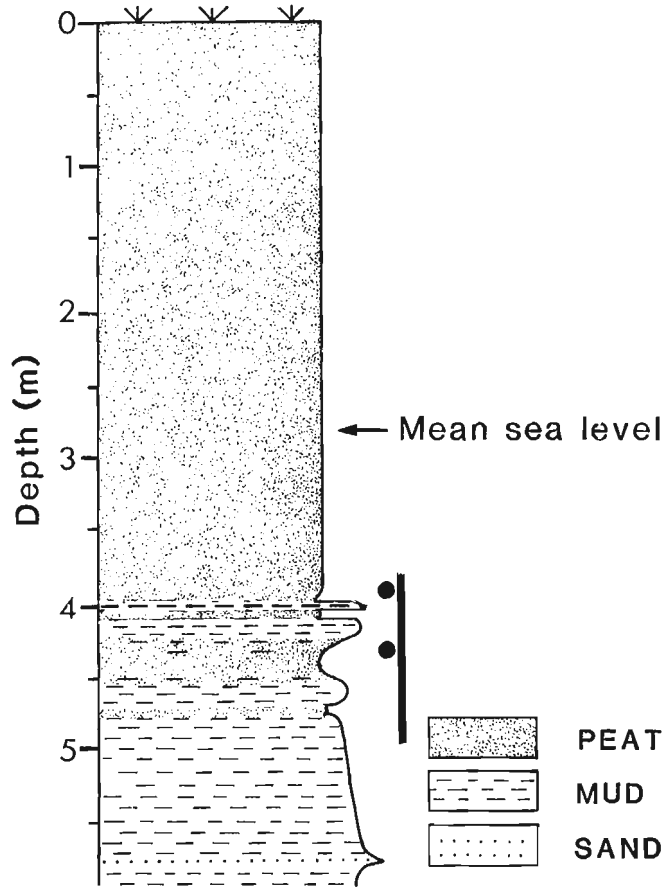

Figure 2. Stratigraphy of the Burns Bog core (49°07.6'N, 123°01.1'W). The vertical bar indicates the analyzed section of the core; dots are the dated horizons (see Fig. 3). Mean and large tidal ranges in the vicinity of the Fraser delta are 3.3 m and 4.9 m, respectively.

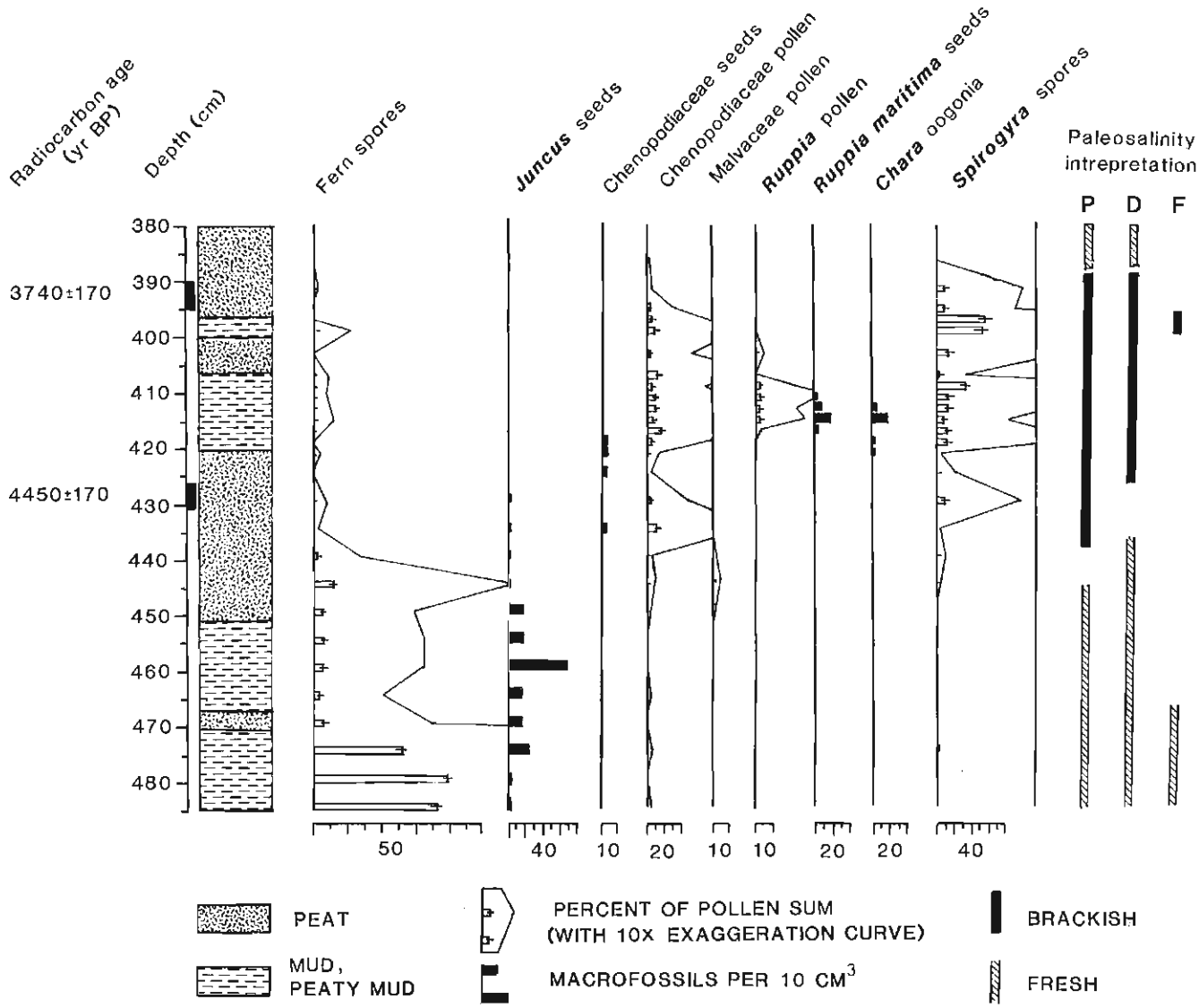

Figure 3. Variations in selected plant macrofossils and microfossils in the lower part of the Burns Bog core. Paleosalinity intrepretations based on pollen, spores, and plant macrofossils (P), diatoms (D), and foraminifera and arcellacea (F) are shown on the right.

hot 10 % HCl and cold 48 % HF to dissolve carbonates and silicates. Clay-rich samples were dispersed in sodium pyrophosphate and sieved through a 7 μm Nitex screen. Palynomorphs were washed, stained with safranin O, and mounted in silicone oil for microscopic analysis, using a Zeiss Photomicroscope II. Pollen percentage calculations were based on sums of all identifiable pollen and spores (range = 331-659 specimens).

Plant macrofossils were concentrated from approximately 10 cm^3 of sediment by wet sieving, and were identified and counted under a dissecting binocular microscope.

Diatom subsamples (10 cm^3 of sediment) were oxidized with 150 mL of 30 % H_2O_2; digestion of highly organic material required boiling. The subsequent addition of small amounts of $K_2Cr_2O_7$ completed the oxidation process. After repeated washings with distilled water, residues were mounted on slides, using Hyrax as a mounting medium. Microscopic examinations were made with a Leitz Ortholux. Critical identifications and taxonomic classification are based on the work of Patrick and Reimer (1966, 1975) and Krammer and Lange-Bertalot (1985, 1986, 1988).

Foraminifera-arcellacea subsamples were stored in a buffered 10 % formaldehyde solution to prevent decay prior to processing; 10-11 cm^3 of sediment were disaggregated by manual shaking and washed through a 63 μm screen. Screen residues were split in a wet state into 8 aliquots, one of which was studied and the remainder stored in reserve in a mixture of methanol and water.

RESULTS

Cores taken from Burns Bog record continuous deposition of peat over the last several thousand years (Hebda, 1977). In the core shown in Figure 2, 4 m of peat overlies interbedded

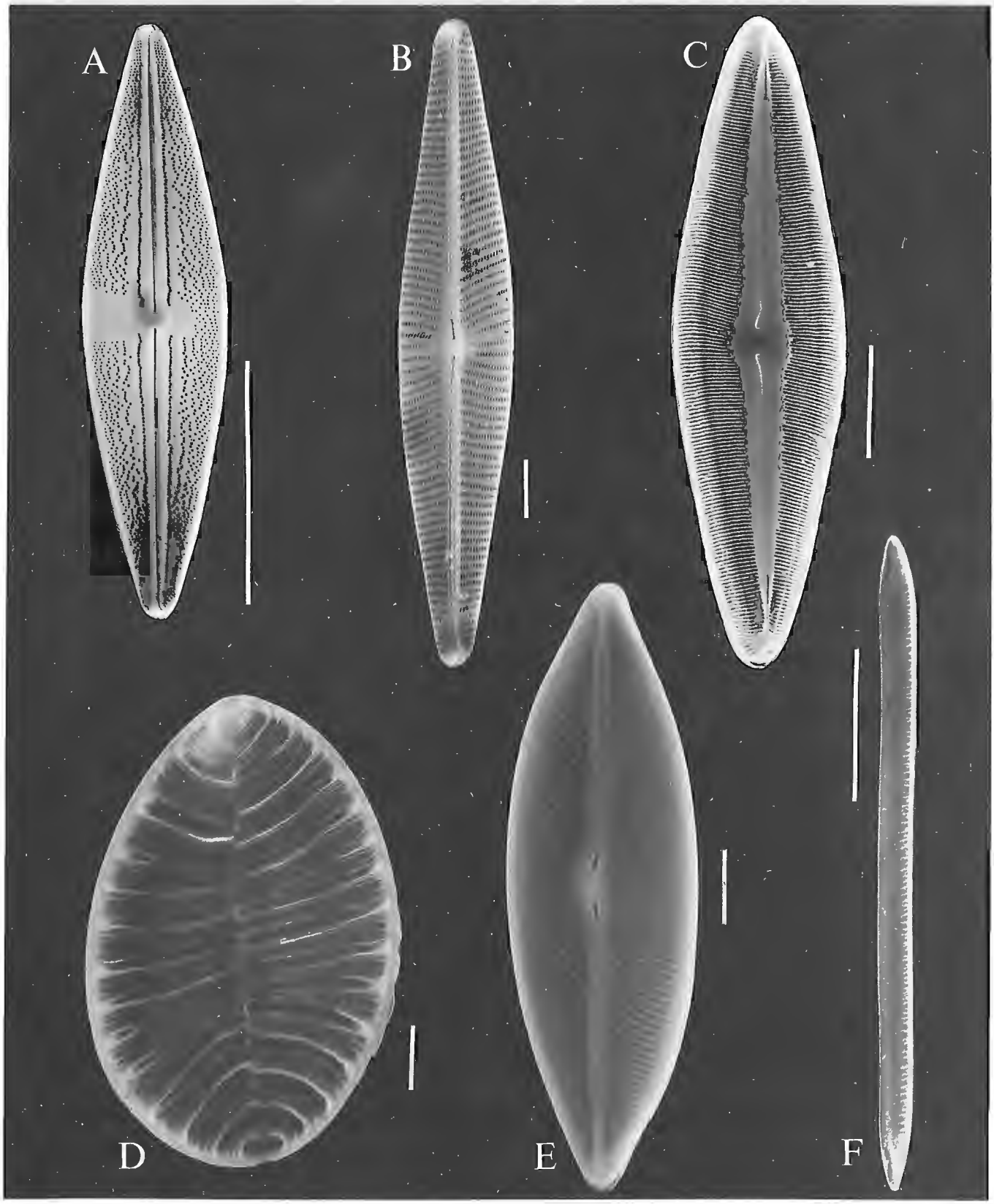

Figure 4. Scanning electron micrographs of selected diatoms from the Burns Bog core. A. *Anomoeoneis sphaerophora* fo. *costata (Kützing)* Schmid (SEM x 861, scale bar = 50 μm, 408-410 cm). B. *Navicula peregrina* (Ehrenberg) Kützing (SEM x 1030, scale bar = 10 μm, 408-410 cm). C. *Caloneis permagna* (Bailey) Cleve (SEM x 660, scale bar = 30 μm, 408-410 cm). D. *Surirella striatula* Turpin (SEM x 1130, scale bar = 10 μm, 406-408 cm). E. *Navicula elegans* W. Smith (SEM x 1270, scale bar = 10 μm, 422-427 cm). F. *Nitzschia scalaris* (Ehrenberg) W. Smith (SEM x 268, scale bar = 100 μm, 422-427 cm).

muddy peat and organic-rich mud. A previous palynological study (Hebda, 1977) indicated that the peat above the uppermost mineral sediments was deposited in freshwater (i.e., swamp, marsh, shrubland, and bog) environments, even though it largely extends below the upper limit of tides. Within this freshwater peat, there are no beds, laminae, or lenses of mineral sediment that might signal a sudden rise in sea level (e.g., due to coseismic subsidence).

Evidence for strongly brackish or marine environments has been found only at the base of the upper thick peat unit, which has yielded a radiocarbon age of 3740 ± 170 BP (S-3190; 1 σ error), and in the immediately underlying zone of interbedded organic-rich mineral sediments and peat (approximately 396-457 cm) (Note: peat at 426-431 cm has been dated at 4450 ± 170 BP, S-3191, 1 σ error). Mud and sand below 457 cm contain freshwater microfossils and seeds.

Pollen and plant macrofossils (R.W. Mathewes)

To date, 45 palynomorph taxa have been identified from the core, representing pollen and spores of vascular plants, algal spores and colonies, and rare foraminifera. Fungi and other organic microfossils are present, but have not been systematically studied. In addition, more than 15 types of macrofossils, mostly seeds and seed-like structures have been identified. Abundances of 9 selected fossil types are plotted in Figure 3. These taxa were selected as useful indicators of local paleoenvironments and paleosalinity.

An abundance of fern spores and seeds of *Juncus* (rushes) and other wetland plants indicates a freshwater depositional environment between 485 cm and 445 cm. The first indication of salinity occurs in peat at about 445-435 cm, where pollen of Malvaceae (mallow) and Chenopodiaceae (chenopod) appear, along with algal spores typical of nutrient-rich waters *(Spirogyra)*.

A strong brackish environment is inferred for peaty sediments between 435 cm and 420 cm, on the basis of seeds and pollen of Chenopodiaceae and pollen of *Rumex* (dock), *Potentilla*-type (silverweed), and Apicaeae (parsley). Macrofossils of the aquatic stonewort *Chara*, seeds and pollen of *Ruppia maritima* (ditchgrass), pollen of Chenopodiaceae, and spores of *Spirogyra* indicate a saline aquatic environment, either a brackish pond or a lagoon, for the mud unit at 406-420 cm. The disappearance of this body of water and the reestablishment of a brackish marsh, represented by the peat bed at 400-406 cm, was followed by renewed mud deposition (396-400 cm). This upper mud bed contains abundant foraminifera and maximum percentages of *Spirogyra* spores, indicating a saline environment of deposition.

Diatoms (S. Lichti-Federovich)

Three diatom floristic units are recognized in the analyzed portion of the Burns Bog core. The lowest diatom unit, which extends from 487 cm to 437 cm depth, records fresh- to slightly brackish-water conditions. The lower part of the unit (up to 457 cm) contains an abundance of the euryhaline taxa *Nitzschia scalaris* (Fig. 4F) and *Navicula peregrina* (Fig. 4B), as well as freshwater diatoms. Above this, there

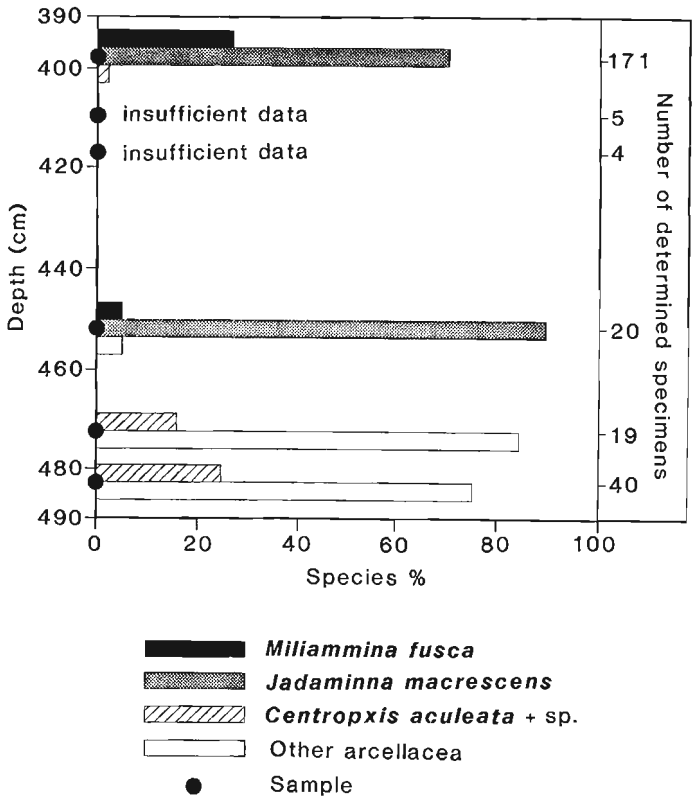

Figure 5. Distribution of foraminifera and arcellacea in the lower part of the Burns Bog core. See Figure 3 for paleosalinity interpretation.

is an increase in the diversity and abundance of the freshwater component *(Stauroneis phonicenteron, Surirella spiralis, Cymatopleura elliptica, Pinnularia, Aulacosira (Melosira), Cymbella, Epithemia)*. Near the top of the unit, diatom frequencies decrease, and the uppermost sample (437-442 cm) contains an impoverished freshwater assemblage.

The gradational transition between the basal and middle diatom units (427-437 cm) is marked by the presence of *N. scalaris* and *N. peregrina*, indicating slightly brackish conditions.

The middle diatom unit (396-427 cm), the most salient of the entire sequence, is characterized by a pronounced brackish element *(Anomoeoneis sphaerophora* fo. *costata* (Fig. 4A), *Caloneis permagna* (Fig. 4C), *Hyalodiscus laevis)*, brackish-marine and marine-littoral forms *(Paralia sulcata, Nitzschia granulata, Navicula lyra)*, and sporadic occurrences in some horizons of freshwater *Aulacosira (Melosira)* valves. This assemblage includes indicator species of brackish-marine mudflat environments *(Scoliopleura tumida, Caloneis westii, Surirella striatula* (Fig. 4D)), as well as members of saltmarsh communities *(Navicula elegans* (Fig. 4E), *N. pusilla, N. peregrina,* and *Nitzschia scalaris)*.

The middle and upper diatom units are separated by a gradational transition zone (394-396 cm), which contains a mixed assemblage of brackish, freshwater, and rare marine elements.

The upper diatom unit (387-394 cm), which is interpreted to be supratidal, is marked by low abundances of *N. scalaris* and *N. peregrina* and low diatom frequencies. The most common diatoms in this unit are freshwater *Aulacosira (Melosira)* valves.

Foraminifera and arcellacea (J.-P. Guilbault)

Four foraminifera species and 4 arcellacean species have been identified in the analyzed part of the Burns Bog core. Only 2 of the foraminifera species, *Jadammina macrescens* and *Miliammina fusca*, occur in appreciable numbers. The first is a typical inhabitant of uppertidal marshes, and the only foraminifer able to survive at the limit of tides. *M. fusca* prefers the lower tidal marsh, but may also be found in lesser numbers higher in the intertidal zone. No foraminifer is known to live in freshwater. (Note: foraminiferal ecology from Scott and Medioli (1980) and Patterson (in press)).

The common arcellacea are *Centropyxis aculeata, Heleopera sphagni,* and *Difflugia globulus.* Arcellacea are strictly freshwater organisms, although *Centropyxis aculeata* can tolerate slight salinity and tends to be dominant immediately above the limit of tides, where saline influence may be felt either through spray (D.B. Scott, personal communication) or during storms. *H. sphagni* lives on mosses and *D. oblonga* in oozes of various freshwater bodies. (Arcellacea ecology from Medioli and Scott (1983) and Bovee (1985)).

The complete absence of foraminifera and the presence of strictly freshwater taxa below 457 cm in the Burns Bog core strongly suggest supratidal conditions (Fig. 3, 5). There is an equally clear indication of an intertidal environment in the mud bed at 396-400 cm (Fig. 5).

The sample at 447-457 cm is dominated by *J. macrescens,* suggesting deposition at the upper limit of the intertidal zone. However, the number of identified specimens (20) is low for an intertidal environment, and the entire assemblage could be allocthonous. Nevertheless, this is the first indication of a marine protozoan assemblage in the core.

The samples at 413-420 cm and 406-413 cm yielded only 4 and 5 identified specimens, respectively, which is not enough for paleoenvironmental interpretation.

DISCUSSION

The sequence in this core appears to be a normal succession deposited in response to a protracted slow rise in relative sea level. The sediments form the top of an extensive delta plain that is graded to present sea level.

The data presented in this report suggest that the lowest cored materials, 3 m below mean sea level, are fluvial overbank sediments dating to ca. 5000 BP and deposited when sea level was lower relative to the land than today (compaction and slow subsidence may account for some, but not most, of the apparent sea level change over this period; see Clague et al. (1982) and Williams and Roberts (1989)).

The presence of upper intertidal foraminifera, brackish- and saline-water diatoms, and pollen and seeds of brackish aquatic plants in the transitional zone between the minerals sediments and the thick upper peat indicates that relative sea level was about 3 m below present when the sediments in this zone were deposited (ca. 4000-4500 BP). Although there are differences in the microfossil content of these transitional sediments, there is no evidence for a large (i.e., more than a few tens of centimetres), rapid change in sea level during the period they were deposited. A small sudden change in sea level, however, may account for the pronounced lithofacies and biofacies changes at ca. 400 cm depth. The mud bed at 396-400 cm contains abundant foraminifera and *Spirogyra* spores and probably was deposited when brackish or saline waters flooded the site ca. 4000 BP. Other lithofacies changes appear to be gradational and do not coincide with changes in microfossil assemblages. Such gradational changes may reflect variations in sediment supply to the site due, for example, to episodic flooding or river channel migration. These changes might be expected under a stable or slowly rising sea level regime as an active floodplain or tidal flat became stabilized with vegetation and transformed into a marsh.

The subsequent accumulation of thick peat over a large area of the eastern Fraser delta and the seral succession of vegetation types in Burns Bog from ca. 4000 BP to the present (Hebda, 1977) indicate that the water table remained high during this period. This, in turn, suggest that sea level was not significantly lower during this period than at the time the bog first formed. On the other hand, available data suggest that there has been no major transgression of Burns Bog by the sea during the last 4000 years (Hebda, 1977).

In summary, the delta plain on which the bog lies apparently has not experienced significant (approximately 1 m) coseismic (or for that matter, aseismic) uplift or subsidence during the last few thousand years. A similar conclusion can be drawn from the somewhat similar peat sequence at Gyro Park on southern Vancouver Island (Fig. 1).

ACKNOWLEDGMENTS

Scanning electron micrographs reproduced in Figure 4 were taken by D.A. Walker and L. Radburn (Geological Survey of Canada, Ottawa). D.B. Scott (Dalhousie University) and R.T. Patterson (Carleton University) provided advice on the foraminifera and arcellacea.

REFERENCES

Bovee, E.C.
1985: Class Lobosea Carpenter, 1861; in An Illustrated Guide to the Protozoa, J.J. Lee, S.H. Hutner, and E.C. Bovee, (ed.), Society of Protozoologists, Lawrence, Kansas, p. 158-211.

Clague, J.J.
1989: Late Quaternary sea level change and crustal deformation, southwestern British Columbia; in Current Research, Part E, Geological Survey of Canada, Paper 89-1E, p. 233-236.

Clague, J.J. and Bobrowsky, P.T.
1990: Holocene sea level change and crustal deformation, southwestern British Columbia; in Current Research, Part E, Geological Survey of Canada, Paper 90-1E, p. 245-250.

Clague, J.J. and Luternauer, J.L.
1982: Excursion 30A: Late Quaternary sedimentary environments, southwestern British Columbia; International Association of Sedimentologists, Field Excursion Guidebook (11th International Congress on Sedimentology, Hamilton, Ontario).

Clague, J.J., Harper, J.R., Hebda, R.J., and Howes, D.E.
1982: Late Quaternary sea levels and crustal movements, coastal British Columbia; Canadian Journal of Earth Sciences, v. 19, p. 597-618.

Hebda, R.J.
1977: The paleoecology of a raised bog and associated deltaic sediments of the Fraser River delta; unpublished Ph.D. thesis, University of British Columbia, Vancouver, B.C.

Krammer, K. and Lange-Bertalot, H.
1985: Naviculaceae; Bibliotheca Diatomologica, Band 9; J. Cramer, Berlin, Stuttgart.
1986: Bacillariophyceae (Naviculaceae); in Suesswasserflora von Mitteleuropa 2, Teil 1, H. Ettl, J. Gerloff, H. Heynig, and D. Mollenhauer, (ed.), Fischer, Stuttgart.
1988: Bacillariophycaea (Bacillariaceae, Epithemiaceae, Surirellaceae; in Suesswasserflora von Mitteleuropa 2, Teil 2, H. Ettl, J. Gerloff, H. Heynig, and D. Mollenhauer, (ed.), Fischer, Stuttgart.

Medioli, F.S. and Scott, D.B.
1983: Holocene arcellacea (thecamoebians) from eastern Canada; Cushman Foundation for Foraminiferal Research, Special Publication 21.

Patrick, R. and Reimer, C.W.
1966: The diatoms of the United States; Academy of Natural Sciences, Philadelphia, v. 1, Monograph no. 13.
1975: The diatoms of the United States; Academy of Natural Sciences, Philadelphia, v. 2, part 1, Monograph no. 13.

Patterson, R.T.
Intertidal benthic foraminiferal biofacies on the Fraser River delta, British Columbia: Modern distribution and paleoecological importance; Micropaleontology, v. 36 (in press).

Scott, D.B. and Medioli, F.S.
1980: Quantitative studies of marsh foraminiferal distributions in Nova Scotia: Implications for sea level studies; Cushman Foundation for Foraminiferal Research, Special Publication 17.

Williams, H.F.L. and Roberts, M.C.
1989: Holocene sea-level change and delta growth: Fraser River delta, British Columbia; Canadian Journal of Earth Sciences, v. 26, p. 1657-1666.

Comparison of surface, borehole and seismic cone penetrometer methods of determining the shallow shear wave velocity structure in the Fraser River delta, British Columbia

J.A. Hunter, D.J. Woeller[1], and J.L. Luternauer[2]
Terrain Sciences Division

Hunter, J.A., Woeller, D.J., and Luternauer, J.L., Comparison of surface, borehole, and seismic cone penetrometer methods of determining the shallow wave velocity structure in the Fraser River delta, British Columbia; in Current Research, Part A, Geological Survey of Canada, Paper 91-1A, p. 23-26, 1991.

Abstract

The shear wave velocity structure of the subsurface is an important input in estimating both ground amplification and liquefaction potential of unconsolidated sediments during an earthquake. Three different methods of measuring the shear wave velocity of shallow sediments have been tested and compared at three sites in the Fraser River delta; these are surface shear wave refraction, surface-to-borehole, and seismic cone penetrometer methods. All three methods indicate the same general trend of shear wave velocity-depth structure, though each is subject to different theoretical or logistical limitations. An evaluation of the potential of each of the three methods is offered.

Résumé

La structure que présente la vitesse des ondes de cisaillement en subsurface est une donnée importante pour estimer à la fois l'amplification des ondes dans le sol et le potentiel de liquéfaction (thixotropie) des sédiments non consolidés durant un séisme. On a mis à l'épreuve trois méthodes différentes de mesure de la vitesse des ondes de cisaillement dans des sédiments peu profonds, et l'on a comparé les résultats de ces méthodes à trois endroits dans le delta du Fraser; il s'agit de la méthode de réfraction des ondes de cisaillement en surface, la méthode de réfraction des ondes de la surface au trou de sondage, et la méthode sismique du pénétromètre à cône. Les trois méthodes indiquent toutes la même tendance générale pour la structure de la vitesse des ondes de cisaillement en fonction de la profondeur, même si chacune de ces méthodes présente des limitations théoriques ou logistiques différentes. Les possibilités que présentent chacune de ces trois méthodes sont évaluées dans cette étude.

[1] Conetec Investigations Ltd, 9113 Shaughnessy Street, Vancouver, B.C. V6P 6R9
[2] Cordilleran Division, Geological Survey of Canada, 100 West Pender Street, Vancouver, B.C. V6B 1R8

INTRODUCTION

For the past few years, the Terrain Geophysics Section has been involved in applied geophysics studies as part of a geohazards program on the west coast of British Columbia. One of the concerns is the response of the Fraser River delta sediments to ground shaking from a moderate earthquake (Richter 6-7). It has been determined that the shear wave velocity structure of the delta sediments is a major parameter in estimating both ground motion amplification and liquefaction potential. For this reason, testing of various methods of measuring the shear wave velocity structure is currently underway and initial results are presented here.

SURFACE REFRACTION METHOD

This method was applied in the standard reversed refraction manner, with an array of 24 transversely oriented horizontal geophones (8 Hz) at 3 m spacings. Both forward and reversed shots were fired into the array before the array was moved to cover a total source-geophone distance of 210 m. A one-geophone overlap was maintained when moving the spread to compensate for possible source timing errors.

Initial tests with a 7.5 kg hammer hitting a block of wood indicated that this source was not sufficiently powerful to maintain an acceptable signal-to-noise ratio over 200 m, even with the stacking capability of an engineering seismograph. Hence, a 12-gauge in-hole shotgun source was configured to shoot a blank load transversely to the line at a depth of 1 m, in an attempt to produce polarized SH energy. For most conditions, one shot with this modified "Buffalo gun" provided sufficient energy.

Although the shear wave packet was a clearly defined, large amplitude event, errors of one-half cycle in the determination of the "first arrival" are probably common, because picking the onset of shear energy can be difficult in the presence of shot generated noise (interpreted to be converted waves from the compressional energy of the source). As well, many records showed evidence of "shingling", suggesting refractions along thin high velocity layers. Qualitative estimates from the seismic records suggested that some degree of velocity reversal was occurring with depth, which was beyond the capability of the refraction method to assess.

Forward and reverse travel-times were compared, and most often were quite close; where differences occurred, these were interpreted to be time shifts resulting from a low velocity layer beneath one of the shotpoints. None of the sites on the delta where this method was applied showed any evidence of dipping layers from the forward and reverse shooting. Hence, it became standard practise to use averaged values of the forward and reverse travel-times for each source-geophone offset in the data analysis.

The travel-time distance data were analyzed using a curve-fitting computer routine (Hunter, 1971). The routine initially assigns a layer to each data point, and uses 3-point least-squares fits to produce a velocity gradient with depth, maintaining distinct velocity layers if they are defined by several data points. The resultant velocity-depth curve is often a mixture of both velocity gradients (single data points layers) and velocity layers.

SURFACE-TO-BOREHOLE METHOD

As part of a geological drilling program on the Fraser River delta, several 10 cm diameter drillholes cased with water-filled, 6 cm, thin-walled plastic pipe are available for geophysical logging. Although no grouting was emplaced around the casing, the holes were left to slump for a period of one or two years before the surface-to-borehole seismic measurements were carried out.

The downhole measurements were conducted using an OYO 3-component well locked geophone, which was lowered down the drillhole in 1 m increments. Since it was not possible to control the orientation of the geophone, the horizontal trace amplitudes and polarities differed between shots; hence, an editing run, consisting of trace and polarity selection, was required prior to analysis of the data.

The source used for the downhole survey was a 60 cm long triangular metal bar welded to a 100 x 60 cm steel step grating (for good ground contact), which was hit on one side with a 7.5 kg hammer to produce polarized shear energy. The source was offset 3 m from the hole for all surveys. Often only one hit was necessary to obtain a good shear wave signal; however, it was possible to use the stacking capability of the seismograph to improve the signal-to-noise ratio as required.

The packet of shear wave energy was plainly visible on all records; however, source-generated noise often resulted in uncertainties of one-half cycle in picking the onset of shear waves. This noise is thought to be coherent coupled P-wave events, since apparent velocities mirrored those of the P-wave first arrival.

The arrival-time data were analyzed using a running least-squares velocity routine after a straight raypath compensation for source offset. Errors arising from the use of a straight-line raypath model are thought to be confined to depths equal to or shallower than the source offset.

SEISMIC CONE PENETROMETER METHOD

The seismic cone penetrometer (SCPT) has been described in detail by Robertson et al. (1986). In essence, the device is a horizontal geophone embedded in the tip of a standard cone penetrometer. The cone is advanced into the soil in 1 m increments using the hydraulics of a drill rig as the pushing force. At each depth location, the rods are disconnected from the rig, to reduce coupled noise, and a shear wave record is obtained using a surface source. For these surveys, the source was a sledge hammer striking a loaded wooden block, situated 1 m from the hole.

A detailed description of the use of this tool in the Fraser delta is given by Finn at el. (1989). Signals are recorded digitally, and two records, with opposite source polarity, are obtained at each depth. Both first arrival and "cross-over" arrivals are picked. Routinely, interval velocities are obtained from arrival time differences across two depth locations, with distances corrected for source offset using a straight raypath. In normal field operations, shear wave data are collected along with the conventional parameters of cone bearing, sleeve friction, pore pressure, etc. In the loose sands of the Fraser

delta, cone penetrations in excess of 30 m are routinely acquired.

RESULTS

Figure 1 shows the shear wave velocity depth structure obtained independently using each of the three techniques described above at a site on the Fraser River delta. The downhole and seismic cone penetrometer tests were carried out within 20 m of each other. The surface refraction line was shot across the site, with the borehole location in the middle of the composite spread.

The velocity-depth function from the surface refraction array shows both velocity gradients and layered structure. The shear wave velocity increases from 90 m/s at surface, to 250 m/s at a depth of 40 m.

The surface-to-borehole (downhole) measurements show the same general trend of increasing velocities with depth; however, substantial velocity reversals are indicated in the 25 to 35 m depth range. The error bars are the standard error of the least squares velocity fit for a 4-point (1.5 m) interval.

The seismic cone penetrometer (SCPT) results also show a similar trend of increasing velocities with depth and significant velocity reversals in the 25 to 35 m range. However, not all velocity reversals correlate with those of the downhole data obtained less than 20 m away.

In general, all three methods show a shear wave velocity structure that increases from approximately 90 m/s at surface to 250 m/s at a depth of 35 m.

DISCUSSION

The surface refraction technique assumes that velocities increase with depth and, although velocity reversals may be suspected if "shingling" or amplitude attenuation is evident on the records, there is no quantitative interpretation technique available to deal with the problem. As well, like any other refraction survey, this method is susceptible to the "hidden layer" problem, where, although velocities increase with depth, certain velocity layers may be masked as first arrivals.

Both the downhole and SCPT methods appear to give results similar to those obtained with the surface refraction

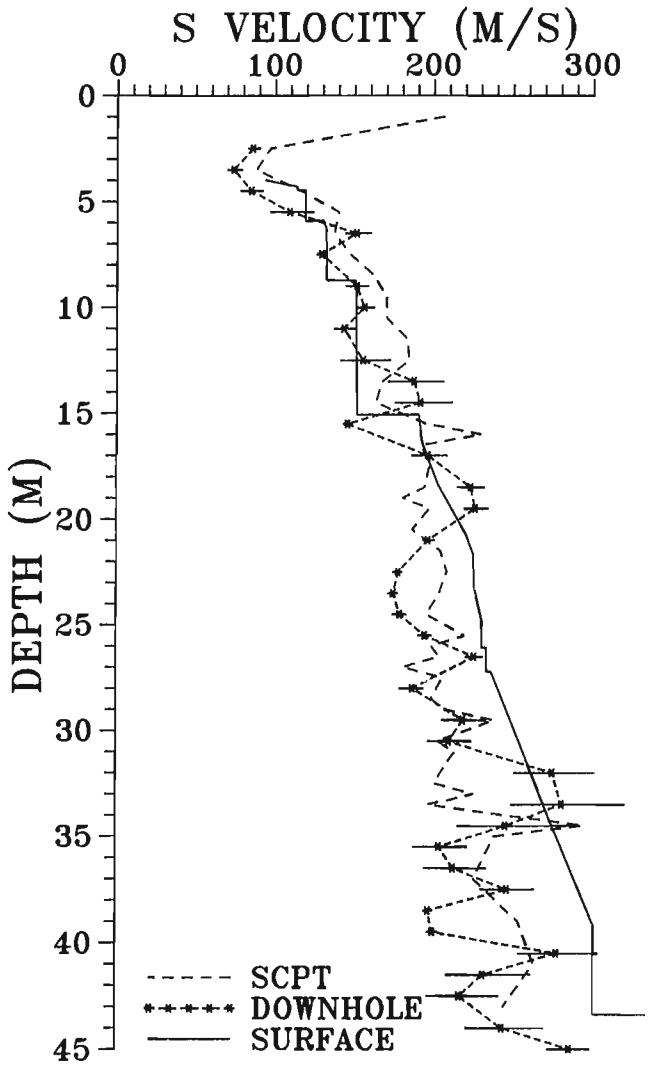

Figure 1. Comparison of the shear wave velocity depth function obtained at a site on the Fraser River delta using the three different methods described in this report.

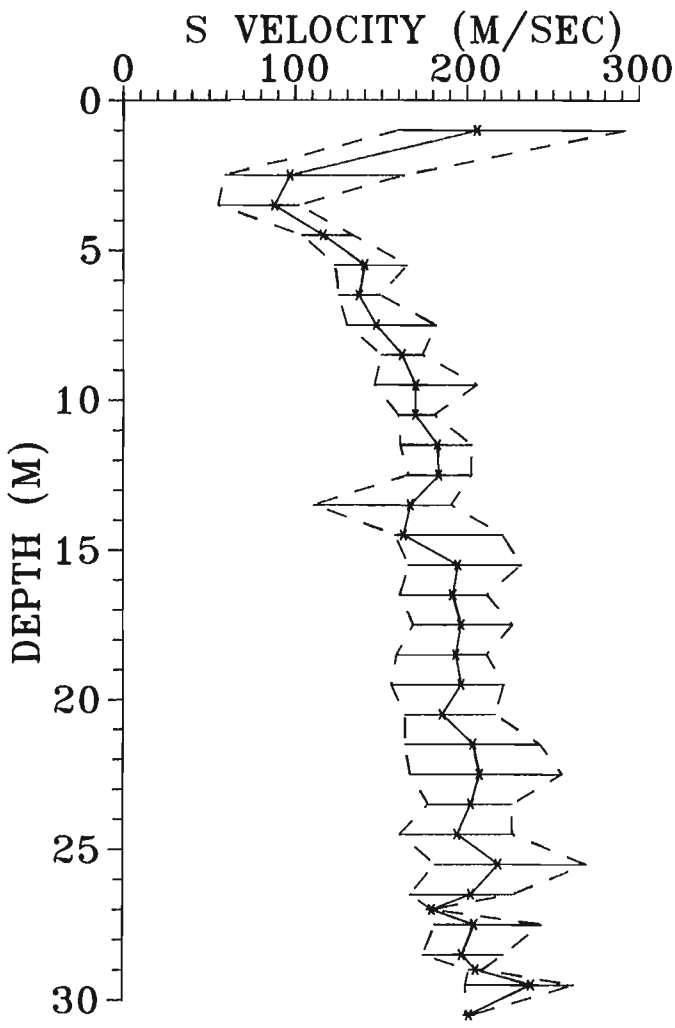

Figure 2. Mean and maximum deviations of the shear wave velocity structure obtained in 8 SCPT holes located within 60 m of each other.

technique at this site. However, much finer detail, including the existence of velocity reversals, is indicated. The downhole data show relatively large standard errors in the area of major velocity reversals, but these errors are not large enough to discount the reversals.

Two questions arise: are these velocity reversals real, and if so, why do adjacent SCPT and downhole measurements show such a different fine-scale velocity structure? It is known that local variations of downhole shear wave velocities are observed in adjacent holes (K. Stokoe, University of Texas, personal communication, 1990). These local variations are also indicated in Figure 2, which is a compilation of the results from 8 seismic cone penetrometer holes from another site in the survey; all 8 holes were within 60 m of each other. In Figure 2, the solid line is the arithmetic mean line of all measurements at that depth, and the bar indicates the maximum observed deviations from the mean. These data suggest that substantial local variations in the shear wave velocity depth function exist in the Fraser delta area, if the assumption is made that the errors in individual velocity measurements are small. To check this assumption, travel-time data from SCPT measurements were analyzed with running least squares fits, in a manner identical to the downhole data analyses. Standard errors of the velocity fits were found to be consistently smaller than the downhole measurements, suggesting better quality first arrival picks.

CONCLUSIONS

Our comparison of surface refraction, downhole, and SCPT methods of determining the shear wave velocity depth function suggests that all three methods indicate the same general trend of shear wave velocity-depth structure. It is possible that the small scale velocity reversals indicated by the downhole and SCPT results are real.

If the objective of a survey is to obtain regional general trends of the shear wave velocity-depth structure, the surface refraction technique may be an economical approach. However, the operator must be aware of the limitations of this approach, such as the requirement for 200 m or more of traverse area, as well as the inability of the technique to determine significant velocity reversals.

The downhole technique, by virtue of its need for a cased borehole, can be a relatively expensive approach. The one advantage of this technique is that it can, if necessary, be used to depths beyond that of the SCPT method which is limited to the depth of cone refusal.

From examination of the data from all sites of this survey, we conclude that the most reliable (although not least expensive) data were obtained from the seismic cone penetrometer.

REFERENCES

Finn, W.D.L., Woeller, D.J., Davies, M.P., Luternauer, J.L., Hunter, J.A., and Pullan, S.E.
1989: New approaches for assessing liquefaction potential of the Fraser River delta, British Columbia; in Current Research, Part E, Geological Survey of Canada, Paper 89-1E, p. 221-231.

Hunter, J.A.
1971: A computer method to obtain the velocity-depth function from seismic refraction data; in Report of Activities, Part B, Geological Survey of Canada, Paper 71-1B, p. 40-48.

Robertson, P.K., Campanella, R.G., Gillespie, D., and Rice, A.
1986: Seismic CPT to measure in situ shear wave velocity; Journal of Geotechnical Engineering Division, ASCE, v. 112, p. 791-803.

Preliminary studies of fluid inclusions in barite from the Middle Valley sulphide mounds, northern Juan de Fuca Ridge

Craig H.B. Leitch
Mineral Resources Division, Vancouver

Leitch, C.H.B., Preliminary studies of fluid inclusions in barite from the Middle Valley sulphide mounds, northern Juan de Fuca Ridge; in Current Research, Part A, Geological Survey of Canada, Paper 91-1A, p. 27-30, 1991.

Abstract

Large, liquid hydrocarbon-bearing fluid inclusions (up to 75 microns long) occur in barite in fractures lined with hydrocarbon cutting hydrothermal sulphide mounds at Middle Valley, on the northern Juan de Fuca Ridge. These inclusions are mainly secondary, trapped after growth of the barite, with homogenization temperatures of 105 to 115°C and an unidentified daughter mineral. Less common primary inclusions containing less petroliferous fluids have homogenization temperatures of 170°C, and also contain a possible daughter mineral. Smaller aqueous fluid inclusions up to 32 microns long are found in barite intergrown with sulphides in the mounds. The aqueous inclusions in barite intergrown with sulphides are probably pseudosecondary, with homogenization temperatures of 250°C and salinities of 3 wt.% NaCl equivalent, roughly equal to seawater (eutectic temperatures of −29 to −23°C indicate the presence of KCl).

Résumé

De grosses inclusions fluides (jusqu'à 75 microns de longueur) contenant des hydrocarbures liquides sont englobées dans la barytine logée dans les fractures dont les parois sont recouvertes d'hydrocarbures et qui recoupent des monticules de sulfures hydrothermaux à la vallée médiane dans le nord de la dorsale Juan de Fuca. Ces inclusions sont principalement de type secondaire, piégées après la croissance de la barytine, et caractérisées par des températures d'homogénéisation de 105 à 115 °C et un minéral de filiation non-identifié. Les températures d'homogénéisation des inclusions primaires moins courantes contenant des fluides moins pétrolifères atteignent 170 °C et peuvent également contenir un minéral de filiation. On trouve des inclusions fluides aqueuses un peu plus petites pouvant atteindre 32 microns de longueur dans la barytine enchevêtrée avec des sulfures dans les monticules. Les inclusions aqueuses dans la barytine enchevêtrée avec des sulfures sont probablement pseudo-secondaires et se caractérisent par des températures d'homogénéisation de 250 °C et des salinités de 3 % en poids d'équivalent NaCl, soit à peu près égal aux valeurs de l'eau de mer (des températures eutectiques de -29 à -23 °C indiquent la présence de KCl).

INTRODUCTION

Sulphides and barite occur in hydrothermal mounds along the eastern margin of Middle Valley, which is a sediment-buried rift near the northern end of the Juan de Fuca Ridge, in the northwestern Pacific Ocean about 300 km due west of Victoria, Brithish Columbia. Active venting is presently occurring at the sites of the hydrothermal mounds, and was observed and sampled during the 1990 Alvin submersible dives. The location, history of exploration, and regional setting of the deposits at Middle Valley are described in Goodfellow and Blaise (1988) and Davis et al. (1987).

This contribution is a summary of preliminary fluid inclusion data from Middle Valley, based on limited samples from pre-1990 piston coring and dredge hauls (donated by W.D. Goodfellow and I.R. Jonasson, respectively, both with Mineral Resources Division in Ottawa), and from 1990 Alvin submersible dives from Atlantis II. All the microthermometric data comes from barite in three samples. Sample ALV 2255-3-2 consists of euhedral barite crystals lining fractures, with hydrocarbon, in the muddy base of a short hydrothermal chimney recovered intact. Sample ALV 2253-1-2 is a doubly polished thin section of barite and minor sulphides from an active vent at R2 Site 1, and TUL88B-13-04 is a doubly polished thin section of fragmental sulphide-minor barite material from piston core.

During exploratory petrographic investigations, fluid inclusions were seen in other samples of barite (TUL88B-20-07, -20-20, -13-04; PAR 85-13 at 110-117.5 cm), carbonate (TUL88B-20-03), and vein quartz (TUL88B-20-13; PAR 85-13 at 110-117.5 cm), but no inclusions were found in the doubly polished plates prepared from these samples. The methods of section preparation, microthermometric measurement, calibration, and estimates of precision and accuracy are given in Leitch (1991; this volume).

FLUID INCLUSIONS

Sample 2255-3-2

This sample consists of euhedral crystals of barite found encrusting fractures cutting the muddy base of a chimney on a mound in the active hydrothermal vent field. The barite is brown due to abundant petroliferous fluid inclusions, and black hydrocarbon commonly coats the same fractures or vugs. The fluid inclusions in barite of this sample are similar to the liquid hydrocarbon-bearing inclusions found in amorphous silica in hydrothermal chimneys and mounds from Guaymas Basin, described by Peter et al. (1990).

Most of the fluid inclusions in this sample appear to be secondary (on planar arrays), and of at least three or possibly four types. The first, most abundant type has a negative crystal shape and is generally up to 25 microns across, although some are large, with irregular shapes up to 75 microns long. They generally contain a striated daughter mineral, a vapour bubble, and a yellow petroliferous fluid with an index of refraction close to that of barite (Fig. 1A); the boundary between the fluid and barite host is indistinct in transmitted light. The vapour to vapour+liquid ratio (V/L) is about 5 to 15% but in some inclusions there is no bubble present. The identity of the daughter mineral is not known, although some partially dissolved on heating to 170°C and did not re-form after cooling. The salinity (if any) of the petroliferous fluid is not known (there were no changes observed on freezing to −60°C and warming). All these inclusions homogenized into a single phase liquid (with or without daughter mineral) at a temperature (Th) of 105 to 115°C. Most then decrepitated or stretched at 130°C.

The second type may be a possible subset of the first type (Fig. 1B); inclusions occur in distinctly planar arrays that must be secondary in origin. These are small (5 micron diameter), diamond-shaped (?negative crystal), and occur in two distinct forms, one orange in colour and apparently petroleum-rich (V/L = 0, no change on freezing to −60°, and all turned brown or baked at T>+125°C), and the other with a vapour bubble in a clear liquid, and V/L = 40. The latter homogenized to liquid at a temperature (Th) of 105°C, and froze at a temperature (Tf) of about −27°C by disappearance of the outer boundary between liquid and barite host. Possible eutectic melting (Te) was observed at about −20°C, followed by vaguely discernible melting. As there was no vapor bubble to observe, melting was defined only by reappearance of the outer inclusion boundary at −10°C, which would imply a salinity of about 14 wt.% eq. NaCl. This is regarded as unlikely given the low salinity (3 wt.%, see below) of inclusions in another sample.

The third, less abundant type is tubular, up to 80 microns long (Fig. 1C), and appears to be primary, since the inclusions are arranged in growth zones. They are composed of a pale yellow liquid, apparently petroliferous, vapour bubble (V/L about 10%), and may have a daughter mineral. The salinity (if any) of the fluid is unknown, since no freezing behaviour was observed to −60°C. These inclusions homogenized to a liquid at a temperature of 169 to 170°C, and this temperature was repeatable.

A possible fourth, least abundant type (Fig. 1D) is rectangular, nonpetroliferous (clear), small (up to 8 microns long), primary or secondary, with no visible daughter minerals and a consistent V/L of about 10%. However, no changes were observable to −60 or +270°C, so it is not clear that these are in fact fluid inclusions.

Sample 2253-1-2 (R2 Site 1)

This sample consists of an interlocking mesh of clear barite laths, generally 0.5 to 1.0 mm long, with minor interstitial sulphides (pyrrhotite laths up to 50 microns long, sphalerite/wurtzite to 5 microns, and rare chalcopyrite/isocubanite of less than 1 micron). Other similar samples of almost pure barite (e.g. 2255-4-1) also contain fluid inclusions, but the epoxy employed in preparation of these sections caused them to buckle during removal from the glass slide, rendering the sections unusable for microthermometry.

Most inclusions in the barite (Fig. 1E) appear to be primary or pseudosecondary: they are not obviously in planar arrays, but instead are aligned parallel to the length of the crystal or perpendicular to it. They have irregular to elongate, flattened teardrop shapes and are up to 32 microns long, with consistent V/L ratios of about 15 to 20%. They contain an aqueous fluid and a vapour bubble; there is no suggestion

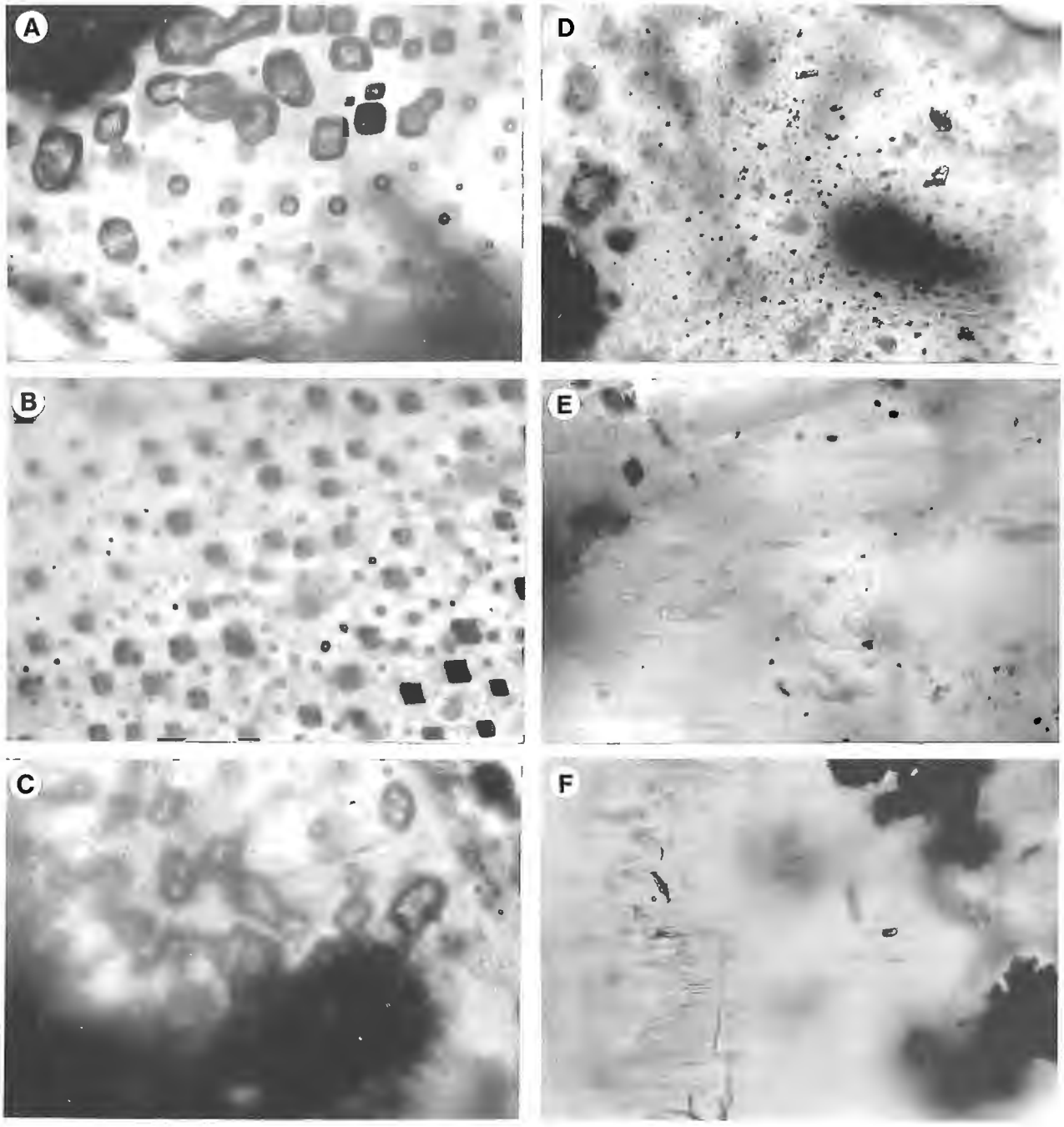

Figure 1. Fluid inclusions in barite from Middle Valley. All photomicrographs are taken in plane polarized, transmitted light.
A. Large hydrocarbon-bearing inclusions (up to 25 microns across) in sample 2255-3-2, with indistinct boundary against the host barite, containing vapour bubble and (in places) daughter mineral. The dark inclusions at the top of the photo have decrepitated during heating.
B. Small diamond-shaped secondary aqueous fluid inclusions (5 microns diameter, with vapour bubble) in a planar array with larger hydrocarbon inclusions (10 microns), in barite of sample 2253-3-2.
C. Two tubular, 50 microns long primary hydrocarbon-bearing inclusions in barite, sample 2253-3-2 (vapour bubble and daughter mineral present). Many other similar inclusions are barely visible in northwest-southeast orientation at lower right of field of view.
D. Rectangular ?fluid inclusions, 8 microns long, in barite from sample 2253-3-2. These appear to contain a vapour bubble and aqueous fluid, but did not homogenize at temperatures up to +270°C.
E. Primary or pseudosecondary flattened inclusions containing aqueous fluid of about the same salinity as seawater and a vapour bubble, in barite from sample 2253-1-2 (R2 Site 1). Large inclusion is 18 microns long.
F. Planar array of single-phase (liquid-rich) secondary inclusions in barite from sample 2253-1-2 (R2 Site 1). One tubular inclusion on the right (with vapour bubble) is 37 microns long. Opaque material is sulphide (mainly pyrrhotite).

of CO_2 being present, either as a visible phase or from phase changes. They all homogenize to liquid at an average temperature of 250°C (n=23, range 245 to 263). Ice melting at about −2.0°C (n=22, range −2.4 to −1.3) suggests that the salinity of the fluid is about that of seawater (3 wt.%). Eutectic temperatures (−20.6°C) suggest mainly NaCl, but with metastable melting observed at −29°C and also several observations around −23°C (n=8, range −24.8 to −22.5), KCl is possibly present.

There are also common planar arrays of one phase (both V-rich and L-rich) inclusions which are probably secondary. They do not demonstrate any changes to −100°C. One tubular inclusion with V/L about 25%, found with this group (Fig. 1F), had leaked by the time it was placed on the stage, so no useful information could be extracted.

Sample TUL88B-13-04

This sample is made up of fragments of massive sulphide (marcasite-pyrite after pyrrhotite laths that were up to 1.5 mm long, with minor sphalerite-wurtzite to 0.2 mm diameter, and interstitial laths of barite up to 0.5 mm long), probably from collapsed chimneys. The barite contains fluid inclusions up to 18 microns long that are similar to those in the barite from active chimneys, described above.

Microthermometric data also suggest that these inclusions are similar to those in the active chimneys. Eutectic temperatures were in the −22 to −30°C range, and final melting took place at −3.6 to −3.0°C, suggesting salinities of about 5 wt.% NaCl equivalent. Most of the inclusions cracked on freezing, causing the vapour bubble to expand; only one inclusion did not crack, but decrepitated at + 208°C. Thus homogenization, while not actually seen, can be inferred to be similar to the 250°C temperatures seen in the active chimney material.

INTERPRETATION

The inclusions in sample 2253-1-2 appear to be primary, and thus represent samples of the fluid that formed the barite and associated minor sulphides of this actively venting chimney. These fluids were therefore trapped at around 265°C (a pressure correction of about +15°C should be applied at the prevailing 2500 m water depth; Roedder, 1984, Fig. 9-4). Fluids were of low salinity (approximately 3 wt.% NaCl + ?minor KCl). Data from barite in fragmental chimney rubble in TUL88B-13-04 are similar (temperature over 208°C and salinity of around 5 wt.% eq. NaCl).

These estimates of trapping temperature and salinity for fluids that deposited the barite forming the framework of the chimneys compare favourably with measurements on fluids currently venting from the chimneys: the highest temperature recorded during the Alvin dives this year was 276°C (R. Mc Duff, pers. comm., 1990). The salinities observed, 3 to 5 wt.% NaCl ± minor KCl, are a good fit for seawater-derived fluids such as noted in Kuroko deposits (Pisutha-Arnond and Ohmoto, 1983).

In the other sample, the barite is from veins that formed after construction of the chimney; the primary (tubular) inclusions in this barite represent temperature of formation of the vein from fluids at over 170°C (a precise pressure correction cannot be applied to these hydrocarbon-bearing fluids) and unknown salinity, with later fluids at over 110°C (again, trapping temperatures cannot be precisely estimated) and variably rich in petroleum. The walls of these veins are also lined with hydrocarbon. Peter et al. (1990) found very similar homogenization temperatures (mode at 115°C) for hydrocarbon-bearing inclusions from the Guaymas Basin hydrothermal mounds; the associated aqueous inclusions had homogenization temperatures ranging from 120 to 180°C with a mean of around 140°C.

ACKNOWLEDGMENTS

The author greatly appreciates the opportunity to accompany the scientific staff of the Mineral Resources Division, Geological Survey of Canada, on the 1990 cruise to Middle Valley and to sample some of the materials from these active vents for fluid inclusion studies. Drs. W.D. Goodfellow and I.R. Jonasson kindly made available samples from piston coring and dredging at Middle Valley, and Dr. R.J.W. Turner critically read the manuscript.

REFERENCES

Davis, E.E., Goodfellow, W.D., Bornhold, B.D., Adshead, J., Blaise, B., Villinger, H., and Le Cheminant, G.
1987: Massive sulphides in a sedimented rift valley, northern Juan de Fuca Ridge; Earth and Planetary Science Letters, v. 82, p.49-61.

Goodfellow, W.D. and Blaise, B.
1988: Sulfide formation and hydrothermal alteration of hemipelagic sediment in Middle Valley, northern Juan de Fuca Ridge; Canadian Mineralogist, v. 26, p. 675-696.

Leitch, C.H.B.
1991: Preliminary fluid inclusion and petrographic studies of the Sullivan sedimentary exhalitive Pb-Zn deposit, southeastern B.C.; in Current Research, Part A, Geological Survey of Canada, Paper 91-1A.

Peter, J.M., Simoneit, B.R.T., and Kawka, O.E.
1990: Liquid hydrocarbon-bearing inclusions in modern hydrothermal chimneys and mounds from the southern trough of Guaymas Basin, Gulf of California; Applied Geochemistry, v. 5, p. 51-63.

Pisutha-Arnond, V., and Ohmoto, H.
1983: Thermal history, and chemical and isotopic compositions of the ore-forming fluids reponsible for the Kuroko massive sulfide deposits in the Hokuroko district of Japan; Economic Geology, Monograph 5, p. 523-558.

Roedder, E.
1984: Fluid inclusions; Mineralogical Society of America, Reviews in Mineralogy, v. 12, 644 p.

Examining fluvial sediments using ground penetrating radar in British Columbia

Brian J. Moorman[1], Alan S. Judge, and Derald G. Smith[1]
Terrain Sciences Division

Moorman, B.J., Judge, A.S., and Smith, D.G., Examining fluvial sediments using ground penetrating radar in British Columbia; in Current Research, Part A, Geological Survey of Canada, Paper 91-1A, p. 31-36, 1991.

Abstract

The feasibility of using ground penetrating radar (GPR) to examine the subsurface structure of fluvial sediments was determined by performing a number of GPR surveys in several different depositional environments. The pulse EKKO III system used was able to image to a depth 34 m in unsaturated gravels while being limited to a depth of only 4 m in saturated mud. Using a inflatable rubber raft as a survey platform while traversing river channels proved to be a quick and easy way of acquiring stratigraphic information on the channel-bottom sediments.

Résumé

Afin de déterminer la faisabilité d'analyser la structure souterraine des sédiments fluviatiles à l'aide du géoradar, on a réalisé un certain nombre de levés au géoradar dans plusieurs milieux de sédimentation différents. Avec le système EKKO III, on a pu produire des images jusqu'à une profondeur de 34 m dans les graviers non saturés mais à une profondeur de seulement 4 m dans les boues saturées. En utilisant un radeau de caoutchouc gonflable comme plate-forme de levé pour traverser les cours d'eau, on a pu obtenir rapidement et facilement des données stratigraphiques sur les sédiments reposant sur leur fond.

[1] Department of Geography, University of Calgary, Calgary, Alberta T2N 1N4

INTRODUCTION

The examination of subsurface sediments using ground penetrating radar (GPR) has several advantages over traditional methods. Using coring methods is costly, time consuming, and only produces point source data. The information gained from examining cutbank and other exposures can be limited by their sparse distribution or the bias of their locations. Shallow seismic methods have also been used to examine subsurface structures (Jol, 1988); however, these methods do not provide stratigraphic information on the top 10 m, and the resolution is often too coarse to delineate heterolithic strata (McCann et al., 1988). Thus, a method is needed that can provide two dimensional information about the stratigraphic structure of the subsurface in a variety of environments, rapidly and at low cost.

Recent developments in GPR have afforded opportunities for geomorphologists and sedimentologists to examine the top 30 m of the subsurface, at a high resolution (as fine as 10 cm). Previous investigations using GPR have included measuring glacier, sea, and lake ice thickness (Bryan, 1974; Campbell and Orange, 1974; Bently et al., 1979), examining permafrost, and massive ground ice (Annan and Davis, 1976; Moorman and Judge, 1989), and mapping bedrock structures in coal, salt, and hard rock mines (Cook, 1973, 1975, 1977; Dellwig and Bare, 1978). Lately, more research has been done on surficial deposits, including archeological and soil science investigations (Collins and Doolittle, 1987; Doolittle, 1982; Vaughan, 1986). Ulriksen (1982) used an analog GPR system to examine massive sand, gravel, and bouldery clay in deltas, eskers, and other depositional environments. His results demonstrated the potential of GPR; however, the quality of the data was limited by the performance of the instrumentation. The state-of-the-art digital GPR systems are proving to be better able to map near surface sediment and rock stratigraphy (Davis and Annan, 1989; Moorman, 1990).

This report discusses the results of GPR surveys carried out across an inactive fan delta in Golden, British Columbia, and surveys run across the channels in the anastomosing Columbia River system in the valley below. Common Mid Point (CMP) soundings were used to calculate depth scales and both 50 and 100 MHz surveys were carried out to compare the information gained by carrying out surveys at different frequencies.

METHODS

Study area

The Rocky Mountain Trench, in the vicinity of Golden, British Columbia, has experienced considerable fluvial activity since the last deglaciation about 11 500 to 11 000 years ago (Fulton, 1971; Harrison, 1976). Since deglaciation and the draining of the glacial lake that occupied the valley during that period, fans have aggraded into the valley, carrying sediment down from the mountains. Much of this sediment has then been transported along and deposited in the valley bottom by Columbia River which flows along the valley floor. The anastomosing river reach, southeast of Golden, is kept active by two large down river crossvalley fans at Nicholson and Golden. These actively aggrading fans raise the local base level such that flooding occurs annually (Locking, 1983). The river is usually above bankfull conditions for a period of one and a half to three months every summer. This situation, and the plentiful supply of sediment, has aided in the creation of a river system (Fig. 1) that has low-energy, multiple interconnected, laterally stable, deep sand-bed channels, confined by prominent silty, forested levees (Smith, 1986).

This setting offered an excellent opportunity to study the ability of GPR to delineate a large number of different facies units with sediment ranging from well sorted sands to organic muds, within a small area. Surveys were also carried out across a Late Pleistocene fan delta on the valley side. This offered the opportunity to examine the internal structure of coarser sediments which, unlike the valley bottom sediments, were not saturated.

Ground penetrating radar profiling

The GPR profiling was carried out using a PulseEKKO III digital GPR system. The system was used with two interchangeable sets of antennae having 50 and 100 MHz centre frequencies. The profiling was done in a step mode with 1 m between stations and antenna separation of 1 m for 100 MHz surveys, and 2 m for 50 MHz surveys. Returns from a time window of 1024 ns were recorded with the signal being digitally sampled every 800 ps. The system used had the ability to automatically stack traces, thus, each recorded trace was an average of 512 traces measured at each station.

On land, the GPR system was towed by hand on a 1 m wooden toboggan. For traverses through heavy brush, a 1 m swath was cleared in preparation for surveying. When crossing active river channels, an inflatable rubber boat was used as a survey platform. All sizable metal and electronic components were removed from the boat to reduce the possibility of electronic noise interfering with the radar returns. This included replacing the metal floor with a custom wood floor. As the current in the channels was not great at the time of surveying (October 1989), the nonmetallic survey chain was strung across the channel and could be used both to move and stabilize the boat (Fig. 2).

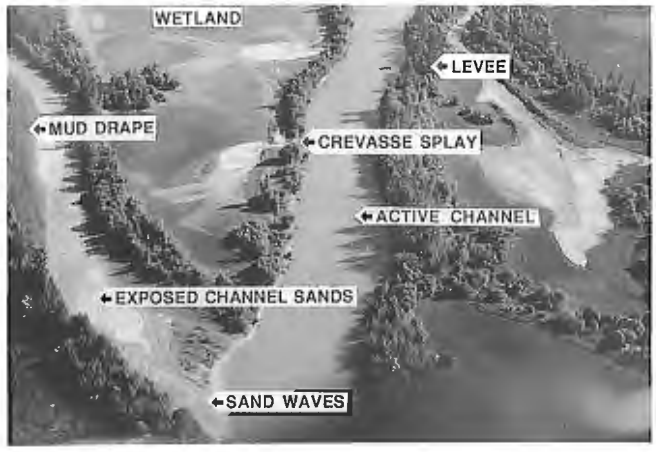

Figure 1. Overview airphoto of an anastomosing reach of the Columbia River.

Figure 2. Profiling channel bottom sediments from an inflatable boat.

Properties of the materials studied

Ground penetrating radar is effective at delineating inter-faces between different geological materials because there is a strong relationship between the physical properties of a material and its dielectric properties (Scott et al., 1978). When a pulse of electromagnetic energy is transmitted into the ground, a portion of the energy is reflected back to the surface from each interface between materials of differing dielectric constant. The strength of the reflection is related to the reflection coefficient which, for vertical incidence between two perfectly dielectric materials is given by:

$$R=(K'_1{}^{0.5}-K'_2{}^{0.5})\ (K'_1{}^{0.5}+K'_2{}^{0.5})^{-1}$$

where K'_1 and K'_2 are the dielectric constants of the two materials (A-CUBED, 1983). Thus, the strength of the reflection is directly proportional to the difference in the dielectric constants of the two materials.

The depth to which GPR is able to image is a function of several parameters including, the attenuation coefficient of the subsurface materials, the frequency used, and reflection coefficients of the interfaces. Annan and Davis (1977) discussed GPR range analysis in detail; however, a simple estimation of the attenuation coefficient of the material examined is sufficient to determine potential effectiveness of GPR. For most geological materials the attenuation coefficient can be estimated by:

$$\alpha=1.64\delta(K')^{-0.5}\times 10^3 \qquad \text{(dB/m)}$$

where $\tan\delta=\sigma_{DC}(fK'\varepsilon_0)^{-1}$, σ_{DC} is the DC conductivity, f is the frequency in radians, and ε_0 is the electric permitivity of free space (A-CUBED, 1983).

The materials encountered in this project can be roughly grouped into three categories; unsaturated sands and gravels (found in the Late Pleistocene delta), saturated sands (found in the channel deposits), and saturated silts, clays, and organics (found in the levee, wetland, and mud drape deposits). The unsaturated gravels had the lowest attenuation coefficients, estimated to be of the order of 0.01 dB/m. The saturated sands had higher attenuation coefficients; however, because the pore water was very fresh, the attenuation coefficient was estimated to be of the order of 0.1 dB/m. The saturated muds had the highest and most variable attenuation coefficients, estimated to be between 1 and 300 dB/m, which resulted in the depth of penetration being only a few metres in the worst cases.

Determining the depth to reflectors can only be accomplished if the propagation velocity of the material is known. In air the propagation velocity of electromagnetic energy is 0.3 m/ns, however, in the ground it is only a fraction of that. The propagation velocity of geological materials can be estimated using their dielectric constant:

$$v=0.3(K')^{-0.5} \qquad \text{(m/ns)}$$

or it can be directly determined by performing a velocity profile at each survey location (A-CUBED, 1983). Common Mid Point (CMP) velocity soundings are stationary profiles that result in an antenna separation vs. travel time plot. The propagation velocity of the ground can then be calculated from the slope of the direct and reflected returns. The propagation velocity of the near surface is the inverse of the slope of the direct ground wave (i.e., the return of energy that travels directly from the transmitter to the receiver along the surface of the ground), while the propagation velocity of deeper materials is calculated from the slope of the reflections from the base of the layer, as given by:

$$v=(d^2+4z^2)^{0.5}t^{-1}$$

where d is the separation distance between the antennae, z the depth to the reflector, and t is the travel time. Common mid point soundings were carried out by recording traces at 0.5 m intervals. Figure 3 is an example of a CMP sounding carried out on the unsaturated gravelly deltaic deposits.

Coring

As the GPR data provide information on the location and strength of reflections produced by material interfaces, but not on the material itself, subsurface samples were collected to verify the GPR records. In most instances, vibracoring techniques, as described by Smith (1984, 1987), were used to acquire the direct subsurface information. Numerous cores were taken from various settings within the area to verify GPR data and to characterize the GPR returns for each of the facies units studied. However, in the case of the Late Pleistocene fan delta in Golden, a nearby railway cutbank exposure provided the suitable information such that coring was not required (Fig. 4).

RESULTS AND DISCUSSION

Of the 25 profiles collected for this project, the examples shown here are representative of the quality of results acquired.

Delta profiles

Both 50 MHz (Fig. 5) and 100 MHz (Fig. 6) surveys were run roughly in the dip direction across the top of a Late Pleistocene fan delta at Golden, British Columbia. The two profiles clearly show strong reflections from the foreset beds. The calculated dip angle, after migration, was 25°, which is the same angle measured at the exposure shown in Figure 4. The strength of reflections and depth of penetration

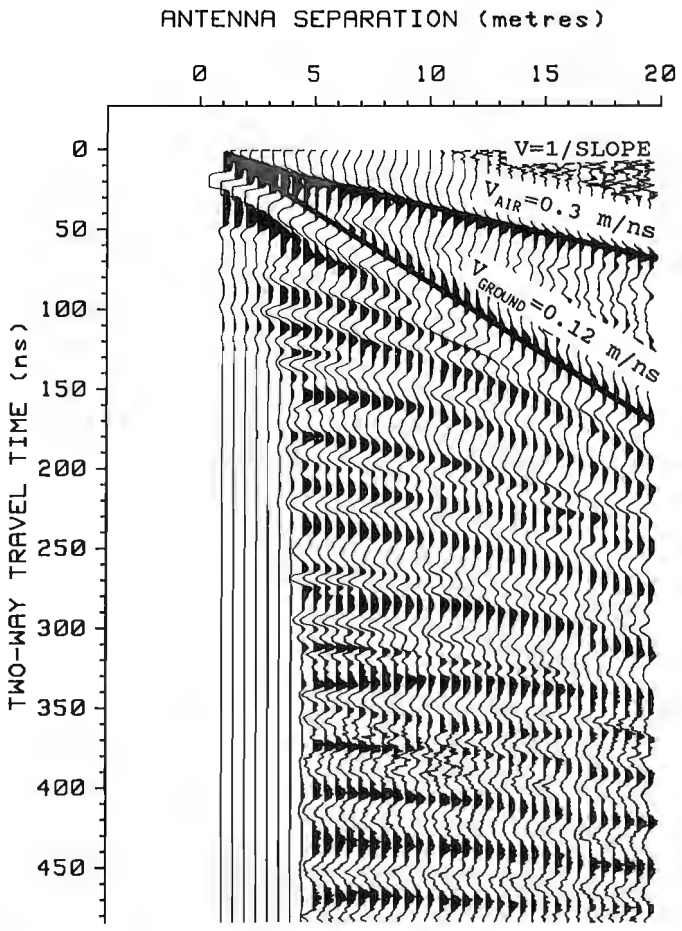

Figure 3. Common mid point velocity sounding of unsaturated gravelly deltaic deposits.

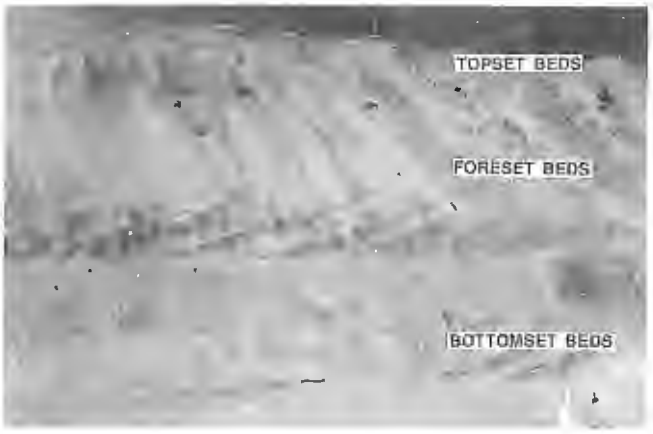

Figure 4. Exposure of the Late Pleistocene fan delta at Golden, British Columbia.

was much greater with the 50 MHz antennae; however, more foreset beds seem to be discernible on the 100 MHz profile. As well, on the 100 MHz profile, reflections observed in the top 4 m of the record suggest the presence of topset beds. The small dip angle of these reflections supports this interpretation.

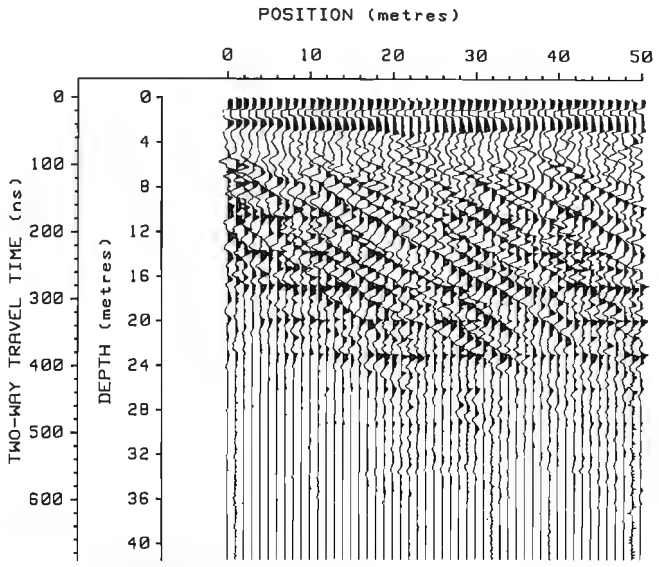

Figure 5. A 50 MHz GPR profile across the delta at Golden, British Columbia.

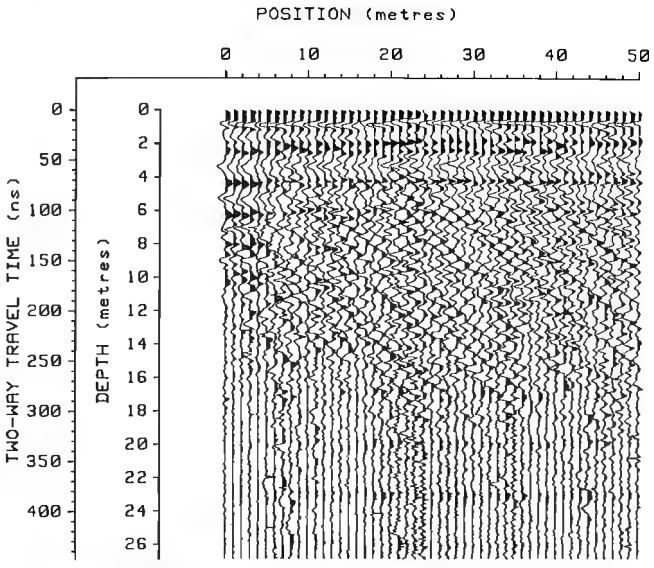

Figure 6. A 100 MHz GPR profile across the delta at Golden, British Columbia.

The first two returns on the 50 MHz profile are the direct air and ground waves. These two returns result from a portion of the energy pulse travelling directly from the transmitter to the receiver through the air (at 0.3 m/ns) and through the surface skin of the ground (at the propagation velocity of the near surface soil), respectively. The depth scales for both these profiles were created using a propagation velocity of 0.12 m/ns as determined from the CMP shown in Figure 3, and correcting for the geometry of the pulse travel path (created by having the antennae separated). The 50 MHz profile indicates the presence of foreset beds to a depth of 34 m; however, the bottomset beds, at a depth of approximately 35 to 40 m, were not detected. The horizontal, evenly spaced pulses (with arrival times of 180, 230, 280, 330, 380, and

430 ns) are thought to be ringing of the signal between the antennae, or complex multiples from near surface soil horizons. These horizontal pulses are much weaker on the 100 MHz profile, due to the change in frequency.

The 100 MHz profile has an effective depth of penetration of approximately 24 m, with as many as 40 foreset beds being indicated. The presence of several small elliptical-shaped reflectors suggests that foreset slope failures may have occurred at the time of deposition.

Open water profile

One of the profiles run in the anastomosing reach of the Columbia River involved crossing a partially filled active channel (Fig. 7). The record was topographically adjusted, as the channel had steep banks which rose up 2 m above the water level. The portion of the profile from the 30 to the 72 m station traversed open water which ranged in depth from 20 cm to 1 m.

Because water has a different propagation velocity than saturated sediment, returns from below the channel had to be vertically transposed. The saturated sediment had a propagation velocity of the order of 0.06 m/ns (as determined from a CMP profile at a nearby similar site with the water table

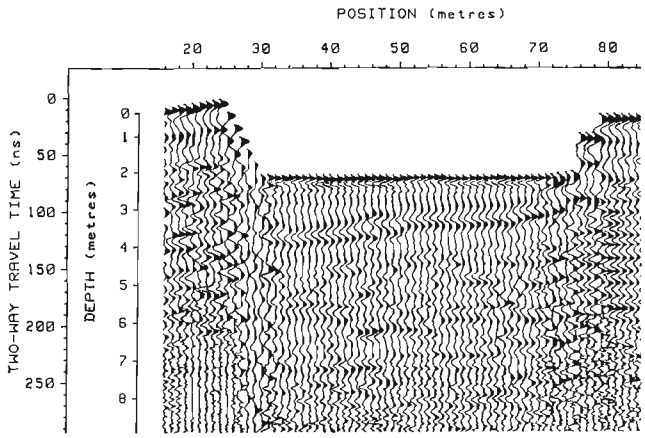

Figure 7. A portion of the 100 MHz GPR profile across an active river channel in the anastomosing reach of the Columbia River.

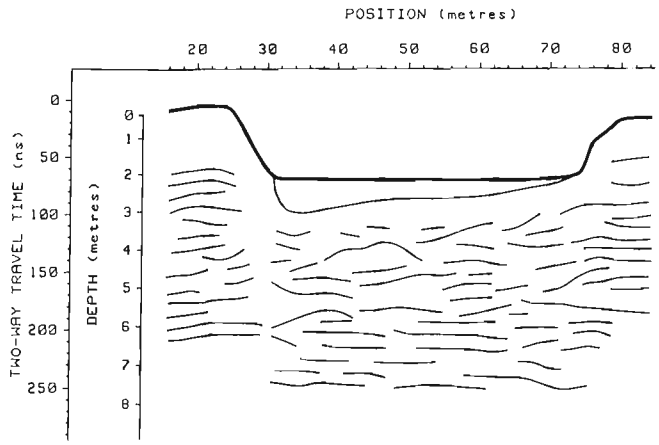

Figure 8. Interpretation of the profile in Figure 7.

at the surface), whereas the velocity in the water was 0.033 m/ns. The velocity of the water was determined using the measured water depth and the travel time on the profile. On the interpretation plot (Fig. 8) the reflections from the channel bottom and below, are vertically transposed such that their positions, relative to the reflections from below the channel banks, are correct.

The reflections from within the buried channel sands result from internal structure produced by sorting of the sediment, as it is deposited. The structure of the deposited channel sands in this reach of the Columbia River is dominated by tabular crossbedded sets with fining upward sequences spaced 0.5 to 1 m apart; however, during bankfull flow conditions, sand waves often form (Fig. 1). These structures are preserved as the channel vertically aggrades and appear on the GPR record as horizontal to undulating reflections. The reflections are laterally continuous for 3 to 10 m. Drill core data were not available for this profile; however, GPR reflections correlated very well with core data at sites where both could be acquired.

On the sides of the channel, the returns are more closely spaced and horizontally parallel. These returns are produced by the thin laminations of overbank deposits that make up the levees (Smith, 1983).

CONCLUSIONS

Ground penetrating radar was able to image the internal structure of fluvially deposited sediment in several different environments. In dry gravels the depth of penetration was up to 34 m, when profiling with 50 MHz antennae, while the depth of penetration in overbank muds was limited to approximately 4 m when profiling with 100 MHz antennae. The pulseEKKO III GPR system also proved to be able to image through fresh water to the sedimentary structures below. Using a small inflatable rubber raft as a survey platform proved to be an efficient system for profiling short distances on calm water.

ACKNOWLEDGMENTS

This research project received additional support from the Department of Geography, and the Faculty of Graduate Studies at the University of Calgary, and an NSERC grant to D. Smith. The field assistance of Harry Jol is also gratefully appreciated.

REFERENCES

A-CUBED
1983: General state of the art review of ground probing radar; A-CUBED Inc. Mississauga, 89 p.

Annan, A.P. and Davis, J.L.
1976: Impulse radar soundings in permafrost; Radio Science, v. 11, p. 383-394.
1977: Radar range analysis for geological materials; in Report of Activities, Geological Survey of Canada, Paper 77-1B, p. 117-124.

Bently, C.R., Clough, J.W., Jezek, E., and Shabtaie, S.
1979: Ice thickness patterns and the dynamics of the Ross Ice Shelf, Antarctica; Journal of Glaciology, v. 24, p. 287-294.

Bryan, M.L.
1974: Ice thickness variability on Silver Lake, Genesee County, Michigan: a radar approach; in Advanced Concepts and techniques in the Study of Snow and Ice Resources: A United States Contribution to the International Hydrological Decade, National Academy of Sciences, p. 213-223.

Campbell, K.J. and Orange, A.S.
1974: A continuous profile of sea ice and freshwater ice thickness by impulse radar; Polar Record, v. 17, p. 31-41.

Collins, M.E. and Doolittle, J.A.
1987: Using ground-penetrating radar to study soil microvariability; Journal of Soil Science Society of America, v. 51, p. 491-493.

Cook, J.C.
1973: Radar exploration through rock in advance of mining; American Institute of Mining Engineers, Transactions, Society of Mining Engineers, v. 254, p. 140-146.
1975: Radar transparencies of mine and tunnel rocks; Geophysics, v. 40, p. 865-885.
1977: Borehole-radar exploration in a coal seam; Geophysics, v. 42, p. 1254-1257.

Davis, J.L. and Annan, A.P.
1989: Ground-penetrating radar for high-resolution mapping of soil and rock stratigraphy; Geophysical Prospecting, v. 37, p. 531-551.

Dellwig, L.F. and Bare, J.E.
1978: A radar investigation of North Louisiana salt domes; Photogrammetric Engineering and Remote Sensing, v. 44, p. 1411-1419.

Doolittle, J.A.
1982: Characterising soil map units with ground-penetrating radar; Soil Survey Horizons, v. 23, p. 3-10.

Fulton, R.J.
1971: Radiocarbon geochronology of southern British Columbia; Geological Survey of Canada, Paper 71-37, 28 p.

Harrison, J.E.
1976: Dated organic material below Mazama(?) tephra: Elk Valley, British Columbia; in Report of Activities, Part C, Geological Survey of Canada, Paper 76-1C, p. 169-170.

Jol, H.M.
1988: Seismic stratigraphic analysis of the Southeastern Fraser River Delta, British Columbia; unpublished MSc thesis, Simon Fraser University, Burnaby, B.C., 176 p.

Locking, T.
1983: Hydrology and sediment transport in an anastomosing Reach of the Upper Columbia River, B.C.; unpublished MSc thesis, University of Calgary, Calgary, Alberta, 107 p.

McCann, D.M., Jackson, P.D., and Flemming, P.J.
1988: Comparison of the seismic and ground probing radar methods in geological surveying; in Institute of Electrical Engineers, Proceedings F. Communications, Radar and Signal Processing, v. 135, p. 380-390.

Moorman, B.J.
1990: Assessing the ability of ground penetrating radar to delineate subsurface fluvial lithofacies; unpublished MSc thesis, University of Calgary, Calgary, Alberta, 124 p.

Moorman, B.J. and Judge, A.S.
1989: Delineating massive ice with ground penetrating radar (abstract); in Program with Abstracts, v. 14, GAC/MAC Joint Annual Meeting, 15-17 May 1989, Montreal, Quebec, Geological Association of Canada and Mineralogical Association of Canada, p. A76.

Scott, W.J., Sellmann, P.V., and Hunter, J.A.
1978: Geophysics in the study of permafrost; in Third International Conference on Permafrost, V. 2, p. 93-115.

Smith, D.G.
1983: Anastomosing fluvial deposits: modern examples from Western Canada; in Modern and Ancient Fluvial Systems, J. Collonson and J. Lewin (eds.); Special Publications of the International Association of Sedimentologists, v. 6, p. 155-168.
1984: Vibracoring fluvial and deltaic sediments: tips on improving penetration and recovery; Journal of Sedimentary Petrology, v. 54, p. 660-663.
1986: Anastomosing river deposits, sedimentation rates and basin subsidence, Magdalena River, Northwestern Colombia, South America; Sedimentary Geology, v. 46, p. 177-196.
1987: A mini-vibracoring system; Journal of Sedimentary Petrology, v. 57, p. 757-758.

Ulriksen, C.P.
1982: Applications of impulse radar to civil engineering; published PhD thesis, Lund University of Technology, Lund. Geophysical Survey Systems, Inc., Hudson, New Hampshire, 175 p.

Vaughan, C.J.
1986: Ground penetrating radar surveys used in archaeological investigations; Geophysics, v. 52, p. 137-150.

Metamorphic terrane east of Denali fault between Kluane Lake and Kusawa Lake, Yukon Territory

P. Erdmer[1]
Cordilleran Division, Vancouver

Erdmer, P., Metamorphic terrane east of Denali fault between Kluane Lake and Kusawa Lake, Yukon Territory; in Current Research, Part A, Geological Survey of Canada, Paper 91-1A, p. 37-42, 1991.

Abstract

Two distinct suites of metamorphic rocks are present east of Denali fault between Kluane Lake and Kusawa Lake, the Kluane and Aishihik assemblages. The Aishihik assemblage includes biotite schist, granitic gneiss, biotite granodiorite gneiss, amphibolite, and minor quartzite, marble, and calc-silicate, and is broadly equivalent to the Nisling terrane. The Kluane assemblage includes graphitic andesine-biotite schist and minor muscovite-chlorite schist, and incorporates the Kluane Schist. Their contact is sharp, and is inferred to be an east-dipping fault welded by metamorphism. Deformation fabrics and mineral phases in the Aishihik assemblage locally record Triassic strain at sillimanite grade. Both assemblages record a sillimanite-grade overprint of inferred Eocene age, related to intrusions of the Coast Plutonic Complex. From metamorphic mineral fabrics and thermobarometry of zoned garnets, the overprint appears to be prograde in the Kluane assemblage and retrograde in the Aishihik assemblage.

Résumé

Deux séquences distinctes de roches métamorphiques sont présentes à l'est de la faille Denali entre le lac Kluane et le lac Kusawa; il s'agit des assemblages de Kluane et d'Aishihik. Ce dernier comprend du schiste à biotite, du gneiss granitique, du gneiss granodioritique à biotite, et en moindres quantités, du quartzite, du marbre et des silicates calciques; on le considère en outre équivalent, dans l'ensemble, au terrane de Nisling. L'assemblage de Kluane comprend du schiste à biotite et andésine graphitique et une faible quantité de schiste à muscovite et chlorite dans lequel s'incorpore le schiste de Kluane. Leur contact est net et l'on a établi par inférence qu'il s'agit d'une faille à pendage vers l'est soudée par métamorphisme. La fabrique de déformation et les phases minérales de l'assemblage d'Aishihik témoignent localement d'une déformation triassique du degré des sillimanites. Les deux assemblages comportent une surimpression du degré des sillimanites que l'on estime d'âge éocène, liée à des intrusions du complexe plutonique côtier. En se fondant sur la fabrique minérale métamorphique et la thermobarométrie des grenats zonés, la surimpression semble être prograde dans l'assemblage de Kluane et rétrograde dans l'assemblage d'Aishihik.

[1] Department of Geology, University of Alberta, Edmonton, Alberta T6G 2E3

INTRODUCTION

High-grade schists and paragneisses outboard from the western margin of "North America" constitute an enigma in the northern Cordillera in Yukon and British Columbia. They are broadly homotaxial with Proterozoic to Paleozoic sequences of continental rocks closer to the foreland in the east, but the correlation is tenuous because their nature and history are not well known. This report presents the results of field and petrological study of the lithology, structural style, and metamorphic history of metamorphic rocks along the eastern margin of the Coast Plutonic Complex, east of Denali fault in southern Yukon, during the summer of 1990. Previous mapping (Erdmer, 1989, 1990) in separate areas showed the possibility of establishing the continuity of regional units and the nature of contacts, and determining whether the rocks were deformed and metamorphosed by mid-Cretaceous to Eocene intrusions of the Coast Plutonic Complex, or earlier.

The metamorphic rocks have been grouped into two regional suites, the Kluane and Aishihik assemblages (Fig. 1). These can be considered as tectonostratigraphic units with separate early histories, that were linked before common metamorphism and uplift in Eocene time. The Kluane assemblage is distinguished by its graphitic nature, coarse schistosity, and abundant blue-grey porphyroblasts of graphite-filled andesine. It includes biotite schist and muscovite schist, which form large, homogeneous units. Biotite schist (unit 1 of Muller, 1967) is commonly garnet- and staurolite-bearing, with tourmaline a characteristic accessory mineral, and weathers brown with a purple hue; muscovite schist (unit 2 of Muller, 1967; "ms" on Fig. 1 in this report) occurs in one area east of Kluane Lake only, essentially as mapped by Muller (1967). The Kluane assemblage appears to be restricted to the area between Kluane and Dezadeash lakes, although its southern boundary is only broadly constrained from present data. The Kluane assemblage includes rocks mapped as hornfelsed schist or Kluane Schist (Tempelman-Kluit, 1974, 1976) in Aishihik map area, rocks of the Yukon Complex in Kluane map area (units 1 and 2 of Muller, 1967), and rocks of the Yukon group of western Dezadeash map area (Kindle, 1952).

The Aishihik assemblage is characteristically heterogeneous. It includes biotite muscovite psammite and pelite that are commonly migmatitic and garnet and (or) sillimanite-bearing, micaceous quartzite, fine grained garnet amphibolite, marble, calc-silicate, and minor granitic orthogneiss. Graphite occurs only locally in minor amount. Contacts between rock types are commonly gradational, and folded in outcrop. Lithological variation within rock units occurs along strike, and may be due to large-scale transposition of primary contacts. The Aishihik assemblage continues along regional strike to the southeast into British Columbia. It was not examined west of 136°30'E, south of Dezadeash Lake (Fig. 1); it is possible that some rocks in that area may be of different affinity, although reconnaissance mapping (Campbell and Dodds, 1979) indicates broad lithological correlation. The Aishihik assemblage includes rocks of the biotite schist and marble units of Tempelman-Kluit (1976) in Aishihik Lake map area, and of the Yukon group in eastern Dezadeash map area. The Aishihik assemblage is part of the Nisling assemblage defined by Wheeler and McFeely (1987); regionally, the Nisling assemblage includes other metamorphic rocks that may have different protoliths.

Both assemblages record a sillimanite-grade overprint, related to Eocene intrusions of the Coast Plutonic Complex, but the overprint appears to be prograde in parts of the Kluane assemblage and retrograde in parts of the Aishihik assemblage, implying different earlier histories. Deformation fabrics and mineral phases locally record Triassic tectonism in the Aishihik assemblage.

VAN BIBBER CREEK-MOUNT BRATNOBER AREA

An area of approximately 200 km^2 in the Dezadeash Range, between Van Bibber Creek and Mount Bratnober, was mapped to locate the contact between different assemblages recognized to the east and west in previous study. The Kluane assemblage in the west is composed of coarse grained, compositionally homogeneous mauve-brown weathering biotite-andesine-sillimanite schist. Sillimanite occurs most commonly as fibrolite and locally as blocky crystals (1-5 cm long). The latter variety occurs locally in variably-oriented bundles in schist along the margins of granitic aplite to pegmatite dykes and apophyses of granitic bodies (Fig. 2) that intrude the schist.

Schistosity defined by biotite flakes and weak mineral segregation has a constant attitude over large areas and dips moderately westward. It is generally characterized by small-amplitude open waviness in outcrop (Fig. 3). In a few places isoclinal folds of thin (a few millimetres across on average) quartz veins or granitic layers were noted.

Rocks of the Aishihik assemblage occur in the eastern part of the area. They are generally more heterogeneous and finer grained than the Kluane assemblage rocks to the west (Fig. 4, 5) and include biotite schist, granitic gneiss, biotite granodiorite gneiss, amphibolite, and minor quartzite, marble, and calc-silicate. Sillimanite is abundant in pelitic layers. Lithological mixing (juxtaposition of different xenoliths in a granitic matrix in outcrop), crosscutting relations (foliated granitic dykes truncating discordant schistosity, in turn cut by massive aplite), schlieren within gneiss layers, and discordance of schistosity in xenoliths and matrix indicate several periods of metamorphic fabric development. Migmatite, and discordant massive aplite to pegmatite granite veins are common. Schistosity is commonly isoclinally folded in outcrop, and locally disharmonic.

The contact with rocks of the Kluane assemblage dips gently west to southwest, is sharp, and parallel to schistosity on either side at the scale of the map. In outcrop, the change of rock type is abrupt, with no mixing of graphitic schist in the more heterogeneous, finer grained rocks in the east. It is interpreted as a fault now welded by metamorphism. Granitic rocks cut both assemblages, and cut the contact north of the area (south of Sekulmun Lake).

KLUANE HILLS

Muscovite and biotite schist units of the Kluane assemblage exposed on Kluane Lake (units 1 and 2 of Muller, 1967) have been traced into the Kluane Hills. The two rock units are

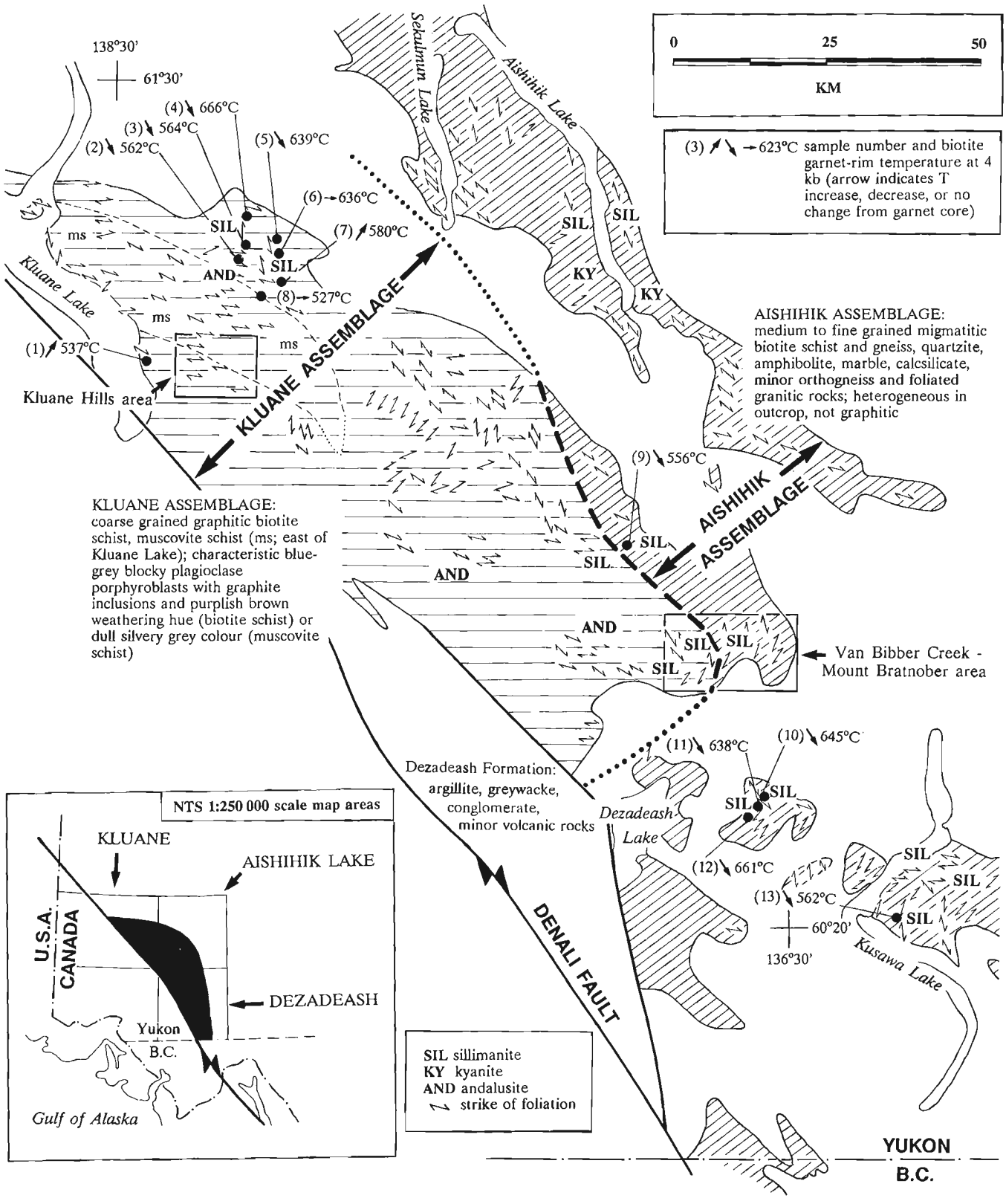

Figure 1. The subdivision of metamorphic rocks east of Denali fault into regional assemblages, in the region between Kusawa Lake and Kluane Lake. Granitic rocks underlie most of the remaining area. Contacts and foliation orientations are based on data collected in 1988-1990, and on work by previous authors (sources given in the text). The approximate extent of the areas mapped in the Kluane Hills and in the Van Bibber Creek-Mount Bratnober area is outlined.

Figure 2. Granite pegmatite dyke (pale rock type) truncating schistosity in the biotite schist of the Kluane assemblage near Van Bibber Creek. Sillimanite crystals up to several centimetres occur in the schist near such contacts.

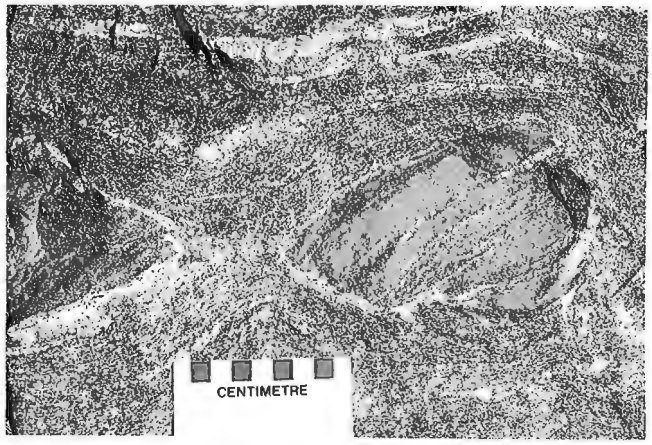

Figure 4. Shear-band boudin of biotite amphibolite in semipelitic schist of the Aishihik assemblage near Van Bibber Creek. The sillimanite-bearing schistosity in the host rock is discordant at the boudin neck and concordant along the top.

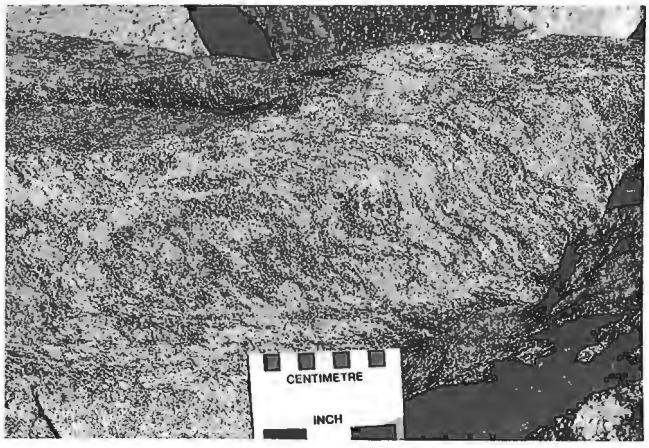

Figure 3. Outcrop face of biotite schist in the Kluane assemblage, near the headwaters of Van Bibber Creek. The schistosity is typically wavy at this scale; it has uniform attitude over several square kilometres on the map scale.

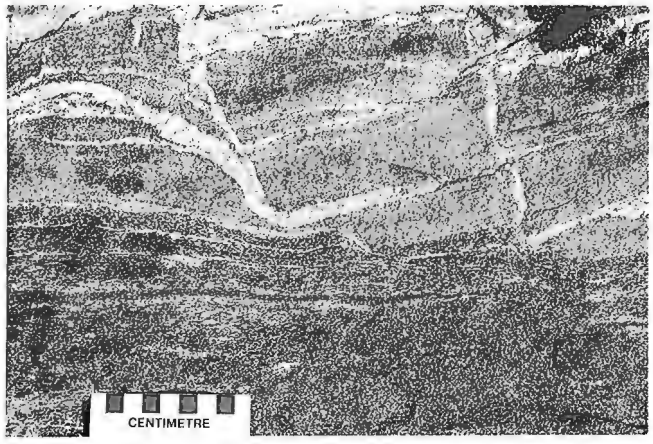

Figure 5. Outcrop of salt-and-pepper granodiorite gneiss and biotite schist cut by several phases of granite pegmatite and aplite, in the Aishihik assemblage near Mount Bratnober.

silvery grey muscovite-chlorite-plagioclase graphitic schist and phyllite (unit ms on Fig. 1) and graphitic biotite-garnet schist, with coarse, even schistosity that dips north to northeast. Most outcrops display asymmetrical folds of the schistosity that are open to closed, have amplitudes of a few to a few tens of centimetres, and are overturned and verge to the south or southwest, with subhorizontal axes. These structures are similar to those in the surrounding area (cf. Erdmer, 1990). The contact between the schist units is gradational over a few tens of metres, with no change in the orientation of schistosity. Because of the distinctive graphitic nature of both units, it is interpreted as an original stratigraphic contact overprinted by metamorphism.

THERMOBAROMETRIC EVOLUTION

Petrological data

Thin section and microprobe analysis showed that porphyroblasts previously reported as cordierite in biotite schist (Erdmer, 1990) are andesine that is tinted characteristically smoky blue-grey from minute graphite inclusions. Cordierite is rare, and appears restricted to true hornfels zones near granitic contacts.

Sillimanite is widely distributed in both the Aishihik and Kluane assemblages in the entire area covered by Figure 1. It is generally fine grained (but not generally fibrolite) and grew at the expense of biotite along the schistosity in many localities. It occurs almost as commonly in the form of isolated bundles of acicular crystals several millimetres long within quartzofeldspathic layers, where needles in the finest grained aggregates are variably oriented, and thus postschistosity. As some of the coarse sillimanite is folded into local crenulations and some has undulatory extinction, it may in part mimic earlier formed metamorphic fabric and in part be contemporaneous. If schistosity is Triassic in age and crenulation is Tertiary, the timing of sillimanite growth is only broadly constrained. Growth is of at least two ages in the metamorphic terrane, as sillimanite occurs both in Eocene- and Triassic-metamorphosed rocks (see below).

Andalusite occurs sporadically in biotite schist of the Kluane assemblage, as porphyroblasts up to 2 mm across that commonly are fringed by fibrolite. It also occurs without sillimanite in the western part of the Kluane assemblage, and as large porphyroblasts (1 cm across or more) in various localities near granitic contacts (cf. Tempelman-Kluit, 1974).

Staurolite is coarse grained and fresh in biotite schist in the Fourth of July Creek area west of the southern end of Kluane Lake (Erdmer, 1990) and is part of the peak equilibrium assemblage together with sillimanite and garnet. This is in contrast to schist farther southeast in Aishihik Lake map area, where Tempelman-Kluit (1974) reported that staurolite is retrograded, and interpreted it to be a product of earlier regional metamorphism.

Kyanite occurs on both sides of the southern part of Aishihik Lake, where it is part of a metamorphic aureole surrounding the Aishihik Batholith, a foliated pluton exposed to the east of the Aishihik assemblage (Johnston, 1988); the plutonic contact was the locus of west-directed, syn-intrusion thrusting. The Aishihik Batholith has yielded Triassic U-Pb zircon ages, and the hot-side up aureole is marked by sillimanite, kyanite, and staurolite zones up to several kilometres wide (S. Johnston, pers. comm; 1990).

Garnet-biotite geothermometry

Microprobe traverses of the largest garnet porphyroblasts in 20 samples show that most are symmetrically zoned, with sharp steps in zoning trends. The typical pattern is of a broad, homogeneous core and a thin, continuously zoned rim, which is interpreted as the sign of at least two periods of garnet growth under differing conditions, i.e. polymetamorphism. The smallest garnets are not zoned, and are compositionally similar to rims of the large, zoned garnets. Garnet-biotite temperatures calculated using garnet rim compositions range between approximately 530 and 660°C at 4 kb (Table 1). Although error on the absolute temperature is at least 50°C (from experimental work, cf. Ferry and Spear, 1978) and likely larger because of microprobe analytical error, the relatively narrow range of garnet-biotite temperature over a large area and the widespread occurrence of sillimanite favour the interpretation that rim garnet and matrix biotite equilibrated under similar pressure-temperature (P-T) conditions in both the Kluane and Aishihik assemblages. Other garnet-biotite geothermometers yield qualitatively comparable results. Given the narrow range of cooling ages in the region (see below), this implies that most or all of the rocks underwent final metamorphism and uplift together.

Geobarometry

Garnet-plagioclase-aluminosilicate geobarometry yielded mixed results in the same samples. Values obtained using the Ghent et al. (1979) expression fall in the range 0.1 to 5.5 kb, with large variation between neighbouring samples. Other expressions yield similar scatter. Assuming that the spread is outside error (which is at least 1.6 kb for the geobarometer (Ghent et al., 1979)), the wide range of pressure observed is at least in part spurious and therefore casts doubt on all results. It is also difficult to reconcile the spread of values with the relatively homogeneous temperature results for the same samples. The main reason for the inconsistency is probably that the plagioclase porphyroblasts are not in equilibrium with the rest of the mineral assemblage; they are inferred to have grown early in the metamorphic history, and appear to not have reacted during later stages. This interpretation is based on the observation that the fine trails of graphite inclusions preserve delicate lamination structure, inferred to be bedding or an early low-grade schistosity. Because of the uncertainty of metamorphic pressure at the time of garnet rim growth, it was not possible to model P-T paths.

Table 1. Garnet rim-matrix biotite temperatures for samples 1-13 (located on Fig. 1), using the geothermometer of Ferry and Spear (1978). The term lnK is the natural log of $(Mg/Fe)_{garnet}/(Mg/Fe)_{biotite}$.

Sample	core lnK	rim lnK	T°C (at 3, 4, 5 kbar)		
1	−2.154	−1.924	533	537	541
2	−1.537	−1.842	558	562	565
3	−1.462	−1.836	560	564	568
4	−1.217	−1.548	661	666	670
5	−1.152	−1.618	635	639	643
6	−1.656	−1.624	632	636	641
7	−1.961	−1.786	576	580	584
8	−1.993	−1.959	523	527	530
9	−1.165	−1.860	553	556	560
10	−1.251	−1.600	641	645	649
11	−1.411	−1.620	634	638	642
12	−1.440	−1.559	657	661	666
13	−1.613	−1.843	558	562	565

DISCUSSION

Although garnet-core matrix-biotite temperature has little geological significance, the direction of temperature change during garnet growth, indicated by compositional zoning, provides a qualitative indication of earlier P-T conditions. In most samples, final temperature is lower than core temperature, with a few samples showing almost no change (garnet not appreciably zoned), and a few with higher rim temperature. Near Kluane Lake, samples showing a temperature increase are located west of the ones showing no change or a decrease. This pattern could result if final metamorphism was (simultaneously) prograde in the western part of the Kluane assemblage and retrograde in the eastern part and in the Aishihik assemblage. When coupled with the observation that the few isotopic ages available are Eocene in the west near Denali fault, and are older in the east (cf. Erdmer, 1989, 1990), this may imply that the western part of the area was uplifted later, heated later, or both buried and uplifted later. However, the small number of both geothermometry and isotopic age data makes this interpretation tentative. Similarly, it is unclear whether (poly)metamorphism in the eastern part of the metamorphic terrane, particularly in the Aishihik assemblage, occurred during separate events or is the result

of a single protracted event, ending with regional uplift. The relation between the protoliths of the Kluane and Aishihik assemblages is unclear. The contact is now welded by metamorphism, and dips east regionally; it may be a thrust surface linked to early movement on Denali fault (cf. Stanley et al., 1990).

K-Ar biotite, hornblende, and whole-rock isotopic dates show that the three youngest intrusive events in the area of Figure 1 are the emplacement of the Nisling Range Granodiorite (102-103 Ma), the Ruby Range Granodiorite (67 Ma, with cooling for the following 15 Ma), and the Nisling Range Alaskite (52-57 Ma) (Stevens et al., 1982; Farrar et al., 1988). Biotite K-Ar dates for the Kluane assemblage fall in the range 53 to 55 Ma (Farrar et al., 1988). From the field relations, thin section textures, and geothermometry results described here, regional sillimanite-grade metamorphism is coeval with either the Ruby Range Granodiorite or the Nisling Alaskite intrusions. As the Nisling suite occupies the northern part of the area only, the Ruby Range suite is likely the direct cause (or result) of metamorphism. The latest metamorphism is thus interpreted to have spanned the period 67 to 52 Ma ago.

The extent of this Eocene overprint is unexpected. If metamorphism is prograde in the western part of the metamorphic terrane, part of the protolith of the Kluane Schist could be as young as Early Eocene. Together with magnetotelluric evidence that flysch of the Late Jurassic to Early Cretaceous Dezadeash Formation underlies the metamorphic rocks, likely in an east-dipping thrust sheet (Stanley et al., 1990), this implies that part of the Kluane Schist is thrust westward over its low-grade protolith, or uplifted in the core of an extensional complex. The hypothesis that the Kluane Schist is the metamorphosed Dezadeash was advanced by Eisbacher (1976); however, as western parts of the Kluane Schist have yielded isotopic dates as old as 180 Ma (Tempelman-Kluit and Wanless, 1975), they have a protolith that is mid-Jurassic or older, which is incompatible with that hypothesis. In the Aishihik assemblage at the margin of the Aishihik Batholith, at least one phase of regional metamorphism is Triassic or older. This early metamorphism may become progressively younger westward, toward the core of the Coast Plutonic Complex; further resolution of the age of metamorphic events requires additional isotopic age data and detailed mapping.

ACKNOWLEDGMENTS

Continuing funding from Energy, Mines and Resources Canada under the Research Agreement program is gratefully acknowledged. Efficient field assistance was provided by B. Keffer. Critical reading of this report prior to its final version was provided by D. Murphy, and is acknowledged with thanks.

REFERENCES

Campbell, R.B. and Dodds, C.J.
1979: Operation Saint Elias, British Columbia; in Current Research, Part A, Geological Survey of Canada, Paper 79-1A, p. 17-20.

Eisbacher, G.H.
1976: Sedimentology of the Dezadeash flysch and its implications for strike-slip faulting along the Denali fault, Yukon Territory and Alaska; Canadian Journal of Earth Sciences, v. 13, p. 1495-1513.

Erdmer, P.
1989: The Nisling Schist in eastern Dezadeash map area, Yukon; in Current Research, Part E, Geological Survey of Canada, Paper 89-1E, p. 139-144.
1990: Studies of the Kluane and Nisling assemblages in Kluane and Dezadeash map areas, Yukon; in Current Research, Part E, Geological Survey of Canada, Paper 90-1E, p. 107-111.

Farrar, E., Clark, A.H., Archibald, D.A., and Way, D.C.
1988: Potassium-argon age of granitoid plutonic rocks, southwest Yukon Territory, Canada; Isochron/West, no. 51, p. 19-23.

Ferry, J.M. and Spear, F.S.
1978: Experimental calibration of the partitioning of Fe and Mg between biotite and garnet; Contributions to Mineralogy and Petrology, v. 66, p. 113-117.

Ghent, E.D., Robbins, D.B., and Stout, M.Z.
1979: Geothermometry, geobarometry, and fluid compositions of metamorphosed calc-silicates and pelites, Mica Creek, British Columbia; The American Mineralogist, v. 64, p. 874-885.

Johnston, S.T.
1988: The tectonic setting of the Aishihik Batholith, southwest Yukon; in Yukon Geology, Volume 2, Exploration and Geological Services Division, Yukon, Indian and Northern Affairs Canada, p. 37-41.

Kindle, E.D.
1952: Dezadeash map-area, Yukon Territory; Geological Survey of Canada, Memoir 268.

Muller, J.E.
1967: Kluane Lake map-area, Yukon Territory (115G, 115F E1/2); Geological Survey of Canada, Memoir 340.

Stanley, W.D., Labson, V.F., Nokleberg, W.J., Csejtley, B., and Fisher, M.A.
1990: The Denali fault system and Alaska Range of Alaska: evidence for underplated Mesozoic flysch from magnetotelluric surveys; Geological Society of America Bulletin, v. 102, p. 160-173.

Stevens, R.D., Delabio, R.N., and Lachance, G.R.
1982: Age determinations and geological studies; Geological Survey of Canada, Paper 82-2.

Tempelman-Kluit, D.J.
1974: Reconnaissance geology of Aishihik Lake, Snag and part of Stewart River map-areas, west-central Yukon; Geological Survey of Canada, Paper 73-41.
1976: The Yukon Crystalline Terrane: enigma in the Canadian Cordillera; Geological Society of America Bulletin, v. 87, p. 1343-1357.

Tempelman-Kluit, D.J. and Wanless, R.K.
1975: Potassium-argon age determinations of metamorphic and plutonic rocks in the Yukon Crystalline Terrane; Canadian Journal of Earth Sciences, v. 12, p. 1895-1909.

Wheeler, J.O. and McFeely, P.A.
1987: Tectonic assemblage map of the Canadian Cordillera and adjacent parts of the United States of America; Geological Survey of Canada, Open File 1565.

1990 field activities and accomplishments, Fraser River delta, British Columbia

John L. Luternauer
Cordilleran Division, Vancouver

Luternauer, J.L., 1990 field activities and accomplishments, Fraser River delta, British Columbia; in Current Research, Part A, Geological Survey of Canada, Paper 91-1A, p. 43-47, 1991.

Abstract

Co-operative investigations of the Fraser River delta were performed to resolve its seismic response and history, further interpret its paleogeographic history, and more precisely measure its sediment budget.

Shallow (<80 m) shear-wave velocities at the western part of the delta generally are significantly less than have been measured for Holocene muds and sands in the southern San Francisco Bay area. Drilling has revealed the first significant evidence of a major paleochannel in the subsurface of the southern part of the delta. Sand boils excavated in central Richmond probably offer the first geological record in the Vancouver area of large earthquakes. Generation of the first analog images of macroturbulent eddies in the Fraser estuary coupled with measurements of suspended sediment suggest eddies are important mechanisms for the transport of suspended sediment.

Résumé

Des études de nature collaborative effectuées dans le delta du fleuve Fraser avaient pour but de déterminer sa réponse sismique et son évolution, d'interpréter de façon plus détaillée son histoire paléogéographique et, en particulier, de mesurer son bilan sédimentaire. Les vitesses des ondes de cisaillement peu profondes (< 80 m) dans la partie ouest du delta sont en général beaucoup moins élevées que celles qui ont été mesurées dans les boues et les sables holocènes dans le sud de la région de la baie de San Francisco. Les forages ont mis à jour les premiers indices significatifs de l'existence d'un important paléochenal dans le sous-sol de la partie sud du delta. Les ostioles de sable excavées dans le centre de Richmond offrent probablement les premières données géologiques dans la région de Vancouver sur les séismes de forte magnitude. Les premières images analogiques des courants tourbillonnaires macroturbulents dans l'estuaire du Fraser conjuguées aux quantités mesurées des sédiments en suspension semblent indiquer que les courants tourbillonnaires sont des mécanismes importants du transport des sédiments en suspension.

INTRODUCTION

Continuing demand for information on the potential earthquake response and present stability of the highly populated, industrialized, and environmentally important Fraser River delta (Fig. 1) has maintained the need for multidisciplinary geological research involving many government, university, and private sector organizations (Luternauer, 1990). These studies have been done in co-operation with and/or coordinated by the Cordilleran Division.

During the summer of 1990, the focus on the subaerial part of the delta was on acquiring data that will help prepare a seismic microzonation map of the area and help recognize evidence of paleoseismicity and sea-level changes. Further to these objectives, we extended our database of subsurface sediment shear-wave velocities and surveyed the subsurface structure and lithology of the delta by coring and continuous seismic profiling and by examining an excavated trench.

Offshore investigations continued to be directed toward improving our understanding of the controls on the stability of the delta front where large ports, a lighthouse, jetties, causeways, power cables, and submarine pipelines are situated and where there are important wildlife habitats (Fig. 1). Attention in 1990 focused on better defining estuarine sedimentary dynamics at the Main Channel mouth which strongly influence the overall sediment budget of the delta front. This program is driven by concerns for the stability of the delta slope arising from the dredging program of Public Works Canada (Stewart and Tassone, 1989) and evidence of massive failure off the mouth of the Main Channel (McKenna and Luternauer, 1987).

In addition to the above programs, the Geological Survey of Canada has shared equipment and samples to assist in a Ph.D. thesis project at the University of Calgary which is examining the early diagenesis of clastics in mixed marine and meteoric water systems.

FIELD ACTIVITIES AND ACCOMPLISHMENTS

The following summaries were prepared in consultation with the individual project chiefs listed in parentheses.

Shear wave and compressional wave velocity surveys and seismic reflection profiling

(J.A. Hunter, S.E. Pullan, and B. Todd, Terrain Sciences Division)

It has been well established that the intensity of ground shaking during an earthquake can be directly related to the thickness and strength of the unconsolidated sediments lying below ground surface. Extensive studies by the U.S. Geological Survey in the San Francisco Bay and Los Angeles basin areas have shown that a relation exists between average shear-wave velocities of unconsolidated materials and earthquake ground motion. Recent investigations in California have also shown a correlation between shear-wave velocities and liquefaction potential of cohesionless soils for moderate earthquakes.

The Fraser River delta consists of a thick sequence of unconsolidated sediments and is in a zone of high seismicity. Shallow seismic reflection surveys have been conducted here on a continuing basis since 1985 (Luternauer, 1988, 1990; Pullan et al., 1989) to map the structure and thickness of the sediment sequence and to compile a database of shear-wave velocity information to be used in the assessment of earthquake hazards in the region (Hunter et al., 1991). This year the coverage of shear-wave velocity measurements made on the delta was extended significantly, and a reflection profile was shot at Boundary Bay in an attempt to map the top of bedrock in that area.

During the 1989 field season, 20 sites in the southern Fraser Delta were shot for surface shear-wave refraction to obtain velocity-depth functions down to a depth of 80 m. The interpretation generally shows that the shallow shear-wave velocities here are significantly less than have been measured for Holocene muds and sands in the southern San Francisco Bay area. In 1990, surface shear-wave refraction data were collected at 30 additional locations to establish sites at a regional spacing of approximately 2 km at the western part of the delta. The shear-wave velocity structure results were similar to those obtained from the 1989 data.

In addition, four deep shear-wave refraction soundings were obtained to a depth of approximately 200 m at Boundary Bay, the Coal Port causeway and approaches, and the northern part of the seaward dyke in Richmond. These data indicate a considerable thickness of low-velocity sediments in the upper section and a lower boundary of high-velocity material. This latter feature possibly correlates with the top of Pleistocene sediments. These soundings are currently being analyzed.

A 1.5 km long seismic reflection profile was shot north-south in the southwestern part of the delta adjacent to Tsawwassen. A strong reflector, interpreted to be the top of Tertiary, was mapped from a depth of approximately 680 m at the north end of the profile to a depth of 450 m at the south end.

Data for calculating compressional wave velocities was collected from three drillholes in co-operation with M.C. Roberts of Simon Fraser University. A 12 channel eel was utilized with a 0.5 m station overlap. The sensors were single hydrophones. The objective of the experiment was to obtain detailed interval velocities in the drillholes. This information is presently being interpreted.

Geoarchitecture and genetic stratigraphy

(M.C. Roberts, Simon Fraser University)

Previous research on the delta (Jol and Roberts, 1988), revealed the presence of a large buried channel (about 1.5 km wide) between Point Roberts Peninsula and onlapping subsurface foreset beds of the delta. Two drilling targets were selected using a previously shot high resolution reflection seismic line (Jol and Roberts, 1988). Mud-rotary drilling was done with a Mobile B-53 rig; core and downhole gamma logs were obtained. Both drill holes were cased with 2'' PVC pipe for subsequent shear measurements by J.A. Hunter (GSC).

A core was also collected at a second site, on Lulu Island (Fig. 1), to serve as lithological control for cone-penetrometer logs that apparently show repetitive turbidite-like units in a silt beneath a tidal-flat sand sequence.

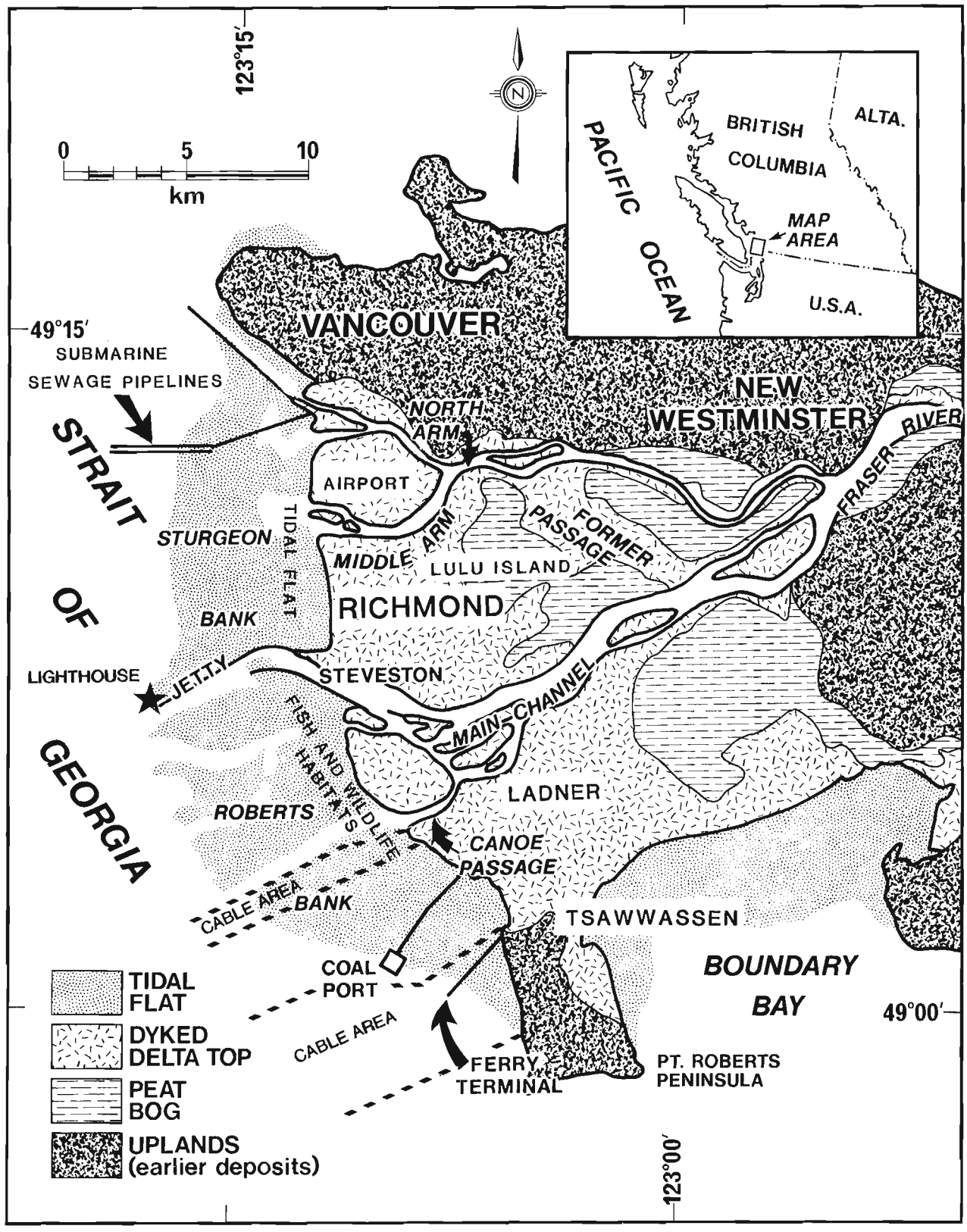

Figure 1. Location map of the study area.

Coring for geophysical and paleoseismicity investigations

(J.L. Luternauer and J.J. Clague, Terrain Sciences Division)

Drilling and coring contracted to Sonic Drilling Ltd. of Surrey, B.C. is underway, as this issue goes to press, to prepare a hole by the (Vancouver International) Airport (Fig. 1) and in central Richmond for shear-wave velocity measurements and to generate lithological control for this and other geophysical surveys. As concerns have been raised about the impact of earthquakes and tsunamis (P. Byrne, University of British Columbia, pers. comm., 1990) at the proposed site for a new runway at the airport, the core taken in this area will be examined for evidence of past earthquakes or related phenomena.

Paleogeography and sea level history

(H. Williams, University of North Texas and J.L. Luternauer)

Seven vibracores were collected along a north-south transect extending from the dyke into the bog at the southeastern part of the delta as a basis for reconstructing the history of this part of the delta. Of particular interest is: 1) identification of any channel that discharged into Boundary Bay to form this part of the delta; and 2) comparison of the local depositional response to the mid-Holocene rise in sea level with that of the northern part of the delta (Williams and Roberts, 1989).

Preliminary evidence in one of the cores, in the form of scattered pebbles, suggests a major distributary channel discharged into Boundary Bay prior to 5000 years ago. Two cores from the margin of the large peat bog reveal that organic-rich silt, up 4 m thick, underlies the surface peat deposits. The silt is lithologically similar to aggraded floodplain sediments underlying Lulu Island (Williams and Roberts, 1989), raising the possibility that a mid-Holocene sea level rise induced a similar style of delta plain aggradation at the southeastern part of the delta (Williams and Luternauer, 1991).

Sea levels and paleoseismicity

(A. Blais, Carleton University and J.J. Clague, Terrain Sciences Division)

A. Blais has undertaken a study of late Holocene sea level change and sedimentary environments at Burns Bog as part of her Ph.D. research at Carleton University. Several vibracores were collected, described, and subsampled for foraminifera during the summer of 1990. One of the objectives of this work, which complements that of J.J. Clague (Clague et al., 1991), is to determine whether or not there has been coseismic subsidence or uplift of the delta top during the late Holocene.

Evidence of paleoseismicity at construction site trench

(J.J. Clague, Terrain Sciences Division and J.L. Luternauer)

Engineering consultants (Klohn Leonoff Ltd.) alerted the authors to sand dykes evident on the trenched face of the surface silts at a construction site in Richmond. Several dykes were noted by the first author. He described and photographed the features and collected wood for radiocarbon dating. At least one of the dykes appears to reach the present surface. However, this could not be confirmed because the surface deposits have been disturbed by human activities. These features are the first indication from the geological record of large earthquakes affecting the Vancouver area.

Estuarine sediment budget

(R.A. Kostaschuk, University of Guelph and M.A. Church, University of British Columbia)

This project to examine sedimentary processes in the lower reaches of the Main Channel of the Fraser River was begun in 1985. The recent focus of the project has been on the interrelationships between flow, bedforms, and sediment transport (Kostaschuk et al., 1990). During the summer of 1990, we examined interactions between macroturbulent eddies, or boils and sediment suspension. A variable-frequency acoustic profiling system provided first-ever analog images of the eddies. These were accompanied by simultaneous measurements of vertical and horizontal velocity fluctuations and suspended sediment concentration. An electromagnetic current meter was used to determine velocity and an optical backscatter probe to measure sediment concentrations. Preliminary results reveal that the eddies have much higher sediment concentrations and turbulent energy than the ambient flow. Eddies are periodically generated on the upstream sides of large bedforms, rise to the surface, then propagate downstream and dissipate. The data suggest that boils are an important factor in the entrainment and transport of suspended bed material.

Early diagenesis of clastics in a deltaic setting

(G. Simpson, University of Calgary)

Sixty-six sediment and pore water samples were collected with a rotary drill and vibracore mainly at the mudflats of the Fraser River delta to study the early diagenesis of clastics in mixed marine and meteoric water systems. The analysis of pore waters from sediments has proved to be a productive approach for understanding the reactions occurring during diagenesis at low and higher temperatures (e.g. Abercrombie, 1989).

REFERENCES

Abercrombie, H.J.
1989: Geochemistry of thermal recovery, Cold Lake, Alberta; Ph.D. thesis, University of Calgary, Calgary, Alberta.

Clague, J.J., Lichti-Federovich, S., Guibault, J.-P., and Mathewes, R.W.
1991: Holocene sea level change, south-coastal British Columbia; in Current Research, Part A, Geological Survey of Canada, Paper 91-1A.

Hunter, J.A., Woeller, D.J., and Luternauer, J.L.
1991: Comparison of surface, borehole and seismic cone penetrometer methods of determining the shallow shear wave velocity structure in the Fraser River delta, British Columbia; in Current Research, Part A, Geological Survey of Canada, Paper 91-1A.

Jol, H.M. and Roberts, M.C.
1988: The seismic facies of a delta onlapping an offshore island: Fraser delta, British Columbia; in Sequences, Stratigraphy, Sedimentology: Surface and Subsurface, edited by D.P. James and D.A. Leckie, Canadian Society of Petroleum Geologists, Memoir 15, p. 137-142.

Kostaschuk, R.A., Ilersich, S.A., and Luternauer, J.L.
1990: Relationship between bed-material load and bedform migration, Fraser River estuary, British Columbia; in Current Research, Part E, Geological Survey of Canada, Paper 90-1E, p. 239-244.

Luternauer, J.L.
1988: Geoarchitecture, evolution and seismic risk assessment of the southern Fraser River delta, B.C.: status of investigations; in Current Research, Part E, Geological Survey of Canada, Paper 88-1E, p. 105-109.
1990: 1989 field activities and accomplishments of geophysical and geotechnical land-based operations and marine/fluvial surveys, Fraser River delta, British Columbia; in Current Research, Part E, Geological Survey of Canada, Paper 90-1E, p. 235-237.

McKenna, G.T. and Luternauer, J.L.
1987: First documented large failure at the Fraser River delta front, B.C.; in Current Research, Part A, Geological Survey of Canada, Paper 87-1A, p. 919-924.

Pullan, S.E., Jol, H.M., Gagne, R.M., and Hunter, J.A.
1989: Compilation of high resolution "optimum offset" shallow seismic reflection profiles from the southern Fraser River delta, British Columbia; Geological Survey of Canada, Open File 1992.

Stewart, I. and Tassone, B.
1989: The Fraser River delta: a review of historic sounding charts; Environment Canada, Conservation and Protection, Inland Waters, Pacific and Yukon Region, March, 1989, 39 p.

Williams, H.F.L. and Luternauer, J.L.
1991: Shallow structure and growth of the southern Fraser River delta: preliminary field results; in Current Research, Part A, Geological Survey of Canada, Paper 91-1A.

Williams, H.F.L. and Roberts, M.C.
1989: Holocene sea-level change and delta growth: Fraser River delta, British Columbia; Canadian Journal of Earth Sciences, v. 26, p. 1657-1666.

Georgia Basin Project: stratigraphy and structure of Gambier Group rocks in the Howe Sound-Mamquam River area, southwest Coast Belt, British Columbia[1]

J.V.G. Lynch[2]
Cordilleran Division, Vancouver

Lynch, J.V.G., Georgia Basin Project: stratigraphy and structure of Gambier Group rocks in the Howe Sound-Mamquam River area, southwest Coast Belt, British Columbia; in Current Research, Part A, Geological Survey of Canada, Paper 91-1A, p. 49-57, 1991.

Abstract

Gambier Group rocks of the Howe Sound region were deposited in an Early Cretaceous continental margin volcanic arc setting. The base of the group rests on a deeply incised unconformity characterized by arkose and conglomerate, overlying eroded Late Jurassic granodiorite. A succession of two composite volcanic complexes both span the complete basalt-andesite-dacite-rhyolite association, and display a variety of depositional textures. Extensive pyroclastic flow deposits record an explosive volcanic environment. Between the two complexes are sediment gravity flow deposits dominated by interbedded shale and wacke, deposited under tectonically unstable marine conditions. Lesser arkose, chert, and limestone occur. Tectonic wedging distinguishes the principal phase of contractional deformation: southwest-directed thrusts emplace Jurassic plutonic rocks and lower Gambier stratigraphy over younger members; concomitant or younger northeast-directed back-thrusts emplace the mid-Cretaceous plutonic roots of the arc above its volcanic derivative.

Résumé

Les roches du groupe de Cambier, dans la région du détroit de Howe, se sont accumulées dans un milieu d'arc volcanique de marge continentale du Crétacé précoce. La base du groupe repose sur une discordance profondément entaillée caractérisée par la présence d'arkose et de conglomérat, au-dessus de granodiorite érodée du Jurassique tardif. Une succession de deux complexes volcaniques composites couvre l'association complète basalte-andésite-dacite-rhyolite et présente diverses textures sédimentaires. La présence étendue d'ignimbrites témoigne d'un milieu volcanique explosif. Entre les deux complexes, on trouve des sédiments provenant d'écoulements par gravité dominés par des shales et des grauwackes interstratifiés qui se sont accumulés dans des conditions marines tectoniquement instables. On trouve également, mais en moindres quantités, de l'arkose, du chert et du calcaire. La phase principale de déformation par contraction se caractérise par un écaillage tectonique : par suite de chevauchements à direction sud-ouest, les roches plutoniques jurassiques et la partie inférieure du groupe de Gambier se se retrouvées au-dessus de membres plus récents; par suite de rétrocharriages concomitants ou plus récents à direction nord-est, les racines plutoniques du Crétacé moyen de l'arc se sont retrouvées au-dessus de ses dérivés volcaniques.

[1] Field work funded in part by the Frontier Geoscience Program (Georgia Basin segment).
[2] Present address: Quebec Geoscience Centre, 2700 rue Einstein, Case postale 7500, Sainte-Foy, Quebec G1V 4C7

INTRODUCTION

The present study serves to upgrade geological mapping at the 1:50 000 scale in the Howe Sound-Mamquam River region immediately north of Vancouver (Fig. 1). Research has been directed towards providing a better stratigraphic and structural framework for the Britannia mining district, through the acquisition of new data as well as integration of past work (Reddy, 1989; McColl, 1987; Heah, 1982; Payne et al., 1980; Roddick and Woodsworth, 1979; McKillop, 1973; Sutherland Brown and Robinson, 1970; Bostock, 1963; Armstrong, 1953; James, 1929). Regional objectives of this study include: (1) extension into Howe Sound of a northeast-southwest geological transect across the southern Coast Belt documenting variations in structural style; (2) stratigraphy and geochemistry of Gambier Group volcanic rocks; and (3) investigation of geological structures which may relate to the adjacent Late Cretaceous-Early Tertiary Georgia Basin (Monger, 1990; England, 1989).

Volcanic and sedimentary rocks of the Gambier Group (Roddick, 1965; Armstrong, 1953), which host the Britannia Cu-Zn-Pb-Ag-Au orebodies, are part of a vast Early Cretaceous subduction related volcanic arc sequence which spans the length of the Coast Belt. Broad correlations can be made in terms of age and lithology to the Gravina-Nutzotin belt of southeast Alaska (Berg et al., 1972), as well as to the Nooksack terrane of Washington State (Monger and Berg, 1987). Within the framework of the subduction model proposed by Berg et al. (1972) for the Gravina-Nutzotin belt, this belt of volcanic rocks is thought to represent the volcanic front related to subduction along the Upper Jurassic-Lower Cretaceous Chugach and Pacific Rim mélange and flysch trench complexes. These trench complexes occur along the western margin of the Insular Belt, with the Insular Belt forming a 100-300 km wide arc-trench gap. Cogenetic intra-arc and back-arc volcanic centres are situated within and along the eastern margin of the Coast Belt, which in the south may include the Brokenback Hill Formation in the Harrison Lake (Arthur, 1986) and Fire Lake areas (Lynch, 1990; Roddick, 1965). However, more age dating and geochemical information is needed to test the facing of the arc and establish links between volcanic centres.

In general volcanic arcs are well known for a diverse suite of ore deposit types, and as an important source of metals. This association reflects increased magmatic activity at varying crustal levels, resultant hydrothermal circulation, and interaction with surficial meteoric or marine environments. Principal deposit types include base and precious metal porphyry and skarn deposits, volcanogenic massive sulphide deposits, as well as epithermal precious metal deposits. In the Howe Sound area, the Gambier volcanic rocks host the Britannia volcanogenic massive sulphide orebodies (Payne et al., 1980). This study attempts to improve knowledge of district scale stratigraphic and structural controls on the orebodies, and provide a model for exploration within the volcanic belt.

STRATIGRAPHY

Stratigraphy of the Gambier Group may be subdivided into two broad volcanic complexes, separated by a predominantly clastic sedimentary interval. These effectively correspond to the "Lower", "Middle", and "Upper" subdivisions of Roddick (1965). The two complexes display similar volcanic features, and span the full range of the basalt-andesite-dacite-rhyolite association typical of composite or stratovolcanoes. However the lower complex is distinct from the upper by the occurrence of plutonic rock fragments, which occur as occasional clasts or accidental ejecta, and form the basal conglomerate.

Within the complexes coarse pyroclastic flows are subdivided on the map (Fig. 1) and provide a useful reference frame from which to describe volcanic stratigraphy. Emphasis on volcanic centres through documentation of vent-proximal facies allows for meaningful reconstructions. However, broad correlations based on flows and coarse pyroclastic units are difficult, due to the linear form or limited areal extent of some flows.

Age determinations

Fossils collected by H.W. Tipper from Gambier Group rocks along the Squamish Highway (99) near Brunswick point were identified by J.A. Jeletzky as hoplitid ammonites belonging to *Cleoniceras (Grycia ?) perezianum* indicating a middle Albian age (J.A. Jeletzky, unpublished GSC report no. Km-3-1970-JAJ). The range in age of the Gamier Group is bracketed by older and younger plutons. In the east the volcanics lie unconformably above the Cloudburst Pluton (Fig. 1), which has been dated by U-Pb zircon geochronometry to be 145 ± 2 Ma (Friedman and Armstrong, 1990); younger intrusions which crosscut the Gambier Group include the Furry and Squamish plutons, these have been determined to be mid-Cretaceous in age, within the interval 107-102 Ma (Friedman and Armstrong, 1990).

Direct dating of the volcanics by Rb-Sr geochronometry has been hampered by large error margins; Rb-Sr isochrons record ages of 114 ± 40 Ma (Heah, 1982), 167 ± 37 Ma (McColl, 1987), and 102 ± 10 Ma (Reddy, 1989). However, major thermal events are effectively recorded by K-Ar dating, and are summarized in Table 1; groupings are as follows: 148-157 Ma, 101-108 Ma, 90-97 Ma, and 81-84 Ma. The first two groupings correspond with pluton intrusion, the other two are thought to reflect deformation and metamorphic events.

Basal unconformity and evidence for early normal faulting

The basal unconformity between Lower Cretaceous Gambier Group rocks and the Jurassic Cloudburst pluton is best exposed along the southeastern ridge of Alpen Mountain, in the eastern study area (Fig. 1). There a 20 m thick section of thickly bedded conglomerate and arkose rests directly upon eroded granodiorite. The conglomerate is well-sorted, clast-supported, and consists of 1-5 cm clasts of rounded granodiorite, and lesser clasts of andesite, basalt, sandstone, and chert. This coarse clastic sequence passes abruptly upwards into interbedded siltstone, shale, and andesitic lapilli tuff with minor breccia. Below the unconformity within the Jurassic pluton, dykes of andesite and basalt are common. These are interpreted to be feeders to the volcanics and are distinguished

from the fresh Tertiary dykes of the region by their contained greenschist metamorphism and foliation.

Clear exposures of the unconformity are rare. However, volcanic flows in the proximity of the unconformity typically contain scattered granodiorite clasts. Such clasts are found in the volcanics east of the Stawamus and Indian rivers, and are absent to the west, with the exception of Alberta Bay in Howe Sound and Gambier Island (Roddick, 1965). This distribution is a useful criterion for segregating broad volcanic packages, and appears to be a feature helpful in discerning relative stratigraphic positions.

On Gambier Island large angular and subangular granodiorite clasts are common within mafic volcanic flows of the Gambier Group in areas near the Jurassic Thornbrough granodiorite. Roddick (1965) reported between 15-90 m of the basal conglomerate along portions of this near vertical contact. The contact is well exposed in the intertidal zone of Halkett Bay where a 50 cm wide mylonitized fault zone separates the volcanic and plutonic assemblages. The fault is steeply dipping and contains a strongly developed down-dip stretching lineation. Small drag folds occur within the volcanics immediately adjacent to the fault, and indicate apparent normal displacement along the fault. The fault plane has been folded by later deformation, is sinuous in outcrop, and is locally overturned. It is not known if the fault extends farther to the west along the rest of the contact; relationships are obscured by intense dyke swarms of Gambier volcanics which penetrate the granodiorite making the exact position and nature of the contact difficult to establish.

Features which indicate that normal faulting and volcanic activity may have been contemporaneous are the occurrence of the coarse angular granodiorite fragments within the mafic flows, which apparently reflect relief and rapid erosion, as well as the occurrence of the dyke swarms along the contact, which formed during extension.

Lower Volcanic Complex

Significant lateral variation in lithology exists within the units immediately above the basal conglomerate. Arkose is present but is subordinate to volcaniclastic sandstone and feldspathic greywacke. The arkose is coarse to pebbly, crumbly, and weathers orange. Siltstone, shale, and phyllite are common. Flame structures, graded bedding and crosslaminations are observed in siltstone. Truncation and scouring of laminations is sometimes seen within shallow gently bevelled troughs. Bedded volcanic tuff and feldspar crystal tuff are also common. Chert is infrequently observed, consisting of microcrystalline quartz in thin grey to white beds forming 2-3 m sequences between shales and siltstone. Interbedded volcanic flows, which in areas dominate the lithology, consist principally of basalt and andesite. Typically these rocks are dark green reflecting an abundance of secondary chlorite and epidote related to regional greenschist metamorphism. The andesite is porphyritic with up to 30 per cent zoned plagioclase in a felted or trachytic microlite groundmass. Basalt contains phenocrysts of plagioclase, pyroxene and hornblende, with the mafic phenocrysts replaced to varying degrees by chlorite. Autoclastic flow breccias locally occur with basalt flows.

Overlapping the sequence of clastic rocks and mafic volcanic flows is an extensive pyroclastic complex. The complex is dominated by poorly sorted heterolithic volcanic breccia. Andesite clasts are dominant, but dacite and rhyolite clasts are also common, and are locally the principal clast type. Fragments are angular, up to 2 m in size, and suspended in a matrix of ash, feldspar crystals, and smaller volcanic rock fragments. Successive pyroclastic flows may show a crude stratification. Internal stratification occurs where ash layers drape over larger ejecta. Most flows are dense. Vesiculation is not particularly common, however beds of felsic pumice and mafic scoria do occur. Degassing is reflected in juvenile bombs as well; these are up to 50 cm across, fluted, almond shaped, and have radial fractures which offset chilled margins due to gas expulsion. Such bombs are evidence of phreatomagmatic processes taking place during volcanic eruption and formation of pyroclastic flows.

Evidence for explosive volcanism and felsic magmatism occurs in the area of Mt. Mulligan where a thick flow banded rhyolite dome is surrounded by felsic pyroclastic deposits. Flow banding in the rhyolite dome is defined by layers of devitrified glass with conchoidal fractures, interlaminated with layers containing quartz phenocrysts and minor feldspar crystals. Flanking pyroclastic deposits include clast supported rhyolite breccia along the flow front, poorly-sorted felsic pyroclastic flows, and distal lapilli tuff, welded tuff, and pumice. The occurrence of several brecciation events are locally recorded by clasts of breccia within andesitic breccias. Thin beds of volcaniclastic conglomerate, sandstone, and siltstone also occur. White clay alteration is widespread.

The sequence of rocks above the breccia complex has been eroded away in the area east of the Stawamus and Indian rivers, but is exposed to the west of the Stawamus River (Reddy, 1989), and on Gambier Island. It consists predominantly of andesite and basalt flows with subordinate breccias tuffs, tuffaceous sediments, and shale.

Middle Sedimentary Interval

The Middle Sedimentary Interval is best exposed at the northeast end of Gambier Island, along the eastern shore of Anvil Island, as well as along the north flank of Goat Ridge, and is reported to occur on Brunswick Mountain (Roddick, 1965). Thickness of the interval ranges widely; on Goat Ridge the Middle Sedimentary Interval is approximately 500 m thick, whereas on Gambier Island it may be greater than 2.3 km thick. Typically the sequence is well bedded, consisting mainly of shale, pyritiferous shale, siltstone, and wacke. Sandstones are commonly moderately or poorly sorted, with angular and subangular clasts up to pebble, or rarely, cobble size. Moderately to poorly sorted breccia and conglomerate also occur. Graded bedding, flame structures, and crosslaminations are common sedimentary structures. Ripple marks, small channel scours and mud rip-up clasts were seen in some places. Structures indicate deposition under high energy conditions, likely as sediment gravity flows. Less common lithologies include limestone, quartzite, arkose, as well as sandstone units with spherical epidote altered carbonate concretions. Fossils include rare unidentified bivalves and

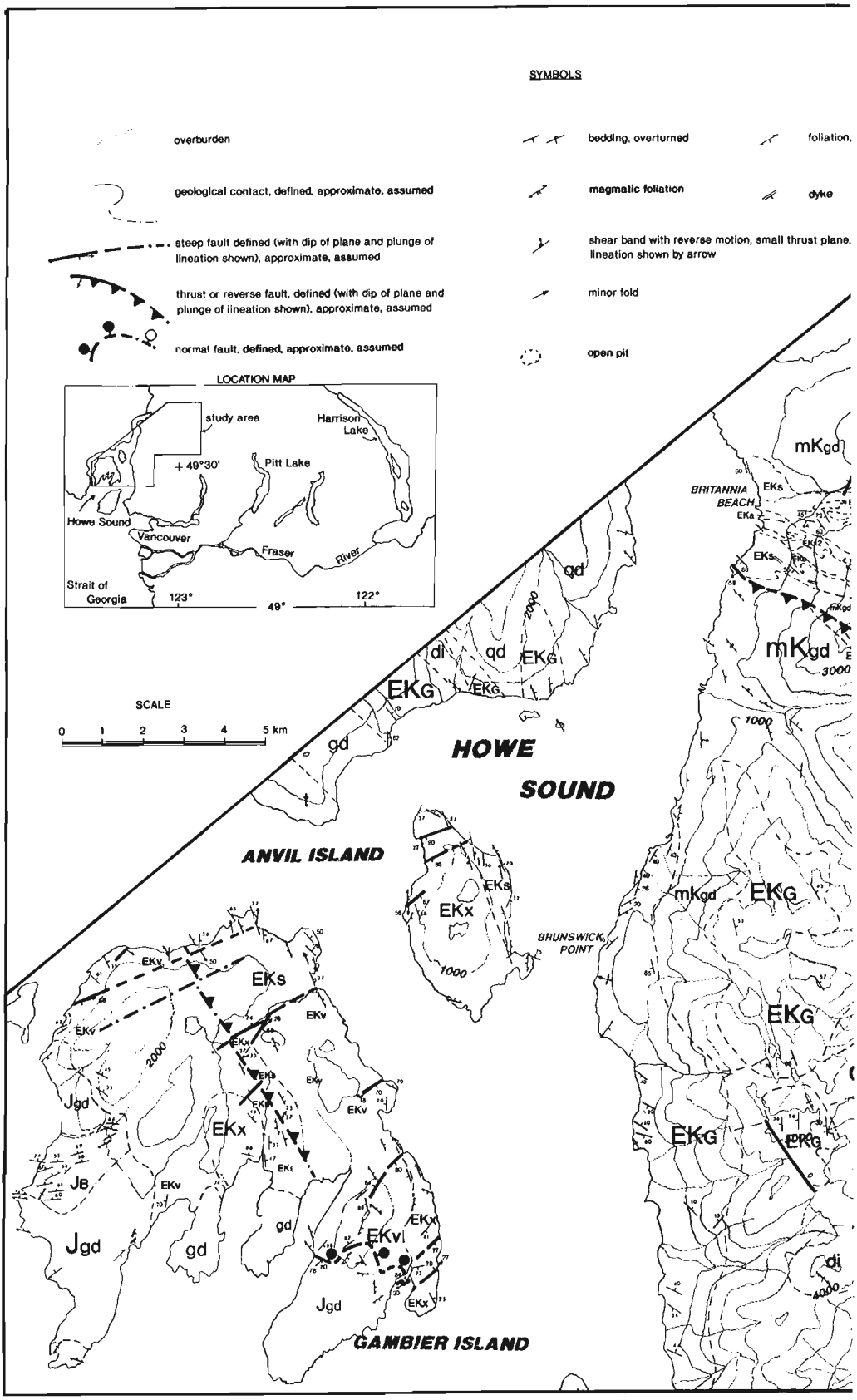

Figure 1. Geology of Gambier Group Rocks in the Howe Sound- Mamquam River region. Map produced from data collected during 1990 field season, and compiled from Reddy (1989), McColl (1987), Payne et al. (1980), Roddick and Woodsworth (1979), McKillop (1973), Bostock (1963), Armstrong (1953), and James (1929).

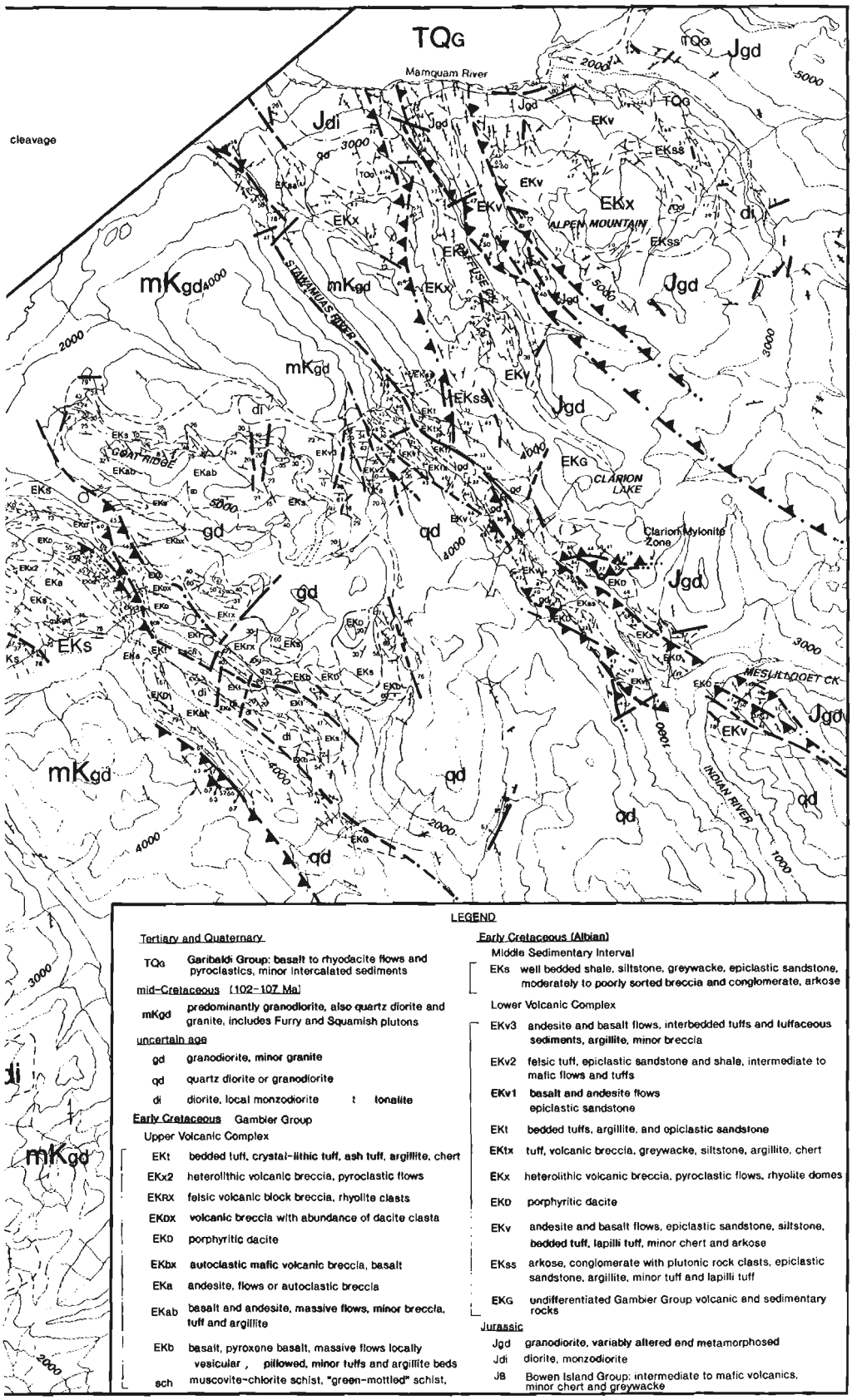
TQG
Mamquam River
cleavage
Jdi
Jgd
EKv
EKx
EKss
ALPEN MOUNTAIN
mKgd
STAWAMUS RIDGE
EKG
CLARION LAKE
Clarion Mylonite Zone
EKs
GOAT RIDGE
EKab
qd
di
MESILLADOET CK.
INDIAN RIVER
LEGEND
Tertiary and Quaternary
TQa Garibaldi Group: basalt to rhyodacite flows and pyroclastics, minor intercalated sediments
mid-Cretaceous (102-107 Ma)
mKgd predominantly granodiorite, also quartz diorite and granite, includes Furry and Squamish plutons
uncertain age
gd granodiorite, minor granite
qd quartz diorite or granodiorite
di diorite, local monzodiorite t tonalite
Early Cretaceous Gambier Group
Upper Volcanic Complex
EKt bedded tuff, crystal-lithic tuff, ash tuff, argillite, chert
EKx2 heterolithic volcanic breccia, pyroclastic flows
EKRx felsic volcanic block breccia, rhyolite clasts
EKDx volcanic breccia with abundance of dacite clasts
EKD porphyritic dacite
EKbx autoclastic mafic volcanic breccia, basalt
EKa andesite, flows or autoclastic breccia
EKab basalt and andesite, massive flows, minor breccia, tuff and argillite
EKb basalt, pyroxene basalt, massive flows locally vesicular, pillowed, minor tuffs and argillite beds
sch muscovite-chlorite schist, "green-mottled" schist,
Early Cretaceous (Albian)
Middle Sedimentary Interval
EKs well bedded shale, siltstone, greywacke, epiclastic sandstone, moderately to poorly sorted breccia and conglomerate, arkose
Lower Volcanic Complex
EKv3 andesite and basalt flows, interbedded tuffs and tuffaceous sediments, argillite, minor breccia
EKv2 felsic tuff, epiclastic sandstone and shale, intermediate to mafic flows and tuffs
EKv1 basalt and andesite flows epiclastic sandstone
EKt bedded tuffs, argillite, and epiclastic sandstone
EKtx tuff, volcanic breccia, greywacke, siltstone, argillite, chert
EKx heterolithic volcanic breccia, pyroclastic flows, rhyolite domes
EKD porphyritic dacite
EKv andesite and basalt flows, epiclastic sandstone, siltstone, bedded tuff, lapilli tuff, minor chert and arkose
EKss arkose, conglomerate with plutonic rock clasts, epiclastic sandstone, argillite, minor tuff and lapilli tuff
EKG undifferentiated Gambier Group volcanic and sedimentary rocks
Jurassic
Jgd granodiorite, variably altered and metamorphosed
Jdi diorite, monzodiorite
JB Bowen Island Group: intermediate to mafic volcanics, minor chert and greywacke

Table 1. Radiometric age determinations (Ma) from the study area. Symbols are (h) hornblende, (b) biotite, (z) zircon, (w) whole rock, (gd) granodiorite, (Gv) Gambier volcanics.

Goups 1	2	3	4	system	
145±2 (gd)	102-107 (gd)			U-Pb(z)	Freedman and
156+2 (gd)				U-Pb(z)	Armstrong (1990)
148±4 (gd)				K-Ar(h)	McKillop (1973)
157±4 (gd)				K-Ar(b)	
167±37 (Gv)				Rb-Sr(w)	McColl (1987)
		90.5±3.2(Gv)	81.4±3(Gv)	K-Ar(w)	
	101±4 (gd)	95.1±3.3 (Gv)		K-Ar(h)	Heah (1982)
	102±15 (gd)			Rb-Sr(w)	
	108±4 (Gv)	96.1±3 (Gv)	83.5±3 (Gv)	K-Ar(w)	Reddy (1989)
		95.6±3.3 (Gv)	84.2±2.9	K-Ar(w)	
	102±10 (Gv)	93±3 (Gv)		Rb-Sr(w)	

belemnites, as well as the previously mentioned ammonite. Minor volcanic units of basalt, andesite, and tuff also occur.

The substantial variation in thickness estimated for the Middle Sedimentary Interval, combined with the sedimentary structures which indicate sediment gravity flow, are interpreted to indicate deposition within a tectonically unstable environment. This may reflect steep slopes constructed along a large volcanic edifice, or possibly indicates syndepositional normal faulting during sedimentation and differential subsidence, or both.

Upper Volcanic Complex

Because the Upper Volcanic Complex is host to the Britannia mining district, numerous geological investigations have been undertaken in this part of the Gambier Group (McColl, 1987; Payne et al., 1980; Sutherland Brown and Robinson, 1970). Most studies attest to the difficulties of stratigraphic analysis.

The Upper Volcanic Complex is intercalated with and overlies the Middle Clastic Interval. As with the Lower Volcanic Complex, the general upward trend appears to progress from mafic and intermediate flows to felsic domes and pyroclastic centres. The start of the cycle is marked by basaltic and andesitic volcanism, erupted under subaqueous conditions producing autoclastic flows, epiclastic sedimentation, and local pillow basalts and agglomerates. Shale and siltstone are abundant, and are interbedded with thin felsic tuff horizons. Andesite is most voluminous. Upward, the sequence is dominated by pyroclastic flows associated with dacite and rhyolite dome complexes, within a sequence of tuffs, shales, siltstones, and chert. The rhyolite and dacite domes are flow banded to massive, porphyritic to phyric, locally spherulitic or vesicular, and mantled by clast supported flow breccias. Surrounding deposits include large heterolithic pyroclastic flows, as well as lapilli, crystal, and ash tuff. An abundance of interbedded sedimentary rocks indicate a predominantly subaqueous regime. However, the identification of accretionary lapilli indicates periods of subareal conditions (McColl, 1987). The pyroclastic flows contain a complete range of volcanic clast types including pumice, dacite, andesite, and basalt fragments. Accidental argillite ejecta reflect explosive extrusion (McColl, 1987), or possibly surficial debris flow processes. Argillite overlies the dome complexes, with some tuff, minor dacite, and andesite.

STRUCTURE

Two sets of northwest-striking thrust faults with opposing senses of shear are recorded in the supracrustal and plutonic rocks of the map area, and are described here. The southwest-verging and northeast-verging fault sets have subparallel trends, and therefore rarely intersect at the present erosional level. As a consequence the relative ages of most thrusts remain uncertain. Small scale opposing shear sets cannot be used to give relative age relations as they appear to be conjugate structures related to individual thrusts. However folded and truncated thrusts have been noted near Indian River south of Clarion Lake, that indicate southwest-directed thrusting preceded northeast-directed thrusting. Such age relationships are consistent with apparent timing relations deduced from map-scale patterns (Fig. 1). Contrasting textural features described here show that the opposing thrust systems may have occurred under different confining conditions, further helping to distinguish groupings. The basic geometric and kinematic features recorded appear to reflect deformation in a regime of tectonic wedging (Price, 1986). However, the two principal post-intrusion thermal events defined by K-Ar geochronology studies (at approximately 93 and 83 Ma, Table 1), may be related to the two thrusting events; they could reflect the long lived nature of the deformation, or possibly indicate separate unrelated thrust systems.

Southwest-verging thrusts

The southwest-verging thrusts are distributed principally within the eastern portion of the district, where the older plutonic rocks and lowest portions of Gambier Group stratigraphy have been juxtaposed against younger strata to the southeast. The two principal southwest verging shear zones occur along Raffuse Creek, and south of Clarion Lake near

Indian River (Fig. 1). The latter constitutes the lowest structural level of the district, represented by a conspicuous white mylonite zone (Clarion Mylonite Zone) displaying a 100-500 m thick section of continuous ultramylonite juxtaposing Upper Jurassic granodiorite in the hanging wall and Gambier Group volcanics in the footwall. The mylonite is highly siliceous, consisting of nearly 100 per cent microcrystalline quartz, and is characterized by a finely laminated planar fabric and strong downdip lineation. Sheath folds are locally abundant. Due to later folding, the orientation of the mylonite is variable, striking from west to northwest, and dipping moderately to steeply north to northeast. A south to southwest direction of thrust transport is indicated by a marked strain gradient, and by curved flattening surfaces within the adjacent granodiorite which rotate into the mylonite when the contact is approached. The western extension of the mylonite is truncated by and buried beneath younger northeast verging thrusts, providing clear evidence of relative timing relations. The eastern extension has not been mapped.

The thrusts which occur along and to the east of Raffuse Creek occur at a higher structural level. Faults are micaceous and characterized by well developed C and S fabrics (Lister and Snoke, 1984). Fault strands crosscut both Jurassic granodiorite and Cretaceous volcanics.

Although major thrusts associated with this phase of deformation have not been mapped within the mid-Cretaceous plutonic bodies, shear bands and smaller southwest-verging thrusts thought to be associated with this phase are recorded locally within the mid-Cretaceous Squamish and Furry plutons.

Folding occurs in the east associated with the thrusting, and is well displayed within the volcanics. Tight to isoclinal folds overturned to the south and southwest occur within a sequence of interbedded tuff, siltstone, and volcanic breccia, in the hanging wall of the Clarion mylonite zone between Mt. Baldwin and Raffuse Creek. Fold axes plunge moderately northwest, to southwest, to southeast, due to refolding associated with later northeast vergent thrusting. A northwest-striking upright crenulation cleavage, thought to be related to younger northeast-directed thrusting, overprints the overturned folds. Along the western flank of Alpen Mountain, exposures of the unconformity between the Upper Jurassic granodiorite and Lower Cretaceous Gambier Group are overturned and dip moderately to the northeast, forming the lower limb of an overturned southwest verging fold.

Greenschist metamorphism is associated with this thrusting. A strong flattening fabric defined by parallel chlorite growth is most intense in the fault zones, and extends as well to the surrounding rocks. The cleavage is typically steep to vertical and strikes northwest-southeast. Associated minerals include epidote, muscovite, albite, and calcite.

Northeast-verging thrusts

The best exposed northeast-verging thrust occurs along the contact between the Upper Cretaceous Furry pluton and Lower Cretaceous Gambier Group (Fig. 1). The fault is particularly well exposed at the headwaters of Downing Creek, as well as on the beach at Howe Sound. The contact is a 50 m thick mylonite. Rotated augen, asymmetric pressure shadows, C and S surfaces, and stretching lineations indicate thrusting of the pluton to the northeast over the volcanic rocks, and locally sinistral dip-slip motion. Faults from this family of thrusts within the volcanics are exposed in the open pits of the Britannia orebodies (Jane Basin), along the northeastern flank of Mt. Mulligan, and to the southeast of Meslillooet Creek. Associated with these faults are flat quartz-filled tension gashes, and en echelon sigmoidal quartz vein arrays containing antitaxial quartz fibres that suggest northeast directed sense of motion, and that thrusting occurred within a regime of high fluid pressures. An abundance of fault horses, and close imbricate stacking of the slices is also common.

Associated folding is open to tight, angular or chevron, and displays similar profiles. Axial planes are upright and strike northwest. Fold axes plunge moderately northwest or southeast. Axial planar cleavage is variably developed, usually as a spaced cleavage with sericite growth.

Pencil structures are formed where cleavages from both principal folding events intersect. These are rare however because the fabrics are typically subparallel. Fold interference patterns are subsequently uncommon, however coaxial or hook refolds have been observed.

Extensive alteration occurs along the northeast-verging thrusts, and within the surrounding rocks. It is typically represented by muscovite-chlorite schist (generally referred to as the "green mottled schist"; Irvine, 1948), or consists of sericitization with variable amounts of silicification and pyritization. Andalusite has also been noted. McColl (1987) has mapped a discontinuous zone of sericite schist which is associated with faults passing through the Britannia orebodies.

The Britannia Shear Zone (Payne et al., 1980; James, 1929) is a northwest trending zone of flattening (pure shear), encompassing the Britannia orebodies. Strain is inhomogeneous and largely controlled by local rock competency. Margins of the shear zone are gradational, or locally fault bounded. Payne et al. (1980) recognized successive stages of progressive deformation within the zone which they classified as D_0 (early flexural-slip folding), D_1 (pervasive cleavage development, parallel mica growth), and D_2 (producing local non-pervasive late cleavage). The late cleavage can be further specified as surfaces accommodating simple shear in the form of discrete shear bands or as significant northeast-verging thrusts; asymmetric deflection of the earlier developed cleavage along these planes provides a useful kinematic indicator.

The association of the orebodies and the zone of northeast-directed thrusting has long been recognized (Irvine, 1946, 1948; Ebbutt, 1935; James, 1929).

Late faults

A late northwest-striking fault runs along the Stawamus-Indian River valley. The fault is steep to vertical, and locally displays two sets of slickensides with accompanying quartz-fibre growth. The early set plunges moderately to the northwest, and combined with tension fractures indicates sinistral

dip-slip motion. The second set is subhorizontal and indicates sinistral motion. More rigorous control on fault movement and offset could not be established.

Steep to vertical northeast-striking faults are well developed on the north end of Gambier Island and Anvil Island. These show up on air photos as thin strongly indented lineaments. In outcrop they form gulleys of intense planar fracture systems. Slickensides on the planes plunge from steep to shallow.

DISCUSSION

Coincidence of reverse faults and volcanogenic massive sulphide deposits

Based on volcanic arc setting, mineralogy, depositional textures of sulphides, alteration, as well as grades and tonnages of metal contents, Payne et al. (1980) have put forward a convincing case for the volcanogenic origin of the Britannia massive sulphide deposits. However the orebodies occur within a zone of intense thrusting, a feature which lead early workers to believe that the deposits originated as shear zone controlled hydrothermal vein and replacement bodies (e.g. Irvine, 1948). A model of structural inversion is presented here, based on stratigraphic observations, which may rationalize these differing interpretations. Structural inversion takes place when basin controlling extensional faults are reactivated as thrust faults during later compressional events (Williams et al., 1989). Such a process of inversion can be identified by thickness changes in stratigraphic intervals across reverse faults, and depositional facies typically related to normal faulting, such as fault scarp breccias or massive sulphide deposits.

In the Britannia mining district, the Middle Sedimentary Interval thickens from approximately 500 m in the footwall of the Britannia Shear Zone (northeast of thrusts) to 700 m or greater in the shear zone (southwest of thrusts). It is not known how much of this apparent thickening is due to strain, but farther to the west the true thickness of the interval exceeds 2.3 km. Volcanic breccias bound portions of the faults. It is speculated that these thrusts originated as basin-controlling normal faults which channelled the original mineralizing fluids. Later contraction resulted in the superposition of reverse shear on the orebodies.

The full extent of the influence that early faults had on the geometry of later shear is unknown and difficult to estimate; but it could potentially have played an important role in establishing the wedge geometry of the later contractional phase.

ACKNOWLEDGMENTS

Research has been made possible through a Post Doctoral Fellowship with the Cordilleran Division of the Geological Survey of Canada. Funds were received during field work from the Georgia Basin segment of the Frontier Geoscience Program. I would like to take this opportunity to extend a heartfelt thanks to the entire staff of the Cordilleran Division, for giving me this truly unique learning opportunity. Mark Gahwens provided competent field assistance.

REFERENCES

Armstrong, J.E.
1953: Preliminary map, Vancouver North, British Columbia; Geological Survey of Canada, Paper 53-28, 7 p.

Arthur, A.J.
1986: Stratigraphy along the west side of Harrison Lake, southwestern British Columbia; in Current Research, Part B, Geological Survey of Canada, Paper 86-1B, p. 715-720.

Berg, H.C., Jones, D.L., and Richter, D.H.
1972: Gravina-Nutzotin Belt — tectonic significance of an Upper Mesozoic sedimentary and volcanic sequence in southern and southeastern Alaska; United States Geological Survey, Professional Paper 800-D, p. D1-D24.

Bostock, H.S.
1963: Squamish map-area; Geological Survey of Canada, Map 42-1963.

Ebbutt, F.
1935: Relationship of structure to ore deposition at Britannia Mine; Transactions of the Canadian Institute of Mining and Metallurgy, v. 38, p. 123-133.

England, T.J.D.
1989: Lithostratigraphy of the Nanaimo Group, Georgia Basin, southwestern British Columbia; in Current Research, Part E, Geological Survey of Canada, Paper 89-1E, p. 197-206.

Friedman, R.M. and Armstrong, R.L.
1990: U-Pb dating, southern Coast Belt, British Columbia; in Southern Canadian Cordillera Transect Workshop, 3-4 March 1990, University of Calgary, p. 146-155.

Heah, T.S.T.
1982: Stratigraphy, geochemistry, and geochronology of the Lower Cretaceous Gambier Group, Sky Pilot area, southwestern British Columbia; unpublished B.Sc. thesis, University of British Columbia, Vancouver, 97 p.

Irvine, W.T.
1946: Geology and development of the No. 8 orebodies, Britannia Mines, B.C.; Bulletin of the Canadian Institute of Mining and Metallurgy, p. 191-214.
1948: Britannia Mine; in Structural Geology of Canadian Ore Deposits, Canadian Institute of Mining and Metallurgy, Special Volume, p. 105-109.

James, H.T.
1929: Britannia Beach map-area, British Columbia; Geological Survey of Canada, Memoir 158, 139 p.

Lister, G.S. and Snoke, A.W.
1984: S-C mylonites; Journal of Structural Geology, v. 6, p. 617-638.

Lynch, J.V.G.
1990: Geology of the Fire Lake Group, southeast Coast Mountains, British Columbia; in Current Research, Part E, Geological Survey of Canada, Paper 90-1E, p. 197- 204.

McColl, K.M.
1987: Geology of Britannia Ridge, east section, southwest British Columbia; unpublished M.Sc. thesis, University of British Columbia, Vancouver, 207 p.

McKillop, G.R.
1973: Geology of southwestern Gambier Island; unpublished B.Sc. thesis, University of British Columbia, Vancouver, 23 p.

Monger, J.W.H.
1990: Georgia Basin: regional setting and adjacent Coast Mountains geology, British Columbia; in Current Research, Part F, Geological Survey of Canada, Paper 90-1F, p. 95-107.

Monger, J.W.H. and Berg, H.C.
1987: Lithotectonic terrain map of western Canada and southeastern Alaska; United States Geological Survey, Field Studies Map 1874-B.

Payne, J.G., Bratt, J.A., and Stone, B.G.
1980: Deformed Mesozoic volcanogenic Cu-Zn sulphide deposits in the Britannia district, British Columbia; Economic Geology, v. 75, p. 700-721.

Price, R.A.
1986: The southeastern Canadian Cordillera: thrust faulting, tectonic wedging, and delamination of the lithosphere; Journal of Structural Geology, v. 8, p. 239-254.

Reddy, D.G.
1989: Geology of the Indian River area; unpublished M.Sc. thesis, University of British Columbia, Vancouver, 166 p.

Roddick, J.A.
1965: Vancouver North, Coquitlam and Pitt Lake map-areas, British Columbia; Geological Survey of Canada, Memoir 335, 276 p.
Roddick, J.A. and Woodsworth, G.J.
1979: Geology of Vancouver west half and mainland part of Alberni; Geological Survey of Canada, Open File 611.
Sutherland Brown, A. and Robinson, J.W.
1970: Britannia Mine; in Geology, Exploration and Mining in British Columbia, British Columbia Department of Mines and Petroleum Resources, p. 233-246.
Williams, G.D., Powell, C.M., and Cooper, M.A.
1989: Geometry and kinematics of inversion tectonics; in Inversion Tectonics, M.A. Cooper and G.D. Williams (ed.), Geological Society Special Publication No. 44, p. 3-15.

Bathonian through Oxfordian (Middle and Upper Jurassic) marine macrofossil assemblages and correlations, Bowser Lake Group, west-central Spatsizi map area, northwestern British Columbia

T.P. Poulton, J.H. Callomon[1], and R.L. Hall[2]
Institute of Sedimentary and Petroleum Geology, Calgary

Poulton, T.P., Callomon, J.H., and Hall, R.L., Bathonian through Oxfordian (Middle and Upper Jurassic) marine macrofossil assemblages and correlations, Bowser Lake Group, west-central Spatsizi map area, northwestern British Columbia; in Current Research, Part A, Geological Survey of Canada, Paper 91-1A, p. 59-63, 1991.

Abstract

Ammonites and bivalves of Middle Bathonian through Oxfordian age permit correlation of strata of the Bowser Lake Group in west-central Spatsizi map area with international standard ammonite zones; others have local or regional significance for correlation within the Bowser Basin. The most useful are ammonites of the boreal Family Cardioceratidae. New species of the Superfamily Perisphinctaceae, unusually abundant in northwestern Bowser Basin, offer further potential for refined correlations. The previously poorly-known stratigraphic ranges of species of the endemic Subfamily Eurycephalitinae are clarified in part, by their association with the cardioceratids and perisphinctids. The biostratigraphic value of certain species of the bivalve Family Trigoniidae is confirmed by their stratigraphic ranges in northwestern Bowser Basin.

Résumé

La présence d'ammonites et de bivalves du Bathonien moyen jusqu'à l'Oxfordien permet de corréler les couches du groupe de Bowser Lake dans le centre-ouest de la région cartographique de Spatsizi avec les zones d'ammonites classiques établies à l'échelle internationale; les autres présentent une importance locale ou régionale permettant une corrélation au sein du bassin de Bowser. Les ammonites de la famille boréale Cardioceratidae sont les plus utiles à cette fin. De nouvelles espèces de la superfamille Perisphinctaceae, excaptionnellement abondantes dans le nord-ouest du bassin de Bowser, pourraient permettre davantage d'établir des corrélations détaillées. Les répartitions stratigraphiques autrefois mal connus des espèces de la sous-famille endémique Eurycephalitinae sont débrouillées en partie, par leur association avec les cardiocératidés et les périsphinctidés. La valeur biostratigraphique de certaines espèces de la famille des bivalves Trigoniidae est confirmée par leur répartition stratigraphique dans le nord-ouest du bassin de Bowser.

[1] Department of Chemistry, University College London, 20 Gordon Street, London WC1H OAJ
[2] Department of Geology and Geophysics, The University of Calgary, Calgary, Alberta T2N 1N4

INTRODUCTION

Fossiliferous marine strata in the vicinity of Tsatia Mountain (Fig. 1), west-central Spatsizi map area (NTS 104 H), contain ammonites and bivalves that permit regional and international correlation. Fossils are particularly important for stratigraphic and structural work in this area, where the Middle and Upper Jurassic strata comprise a structurally deformed sequence in which complex facies changes result in abrupt lateral variations and vertical repetition of similar lithologies (Fig. 2).

The strata comprise interbedded sandstones, siltstones, and conglomerates of the Bowser Lake Group (Tipper and Richards, 1976; Evenchick and Green, 1990; Ricketts, 1990). It has not yet been possible to identify mappable units having regional continuity, so that the Bowser Lake Group is not presently subdivided into formations in this area.

This preliminary report is based on fieldwork in 1983 by Poulton, in 1989 by Poulton, Hall, and Callomon and in 1990 by Poulton and Hall. It involves continuing study of previously available collections, mainly those of H.W. Tipper, H. Gabrielse, and C. Evenchick, and comparison of some of the significant specimens with European equivalents by Callomon. Geological discussions and logistical support were provided by C. Evenchick, B. Ricketts, H.W. Tipper, and H. Gabrielse.

Compilation of the ammonite and bivalve occurrences in several stratigraphic sections allows the proposal of a preliminary biostratigraphic zonation applicable to much of west-central and northwestern British Columbia (Fig. 3). It also contributes to our understanding of the still incompletely known stratigraphic ranges of certain endemic northern East Pacific ammonites that are important in British Columbia,

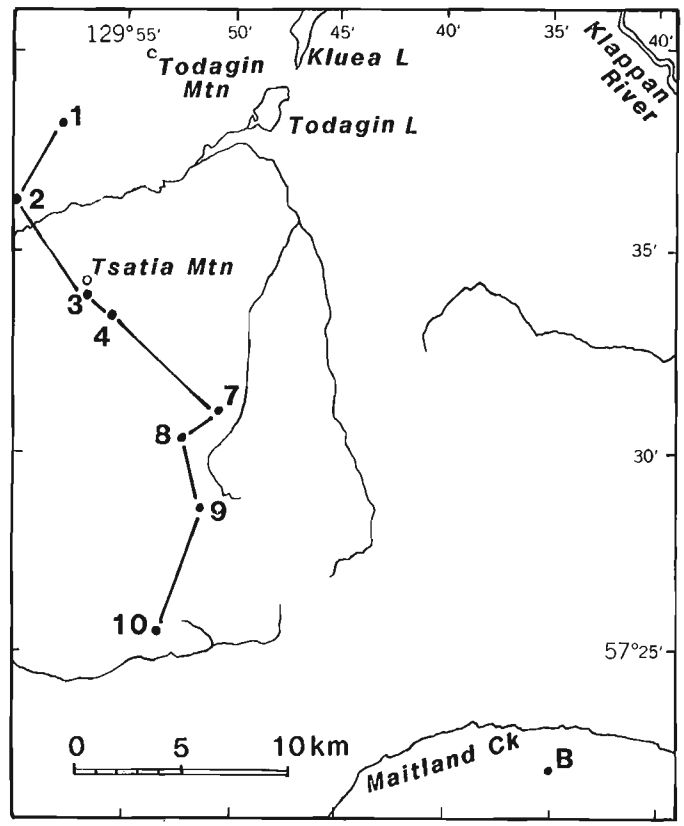

Figure 1. Index map, Tsatia Mountain area, west-central Spatsizi map area (NTS 104H/5,12). The numbered localities indicate stratigraphic sections shown on Figure 2. H. Cookenboo collected the Late Oxfordian or Early Kimmeridgian bivalve *Buchia concentrica* (Sowerby) at Locality "B" south of Maitland Creek.

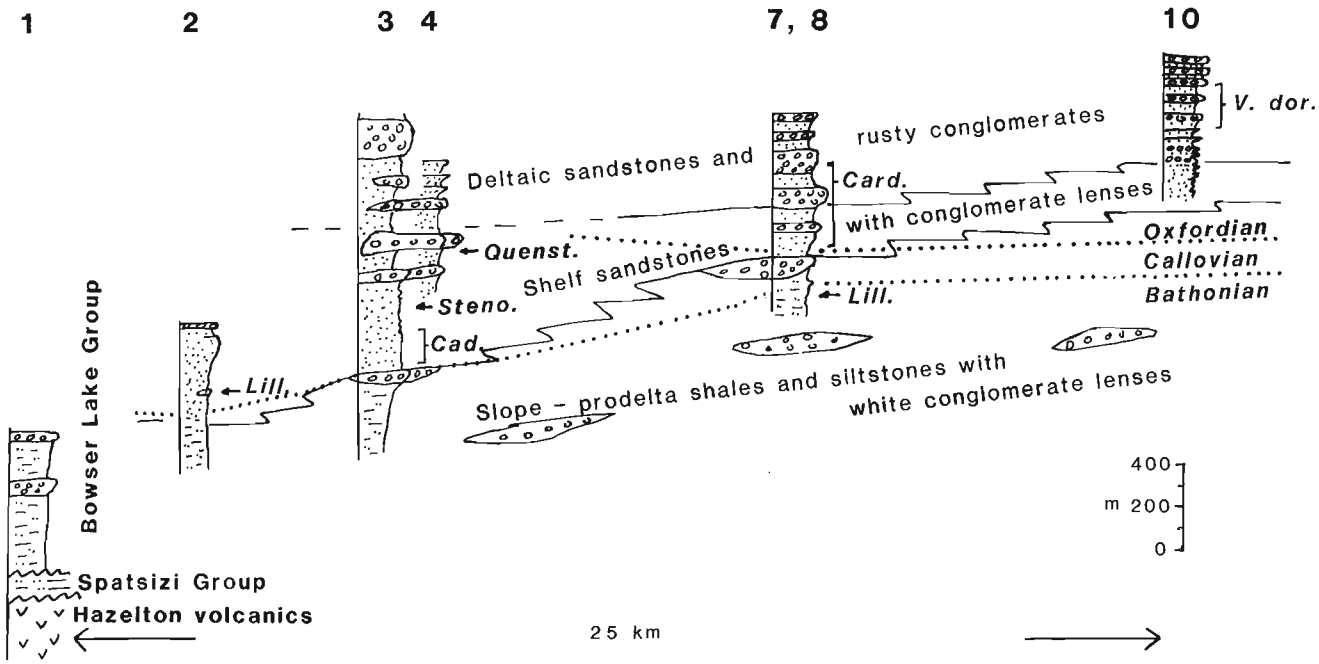

Figure 2. Schematic generalized stratigraphic cross-section, showing the correlation of the sections studied in detail in 1989 and 1990, and their major ammonite occurrences. The localities of the sections are shown in Figure 1. The interpretation of the major lithological facies assemblages is modified from a sketch by B. Ricketts.

such as *Iniskinites, Lilloettia,* and *Xenocephalites*. This preliminary zonation generally confirms structural interpretations that the thick series of Middle and Upper Jurassic strata are exposed in sequences becoming progressively younger to the south within western Spatsizi map area, toward more axial parts of the "Bowser Basin" (Evenchick and Green, 1990). Sedimentological studies indicate that the Tsatia and Todagin mountains area lies close to the northern margin of the Bowser Basin, with chert-dominated sediments having been derived from a northerly source (Ricketts, 1990).

BIOSTRATIGRAPHIC TOOLS

Ammonite genera of the boreal family Cardioceratidae, occurring at several levels in the Tsatia Mountain area, are the basis for correlation throughout much of northern North America, Europe, and Asia, and with international standard zones. They comprise an evolutionary lineage that includes the genera *Cadoceras, Quenstedtoceras,* and *Cardioceras* in the western Spatsizi map area. Perisphinctid ammonites common at many levels also resemble biostratigraphically important forms from Europe, but their significance in western Canada awaits detailed taxonomic and biostratigraphic study. Their newly recognized abundance in northern Bowser Basin is anomalous with respect to other areas of the western Cordillera. Associated ammonites in the western Spatsizi area include species of the eurycephalitinid genera *Iniskinites, Lilloettia,* and *Xenocephalites*, which are endemic to western North America and the biostratigraphic value of which remains unclear. Finally, the phylloceratid ammonites *Adabofoloceras* (included in *Partschiceras* in older literature; very abundant at many levels), *Phylloceras*, and *Calliphylloceras* (both rare) have no significance for detailed correlation within the Jurassic. Surprisingly, the invaluable index ammonite *Kepplerites*, abundant elsewhere in the Callovian of British Columbia, including Smithers map area at the south end of Bowser Basin, has not yet been found in the Tsatia Mountain area.

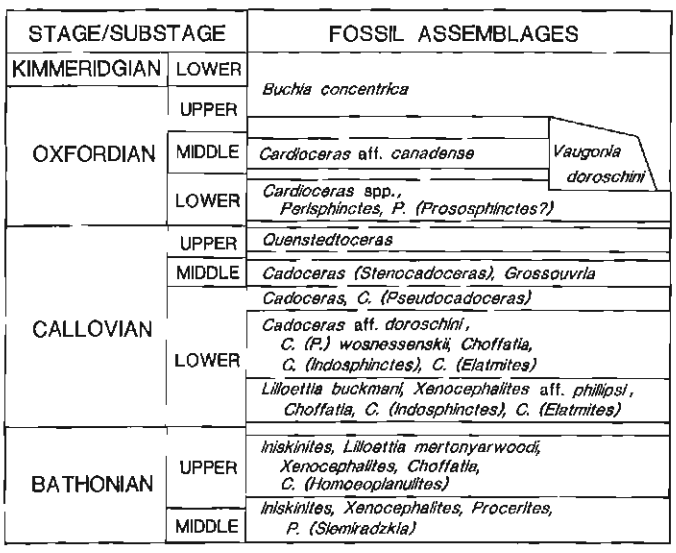

Figure 3. Macrofossil assemblages, and their approximate correlation with standard stages and substages.

Bivalves occur in great abundance and variety at many levels. Most are long-ranging and not of biostratigraphic significance at present, and include the common Jurassic genera *Astarte, Pinna, Pleuromya, Meleagrinella,* etc. However, the succession of several species of the family Trigoniidae in western Spatsizi map area is regionally consistent with, and augments, that described from other areas of western North America (Poulton, 1979). Of particular stratigraphic significance for Spatsizi area are the species *Myophorella packardi* (Crickmay), *Anditrigonia plumasensis* (Hyatt), *Myophorella devexa* (Eichwald) and similar forms, and *Vaugonia doroschini* (Eichwald). Nevertheless, the precise ranges of some of these species appear to vary between different parts of western British Columbia and perhaps partly result from facies distributions and position on the Jurassic shelf.

Other macrofossils present include locally abundant terebratulid and rhynchonellid brachiopods, scaphopods and belemnites, and rare bryozoa and serpulid worm tubes, none of which have major biostratigraphic significance at present.

BIOSTRATIGRAPHY

The discussion below includes "International standard zones" where the guide ammonites permit correlation with zones of Northwest Europe, in addition to empirically observed local assemblage zones.

Middle and Upper Bathonian

Most localities are east of Tsatia and Todagin mountains, and low in the Klappan and Little Klappan river valleys west and southwest of Mount Cartmel.

None of the ammonites is sufficiently well known to allow correlation with any precise level within the Bathonian and the position of the base of the Callovian also remains uncertain. Callomon (1984) has proposed general ranges for some of the species. The various perisphinctid ammonites, occurring in association with *Iniskinites* and *Xenocephalites*, are apparently entirely new. They have some general resemblances to European Middle or Upper Bathonian Zigzagiceratinae, such as species of the genera *Procerites, P. (Siemiradzkia), Zigzagiceras (Procerozigzag),* and *Choffatia.*

Other perisphinctids, in association with *Lilloettia mertonyarwoodi* Crickmay, *Xenocephalites* and *Adabofoloceras pacificum* (Frebold and Tipper), are closely similar to, and almost certainly correlative with, European Upper Bathonian species of *Choffatia* and *C. (Homoeoplanulites).*

Early Callovian

The Early Callovian is indicated primarily by species of the cardioceratid genus *Cadoceras*. Associated macrofossils include the probable microconch dimorph *Pseudocadoceras,* the perisphinctid ammonite *Choffatia,* and a wide variety of bivalves including particularly the trigoniid *Myophorella packardi* (Crickmay). This distinctive bivalve is apparently

mainly restricted to, and characteristic of, the Lower Callovian throughout western British Columbia, although it may occur also in Middle Callovian beds in its type area at Harrison Lake (Crickmay, 1930; Poulton, 1979).

Cadoceras-bearing beds occur in a sequence of shelf sandstones on the south side of Tsatia Peak above a major conglomerate lens (forming a waterfall) that overlies a banded siltstone facies with slope characteristics (Fig. 2).

There are perhaps three distinct Lower Callovian faunas, the lowest assemblages already perhaps from the middle Lower Callovian. These assemblages contain, in addition to *Lilloettia buckmani* Crickmay, *Xenocephalites* cf. *phillipsi* Imlay and *Calliphylloceras*, a variety of perisphinctids (which may all be variants of a single species) comparable with European mid-Lower Callovian species of *Choffatia, C. (Indosphinctes)*, and the microconch *C. (Elatmites)*. Another assemblage contains *Cadoceras* aff. *doroschini* (Eichwald), *C. (Pseudocadoceras) wosnessenskii* (Grewingk), *Adabofoloceras pacificum* (Frebold and Tipper), and species of *Choffatia (Indosphinctes), C. (Choffatia)*, and *C. (Elatmites)*. This assemblage is probably about the same age as the first, and some of the cadoceratids resemble those of the English Koenigi Zone. Other beds, higher in the Tsatia Mountain succession, but with less abundant and less distinctive faunas contain *Cadoceras, C. (Pseudocadoceras)*, and *Adabolofoceras*.

Middle Callovian

Cadoceras (Stenocadoceras) sp. probably indicates the Middle Callovian, perhaps the Jason zone. It occurs in association with *Grossouvria, Phylloceras*, and *Adabofoloceras*.

Late Callovian

Quenstedtoceras indicates the presence of the Upper Callovian Lamberti Zone.

Early Oxfordian

Six successive faunas containing species of the ammonite *Cardioceras* are unequivocally correlative with the Praecordatum and Bukowskii subzones of the Mariae and Cordatum zones of the Lower Oxfordian. They include *Cardioceras (Scarburgiceras)* aff. *praecordatum, C. (S.)* cf. *martini* Reeside, *C. (S.)* cf. *bukowskii* Maire, and *C. (Subvertebriceras)* spp., *C. (Cardioceras)* aff. *alphacordatum* Spath, *C. (Scoticardioceras)* cf. *harmonicum* Maire, and *C. (S.)* cf. *alaskense* Reeside. Other ammonites include *Perisphinctes* sp., *P. (Prososphinctes?)* sp., and *Adabofoloceras* sp.

A suite of distinctive trigoniid bivalves occurs with *Cardioceras* in sections south of Tsatia Mountain (sections 7, 8 of Fig. 1, 2). These species include *Anditrigonia plumasensis* (Hyatt), a higher than wide form of *Myophorella* aff. *devexa* (Eichwald), and *Scaphotrigonia* aff. *naviformis* (Hyatt). This association may be biostratigraphically useful in the Tsatia Mountain area to indicate the Lower Oxfordian even where *Cardioceras* is absent. However, the nominal species are known to range into the Callovian elsewhere in British Columbia and western U.S.A. (Poulton, 1979), and their distribution in Spatsizi map area may reflect ecological restriction rather than biostratigraphic range.

Middle Oxfordian

The Middle Oxfordian Densiplicatum Zone is perhaps represented by the ammonite *Cardioceras* aff. *canadense* Whiteaves (see also Callomon, 1984; Poulton, 1989).

The highest marine Jurassic beds in the Tsatia Mountain area are characterized by the trigoniid bivalve *Vaugonia doroschini* (Eichwald) which occurs, sometimes in great abundance, above strata with *Cardioceras*. *V. doroschini* (Eichwald) is characteristic of the "Trout Creek facies" or "Trout Creek assemblage" of the lower Bowser Lake Group around the presumed southern margin of Bowser Basin in Hazelton and Smithers map area (Richards and Jeletzky, 1975; Tipper and Richards, 1976). Lower Oxfordian *Cardioceras* occurs in this assemblage at one locality (T. Richards, *in* Poulton, 1979). *Myophorella* aff. *devexa* (Eichwald) is associated with *V. doroschini* at certain localities in the Smithers map area. Some beds in the lower part of the zone of *V. doroschini* in Tsatia Mountain area also contain *Myophorella* sp. aff. *devexa* (Eichwald). The younger age limit (Fig. 3) of the *V. doroschini* beds is suggested by the absence of associated *Buchia* which dominates Upper Oxfordian and younger Jurassic strata throughout British Columbia.

Upper Oxfordian and Lower Kimmeridgian

The Upper Oxfordian or Lower Kimmeridgian index bivalve *Buchia concentrica* (Sowerby) was collected in 1990 by H. Cookenboo about 30 km southeast of Tsatia Mountain, south of Maitland Creek (latitude 57°22'N, longitude 129°35'W; locality "B" of Fig. 1). This marine bivalve occurs in a structurally complex succession that is probably high in the transitional interval to the major coal-bearing unit of Bowser Basin (F.M. Dawson, pers. comm., 1990). Beds of this age are dominated by *Buchia concentrica* (Sowerby) throughout western British Columbia and also rarely contain *Amoeboceras* and *Rasenia(?)*.

Younger Jurassic

Marine strata younger than Upper Oxfordian or Early Kimmeridgian are thought to be absent in the Tsatia Mountain area, because of the apparent absence of any species of the bivalve *Buchia* (except the occurrence mentioned above) and of diagnostic ammonites. Indeed, the transition into nonmarine coal-bearing beds in Bowser Basin makes it unlikely that younger marine beds will be found in a continuous sequence with those described in this report. In contrast, MacLeod and Hills (1990) have interpreted a complete sequence of marine strata from the Oxfordian into the Early Cretaceous somewhat farther south in the northern Bowser Basin, on the basis of several species of *Buchia*, which indicate Late Oxfordian through Neocomian ages.

REFERENCES

Callomon, J.H.
1984: A review of the biostratigraphy of the post-Lower Bajocian ammonites of western and northern North America; in Jurassic-Cretaceous Biochronology and Biogeography of North America, edited by G.E.G. Westermann, Geological Association of Canada, Special Paper 27, p. 143-174.

Crickmay, C.H.
1930: Fossils from Harrison Lake area, British Columbia; National Museum of Canada, Bulletin 63, p. 33-113.

Evenchick, C.A. and Green, G.M.
1990: Structural style and stratigraphy of southwest Spatsizi map area, British Columbia; in Current Research, Part F, Geological Survey of Canada, Paper 90-1F, p. 135-144.

MacLeod, S.E. and Hills, L.V.
1990: Conformable Late Jurassic (Oxfordian) to Early Cretaceous strata, northern Bowser Basin, British Columbia: a sedimentological and paleontological model; Canadian Journal of Earth Sciences, v. 27, p. 988-998.

Poulton, T.P.
1979: Jurassic trigoniid bivalves from Canada and western United States of America; Geological Survey of Canada, Bulletin 282.
1989: Jurassic (Oxfordian) ammonites from the Fernie Formation of western Canada: a giant peltoceratinid, and Cardioceras canadense Whiteaves; in Contributions to Canadian Paleontology, Geological Survey of Canada, Bulletin 396, p. 173-179.

Richards, T.A. and Jeletzky, O.L.
1975: A preliminary study of the Upper Jurassic Bowser assemblage in the Hazelton west half map-area, British Columbia (93M-W1/2); in Geological Survey of Canada, Report of Activities, Paper 75-1A, 1975, p. 31-36.

Ricketts, B.D.
1990: A preliminary account of sedimentation in the lower Bowser Lake Group, northern British Columbia; in Current Research, Part F, Geological Survey of Canada, Paper 90-1F, p. 145-150.

Tipper, H.W. and Richards, T.A.
1976: Jurassic stratigraphy and history of north-central British Columbia; Geological Survey of Canada, Bulletin 270.

Analysis of the Middle to Upper Jurassic Bowser Basin, northern British Columbia

B.D. Ricketts and C.A. Evenchick
Cordilleran Division, Vancouver

Ricketts, B.D. and Evenchick, C.A., Analysis of the Middle to Upper Jurassic Bowser Basin, northern British Columbia; in Current Research, Part A, Geological Survey of Canada, Paper 91-1A, p. 65-73, 1991.

Abstract

The Middle to Late Jurassic coarse grained facies belt of the northern Bowser Basin foredeep consists of fan delta (including braid delta and Gilbert delta), interfan shelf, submarine canyon and gully, slope and submarine fan facies assemblages. Progradation was rapid, with up to 50 km in 2 Ma estimated for the Lower Callovian part of the succession. Four major pulses of sedimentation are recorded: (1) post-Toarcian shale (Spatsizi Group); (2) Bathonian (base of the Ashman Formation); (3) Lower Callovian; and (4) uppermost Callovian-Lower Oxfordian.

Subsidence of the Bowser foredeep may have begun toward the end of the Toarcian, with initial sediments being dominated by the post-Toarcian shale component of the Spatsizi Group. However, coarse grained sediment derived from oceanic Cache Creek rocks uplifted in southwest-verging thrusts was delayed until the Bathonian.

Résumé

La zone de faciès à grain grossier du Jurassique moyen à tardif de l'avant-fosse de la partie nord du basin de Bowser est composée d'assemblages à faciès de cône alluvial (y compris de delta anastomosé et du delta de Gilbert), de zones de plate-forme situées entre des cônes, de canyon et de ravin sous-marins, de talus et de cône sous-marins. La progradation a été rapide, ayant atteint 50 km en 2 Ma dans la partie du Callovien inférieur de la succession. Quatre impulsions importantes de sédimentation ont eu lieu comme en témoignent : 1) le shale post-toarcien (groupe de Spatsizi); 2) le Bathonien (base de la formation d'Ashman); 3) le Callovien inférieur; et 4) la partie sommitale du Callovien à l'Oxfordien inférieur. L'effondrement de l'avant-fosse de Bowser a pu s'amorcer vers la fin du Toarcin, les sédiments initiaux étant surtout composés du shale post-toarcien du groupe de Spatsizi. Cependant, les sédiments à grain grossier provenant des roches océaniques de Cache Creek soulevées dans les chevauchements à vergence sud-ouest ne se sont pas accumulés avant le Bathonien.

INTRODUCTION

Bowser Basin strata provide the critical record of accretionary tectonics and related patterns of erosion and deposition within Stikinia and Cache Creek terranes of the northern Intermontane Belt. Current investigations on the Middle to Upper Jurassic succession in northern Bowser Basin aim to resolve questions that have a direct bearing on our understanding of Bowser depocentre evolution (Fig. 1 and 2). These questions, some of which are broached in this report, are concerned with: 1) definition of the limits, style, and timing of Bowser sedimentation; 2) the paleogeography of the basin, especially the presence or absence of a western basin margin; 3) the dichotomous relations among provenance, lithofacies, sediment composition, and the palinspastic position of potential source rocks; and 4) how several kilometres of Bowser strata were accommodated in the basin with respect to regional tectonism and subsidence.

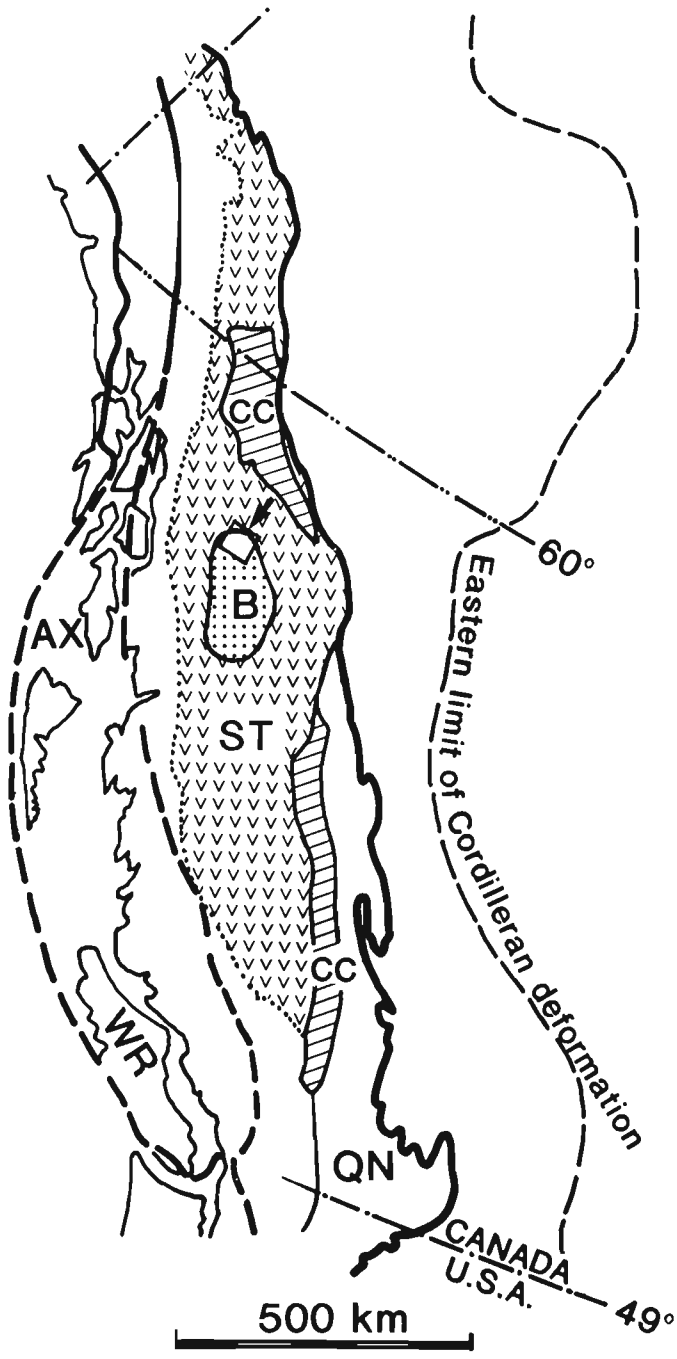

Figure 1. Location map showing tectonic position of preserved Bowser Basin (B) and study area (arrow), in relation to Stikinia (ST), Cache Creek (CC), Quesnellia (QN), Wrangellia (WR), and Alexander terranes (AX). Heavy dashed and solid lines outline Insular and Intermontane superterrane assemblages.

Map units

The stratigraphic profiles presented in Figures 3 and 4 have been constructed from measured sections, traverses, and aerial photographs (Evenchick, 1988, 1989; Evenchick and Green, 1990; Ricketts, 1990). Sandy and conglomeratic strata that overlie and partly interfinger with the Ashman Formation (Tipper and Richards, 1976), constitute lithologically variable and highly diachronous rock units, referred to here as lithosomes. The lithosomes in turn can be subdivided into lithofacies assemblages and their constituent facies (Table 1).

SEDIMENTARY FACIES

The Bowser Lake Group facies listed in Table 1 were described by Ricketts (1990). Some of the facies names have been changed or expanded to more appropriate labels:

Sandy turbidite	= Mid- (submarine) fan
Tabular conglomerate	= Proximal (submarine) fan
Shale	= Slope, Overbank
Lenticular conglomerate	= Channel (submarine canyon/gully)
Tabular rusty cong.	= Fan delta
Trough crossbedded cong.	= Braid delta

Table 1. Components of the Ashman Formation, rusty and sandy lithosomes, and facies assemblages, northern Bowser Basin.

Map Unit	Facies assemblage	Lithofacies
Ashman Fm.	**Deep basin**	Most distal turbidites Pelagic
	Submarine fan	Proximal, middle & distal fan
	Prodelta-slope	Slope Overbank (channel) Slump
	Submarine canyon/ gully	Channel Overbank
Rusty lithosome	**Fan delta**	Fan delta Braid delta Gilbert delta
	Coastal	Gravel Barrier-lagoon Beach
Sandy lithosome	**Shelf**	Outer/inner shelf cycles transgressive lags

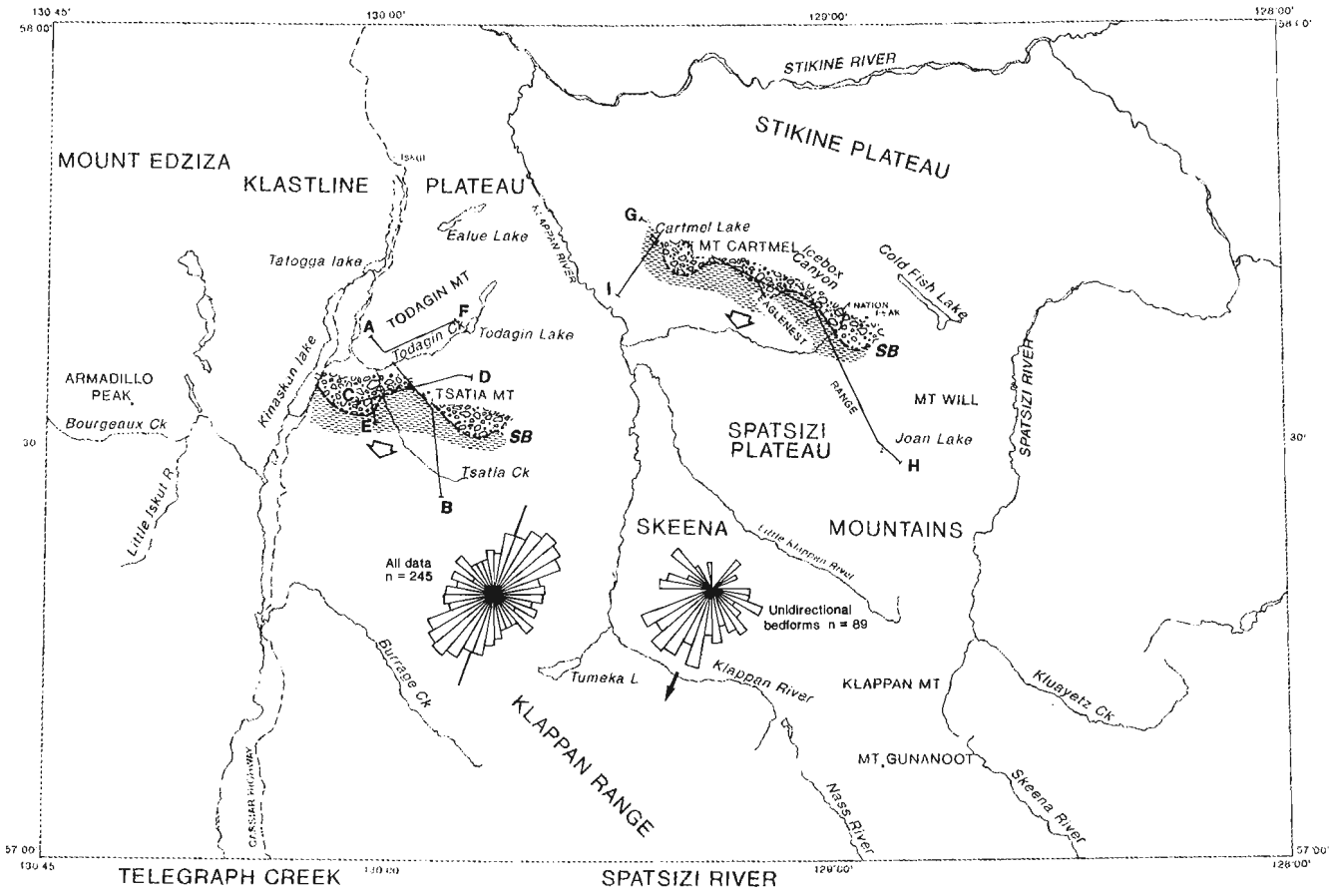

Figure 2. Stratigraphic profiles (Fig. 3 and 4) are located in Spatsizi and the eastern portion of Telegraph map areas. The preserved positions of the Early Callovian shelf/slope break (SB) are shown, in relation to general paleocurrent trends, from which progradation rates can be estimated. The two rose diagrams depict general trends of sediment transport indicated by all paleocurrent data (with and without sense of flow), and unidirectional flow indicators (e.g. crossbeds, flute casts); n = number of measurements. Vector means are 201° and 202° respectively.

Attention here will be directed only toward additional facies, primarily those in the rusty lithosome-Gilbert delta facies in the Fan delta assemblage, and the barrier and beach facies in the Coastal assemblage.

Gilbert delta facies

Huge conglomerate foresets, in crossbed sets 50 to 100 m thick, form a highly distinctive facies within the rusty lithosome (Fig. 5). To date, the facies has only been encountered close to or at the base of the rusty lithosome, where it abruptly overlies Ashman Formation slope and submarine canyon deposits. Foresets have been observed at four localities along a trend from Icebox Canyon to Cartmel Lake, and at a locality about 4 km due west of Tsatia Mountain (RAK 10-90). Erosional relief at the base of foresets in places exceeds 12 m. The basal contact is thus a disconformity, which although of local extent in any one foreset package, seems to occur at similar stratigraphic levels throughout the region. The foreset conglomerates grade laterally and vertically into conglomeratic braid delta, fan delta (Fig. 6), and sandy shelf facies.

Foreset toes in the west Tsatia example are moderately tangential where the basal contact is planar, but abrupt where the contact has erosional relief. Foreset tops also are tangential, and in the Cartmel Lake examples (Fig. 5), top-set conglomerate beds are 1 to 2 m thick. Foresets dip between 20 and 25°. Individual foresets range in thickness from 1 to 3 m and internally consist of several layers 10 to 80 cm thick. Some layers are normally size graded; some show inverse grading in the lower few centimetres. Conglomerates are fully to partly clast-supported and crudely laminated; clasts commonly display long axis alignment and imbrication. Framework clast size ranges from averages of about 1 cm in some layers, to 5 to 6 cm in other layers, with maximum widths up to 15 cm. Foresets are separated by thin, frequently discontinuous sandy beds and lenses. Crossbedding has not been seen. Plant fragments are common on bedding. Marine fossils in the foreset packages are rare, but do occur in bounding strata.

Interpretation

Scale and geometry of the conglomerate foreset packages suggest a comparison with Gilbert deltas, known in the Recent and interpreted in the rock record to be associated with steep depositional gradients and rapid sediment supply (Massari and Colella, 1988; Postma et al., 1988; Postma, 1990).

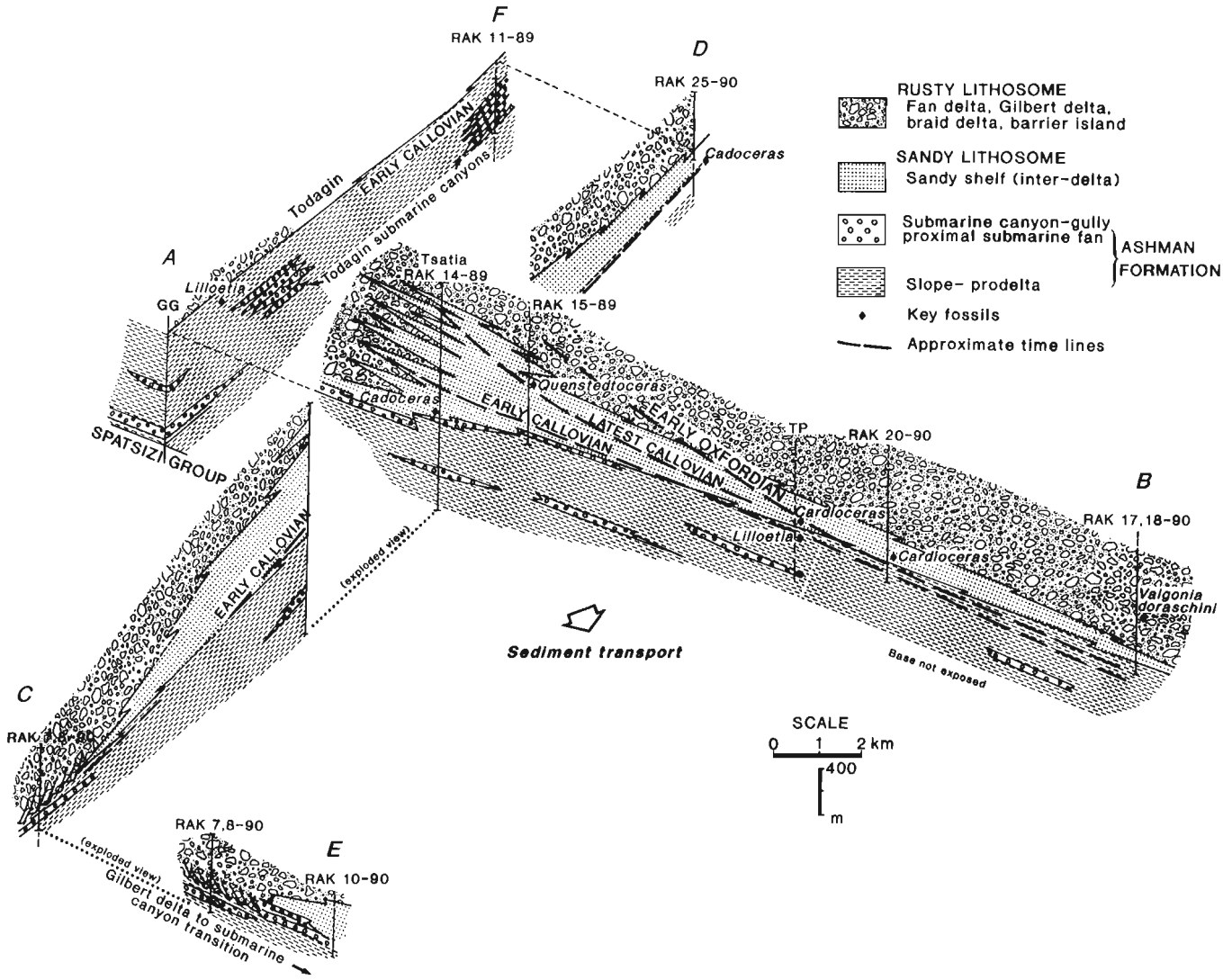

Figure 3. Lithostratigraphic profiles, key fossils, and time lines for the Jurassic Bowser succession in the west-central part of Spatsizi map area illustrate the diachroneity and complex interfingering relationships among lithosomes. RAK numbers indicate measured or traversed sections. The profiles are located in Figure 2. Data for the west Todagin Mountain area is from G. Green (pers. comm., 1990). Section labelled TP is courtesy of T. Poulton (pers. comm., 1990).

Sedimentation was dominated by sediment gravity flow processes, especially rapid, noncohesive surging debris flows. Cohesive muddy flows (pebbly mudstone, Ricketts, 1990) are less common and generally occur in the upper portions of foresets. In one example at Cartmel Lake, a single flow unit, being cohesive with a mud-supported framework at the top, becomes progressively more clast-supported and laminated with imbricated fabrics downdip toward the toeset. In comparison to Gilbert deltas described by Postma et al. (1988), there is no evidence for significant delta-front failure. Top set beds, where present, share some of the characteristics of braided stream deposits but clear distinction between fluvial and possible reworked shallow marine gravels is difficult. The significance of the Gilbert deltas in terms of paleogeography and sediment provenance will be discussed below.

Barrier and beach facies

Type 1

Coarsening and thickening upward units (cycles) of shale, sandstone, and conglomerate, up to 25 m thick, are common in the rusty lithosome, grading laterally and vertically into sandy shelf, fan, braid, and Gilbert delta facies. Typically, basal deposits consist of a muddy, pebbly, and commonly fossiliferous lag which abruptly overlies the subjacent cycle. The basal lag grades upward into shale, which in turn becomes progressively sandy. Sandstone beds are parallel laminated, with hummocky crossbedding becoming more common in the cycles. The uppermost sandstone beds in each cycle commonly contain low-angle planar stratification and some planar-tabular crossbeds. Hummocky crossbeds also occur, some associated with thin matrix-supported conglomerate beds. At localities north of Maitland Creek (sections RAK 18,20-90) buff sandy coquinas occur below the conglomerate units,

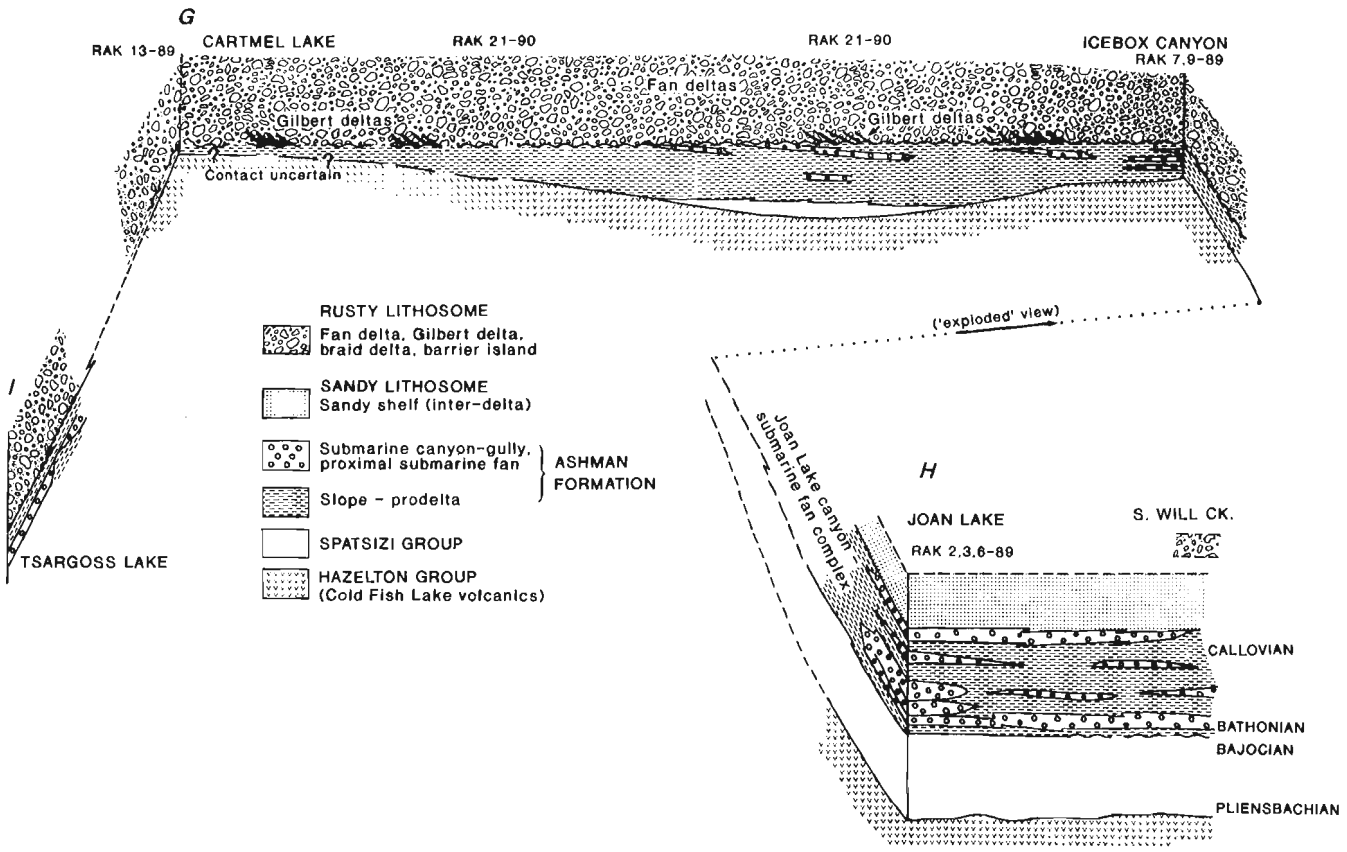

Figure 4. Lithostratigraphic profiles for the Jurassic Bowser and Spatsizi successions in the northern part of Spatsizi map area illustrate the complexity of lateral and vertical facies changes. Time lines are less well constrained than in Figure 3. Age designation for the Spatsizi Group at Joan Lake is from Thomson et al. (1986). Note the lateral extent of the rusty lithosome along the Cartmel Lakelcebox Canyon trend. The profiles are located in Figure 2. Scale and symbols as in Figure 3.

commonly having eroded bases; bivalves predominate, but locally abundant scaphopods exhibit good current alignment. Sandstone beds pass, usually gradationally but locally with erosional contact, into conglomerate units up to 5 m thick and are characterized by tabular or wedge-shaped beds plus a few planar-tabular sets up to 2 m thick. Interfingering of sandstone beds and lenses is common. Trace fossils are similar to those seen in the sandy shelf facies (Ricketts, 1990).

Type 2

A variation on the theme of Type 1 and generally encountered in sections stratigraphically above Type 1, includes cycles that contain a fining upward component 1 to 3 m thick overlying the conglomerate. This component contains grey-brown shale and thin carbonaceous, coaly shale with root structures. Contact with the succeeding coarsening upward cycle is abrupt but conformable, with bioturbated noncarbonaceous, sparsely fossiliferous shale overlying the coaly layers. In some cycles the marine shale/coaly shale contact is defined by a thin bed of poorly sorted conglomerate, locally fossiliferous and generally less than 10 to 15 cm thick; the conglomerate bed has an erosional base.

Interpretation

The coarsening upward cycles are marine, interdigitate with, and indeed constitute a part of the facies spectrum that includes sandy shelf and gravelly fan delta deposits. Shale and sandstone lithologies contain the hallmarks of outer shelf to shoreface transitions. In particular, the surface underlying thin conglomerate beds at the base of several cycles is interpreted as a ravinement surface — the product of shoreface migration during transgression, subsequently overlain by shelf deposits. The remaining coarsening upward component in each cycle represents the progradational episode. Thick conglomerate units in Type 1 cycles developed as upper shoreface and beach deposits, and perhaps as gravel bars. Hummocky crossbedding and the coquina beds indicate storm deposition below fairweather wave base, and in the upper shoreface, respectively. Type 2 cycles capped by a fining upward, coaly unit reflect the development of lagoonal environments, including vegetated marshes, which accumulated landward of gravel bars or barriers (e.g. Carter et al., 1987).

STRATIGRAPHIC PROFILES AND PALEOCURRENTS

The fence diagrams in Figures 3 and 4 illustrate the complexity of lithological and facies relationships. Interfingering of facies is common in the generally shallow marine and

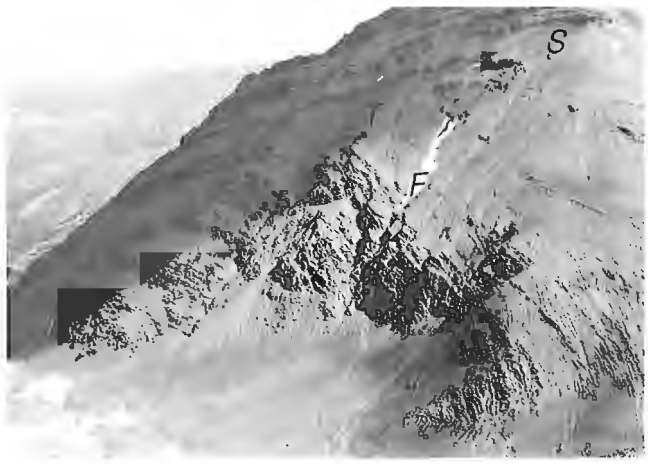

Figure 5. Huge, south-dipping foresets (F) and associated topset beds (T) in the Gilbert delta facies near Cartmel Lake contain mud-supported and clast-supported debris flow units having a depositional dip of about 20°. The foreset unit occurs near the base of the rusty lithosome; it is overlain by shallow shelf sandstone, and conglomerate beds which represent encroaching fan deltas.

Figure 6. Tabular conglomerate units and intervening coarsening upward shale-sandstone in packages averaging 20 m thick, and stacked into a succession approximately 400 m thick (near Cartmel Lake). The succession in part is laterally equivalent to the Gilbert delta facies in Figure 5. Stratigraphic top is to the left.

paralic, rusty, and sandy lithosomes so that lateral transitions commonly are abrupt. For example, sandy shelf facies in the Tsatia Mountain area thin by more than 60 % (from about 1100 m to 300-400 m) over as little as 2 km distance (Fig. 3). Likewise, contact between the Ashman Formation and rusty lithosome is disconformable in places, especially beneath Gilbert delta facies, and gradational in other places. Again in Figure 3, 500 m of shelf facies rocks at Joan Lake (of probable Middle to Callovian age) are replaced by at least 900 m of rusty lithosome facies in the Cartmel Lake area.

Overall, paleocurrent azimuths (Fig. 2) indicate predominant sediment transport toward the south-southwest, in general agreement with determinations by Eisbacher (1974, 1981).

Time lines

Time lines schematically presented in Figure 3 are based on key ammonite and pelecypod identifications (T. Poulton and R. Hall, pers. comm., 1989, 1990). Given the pronounced lithofacies changes and diachroneity of the Bowser rocks, the biostratigraphic database is indispensable for unravelling the depositional and paleogeographic history. Time lines are best constrained in the area extending from Todagin Mountain to Maitland Creek. Significant points to note are: 1) the Callovian to Early Oxfordian time lines converge towards the south ; 2) the rusty lithosome ranges in age from Early Callovian to Oxfordian ; and 3) Ashman strata are at least as young as Early Oxfordian toward the southern edge of the map area.

West of Tsatia Mountain (sections RAK 8-90, 10-90, Fig. 3) Gilbert delta conglomerate beds (described above) are in abrupt, eroded contact with Ashman beds, locally with 12 m and more relief. The conglomerate beds, when traced southward over a distance of about 3 km, grade laterally into grey conglomerate that fills large channels identical to those occurring in the submarine canyon/gully facies assemblage elsewhere in the Ashman Formation. A similar transition from rusty conglomerate to channelized facies has also been seen on Tsatia at the upper Ashman contact (G. Green, pers. comm., 1990). In the Tsatia example the transition is known to occur in Lower Callovian beds, below *Cadoceras*-bearing shelf facies (Ricketts, 1990). The Gilbert delta-to-canyon/gully transition is regarded as a significant sedimentological break, the *shelf/slope break*, that can be traced over a wide area of the northern Bowser Basin. It is also prominent in the Icebox Canyon-Cartmel Lake area, where thick, tabular bedded fan delta and Gilbert delta facies abruptly (and at least locally erosionally) overlie Ashman slope and channel facies (Fig. 4).

REGIONAL PICTURE, NORTHERN BOWSER BASIN

The paleoenvironmental reconstruction illustrated in Figure 7 is a more elaborate version of that presented in Ricketts (Fig. 5, 1990). An extensive system of prograding fan deltas, braid deltas, and Gilbert deltas resulted in a highly irregular coastline that was subject to frequent and abrupt changes. Inter-delta areas were the sites of shelf-like deposition, sand-dominated in areas only a few kilometres distance from the principal gravel deltas. Shelf deposits that accumulated closer to the deltas are commonly associated with gravel beaches and bars. Gravel-dominated barrier and lagoonal settings probably developed on abandoned segments of fan deltas. Gravels on the delta bodies were fed directly into submarine canyons and gullies, primarily by fast-flowing, noncohesive debris flows, bypassing the slope (Ashman Formation), and continuing into base-of-slope submarine fans.

Progradation of the shelf/slope break

Rates of sedimentation during Middle and Late Jurassic time in Bowser Basin generally were rapid, as indicated by the huge volumes of conglomerate in environments ranging from paralic to relatively deep basin. Sediment influx appears to have been particularly rapid during two periods: 1) Early Callovian — indicated by the presence of Gilbert delta and

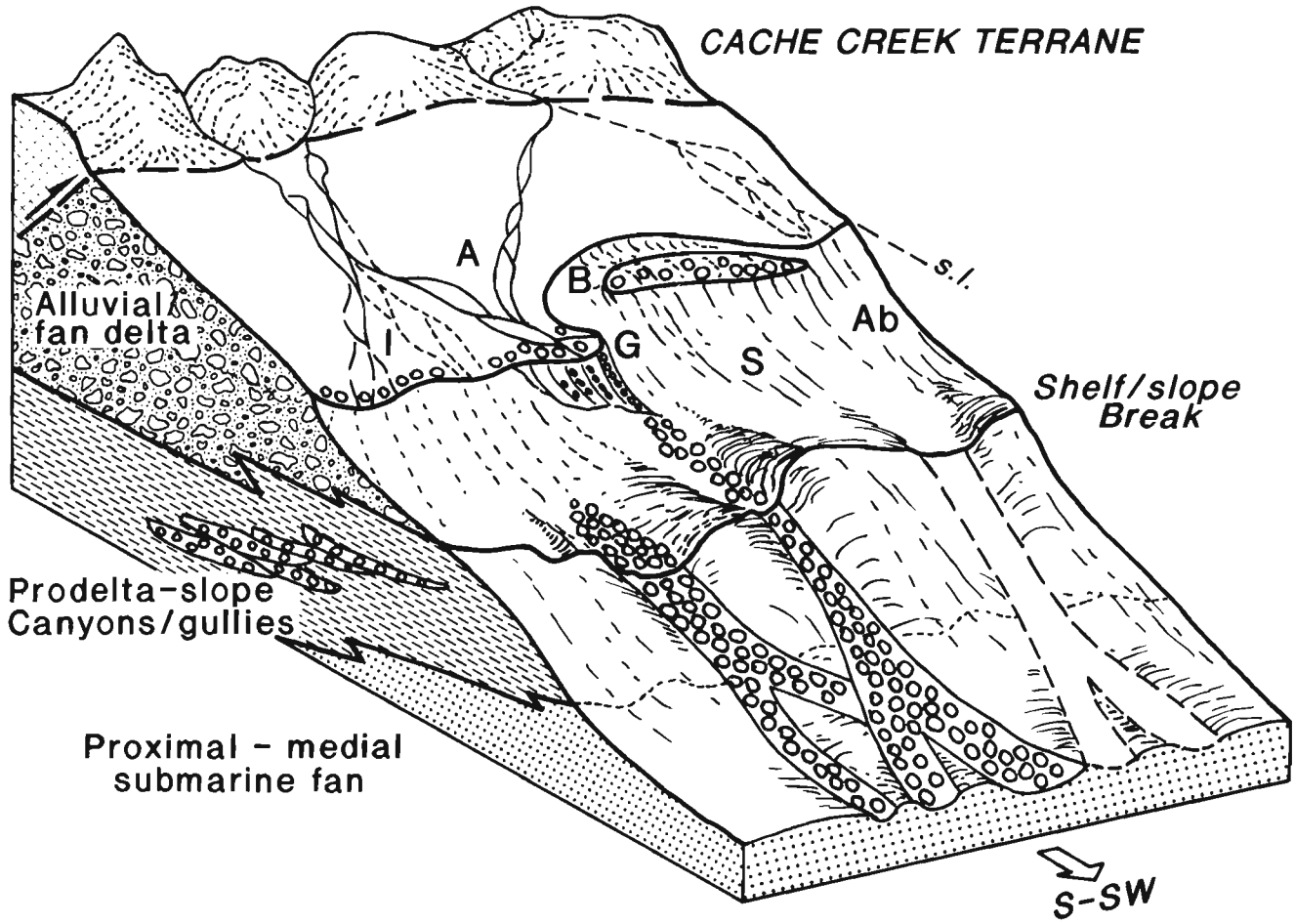

Figure 7. Paleoenvironmental reconstruction depicts a highly irregular coastline, characterized by frequent shifting, abandonment, and reactivation of gravelly fan deltas and sandy interfan shelves. Gravel from the deltas was funnelled through shelf-edge gullies and canyons, feeding base-of-slope submarine fans. The submarine channel-fan systems also were frequently abandoned in concert with changes in the locus of landward sediment supply. A = active alluvial channels; I = inactive alluvial channels; B = gravel bars, barriers, and lagoons; G = Gilbert delta; S = interfan shelf; Ab = abandoned fan delta/submarine canyon/fan.

thick fan delta conglomerate that conformably and locally disconformably overlie the slope/canyon assemblage; and 2) latest Callovian and Early Oxfordian, again indicated by a few Gilbert deltas and by a thick (at least 1 km), conglomerate-dominated Lower Oxfordian succession (south of Tsatia Mountain area).

The Early Callovian shelf/slope break, striking approximately east-southeast in the northern coarse grained facies belt of Bowser Basin, can be traced from the Icebox Canyon/Mount Cartmel area south to the Tsatia Mountain area, along a trend almost parallel with regional paleoslope. Present separation of the two areas is about 40 km, and therefore the paleogeographic distance was a minimum of about 50 km (based on estimates of structural shortening; Evenchick, in press). This value therefore represents a minimum distance of shelf and fan delta progradation over a period of about 2 million years for the early part of Bowser Basin filling.

Western limits of northern Bowser strata

Outcrops of Bowser strata at Raspberry Pass and Bourgeaux Creek (south of Mount Edziza, Telegraph map area; Fig. 2) represent the westernmost preserved limits of northern Bowser Basin. Up to 400 m of Ashman strata consisting of shale, siltstone, fine sandstone, and conglomerate belong to the prodelta/slope and submarine canyon/gully facies assemblages. Facies are identical to those seen in other parts of Bowser Basin. Shallow water deposits are not present. Sandstone and conglomerate clast types are predominantly chert, as is the case elsewhere in the northern Bowser depocentre. There is no evidence for a western basin margin in either the sedimentary facies or sediment composition. However, it is possible that some kind of western margin existed in the central part of Bowser Basin. For example Anderson (1989) reports plagioclase-rich greywacke in Iskut map area, that likely was derived from exposed Hazelton or older Stikinian volcanic rocks.

Sedimentary facies, composition, and provenance — a dilemma

Modern analogues of Gilbert deltas and various kinds of fan delta usually accumulate close to sediment source regions of high topographic relief. Fan deltas in general are usually associated with rapid influxes of coarse sediment in tectonically active basins, particularly those bounded by faults; the more than 900 m of gravelly fan delta strata in many parts of the northern Bowser certainly attest to rapid rates of sedimentation. Gilbert deltas in particular are commonly associated with faulted basin margins and failed slopes (e.g. Massari and Colella, 1988) and rarely are more than a few kilometres from their source of sediment. Another quality of fan deltas is their susceptibility to cannibalization during relative lowering of sea levels. This leads to reworking of sediment and the development of unconformities between progradational events. These disconformities may or may not be of regional extent, depending on the relationships among local sediment supply rates, basin subsidence and sea level change.

In contrast, the uniform compositional maturity of coarse grained Middle and Upper Jurassic Bowser sediments suggest considerable reworking of sand and gravel. Chert clasts predominate with felsic volcanic clasts generally less than 3 to 4%, and frequently absent. Bedded chert of oceanic affinity in the Cache Creek Terrane, an accretionary subduction complex, is the most likely source candidate (Souther and Armstrong, 1966; Wheeler and Gabrielse, 1972; Monger, 1977; Eisbacher, 1981, 1985). Of particular note in the Cache Creek Terrane is the common occurrence of basic and ultramafic volcanic rocks and minor reefal limestone, lithologies that have not found their way into Bowser sediments in the Spatsizi or Telegraph map areas. Current separation of Cache Creek rocks from these map areas is between 80 to 100 km (tectonic shortening not taken into account). This geographic separation, in concert with the ensuing high degree of mechanical attrition during sediment transport, would be sufficient to explain the paucity of labile sediments deposited if it were not for the sedimentary facies which indicate much closer proximity to source terrain.

Three solutions to this dilemma might be: 1) the Cache Creek rocks were much closer to the depositional sites than presently disposed; or 2) Bowser sediments were cannibalized by intrabasin tectonics; 3) a combination of the above.

A major problem with the first case is that significantly closer proximity of Cache Creek source rocks should have resulted in greater proportions of volcanic- and carbonate-derived sediment. In the second case, cannibalization would have resulted in at least local development of disconformities, like those encountered below the Gilbert delta facies in several places. Although this criterion confirms to some extent the viability of option 2, the verification of synsedimentary faults poses more difficult problems. Both normal faults and thrust faults occur in the Skeena Fold and Thrust Belt (Evenchick, in press), but it cannot yet be established whether any of these are reactivated intrabasinal faults.

SOME CONSTRAINTS ON THE EVOLUTION OF BOWSER BASIN

When did Bowser sedimentation begin?

Opinions regarding the crustal position of Bowser Basin in western Cordillera generally consider it to have been in a back arc, marginal, or back basin position (Wheeler and Gabrielse, 1972; Eisbacher, 1974; Bustin and Moffat, 1989). Eisbacher (1974, 1981) employed the term "successor basin" for the Bowser (and other Intermontane basins); a rapidly subsiding trough developed on deformed and intruded basement (in this case Stikine arc volcanics). In most of these scenarios, Bowser deposition is inferred to have begun in the Bathonian, in a rapidly subsiding foredeep on Stikinian crust that was loaded by Cache Creek rocks carried on west- to southwest-verging thrusts (Monger, 1977; Eisbacher, 1985).

Application of a foredeep model (analogous at least to the general style of thrust-related crustal loading and flexure, e.g. Price, 1973; Beaumont, 1981), predicts that the initial pulse of sediment is dominated by shale. During the early stages of thrusting and loading, Cache Creek (oceanic) rocks transported over the east-dipping Stikinian crustal ramp would have remained below sea level. Only when sufficient relief was created would substantial erosion and coarse clastics have been introduced into the subsiding basin. In this scenario, the shale, or starved basin stage occurs in the Spatsizi Group, analogous to the Fernie Group in the Foreland Basin. In particular, the Abou Formation of Aalenian age (Thomson et al., 1986) is a dark, organic and siliceous shale overlying a disconformity that in the Spatsizi area is locally erosional. The Abou has the hallmarks of a condensed stratigraphic succession, that accumulated in a starved basin and overlying a transgressive hiatus. If the Abou flood event marks the beginning of Bowser Basin subsidence, then the thrusting event, and therefore stacking of the Cache Creek accretionary subduction prism, also began in the Aalenian or perhaps latest Toarcian. Introduction of coarse clastic sediment (Ashman Formation) into the Spatsizi map area, and derived from uplifted and exposed Cache Creek strata above the King Salmon and Nahlin thrusts was delayed until the Bathonian. Thrusting along the King Salmon Fault is bracketed between Toarcian and middle Bajocian (Thorstad and Gabrielse, 1986).

Additional support for this timing has been discovered by Cordey et al. (1987) who found Early to Middle Jurassic (Pliensbachian to Bajocian) radiolaria in bedded chert in the type area of the Cache Creek Group, and more recently in chert pebbles from the Bowser Lake Group (F. Cordey, pers. comm., 1990). This implies that Cache Creek sedimentation may have continued until earliest Middle Jurassic time, at least locally, but does not preclude the possibility that subduction deformation of Cache Creek rocks could have begun somewhat earlier at the leading edge of the upper plate.

The Bowser Basin precursor

A corollary of the above hypothesis is that the Bowser depocentre developed within a pre-existing basin or trough, represented by pre-Abou Formation (pre-Aalenian) units in

the Spatsizi Group and Hazelton Group (including Cold Fish volcanics). Corresponding (at least in part) to the Hazelton Trough of Tipper and Richards (1976), the pre-accretionary basin conceivably represents an inter-arc or back-arc setting associated with Hazelton volcanics. The pre-Aalenian Spatsizi Group and related volcanic rocks must also represent the youngest pre-accretionary deposits in Stikinia, forming immediately prior to accumulation of the autochthonous Bowser succession — the overlap assemblage of Monger and Berg (1984) and Wheeler and McFeely (1987).

Pulses of sediment in the Jurassic Bowser Basin

From its inception in earliest Middle Jurassic (or perhaps Toarcian) to the Oxfordian, at least four significant pulses of sediment are recorded in Bowser Basin: 1) shale and water-laid tuff characterizing the Quock Formation/Pyjama succession; 2) the first major influx of conglomerate in the Bathonian near the base of the Ashman Formation at Joan Lake; 3) a Lower Callovian event, signalled by Gilbert deltas and local erosional disconformities, and thick fan deltas; and 4) a latest Callovian-Early Oxfordian event, also indicated by renewed Gilbert delta formation and a great thickness of coarse grained, shallow water sediment.

The first event corresponds to earliest Bowser Basin flexural subsidence resulting from Cache Creek accretion, whereas the second event records eventual exposure and erosion of Cache Creek strata above the subduction zone. The latter two events are inferred to reflect within-basin adjustments, perhaps by intrabasin faulting.

ACKNOWLEDGMENTS

Thanks go to Lynn McFarland, Andrew Kaip, and Michael Toolan for assistance in the field, and to George Green for providing stratigraphic information in Todagin Mountain area. Critical biostratigraphic information was provided by Terry Poulton (ISPG) and Russell Hall (University of Calgary). The constructive review by Hu Gabrielse is gratefully acknowledged.

REFERENCES

Anderson, R.G.
1989: A stratigraphic, plutonic, and structural framework for the Iskut River map area, northwest British Columbia; *in* Current Research, Part E, Geological Survey of Canada, Paper 89-1E, p. 145-154.

Beaumont, C.
1981: Foreland basins; Geophysical Journal of the Royal Astronomical Society, v. 65, p. 291-329.

Bustin, R.M. and Moffat, I.
1989: Semianthracite, anthracite and meta-anthracite in the central Canadian Cordillera: their geology, characteristics and coalification history; International Journal of Coal Geology, v. 13, p. 303-326.

Carter, R.W.G., Orford, J.D., Forbes, D.L., and Taylor, R.B.
1987: Gravel barriers, headlands and lagoons: an evolutionary model; in Coastal Sediments '87, edited by N.C. Kraus, Proceedings, p. 1776-1792.

Cordey, F., Mortimer, N., DeWever, P., and Monger, J.W.H.
1987: Significance of Jurassic radiolarians from the Cache Creek Terrane, British Columbia; Geology, v. 15 , p. 1151-1154.

Eisbacher, G.H.
1974: Deltaic sedimentation in the northeastern Bowser Basin, British Columbia; Geological Survey of Canada, Paper 73-33, 13 p.
1981: Late Mesozoic-Paleogene Bowser Basin molasse and Cordilleran tectonics, Western Canada; in Sedimentation and Tectonics in Alluvial Basin, edited by A.D. Miall, Geological Association of Canada, Special Paper 23, p. 126-151.
1985: Pericollisional strike-slip faults and synorogenic basins, Canadian Cordillera; in Strike-Slip Deformation, Basin Formation, and Sedimentation, edited by K.T. Biddle and N. Christie-Blick, Society of Economic Paleontologists, Special Publication 37, p. 265-282.

Evenchick, C.A.
1988: Structural style and stratigraphy in northeast Bowser and Sustut basins, north-central British Columbia; *in* Current Research, Part E, Geological Survey of Canada, Paper 88-1E, p. 91-95.
1989: Stratigraphy and structure in east Spatsizi map area, north-central British Columbia; *in* Current Research, Part E, Geological Survey of Canada, Paper 89-1E, p. 133-138.
in press: Geometry, evolution and tectonic framework of the Skeena Fold Belt, north-central British Columbia; Tectonics.

Evenchick, C.A. and Green, G.M.
1990: Structural style and stratigraphy of southwest Spatsizi map area, British Columbia; *in* Current Research, Part F, Geological Survey of Canada, Paper 90-1F, p. 135-144.

Massari, F. and Colella, A.
1988: Evolution and types of fan-delta systems in some major tectonic settings; in Fan Deltas: Sedimentology and Tectonic Settings, edited by W. Nemec and R.J. Steel, Blackie and Son, p. 103-122.

Monger, J.W.H.
1977: Upper Paleozoic rocks of the western Canadian Cordillera and their bearing on Cordilleran evolution; Canadian Journal of Earth Sciences, v. 14, p. 1832-1859.

Monger, J.W.H. and Berg, H.C.
1984: Part B — Lithotectonic terrane map of western Canada and southeastern Alaska; in Lithotectonic Terrane Maps of the North American Cordillera, edited by N.J. Silberling and D.L. Jones, United States Geological Survey, Open File Report 84-523.

Postma, G.
1990: An analysis of the variation in delta architecture; Terra Review, v. 2, p. 124-130.

Postma, G., Babic, L., Zupanic, J., and Roe, S.-L.
1988: Delta-front failure and associated bottomset deformation in a marine, gravelly Gilbert type fan delta; in Fan Deltas: Sedimentology and Tectonic Setting, edited by W. Nemec and R.J. Steel, Blackie and Son, p. 91-102.

Price, R.A.
1973: Large-scale gravitational flow of supracrustal rocks, southern Canadian Rockies; in Gravity and Tectonics, edited by K.A. DeLong and R. Scholten, Wiley and Sons, New York, p. 491-502.

Ricketts, B.D.
1990: A preliminary account of sedimentation in the lower Bowser Lake Group, northern British Columbia; in Current Research, Part F, Geological Survey of Canada, Paper 90-1F, p. 145-150.

Souther, J.G. and Armstrong, J.E.
1966: North-central belt of the Cordillera of British Columbia; Canadian Institute of Mining and Metallurgy, Special Volume No. 8, p. 171-184.

Thomson, R.C., Smith, P.L., and Tipper, H.W.
1986: Lower to Middle Jurassic (Pliensbachian to Bajocian) stratigraphy of the northern Spatsizi area, north-central British Columbia; Canadian Journal of Earth Sciences, v. 23, p. 1963-1973.

Thorstad, L.E. and Gabrielse, H.
1986: The Upper Triassic Kutcho Formation Cassiar Mountains, north-central British Columbia; Geological Survey of Canada, Paper 86-16.

Tipper, H.W. and Richards, T.A.
1976: Jurassic stratigraphy and history of north-central British Columbia; Geological Survey of Canada, Bulletin 270.

Wheeler, J.O. and Gabrielse, H.
1972: The Cordilleran Structural Province; in Variations in Tectonic Styles in Canada, edited by R.A. Price and R.J.W. Douglas, The Geological Association of Canada, Special Paper No. 11, p. 1-81.

Wheeler, J.O. and McFeely, P.
1987: Tectonic assemblage map of the Canadian Cordillera and adjacent parts of the United States of America; Geological Survey of Canada, Open File 1565.

Stratigraphic studies of Lower to Middle Jurassic rocks in the Mt. Waddington and Taseko Lakes map areas, British Columbia

Paul J. Umhoefer[1] and H.W. Tipper
Cordilleran Division, Vancouver

Umhoefer, P.J. and Tipper, H.W., Stratigraphic studies of Lower to Middle Jurassic rocks in the Mt. Waddington and Taseko Lakes map areas, British Columbia; in Current Research, Part A, Geological Survey of Canada, Paper 91-1A, p. 75-78, 1991.

Abstract

Lower Jurassic and lower Middle Jurassic rocks underlie parts of the Mt. Waddington area near Mt. Nemaia and westward to Tatlayoko Lake (NTS 92N,92O) forming a thick sequence of volcanogenic sediments consisting of lithic sandstone, siltstone, shale, and minor tuff(?), limy beds and fine grained conglomerate. So far as can be determined, it is a conformable sequence from Early Sinemurian to Early Bajocian time but fossils are sparse and paleontological control is barely adequate. The Lower Sinemurian to Aalenian rocks are mainly siltstone and shale whereas the Lower Bajocian is a coarsening upward sequence of siltstone and sandstone. The sequence is 2-3 km thick.

Résumé

Les roches du Jurassique inférieur et de la base du Jurassique moyen reposent sous des parties de la région du mont Waddington près du mont Nemaia et à l'ouest du lac Tatlayoko (SNRC 92N, 92O), formant une épaisse séquence de sédiments d'origine volcanique composés de grès lithique, de siltstone, de shale ainsi que d'une petite quantité de tuf (?), de couches calcaires et de conglomérat à grain fin. Selon les données recueillies jusqu'à présent, il s'agit d'une séquence concordante datant du Sinémurien précoce au Bajocien précoce mais les fossiles étant disséminés, les données paléontologiques manquent de précision. Les roches du Sinémurien inférieur à l'Aalénien se composent principalement de siltstone et de shale tandis que celles du Bajocien inférieur forment une séquence à granoclassement inverse de siltstone et de grès. La séquence mesure entre 2 et 3 km d'épaisseur.

[1] 101 East Arrowhead Road, Duluth, Minnesota, U.S.A. 55803

INTRODUCTION

In 1990 eight days were spent in the Mt. Waddington map area to revise and update the available stratigraphic information on the Middle and Lower Jurassic strata. Although these rocks were briefly mentioned in early reports by Dawson (1877), Dolmage (1925) and Galloway (1917) they were not systematically studied until 1967 (Tipper, 1969; Roddick and Tipper, 1985). Here they were briefly described but not subdivided or named and their relation to other units of similar age was not suggested.

This study is a part of the Nechako-Chilcotin Project in which a report on the Upper Norian to Bajocian rocks for the Mt. Waddington (92N) and Taseko Lakes (92O) will be produced based on a doctoral dissertation by Umhoefer (1989), on unpublished work by Tipper and some minor field work in 1990. The lithostratigraphy and biostratigraphy are the main parts of this study.

STRATIGRAPHY

Strata of Early Jurassic (Early Sinemurian) to Middle Jurassic (Early Bajocian) age have been identified (Fig. 1) and tentatively divided into three members; the whole unit is considered to be one conformable formation at least 2-3 km thick. The best exposed part of the formation (Aalenian to Early Bajocian age) forms a generally coarsening-upward sequence. The lower member is dominantly shale, siltstone and minor sandstone and conglomerate, the middle member is typically siltstone and shale with subordinate sandstone, and the upper member is mainly coarse grained lithic sandstone and arkosic sandstone with lesser siltstone and minor conglomerate. The base and top of the formation have not been clearly delineated.

Lower Member

Finer clastic rocks characterize this unit but lack of unfaulted good exposures and the scarcity of fossils precludes a full understanding of the stratigraphy. The uppermost beds are of Aalenian age and comprise black to dark grey finely laminated and banded shales with a few interbeds of lithic sandstone and rare brown weathering limy lenses (Fig. 2). Sedimentary structures are rare. The best exposures of these rocks are on the south side of "Huckleberry Mountain" but unfossiliferous beds on Mt. Nemaia are probably correlative.

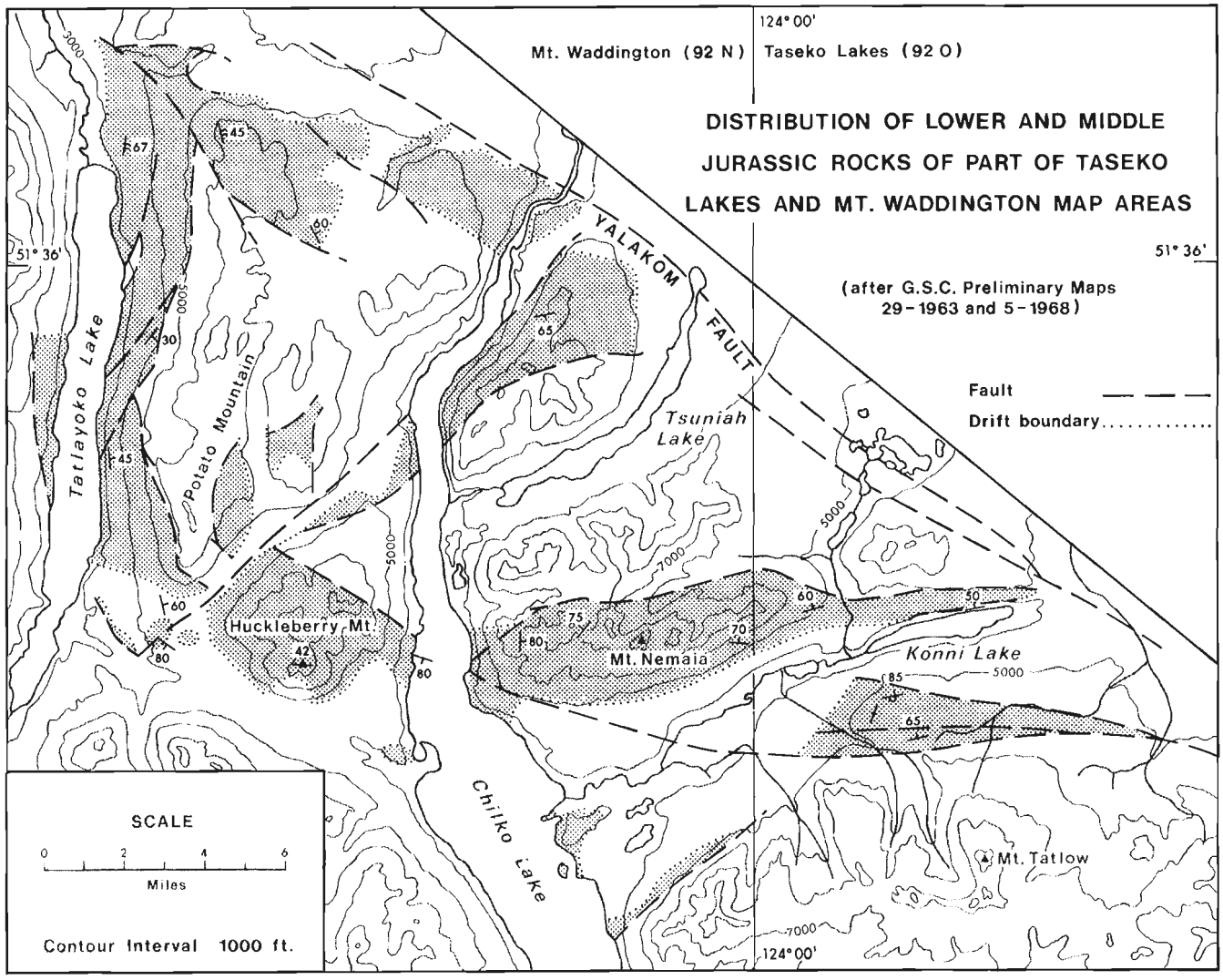

Figure 1. Lower and Middle Jurassic rocks of the map area.

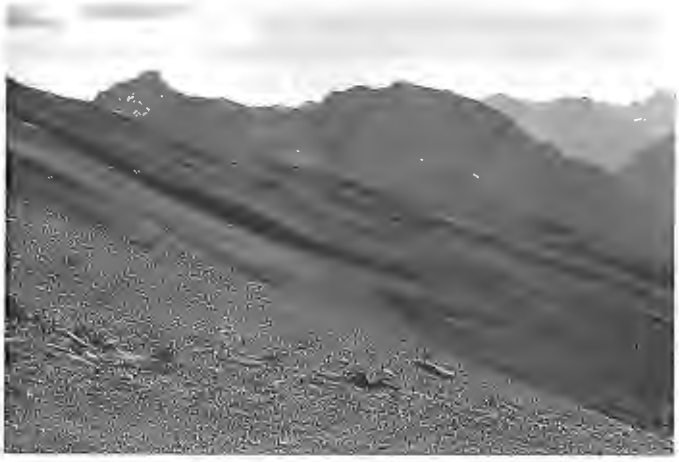

Figure 2. Aalenian shales of the Lower Member, Huckleberry Mountain.

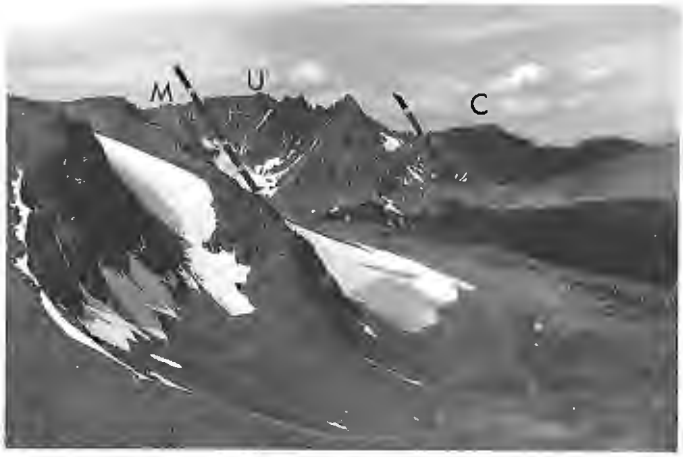

Figure 4. North of Mt. Nemaia; Middle Member overlain by Upper Member, the more rugged part of the ridge. Callovian sediments (C) overlie the Upper Member disconformably(?).

Figure 3. Finer talus of the Middle Member (M) overlain by the Upper Member (U) near Mt. Nemaia.

Figure 5. Typical rough outcrops of the Upper Member east of Mt. Nemaia.

In a creek near the north end of Tatlayoko Lake a short section of Early Pliensbachian age consists of siltstone, sandstone and fine gritty conglomerate. Similar rocks, but lacking fossils are present on the Mt. Nemaia ridge low in the section.

On the north side of Mt. Tatlow, in the Taseko Lakes area a fault bounded exposure of Lower Sinemurian rocks consists of black to dark grey shale or siltstone with greenish tuff(?) or lithic sandstone and minor limy beds. A few fossils indicate an Early Sinemurian age. Similar strata occur near the base of Mt. Nemaia but are unfossiliferous. The base of the formation is nowhere exposed. Although the complete section cannot be documented there is a section of dominantly silty strata on the southern flank of Mt. Nemaia that could be up to 2 km thick and represent most, if not all Early Jurassic time.

Middle Member

Conformably overlying the Lower Member is a mainly siltstone and fine sandstone unit (Fig. 3, 4); the transition is abrupt. The unit is best exposed on the south side of "Huckleberry Mountain", on Mt. Nemaia, and on the road at the north end of Tatlayoko Lake. Fossils are scarce but a few sonninid ammonites suggest a basal Early Bajocian age.

Blue-green and greenish-grey siltstone are present in beds of varying thickness up to 3 or 4 m. Some show no sedimentary structures but others are crossbedded or have irregular laminations. Regularly laminated beds and a few beds with fine tuff(?) bands are not uncommon. Medium- to coarse-grained sandstones to 50 cm and shale in thin beds a few centimetres thick are uncommon.

Upper Member

Conformably overlying, and abruptly gradational with the middle member is a coarse grained unit of medium- to coarse-grained sandstones and fine-pebble conglomerates interbedded with laminated silty shale and 1 cm scale turbiditic sandstones (Fig. 3, 4, 5). The upper member is greater than 500 m thick, and is most likely at least a kilometre thick based on partial sections examined on "Huckleberry Mountain" and Mt. Nemaia. The lower 45 m at each location was examined in the most detail. Fossils of the upper member are uncommon stephanoceratids and represent the

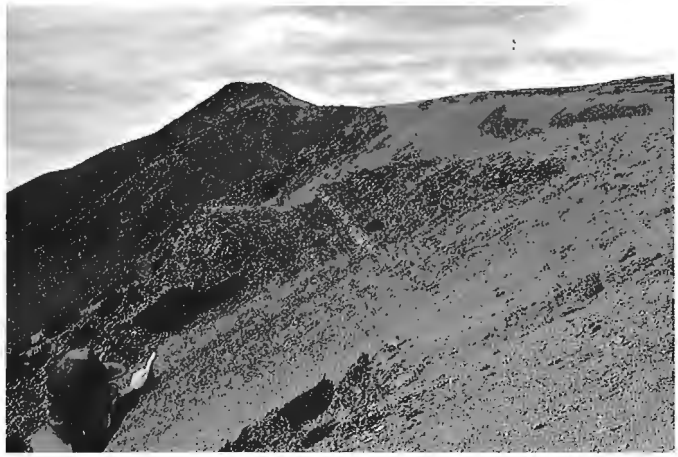

Figure 6. Rare tuff bands (light grey) in the Upper Member.

late Early Bajocian. The upper contact of the member (and formation) is overlain by Callovian-age strata (Fig. 4) containing fine-pebble conglomerate, sandstone, and siltstone (Tipper, 1969).

In the lower part of the member, lithic to arkosic sandstones and volcanic-pebble conglomerates are generally graded in decimetre-scale beds, with common mudstone clasts, and minor erosional bases. Thick sandstones in the finer grained beds commonly show ripple and convolute lamination. Carbonaceous and shelly material is rare to absent low in the member, and increases upsection. Buff to white weathering siltstone layers in the fine grained, laminated facies are possibly ash or tuffaceous in part (Fig. 6). A few, minor calcareous sandstones to calcarenites are present in the upper part of the section.

REFERENCES

Dawson, G.M.
1877: Report on explorations in British Columbia; Geological Survey of Canada, Report of Progress 1875-76, p. 233- 265.

Dolmage, V.
1925: Chilko Lake and vicinity, British Columbia; Geological Survey of Canada, Summary Report 1924, Part A, p. 59-75.

Galloway, J.D.
1917: Bulkley Valley to Chilcotin District; British Columbia, Report of Minister of Mines, 1916, p. 134-186.

Roddick, J.A. and Tipper, H.W.
1985: Mount Waddington, B.C.; Geological Survey of Canada, Open File 1163.

Tipper, H.W.
1969: Mesozoic and Cenozoic geology of the northeast part of Mt. Waddington map-area (92N), Coast District, British Columbia; Geological Survey of Canada, Paper 68-33.

Umhoefer, P.J.
1989: Stratigraphy and tectonic setting of the Upper Cadwallader Terrane and overlying Relay Mountain Group, and the Cretaceous to Eocene structural evolution of the eastern Tyaughton Basin, British Columbia; unpublished Ph.D. thesis, University of Washington, Seattle.

Preliminary U-Pb dates and field observations from the eastern Coast Belt near 52°N, British Columbia

Peter van der Heyden
Cordilleran Division, Vancouver

van der Heyden, P., Preliminary U-Pb dates and field observations from the eastern Coast Belt near 52°N, British Columbia; in Current Research, Part A, Geological Survey of Canada, Paper 91-1A, p. 79-84, 1991.

Abstract

New U-Pb data and field observations show that the eastern Coast Belt near 52°N consists predominantly of late Middle Jurassic and Early Cretaceous plutons, which form crystalline basement to nonconformably overlying Middle-Late Jurassic and Early Cretaceous volcanic sequences, respectively. The Atnarko Complex represents a separate tectonized domain, superimposed on the composite plutonic mass, with a poorly understood structural history. Synkinematic Middle-Late Jurassic and Early Cretaceous plutons, and a pre- or syn-kinematic mid-Cretaceous pluton, indicate three major, apparently localized deformation episodes.

Middle-Late Jurassic and Early Cretaceous magmatic rocks in the eastern Coast Belt augment known regional distribution patterns which suggest pre-late Middle Jurassic amalgamation and accretion of the major allochthonous Cordilleran terranes to continental North America. Inherited radiogenic Pb in zircons from Early Jurassic(?) and Middle-Late Jurassic volcanic rocks suggests involvement, however indirect, of Late Proterozoic crust in the Mesozoic evolution of this part of the western Canadian Cordillera.

Résumé

De nouvelles données U-Pb et des observations sur le terrain indiquent que la zone côtière de l'Est, près de 52°N, est surtout composée de plutons de la fin du Jurassique moyen et du Crétacé précoce qui forment le socle cristallin des séquences volcaniques discordantes sus-jacentes du Jurassique moyen à tardif et du Crétacé précoce, respectivement. Le complexe d'Atnarko représente un domaine tectonisé distinct, superposé au massif plutonique composite, dont l'histoire structurale est mal connue. Les plutons syncinématiques du Jurassique moyen à tardif et du Crétacé précoce ainsi que les plutons précinématiques ou syncinématiques du Crétacé moyen, indiquent trois épisodes importants de déformation apparemment localisés.

Les roches magmatiques du Jurassique moyen à tardif et du Crétacé précoce dans la zone côtière de l'Est renforcent les configurations connues de répartition régionale qui révèlent une amalgamation, avant la fin du Jurassique moyen, des principaux terranes allochtones de la Cordillère à l'Amérique du Nord continentale et leur accrétion. La présence de Pb radiogénique hérité dans les zircons des roches volcaniques du Jurassique précoce(?) et du Jurassique moyen à tardif semble indiquer une participation, quoique indirecte, de la croûte du Protérozoïque tardif à l'évolution mésozoïque de cette partie de la Cordillère de l'ouest du Canada canadienne occidentale.

INTRODUCTION

This progress report summarizes preliminary geochronometry results and new field observations for the eastern Coast Belt near 52°N (Fig. 1). An introduction to the study area and preliminary conclusions were presented previously (van der Heyden, 1990). The study area is centred on the Atnarko Complex, a north-northwest trending structural and metamorphic culmination dominated by penetratively deformed, commonly mylonitic plutons and lesser metavolcanic country rocks (Fig. 2). The deformed plutons grade into relatively undeformed plutonic protoliths along the margins of the Atnarko Complex. These marginal plutons are nonconformably overlain by Early Cretaceous volcanic rocks to the west (Monarch volcanics) and probably by Middle-Late Jurassic volcanic rocks to the north and east (Hotnarko volcanics). These field relations, and the resemblance of the Atnarko Complex to the Late Jurassic Gamsby Complex in the Whitesail Lake area (van der Heyden, 1982, 1989), initially suggested that much of the Atnarko Complex could be a Late Jurassic tectonite zone superimposed on Middle Jurassic plutons and their older country rocks (van der Heyden, 1990), but recent revision of the geological time scale (Harland et al., 1989) implies a possible late Middle Jurassic (Bathonian) maximum age for both tectonite complexes.

Recently completed geochronometry (done at the GSC geochronology laboratory, Ottawa), fossil identification, and additional field work generally substantiate the preliminary conclusions outlined above, but they also indicate a considerably more complex post-Middle Jurassic magmatic and structural evolution than was initially recognized. Additional geochronometry and, especially, careful 1:50 000 scale mapping must be done to obtain a better understanding of this area, which has been subjected only to regional study. New results are summarized below (Table 1, Fig. 2); complete analytical data, regional implications, and final conclusions will be presented elsewhere (van der Heyden and Parrish, in prep.).

JURASSIC PLUTONS AND VOLCANIC ROCKS

Early Jurassic(?) volcanic rocks

Structureless volcaniclastic rocks, volcanic flows, and lesser epiclastic sediments along the northern and eastern margin of the study area, previously collectively referred to as the Hotnarko volcanics, were inferred to be Callovian-Oxfordian on the basis of fossils collected on Hotnarko Mountain (van der Heyden, 1990). Two zircon fractions from a rhyolitic tuff collected along the north shore of Charlotte Lake (sample V89-2, Fig. 1) are near-concordant, with 189 ± 2 and 191 ± 2 Ma Pb/Pb dates. The zircons are fragmental and thus may indicate an Early Jurassic clastic or xenocrystic component in a younger rhyolite, but because they form a single population the preferred interpretation is that the rhyolite is Early Jurassic. Volcanic rocks south of Charlotte Lake are also inferred to be Early Jurassic, because they are intruded (Tipper, 1969) by the Middle Jurassic McClinchy pluton (sample V89-141, below).

Metavolcanic rocks within the Atnarko Complex are believed to have been derived from Early Jurassic protoliths.

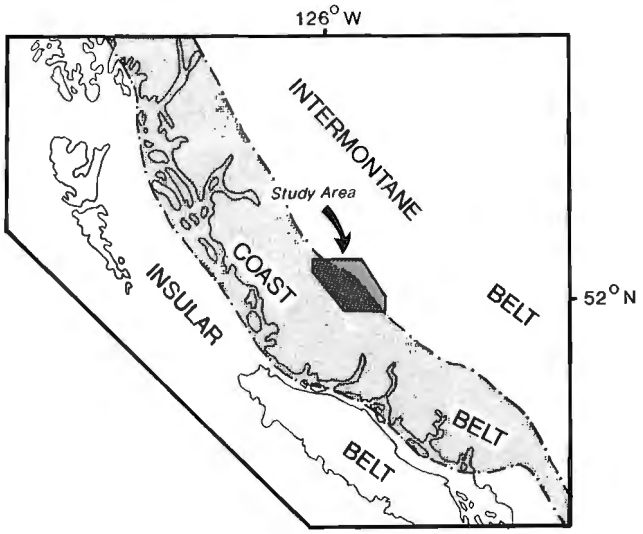

Figure 1. Location of the study area along the eastern margin of the Coast Belt, British Columbia.

Three zircon fractions from a metarhyolite (sample V89-115-1) unfortunately gave widely scattered and inconclusive Pb/U ratios. Highly discordant Pb/U ratios for a fraction containing faint cores suggest Late Proterozoic inheritance; the age of the rhyolite remains unknown. However, the volcanic rocks are intruded by a Middle-Late Jurassic quartz diorite pluton (sample V89-112-3, below), and they are lithologically and structurally remarkably similar to penetratively deformed, greenschist facies metavolcanic rocks of the Gamsby Complex in the Whitesail Lake area, which have been dated as Early Jurassic.

These data and the lithological character of the volcanic rocks invite correlation with the Early Jurassic Hazelton Group. The Early Jurassic volcanics are here excluded from the Hotnarko volcanics; that name is reserved for rocks known or presently inferred to be Middle-Late Jurassic in age. Due to difficulties distinguishing between the two volcanic packages in the field, some areas mapped as Hazelton Group (Fig. 2) may in fact belong to the younger unit and vice-versa.

Middle-Late Jurassic volcanic rocks (Hotnarko volcanics)

The Hotnarko volcanics are a marine to nonmarine sequence of volcaniclastic rocks, volcanic flows, and minor intercalated epiclastic sediments that flank the Atnarko Complex to the north and northeast. Local intervals in the Hotnarko volcanics with well developed bedding may serve to distinguish them from the generally structureless Early Jurassic volcanics. The sequence dips gently to moderately to the north, but it is locally strongly disrupted by northeast trending faults. The apparent base of the sequence against underlying plutonic rocks generally follows topographic contours. Absence of contact metamorphism and granitoid dykes, and local presence of granitoid cobbles and arkosic debris near the base of the sequence indicates that the Hotnarko volcanics sit nonconformably on the plutonic rocks.

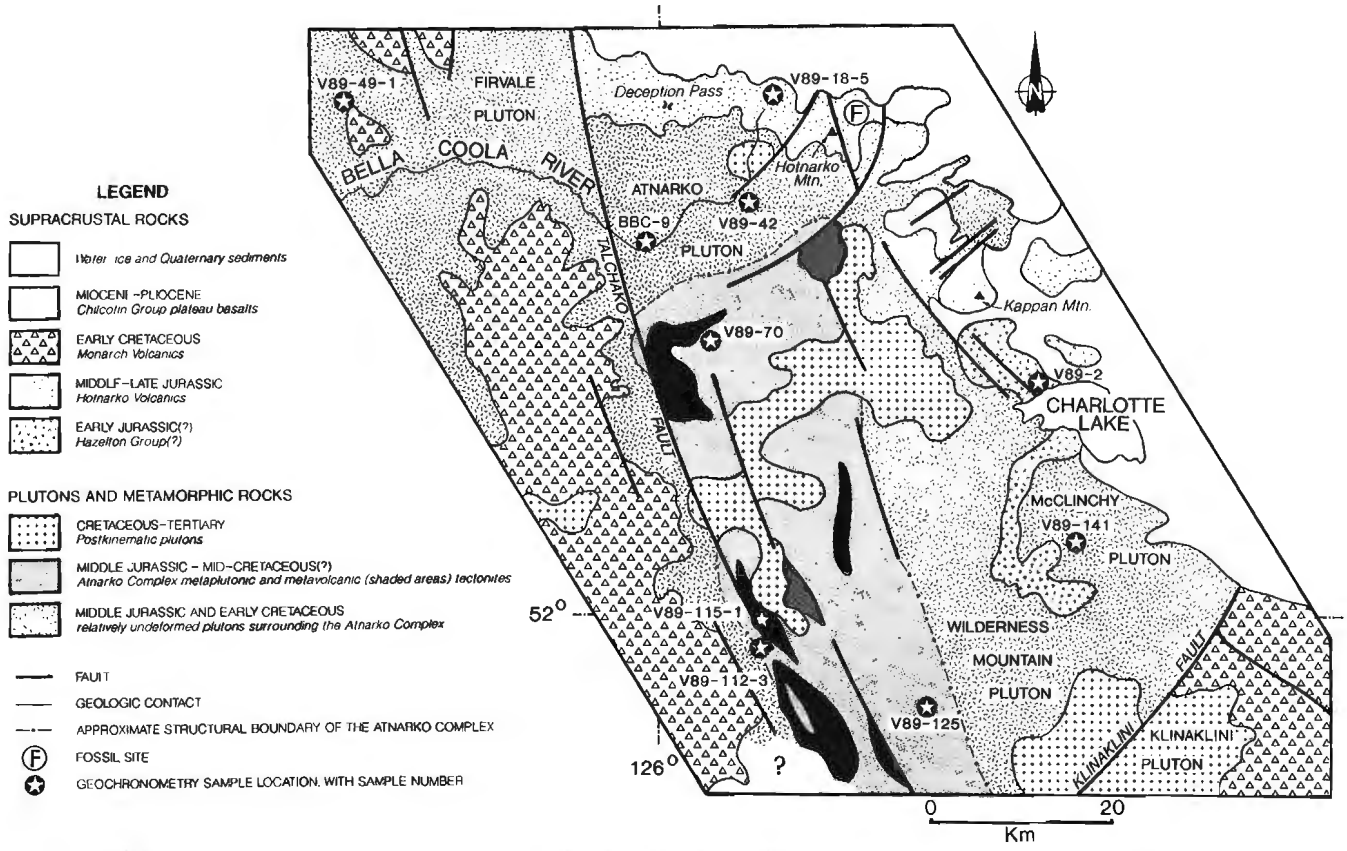

Figure 2. Simplified geological map of the study area, updated to reflect results of geochronometry, fossil identification, and field data obtained since 1989.

Table 1. Preliminary U-Pb and Pb/Pb dates of plutons and volcanic rocks, eastern Coast Belt near 52°N.

Sample #	Rock type	Map Unit	Date (Ma)[1]
V89-2	Rhyolite	Hazelton Group	189 ± 2[p] and 191 ± 2[p]
V89-115-1	Metarhyolite	Atnarko Complex	? Late Proterozoic inheritance
V89-18-5	Rhyolitic tuff	Hotnarko volcanics	154.4 ± 1.2[i], 1016 ± 76 upper intercept
V89-42	Quartz diorite	undeformed pluton	162.5 +15.2/-8.7[i]
V89-112-3	Quartz diorite	Atnarko Complex	156 ± 2[i]
V89-141	Granodiorite	undeformed pluton	163 ± 1.4[p] and 165.4 ± 1.6[p]
V89-49-1	Quartz diorite	undeformed pluton	134 ± 0.3[c]
BBC-9	Quartz diorite	undeformed pluton	138 ± 2[p] and 143 ± 11[p]
V89-125	Quartz diorite	Atnarko Complex	142 ± 0.5[c]
V89-70	Quartz diorite	Atnarko Complex	114.8 ± 0.3[c]
	[1] Errors are 2 sigma [p] Pb/Pb date		[i] Concordia intercept [c] Concordant date

A thick succession of flowbanded rhyolites, dacites, andesites, and intercalated tuffs and breccias, locally with beautifully preserved primary textures, was discovered near Deception Pass (Fig. 2) during the 1990 field season. These rocks form a direct westerly extension of the volcanics of Hotnarko Mountain, but they are generally more acid. Three zircon fractions from a sample of rhyolitic tuff (sample V89-18-5, collected along Highway 20) yielded a discordant array with a lower intercept (crystallization age) of 154.4 ± 1.2 Ma, and an upper intercept of 1016 ± 76 Ma. The Late Jurassic age for this rhyolite confirms previous conjecture based on preliminary identification of *Trigonia* sp. from Hotnarko Mountain (T. Poulton, in van der Heyden, 1990). That result is now definite: several bivalve fragments, collected from volcaniclastic rocks close to the base of the succession, belong to *Anditrigonia* sp. aff. *plumasensis* (Hyatt), which are probably Callovian but may be as young as middle Oxfordian (T. Poulton, pers. comm., 1990; complete fossil data will be published in a manuscript by van der Heyden and Parrish, in prep.). The rhyolite was collected

higher in the stratigraphic package, and could therefore be a Late Jurassic component of a Callovian-Kimmeridgian succession. However, the Middle-Late Jurassic part of the time scale is poorly calibrated, and a Callovian age for the entire succession cannot be ruled out.

The presence of Late Proterozoic inherited radiogenic Pb in zircons from Late Jurassic (sample V89-18-5) and Early Jurassic (sample V89-115-1) volcanic rocks indicates involvement, however indirect, of Late Proterozoic crust in the evolution of west-central British Columbia. Such inheritance has not previously been documented in volcanic rocks associated with Stikinia, although not many U-Pb analyses have been done on volcanic rocks of this terrane. Until more isotopic data are available, the meaning of this inheritance will remain uncertain.

Middle Jurassic plutons

With the exception of clearly younger and generally more leucocratic plutons, most granitoid rocks in the study area, both within and external to the Atnarko Complex, were previously inferred to be Middle Jurassic (van der Heyden, 1990). Collectively they appeared to form crystalline basement to nonconformably overlying Late Jurassic Hotnarko volcanics and Early Cretaceous Monarch volcanics. Of six pluton samples subjected to U-Pb analysis, three are Middle Jurassic, and the remaining three are Cretaceous. Additional samples are in process, but these initial results clearly indicate a more complex magmatic and structural history than initially envisioned.

Four zircon fractions from altered quartz diorite (sample V89-42) underlying the Hotnarko volcanics (Fig. 2, Atnarko pluton) yielded a discordant array with a 162.5+15.2/−8.7 Ma upper intercept, and a 109+15/−21 Ma lower intercept. Three zircon fractions from locally strongly foliated, syn- to late-kinematic quartz diorite along the western margin of the Atnarko Complex (sample V89-112-3) yielded a discordant array with upper intercept of 156 ± 2 Ma and a present-day lower intercept. The 156 Ma date is probably a minimum age; ductile deformation along the western edge of the Atnarko Complex is therefore broadly constrained to be late Middle Jurassic to early Late Jurassic in age.

Two slightly discordant zircon fractions from a biotite granodiorite pluton south of Charlotte Lake (sample V89-141, McClinchy pluton) gave Pb/Pb dates of 165.4 ± 1.6 and 163.1 ± 1.4 Ma. The interpreted late Middle Jurassic age for this pluton represents a revision from a previously inferred Late Cretaceous or Early Tertiary age (van der Heyden, 1990). Pending additional geochronometry, this result also casts doubt on the inferred ages of similar plutons elsewhere in the study area.

CRETACEOUS PLUTONS

The geochronometric identification of Early Cretaceous plutons is among the more surprising results of this study, emphasizing the difficulties inherent in distinguishing plutons of different ages in the field. For instance, the Firvale pluton, west of the Talchako fault, is identical in many respects to the Middle Jurassic Atnarko pluton, and it unambiguously forms the basement to nonconformably overlying Early Cretaceous volcanic rocks (Baer, 1973; van der Heyden, 1990). However, four zircon fractions from quartz diorite immediately below the nonconformity (sample V89-49-1) are concordant at 134 ± 0.3 Ma (Hauterivian). Whether this Early Cretaceous age is representative of the Firvale pluton as a whole, or whether it implies an Early Cretaceous intrusion in an older, Middle Jurassic pluton, is not yet clear. In any case, the nonconformable Hauterivian-Barremian strata on the Early Cretaceous (Hauterivian) pluton suggest rapid unroofing shortly after pluton emplacement, within an active marine magmatic arc.

Preliminary results for zircons from quartz diorite east of the Talchako fault (sample BBC-9, zircons donated by R.L. Armstrong and R. Parrish), also indicate an Early Cretaceous emplacement age. Two discordant fractions gave Pb/Pb dates of 143 ± 11 and 138 ± 2 Ma. Baer (1973) distinguished the unit from which this sample was collected from rocks here assigned to the older Atnarko pluton. The Firvale and Atnarko plutons may thus in fact be parts of the same Middle Jurassic-Lower Cretaceous composite pluton, dissected by the Talchako Fault.

The large and locally strongly deformed Wilderness Mountain pluton, which contains the eastern structural margin of the Atnarko Complex, is also Early Cretaceous. Three zircon fractions (sample V89-125) are concordant at 142 ± 0.5 Ma. This confirms the age previously assigned to this pluton on the basis of a 140 Ma hornblende K-Ar date (Roddick and Tipper, 1985; Wanless et al., 1979); the Jurassic age suggested in van der Heyden (1990) is not substantiated by the combined isotopic data. Because the pluton was involved in amphibolite facies tectonism along the eastern margin of the Atnarko Complex, this deformation is also constrained to be Early Cretaceous. The Atnarko Complex was evidently affected by more than one phase of ductile deformation.

A third phase of deformation is hinted at by locally strongly deformed pluton which contains the northern structural margin of the Atnarko Complex. Four zircon fractions from a foliated, locally mylonitic quartz diorite (sample V89-70) are essentially concordant at 114.8 ± 0.3 Ma (this age is based on superb agreement of $^{206}Pb/^{238}U$ dates; there is slight "sideways" dispersion possibly due to incorrect common Pb correction). The age of the deformation in this case is constrained only to mid-Cretaceous or younger.

The Early and mid-Cretaceous ages for deformed plutons came as a surprise, because preliminary work in the study area had suggested that the Atnarko Complex as a whole represented pre-Early Cretaceous crystalline basement (van der Heyden, 1990). Therefore, as presently known, the Atnarko Complex must be viewed as a tectonized complex consisting of discrete domains, each characterized by magmatic and structural elements of different age. Since the area underlain by the Atnarko Complex has never been mapped in any detail, the nature and precise locations of contacts or transitions between these domains are presently unknown. The boundaries between lower grade magmatic and structural domains adjacent to the Atnarko Complex are likewise poorly known and not accurately located.

AGE OF STRUCTURES IN AND ADJACENT TO THE ATNARKO COMPLEX

Steeply dipping, north-northwest trending dextral ductile shear fabrics characterize most of the Atnarko Complex. Results of geochronometry, presented above, suggest that dextral shear along the western margin of the Atnarko Complex occurred in late Middle Jurassic or early Late Jurassic time. Dextral ductile shear along the eastern margin of the Atnarko Complex, where it appears to be coincident with the western margin of the Wilderness Mountain pluton, is Early Cretaceous. The age of northeast-trending ductile fabrics along the northern margin of the Atnarko Complex appears to be mid-Cretaceous or younger.

East of the Atnarko Complex several areas underlain by plutonic and volcanic rocks are characterized by steeply-dipping, northeasterly-trending penetrative foliations. Some of these foliations clearly formed as a result of localized dextral ductile shearing; parts of the eastern Wilderness Mountain pluton, for instance, are characterized by northeast trending, dextral mylonitic fabrics. North of Kappan Mountain an apophysis of the Atnarko pluton and overlying Hotnarko volcanics were sheared along northeasterly-trending faults. Structures along these faults range from well developed gneissosity in the pluton to discrete slickensided surfaces, some of which appear to represent a faulted nonconformity. Northeast-trending brittle faults, such as the Klinaklini Fault and the Hotnarko Fault (Fig. 2), may be related to these structures, as may the northeast-trending fabrics along the northern margin of the Atnarko Complex.

If the northeast-trending structures east of the Atnarko Complex are related, they must be Early-Cretaceous or younger, because they are present in the Wilderness Mountain pluton. They also appear to locally affect the younger Klinaklini pluton, which intrudes Early Cretaceous volcanic and sedimentary rocks. If the structures in the northern Atnarko Complex are also related, then the northeast-trending structures are mid-Cretaceous or younger. Microfabric analysis and additional geochronometry may further clarify the significance of these poorly known structures.

DISCUSSION

The presence of Middle-Late Jurassic plutons and structures in the study area has important implications for the tectonic evolution and terrane reconstructions of the western Canadian Cordillera. Plutons and structures of this age are present along both margins of the Coast Belt, affecting both Insular and Intermontane superterranes. They appear to have formed within a single, west-facing magmatic arc (van der Heyden, 1989), suggesting that the diverse components of Monger et al.'s (1982) superterranes were already amalgamated long before mid-Cretaceous time.

As elsewhere, the evidence for this older history in the study area is incompletely preserved amongst younger magmatic and structural overprints of the Coast Belt. The Atnarko Complex and adjacent areas, as presently known, are clearly the product of multiple magmatic, structural, and metamorphic episodes. Previous correlation of mylonitic rocks along its western margin to strikingly similar rocks of the Gamsby Complex in the Whitesail Lake area (van der Heyden, 1990) is supported by identical ages of late Middle Jurassic to early Late Jurassic, syn- to late-kinematic plutons in both areas. The western margin of the Atnarko Complex is interpreted as the locus of a major Middle-Late Jurassic, dextral ductile shear zone, which may be related to similar shear zones in and along the eastern margin of the Gamsby Complex.

The eastern and northern parts of the Atnarko Complex were deformed much later, in Early Cretaceous and mid-Cretaceous or later time, respectively. Early Cretaceous dextral ductile shear fabrics along the eastern margin of the Atnarko Complex suggest either episodic reactivation or a relatively steady-state stress regime between late Middle Jurassic and Early Cretaceous, with the locus of deformation migrating easterly with time. Steeply dipping northeast trending ductile and brittle fabrics, both in and adjacent to the Atnarko Complex, are probably mid-Cretaceous or younger, and are interpreted to reflect a significant change in the regional stress regime.

Early Cretaceous plutons in the study area are thought to represent the magmatic roots of the Gambier volcanic arc (for regional distribution of Early Cretaceous volcanic rocks, see Wheeler and McFeely, 1987). Early Cretaceous magmatic rocks, like their Middle-Late Jurassic predecessors, are thought to link and overlap both Insular and Intermontane superterranes. In the southern Coast Belt, the Gambier Group and associated Early Cretaceous plutons occur in Wrangellia (Monger, 1991). In the study area, and further north in the Whitesail Lake area (Woodsworth, 1980; van der Heyden, 1989), Early Cretaceous plutons and volcanic rocks intrude and overly rocks associated with Stikinia.

CONCLUSIONS

The Atnarko Complex is a metamorphic and structural culmination which, together with adjacent, relatively undeformed plutons, constitutes the eastern margin of the Coast Belt near 52°N. It represents a tectonized domain within a large plutonic mass dominated by late Middle Jurassic and Early Cretaceous intrusions. Relatively undeformed Jurassic and Cretaceous plutonic protoliths adjacent to the Atnarko Complex constitute the respective crystalline basements to only slightly younger, nonconformably overlying volcanic and sedimentary sequences.

Although boundaries between plutons and structural domains of different ages are poorly known, three episodes of plutonism and ductile deformation can be distinguished based on U-Pb ages of pre- and syn-kinematic plutons in the Atnarko Complex. An important Middle-Late Jurassic episode correlates with a synchronous episode in the Gamsby Complex, approximately 150 km north-northwest of the study area, and with episodes in other areas along the margins of the Coast Belt (van der Heyden, 1989). Early Cretaceous plutons represent roots to nearby Gambier Group volcanic rocks. Well developed dextral tectonite fabrics in one of these plutons represent a deformation episode not previously recognized in the eastern Coast Belt. Mid-Cretaceous or younger deformation is represented by a locally strongly deformed mid-Cretaceous pluton along the northern margin of the Atnarko Complex.

From a regional perspective the Middle-Late Jurassic and Early Cretaceous episodes are quite important. They augment known magmatic and structural distribution patterns which suggest pre-late Middle Jurassic amalgamation and accretion of the major allochthonous terranes of the Canadian Cordillera to continental North America (van der Heyden, 1989; van der Heyden and Woodsworth, in prep.). Inherited radiogenic lead in zircons from Jurassic volcanic rocks in and adjacent to the Atnarko Complex may also have tectonic implications, suggesting the involvement of Late Proterozoic crust in the evolution of this part of the western Canadian Cordillera. The significance of this involvement, however, is presently not understood.

ACKNOWLEDGMENTS

The writer wishes to thank C.J. Hickson for generous support and encouragement of this PDF project, Mort Grass, Donna and Dudley Klopfer, Rosemary and Dave Neads, and Rob Berman for lodging, food, and company, and the pilots of Wayco Aviation for excellent flying. Randy Parrish was instrumental in seeing the U-Pb analyses through to completion and is thanked, in addition, for his ongoing co-operation and support of this project.

REFERENCES

Baer, A.J.
1973: Bella Coola-Laredo Sound map areas, British Columbia; Geological Survey of Canada, Memoir 372, 122 p.

Harland, W.B., Armstrong, R.L., Cox, A.V., Craig, L.E., Smith, A.G., and Smith, D.G.
1989: A Geologic Time Scale 1989; Cambridge University Press.

Monger, J.W.H.
1991: Georgia Basin Project: structural evolution of parts of southern Insular and southwestern Coast belts, British Columbia; in Current Research, Part A, Geological Survey of Canada, Paper 91-1A.

Monger, J.W.H., Price, R.A., and Tempelman-Kluit, D.J.
1982: Tectonic accretion and the origin of the two metamorphic and plutonic welts in the Canadian Cordillera; Geology, v. 10, p. 70-75.

Roddick, J.A. and Tipper, H.W.
1985: Geology of the Mt. Waddington map area; Geological Survey of Canada, Open File 1163.

Tipper, H.W.
1969: Geology, Anahim Lake map area, Geological Survey of Canada, Map 1202A.

van der Heyden, P.
1982: Tectonic and stratigraphic relations between the Coast Plutonic Complex and the Intermontane Belt, west-central Whitesail Lake map area, British Columbia; unpublished M.Sc. thesis, University of British Columbia, Vancouver, 172 p.
1989: U-Pb and K-Ar geochronometry of the Coast Plutonic Complex, 53°N to 54°N, British Columbia, and implications for the Insular-Intermontane superterrane boundary; unpublished Ph.D. thesis, University of British Columbia, Vancouver, 392 p.
1990: Eastern margin of the Coast Belt in west-central British Columbia; in Current Research, Part E, Geological Survey of Canada, Paper 90-1E, p. 171-182.

Wanless, R.K., Stevens, R.D., Lachance, G.R., and Delabio, R.N.
1979: Age determinations and geological studies: K-Ar ages, report A; Geological Survey of Canada, Paper 79-2, 67 p.

Wheeler, J.O. and McFeely, P.
1987: Tectonic assemblage map of the Canadian Cordillera and adjacent parts of the United States of America; Geological Survey of Canada, Open File 1565.

Woodsworth, G.J.
1980: Geology of Whitesail Lake (93E) map-area; Geological Survey of Canada, Open File 708.

Shallow structure and growth of the southern Fraser River delta: preliminary field results

Harry F.L. Williams[1] and John L. Luternauer
Cordilleran Division, Vancouver

Williams, H.F.L. and Luternauer, J.L., Shallow structure and growth of the southern Fraser River delta: preliminary field results; in Current Research, Part A, Geological Survey of Canada, Paper 91-1A, p. 85-90, 1991.

Abstract

Preliminary interpretations of lithofacies revealed by a series of drill cores from the southern part of the Fraser River delta are presented. Lithological evidence encountered in one of the cores indicates a fluvial origin for the subsurface deposits and suggests that a major distributary channel discharged into Boundary Bay prior to 5000 years ago. Two cores from the margin of a large peat bog reveal organic-rich silt, up to 4 m thick, underlying the surface peat deposits. The silt contains interbeds of peat and, in places, alternations of silt and fine sand. Similar lithology was observed in aggraded floodplain sediments underlying the northern part of the delta (Lulu Island). This raises the possibility that a mid-Holocene sea level rise induced a similar style of delta plain aggradation in the study area as occurred at the northern part of the delta. Samples have been submitted for micropalaeontological analyses and radiocarbon dating.

Résumé

Des interprétations préliminaires de lithofaciès révélés par une série de carottes de sondage provenant de la partie sud du delta du fleuve Fraser sont présentées. Des indices lithologiques recueillis dans l'une des carottes indiquent que les sédiments souterrains sont d'origine fluviatile et portent à croire qu'un important défluent se jetait dans la baie Boundary il y a plus de 5 000 ans. Deux carottes prélevées dans la bordure d'une grande tourbière révèlent l'existence d'un silt riche en matières organiques mesurant jusqu'à 4 m d'épaisseur sous la surface de la tourbe. Le silt contient des interstratifications de tourbe et, par endroits, des alternances de silt et de sable fin. On observe une lithologie semblable dans les alluvions de plaine d'inondation reposant sous la partie nord du delta (île Lulu). Ces observations soulèvent la possibilité qu'une hausse du niveau de la mer à l'Holocène moyen aurait provoqué un style semblable d'alluvionnement de plaine deltaïque dans la zone à l'étude, tel qu'il s'est produit dans la partie sud du delta. Des échantillons ont fait l'objet d'analyses micropaléontologiques et de datations au carbone radioactif.

[1] Department of Geography, University of North Texas, Denton, Texas 76203, U.S.A.

INTRODUCTION

As part of a continuing research effort on the structure and growth of the Fraser River delta, British Columbia, a series of drill cores was obtained along a north-south transect across the southern portion of the delta (Fig. 1). The specific objectives of the study are, firstly, to reconstruct the paleogeography of the delta; secondly, to more fully develop the lithostratigraphy of the southern part of the delta, especially in terms of the delta's depositional response to rising sea level during the Holocene; and, thirdly, to better establish the chronology of the delta's growth.

The results of this, and other such studies, have a number of important applications. Interpretation of the environment of deposition of sediments within the Fraser River delta, provides a means to track former sea level positions and thereby reconstruct local relative sea level history during the Holocene epoch. Documentation of sea level changes for this, and other sites along the Canadian west coast, is important for improving our understanding of the complex isostatic and eustatic adjustments that occurred at the close of the Late Wisconsinan Fraser Glaciation (Armstrong, 1981; Clague et al., 1982) and for exploring the possibility that potentially devastating megathrust earthquakes have occurred recently in this region, which is the most seismically active in Canada (Dragert and Rogers, 1988; Clague and Bobrowsky, 1990).

Previous studies on the northern portion of the delta (Lulu Island) have demonstrated that knowledge of the environment of deposition of subsurface deposits and their relative positioning and age, can be used to provide insights into the response of the deltaic depositional system to changes in sea level and the pattern of growth of deltaic deposits during the Holocene (Williams and Roberts, 1989).

On Lulu Island these studies have shown that this part of the delta aggraded in concert with sea level rise and that a substantial marine transgression did not occur. Consequently, much of the eastern part of Lulu Island is underlain by a thick sequence of floodplain deposits which formed during the episode of aggradation (Williams, 1988).

In contrast to Lulu Island, the pattern of growth of the southern portion of the delta remains largely unknown. The following questions remain to be answered: 1) did the southern delta undergo a period of aggradation similar to that which occurred on Lulu Island?; 2) did a major marine transgression occur in response to the Holocene sea level rise?; 3) how was sediment supplied to the growing Boundary Bay delta front?; 4) did the northern and southern portions of the delta grow concurrently, or did the growth of the southern part of the delta predate or postdate growth of Lulu Island? The answers to these questions will be of relevance to related fields of study, including geomorphology, geophysics, sedimentology and archaeology.

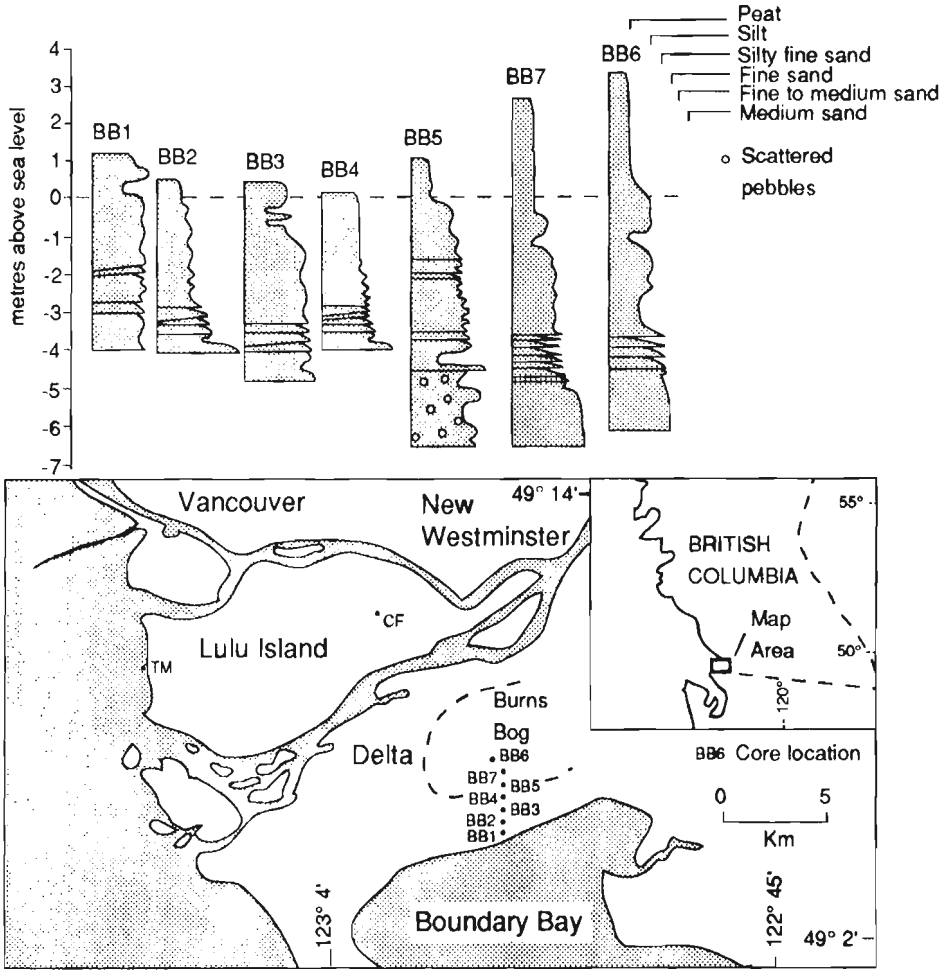

Figure 1. Location of core sites and core profiles (TM: Tidal marsh core site; CF: Channel fill core site — Fig. 2). Datum is mean sea level.

METHODS

Seven cores were obtained from the southeast part of the delta with a vibracorer, which provides continuous 7.5 cm diameter cores up to about 9 m in length. The following features were logged (visually) in the field: grain size and sorting, organic matter content, and sedimentary structures. Selected core samples were retained for laboratory analysis of their foraminifera and pollen contents, to aid in paleoenvironmental interpretation. Wood fragments and concentrations of organic material (such as buried peat layers) were retained for possible radiocarbon dating. Core profiles, levelled with respect to nearby benchmarks, are shown in Figure 1.

It is difficult to interpret the environment of deposition of subsurface deposits within the Fraser delta based on lithofacies characteristics alone. Cores from two contrasting environments, the tidal marsh bordering western Lulu Island and channel fill deposits from an abandoned distributary channel on Lulu Island (sites TM and CF respectively, Fig. 1), are presented for comparison (Fig. 2). These cores contain the major lithofacies types found within the topset deposits of the delta, with the exception of the peat bog facies (Williams, 1988; Williams and Roberts, 1989).

The tidal marsh core contains bioturbated, horizontally bedded, organic-rich silt in its upper part, representing the well-vegetated, upper-tidal marsh environment. Below this are interbedded silts and sands of the mid-tidal environment. Bedding within this part of the core is mainly horizontal, although some gently inclined bedding is also present. Some contacts between the silts and sands are gradational, whereas others are erosional — probably the result of shifting tidal channels. The lower part of the core contains clean fine to medium sand with shell fragments, deposited in the lower-tidal sand flat environment (Williams, 1986, 1988).

The channel fill core (Fig. 2) also fines upward into horizontally bedded organic-rich silt, representing delta top floodplain sedimentation (i.e. overbank flood deposits accumulated on the terrestrial delta plain). The remainder of the core is characterized by numerous erosional contacts, horizontal to gently inclined bedding, generally coarse-textured sediment and scattered gravel.

Unfortunately, the lithological characteristics outlined above, with the possible exception of sediment coarseness, are not sufficiently distinctive to allow deposits of these environments to be readily distinguished in core. Bioturbation, caused by burrowing organisms or root action, is present to a greater or lesser degree in most cores obtained from the delta, and so the bioturbation prevalent in the tidal marsh core is not in itself diagnostic. The shell fragments common in recent intertidal sediments, such as the lower part of the tidal marsh core, are only rarely encountered in older intertidal deposits within the delta, presumably due to poor preservation (Williams, 1989; Williams and Roberts, 1989). The alternating sand and silt beds, erosional contacts, and inclined bedding that characterize the fluvial channel fill deposits, can

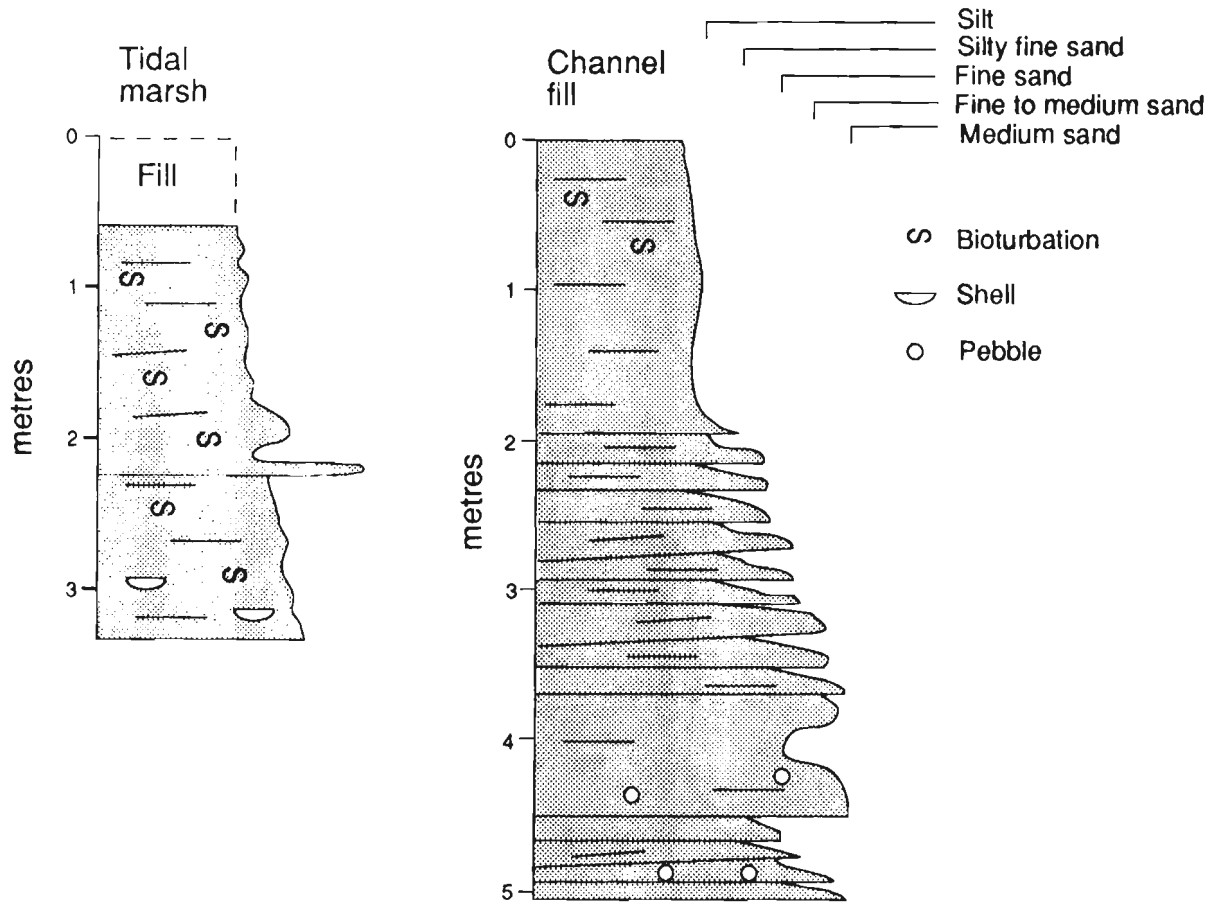

Figure 2. Core profiles: tidal marsh and channel fill deposits (see Fig. 1 for core site locations).

also be found in the mid-tidal environment, where the silty marsh deposits are encroaching on the sandy tidal flat environment (Fig. 3).

Due to these similarities in lithology, paleoenvironmental interpretation of Fraser delta core samples is best accomplished by incorporating additional evidence from microfossil analyses. Palynological and, to a lesser degree, foraminiferal studies, have helped in the interpretation of the environments of deposition of Lulu Island core samples, particularly where tidal marsh and delta top floodplain deposits are lithologically similar (Williams, 1989; Williams and Roberts, 1989; Clague et al., 1991; Williams and Hebda, in prep.).

SOUTHERN DELTA CORE DESCRIPTIONS AND INTERPRETATIONS

Cores BB1, BB2, BB3 and BB4 all contain interbedded silts and sands in their lower parts, which grade upwards to mostly horizontally bedded organic-rich silt (Fig. 1). As these lithofacies sequences are characteristic of both intertidal and channel fill deposits, a clear interpretation of the environment of deposition cannot be made without additional evidence from micropalaeontological analyses.

Core BB1 is unusual in that it contains a clear reversal in the usual fining upward trend — a silty clay layer at a depth of about 1 m is overlain by silty fine sand, which grades upwards into silt. This may represent a marine transgression caused by the Holocene rise in sea level, at least around the margin of Boundary Bay. We do not, however, have microfossil evidence to substantiate this. The silty fine sand layer may represent mid-tidal deposits which have migrated over the silty clay tidal marsh and/or delta top floodplain deposits. A similar sequence has been reported by Kellerhals and Murray (1969), who found tidal marsh peat overlain by mid-tidal sand in Boundary Bay, although this was attributed to subsidence of the delta rather than rising sea level.

The lower part of core BB5 contains well-defined erosional contacts, has the coarsest sediment encountered in any of the cores and is the only core to contain scattered pebbles, which are up to about 2 cm in diameter. Such relatively large pebbles may offer the first documented evidence of a major distributary channel that could have supplied sediment to the Boundary Bay delta front.

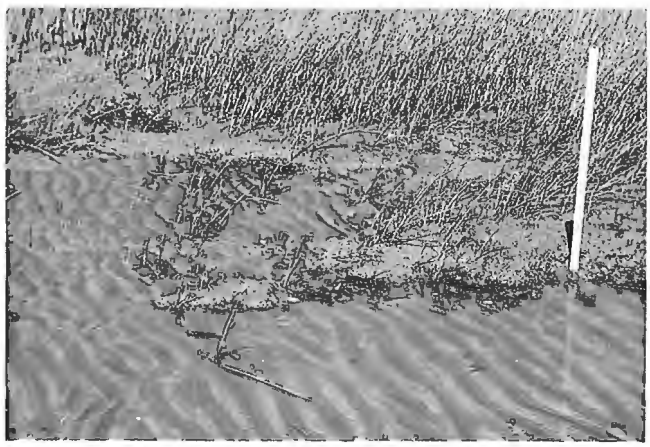

Figure 3. Vegetated tidal marsh silts encroaching on sandy tidal flat deposits in the mid-tidal zone of western Lulu Island (1 m rule for scale).

The location of core BB5 on the southern margin of Burns Bog (a domed peat bog covering much of the eastern part of the southern delta — Fig. 1) suggests that such a channel would be older than about 5000 years — the age of the base of the peat bog (Hebda, 1977). This suggests that growth of the Boundary Bay delta front was mostly completed prior to 5000 years ago, by which time the channel was presumably abandoned and the supply of Fraser River sediment was cut off.

Thick surface peat layers, part of the Burns Bog domed peat bog, in cores BB7 and BB6 grade into underlying horizontally bedded, organic-rich silt. The silt units of both these cores extend to a depth of about 4 m below sea level (bsl) and both contain a buried peat bed at about 1 m bsl (Fig. 1). The position of this peat bed relative to the ca 5000 year old surface peat bog, suggests that it may be correlative to a 6000 year old peat bed found below eastern Lulu Island (Williams, 1988; Williams and Roberts, 1990). However, the existence of more than one such peat bed cannot be precluded at this stage.

The organic-rich silt unit in core BB7 also contains well-defined, regular couplets of fine sand and silt. Each couplet has a sharp base overlain by fine sand which grades up into silt, and is commonly capped by organic detritus (Fig. 4A). A similar feature has been found in aggraded floodplain deposits underlying eastern Lulu Island (Fig. 4B).

Given the regularity of these silt-sand couplets, it is possible that they represent seasonal flood deposits associated with aggradation of the delta plain under conditions of a steadily rising sea level. The basal fine sand may represent sediment carried onto the terrestrial delta plain by large freshet floods, whereas the silt may represent deposits of smaller floods occurring throughout the remainder of the year. If this is the case, then each couplet represents one year of deposition. A count of the number of couplets in a 61 cm length of core revealed 78, giving an average sedimentation rate of 7.8 mm/year — which is comparable to the maximum rate of sedimentation of about 6-7 mm/year calculated for the Lulu Island aggraded floodplain deposits (Williams and Roberts, 1989).

The presence of the buried peat beds in cores BB7 and BB6, and the similarity between the silt units underlying the northern and southern parts of the delta, suggest that the southern portion of the delta may also contain aggraded terrestrial deposits, which formed in response to rising sea level. The overall lithofacies sequence in cores BB7 and BB6 is in fact very similar to that of cores from the margins of the peat bog on Lulu Island (e.g. Williams and Roberts, 1989, Fig. 5, core D26).

ONGOING ANALYSES

Laboratory analyses of the microfossil contents of selected core samples are being conducted to provide additional evidence on which to base paleoenvironmental interpretations.

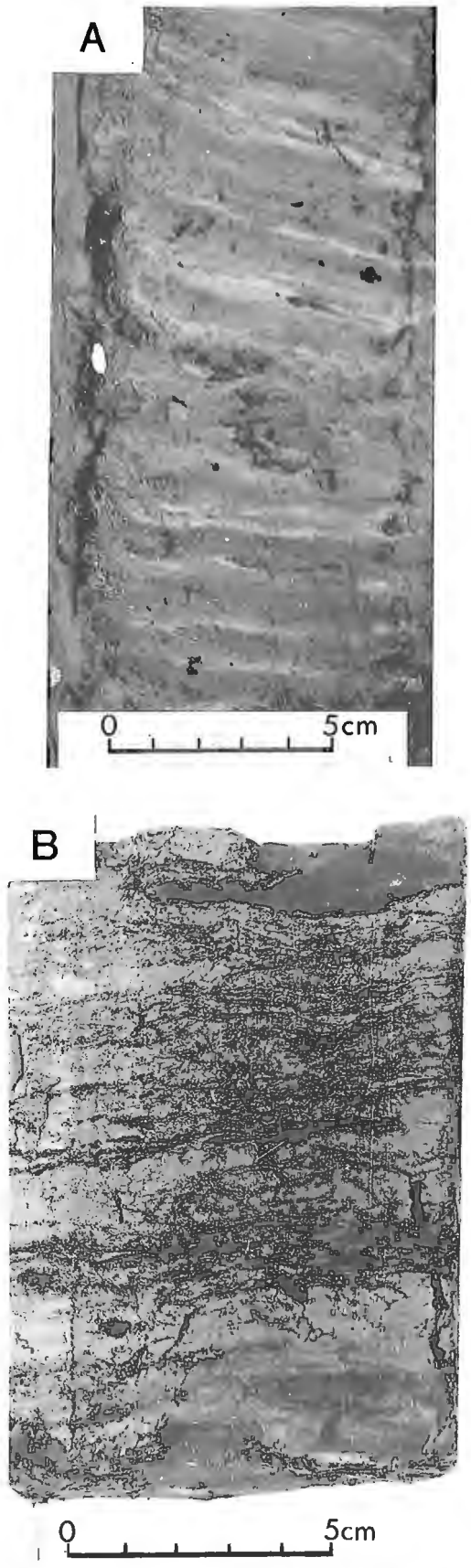

Figure 4 A. Silt-sand couplets 5.8 m below the surface in core BB7, presumably representing annual sediment accumulations. B. Aggraded delta top floodplain deposits in a core from eastern Lulu Island supplied by British Columbia Department of Highways.

Palynological analysis is being carried out on a set of samples from core BB7. Characteristic pollen and spore spectra have been used successfully to identify intertidal deposits in cores from Lulu Island and to distinguish between lithologically similar tidal marsh and delta top floodplain sediments (Williams, 1988; Williams and Hebda, in prep.).

Selected samples from cores BB1 through BB6 are also being examined for their foraminifera contents. This method has also been successfully employed in the study of Lulu Island core samples, primarily in the identification of intertidal sediments (Williams, 1989).

In order to provide a chronological framework for the sediments and allow attempts at correlation with Lulu Island deposits, three samples have been submitted for radiocarbon dating: a wood sample from core BB1 at a depth of 3.4 m below the surface; the buried peat bed from core BB6 at a depth of 4.32 m below the surface; and another wood sample, also from core BB6, at a depth of 4.88 m below the surface.

CONCLUSIONS

It is clear from the foregoing discussion that lithological evidence alone is often insufficient to provide unequivocal interpretations of the environment of deposition of subsurface deposits within the Fraser River delta. However, the combination of lithological and microfossil evidence has proved successful in the past and is expected to provide a means of interpreting the core samples obtained in this study.

The preliminary results from this study suggest that a hitherto undiscovered major distributary channel discharged into Boundary Bay prior to 5000 years ago, building the Boundary Bay delta front, which has remained relatively inactive since that time. The lithological similarities between the silt units underlying the northern and southern parts of the delta, suggest that rising sea level induced a similar style of delta top aggradation on the southern part of the Fraser delta as occurred on the northern portion of the delta.

ACKNOWLEDGMENTS

The authors wish to thank the Bremner family, J. Clague, A. Blais and R. Atkinson for help with the field work. M.C. Roberts is thanked for the loan of the vibracore equipment. R. Davidson helped prepare the illustrations.

REFERENCES

Armstrong, J.E.
1981: Post-Vashon Wisconsin Glaciation, Fraser Lowland, British Columbia; Geological Survey of Canada, Bulletin 322.

Clague, J.J. and Bobrowsky, P.T.
1990: Holocene sea level change and crustal deformation, southwestern British Columbia; in Current Research, Part E, Geological Survey of Canada, Paper 90-1E, p. 245-250.

Clague, J.J., Harper, J.R., Hebda, R.J., and Howes, D.E.
1982: Late Quaternary sea levels and crustal movements, coastal British Columbia; Canadian Journal of Earth Sciences, v. 19, p. 597-618.

Clague, J.J., Lichti-Federovich, S., Guibault, J.-P., and Mathewes, R.W.
1991: Holocene sea level change, south-coastal British Columbia; in Current Research, Part A, Geological Survey of Canada, Paper 91-1A.

Dragert, H. and Rogers, G.C.
1988: Could a megathrust earthquake strike southwestern British Columbia?; Geos, v. 17, p. 5-8.

Hebda, R.J.
1977: The paleoecology of a raised bog and associated deltaic sediments of the Fraser River delta; unpublished Ph.D. thesis, University of British Columbia, Vancouver.
Kellerhals, J. and Murray, J.W.
1969: Tidal flats at Boundary Bay, Fraser River delta, British Columbia; Bulletin of Canadian Petroleum Geologists, v. 17, p. 67-91.
Williams, H.F.L.
1986: Depositional facies and evolution of Lulu Island topset deposits, Fraser River delta, British Columbia; in Current Research, Part A, Geological Survey of Canada, Paper 86-1A, p. 559-564.
1988: Sea-level change and delta growth: Fraser delta, British Columbia; unpublished Ph.D. thesis, Simon Fraser University, Burnaby, B.C.
1989: Foraminiferal zonations on the Fraser River delta and their application to paleoenvironmental interpretations; Paleogeography, Paleoclimatology, Paleoecology, v. 73, p. 9-50.
Williams, H.F.L. and Roberts, M.C.
1989: Holocene sea level change and delta growth: Fraser River delta, British Columbia; Canadian Journal of Earth Sciences, v. 26, p. 1657-1666.
1990: Two Mid-Holocene marker beds in aggraded floodplain deposits, Fraser River delta, British Columbia; Géographie Physique et Quaternaire, v. 44, p. 27-32.

Preliminary fluid inclusion and petrographic studies of parts of the Sullivan stratiform sediment-hosted Pb-Zn deposit, southeastern British Columbia

Craig H.B. Leitch
Mineral Resources Division, Vancouver

Leitch, C.H.B., Preliminary fluid inclusion and petrographic studies of parts of the Sullivan stratiform sediment-hosted Pb-Zn deposit, southeastern British Columbia; in Current Research, Part A, Geological Survey of Canada, Paper 91-1A, p. 91-101, 1991.

Abstract

Preliminary fluid inclusion and petrographic studies on parts of the Sullivan deposit have identified at least 5 different fluids trapped within quartz, carbonate, albite and cassiterite. Fluids trapped in pseudosecondary inclusions of possible pre- or syn-metamorphic age include (1) liquid-rich very high-temperature and high-salinity aqueous (415°C, 35-40 wt. % NaCl equivalent), (2) liquid-rich moderate temperature and salinity aqueous (275 and 200°C, 10-20 wt. % or 5 wt. % NaCl equivalent), (3) transitional (315°C, 5 wt. % NaCl equivalent with moderate CO_2 and minor CH_4) and (4) vapour-rich carbonic (300°C, 5 wt. % NaCl equivalent with major CO_2 and minor CH_4). Fluids trapped in secondary inclusions of probable post-metamorphic age are (5) liquid-rich low-temperature (105-130°C, 10-20 wt. % NaCl equivalent).

Résumé

Des études préliminaires sur les inclusions fluides et la pétrographie de certaines parties du gisement Sullivan ont permis d'identifier au moins cinq fluides différents piégés au sein du quartz, des roches carbonatées, de l'albite et de la cassitérite. Les fluides piégés dans des inclusions pseudosecondaires d'âge probablement prémétamorphique ou synmétamorphique sont notamment (1) aqueux, à température très élevée et forte salinité, à haute teneur en liquides (415°C, 35-40 % poids d'équivalent de NaCl), (2) aqueux, à salinité et température moyennes, à haute teneur en liquides (275 et 200°C, 10-20 % poids ou 5 % poids d'équivalent de NaCl), (3) transitoires (315°C, 5 % poids d'équivalent de NaCl avec teneur moyenne en CO_2 et faible teneur en CH_4) et (4) carbonique à haute teneur en vapeurs (300°C, 5 % poids d'équivalent de NaCl avec teneur importante en CO_2 et faible teneur en CH_4). Les fluides piégés dans des inclusions secondaires d'âge probablement postmétamorphique présentent (5) une basse température et ont une forte teneur en liquides (105-130°C, 10-20 % poids d'équivalent de NaCl).

INTRODUCTION

The Sullivan deposit has been the subject of extensive studies by Cominco staff and other researchers (Hamilton et al., 1982). However, there is still little information on the character of the mineralizing fluids at Sullivan. Therefore, reconnaissance petrographic studies were initiated to locate suitable fluid inclusions and to understand their paragenetic setting, especially in the fossil hydrothermal upflow zone. Previously, temperatures of mineralization (?of metamorphism) have been estimated by (1) fluid inclusions (200-250°C: Shaw and Hodgson, 1986); (2) mineral equilibria: biotite-garnet = 400-450°C, arsenopyrite-pyrite-pyrrhotite = 430-460°C; (3) O isotopes of coexisting magnetite-quartz assemblages: 400-560°C (Ethier et al., 1976); (3) S isotopes: 250-550°C, mean 340, or 210-500, mean 300, using alternate equations for fractionation (Campbell et al., 1978). Pressure of mineralization (?of metamorphism) has been estimated by the sphalerite-pyrrhotite-pyrite equilibria, which suggests 5 kb or 19 km depth. This is unlikely; Edmunds (1977) estimated maximum burial of 5.8-7.6 km or 2 kb, so it seems likely that the sphalerite has reequilibrated with monoclinic pyrrhotite and pyrite at 250°C (Ethier et al., 1976). The 90°C difference between fluid inclusion and mean S isotope temperatures suggests a pressure correction of about 1 kb (Roedder, 1984). The only previous information on the composition of the ore fluid is a salinity of 22-29 wt. % NaCl equivalent (Shaw and Hodgson, 1976); the possible presence of CO_2, CH_4 and (K-Ca-Mg)Cl has not been described.

SAMPLING AND ANALYTICAL PROCEDURE

The current study is limited to existing collections held by R.J.W. Turner (Mineral Resources Division, Vancouver) and the University of British Columbia (Table 1). Samples include 7 thin, 7 polished and 11 polished thin sections from (1) arsenopyrite and cassiterite veins cutting tourmalinite, and (2) massive pyrrhotite (±pyrite) and chlorite, both from below the orebody; (3) albite-chlorite-pyrite alteration above the orebody; (4) laminated pyritic ore from the southeastern fringe of the deposit; and (5) laminated galena-sphalerite ore. Following initial petrographic studies, 8 samples were chosen for fluid inclusion investigations from which 100 micron doubly-polished "thick" sections were prepared by standard methods (Holland et al., 1978). A USGS gas-flow heating and freezing stage, calibrated in accordance with the manufacturer's recommendations, was used to make microthermometric measurements. The accuracy when so calibrated is better than ±0.4°C from −56.6 to +660.4°C (T.J. Reynolds, pers. comm. and unpublished manuscript, 1988). Precision was estimated by replicate measurements to be ±1 % up to 200°C and ±2 % from 200 to 500°C. Inclusions in both quartz and carbonate were subjected to freezing measurements first, to avoid stretching and false homogenization temperatures; inclusions in carbonate could not be heated first because they were found to decrepitate.

CLASSIFICATION AND DESCRIPTION OF FLUID INCLUSIONS

Fluid inclusions suitable for microthermometry were found in all samples except the laminated ore. Fluid inclusions are found mainly in quartz, but also in carbonate, albite, and cassiterite. Solid inclusions but no fluid inclusions were found in sphalerite (Fig. 1A and 1B). Inclusions were classified as primary, pseudosecondary and secondary by the criteria in Roedder (1984). There are no obviously primary inclusions in growth zones, although large isolated inclusions (15-30 μm diameter) do occur. Most inclusions occur in groups or along microfractures that do not cross grain boundaries and are pseudosecondary. A few are in distinctly planar arrays that cross grain boundaries and have decrepitation temperatures (150-160°C) well below metamorphic temperatures; these must be secondary inclusions.

There is a wide variety of fluid inclusions in the samples from the Sullivan deposit (Table 2 and Fig. 1). The pseudosecondary inclusions are divided into two groups: (1) common liquid-rich, two-phase aqueous inclusions and (2) less common vapour-rich, three-phase carbonic, or CO_2-CH_4 bearing, inclusions. Associated with the latter are rare inclusions of a transitional group with intermediate characteristics. Although the liquid-rich and vapour-rich inclusions commonly occur immediately adjacent to each other, they have not been seen in the same microfracture.

The fluid inclusions selected for measurement in this study range from 3 to 45 μm in diameter, although most are between 5 and 10 μm. In quartz, inclusion shapes vary from small irregular or "star" shapes in Type 1 (Fig. 1C) to small or large regular, "star" or negative-crystal shapes in Type 2 (Fig. 1D, 1F) to larger, tear-drop or ovoid shapes in Type 3 and 4 (Fig. 1F, 1G, 1H). Type 2a inclusions in cassiterite and in calcite are commonly negative crystal shapes (Fig. 1J and 1K). Type 5 secondary inclusions have small rounded shapes in both quartz and albite (Fig. 1D, 1E).

Daughter minerals, probably all halite by their cubic shape, are seen in all Type 1 (Fig. 1C) and some Type 2a inclusions, where their size indicates salinities of 35-40 and 25-35 wt % NaCl equivalent respectively (Roedder, 1984).

In the liquid-rich inclusions, there is a trend of decreasing vapour to liquid ratio from Type 1 to 2a to 2b (from 15-20 % to 10-15 % to 10 %). Vapour-rich Type 4 inclusions (Fig. 1F, 1G, 1H) range from 70-100 %, averaging 90 %, whereas transitional Type 3 range from 30-60 %, averaging 40 %. Vapour to liquid ratios were estimated as areal percent at 25°C, and converted to volume percent (Hollister et al., 1981).

A striking feature in the Sullivan samples is the widespread presence of auto-decrepitated inclusions, especially those having a secondary habit (Fig. 1L, 1M). The significance of these abundant decrepitated inclusions is discussed below.

MICROTHERMOMETRY

Final homogenization temperatures

Microthermometric measurements are summarized by inclusion type in Table 2. Homogenization temperatures for all the pseudosecondary inclusions (two and three-phase) range from 165 to 465°C, with well-defined modes at about 200, 300 and 415°C for Type 2b, 2a and 1 inclusions respectively. Most of these inclusions homogenize to liquid. Type

Table 1. Summary of samples for petrographic study, Sullivan deposit

SAMPLE[1]	Ore Type[2]	Mineralogy[3]	Special Features
SULIV 1	HW albite	ab-ch-sp-ap-qz py (TS only)	Chlorite replaces biotite and muscovite
SULIV 2	HW albite	ab-qz-ch-sp-ca py	Fluid inclusions in quartz and albite
SULIV 3	HW High-Fe core zone	ca-qz py-sl-gn (TS only)	Rare fluid inclusions in calcite
SULIV 4	Pyrite-rich massive ore	qz-ms-ch-hbi-ca-gt py-po-gn-sl-cp-ru-il	Many fluid inclusions (possibly metamorphic)
83SVT6	Distal Main pyrrhotite	ca-qz-ch-hbi-ms-gt po-py-mt-sl-gn	Fluid inclusions in calcite (?metamorphic)
83SVH5	FW fragmental chlorite rock	qz-bi-gt-ms-chl-tm po-gn-sl-pb-bl-il-ru	Qz mainly detrital; bi is chloritized (±sx)
83SVH6	FW fragmental pyrrhotite	qz-ba-ca-tr-ap-px po-gn-cp-as-tt-pb-sl	Included barite, apatite, tremolite, diopside
85SVT1 G-13-30	FW fragmental tourmalinite	qz-tm-ms-sp-zr py? (TS only)	Darkening of tourmaline along fractures
85SVT3 P-10-4	FW tourmalinite	tm-qz-sp-ru po-as-il-cp-bl-Bi	?2 generations of rutile (il to ru, po to as)
85SVT3A P-10-4	FW foliated chlorite rock	ch-ca-bi-sp-zr po-gn-sl-cp-ru-il	Coarse sphene, wispy foliated sx
89SVT3 #2Cutout	FW alteration	qz-gt-ep-ms-ch	Porphyroblastic garnet and ?chloritoid
89SVT9	FW chlorite-pyrrhotite	ch-qz-ms-sp-ca-tr-zr po-sl	Fluid inclusions in quartz
89SVT15 R-10	FW massive pyrrhotite	qz-ca?-mt (PS only) po-gn-sl-cp-tt-bl-as	Massive po replacement ("wispy" texture)
89SVT20 3259Xcut	FW massive pyrrhotite	qz-ca? (PS only) po-sl-gn-tt-as-cp-bl	Other minerals as inclusions in po
89SVT23	FW conglomerate	qz-ms-bi-gt-ca-ep po (TS only)	Protolith control on metamorphic assemblage
89SVT28	Laminated ore (Mid-"A" band)	qz-ms-ca-ap sl-gn-po-bl-jm	Abundant ?apatite, high content of Sb-minerals
89SVR1	FW tin zone (cassiterite)	tm-qz-cs as-po-gn-bl-tt-cp-Bi-pg	Many fluid inclusions in cassiterite; note sxsalt
SUL13	SE fringe bedded pyrite	qz-ch-ms-bi-gt py-po-sl-mt-gn-cp	Very fine-grained almost framboidal pyrite
E9303	Laminated ore (Main band)	qz-ch-ms-sp-ba sl-gn-po	Fluid inclusions in qz not in F.I. section
G79SL4	FW tourmalinite	tm-qz-ms-ca-sp-il-ru-hm as-po-py-mc-gn-cp-bl	High-T fluid inclusions in qz-as vein

[1] Designation is by year of collection (79, 83, 85, 89) and collector (T = R.J.W. Turner, H = G. Hahn, R = P. Ransom, G = C.I. Godwin). Samples SULIV 1, 2, 3, 4, SUL13, and E9303 are from UBC 'E' (Economic Geology) Collection and/or Geology 418/428 collections. Boldface indicates sample chosen for fluid inclusion microthermometry. Detailed location in the mine (where known) is underlined.

[2] Abbreviations: HW = hanging wall, FW = footwall, SE = southeast.

[3] Minerals are listed in approximate order of decreasing abundance. Abbreviations: TS = thin section, PS = polished section, F.I. = fluid inclusion (doubly polished) section; sx = sulphides, sxsalt = sulphosalt. Underlined minerals have a potential for radiometric dating.

Transparent minerals are: ab = albite, ap= ?apatite, ba = ?barite, bi = biotite, ca = carbonate, ch = chlorite, ep = epidote, gt = garnet, hbl = hydrobiotite, ms = muscovite, px = pyroxene, qz = quartz, sp = sphene, tm = tourmaline, tr = ?tremolite, zr = zircon.

Opaque minerals are: as = arsenopyrite, Bi = ?Bi-sulphosalt, bl = ?boulangerite, cs = cassiterite, cp = chalcopyrite, gn = galena, hm = hematite, il = ilmenite, jm = ?jamesonite, mc = marcasite, mt = magnetite, pb = ?pearcite-polybasite, pg = ?pyrargyrite, po = pyrrhotite, py = pyrite, ru = rutile, sl = sphalerite, tt = tetrahedrite-tennantite. Question marks indicate optical determination only.

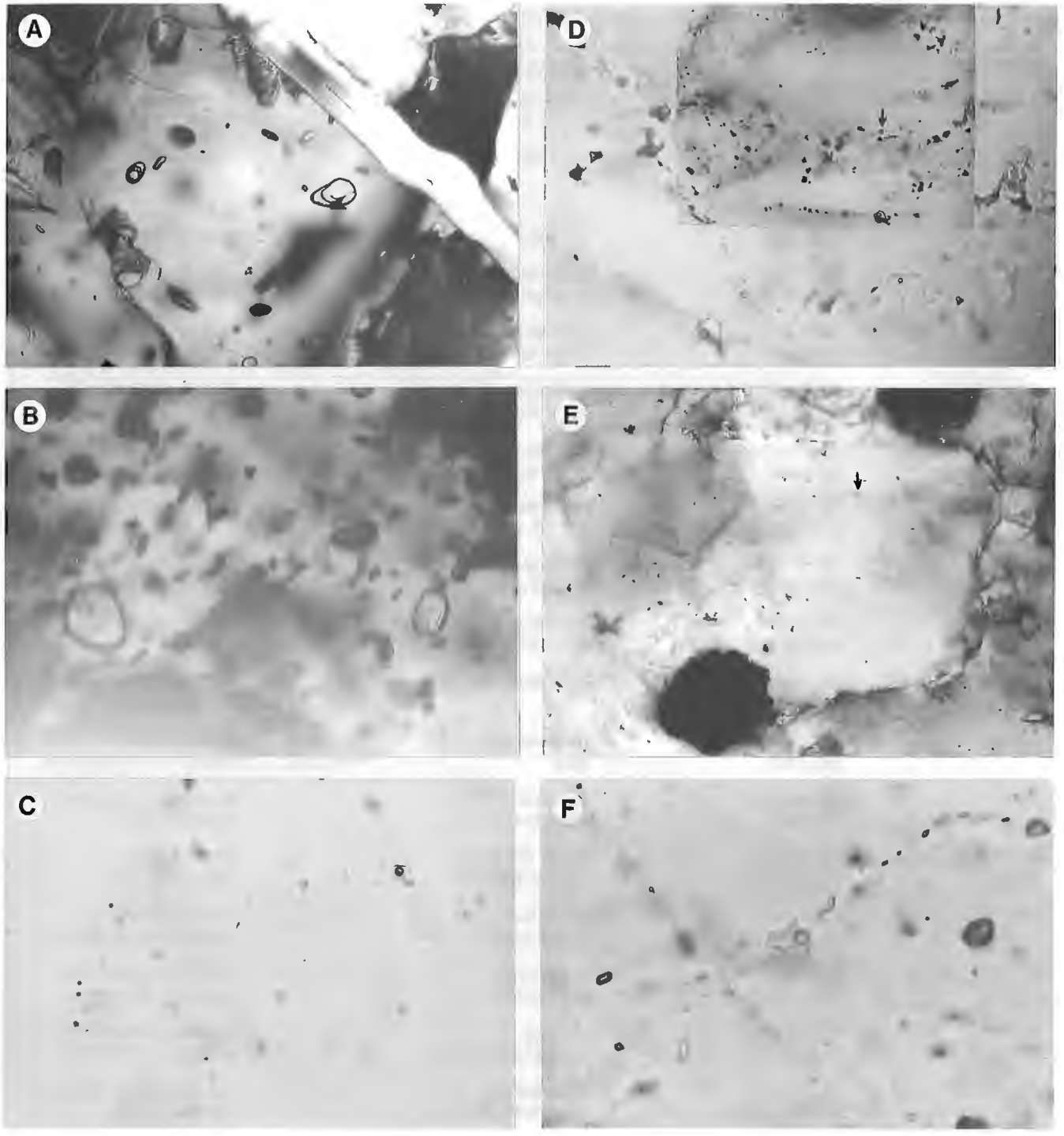

Figure 1. Photomicrographs of fluid inclusions in specimens from the Sullivan deposit. All photos taken in transmitted light, uncrossed polars.

A and **B)** Solid inclusions in sphalerite from massive chlorite-pyrrhotite below the orebody that appear to contain a flat, angular daughter mineral and an inner vapor bubble. Sample 89SVT9, width of field of view is 130 μm.

C) Type 1 high-T, high salinity fluid inclusions containing halite daughter crystal, in quartz from arsenopyrite vein cutting tourmalinite, sample G79SL4. Largest inclusion is 7 μm long.

D) Type 2b and rare Type 2a (inset, arrowed) moderate-T, moderate salinity fluid inclusions in quartz from sample SULIV 2 from hanging wall albite-chlorite-pyrite-quartz alteration. Note how arrays of inclusions do not cross grain boundaries, and are therefore probably pseudosecondary. Arrowed inclusion is 10 μm long.

E) Secondary Type 5 (low-T, moderate salinity) fluid inclusions in albite, also from SULIV 2. Longest inclusion (arrowed) is 7 μm.

F) Type 2 two-phase, aqueous liquid-rich (large star-shape and smaller regular shapes along microfractures) and Type 4 three-phase, carbonic vapour-rich (dark) fluid inclusions in quartz from massive pyritic ore, sample SULIV 4. Largest inclusion is 15 μm across.

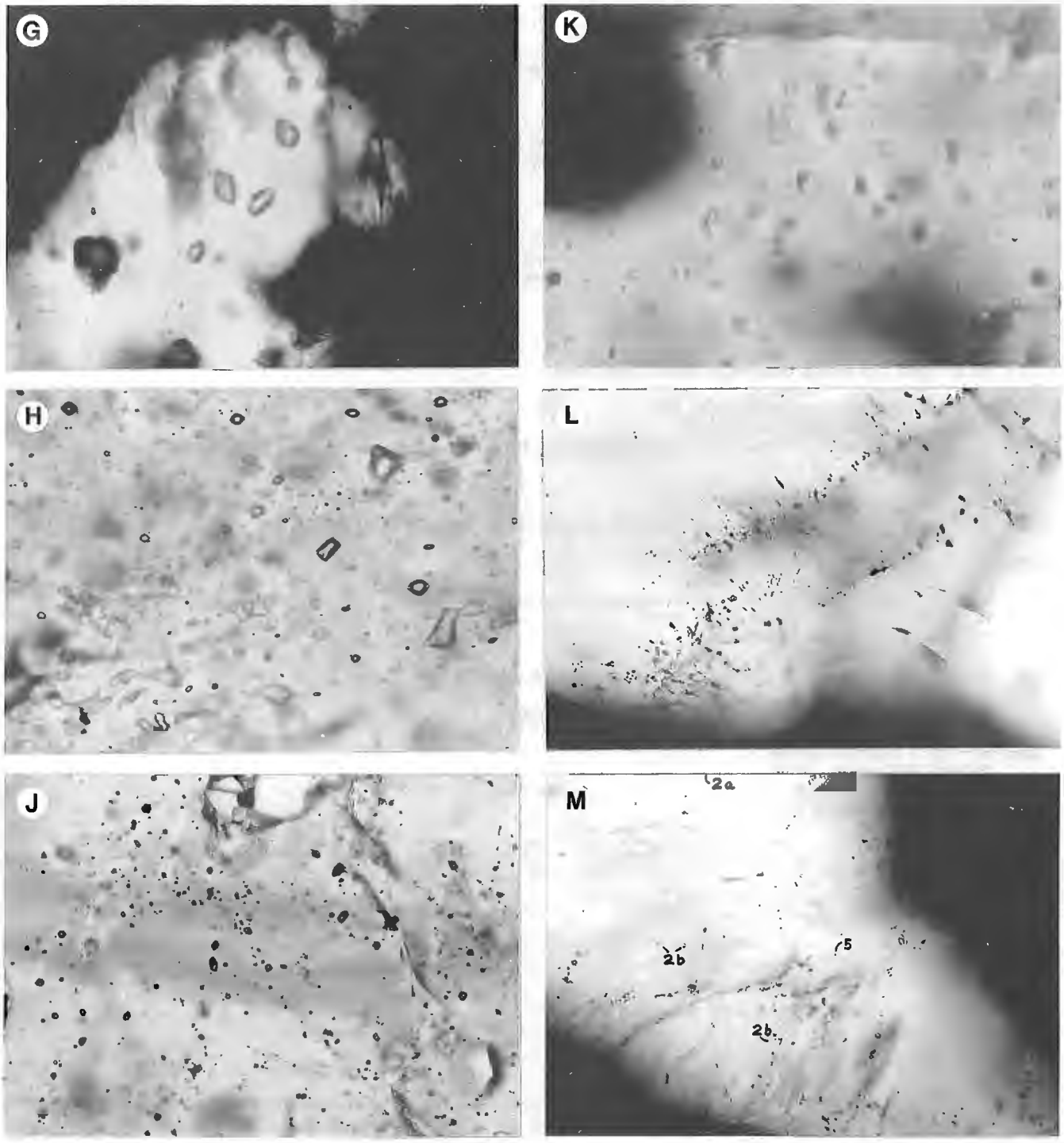

G) Type 4 three-phase, vapour-rich fluid inclusions containing outer aqueous liquid, inner carbonic (CO_2 + CH_4) liquid, and innermost carbonic vapor bubble. In quartz from sample SULIV 4; largest inclusion is 28 μm long.

H) Abundant Type 2a two-phase liquid-rich, moderate T and low salinity (large, irregular shapes) and Type 4 three-phase vapour-rich, moderate to high T and low salinity fluid inclusions in sample SULIV 4. Largest inclusion is 45 μm long. These inclusions, and those shown in F and G, could be metamorphic in origin.

J) Swarms of Type 2a pseudosecondary fluid inclusions with strong negative crystal shape in cassiterite, with quartz inclusions and associated arsenopyrite, in sample 89SVR1 from the tin zone. These inclusions have salinities of about 10 wt% NaCl equivalent and traces of CO_2 which were detected by clathrate melting at +6°C. The largest fluid inclusion is about 10 μm long.

K) Rhombic, 5 μm diameter Type 2a (moderate T, low salinity of <5 wt. %) fluid inclusions in carbonate, sample 83SVT6 from the massive pyrrhotite body. There are traces of CO_2 detected by clathrate melting of around +9°C, and $CaCl_2$ ± KCl may be present in addition to NaCl.

L and **M)** Trails of decrepitated secondary or pseudosecondary fluid inclusions in quartz from hanging wall albite-chlorite alteration, sample SULIV 2. Undecrepitated inclusions are labelled as to type in M; field of view is about 300 μm across in both photos.

Table 2. Summary of fluid inclusion characteristics, Sullivan deposit

Pseudosecondary

Liquid-rich: Type 1 Two-phase aqueous
(H_2O-NaCl-?KCl), salinity = 35-40%
Th: range 367-465, average 415 (n=11). Most homogenize to liquid, rarely to vapour (decrepitate)
Tm: at eutectic (−20 to −23) or metastable eutectic (−29 to −35)
V/V+L: 15-20%, 3-10 um size, "star" shaped, halite daughter

Type 2a Two-phase aqueous
(H_2O-NaCl), salinity = 25-35% or 10-20% or 3-5%
Th: range 238-319, average 275 (n=43). Most homogenize to liquid, rarely to vapour
Tm: at eutectic (−20), or −17 to −7.4 or −1.9 to −4.5 (Tm_c=+6 to +9)
V/V+L: 10-15%, 2-16 um size, small regular negative crystal shapes

Type 2b Two-phase aqueous
(H_2O-NaCl-?KCl), salinity = 15-20% or 3-5%
Th: range 165-237, average 200 (n=46). All homogenize to liquid
Tm: range −17 to −10 or −2.0 to −2.8, eutectic −23 to −20
V/V+L: 10%, 3-23 um size, small regular negative crystal shapes

Transitional: Type 3a Three-phase aqueous ($\pm CO_2$, CH_4)
(approximately $.55H_2O/.35CO_2/.05CH_4/.05NaCl$)
Th: range 308-327, average 315 (n=10) or range 400-435, average 415 (n=4). All homogenize to vapour (or decrepitate)
Th_{CO2}: either +7.8 or +27 to +31
Tm_c: range +7.9 to +10.1, average 8.5
Tm_{CO2}: range −57.6 to −57.1, average −57.4
V/V+L: range 30-60, average 40%, 5-14 um size, small, tear-drop shaped or negative crystal shapes

Vapour-rich: Type 4 Three-phase carbonic
(approximately $.05H_2O/.85CO_2/.05CH_4/.05NaCl$)
Th: range 220-425, average 300 (n=17). All homogenize to vapour (rarely decrepitate)
Th_{CO2}: either +7.8 (vapour) or +24 to +31 (liquid)
Tm_c: range +8.4 to +10.4, average 9.0
Tm_{CO2}: range −59 to −56.6, average −58
V/V+L: range 70-100, average 90%, 5-45 um, large, irregular, oval or negative crystal shapes

Secondary

Liquid-rich: Type 5 Two-phase aqueous
(H_2O-NaCl-?KCl), salinity 10-20%
Th: range 85-105, average 95 (n=6 in quartz) or 124-141, average 130 (n=6 in albite)
Tm: -17 to −7.5, eutectic −20 to −34
V/V+L: 5-10%, 3-8 um size, small, irregular to rounded shapes

Abbreviations: Th = final homogenization temperature, Th_{CO2} = homogenization temperature of CO_2, Tmc = melting temperature of clathrate, Tm = final melting temperature of ice, Tm_{CO2} = final melting temperature of CO_2, V/V+L = ratio of vapour bubble to liquid at 25°C, um = micron, n = number of measurements. All temperatures in °C.

3 and 4 three-phase inclusions, which are vapour-rich, contain significant CO_2 + CH_4, and homogenize to vapour at about 300°C (range 220-425) or less commonly decrepitate, making determination of homogenization temperature difficult. Homogenization temperatures for secondary inclusions (all to liquid) range from 85 to 141°C, with modes at 95°C for inclusions in quartz and 130°C for inclusions in albite.

CO_2 homogenization temperatures

Homogenization temperatures for the carbonic portion of Type 3 and 4 inclusions vary from +7.8 to +31.1°C, all to liquid. There are several modes within this range, at +7.8 for a few Type 3 inclusions, +16.8 to 20.5 (average +18.0) for a few Type 4 inclusions, and +24 to +31.1 (average +28.5) for most Type 4 inclusions. These indicate densities of the carbonic fluid of 0.89, 0.83 and 0.75 g/cm^3 respectively (Roedder, 1984).

Ice and clathrate melting temperatures

Salinities are also widely variable, ranging from less than 5 up to 40 wt. % NaCl equivalent (hereafter abbreviated to simply %). Type 1 inclusions are the most saline (35-40 %), as indicated above. Ice melting at the eutectic (−20 to −23°C) or metastable eutectic (−29 to −39°C) suggests possible KCl in addition to NaCl (Davis et al., 1988).

Type 2 inclusions have the most variation in salinity, with a general trend (Table 2) of decreasing salinity with decreasing homogenization temperature from Type 2a (25-35 %) to 2b (15-20 %). However, there are two other groups of differing salinities included with Type 2a on the basis of their homogenization temperatures; these have lower (10-20 %) and very low (<5 %) salinities. Ice melting for moderate to high salinity Type 2a and 2b is at the eutectic (−20 to −23°C) or metastable eutectic (−55 to −29°C), indicating possible KCl and/or $CaCl_2$ present with NaCl. Ice melting for the low-salinity Type 2a inclusions is generally −2 to −3°C, with eutectic/metastable eutectics at −20 to −39°C (rarely −49°C) also indicating the possible presence of KCl and/or $CaCl_2$.

Type 3 and 4 (carbonic) inclusions have low salinities of <5 %, as shown by clathrate melting temperatures of +7.9 to +10.4°C (averages +8.5 and +9.0°C, respectively). Both types contain another gas in addition to CO_2, probably CH_4, as indicated by depression of the CO_2 melting point (see below). The presence of CH_4 opposes the depression of clathrate melting from 10.0°C; therefore the actual salinities are approximated by plotting clathrate melting temperatures versus CO_2 melting temperatures and extrapolating to the clathrate melting temperature corresponding to pure CO_2 (Linnen, 1985). Ice melting temperatures of −7 to −10°C, that are depressed by the withdrawal of water during clathrate formation, and therefore give erroneous salinities (Collins, 1979) are only rarely observed in these inclusions. Rarely observed eutectic or metastable eutectic temperatures of −39 to −22°C suggest that there may be minor KCl present with the NaCl in these vapour-rich inclusions.

CO_2 melting temperatures

The carbonic (CO_2+CH_4) portion of Type 3 and 4 inclusions freezes at −93 to −98°C, and the depression of the melting point below that of pure CO_2 at −56.6°C indicates the presence of another gaseous component, most probably CH_4. The depression is slightly greater for Type 4 inclusions (−58°C) than for Type 3 inclusions (−57.4°C), indicating slightly greater concentrations of CH_4 in the former. Due to the much greater proportion of vapour in Type 4, they are also much richer in CO_2, with about 85 % CO_2 and 5 % CH_4, whereas Type 3 contain perhaps 35 % CO_2 and <5 % CH_4.

PETROGRAPHY

The petrography of 20 samples was studied in detail to aid in interpretation of the fluid inclusion data (Table 1 and Fig. 2). Emphasis was placed on samples from the footwall zones, where hydrothermal processes are expected to have left the best imprint. Fluid inclusions are not common in the bedded ores examined to date, and none have been found in sphalerite.

Hanging wall alteration

Hanging wall alteration is characterized by a zone of massive "albitite" (albite-chlorite-quartz-pyrite: Hamilton et al., 1982). Samples SULIV 1 and 2 from this zone above the orebody contain abundant sphene and apatite, which may be suitable for radiometric dating. Fluid inclusions in quartz are almost entirely Type 2b, moderate temperature and salinity (200°C and 15-20 % NaCl). Rare inclusions of Type 1 and 2a (higher temperature, higher salinity) are found, and there are secondary (Type 5) very low temperature, moderate salinity inclusions (95-130°C, 10-20 % NaCl) in both quartz and albite (Fig. 1E).

An unlocated sample of semi-massive pyrite and calcite with minor sphalerite and galena that likely comes from the pyritic portion of the orebody, contains only rare fluid inclusions in the carbonate. These inclusions have small negative crystal (rhomb) shapes to 8 μm long and vapour to liquid ratios of about 20 %. Although not subjected to microthermometry, they are similar to inclusions in carbonate in sample 89SVT6 (see below) that may be metamorphic in origin.

Footwall alteration

Footwall alteration includes early, lower temperature tourmalinite (Nesbitt et al., 1984), later, higher temperature chlorite-pyrrhotite-pyrite (Shaw and Hodgson, 1986), and finally highest temperature arsenopyrite-chalcopyrite-sulphosalt (this study). Samples from the footwall zone include footwall alteration (89SVT3) and footwall conglomerate (89SVT23), tourmalinite (85SVT1, 85SVT3, G79SL4), foliated or fragmental chlorite rock (85SVT3A, 85SVH5), chlorite-pyrrhotite rock (89SVT9), massive and fragmental pyrrhotite (83SVT6, 83SVH6, 89SVT15, 89SVT20), and pyritic high-iron core zone (SULIV 3). There are also samples of the footwall tin zone (89SVR1).

Alteration in the footwall zone (89SVT3) has been metamorphosed in the specimen studied to a quartz-garnet-epidote-muscovite-chlorite assemblage. Fragmental rocks in the footwall (89SVT23) have an assemblage similar to that in 89SVT3 and appear to have exerted a protolith control on the metamorphic assemblage (Fig. 2A).

The tourmalinite samples contain sphene and minor zircon, rutile and apatite, possibly suitable for radiometric dating (Fig. 2B). However, there may be two generations of rutile present, one of detrital origin with quartz, and the other formed by hydrothermal alteration of ilmenite. Darker, more schorl-rich tourmaline along fractures may indicate a late stage, more Fe-rich fluid. This may be similar to late-stage, possibly more Fe-rich chlorite also seen in footwall rocks (see below).

Pyrrhotite replacements are noted to "bed out" into adjacent finely laminated tourmalinite, or replace laminations in fragments of tourmaline. Cross-cutting this pyrrhotite are arsenopyrite-quartz veins (G79SL4, 85SVT3) that contain lesser pyrite, pyrrhotite, marcasite, chalcopyrite and boulangerite and have ilmenite, rutile, sphene and carbonate in their envelopes (Fig. 2C). The association of arsenopyrite with sulphosalts, including a possible Bi-bearing phase, is noteworthy, and is seen elsewhere (Fig. 2D, from tin zone sample 89SVR1). Quartz in these veins (G79SL4) hosts several types of fluid inclusions, notably very high-T, high-salinity Type 1 but also Type 2, and Type 5 secondary inclusions. The temperatures of the Type 1 inclusions (up to 450°C) and their very high salinity are more typical of a porphyry-copper environment (T.J. Reynolds, pers. comm., 1990). Reasonable pressure corrections for the depth of cover postulated by Edmunds (1977; see above) would be 1.75 kb, or 225°C (Figure 9-4 of Roedder, 1984). This would imply trapping temperatures of 675°C for the Type 1 inclusions. It is therefore unlikely that these inclusions are of metamorphic origin (temperature at the biotite-garnet greenschist grade indicated at Sullivan is 450°C; Winkler, 1971).

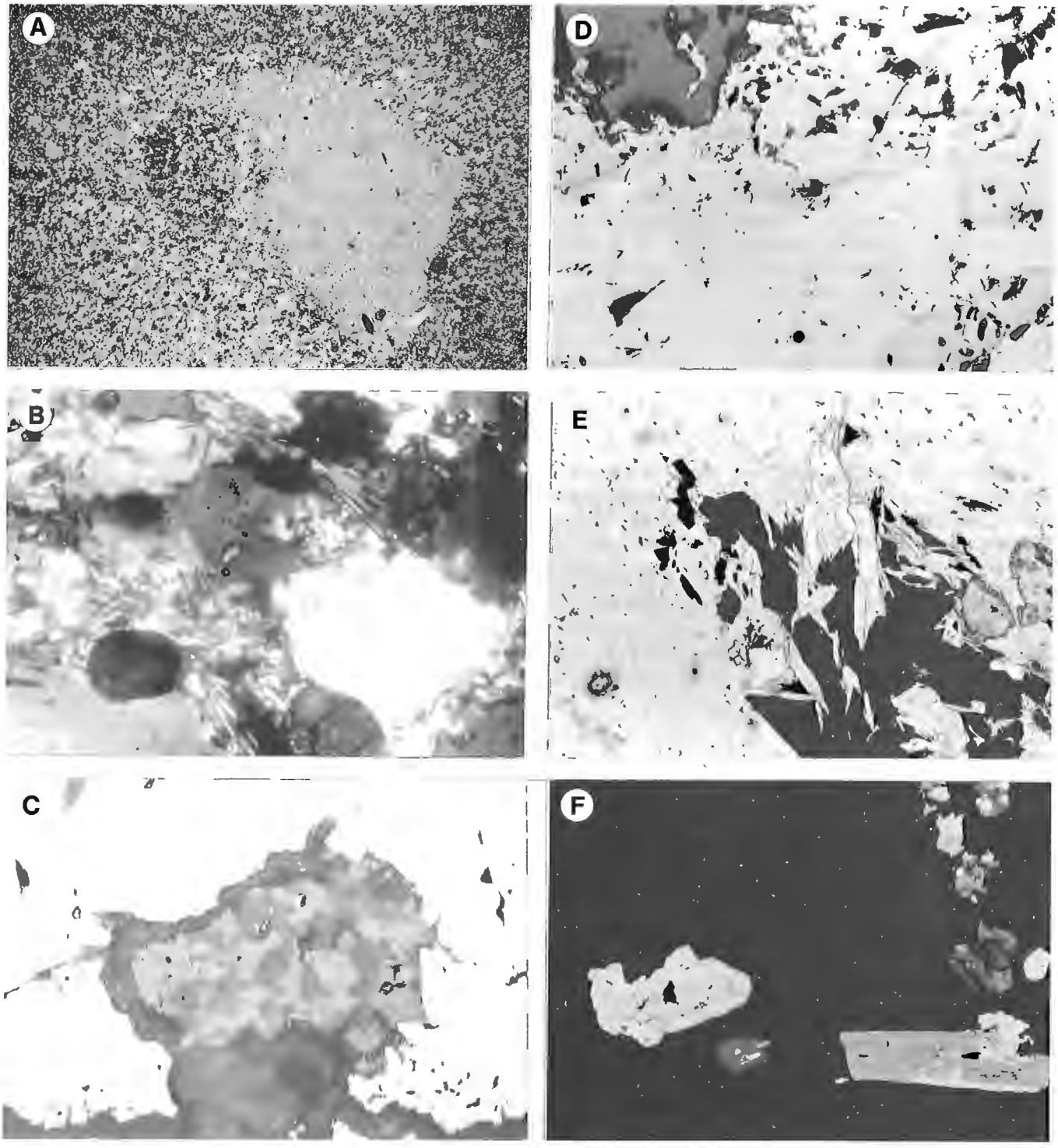

Figure 2. Photomicrographs of minerals and textures in samples studied from the Sullivan deposit.

A) Biotite-rich (small clast) and biotite-absent (large clast) in altered footwall conglomerate, sample 89SVT23, possibly indicating a protolith control on metamorphic mineralogy. Transmitted light, uncrossed polars, field of view = 5 mm.
B) Coarse sphene (0.05 mm) and fine needle-like sprays of zircons (up to 0.05 mm long) in quartz-tourmaline matrix, sample 85SVT1 from fragmental-textured tourmalinite. Transmitted light, crossed polars.
C) Multiple oxide grain in envelope to quartz (dark) -arsenopyrite (white) vein cutting footwall tourmalinite, sample G79SL4. Within the grain, which is 70 μm across, darkest is sphene; next shade of grey is ilmenite; lightest are rutile and laminated hematite-?titanhematite. Reflected light, uncrossed polars.
D) Banded galena-cassiterite-arsenopyrite-pyrrhotite-chalcopyrite-?Bi-sulphosalt ore from the tin zone, sample 89SVR1. Darkest grey is cassiterite; next is pyrrhotite, with lighter galena and boulangerite (boundary not visible); lightest is the Bi-bearing phase, largest of which is 25 μm long. Reflected light, uncrossed polars.

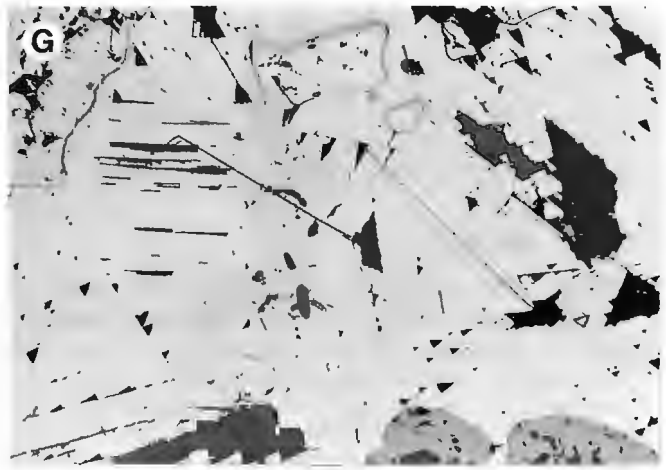

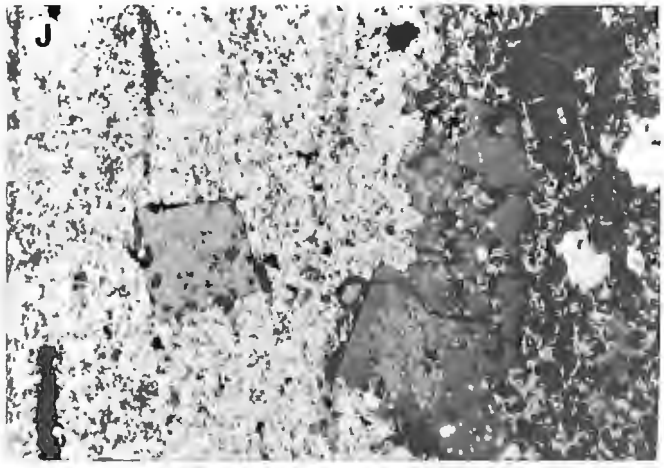

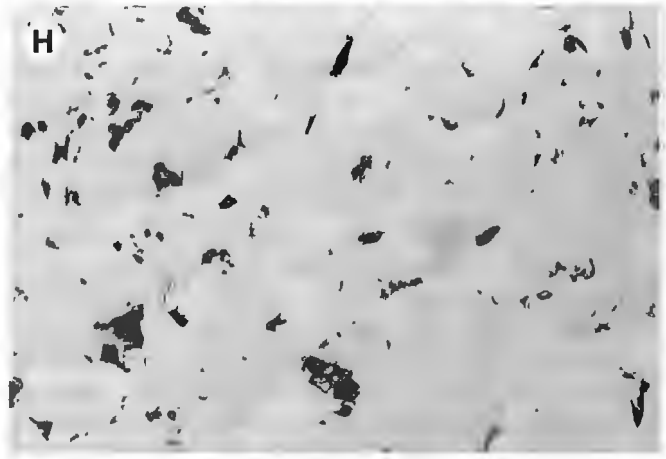

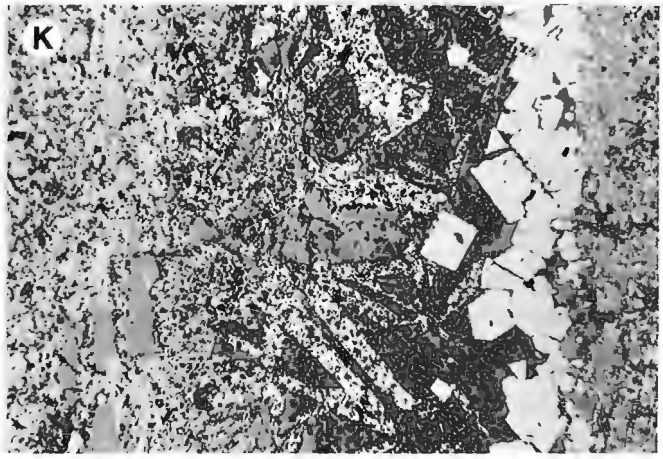

E) Foliated chlorite rock from below massive pyrrhotite body, sample 85SVT3A, showing coarse 0.25 mm sphene (high relief, to right of black pyrrhotite and bladed carbonate grain), and 0.07 mm long zircon (with metamict halo, to lower left). Transmitted light, uncrossed polars.

F) Bladed ?tremolite (right) and stubby barite (left) as euhedral crystals in fragmental massive pyrrhotite from sample 83SVH6. Width of field of view is 1.3 mm; transmitted light, crossed polars.

G) Large grain (0.7 mm long, oriented north-south) of boulangerite (mid-grey) with rim of ?pearcite-polybasite (slightly darker grey) in galena (lightest) and minor pyrrhotite (high relief) - sphalerite (darkest) from sample 85SVH5, footwall fragmental chlorite rock. Reflected light, uncrossed polars.

H) Massive pyrrhotite (mid-grey) from sample 83SVH6, with interstitial galena (lightest), minor chalcopyrite, and rare sulphosalts including larger grain of ?tetrahedrite (darker, 35 μ across) and smaller grains of ?pearcite-polybasite. Reflected light, uncrossed polars.

J) Magnetite (lighter grey, center) and garnet (darker, to right) porphyroblasts in massive very fine-grained pyrite from southeast fringe of laminated ore zone, sample SUL13. Width of view is 2.5 mm; reflected light, uncrossed polars.

K) Unusual bladed pyrrhotite laths, up to 2 mm long, from massive fine-grained pyrite, southeast fringe of laminated ore zone, sample SUL13. Width of view is 5 mm; reflected light, uncrossed polars.

Hamilton et al. (1982) described massive chlorite-pyrrhotite bodies at the base and top of the massive pyrrhotite body. Samples from these bodies are massive, foliated to fragmental, and composed of chlorite-pyrrhotite$\pm$sphalerite-galena, lesser quartz-muscovite-carbonate and minor arsenopyrite-sulphosalt. Samples from below the massive pyrrhotite body (85SVT3A, 85SVH5, 89SVT9) also contain sphene, rutile and zircon (Fig. 2E). In places, garnet porphyroblasts are also present. Chlorite appears to replace biotite and possibly muscovite (also noted in hanging wall alteration, SULIV 1), especially where the chlorite is associated with sulphides. Chlorite lacking anomalous interference colours, probably Mg-rich, is replaced by a chlorite with anomalous interference colours (more Fe-rich) around sulphides.

The massive to foliated samples from the pyrrhotite body (83SVT6, 83SVH6, 89SVT15, 89SVT20) also contain grains or layers of sphalerite and galena, and locally chalcopyrite, arsenopyrite, and sulphosalts (tetrahedrite-tennantite, pearcite-polybasite, and boulangerite: Fig. 2G, 2H). They generally show a strong fabric (cf. Campbell et al., 1980), with magnetite porphyroblasts in places. Fragmental massive pyrrhotite contains clasts or augens of pyrite, carbonate, plagioclase and several tentatively identified minerals: apatite, barite, tremolite and clinopyroxene (Fig. 2F).

Four paragenetic assemblages are seen in the samples studied from the footwall zones: early tourmaline-quartz, replaced by later pyrrhotite-ilmenite, cut by arsenopyrite-sphene, and finally cut by chalcopyrite-boulangerite-rutile

(±?Bi sulphosalt in other samples). Ilmenite is replaced by rutile, and pyrrhotite by arsenopyrite. Quartz in the footwall pyrrhotite-chlorite samples (89SVT9) hosts moderate salinity Type 2b and secondary Type 5 inclusions. Carbonate, on the other hand, found in 89SVT6 hosts Type 2a inclusions with the lowest salinities (5 %) observed in this group. These inclusions also appear to contain minor amounts of CO_2, as indicated by clathrate melting. Such low salinities, and the CO_2 component, are only seen elsewhere in the inclusions in SULIV 4, which may be metamorphic in origin.

The sample from the tin zone (89SVR1) contains the assemblage cassiterite-arsenopyrite-quartz (±galena, boulangerite, tetrahedrite, pyrargyrite, ?Bi sulphosalt or telluride: Fig. 2D) cutting tourmalinite. The cassiterite contains abundant pseudosecondary inclusions of Type 2a: 275-305°C, 10 % NaCl); quartz contains Type 2a as well, and also contains scattered Type 2b (200°C) inclusions and some planar swarms of secondary Type 5 inclusions.

Massive pyritic ore

One unlocated sample (SULIV 4) of massive pyritic ore consists of augen of pyrite, quartz, and garnet, with albite, carbonate and lesser muscovite, chlorite and hydrobiotite, in a matrix of fine pyrrhotite-galena-sphalerite-minor chalcopyrite-rutile-ilmenite. The quartz and carbonate contain abundant moderate T (300°C) fluid inclusions of two widely different types, Type 2 (liquid-rich aqueous, moderate salinity, 5 % to rarely 18 %) and Type 4 (vapour-rich, carbonic, low salinity, 5wt. %) plus a transitional Type 3. Both Type 3 and 4 contain significant amounts of CO_2 and CH_4. The presence of carbonic fluid and much lower salinities compared to the other inclusions implies that these (Type 3 and 4) have trapped metamorphic fluids.

Bedded ore

Samples SUL13, E9303 and 89SVT28 from well-laminated ore appeared to contain fluid inclusions in sphalerite (Fig. 1A, 1B) in preliminary studies in polished thin section, but none were found in the doubly polished plates. SUL13, from the southeastern fringe of the deposit, is composed of interlayered quartz-chlorite-muscovite-biotite waste bands and sulphide-rich bands of very fine grained, almost framboidal-looking pyrite, with lesser pyrrhotite, sphalerite, galena and chalcopyrite. There are local concentrations of porphyroblastic garnet and magnetite in the sulphide and intervening waste bands respectively (Fig. 2J). Pyrrhotite also occurs as bladed laths in this specimen (Fig. 2K), similar to descriptions by Hamilton et al. (1982). This feature is similar to pyrrhotite laths in modern sea-floor systems (e.g. Goodfellow and Blaise, 1988). Laminated sphalerite-galena-pyrrhotite ore from the middle of the "A" band (89SVT28) contains coarse-grained (0.5 mm) boulangerite and lesser ?jamesonite, plus gangues of quartz, muscovite, carbonate and ?apatite. The sulphosalts appear to be concentrated in layers parallel to the lamination, possibly suggesting deposition with the layered sulphides. E9303 consists of laminated sphalerite-galena-pyrrhotite with minor quartz-chlorite-muscovite-sphene and possible ?barite. All the inclusions in sphalerite are solid (no changes are observed on cooling to −140°C or heating to +400°C). Coarse, non-detrital quartz found in "sweats" or porphyroblasts contains rare fluid inclusions that have features typical of Type 2 (moderate T, moderate salinity), but none could be measured in the doubly polished section.

CONCLUSIONS

The data gathered during this preliminary study are too scant to warrant detailed interpretation, but encourage further study, and a few tentative conclusions may be drawn. Since there are evidently many different fluids trapped in these rocks, it seems likely that at least some represent fluids associated with ore deposition; the problem is to sort out which. The secondary Type 5 inclusions are clearly post-metamorphic and can be disregarded in terms of ore genesis. The Type 1 inclusions are clearly too hot for metamorphic fluids, given a pressure correction of at least 200 degrees that would result in trapping temperatures of 600-650°C for 2 kb. The Type 2 fluids with low salinities (<5 wt %) and the Type 3 and 4 fluids, rich in CO_2/CH_4 and also with low salinities, may be appropriate for metamorphic fluids. Homogenization temperatures for these inclusions of up to 325°, rarely to 425°C, imply trapping temperatures of 500° to rarely 675°C that might also exceed metamorphic temperatures. It is significant that there are so many different fluids represented. This suggests that metamorphism has not overprinted all earlier fluids, or they would all be the same. The widespread occurrence of decrepitated fluid inclusions, especially those with a secondary habit that would be expected to be lower-temperature, suggests decrepitation during metamorphism. Therefore the adjacent inclusions, many of which did not decrepitate on heating the stage to 450°C, may have survived metamorphism.

Based on the data currently available, it seems likely that (1) previous conclusions regarding fluids reponsible for the post-ore albite-chlorite-pyrite alteration (200-250°C and 22-29 wt. % NaCl equivalent: C.J. Hodgson, unpublished data; cf. Nesbitt et al., 1984) are supportable from the present data (180-230°C and 15-20 wt % NaCl + lesser KCl); (2) very hot, highly saline fluids (450°C, 35-40 wt. % NaCl + lesser KCl and possibly $CaCl_2$) may have been involved during an episode that deposited quartz-arsenopyrite veining in the lower parts of the deposit; (3) hot, moderate salinity fluids (275-300°C and 15-35 wt. % NaCl + lesser KCl) may be associated with deposition of cassiterite-quartz-arsenopyrite, again in lower parts of the deposit.

Fluids responsible for deposition of the major portion of the orebody (massive and laminated pyrrhotite-sphalerite-galena) are difficult to delineate directly due to the absence of fluid inclusions in sphalerite. This could be because dynamic metamorphism of the orebody (McClay, 1983) has recrystallized the sulphides and thus destroyed the fluid inclusions. However, quartz associated with both massive and laminated ore appears to have been deposited from Type 2b fluids of lower temperature and moderate salinity (165 to 240°C and 15-20 wt % NaCl equivalent).

ACKNOWLEDGMENTS

The geology department at The University of British Columbia, and in particular C.I. Godwin, are thanked for access to their collections of Sullivan material. R.J.W. Turner also made available his collections of Sullivan rocks, and is thanked for his critical reading of the manuscript.

REFERENCES

Campbell, F.A., Ethier, V.G., Krouse, H.R., and Both, R.A.
1978: Isotopic composition of sulfur in the Sullivan orebody, British Columbia; Economic Geology, v. 73, p. 246-268.

Campbell, F.A., Ethier, V.G., and Krouse, H.R.
1980: The massive sulfide zone: Sullivan orebody; Economic Geology, v. 75, p. 916-926.

Collins, P.L.F.
1979: Gas hydrates in CO_2-bearing fluid inclusions and the use of freezing data for estimation of salinity; Economic Geology, v. 74, p. 1435-1444.

Davis, D.W., Lowenstein, T.K., and Spencer, R.J.
1988: Melting behaviour of fluid inclusions in laboratory-grown halite crystals in the systems NaCl-H_2O, NaCl-KCl-H_2O, and NaCl-$MgCl_2$-H_2O (abstract); Geological Society of America, Abstracts with Programs, v. 20, no. 7, p. A152.

Edmunds, F.R.
1977: The Aldridge Formation, B.C., Canada; Ph. D. thesis, Pennsylvania State University, University Park, Pennsylvania, 368 p.

Ethier, V.G., Campbell, F.A., Both, R.A., and Krouse, H.R.
1976: Geological setting of the Sullivan orebody and estimates of temperature and pressure of metamorphism; Economic Geology, v. 71, p. 1570-1588.

Goodfellow, W.D. and Blaise, B.
1988: Sulfide formation and hydrothermal alteration of hemipelagic sediment in Middle Valley, northern Juan de Fuca Ridge; Canadian Mineralogist, v. 26, p. 675-696.

Hamilton, J.M., Bishop, D.T., Morris, H.C., and Owens, O.E.
1982: Geology of the Sullivan orebody, Canada, in Precambrian Sulphide Deposits (H.S. Robinson Memorial volume: R.W. Hutchinson, C.D. Spence, and J.M. Franklin, ed.). Geological Association of Canada, Special Paper 25, p. 597-665.

Holland, R.A.G., Rey, C.J., and Spooner, E.T.C.
1978: A method for preparing doubly polished thin sections suitable for microthermometric examination of fluid inclusions; Mineralogical Magazine, v. 42, p. 407-408.

Hollister, L.S., Crawford, M.L., Roedder, E., Burruss, R.C., Spooner, E.T.C., and Touret, J.
1981: Practical aspects of microthermometry, in Short Course in Fluid Inclusions, Hollister, L.S. and Crawford, M.L. (ed.), Mineralogical Association of Canada, v. 6, p. 278-304.

Linnen, R.
1985: Contact metamorphism, wallrock alteration, and mineralization at the Trout Lake stockwork molybdenum deposit, southeastern British Columbia; M. Sc. thesis, McGill University, Montreal, Quebec, 220 p.

McClay, K.R.
1983: Structural evolution of the Sullivan Fe-Pb-Zn-Ag orebody, Kimberley, British Columbia, Canada; Economic Geology, v. 78, p. 1398-1424.

Nesbitt, B.E., Longstaffe, F.J., and Muehlenbachs, K.
1984: Oxygen isotope geochemistry of the Sullivan massive sulfide deposit, Kimberley, British Columbia; Economic Geology, v. 79, p. 933-946.

Roedder, E.
1984: Fluid Inclusions; Mineralogical Society of America, Reviews in Mineralogy, v. 12, 644 p.

Shaw, D.R. and Hodgson, C.J.
1986: Wall-rock alteration at the Sullivan mine, Kimberley, B.C., in The genesis of stratiform sediment-hosted lead and zinc deposits: conference proceedings (R.J.W. Turner and M.T. Einaudi, ed.), Stanford University Publications, School of Earth Sciences, Volume XX, p. 13-21.

Winkler, H.G.F.
1971: Petrogenesis of Metamorphic Rocks; New York, Springer-Verlag, 3rd Ed., 237 p.

Preliminary report on structural evolution and stratigraphic correlations, northern Cariboo Mountains, British Columbia

Charles A. Ferguson[1] and Philip S. Simony[1]
Institute of Sedimentary and Petroleum Geology, Calgary

Ferguson, C.A. and Simony, P.S., Preliminary report on structural evolution and stratigraphic correlations, northern Cariboo Mountains, British Columbia; in Current Research, Part A, Geological Survey of Canada, Paper 91-1A, p. 103-110, 1991.

Abstract

The Upper Proterozoic and Lower Cambrian Kaza and Cariboo groups of the northern Cariboo Mountains comprise a shallowing-upward sequence of deep marine turbidites, west-facing slope deposits, and a carbonate/siliciclastic platform. Four phases of deformation and two episodes of greenschist facies metamorphism are recognized. Northeast-vergent folds and a widespread bedding-parallel cleavage constitute the first phase. Phase 2 is represented by two styles of compressional deformation: 1) kilometre-scale upright folding in the turbidites and slope deposits, and 2) reverse faults in the relatively rigid platformal strata. Oblique dextral faults within the platformal sequence constitute Phase 3 deformation, and could account for up to 10 km of distributed strike-slip displacement between Isaac Lake and the Rocky Mountain Trench. The youngest deformation is represented by an upright crenulation cleavage. The Phase 1 and 2 deformations are pre-Middle Jurassic in age and are closely related to metamorphism, but the lower age limit of the younger events is unconstrained.

Résumé

Les groupes de Kaza et de Cariboo du Protérozoïque supérieur et du Cambrien inférieur dans le nord des monts Cariboo renferment une séquence à granoclassement normal composée de turbidites marines d'eau profonde, de dépôts de pente orientés vers l'ouest et d'une plate-forme de roches silicoclastiques et carbonatées. Quatre phases de déformation et deux épisodes de métamorphisme au faciès des schistes verts sont reconnus. Des plis d'orientation nord-est et une important clivage parallèle à la stratification constituent la première phase. La phase 2 est représentée par deux styles de déformation causée par la compression: (1) un plissement droit de l'ordre du kilomètre dans les turbidites et les dépôts de pente, et (2) des failles inverses dans les couches de plate-forme plus jeunes et moins ductiles. Des failles dextres obliques à l'intérieur de la séquence de la plate-forme constituent la déformation de la phase 3 et pourraient expliquer un décrochement atteignant 10 km entre le lac Isaac et le sillon des Rocheuses. La déformation la plus récente est un clivage de rides droites. Les déformations des phase 1 et 2 sont antérieures au Jurassique moyen et sont étroitement liées au métamorphisme, mais la limite d'âge inférieure des événements récents est inexistante.

[1] Department of Geology and Geophysics, University of Calgary, Calgary, Alberta T2N 1N4

INTRODUCTION

A thick sequence of Upper Proterozoic and lower Paleozoic North American continental margin strata, at greenschist metamorphic grade or lower, are preserved in the northern Cariboo Mountains. The stratigraphic succession is at least 6 km thick, and is important because it records the construction of a west-facing margin that predates the early Paleozoic Cordilleran miogeocline.

Structurally, the Cariboo Mountains represent the highest level of the Omineca belt preserved. The northern "Cariboos" consist of two fold domains with opposing plunges (Fig. 1), separated by a northwest trending east-side-down oblique dextral slip fault zone that runs through the trough occupied by Isaac Lake (Ross and Ferguson, unpublished mapping). The narrower western domain is dominated by northeast-verging, open, first phase folds plunging 10° southeast. The larger eastern domain is dominated by upright, slightly tighter, mostly southwest-verging, second phase folds plunging 10° northwest. The folding is constrained to be older than the 174 Ma age of the Hobson Lake pluton (Gerasimoff, 1988), by comparison to relationships in the southern Cariboos (Murphy, 1987). The Isaac Lake fault zone clearly postdates the Mesozoic folding event.

An area (1400 km^2) of the eastern structural domain (between Isaac Lake and the Rocky Mountain Trench) was mapped at a scale of 1:50 000 during the 1989 and 1990 field seasons (Fig. 2). The regional northwest plunge exposes the upward transition from Upper Proterozoic, pelite dominated, deep water, marine turbidites into relatively rigid Upper Proterozoic and Lower Cambrian platformal limestones and littoral quartzites. Tectonic shortening is accommodated in the pelitic strata by an unbroken series of large amplitude, kilometre-scale folds. Shortening in the younger, more competent, limestones and quartzites is achieved partly through broad folding, but to a large extent by reverse and thrust faulting along fault planes dipping at moderate angles (< 50°).

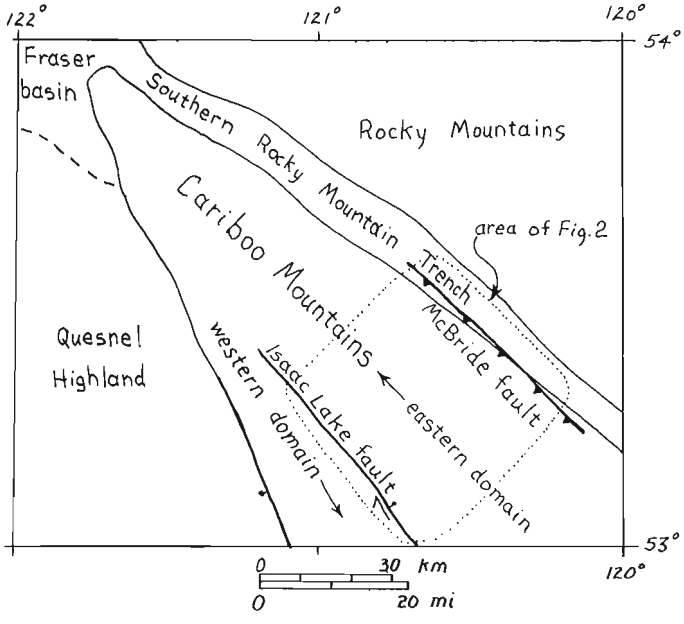

Figure 1. Location of the study area in the northern Cariboo Mountains of British Columbia, and definition of the eastern and western structural domains. Long arrows indicate direction of regional plunge.

The objective of this paper is to present preliminary structural cross-sections, and describe the relationship of the large structures to microstructural fabric and metamorphic mineral growth. Some important stratigraphic observations are also reported.

STRATIGRAPHY

The northern Cariboo Mountains are underlain by Upper Proterozoic Kaza Group and Upper Proterozoic through Lower Cambrian Cariboo Group strata (Fig. 3). The lower two thirds of the sequence records filling of a deep marine basin that was oriented crudely parallel to the present structural grain of the Cordillera. The basin was filled by medium and thick bedded feldspathic and quartzose axial turbidites (Ross et al., 1989) of the Kaza Group and lower Isaac Formation. The turbidites were succeeded by, and to some extent interfinger with, southwest-directed slope deposits of the Isaac Formation. The slope deposits consist mostly of calcareous and carbonaceous pelites, with lesser amounts of medium and thin bedded, quartzose, turbidite sandstone and siltstone units. A wide variety of coarse grained olistostromes containing platformal carbonate clasts along with limestone turbidites and southwest-directed slump deposits are characteristic of the middle and upper parts of the Isaac Formation, and provide evidence of the slope environment.

The Isaac Formation is conformably overlain by, and in part interfingers with, platformal limestones (mostly peloidal packstones with rare stromatolitic boundstone intervals) of the Cunningham Formation, which in turn is succeeded by platformal limestones interbedded with fine quartzose sandstones and muddy siltstones of the Yankee Belle Formation. Sedimentary structures in the Yankee Belle sandstones suggest a stormy siliciclastic/carbonate shelf environment. The Yankee Belle is abruptly overlain by medium and thick bedded, cross-stratified, medium and coarse grained quartzites of the Yanks Peak Formation. Most of these quartzites are interpreted as fluvial deposits and, in some cases, as marginal marine sand bodies (Young, 1979). In the western Cariboo Mountains, quartzites in the Yanks Peak Formation are interleaved with one, two, or three thin bedded, ripple crosslaminated, sandstone/siltstone and pelite units between 5 and 30 m thick. These fine grained intervals are interpreted as shallow water, subtidal marine deposits (Young, 1979). The Yanks Peak Formation is overlain by the Midas Formation, a pelite dominated, marine, quartzite-pelite unit, and the Mural Formation, a thin bedded, silty, ripple crosslaminated limestone.

Stratigraphic transitions

The upward transition from a deep water, marine, axial turbidite basin (Kaza Group and lower Isaac Formation); through a continental slope sequence (Isaac Formation); into a carbonate (Cunningham Formation) and siliciclastic (Yankee Belle Formation) platformal shelf, is characterized by gradational contacts all along the western edge of the study

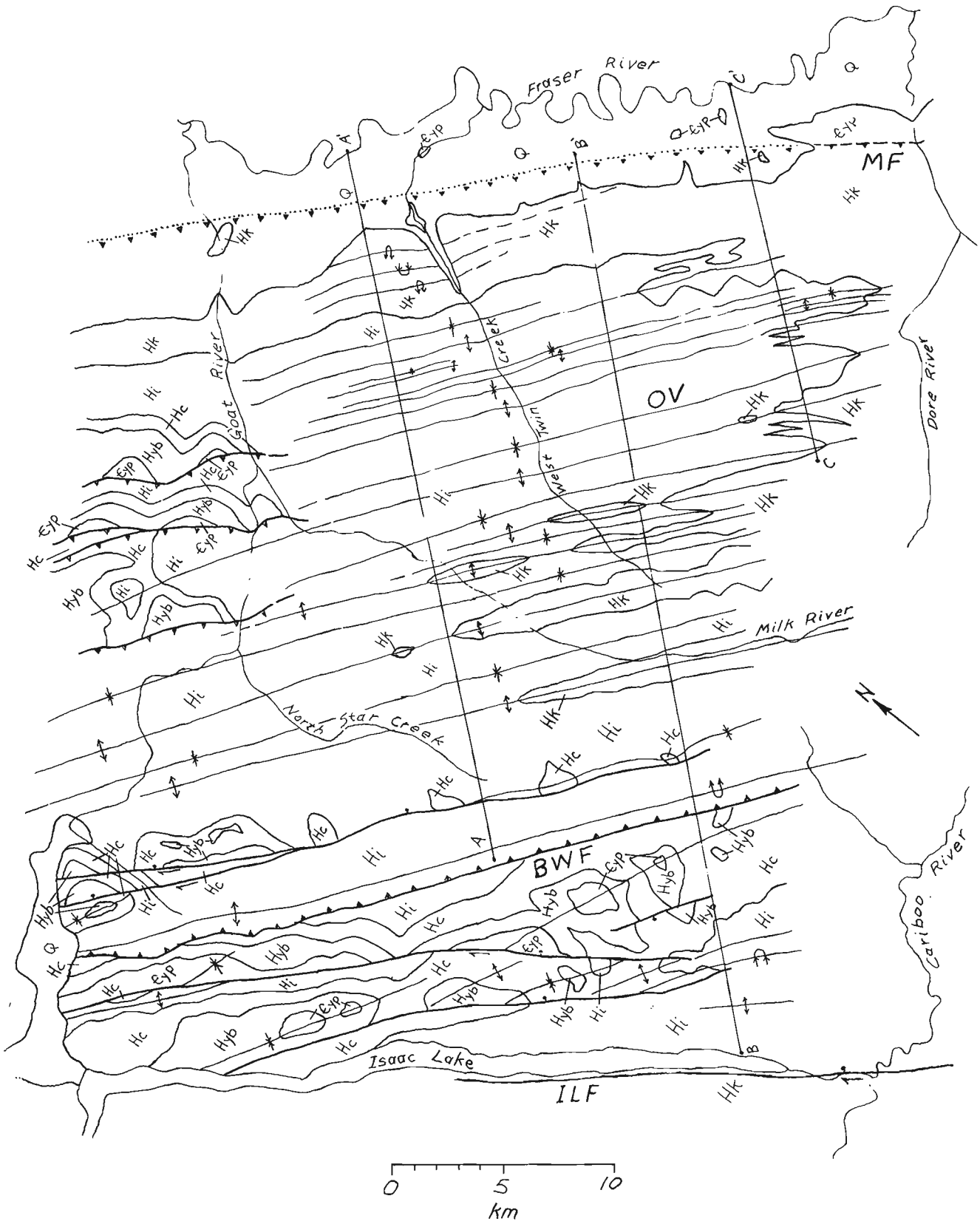

Figure 2. Geology of area mapped during the 1989 and 1990 field seasons, northern Cariboo Mountains, British Columbia. Hadrynian (latest Proterozoic) strata, from oldest to youngest: Hk = Kaza Group, Hi = Isaac Formation, Hc = Cunningham Formation, Hyb = Yankee Belle Formation. Cambrian strata: Cyp = Yanks Peak Formation (in some areas includes the Midas and Mural formations). Q = Quaternary sediments, OV = Ozalenka valley, BWF = Betty Wendle Fault, MF = McBride Fault, ILF = Isaac Lake Fault.

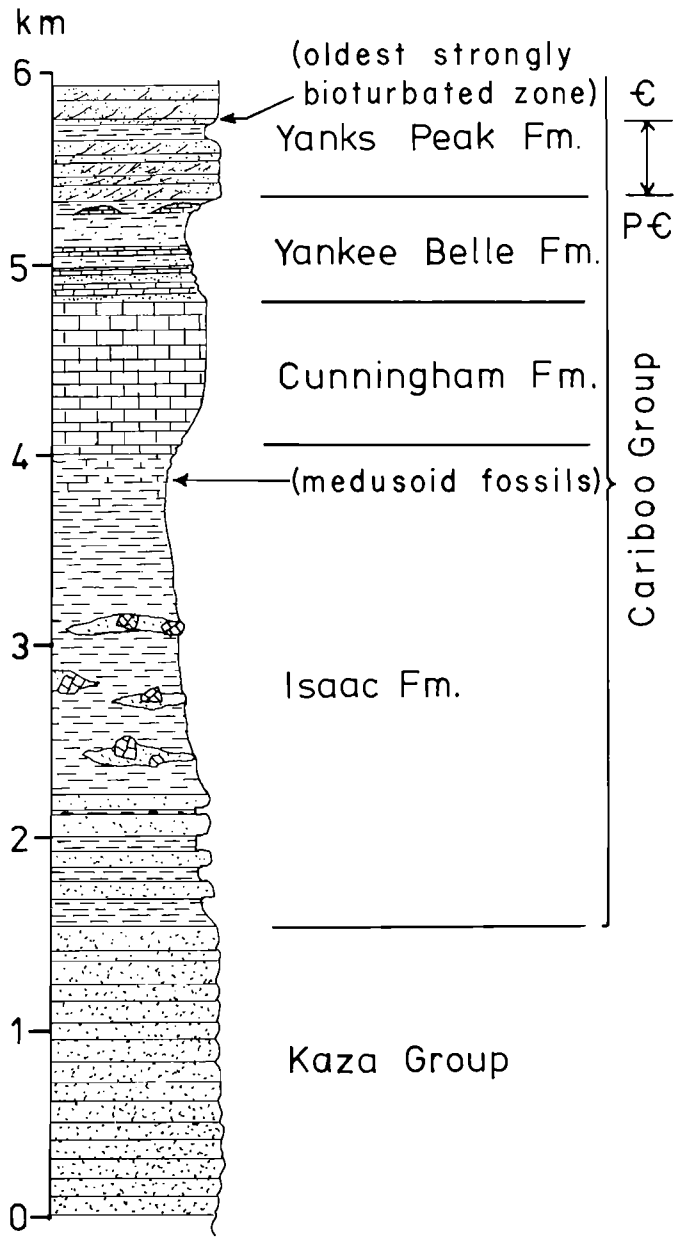

Figure 3. Generalized stratigraphy in the northern Cariboo Mountains, British Columbia. Important biostratigraphic intervals (discussed in text) are indicated.

area. The only obvious depositional hiatus is at the base of the Yanks Peak Formation where a fluvial quartzite unit overlies low-angle, undulose, crossbedded, calcareous, subtidal sandstones and silty mudstones of the Yankee Belle Formation.

The transitions from Kaza Group to Isaac Formation, and upward into the Cunningham Formation are gradational and appear to be completely conformable everywhere in the study area. Locally, however, they display a good deal of relief through rapid lateral facies changes. For example, in the southeast corner of the study area, the Kaza Group/Isaac Formation contact is marked by a gradual transition from grit dominated turbidites to pelite dominated and generally thinner bedded turbidites. The contact climbs upsection to the west, so that it is at least 500 m, and perhaps as much as 1000 m, higher stratigraphically over a distance of 5 to 10 km (palinspastically restored). The climb is achieved by intertonguing of Isaac Formation pelites with Kaza grits (see structure cross-sections, Fig. 4). This fairly steep facies transition probably represents a strike parallel (NW-SE oriented) boundary between an axial grit and coarse, sandy turbidite channel-system, and fine grained west-directed slope deposits.

The transition from Isaac Formation to Cunningham Formation is very gradual. Thin and medium bedded siliciclastic and carbonate turbidites, interbedded with dark pelites, change gradually upward into a continuous sequence of medium bedded, mostly recrystallized, limestone with rare greenish pelite interbeds. In the northeast corner of the study area, the upper Isaac Formation contains at least one massive, shallow water, platformal limestone sequence that pinches out rapidly westward into "below-storm-wave-base" calcareous pelites and limestone turbidites (Fig. 5). If this intertonguing relationship continues eastward into stratigraphically older strata of the Isaac Formation, it would imply that a source for the carbonate-clast olistostromes and calcareous turbidites of the middle Isaac Formation was probably a contemporaneous limestone platform that prograded westward during late Isaac time (Ross et al., 1989).

In the northeast corner of the study area (along the Rocky Mountain Trench north of Goat River), abrupt and disconformable contacts separate the Cunningham, Yankee Belle, and Yanks Peak formations. The upper contacts of both the Cunningham and Yankee Belle formations are karst surfaces overlain by fluvial quartzites of the Yankee Belle and Yanks Peak formations, respectively. The terrigenous clastic component of the Cunningham Formation, and the proportion of terrestrial lithofacies in the Yankee Belle Formation are both much higher in this area than in the western Cariboo Mountains. In addition, two of these units (Cunningham and Yanks Peak) are significantly thinner here than they are to the west.

BIOSTRATIGRAPHY

The earliest occurrence of abundant trace fossils in the northern Cariboo Mountains is at the top of a prominent thin bedded quartzite-pelite interval in the lower third of the Yanks Peak Formation. Traces are mostly *Planolites*, with rarer examples of *Cruziana*, and *Didymaulichnus*. The interval is just above either the first or second pelite in the Yanks Peak Formation, which implies that the Precambrian/Cambrian boundary is either within the lower part of the Yanks Peak Formation or at its disconformable lower contact with the Yankee Belle Formation. Body fossils from the Yanks Peak Formation or younger Cambrian strata were not found, but Campbell et al. (1973) reported Archeocyathids and other Early Cambrian fossils from the Midas and Mural formations just to the north of the study area.

Disc shaped medusoid traces, between 1 and 15 cm in diameter, were discovered in a very thin bedded, silty, dark grey slate of the upper Isaac Formation (Fig. 3). The traces (Fig. 6) bear resemblance to Ediacaran fossils found elsewhere in the Cordillera (Hofmann et al., 1985; Narbonne and Hofmann, 1987). The fossil locality will be studied in

detail during the 1991 field season by Guy Narbonne of Queen's University. If the biogenic origin of the impressions is substantiated, regional correlations will be significantly improved.

STRUCTURAL GEOLOGY

Preliminary structural cross-sections have been constructed for the study area (Fig. 4). The sections transect the eastern structural domain between Isaac Lake and the Rocky Mountain Trench, where the domain is about 40 km wide. These sections illustrate the fold structure typical of the Kaza Group and Isaac Formation. Cross-sections of the northern part of the study area, where brittle deformation is more important, have not been completed.

Fold structure

In the southern two thirds of the study area, structure is dominated by open megascopic folds the axial planes of which define a broad fan structure, herein called the "Ozalenka Fan" (Ozalenka is the name of a large alpine valley, between West Twin Creek and the Dore River). A zone of upright folds, about 10 km wide, forms the axis of the fan in the east-central part of the eastern domain (Fig. 4). Axial planes gradually tilt away from the central zone, their dips decreasing to about 50° in southwesterly (along the west wall of the Rocky Mountain Trench) and northeasterly (along Isaac Lake) directions.

The Ozalenka Fan produces a broad arch in the enveloping surface of megascopic folds in the eastern structural domain. To the west, the enveloping surface eventually flattens out into the Isaac Synclinorium (Campbell et al., 1973) along the transition zone between the eastern and western structural domains. The shape of the enveloping surface near the Rocky Mountain Trench is poorly defined, chiefly owing to the lack of continuous exposure. It is, however, thought to curve sharply over a large, northeast-vergent, nappe-like anticline (Fig. 4). The hinge area for this structure has not been located, but is inferred to run just west of a relatively thick panel of overturned Kaza Group strata along the west wall of the Trench.

Faults

Three different styles of faulting were recognized in the study area. One style, the oldest and perhaps most difficult to interpret, occurs along the west wall of the Rocky Mountain Trench, in a structure herein called the McBride Fault. This fault was recognized by Campbell et al. (1973) because of large east-side-down stratigraphic offset (juxtaposition of Kaza Group and Cambrian strata). The fault surface has not been located, but a dip of 40 to 50° to the southwest is inferred from the attitude of an intense shear fabric in the footwall.

The other two fault systems are confined to the more rigid units of the Cariboo Group in the western and northern parts of the study area. The oldest of these two systems comprises a set of moderate angle (30 to 50°) reverse and thrust faults. The faults are southwest-directed to the west of the Ozalenka Fan and northeast-directed east of the fan. The most important fault west of the fan runs through the valley of Betty Wendle Creek near Isaac Lake. It grows out of the overturned limb of a large, southwest-verging anticline cored by upper Kaza Group strata in the southwest corner of the study area (Ross and Ferguson, unpublished mapping). The fault displaces lower Isaac Formation over lower Yankee Belle Formation or upper Cunningham Formation, and is inferred to dip about 50° northeast (parallel to the axial plane of the fold from which it emerges). To the north, the fault trace is well exposed above tree line, and its dip decreases progressively to 34° near the headwaters of Goat River. Stratigraphic offset across the Betty Wendle fault remains constant throughout its entire length in this study area.

In the northeast corner of the area, a series of three southwest dipping reverse or thrust faults repeat an unfolded southwest dipping homoclinal sequence of upper Isaac Formation through Yanks Peak Formation. These faults die out downsection, to the south, into folded pelites of the Isaac Formation.

Contractional faults in the Cariboo Group are mostly coplanar with the axial planes of the megascopic folds from which they emerge throughout the study area. They are probably syn- to slightly post-kinematic with respect to the folds. The faults could help balance the tectonic shortening of the rigid upper Cariboo Group, which is only broadly folded, relative to the relatively tight high amplitude folds of the underlying Isaac and Kaza turbidites.

The third type of fault system in the study area consists of high angle (> 65°) oblique slip faults in the competent units of the Cariboo Group. West of the Ozalenka Fan, a series of four "down-to-the-east", dextral, oblique slip faults trend crudely parallel to the regional structure and, in at least one locality, truncate contractional faults. All of these faults emerge upward from unfaulted upper Isaac Formation pelites, and they dip between 60 and 80° northeast. The faults consistently exhibit dextral slip kinematic indicators, and slickensided surfaces with slickenline rake angles between 20 and 60° from the southeast. Stratigraphic separations in the fault planes range between 0.3 and 2 km, and total dip slip across all the faults is just under 4 km. The range of the possible total dextral strike slip component is between 3 and 9 km (using the range of slickenline rake angles for each fault). These faults are kinematically akin to the Isaac Lake fault and, as a group, have a similar net slip. The Isaac Lake fault places upper Isaac Formation against middle and lower Kaza Group (Ross and Ferguson, unpublished mapping).

Dextral strike slip faults also occur east of the Ozalenka Fan axis, but they are always high angle (> 80°), and slickenline orientations are consistently parallel to the regional plunge. The net strike slip component of these faults cannot be estimated, but is probably not very significant, because the faults grow out of unfaulted Isaac pelites to the south. Apparent stratigraphic offsets are less than one kilometre, usually west-side-down.

Structural fabrics

The pelitic strata of the northern Cariboo Mountains show at least three, and in some areas four, structural fabrics defined by the parallel alignment and or crenulation of micaceous minerals formed during low grade regional metamorphism.

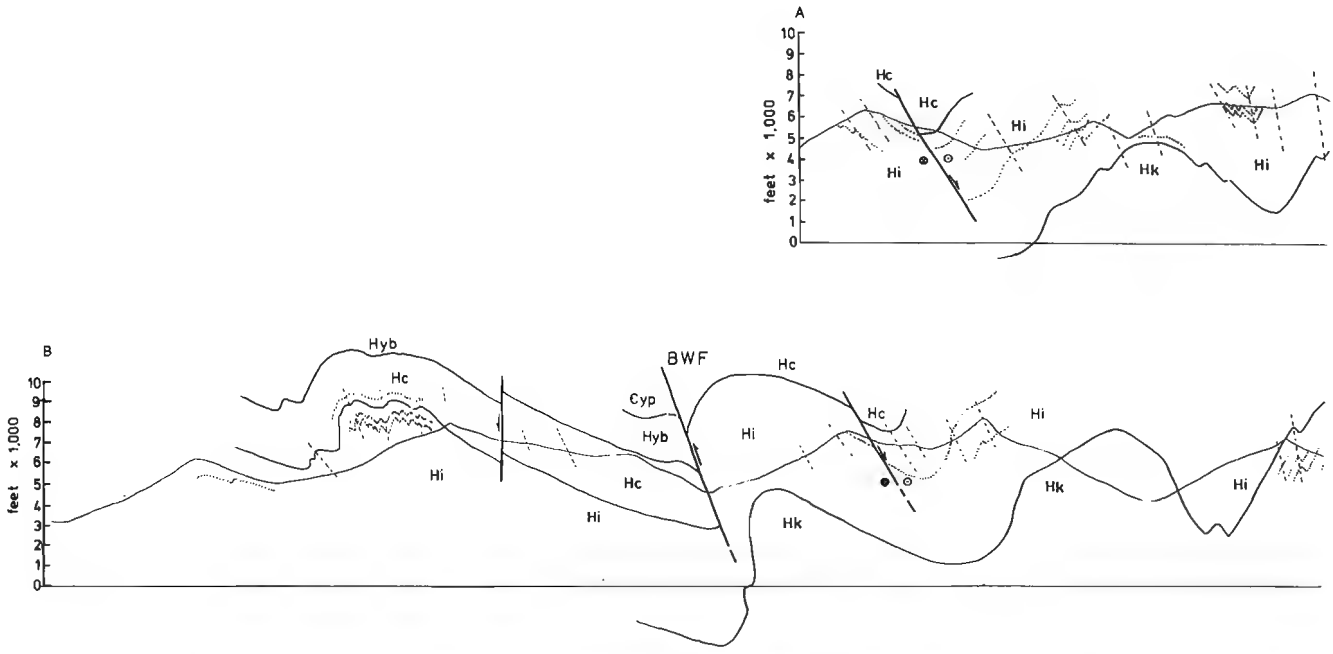

Figure 4. Preliminary structural cross-sections across the eastern structural domain of the northern Cariboo Mountains, British Columbia (no vertical exaggeration). Location of section lines given in Figure 2. Orientation of prominent cleavage(s) shown with dashed lines, dotted lines represent bedding planes. OF = Ozalenka Fan axis, BWF = Betty Wendle Fault, MF = McBride Fault.

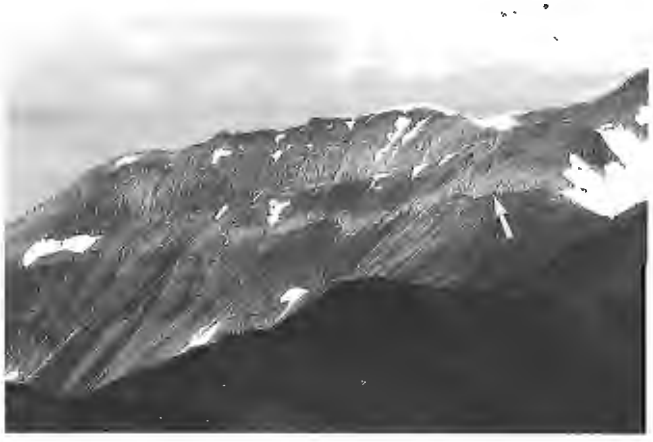

Figure 5. View to the north of an upper Isaac Formation platformal limestone. The limestone pinches out to the west into sub-storm-wave-base limestone units below a prominent cliff that represents the base of the Cunningham Formation. Ridge is at the headwaters of Whitehorse Creek, northern Cariboo Mountains, British Columbia.

Figure 6. Medusoid-like impressions in a thin bedded, dark grey slate of the upper Isaac Formation, northern Cariboo Mountains, British Columbia. The traces resemble Ediacaran fossils described elsewhere from the Canadian Cordillera.

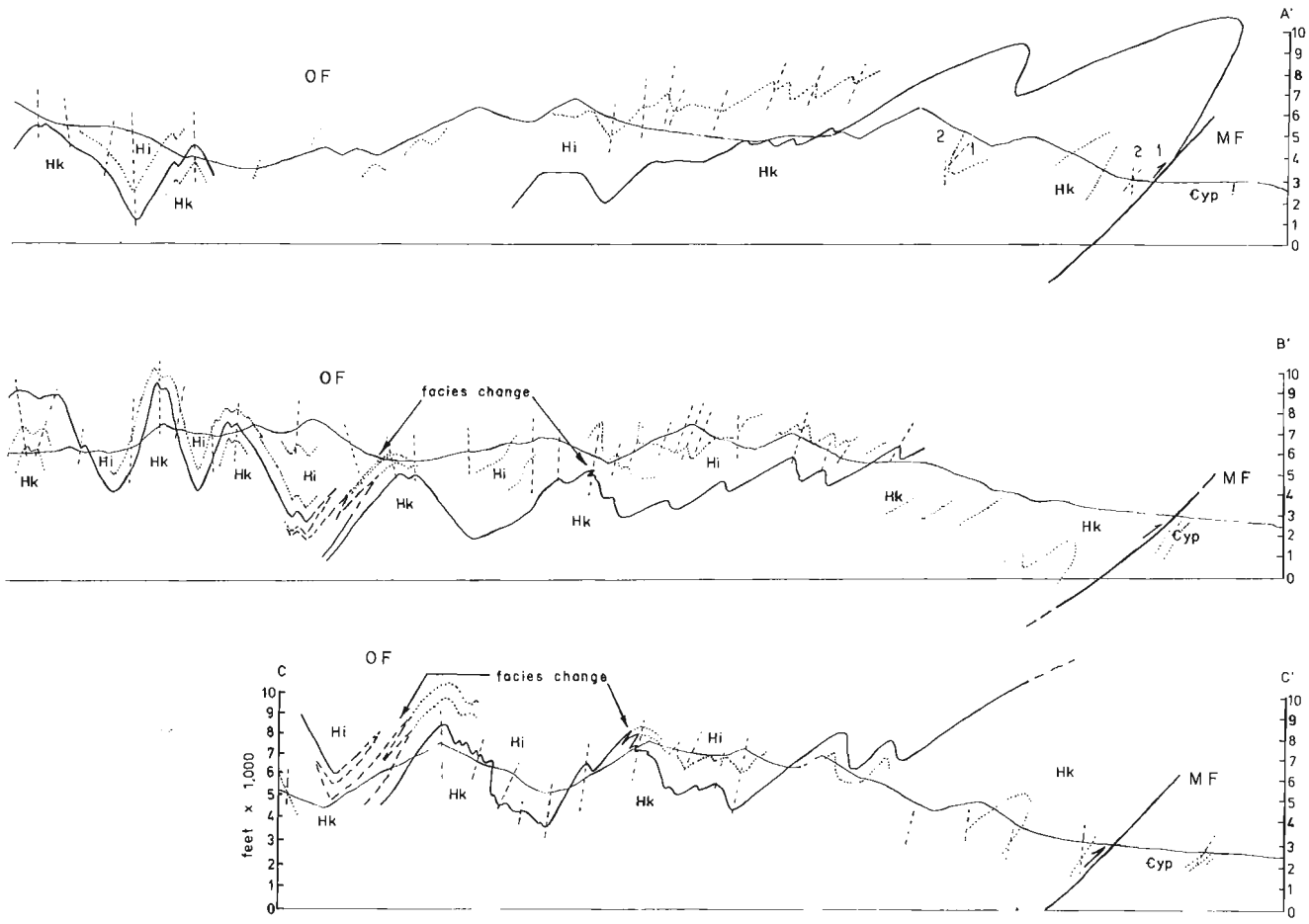

The earliest fabric recognized is a foliation defined by fine grained muscovite and chlorite grains, and aligned chloritoid porphyroblasts. Through most of the eastern domain (west of the Ozalenka Fan) this fabric (S_1) is almost always bedding parallel and crenulated into a younger cleavage, axial planar to the megascopic fold structure. East of the fan axis, S_1 commonly dips more steeply to the west relative to S_0, and is associated with minor northeast-verging F_1 folds. The only megascopic F_1 fold in the eastern domain is the large overturned anticline adjacent to the Trench (Fig. 4).

Structural fabrics in the footwall of the McBride Fault are dominated by an intense shear foliation, defined by axial planes of transposed fold hinges and isolated mesoscopic isoclinal folds in thin bedded units. This fabric is interpreted as being coeval with S_1 because it is locally deformed by two steeply dipping crenulation cleavages.

The second oldest structural fabric (S_2) is a crenulation cleavage that is axial planar to the megascopic (F_2) folds throughout the study area. The S_2 fabric is defined by crenulated S_1 micas and the growth of syn-kinematic micas. Along the west wall of the Trench, S_2 is oriented at a high angle to the axial plane of the F_1 overturned anticline.

A faint crenulation cleavage (S_3) parallels the axial planes of east-west trending broad folds (F_3) associated with the Isaac Lake Fault zone just to the south of the study area. The fabric (S_3) and folds (F_3) are interpreted as ductile deformation associated with strike-slip motion along the Isaac Lake Fault zone (Ross and Ferguson, unpublished data).

The youngest fabric recognized in the Cariboos is a widespread upright crenulation (S_4) typically oriented about 020 to 080°. This fabric is usually expressed as millimetre- to centimetre-scale, steeply plunging crenulations developed on the prominent (usually S_2) cleavage plane, and occasionally as decimetre- to metre-scale kink folds (F_4). Particularly large amplitude (tens of metres) F_4 folds, associated with S_4, were noted in some areas, usually underlain by Isaac Formation pelites.

METAMORPHISM

Two episodes of metamorphism were recognized. The metamorphic assemblage in pelites formed during both episodes is dominated by chlorite and muscovite. Chloritoid porphyroblasts appear to be associated only with the first episode of metamorphism (M_1). M_1 is syn-kinematic with respect to

F_1 folding and characterized by growth of S_1 parallel micaceous minerals and chloritoid porphyroblasts. M_2 metamorphism is syn-kinematic with respect to F_2 folding and crenulation cleavage (S_2) development. Fabrics related to the McBride Fault are deformed by two steep crenulation cleavages, tentatively correlated with the S_2 and S_4 fabrics seen elsewhere in the study area. If correct, this correlation would constrain the timing of at least some motion along the McBride Fault to predate M_2 metamorphism. Upright F_3 folds and S_3 crenulations are clearly post M_2.

INTERPRETATION OF STRUCTURAL EVOLUTION IN THE NORTHERN CARIBOO MOUNTAINS

The structural evolution of the northern Cariboo Mountains is broken into four (D_{1-4}) deformational phases, each associated with folding events (F_{1-4}), and structural fabrics (S_{1-4}). The first two phases were associated with large-scale folding and compressional faulting events linked to the obduction and subduction of oceanic terranes along the western margin of North America during the mid-Mesozoic Columbian Orogeny (Murphy, 1987). The third phase (D_3) was a dextral, oblique slip, faulting event, and the fourth (D_4) produced widespread transverse crenulations.

Three of the four phases (D_1, D_2, and D_4) are directly correlative with deformational phases recognized by Murphy (1987) in the southern Cariboo Mountains. Murphy's (1987) D_3 phase is a northwest-trending, broad folding event that does not appear to manifest itself in the northern Cariboos. Likewise, the brittle faulting event recognized as D_3 in this study area is not expressed in the southern Cariboos.

The first phase of deformation (D_1) resulted in the formation of a bedding parallel structural fabric (S_1) in most of the study area, and a large northeast-verging anticline along the west wall of the Rocky Mountain Trench. The (S_1) fabric gradually diverges from the bedding from west to east near the Trench until it is axial planar with folds in the core of this anticline.

The D_1 deformation described here corresponds with Murphy's (1987) D_1 northeast-vergent nappe structure in the central Cariboo Mountains. Murphy (1990) also described a northeast-vergent thrust fault that is younger than his D_1 nappe structure along the west side of the Trench, in the vicinity of Valemont. Murphy (1990) correlated this fault, originally interpreted as a normal fault (Campbell et al., 1973; Murphy, 1984), with the post-metamorphic Purcell Thrust. The McBride Fault (this report), which occupies a similar geomorphic position along the west wall of the Trench, may be post-metamorphic with respect to M_1, but from evidence found so far in the McBride area, it is probably pre-D_2, and therefore pre- to syn-kinematic with respect to M_2 metamorphism. The McBride Fault may have been reactivated as a post-metamorphic (M_1 and M_2) Purcell-Thrust-type structure. Current investigations will hopefully shed more light on this problem.

The second phase of deformation (D_2) is expressed by megascopic folds (F_2) with an axial planar crenulation cleavage (S_2) throughout the study area, and by contractional faults in younger units of the Cariboo Group. This D_2 event is correlated with the D_2 event of Murphy (1987) in the central Cariboo Mountains.

Dextral oblique-slip faulting constitutes the third phase (D_3) of deformation recognized in the study area. D_3 faulting clearly postdates D_2 fold and fault structures, and predates a transverse upright crenulation (S_4) event. The S_4 fabric crenulates a faint cleavage (S_3) associated with the dextral oblique faults south of the study area, and S_4 shear planes offset similar faults near North Star Mountain.

The youngest deformational event (D_4) in the northern Cariboo Mountains is linked to the formation of upright, steeply plunging F_4 folds and S_4 crenulations.

ACKNOWLEDGMENTS

Research for this project is supported by Department of Energy, Mines and Resources Contract 23294-0-0618/01-XSG. Gerald Ross contributed greatly to this research through his visits to the study area and by numerous discussions. Gerald Ross and Mike McDonough critically reviewed the manuscript. Peter Gibson, Elizabet Kruit, and Jeff Nazarchuck provided very capable and enthusiastic field assistance. We would also like to thank our helicopter pilot Ron Eland, and our fixed-wing pilot Charles Leake for their safe and reliable field support. Sharon and Ron Hawkins provided a great service to our field party with reliable radio contact. The British Columbia Parks Service are acknowledged for allowing helicopter access to parts of Bowron Lake Provincial Park, and for permission to collect samples within the Park boundary.

REFERENCES

Campbell, R.B., Mountjoy, E.W., and Young, F.G.
1973: Geology of the McBride map-area, British Columbia; Geological Survey of Canada, Paper 72-35, 104 p.

Gerasimoff, M.
1988: The Hobson Lake pluton, Cariboo Mountains, British Columbia, and its significance to Mesozoic and early Cenozoic cordilleran tectonics; M.Sc. thesis, Queens University, Kingston, Ontario, 196 p.

Hofmann, H.J., Mountjoy, E.W., and Teitz, M.W.
1985: Ediacaran fossils from the Miette Group, Rocky Mountains, British Columbia, Canada; Geology, v. 13, p. 819-821.

Murphy, D.C.
1984: A note on faulting in the southern Rocky Mountain Trench between McBride and Canoe Reach, British Columbia; Geological Survey of Canada, Paper 84-1A, p. 627-630.
1987: Suprastructure/infrastructure transition, east-central Cariboo Mountains, British Columbia: geometry, kinematics, and tectonic implications; Journal of Structural Geology, v. 9, p. 13-29.
1990: Direct evidence for dextral strike-slip displacement from mylonites in the southern Rocky Mountain Trench near Valemont, British Columbia; in Current Research, Part E, Geological Survey of Canada, Paper 90-1E, p. 91-95.

Narbonne, G.M., and Hofmann, H.J.
1987: Ediacaran biota of the Wernicke Mountains, Yukon, Canada; Paleontology, v. 30, p. 647-676.

Ross, G.M., McMechan, M.E., and Hein, F.J.
1989: Proterozoic history: the birth of the miogeocline; in Western Canada Sedimentary Basin, Ricketts, B.D. (ed.); Canadian Society of Petroleum Geologists, p. 79-99.

Young, F.G.
1979: The lowermost Paleozoic McNaughton Formation and equivalent Cariboo Group of eastern British Columbia: piedmont and tidal complex; Geological Survey of Canada, Bulletin 188, 60 p.

Preliminary report on stratigraphy and structure, northeastern Brooks Range, Alaska and Yukon: a USGS—GSC co-operative project

Larry S. Lane, John S. Kelley[1], and Chester T. Wrucke[2]
Institute of Sedimentary and Petroleum Geology, Calgary

Lane, L.S., Kelley, J.S., and Wrucke, C.T., Preliminary report on stratigraphy and structure, northeastern Brooks Range, Alaska and Yukon: a USGS—GSC co-operative project; in Current Research, Part A, Geological Survey of Canada, Paper 91-1A, p. 111-117, 1991.

Abstract

Four weeks of structural and stratigraphic mapping, along the Alaska/Yukon border, have revealed positive correlations between Proterozoic(?) and Paleozoic units in northeastern Alaska and northwestern Yukon.

A Cambrian, Oldhamia-bearing, maroon and green argillite underlies a bioturbated chert/argillite unit that is correlative with a fossiliferous Lower Ordovician unit previously mapped farther east. Interlayered with the lower part of the chert/argillite is a succession of argillaceous lithic arenites, mudstones, and conglomerates containing abundant volcanic clasts, associated with mafic tuffs. The stratigraphic position of this unit, correlative with the Whale Mountain volcanic succession, is consistent with published fossil evidence indicating a Late Cambrian age for the latter. The definition of facies changes will be important in determining the stratigraphic succession and basin geometry.

Two sets of structures control outcrop geometry. Upright to north-verging tight to isoclinal folds and thrust faults predate Mississippian sedimentation. North- and south-verging faults and minor folds crenulate earlier fabrics and locally involve Mississippian strata.

Résumé

Après quatre semaines de travaux, la cartographie structurale et stratigraphique de la région chevauchant la frontière de l'Alaska et du Yukon a révélé des corrélations positives entre des unités paléozoïques et (?)protérozoïques dans le nord-est de l'Alaska et le nord-ouest du Yukon.

Une argilite marron et vert du Cambrien, contenant l'espèce Oldhamia, repose sous une unité d'argilite à chert bioturbée qui est en corrélation avec une unité fossilifère de l'Ordovicien précoce déjà cartographiée plus à l'est. La partie inférieure de l'unité d'argilite à chert est interstratifiée avec une succession d'arénites, de mudstones et de conglomérats à caractère lithique et argileux, contenant d'abondants fragments de roche détritique volcanique, associés à des tufs mafiques. La position stratigraphique de cette unité, par rapport aux roches volcaniques de Whale Mountain, concorde avec les données publiées sur les fossiles, indiquant que les roches volcaniques datent du Cambrien tardif. La définition des changements de faciès s'avérera importante lorsqu'il s'agira de déterminer la succession stratigraphique et la géométrie du bassin.

Deux ensembles de structures contrôlent la géométrie de l'affleurement. Des plis et des failles chevauchantes, serrés à isoclinaux et à vergence droite ou orientés vers le nord, sont antérieurs à la sédimentation mississipienne. Des failles et des plis mineurs d'orientation nord et sud rident des fabriques plus anciennes et renferment par endroits des couches mississipiennes.

[1] United States Geological Survey, 4200 University Drive, Anchorage, Alaska, USA 99508.
[2] United States Geological Survey, Mail Stop 901, 345 Middlefield Road, Menlo Park, California, USA 94025

INTRODUCTION

A joint United States Geological Survey—Geological Survey of Canada geological mapping project along the Alaska-Yukon border was first proposed (by JSK) in March 1988, during a Canadian—American workshop in Calgary on progress and problems in Beaufort Sea and North Slope geology. Subsequently, the project was included by GSC and USGS management as one of five potential co-operative studies in Arctic geoscience. Approval to proceed with fieldwork was obtained in the spring of 1990.

The purpose of a co-ordinated joint project (as opposed to separate individual projects) was to produce a single "standard" map covering both sides of the international boundary, as a basis for future more detailed work, thus assuring a positive correlation of stratigraphic and structural interpretation to facilitate future mapping in both countries. The initial objective of this project will be to document the ages and succession of units, and the role of facies changes in the border area, as well as to normalize the contrasting stratigraphic interpretations of Reiser et al. (1980) and Norris (1981). In addition, we hope that the results of this project will stimulate further studies of pre-Mississippian stratigraphy which has been largely neglected on both sides of the border.

Reiser et al. (1980) identified 34 separate (meta)sedimentary units predating deposition of Lower Mississippian strata of the Endicott Group, and interpreted many of them as early Paleozoic in age. In contrast, Norris (1981) grouped all the pre-Mississippian strata into nine broad units, and interpreted a Proterozoic age for all but two (the Whale Mountain and Road River successions), although he later recognized that Paleozoic rocks might be included locally within his Proterozoic units (Norris, 1985, 1986).

Recent detailed fieldwork in northwestern Yukon indicates that these pre-Mississippian strata may contain more Paleozoic strata than previously supposed for that area, and that the stratigraphy may represent regionally mappable units (Cecile, 1988; Lane and Cecile, 1989). In addition, these studies documented intense structural imbrication that predates Mississippian sedimentation.

The objective of this project is to map bedrock geology from the Arctic coast to the vicinity of latitude 69°N during two field seasons, consisting of six weeks each. However, owing to other field commitments, only four weeks of structural and stratigraphic mapping, at a scale of 1:50 000, were carried out in 1990. This phase, near the Arctic coast (Fig. 1), focused on the northernmost exposures of pre-Mississipian rocks and consisted of detailed ground traverses from fly camps, alternating with helicopter "setouts" from a common base camp. United States Geological Survey personnel were principally responsible for mapping in Alaska, and Geological Survey of Canada personnel for mapping in Yukon. Several joint traverses on foot and by helicopter, together with the daily exchange of information, ensured that the results of fieldwork evolved into a single map (Fig. 2).

STRATIGRAPHY

A prominent ridge-forming syncline of Carboniferous limestone of the Lisburne Group divides the field area into

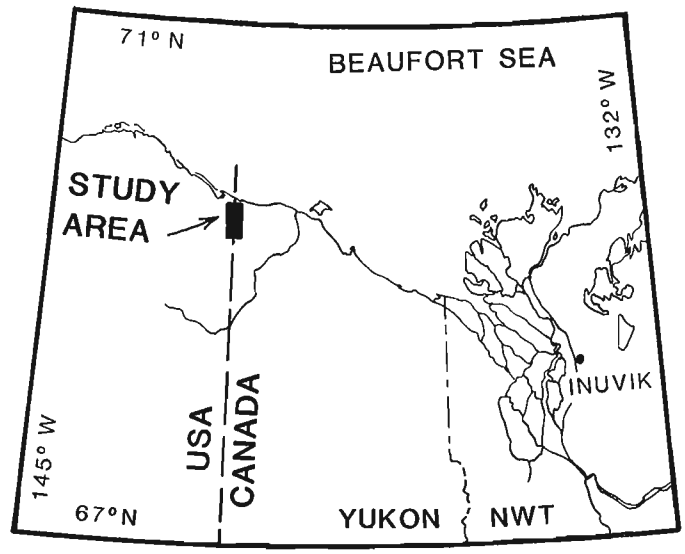

Figure 1. Location map of the Beaufort-Mackenzie region, showing the field area along the Yukon/Alaska boundary.

northern and southern parts, and is the only exposure of Mississippian and younger rocks in the field area. At its base, Kekiktuk Conglomerate is discontinuously exposed beneath silty shale and sandstone of the Kayak Shale. Together, these two Endicott Group units overlie several pre-Mississippian units with angular unconformity. The unconformity is poorly exposed. Pre-Mississippian limestone is locally and irregularly silicified in a zone immediately beneath the unconformity. The Kekiktuk Conglomerate does not appear to be more than a few metres thick in this area, whereas the Kayak Shale attains a thickness of approximately 150 m (without much apparent structural thickening) along the southern margin of the Mississippian exposures. The youngest rocks exposed in the area are Permian and Triassic units of the Sadlerochit Group (Reiser et al., 1980) lying at the hinge of the syncline (Fig. 2).

The pre-Mississippian strata exposed in the northern part of the field area (Fig. 2), are predominantly early Paleozoic in age. In general, the oldest strata are exposed in the north with progressively younger rocks exposed southward, toward the Lisburne limestone. All pre-Mississippian units are involved in isoclinal folds and thrust faults, so that many stratigraphic details are uncertain. The succession is similar to one for which a well constrained stratigraphy was documented previously, in the Firth River area 60 km to the southeast (Lane and Cecile, 1989). There, a succession of *Oldhamia*-bearing Cambrian argillites, quartzites, and minor limestones are overlain by graptolitic Lower Ordovician chert and argillite, Upper Ordovician black argillite, and Lower Silurian graptolitic, rusty weathering argillite.

In the border area, a distinctive, maroon and green argillite unit, containing the Early Cambrian trace fossil *Oldhamia* (Hofmann and Cecile, 1981), strikes east-west across the central part of the field area (Fig. 2). It is underlain by a white weathering, pale green, siliceous, argillite and chert unit containing limestone beds a few metres thick (collectively Unit Ꞓac). This in turn is underlain by a maroon and green argillite followed by a dark grey limestone (PꞒl) tentatively dated as latest Proterozoic or Cambrian on

the basis of its position beneath the fossiliferous Cambrian argillite. The limestone contains a variety of sedimentary structures. These include well rounded to subangular quartz sand grains floating in a fine crystalline limestone matrix; coarse clastic limestone beds (sandstone, grit, and matrix supported conglomerate); graded beds; ripple crosslaminae; tabular crossbeds; debris flows; and small-scale scours. The northernmost, poorly exposed, part of the area is underlain by structural repetitions of the siliceous argillite, maroon and green argillite, and limestone units. Owing to the poor exposure, little information is available as to contact relationships and internal structure.

Depositionally overlying the fossiliferous Cambrian argillite/chert unit is a succession of lithic wackes and sandstones; dark green, grey and burgundy coloured mudstones; volcanic-clast conglomerates; chloritic tuffs; and minor limestones (Ow) with a total estimated thickness of 40 to 70 m. These rocks are interbedded with dark grey argillite and bedded chert. The volcanic clasts are consistently mafic, very dark green to black, and commonly amygdaloidal. Rare red amygdaloidal volcanic cobbles are present. The clasts, in particular the distinctive red amygdaloidal cobbles, are indistinguishable in appearance from volcanic rocks exposed 25 km to the south in the Whale Mountain volcanic succession, which has been dated as Late Cambrian on the basis of a trilobite fauna recovered from a limestone in the basal part of the succession (Dutro et al., 1971, 1972).

This volcanic/clastic unit (Ow) is depositionally overlain by a ridge-forming, bedded chert approximately 30 m thick. The chert is principally dark grey on fresh surfaces, weathering medium to light grey, locally weathering medium green. It is commonly, locally conspicuously, bioturbated. This thick chert unit probably correlates with chert mapped farther east (Lane and Cecile, 1989) at the top of a graptolitic Lower Ordovician chert/argillite unit. If this correlation is correct, the underlying volcanic/clastic unit is depositionally bracketed between a fossiliferous Lower Cambrian argillite and a Lower Ordovician chert. The fact that the volcanic sedimentary rocks depositionally interfinger with the dark grey chert/argillite unit suggests that the volcanic sedimentary rocks have an age near the upper end of the bracketed range. This bracketed biostratigraphic age for rocks believed to be correlative with the Whale Mountain volcanic succession provides the first independent corroboration of the published Late Cambrian age of the latter.

Overlying the ridge-forming chert is a cherty argillite with thin chert interbeds, characterized by the occurrence of manganese coatings on fracture surfaces. The manganiferous unit is commonly only a few metres thick, and is overlain by pale grey and green, siliceous argillite that weathers white and rusty; dark grey argillite and interbedded chert; and minor brown weathering limestone beds. Overlying these units, with apparent conformity, is a succession with a structural thickness of some 200 m, consisting of black silty argillite containing ripple crosslaminated, fine sandstone beds generally less than 3 cm thick. Unidentified feeding and locomotion traces are sparsely distributed on bedding surfaces throughout the unit. A single Upper Ordovician graptolite fossil, together with several varieties of trace fossil, have been collected from near the southern contact of this unit at the international boundary (Dutro et al., 1971, 1972). All strata between the ridge-forming chert and the Upper Ordovician argillite have been included as one undifferentiated unit (Oca) in Figure 2. The ridge-forming chert unit (Oc) has been separated locally, depending on outcrop width and structural complexity (Fig. 2).

Overlying the dated Ordovician units with apparent conformity are three Paleozoic units (Pzw, Pzl, and Pza) that are possibly a structural repetition of part of the underlying Ordovician succession. The unit designated Pzw consists of lithic arenite; volcanic-clast conglomerate; mafic tuff; finely laminated dark mudstone (locally a magnetite iron-formation); and muddy limestone, all of which are interbedded with chert and argillite. A one metre thick sill of intermediate (?) composition, exposed only as frost heaved blocks, occurs near the base at one site. The top part of this unit is a blue-grey, siliceous argillite 15 to 20 m thick. Unit Pzw does not persist westward to the Clarence River at the western edge of the field area. Unit Pzl is a dark grey, fine grained limestone, locally recrystallized to very coarse grain size, and which emits a sulphurous odor from fresh breaks. Some beds contain fine grained, floating, quartz clasts. At one site a 2 m thick, rusty weathering, carbonate-matrix tuff(?) is exposed at the base of this unit. Above Unit Pzl, but north of the Lisburne Ridge, is a pale green siliceous argillite (Unit Pza) seen only as frost heaved fragments in the field area.

If these units are part of an intact, normal stratigraphic succession, they must be Late Ordovician or younger in age, based on a fossil locality in the underlying beds (Dutro et al., 1971, 1972). If the succession was formed by structural repetition (Unit Pzw being equivalent to Unit Ow), the limestone (Pzl) would necessarily be a southern carbonate facies equivalent to thin limestone beds associated with Unit Ow. At present, we cannot distinguish between these alternative interpretations.

Mapping south of Lisburne ridge has not yet been compiled on Figure 2. In this area, the pre-Mississippian units differ significantly from those on the north side. However, several similarities suggest that there is at least a partial overlap of stratigraphy, complicated by facies variations. The principal differences are the greater proportion of carbonate rocks in the south, and the change from mainly basinal deposits in the north to predominantly turbiditic deposits in the south. A partial stratigraphic succession consists of (progressing upward) thin bedded, grey chert and minor argillite, gradationally overlain by maroon and green argillite with minor rippled siltstone and limestone beds. These strata grade upward through siliceous rippled siltstone and minor limestone into clearly turbiditic sandstone and siltstone with minor limestone; followed by a buff weathering turbiditic limestone; then a grey weathering, grey limestone locally containing pisolitic beds, trough crossbeds and a lens of massive limestone three metres thick. This succession is structurally repeated at least once. Other units whose stratigraphic positions are currently uncertain are: a thick succession of interbedded cherts and argillites; a thick quartzite and quartz-feldspar wacke succession; and an argillite/chert/volcanic (tuff?) unit. Several smaller limestone units appear to thin and pinch out across the field area. The southern part of the area requires further detailed mapping in order to resolve the stratigraphic and structural complexities identified there.

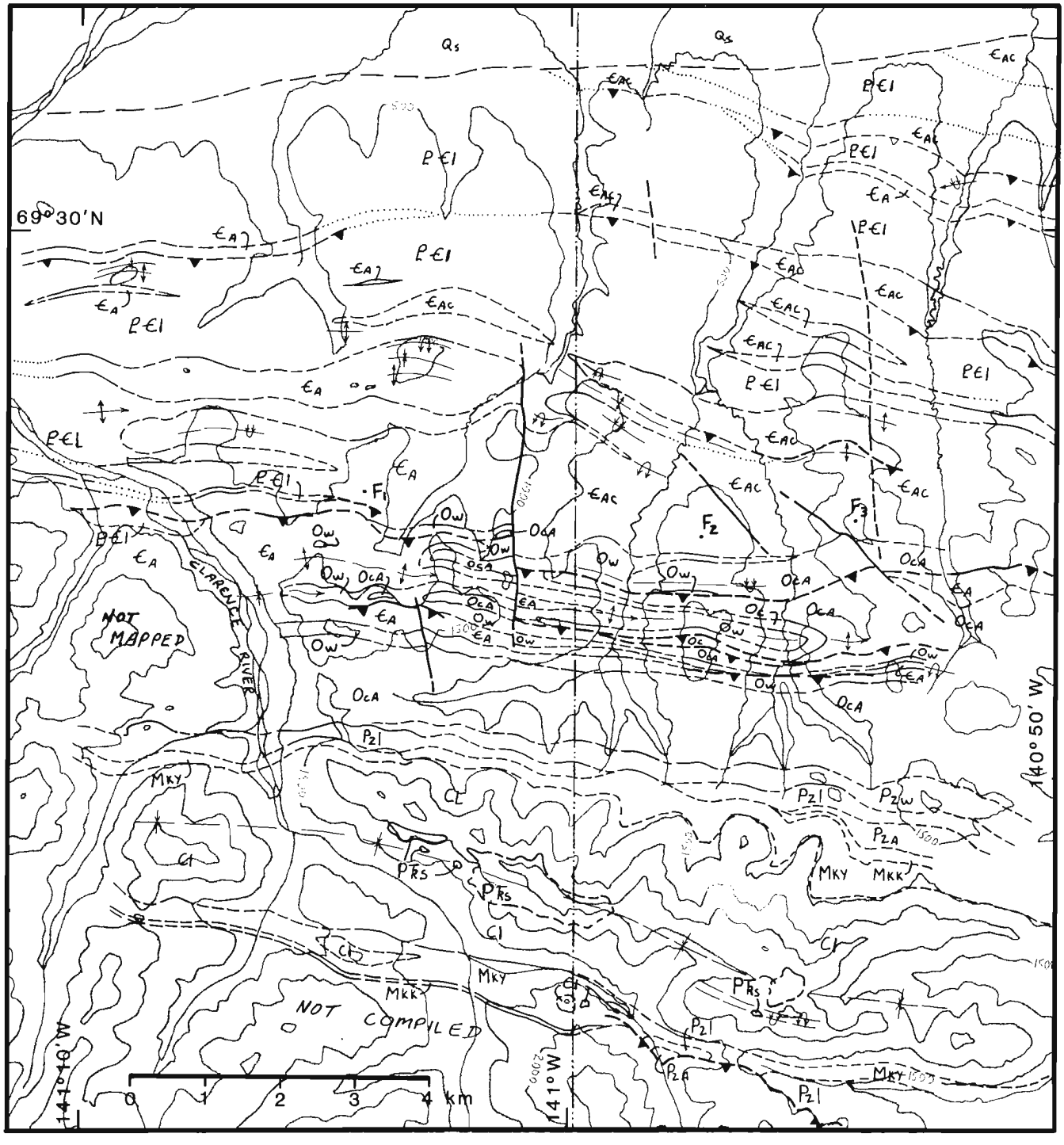

Figure 2. Preliminary compilation map of the field area. A 5 km wide strip of stratigraphically and structurally complex geology along the southern margin is not yet compiled.

LEGEND

Qs	Surficial deposits (Quaternary)
PTs	Sadlerochit Group (Permian and Triassic): sandstone and shale
Cl	Lisburne Group (Carboniferous): limestone
Mky	Kayak Shale (Mississippian): silty shale
Mkk	Kekiktuk Conglomerate (Mississippian)
Pzl	Limestone (Paleozoic)
Pzw	Wacke, volcaniclastic rocks, and tuff (Paleozoic)
Pza	Argillite (Paleozoic)
Oca	Chert and argillite (Ordovician)
Oc	Chert (Ordovician)
Ow	Wacke, mudstone, and volcaniclastic rocks
Ca	Argillite (Cambrian)
Cac	Argillite and chert (Cambrian)
PCl	Limestone (latest Proterozoic or Cambrian)
	Anticline, overturned
	Syncline, overturned
	Contact defined, approximate, assumed
	Thrust fault, teeth on upper plate
	International boundary
F_1	New *Oldhamia* fossil locality
	Contour interval is 500 feet

STRUCTURE

Strata in the area have been intensely deformed by thrust faulting and isoclinal folding. In the pre-Mississippian succession, the dominant structures are similar to those documented by detailed mapping farther east in the British Mountains, and to the southeast in the Barn Mountains (Lane and Cecile, 1989; Cecile, 1988). Structural style is dependent on rock type (i.e., competence). In argillaceous rocks, the structures are upright or steeply northward-overturned, tight to isoclinal folds but, in competent rocks, thrust faults dominate. The older argillaceous Cambrian succession, which deformed by isoclinal folding, is exposed in the west. However, down plunge eastward, the more competent, chert dominated, Ordovician units accommodated the same strain by thrust imbrication as well as by folding. Consequently, simple anticline/syncline fold trains exposed in the west pass eastward into complex imbricated structures in which the anticline hinges are preserved but the syncline hinges are sheared out (Fig. 2). In the limestone dominated northern exposures (Fig. 2), and in the structurally complex area south of the Lisburne Ridge (not included in the compilation), the strata tend to have homoclinal southward dips. In the north, the limestone and argillite units are repeated several times, presumably on thrust faults. There is no stratigraphic or structural evidence of large-scale folds although mesoscopic folding is common. Poor exposure seriously limits any attempt to interpret the structures there.

South of Lisburne Ridge, slaty cleavage is pervasive in argillaceous units, and is axial planar to tight chevron folds—on scales up to several metres between axial surfaces. However, stratigraphic tops are predominantly southward and mappable thrust faults, which truncate the strata, are locally exposed, together suggesting that thrust faulting is relatively more important there than folding.

The only structures whose ages can be definitively constrained are those affecting the Mississippian and younger rocks. The thick Lisburne limestone contains a single, tight, upright syncline with local detachments at its base and, on its south limb, at least one minor fold steeply overturned toward the north. In the Kayak Shale, a non-penetrative cleavage crenulates the fine silt/shale laminae. Moderate southward dips are common, although a northward dipping fabric is locally developed. In local high-strain zones, the bedding is transposed into the plane of the cleavage.

A north-directed thrust fault displaces pre-Mississippian argillite and limestone (not compiled in Fig. 2) onto the Kayak Shale along the south margin of the exposed Mississippian strata. The displacement is not well documented, but does not appear to exceed several hundred metres. Just east of the field area, a south-directed, prominently exposed, thrust fault repeats parts of the Kayak/Lisburne succession (Norris, 1981).

Mesoscopic structures similar to those involving Mississippian strata were locally observed in the older rocks, where pre-Mississippian structures have been refolded on gently to moderately north dipping axial surfaces. At one locality south of Lisburne Ridge, a tight, north-verging, second generation structure has refolded a first generation mesoscopic fold. The second generation axial planar fabric

in argillite beds is cataclastic, whereas the overprinted first generation fabric is a slaty cleavage.

In contrast, structures characteristic of the older succession were not observed in the younger rocks. Notably absent from the Kayak Shale are the pervasive slaty cleavage and common mesoscopic minor folding seen in argillaceous rocks of the pre-Mississippian succession. Similarly, superposition of several generations of structures is widespread in the older rocks, but absent from the younger succession.

Several north-trending and northwest-trending, steep, transverse faults, many with displacements of only tens of metres, were mapped in the field area. Air photographs reveal prominent lineaments whose abundance suggests that transverse faults are common. These faults involve Lisburne and younger rocks in adjacent areas (Reiser et al., 1980; Norris, 1981). Because of limited exposure, kinematic information is sparse, but the map separation of stratigraphic units suggests oblique motion with west sides displaced northward and down.

DISCUSSION

The distinctly different structural styles exhibited by the pre-Mississippian and younger successions indicate that the intense strain preserved in the older rocks is predominantly due to pre-Mississippian deformation, with only local modifications by Cretaceous to Tertiary Brookian deformation. This is consistent with previous observations in the British Mountains (Norris, 1981, 1986; Lane and Cecile, 1989), and farther southeast in the Barn Mountains (Cecile, 1988). Widespread preservation of Paleozoic structures with local modification by Brookian structures tends to support a model of Brookian structural evolution which suggests that Brookian crustal shortening was transmitted to Mississippian and younger strata via localized structures such as (reactivated) thrust faults, as opposed to Brookian penetrative strain in the older rocks (e.g., Kelley and Foland, 1987; see also the review by Wallace and Hanks, 1990).

A principal purpose of a co-ordinated international effort was to rationalize published reconnaissance work on both sides of the border. Whereas Norris (1981) presented a highly generalized summary of pre-Mississippian lithology and structure, Reiser et al. (1980) showed detailed rock distributions for pre-Mississippian strata with only limited success in stratigraphic correlations across strike. Both maps reflect a lack of stratigraphic and structural control. Although both compilations may be valid approaches to regional reconnaissance mapping, we are now able to suggest a partial (preliminary) rationalization of the two apparently conflicting stratigraphic schemes.

On the Canadian side, pre-Mississippian units included in the 1990 fieldwork are Pn2, Pn4, Pn5 and the lower Paleozoic Road River Formation (Norris, 1981). It is apparent from 1990 and previous fieldwork (Norris, 1986; Lane and Cecile, 1989) that Unit Pn2 consists largely of Ordovician, Silurian, and Lower Devonian Road River equivalent strata, with the structural inclusion of some older rocks, particularly in the border area. North of Lisburne Ridge Unit Pn4 is equivalent to the Road River Formation. South of Lisburne Ridge, areas of both Units Pn4 and Pn5 are tentatively interpreted as predominantly Cambrian and older. The strata south of Lisburne Ridge appear to belong to a more calcareous and turbiditic facies than farther north.

The principal outcrop belt of Norris' Pn4 unit lies south of our present coverage. Norris (1985) correlated this unit (in part) with the Neruokpuk Quartzite (Reiser et al., 1978), as well as with a broad belt of calcareous sandstone, siltstone, and phyllite interpreted as Cambrian in age by Reiser et al. (1980).

On the American side, our field area includes eight of the pre-Mississippian map units of Reiser et al. (1980). These include: three units assigned Ordovician ages on the basis of a single Upper Ordovician graptolite recovered from a site at the border (Dutro et al., 1971, 1972); one unit interpreted as Precambrian; three units of unknown stratigraphic position; and one undifferentiated unit. Our results are consistent with an interpreted Ordovician age for Units Opc, Ovc, and Os of Reiser et al. (1980), and indicate the equivalence of Units Opc and Os to the Road River basinal facies. The volcanic-derived unit (Ovc) appears to be largely restricted to the border area. Unit ph of Reiser et al. (1980) belongs to the Cambrian maroon and green argillite succession, as documented by three new *Oldhamia* localities straddling the border, allowing definite correlation with *Oldhamia*-bearing maroon and green argillites as far away as the Selwyn Basin (Lane and Cecile, 1989; Gordey, 1980, in press).

Unit sc of Reiser et al. (1980) appears to be a structural mixture of Cambrian and Ordovician strata, except near the northern limit of its exposure where it appears to correlate with Cambrian argillite and chert. The Precambrian limestone unit of Reiser et al. (1980) correlates with the dark grey limestone characteristic of Norris' Unit Pn5 (Norris, 1981, 1985). This unit lies structurally below (or within?) the Cambrian maroon and green argillite, and therefore is presumably latest Proterozoic or Cambrian in age. Structural complications and lack of exposure preclude a definite stratigraphic interpretation. Finally, the local aq unit and the undifferentiated Precambrian and Paleozoic rocks, correlate with a succession that we believe to be predominantly Cambrian and older. However, this area south of Lisburne Ridge is stratigraphically and structurally complex, and exposure is limited. This area requires further detailed work along strike before definitive stratigraphic correlations can be attempted.

CONCLUSIONS

Approximately one third of the total project area has been mapped, and the preliminary results of this co-operative international project have led to significant positive correlations of stratigraphy across the international boundary.

Much of the area mapped in 1990 is correlative with basinal facies of the lower Paleozoic Road River Formation, including much of Unit Pn2 (Norris, 1981) and several units interpreted as Ordovician in age by Reiser et al. (1980). This correlation is applicable to a belt of exposure extending from longitude 139°W to 142° 30'W, some 140 km along strike.

Discovery of three new *Oldhamia* trace fossil localities extends the range of a distinctive lower Cambrian maroon

and green argillite unit to include a widely exposed phyllite unit (ph) in northeastern Alaska.

A dark grey limestone, presumably of latest Proterozoic or Cambrian age, structurally underlies the fossiliferous Cambrian argillite succession at the northern limit of exposures. The precise stratigraphic position of this unit, and possible correlative units farther south, is uncertain.

Lying above the Cambrian argillite is a succession of lithic arenites, volcanic-clast conglomerates, chloritic tuffs, and dark mudstones, interbedded with the lower part of the Lower Ordovician chert and argillite unit. Cobbles of distinctive, dark red, amygdaloidal volcanic rocks, indistinguishable in appearance from volcanic rocks exposed farther south, strongly indicate a definite correlation with the Whale Mountain volcanic succession. The stratigraphic position of the volcanic-derived clastic rocks mapped in 1990 is consistent with the Late Cambrian age of fossil debris from carbonate rocks within the basal part of the Whale Mountain volcanic succession (Dutro et al., 1971, 1972). If the lithological correlation between the Whale Mountain volcanic succession and these volcaniclastic rocks is correct, this would be the first independent corroboration of the age of the Whale Mountain volcanic succession.

The structural geometry of pre-Mississippian rocks differs significantly from that of younger strata, supporting the interpretation that much of the strain preserved in the older rocks reflects pre-Mississippian deformation.

ACKNOWLEDGMENTS

GSC funding was provided through the Frontier Geoscience Program (FGP). Helicopter support was provided by the Polar Continental Shelf Project (PCSP) and by Sunrise Helicopters. Logistical support was provided by the Inuvik Research Centre (Science Institute of the Northwest Territories). Efficient and cheerful assistance in the field was provided by R.A. Stevens. Bill Dolan and Dan Frandsen (warden's staff, North Yukon National Park) very kindly allowed us to use the wardens' facilities in the park during our fieldwork. The manuscript was thoroughly reviewed by M.P. Cecile (GSC), and A.B. Till and K.J. Bird (USGS).

REFERENCES

Cecile, M.P.
1988: Corridor traverse through Barn Mountains, northernmost Yukon; in Current Research, Part D, Geological Survey of Canada Paper 88-1D, p. 99-103.

Dutro, J.T. Jr., Reiser, H.N., Detterman, R.L., and Brosgé, W.P.
1971: Early Paleozoic fossils in the Neruokpuk Formation, northeast Alaska. U.S. Geological Survey, Open File Report 499, 4 p.

Dutro, J.T. Jr., Brosgé, W.P., and Reiser, H.N.
1972: Significance of recently discovered Cambrian fossils and reinterpretation of Neruokpuk Formation, northeastern Alaska. American Association of Petroleum Geologists, Bulletin, v. 56, p. 808-815.

Gordey, S.P.
1980: Selwyn Basin to Mackenzie Platform, Nahanni Map area, Yukon Territory and District of Mackenzie; in Current Research, Part A, Geological Survey of Canada, Paper 80-1A, p. 353-355.
in press: Evolution of the northern Cordilleran Miogeocline, Nahanni Map area (105-I), Yukon Territory and District of Mackenzie. Geological Survey of Canada, Memoir.

Hofmann, H.J., and Cecile, M.P.
1981: Occurrence of *Oldhamia* and other trace fossils in Lower Cambrian(?) argillites, Niddery Lake Map Area, Selwyn Mountains, Yukon Territory; in Current Research, Part A, Geological Survey of Canada, Paper 81-1A, p. 281-289.

Kelley, J.S. and Foland, R.L.
1987: Structural style and framework geology of the Coastal Plain and adjacent Brooks Range. Chapter 20; in Petroleum Geology of the Northern Part of the Arctic National Wildlife Refuge, Northeastern Alaska, Bird, K.J. and Magoon, L.B. (eds.); U.S. Geological Survey, Bulletin 1778, p. 255-270.

Lane, L.S. and Cecile, M.P.
1989: Stratigraphy and structure of the Neruokpuk Formation, northern Yukon; in Current Research, Part G, Geological Survey of Canada, Paper 89-1G, p. 57-62.

Norris, D.K.
1981: Geology, Herschel Island and Demarcation Point, Yukon Territory. Geological Survey of Canada, Map 1514A. (Scale 1:250 000.)
1985: The Neruokpuk Formation, Yukon Territory and Alaska; in Current Research, Part B, Geological Survey of Canada, Paper 85-1B, p. 223-229.
1986: Lower Devonian Road River Formation on the north flank of Romanzof Uplift, northern Yukon Territory; in Current Research, Part A, Geological Survey of Canada, Paper 86-1A, p. 801-802.

Reiser, H.L., Norris, D.K., Dutro, J.T. Jr., and Brosgé, W.P.
1978: Restriction and renaming of the Neruokpuk Formation, northeastern Alaska: changes in stratigraphic nomenclature by the U.S. Geological Survey, 1977. U.S. Geological Survey, Bulletin 1457A, p. A106-A107.

Reiser, H.L., Brosgé, W.P., Dutro, J.T. Jr., and Detterman, R.L.
1980: Geologic map of the Demarcation Point Quadrangle, Alaska. U.S. Geological Survey, Miscellaneous Investigation Series, Map I-1133. (Scale 1:250 000.)

Wallace, W.K. and Hanks, C.L.
1990: Structural provinces of the northeastern Brooks Range, Arctic National Wildlife Refuge, Alaska. American Association of Petroleum Geologists, Bulletin, v. 74, p. 1100-1118.

An investigation of platinum-bearing alluvium from Florence Creek, Yukon

S.B. Ballantyne and D.C. Harris
Mineral Resources Division

Ballantyne, S.B. and Harris, D.C., An investigation of platinum-bearing alluvium from Florence Creek, Yukon; in Current Research, Part A, Geological Survey of Canada, Paper 91-1A, p. 119-129, 1991.

Abstract

A sample of gold- and platinum-bearing placer heavy mineral concentrate from Florence Creek, Yukon is being studied in detail. This report presents quantitative microprobe data and scanning electron microscope images of twelve of the largest (average 844 x 806 μm) PGM grains. Surface texture is variably smooth, pitted and even jagged.

Microprobe data confirmed all grains to be isoferroplatinum (Pt_3Fe) in composition. One Pt-Fe alloy contained four bornite-digenite, 50 μm drop-like, inclusions which host (Pt, Pd)S (braggite ?) and an unnamed Rh-Cu-Pt-S phase. Three placer grains contain several equidimensional to lath shaped native osmium inclusions. Drop-like silicate inclusions and fracture-filled altered silicate gangue were noted in many grains.

This study supports the economics of platinoid placer recovery and points to the undiscovered PGM potential of the area.

Résumé

Un échantillon de concentré de minéraux lourds d'un gisement alluvial aurifère et platinifère à Florence Creek au Yukon fait l'objet d'une étude détaillée. Le présent rapport fournit des données quantitatives obtenues à la microsonde et des images des douze plus gros grains (moyenne 844 x 806 micromètres) de MGP obtenues au microscope électronique à balayage. La texture superficielle est plus ou moins lisse, picotée et même déchiquetée.

Les données fournies par la microsonde confirment que tous les grains présentent la composition de l'isoferroplatine (Pt_3Fe). Un alliage de Pt et de Fe renfermait quatre inclusions de bornite et néodigénite en forme de goutte de 50 micromètres qui renfermaient (Pt, Pd)S (braggite ?) et une phase de Rh-Cu-Pt-S non nommée. Trois des grains du gisement alluvial renfermaient plusieurs inclusions d'osmium natif dont la forme variait d'équidimensionnelle à prismatique. On a noté dans plusieurs des grains la présence d'inclusions de silicate en forme de goutte et d'une gangue de silicate altéré.

Cette étude reconnaît la rentabilité de la récupération de métaux platinoïdes au gisement alluvial et met en valeur le fait que cette région recèle peut-être d'autres ressources en MGP non découvertes.

INTRODUCTION

Although studies of placer gold in the Canadian Cordillera are in progress or have been reported recently (Ballantyne and MacKinnon, 1986; Eyles, 1990; Giusti, 1986; Knight and McTaggart, 1986, 1990) few investigations of alluvial grains bearing platinum group elements (PGE) are available. At this stage of research, placer gold studies have generally emphasized morphology and gold grain compositions. Rarely has discussion included detailed data of the geochemical composition of the accompanying heavy mineral suite or gangue mineralogy within the placer gold grains. There have been few descriptive and quantitative studies of alluvial platinum group mineral (PGM) grains (Cabri and Harris, 1975; Cousins and Kinloch, 1976; Feather, 1976; Hagen et al., 1990; Johan et al., 1990; and Nixon et al., 1989). No similar study has been reported for the Yukon. Compared to placer gold, alluvial grains bearing PGE enrichments are relatively rare. Placer gold mining in the Yukon has produced oral communication reports of PGE alluvial nugget recoveries, but, their poor documentation and identification is the norm.

Systematic characterization of PGE alluvial material must include basic mineral (PGM) identification, determination of inclusion material and gangue composition found within PGM grains and most importantly detailed examination of the accompanying heavy mineral suite. This approach can provide the fundamental economic and geological data required for exploration for PGM placers and the source of the primary PGE ores or host rocks.

In this preliminary report, we identify and describe our investigations of selected large PGM placer grains from a single heavy mineral concentrate (HMC) sample recovered from the Florence Creek drainage, Yukon. This is significant since no potential source rocks for primary PGE occurrences or PGM mineralization is now known in the area. Study of the smaller PGE particles, the placer gold and the complete placer heavy mineral concentrate suite of minerals is in progress. Bob Wondga collected the sample and kindly donated a portion for our studies.

Scientific study of placer PGE grains is important since it can provide:

1. the first proof of the PGE potential of a drainage basin. It can guide exploration strategy for specific genetic types of primary PGE deposits. For example, the relative abundance of Os-Ir-Ru versus Pt-Pd in the alluvial grains, the presence or absence of chromitities and/or sulphides in the accompanying heavy mineral suite can have direct economic significance as well as govern geochemical and geophysical exploration methods.
2. fundamental geochemical and geological knowledge of primary ore and source rock mineralogy, assuming that the alluvial grains themselves and entrapped silicate gangue and inclusions are not altered. The shapes of preserved PGM sulphides as individual alluvial grains or as inclusions in PGM alloys would provide proof of primary heritage of alluvial grains.
3. the opportunity to better understand anomalous PGE geochemical signatures in the surficial environment. Detailed studies can provide a better understanding of the effects of chemical and mechanical weathering on primary PGE enrichments and their dispersion characteristics away from source. Many of the unresolved arguments concerning placer gold formation are repeated in our lack of understanding of the relative stability of PGE under low temperature conditions, maturity cycles and PGE dispersion, colloidal and in situ accretion of platinoids (i.e. nugget formation). A clear definition of processes acting upon different genetic types of PGE mineralization during changing or different climatic conditions are obviously important aspects requiring further study.
4. insight into specific aspects of PGE genesis. Compared to primary PGE ores now under detailed scientific examination, alluvial platinoid grains are often much larger in size and thus easier to find and to characterize when utilizing microprobe or SEM systems. It remains to be seen if meaningful micro-mineral chemistry including isotopic and fluid inclusion data can be obtained from the alluvial PGM and their associated heavy mineral suite. Alluvial grains could be used to a greater degree in genetic modelling studies considering the controversy surrounding PGE sources, fluid-volatile transport, precipitation and crystallization mechanisms, and hydrothermal-magmatic genesis.

LOCATION AND REGIONAL SETTING

The Florence Creek drainage is located in NTS 115H/15, 16 approximately 3 km south of Little Buffalo Lake. Limited placer bench-mining activity has taken place. However, remarkable concentrations of "black sand" can be recovered and non-magnetic HMC assay 32 oz/t gold and 70 ppm platinum (Wondga, pers. comm).

The area is underlain by hornblende granodiorite and porphyritic quartz monzonite granitoid rocks (Tempelman-Kluit, 1974). Regional aeromagnetic data do not reveal strong magnetic features often characteristic of ultramafic-mafic rocks (GSC-Aeromagnetic Series, Maps 3329G, 3347G, 1966a, b). National Geochemical Reconnaissance (NGR) regional stream sediment geochemistry reveals a single sample, multi-element anomaly of Cu, Fe, Ni, As, Co, V on a tributary entering Florence Creek from the south (GSC Open Files 1219, 1986). This element association may be important in characterizing source rocks for the alluvial PGM grains.

Studies of the surficial geology of the Florence Creek drainage south of Little Buffalo Lake show that McConnell age glacial and glaciofluvial deposits predominate (Hughes, 1989). Glacial deposits are generally composed of moraine-colluvial blankets and moraine veneers on bedrock. However, glaciofluvial plain, glaciofluvial terrace and complexes of both are also present. Northerly directed meltwater channels of variable length follow topographic lows.

It is important to note that the anomalous stream sediment sample noted above was collected from the glaciofluvial terrace which yielded the gold-PGE bearing material examined in this study. This same stream drains a topographic high of bedrock and moraine veneer which could also be an anomaly source.

To date, limited prospecting by Mr. Wondga has failed to pinpoint mineralization or obvious source rocks for the PGE-gold enrichment found in the placers.

METHODS

The PGM grains used in this study were first separated from the placer gold and heavy-mineral concentrate under a low-power stereo microscope. Twelve of the largest PGM grains have been studied for this report. Smaller PGM grains, gold grains and the HMC are being investigated in detail and results will be reported in the future.

Distinct shape factors, external texture and structure, and the detailed resolution of the dimensions of the grains are best studied using the scanning electron microscope (SEM). The grains were mounted on double-sided tape on four mounting stubs, carbon coated and then examined using both secondary and back-scattered electron modes of a Cambridge S-200 SEM. Polaroid photo images of each grain were taken to document size and shape. Close up images of a variety of surface textures, embayments and concave depressions, protrusions and knobby or nodular features were noted, measured and photographed. Qualitative chemical analyses of gangue and inclusions observed in back-scatter mode, and the surface chemistry of the grains themselves were determined using a Link Analytical AN 10000 energy dispersive X-ray spectrometer.

The grains were removed from the SEM holders and moulded in an araldite mount for polishing. After polishing, the mount was examined under oil immersion with a reflecting ore microscope. Colour photographs of the interiors of the grains were taken to record the various types of inclusions and the phases now revealed within them.

The polished mount was then carbon-coated and detailed investigations utilizing SEM, image analysis, energy dispersive and electron microprobe systems were completed on each grain.

Analyses of the PGE alluvial grains were made using a Cameca SX 50 microprobe using wavelength spectrometers. The operating voltage was 20 kilovolts at beam current of 20 nanoamperes. Pure metals and synthetic compounds were used as standards with raw data corrected by an on-line PAP correction program.

RESULTS

Size, shape and surface texture observations

Length and width dimensions of the twelve grains examined during the SEM study average 844 x 806 μm, respectively. The largest grain measured 1.8 x 1.4 mm (Fig. 10) and the smallest was 300 x 700 μm (Fig. 2).

The general shape of these grains can be described as tabular, rounded plates or discoid (Fig. 1-4, 7-15). However, although they are generally flat and approximately equal in length and width, some grains do have subangular knobs, nodules or lobes protruding from the disc-shaped body (Fig. 11, 12, 15). The lobate features observed in Figures 5 and 6 may be partially rounded octahedral or cubic shapes commonly ascribed to Pt-Fe alloys.

Table 1. Microprobe analyses of Pt-Fe Alloys

Stub-grain	Rh %	Pd %	Os %	Ir %	Pt %	Fe %	Cu %	Total %
1662-1	2.1	1.3	1.0	0.4	90.6	5.2	0.6	101.2
1662-3	2.0	0.9	1.5	0.7	90.4	5.0	0.4	100.9
1663-1	1.7	0.9	0.2	0.3	92.2	5.0	0.4	100.7
1663-2	1.6	1.1	0.8	-	89.4	5.7	2.0	100.6
1663-3	0.6	0.5	0.3	1.7	88.6	7.5	1.2	100.4
1663-5	0.7	0.8	0.2	2.4	87.4	8.0	0.6	100.1
1664-1	1.2	1.6	0.3	0.7	89.7	5.6	0.7	99.8
1664-2	1.2	0.6	0.4	-	88.9	6.9	2.3	100.3
1664-5	1.8	0.8	0.8	3.7	85.1	8.0	0.7	100.0
1664-6	1.5	1.0	1.0	0.6	90.7	4.7	0.8	100.3

not detected - Ru, Ni, Ag, Au, Te, Sb

The suite of grains exhibited a variety of surface textures which are difficult to interpret (see Fig. 1-18).

Some grains appear smooth (Fig. 1-8) whereas others have pitted surfaces. Some detrital fracturing may have occurred as evidenced by the cup-shaped and concentric indentations seen in Figures 9 and 10. Intergrowth structures (parallel lines on shrinkage folds) are also present at the surface of some grains giving a somewhat layered appearance (Fig. 11-12).

The surface irregularities of the grains were examined in detail (close up micrometre imaging, Fig. 16-18). Ragged surface textures are often inferred to have been caused by unstable preferential chemical leaching of alloy phases and chemical etching.

The bright back-scattered electron images (BEI) shown in Figures 1 to 18 are all Pt-Fe alloys in surface composition. The surface black blotches and seams appearing in these SEM photomicrographs are silicate phases of variable composition (qualitative data from SEM-energy dispersive analysis system).

Interior grain composition

Matrix

Our investigations (SEM, image analysis, microprobe, wavelength dispersive analysis) confirmed that all of the grains are the Pt-Fe alloy isoferroplatinum (Pt3Fe). Some grains contained rare to frequent inclusions. We found no evidence of alteration of the Pt-Fe alloy portion of the grains (e.g. no preferential leaching causing zonation). The Pt-Fe alloy portion of each grain is homogeneous showing little variation in composition (rim to core), although the Pt, Rh, Ir, Os, Pd, Fe and Cu contents were found to vary among grains (Table 1). Colloform or zoned Pt-Fe alloy grains were not observed. Chemical accretion of alloy grains either in situ or from dispersed colloidal PGE particles would appear not to have played a role in the creation of these alluvial grains or their irregular surface textures (Fig. 21, 25-27).

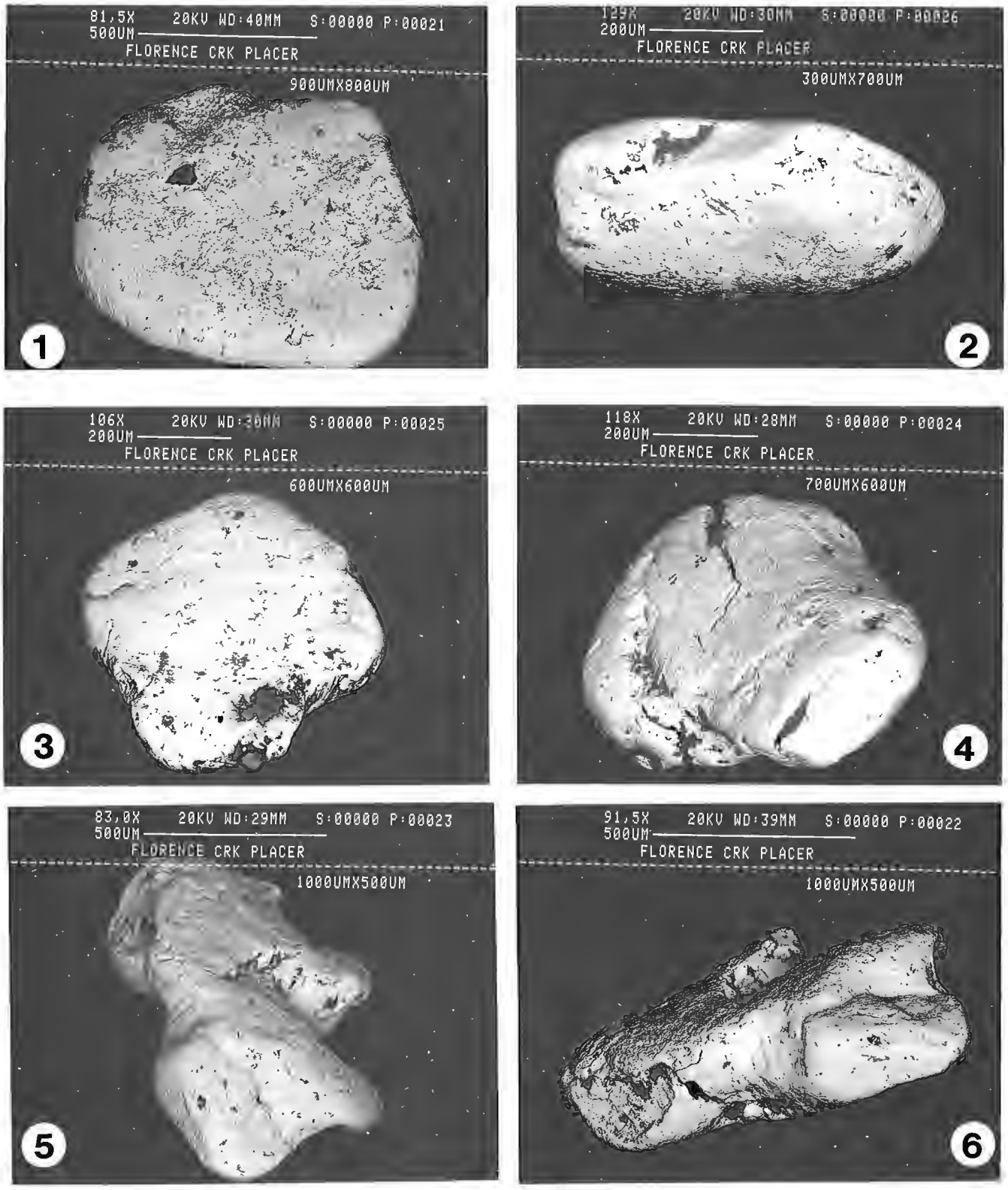

Figures 1-6.

Back-scattered electron images (BEI) of isoferroplatinum grains Florence Creek Yukon. Figures 1-4 show tabular, disc shapes. Figures 5-6 show lobed features of the same grain illustrating partially rounded octahedral or cubic shapes ascribed to primary Pt-Fe alloys.

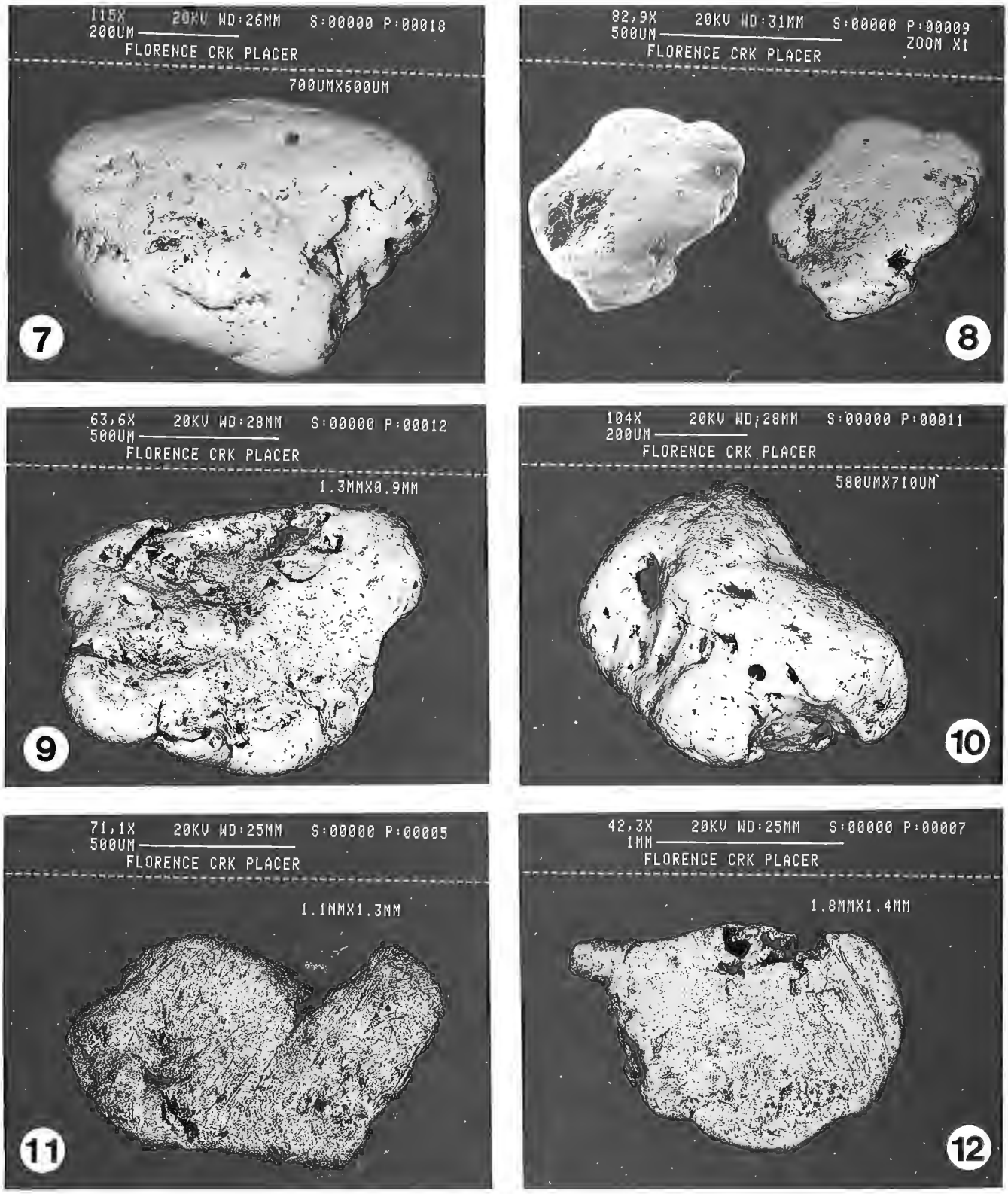

Figures 7-12.

BEI of isoferroplatinum grains. Note the scale bar in millimetres or micrometres above the title of each figure. Suite of grains shows variety of surface textures: Figures 7-8 smooth; Figures 9-10 concentric indentations from detrital fracturing; Figures 11-12 protrusions from disc-shaped body and layered surface appearance (intergrowth structures ?).

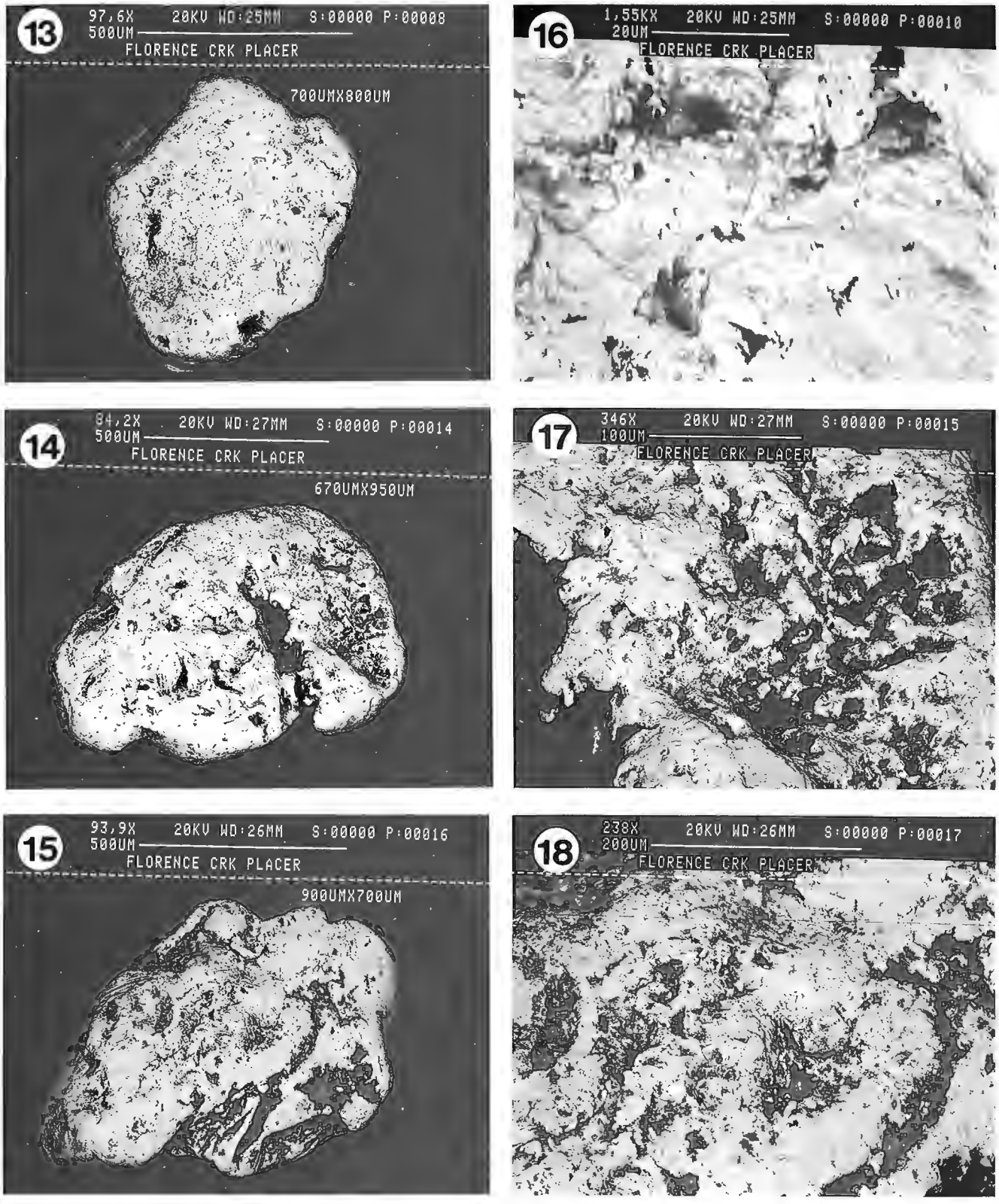

Figures 13-18.

BEI of grains and detailed micrometre imagery of surface irregularities of portions of the same grain (Fig. 13 and 16; 14 and 17; 15 and 18). Note jagged and pitted surface of isoferroplatinum (bright) and silicate phases (black).

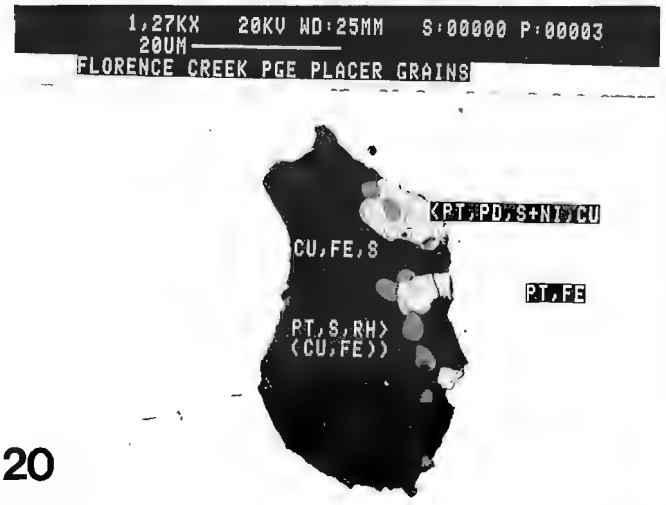

Figures 19-22

BEI of polished mount showing interior of the grain matrix, inclusions and embayments or seams of silicate phases. Figures 19 and 20 are close-ups of the two bornite-digenite inclusions shown in Figure 20. Figure 22 is close-up of the droplet-shaped (braggite (?)) and rounded crystals of the unknown Rh-rich phase found in the upper right of the Cu-sulphide inclusion in Figure 21.

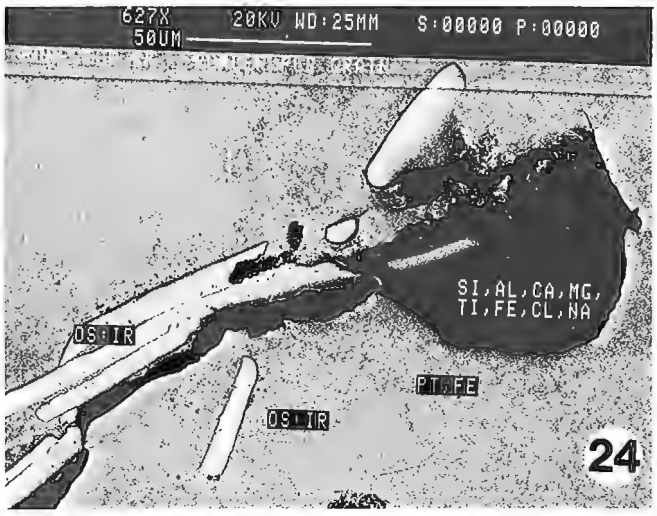

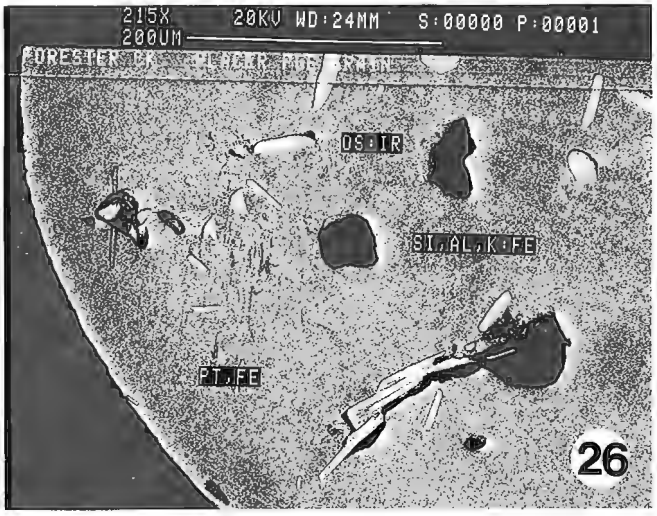

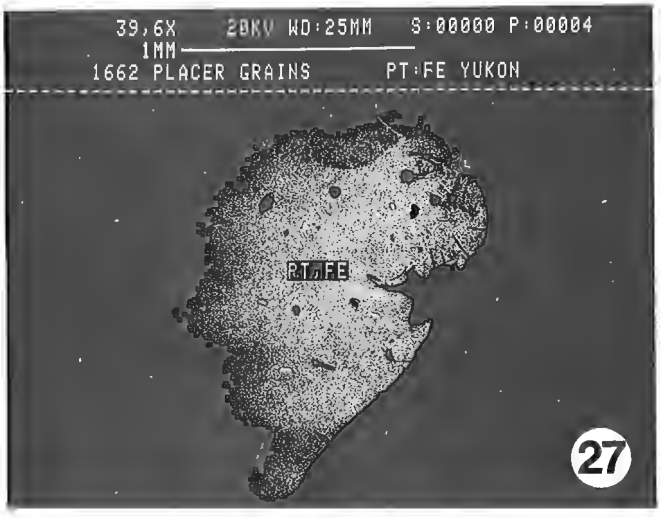

Figures 23-27.

BEI of interior matrix and inclusions of PGM and silicate phases. Figure 23 is photographed in reverse polarity to enhance silicate phase (bright) which encapsulates the complex Os:Ir phase (dark). Note native osmium lath-rod shapes in isoferroplatinum matrix with silicate inclusions or as disoriented separate inclusions (Fig. 24, 26). Figure 25 illustrates silicate inclusions and seams in isoferroplatinum matrix without PGM inclusions whereas Figure 27 shows the presence of both types (close-up Fig. 24, 26).

Table 2. Microprobe analyses of bornite and digenite inclusions

Stub-grain	S %	Fe %	Cu %	Total %
bornite 1664-2	26.2	10.4	63.3	99.9
digenite 1664-2	21.8	0.4	78.5	100.7

not detected - Rh, Pd, Os, Ir, Pt, Ni, As

Detailed polished mount study of the Pt-Fe alloy grains revealed three types of inclusions: I) sulphide, II) PGM and III) silicate. The sulphide inclusions are rare and are multi-phase mixes of Cu-sulphide and PGM sulphides. Inclusions of PGM and silicates are much more abundant than sulphide inclusions. Silicate inclusions and seams of gangue were found in four grains.

Sulphide inclusions

Base-metal sulphide inclusions exhibiting globular and/or drop-like shapes measuring less than 50 μm in length were observed in the polished surface of one grain (Fig. 21). The four inclusions are essentially bornite-digenite (Table 2). Further polishing of the mount may expose more inclusions in other grains and it may provide further dimensional data on the inclusions reported here.

Bornite and digenite occur together in all sulphide inclusions. SEM study revealed that these Cu-sulphide phases are highly variable in relative Cu:Fe contents which would suggest an intergrowth and/or solid solution series (Fig. 19, 20). Johan et al. (1990) reported that similar Cu-sulphide inclusions were found in alluvial Pt-Fe alloys of the Durance River, France. He noted that excess Cu in the presence of bornite would indicate higher temperature formation and stabilization by rapid cooling (Cabri, 1973) and that the presence of Pd sulphides also supports high temperature formation.

The bornite-digenite inclusions also contain noteworthy PGE sulphide bearing phases of generally less than 5 μm in size (Fig. 22). The PGE sulphides exhibit rounded to euhedral crystal shapes. SEM and microprobe analysis characterized them to be of two distinct types. Analysis of the euhedral crystals gave compositions of $Pt_{.50}Pd_{.41}Cu_{.05}S_{1.04}$, $Pt_{.53}Pt_{.39}Cu_{.04}S_{1.03}$ and $Pd_{.40}Pt_{.38}Cu_{.15}S_{1.06}$, which are close to the mineral braggite (Pt, Pd)S. The rounded crystals are a Rh-rich unknown phase of approximate composition $Rh_{.29}Cu_{.27}Pt_{.23}Pd_{.06}S_{1.14}$ (Fig. 19, 20). Image analysis and detailed SEM study revealed that Cu:Fe ratios were variable within some Rh-rich droplets. Exsolution or solid solution variability may explain these differences. The discrete rounded shapes would indicate rapid cooling much like the Cu-sulphide host inclusions themselves (Fig. 22).

Table 3. Microprobe analyses of native Osmium inclusions

Stub-grain	Os %	Pt* %	Ir %	Ru %	Rh %	Pd %	Total %
1662-3	93.3	2.3	2.9	1.0	1.1	0.4	101.0
1662-3	96.7	1.2	4.2	-	0.7	0.2	102.9
1662-3	94.1	2.5	4.1	0.2	1.0	0.3	102.2
1662-3	94.0	1.5	4.8	0.9	0.8	0.4	102.4
1662-3	96.7	1.9	3.1	0.4	1.1	0.2	101.5
1662-3	100.1	1.8	-	0.5	-	0.2	102.6

not detected - Fe, Cu, Ni, As, Ag, S, Au, Te, Sb
*Pt values are probably high due to interference from the Pt-Fe matrix

Palladium and Rh enrichment (Fig. 19, 20) is dominantly associated with Cu-sulphides, however, minor concentrations of Pd and Rh were detected in PGM inclusions (Table 3).

PGM inclusions

Inclusions of native osmium are disseminated throughout the Pt-Fe grain hosting the sulphide inclusions and in two other grains (e.g. Fig. 27).

Shapes vary from equi-dimensional to predominant, non-oriented, laths (Fig. 26). The largest inclusion was 15 x 50 μm (Fig. 24). Most Os-rich laths are less than 5 μm wide, and are generally less than 50 μm in length (Fig. 23, 24, 26).

The small size of PGM inclusions made microprobe analysis difficult to obtain. Compositions of some PGM inclusions are given in Table 3. No compositional differences were determined for equi-dimensional versus lath-shaped inclusions. PGM inclusions in one of the Pt-Fe alloy grains appear to be pure native osmium.

Early crystallization of native osmium is inferred from the shapes of inclusions and Os depletion in the host Pt-Fe alloys. Laurite has not been observed as individual crystals or as intergrowths, and SEM studies confirmed Ru depletion.

PGM and silicate phases commonly share inclusion space either as complex intergrowths or as separate laths and droplets (see Fig. 23, 24). A single silicate inclusion (Fig. 23) contained an Ir-rich complex phase, and other phases with variable Ir/Os ratios.

PGM inclusions appear to have solidified before formation of Pt-Fe alloys. However, the lath-shapes of these inclusions may also be interpreted as disrupted lamellar intergrowths in the Pt-Fe alloy.

Silicate inclusion

Silicate phases were found in 4 of the 10 grains examined. They occur as droplets, as fracture fillings, or embayments extending from the exterior of the grains into the Pt-Fe alloys (Fig. 21, 25, 26). Microprobe analyses were often difficult

due to small grain size and/or alteration or differential polishing giving pitted surfaces. Quartz and albite were identified as angular fragments within the fracture of one grain, but these are considered as impurities. Silicates associated with the Pt-Fe alloys consist of rims of a silica-rich phase with as much as 7% Al_2O_3, 1% SrO, 1.8% P_2O_5; inclusions of kaolinite with 3% FeO; a chloritized mica and sodic-calcic amphiboles with compositions of winchite to richterite to a calcic amphibole of edenitic hornblende composition. Fluorine occurs in some of the amphiboles and may be important in resolving primary ore-forming conditions.

CONCLUSIONS

Our observations and data as presented for this selected suite of large PGM grains from Florence Creek, Yukon, show the following characteristics:

1. All of the grains are isoferroplatinum (Pt_3Fe) in composition. They are generally tabular, flattened or discoid in shape. Since the primary crystal shape of isoferroplatinum is generally cubic or octahedral these particles would appear to be deformed possibly by a tectonic-metamorphic event(s). The preservation of nodular and lobe-shaped protrusions from the discoid body and the ragged surface texture of some grains or portions of grains seem to preclude detrital transport flattening.
2. The chemical and shape characteristics of the three types of inclusions and the presence of gangue mineral phases found within the Pt-Fe hosts unambiguously indicate the primary origin of these grains. Distance to the primary ore source is difficult to assess since some of these hard grains show strong wear (polish, fracture pits) while others exhibit delicate and jagged surface textures. The examination of the accompanying alluvial gold and heavy mineral particles may yield more conclusive evidence of distance to and type of source area.
3. The cohabitation of discrete Cu-sulphide and PGE-sulphides in inclusions, the presence as inclusions of native osmium, the absence of Os, Ir, and Ru sulphides, and the absence of PGM phases of As, Te and Sb suggest that grain formation was complex. Of particular interest is the high concentration of Cu, S, Pd and Rh of some phases. Ore forming processes involving volatile components, solid-liquid, solid-solution series, exsolution, liquid-liquid immiscibility all may have to be used to explain predominant and absent phases, and entrapment. Meaningful discussion of these aspects must await the results of the continuing detailed examination and data collection from smaller PGM grains and the alluvial gold and heavy minerals.
4. Reports in recent scientific literature address the geochemical behaviour of low and high temperature transport of PGEs and discuss ore-formation of PGM in ophiolite complexes, stratiform intrusions and mafic-ultramafic Alaskan-type intrusions and describe the affects of metamorphic, serpentinization and hydrothermal processes on PGEs and PGMs. These new data have aroused much debate. Researchers should consider the benefits of using large PGM particles found in placers when they can be attributed to primary derivation. It would seem prudent to advance the study of alluvium related to platinoid-gold bearing placers.
5. This study has direct exploration and economic implications. Firstly, recovery methods designed for placer gold should be enhanced to maximize the recovery of platinoids. Platinum, Pd and Rh could be of substantial economic benefit to the miners of Florence Creek.
   Secondly, the inclusion of Cu-sulphides in the PGM grains may indicate that copper sulphide mineralization in host rocks is a potential source of PGE enrichments. However, since further study of the concentrate is required and no PGM sources are yet known in the Florence Creek drainage, speculation constraining sources based on geochemical signatures is premature.

ACKNOWLEDGMENTS

We would like to thank Bob Wondga who, while placer gold testing on Florence Creek, collected and donated the concentrate examined in this study. We as researchers are indebted to the curiosity of the placer miner — prospector. We wish also to acknowledge Dave Walker for the careful SEM and image analysis work absolutely required at this stage of research. The objective of this work is to develop and test in a variety of geological and surficial environments geochemical exploration methods applicable to the discovery of concealed ore deposits (GSC project "Applied Geochemistry for the Cordillera", S.B. Ballantyne).

REFERENCES

Ballantyne, S.B. and MacKinnon, H.
1986: Gold in the Atlin Terrane, British Columbia; in Gold 86, An International Symposium on the Geology of Gold Deposits, Poster Volume, Ed. A.M. Chater, p. 16-17.

Cabri, L.J.
1973: New data on phase relations in the Cu-Fe-S system; Economic Geology, v. 68, p. 443-454.

Cabri, L.J. and Harris, D.C.
1975: Zoning in Os-Ir alloys and the relation of the geological and tectonic environment of the source rocks to the bulk Pt: Pt + Ir + Os ratio for placers; Canadian Mineralogist, v. 13, p. 266-274.

Cousins, C.A. and Kinloch, E.D.
1976: Some observations on textures and inclusions in alluvial platinoids; Economic Geology, v. 71, p. 1377-1398.

Eyles, N.
1990: Post-depositional nugget accretion in Cenozoic placer gold deposits, Cariboo mining district, British Columbia; in Exploration in British Columbia, 1989, Part B, Geological Descriptions of Properties, p. 147-169.

Feather, C.E.
1976: Mineralogy of platinum-group minerals in the Witwatersrand, South Africa; Economic Geology, v. 71, p. 1399-1428.

Giusti, L.
1986: The morphology, mineralogy and behavior of "fine-grained" gold from placer deposits of Alberta: Sampling and implications for mineral exploration; Canadian Journal of Earth Sciences, v. 23, p. 1662-1672.

Geological Survey of Canada — Aeromagnetic Series
1966a: Geophysics paper 3329, Upper Nisling River, Yukon Territory; Map 3329G, Sheet 115H/15.
1966b: Geophysics paper 3347, Mount Morrison, Yukon Territory; Map 3347G, Sheet 115H/16.

Geological Survey of Canada
1986: Regional stream sediment and water geochemical reconnaissance data, Yukon 1985; Geological Survey of Canada, Open File 1219, NTS 115H, p. 103.

Hagen, D., Weiser, T. and Htay, T.
1990: Platinum-group minerals in Quaternary gold placers in the Upper Chindwin area of northern Burma; Mineralogy and Petrology, v. 42, p. 265-286.

Hughes, O.L.
1989: Surficial geology, Little Buffalo Lake, Yukon Territory; Geological Survey of Canada, Map 23-1987, scale 1:100 000

Johan, Z., Ohnenstetter, M., Fischer, W. and Amossé, J.
1990: Platinum-group minerals from the Durance River Alluvium France; Mineralogy and Petrology, v. 42, p. 287-306.

Knight, J. and McTaggart, K.C.
1986: The composition of placer and lode gold from the Fraser River drainage area, southwestern British Columbia; Canadian Institute of Mining and Metallurgy, v. 1, p. 21-30.

1990: Lode and placer gold of the Coquihalla and Wells areas, British Columbia (92H, 93H); in Exploration in British Columbia 1989, Part B, Geological Descriptions of Properties, p. 105-118.

Nixon, G.T., Cabri, L.J. and Laflamme, J.H.G.
1989: Origin of platinum nuggets in Tulameen placers: A mineral chemistry approach with potential for exploration; in Exploration in British Columbia 1988, Part B, 1988, Part B, p. B83-B89.

Templeman-Kluit, D.J.
1974: Reconnaissance geology of Aishihik Lake, Snag and part of Stewart River map areas, West-Central Yukon; Geological Survey of Canada Paper 73-41, p. 97.

Preliminary results of the sedimentology of the Skeena Group in west-central British Columbia

Kari N. Bassett[1]
Cordilleran Division, Vancouver

Bassett, K.N., Preliminary results of the sedimentology of the Skeena Group in west-central British Columbia; in Current Research, Part A, Geological Survey of Canada, Paper 91-1A, p. 131-141, 1991.

Abstract

The Skeena Group in west-central British Columbia was deposited in fluvio-deltaic, deltaic, and nearshore marine environments. In the northeastern area, the sediments were transported to the southwest and deposited in lower deltaic coal swamps. The southeastern area contains sediments deposited in a southwestward prograding delta front. The westernmost occurrences of the Skeena Group vary in depositional environment from subtidal sand wave to deltaic with transport direction to the northeast, southeast and northwest. Previously described paleocurrent data indicate sediment transport solely to the southwest. However, paleocurrent data from the westernmost area of this study indicate transport toward the southeast and northeast. This suggests proximity of the western margin of the marine basin in which the Skeena Group was deposited. Primary volcanic deposits in the westernmost occurrences of the Skeena Group suggest active volcanism on the western margin of the basin.

Résumé

Le groupe de Skeena, situé dans le centre ouest de la Colombie-Britannique, a été mis en place dans des milieux fluvio-deltaïques, deltaïques et marins littoraux. Dans la partie nord-est, les sédiments ont été transportés vers le sud-ouest et déposés dans des marécages carbonifères de bas delta. Le secteur sud-est renferme des sédiments déposés dans un front deltaïque en progression vers le sud-ouest. Les venues les plus occidentales du groupe de Skeena ont été déposées dans des milieux de sédimentation variant des ondes de sable subtidales aux deltas avec transports en direction du nord-est, du sud-est et du nord-ouest. Les données sur les paléocourants précédemment décrites indiquent un transport de sédiments uniquement en direction du sud-ouest. Cependant, les données sur les paléocourants dans la partie la plus occidentale de cette région levée indiquent qu'il y a eu transport vers le sud-est et le nord-est. Cela suggère la proximité de la marge occidentale du bassin marin dans lequel a été déposé le groupe de Skeena. Les gisements volcaniques primaires dans les venues les plus occidentales du groupe de Skeena suggèrent l'existence d'un volcanisme actif sur la marge occidentale du bassin.

[1] Department of Geology and Geophysics, University of Minnesota, Minneapolis, Minnesota 55455, U.S.A.

INTRODUCTION

This report describes field research completed during 1990 on the sedimentology of the Lower Cretaceous Skeena Group. The Group has been previously described as part of regional mapping projects (Whitesail Lake (93E), Woodsworth, 1980; Diakow, 1990; Terrace (103I), Woodsworth et al., 1985; Smithers (93L), Tipper, 1976; Hazelton (93M), Richards, 1980, in press) and in theses on stratigraphically adjacent units (MacIntyre, 1985) but little detailed sedimentology has been done. The purpose of this study is to interpret the depositional environments and paleogeography of the Skeena Group in the western part of its outcrop belt, an area corresponding to the southwest part of the Jurassic Bowser Basin.

GEOLOGICAL SETTING

The study area occupies a key location at the junction between the Bowser and Nechako basins of British Columbia, in a position superimposed on the northern margin of the east-trending Skeena Arch that separated the two basins from Callovian (Late Jurassic) to Hauterivian (Early Cretaceous) time. The study is of the Lower Cretaceous Skeena Group that was deposited over the then subsiding Skeena Arch. Results from this study will have implications not only for the uplift and subsidence history of the Skeena Arch, but also for the changing geometries of the Bowser Basin to the north and the Nechako basin to the south. Although the Jurassic paleogeography has been reconstructed (Tipper and Richards, 1976), little is known about the paleogeography and tectonic setting of the area during Early to mid-Cretaceous time because the Skeena Group has not been studied beyond general geological field mapping.

The Skeena Group has been mapped and briefly described (Duffell, 1959; Brown, 1960; Richards and Jeletsky, 1975; Tipper and Richards, 1976; Richards, 1977, 1978, 1980; Woodsworth, 1978, 1979, 1980; Eisbacher, 1981; Koo, 1984; MacIntyre, 1985; Diakow and Mihalynuk, 1987; Diakow and Koyanagi, 1988; Diakow and Drobe, 1989; Diakow, 1990), but no detailed sedimentological studies have been conducted. The Skeena Group is composed of chert-rich conglomerates, lithic-wackes and arkosic lithic-wackes, siltstones, carbonaceous shales, and coal with minor interbedded volcanics of basaltic to rhyolitic composition (Duffell, 1959; Brown, 1960; Tipper and Richards, 1976; MacIntyre, 1985). The sandstones and siltstones contain abundant detrital muscovite, distinguishing them from the underlying Jurassic Bowser Lake and Hazelton groups.

The Skeena Group has been assigned to the Early Cretaceous (Hauterivian) to earliest Late Cretaceous (Albian or Cenomanian) based on marine macrofauna (Duffell, 1959; Brown, 1960; Tipper and Richards, 1976). It is thought to be correlative with the Taylor Creek, Jackass Mountain, and Gambier groups to the south in the Nechako and Tyaughton basins (Tipper and Richards, 1976) and with the Gunanoot Group (Richards and Gilchrist, 1979), the lower part of the Bowser Lake and Sustut groups to the east and north in the Bowser Basin (Tipper and Richards, 1976; Eisbacher, 1981, 1985; Moffat et al., 1988; Bustin and McKenzie, 1989).

The few previously published paleocurrent data generally indicate west to southwestward dispersal from an eastern sediment source. This pattern is distinct from the north to northeastward transport determined for the underlying Upper Jurassic Bowser Lake sediments (Tipper and Richards, 1976; Richards, 1978; Woodsworth, 1979; Eisbacher, 1981; Tipper, 1984). However, a western source for part of the Skeena Group has also been suggested (Richards and Dodds, 1973). The interpretation of an eastern Skeena paleo-source has been based as much on a detrital muscovite component in the sandstones as the sparse paleocurrent data. The detrital muscovite was interpreted as derived from the Omineca Crystalline Belt, a mid-Jurassic metamorphic complex east of the Bowser and Nechako basins (Eisbacher, 1981). Mid-Cretaceous and older plutons and metamorphic bodies of the Coast Plutonic Complex to the west do not contain a sufficiently high concentration of muscovite to provide the abundant muscovite in the Skeena Group (Armstrong, 1988; G.J. Woodsworth, pers. comm., 1989).

Several depositional environments have been postulated for different parts of the Skeena Group: 1) proximal turbidites in a shallow marine setting (MacIntyre, 1985); 2) a combination of low-gradient clastic shorelines, deltas, and lagoonal coal swamps grading eastward into alluvial plains (Eisbacher, 1981); and 3) fluvial settings with coal-forming swamps in the floodplains (Brown, 1960; Koo, 1984). The presence of marine macrofauna restrict at least part of the Skeena Group to a marine setting (Duffell, 1959; Brown, 1960; Tipper, 1963; Tipper and Richards, 1976). Disparate views also exist regarding the regional-scale paleogeography. The Skeena Group has been interpreted to represent a mid-Early Cretaceous (Hauterivian) marine transgression from the west over an area of low relief in which portions of the Jurassic Skeena Arch had collapsed for unspecified reasons (Tipper and Richards, 1976; Tipper, 1984). An alternative interpretation is that the Skeena Group was deposited in near shore and deltaic environments on an eroded, but still existing, east-west Skeena Arch separating the Bowser and Nechako basins (Eisbacher, 1981, 1985). Coeval intermediate volcanics and plutonic bodies are concentrated west of the study area as well as interspersed with Skeena outcrop belts (Wheeler and McFeely, 1987) suggesting that Skeena deposition may have occurred under the influence of contemporaneous arc volcanism.

LOCATION

Skeena Group outcrops were examined in three different map areas, Whitesail Lake (93E), Hazelton (93M), and Terrace (103I), in order to provide geographically widespread data for determining the paleogeography of the western occurrences of the Skeena Group (Fig. 1). The Skeena Group is well exposed in the area, particularly above treeline, and, although brittley deformed regionally, the Skeena Group locally displays stratigraphic continuity and only zeolite-grade metamorphism. A section was measured in the Whitesail Lake map ares, on Rhine Ridge in the Sibola Range just north of Tahtsa Lake (Locality Wa, Fig. 1), where the Skeena Group outcrops below the volcanic Upper Cretaceous Kasalka Group. Sections were also examined in two parts of the Hazelton map area, in the Bulkley Canyon along the railroad tracks 2-3 km east of the town of New Hazelton, B.C. (Localities Ha and Hd, Fig. 1). The Bulkley Canyon contains a well exposed, continuous section that is highly

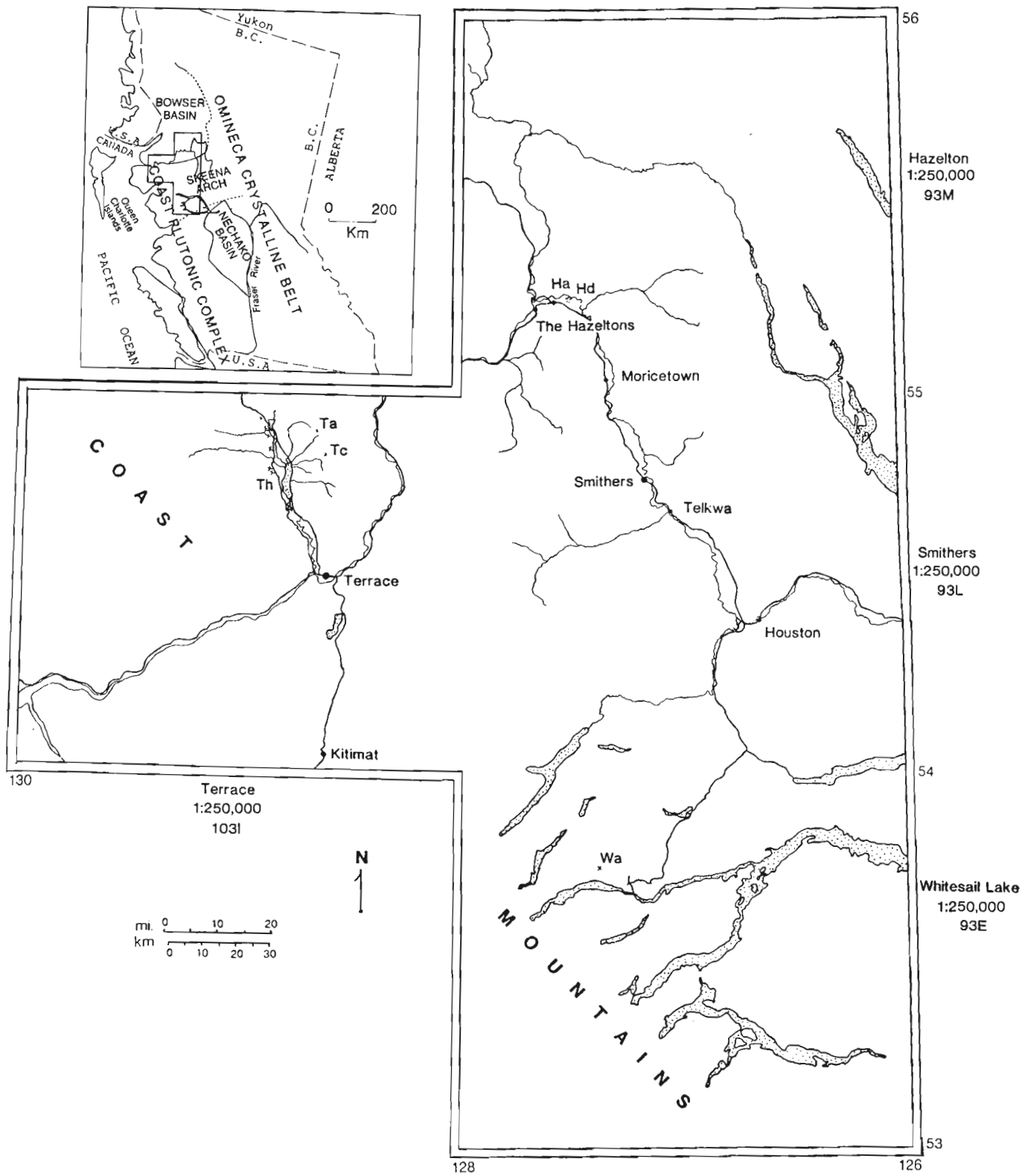

Figure 1. Location map showing the study area and the various localities.

deformed less than 1 km farther to the east of the easternmost study locality. The sections appeared to have coherent stratigraphy between faults several hundreds of metres apart with offsets of up to 30 m.

In the Terrace map area work focused on three locations near Kitsumkalum Lake: Mount Couture (Locality Ta, Fig. 1) and Wesach Mountain (Locality Tc, Fig. 1) to the east of the lake and along roadcuts on the road on the western side of the lake (Locality Th, Fig. 1). Mount Couture includes several major thrust faults and thus the Skeena Group is both extensively faulted and folded. However, it was possible to measure one continuous section and nearby deformed outcrops yielded additional information on the depositional environment. The eastern shoulder of Wesach Mountain contains a continuous stratigraphic sequence that has little internal deformation, although it is cut by dykes and minor high-angle normal faults. Several thin sequences exposed in roadcuts along the western side of Kitsumkalum Lake provided the information on the westernmost depositional environment of the Skeena Group. The roadcuts follow a north-south trend

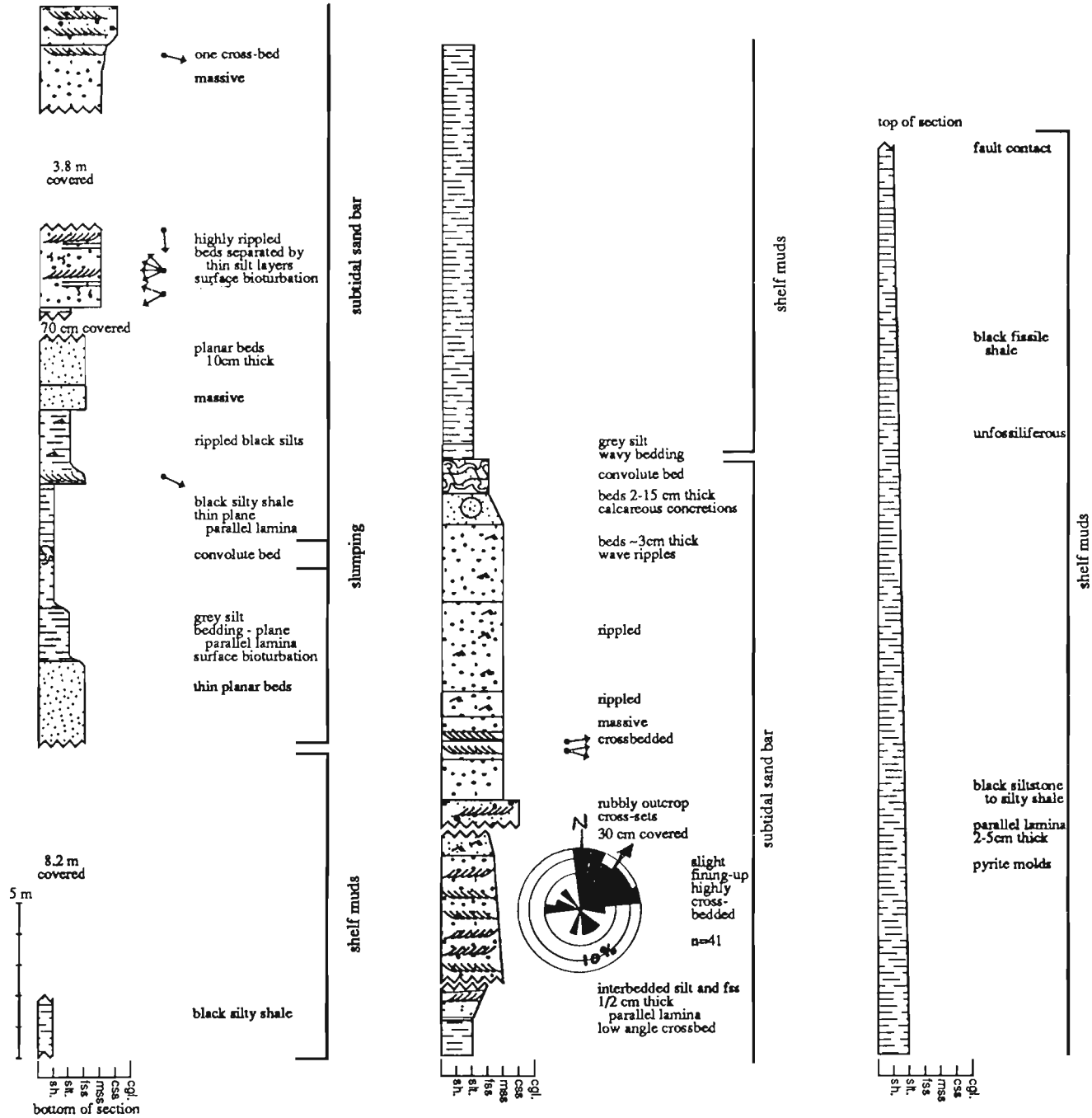

Figure 2. Section measured at locality Ta on Mount Couture in the Terrace map area. The section contains crossbedded sandstones with double mud drapes indicating deposition by a subtidal sandwave. The patterns used in the figure are shown in Figure 3.

that is not crosscut by any major faults (Woodsworth et al., 1985). Therefore, little major lateral or vertical displacement between consecutive roadcuts is assumed, although minor faults were observed.

METHODS

The summer of 1990 consisted of detailed measurement and sedimentological description of continuous stratigraphic sections to determine the depositional environment of the sediments and the paleogeography of the region. Included in the sedimentological descriptions are paleocurrent data measured to decipher the local and regional sediment dispersal directions. Determination of the provenance and diagenetic history of the sediments will constitute later phases of this ongoing study.

The lack of macrofossils in the Skeena Group and extensive regional faulting that isolates the studied outcrop belts present problems for regional chronostratigraphic correlation. To address these problems, samples for both pollen and foraminifera identification will be examined by Arthur Sweet, GSC, Calgary, and Timothy Patterson, Carleton University, Ottawa.

DEPOSITIONAL SETTINGS

Subtidal sandwaves

At Mount Couture, the Skeena Group is mapped with a possible conformable contact between the Bowser Lake Group and overlying Skeena Group (Woodsworth et al., 1985). However, the lower contact appears to be a fault contact in highly sheared black shales, possibly a splay of the thrust fault mapped in the Bowser Group shales below (Woodsworth et al., 1985). A Kimmeridgian (Lower Jurassic) fossil was collected from the Bowser Lake Group immediately below the micaceous sandstones of the Skeena Group (G.J. Woodsworth, pers. comm., 1990). One cohesive section was measured in the Skeena Group above the fault contact (Fig. 2). The measured section is overlain by 200-300 m of unfossiliferous, massive black shales that are probably thickened by thrust fault repetition. It is also possible that these overlying shales are Bowser Lake Group black shales thrust over the Skeena Group as Bowser Lake and Skeena black shales appear lithologically indistinguishable. As no fossils were found it is not possible to assign the overlying black shales to a stratigraphic unit.

The Skeena Group on Mount Couture contains thick, crossbedded, slightly micaceous, medium grained lithic-wackes and thinly interlaminated and rippled black siltstones and fine sandstones (Locality Ta, Fig. 1; Fig. 2; Fig. 3). Cross-strata within the sandstones range in amplitude from 0.5-2 m and are predominantly planar. The crossbedded sands contain double mud drapes throughout the locality (Fig. 4). Double mud drapes form in a subtidal environment where the asymmetric flow velocity and the resultant cyclical variation in grain size of the deposits are controlled by the daily tidal cycle (Visser, 1980; deMowbray and Visser, 1984). The sandstones were probably deposited in a subtidal sand bar migrating to the northeast, as indicated by a combined total of 112 paleocurrent measurements. The uppermost 2 m of the sandstone unit displays convolute bedding in fine sandstone which was probably formed by a slump down the slip-face of the bar (Fig. 2). The fine sands and silts were deposited in areas between sand bars by small migrating ripples with

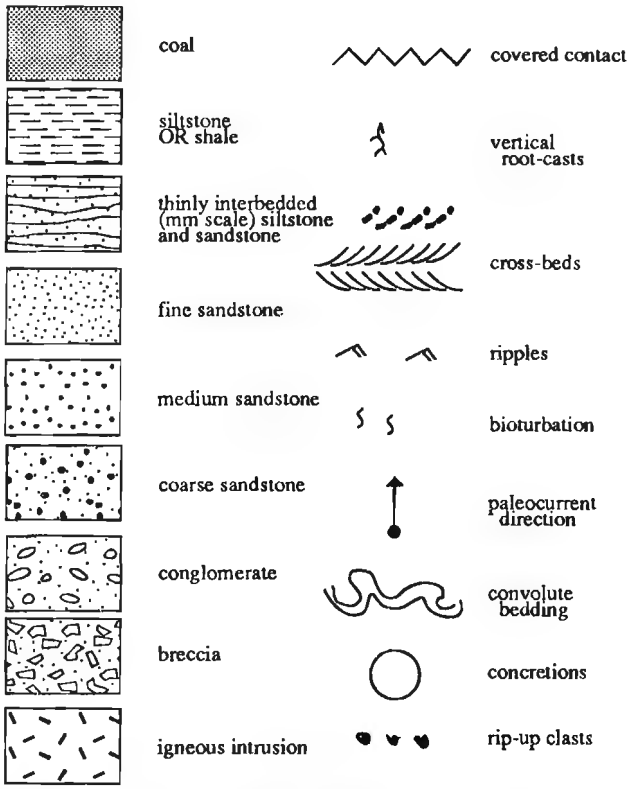

Figure 3. Legend for measured sections (Fig. 2, 5, 6, 7).

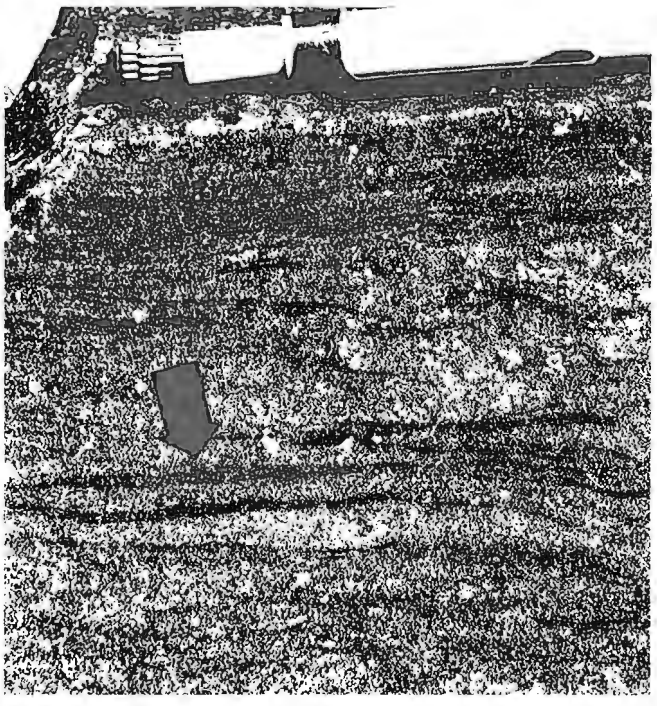

Figure 4. Photograph showing the double mud drapes found in the crossbedded sandstones in section Ta on Mount Couture in the Terrace map area.

silt filling the troughs. The 21 m black siltstone in the upper part of the measured profile represents unfossiliferous shelf muds probably deposited under anoxic conditions (Fig. 2).

Prodelta to delta plain

Interpretation of the depositional environment for the west side of Kitsumkalum Lake (Fig. 1) are consistent with a deltaic deposit that becomes more proximal 18 km to the south. Prodelta to delta front characteristics occur in the northernmost deposits changing to a lower delta plain to upper delta plain environment to the south, separated by a large interdistributary bay of approximately 10 km width. Only two paleocurrent indicators were observed, both suggesting dispersal to the northwest. Belemnites collected by previous researchers suggest that the delta is of Hauterivian (Early Cretaceous) age (G.J. Woodsworth, pers. comm., 1990). Localities will be discussed in order from north to south.

The northernmost localities (Locality Th, Fig. 1) contain interlaminated (2-10 mm thick) and rippled black siltstones and fine sandstones with thicker, normally graded sandstone beds becoming coarser grained to the south. The ripples in the siltstones and fine sandstones are unidirectional current ripples. The depositional environment is interpreted to be shallow-water turbidite deposits over subtidal, prodelta sediments deposited by migrating ripples. Hydroplastic slickensides, formed due to faulting in unlithified or partially lithified sediments, are also found in the silts (sensu Petit and Laville, 1987). These may have formed in response to tectonic activity, growth faulting, or slumping, although convolute bedding was not seen in outcrop. Several sandstones contain euhedral feldspar crystals suggesting a volcanic source in part.

Four kilometres farther south (Locality Th, Fig. 1) the outcrops consist of fine grained, rippled sandstones, black siltstones and shales, and coals in both fining-up and coarsening-up sequences. Two to 8 m sequences coarsen-up from siltstone to fine sandstone and represent crevasse splay or mouth bar deposits. Carbonaceous bimodal siltstones and sandstones, which are typical of saltmarshes behind a barrier island or in interdistributary bays, are also present in the section. The 2-3 m thick fining-up sequences fine upward from fine sandstone to coal with flaser bedding and organic-rich lamina in the sandstones and are consistent with deposition in small distributary channels on a lower delta plain. Two 20 cm crossbed measurements at one locality 2 km farther

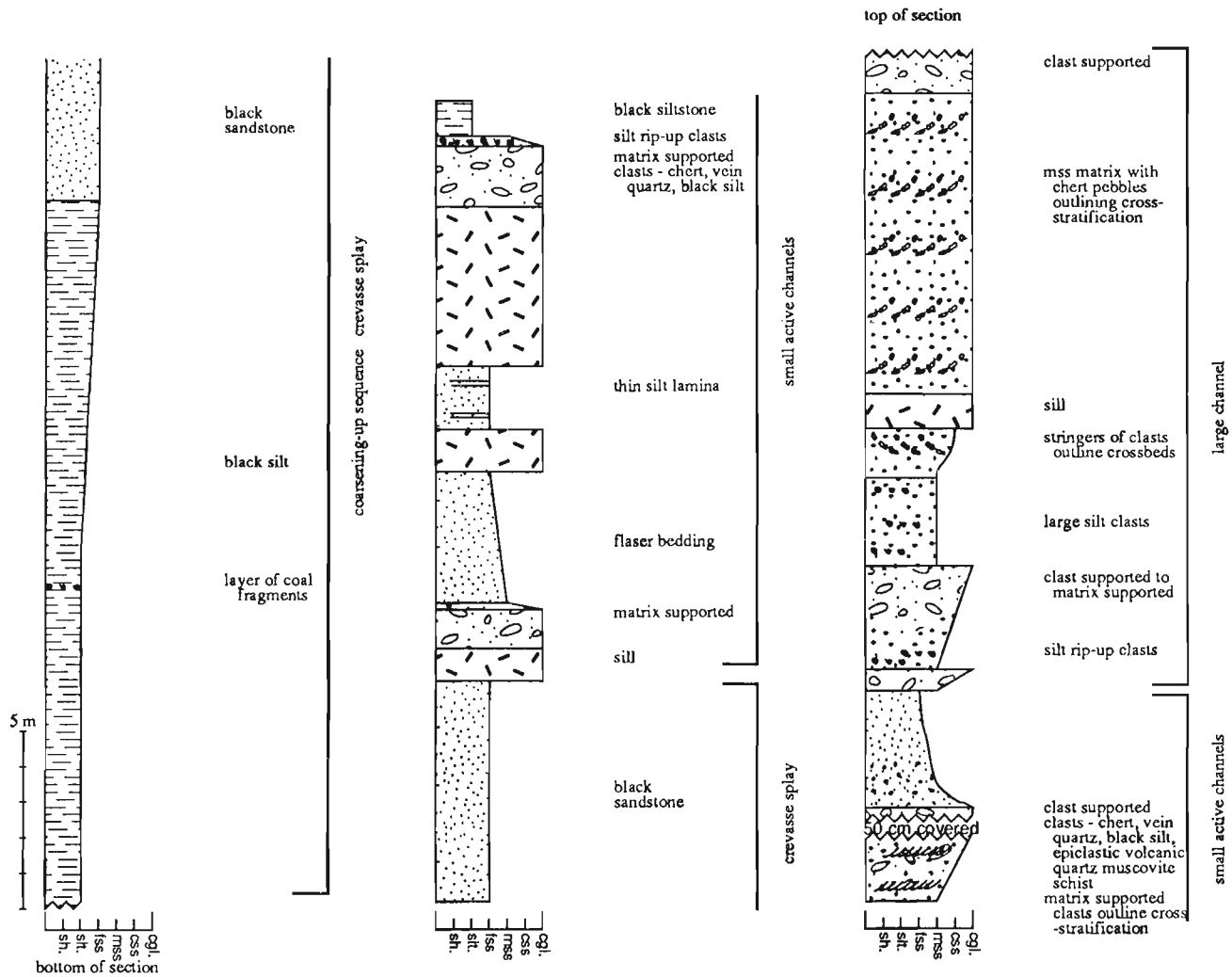

Figure 5. Section measured at locality Th, the southernmost locality on the western side of Kitsumkalum Lake in the Terrace map area. Deposition probably occurred in a delta plain environment.

south (Fig. 1) suggest local flow was to the northwest. The upper 3 m of the section contain root casts suggesting that the area was at least intermittently subaerial.

Three kilometres farther south and continuing for another 8 km the deposits again become primarily black siltstones and shales with approximately 60 m of massive black siltstone to shale with no fossils, root casts, or bioturbation (Fig. 1). The thickness of mudstones and their proximity to strata interpreted as delta plain deposits suggest deposition in a deltaic interdistributary bay or lagoon that was hostile to life as no bioturbation or macrofauna were observed. Hydroplastic slickensides are also present at this locality.

The southernmost locality (Locality Th, Fig. 1; Fig. 5) contains much coarser grained clastics than those found 1 km to the north. The section is a 32 m thick coarsening-upward sequence from black siltstone to fine black sandstone capped by crossbedded conglomerate. Well-rounded clasts are 1-3 cm in diameter and are composed of chert, vein quartz,

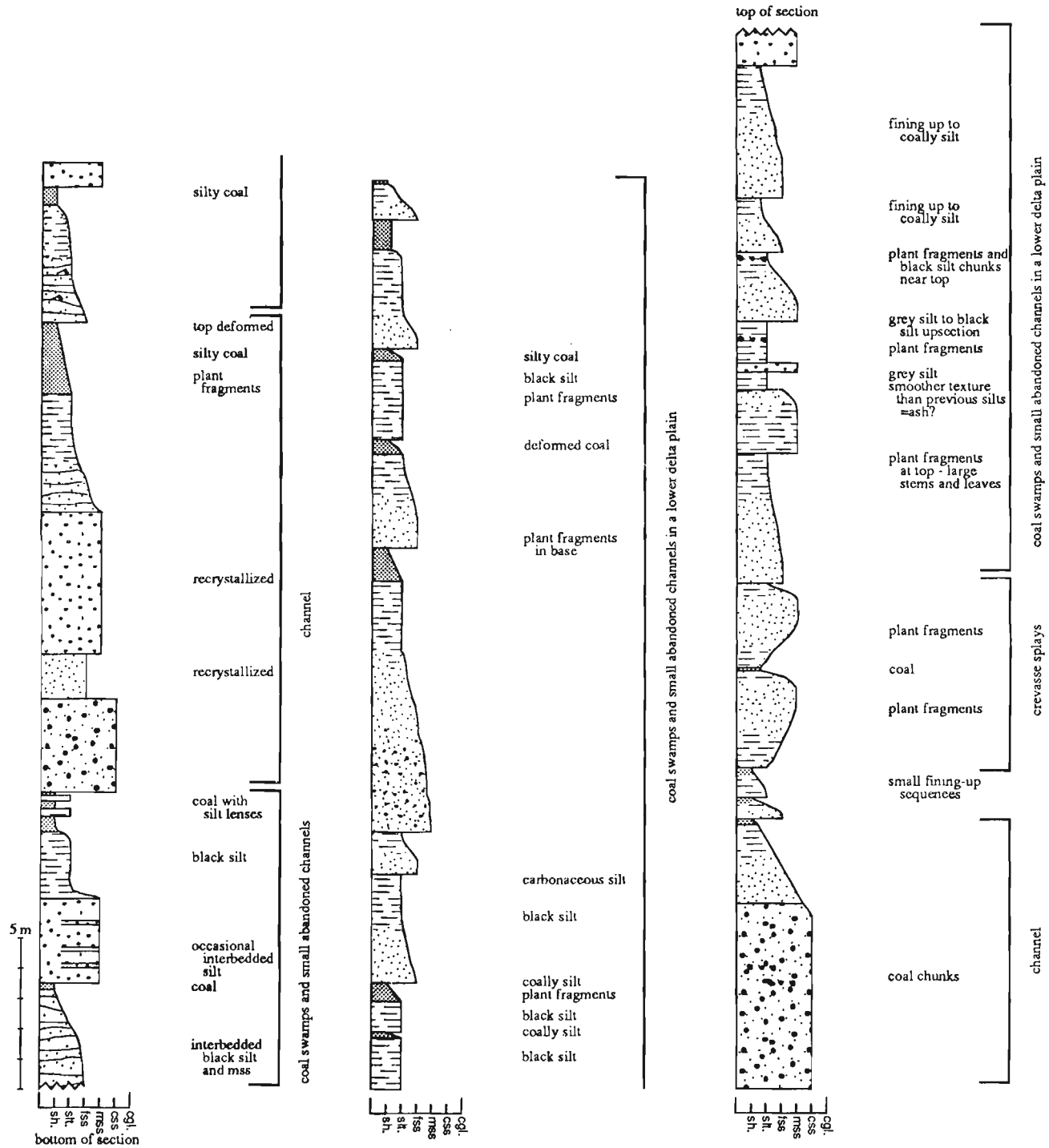

Figure 6. Section measured at locality Ha in the Bulkley Canyon to the east of New Hazelton in the Hazelton map area. The sediments were probably deposited in lower deltaic coal swamps.

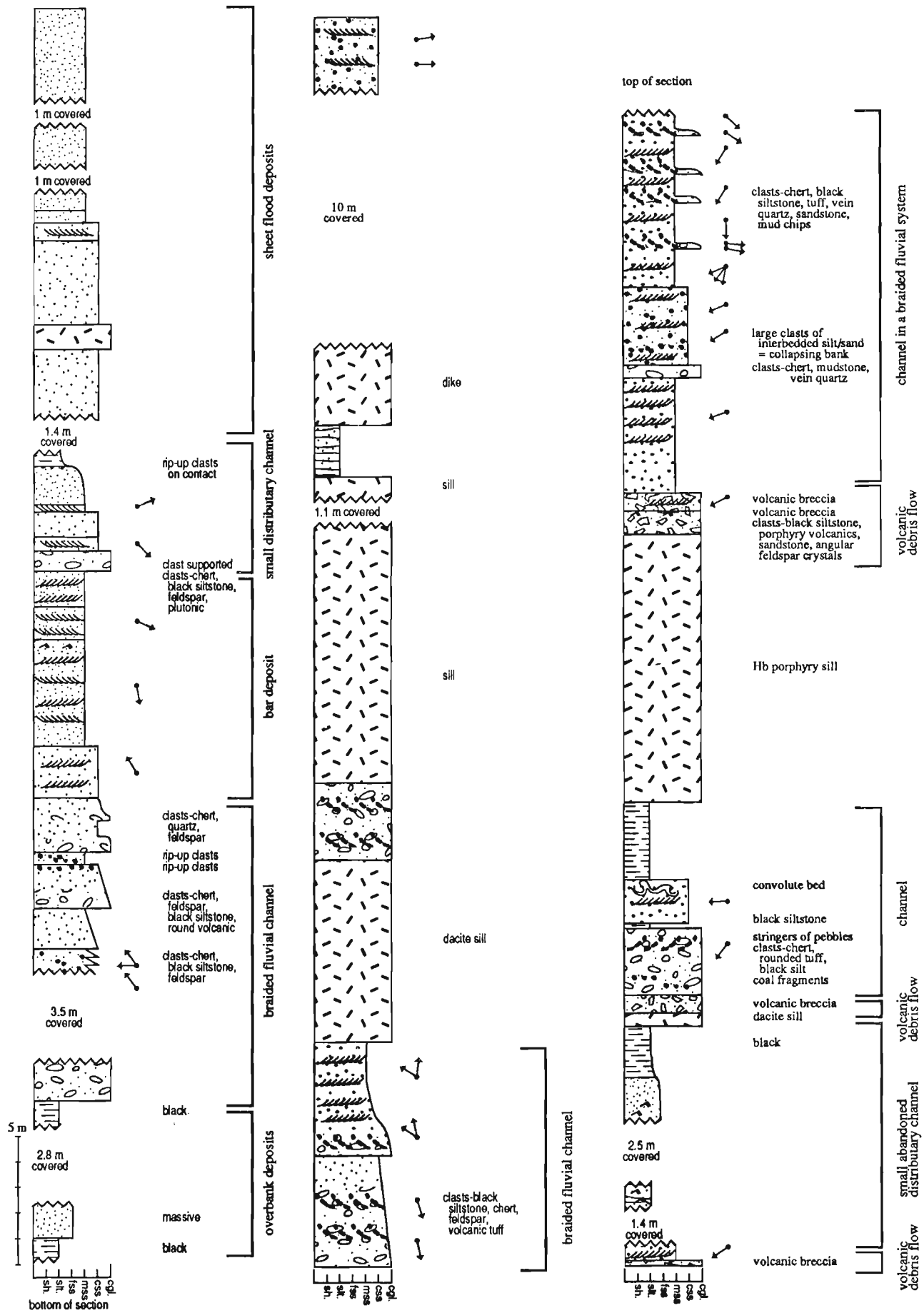
1 m covered
1 m covered
1.4 m covered
3.5 m covered
5 m
2.8 m covered
bottom of section
sh.
slt.
fss
mss
css
cgl.
rip-up clasts on contact
clast supported clasts-chert, black siltstone, feldspar, plutonic
clasts-chert, quartz, feldspar
rip-up clasts
rip-up clasts
clasts-chert, feldspar, black siltstone, round volcanic
clasts-chert, black siltstone, feldspar
black
massive
black
sheet flood deposits
small distributary channel
bar deposit
braided fluvial channel
overbank deposits
10 m covered
dike
sill
1.1 m covered
sill
dacite sill
clasts-black siltstone, chert, feldspar, volcanic tuff
braided fluvial channel
top of section
clasts-chert, black siltstone, tuff, vein quartz, sandstone, mud chips
large clasts of interbedded silt/sand = collapsing bank
clasts-chert, mudstone, vein quartz
channel in a braided fluvial system
volcanic breccia
volcanic breccia
clasts-black siltstone, porphyry volcanics, sandstone, angular feldspar crystals
volcanic debris flow
Hb porphyry sill
convolute bed
black siltstone
stringers of pebbles
clasts-chert, rounded tuff, black silt
coal fragments
channel
volcanic breccia
dacite sill
volcanic debris flow
black
2.5 m covered
1.4 m covered
small abandoned distributary channel
volcanic breccia
volcanic debris flow
sh.
slt.
fss
mss
css
cgl.

and black siltstone. Abundant 10-60 cm siltstone intraclasts occur at the base of some of the conglomeratic strata. Deposition records migration of a deltaic channel with deposition changing from interdistributary bay muds to crevasse splay and levee deposits and finally to channel conglomerates deposited by a fluvial channel on the lower delta plain.

Delta front

On Rhine Ridge four sections were measured for a combined stratigraphic thickness of approximately 800 m (Locality Wa, Fig. 1). Outcrops are lichen covered and rubbly, and thus detail is lacking in the description of the units. The lower contact was not observed and the upper contact with the Upper Cretaceous Kasalka Group is poorly exposed preventing detailed sedimentological description of that contact. The contact has been previously described as an angular unconformity (MacIntyre, 1985; Woodsworth, 1979). The section is composed primarily of 10-30 m thick units of crossbedded, lithic-wackes commonly with 3-dimensional ripples superimposed on the larger cross-strata. Two-dimensional cross-strata range in amplitude from 20 cm to approximately 1 m. The thick sandstones are interbedded with thinner units of highly micaceous, black siltstones or thinly interlaminated and rippled black siltstones and fine sandstones. The sequence coarsens upward overall and contains smaller coarsening-upward and fining-upward sequences 10-20 m thick.

Occasional woody fragments and intraclasts are contained in the sandstones. With the exception of rare surface-feeding traces found near the top of the section, little bioturbation is recorded in the section. Dewatering and load structures such as sand dykes and flame structures are common in the basal part of the sequence.

The lack of bioturbation and the common load structures are consistent with a rapid sedimentation rate. In addition to the overall coarsening-upward of the section and the thickness of the crossbedded sandstone units, these observations suggest deposition on a prograding delta front. Sediment dispersal to the southwest is suggested by 8 paleocurrent measurements.

Lower delta plain

Figure 6 displays a profile measured along the railroad tracks 2-3 km east of New Hazelton, B.C. (Localities Ha and Hd, Fig. 1) in coal-bearing sediments that Richards has informally called the "Kitsuns Creek formation" within the Skeena Group (T.A. Richards, in press, pers. comm., 1990). Section Ha comprises approximately 100 continuous metres with very little internal deformation except within the coal layers. Section Hd (Fig. 1) has two normal faults with offsets of approximately 30 m cutting the 200 m thick section. Between the faults, the section appears continuous with little internal deformation. Both sections are not overturned although steeply dipping approximately 70° to the west.

Section Ha (Fig. 5) is composed primarily of 5-20 m thick fining-upward sequences from medium grained, micaceous, lithic-wackes to carbonaceous silt and coal. The sandstones and siltstones contain abundant plant fragments but lack root casts. Two beds contain inverse to normal grading typical of proximal crevasse-splays in subaerial coal swamps. The fining-up sequences, lack of root casts, and crevasse splay deposits suggest a lower delta-plain depositional environment with the fining-up sequences developed in small, abandoned distributary channels. No macrofaunal fossils were found but macrofloral fossils were collected for identification and dating and samples were collected for palynological analysis.

A second section, Hd (Fig. 1), is an upper delta plain or fluvial deposit ranging from chert-pebble conglomerates and micaceous lithic-wackes to carbonaceous siltstones and coals. The conglomerates and coarse sandstone beds mark erosional bases of 20-30 m fining-upward sequences capped by black siltstone indicative of channel deposits. The conglomerates are primarily matrix-supported with clasts composed of chert, vein quartz, and black silt clasts of 2-5 cm diameter in a medium to coarse sand matrix. One conglomerate layer shows a slight imbrication of the clasts, but was unmeasurable. Smaller 2-6 m fining-upward sequences generally start at fine to medium sandstone that fines to coal indicating abandonment, probably in minor distributary channels. Present in the section are thin (8-10 cm), interbedded, laterally continuous siltstones and sandstones which are typical of levee deposits. Numerous inversely to normally graded beds of rippled siltstone and sandstone indicate crevasse splays. Beds of bimodal carbonaceous siltstone and medium sandstone, one of which has convolute bedding indicating slumping, may have been deposited by overbank flooding. There are plant fragments throughout as well as abundant root casts indicating subaerial and freshwater conditions. Although rippled, the strata contains no unambiguous paleocurrent indicators. Richards (1980, in press) presents one paleocurrent measurement indicating transport towards the southwest.

The two sections measured in the Bulkley Canyon are interpreted to be deltaic deposits of differing lateral facies. These represent typical deposits of the widespread informal "Kitsuns Creek formation" (T.A. Richards, pers. comm., 1990). The widespread nature of the formation may indicate that the delta was both a large paleogeographic feature and fairly continuous through time.

Fluvial to upper delta plain of Gilbert-Type delta

The Skeena Group on Wesach Mountain (Locality Tc, Fig. 1; Fig. 7) is composed primarily of crossbedded, chert-pebble conglomerate and arkosic sandstone with few interbedded black siltstone or interlaminated micaceous siltstone and fine sandstone. The conglomerate is composed of rounded chert, black siltstone, vein quartz, volcanic tuff, plutonic, and feldspar clasts, typically of 1-5 cm diameter. The clasts are matrix-supported and define two- and three-dimensional cross-strata ranging in amplitude from 50 cm to 5 m. The conglomerate generally fine up to crossbedded sandstone with overlying siltstone in a few places. Both the sandstone and the conglomerate contain large rip-up clasts of black siltstone.

Figure 7. Section measured at locality Tc on Wesach Mountain in the Terrace map area. The section contains primary volcanic debris flows and is interpreted as a Gilbert delta deposit.

One coarse sandstone near the top of section Td (Fig. 7) contains very large (50-70 cm diameter), bedded silt clasts interpreted as having been deposited as colluvium during bank collapse or slumping. The section coarsens-up overall from shales below the measured profile to the conglomerates.

This profile is interpreted as a braided fluvial deposit probably on a Gilbert delta plain, an interpretation enhanced by approximately 5 m high cross-strata. The paleocurrent directions are compatible with a sediment source to the north or northwest.

Several volcanic breccia units, ranging from 20 cm to 1 m thick, are interbedded with the sandstones and conglomerates of the section (Fig. 7). These breccias are matrix-supported with angular volcanic clasts up to 12 cm in diameter. Clasts include hornblende porphyry, black siltstone, and angular tuffs as well as zoned euhedral feldspar crystals (1-5 mm). Several irregularly shaped clasts (2-4 cm) that were probably vesiculated pumice have fractured in situ and appear to have been soft, but brittle, at time of deposition. The observations support an interpretation of active volcanism rather than reworking of epiclastic detritus. The breccias have very slightly erosional basal contacts and lack internal grading, suggesting deposition by debris-flow. One breccia thins and fines to the east, suggesting possible dispersal in that direction, consistent with the paleocurrent data from the conglomerates.

DISCUSSION

The depositional environment of the Skeena Group appears to be consistently shallow subtidal marine to fluvio-deltaic with possibly little change in depositional environment from the Late Jurassic Bowser Lake Group through the Early Cretaceous Skeena Group. The primary differences appear to be the inclusion of detrital muscovite in the Skeena sediments, suggesting a change in the source area; a change in dispersal direction from south to north in the Bowser Lake Group (Eisbacher, 1981) to primarily northeast to southwest in the Skeena Group with some north-south components; and the inclusion of primary volcanic detritus in the Skeena Group. Forthcoming chronostratigraphic data will hopefully permit correlation of coeval deposits among the studied outcrop belts which will enable more sophisticated paleogeographic reconstructions.

Paleocurrent data published prior to this study indicate sediment transport to the southwest (Richards, 1980, in press; Eisbacher, 1981). In contrast, some of the data from the westernmost occurrences of the Skeena Group on Wesach Mountain and Mount Couture (Localities Ta and Tc, Fig. 1) indicate transport towards the northeast and southeast suggesting the possible proximity of the western margin of the marine basin during part of the deposition of the Skeena Group.

Volcanic debris-flow deposits with angular, pumiceous clasts on Wesach Mountain and euhedral feldspar crystals in the overbank deposits observed on Wesach Mountain and near Kitsumkalum Lake imply coeval volcanism on the western margin of the Early Cretaceous marine basin. Volcanic tuffaceous clasts in most Skeena Group conglomerates are rounded whereas the angular tuffaceous and pumiceous clasts in the few Wesach debris-flow breccias suggest sporadic events, such as eruptions, which may have both caused the debris flows and provided the fresh volcanic detritus.

ACKNOWLEDGMENTS

Financial support by the GSC for my first summer of fieldwork is gratefully acknowledged. I would also like to thank my advisor, Karen Kleinspehn for her company and expertise in the field and critical reading of this paper; Tom Richards for his advise and lodgings; Glenn Woodsworth for the same; and my field assistants, Jinx Bryant and Peg Chappars, for their enthusiasm and company.

REFERENCES

Armstrong, R.L.
1988: Mesozoic and Early Cenozoic magmatic evolution of the Canadian Cordillera; Geological Society of America, Special Paper 218, p. 55-91.

Brown, A.S.
1960: Geology of the Rocher Deboule Range; B.C. Department of Mines and Petroleum Resources, Bulletin 43, 78 p.

Bustin, R.M. and McKenzie, K.M.
1989: Stratigraphy and depositional environments of the Sustut Group, southern Sustut Basin, north-central British Columbia; Bulletin, Canadian Petroleum Geology, v. 37, p. 210-223.

deMowbray, T. and Visser, R.
1984: Reactivation surfaces in subtidal channel deposits, Oosterschelde, SW Netherlands; Journal of Sedimentary Petrology, v. 54, p. 811-824.

Diakow, L.J.
1990: Geology of the Nanika Lake map area; in Geological Fieldwork 1989, British Columbia Ministry of Energy, Mines and Petroleum Resources, Paper 1990-1, p. 83-89.

Diakow, L.J. and Drobe, J.
1989: Geology and mineral occurrences in North Newcombe Lake map sheet; in Geological Fieldwork 1988, British Columbia Ministry of Energy, Mines and Petroleum Resources, Paper 1989-1, p. 183-188.

Diakow, L.J. and Koyanagi, V.
1988: Stratigraphy and mineral occurrences of Chikamin Mountain and Whitesail Reach map areas; in Geological Fieldwork 1987, British Columbia Ministry Energy, Mines and Petroleum Resources, Paper 1988-1, p. 155-168.

Diakow, L. and Mihalynuk, M.
1987: Geology of Whitesail Reach and Troitsa Lake map areas; in Geological Fieldwork 1986, British Columbia Ministry of Energy, Mines and Petroleum Resources, Paper 1987-1, p. 171-179.

Duffell, S.
1959: Whitesail Lake map-area, British Columbia; Geological Survey Canada, Memoir 299, 119 p.

Eisbacher, G.H.
1981: Late Mesozoic-Paleogene Bowser Basin molasse and Cordilleran tectonics, western Canada; in Sedimentation and Tectonics in Alluvial Basins, A.D. Miall (ed.), Geological Association Canada, Special Paper 23, p. 125-151.
1985: Pericollisional strike-slip faults and synorogenic basins, Canadian Cordillera; in Strike-Slip Deformation, Basin Formation, and Sedimentation, K.T. Biddle and N. Christie-Blick (ed.), Society of Economic Paleontologists and Mineralogists, Special Publication 37, p. 265-283.

Koo, J.
1984: The Telkwa, Red Rose, and Klappan coal measures in northwestern British Columbia; in Geological Fieldwork 1983, British Columbia Ministry of Energy, Mines and Petroleum Resources, Paper 1984-1, p. 81-90.

MacIntyre, D.G.
1985: Geology and mineral deposits of the Tahtsa Lake District west-central British Columbia; British Columbia Ministry of Energy, Mines and Petroleum Resources, Bulletin 75, 82 p.

Moffat, I.W., Bustin, R.M., and Rouse, G.E.
1988: Biochronology of selected Bowser Basin strata: tectonic significance; Canadian Journal Earth Sciences, v. 25, p. 1571-1578.

Petit, J.P. and Laville, E.
1987: Morphology and microstructures of hydroplastic slickensides in sandstone; in Deformation of Sediments and Sedimentary Rocks, M.E. Jones and R.M.F. Preston (ed.), Geological Society of London, Special Publication 29, p. 107-121.

Richards, T.A.
1977: Geology of Hazelton map-area, British Columbia; in Current Research, Part A, Geological Survey of Canada, Paper 77-1A, p. 247.
1978: Geology of Hazelton (west-half) map-area, British Columbia; in Current Research, Part A, Geological Survey of Canada, Paper 78-1A, p. 59-60.
1980: Geology of Hazelton (93M) map area; Geological Survey of Canada, Open File 720.
in press: Geology of Hazelton (93M) map area; Geological Survey of Canada.

Richards, T.A. and Dodds, C.J.
1973: Hazelton (east-half) map-area, British Columbia; in Reports of Activities, Geological Survey of Canada, Paper 73-1, p. 38-42.

Richards, T.A. and Gilchrist, R.D.
1979: Groundhog coal area, British Columbia; in Current Research, Part B, Geological Survey of Canada, Paper 79-1B, p. 411-414.

Richards, T.A. and Jeletsky, G.L.
1975: A preliminary study of the Upper Jurassic Bowser Assemblage in the Hazelton west half map-area, British Columbia; in Current Research, Part A, Geological Survey of Canada, Paper 75-1A, p. 31-36.

Tipper, H.W.
1963: Nechako River map-area, British Columbia; Geological Survey of Canada, Memoir 324, 59 p.
1976: Smithers B.C. (93L); Geological Survey of Canada, Open File 351.
1984: The allochthonous Jurassic-Lower Cretaceous terranes of the Canadian Cordillera and their relation to correlative strata of the North American craton; in Jurassic-Cretaceous Biochronology and Paleogeography of North America, G.E.G. Westermann (ed.), Geological Association of Canada, Special Paper 27, p. 113-120.

Tipper, H.W. and Richards, T.A.
1976: Jurassic stratigraphy and history of north-central British Columbia; Geological Survey of Canada, Bulletin 270, 73 p.

Visser, M.J.
1980: Neap-spring cycles reflected in Holocene subtidal large-scale bedform deposits: a preliminary note; Geology, v. 8, p. 543-546.

Wheeler, J.O. and McFeely, P.
1987: Tectonic assemblage map of the Canadian Cordillera and adjacent parts of the United States of America; Geological Survey of Canada, Open File 1565, scale 1:2,000,000.

Woodsworth, G.J.
1978: Eastern margin of the Coast Plutonic Complex in Whitesail Lake map-area, British Columbia; in Current Research, Part A, Geological Survey of Canada, Paper 78-1A, p. 71-75.
1979: Geology of Whitesail Lake map area, British Columbia; in Current Research, Part A, Geological Survey of Canada, Paper 79-1A, p. 25-29.
1980: Geology of Whitesail Lake (93E) map-area B.C.; Geological Survey of Canada, Open File 708.

Woodsworth, G.J., Hill, M.L., and van der Heyden, P.
1985: Preliminary geologic map of Terrace (NTS 103I east half) map area, British Columbia; Geological Survey of Canada, Open File 1136.

Petroleum source rock potential of the Nanaimo Group, western margin of the Georgia Basin, southwestern British Columbia

R.M. Bustin[1] and T.D.J. England[2,3]
Cordilleran Division, Vancouver

Bustin, R.M. and England, T.D.J., Petroleum source rock potential of the Nanaimo Group, western margin of the Georgia Basin, southwestern British Columbia; in Current Research, Part A, Geological Survey of Canada, Paper 91-1A, p. 143-145, 1990.

Abstract

The petroleum source rock potential of Upper Cretaceous strata of the Nanaimo Group on Vancouver Island and the Gulf Islands is generally poor. The level of organic maturation is highly variable ranging from immature to overmature (<0.4-4.5 % Ro) with respect to the oil window. In the Comox and Nanaimo sub-basins of the Georgia Basin much of the succession is within the oil window (0.6-1.35 % Ro) except adjacent to the Eocene Catface Intrusives where strata are overmature. For the most part the strata are characterized by uniformly low total organic carbon contents (<1 %) and moderate to low hydrogen and oxygen indices as measured by Rock-Eval pyrolysis. The organic matter is principally Type II and Type III with little liquid hydrocarbon generating potential. Within the sample suite little significant variation in source rock quality exists; exceptions are the Extension and Pender formations which locally include intervals with up to 5.5 % TOC and hydrogen indices up to 373 mg HC/g TOC.

Résumé

Les couches du groupe de Nanaïmo du Crétacé supérieur sur l'île de Vancouver et dans les îles Gulf présentent des possibilités généralement faibles quant aux roches mères pétrolifères. Le degré de maturation organique est très variable et il y a immaturité à surmaturité (Ro <0,4 à 4,5 %) pour ce qui est de l'enclave de pétrole. Dans les sous-bassins de Comox et de Nanaïmo du bassin de Géorgie, une partie importante de la succession se trouve à l'intérieur de l'enclave de pétrole (Ro 0,6 à 1,35 %), s'il est fait exception des roches intrusives éocènes adjacentes de Catface dont les couches sont à surmaturité. Les couches sont principalement caractérisées par des teneurs uniformément faibles en carbone organique total (moins de 1 % et des indices modérés à faibles pour l'hydrogène et l'oxygène, tels que mesurés par pyrolyse Rock-Eval. La matière organique est principalement de types II et III et présente peu de possibilités quant à la génération d'hydrocarbures liquides. À l'intérieur de la suite échantillon, la qualité de la roche mère varie peu; les formations d'Extension et de Pender constituent des exceptions et englobent par endroits des intervalles présentant jusqu'à 5,5 % de COT et des indices d'hydrogène atteignant 373 mg HC/g COT.

[1] Department of Geological Sciences, University of British Columbia, 6339 Stores Road, Vancouver, B.C. V6T 2B4
[2] Department of Earth Sciences, Memorial University of, Newfoundland, St. John's NewFoundland, A1B 3X5
[3] Current address: BP Exploration Inc., P.O. Box 4587, Houston, Texas 77210, U.S.A.

INTRODUCTION

The Upper Cretaceous Nanaimo Group on Vancouver Island and the Gulf Islands comprises the western edge of the Cretaceous and Tertiary Georgia Basin. The Nanaimo Group was deposited in three major sub-basins: the Comox, Nanaimo and Suquash (Fig. 1 and 2). In these basins a diverse succession of marine, transitional marine and nonmarine clastics in excess of 4 km in thickness accumulated. The strata include important coal deposits and have long been considered as potential petroleum source and reservoir rocks. As part of a study to assess the lateral and stratigraphic variations in organic maturation and petroleum source rock potential in the George Basin (Bustin, 1990), samples from the Nanaimo Group on Vancouver Island and the Gulf Islands were analyzed by Rock-Eval pyrolysis, total organic carbon analysis and organic petrography. The purpose of this paper is to provide a brief overview of the source rock potential of the strata.

Samples utilized in this study were collected from outcrop samples complemented by well cuttings from the Harmac c-36-f and Yellow Point d-84-c bore holes located in the Nanaimo sub-basin. The samples are principally claystones and represent most of the stratigraphic succession in the Nanaimo sub-basin and the Trent River and Comox formations from the Comox sub-basin (Fig. 1).

RESULTS AND DISCUSSION

The results of Rock-Eval and total organic carbon analyses for all formations are summarized in Table 1. It must be emphasized that for some formations few samples have been processed and as additional analyses are made the values summarized in Table 1 may change significantly. The level of organic maturation of the strata, based on vitrinite reflectance (Bustin, unpub. data) and Tmax from Rock-Eval analyses, ranges from mature (0.4 % mean maximum vitrinite reflectance –Ro %.) to overmature (up to 2.7 %Ro). Vitrinite reflectance values up to about 5 % occur where the strata are proximal to, or cut by Eocene Catface Intrusives Throughout much of the Comox and Nanaimo sub-basins the strata are within the oil window whereas in the Suquash sub-basin the strata are mainly immature.

The quality of the organic matter is remarkably uniform within and between formations. For the most part the strata are characterized by low average total organic carbon (TOC) contents (<1 %), moderate to low average hydrogen indices (38-122 mg HC/g TOC) and moderate to low average oxygen indices (24-59 mg CO_2/g TOC; Table 1, Fig. 3). The highest TOC values occur in the Comox Formation (average 5 %), Extension Formation (values to 1.85 %) and in the Pender Formation (values up to 5.5 %). The rest of the strata show little significant variation in TOC, with all average values

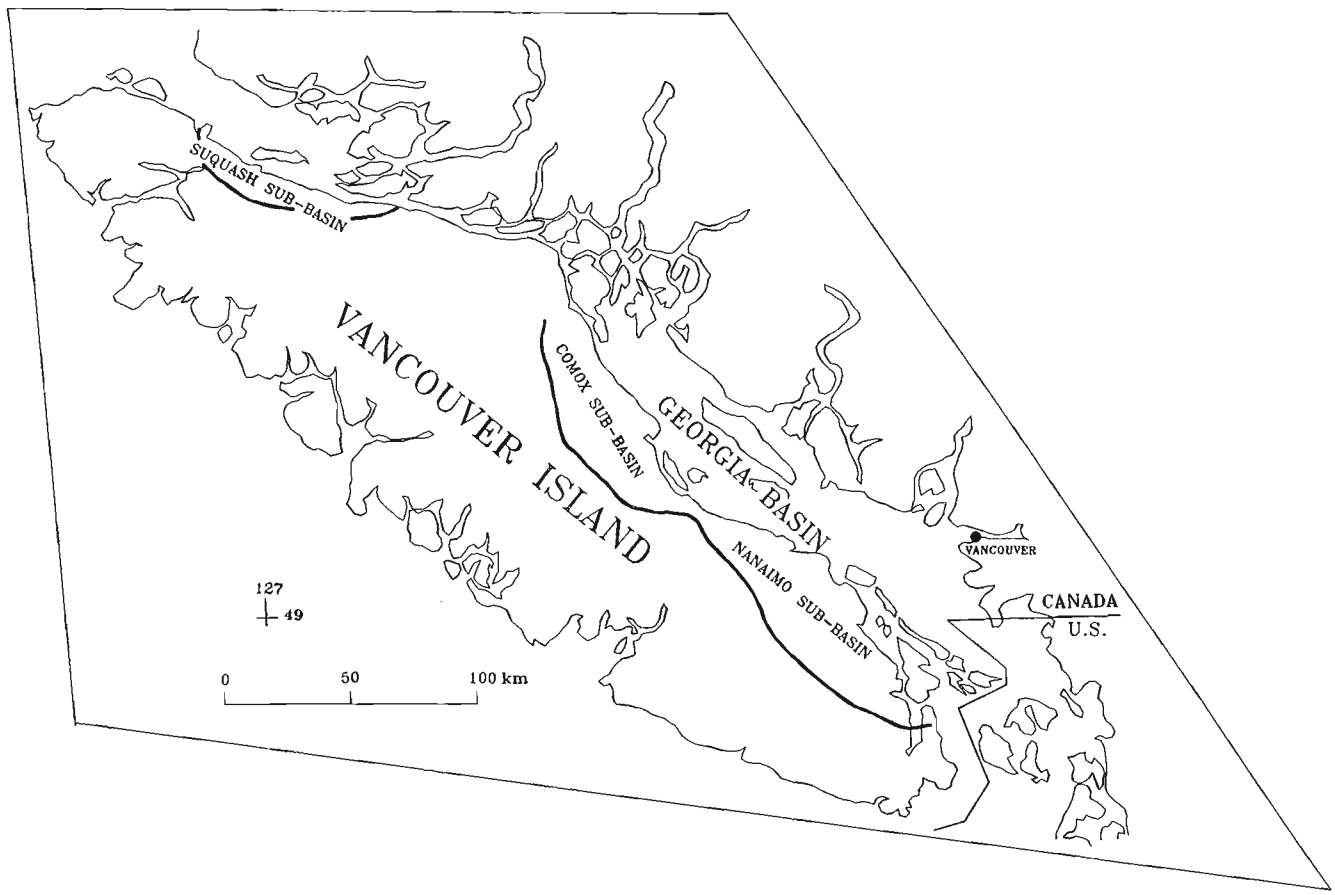

Figure 1. Index map showing the geographic location of the Nanaimo, Comox and Suquash sub-basins of the George Basin.

Table 1. Average Tmax, total organic carbon (TOC), Hydrogen index (HI; mg hydrocarbon/g TOC) Oxygen index (OI; mg CO_2/g TOC) and number of samples (N). Tmax (°C, HI and OI) are values obtained from Rock-Eval pyrolysis and are utilized in interpreting the source rock potential (refer to Espitalie et al., 1977).

FORMATION	Tmax	TOC	HI	OI	N
Gabriola	432	0.67	122	56	4
Mayne	430	0.36	77	36	9
Northumbland	420	0.48	58	38	16
De Courcy	440	0.58	52	59	9
Cedar Dist.	437	0.48	83	74	36
Protection	445	0.72	78	33	29
Pender	450	0.74	60	31	23
Extension	422	0.72	117	31	6
Haslam	455	0.62	46	32	65
Trent River	467	0.59	38	24	9
Comox	468	5.01	106	31	6
Bensen	454	0.98	44	49	3

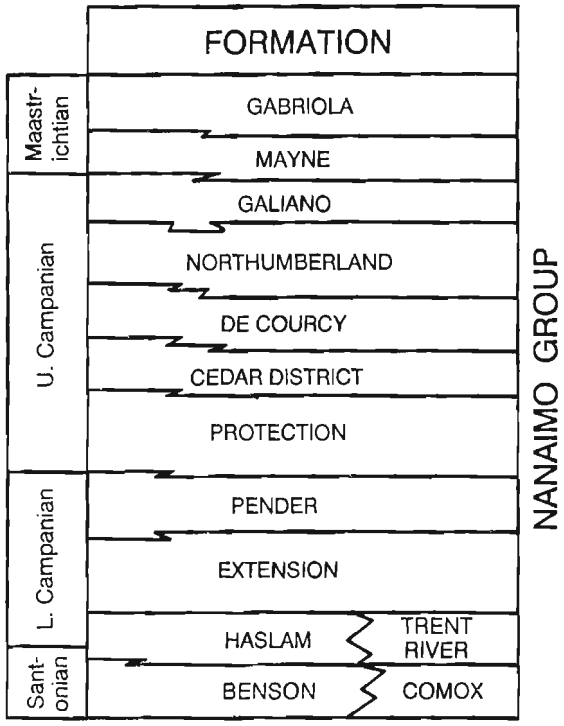

Figure 2. Lithostratigraphy of formations discussed in this paper. The samples in this study are mainly from the Nanaimo sub-basin with the exception of the Trent River and Comox formations which are from the Comox sub-basin (modified after England (1989) and Bickford and Kenyon (1988)).

in the range from 0.36-0.74 %. Overall the strata are composed mainly of Type II (oil and gas prone) and Type III (gas prone) organic matter (Fig. 3). Samples with the highest hydrogen index occur in the Extension (HI up to 365) and Pender (HI up to 373) formations but even these strata are characterized by low average values (Table 1).

The low average TOC and moderate to low hydrogen indices obtained to date indicate that, although much of the Nanaimo Group is within the oil window, the potential for the generation of substantial quantities of liquid hydrocarbon

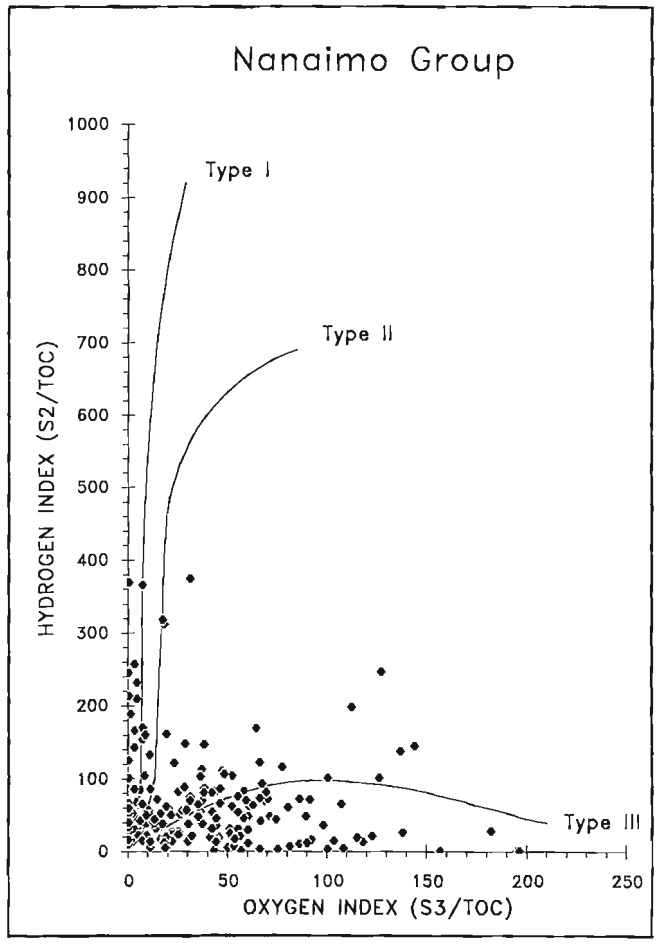

Figure 3. Modified van Krevelen diagram (hydrogen index, HI, vs Oxygen Index, OI) for samples from the Nanaimo Group. HI units = mg HC/g TOC, OI units = mg CO_2/g TOC.

is poor. There is a greater potential for generation of substantial gaseous hydrocarbons based on the presence of major coal deposits and dispersed Type III organic matter. Further sample collection and more detailed chemical analyses are required to fully document the spatial variation in organic maturation and source rock quality within specific formations.

REFERENCES

Bickford, C. and Kenyon, C.
1988: Coalfield geology of eastern Vancouver Island (92F); in Geological Fieldwork Paper 1988-1, British Columbia Ministry of Energy, Mines and Petroleum Resources, p. 441-450.

Bustin, R.M.
1990: Stratigraphy, sedimentology and petroleum source rock potential of the Georgia Basin, southwest British Columbia and northwest Washington State; in Current Research, Part F, Geological Survey of Canada, Paper 90-1F, p. 103-108.

England, T.D.J.
1989: Lithostratigraphy of the Nanaimo Group, Georgia Basin, southwestern British Columbia; in Current Research, Part E, Geological Survey of Canada, Paper 89-1E, p. 197-206.

Espitalie, R., Madec, M., and Tissot, B.
1977: Source rock characterization method for petroleum exploration; 9th Annual Offshore Technology Conference, Houston, Texas, p. 439-444.

Geology of the Tagish Lake area, northern Coast Mountains, northwestern British Columbia

Lisel D. Currie[1]
Continental Geoscience Division, Ottawa

Currie, L.D., Geology of the Tagish Lake area, northern Coast Mountains, northwestern British Columbia; in Current Research, Part A, Geological Survey of Canada, Paper 91-1A, p. 147-153, 1991.

Abstract

The structurally lowest lithological units of the Nisling Terrane exposed in this area include the Late Devonian to Early Mississippian Bighorn Creek orthogneiss, the Mt. Lawson gneiss, and the Mt. Lawson metamorphic suite. They lie structurally below the Boundary Ranges metamorphic suite. Metamorphic rocks of the Nisling Terrane in the Tagish Lake area were ductilely deformed between Early Jurassic and Early Cretaceous time, based on deformation of Early Jurassic Hale Mountain granodiorite, which is intruded by undeformed Early Cretaceous granite. Fabrics associated with this deformation are concordant with the Wann River Shear Zone (WRSZ) and Hoboe Glacier Shear Zone and are truncated by the Willison Creek Shear Zone (WCSZ), Chicken Creek Fault, Wann River Fault (WRF) and Llewellyn Fault. Consequently, some movement on these faults occurred after Early Jurassic time. A Paleocene syenite intrudes the WRSZ, placing a younger age limit on movement on the WRSZ and likely the WCSZ.

Résumé

Les unités lithologiques structuralement les plus basses du terrane de Nisling mises à nu dans cette région englobent l'orthogneiss de Bighorn Creek du Dévonien supérieur au Mississipien inférieur, le gneiss de Mount Lawson et la suite métamorphique de Mt Lawson. Elles se trouvent structuralement sous la suite métamorphique des chaînons Boundary. Les roches métamorphiques du terrane de Nisling dans la région du lac Tagish ont été ductilement déformées entre le Jurassique inférieur et le Crétacé inférieur, d'après la déformation de la granodiorite de Hale Mountain du Jurassique inférieur qui est pénétrée par un granite non déformé du Crétacé inférieur. Les éléments structuraux associés à cette déformation sont en concordance avec la zone de cisaillement de Wann River et la zone de cisaillement de Hoboe Glacier ainsi que tronqués par la zone de cisaillement de Willison Creek, la faille Chicken Creek, la faille Wann River et la faille Llewellyn. En conséquence, il y a eu un certain déplacement le long de ces failles après le Jurassique inférieur. Une syénite paléocène pénètre la zone de cisaillement de Wann River, ce qui repousse dans le temps la limite du déplacement dans la zone de cisaillement de Wann River, et vraisemblablement dans la zone de cisaillement de William Creek.

[1] Ottawa-Carleton Geoscience Center, Department of Earth Sciences, Carleton University, Ottawa, Ontario K1S 5B6

INTRODUCTION

Geological mapping and preliminary U-Pb zircon geochronology in the Tagish Lake area have helped to constrain the tectonic history of metamorphic rocks that belong to the Nisling Terrane (Wheeler and McFeely, 1987) in northwestern British Columbia. The study area is located adjacent to, and primarily west of the Llewellyn Fault, which forms the boundary between the Nisling Terrane (Wheeler and McFeely, 1987) and Stikine Terrane to the east (Fig. 1).

During the 1990 field season 1 : 20 000 geological mapping of the Tagish Lake area was conducted as a continuation of a mapping project initiated in 1988 (Mihalynuk et al., 1989a,b; Currie, 1990). Fieldwork focused on mapping the continuation of geologic units recognized during the 1989 field season, more precisely locating contacts between these units, and investigating metamorphic rocks that are exposed east of the trace of the Llewellyn Fault. Mapping was extended toward the west to the headwaters of the Swanson River (NTS 104M/7), Chicken Creek and Bighorn Creek (NTS 104M/10), and toward the south to the headwaters of Hoboe Creek and Willison Creek (NTS 104M/1; Fig. 2). This area was previously mapped at 1 : 250 000 scale by Christie (1957) and parts of NTS 104M/1 were mapped at 1 : 30 000 scale by Werner (1977, 1978).

Age constraints presented here are preliminary results based on U-Pb geochronometry presently in progress. More precise ages for the Bighorn Creek orthogneiss (Late Devonian to Early Mississippian), Wann River Gneiss (Permian?), Hale Mountain granodiorite (Early Jurassic), the granite on the south shore of Tagish Lake (Early Cretaceous), and the syenite north of the Wann River (Paleocene) will be presented elsewhere in the near future.

General geology and previous work

The Nisling Terrane, as it is presently defined in northern British Columbia (Wheeler and McFeely, 1987), comprises: (1) metasediments of probable continental affinity that belong to the Florence Range metamorphic suite (Currie, 1990); (2) the Permian (or older?) Wann River gneiss (Currie, 1990 and unpub. data, 1990); (3) metavolcanic rocks of the Boundary Ranges metamorphic suite (Mihalynuk and Rouse, 1988a,b); (4) metasediments of the Mt. Lawson metamorphic suite (this paper) and (5) deformed plutons, which include the Mt. Caplice granite, Hale Mountain granodiorite and Bighorn Creek orthogneiss (Currie, 1990, and this paper). These lithological units are commonly juxtaposed by shear zones that are concordant with the metamorphic fabric in the rocks adjacent to the shear zone (Currie, 1990; Fig. 2). The Boundary Ranges metamorphic suite has experienced at least three phases of deformation, and the Florence Range and Mt. Lawson metamorphic suites preserve evidence of two major phases of deformation. The presence of only one fabric in the Wann River gneiss, Hale Mountain granodiorite, and Mt. Caplice granite may be due to the lack of rheological variation within these units.

The foliated rocks have been intruded by undeformed Mesozoic and Tertiary plutons and are overlain by undeformed Mesozoic Mt. Switzer volcanic rocks (Currie, 1990; Mihalynuk and Mountjoy, 1990; Mihalynuk et al., 1990) and Tertiary Sloko volcanic rocks (Werner, 1977).

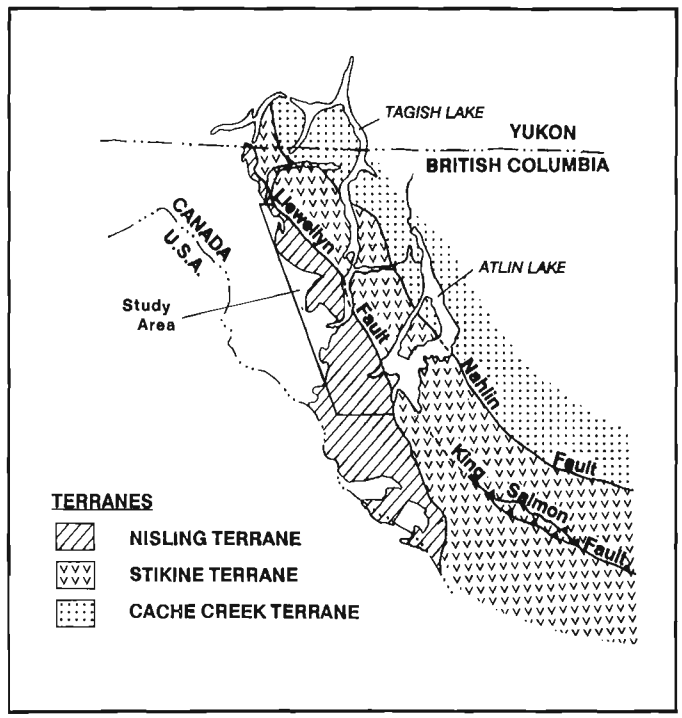

Figure 1. Map showing the location of the study area, and the boundaries of the Nisling, Stikine and Cache Creek terranes.

East of the Llewellyn Fault there are variably deformed Late Triassic volcanic rocks of the Stuhini Group, mildly deformed Early Jurassic sedimentary rocks of the Laberge Group, and flat-lying undeformed Tertiary Sloko Group volcanic rocks (Fig. 2). Metamorphic rocks have been reported east of the southern projection of the Llewellyn Fault (Christie, 1957; Aitken, 1959a,b; Werner, 1977 and 1978; and Bultman, 1979).

STRATIGRAPHY

The Florence Range metamorphic suite, Boundary Ranges metamorphic suite, Wann River gneiss, Hale Mountain granodiorite, and Bighorn Creek orthogneiss have been described previously (Currie, 1990). The Mt. Lawson metamorphic suite, Mt. Lawson gneiss, and Chicken Creek gneiss (Fig. 2) are described here for the first time.

Northwest of Chicken Creek, on the southeast side of Mt. Lawson, the Mt. Lawson gneiss and the Mt. Lawson metamorphic suite are exposed, structurally below the Late Devonian to Early Mississippian Bighorn Creek orthogneiss (Currie, unpub. data, 1990; Fig. 2). The Mt. Lawson gneiss is a fine grained leucocratic feldspar-quartz-muscovite gneiss that is at least 400 m thick. It was originally mapped as a quartzite (Mihalynuk et al., 1989a), but is probably made up of meta-tuffs or meta-flows, since it is feldspar-rich and well layered.

Structurally below the Mt. Lawson gneiss is the Mt. Lawson metamorphic suite, which is the structurally lowest

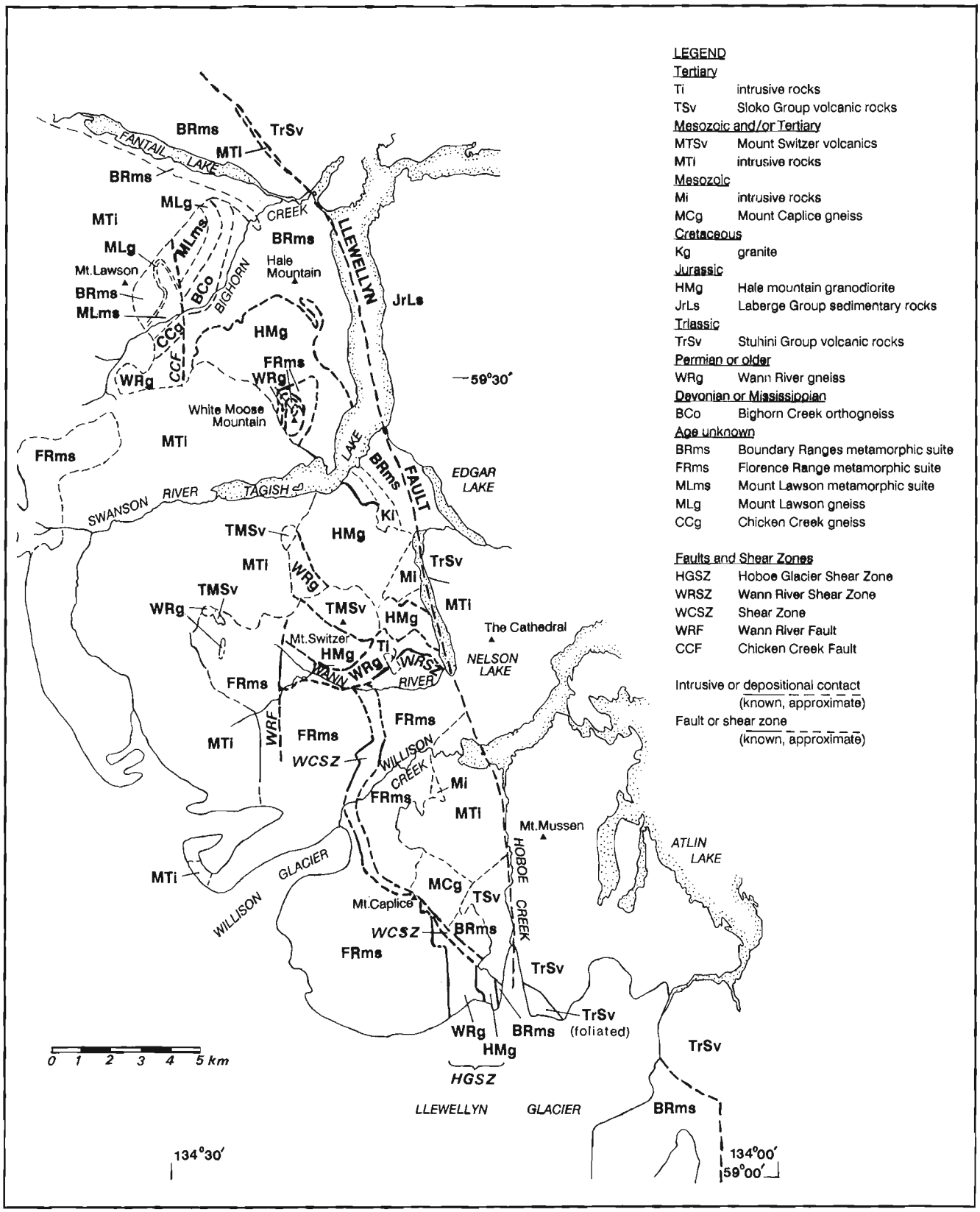

Figure 2. Geological map for Nisling Terrane lithologies from Fantail Lake south to the Llewellyn Glacier.

lithological unit of the Nisling Terrane that has been observed in northern British Columbia. It comprises biotite schist, muscovite schist, garnet-biotite schist and minor carbonate, and is at least 300 m thick. These rocks have been deformed at least twice and exhibit a strong top-to-the-southeast, shallowly plunging lineation.

West of the Chicken Creek Fault the Mt. Lawson metamorphic suite is overlain by the Mt. Lawson gneiss. They are in turn overlain by chlorite schist and distinctive pyroxene phyric chlorite schist, which are lithologically similar to schists in the Boundary Ranges metamorphic suite. Here, in contrast with the area east of the Chicken Creek Fault, the Bighorn Creek orthogneiss is apparently not present between the Mt. Lawson gneiss and the Boundary Ranges metamorphic suite.

The Chicken Creek gneiss is exposed south of Bighorn Creek and west of the Chicken Creek Fault. It is a fine grained leucocratic feldspar-quartz-muscovite gneiss that resembles the Mt. Lawson gneiss. Unlike the Mt. Lawson gneiss, the Chicken Creek gneiss is overlain by hornblende-plagioclase gneisses that are correlated with the Wann River gneiss. The contact between the Chicken Creek gneiss and the overlying gneisses has not been observed.

CONSTRAINTS ON THE AGE OF DEFORMATION

Previously, the age of penetrative deformation of the metamorphic rocks in the Tagish Lake area was thought to be older than Late Triassic (Bultman, 1979; Werner, 1977; Mihalynuk and Mountjoy, 1990), based on the presence of foliated clasts in Late Triassic conglomerates in the Stuhini Group at the south end of Atlin Lake. However, an Early Jurassic U-Pb zircon age for the deformed Hale Mountain granodiorite (Currie, unpub. data, 1990) indicates that most or all of the deformation and movement on the shear zones that bound the Hale Mountain granodiorite must have occurred after Late Triassic time. The Hale Mountain granodiorite is intruded by an undeformed Early Cretaceous granite (Currie, unpub. data, 1990), and therefore penetrative deformation at this locality must have ceased before the end of the Early Cretaceous.

Early Jurassic to Early Cretaceous deformation in the Tagish Lake area does not preclude older phases of deformation affecting Nisling Terrane rocks. The Mt. Lawson, Boundary Ranges and Florence Range metamorphic suites and the Wann River gneiss have experienced more than one period of deformation, and one or more of the deformational events may predate the deformation that affected the Hale Mountain granodiorite.

North of the Wann River (above Nelson Lake) the Wann River Shear Zone juxtaposes the Permian (or older?; Currie, unpub. data, 1990) Wann River gneiss and the Florence Range metamorphic suite. There, the shear zone is intruded by an undeformed Paleocene syenite (Currie, unpub. data, 1990; Fig. 2), which places a younger age limit on the timing of movement on the Wann River Shear Zone and fabrics within the Wann River gneiss. The older age limit for the foliation in the Wann River gneiss is less easily constrained. It has the same orientation as the foliation in the Early Jurassic Hale Mountain granodiorite, where these two units are in contact, and therefore the fabrics in these two units are probably correlative. This suggests that the foliation in the Wann River Gneiss formed during or after the Early Jurassic.

FAULTS AND SHEAR ZONES

Within the Nisling Terrane of the Tagish Lake area the oldest faults are those within individual lithological units (Currie, 1990). They are at least as old as the shear zones that juxtapose the different lithological units, such as the Wann River Shear Zone (Fig. 2). The boundary shear zones are truncated by younger structures, including the Llewellyn Fault (Fig. 2).

Hoboe Glacier Shear Zone

The Hoboe Glacier Shear Zone is a 3 km wide zone characterized by north-striking, subvertical, sinistral ductile fabrics that affect lithologies belonging to the Boundary Ranges metamorphic suite, the Hale Mountain granodiorite and Wann River gneiss (Fig. 2). Kinematic indicators include C-S fabrics and rotated porphyroblasts. The fabrics increase in intensity eastward, toward the Llewellyn Fault. To the north the shear zone may be truncated by the Willison Creek Shear Zone. However, this relationship is obscured by the overlying Sloko Group volcanic rocks. Since shearing affects the Hale Mountain granodiorite, the Hoboe Glacier Shear Zone is younger than Early Jurassic, but it must be older than Tertiary, because the Sloko volcanic rocks are not deformed.

Chicken Creek and Wann River faults

The Chicken Creek Fault is a north-striking, steep fault that extends from near the headwaters of Chicken Creek, northward across Bighorn Creek. The offset and sense of motion on this fault are not known. Both the northern and southern terminations are intruded by Mesozoic to Tertiary igneous rocks (Fig. 2, Mihalynuk et al., 1989a,b).

The Wann River Fault is a north-striking, steep, west-side-down fault that is exposed from north of Willison Glacier, across the Wann River, to west of Mt. Switzer. The southern terminus of the fault is covered by a glacier and the northern terminus is intruded by a Mesozoic to Tertiary granite. Movement on the Wann River fault occurred between Early Jurassic and Paleocene time.

The Chicken Creek and Wann River Faults are parallel (Fig. 2, Currie, 1990; Mihalynuk et al., 1990), both faults truncate metamorphic foliations and the shear zones that juxtapose lithological units, and neither fault affects undeformed Mesozoic to Tertiary intrusive rocks. Thus, these faults may be the same age. The relationship between these faults and the Llewellyn Fault is not presently known.

Willison Creek Shear Zone

The Willison Creek Shear Zone (Fig. 3) is a previously unrecognized shear zone that is exposed from the Wann River above Nelson Lake, toward the southeast to near the north end of Hoboe Creek (Fig. 2). It dips toward the southwest and truncates the Florence Range metamorphic suite, Boundary Ranges metamorphic suite, Wann River gneiss,

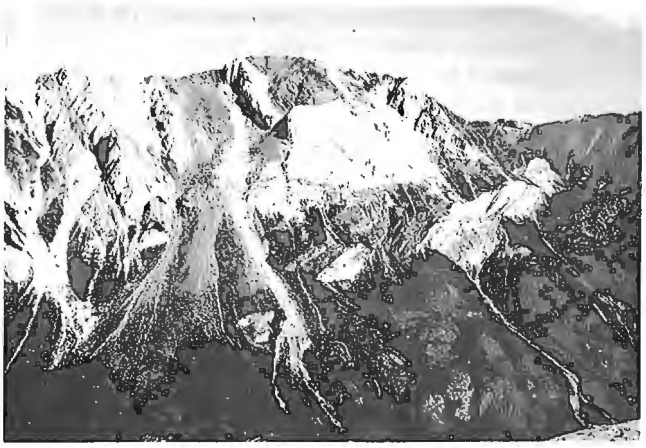

Figure 3. View north from Willison Creek to the Willison Creek Shear Zone. To the west a coherent stratigraphy is preserved, but within the Willison Creek Shear Zone, blocks of carbonate and schist are faulted and rotated.

Hale Mountain granodiorite, the shear zones that separate them and the Mt. Caplice granite, but does not affect the unconformably overlying Tertiary Sloko volcanic rocks. Movement on the shear zone must have occurred between Early Jurassic and the end of the Tertiary.

The fault zone contains in part large horses (up to 250 m^3; Fig. 3). They are fault-bounded blocks of carbonate, calc-silicate, schist, and plutonic rocks that are not penetratively deformed. Faults within the shear zone truncate metamorphic fabrics within the horses, but the sense of movement for these faults or for the entire shear zone is not known.

In the south, the Willison Creek Shear Zone disappears beneath the Sloko volcanic rocks, and the Hoboe Glacier where it intersects the southern projection of the Llewellyn Fault. Either the Willison Creek Shear zone is truncated by the Llewellyn Fault, or it offsets the Llewellyn fault and continues to the east.

On the east side of Hoboe Glacier there is a shear zone that deforms Late Triassic Stuhini Group pyroxene phyric mafic volcanic rocks, volcanic greywacke, and carbonate may be continuous with the Willison Creek Shear Zone (Fig. 2). Due to their strong fabric, these rocks were originally mapped as metamorphic rocks by Werner (1977, 1978), but with the exception of a sliver of possible Boundary Ranges metamorphic suite rocks within the shear zone, these rocks are interpreted to be ductilely deformed equivalents of the Stuhini Group.

The Willison Creek Shear Zone has not been recognized north of the Wann River. It may be a splay of the Wann River Shear Zone, in which case movement on the Willison Lake Shear Zone may have occurred at the same time as movement on the Wann River Shear Zone, between the Early Jurassic and the Late Tertiary.

Llewellyn Fault

In map area 104M/1 the Llewellyn Fault strikes north-south and follows the Hoboe Creek valley. East of the fault Mesozoic and/or Tertiary intrusive rocks and Late Triassic Stuhini Group volcanic rocks are exposed. Since the Stuhini Group is not exposed west of the Llewellyn Fault in this area, at least some movement on this portion of the fault occurred after Late Triassic time.

West of the Llewellyn Fault brittley deformed Mesozoic-Tertiary granites, gently dipping Sloko volcanic rocks, and potassium feldspar megacrystic granite have been observed near the trace of the fault (Fig. 2). Presently included with the Sloko volcanic rocks are steeply dipping volcanic rocks exposed near Hoboe Creek that may be older than the Sloko volcanic rocks.

DISCUSSION

In the Tagish Lake area, rocks west of the Llewellyn Fault have been included in the Nisling Terrane (Wheeler and McFeely, 1987). There, at least five distinct lithological units are exposed. They are the Mt. Lawson, Boundary Ranges, and Florence Range metamorphic suites, the Wann River gneiss and the Hale Mountain granodiorite. These units, with the possible exception of the Mt. Lawson and Boundary Ranges metamorphic suites, are juxtaposed by shear zones. If the lithological units did not form adjacent to one another, then the Nisling Terrane may be a composite terrane. Alternatively, the different lithological units may have formed adjacent to one another or at different times, and the Nisling Terrane may be a single terrane that has been imbricated by shear zones. In either case, movement on the shear zones that separate the different units occurred before movement on the Llewellyn Fault ceased since the Llewellyn Fault truncates both the ductile fabrics within the Hale Mountain granodiorite and the shear zones that bound the lithological units in the Nisling Terrane.

The significance of the Llewellyn Fault is brought into question by the presence of metamorphic rocks that are correlated with the Boundary Ranges metamorphic suite, east of the southern projection of the Llewellyn Fault (Fig. 2). The presence of Nisling Terrane rocks east of the Llewellyn Fault implies that either the Llewellyn Fault is not a major terrane boundary separating the Nisling and Stikine terranes as shown in Figure 1, or the Llewellyn Fault has been offset to the east by a younger fault. The lack of penetrative deformation throughout upper Triassic Stuhini Group volcanic rocks east of the Llewellyn Fault suggests that these rocks did not experience a strong deformational event between Early Jurassic and Early Cretaceous time, and therefore at that time were not adjacent to rocks of the Nisling Terrane that are exposed today.

Since the fabrics in the Hale Mountain granodiorite parallel the shear zones that bound this unit, the Early Jurassic to Early Cretaceous deformation may be associated with the juxtaposition of at least the Hale Mountain granodiorite, Boundary Ranges metamorphic suite and the Wann River gneiss, which make up part of the Nisling Terrane.

Fabrics within the Hoboe Creek Shear Zone are not truncated by the Llewellyn Fault, and therefore it is not clear whether the fabrics are related to ductile sinistral motion on the Llewellyn Fault, or whether they may be correlative with penetrative fabrics observed in these units to the north, such

as the top-to-the-southeast fabrics in the Mt. Lawson metamorphic suite north of Bighorn Creek.

The Early Jurassic to Early Cretaceous deformation documented for the Nisling Terrane of northern British Columbia is not unique in the western Canadian Cordillera. It may be related to Early Jurassic deformation to the north in Yukon, and to the south on the eastern margin of the Coast Plutonic Complex of central British Columbia. In the Aishihik Lake area, Yukon, the penetratively deformed Early Jurassic Aishihik Batholith (J.M. Mortensen, pers. comm., 1989) is thrust over amphibolite grade metasediments of the Nisling Terrane (Johnston, 1988; Wheeler and McFeely, 1987). An Early Jurassic pink quartz monzonite cuts the mylonitic contact at the base of the penetratively deformed Early Jurassic Aishihik Batholith (J.M. Mortensen, pers. comm., 1989), thus constraining the age of deformation to Early Jurassic.

Jurassic deformation has also been documented on the eastern margin of the Coast Belt in west-central British Columbia. The Gamsby Complex comprises Early Jurassic volcanic rocks, Middle Jurassic plutonic rocks, and possibly Late Triassic intrusions and Paleozoic strata, which were deformed and metamorphosed in early Late Jurassic time (van der Heyden, 1982). Deformation of the Atnarko Complex occurred before Early Cretaceous time, based on cooling ages, and probably after Middle Jurassic time, based on a possible lithological correlation with Middle Jurassic plutonic protoliths of the Gamsby Complex (van der Heyden, 1990).

CONCLUSIONS

The newly described Mt. Lawson metamorphic suite, Mt. Lawson gneiss, and possibly the Chicken Creek gneiss are the structurally lowest units of the Nisling Terrane recognized in the Tagish Lake area. Their original tectonic relationship with the Boundary Ranges and Florence Range metamorphic suites is not known.

New U-Pb zircon age data for the Bighorn Creek orthogneiss (Late Devonian to Early Mississippian), Wann River Gneiss (Permian or older?), Hale Mountain granodiorite (Early Jurassic), the granite on the south shore of Tagish Lake (Early Cretaceous), and the syenite north of the Wann River (Paleocene) provide constraints for some of the deformation that affected metamorphic rocks of the Nisling Terrane in the Tagish Lake area. There, some, but not necessarily all, of the deformation occurred between Early Jurassic and Early Cretaceous time, and no penetrative deformation affected these rocks after Early Cretaceous time. At least some of the movement on the Wann River Shear Zone, Hoboe Glacier Shear Zone, Willison Creek Shear Zone, Wann River Fault and Llewellyn Fault, and possibly the Chicken Creek Fault, occurred after Early Jurassic time. Movement on these faults ceased before the end of the Tertiary, with the possible exception of the Llewellyn fault, which may have been active after deposition of Sloko volcanic rocks.

ACKNOWLEDGMENTS

Fieldwork was funded by Geological Survey of Canada Project 850001 and a Natural Sciences and Engineering Research Council Operating Grant awarded to R.R. Parrish, and a Northern Scientist Training Program Grant from the Department of Indian and Northern Affairs and a Geological Society of America Grant awarded to L.D. Currie. Geochronology was performed at the Geological Survey of Canada in Ottawa.

While in the field I enjoyed visits by Randy Parrish and Dick Brown, who shared their expertise. Norm Graham, Haley Holzer, and Jacqueline Storey of Capital Helicopters provided field support above and beyond the expectations of any field geologist. Pierre Maheux and crew of Placer Dome made us welcome at their camp on White Moose Mountain. Debbie van der Wettering and Dave Sarkany provided able assistance and companionship in the field. Ideas presented in this paper were aided by discussions with Randy Parrish, Dick Brown, Jay Jackson, and Mitch Mihalynuk and comments by Peter van der Heyden.

REFERENCES

Aitken, J.D.
1959a: Geology, Atlin, Cassiar District, British Columbia; Geological Survey of Canada, Map 1082A.
1959b: Geology of Atlin map area; Geological Survey of Canada, Memoir 307, 89 p.

Bultman, T.R.
1979: Geology and tectonic history of the Whitehorse Trough west of Atlin, British Columbia; unpublished Ph.D. thesis, Yale University, New Haven, Conneticut, 284 p.

Christie, R.L.
1957: Bennett, Cassiar District, British Columbia; Geological Survey of Canada, Map 19-1957.

Currie, L.D.
1990: Metamorphic rocks in the Florence Range, Coast Mountains, northwestern British Columbia; in Current Research, Part E, Geological Survey of Canada, Paper 90-1E, p. 113-119.

Johnston, S.T.
1988: The tectonic setting of the Aishihik Batholith, SW Yukon; in Yukon Geology, Vol. 2, Exploration and Geological Services Division, Yukon, Indian and Northern Affairs Canada, p. 37-41.

Mihalynuk, M.G. and Rouse, J.N.
1988a: Geology of the Tutshi Lake area, British Columbia; British Columbia Geological Survey, Open File Map 1988-5 (104M/15).
1988b: Preliminary geology of the Tutshi Lake area, northwestern British Columbia (104M/15); in Geological Fieldwork 1987, British Columbia Ministry of Energy, Mines and Petroleum Resources, Paper 1988-1, p. 217-231.

Mihalynuk, M.G., Currie, L.D., Mountjoy, K.M., and Wallace, C.
1989a: Geology of the Fantail Lake (west) and Warm Creek (east) map area; British Columbia Geological Survey, Open File Map 1989-13 (104M/9W and 10E).

Mihalynuk, M.G., Currie, L.C., and Arksey, R.L.
1989b: Geology of the Tagish Lake area (Fantail Lake and Warm Creek) (104M/9W and 10E); in Geological Fieldwork 1988, British Columbia Ministry of Energy, Mines and Petroleum Resources, Paper 1989-1, p. 293-310.

Mihalynuk, M.G. and Mountjoy, K.J.
1990: Geology of the Tagish Lake area (104M/8, 9E); in Geological Fieldwork 1989, British Columbia Ministry of Energy, Mines and Petroleum Resources, Paper 1990-1, p. 181-196.

Mihalynuk, M.G., Mountjoy, K.J., Currie, L.D., Lofthouse, D.L., and Winder, N.
1990: Geology of the Tagish Lake area (Fantail Lake and Warm Creek) (104M/9W and 10E); British Columbia Geological Survey, Open File Map 1990-4.

van der Heyden, P.
1982: Tectonic and stratigraphic relations between the Coast Plutonic Complex and the Intermontane Belt, west-central Whitesail Lake map area; unpublished M.Sc. thesis, University of British Columbia, Vancouver, 253 p.

1990: Eastern margin of the Coast Belt in west-central British Columbia; in Current Research, Part E, Geological Survey of Canada, Paper 90-1E, p. 171-182.

Werner, L.J.

1977: Metamorphic terrane, northern Coast Mountains west of Atlin Lake, British Columbia; in Current Research, Part A, Geological Survey of Canada, Paper 77-1A, p. 267-269.

1978: Metamorphic terrane, north Coast Mountains west of Atlin Lake, British Columbia; in Current Research, Part A, Geological Survey of Canada, Paper 78-1A, p. 69-70.

Wheeler, J.O. and McFeely, P.

1987: Tectonic assemblage map of the Canadian Cordillera; Geological Survey of Canada, Open File 1565.

Jurassic stratigraphy of east Telegraph Creek and west Spatsizi map areas, British Columbia

C.A. Evenchick[1]
Cordilleran Division, Vancouver

Evenchick, C.A., Jurassic stratigraphy of east Telegraph Creek and west Spatsizi map areas, British Columbia; in Current Research, Part A, Geological Survey of Cdnada, Paper 91-1A, p. 155-162, 1991.

Abstract

The Middle Jurassic to Cretaceous Bowser Lake Group is underlain by a Lower to lower Middle Jurassic succession called the Hazelton Group. The lower stratigraphic interval exhibits a wide variety of proportions of volcanic and sedimentary rock west and north of the Bowser Basin. In Telegraph Creek area, its dominantly clastic nature is most similar to the Eskay Creek facies of the Salmon River Formation, but the presence of felsic to mafic volcanic rocks also reflects affinity to the Snippaker Mountain facies. The strata are tightly folded about northwest-trending fold axes, and probably have a similar structural history to the Bowser Lake Group.

The Bowser Lake Group in Telegraph Creek area is entirely marine. Mid-fan turbidites are present in the southeast corner of the map area, and Ashman Formation is everywhere the westernmost Bowser Lake Group.

Résumé

Le groupe de Bowser Lake, datant du Jurassique moyen au Crétacé, repose sur une succession datant du Jurassique inférieur au Jurassique moyen inférieur qui est appelée groupe de Hazelton. L'intervalle stratigraphique inférieur présente des proportions très variables de roches volcaniques et sédimentaires à l'ouest et au nord du bassin de Bowser. Dans la région de Telegraph Creek, sa nature à prédominance clastique est des plus similaires au faciès d'Eskay Creek de la formation de Salmon River, mais la présence de roches volcaniques felsiques à mafiques reflète également une affinité avec le faciès de Snippaker Mountain. Les couches sont plissées serrées autour d'axes de plis d'orientation nord-est et ont probablement une histoire structurale similaire à celle du groupe de Bowser Lake.

Le groupe de Bowser Lake est entièrement marin dans la région de Telegraph Creek. Des turbidites de type «mid-fan» sont présentes à l'angle sud-est de la région cartographiée et la formation d'Ashman est partout la partie la plus occidentale du groupe de Bowser Lake.

[1] Contribution to Frontier Geoscience Program

INTRODUCTION

The Bowser Basin project is designed to provide a sedimentological, stratigraphic, and structural framework for the large area of north-central British Columbia that is referred to as the Bowser Basin. Strata considered are primarily the Middle Jurassic to Cretaceous Bowser Lake Group, but include the Cretaceous Sustut Group and the Lower and Middle Jurassic Hazelton Group (Fig. 1). Past work in Spatsizi map area focused on stratigraphy of the marine and nonmarine Bowser Lake Group and the nonmarine Sustut Group, as well as outlining the regional framework of a fold and thrust belt (Skeena Fold Belt) which involved all of these strata (Evenchick, 1986, 1987, 1988, 1989; Evenchick and Green, 1990; Ricketts, 1990; Evenchick, in press). These regional studies incorporate past regional work (Tipper and Richards, 1976; Gabrielse and Tipper, 1984), as well as ongoing more detailed research (Cookenboo and Bustin, 1989; MacLeod and Hills, 1990).

This report presents the results of regional mapping in southwest Spatsizi and east Telegraph Creek map areas (dashed area on Fig. 1). The region is underlain by Bowser Lake Group (Tipper and Richards, 1976) and island arc volcanic rocks and related sedimentary rocks of the Hazelton Group. The lower succession is currently the focus of intense mineral exploration (eg. Mining Review staff, 1990).

Additional research associated with this project includes a sedimentological analysis of the northern margin of the basin (Green, 1991; Ricketts and Evenchick, 1991), regional mapping in the Oweegee Dome and Kitsault Lake areas (Greig, 1991), and biostratigraphic studies of the northern margin of the basin (Poulton et al., 1991). An ongoing study of thermal maturation will be reported on in the near future (Goodarzi and Evenchick). M. Dawson (GSC) and B. Ryan (BCGS) conducted regional coal quality studies of the northern basin.

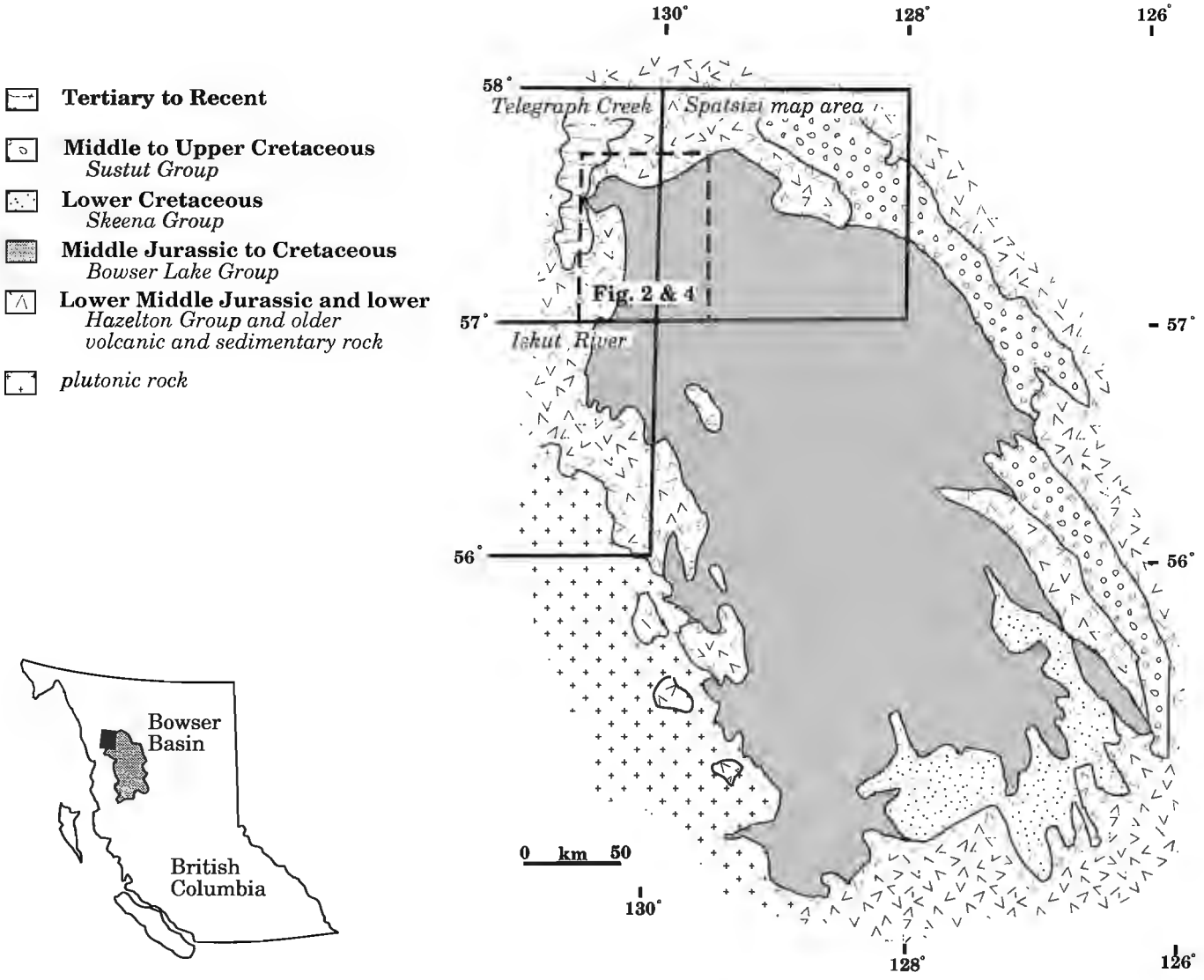

Figure 1. Location of the Bowser Basin, Telegraph and Spatsizi map areas. The location of Figures 2 and 4 is outlined by dashes.

LOWER AND MIDDLE JURASSIC CLASTIC ROCKS IN TELEGRAPH CREEK MAP AREA

Lower and lower Middle Jurassic island arc volcanic rocks and related sedimentary rocks of the Hazelton Group occur in a broad belt around the north and west margins of the Bowser Basin (Fig. 1; Souther, 1972; Grove, 1986; Alldrick and Britton, 1988; Alldrick et al., 1989; Anderson and Thorkelson, 1990). The Hazelton Group has been divided into regionally mappable units and facies in Iskut map area (summarized in Anderson and Thorkelson, 1990). In Spatsizi map area, upper Lower and lower Middle Jurassic clastic rocks were formally defined as the Spatsizi Group (Thomson et al., 1986). Between these regions, in the intervening Telegraph Creek map area, strata of this age have not been studied since the regional mapping of Souther (1972).

In Telegraph Creek map area Souther (1972) recognized two Jurassic map units below the Bowser Lake Group. He outlined three areas of Toarcian to Bajocian friable black shale with minor ironstone, sandstone, siliceous siltstone and quartzose sandstone (unit 14). Northeast of 180 Lake (Fig. 2) they are overlain by Middle Jurassic basalt or andesite pillow lavas and flows of unit 15. A second body of unit 15 (west of Kinaskan Lake) is dominantly tuff, tuff breccia, and volcanic sandstone, and is overlain by Bowser Lake Group.

This report clarifies the stratigraphic position and relationships of the clastic part of the Hazelton Group (Souther's unit 14) in Telegraph Creek map area. It is an attempt to compare the lithology and stratigraphy with coeval strata in Iskut and Spatsizi map areas. Five schematic sections are shown in Figure 3 aligned with sections from Spatsizi and Iskut map areas. A persistent problem is that only partial sections are exposed, so that thickness and contact relations of units 14 and 15 with bounding strata are not well defined. A combination of folding, faulting, and discontinuous outcrop further thwart stratigraphic studies.

Lithology of unit 14

The most common lithology is friable to well indurated black/brown/grey siltstone, with parallel lamination as the most persistent sedimentary structure. Crossbedding and graded bedding are rare. The fine grained clastic rocks in each section include 10-60% felsic to mafic volcanic component (see Fig. 3). Volcanic rocks within the unit include pillowed basalt or andesite, vesicular basalt or andesite, heterolithic and monolithic breccia, tuff, rhyolite breccia and flows, and medium- to coarse-grained volcaniclastic rocks. Many volcanic intervals vary in thickness laterally, and are intercalated with the fine grained clastic rocks.

Laminated, varicoloured, siliceous siltstone constitutes a regionally distinctive lithology. It is formally called Quock Formation of the Spatsizi Group in Spatsizi map area (Thomson et al., 1986), but is more commonly known as the 'pyjama beds' throughout the region. This lithology also comprises the Troy Ridge facies of the Salmon River Formation in Iskut map area (Anderson and Thorkelson, 1990), and is inferred to represent distal turbidites. The term 'pyjama beds' refers to a specific lithology, and is used instead of formalized terms in Telegraph Creek area because it occurs at more than one stratigraphic level, and is a minor component of unit 14. An exception is the Esja Peak section, which has at least 150 m of the siliceous siltstone. The Todagin Mountain section has a large proportion of pyjama beds, but it is much thinner than both the Esja Peak section, and the type section of Spatsizi Group to the east.

Basal contact of unit 14

The part of the Hazelton Group that is dominantly clastic has both gradational and abrupt contacts with underlying dominantly volcanic strata. In the section east of Hankin Peak, the clastic rocks overlie intermediate volcanic rock of Pliensbachian age (Souther, 1972). In the Esja Peak section, siliceous siltstone grades down into well layered volcaniclastics interbedded with mafic volcanic rock. Clastic rocks are intercalated with volcanic rocks in the lower part of the 180 Lake section. On Todagin Mountain, pyjama beds are 10 m above a section of volcanic and volcaniclastic strata, which has up to 10% fine grained, dark clastic rock. In this case the contact is relatively abrupt, and the section (unit 14 or Spatsizi Group) is entirely clastic.

Upper contact of unit 14

The only exposed contact between units 14 and 15 is east of 180 Lake. There, unit 15 appears to be in the hanging wall of a fault that truncates tightly folded unit 14 in the footwall. Although the contact appears to be a fault, it need not represent great stratigraphic offset. Interpretation of this contact is critical to the stratigraphy. Souther (1972) considered that unit 15 was Bajocian based on his interpretation of a stratigraphic contact with unit 14 (which is known to be Bajocian). If, however, the contact is a fault, the relative stratigraphic position and age of unit 15 is open to question. It is possible that unit 15 is a volcanic facies of unit 14. In support of this possibility, pillow basalt in Ball Creek (near its confluence with Iskut River valley) is intercalated with sedimentary rocks which are overlain by an entirely clastic section (of unit 14), and then by Bowser Lake Group.

More doubt is cast on the stratigraphic position of unit 15 by uncertainty in the nature of its contact with the Bowser Lake Group west of Kinaskan Lake. Furthermore, Pliensbachian fossils (H.W. Tipper, pers. comm., 1990) near the top of the dominantly volcanic succession east of Kinaskan Lake clearly indicate that rocks stratigraphically correlated with unit 15, and along trend with unit 15, are older than unit 14. A stratigraphic contact between the volcanic succession and the clastic succession (unit 14 in Telegraph area, Spatsizi Group in Spatsizi area) can be traced from Todagin Creek in west Telegraph Creek area, east to the east slopes of Todagin Mountain. There, pyjama beds are overlain by 3 m of fine- and medium-grained sandstone, then by siltstone and chert-pebble conglomerate assigned to the Bowser Lake Group (Evenchick and Green, 1990). Although there are stratigraphic contacts between volcanic rocks, a clastic section (Spatsizi Group), and the Bowser Lake Group east of Kinaskan Lake, the same cannot be said west of Kinaskan Lake. If unit 14 is present it is thin and covered by overburden. Alternatively, it may have been removed from the present erosion level by a fault between the Bowser Lake Group and volcanics.

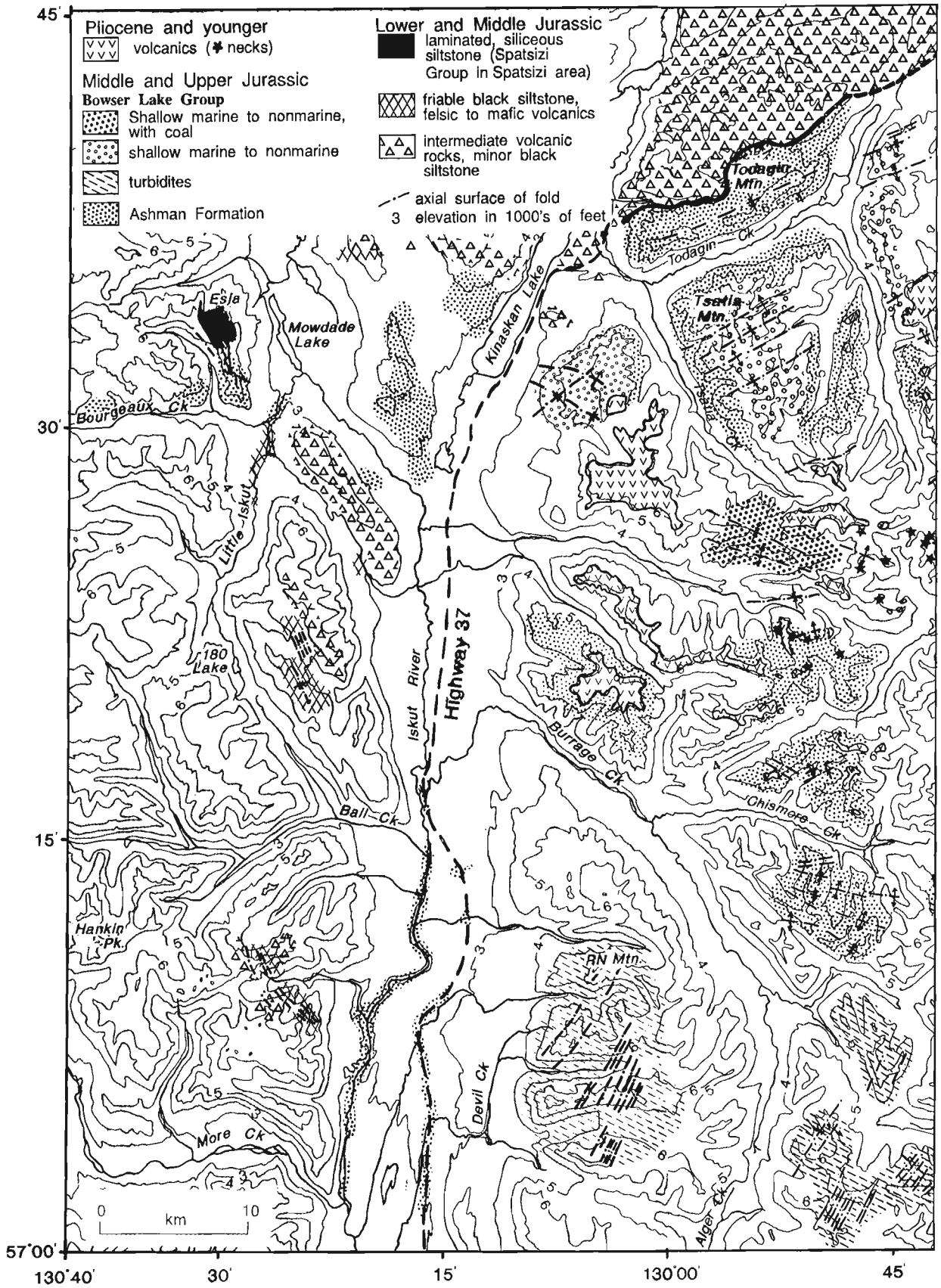

Figure 2. Geology of east Telegraph Creek and west Spatsizi map areas. The map has the same scale and legend as the map of west Spatsizi area presented in Evenchick and Green (Fig. 2; 1990).

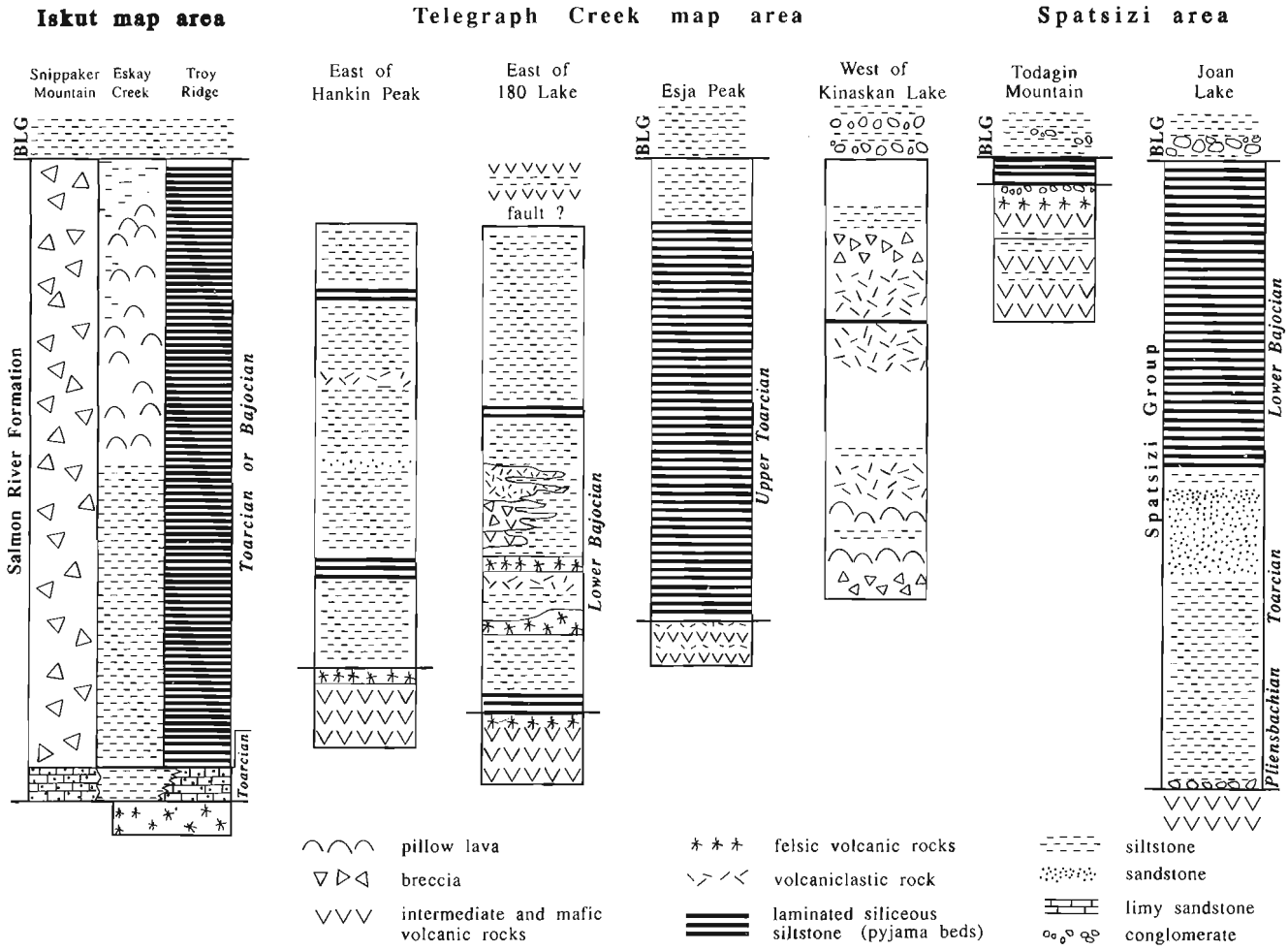

Figure 3. Schematic sections of the regions examined in Telegraph Creek map area. Included are simplified sections of Lower and lower Middle Jurassic strata in Iskut map area (modified after Anderson and Thorkelson, 1990), and the Spatsizi Group in Spatsizi map area (modified after Thomson et al., 1986). BLG - Bowser Lake Group.

The nature of the upper contact of unit 14 where unit 15 is absent is also equivocal. At Hankin Peak, the northeast contact of unit 14 is probably a stratigraphic contact with underlying volcanics, as shown by Souther (1972). However, with the exception of minor folds, the entire clastic section dips to the southwest rather than close in a syncline as shown by Souther (1972). The southwest contact is likely a thrust or reverse fault, and the upper stratigraphic contact of unit 14 is therefore eroded. Esja Peak is another case where unit 15 is not present. Pyjama beds grade up into black siltstone which is at the present erosion surface. In another exposure, black siltstone grades up into sandstone typical of the Bowser Lake Group. The contact between siltstone above the pyjama beds and Bowser Lake Group is probably gradational, but no complete section was observed.

Age of unit 14

Ages for diagnostic macrofossils in unit 14 are shown on Figure 3. A Late Toarcian age is reported for the three fossil localities in unit 14 (pyjama beds) on Esja Peak. An Early Bajocian age is indicated for the 180 Lake section by Souther (1972), and was confirmed with additional collections by H.W. Tipper (pers. comm., 1990). No diagnostic fossils are reported from the section east of Hankin Peak, or the volcanic and clastic section west of Kinaskan Lake, although Pliensbachian fossils were collected from the dominantly volcanic section east of Kinaskan Lake (H.W. Tipper, pers. comm., 1990).

Discussion of Lower and Middle Jurassic strata in Telegraph Creek, Iskut, and Spatsizi map areas

In Spatsizi map area, 730 m of siltstone, conglomerate, and shale which overlie felsic units of the Cold Fish volcanics (part of the Hazelton Group) and underlie Bowser Lake Group were formally defined as Spatsizi Group (Thomson et al., 1986). In contrast with contemporaneous strata in Telegraph Creek map area, the Spatsizi Group generally lacks volcanic rock, but has a persistently mappable interval of pyjama beds (Quock Formation). The pyjama beds are Early Bajocian in age, whereas those on Esja Peak are of Late Toarcian age.

Upper Lower to lower Middle Jurassic strata in Iskut area are called the Salmon River Formation (Alldrick and Britton, 1988; Alldrick et al., 1989; Anderson and

Thorkelson, 1990). Anderson and Thorkelson (1990) excluded Bowser Lake Group strata from the Salmon River Formation. This more restricted usage is followed here. Three facies of the formation overlie a regionally mappable rhyolitic unit called the Mt. Dilworth formation (Fig. 3). The eastern facies (Troy Ridge) is dominantly pyjama beds. A central facies (Eskay Creek) contains shale and siliceous shale with minor limy shale, capped by pillow lava. The western facies (Snippaker Mountain) consists of limy sandstone and conglomerate overlain by andesite lava and breccia. Although these facies are not directly correlative with unit 14, the fine grained clastic rocks (and local intercalations of pillowed lavas) which are typical of the Telegraph Creek sections compare best with the dominantly clastic Eskay Creek facies. Felsic to mafic volcanic rocks within the Hankin Peak and 180 Lake sections illustrate aspects of the Snippaker Mountain facies.

BOWSER LAKE GROUP

Stratigraphy

The Bowser Lake Group was examined in east Telegraph Creek and southwest Spatsizi areas (Fig. 2). The units on Figure 2 are not conventional rock-stratigraphic units, but represent units of common lithology, sequences, sedimentary structures, and fossil assemblages. Description of these units, and their association with units defined to the east (Cookenboo and Bustin, 1989) are outlined by Evenchick and Green (1990). The only conventional stratigraphic unit is the Ashman Formation. It is composed of black siltstone and fine grained sandstone with minor to large proportions of chert pebble conglomerate, and can also be divided into a number of facies (eg. Evenchick and Green, 1990; Ricketts, 1990), but is undivided on Figure 2.

Regions underlain by Bowser Lake Group are described briefly below, from north to south. Southwest of Tsatia Mountain is one of the few areas where facies changes can be observed. East facing cirques reveal shallow marine rusty conglomerate interfingering with Ashman Formation containing lenses of grey conglomerate (see Ricketts and Evenchick, 1991).

The region north of Burrage Creek is dominated by black siltstone, and fine grained sandstone with numerous soft sedimentary folds and faults. This may be the slope facies of the Ashman Formation.

Mid-fan turbidites similar to those described in southwest Spatsizi area (Evenchick and Green, 1990) extend westward to RN Mountain and farther south in Telegraph Creek map area. In southeast Telegraph Creek area at least 1500 m of turbidites are present.

Western outcrops of Bowser Lake Group were examined at several places, from Bourgeaux Creek to the south boundary of Spatsizi map area. In all cases, the exposures are Ashman Formation. They have the same marine character as the Ashman Formation in Spatsizi area, and a western depositional margin is not evident. Outcrops in Iskut River canyon are also Ashman Formation, in this case with little or no conglomerate. Farther west, roadcuts on Highway 37 expose turbidites with minor conglomerate. North of Bourgeaux Creek is conglomerate, siltstone and sandstone of the Ashman Formation. In the large region between Kinaskan Lake and Mowdade Lake conglomerate forms resistant ribs, but large recessive intervals are covered. This area is assumed to be underlain by Ashman Formation because of the high proportion of grey weathering conglomerate.

STRUCTURAL GEOLOGY NOTES

Compilations of axial surfaces of folds and stereonets of poles to bedding are shown in Figures 2 and 4 respectively. Southeast of Kinaskan Lake, large-scale interference of folds has resulted in a basinal structure 3 km across, and the dispersion of poles to bedding away from a great circle (Fig. 4). Interference of folds has probably also resulted in the irregular contact between the Bowser Lake Group and older strata in west Spatsizi and east Telegraph Creek areas.

The folds in southeast Telegraph Creek, combined with those in southwest Spatsizi area (Fig. 4) delineate a large region of northeast- to north-northeast-trending folds that appear to end abruptly at Burrage Creek. To the north, northwest-trending folds dominate. Resolution of the significance and origin of different fold trends is part of an ongoing analysis of the Skeena Fold Belt.

Pre-Bowser strata were clearly affected by the same intense shortening that affected the Bowser Lake Group. Unit 14 forms large-scale southwest-verging chevron folds east of 180 Lake, and upright, open to tight northeast-verging folds east of Hankin Peak. In this region tight folds and faults are also well exposed in the volcanic rocks southwest of unit 14.

DISCUSSION AND SUMMARY

The fine grained Lower to Middle Jurassic clastic unit in Telegraph Creek map area varies in proportion of intercalated volcanics, nature of basal contact, and lithology. It does not directly compare with coeval strata to the east and south. Although it is most similar to the Eskay Creek facies of the Salmon River Formation in Iskut map area, it also has elements of the Snippaker Mountain facies. In addition, the Esja Peak section is remarkably similar to the Troy Ridge facies.

The three facies of the Salmon River Formation form north-trending belts (Anderson and Thorkelson, 1990). The Troy Ridge facies is easternmost, the Eskay Creek facies central, and the Snippaker Mountain facies westernmost. The general similarity between strata in Telegraph Creek and the Eskay Creek facies, and of Spatsizi Group with Troy Ridge facies illustrate a gross similarity in the distribution of belts between the Iskut area and regions to the north. However, the facies in Telegraph Creek are clearly not distributed in belts in a simple fashion. For example, the Esja Peak section is typical of the Troy Ridge facies, but is the westernmost of the sections.

The term Spatsizi Group is meant to apply to clastic rocks between the Hazelton Group volcanics and Bowser Lake Group (Thomson et al., 1986). There is an obvious problem

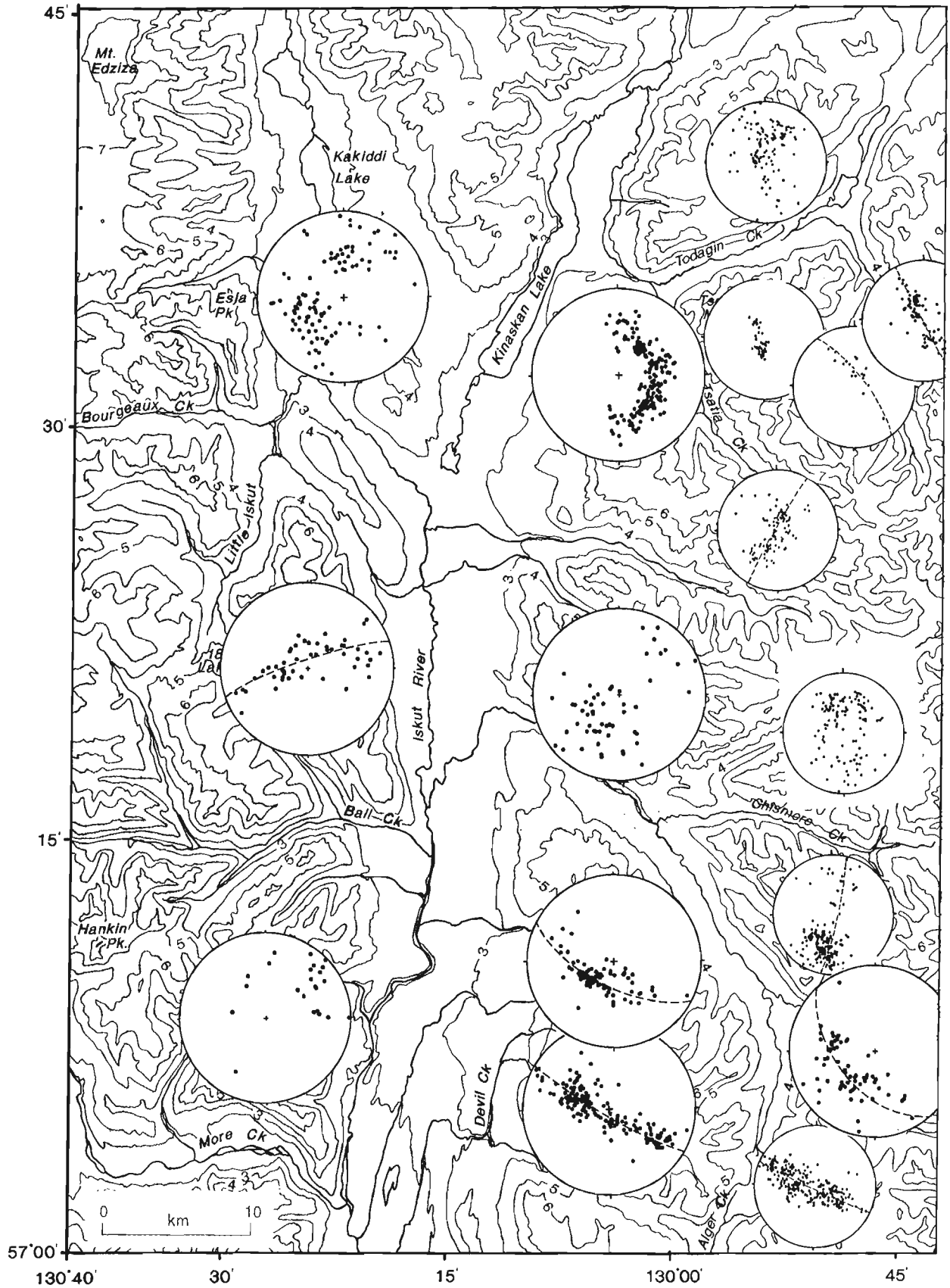

Figure 4. Equal angle projections of poles to bedding in east Telegraph Creek and west Spatsizi map area. Large stereonets are from the 1990 season, small stereonets are from the 1989 field season (Evenchick and Green, 1990).

in applying this terminology to sections with intercalated volcanic and sedimentary rocks, particularly when the volcanic rocks are thick, and their association with a clastic section is unclear. The relationships between different sections of pre-Bowser Lake Group strata along the west side of the Bowser Basin is an intriguing stratigraphic problem that requires more detailed study, and increased biostratigraphic control to resolve.

Bowser Lake Group in Telegraph Creek area is entirely marine, and units are continuous with those mapped in Spatsizi area. The westernmost outcrops are Ashman Formation, and do not reflect proximity to a western depositional margin.

ACKNOWLEDGMENTS

I appreciate the fine assistance in the field by Andrew Kaip and Michael Toolin. Mike Jones and his staff at Tatogga Lake Resort helped in aspects of base camp operation. Once again, the co-operation and professional effort of Brian McCarthy of Canadian Helicopters Inc. was a substantial factor in the success of the field program. I appreciate the helpful comments of Charlie Roots as reviewer of the manuscript.

REFERENCES

Alldrick, D.J. and Britton, J.M.
1988: Geology and mineral deposits of the Sulphurets area (NTS 104 A/5, 104 A/12, 104 B/8, and 104 B/9); British Columbia Geological Survey Branch, Open File Map 1988-4.

Alldrick, D.J., Britton, J.M., Webster, I.C.L., and Russell, C.W.P.
1989: Geology and mineral deposits of the Unuk area; British Columbia Geological Survey Branch, Open File Map 1989-10.

Anderson, R.G. and Thorkelson, D.J.
1990: Mesozoic stratigraphy and setting for some mineral deposits in Iskut River map area, northwestern British Columbia; in Current Research, Part E, Geological Survey of Canada, Paper 90-1E, p. 131-139.

Cookenboo, H.O. and Bustin, R.M.
1989: Jura-Cretaceous (Oxfordian to Cenomanian) stratigraphy of the north-central Bowser Basin, northern British Columbia; Canadian Journal of Earth Sciences, v. 26, p. 1001-1012.

Evenchick, C.A.
1986: Structural style of the northeast margin of the Bowser Basin, Spatsizi map area, north-central British Columbia; in Current Research, Part B, Geological Survey of Canada, Paper 86-1B, p. 733- 739.
1987: Stratigraphy and structure of the northeast margin of the Bowser Basin, Spatsizi map area, north- central British Columbia; in Current Research, Part A, Geological Survey of Canada, Paper 87-1A, p. 719- 726.
1988: Structural style and stratigraphy in northeast Bowser and Sustut basins, north-central British Columbia; in Current Research, Part E, Geological Survey of Canada, Paper 88-1E, p. 91-95.
1989: Stratigraphy and structure in east Spatsizi map area, north-central British Columbia; in Current Research, Part E, Geological Survey of Canada, Paper 89-1E, p. 133-138.
in press: Geometry, evolution, and tectonic framework of the Skeena Fold Belt, north-central British Columbia; Tectonics.

Evenchick, C.A. and Green, G.M.
1990: Structural style and stratigraphy of southwest Spatsizi map area, British Columbia; in Current Research, Part F, Geological Survey of Canada, Paper 90-1F, p. 135-144.

Gabrielse, H. and Tipper, H.W.
1984: Bedrock geology of Spatsizi map area (104H); Geological Survey of Canada, Open File 1005.

Green, G.M.
1991: Detailed sedimentology of the Bowser Lake Group, northern Bowser Basin, British Columbia; in Current Research, Part A, Geological Survey of Canada, Paper 91-1A.

Greig, C.J.
1991: Stratigraphic and structural relations along the west-central margin of the Bowser Basin, Oweegee and Kinskuch areas, northwestern British Columbia; in Current Research, Part A, Geological Survey of Canada, Paper 91-1A.

Grove, E.W.
1986: Geology and mineral deposits of the Unuk River- Salmon River-Anyox area; British Columbia Ministry of Energy, Mines and Petroleum Resources, Bulletin 63, 434 p.

MacLeod, S. and Hills, L.V.
1990: Sedimentology and paleontology of Late Jurassic (Oxfordian) to Early Cretaceous (Aptian) strata, northern Bowser Basin; Canadian Journal of Earth Sciences, v. 27, p. 988-998.

Mining Review staff
1990: On the gold trail; Mining Review, v. 10, p. 4-7.

Poulton, T.P., Callomon, J.H., and Hall, R.L.
1991: Bathonian through Oxfordian (Middle and Upper Jurassic) marine macrofossil assemblages and correlations, Bowser Lake Group, west-central Spatsizi map area, northwestern British Columbia; in Current Research, Part A, Geological Survey of Canada, Paper 91-1A.

Ricketts, B.D.
1990: A preliminary account of sedimentation in the lower Bowser Lake Group, northern British Columbia; in Current Research, Part F, Geological Survey of Canada, Paper 90-1F, p. 145-150.

Ricketts, B.D. and Evenchick, C.A.
1991: Analysis of the Middle to Upper Jurassic Bowser Basin, northern British Columbia; in Current Research, Part A, Geological Survey of Canada, Paper 91-1A.

Souther, J.G.
1972: Telegraph Creek map-area, British Columbia; Geological Survey of Canada, Paper 71-44.

Thomson, R.C., Smith, P.L., and Tipper, H.W.
1986: Lower to Middle Jurassic (Pliensbachian to Bajocian) stratigraphy of the northern Spatsizi area, north- central British Columbia; Canadian Journal of Earth Sciences, v. 23, p. 1963-1973.

Tipper, H.W. and Richards, T.A.
1976: Jurassic stratigraphy and history of north-central British Columbia; Geological Survey of Canada, Bulletin 270, 73 p.

Structure and stratigraphy of the northern Porcupine Creek Anticlinorium, western Main Ranges between the Sullivan and Wood rivers, British Columbia[1]

W.H. Lickorish[2] and P.S. Simony[2]
Cordilleran Division, Vancouver

Lickorish, W.H. and Simony, P.S., Structure and stratigraphy of the northern Porcupine Creek Anticlinorium, western Main Ranges between the Sullivan and Wood rivers, British Columbia; in Current Research, Part A, Geological Survey of Canada, Paper 91-1A, p. 163-169, 1991.

Abstract

A distinct lithostratigraphic unit has been recognized between the Upper Proterozoic Miette Group and the Lower Cambrian Gog Group. It consists of a sequence of coarse, quartzofeldspathic, crossbedded, sandstones and conglomerates with thin interbedded slates. The thickness of the unit varies from a few metres or absent altogether to more than 700 m and such changes in thickness can take place over a distance of less than 2 km. A small thickness of upper Miette slates was identified in the northern part of the study area but was absent in the south, demonstrating the unconformable nature of the top of the Miette Group. Structurally the study area is dominated by the Porcupine Creek Anticlinorium which is composed of large upright folds, although an early phase of east-verging folds and thrusts is exposed in the core. The late phase Chatter Creek Thrust is shown to have only small displacements.

Résumé

Une unité lithostratigraphique distincte a été relevée entre le groupe de Miette du Protérozoïque supérieur et le groupe de Gog du Cambrien inférieur. Elle est composée d'une séquence de grès et de conglomérat grossier, quartzofeldspathique et à stratification oblique au sein de laquelle on remarque la présence de minces interstratifications d'ardoise. L'épaisseur de l'unité passe de quelques mètres ou de nul à plus de 700 m, et ces différences d'épaisseur peuvent s'étaler sur une distance de moins de 2 km. On a relevé une petite couche d'ardoise de la partie supérieure du groupe de Miette dans le nord de la zone à l'étude mais aucune dans le sud, témoignant ainsi de la nature discordante du sommet du groupe de Miette. Du point de vue structural, la zone à l'étude est dominée par la présence de l'anticlinorium de Porcupine Creek qui se compose de grands plis droits, bien qu'une phase précoce de plis à vergence est et de chevauchements se distingue dans le noyau. Le chevauchement de Chatter Creek de phase tardive n'accuse que de faibles déplacements.

[1] EMR Research Agreement 90-4-67
[2] Department of Geology and Geophysics, University of Calgary, Calgary, Alberta T2N 1N4

INTRODUCTION

Field work done in 1989 and 1990 has helped to refine stratigraphy of Lower Cambrian and Upper Proterozoic rocks of the Gog and Miette groups, and to establish structural control on the formation of the Porcupine Creek Anticlinorium (PCA). The area studied consists of about 700 km^2 of the Western Main Ranges about half way between Golden and Valemount on the eastern side of the Southern Rocky Mountain Trench (SRMT) between the Sullivan and Wood rivers (Fig. 1). This area lies on the boundaries of the following 1:250 000 map sheets: Rogers Pass 82N-W1/2 (Wheeler, 1963); Big Bend 82M-E1/2 (Wheeler, 1965) and Canoe River 83D (Campbell, 1968).

REGIONAL GEOLOGY

The Western Main Ranges of the Rocky Mountains lie directly east of the Southern Rocky Mountain Trench at this latitude, the overturned west-facing package of the Western Ranges being absent. They are separated on the west from the metamorphic rocks of the Selkirk and Monashee mountains by the Purcell and Chancellor faults in the Southern Rocky Mountain Trench; and bounded on the east by the structurally competent rocks of the lower Paleozoic carbonate facies. The rocks of the Western Main Ranges consist of the lower Paleozoic and Upper Proterozoic sedimentary strata of the western North American miogeoclinal wedge. The Upper Proterozoic Miette Group is divided into the upper, middle and lower Miette (Mountjoy, 1962). It is unconformably overlain by the Gog Group which rests on up to 2 km of upper Miette in the Jasper area (Charlesworth et al., 1967) and in the Cushing Creek area (Carey and Simony, 1985), and overlies the middle part of the middle Miette at Lake Louise (Aitken, 1969). Although hard to detect locally the contact is therefore regionally a major unconformity.

The Porcupine Creek Anticlinorium is a large, somewhat conical, gently southeast plunging fold structure. At the latitude of the Blaeberry River (51°30'N) it rests above a detachment that overlies the Lower Cambrian Gog Group (Balkwill, 1972) with very little involvement of the Gog Group itself (Gardner, 1977). North of the Bush River (51°45'N) rocks of the Gog Group and below are included in the core of the Porcupine Creek Anticlinorium (Meilliez, 1972; Ferri, 1984). Between the Bush and Sullivan rivers it has been demonstrated that the detachment that separates Chancellor Group from Gog strata cuts down to involve the Gog Group on the west (Gal et al., 1989; Gal, 1990). The rocks of the Upper Proterozoic Miette Group in the Selwyn Range to the north clearly show at least two phases of deformation (Mountjoy et al., 1985). However between the Bush River and Tsar Creek only one major phase was identified in Proterozoic and Lower Cambrian strata, whereas two distinct phases were identified in strata that overlie the major sub-Chancellor detachment. The Ptarmigan and Selwyn Range Detachment proposed in the Hugh Allan Creek area (Dechesne and Mountjoy, in press) could be the detachment zone on which the Porcupine Creek Anticlinorium is carried. On the eastern edge of the Porcupine Creek Anticlinorium the out-of-sequence Chatter Creek Thrust places the anticlinorium against the carbonate platform facies of the Eastern Main Ranges.

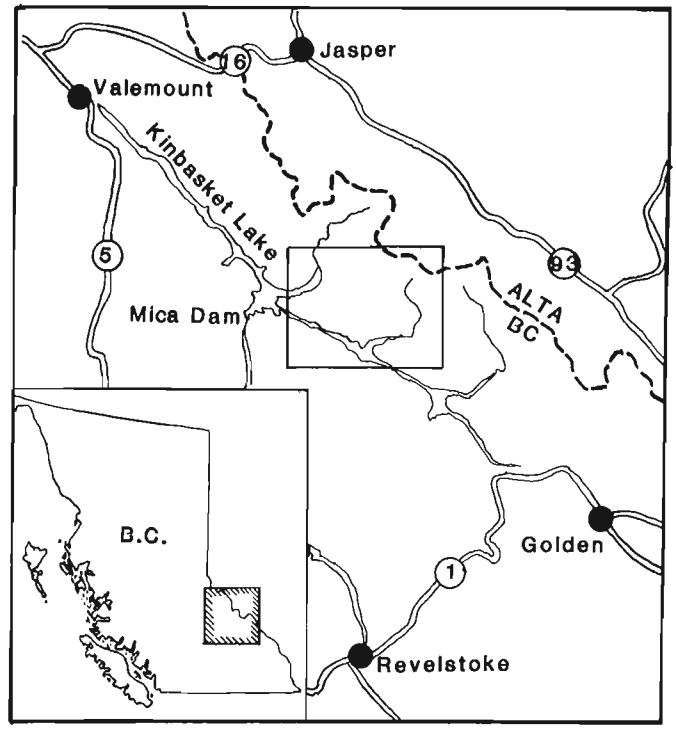

Figure 1. Location of study area in British Columbia and within the Valemount-Golden area.

STRATIGRAPHY

The oldest rocks in the study area are middle Miette forming a sequence of just over 1 km in thickness of slates and grits exposed in the core of the Porcupine Creek Anticlinorium (Fig. 2). There, on "Cummins Ridge" and southwest of Mount Shackleton in the immediate hanging wall of the Chatter Creek Thrust, is a characteristic sequence of green slate, carbonate rhythmite and black slate that is probably correlative with the Old Fort Point marker horizon found elsewhere in the middle of the middle Miette grits (Ross and Murphy, 1988). On "Cummins Ridge" the marker is underlain by some 50 m of grit. The thickness of upper Miette probably increases northward. Gal (1990) documented an absence of upper Miette in the Solitude Range where the Lower Cambrian McNaughton Formation lies directly on 400 m of middle Miette grits. Whereas along "Cummins Ridge" just south of the Wood River there is probably a maximum of 500 m of upper Miette slates. Two 15 m beds of grit and calcareous conglomerate in a carbonate matrix appear within the upper Miette and are capped by a limestone bed from 2-5 m thick, which possibly continues southward to the ridges by Tsar Creek, where it is represented by a brown weathering calcareous slate.

Above the slates of the Miette Group and beneath the white quartzite marker of the base of the McNaughton Formation is a sequence of crossbedded quartzofeldspathic grits and conglomerates with thin slate partings. The grits can be distinguished from the Miette grits by being much more quartzose and lacking plagioclase feldspar. These strata were first mapped by Fyles (1960) who referred to them as the Sullivan quartzite in which he also included all of the Gog Group; at Jasper a similar unit was observed in the same

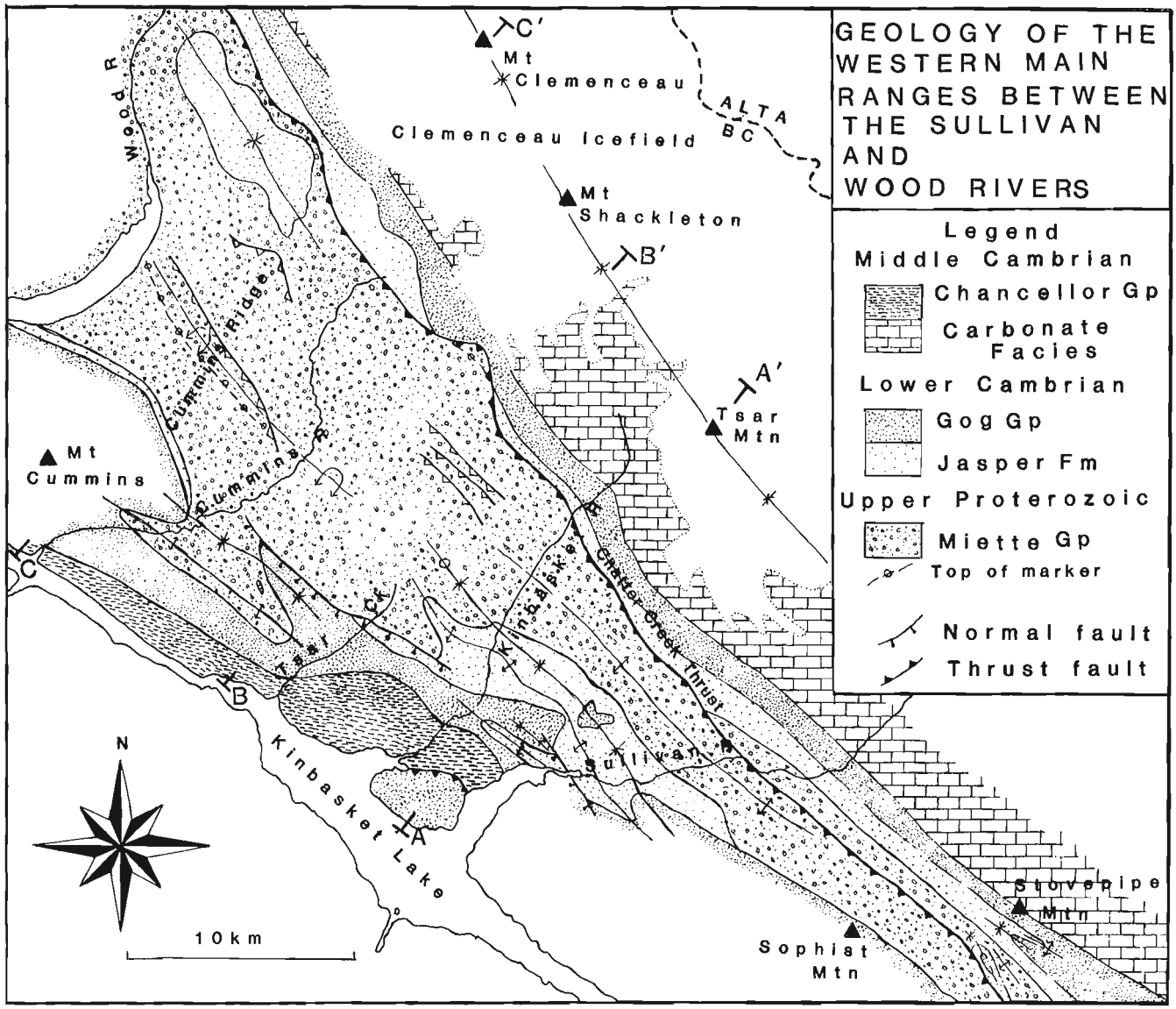

Figure 2. Simplified geological map of the area between the Sullivan and Wood rivers. Kinbasket Lake occupies the Rocky Mountain Trench. The strip of Miette Group marks the core of the Porcupine Creek Anticlinorium.

stratigraphic position: between the Miette and Gog groups (Charlesworth et al., 1967) and was referred to as the Jasper Formation. Recently Bond et al. (1985) described what is probably the same sequence in parts of the Eastern Main Ranges and they included it with the McNaughton Formation.

In the study area this sequence consists of quartzofeldspathic grit and conglomerate beds fining upwards with planar crossbedding ranging in thickness from 20-150 cm. These beds are generally separated by thin beds of slate from 1-10 cm thick. Locally channel-like structures consisting of trough crossbedded quartzite scour the lower beds. The base of the unit contains interbedded grits and slates not too dissimilar from the Miette Group except for the increased quartzose nature of the grits, which then grade rapidly upward into the main succession. Also, near the base, two or three calcareous layers up to 2 m thick are traceable for several kilometres. Near the top of the unit thicker slate beds up to 3 m thick start to reappear, commonly with a black or dark purple colour. Also appearing in the top part of the unit are thin, well-rounded and sorted conglomerates, with pebbles up to 5 cm in size, in beds up to 10 cm thick. A carbonate bed 3-4 m thick occurs near the top of the sequence northeast of the Wood River. The thickness of the unit varies considerably (Fig. 3). In an area south of the Sullivan River over 700 m of strata disappear southeastward in less than 2 km. Considering the absence of thrust repetition of the stratigraphy, such rapid thickness changes suggest tectonic control of the sedimentation. Both the top and the base of this unit may be unconformable.

Three formations of the Lower Cambrian Gog Group were recognized (Mountjoy, 1962). The lowest formation in the Gog Group is the McNaughton which displays a prominent tripartite division. At its base is a distinctive almost pure quartzite band about 100 m thick. Above this is approximately another 100 m of quartzite, but considerably less clean, and with interbedded shale beds. The upper McNaughton has

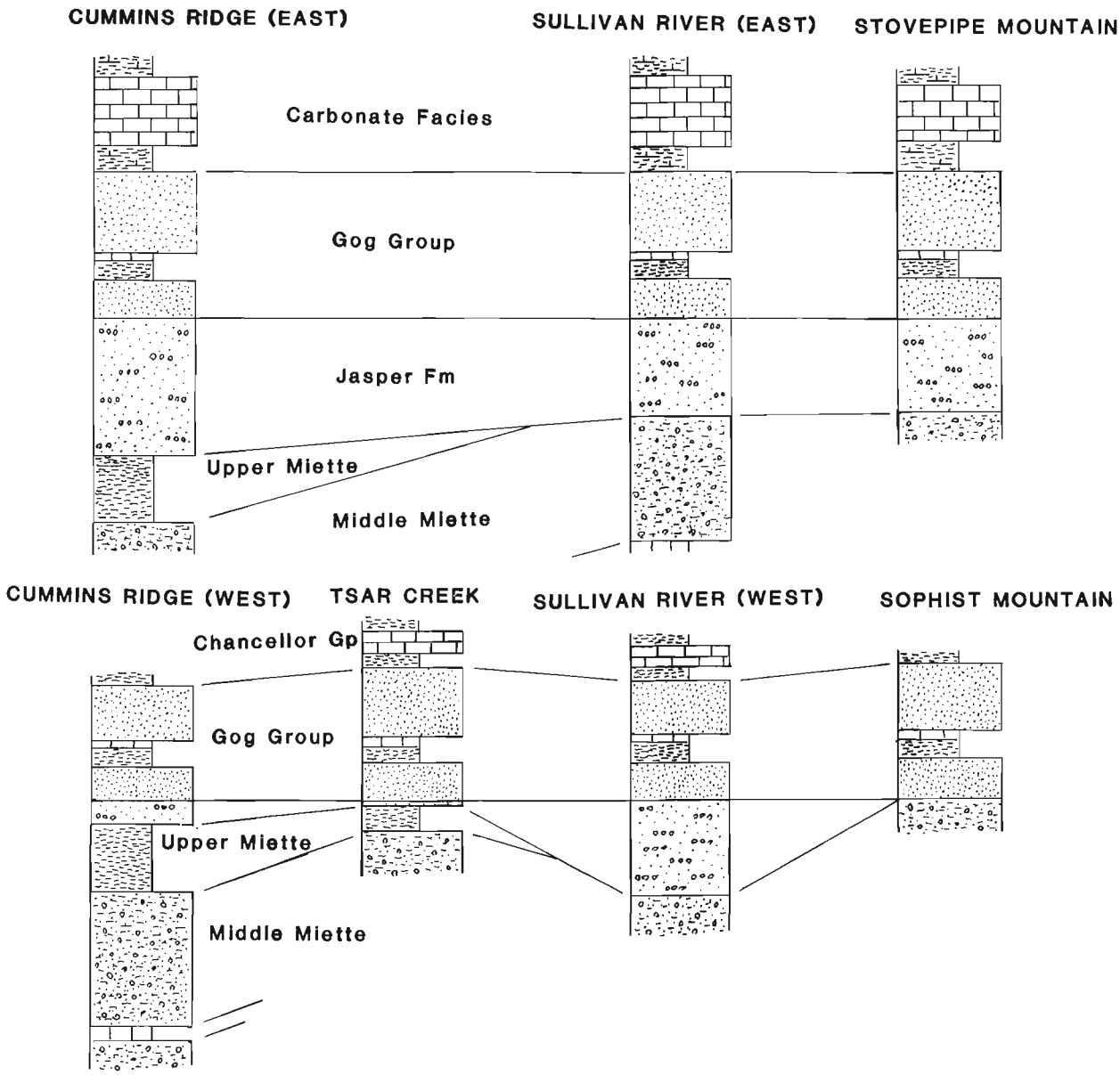

Figure 3. Stratigraphic cross-sections along the northeast and southwest flanks of the Porcupine Creek Anticlinorium illustrating the relations of the "Jasper" Formation and upper Miette to the unconformity at the base of the Gog Group.

clean quartzite beds interbedded with thin shales. Towards the top minor calcareous beds are usually present, and bioturbation becomes significant.

In the middle of the Gog Group is the Mural Formation, which is about 170 m of slightly calcareous and usually green shales and slates. At the base of the Mural a limestone band is locally developed varying from 0-10 m in thickness. Characteristically in the middle of the Mural Formation is a band of bioturbated quartzites from 20-50 m thick, and at the top is another 15-20 m of limestone.

The highest, Mahto Formation, consists of about 660 m of quartzites, with a general increasing shale content upwards, and minor carbonate beds, up to 1 m thick, in the topmost 50 m. Trace fossils are common throughout the Mahto including burrows (e.g. *Skolithus*) and feeding traces.

The stratigraphically highest rocks exposed in the area are Middle Cambrian in age. They are divided into an eastern carbonate facies and a western shale facies. The western facies is divided into the Tsar Creek and Kinbasket units (Fyles, 1960). The Tsar Creek is a dark grey pelitic unit and underlies the pale grey micritic limestones of the Kinbasket unit. Due to intense structural thickening stratigraphic thicknesses are very hard to establish but Meilliez (1972) estimated approximately 100 m for the Tsar Creek and 150 m for the Kinbasket. The eastern facies consists of a more competent package of carbonates, map unit 13 of Wheeler (1963), but divisible into the formations of Walcott (1908), the lowest being the Mount Whyte Formation comprising about 200 m of shaly micritic carbonates, above which is the Cathedral Formation, consisting of 400-500 m of limestone and dolomite. Also developed in the Cathedral, but not traceable over

large distances, are shale beds up to 50 m thick. The Cathedral is then followed by up to 300 m of recessive shaly limestones of the Stephen Formation, which in turn is overlain by the large cliff-forming limestones of the Eldon and Pika formations.

STRUCTURE

The Porcupine Creek Anticlinorium is the dominant structural feature in the area exposing Chancellor Group rocks on the western flank and the carbonate facies rocks to the east, with the Gog and Miette groups in the core (Fig. 4). An upright cleavage pervades the whole structure and is axial planar to the large scale folds that make up the anticlinorium.

The style of folding is influenced by the structural competence of the lithostratigraphic units, and probably also the grade of metamorphism. The incompetent high-grade rocks of the Chancellor Group form small tight folds, locally almost isoclinal. The more competent rocks of the Gog Group form the large folds that outline the main structure of the Porcupine Creek Anticlinorium. The relatively incompetent Mural Formation acts as a zone of disharmony in some structures between the more competent Mahto and McNaughton formations. On the eastern flank the rocks of the carbonate facies form a single structural package that is folded into a very large syncline; the more incompetent formations in this package only serve to take up bedding slip due to the folding.

In the northern part of the core of the Porcupine Creek Anticlinorium the rocks of the Miette Group also show an early cleavage generally dipping westward at about 30°, with the main upright cleavage being present as a crenulation. Occasionally associated with this early cleavage are small folds and thrust faults.

The rocks of the Chancellor Group on the western flank of the anticlinorium also have an earlier bedding-parallel cleavage, and many small refolded isoclines. With the exception of a small amount of the Mahto Formation (Gal, 1990) this deformation does not penetrate the Gog Group and is presumed to be due to a detachment horizon in the basal Tsar Creek unit (Meilliez, 1972). The formations of

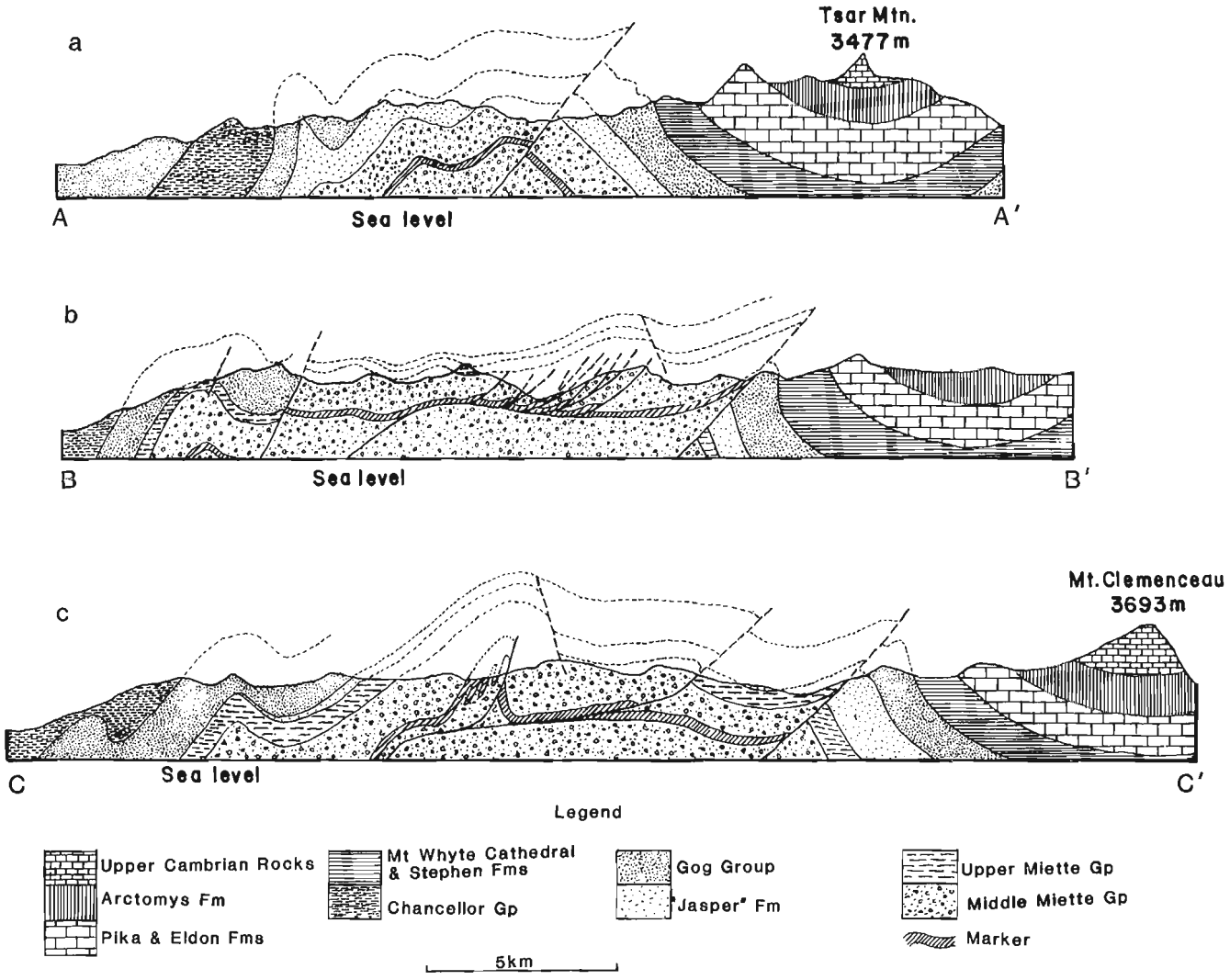

Figure 4. Three structural sections illustrating the structure of the Porcupine Creek Anticlinorium and the broad flanking syncline in the eastern carbonate facies belt. The lines of section are marked in Figure 3.

the eastern carbonate facies show no evidence of this early deformation, and so the detachment must end somewhere near the facies change, or cut very steeply upsection.

A later crenulation is faintly developed in many of the slates of the Gog and Miette groups. It lies transverse to the main structural strike of the area and is apparently associated with no larger scale structures in the study area.

The Chatter Creek Thrust runs along the eastern edge of the study area. It dips to the west at about 30° and has a small stratigraphic throw placing rocks of the Miette Group over the Gog Group. Maximum estimates of thrust displacement are only a few kilometres.

METAMORPHISM

Most of the rocks contain no metamorphic minerals other than white mica and chlorite. The metamorphic grade, however, increases to the west with the highest grade assemblage, containing staurolite, found on the shores of Kinbasket Lake in the Southern Rocky Mountain Trench. The garnet zone is also confined to the lower slopes of the trench. Biotite, although common in association with garnet, is rarely found by itself. Chloritoid, although distributed over a wide range is only developed in pelites of suitable composition such as the greenish pelites of the upper Miette slates.

SUMMARY

Beneath the prominent quartzite marker of the McNaughton Formation there is a distinctive sequence of quartzofeldspathic crossbedded grits and conglomerates. Although the sequence is locally absent altogether it attains thicknesses of up to 700 m with rapid changes of thickness. This kind of distribution may suggest filling of fault controlled basins possibly related to Late Proterozoic rifting.

A carbonate marker unit found elsewhere in Windermere stratigraphy in the middle of the thick grit sequence has been located in the core of the Porcupine Creek Anticlinorium providing control on the stratigraphic position of the Miette grits exposed in the study area. They belong to the upper division of the middle Miette. Although Gal (1990) found no upper Miette in the Sullivan River area, up to 500 m of this unit is preserved near the Wood River, and possibly 100 m near Tsar Creek suggesting that at the Sullivan River there is probably no more than 200 m of middle Miette missing beneath the sub-Cambrian unconformity.

The deformation of the strata overlying the Gog Group above a detachment at the base of the Middle Cambrian rocks is an important structural element of the western PCA. This detachment is not evident in the eastern carbonate facies, and motion on it must be lost near the facies change. Activation of a lower detachment produced an early deformation in the Miette Group at a deep structural level. Structures associated with this deformation are not seen everywhere, and are particularly absent immediately beneath the competent Gog Group, which is itself never affected. The growth of the large scale structures which constitute the Porcupine Creek Anticlinorium must be associated with the activation of a yet lower detachment, well below sea-level in the study area. The whole structure was later cut by the out-of-sequence Chatter Creek Thrust.

ACKNOWLEDGMENTS

Valuable support was provided by Don McTighe and Rob Graham of Canadian Helicopters in Golden. Rich Hannah and Brent McNiven provided assistance in the field. Financial Support came from EMR Research Agreement 90-4-67 to P. Simony.

REFERENCES

Aitken, J.D.
1969: Documentation of the sub-Cambrian unconformity, Rocky Mountains Main Ranges, Alberta; Canadian Journal of Earth Sciences, v. 6, p. 193-200.

Balkwill, H.R.
1972: Structural geology, lower Kicking Horse River region, Rocky Mountains, British Columbia; Bulletin of Canadian Petroleum Geology, v. 20, p. 608-633.

Bond, G.C., Christie-Blick, N., Kominz, M.A., and Devlin, W.J.
1985: An early Cambrian rift to post-rift transition in the Cordillera of western North America; Nature, v. 315, p. 742-746.

Campbell, R.B.
1968: Canoe River (83D), British Columbia; Geological Survey of Canada, Map 15-1967, scale 1:250 000 (Part of GSC Open File 290).

Carey, J.A. and Simony, P.S.
1985: Stratigraphy, sedimentology and structure of the late Proterozoic Miette Group, Cushing Creek area, British Columbia; Bulletin of Canadian Petroleum Geology, v. 33, p. 184-203.

Charlesworth, H.A.K., Weiner, J.L., Akehurst, A.J., Bielenstein, H.U., Evans, C.R., Griffiths, R.E., Remington, D.B., Stauffer, M.R., and Steiner, J.
1967: Precambrian geology of the Jasper region, Alberta; Research Council of Alberta, Bulletin 23, 74 p.

Dechesne, R.G. and Mountjoy, E.W.
in press: Multiple décollements at deep levels of the southern Canadian Rocky Mountain Main Ranges, Alberta and British Columbia; in Structural Geology of Fold and Thrust Belts, S. Mitra, (ed.), Dave Elliott Volume, John Hopkins University Press.

Ferri, F.
1984: Structure of the Blackwater Range, British Columbia; unpublished M.Sc. thesis, University of Calgary, Alberta, 143 p.

Fyles, J.T.
1960: Geological reconnaissance of the Columbia River between Bluewater Creek and Mica Creek, British Columbia; British Columbia Minister of Mines, Annual Report, 1959, p. 90-105.

Gal, L.P.
1990: Metamorphic and structural geology of the northern Solitude Range, Western Rocky Mountains, British Columbia; unpublished M.Sc. thesis, University of Calgary, Alberta, 282 p.

Gal, L.P., Ghent, E.D., and Simony, P.S.
1989: Geology of the Northern Solitude Range, Western Rocky Mountains, British Columbia; in Current Research, Part D, Geological Survey of Canada, Paper 89-1D, p. 55-60.

Gardner, D.A.C.
1977: Structural geology and metamorphism of calcareous lower Paleozoic slates, Blaeberry River - Redburn Creek area, near Golden, British Columbia; unpublished Ph.D. thesis, Queens University, Kingston, Ontario, 224 p.

Meilliez, F.
1972: Structure of the southern Solitude Range, British Columbia; unpublished M.Sc. thesis, University of Calgary, Alberta, 112 p.

Mountjoy, E.W.
1962: Mount Robson (southeast) map-area, Rocky Mountains of Alberta and British Columbia 83E/SE; Geological Survey of Canada, Paper 61-31, 114 p.

Mountjoy, E.W., Forest, R., and Leonard, R.
1985: Structure and stratigraphy of Miette Group, Selwyn Range, between Ptarmigan and Hugh Allan creeks, British Columbia - an antiformal stack of thrusts; in Current Research, Part A, Geological Survey of Canada, Paper 85-1A, p. 485-490.

Ross, G.M. and Murphy, D.C.
1988: Transgressive stratigraphy, anoxia, and regional correlations within the late Precambrian Windermere grit of the southern Canadian Cordillera; Geology, v. 16, p. 139-143.

Walcott, C.D.
1908: Nomenclature of some Cambrian Cordilleran formations; Smithsonian Miscellaneous Collection, v. 53, no. 1, p. 1-12.

Wheeler, J.O.
1963: Rogers Pass map-area, British Columbia and Alberta (82N W1/2); Geological Survey of Canada, Paper 62-32, 32 p.
1965: Big Bend map-area, British Columbia (82M E1/2); Geological Survey of Canada, Paper 64-32, 37 p.

Teslin map area, a new geological mapping project in southern Yukon

S.P. Gordey
Cordilleran Division, Vancouver

Gordey, S.P., Teslin map area, a new geological mapping project in southern Yukon; in Current Research, Part A, Geological Survey of Canada, Paper 91-1A, p. 171-178, 1991.

Abstract

The aim of this five-year project is to produce revised 1:250 000 and selected 1:50 000 maps and reports for the Teslin map area (105C) in order to understand the stratigraphic, structural and tectonic setting of the region's mineral resources. Preliminary study of selected areas within the Teslin region focused on: 1) structure and sedimentology of the Inklin assemblage, and relations and lithology of ultramafic bodies within it, 2) structure and sedimentology of the Lewes River assemblage and Cache Creek strata, 3) intensely deformed strata of the North American margin within the Thirtymile Range, and 4) a transect across southern Big Salmon Range, which exposes mylonitic plutonic and metasedimentary rocks in fault contact with Mesozoic(?) volcaniclastics.

Résumé

Ce projet quinquennal a comme objet la production de cartes révisées au 1:250 000 et de cartes choisies au 1:50 000 ainsi que de rapports pour la région cartographiée de Teslin (105C) permettant de comprendre le cadre stratigraphique, structural et tectonique des ressources minérales de la région. L'étude préliminaire de secteurs choisis de la région de Teslin a été concentrée sur : 1) la structure et la sédimentologie de l'assemblage d'Inklin ainsi que les relations entre les corps ultramafiques qu'il renferme et leur lithologie, 2) la structure et la sédimentologie de l'assemblage de Lewes River et des couches de Cache Creek, 3) les couches très déformées de la marge nord-américaine dans la chaîne Thirtymile et 4) un transect recoupant la partie méridionale de la chaîne Big Salmon et qui révèle l'existence de roches plutoniques et sédimentaires métamorphisées mylonitiques en contact avec des roches volcaniclastiques mésozoïques (?) à l'emplacement d'une faille.

INTRODUCTION

Fieldwork in 1990 comprised the first field season of a five-year project to map the geology of the Teslin area (NTS 105C; 60-61°N; 132-134°W) in southern Yukon (Fig. 1). The aim of this project is to produce a revised 1:250 000 scale map and reports as well as 1:50 000 scale maps of selected areas, in order to understand the regional stratigraphic, structural and tectonic context of the area's mineral resources. The fieldwork of Mulligan in the early 1950s (Mulligan, 1963) established a geological framework, but little geological work has been done since. Many map units and their relationships remain poorly understood and need critical re-examination in light of modern techniques and concepts in radiometric dating, paleontology, sedimentology and tectonics.

Four main areas were examined this season (Fig. 2) to provide a representative sampling of the geology and lay the groundwork for future field studies. Logistical help was provided to Rob Stevens (University of Alberta) who examined strongly mylonitized metamorphic rocks in the Big Salmon Range northwest of the Canol Road (Fig. 2) for a Ph.D. thesis (see Stevens, 1991).

REGIONAL SETTING

The Teslin map area is underlain by numerous terranes of the Intermontane and Omineca belts that originated in continental margin, oceanic, and island arc settings (see Wheeler et al., 1988) and which have undergone strikingly different structural and metamorphic modification during the Mesozoic. However, if viewed in a simplified fashion, the map area can be divided into three geological segments by a narrow fault-bounded panel trending diagonally northwest across the area (Fig. 2). To the southwest, upper Paleozoic greenstone, chert, and limestone of the Cache Creek Group is basement to varied volcanics and sediments. Northwest of the Alaska Highway its cover comprises Triassic(?) and Jurassic sediments and minor volcanics of the Inklin assemblage (Wheeler and McFeely, 1987) that are intruded by several ultramafic plutons. Southeast of the highway the overlying sediments are Triassic and(?) Jurassic chert and clastic rocks of the Lewes River assemblage (Wheeler and McFeely, 1987). The northeast part of the map area is underlain by variably sheared Proterozoic and Paleozoic strata deposited along the margin of ancient North America. These are overlain by allochthons of Upper Paleozoic greenstone, sheared and metamorphosed Paleozoic siliceous sediments and mylonitized granitic rock. Isotopic age data from other regions to the northwest (Hansen et al., 1989) indicate the mylonitic fabric and metamorphism in allochthonous rocks are post-Permian and pre-Early Jurassic in age. The central fault bounded panel consists of poorly understood Mesozoic(?) volcanics and volcaniclastics. Its southwest boundary, the Teslin fault, may have 150 km of pre-Late Cretaceous dextral displacement as indicated by offset along the Thibert Fault in northwestern British Columbia to which it may connect (Gabrielse, 1985, Fig. 9). The northeast bounding fault (unnamed) separates unmetamorphosed and weakly deformed strata on the southwest from mylonitized sedimentary and granitic rocks of high metamorphic rank on the northeast. Regional folding and faulting of strata across the map area was broadly Jura-Cretaceous, as was obduction of allochthons

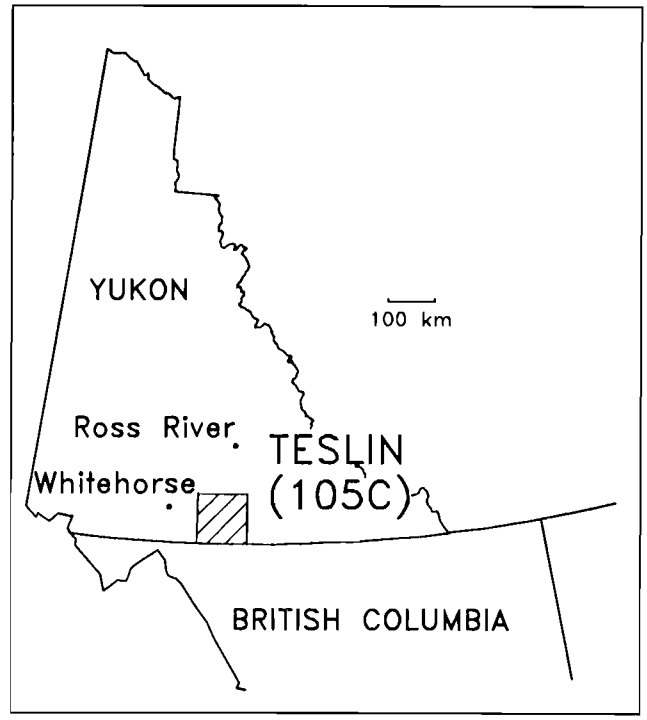

Figure 1. Location of Teslin map area, southern Yukon.

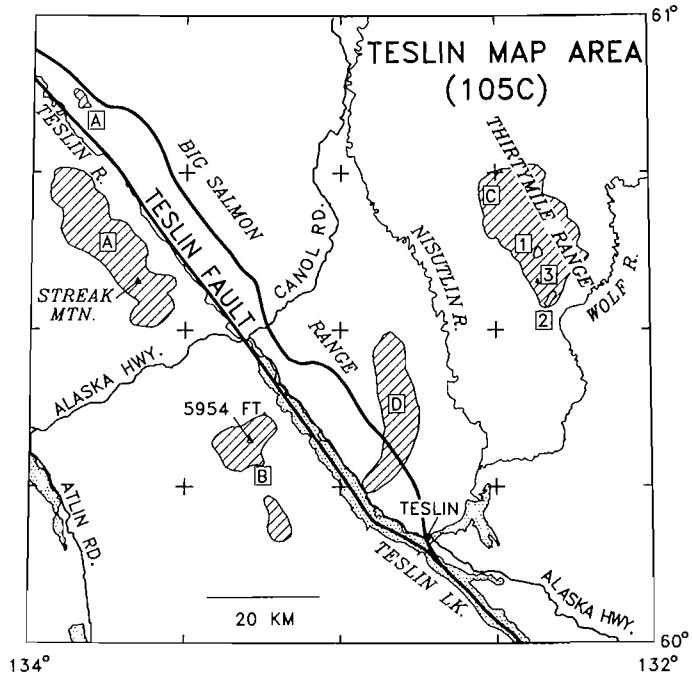

Figure 2. Areas examined in Teslin map area during 1990 fieldwork (diagonal hatching). Letters and numbers in squares are referenced in text. Heavy lines are major faults (Teslin fault and unnamed fault to the northeast) discussed in text. Small crosses indicate corners of 1:50 000 scale map areas.

of already metamorphosed and mylonitized rock onto North American strata. Unfoliated, post-tectonic mid-Cretaceous granitic plutons occur across the map area.

INKLIN ASSEMBLAGE

Mesozoic sedimentary and minor volcanic strata and local ultramafic intrusions were examined flanking the Teslin River and northwest of the Alaska Highway (area A, Fig. 2). The sediments (unit 9 of Mulligan, 1963) consist predominantly of sandstone and lesser interbedded argillite. The sandstone is well indurated and weathers dark grey to orange grey; on fresh surfaces it is blue-grey to light-grey. It may occur as individual thin to thick beds sharply bounded by argillite but typically forms massive, uniformly fine- to medium-grained packets from 10 m to as much as 150 m thick. Sedimentary structures include fist-sized argillite rip-up clasts, graded bedding, and lamination. Cursory petrographic examination shows framework grains to consist mostly of plagioclase, lesser monocrystalline quartz and minor orthoclase, hornblende, pyroxene and rock fragments, the last including chert(?) and aphanitic volcanics.

Thinly interbedded grey, green and tan laminated argillite and siltstone form members up to 100 m thick that separate the sand bodies described above. Graded thin to thick, fine- to coarse-grained sandstone interbeds are common. Locally the argillite is highly siliceous and grades into grey to green-grey chert.

The clastic succession also contains scattered occurrences of conglomerate. One type consists of pebble to cobble conglomerate with clasts of limestone, granitic rock, feldspar porphyry, green to grey-green volcanic(?) and argillite(?), chert, and dark grey argillite. All clasts are well rounded, the largest reaching up to 50 cm across, and are typically matrix supported within dark grey to black mudstone. A second type consists almost entirely of rounded limestone clasts, matrix supported within black calcareous mudstone (Fig. 3a), but also carrying rare granitoid and volcanic clasts. Clast size ranges from small pebbles to boulders up to 1.5 m across. The thickness of the conglomeratic units ranges from a few metres to up to 200 m thick. Most of the occurrences of limestone mapped by Mulligan (unit 9b, 1963) probably comprise limestone conglomerate.

Volcanic rocks within the succession are rare. Pillowed andesite, estimated at up to 200 m thick, was seen at one locality but could not be traced more than a few kilometres along strike. Scattered occurrences of white to orange weathering, locally quartz phyric felsite range up to 30 m across and have a trend that parallels bedding. The origin of most of these bodies, whether as dykes sills or flows is unresolved, as is whether the felsite was broadly contemporaneous with sedimentation, or younger.

The coarse clastics, including conglomerates, were likely deposited as sediment gravity flows. The preponderance of sand over shale and the thickness of the sand bodies are suggestive of mid-fan deposits. Fan-channel migration probably lead to times of diminished sediment supply, and could account for deposition of the finer clastic members. Massive, thick sandstone sections are likely composed of amalgamated beds where intervening shale has been eroded or has not had time to accumulate between sedimentation events.

An area examined northeast of Teslin fault (A, Fig. 2) is lithologically and structurally similar to the clastic succession described above. These strata within the central fault-bounded panel (unit 9 of Mulligan, 1963), may represent an offset part of the same basin displaced by dextral movement along Teslin fault.

The structure of the clastic rocks in the area is relatively simple. Dips of bedding vary from shallow to up to 70°, and reversals of dip direction indicate northwest trending upright folds with wavelengths of a kilometre or more. Wherever facing could be determined, bedding proved to be upright. There is no slaty cleavage. Small- to outcrop scale folds are absent, nor are there markers within the succession whereby the geometry of large scale folds can be mapped.

Two occurrences of ultramafic rocks are partly to completely surrounded by the sediments described above; both bodies have been previously mapped by Mulligan (unit 11, 1963). The largest one, about 2.5 km across, is located 6.3 km north of Streak Mountain and consists of a fresh, foliated pyroxenite core, partially enveloped by serpentinite. Magmatic foliation is defined by horizons of coarse pyroxene crystals up to a few centimetres thick within a background of finer grained pyroxene (Fig. 3b). The magmatic foliation is crosscut by planar veins and pods of coarse grained altered pyroxenite up to 8 cm thick. The second ultramafic body, located 18 km northwest of Streak Mountain is slightly smaller and elliptical in plan view. It is composed of pyroxenite and peridotite (see Mulligan, 1963, p. 61). The circular to elliptical shapes of the bodies and their steep contacts as indicated by intersection with topography show them to be intrusive and not emplaced along thrust faults.

CACHE CREEK GROUP AND LEWES RIVER ASSEMBLAGE

Strata examined south of the Alaska Highway and southwest of Teslin Lake (Fig. 2) include volcanics, argillite and limestone of the Cache Creek Group and overlying(?) chert and greywacke of the Lewes River assemblage (areas labelled B, Fig. 2; see also Jackson, 1990). The southern of the two areas indicated is underlain entirely by chert and greywacke.

Greenstone, mélange(?) and carbonate are the components of the Cache Creek Group in the small area examined. The greenstone (CPv, Fig. 4; unit 7 of Mulligan, 1963) is aphanitic, massive, well indurated, and weathers dark grey-brown. Fresh surfaces are light to dark grey-green. Amygdaloidal textures were seen locally. On the west flank of peak 5954 ft. the greenstone contains blocks of light grey weathering, dark grey limestone up to 20 m across. On the ridge leading northeast from the peak it encloses a carbonate debris flow at least 5 m thick comprising 1-15 cm sized clasts of light grey weathering, grey to black limestone that are matrix-supported within a calcareous tuff(?) or mudstone. At another location about 1 km north of peak 5954 ft. a house-sized block of dark blue-grey, bedded chert is surrounded by greenstone. In uncertain but probably intrusive contact with the greenstone is a small body of unfoliated fine- to medium-grained diorite of uncertain age (PMg, Fig. 4)


a

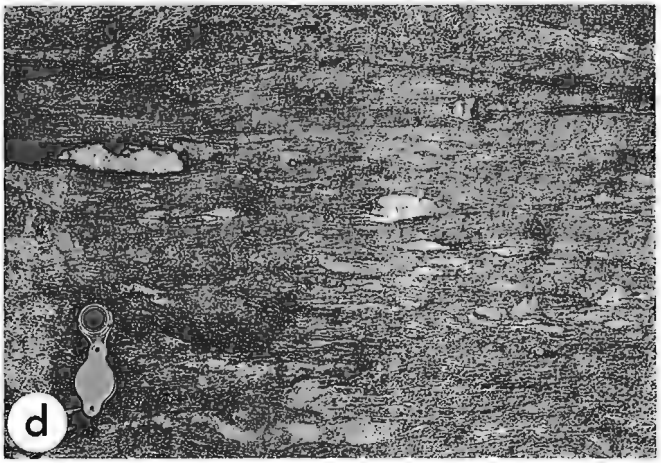
d

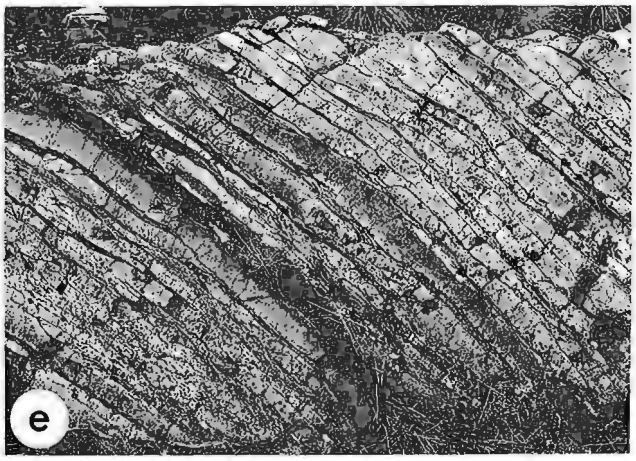
e


b

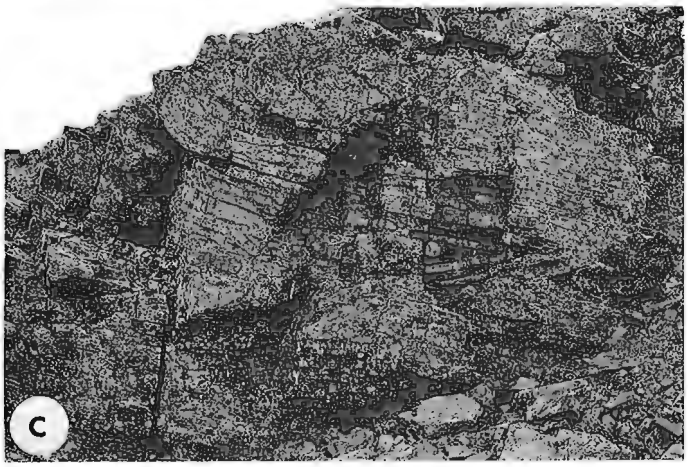
c

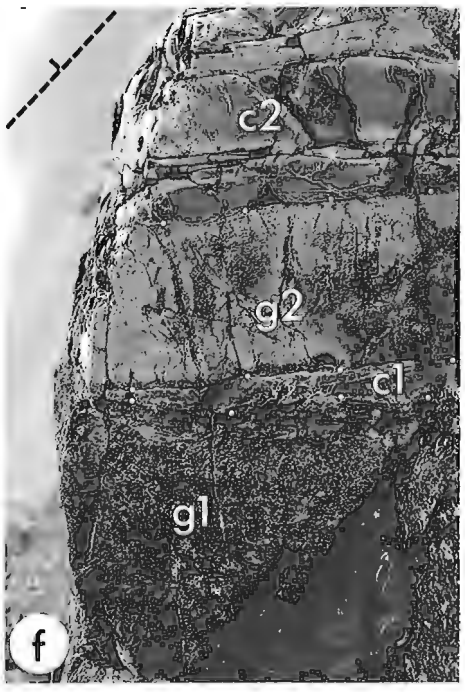
c2
g2
c1
g1
f

consisting of about 40% hornblende and the remainder of feldspar. An adjacent body of altered quartz-bearing felsite (Kg, Fig. 4) is also of uncertain age, but its composition suggests it may be satellitic to the nearby Cretaceous Mt. Hayes granitic pluton.

Southwest of the massive greenstone is a belt up to 2 km wide composed of alternating members of black siliceous argillite to dark grey chert, and light chrome green tuffaceous(?) argillite or greenstone (CPpv, Fig. 4; unit 4 of Mulligan, 1963). Swirly, disrupted lamination is characteristic of all rock types. The relations between these two members are obscure, however they generally form alternating, in places lensoid intervals from 5-100 m thick. Locally, in the black argillite are pebble-size clasts of chert, rare round limestone clasts, and rare blocks of sandstone, suggestive of a matrix supported debris-flow deposit. At one locality the tuffaceous argillite or greenstone encloses(?) a small body of black weathering, black serpentinite, about 50 m across. This unit is tentatively interpreted as a mélange and to have originated from tectonic disruption of an original succession of black and green argillite, chert, greenstone and possibly debris flow deposits. This would account for the unbedded and chaotic mixture of lithologies, and incorporation of the small ultramafic body.

Southwest of the above unit is medium grey weathering, light to dark grey, fine crystalline limestone that is typically massive and poorly bedded (CPl, Fig. 4; unit 5(?) of Mulligan, 1963). Crinoid ossicles are locally abundant. The carbonate may be as much as 200 m thick but pinches out structurally along strike. Both upper and lower contacts are moderately southwest dipping and structurally concordant with bounding units.

Southwest of the carbonate and also comprising the southern exposure of area B (Fig. 2) is a succession of ribbon-bedded, radiolarian chert and greywacke (TJts, Fig. 4; unit 4 of Mulligan, 1963). The chert dominantly weathers grey, white, black, or rust and is medium grey to black on fresh surfaces. Beds range from 3-10 cm thick, and are even

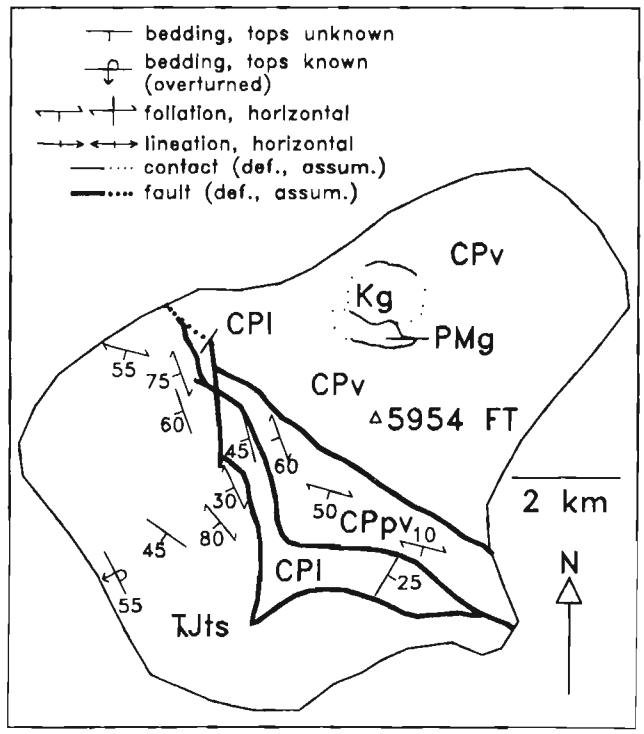

Figure 4. Geological sketch map for northern of two areas labelled B in Figure 2. Cache Creek Group includes Carboniferous to Permian greenstone (CPv), limestone (CPl), and mixed chert, shale, and tuffaceous greenstone (CPpv). The Lewes River assemblage includes Triassic and(?) Jurassic chert and greywacke (undivided; TJts). Symbols indicated pertain to Figures 4 and 5.

bedded to lensoid (Fig. 3e). Interbedded shale ranges from partings, to beds usually less than 3 cm thick. The greywacke is light grey-green to locally orange-white weathering, and well indurated. Fresh surfaces are medium grey. The sandstone was massive wherever encountered, even in members as much as 200 m thick. Rare sedimentary structures include shale rip-up clasts, convolute bedding, planar lamination, and graded bedding. Grain size in the sandstone is typically fine to coarse grained. Angular lithic clasts are locally abundant, range up to 5 cm in diameter, and are dominated by grey to white weathering chert, some radiolarian-bearing, and lesser argillite. Cursory petrographic examination shows the sandstone to comprise subequal proportions of quartz and plagioclase, and minor orthoclase, hornblende and lithic clasts. Late Triassic conodonts and radiolaria have been recently recovered from the Inklin assemblage chert (reported in Cordey, 1990, p. 123).

Although the greywacke and chert form alternating packets from 20-200 m thick, at only one locality were these lithologies proven to be interbedded. There, about six greywacke beds ranging from 15 cm to 3 m thick punctuated a succession of thin bedded chert (eg. Fig. 3f). Scour at the base of two of the greywacke beds and excellent graded bedding show this part of the succession, moderately southwest dipping, to be overturned.

The greenstone (CPv), mélange(?) (CPpv) and carbonate (CPl) are interpreted as large fault-bounded panels or

Figure 3. **a.** Matrix supported limestone clast conglomerate of the Inklin assemblage.
b. Igneous foliation defined by concentrations of coarse pyroxene in pyroxenite from ultramafic intrusion located 6.3 km north of Streak Mountain.
c. Thin bedded folded chert of possible early Paleozoic age, Thirtymile Range.
d. Mylonitic fabric in fine grained quartz sandstone, Thirtymile Range.
e. Thin bedded, planar to lensoid bedded grey chert of the Lewes River greywacke-chert succession (hand lens for scale in upper right corner).
f. Interbedded chert (c1,2) and greywacke (g1,2) in Lewes River greywacke-chert succession. White dots indicate bedding planes. Photograph is rotated with respect to horizontal; for correct orientation view the photo with the dashed black line horizontal and with the black bar on this line directed upwards. Bedding at this locality is overturned. Pinchout of thin chert bed (c1) is likely caused by scour at stratigraphic base of the coarse grained greywacke bed (g1), which near its stratigraphic base contains angular small fragments of chert.

megablocks of differing lithology within the Cache Creek Group. The unfoliated character of the greenstone (CPv) and the contained large blocks of chert and carbonate indicate a sedimentary debris flow or rock-fall origin for the latter, perhaps from fault scarps active during volcanism. The limestone unit, although deceptively like a moderately dipping stratigraphic marker in its structural concordance and distribution, may be a giant fault bounded lozenge. At its southeast end for example, bedding within the carbonate is perpendicular to its bounding contacts (Fig. 4). Siliceous argillite immediately above the carbonate is strongly cleaved in contrast to cleavage being poor or absent in the chert-greywacke succession elsewhere.

Sedimentary features of the greywacke are indicative of deposition from sediment gravity flows. The thick intervals of apparently massive sandstone, probably represent amalgamated beds, with no intervening shale deposited or preserved between depositional events. Greywacke within bedded chert is an unusual sedimentological association (see eg. Blake et al., 1984, p. 10). The greywacke beds are interpreted to represent brief pulses of clastic input within a starved setting.

The alternating packets of chert and greywacke of the Inklin assemblage, generally dip southwest in the southwest quadrant of the Teslin map area (Mulligan, 1963). If structural disruption were neglected thickness of the greywacke-chert succession would amount to an unreasonable(?) thousands of metres. Much of the alternation of chert and greywacke could be produced by thrust imbrication and tight folding of an original stratigraphic succession consisting of bedded chert overlain by a transitional sequence of interbedded chert and greywacke, in turn overlain by greywacke. The possibility of such a structural style is suggested by locally documented overturned bedding and tight small scale folding within chert members.

THIRTYMILE RANGE

The Thirtymile Range (area C, Fig. 2) is underlain by quartz sandstone, chert, chert pebble conglomerate, andesite and carbonate. Carbonate of Mississippian age comprises unit 2 of Mulligan (1963). The other rock types, for which no age control exists, are only locally subdivided (within unit 3 of Mulligan, 1963). Despite an overprint of variable and locally intense mylonitization, and disruption by numerous steep normal faults, a stratigraphy can be pieced together from different parts of the range (areas 1, 2, 3 of C, Fig. 2). Mylonitic fabrics are concordant with bedding, and have shallow to moderate dips. Large parts of the range are metamorphosed adjacent to unfoliated, mid-Cretaceous granite.

The structurally and stratigraphically lowest part of the range (C1, Fig. 2) consists of grey to black weathering, foliated, fine- to coarse-grained quartz sandstone and mudstone. Typically the sands are bimodal, containing large blue or clear quartz and minor feldspar within a matrix of finer grained quartz sand. Locally, the rock is a quartz feldspar pebble conglomerate. Mylonitic fabric is preferentially developed within fine grained clastics and is displayed as disrupted lenses and nodules of sandstone within siltstone and very fine grained sandstone (Fig. 3d). At only one locality were primary sedimentary structures clearly seen through the overprinting of metamorphism, mylonitization and weathering. There, six coarse grained beds from 0.5-3 m thick, all possessed sharp "bases" and well defined grading that indicate bedding in this subhorizontal succession is overturned. Within the sandstone is a 50(?) m thick member of white carbonate, dominated by relatively pure coarse grained marble but including zones of radiating tremolite, apple green diopside, garnet, and diopside-pyrrhotite skarn.

Topographically and stratigraphically(?) overlying the quartzose clastics is thin to thick-bedded, medium grey chert with shaly partings (area C1, Fig. 2). In several places the chert is deformed by recumbent tight folds (Fig. 3c), and in one locality the chert graded by increased intensity of flattening into strongly foliated siliceous mylonite.

Resting above the bedded chert (area C1, Fig. 2), and found at numerous other places in uncertain stratigraphic context is chert pebble conglomerate. Chert clasts are dominantly dark grey to black and gritty quartz sandstone clasts are seen locally. Clast diameters average about 1 cm, but are as large as 2-3 cm. At many places strain has almost completely obscured the original conglomeratic fabric.

In another part of the range (area C2, Fig. 2) chert quartzite cobble conglomerate and brown weathering, black slate overly grey weathering, sparsely coralline limestone. Relations to the strata previously described (ie. to area C1, Fig. 2) are uncertain. In the cobble to boulder conglomerate, chert clasts are dominantly grey. About 10% of the clasts are fine to coarse grained, gritty quartzose sandstone, with characteristic blue quartz. All clasts are well rounded, poorly sorted, and clast-supported within a muddy matrix. The carbonate (unit 2 of Mulligan, 1963) stratigraphically beneath the conglomerate and slate is massive, light grey to white weathering, and carries irregular masses and nodules of light to dark grey chert (5-15%). The limestone is fetid, and contains rare poorly preserved cup corals, and scattered crinoid debris. The slate has a gently dipping, bedding-parallel cleavage, but the conglomerate and carbonate have no cleavage, and the mylonitic fabric so pervasive elsewhere in the range is absent.

Volcanic rocks occur at several localities in the range and contain spectacular olistoliths. At one place (area C3, Fig. 2), a giant carbonate block 80-100 m across sits within green foliated volcanic tuff. The upper irregular surface of the carbonate block, with up to 10 m of relief, is covered by aphyric andesite. The andesite is in turn overlain by volcanic tuff containing centimetre to boulder-sized (3 m across) clasts of grey limestone. Nearby, but in uncertain stratigraphic relationship are exposures of carbonate-volcanic tuff debris flow(s) within which are entrained blocks of andesite, white to grey chert and carbonate.

Neglecting their structural overprint, Thirtymile Range strata have a striking resemblance to Proterozoic to mid-Paleozoic successions of the outer Northern Cordilleran margin. The gritty quartzose clastic rocks are similar to Upper Proterozoic clastics of the Ingenika Group (Mansy and Gabrielse, 1978) in Cassiar Mountains and the Hyland Group in the Selwyn Mountains of east-central Yukon (Gordey and

Irwin, 1987). The bedded chert is like that found in Cambrian to Devonian strata typifying outermost miogeoclinal strata in the Selwyn Mountains area of central Yukon (Gordey and Irwin, 1987). The chert and chert-quartzite clast conglomerate, and associated Mississippian carbonate, are akin to Devono-Mississippian strata found throughout the northern Cordillera (Gordey, 1988). The andesite described herein may be a local manifestation of extension that also accompanied Devono-Mississippian sedimentation elsewhere (Gordey, 1988). They may have intruded upward along faults that controlled scarps from which the carbonate slide blocks and the carbonate-tuff debris flow deposits (derived from Mississippian(?) carbonate described above) may have originated.

Recumbent tight folds within the chert, the presence of recumbent fold nappes in the gritty quartz sandstone indicated by subhorizontal yet overturned bedding, and the locally intense mylonitic fabrics reflect severe deformation. Although thicknesses of individual units have been structurally modified, gross stratigraphic order has been preserved. The age of deformation is uncertain but may be Jura-Cretaceous and related to the emplacement of allochthons above the North American margin.

BIG SALMON TRANSECT

A transect across the Big Salmon Range crossed several types of granitic rock, metasediments, and unmetamorphosed volcaniclastic sediments, most of uncertain age. At the north end of the transect (area D, Fig. 2; Fig. 5), medium grained equigranular to potash feldspar megacrystic granite (Kg, Fig. 5) intrudes hornblende quartz diorite (PMqd, Fig. 5). The diorite has a strong mylonitic foliation, and a lineation defined by streaking of the mafic minerals. South of, and structurally concordant with the diorite is a metasedimentary succession (Psq, Fig. 5) including minor tremolite-bearing and grossular-diopside bearing marble, but composed mostly of fine grained biotite quartzite and biotite quartz feldspar schist. Its strong foliation is defined by alignment of mica, and a lineation by mineral streaking and crenulation. Sillimanite was noted at one locality. South of the metasediments and intrusive into them is a strongly foliated biotite-hornblende granite. The foliation is a mylonitic fabric defined by laminae and aggregations of biotite and hornblende separating augen of feldspar and folia of fine grained quartz and feldspar. A variably developed lineation is seen as a streaking of mafic minerals on the foliation surface. Foliation-concordant screens of metasediment up to 10 m thick and less are common within the granite and along its northern contact. On the south side of the foliated granite, and concordantly above it is very fine grained, rusty weathering, dark grey to black muscovitic quartz-feldspar phyllite (Psq, Fig. 5). Lineation and foliation in these rocks have attitudes consistent with those seen in the granite. The most southerly unit of the transect consisted of brown weathering siltstone and shale, grey and blue-grey laminated siliceous argillite, and medium grey to greenish-grey fine- to medium-grained sandstone (Mps, Fig. 5).

Foliation attitudes across the transect define a broad antiform; lineations consistently plunge shallowly to moderately southeast. The shallow attitude of foliation and

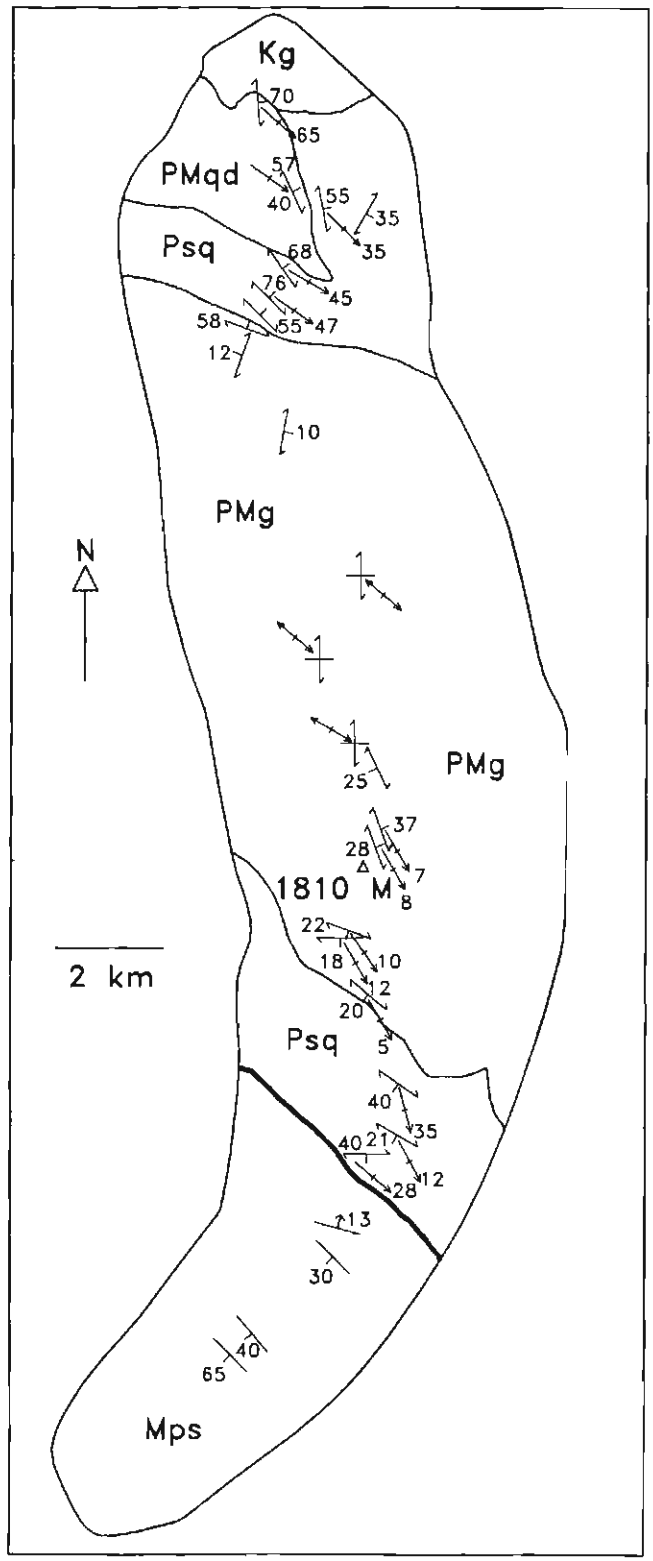

Figure 5. Geological sketch map for area labelled D in Figure 2. From north to south the rock units include Cretaceous unfoliated granite (Kg), Paleozoic or Mesozoic quartz diorite (PMqd), Paleozoic quartzose metasediments and minor marble (Psq), Paleozoic or Mesozoic strongly foliated granite (PMg), and Mesozoic(?) sandstone and shale. For symbol explanation see Figure 4. See text for discussion.

abundant metasedimentary screens in the foliated granite suggest that only the upper parts or roof of this intrusive are exposed.

The foliated quartz diorite (PMqd, Fig. 5) and metasedimentary rocks (Psq, Fig. 5) resemble similar rock types northwest of the Canol Road in the Big Salmon Range (see Stevens, 1991). Regional evidence suggests that those rocks are allochthonous and received their fabric and metamorphism in pre-Early Jurassic time. The foliated granite (PMg, Fig. 5) compositionally resembles widespread mid-Cretaceous plutons, but these latter types are typically bereft of fabric. This granite is therefore possibly Triassic or older in age, allochthonous, and achieved its foliation along with the metasediments through pre-Early Jurassic deformation.

The fault crossing the southern part of the transect (Fig. 2 and 5) is not exposed but its trace is well constrained by contrasting rock types. On its northeast side are foliated muscovitic phyllite, in which bedding is not preserved, whereas rocks on the southwest side consist of unmetamorphosed and uncleaved sandstone, siltstone and shale (unit 10 of Mulligan, 1963). The sediments had only cursory examination. Moderate dips and reversals in dip direction show them to be folded, but the severity of shortening is uncertain. Their depositional environments and possible relationships to the previously described Inklin and Lewes River assemblages are also uncertain (see Mulligan, 1963, p. 53).

GUIDE TO MINERAL EXPLORATION

No new mineral showings were discovered during the present work. The ultramafic intrusions mentioned above contain no noted asbestos, nor, because of their lack of mineral segregation do they seem promising for economic platinum or chromium deposits. The Inklin and Lewes River sedimentary successions are notably barren of mineral occurrences (INAC, 1989, p. 32).

Occurrences of probable Devono-Mississippian clastic strata in Thirtymile Range represent a previously unrecognized potential for stratiform base metal deposits, and a new option for interpreting existing and future discoveries. A hallmark of these strata in other parts of the Cordillera are associated deposits of stratiform Ag-Pb-Zn-barite such as at Macmillan Pass, Yukon (Bailes et al., 1986) and at the Cirque deposit (Pigage, 1986) in northern British Columbia. Correlations presented herein of the Thirtymile Range, associate the Ork and Mindy tin-tungsten skarn deposits with a carbonate host of late Proterozoic age.

ACKNOWLEDGMENTS

Excellent helicopter support was provided by TransNorth Helicopters (Whitehorse) and Capital Helicopters (Atlin). The use of facilities and co-operation of Steve Morison of Indian and Northern Affairs Canada in Whitehorse is sincerely appreciated. Dave Scott provided superb assistance in the field.

REFERENCES

Bailes, R.J., Smee, B.W., Blackadar, D.W., and Gardner, H.D.
1986: Geology of the Jason lead-zinc-silver deposits, Macmillan Pass, Yukon; in Mineral Deposits of the Northern Canadian Cordillera, J.A. Morin (ed.), Canadian Institute of Mining and Metallurgy, Special Volume 37, p. 87-99.

Blake, M.C., Howell, D.G., and Jayko, A.S.
1984: Tectonostratigraphic terranes of the San Francisco Bay region; in Franciscan Geology of Northern California, M.C. Blake, Jr. (ed.), Pacific Section Society of Economic Paleontologists and Mineralogists, v. 43, p. 5- 22.

Cordey, F.
1990: Radiolarian age determinations from the Canadian Cordillera; in Current Research, Part E, Geological Survey of Canada, Paper 90-1E, p. 121- 126.

Gabrielse, H.
1985: Major dextral transcurrent displacements along the Northern Rocky Mountain Trench and related lineaments in north-central British Columbia; Geological Society of America Bulletin, v. 96, p. 1-14.

Gordey, S.P.
1988: Devono-Mississippian clastic sedimentation and tectonism in the Canadian Cordilleran miogeocline; in Devonian of the World, N.J. McMillan, A.F. Embry, and D.J. Glass (ed.), Canadian Society of Petroleum Geologists, Memoir 14, vol. II, p. 1-14.

Gordey, S.P. and Irwin, S.E.B.
1987: Geology of Sheldon Lake and Tay River map areas, Yukon Territory, Yukon Territory; Geological Survey of Canada, Map 19-1987.

Hansen, V.L., Armstrong, R.L., and Mortensen, J.K.
1989: Pre-Jurassic ductile deformation and synchronous metamorphism of the Yukon Tanana terrane: geochronologic constraints from the Teslin suture zone, Yukon; Canadian Journal of Earth Sciences, v. 26, p. 2224-2235.

INAC
1989: Yukon exploration, 1988; Exploration and Geological Services Division, Yukon, Indian and Northern Affairs Canada.

Jackson, J.
1990: Geology and Nd isotope geochemistry of part of the northern Cache Creek terrane, Yukon: implications for tectonic relations between Cache Creek and Stikine; in Geological Association of Canada/ Mineralogical Association of Canada, Joint Annual Meeting, Program with Abstracts, v. 15, p. A64.

Mansy, J.L. and Gabrielse, H.
1978: Stratigraphy, terminology, and correlation of upper Proterozoic rocks in Omineca and Cassiar mountains, north-central British Columbia; Geological Survey of Canada, Paper 77-19, 17 p.

Mulligan, R.
1963: Geology of Teslin map area, Yukon Territory (105C); Geological Survey of Canada, Memoir 326.

Pigage, L.C.
1986: Geology of the Cirque barite-zinc-lead-silver deposits, northeastern British Columbia; in Mineral Deposits of the Northern Canadian Cordillera, J.A. Morin (ed.), Canadian Institute of Mining and Metallurgy, Special Volume 37, p. 71-86.

Stevens, R.A.
1991: The Teslin suture zone in northwest Teslin map area, Yukon; in Current Research, Part A, Geological Survey of Canada, Paper 91-1A.

Wheeler, J.O. and McFeely, P.
1987: Tectonic assemblage map of the Canadian Cordillera and adjacent parts of the United States of America; Geological Survey of Canada, Open File 1565.

Wheeler, J.O., Brookfield, A.J., Gabrielse, H., Monger, J.W.H., Tipper, H.W., and Woodsworth, G.J.
1988: Terrane map of the Canadian Cordillera; Geological Survey of Canada, Open File 1894.

Geology of the footwall of the Blackman Thrust and facies variations in middle Miette Group, southern Selwyn Range, British Columbia

Eric W. Mountjoy[1] and Stephen E. Grasby[1]
Cordilleran Division, Vancouver

Mountjoy, E.W. and Grasby, S.E., Geology of the footwall of the Blackman Thrust and facies variations in middle Miette Group, southern Selwyn Range, British Columbia; in Current Research, Part A, Geological Survey of Canada, Paper 91-1A, p. 179-185, 1991.

Abstract

New mapping between the Selwyn Range and Hugh Allan thrusts near Blackman Creek indicates the presence of two additional thrust faults in the footwall of the Blackman Thrust. These thrusts are identified by the repetition of the distinctive Old Fort Point Formation which was recently discovered in the region. Correlation of stratigraphy across this area, using the Old Fort Point Formation as a datum, shows that the middle Miette Group "shales-out" from east to west across the southwest part of the Fraser River Antiform, and also at the top of the middle Miette near Athabasca and Canoe passes.

Résumé

De nouveaux travaux cartographiques de la zone située entre les chevauchements de Selwyn Range et de Hugh Allan près du ruisseau Blackman indiquent la présence de deux failles chevauchantes supplémentaires dans la paroi inférieure du chevauchement de Blackman. Ces chevauchements sont révélés par la répétition de la formation d'Old Fort Point, formation distinctive récemment découverte dans cette région. La corrélation de la stratigraphie de toute cette zone, en utilisant la formation d'Old Fort Point comme référence, indique que la partie intermédiaire du groupe de Miette se transforme en biseau de shale de l'est à l'ouest à travers la partie sud-ouest de l'antiforme de Fraser River, et également au sommet de la partie intermédiaire du groupe de Miette, près des cols Athabasca et Canoe.

[1] Department of Geological Sciences, McGill University, 3450 University Street, Montreal, Quebec H3A 2A7

INTRODUCTION

The area between Hugh Allan and Ptarmigan creeks is underlain by rocks of the Miette Group (Fig. 1, Leonard, 1985; Mountjoy et al., 1985; Mountjoy and Forest, 1986). The Miette Group has been divided into three informal map units: lower, middle, and upper Miette Group (Campbell et al., 1973; Charlesworth et al., 1967; Carey and Simony, 1985). This report deals only with the middle Miette Group.

As traditionally defined, the middle Miette Group consists of three sequences, two thick (1000-1500 m) sequences of dominantly composite-bedded grit units 10-100 m-thick, interbedded with thick (10-40 m) pelites and an intervening thin (50-100 m), but distinctive and regionally persistent carbonate-bearing Old Fort Point Formation (Charlesworth et al., 1967; Ross and Murphy, 1988; McDonough and Simony, 1988; Dechesne and Mountjoy, 1990; Kubli, 1990). Individual grit beds (10-30 cm) are poorly sorted, and grade upward from granule- to pebble-conglomerate into coarse sandstones (Bouma T_{aa}, T_{ab}). Clasts are angular and dominantly consist of white, smokey, and blue quartz, in order of decreasing abundance. Feldspar is common, ranging from 3-15 %. Clasts are supported in an argillaceous to calcareous matrix. Interbedded with the composite grit units are distinctive grey-green, chloritic pelites, with abundant green silty laminations. Pelite units (10-40 m-thick) generally show sharp contacts with underlying and overlying grit units.

Early mapping in this area (Leonard, 1985) indicated that continuous carbonates occur in the immediate hanging wall of a 100 m-thick shear zone, now referred to as the Selwyn Range Thrust (Fig. 2). These carbonates are now known to be the Old Fort Point Formation (Mountjoy and Grasby, 1990; and this paper). Overlying the Old Fort Point Formation is a relatively thin (200 m) sequence of medium grained grits which pass upward into a thick (about 1000 m) silty pelite sequence assigned by Leonard (1985) to the upper Miette Group.

This summer, however, two bands of carbonate assigned to the Old Fort Point Formation were discovered within this thick pelite sequence north and south of Blackman Creek (Fig. 2, 3). The occurrence of these two bands indicates: 1) that two thrust faults occur between the Blackman and Selwyn Range thrusts; 2) that the thick pelite sequence is middle Miette Group, not upper; and 3) that the upper middle Miette Group 'shales-out' to the west (Fig. 4). A similar east to west 'shale-out' at the top of the middle Miette Group was also discovered near Athabasca and Canoe passes.

We questionably assign black pelites in the footwall of the Selwyn Range Thrust to the upper Miette Group

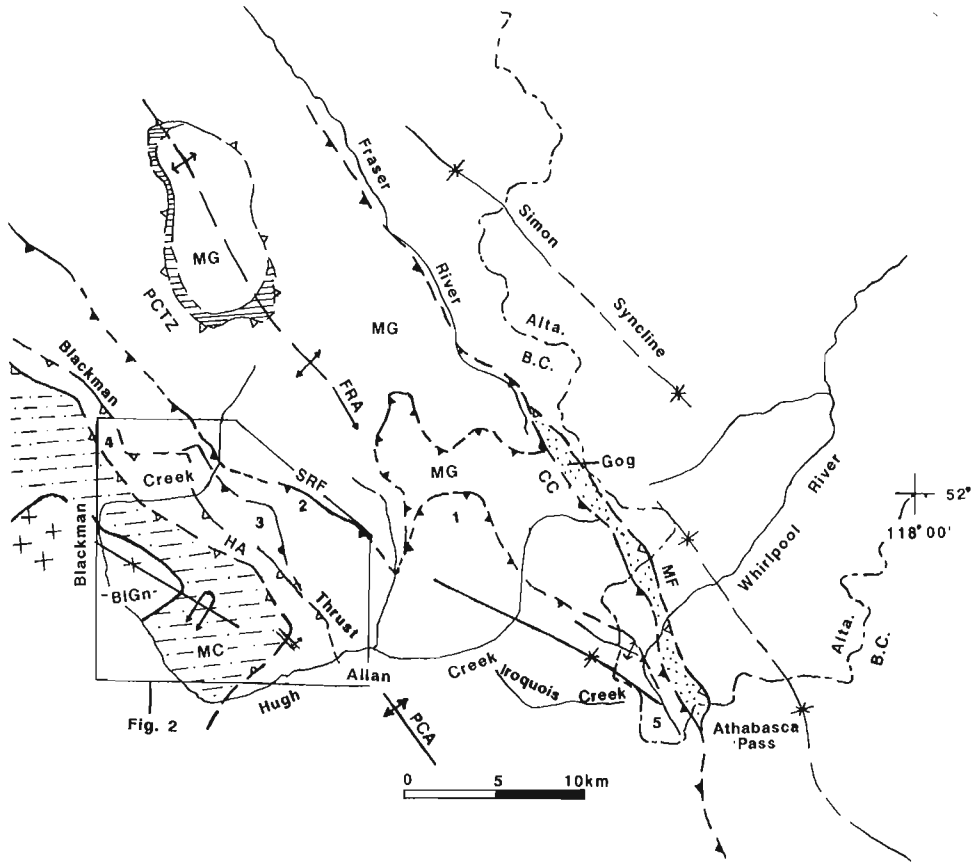

Figure 1. Regional geological map showing locations of major structural elements and stratigraphic locations (numbered). MF = McGillivary Fault, CC = Chatter Creek Fault, FRA = Fraser River Antiform, PCTZ = Ptarmigan Creek Thrust zone, SRT = Sewlyn Range Thrust. 1 - Saddle Mountain, 2 - Selwyn Range Thrust, 3 - Unnamed thrust slice, 4 - Blackman Thrust sheet, 5 - Athabasca Pass.

(Fig. 2), but they may also represent lower Miette Group strata (the thin versus thick stratigraphy of Mountjoy and Grasby, 1990). The proper stratigraphic assignment of these strata depends on working out a consistent structural picture of the southern Selwyn Range, which is beyond the scope of the present paper. Dechesne (1990) and Mountjoy and Grasby (1990) favoured assigning these strata to the upper Miette Group and connecting the Selwyn Range Thrust with a bedding glide zone beneath a thick sequence of middle Miette grits on the east flank of the Fraser River Antiform. However, it is difficult to find this thrust on the east flank of the Fraser River Antiform north of the Cube Ridge Thrust (Mountjoy and Grasby, 1990, Fig. 3). Mesoscopic structures observed along the Selwyn Range Thrust on the west flank of the Fraser River Antiform have so far not been observed on the east flank. McDonough and Simony (1988) favoured assigning these strata to the lower Miette Group. Such an assignment creates difficulties with respect to the Selwyn Range Thrust which cuts out the lower two thirds of the middle Miette Group including the Old Fort Point Formation in the present map area (Fig. 2, 3). Previously this inferred stratigraphic omission was the main reason why Leonard (1985) and the senior author (Mountjoy et al., 1985) interpreted the Selwyn Range Thrust to be a normal fault. Our stratigraphic and structural research is attempting to resolve these problems.

Thrust slices between Selwyn Range and Hugh Allan thrusts

The latest version of the geology of the area around Blackman Creek, including the distribution of the carbonate-bearing strata assigned to the Old Fort Point Formation, is shown in Figure 2. The Old Fort Point consists of the same diagnostic tri-part sequence as observed in the northern part of the Selwyn Range (McDonough and Simony, 1988), the type

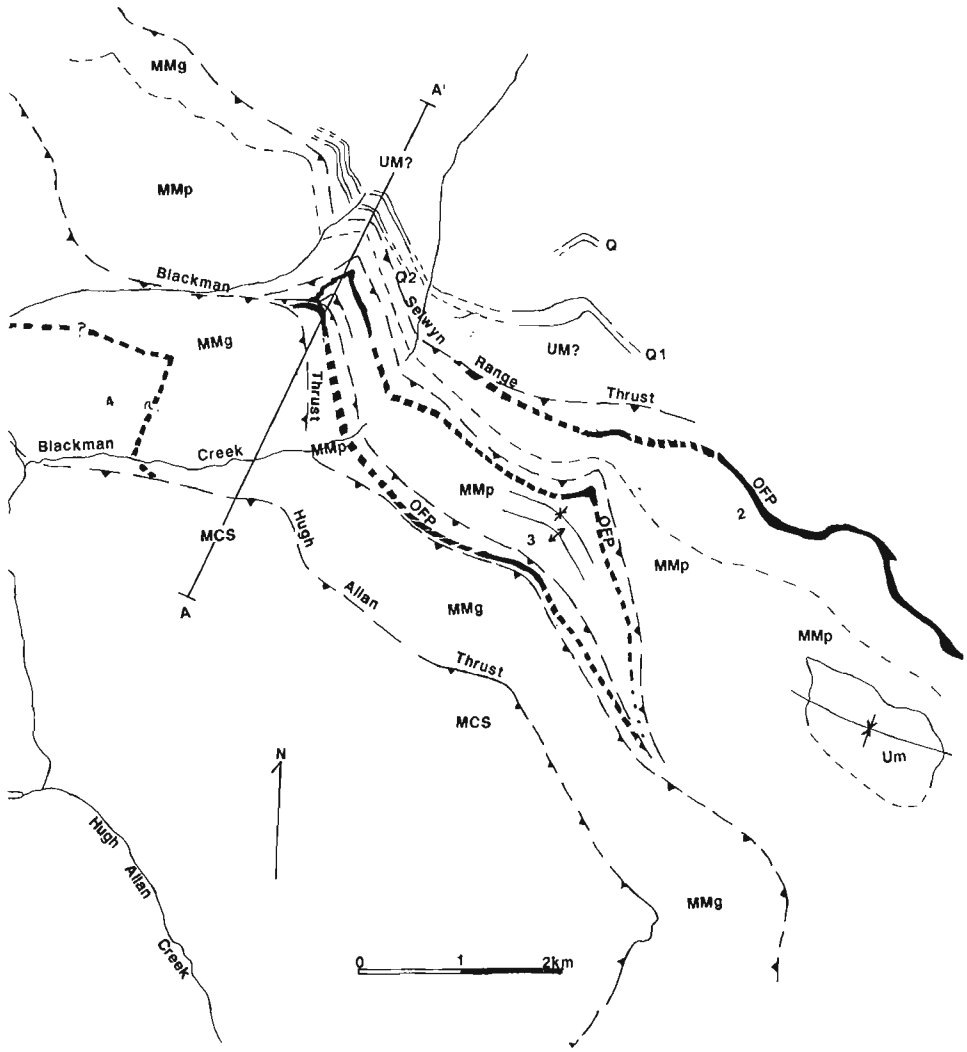

Figure 2. Geological map of area between Blackman and Hugh Allan creeks. Showing, from east to west, Selwyn Range Thrust, unnamed thrust, Blackman Thrust and Hugh Allan Thrust. UM? = black pelites tentatively assigned to upper Miette Group (see text), MMg = middle Miette Group grits, MMp = middle Miette Group pelites, Q_1 & Q_2 = quartzite and quartz- pebble conglomerate units, MCS = Mica Creek Succession of Horsethief Creek Group (McDonough and Murphy, 1990), BlGn = Blackman Gneiss.

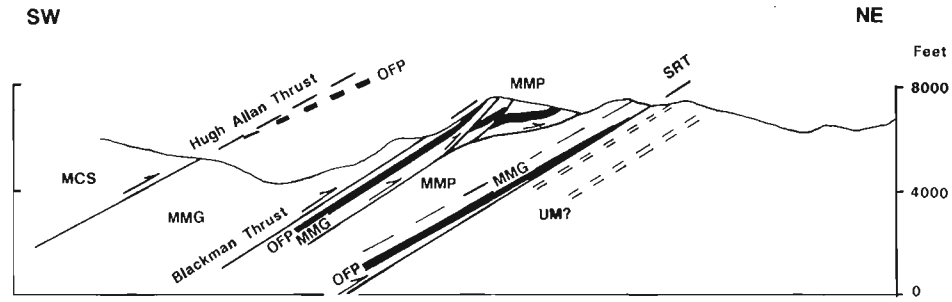

Figure 3. Cross-section immediately northwest of Blackman Creek (Fig. 2) showing thrust slices that duplicate Old Fort Point Formation and distribution of the middle Miette Group pelite sequence between the Selwyn Range and Blackman thrusts. Legend accompanies Figure 2.

section near Jasper (Dechesne and Mountjoy, 1990), and elsewhere (Ross and Murphy, 1988). A basal silty green pelite is overlain by a banded, silty carbonate unit that is capped by a black graphitic pelite. At Saddle Mountain this sequence consists of: 1) a basal 50 m green, silty pelite, 2) 28.5 m of rhythmically banded orange weathering carbonate and reddish brown siltstone, and 3) at the top, 15 m of black, graphitic pelites. The same three distinctive units occur in the Selwyn Range thrust sheet and overlying thrust slices, but are generally deformed and tectonically thinned. They are assigned to the Old Fort Point Formation.

The two thrust splays follow a detachment horizon at a stratigraphic level just below the base of the Old Fort Point Formation. This aspect is well exposed on the north side of the ridge immediately northwest of Blackman Creek, and is sketched in Figure 4. Although covered, a similar relationship of these thrusts with respect to the stratigraphy fits the known geology near the southern limits of these thrust slices (Fig. 2). Thus it appears that the thrust faults in these two splays follow this stratigraphic level for a lateral strike distance of about 6 km, and a minimum of 5 km perpendicular to strike (Fig. 3).

These thrust slices must merge with the Blackman Thrust to the northwest, as they do not continue across an unnamed creek 2.5 km northwest of Blackman Creek (118°35', 52°31'). The southern limit of these thrust slices is uncertain. The east limb of the Porcupine Creek Anticlinorium (along strike to the south of Hugh Allan Creek) is unfaulted, suggesting that these fault slices merge with the Blackman Thrust to the south (Fig. 1).

As shown by the map and cross-sections (Fig. 2, 3), the two unnamed thrust slices probably represent a more forward part of the Blackman Thrust sheet that was overridden by the main part of the sheet. Minimum displacements of these thrust slices and the Blackman Thrust can be estimated, depending on the location of the Old Fort Point Formation cutoffs in these structures (Fig. 3), as follows: basal slice, 6 km; upper slice, 1 km; Blackman Thrust sheet, 4 km for a total of 11 km.

The Blackman Thrust and these associated unnamed thrusts occur along strike from the core of the Porcupine Creek Anticlinorium south of Hugh Allan Creek (Fig. 1). These structures appear to root in the core of the Porcupine Creek Anticlinorium (Klein and Mountjoy, 1988; Mountjoy, 1988), hence the displacement of the Blackman Thrust must increase rapidly northwestwards.

Shale-out in the middle Miette Group

From east to west, a gradual facies change from normal coarse grits and silty pelites to pelites lacking grits is inferred in the middle Miette in two locations in the southern Selwyn Range; in the northern area across the three thrust sheets just described, and in the southern area near Canoe and Athabasca passes (Fig. 1, 2, 7). In the northern area, the transition from grit-dominated to shale-dominated sedimentation is shown in sections from 4 locations, from east to west: (1) the hanging wall of the Selwyn Range Thrust at Saddle Mountain (locality 1, Fig. 1, 5); (2) hanging wall of the Selwyn Range Thrust on the west flank of the Fraser River Antiform (locality 2, Fig. 1, 5); (3) hanging wall of the lower unnamed thrust (locality 3, Fig. 1, 5); (4) hanging wall of Blackman Thrust (locality 4, Fig. 1, 5). In the southern area the transition occurs between the heads of Hugh Allan Creek and the Whirlpool River just northwest of Athabasca Pass (locality 5, Fig. 1, 5, 6, 7).

Saddle Mountain (Fig. 1, 5; locality 1)

A complete stratigraphic sequence above the Old Fort Point Formation is exposed at Saddle Mountain on the southern plunge of the Fraser River Antiform. Amalgamated grit units range from 10-40 m-thick. Individual beds (10-30 cm-thick) are poorly sorted, grading upwards from basal granule- to pebble-conglomerate to a coarse grained sandstone. Interbedded with grit units are green pelite units (10-20 m-thick), with abundant green silty laminations.

Hanging wall of Selwyn Range Thrust (Fig. 1, 5; locality 2)

Much of the hanging wall of the Selwyn Range Thrust comprises a thick (1000 m) sequence of green, silty pelites. Originally assigned to the upper Miette Group by Leonard (1985), this unit is now considered to be middle Miette Group due to the presence of the Old Fort Point Formation as just discussed. Most of the lower part of the middle Miette Group is cut out by the Selwyn Range Thrust, including the Old

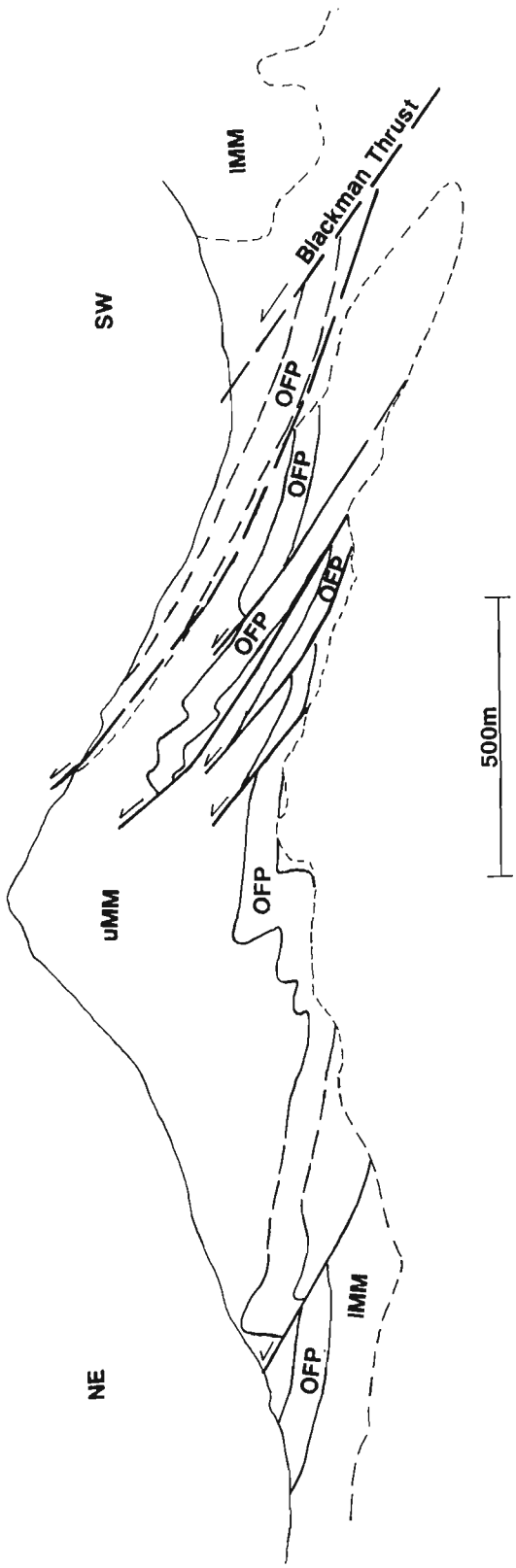

Figure 4. Sketch from photographs looking southeast along strike showing thrust slices of Old Fort Point Formation immediately beneath the Blackman Thrust (right). Lower middle Miette = 1MM, upper middle Miette = uMM, OFP = Old Fort Point Formation.

Fort Point Formation northwest of Blackman Creek (Fig. 2). Above the Old Fort Point Formation, grit packages are notably thinner (10-15 m-thick), more widely spaced, and finer grained than on Saddle Mountain to the southeast. About 200 m above the Old Fort Point Formation, grits are absent and silty green pelite becomes predominant, with only minor units of coarse grained, calcareous sandstone (up to 6 m-thick) present. Pelites are greyish-green, chloritic, and contain the abundant silty laminations that are characteristic of pelites in the middle Miette Group. This sequence appears to be transitional to the pelite lacking grits in the unnamed thrust slice to the southwest.

Unnamed lower thrust slice (Fig. 1, 5; locality 3)

Strata in this thrust slice are almost entirely silver-grey to green pelite with abundant green silty laminations characteristic of the middle Miette Group. However, unique to this facies are isolated thin beds (centimetre- to decimetre-scale) of calcareous, brown weathering coarse- to fine-grained sandstone. Less common are isolated ripple-laminated lenses of fine sandstone or siltstone inferred to be starved ripples. Occasionally sandstone beds occur in composite units up to 5 m-thick. A thickness of over a kilometre is estimated for these strata.

Blackman Thrust Sheet (Fig. 1, 5; locality 4)

Approximately 1.4 km of middle Miette strata are exposed in the hanging wall of the Blackman Thrust. As the Old Fort Point occurs in the upper part of the thrust sheet (Fig. 2), these strata belong mainly to the lower part of the middle Miette Group. The lower middle Miette strata are dominantly amalgamated grit units (10-30 m-thick) composed of coarse sand- to granule-conglomerate (10-20 cm-thick) and lesser interbedded green to grey silt-laminated pelite units (10-20 m-thick).

Strata above the Old Fort Point Formation can only be observed on the ridges between Blackman and Ptarmigan creeks, northeast of Mount Blackman beneath the Hugh Allan Thrust. The upper middle Miette consists of between 100 and 200 m of predominantly pelites containing a few grit units up to 5-10 m thick. It appears to represent part of the 'shaled out' upper middle Miette Group.

Athabasca Pass (Fig. 1, 5; locality 5)

Excellent exposures of the Miette Group outcrop in the hanging wall of the Chatter Creek Thrust (Fig. 1). About 5 km northwest of Athabasca Pass, the topmost 300 m of middle Miette grits thin and change rapidly into pelites over a distance of about 1 km in an area which has only been moderately deformed by upright open folds. These relationships are shown schematically in a sketch taken from field and air photographs illustrating the distribution of the thickest composite grit units (Fig. 6). A similar rapid westward change from grits to pelite also occurs in the next valley about 4 km to the north-northwest near Canoe Pass. This facies change appears to mark the continuation of the western margin of the same submarine fan or channel at the top of the middle Miette Group. Thus the margin has a northerly orientation

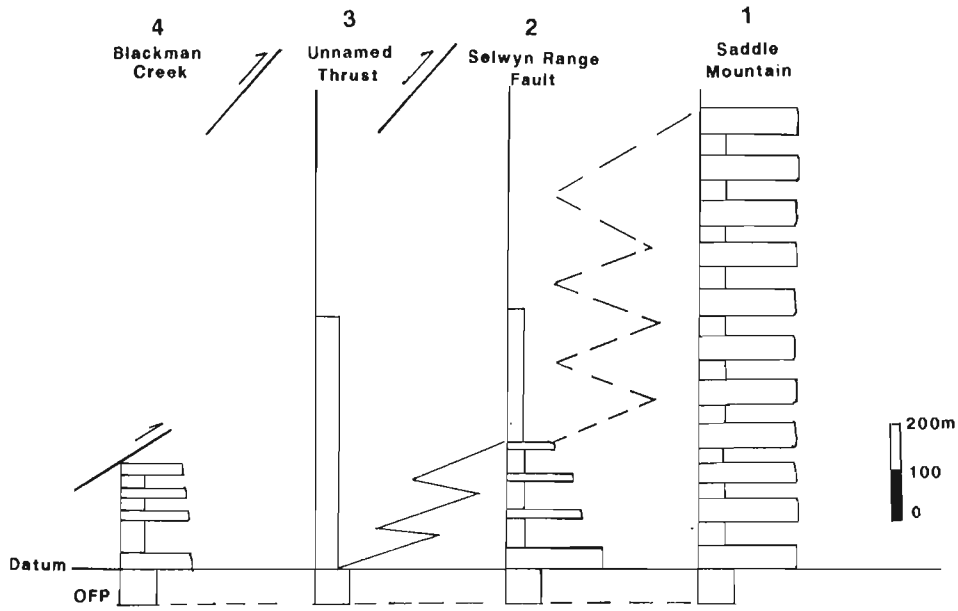

Figure 5. Schematic stratigraphic columns of middle Miette Group above the Old Fort Point in four areas: 1) Saddle Mountain, 2) Selwyn Range Thrust, 3) unnamed lower thrust slice, and 4) Blackman Thrust sheet. Note that sections 1 and 2 are both located in the hanging wall of the Selwyn Range Thrust.

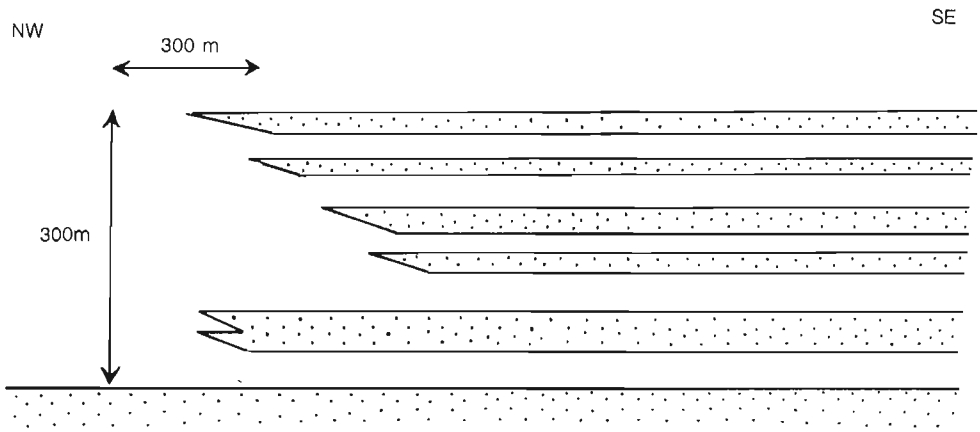

Figure 6. Sketch from photographs showing shaling out westward of composite grit units in the uppermost 300 m of the middle Miette strata on the north side of unnamed pass at the head of Iroquois Creek, 5 km northwest of Athabasca Pass (see Fig. 7 for location). Cross-section has about 2 times vertical exaggeration, and is oriented west-northwest - east-northeast.

and is similar to channel orientations observed by McDonough and Simony (1988) in the lowermost middle Miette Group of the northern Selwyn Range.

CONCLUSIONS

The presence of several bands of Old Fort Point Formation in the Blackman Creek area provide a means for identifying two new thrust slices between the Selwyn Range and Blackman thrusts and for correlating the middle Miette Group across these slices. The presence of Old Fort Point Formation within a thick green-grey pelite succession conclusively indicates that typical middle Miette Group composite grit units have 'shaled-out' westwards. 'Shaling-out' of the upper half of the middle Miette Group occurs in two areas, in the hanging wall of the Selwyn Range Thrust, and northwest of Athabasca Pass at the head of Iroquois Creek.

The above relationships help to explain the difficulties in mapping a consistent upper/middle Miette Group contact in this region. Traditionally the top of the middle Miette Group has been placed at the top of the last thick composite grit. In several sections grits become thinner and the pelitic units thicker over a vertical interval of 100-200 m, making it arbitrary as to where to draw this boundary. Perhaps using the upward gradual change in colour of the pelites from greenish-grey to black might be a better criteria for mapping a more consistent boundary, following the suggestion of

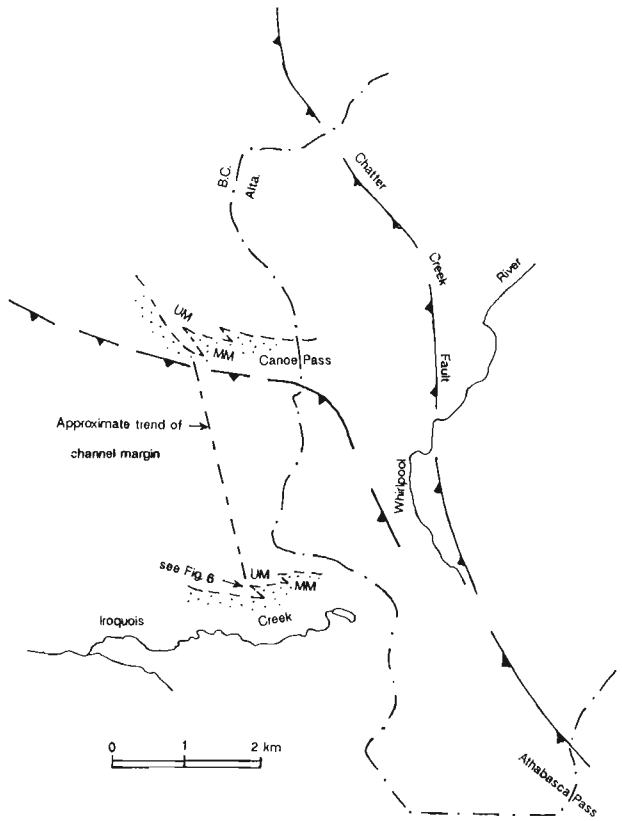

Figure 7. Generalized geological map of Canoe and Athabasca passes showing top of massive middle Miette grits changing rapidly westward into pelites (labelled UM). Dashed line represents the approximate location and orientation of the channel margin. Location of the cross-section in Figure 6 is also shown.

McDonough and Simony (1988). This would require the walking out of this contact.

ACKNOWLEDGMENTS

Financial support for this work comes from EMR research agreement (90/4/250) and NSERC's collaborative research grant, and Mountjoy's NSERC grant no A2128. We express our special thanks to Yellowhead Helicopters for their excellent flying services and field support. Brian Hannis and Niki and Carl Forman provided excellent expediting services. T. Waller and L. Roman where of great assistance in the field. We appreciate the helpful comments and suggestions on the manuscript by D. Murphy.

REFERENCES

Campbell, R.B., Mountjoy, E.W., and Young, F.G.
1973: Geology of McBride map-area, British Columbia; Geological Survey of Canada, Paper 72-35, 104 p.

Carey, J.A. and Simony, P.S.
1985: Stratigraphy, sedimentology and structure of Late Proterozoic Miette Group, Cushing Creek area, B.C.; Bulletin of Canadian Petroleum Geology, v. 33, p. 184-203.

Charlesworth, H.A.K., Weiner, J.L., Akehurst, A.J., Bielenstein, H.U., Evans, C.R., Griffiths, R.E., Remington, R.E., Stauffer, M.R., and Steiner, J.
1967: Precambrian geology of the Jasper region, Alberta; Research Council of Alberta, Bulletin 23.

Dechesne, R.G.
1990: Geology of the Ptarmigan Creek map area (east half) and adjacent regions, Main Ranges, Rocky Mountains, British Columbia; in Current Research, Part E, Geological Survey of Canada, Paper 90-1E, p. 81-89.

Dechesne, R.G. and Mountjoy, E.W.
1990: Miette Group in its type region: fill for a multiply extended basin; in Geological Association of Canada, Nuna Conference, Abstracts, p. 10.

Klein, G.A. and Mountjoy, E.W.
1988: Northern Porcupine Creek anticlinorium and footwall of the Purcell Thrust, northern Park Ranges, British Columbia; in Current Research, Part E, Geological Survey of Canada, Paper 88-1E, p. 163-170.

Kubli, T.
1990: The Baird Brook Division: a new recognized time stratigraphic marker in the Windermere Supergroup of the northern Purcell Mountains; in Geological Association of Canada, Nuna Conference, Abstracts, p. 22.

Leonard, R.
1985: Variable structural style, stratigraphy, total strain and metamorphism adjacent to the Purcell thrust, near Blackman Creek, British Columbia; unpublished M.Sc. thesis, McGill University, Montreal, Quebec.

McDonough, M.R. and Murphy, D.C.
1990: Valemount, British Columbia, 83 D/14; Geological Survey of Canada, Open File 2259, 1:50 000 scale.

McDonough, M.R. and Simony, P.S.
1988: Stratigraphy and structure of late Proterozoic Miette Group, northern Selwyn Range, Rocky Mountains, British Columbia; in Current Research, Part D, Geological Survey of Canada, Paper 88-1D, p. 105-113.

Mountjoy, E.W.
1988: The Hugh Allan (Purcell) fault (a low-angle west- dipping thrust) at Hugh Allan Creek, British Columbia; in Current Research, Part E, Geological Survey of Canada, Paper 88-1E, p. 97-104.

Mountjoy, E.W. and Forest, R.
1986: Revised structural interpretation, Selwyn Range between Ptarmigan and Hugh Allan creeks, British Columbia - an antiformal stack of thrusts; in Current Research, Part A, Geological Survey of Canada, Paper 86-1A, p. 177-183.

Mountjoy, E.W. and Grasby, S.E.
1990: Revised stratigraphic and structural interpretation of folded décollements, southern Fraser River Antiform, Selwyn Range, British Columbia; in Current Research, Part E, Geological Survey of Canada, Paper 90-1E, p. 359-367.

Mountjoy, E.W., Forest, R., and Leonard, R.
1985: Structure and stratigraphy of the Miette Group, Selwyn Range, between Ptarmigan and Hugh Allan creeks, British Columbia; in Current Research, Part A, Geological Survey of Canada, Paper 85-1A, p. 485-490.

Ross, G.M. and Murphy, D.C.
1988: Transgressive stratigraphy, anoxia, and regional correlations with the Late Precambrian Windermere grit of the southern Canadian Cordillera; Geology, v. 16, p. 139-143.

Detailed sedimentology of the Bowser Lake Group, northern Bowser Basin, British Columbia[1]

G.M. Green[2]
Cordilleran Division, Vancouver

Green, G.M., Detailed sedimentology of the Bowser Lake Group, northern Bowser Basin, British Columbia; in Current Research, Part A, Geological Survey of Canada, Paper 91-1A, p. 187-195, 1991.

Abstract

In the northeastern part of Spatsizi map area (104H), the lower Bowser Lake Group comprises coastal, fan delta, shelf, prodelta-slope, and submarine canyon/gully assemblages. A shale/siltstone facies within the prodelta-slope assemblage contains a sandstone subfacies which is inferred to represent overbank deposits of submarine fan channels. Coalesced, offstacked conglomerates of the submarine canyon/gully assemblage may represent major supply routes from a source to the north. In the shelf assemblage, repetitive coarsening-up cycles containing fossiliferous beds represent a persistent shallow marine shelf. Bedform geometries and internal fabrics in rusty conglomerates suggest coalesced fan deltas or gravel bars on braid deltas. Association with carbonaceous shales is compatible with a barrier bar-lagoonal setting. Paleocurrent data from ripple cross-stratification and clast imbrication indicate south-southwesterly sediment transport. Megascopic point counts of conglomerates indicate no significant lateral or vertical changes in clast compositions.

Résumé

Dans la partie nord-est de la région cartographique de Spatsizi (104H), la partie inférieure du groupe de Bowser Lake comprend des assemblages de sédiments littoraux, de cône de déjection, de plate-forme continentale, de prodelta-talus et de canyon et ravin sous-marins. Un faciès de shale et siltstone au sein d'un assemblage de prodelta-talus renferme un sous-faciès de grès qui représenterait, on suppose, des sédiments de débordement de chenaux de cônes sous-marins. Les conglomérats hors séquence fusionnés de l'assemblage de sédiments de canyon et ravin sous-marins pourraient représenter d'importants parcours d'alimentation à partir d'une source située au nord. Dans l'assemblage de plate-forme continentale, la présence de cycles répétitifs à granoclassement inverse et contenant des couches fossilifères, indique qu'il s'agit d'un milieu de plate-forme épicontinentale continue. La géométrie des formes sous-marines et la fabrique interne des conglomérats rouillés laissent supposer la présence de cônes de déjection fusionnés ou de bancs de gravier sur des deltas à chenaux anastomosés. Leur association à des shales carbonés est conforme à un milieu de banc prélittoral et lagune. Les données sur les paléocourants révélées par la stratification oblique à rides et l'imbrication des clastes établissent que le transport sédimentaire s'est effectué vers le sud-sud-ouest. Le dénombrement ponctuel mégascopique des conglomérats n'indique aucun changement latéral ou vertical important dans la composition des clastes.

[1] Contribution to Frontier Geoscience Program
[2] Ottawa-Carleton Geoscience Centre, Department of Earth Sciences, Carleton University, Ottawa, Ontario K1S 5B6

INTRODUCTION

The Bowser Basin is a thick accumulation of syn- to late-orogenic, marine to nonmarine sedimentary rocks within the Intermontane Belt of the Canadian Cordillera (Fig. 1; Eisbacher, 1974a,b, 1981, 1985; Eisbacher et al., 1974). The basin fill preserves an indirect record of terrane interactions and contains voluminous chert detritus believed to have been derived from the Cache Creek Terrane (Souther and Armstrong, 1966; Eisbacher, 1981). The present study is part of a regional Frontier Geoscience Program designed to place better constraints on the evolution of the basin. Recent studies of the basin include Cookenboo and Bustin (1990), Evenchick and Green (1990), Evenchick (in press), Ricketts (1990), and Ricketts and Evenchick (1991).

The term Bowser Lake Group was first used by Tipper and Richards (1976) for Middle to Upper Jurassic strata in the southern part of the Bowser Basin. The Ashman Formation has been formally recognized as the lowest formation within the Bowser Lake Group. This unit includes Upper Bajocian to Lower Oxfordian strata in the southern part of the basin (Tipper and Richards, 1976), and Late Bathonian to Early Oxfordian strata in the northern part of the basin (Gabrielse and Tipper, 1984). The present study is based on six stratigraphic sections measured through upper parts of the Ashman Formation and overlying undivided strata of the Bowser Lake Group in and around Todagin and Tsatia mountains (Fig. 2). A total of 6400 m was measured at a scale of 1:400. The underlying Hazelton and Spatsizi groups and the overlying Maitland volcanic rocks are briefly described in Evenchick and Green (1990). The purpose of this paper is to: (1) provide detailed descriptions and interpretations of selected facies and assemblages delineated by Ricketts (1990), and Ricketts and Evenchick (1991); (2) present paleocurrent data from three selected facies; and (3) provide preliminary clast composition data from conglomerate units within the study area.

FACIES/ASSEMBLAGE ANALYSIS

Preliminary examination of the Middle to Upper Jurassic Bowser Lake Group led Ricketts (1990) to develop a depositional model for the northern part of the Bowser Basin. His model comprises a spectrum of environments including deep-sea submarine fans, prodelta-slope with incised submarine canyons, interfan shelves, and fan deltas with possible alluvial equivalents (Fig. 5 in Ricketts, 1990). Bathonian to possibly Oxfordian strata are subdivided into corresponding broad facies assemblages which include fan delta, shelf, prodelta-slope, and submarine fan. The depositional model has been modified by Ricketts and Evenchick (1991) to include a deep basin, coastal, and submarine canyon/gully assemblage (formerly part of the prodelta-slope assemblage). Table 1 in Ricketts and Evenchick (1991) presents an updated version of the depositional model. Below are descriptions and interpretations of selected facies and assemblages.

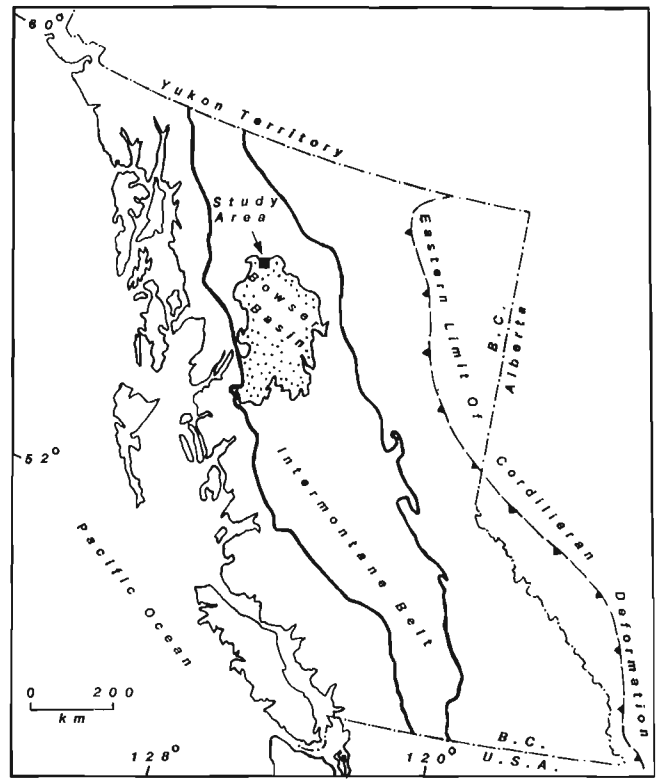

Figure 1. Location of the Bowser Basin and study area within the Intermontane Belt (modified after Wheeler and McFeely, 1987).

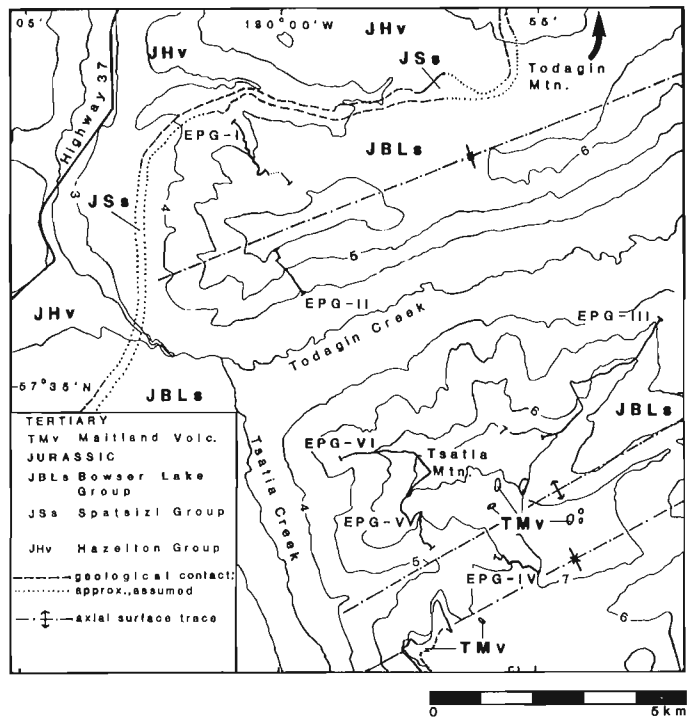

Figure 2. Generalized geological map of the study area, showing the gross stratigraphy, location of measured sections (EPG-I-VI), and axial surface traces of major folds (most geological contacts and axial surface traces adapted from Evenchick and Green, 1990).

PRODELTA-SLOPE ASSEMBLAGE

Shale/Siltstone facies

Dark grey siltstones and shales monotonously interbedded with buff-weathered mudstones and very fine grained sandstones were observed in all stratigraphic sections. This facies reaches a maximum thickness of 800 m in section EPG-I (total = 1051 m). Its striped appearance (Fig. 3) is typical of parts the Ashman Formation, originally defined by Tipper and Richards (1976). Most beds are laterally continuous and average 2-5 mm in thickness, but beds up to 20 cm occur sporadically. Normal grading is common, with tan weathered fine grained sandstones grading to grey siltstones and shales. Each shale bed is abruptly overlain by the sandstone base of the next bed. Pinch and swell of individual beds is common; in extreme cases, beds are boudinaged. Micro-flame structures verge consistently to the south.

Soft sediment slumps exist within the shale/siltstone facies. Slumps range from low-angle discordances to abruptly truncated intact sandstone units up to 20 m high and 150 m in length (Fig. 4). Most slumps on the prodelta-slope are composed of relatively coarse units (fine grained sandstone to conglomerate) within finer grained host rocks. Most slump contacts are sharp, and truncate adjacent bedding planes. Syn-sedimentary faults (most penetrating less than 5 cm into the sediment), flame structures and convolute bedding occur in sediments directly underlying slump structures. Folds within slumps range from gentle to tight and tend to verge to the south. Fold axes in slumps within section EPG-II trend northwest.

Sandstone subfacies

Intermittent sandstone units within the shale/siltstone facies, ranging from 2-22 m thick, are distinguished from the relatively fine grained rocks by positive relief of the sandstone units (Fig. 3). The tan to light grey very fine- to fine-grained sandstone beds are laterally continuous, averaging 5-30 cm

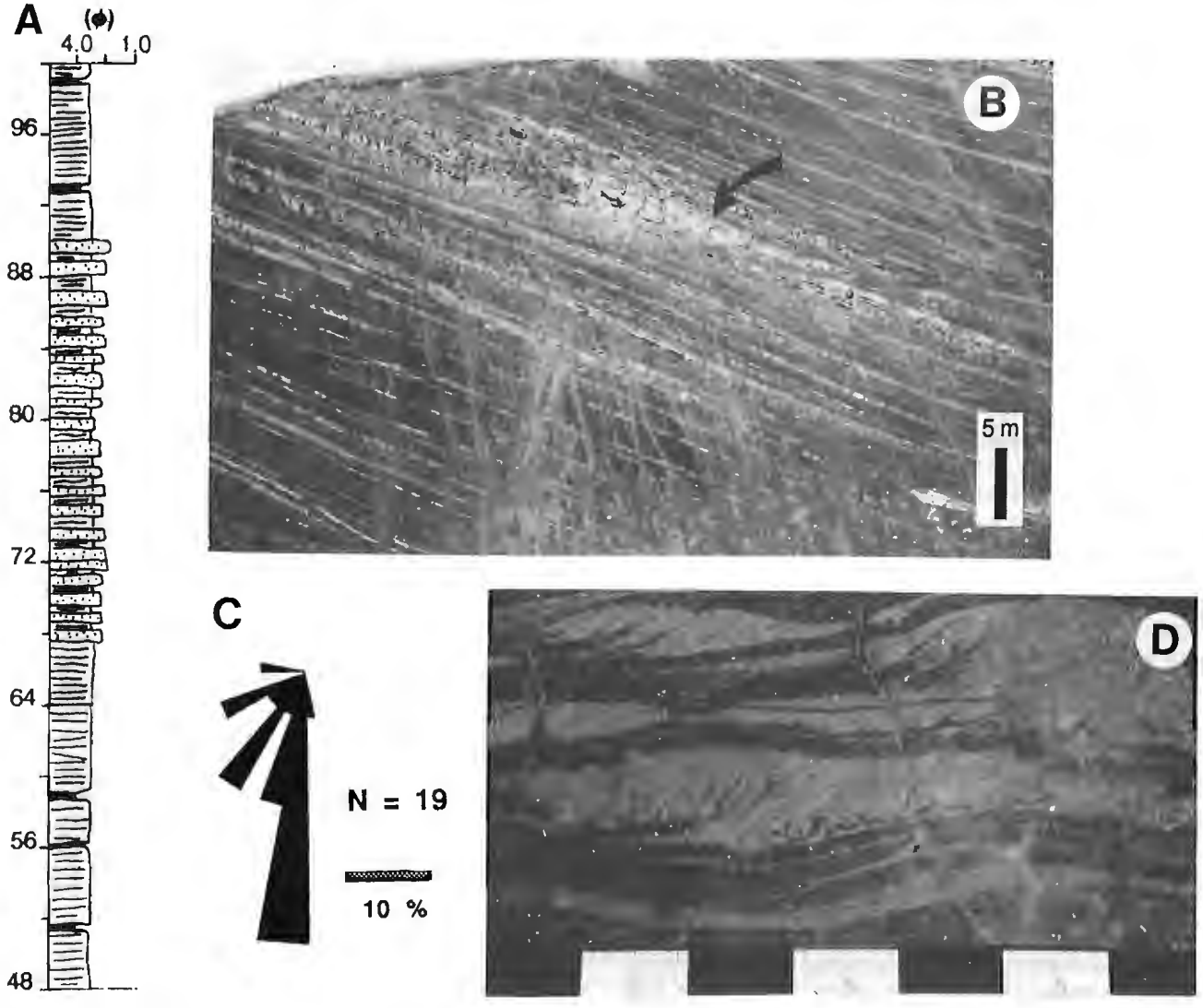

Figure 3. A. Stratigraphic section of the shale/siltstone facies of the prodelta-slope assemblage (section EPG-V, interval 048-100 m). Vertical scale is calibrated in metres. B. Typical striped appearance of the Ashman Formation. Note the fine grained sandstone intervals (arrow). C. Rose diagram of foresets of ripple cross- stratification (Section EPG-V at 076 m). D. Ripple cross-stratification within the sandstone subfacies (section EPG-V at 076 m).

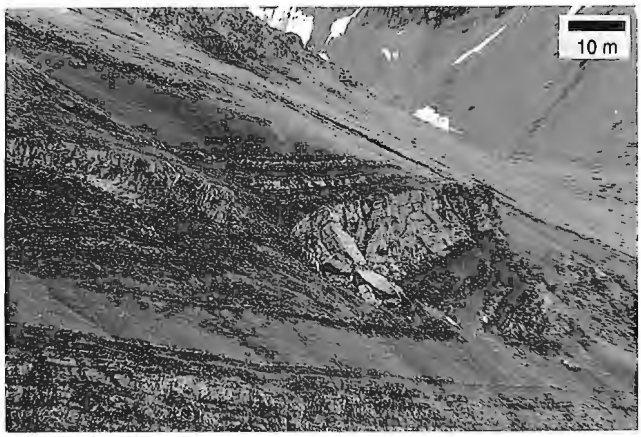

Figure 4. View looking southeast at a soft-sediment slump structure within the prodelta-slope assemblage, approximately 1 km west of section EPG-IV. Note the sharp detachment surface that truncates the slump folds.

thick. Individual beds display parallel to wavy bedding as well as pinch and swell geometries; ripple cross-stratification is common (Fig. 3). Rare siltstone rip-up clasts up to 3 cm long are elongate, rounded, and oriented parallel to bedding. A section from the prodelta-slope assemblage is shown in Figure 3.

Interpretation

The fine grained nature of the shale/siltstone facies suggests low sedimentation rates. According to Ricketts (1990), most of the sediments were introduced to the deeper, quieter portions of the basin via submarine fan systems. On the prodelta slopes, inter-submarine channel regions would receive most sediments from hemipelagic and pelagic sources. Turbiditic beds incorporating very fine grained sandstones and siltstones may represent overbank deposition from submarine channelways (Ricketts, 1990). Rip-ups and ripple cross-stratification in the sandstone subfacies may represent overbank deposits where sediment supply rates were increased. Overbank deposits probably accumulated as minor lobes or sheets where slope topography permitted. The vertical and lateral repetition of the sandstone subfacies reflects a dynamic depositional system with frequent changes in sedimentation rates and lateral migration of submarine fan channelways. Consistent southward vergence of flame structures and slump folds suggests a southerly dipping paleoslope.

SUBMARINE CANYON/GULLY ASSEMBLAGE

Channel facies

Significant amounts of conglomerate are spatially associated with the prodelta-slope facies. On Tsatia and Todagin mountains, conglomerate bodies occur as wedges from 5 m thick and 20 m wide (cross-section viewed down depositional axis) to coalesced offstacked wedges 100 m thick and 400 m across. Conglomerate bases are extremely abrupt, and typically show scouring into the underlying fine-grained rocks (Fig. 5). Conglomerate bodies are not associated with coarsening-up trends within the sedimentary sequence. Channel margins tend to pinch out laterally. Thick conglomerates (>30 m) represent a series of offstacked wedges overlapping one another. Successive wedges may even scour into underlying bodies. They are in a few places separated by thin units of siltstone and fine sandstone, generally less than 50 cm thick. Internally, conglomerates are well stratified, manifested by alternating discontinuous fine- to medium-grained sandstone interbeds (Fig. 5). Beds range from 5-40 cm thick. Bedform geometries are typically planar to slightly wavy and contain low-angle foresets; discontinuous sandstone beds commonly occur between foresets. Trough cross-stratification is rare. Inverse to normal grading is common in individual conglomerate beds, although ungraded varieties exist. Sorting of clasts is moderate to well developed. Subrounded to well-rounded, bladed clasts produce a pronounced a/b plane imbrication. Most imbricated beds display a-axis orientation parallel to flow direction (north-northeast, south-southwest direction). Clast frameworks are intact to condensed; framework to matrix ratios range from 80:20 to 70:30. The matrix is composed of fine- to medium-grained poorly sorted cherty sandstone.

Lateral exposure of a 10-50 m thick conglomerate in the upper part of the shale/siltstone facies on Tsatia Mountain reveals that the character of the channelized conglomerates changes down depositional axis (south-southwest). At the north end of Tsatia Mountain, the conglomerate unit is poorly sorted and is pervasively rusty weathered. To the south, the conglomerates become grey weathered, display clast sorting and are more distinctly stratified. At the south tip of Tsatia Mountain, approximately 1.5 km along the unit, the conglomerate beds are strongly imbricated, clast sizes are relatively small, and the proportion of interstratified sandstone increases. Viewed perpendicular to the depositional axis, the conglomerates show a change in geometry from sheetlike to a series of prograding lobes.

Interpretation

Channelized conglomerates of the submarine canyon/gully assemblage represent infillings of incised canyons and gullies (Ricketts, 1990). Coarse clastics shed from the north are inferred to have bypassed the shelf accumulations, and funnelled down the slope along depressions which may represent slump scars on the prodelta-slope. In a fluidized environment, coarse coastal sediments can be expected to eventually become well sorted and stratified with increased time and distance travelled down canyons. Channelized conglomerates tend to occur as coalesced units on Tsatia and Todagin mountains; this may reflect the location of major source supply routes from the north. The lateral offstacking of individual wedges probably reflects the sinuosity of such routes, and the repetitive vertical stacking probably records periodic increases in rates of sediment influx. Erosive channel bases and possible cannibalization of pre-existing deposits indicate high-energy episodes.

SHELF ASSEMBLAGE

On Tsatia Mountain, the shelf assemblage is documented in all four sections (EPG-III,IV,V,VI). In section EPG-III, 900 m of shelf deposits interfinger with rusty weathered conglomerates of the fan delta and coastal assemblages (discussed

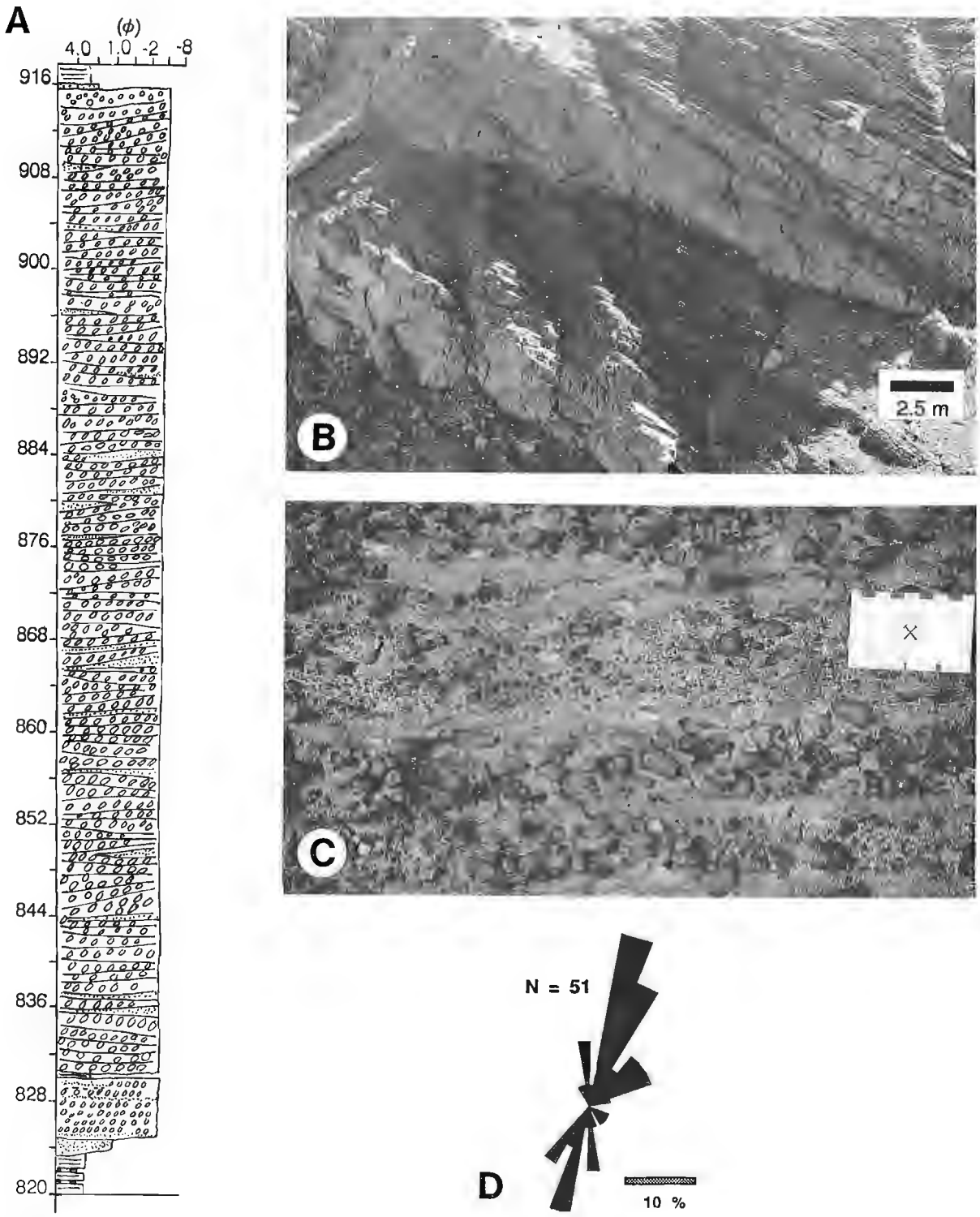

Figure 5. A. Stratigraphic section of the channelized slope-canyon conglomerate facies of the prodelta-slope assemblage (section EPG-I, interval 820-916 m). Vertical scale is calibrated in metres. B. Wedge geometry of the stacked conglomerates (section EPG-I at 484 m). C. Well-stratified conglomerate and sandstone beds (section EPG-I at 900 m). D. Rose diagram of a/b plane clast imbrication in conglomerates (section EPG-I at 828 m).

in next section). Section EPG-IV contains the thinnest shelf assemblage, measuring 116 m. Sections EPG-V and VI exhibit similar shelf thicknesses of approximately 640 m. The shelf assemblage contains cyclical coarsening-up packages of siltstone, sandstone, and sporadic caps of conglomerate. Individual cycles range from 5 m (Fig. 6) up to 30 m thick. Cycle bases are characterized by recessive thinly bedded shales containing minor amounts (<10 %) of mudstone and chert pebbles. Grain size and bed thickness increase upwards. Towards the top of the cycles, fine- to medium-grained sandstones contain abundant concretions that range from perfectly spherical to oblong. Ranging from 1 cm to 1 m in diameter, they are post-compactional and tend to obscure primary sedimentary structures. Brown to tan weathered calcareous (dolomitic?) horizons best preserve sedimentary structures. Low-angle planar cross-stratification is a common bedform in coarse grained parts of the cycles. Wavy cross-stratification and planar beds also are common. Fossil-rich beds near the tops of cycles are up to 20 cm thick, and contain up to 60 % disarticulated pelecypods, belemnites, ammonites and rare gastropods. Sporadic rounded chert pebbles and sandstone rip-ups are associated with these beds. Apart from the capping conglomerates described by Ricketts (1990), poorly sorted chert-lithic pebble conglomerates occur sporadically throughout the shelf assemblage. These 20-40 cm thick conglomerate beds occur in shale and sandstone components of cycles. Characterized by abrupt, undulatory erosive bases with pebble-filled scours and flat tops, the conglomerates commonly grade into sandstones. Frameworks are intact to condensed, and clasts show extreme ranges in size, shape and composition. The largest clasts tend to 'float' in the middle of beds. Mud clasts and fossil fragments are locally abundant; the matrix is composed of mud and medium grained poorly sorted cherty sandstone. Matrix content tends to increase towards the tops of beds, and towards the top of each shelf assemblage section, the abundance of carbonaceous plant fragments shows a subtle increase. Plant fragments, which rarely compose more than 3 % of the rocks, are generally less than 1 cm thick, and occur throughout the siltstone and sandstone beds. The ratio of rusty to grey weathering in sandstones also increases as the conglomerates of the fan delta/coastal assemblage are approached. This is particularly obvious in the concretionary sandstones at the tops of cycles.

Interpretation

The lateral variation in shelf thickness over a relatively small region indicates either a complex margin with different shelf widths or regions of selective preservation (eg. inter-fan shelves). The cyclicity in both lithology and fossil content

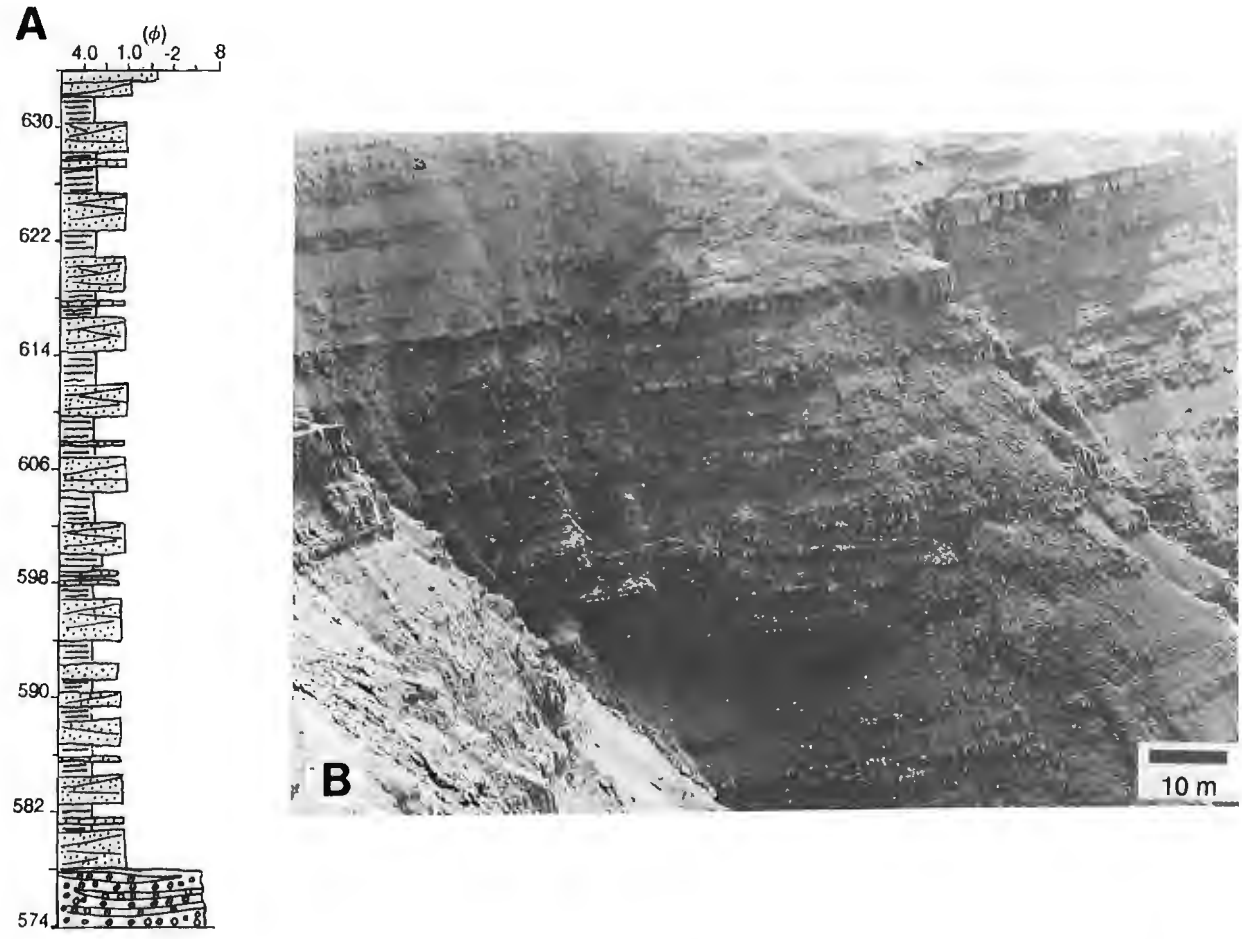

Figure 6. A. Typical section of the shelf assemblage (section EPG-III, interval 574-634 m). Vertical scale is calibrated in metres. B. View looking southeast showing the cyclical nature of shelf assemblage (laterally equivalent to section EPG-VI at 300 m).

suggests relatively shallow waters which were sensitive to transgressive and regressive events. The upward increase in carbonaceous matter supports proximity to coastal regions. Randomly distributed, poorly sorted conglomerates are interpreted as storm or seismic deposits.

FAN DELTA/COASTAL ASSEMBLAGES

Rusty weathered chert pebble- to cobble-conglomerates comprise several lithofacies within the Bowser Lake Group. A 5 m-thick unit occurs at the top of section EPG-II on Todagin Mountain; rusty conglomerates and sandstones also occur in all four sections measured on Tsatia Mountain. These conglomerates are sheetlike and extend for several kilometres within the Tsatia Mountain massif; amalgamated conglomerate units on the north side of Tsatia diverge southward into the shelf assemblage. A 14° discordance between the rusty conglomerate facies and the shelf assemblage can be seen 1 km southwest of section EPG-IV (Fig. 7). Rusty conglomerate units (some up to 50 m thick) are separated by siltstones and shales which tend to coarsen upwards. Medium grained sandstones at the base of the conglomerates are pervasively rusty weathered and tend to be concretionary. Towards the top of Tsatia Mountain, carbonaceous shales less than 1 m thick occur between the upper two units of rusty conglomerate. The internal fabric of the rusty conglomerates is diverse and differs from the channel conglomerates. Bed thicknesses range from 10-40 cm. Bedforms include planar cross-stratification (Fig. 8) and trough cross-stratification inclined 10°-20°. Non-graded beds are most common, although normal grading exists up foreset dip. Clast sorting and imbrication are moderate to poor, and outsized clasts are common (Fig. 8). Clasts range from rounded to subangular and display a wide range of sphericities. Discontinuous sandstone beds occur less frequently than in the channelized conglomerate facies. Framework to matrix ratios are similar to the above channelized conglomerate facies, but openwork conglomerates occur in the upper parts of some beds. Carbonaceous plant fragments are common within the rusty conglomerates. A displaced 2 m x 10 cm tree trunk was observed near the top of section EPG-III. Marine fossils such as pelecypods and ammonites occur sporadically within the conglomerates, generally as fragments.

Interpretation

Rusty conglomerates and their lithological associations in the Tsatia Mountain area are consistent with lithofacies divisions of the rusty lithosome shown in Table 1 of Ricketts and Evenchick (1991). For example, a gravel barrier-lagoon facies within the coastal assemblage is supported by the presence of carbonaceous shales between rusty conglomerate units. On Tsatia Mountain, the presence of diversely oriented and locally opposed foresets within sheetlike units may represent coalesced fan deltas, or gravel bars on braid deltas. Marine fossils could be introduced onto coastal regions by short-lived transgressions. Evidence of Gilbert-type fan deltas within the immediate study area is lacking. The discordance between the rusty conglomerates and shelf assemblage on Tsatia Mountain, representing one of the local discordances described by Ricketts and Evenchick (1991), may have developed in response to intrabasinal faulting, although this has yet to be proven.

Figure 7. View looking southeast showing local discordance between the rusty conglomerates and the shelf assemblage (1 km southwest of section EPG-IV).

PALEOCURRENT DATA

Data from three different facies provide a sampling of paleocurrent trends within the study area. Foresets in ripple cross-stratification of the prodelta-slope sandstone subfacies indicate sediment transport in a south to southwesterly direction (Fig. 3). Clast imbrication studies in beds of conglomerate where preferential erosion provides three dimensional views of clasts, were based on clasts with a/b ratios greater than 2:1 and a-axes greater than 2 cm. Imbrication data from one locality of the channelized conglomerates indicate strongly bipolar north-northeast to south-southwest dip directions with a-axes aligned parallel to flow (Fig. 5). Braid bars in deep sea valley fill deposits also show bipolar imbrication, with a-axes parallel to flow (cf. Hein, 1984). The facies association of conglomerates in concert with a-axes parallel to flow, supports an interpretation of deep sea braid bars. Thus bipolar paleocurrent trends are expected (Fig. 5). An example of imbrication within rusty conglomerates of the coastal assemblage is illustrated in Figure 8. A bipolar northwest-southeast a-axis imbrication with minor trends towards the southwest and east-northeast indicates complex flow directions. Such trends might reflect currents flowing across gravel bar fronts (cf. Hein, 1984). Regardless, the dominant north to south trend is consistent with the above data, which support the findings of Eisbacher (1974a, 1981) of a southerly sediment transport direction for the northern part of the basin.

CLAST COMPOSITIONS

An examination of vertical and lateral clast composition changes within measured sections was conducted by means of megascopic point counts of conglomerates in section EPG-I (Fig. 5). Division of clast types is based on volcanics versus chert, the latter divided by colour into black, green, and grey. Most of the volcanic clasts are felsic, and commonly contain feldspar phenocrysts. A preliminary examination of clast abundances (normalized to 100%) reveals no appreciable

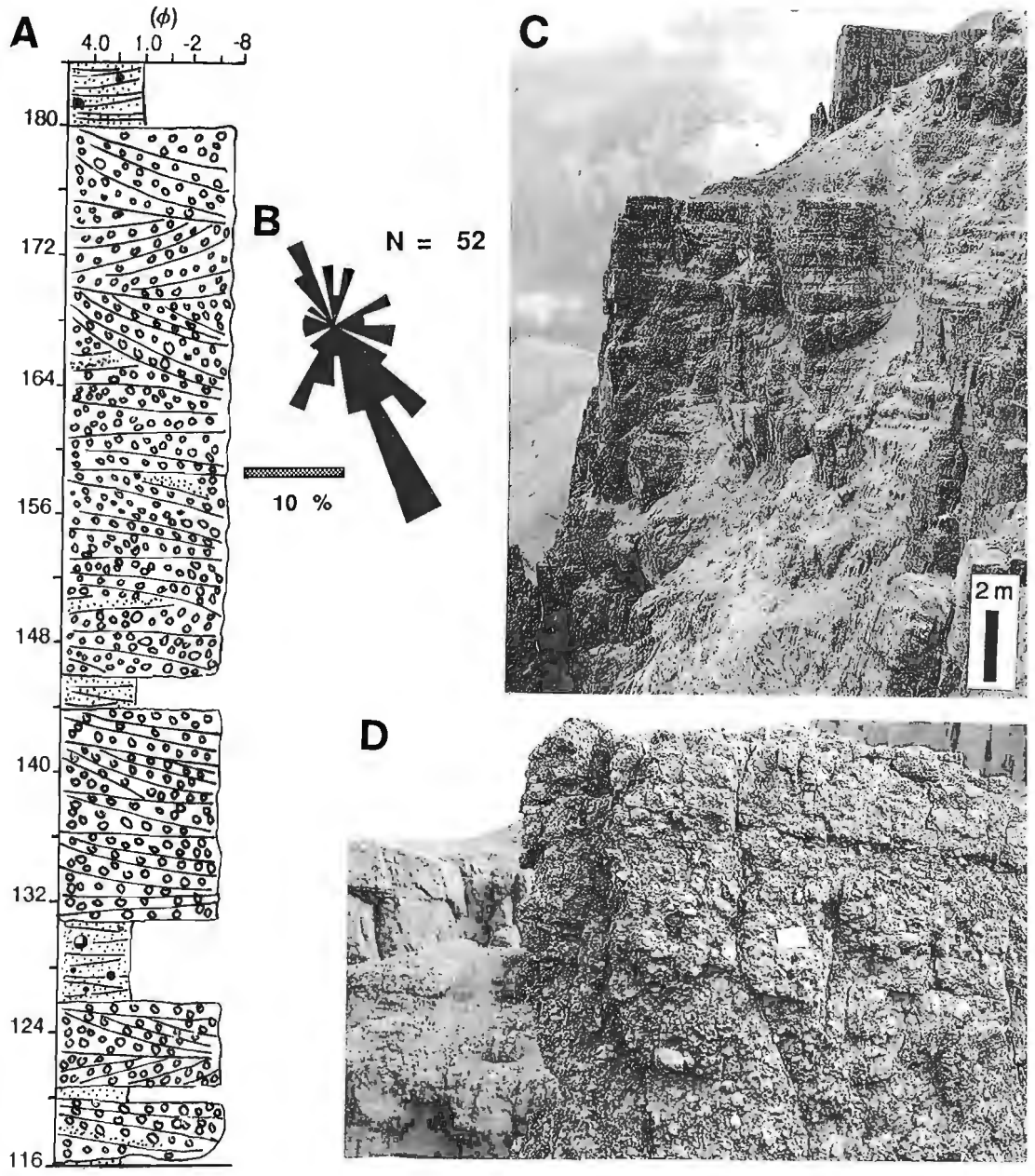

Figure 8. A. Stratigraphic section through rusty conglomerates of the fan delta/coastal assemblages (section EPG-IV, interval 116-184 m). Vertical scale is calibrated in metres. Solid black circles represent concretions. B. Rose diagram of a/b plane clast imbrication (section EPG-IV at 125 m). C. Foresets truncated by topset beds. D. Poor sorting typical of the rusty conglomerates.

vertical trends within the measured section (Fig. 9). Lateral studies of an extensive conglomerate on Tsatia Mountain at the top of the shale/siltstone facies produced similar results.

SUMMARY

Data based on preliminary examination of selected measured sections representing the prodelta-slope (shale/siltstone facies), submarine canyon/gully (channel facies), shelf, and fan delta/coastal assemblages are consistent with the findings of Ricketts (1990), and Ricketts and Evenchick (1991). A sandstone subfacies added to the shale/siltstone facies is inferred to represent overbank deposits from submarine channelways.

Paleocurrent data including ripple cross-stratification foresets and a/b plane clast imbrication in conglomerates suggest that the main flow direction was to the south-southwest. Data from the rusty conglomerates suggest that complex flow patterns were produced by sedimentation in submarine gravel bars.

Preliminary examination of vertical and lateral clast composition changes in conglomerates within the study area revealed no significant trends.

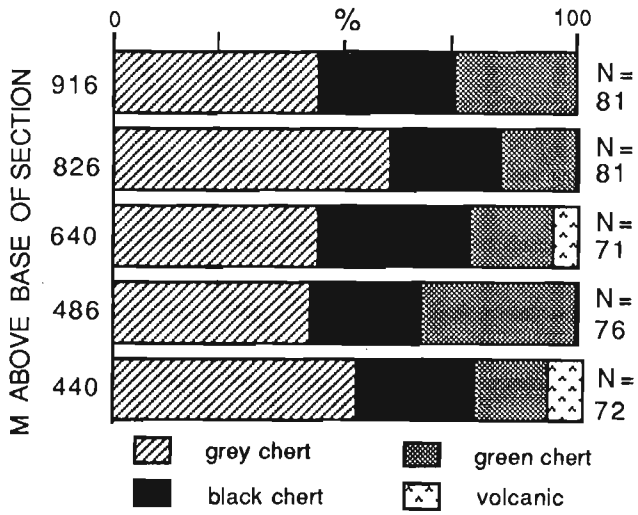

Figure 9. Clast compositions from section EPG-I. Note that the relative abundance of clast types remains constant throughout the section.

ACKNOWLEDGMENTS

I thank Carol Evenchick (GSC-Vancouver) for introducing me to Cordilleran geology. Also, Al Donaldson (Carleton University) and Larry Aspler provided invaluable assistance in preparation of this report. Brian Ricketts (GSC-Vancouver) taught me a great deal about sedimentology. I thank Andrew Kaip, Randy Castelleran, and Mike Toolan for their assistance in collection of data. Financial assistance from J.A. Donaldson's NSERC Operating Grant, and from a Northern and Native Studies Northern Science Training Grant, is appreciated.

REFERENCES

Cookenboo, H.O. and Bustin, R.M.
1990: Lithostratigraphy of the northern Skeena Mountains, British Columbia; in Current Research, Part F, Geological Survey of Canada, Paper 90-1F, p. 151-156.

Eisbacher, G.H.
1974a: Deltaic sedimentation in the northeastern Bowser Basin, British Columbia; Geological Survey of Canada, Paper 73-33, 13 p.
1974b: Evolution of successor basins in the Canadian Cordillera; in Modern and Ancient Geosynclinal Sedimentation, R.H. Dott, Jr. and R.H. Shaver (ed.), Society of Economic Paleontologists and Mineralogists, Special Publication 19, p. 274-291.
1981: Late Mesozoic-Paleogene Bowser Basin molasse and Cordilleran tectonics, western Canada; in Sedimentation and Tectonics in Alluvial Basins, A.D. Miall (ed.), Geological Association of Canada, Special Paper 23, p. 125-151.
1985: Pericollisional strike-slip faults of synorogenic basins, Canadian Cordillera; in Strike-Slip Deformation, Basin Formation, and Sedimentation, K.T. Biddle and N. Christie-Blick (ed.), Society of Economic Paleontologists and Mineralogists, Special Publication 37, p. 265-282.

Eisbacher, G.H., Carrigy, M.A., and Campbell, R.B.
1974: Paleodrainage patterns and late-orogenic basins of the Canadian Cordillera; in Tectonics and Sedimentation, W.R. Dickinson (ed.), Society of Economic Paleontologists and Mineralogists, Special Publication 22, p. 143-166.

Evenchick, C.A.
in press: Geometry, evolution, and tectonic framework of the Skeena fold belt, north-central British Columbia; Tectonics.

Evenchick, C.A. and Green, G.M.
1990: Structural style and stratigraphy of southwest Spatsizi map area, British Columbia; in Current Research, Part F, Geological Survey of Canada, Paper 90-1F, p. 135-144.

Gabrielse, H. and Tipper, H.W.
1984: Bedrock geology of Spatsizi map area (104H); Geological Survey of Canada, Open File 1005.

Hein, F.J.
1984: Deep sea and fluvial braided channel conglomerates: a comparison of two case studies; in Sedimentology of Gravels and Conglomerates, E.H. Koster and R.J. Steel (ed.), Canadian Society of Petroleum Geologists, Memoir 10, p. 33-49.

Ricketts, B.D.
1990: A preliminary account of sedimentation in the lower Bowser Lake Group, northern British Columbia; in Current Research, Part F, Geological Survey of Canada, Paper 90-1F, p. 145-150.

Ricketts, B.D. and Evenchick, C.A.
1991: Analysis of the Middle to Upper Jurassic Bowser Basin, northern British Columbia; in Current Research, Part A, Geological Survey of Canada, Paper 91-1A.

Souther J.G. and Armstrong, J.E.
1966: North-central belt of the Cordillera of British Columbia; in Canadian Institute of Mining and Metallurgy, Special Volume 8, p. 171-184.

Tipper, H.W. and Richards, T.A.
1976: Jurassic stratigraphy and history of north-central British Columbia; Geological Survey of Canada, Bulletin 270, 73 p.

Wheeler, J.O. and McFeely, P. (compilers)
1987: Tectonic assemblage map of the Canadian Cordillera and adjacent parts of the United States of America; Geological Survey of Canada, Open File 1565.

Stratigraphic and structural relations along the west-central margin of the Bowser Basin, Oweegee and Kinskuch areas, northwestern British Columbia[1]

C.J. Greig[2]
Cordilleran Division, Vancouver

Greig, C.J., Stratigraphic and structural relations along the west-central margin of the Bowser Basin, Oweegee and Kinskuch areas, northwestern British Columbia; in Current Research, Part A, Geological Survey of Canada, Paper 91-1A, p. 197-205, 1991.

Abstract

In the Oweegee and Kinskuch areas, southwest vergent structures predominate within the Jurassic and Lower Cretaceous Bowser Lake Group along the northeast margins of basement culminations. In basement rocks in the Oweegee Range, structures pre- and postdate the Lower and lower Middle Jurassic Spatsizi Group. The younger structures may not link kinematically with those in the Bowser Lake Group. In the Kinskuch area, basement structures have southwest-directed shortening.

New fossil localities in the Oweegee and Kinskuch areas contain faunas diagnostic of the Lower Jurassic, thus confirming the presence of Hazelton Group rocks. The Hazelton Group appears to underlie much of the Oweegee dome. Map relations with Permian limestone and the Stuhini and Spatsizi groups suggest that the Hazelton Group was deposited on a surface with significant relief.

Résumé

Dans la région d'Oweegee et de Kinskuch, on remarque la présence dominante de structures à vergence sud-ouest au sein du groupe de Bowser Lake, du Jurassique et du Crétacé inférieur le long des marges nord-est des culminations de socle. Dans les roches de socle du chaînon Oweegee, les structures sont antérieures et postérieures au groupe de Spatsizi du Jurassique inférieur et de la base du Jurassique moyen. Les structures plus récentes ne présentent aucun lien cinématique avec celles du groupe de Bowser Lake. Dans la région de Kinskuch, les structures de socle présentent un raccourcissement à direction sud-ouest.

Les nouvelles localités de fossiles découvertes dans les régions d'Oweegee et de Kinskuch contiennent des faunes caractéristiques du Jurassique inférieur, confirmant ainsi la présence de roches du groupe de Hazelton. Ce dernier semble s'étendre sous la grande partie du dôme Oweegee. Des corrélations cartographiques avec le calcaire permien et les groupes de Stuhini et de Spatsizi semblent indiquer que le groupe de Hazelton a été mis en place sur une surface à relief important.

[1] Contribution to the Frontier Geoscience Program (Bowser Basin project)
[2] Department of Geosciences, University of Arizona, Building #77, Tucson, Arizona 85721, U.S.A.

INTRODUCTION

This report describes preliminary results of 1990 mapping in the Oweegee Range and Kinskuch Lake area, northwestern British Columbia (Fig. 1). The work represents the initiation of a three season mapping program focusing on the stratigraphic and structural relationships between the Jurassic and Lower Cretaceous Bowser Lake Group and its Paleozoic and earlier Mesozoic Stikine terrane basement rocks in west-central Bowser Basin.

Evenchick (in press) has proposed that the northern part of the Bowser Basin consists of a latest Jurassic(?) to latest Cretaceous northeast-directed fold belt (Skeena Fold Belt) with shortening of up to 50 % across its greater than 200 km width. This proposal has significant implications for local and regional structural studies and for tectonic reconstructions, and provides the impetus for the present project. The mandate of this study is to examine the poorly known west-central part of the Skeena Fold Belt and Bowser Basin and to investigate how shortening is accommodated in the basement rocks. Thus, the structural transition between the Bowser Lake Group and its basement has been the focus for initial mapping. The stratigraphic transition is also important because rocks underlying the Bowser Lake Group along much of its western margin include precious and base metal-rich rocks of the Lower and Middle Jurassic Hazelton Group and the lower to lower Middle Jurassic Spatsizi Group. Recent discoveries of significant stratabound mineral occurrences have refocussed exploration activity on this stratigraphy and, as a consequence, a better understanding of the distribution of the Hazelton Spatsizi and Bowser Lake groups and of their structural style, may prove of use to mineral explorationists.

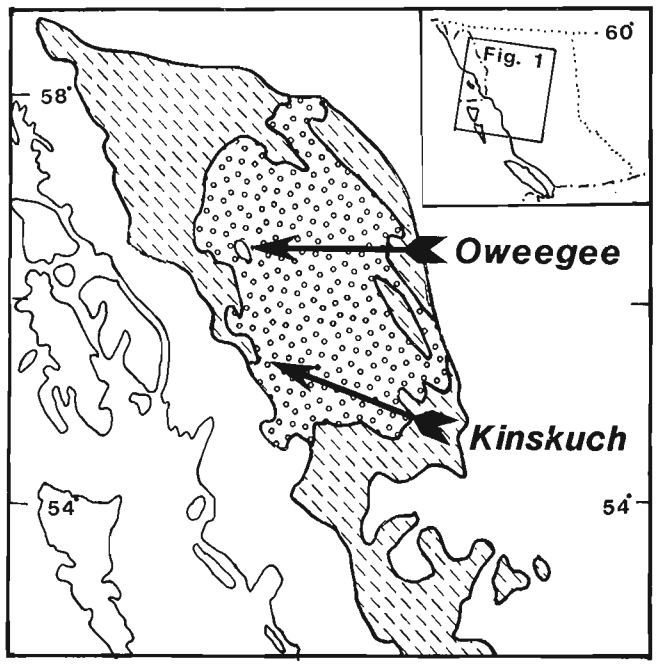

Figure 1. Location map of Oweegee and Kinskuch areas, north-central British Columbia. Stippled pattern represents Bowser Lake Group strata; hachured pattern represents Middle Jurassic and older basement rocks of the Stikine terrane (after Evenchick, manuscript in prep.).

This study is funded by the Frontier Geoscience Program as part of the Bowser Basin project, which is under the direction of C.A. Evenchick. The mapping and associated research forms part of doctoral studies being undertaken at the University of Arizona under the supervision of G.E. Gehrels.

OWEEGEE RANGE

In the Oweegee Range, a structural culmination, commonly referred to as the "Oweegee dome (Koch/1973)," forms one of the few places where basement rocks are exposed in the Bowser Basin. The Oweegee dome has been described previously by Koch (1973) and by Monger (1977). Mapping during July of 1990 focused on the northeastern side of the Oweegee dome and on Bowser Lake Group rocks to the east. Figure 2 shows the distribution of map units in the northern Oweegee Range.

Stratigraphy

Permian limestone

Pale grey weathering Permian limestone occurs on the ridge system northeast of Oweegee Peak, and in several exposures on both sides of the Skowill Creek valley. Exposures low in Skowill Creek valley were not examined. Layering in the dark grey, massive to thick bedded but predominantly medium bedded bioclastic limestone is commonly outlined by discontinuous layers of tan weathering black chert. Fossils are common and include solitary and colonial corals, fusulinids, bryozoans and crinoids.

The limestone body northeast of Oweegee Peak is in fault contact with Upper Triassic Stuhini Group rocks and in most places, with Lower and Middle Jurassic rocks of the Hazelton Group as well. Faulted contacts with Hazelton Group rocks were likely originally depositional, as tuffaceous rocks near the contact contain local carbonate fragments and locally, such as at the northernmost end of the limestone, rocks correlative (?) with the Hazelton Group overlie the Permian rocks. Previously, some of the rocks assigned to the Hazelton Group in this study were thought to be older than the limestone (Koch, 1973; Monger, 1977). The complexity of Hazelton Group-limestone contact relationships, both at this locality and west of Skowill Creek, is considered to result from deposition on a surface with considerable relief and from later modification by faults.

Stuhini Group

The Stuhini Group includes abundant medium to dark green, thick bedded turbiditic tuffaceous(?) sandstone, somewhat less common black siliceous siltstone, dark green crystal lithic dacite or andesite ash and lapilli tuff, and rare pyritic siliceous tuff, pyroxene-plagioclase phyric basalt, and thin (<30 cm) carbonate lenses. No fossils were found, although Monger (1977) reported the presence of Late Triassic ribbed belemnites from northeast of Oweegee Peak. Stuhini Group rocks are in fault contact with Permian limestone to the north and Hazelton Group volcanic rocks to the south and are overlain

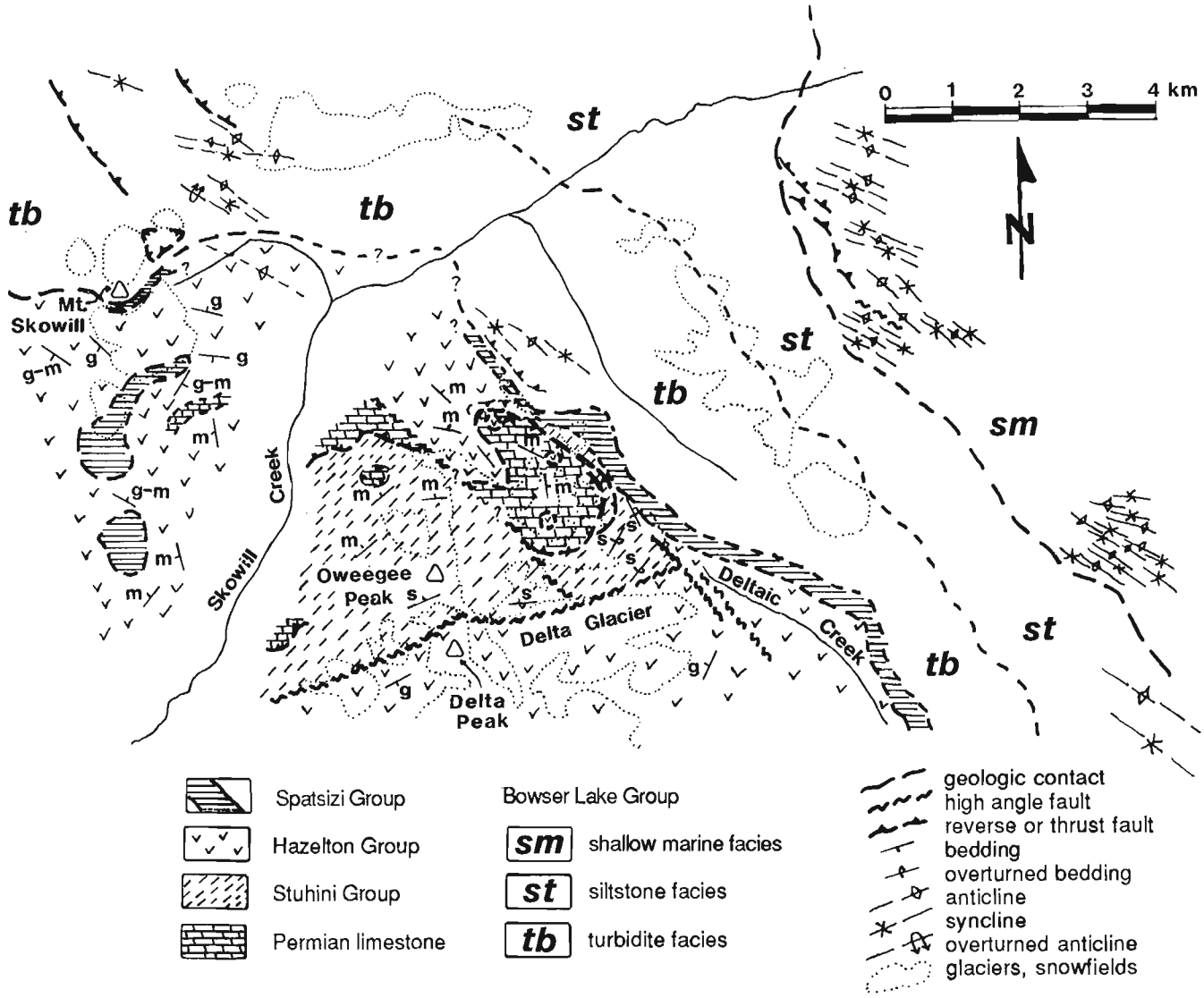

Figure 2. Generalized geology, northern Oweegee range.

unconformably along their northeast margin by the Spatsizi Group. Stuhini Group rocks reported by Monger (1977) to lie west of Skowill Creek were examined only briefly. They appear to be indistinguishable from overlying Hazelton Group rocks and are tentatively assigned to that map unit.

Hazelton Group

Much of the Oweegee dome is underlain by a thick succession of volcanic and subordinate volcaniclastic rocks of the Lower and Middle Jurassic Hazelton Group. Lower and Middle Jurassic fossils, heretofore unknown from the Oweegee dome, were found west of Skowill Creek and northeast of the toe of Delta glacier.

In exposures of Hazelton Group west of Skowill Creek and south of Mt. Skowill, well-layered and typically gently dipping maroon and green feldspathic crystal lithic ash and lapilli tuff predominate. Farther to the south, more varied lithologies occur. They include abundant tuff-breccia limy lapilli and ash tuff, polymictic boulder conglomerate, and distinctive buff weathering coarse arkosic wacke that is locally fossiliferous. Near the upper part of the section, rusty and pale weathering dacite to rhyolite flows are common.

Hazelton Group rocks east of Skowill Creek and north of Oweegee Peak, in part previously referred to as pre-Permian (Monger, 1977), consist mainly of dark green and maroon feldspathic basaltic(?)-andesite lapilli tuff and tuff-breccia, but also include subordinate feldspar porphyritic amygdaloidal andesite flows and flow breccia as well as pale weathering dacite to rhyolite flows(?) and flow breccia.

South of Oweegee Peak, the Hazelton Group was examined in detail only in two areas: at its northern end and at the southernmost end of the Oweegee dome. However, it appears that the intervening area is underlain by gently to moderately dipping massive volcanic units of the Hazelton Group. As with Hazelton Group exposures north of Oweegee Peak, green and maroon feldspathic crystal lithic andesite ash and lapilli tuff dominate; more felsic(?) dust tuff and more mafic (basaltic-andesite?) tuff-breccia are subordinate.

Northeast of Delta glacier, near the fault separating the Hazelton and Stuhini groups, lithologies of the Hazelton Group are more varied and more deformed. In addition to the ubiquitous green andesite ash tuff, lapilli tuff and tuff-breccia are local pyroxene feldspar porphyritic basaltic volcanic breccia, fossiliferous medium bedded, pale brown weathering limestone, green to black laminated to thin bedded siltstone and sandstone, and massive pale green to black silty (locally tuffaceous and/or limy) mudstone. Most of the finer grained rocks in this area, both sedimentary and pyroclastic, display abundant evidence for synsedimentary deformation.

Spatsizi Group

Rocks assigned to the Lower to lower Middle Jurassic Spatsizi Group (Thomson et al., 1986) outcrop in a thin (30-250 m) but relatively continuous belt around the northern margin of the Oweegee dome. Thus, they appear to form the basal unit of the "cover" rocks to the basement rocks in the Oweegee dome. Spatsizi Group rocks are characterized by their relatively thin bedded and siliceous character compared to overlying clastic rocks of the Bowser Lake Group. Laminated and thin bedded black siliceous siltstone is the most common lithology, but discontinuous silty limestone layers up to 0.5 m thick, thin bedded chert, and pale weathering pyritic clay-altered dust tuff(?) are also commonly present.

Along the northeast margin of the Oweegee dome, near the headwaters of Deltaic Creek, moderately northeast dipping Spatsizi Group rocks unconformably overlie overturned Stuhini Group rocks steeply west dipping. The lowermost bed of the Spatsizi Group in this area is a pebbly siltstone which has up to 10 cm of relief at its base. Immediately overlying rocks are typical of the Spatsizi Group elsewhere in the Oweegee area. The unconformable relationship of Spatsizi with Stuhini Group rocks indicates that either Hazelton Group rocks were never deposited on this part of the Stuhini Group or that considerable uplift (and deformation?) must have occurred during or following deposition of the Hazelton Group and prior to deposition of the Spatsizi Group. Contacts with the Hazelton and Bowser Lake groups were not directly observed, but from the distribution of map units and from a general lack of evidence for deformation in the Spatsizi Group, the contacts are inferred to be stratigraphic.

Bowser Lake Group

North and east of the Oweegee dome, the Jurassic and Lower Cretaceous Bowser Lake Group has been tentatively subdivided into three facies: a turbidite facies on the west, a shallow marine facies on the east, and an intervening siltstone-rich facies. The turbidite facies appears to be the oldest of the three, and in general grades upward into the siltstone facies. The siltstone facies appears to grade both upward and laterally into the shallow marine facies. The relationships are consistent with the predominant eastward dips in the units and with their map distribution, but their relative ages are somewhat uncertain because of complex structure and a lack of marker units.

Rocks of the turbidite facies are characterized by thin, medium and thick bedded, fine to medium grained dark grey to black silty sandstone beds with few internal sedimentary structures (AE turbidites). These are interbedded with abundant dark grey to black laminated to massive siltstone. The siltstone facies consists of thick sequences of black siltstone with regularly interbedded (5-10 m) buff weathering, iron carbonate cemented, fine grained sandstones (Fig. 3). Rocks of this facies also display abundant evidence for bioturbation. The shallow marine facies, like the turbidite facies, contains a relatively greater proportion of sandstone than does the siltstone facies. Sandstone of the shallow marine facies, however, is relatively well sorted compared to that of the turbidite facies. Crossbeds are also common and bedding surfaces commonly contain ripple marks. The unit is further distinguished from rocks of the other facies by common bivalve and oyster coquinas.

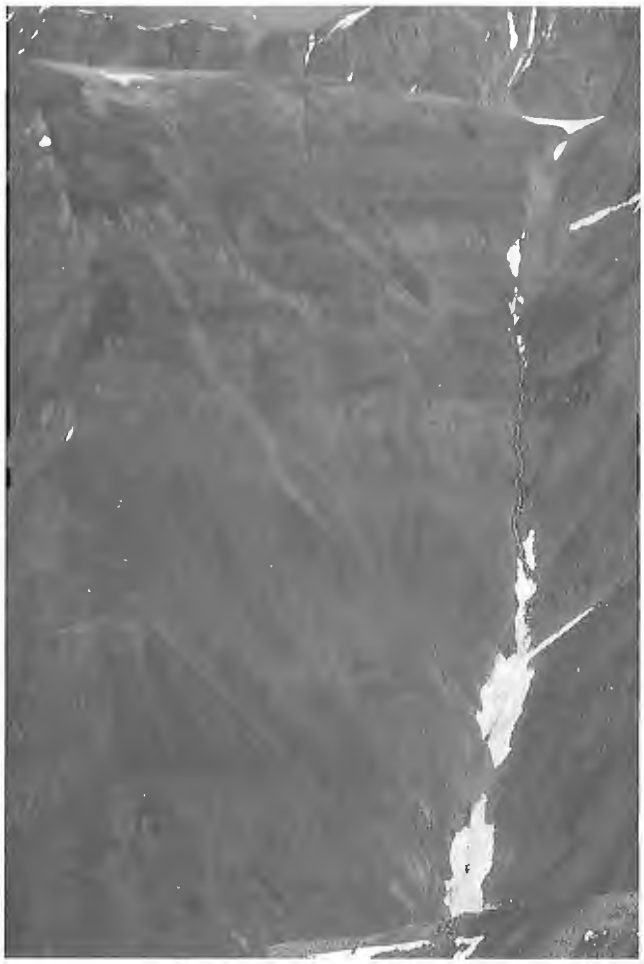

Figure 3. Gradational contact between rocks of the siltstone facies (lower half) and shallow marine facies of the Bowser Lake Group, Oweegee Range. View is to northeast; beds dip moderately to steeply northeast; difference in elevation between top and bottom of section is 450 m.

Structure

Structures in the Oweegee Range may be subdivided on the basis of whether or not they involve the Spatsizi Group. Structures which do not are restricted to rocks within the

Figure 4. Fault contact between near-vertical volcaniclastic rocks of the Stuhini Group and massive gently dipping volcanic rocks of the Hazelton Group on the north side of Delta Peak (high point in photo), Oweegee Range. View is to west-southwest. The moderately to steeply south dipping fault is near the centre of the photo and is marked by a thin linear snowpatch which trends from the saddle toward the lower left corner of the photo. Difference in elevation between cirque and peak is 500 m.

Figure 5. Southwest dipping reverse fault juxtaposing pale grey Permian limestone (forming cliffs, ~150 m high) with dark weathering Stuhini Group volcaniclastic rocks, north-east margin of Oweegee dome.

dome, but may, however, be difficult to distinguish from younger structures because all are brittle and later structures may have reactivated earlier ones. At this preliminary stage it is difficult to establish a kinematic link between structures within the dome and those in the Bowser Lake Group.

Within the Oweegee dome, the most notable pre-Spatsizi structures are northwest dipping fault(s) which place Permian limestone on Stuhini Group rocks, and a steeply south dipping fault which juxtaposes the Stuhini Group on the north with Hazelton Group rocks on the south (Fig. 4). The faults are unrelated. The fault separating the Stuhini and Hazelton groups locally truncates structures which conform to the Permian limestone-Stuhini Group fault contact. Near the northeast margin of the dome are several steeply southwest to south dipping faults (Fig. 5), some of which have components of southwest side up and dextral motion.

Folds and faults in the Bowser Lake Group are best outlined by relatively resistant rocks of the shallow marine facies. Chevron folds, in most cases more tightly-spaced than those shown in Figure 6, typically verge southwest. A number of thrust faults of small displacement (10-100 m) were noted, but could not be traced for any significant distance; most verge southwest. Nearer to the dome, in the siltstone and turbidite facies, structures are more difficult to identify because of the recessive character of the rocks, but in general, folds appear to be tighter, more upright, and hinges are more commonly disrupted.

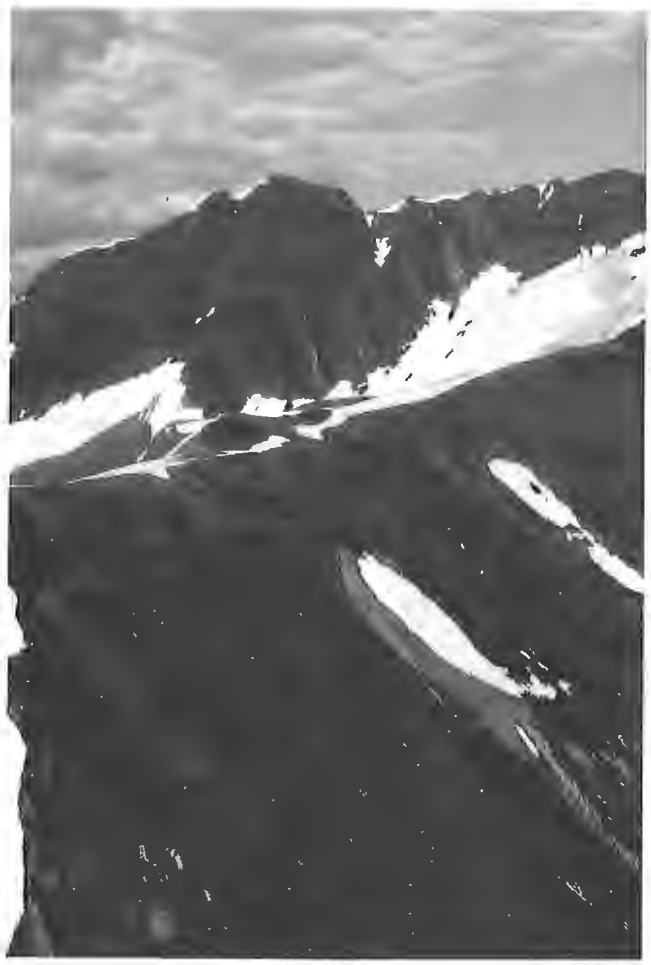

Figure 6. Southwest vergent chevron folds in the shallow marine facies of the Bowser Lake Group, Oweegee Range. Recessive rocks of the siltstone facies underlie the ridge in foreground. Cliff with fold is 150 m high.

KINSKUCH LAKE

The Kinskuch Lake area lies approximately 100 km due south of the Oweegee Range (Fig. 1). Although not truly forming an inlier in the Bowser Basin, basement rocks in the Kinskuch area are nearly surrounded by rocks considered age-equivalent with the Jurassic and Lower Cretaceous Bowser Lake Group.

In an attempt to trace structures from the Bowser Lake Group into the older rocks, a well-exposed area extending across the structural grain outlined by previous workers (Alldrick et al., 1986; Grove, 1986; Hanson, 1935) was mapped in August and early September of 1990. Results of the mapping are shown in Figure 7.

Stratigraphy

In spite of the relative abundance of sedimentary rocks in the Kinskuch area, fossils are rare, and therefore absolute ages of map units are poorly constrained. However, regional correlations and limited paleontological data suggest that rocks of units 1, 2 and 3 are equivalents of the Upper Triassic Stuhini Group and rocks of units 4 and 5 are equivalents of the Lower and Middle Jurassic Hazelton Group (D.J. Alldrick, pers. comm., 1990; Anderson, 1989). Based on similar reasoning, units 6 and 7 are probable equivalents of the Lower and Middle Jurassic Salmon River Formation and the Jurassic and Lower Cretaceous Bowser Lake Group. Using the stratigraphic nomenclature of Anderson and Thorkelson (1990), unit 5 would correlate, in part, with the Lower and Middle Jurassic Salmon River Formation.

On both the east and west margins of the study area, the relative ages of units are known, but this is not so in the central part. Most of the doubt arises from the uncertain affinity of rocks and uncertain nature of faults near the north end of Kinskuch Lake. This area received little attention and further mapping is necessary.

Stuhini Group

Unit 1: Deformed black clastic rocks

The western margin of the study area is underlain by thin bedded silty argillite and fine grained sandstone, and by rare rusty weathering siliceous siltstone and lenses and discontinuous beds of tan to medium grey silty limestone up to 40 cm thick. The unit is characterized by steeply dipping, commonly contorted and highly veined and fractured beds. Alteration related to iron carbonate veining locally gives the rocks a striped black and tan or orange appearance. The contact with mafic rocks to the east (unit 2), where observed, is commonly marked by orange limonitic zones, probably related to dyke intrusion and iron carbonate alteration. In several localities, the contact is marked by a steeply northeast dipping reverse fault putting mafic rocks on black siltstone. Nowhere along the contact with unit 2 was evidence for a stratigraphic contact observed.

Unit 2: Mafic volcanic and volcaniclastic rocks

On the west, most of this unit consists of very distinctive, resistant, dark green volcanic and subordinate volcaniclastic rocks that are characterized by their mafic composition and the presence of pyroxene. Lithologies include very massive monomictic mafic lahar or flow-breccia, locally with fragments up to 1 m across. Pyroxene feldspar crystal lithic lapilli and ash tuff, mafic wacke, local black siltstone and rare mafic volcanic conglomerate, green siltstone and augite porphyritic

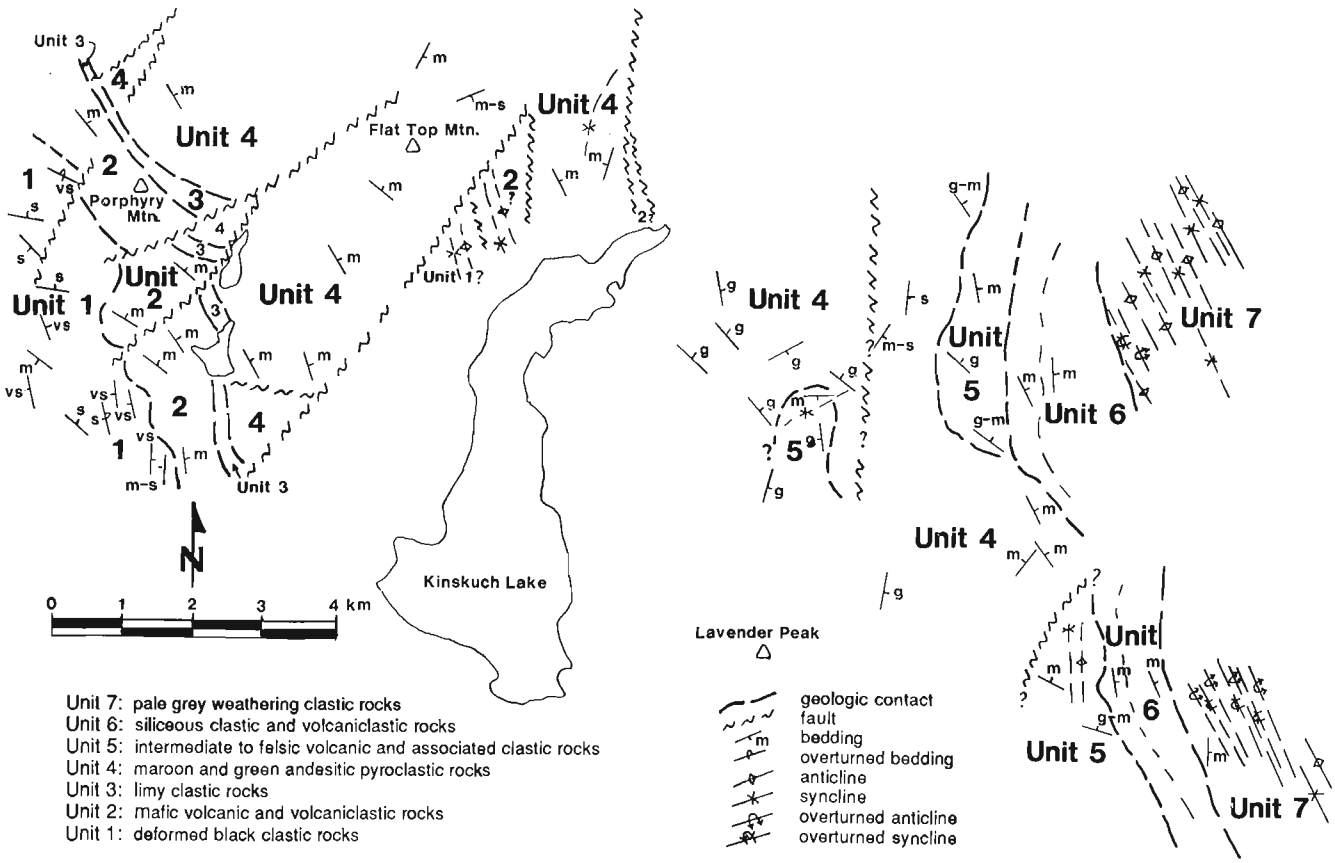

Figure 7. Generalized geology, Kinskuch River area.

flows are also present. Along the western margin of the unit, near its base, is an approximately 50 m thick section where finer grained rocks predominate. There, mafic wacke and/or ash tuff are interbedded with pale green laminated tuffaceous chert or felsic dust tuff and thin to medium bedded green-grey felsic ash and dust tuff.

In the central part of the study area, rocks immediately to the east of Flat Top Mountain have been (speculatively) correlated with rocks of unit 2. To the west, they are in fault contact with tuff-breccia of unit 4, and to the east they are overlain conformably(?) by similar unit 4 tuff-breccia. In general, they comprise a very resistant package of volcaniclastic rocks which bear similarities with the finer grained mafic and felsic rocks at the base of unit 2 to the west. They comprise abundant thick bedded, medium to coarse grained, tuffaceous(?) mafic to arkosic wacke, as well as laminated to thin bedded, medium to dark grey-green tuffaceous(?) siltstone and thin bedded siliceous ash and dust tuff.

Unit 3: Limy clastic rocks

This unit, locally up to 150 m thick, conformably overlies unit 2 in the western part of the study area. It comprises rusty weathering, coarse grained, commonly limy arkosic wacke, dark grey, moderately siliceous siltstone, and limy sedimentary breccia. Coarser grained lithologies are more common toward the base of the unit. The breccia is commonly bioclastic and locally contains fragments of colonial corals. Most breccia fragments are siltstone. On Porphyry Mountain, the wacke unit is conformably overlain by andesite tuff-breccia, which at its base contains abundant sedimentary lithic fragments, commonly in a limy matrix.

Hazelton Group

Unit 4: Maroon and green andesite pyroclastic rocks

This unit is a very thick sequence in which pale green and mauve weathering green and maroon massive andesite lapilli tuff-breccia predominates. Tuff-breccia is typically monomictic and locally contains fragments up to 1.5 m across. It is interbedded with subordinate andesite lapilli and ash tuff, rare dust tuff and local lahar of similar composition and maroon to green coloration. Between Porphyry and Flat Top mountains, the breccia unit contains continuous and undeformed (except in narrow zones adjacent to northeast trending faults) sequences up to 50-100 m thick of thin-bedded dark grey siltstone and fine to locally coarse grained, thin bedded turbiditic sandstone. Overlying tuff-breccia has downcut up to several metres into the sedimentary rocks.

Although the relationship between rocks in the continuous Porphyry-Flat Top section to rocks farther east is uncertain, much of the area southeast of Flat Top Mountain and north of Lavender Peak is underlain by lithologically similar tuff-breccia. In several places, particularly near the contact with unit 6, but also north of Lavender Peak, unit 4 grades upward into more heterogeneous and typically more felsic volcanic rocks of unit 5.

Unit 5: Intermediate to felsic volcanic and associated clastic rocks

Volcanic rocks of dacitic-andesite or rhyodacitic composition are consistently present within this unit, but it is perhaps best distinguished by its varied lithologies. The unit is volumetrically insignificant compared to unit 4. Intermediate to felsic volcanic rocks include rusty, buff, cream and very pale green weathering medium green, grey or tan lapilli tuff, tuff-breccia, flow-breccia, dust tuff and welded tuff. Rare buff weathering, pale grey, metre-scale felsic flows containing well-developed flow-layering also occur, as do local massive green (hornblende) feldspar (rarely megacrystic) andesite porphyry flows.

Volcanic rocks of unit 5 are interlayered with a wide variety of sedimentary rocks that range from laminated to thick bedded and lens-shaped black or green limy mudstone, to medium bedded, brown weathering limestone with discontinuous millimetre- to centimetre-scale black chert layers, to coarse monomictic sedimentary breccia containing either siltstone or felsic volcanic clasts in a silty mudstone matrix. At one locality, adjacent to the contact with Salmon River Formation rocks, coarse grained tuffaceous wacke contains fossils of Toarcian age (late Early Jurassic, H.W. Tipper, pers. comm., 1990).

Locally, the intermediate to felsic volcanic rocks of this unit are interlayered with and(or) overlain by thin bedded to massive mauve to maroon and green andesite lapilli tuff, ash tuff, and tuff-breccia indistinguishable from lithologies of unit 4. However, where this is the case, coarser grained pyroclastic rocks are less abundant and in total, maroon and green pyroclastic rocks of unit 5 do not comprise the great thicknesses observed in unit 4.

Salmon River Formation

Unit 6: Siliceous clastic and volcaniclastic rocks

Siliceous clastic and volcaniclastic rocks of unit 6, the Salmon River Formation, disconformably overlie Toarcian and older rocks of unit 5 on the east side of the study area. The Salmon River Formation is subdivided into a typically thin bedded and finer grained lower package which is gradational with a thick bedded and coarser grained upper package. The coarse grained rocks in turn grade upward (and laterally?) into sedimentologically more mature clastic rocks of the Bowser Lake Group. In general, rocks in both the lower and upper parts of unit 6 are relatively siliceous compared to overlying Bowser Lake Group rocks. They can also be distinguished from the pale grey weathering Bowser Lake Group rocks by their common rusty or dark grey-green weathering surfaces.

Rocks of the lower part of the Salmon River Formation are similar in many respects to rocks of the Spatsizi Group seen in the Oweegee Range. They are dominated by laminated to thin bedded black pyritic siliceous siltstone and subordinate fine grained sandstone and argillite. Discontinuous lenses of

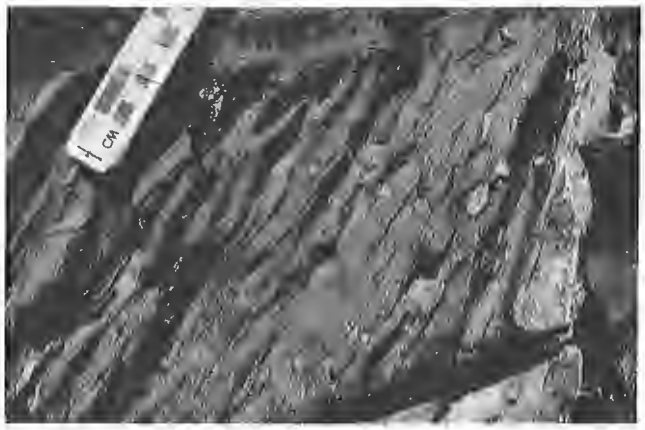

Figure 8. Flaggy, black, fine grained tuffaceous wacke of the upper part of the Salmon River Formation; note scattered pale weathering, angular volcanic lithic fragments, Kinskuch River area.

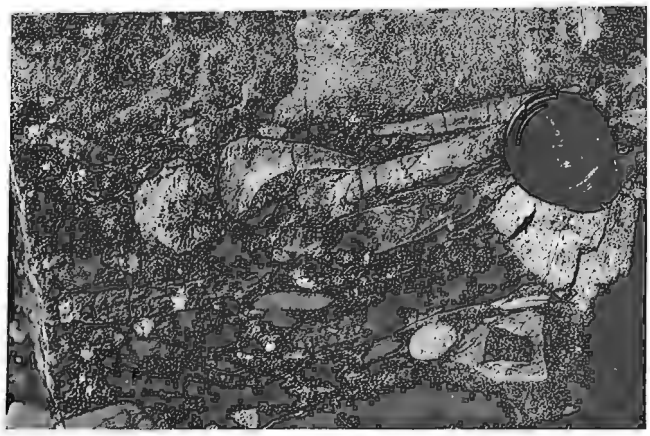

Figure 9. Poorly sorted cobble conglomerate containing abundant angular siltstone clasts, Salmon River Formation-Bowser Lake Group contact, Kinskuch River area.

tan to grey weathering silty limestone occur locally. Where exposed, the contact with underlying rocks of unit 5 exhibits very little relief. Basal beds contain scattered angular centimetre- to sub-centimetre size clasts in a matrix of siltstone or fine grained sandstone. Along the contact, pale grey weathering hornblende feldspar andesite porphyry sills are common.

The overlying thick bedded part of the Salmon River Formation is typified by the presence of very massive, thick bedded, medium grained turbiditic arkose. Also typifying this subunit are tuffaceous(?) siltstone and fine grained wacke containing distinctive recessive weathering lithic fragments (altered felsic volcanic lithic fragments?), locally up to 2 cm across (Fig. 8), and abundant broken feldspar and quartz grains.

Thick bedded Salmon River rocks grade upward and laterally into rocks of the Bowser Lake Group. Compositions and textures of clastic rocks support this interpretation and suggest a mixing of sedimentary provenance between a more proximal volcanic source and a more distal chert-rich source. In several places within the Bowser Lake Group, tuffaceous(?) dark grey siltstone and fine grained wacke with angular altered lithic fragments, common within the upper part of the Salmon River Formation, are found interbedded with the typically more mature rocks characteristic of the Bowser Lake Group. In addition, pale grey weathering, well sorted, chert-rich turbiditic sandstone typical of the Bowser Lake Group is locally interbedded with rocks of the upper part of the Salmon River Formation. Indications of provenance mixing are also evident in rare granule to pebble conglomerate beds near the Salmon River-Bowser Lake Group contact. Two conglomerate beds of contrasting textural and compositional makeup occur (Fig. 9, 10). One is poorly sorted, calcareous and contains highly angular siltstone clasts and scattered belemnite fragments of local derivation, and the other is well sorted and siliceous, and contains well-rounded, resistant and relatively far-travelled clasts.

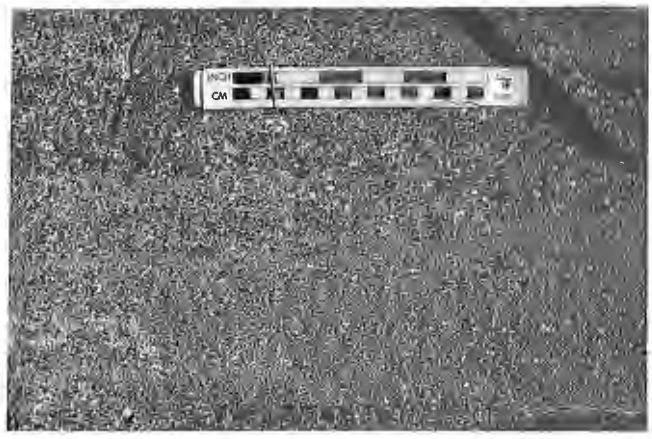

Figure 10. Granule conglomerate/conglomeratic sandstone containing abundant well-rounded chert clasts, Salmon River Formation- Bowser Lake Group contact, Kinskuch River area.

Bowser Lake Group

Unit 7: Pale grey weathering clastic rocks

Bowser Lake Group rocks in the Kinskuch area are characterized by pale grey weathering medium to thick bedded, medium and rarely coarse grained dark grey turbiditic sandstone. Also present are abundant pale grey weathering, laminated and thin bedded, moderately siliceous black siltstone and fine grained sandstone, and rare chert granule conglomerate.

Structure

Bowser Lake Group rocks in the study area have been folded into tight chevron shapes with a strong west vergence. The folds have short, steeply east dipping overturned southwestern limbs, and relatively long, moderately east dipping northeastern limbs. Local moderate to steep, west dipping reverse faults cut the southwest vergent folds. Drag into the faults may account for local anomalous northeast vergent folds.

Shortening evident in the Bowser Lake Group is not expressed in the Salmon River Formation, which forms a northeast dipping homoclinal sequence beneath the Bowser Lake Group. Shortening must therefore have taken place within structurally lower rocks of the Hazelton and Stuhini groups, or along a detachment between the Bowser Lake Group and the Salmon River Formation. The former alternative is preferred, and given the massive nature of Stuhini and Hazelton Group volcanic rocks, it is probable that shortening was accommodated primarily by faults rather than by folds.

Faults within the Hazelton Group east of Kinskuch Lake and within the Stuhini and Hazelton groups between Porphyry and Flat Top mountains do not exhibit vergence compatible with significant southwest directed shortening. Farther to the southwest, however, fine grained black clastic rocks of unit 1 are characteristically highly disrupted. In general, they strike northwest and have steep dips. Where observed, folds are typically disharmonic, with thickened or faulted hinges, and thinned or sheared out limbs. Together with evidence for a faulted contact with the overlying mafic volcanic rocks of unit 2, this suggests that the contact might mark the trace of a significant southwest vergent contractional fault. It may also imply that rocks of unit 1 are younger than rocks of unit 2.

A similar case may be argued for contacts and structures near the north end of Kinskuch Lake. If rocks mapped as unit 2 in that area correlate with rocks of unit 2 to the west, then the faults shown near the north end of the lake may also account for some of the shortening observed in Bowser Lake Group rocks. This possibility will be evaluated by further mapping and by attempting, via microfossil and geochronological work, to place absolute age constraints on the map units.

ACKNOWLEDGMENTS

Carol Evenchick, Brian Ricketts, Bob Anderson, Howard Tipper and Rodney Kirkham of the Geological Survey of Canada and Dani Alldrick, Dave Lefebure and Mary Lou Mallott of the British Columbia Geological Survey Branch are thanked for their encouragement and valuable geological input. Capable field assistance was provided by Randy Castellarin and Michael C. Toolan. Keewatin Engineering is gratefully acknowledged for logistical support in the Kinskuch area; special thanks go to Dave Tupper and the crew at Keewatin's Kitsault Lake camp for stimulating geological discussions and generous hospitality. Bert Struik and Bev Vanlier of the Geological Survey of Canada carefully edited and proofread the manuscript.

REFERENCES

Alldrick, D.J., Dawson, G.L., Bosher, J.A., and Webster, I.C.L.
1986: Geology of the Kitsault River area, NTS 103P; British Columbia Ministry of Energy, Mines and Petroleum Resources, Open File Map 1986/2.

Anderson, R.G.
1989: A stratigraphic, plutonic, and structural framework for the Iskut River map area, northwestern British Columbia; in Current Research, Part E, Geological Survey of Canada, Paper 89-1E, p. 145-154.

Anderson, R.G. and Thorkelson, D.J.
1990: Mesozoic stratigraphy and setting for some mineral deposits in Iskut River map area, northwestern British Columbia; in Current Research, Part E, Geological Survey of Canada, Paper 90-1E, p. 131-139.

Evencheck, C.A.
in press: Geometry, evolution, and tectonic framework of the Skeena Fold Belt, north-central British Columbia; Tectonics.

Grove, E.W.
1986: Geology and mineral deposits of the Stewart area, British Columbia; British Columbia Ministry of Energy, Mines and Petroleum Resources, Bulletin 63, 434 p.

Hanson, G.
1935: Portland Canal area, British Columbia; Geological Survey of Canada, Memoir 175, 175 p.

Koch, N.G.
1973: The central Cordilleran Region; *in* Future Petroleum Provinces of Canada; Canadian Society of Petroleum Geologists, Memoir 1, p. 37-71.

Monger, J.W.H.
1977: Upper Paleozoic rocks of northwestern British Columbia; in Report of Activities, Part A, Geological Survey of Canada, Paper 77-1A, p. 255-262.

Thomson, R.C., Smith, P.L., and Tipper, H.W.
1986: Lower to Middle Jurassic (Pliensbachian to Bajocian) stratigraphy of the northern Spatsizi area, north-central British Columbia; Canadian Journal of Earth Sciences, v. 23, p. 1963-1973.

Revised geological mapping of northeastern Taseko Lakes map area, British Columbia

C.J. Hickson, P. Read[1], W.H. Mathews[2], J.A. Hunt[2], G. Johansson[2], and G.E. Rouse[3]
Cordilleran Division, Vancouver

Hickson, C.J., Read, P., Mathews, W.H., Hunt, J.A., Johansson, G., and Rouse, G.E., Revised geological mapping of northeastern Taseko Lakes map area, British Columbia; in Current Research, Part A, Geological Survey of Canada, Paper 91-1A, p. 207-217, 1991.

Abstract

Regional mapping in Taseko Lakes (NTS 92O/NE) straddles the dextral strike-slip Fraser Fault. Although the western belt of Cache Creek Complex underlies both sides of the fault, only to the west is it intruded by the Late Permian Farwell Pluton. Southwest of the pluton, leucoquartz monzonite intrudes Lower Jurassic(?) volcanics, but does not contact fossiliferous Lower Jurassic sediments. Farther southwest, the mid-Jurassic(?) Mount Alex plutonic complex nonconformably underlies Upper(?) Jurassic volcanics. In the south, Paleozoic and lower Mesozoic rocks disappear under a cover of Cretaceous, Eocene, and Miocene-Pleistocene volcanics and sediments. In Churn Creek, uppermost Albian to Cenomanian sediments of the Silverquick formation unconformably underlie Eocene volcanics. Near the Fraser River, Pliocene and Pleistocene basalts and underlying Miocene-Pliocene sediments and rhyolite ash comprise the Chilcotin Group. Four eruptive centres, 10-35 km west of the river, were the source of the flows that covered the sediments deposited in a northerly flowing river.

Résumé

Des travaux de cartographie régionale dans la région des lacs Taseko (SNRC 92-O/NE) ont recoupé le décrochement dextre de la faille Fraser. Bien que la zone occidentale du complexe de Cache Creek soit sous-jacente aux deux côtés de la faille, elle n'est pénétrée par le pluton Farwell du Permien supérieur que du côté ouest. Au sud-ouest du pluton, de la monzonite leucoquartzique pénètre des roches volcaniques du Jurassique inférieur (?), mais ne vient pas en contact avec des sédiments fossilifères du du même âge. Plus loin au sud-ouest, le complexe plutonique Mount Alex du Jurassique moyen (?) repose en discordance sous des roches volcaniques du Jurassique supérieur (?). Au sud, des roches du Paléozoïque et du Mésozoïque inférieur disparaissent sous une couverture de roches volcaniques et sédimentaires du Crétacé, de l'Éocène et du Miocène-Pléistocène. Au Ruisseau Churn, les sédiments supérieurs de l'Albien au Cénomanien de la formation de Silverquick reposent en discordance sous des roches volcaniques de l'Éocène. Près du fleuve Fraser, des basaltes du Pliocène et du Pléistocène composent, avec des sédiments du Miocène-Pléistocène et des cendres rhyolitiques sous-jacentes, le groupe de Chilcotin. Les coulées qui ont recouvert les sédiments déposés dans un cours d'eau se déversant vers le nord provenaient de quatre centres d'éruption situés de 10 à 35 km à l'ouest du fleuve.

[1] Contribution to the Frontier Geoscience Program
[2] Geotex Consultants Ltd., #1200 - 100 West Pender Street, Vancouver, B.C. V6B 1R8
[3] Department of Geological Sciences, University of British Columbia, 6339 Stores Road, Vancouver, B.C. V6T 2B9
[4] PCI Palynorox Consulting Inc., 2134 West 53rd Avenue, Vancouver, B.C. V6P 1L6

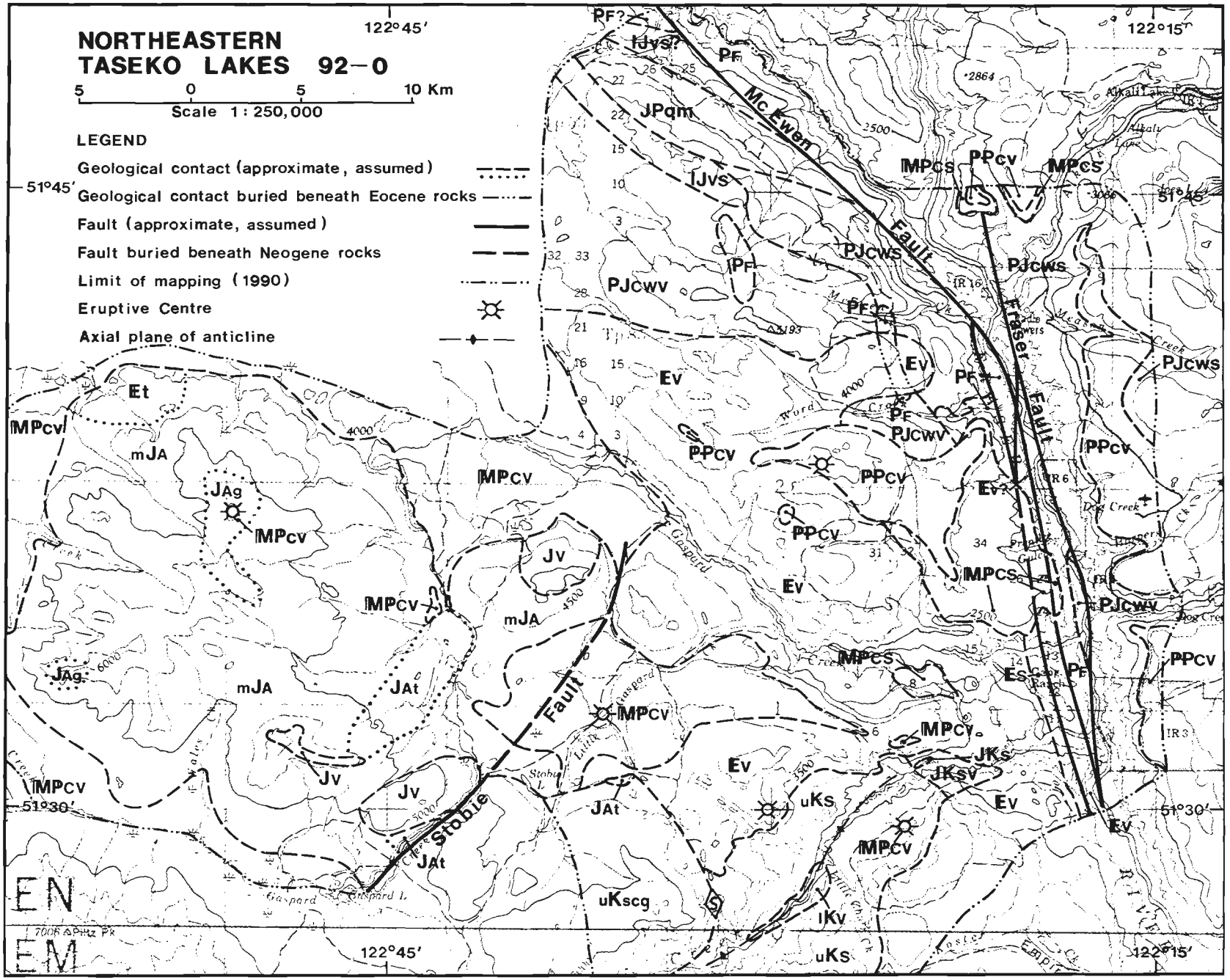
NORTHEASTERN
TASEKO LAKES 92–O
5 0 5 10 Km
Scale 1:250,000
LEGEND
Geological contact (approximate, assumed)
Geological contact buried beneath Eocene rocks
Fault (approximate, assumed)
Fault buried beneath Neogene rocks
Limit of mapping (1990)
Eruptive Centre
Axial plane of anticline
122°45′
122°15′
51°45′
51°30′
Et
MPcv
mJA
JAg
JAt
Jv
JPqm
IJvs
PF
PPcv
PJcwv
PJcws
Ev
MPcs
JMPcs
Es
JKs
JKsv
uKs
uKscg
IKv
Mc Ewen Fault
Fraser Fault
Stobie Fault
Gaspard
Stobie
Dog Creek
Alkali Lake
EN
EM

CENOZOIC
Quaternary and Tertiary
Pliocene and Pleistocene
PPcv — CHILCOTIN GROUP (PPcv to lMPcs)
Grey olivine basalt flows; locally basal palagonite tuff and pillow breccia

Tertiary
Miocene to Pleistocene
lMPcv — Grey olivine- and/or plagioclase-phyric subaerial basalt flows; minor interflow breccia

Miocene and(?) Pliocene
lMPcs — Unconsolidated fluviatile sediments; minor rhyolite ash and diatomaceous earth

Eocene
Es — Conglomerate, sandstone; minor siltstone and bentonitic shale; rare coal

Ev — Hornblende-plagioclase-phyric dacite and hornblende-biotite-quartz-phyric rhyolite flows; minor basalt, andesite, pyroclastic flows and ash; rare sediments

Et — Biotite-muscovite tonalite

MESOZOIC
Cretaceous
upper Lower Cretaceous and Upper Cretaceous
uKscg — Silverquick formation (uKscg to uKs)
Maroon volcanic conglomerate; minor sandstone

uKs — Green to buff chert pebble conglomerate, green to maroon sandstone; minor siltstone

Lower Cretaceous
lKv — Amygdaloidal plagioclase-phyric andesite(?) flows; minor pyroclastic rocks

Jurassic and/or Cretaceous
Lower Jurassic to Lower Cretaceous
JKsv — Plagioclase-phyric andesite(?) flows; green sandstone and minor siltstone

JKs — Argillaceous, well lithified dark grey siltstone

Jurassic
Middle and Upper Jurassic
Jv — Maroon to green sparsely feldspar-phyric andesite (?) flows, breccia; minor welded rhyolite ash flows

MOUNT ALEX PLUTONIC COMPLEX (JAg to mJA)
JAg — Hornblende monzogranite and granodiorite

JAt — Chloritized hornblende leucotonalite

mJA — Weakly to strongly foliated, chloritized hornblende quartz monzodiorite, quartz diorite and diorite

Lower Jurassic
lJvs — Grey-green and locally maroon porphyritic (plagioclase) andesite flows and tuffs, felsite- and quartz-feldspar porphyry-bearing tuff; minor fossiliferous grey siltstone

Jurassic or Permian
JPqm — Chloritized leucoquartz monzonite

PALEOZOIC
Permian
Late Permian
PF — FARWELL PLUTON
Chloritized and locally foliated granodiorite, quartz diorite and diorite

Permian to Jurassic
Lower Permian to Middle(?) Jurassic
PJcws — CACHE CREEK COMPLEX (PJcws to PJcwv)
Western Belt: Grey phyllite, siltstone, greywacke; grey, green and white chert and ribbon chert; minor greenstone and limestone

PJcwv — Western Belt: Greenstone, lithic ash and lapilli meta-andesite tuff; rare limestone and chert

Figure 1. Preliminary geological map of all or parts of 92O/7, 8, 9, 10, 15, and 16. Diamond enclosing an S (middle of southern edge of map) is the location of the measured section.

INTRODUCTION

The work reported in this paper is part of the Frontier Geoscience Program to study the Chilcotin-Nechako Hydrocarbon Province. An overview of the study can be found in Hickson (1990). Field work this year focused on the northeastern part of Taseko Lakes (92O), southwestern British Columbia; the eventual aim is to complete a new 1:250 000 geological map of 92O. This report outlines the results of the season's mapping, and preliminary petrological and petrographic work. Geological mapping at a scale of 1:50 000 extended southwest from the junction of the Chilcotin and Fraser rivers to Gaspard Lake and Churn Creek in 92O/10 and included all or parts of 92O/7, 8, 9, 15 and 16 (Fig. 1). Samples for radiometric dating, palynology and whole-rock geochemistry were collected from a larger area that extended southward to Lone Cabin Creek and Black Dome Mine (Fig. 2). Read mapped the area north of Gaspard Creek, and Hickson and the others investigated the region south of the creek.

Earlier regional mapping in the study area (Tipper, 1978) indicated that southwest of the Chilcotin River, Upper Triassic and Middle Jurassic stratified rocks host Jurassic plutonic rocks. South of Word Creek, Tipper mapped Eocene, Oligocene, Miocene and Pliocene rocks that covered the older rocks, including a sliver of Upper Cretaceous sediments. The more recent investigations of Mathews and Rouse (1984 and 1986) and Rouse et al. (1990) in Churn and Dog creeks, clearly defined and dated the Cretaceous, Tertiary and Quaternary units, and found that Oligocene volcanics are absent. The present work builds upon and modifies these earlier findings.

STRATIGRAPHY

Paleozoic to early Mesozoic

Cache Creek Complex

East of Fraser Fault to the limit of mapping, the western belt of the Cache Creek Complex (Trettin, 1980) consists of grey phyllite, indistinctly bedded siltstone and wacke, varicoloured ribbon chert and chert, and light green phyllite and siliceous phyllite. Grey crystalline limestone and dark green greenstone and phyllite are rare, thin, and lenticular. Beyond the limit of mapping to the east, the complex is dominated by limestone (Tipper, 1978) of the Marble Canyon Formation. West of Fraser Fault, the greater abundance of volcanic rocks permits a subdivision of the western belt of the Cache Creek Complex into volcanic (**PJcwv**) and sedimentary (**PJcws**) dominated units. The volcanic unit (**PJcwv**) contains mafic greenstone which has few primary volcanic textures preserved, and rare thin limestone lenses and chert layers. The sedimentary unit (**PJcws**) is mainly grey phyllite, siliceous phyllite, ribbon chert and chert. It also contains some greenstone (which may include sills and dykes) and rare limestone lenses. The stratigraphic order of the two units is unknown. At present, the complex ranges in age from Permian to mid(?)-Jurassic, but refinement of the time interval is probable with additional dating.

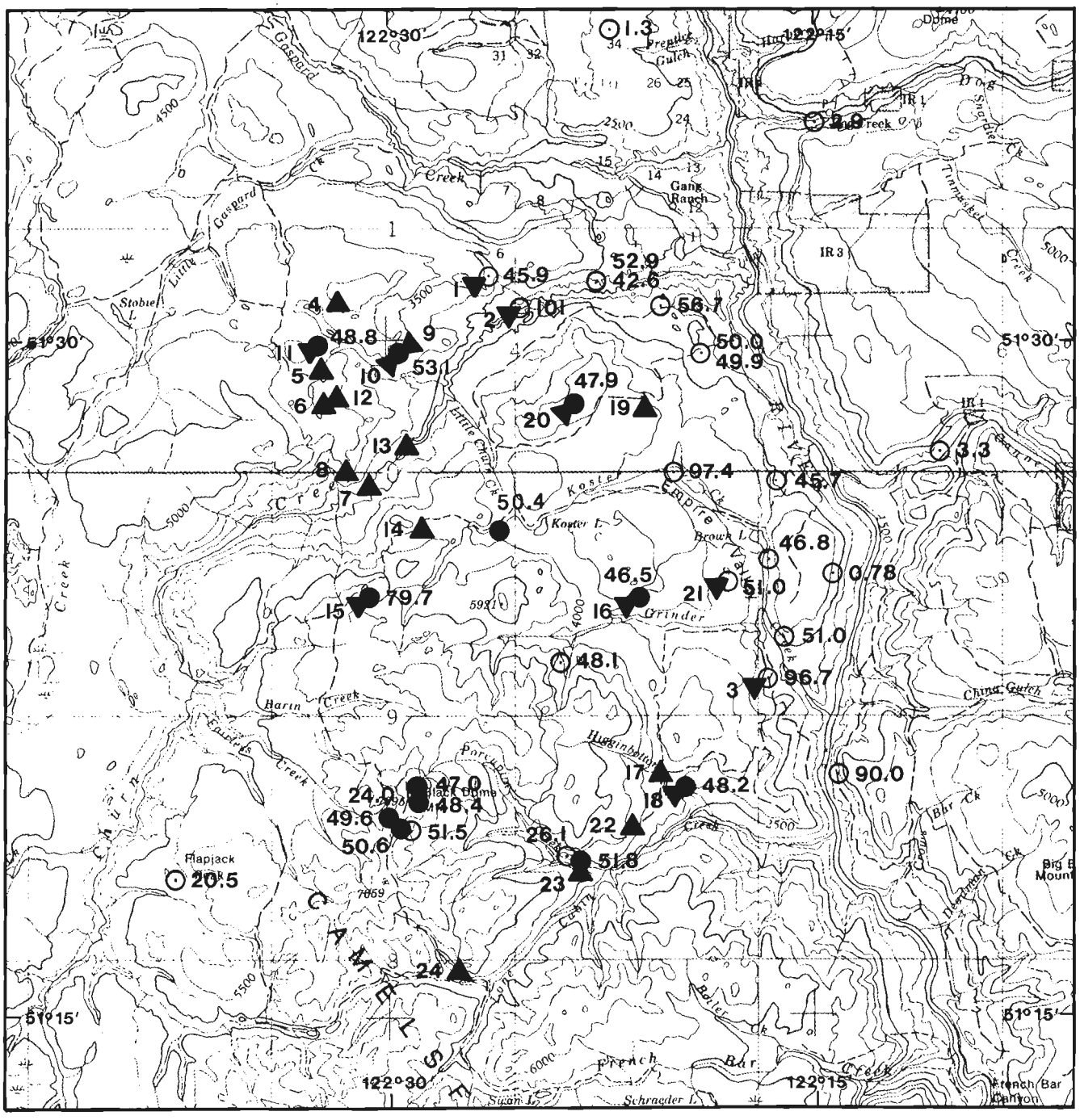

15 ▼ K-Ar date and whole-rock analysis

1 ▲ Chemical analysis: see table 2

48.8 ⊙ Previously published K-Ar date

51.0 ● K-Ar date: see table 1

Figure 2. Location of samples for radiometric dates and whole-rock chemical analyses. Analytical information on previously published K-Ar dates is in Mathews and Rouse (1984) and Mathews (1989).

Farwell Pluton

The Chilcotin and Fraser rivers, from Farwell Canyon to the mouth of Gaspard Creek, expose Farwell Pluton (**Pf**) and similar rocks. In the map area, the pluton and lithologically similar rocks lie only west of Fraser Fault. The pluton ranges in composition from altered granodiorite through quartz diorite to diorite. U-Pb dating of zircons from a sample collected at Farwell Canyon yielded a Late Permian age (Friedman and Armstrong, 1989). The McEwen fault separates this pluton from the lithologically similar, but undated, stocks to the south where they intrude and metamorphose rocks of the western belt of the Cache Creek Complex.

Jurassic

A fossiliferous grey siltstone of Early Jurassic (Toarcian) age (Hickson, 1990) and intercalated tuff are part of a Lower Jurassic sedimentary and volcanic assemblage (**lJvs**). Porphyritic (plagioclase) meta-andesite flows and tuffs, retaining primary textures and only locally foliated, are tentatively included within this unit. These sedimentary and volcanic rocks comprise a northwesterly trending zone a few kilometres southwest of Chilcotin River. Dykes from a leucoquartz monzonite (**JPqm**) intrude these undated volcanic rocks but do not come in contact with the fossiliferous sediments.

In the western part of the map area rocks of the Mount Alex plutonic complex are exposed. The complex is of possible mid-Jurassic age (Tipper, 1978) and is mapped as three zones (Fig. 1, 3). The most extensive zone is chloritized quartz monzodiorite, quartz diorite and diorite (**mJa**). The principal mafic phase of this zone is hornblende. In places the rock is extensively altered and the hornblende replaced by chlorite. Locally, epidote and quartz veining is present and the rock is weakly to strongly foliated. Mafic and felsic dykes cut rocks of the zone, locally exceeding 50 % of the outcrop. Weakly to moderately sheared metavolcanic and metaplutonic rocks are also present. In thin section, these rocks are noted to contain strained plagioclase crystals and many show cataclasite textures.

The second zone, equigranular, medium- to coarsely-crystalline, leucoquartz tonalite (**Jat**) is present along the southeastern side of the complex. The third zone is unaltered

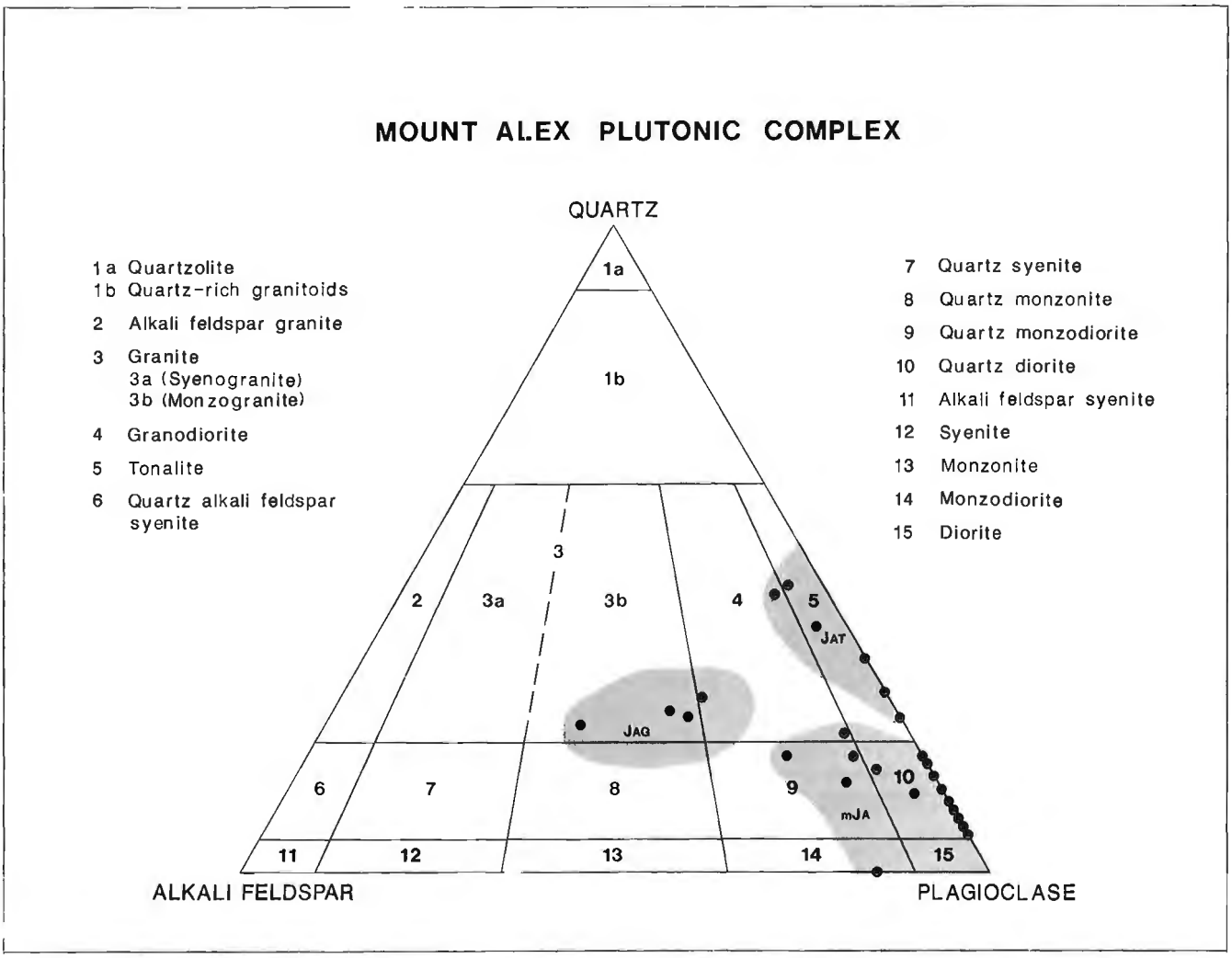

Figure 3. Streckeisen classification of plutonic rocks from the Mount Alex plutonic complex. Location of points is based on visual estimates made from thin-sections and stained slabs. **JAG**, **JAT**, and **mJA** refer to map units **JAg**, **JAt** and **mJA** respectively.

monzogranite and granodiorite (**JAg**) found in the central part of the complex. The principal mafic mineral in these zones is hornblende, but biotite is also found. In zone **JAg**, hornblende, several centimetres in length and 1-2 cm in diameter, is locally present. Secondary, tectonic foliation was not found in either of these zones.

Nonconformably overlying the Mount Alex plutonic complex, in short and poorly exposed sections, are porphyritic (feldspar) basic to siliceous volcanic flows, breccia, and welded pyroclastic rocks (**Jv**). The rocks are dominantly maroon, but locally green is also common. In places, tuff and lapilli breccia are composed of both green and maroon coloured clasts. Primary textures are well preserved. No evidence of hornfelsing or intrusion of the underlying pluton was noted. In two localities, close to the contact with the underlying plutonic rocks, breccia containing plutonic clasts was found.

Jurassic and/or Cretaceous

In the lower part of Churn Creek, argillaceous, well lithified, dark grey, siltstone (**JKs**) is exposed. It is not in stratigraphic continuity with rocks of presumed early Cretaceous age and no macrofossils have been found. The unit may be as old as Jurassic. Unconformably above this siltstone are green-weathering sandstones, minor siltstone and plagioclase-phyric andesite(?) volcanic flows and maroon to green lapilli-tuff breccia (**JKvs**). Lowermost in the section is a lapilli-block breccia composed of feldsparphyric volcanic clasts and 10 % angular clasts (up to 6 cm in diameter) of siltstone.

Cretaceous

Cretaceous sedimentary and volcanic rocks are exposed in Churn Creek (Fig. 1). At creek level and lowermost in the section exposed in the core of an anticline (Rouse et al., 1990) (Fig. 1), is amygdaloidal, extensively fractured and weathered, plagioclasephyric brown-weathering andesite and maroon to green lavas and pyroclastic rocks (**lKv**).

Above the core rocks, are late Albian to Cenomanian conglomerate and sediments (**uKs**) exposed in a section at least 600 m thick. A 240 m thick section was measured (Fig. 4) through the thickest continuous part of these sediments (Fig. 1). Above this measured section, continuing for at least another 200 m, volcanic-clast-rich conglomerate grades into massive volcanic lahar. Below the measured section a further 200 m of interbedded chert pebble conglomerate and sandstone is exposed. Downstream, about 150 m of green volcanic sandstone and minor buff coloured siltstone outcrops.

A thin siltstone, interbedded in the sandstone (10U EN 540750mE, 5707920mN), yielded the following, late Albian-early Cenomanian palynomorph assemblage:

Dinocysts	*Pseudoceratium expolitum*
	Aptea cf. *rugulosum*
	cf. *Carpodinium obliquocostatum*
Fern spores	*Distaltriangulisporites irregularis*
	Cyathidites minor
	Concavisporites sp.
Gymnosperm pollen	*Eucommiidites troedssonii*
	Vitreisporites pallidus

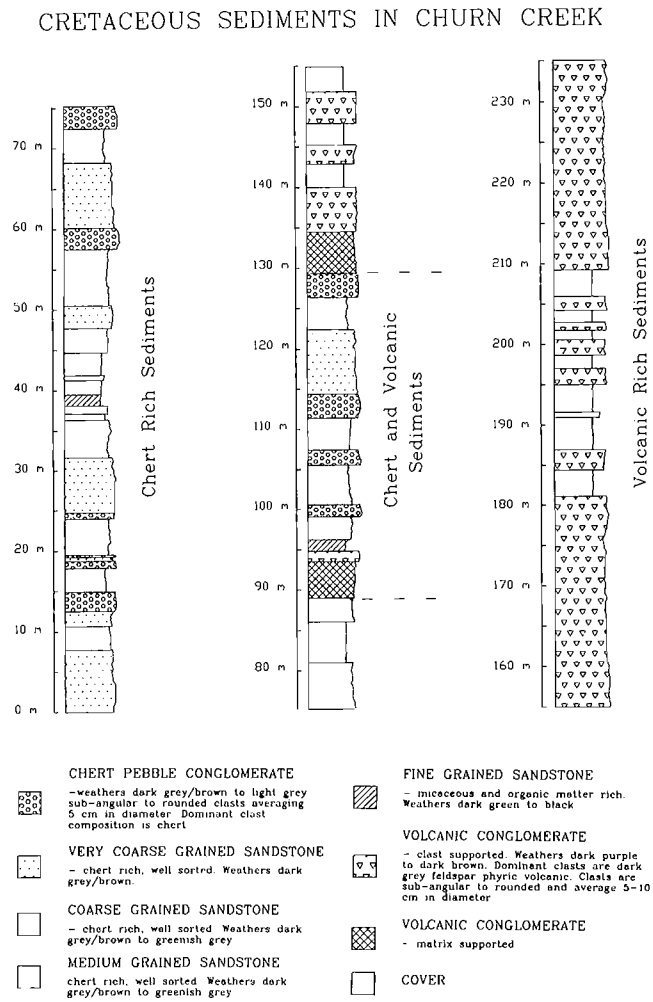

Figure 4. Stratigraphic section measured through the thickest continuous section of Cretaceous sediment found along Churn Creek.

Angiosperm pollen	*Tricolpites crassimurus*
	T. micromunus
	T. minimus

Within the area mapped this field season, unit **uKs** is the only unit that may contain potential hydrocarbon reservoir rocks. Samples for vitrinite reflectance, permeability and porosity measurements have been collected from the succession. The following are detailed lithological descriptions of the section measured along the north side of Churn Creek (Fig. 1).

Lower Chert Rich Sediments (uKs)

Conglomerate

The lower conglomerate in the measured section is composed primarily of varicoloured chert (commonly grey) and rare pink and white granitic clasts. It varies from clast to matrix supported. The matrix is well sorted, very coarse to coarse grained chert-rich sandstone. Weathered exposures are friable to crumbly and dark grey-brown to light grey; fresh surfaces are light brown to grey. Clasts are angular to subrounded, vary from 0.5-5 cm in diameter.

Pebble rich layers grade up to sand layers, commonly in repetitive cycles 10-15 cm thick. Similar fining upward sequences define channels, up to a few metres wide, which grade from large pebbles to coarse sand, above a base scoured into underlying sandstone. In some matrix supported conglomerate beds, the percentage of pebbles increases upwards, but their size diminishes.

Sandstone

The sandstone layers within the conglomerate are well sorted and vary from very coarse grained to fine grained. Coarse to medium grained sandstone weathers dark grey-brown to greenish-grey; fresh surfaces are pale green to pale greenish-grey, commonly with rusty blebs around plant fragments. Some medium grained sandstone and the fine grained sandstone weathers dark brown to dark green-black.

Typically, the sandstone is massive and lacks internal sedimentary structures. However, some sandstone beds show cyclic, 10 cm thick, fining upward sequences. Others are crudely laminated, on a scale of 5-15 cm, and some fine upwards, being more pebble-rich at the base. Pebbles found in the sandstone are commonly aligned with bedding or rarely parallel to crossbedding. The maximum pebble size in coarse grained sandstone is 1.0 cm in diameter, in medium grained sandstone, 0.5 cm. Pebbly channels, from 2-6 m wide and up to 0.7 m deep, cut the sandstone. Pebbles are absent in the fine grained sandstone which is micaceous and rich in organic matter. This sandstone is flaggy weathering due to thin (0.1 cm thick) layers spaced 0.3 cm apart. Higher in the section (Fig. 4), close to the volcanic conglomerate contact, micaceous, medium grained sandstone contains angular shale clasts up to 15 cm long.

***Upper Volcanic-clast Rich Sediments* (uKscg)**

The upper conglomerate of the measured section is almost entirely clast supported and the clasts are dominantly volcanic in origin. Minor sandstone and matrix supported conglomerate are also present. The unit as a whole is well bedded and strongly jointed with calcite and zeolite(?) filling the fractures.

The transition upwards from chert-clast rich to volcanic-clast-rich sediments occurs across a 40 m interval in which the two lithologies alternate. Close to the transition zone, the sediments weather dark grey to dark brown; fresh surfaces are light grey. Clasts are poorly sorted, rounded to subrounded and average 3-5 cm in diameter, but range from 1-20 cm across. Higher in the section the volcanic-clast conglomerate weathers dark purple to dark brown; fresh surfaces are dark grey-brown. Here clasts are subangular to rounded and average 5-10 cm in diameter varying from 1-70 cm.

At the base of the volcanic-clast rich sediments, dark-grey, fine grained, green and red mottled volcanic clasts dominate. Higher in the section, fine grained, dark-grey feldsparphyric volcanic clasts and fine grained maroon, grey or dark-brown volcanic rocks are prevalent. Near the top, fine grained, grey recessive-weathering clasts are a major constituent. Throughout the section minor amounts of the following rock types are found: white, flow-banded rhyolite; pink chert and quartz; white quartz; red chert; creamy to pale brown chert; white chert with black veins; fine grained maroon volcanic rock with feldspar and mafic phenocrysts; dark brown vesicular volcanic rock; purple vesicular volcanic rock; fine grained pink or green volcanic rock; maroon and black flowbanded volcanic rock with feldspar phenocrysts; fine grained, maroon, amygdaloidal volcanic rocks; brown amygdaloidal volcanic rock; and soft, fine grained, yellowish-green rock.

Within the conglomerate, layers are clast supported at the base but fine upwards to coarse grained, laminated sandstone in the top 15 cm. Laminations within these sandstones are parallel to bedding, about 1 cm apart and outlined by magnetite. Rare crossbedded sandy layers, up to 50 cm thick, and highly fractured sandy lenses, 30 cm thick by 1 m wide, occur within the conglomerate. The sandstone weathers dark grey-purple; fresh surfaces are similar but have pale green and white grains. Some of the sandstone has small (0.3 cm long) oval clasts of fine grained grey rock.

Sedimentary Structure and Correlation

Throughout the section shown in Figure 4 crossbeds are scarce and decrease in abundance upsection. The lower chert rich sedimentary rocks are generally well bedded and have little internal structure. Where crossbeds are present (between 72 m and 78 m on Fig. 4) an average south-southwest paleocurrent direction is indicated (Fig. 5).

The overlying volcanic-clast rich sedimentary rocks are also well bedded. Crossbeds are scarce. Five which were measured (between 160 m and 162 m in Fig. 4) suggest a paleocurrent direction of north-northeast.

Varying lithologies and paleocurrent directions within the Cretaceous sedimentary rocks in the Churn Creek area suggest two distinct sediment sources. Paleocurrent directions suggest a chert rich source to the north and a later volcanic rich source to the south. Internal structure of these sedimentary rocks suggests a braided stream environment (Rust and Koster, 1984).

Age and lithological considerations suggest that the sediments are correlative with the Silverquick formation, of the informal Battlement Ridge group, mapped to the south in the Noaxe Creek (92O/02) map area (Glover *et al.*, 1988).

Tertiary

From north of Word Creek to south of Churn Creek, Eocene volcanic (**Ev**) and overlying sedimentary rocks (**Es**) comprise a succession that Mathews and Rouse (1984) estimated as 1600 m thick. From north of Word Creek to north of Gaspard Creek, the isolated outcrops are exclusively porphyritic (hornblende, ±feldspar, ±biotite) rhyodacite flows. In Gaspard and Churn creeks, more complete sections allow the sequence to be divided into a lower, mixed unit of subaerial andesite and dacite flows and minor basalt flows and breccia; a middle, porphyritic hornblende (±biotite±quartz±feldspar) unit of dacite flows and thick breccias; and an upper mixed (andesite, dacite and minor rhyolite and basalt) unit with locally thick airfall, pyroclastic and lahar deposits. The following

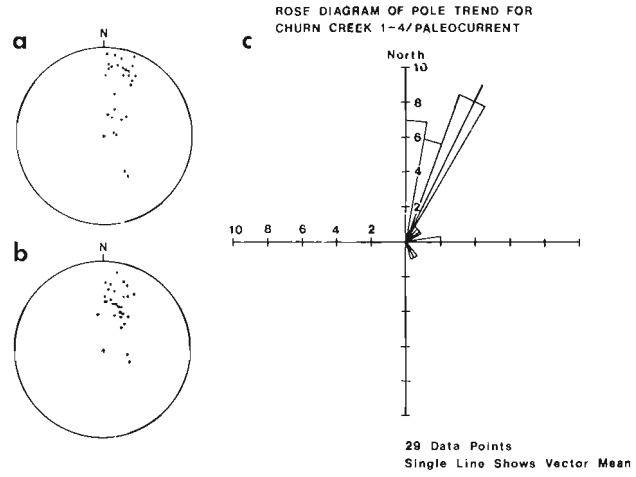

Figure 5. Paleocurrent data for the section shown in Figure 4.
a: Stereoplot of the poles to crossbedding;
b: Stereoplot of rotated poles to crossbedding;
c: Rose diagram based on the data in b, giving a plot of trends paleocurrent directions.

palynomorphs were obtained from the upper unit (10U EN 543225mE, 5708575mN):

Fungal spores	*Dicellaesporites "inaequalis"*
	D. popovii
	D. aculeolatus
	Diporisporites - A.
	Staphlosporonites conoideus
	Multicellaesporites didymus
	Callimothallus pertusus
	"Circulosporites" sp.
Fungal hypha	Fungal hypha - type B (Norris)
Fern spores	*Polypodiisporites favus*
	Deltoidospora diaphana
Conifer pollen	*Pinus diploxylon* - type
Angiosperm	*Alnus vera*

This assemblage corresponds to those from the Middle Eocene of the Gang Ranch-Big Bar exposures, and correlatives from the south-central region of B.C. (Mathews and Rouse, 1984; Rouse et al., 1990).

Chemical analyses of Cretaceous and Eocene volcanic rocks from the map area indicate the rocks are calc-alkaline andesite to rhyolite (Table 1, Fig. 2). Previous radiometric dating (Mathews and Rouse, 1984; Mathews, 1989; Rouse et al., 1990) and new dating (Table 2) have established that the majority of the volcanic rocks are Eocene, but there are an unknown number of Cretaceous volcanic rock outcrops in the southern part of the study area.

In the lower part of Gaspard Creek and south of Churn Creek along the west side of the Fraser River, outcrops and slide blocks expose Eocene (Mathews and Rouse, 1984; Rouse et al., 1990) conglomerate, sandstone, siltstone, bentonitic shale, and rare thin coal seams (**Es**). Fraser Fault and its splays truncate and form the eastern limit of the Eocene rocks.

Farther west, along the northwestern edge of the Mount Alex plutonic complex, a dated Eocene (R. Friedman, pers. comm., 1990) tonalite plutonic body crops out (**Et**). The equigranular texture, lack of alteration and biotite+muscovite mineralogy distinguish it from other plutonic rocks in the region.

Chilcotin Group

Erosional remnants of sedimentary and overlying volcanic rocks of the Chilcotin Group form parts of the valley walls on both sides of the Fraser River. Here and there small outcrops of pebble to cobble conglomerate, sandstone, rhyolite ash and rare diatomite, form a 10- to 30-m thick lenticular sedimentary sequence (**MPcs**). Along the east side of the Fraser River, sediments are too thin to show in Figure 1. Between Churn and Word creeks, sediments are up to 350 m thick and outcrop in widely scattered stream cuts and slide scarps to as low as 556 m (1825 ft) on the west side of the river, and as low as 520 m (1700 ft) on the east side, opposite Word Creek. Pebbles and cobbles in the conglomerate include subrounded to rounded clasts of buff, cream or pink quartzite, and locally, olivine basalt. Small exposures of rhyolite ash and diatomaceous earth are present between Gaspard and Churn creeks, and the occurrence of more than 40 m of rhyolite lapilli tuff with clasts up to 1.5 cm in length between Prentice Gulch and Word Creek may indicate a nearby rhyolite vent. Although a Miocene age for these rocks has been indicated by Mathews and Rouse (1984) and Rouse et al. (1990), a Pliocene age cannot be excluded for parts of the unit. At several localities, pebble imbrication and crossbedding indicate that the sediments were deposited in a northward flowing drainage system (Mathews and Rouse 1984; this study).

Near Harper and Dog creeks on the east side of the Fraser River and above 853 m (2800 ft) is a 40-150 m high escarpment of grey olivine basalt flows (**PPcv**). North of Dog Creek and immediately east of the map area, Mathews and Rouse (1986) defined a 150-200 m thick Pleistocene succession of fluviatile sediments and till capped by up to 15 m of olivine basalt. This Pleistocene succession occurs on the ridge between Dog and Harper creeks, but is not distinguished in Figure 1. West of the Fraser River, olivine basalt flows probably cover the valley wall south of Word Creek and form flow remnants up to the 1463 m (4800 ft) level on a few ridges close to the river. On the west side, four eruptive centres are known or inferred (Fig. 1) and at least two of these are likely sources for the olivine basalt on the east side of the river within the map area.

The flows near the Fraser River have been radiometrically dated as Pliocene or Pleistocene age (Fig. 2; Mathews and Rouse 1984, 1986; Mathews, 1989), but to the west, olivine-phyric and plagioclase-phyric basalt (**Pcv**) flows are undated but unconformably overlie Eocene volcanic flows. In one location a well developed paleosol was found below the basalt flows. The flows cover extensive areas around Little Gaspard Creek and the Mount Alex plutonic complex. Possible sources for some of these flows are the inferred eruptive centre at 1707 m (5600 ft) elevation, south of Word Creek and "Little Devils Postpile" close to Little Gaspard Creek (Fig. 1).

Table 1. Whole-rock chemical analyses.

Fig. 2, Ref.#	1	2	3	4	5	6	7	8
Rock Name	Dacite	Dacite	Dacite	Andesite	Dacite	Dacite	Andesite	Rhyolite
Sample #	CH2A	CH32	CH40	CH53A	CH55	CH56	CH59	CH61
Age (Ma)	45.9	101	96.7	Eocene	Eocene	Eocene	Cret.	Cret.
SIO_2	66.36	72.48	63.06	61.88	67.56	64.23	60.23	72.01
TIO_2	0.48	0.35	0.53	0.63	0.33	0.62	0.97	0.17
AL_2O_3	17.34	15.01	19.06	18.25	18.80	18.37	18.76	16.18
FE_2O_3	1.39	1.40	2.51	4.55	1.99	2.28	5.00	0.95
FEO	1.46	0.65	1.69	0.48	0.56	0.89	0.95	0.41
MNO	0.05	0.05	0.06	0.08	0.05	0.05	0.12	0.04
MGO	2.65	1.38	3.26	4.07	1.39	2.66	3.69	0.66
CAO	3.17	2.06	3.41	4.65	2.74	3.36	5.56	1.59
NA_2O	3.47	3.48	5.51	3.98	3.87	4.21	4.03	3.99
K_2O	3.06	2.92	0.80	1.75	2.20	2.27	1.09	2.96
P_2O_5	0.23	0.19	0.22	0.24	0.19	0.18	0.35	0.05
TOTAL	99.65	99.98	100.11	100.56	99.67	99.12	100.74	99.02
LOI %	2.39	1.92	1.36	3.83	1.37	1.99	4.14	0.66
FE_2O_3	3.01	2.13	4.39	5.09	2.61	3.27	6.05	1.41

Fig. 2, Ref.#	9	10	11	12	13	14	15	16
Rock Name	Andesite	Dacite	Dacite	Dacite	Andesite	Andesite	Dacite	Dacite
Sample #	CH63	CH64	CH73	CH75	CH76	CH78	CH83	CH86
Age (Ma)	53.1	Eocene?	48.8	Eocene	Cret.?	Cret.?	79.7	46.5
SIO_2	65.02	64.27	66.81	67.51	60.60	60.51	67.91	62.69
TIO_2	0.56	0.36	0.32	0.42	0.73	0.63	0.37	0.89
AL_2O_3	17.56	20.55	18.26	18.16	19.08	18.69	18.17	18.79
FE_2O_3	1.94	2.43	1.78	1.31	3.87	3.55	2.87	2.71
FEO	1.56	0.26	0.66	1.28	1.36	1.28	0.14	1.57
MNO	0.05	0.05	0.05	0.05	0.08	0.08	0.06	0.06
MGO	3.02	2.02	1.86	2.17	2.65	3.74	1.54	2.19
CAO	3.66	3.51	2.73	2.62	5.16	4.89	3.40	3.68
NA_2O	3.94	4.81	4.41	4.08	4.69	4.75	4.78	4.71
K_2O	2.41	1.71	2.42	2.70	1.37	1.73	1.05	2.20
P_2O_5	0.18	0.22	0.21	0.18	0.31	0.33	0.20	0.21
TOTAL	99.91	100.18	99.52	100.49	99.91	100.18	100.49	99.70
LOI %	2.24	4.94	1.47	0.99	3.53	3.69	0.89	1.29
FE_2O_3	3.67	2.72	2.52	2.73	5.39	4.97	3.03	4.45

Fig. 2, Ref.#	17	18	19	20	21	22	23	24
Rock Name	Dacite	Dacite	Dacite	Dacite	Dacite	Rhyolite	Rhyolite	Andesite
Sample #	CH89	CH91	CH93	CH96	CH97	CH98	CH100	CH102
Age (Ma)	Eocene	48.2	Eocene	47.9	51.0	Eocene	51.8	Eocene
SIO_2	76.97	61.95	63.03	66.80	64.11	77.30	74.04	64.02
TIO_2	0.14	1.04	0.74	0.62	0.63	0.14	0.25	0.51
AL_2O_3	14.01	18.76	19.12	17.42	18.47	12.51	15.41	16.86
FE_2O_3	0.85	4.53	2.61	2.94	3.25	1.09	0.69	2.27
FEO	0.21	0.41	1.69	0.55	0.50	0.29	0.28	2.18
MNO	0.03	0.08	0.06	0.05	0.06	0.02	0.02	0.06
MGO	0.97	2.61	2.41	1.93	2.57	0.84	0.83	3.28
CAO	1.48	2.52	4.02	3.28	3.48	0.64	1.12	4.76
NA_2O	2.59	3.63	4.63	4.17	4.42	3.39	3.61	3.53
K_2O	3.33	4.92	2.04	2.34	2.53	3.99	4.14	1.98
P_2O_5	0.03	0.26	0.21	0.21	0.25	0.04	0.04	0.12
TOTAL	100.62	100.71	100.56	100.30	100.28	100.27	100.44	99.56
LOI %	10.25	4.02	1.26	2.03	2.52	1.08	0.63	4.21
FE_2O_3	1.08	4.98	4.49	3.56	3.81	1.42	1.00	4.69

Table 2. Radiometric dating results.

Sample #	Rock	Material Dated	UTM: Zone 10 E	N	K%	$^{40}Ar^*$ / ^{40}Ar tot	$^{40}Ar^*$ ($STDcm^3/gx10^{-5}$)	Date (Ma)
CH83	Dacite	whole-rock	5337	57950	1.03	58.4	.3264	79.7 ± 2.8
CH91	Dacite	whole-rock	5468	56874	4.41	85.8	.8368	48.2 ± 1.7
CH97A	Andesite	whole-rock	5487	57958	2.50	94.3	.5026	51.0 ± 1.8
CH100	Rhyolite	whole-rock	5419	56843	3.69	77.3	.7538	51.8 ± 1.9
*88-2KAR	Dacite	whole-rock	535710	5686660	1.96	81.3	.3626	47.0 ± 1.6
*88-2KAR	Dacite	hornblende	535710	5686660	0.538	73.0	.1026	48.4 ± 1.6
*88-1KAR	Dacite	hornblende	534670	5684410	0.437	71.8	.0876	50.6 ± 1.8
*D40E	Basalt	whole-rock	534245	5686160	0.796	64.8	.1556	49.6 ± 1.7
CH86	Dacite	whole-rock	5451	56961	2.21	90.0	.4042	46.5 ± 1.6
CH63	Andesite	whole-rock	5350	57051	0.662	80.0	.1386	53.1 ± 1.8
CH79	Dacite	whole-rock	5390	56975	2.97	93.4	.5902	50.4 ± 1.8
CH96	Dacite	whole-rock	5421	57030	2.32	90.2	.4379	47.9 ± 1.7
CH73	Dacite	biotite	531622	5705309	6.35	64.6	1.2217	48.8 ± 1.7

Analyses are by D. Runkle (K) and J. Harakal (Ar), Department of Geological Sciences, University of British Columbia. K is determined in duplicate by atomic absorption using a Techtron AA4 spectrophotometer. Ar is determined by isotope dilution using an AEI MS-10 mass spectrometer and high-purity ^{38}Ar spike. Errors reported are one standard deviation. The constants used are $K_{\lambda_\varepsilon} = 0.581\times10^{-10}year^{-1}$; $^{40}K/K = 0.01167$ at.%; and $K_{\lambda_\beta} = 4.962\times10^{-10}year^{-1}$.

* Permission to publish dates was kindly given by Blackdome Mining Corporation.

STRUCTURE

Strong folding affects stratified rocks older than Lower Jurassic, and faulting with large displacements controls the distribution of Eocene and older rocks. Within the map area, only rocks of the western belt of the Cache Creek Complex are strongly folded. East of the Fraser River, the rocks of the complex mostly dip steeply eastward, and in a few places where facing can be determined, they also are upright to the east. A steep east to southeasterly dipping axial-plane foliation cuts the rocks and indicates a phase of folding with moderate to steep northeasterly plunges. West of the Fraser Fault rocks of the complex are strongly folded and steep dips are common, but with no obvious pattern of folding. In contrast, the Lower Jurassic siltstone and tuff show gently dipping bedding and only an incipient fracture cleavage striking northwesterly and dipping steeply. In Churn Creek bedding of the gently dipping Cretaceous Silverquick formation outlines a southwesterly trending and gently dipping anticline. North of Gaspard Creek, flow layering present in Eocene volcanic rocks is consistent with the distribution of outcrops indicating that the Eocene succession dips gently south towards Gaspard Creek. The gentle eastward dips in Gaspard and Churn creeks outline either (a) the northern end of an open, gently southerly plunging syncline that is partly truncated to the south by the Fraser Fault so that only its western limb remains, or (b) the present distribution reflects Eocene paleotopography with high areas near McEwen Creek and east of Stobie Lake (where flow layering and questa like forms indicate northerly dips). South of Churn Creek the Eocene succession is strongly deformed close to the Fraser Fault and strike and dip nearly parallel to it.

Fraser Fault and its splays are the northward continuation of the Fraser River fault system. Veering off from the system, south of the map area, are the northwesterly trending Yalakom, Slok Creek-Hungry Valley faults, and within the map area, McEwen Fault. Although the splays of Fraser Fault locally bound slices of Eocene volcanic rocks, the easternmost fault forms the eastern limit of Farwell Pluton and Eocene rocks. Fault movement indicators are absent within the area, but strike-slip slickensides are known to the south (Read, 1988) and workers such as Misch (1977), Davis et al. (1978), Monger and Price (1979), and Kleinspehn (1985) have suggested dextral strike-slip displacement in the order of 110 km (Kleinspehn, 1985) to 190 km (Misch, 1977) or more (Norris, 1980). Read (1988) noted that Fraser Fault truncates an undated granodiorite pluton near Leon Creek east of the fault and a pluton, now called Farwell Pluton, near the mouth of the Chilcotin River west of the fault. In both places, the faulted plutons intrude rocks of the western belt of the Cache Creek Complex, and if prior to faulting, they were one pluton, the offset would indicate a post-Late Permian dextral strike-slip displacement of some 90 km.

McEwen Fault is subparallel to other major northwesterly trending faults that veer away from the Fraser River fault system. At McEwen Creek, a 100-200 m-thick zone of white quartz-sericite-pyrite schist follows the fault zone and dips 70-80°SW. Fault motion indicators are absent, but the presence in the fault zone of a slice of undeformed felsite pebble conglomerate and overlying limestone, unlike all other rocks in the map area, suggests that displacement may be large. Near Word Creek, Tipper (1978) mapped the northwesterly striking Chilcotin Fault, but because Eocene volcanic rocks and rocks of the western belt of the Cache Creek Complex seem unaffected along the presumed fault trace, the fault has been discounted.

MINERAL OCCURRENCES

The 1990 field area lies immediately north of the epithermal Au-Ag deposit developed in Eocene volcanic rocks at Black Dome mine. In the course of fieldwork south of Little Gaspard Creek (10U EN 529780mE, 5707075mN) and 5 km northwest of a suggested volcanic centre (Fig. 1), a 40 m wide zone of hydrothermally altered and veined hornblende-phyric dacite was discovered. The dacite is most likely Eocene in age. The zone is brecciated and fractured with quartz veins up to 40 cm wide. Vein and fracture directions vary between north-northeast and north-northwest. Six surface grab samples were taken and fire assayed, but Au values were at or below the detection limit of 5 ppb for each sample. Twelve kilometres west of this location, exploration and drilling is currently underway on the Gaspard Lake property. The target is auriferous quartz-chalcedony stockworks developed in the Mount Alex plutonic complex. The mineralization is of presumed Eocene age and may be associated with fractures on a splay of a Stobie fault.

Of the other recorded mineral occurrences in the map area (Fields et al., 1990), most lie on sheared and hydrothermally altered fault splays associated with the Fraser and McEwen faults. Trenching and drilling have been done in at least three other locations. On the Dry Farm showing, a 100-200 m-wide zone of hydrothermal alteration associated with McEwen Fault produced a quartz-sericite-pyrite schist that has been trenched extensively and apparently drilled about 2 km west of the mouth of the Chilcotin River at EN0539400mE, EN5732100mN. At the Gang showing (10U EN0544600mE, EN5722500mN), a crush zone associated with one of the splays of Fraser Fault was drilled. Rusty skarn, developed in the contact aureole in unit **PJcwv**, has been drilled at EN0541700mE, EN5723400mN.

Occurrences of industrial minerals are restricted to the Eocene sedimentary rocks which locally contain bentonite and zeolites (heulandite-clinoptilolite), and to sediments of the Chilcotin Group which have scattered occurrences of diatomaceous earth (Green, 1989). Several new occurrences of diatomaceous earth in unit **MPcs** outcrop between the 610-838 m (2000-2750 ft) levels up to 2 km north of Prentice Gulch on the west side of the Fraser River, and on the east side of the Fraser immediately beneath the basalt flows 2.5 km north of Harpers Creek.

ACKNOWLEDGMENTS

The kind assistance and generosity of Larry Ramsted, Steve Oswald and other employees of Rudigers Ranch (Gang Ranch) were most appreciated. Eitha and Robert Pepperlling of Empire Valley Ranch were most helpful and allowed access to private property. Whole-rock chemical analyses were done by Stanya Horsky, University of British Columbia. The able assistance of Kathi Hoffman is most appreciated. Reviews by D. Tempelman-Kluit and H.W. Tipper were most helpful.

REFERENCES

Davis, G.A., Monger, J.W.H., and Burchfiel, B.C.
1978: Mesozoic construction of the Cordilleran "collage", central British Columbia to central California; in Mesozoic Paleogeography of the Western United States, D.G. Howell and K.A. McDougall (ed.), Society of Economic Paleontologists and Mineralogists, Pacific Coast Paleogeography Symposium, v. 2, p. 1-32.

Fields, M.F., Carlson, G.G., and Hickson, C.J.
1990: Mineral showings in the Taseko Lakes (92/O) map area; Geological Survey of Canada, Open File 2207.

Friedman, R.M. and Armstrong, R.L.
1989: U-Pb dating of Permian, Jurassic, and Eocene granitic rocks between the Coast Plutonic Complex and Fraser- Pinchi fault system (51°-54°N), B.C.; in Abstracts with Programs 1989, Geological Society of America, Cordilleran and Rocky Mountain Section Meetings, v. 21, no. 5, p. 81.

Glover, J.K., Schiarizza P., and Garver, J.I.
1988: Geology of the Noaxe Creek map area (92O/02); in Geological Fieldwork 1987, British Columbia Ministry of Energy, Mines and Petroleum Resources, Paper 1988- 1, p. 105-123.

Green, K.C.
1989: Geology and industrial minerals in the Gang Ranch area; British Columbia Ministry of Energy, Mines and Petroleum Resources, Open File 1989-27.

Hickson, C.J.
1990: A new Frontier Geoscience Project: Chilcotin-Nechako region, central British Columbia; in Current Research, Part F, Geological Survey of Canada, Paper 90-1F, p. 115-120.

Kleinspehn, K.L.
1985: Cretaceous sedimentation and tectonics, Tyaughton-Methow asin, southwestern British Columbia; Canadian Journal of Earth Sciences, v. 22, p. 154-174.

Mathews, W.H.
1989: Neogene Chilcotin basalts in south-central British Columbia: geology, ages, and geomorphic history; Canadian Journal of Earth Sciences, v. 26, p. 969-982.

Mathews, W.H. and Rouse, G.E.
1984: The Gang Ranch-Big Bar area, south-central British Columbia: stratigraphy, geochronology, and palynology of the Tertiary beds and their relationship to the Fraser Fault; Canadian Journal of Earth Sciences, v. 21, p. 1132-1144.
1986: An Early Pleistocene proglacial succession in south-central British Columbia; Canadian Journal of Earth Sciences, v. 23, p. 1796-1803.

Misch, P.
1977: Dextral displacements of some major strike faults in the northern Cascades; Geological Society of America, v. 2, p. 37.

Monger, J.W.H. and Price, R.A.
1979: Geodynamic evolution of the Canadian Cordillera - progress and problems; Canadian Journal of Earth Sciences, v. 16, p. 770-791.

Norris, D.K.
1980: Transform, contraction and extension faults in the northern Cordillera of Canada - their spatial and temporal relationships since mid-Cretaceous time; in The Last 100 Million Years of Geology and Mineral Deposits in the Canadian Cordillera, Programme and Abstracts, Cordilleran Section, Geological Association of Canada, p. 29.

Read, P.B.
1988: Tertiary stratigraphy and industrial minerals, Fraser River: Lytton to Gang Ranch, southwestern British Columbia; British Columbia Ministry of Energy, Mines and Petroleum Resources, Open File 1988-29.

Rouse, G.E., Mathews, W.H., and Lesack, K.A.
1990: A palynological and geochronological investigation of Mesozoic and Cenozoic rocks in the Chilcotin-Nechako region of central British Columbia; in Current Research, Part F, Geological Survey of Canada, Paper 90-1F, p. 129-133.

Rust, B.R. and Koster, E.H.
1984: Coarse alluvial deposits; in Facies Models, R.G. Walker (ed.), Geoscience Canada Reprint series 1, p. 53-118.

Tipper, H.W.
1978: Taseko Lakes (92O) map-area; Geological Survey of Canada, Open File 534.

Trettin, H.P.
1980: Permian rocks of the Cache Creek Group in the Marble Range, Clinton area, British Columbia; Geological Survey of Canada, Paper 79-17, 17 p.

Georgia Basin Project: structural evolution of parts of southern Insular and southwestern Coast belts, British Columbia

J.W.H. Monger
Cordilleran Division, Vancouver

Monger, J.W.H., Georgia Basin Project: structural evolution of parts of southern Insular and southwestern Coast belts, British Columbia; in Current Research, Part A, Geological Survey of Canada, Paper 91-1A, p. 219-228, 1991.

Abstract

Vancouver Island and southwestern Coast Belt are divided, from west to east, into northwest-trending, Insular, Sechelt, Howe Sound and Squamish River tracts. The age of stratified rocks within each tract is used as an indicator of structural level. The boundary between Insular tract (mainly Triassic strata) and Sechelt tract (mainly Jurassic strata) appears to be a Late Jurassic magmatic front coextensive with syn(?)-plutonic faults. Within Sechelt tract westernmost tract of the granitic rock dominated Coast Belt, folds in Lower and (?)Middle Jurassic Bowen Island Group predate 155 Ma granitic intrusions. Eastern boundary of Sechelt tract is a probable Early Cretaceous normal fault, east of which Howe Sound tract is structurally the lowest tract, and comprises Lower Cretaceous Gambier Group and coeval plutons. Eastern boundary of Howe Sound tract features contraction faults congruent with early Late Cretaceous mainly southwest-directed structures in Triassic through Cretaceous rocks of Squamish River tract, that are western elements of the major structural and metamorphic culmination in eastern Coast Belt.

Résumé

L'île de Vancouver et le sud-ouest de la zone littorale ont été divisés, de l'ouest à l'est, en bandes orientées vers le nord-ouest : Insular (I), Sechelt (S), Howe Sound (HS) et Squamish River (SR). L'âge des roches stratifiées au sein de chacune des bandes est utilisé comme indicateur du niveau structural. La limite entre Insular (couches principalement triassiques) et Sechelt (couches principalement jurassiques) semble être un front magmatique du Jurassique tardif coextensif à des failles syn(?)plutoniques. Au sein de Sechelt, bande d'extrême ouest de la zone littorale principalement granitique, les plis dans le groupe de Bowen Island du Jurassique inférieur et (?) moyen sont antérieurs aux intrusions granitiques d'il y a 155 Ma. La limite orientale de Sechelt est probablement une faille normale du Crétacé précoce, à l'est de laquelle Howe Sound est, du point de vue structural, la bande la plus basse, et elle comprend aussi les plutons du groupe de Gambier du Crétacé inférieur et des plutons contemporains. La limite orientale de Howe Sound est découpée par des failles de contraction conformes à des structures principalement orientées vers le sud-ouest et datant du début du Crétacé tardif dans les roches triassiques à crétacées de Squamish River, qui sont les éléments occidentaux de la principale culmination structurale et méthamorphique de la partie est de la zone littorale.

INTRODUCTION

One component of Georgia Basin project attempts to determine the regional structural setting within which Upper Cretaceous and lower Tertiary sedimentary strata comprising the fill of Georgia Basin were deposited, by examination of not only of basinal rocks and structures, but also rocks and structures of the generally better exposed basements to the basin. The latter are Wrangellian terrane of the Insular Belt to the west, Coast Belt to the northeast, and Cascade Mountains to the southwest (Monger, 1990). To this end, the field season of 1990 was spent in mapping rock units and their relationships to one another in the structurally poorly known western part of southwestern Coast Belt from Sechelt Peninsula (lat. 49°30') to northern Quadra Island (50°15'), in areas mapped regionally by Roddick and Woodsworth (1977, 1979). Attention was paid to the contact between southwestern Coast and Insular belts, where exposed on islands at the north end of Strait of Georgia and there mapped in detail by Carlisle and Suzuki (1965) and Nelson (1976, 1979). New U-Pb dates from the southern Coast Mountains, mainly from granitic rocks collected by several workers, including the writer, as part of the Southern Cordilleran LITHOPROBE project, give ages of crystallization of the abundant plutonic rocks, and thus precision to interpretations of the structural history (Friedman and Armstrong, 1990).

DISTRIBUTION AND AGES OF ROCKS IN INSULAR TO CENTRAL COAST BELTS

The Insular Belt and southwestern Coast Belt region is divisible into four north-northwest-trending "tracts", described below from west to east (Fig. 1). Each tract is distinguished by predominance of stratified and intrusive rocks of ages different from those of rocks in adjacent tracts, although most stratigraphic units can be correlated from one tract to another (Fig. 2). It should be noted that the proportion of granitic to stratified rocks in the three Coast Belt tracts is approximately 4:1, a ratio reversed in the Insular Belt. Typically, grade of metamorphism of rocks within southwestern Coast Belt is greenschist, whereas that in Insular Belt is subgreenschist (Read, 1988). Grade differences appear to be due mainly to temperature rather than depth of burial during metamorphism, and caused by addition of heat from abundant Coast Belt granitic intrusions, although this has not been rigorously tested regionally. Georgia Basin strata lie mainly on the Insular tract, but overlap the other three.

(1) Insular tract

Predominantly Upper Triassic strata (Karmutsen Formation) but locally Paleozoic through Jurassic strata (Sicker to Bonanza groups) are exposed on Vancouver Island (Fig. 2; Muller, 1977). Intrusive rocks within Insular tract are mainly of Early to Middle Jurassic, locally Tertiary ages (*ca.* 200-175 Ma; 50?, 45-36 Ma; Armstrong, 1988; Webster and Ray, 1990).

Most of Georgia Strait appears to be underlain by Insular tract. The eastern boundary of the tract is exposed only on Quadra Island and other islands near Johnstone Strait, but is submerged west of Twin (Ulloa) Islands (between Mitlenach and Hernando islands), and lies between Texada and Thormanby islands and the mainland (Fig. 1). Although White and Clowes (1984) suggested that their seismic data from Georgia Strait cannot be used to differentiate between Karmutsen and Coast Belt rocks in the subsurface, their data appear to be largely (entirely?) from the Insular tract.

(2) Sechelt tract

The southwesternmost Coast Belt tract underlies southern Howe Sound, extends north-northwestwards through Sechelt Peninsula and the ranges between the town of Powell River and Prince of Wales Reach of Jervis Inlet, to Cortes, Read and northeastern Quadra islands in northern Georgia Strait (Fig. 1). Stratified rocks are mainly Lower and(?) Middle Jurassic (Bowen Island Group), but locally include minor, locally pillowed metabasalt and marble probably correlative with Upper Triassic Karmutsen and Quatsino formations of Insular tract (Fig. 2; Friedman et al., 1990). Plutonic rocks are of Late Jurassic (*ca.* 156-153 Ma) and Early Cretaceous ages (*ca.* 118-114 Ma; Friedman and Armstrong, 1990).

The eastern boundary of the tract crosses Gambier Island in lower Howe Sound, Tzoonie Narrows in Narrows Inlet, and extends north-northwestwards along Prince of Wales Reach of Jervis Inlet and Brittain River (Fig. 1).

(3) Howe Sound tract

East of this, the tract occupying much of the area between Howe Sound and Princess Royal Reach of Jervis Inlet comprises Lower Cretaceous volcanic and sedimentary rock (Gambier Group), and Early Cretaceous plutons (118-114 Ma; 100-102 Ma; Friedman and Armstrong, 1990).

The eastern boundary of Howe Sound tract extends along Indian and Stawamus rivers in the south, through Ashlu Creek northwest of Squamish, to the east side of Queens Reach of upper Jervis Inlet in the north (Fig. 1; Monger, 1990; Lynch, 1991).

(4) Squamish River tract

Easternmost is a tract extending at least as far east as Harrison Lake and Pemberton valleys (Fig. 1), east of which partly correlative strata are penetratively deformed, highly metamorphosed, and structurally imbricated with other rocks including Late Cretaceous granitic rocks, within the core of the "Central Coast Belt-Northwest Cascade System" of Journeay and Friedman (manuscript in prep.; Monger, 1989; Journeay, 1990). Squamish River tract contains stratified rocks ranging in age from Late Triassic to Early Cretaceous (Roddick, 1965; Arthur, 1986; Monger, 1990; Lynch, 1990). Plutons are Late Jurassic to mid-Cretaceous in age (162-145 Ma; 113-111 Ma; 107-102 Ma; 91 Ma; Friedman and Armstrong, 1990).

There are no compelling stratigraphic or plutonic reasons to suspect the existence of different (post-Triassic?) terranes anywhere between western Vancouver Island and Harrison Lake (Fig. 2). Jurassic stratified rock units in Insular and Sechelt tracts can be correlated (Bonanza and Harbledown with Bowen Island), and are similar in composition and overlap in age with Harrison Lake volcanics of Squamish River

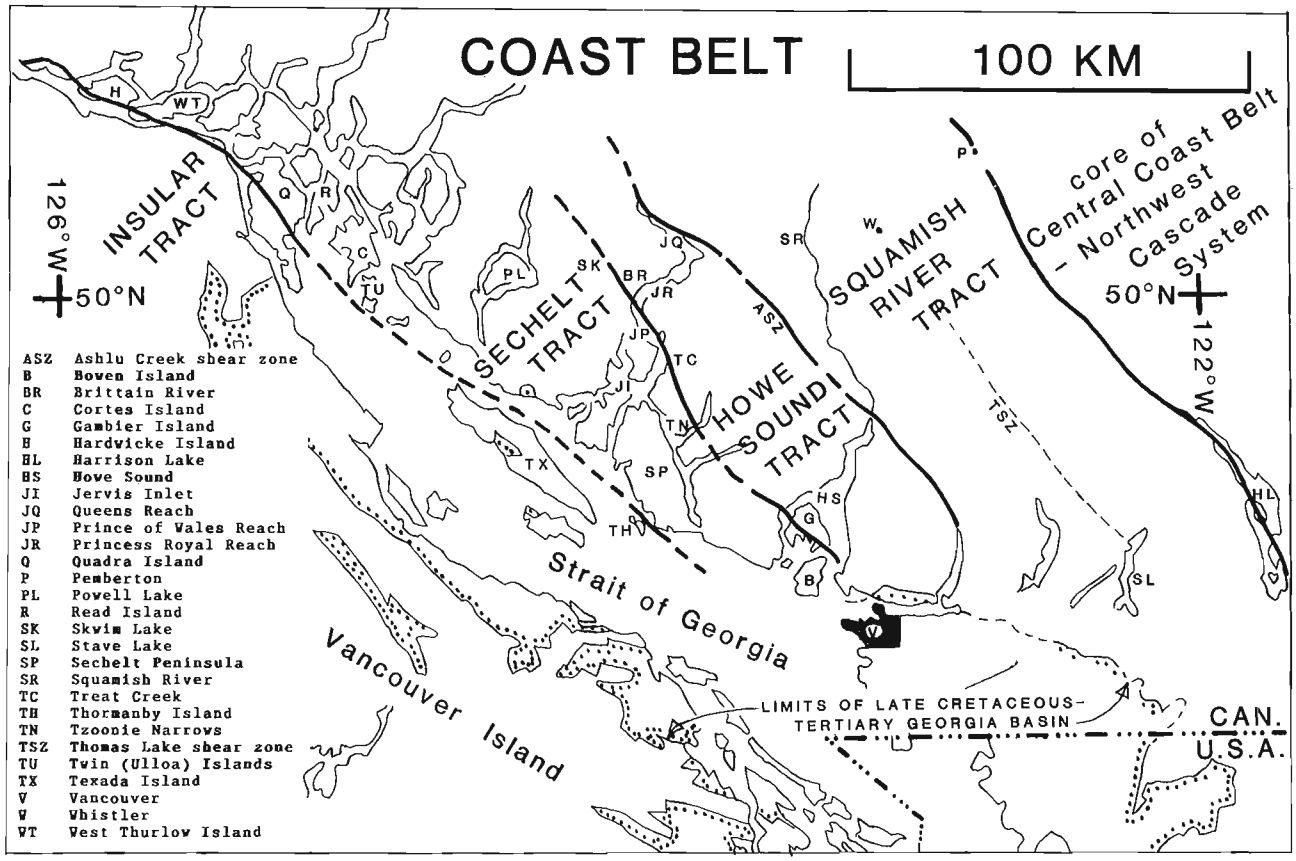

Figure 1. Index map showing tracts, geographic localities in text, and limits of Georgia Basin strata.

tract. Lower Cretaceous intrusive rocks occur in Sechelt, Howe Sound and Squamish River tracts, and Howe Sound and Squamish River tracts have Lower Cretaceous stratified rocks in common. The only Upper Triassic strata recognized in Squamish River tract (Fissile Peak argillite; Monger, 1990) are different from most Upper Triassic rocks in Insular and (?)Sechelt tracts in age and lithology, but arguably they could be a facies of uppermost Triassic Parsons Bay Formation.

The differing ages of rocks within the tracts reflect both varying locations of magmatic fronts in the case of plutonic rocks (Armstrong, 1988; Friedman and Armstrong, 1990), and probable different structural levels in the case of stratified rocks. Howe Sound tract, with its Lower Cretaceous strata, is more than 2 km structurally lower than Sechelt tract to the west of it (see below), and structurally lower than Squamish River tract to the east, in which pre-Cretaceous rocks are widely exposed. Sechelt tract, with its Jurassic strata, appears to be structurally lower than Insular tract, with its predominant Triassic strata. The occurrence of a major structural low well within the Coast Belt is surprising, as much of the belt underwent more than 3 km of uplift in late Neogene-Quaternary time, and an unknown amount of Eocene uplift (Parrish, 1983).

SOME ROCK UNITS AND STRUCTURES WITHIN AND BOUNDING TRACTS

(1) Insular tract

Earlier mapping on Vancouver Island (e.g. Muller, 1977) emphasized block faulting. Later studies combine surface mapping and deep seismic reflection profiling to suggest that the crustal structure of central and southern Vancouver Island consists of imbricated, predominantly northeast-dipping, thrust and reverse faults (Yorath et al., 1985; Clowes et al., 1987). In part (entirely?), the latter structures must be of Tertiary age, as they involve uppermost Cretaceous rocks (Nanaimo Group) which form western parts of Georgia Basin (England, 1989).

According to Webster and Ray (1990), Texada Island features broad northwest-trending open folds with locally intense deformation along three northwest-trending sinistral fault zones. They suggested that emplacement of Middle Jurassic (175 Ma) intrusions has been controlled by these faults. The writer has little to add to this, other than to say that slickensides associated with fibrous calcite steps in fractures in Triassic Marble Bay Formation at the Canada Lafarge Quarry on Texada Island show both sinistral and dextral displacements.

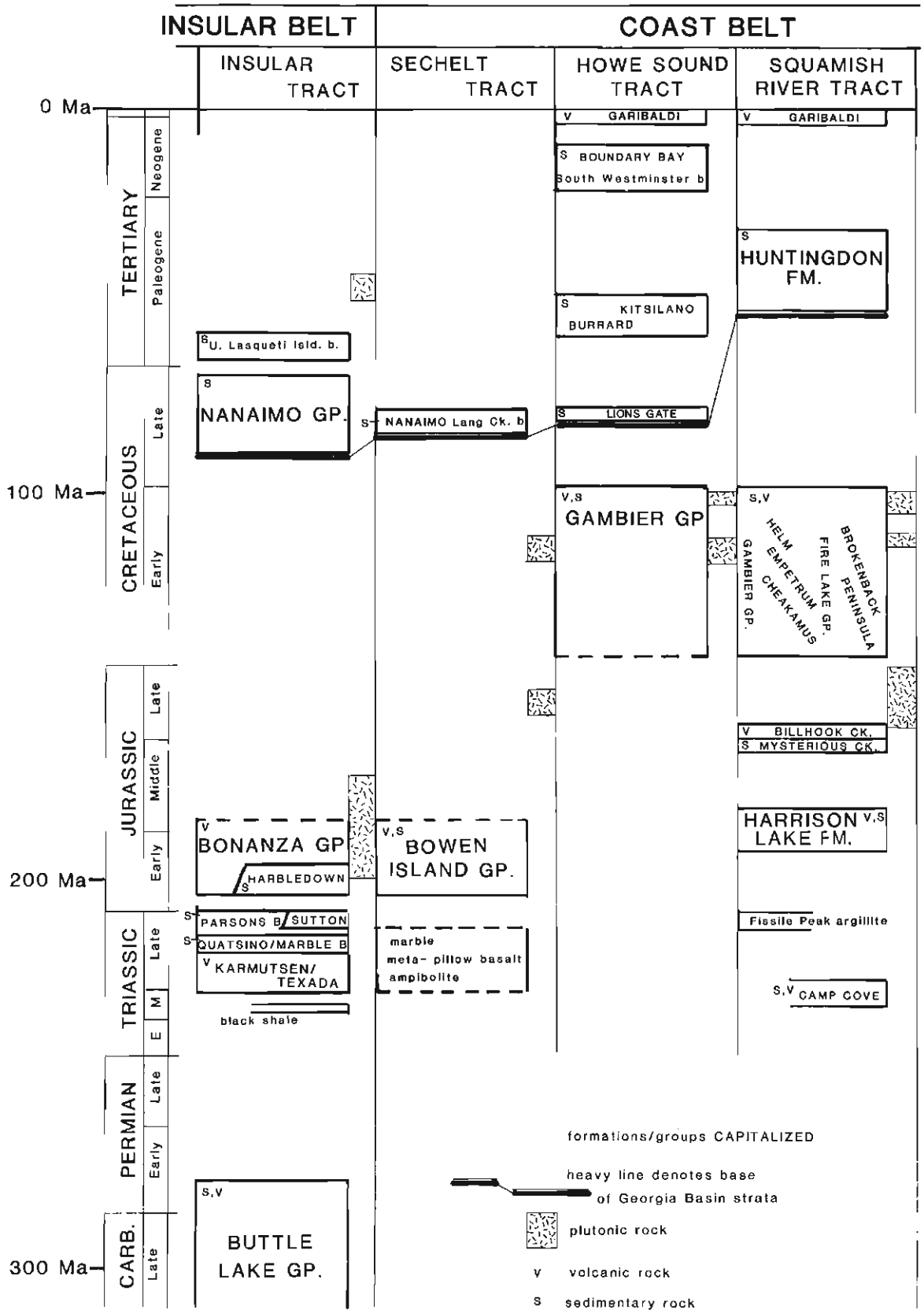

Figure 2. Correlation chart of stratified and intrusive rocks within southern Insular and southwestern Coast belts

The boundary between Insular and Sechelt tracts, which is the western margin of the Coast Belt, is exposed on Quadra Island (Fig. 1), where it has been mapped in detail at Open Bay by Carlisle and Suzuki (1965). The southwestern part of Quadra Island is underlain by little deformed, (bedding dips 20° or less), typically subgreenschist grade, massive and pillowed Karmutsen basalt, and the northeastern part by granitic rocks which yield an Early Cretaceous K-Ar date (104 Ma; Roddick and Woodsworth, 1977). The two lithologies are partly separated by a narrow linear belt of Upper Triassic and(?) earliest Jurassic highly deformed limestone, metabasalt, shale and siltstone. In correlative normal stratigraphic sequences 40 km to west in the Memekay River area on Vancouver Island, similar rocks overlie the Karmutsen. Rocks of this belt are intruded by rusty-weathering diabasic bodies, which are deformed along with the hosting country rock. These rocks are intensely folded into complex tight folds whose axes dip gently northwestward or southeastward. The folds are crosscut by Cretaceous(?) granitic intrusions that underlie northeastern Quadra Island. Near Bodega Point, northwestern Quadra Island, granitic rocks transgress westwards across the belt of the post-Karmutsen strata to intrude Karmutsen. There, the Karmutsen is a foliated fine grained black amphibolite with flattened quartz amygdules. The foliation rapidly diminishes away from the contact and the metamorphic grade changes southwards over a distance of about 2 km, from amphibolite to typical subgreenschist grade, nonfoliated Karmutsen volcanics.

On Quadra Island a close spatial relationship exists between granitic intrusion and deformation, although (most?) deformation appears to predate intrusion. Furthermore, the granitic rocks are mainly hosted by post-Karmutsen strata and thus emplaced within a structurally lower tract than the little deformed more-or-less continuously exposed Karmutsen Formation to the southwest.

On West Thurlow and Hardwicke islands, located 30-40 km northwest of Quadra Island (Fig. 1), similar relationships were reported earlier by Nelson (1976, 1979). Granitic intrusions are hosted locally in Karmutsen Formation but mainly in units that stratigraphically overlie it (Quatsino, Bonanza, Harbledown). On West Thurlow Island, Late Jurassic (K-Ar 155 Ma) granitic rocks intrude a north northeast dipping homoclinal succession correlative with that at Open Bay on Quadra Island. On Hardwicke Island, Upper Jurassic (Rb-Sr 154 Ma) granitic rock clearly crosscuts the steep northwest-trending Telegraph Hill Fault, northeast of which Jurassic strata (Bonanza Group, Harbledown Formation) are downdropped against the Karmutsen.

The evidence supports Nelson's (1979) contention that the western boundary of the Coast Belt at these latitudes is a Late Jurassic magmatic front, probably intruded along pre- or synplutonic faults. The apparent regional linearity of the front, and the observation that west of it mainly Upper Triassic strata are exposed whereas east of it stratified rocks are mainly Jurassic, suggest that a regional system of northeast- side-down Jurassic faults controlled location of the front.

(2) Sechelt tract

Stratified rocks within this tract form a series of pendants that trend north-northwestward within Late Jurassic and Early Cretaceous granitic rocks. Formerly mapped as Lower Cretaceous Gambier Group, these strata are included by the writer in Bowen Island Group, of Early to Middle(?) Jurassic age. The age is based on one U-Pb date of 185 Ma from felsic metavolcanics on Mount Elphinstone, northwest of Bowen Island, and two Early Jurassic fossil localities, one near Skwim Lake, 40 km northeast of the town of Powell River and the other near Iron Point on Twin (Ulloa) Islands, 30 km northwest of Powell River (Friedman et al., 1990; G.J. Woodsworth, pers. comm., 1990). The Bowen Island Group is correlative in age and lithology both with the largely sedimentary Lower Jurassic Harbledown Formation (type area: Harbledown Island, western Johnstone Strait) and the largely volcanic Bonanza Group of Vancouver Island.

Characteristic lithologies of Bowen Island Group are thin layered light and dark grey, white, less commonly green and rarely pink, variably silicified and skarnified fine grained tuff and argillite and siliceous phyllite. Within this facies are rare thin marble layers or local grits and fine grained conglomerates composed of volcanic fragments and rare granitic clasts. Elsewhere are massive or schistose dark to light green volcanics, silicified volcanics, volcaniclastics typically with flattened fragments (Fig. 3) and rare probable ignimbrites.

In places, the thin layering in these rocks can be identified by grading and local rip-up clasts as bedding, but typically it is a layer parallel foliation and accompanied by flattening of clasts in appropriate lithologies. Commonly, it is difficult to distinguish bedding from foliation in the field (Fig. 4). Isoclinal to tight upright folds, generally with plunges less than 35° and no consistent regional vergence, are rare but have been observed in the Bowen Island Group from southeast of lower Jervis Inlet in the south to Twin (Ulloa) Islands in the north (Fig. 5a, b, c). It is not certain whether the folds represent the same contraction episode, because they are in widely separated pendants.

Figure 3. Fragmental volcanic rocks of Bowen Island Group, interbedded with argillite; note flattening of clasts in plane of compositional layering; outcrop about 4 m across; southeast side of northern arm of Powell Lake.

Figure 4. Compositional layering in thin-bedded tuffs and argillites, McMurray Bay, west side of Princess Royal Reach, Jervis Inlet.

On the east side of Jervis Inlet, 7 km northeast of Skookumchuk Narrows, foliated, folded rocks (Fig. 5a) are intruded by a dioritic pluton dated by U-Pb at 155 Ma (Friedman and Armstrong, 1990). The margin of the pluton has a weak fabric and both it and the country rock are cross-cut by felsic dykes which are pulled apart in places. This relationship provides firm evidence for post-185 Ma, pre-155 Ma regional contractional deformation within Sechelt tract. No evidence for Jurassic contraction is recognized in coeval rocks of the Squamish River and Insular tracts at these latitudes.

The eastern margin of Sechelt tract is exposed locally between the east side of Jervis Inlet near Treat Creek, and Tzoonie Narrows on Narrows Inlet, 20 km to the southeast, over a vertical distance of 2000 m (Fig. 1). The contact between Bowen Island Group and Lower Cretaceous Gambier Group is vertical and marked by small bodies of quartz feldspar porphyry and hornblende diorite, and by local intense pyritic alteration, as at the "Copper" property above Treat Creek. West of the contact, foliation in Bowen Island Group is steep to vertical. East of it, massively bedded volcaniclastics and intercalated non-foliated argillites of the Gambier Group dip northeastward and locally southwestward at angles up to about 60°, although typically dips are less (30-40°).

North-northwest of Treat Creek, the contact is submerged in Prince of Wales Reach of Jervis Inlet, with Bowen Island rocks exposed on the west side of Jervis Inlet at Saumarez Bluff, and Gambier Group on the east side, south of Vancouver Bay. North of Vancouver Bay, on the east side of the Inlet, is a complex zone in which Gambier and(?) Bowen Island rocks are intruded by and faulted against numerous granitic and quartz feldspar porphyry bodies. Just east of the bend between north-northwest trending Prince of Wales Reach and northeast trending Princess Royal Reach are (undated) mylonitic granitic rocks that in a zone up to 2 km wide are cut by (undated) amphibolite dykes. In places these form over 30 % of the outcrop, indicating considerable extension across the zone (Fig. 6).

Northwest of this bend, on the north side of Jervis Inlet, the contact between Bowen Island strata and granitic rocks is just east of the debouchment of Brittain River into the Inlet. Foliated and extensively dyked granitic rocks east of this contact are the continuation of the zone southeast of Jervis Inlet shown in Figure 6. East of this again, on the north side of Princes Royal Reach, massive, non-foliated granodiorite is dated by U-Pb at 102 Ma (Friedman and Armstrong, 1990).

On Gambier Island in Howe Sound, easternmost exposures of the Bowen Island Group, cut by Late Jurassic (U-Pb date of 156 Ma; Friedman and Armstrong, 1990) Thornborough Intrusions, have long been regarded as being overlain stratigraphically by the Gambier Group (e.g. Roddick, 1965). The map-pattern suggests the contact is nearly vertical with Gambier bedding dipping away from it at angles between 70° and 35°. The contact is marked locally by conglomerate (and breccia) composed of volcanic and granitic clasts, which grades into Gambier volcanics (Roddick, 1965). Near Halkett Bay, southeastern Bowen Island, where the contact can be approached very closely, Lynch (1991) reported a mylonite 50 cm wide with a near-vertical fabric at the contact, and small drag folds in volcanics close to the contact, suggesting that there the contact is a normal fault.

In conclusion, the eastern boundary of Sechelt tract is best explained as a near-vertical, normal fault zone of regional extent, across which there is a minimum of 2 km of down-to-the-northeast displacement. Exposures in Jervis Inlet indicate that faulting was accompanied by intrusion, and faulting may have attended Early Cretaceous eruption and deposition of Gambier strata. This boundary is not a magmatic front, as Early Cretaceous plutonic rocks occur west of it.

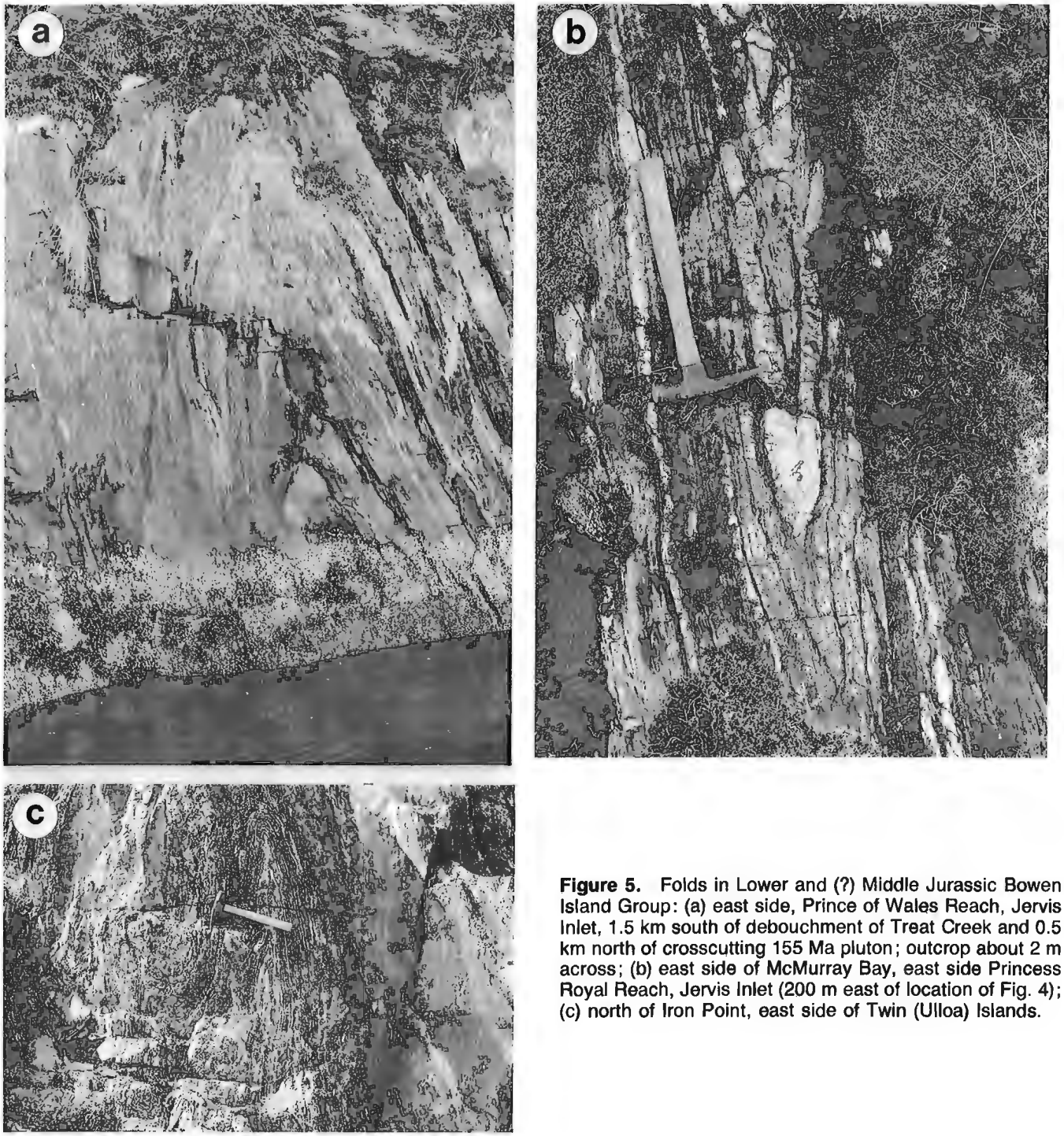

Figure 5. Folds in Lower and (?) Middle Jurassic Bowen Island Group: (a) east side, Prince of Wales Reach, Jervis Inlet, 1.5 km south of debouchment of Treat Creek and 0.5 km north of crosscutting 155 Ma pluton; outcrop about 2 m across; (b) east side of McMurray Bay, east side Princess Royal Reach, Jervis Inlet (200 m east of location of Fig. 4); (c) north of Iron Point, east side of Twin (Ulloa) Islands.

(3) Howe Sound tract

Rocks and structures of Howe Sound tract are described in some detail in several reports and theses on the Britannia mining area, and most recently by Lynch (1991). Much of this tract consists of granitic rock that is of Early Cretaceous age, with pendants of massively bedded intermediate to felsic volcaniclastics, local flows and interbedded fine grained tuff and argillite of the Lower Cretaceous (Albian fossils from this tract) Gambier Group. The latter rocks are typically tilted or folded into broad open folds, and cleavage and/or grain flattening generally are restricted to local zones of intense deformation, some of which accompany southwest- and locally northeast-directed contraction faults (Lynch, 1991).

The eastern boundary of the tract, where exposed in Ashlu Creek valley 40 km northwest of the town of Squamish, is a reverse fault called Ashlu Creek shear zone (Monger, 1990). Cretaceous granitic rocks and foliated volcaniclastic Gambier strata to the southwest are juxtaposed against fractured and locally mylonitic Cloudburst quartz diorite of Late Jurassic age (U-Pb date, 145 Ma; Friedman and Armstrong, 1990). The fault dips steeply to the northeast and fabrics along it indicate northeast-side-up movement.

Figure 6. Foliated granitic rocks extensively dyked by mafic dykes, southeast side of Princess Royal Reach, Jervis Inlet. The dykes and host granite are not dated, but are close to the western boundary of Howe Sound tract; speculatively they could be related to Early Cretaceous extension recorded by a fault along Treat Creek, 15 km south along strike; outcrop about 5 m across.

Farther northeast, the 158 Ma Malibu diorite (U-Pb date; Friedman and Armstrong, 1990) is juxtaposed against black slate to the southwest which has a vertical and steeply northeast-dipping cleavage, and was mapped as Gambier Group by Roddick and Woodsworth (1979). The eastern contact is sharp, although not obviously a fault. No contact metamorphic minerals were seen in the slate, and within the adjacent margin of the diorite are large xenoliths of volcanic breccia not present in the black slate. The slate is intruded on the west by a 102 Ma pluton (Friedman and Armstrong, 1990).

East of Howe Sound, the contact is a complex structural boundary, that extends along the valley containing Stawamus and Indian rivers. East of this boundary are Upper Jurassic granitic rocks (U-Pb date of 147 Ma from north side of Ring Creek, 9 km northeast of Squamish; R.M. Friedman, pers. comm., 1990) cut by Gambier dykes and capped stratigraphically by Gambier volcanics. Lynch (1991) mapped this boundary as a complex fault zone featuring southeast- and northwest-directed thrusts that involve Gambier and older rocks, and late, brittle lateral translation.

The northeastern margin of the Howe Sound tract is of different character from that to the southwest. It is post-Gambier, that is Late Cretaceous, and dominantly contractional, whereas that to the southwest is probably syn-Gambier, Early Cretaceous, and extensional.

(4) Squamish River tract

Summary descriptions of rocks and structures within this tract are given by Journeay (1990), Lynch (1990) and Monger (1990). In general, the tract is structurally higher than Howe Sound tract, so that exposed within it are stratified volcanic and sedimentary rocks as old as Triassic, and pre-Gambier rocks are common (Mathews, 1958; Arthur, 1986; Friedman and Armstrong, 1990). A valuable regional stratigraphic and structural marker within the tract is the basal Cretaceous granite cobble and boulder conglomerate, that at several localities lies stratigraphically on Jurassic granitic and stratified rocks.

Rocks within the tract are cut by several contractional shear zones (Monger, 1990). They increase in frequency towards the northeast and are congruent with thrust faults involving high-grade metamorphic rocks and Late Cretaceous granites east of Harrison Lake-Pemberton valleys. There, between Harrison Lake and Fraser River valleys, is the major structural and metamorphic culmination in the southern Coast Belt, most recently described by Journeay (1990). One of the structures in Squamish River tract, the Thomas Lake shear zone, a northeast-side-up, northeast-dipping reverse fault, has been traced from the head of Stave Lake in the southeast, to 20 km southeast of the village of Whistler in the northwest (Fig. 1; Monger, 1990). Lower Cretaceous Helm Formation (Fig. 2) forms the footwall 20 km southeast of Whistler, and granitic rock dated by U-Pb at 94 Ma (R.M. Friedman, pers. comm., 1990) forms the hanging wall near Thomas Lake. The shear zone is intruded by the Castle Towers pluton, dated by U-Pb at 92 Ma (R.M. Friedman, pers. comm., 1990), clearly dating Thomas Lake shear zone at 93 Ma.

SUMMARY OF REGIONAL STRUCTURAL HISTORY, SOUTHERN INSULAR AND SOUTHWESTERN COAST BELTS

The preliminary work reported here suggests that southern Insular and southwestern Coast belts record a complex structural history of contraction and extension, extending back to at least early Late Jurassic time (pre-155 Ma). Transcurrent structures do not appear to be of major importance here, unlike the southeastern Coast Belt and Cascade Mountains, where they play a major role in creating the regional structural fabric (e.g. Monger, 1986; Brown and Talbot, 1987). Faults with sinistral displacements have been recognized in only two areas. They are of Early to Middle Jurassic age on Texada Island (Webster and Ray, 1990), and post-early Late Cretaceous age along the boundary between Howe Sound and Squamish River tracts (Lynch, 1991). Any pre-Late Jurassic transcurrent structures within the Coast Belt may have been obliterated by the abundant Late Jurassic and Cretaceous plutonic rocks.

The oldest structural event recognized is contractional and represented by folds within the Lower and (?)Middle Jurassic (185 Ma) Bowen Island Group of Sechelt tract. The folds formed prior to intrusion of a 155 Ma pluton. Analogous structures have not been recognized to the east in Squamish River tract, or to the west on Vancouver Island.

As suggested by Nelson (1976, 1979) intrusion of Upper Jurassic (154-155 Ma) plutonic rocks, along a magmatic front which delineates the western margin of the southern Coast Belt, was preceded or accompanied by faulting, that appears to downdrop Sechelt tract to the east relative to Insular tract. The (lithological as opposed to physiographic) western boundary of the Coast Belt at these latitudes thus appears to be

a Late Jurassic feature. As such it may have little significance in terms of the evolution of Georgia Basin.

Subsequently, all southwestern Coast Belt tracts (west of Harrison Lake) were intruded by Lower Cretaceous plutonic rocks, whose surface expression appears to be Gambier Group volcanism. This was probably accompanied by extensional faulting, during which Lower Cretaceous volcanic and plutonic rocks of Howe Sound tract were dropped down relative to Sechelt tract to the west. The granite cobble and boulder conglomerates near the base of the Gambier Group, widespread in Howe Sound and Squamish River tracts, may be the sedimentary expression of such faulting.

The stratigraphic similarity between Vancouver Island and Queen Charlotte Islands has long been recognized. Recent work in the latter location has demonstrated a structural history of Middle Jurassic contraction and Late Jurassic and probable Cretaceous extension (Lewis and Ross, 1991; Thompson et al., 1991) that tantalizingly appears to have more similarities with the fragmentary structural record of Sechelt tract than that reported from Vancouver Island. Jurassic plutonism in Queen Charlotte Islands (Anderson and Reichenbach, 1991) appears to be intermediate in age (172-158 Ma) between ages of Jurassic intrusions in Insular and Sechelt tracts. A major difference is the absence in Queen Charlotte Islands of the Early Cretaceous magmatism so important in the southwestern Coast Belt.

In early Late Cretaceous time (93 Ma), eastern parts of the region underwent contraction, expressed by southwest-directed reverse and thrust faults within Squamish River tract. Squamish River tract was elevated with respect to Howe Sound tract. Congruent contraction structures occur locally within the latter (Lynch, 1991), but have not been recognized farther west. The most intense deformation, highest grade of regional metamorphism, and tract of greatest uplift in the southern Coast Mountains, occur east of the region discussed here, between Harrison Lake and Fraser River (e.g. Journeay, 1990).

For the Insular Belt, England (1989) showed that central and southern Vancouver Island underwent an episode of contraction in post-Nanaimo, early(?) Tertiary time. Southwest directed, thick skinned thrust faults imbricate Upper Cretaceous Nanaimo Group strata with stratigraphically underlying Wrangellian terrane. These structures root beneath Georgia Strait and/or western Coast Mountains, carrying a thin (*ca.* 2 km; White and Clowes, 1984) layer of Georgia Basin strata in their hanging wall. Local preserved remnants of this layer lap on to the Coast Belt (Mustard and Rouse, 1991), but have nowhere been recognized within it.

Northeast-trending faults offset Cretaceous structures in eastern parts of the region, and linear features with this orientation are common in the southern margin of the Coast Belt and Fraser Lowland (Monger, 1990). Such structures are probably of late Tertiary age, as east of the region they involve rocks dated between 24 and 16 Ma as well as mid-Tertiary rocks (Huntingdon Formation) of Georgia Basin (Monger, 1989; J.M. Journeay, pers. comm., 1990).

Uplift of the Coast Mountains in excess of 3 km, occurred in late Tertiary-Quaternary time (Parrish, 1983).

ACKNOWLEDGMENTS

The writer wishes to thank Steve Phillips for the generous offer and use of his boat "Galatea" as a mobile base for field work in northern Georgia Strait and Jervis Inlet, and for his and Andrew Showbridge's enthusiastic assistance in the field. Rich Friedman rapidly produced U-Pb dates on specimens collected by the writer, and freely discussed dates on his own material from the southern Coast Mountains.

REFERENCES

Anderson, R.G. and Reichenbach, I.
1991: U-Pb and K-Ar framework for Middle to Late Jurassic (172-≥158 Ma) and Tertiary (46-27 Ma) plutons in Queen Charlotte Islands, British Columbia; in Evolution and Hydrocarbon Potential of the Queen Charlotte Basin, British Columbia, Geological Survey of Canada, Paper 90-10.

Armstrong, R.L.
1988: Mesozoic and early Cenozoic magmatic evolution of the Canadian Cordillera; Geological Society of America, Special Paper 218, p. 55-91.

Arthur, A.
1986: Stratigraphy along the west side of Harrison Lake, southwestern British Columbia; in Current Research, Part B, Geological Survey of Canada, Paper 86-1B, p. 715-720.

Brown, E.H. and Talbot, J.L.
1987: Orogen-parallel extension in the North Cascades Crystalline Core, Washington; Tectonics, v. 8, p. 1105-1154.

Carlisle, D. and Suzuki, T.
1965: Structure, stratigraphy, and paleontology of an Upper Triassic section on the west coast of British Columbia; Canadian Journal of Earth Sciences, v. 2, p. 442-484.

Clowes, R.M., Brandon, M.T., Green, A.G., Yorath, C.J., Sutherland Brown, A., Kanasewich, E.R., and Spencer, C.
1987: LITHOPROBE-southern Vancouver Island: Cenozoic subduction complex imaged by deep seismic reflections; Canadian Journal of Earth Sciences, v. 24, p. 31-51.

England, T.J.D.
1989: Lithostratigraphy of the Nanaimo Group, Georgia Basin, southwestern British Columbia; in Current Research, Part E, Geological Survey of Canada, Paper 89-1E, p. 197-206.

Friedman, R.M. and Armstrong, R.L.
1990: U-Pb dating, southern Coast Belt, British Columbia; in Project Lithoprobe: Southern Canadian Cordilleran Workshop volume, University of Calgary, p. 146-155.

Friedman, R.M., Monger, J.W.H., and Tipper, H.W.
1990: Age of the Bowen Island Group, southwestern Coast Mountains, British Columbia; Canadian Journal of Earth Sciences.

Journeay, J.M.
1990: A progress report on the structural and tectonic framework of the southern Coast Belt, British Columbia; in Current Research, Part E, Geological Survey of Canada, Paper 90-1E, p. 183-195.

Lewis, P.D. and Ross, J.V.
1991: Mesozoic and Cenozoic structural history of the central Queen Charlotte Islands, British Columbia; in Evolution and Hydrocarbon Potential of the Queen Charlotte Basin, British Columbia, Geological Survey of Canada, Paper 90-10.

Lynch, J.V.G.
1990: Geology of the Fire Lake Group, southeast Coast Mountains, British Columbia; in Current Research, Part E, Geological Survey of Canada, Paper 90-1E, p. 197-204.
1991: Georgia Basin Project: stratigraphy and structure of Gambier Group rocks in the Howe Sound-Mamquam River area, southwest Coast Belt, British Columbia; in Current Research, Part A, Geological Survey of Canada, Paper 91-1A.

Mathews, W.H.
1958: Geology of the Mount Garibaldi area, southwestern British Columbia, Canada; Geological Society of America Bulletin, v. 69, p. 161-178.

Monger, J.W.H.
1986: Geology between Harrison Lake and Fraser River, Hope map-area, southwestern British Columbia; in Current Research Part B, Geological Survey of Canada, Paper 86-1B, p. 699-706.
1989: Geology of Hope and Ashcroft map areas, British Columbia; Geological Survey of Canada, Maps 41-1989 and 42-1989; scale 1:250 000.
1990: Georgia Basin: regional setting and adjacent Coast Mountains geology, British Columbia; in Current Research, Part F, Geological Survey of Canada, Paper 90-1F, p. 95-107.

Muller, J.E.
1977: Geology of Vancouver Island; Geological Survey of Canada, Open File 463; scale 1:250 000.

Mustard, P.S. and Rouse, G.E.
1991: Sedimentary outliers of the eastern Georgia Basin margin British Columbia; in Current Research, Part A, Geological Survey of Canada, Paper 91-1A.

Nelson, J.L.
1976: The origin of Georgia Depression and the Coast Plutonic Complex/Insular Belt province belt boundary on Hardwicke and West Thurlow Islands, B.C.; unpublished M.Sc. thesis, University of British Columbia, Vancouver, 179 p.
1979: The western margin of the Coast Plutonic Complex on Hardwicke and West Thurlow islands, British Columbia; Canadian Journal of Earth Sciences, v. 16, p. 1166-1175.

Parrish, R.R.
1983: Cenozoic thermal evolution and tectonics of the Coast Mountains of British Columbia: 1. Fission track dating, apparent uplift rates, and patterns of uplift; Tectonics, v. 2, p. 601-631.

Read, P.B.
1988: Metamorphic map of the Canadian Cordillera; Geological Survey of Canada, Open File 1893, scale 1:2,000,000.

Roddick, J.A.
1965: Vancouver North, Coquitlam, and Pitt Lake map-areas, British Columbia; Geological Survey of Canada, Memoir 335, 276 p.

Roddick, J.A. and Woodsworth, G.J.
1977: Bute Inlet; Geological Survey of Canada, Open File 480; geological map, scale 1:250,000, with notes on the stratified rocks of Bute Inlet map-area.
1979: Geology of Vancouver, west half, and mainland part of Alberni; Geological Survey of Canada, Open File 611.

Thompson, R.I., Haggart, J.W., and Lewis, P.D.
1991: Late Triassic through early Tertiary evolution of the Queen Charlotte Basin, British Columbia, with a perspective on hydrocarbon potential; in Evolution and Hydrocarbon Potential of the Queen Charlotte Basin, British Columbia, Geological Survey of Canada, Paper 90-10.

Webster, I.C.L. and Ray, G.E.
1990: Geology and mineral occurrences of northern Texada Island; British Columbia Ministry of Energy, Mines and Petroleum Resources, Open File 1990-3; map, scale 1:20,000.

White, D.J. and Clowes, R.M.
1984: Seismic investigation of the Coast Plutonic Complex - Insular Belt boundary beneath Georgia Strait; Canadian Journal of Earth Sciences, v. 21, p. 1033-1049.

Yorath, C.J., Green, A.G., Clowes, R.M., Sutherland Brown, A., Brandon, M.T., Kanasewich, E.R., Hyndman, R.D., and Spencer, C.
1985: Lithoprobe, southern Vancouver Island: seismic reflection sees through Wrangellia to the Juan de Fuca plate; Geology, v. 13, p. 759-762.

Sedimentary outliers of the eastern Georgia Basin margin, British Columbia[1]

Peter S. Mustard and Glenn E. Rouse[2]
Cordilleran Division, Vancouver

Mustard, P.S. and Rouse, G.E., Sedimentary outliers of the eastern Georgia Basin margin, British Columbia; in Current Research, Part A, Geological Survey of Canada, Paper 91-1A, p. 229-240, 1991.

Abstract

Eastern outliers of Georgia Basin were re-examined. At Lang Bay, a floodplain sequence contains Santonian-Campanian palynomorphs, compatible with lower Nanaimo Group correlation. On Texada Island, a conglomeratic unit contains features of fluvial deposition, but reportedly includes early Campanian marine bivalves. An overlying mudstone contains fossils supporting correlation with the Pender Formation, Nanaimo Group. The north end of Lasqueti Island comprises three units. A lower calcarenite contains early Coniacian-Campanian fossils, supporting correlation with the Comox Formation, Nanaimo Group. A middle unit of siliciclastic sandstone contains late Santonian-early Campanian pelecypods. An upper conglomerate-rich unit contains late Paleocene palynomorphs, requiring an unconformity between the siliciclastic units. An outlier at Blue Mountain near Vancouver, previously considered Tertiary, contains Albian palynomorphs. The deepest core from a Fraser Delta well also contains previously unrecognized Albian strata. Thus, Albian sediments are preserved below Upper Cretaceous strata formerly believed the Georgia Basin base.

Résumé

Les buttes témoins orientales du bassin de Géorgie ont été examinés de nouveau. À Lang Bay, une séquence de plaine inondable renferme des palynomorphes du Santonien et du Campanien en accord avec une corrélation avec le groupe de Nanaïmo inférieur. Sur l'île Texada, une unité conglomératique renferme des éléments de dépôt fluvial, mais il aurait été signalé qu'elle comporte des bivalves marins du Campanien précoce. Une mudstone sus-jacente renferme des fossiles appuyant la corrélation avec la formation de Pender du groupe de Nanaïmo. L'extrémité septentrionale de l'île Lasqueti se compose de trois unités. Une calcarénite inférieure renferme des fossiles du Coniacien précoce et du Campanien appuyant la corrélation avec la formation de Comox du groupe de Nanaïmo. Une unité centrale de grès siliciclastique renferme des pélécypodes du Santonien supérieur et du Campanien inférieur. Une unité supérieure riche en conglomérat renferme des palynomorphes du Paléocène supérieur, ce qui exigerait la présence d'une discordance entre les unités siliciclastiques. Une butte témoin au mont Blue près de Vancouver, antérieurement considéré comme appartenant au Tertiaire, renferme des palynomorphes de l'Albien. La carotte la plus profonde provenant d'un puits foré dans le delta du Fraser renferme également des couches de l'Albien non antérieurement reconnues. Ainsi, des sédiments de l'Albien sont conservés sous des couches du Crétacé supérieur que l'on croyait antérieurement la base du bassin de Géorgie.

[1] Contribution to Frontier Geoscience Program
[2] PCI Palynorox Consulting Inc., 2134 West 53rd Avenue, Vancouver, B.C. V6P 1L6

INTRODUCTION

The Georgia Basin is a northwest oriented structural and topographic depression which encompasses Georgia Strait, eastern Vancouver Island and the Fraser River lowlands of British Columbia and northwest Washington State. Sedimentary rocks of the Georgia Basin comprise three main packages: the Upper Cretaceous Nanaimo Group, exposed mainly on eastern Vancouver Island and the Gulf Islands of Georgia Strait; a superimposed Tertiary basin of Eocene (locally Paleocene and Oligocene) rocks exposed in the Vancouver area and northwest Washington; and Miocene rocks in the Fraser River delta area (Fig. 1).

The Nanaimo Group has been extensively studied in the well-exposed western part of the basin (Vancouver Island and main Gulf Islands). England (1989, 1990) provided a recent review. Less documented are upper Cretaceous rocks on the present eastern basin margin and on the more remote Georgia Strait islands. Most of these exposures were examined during 1990 and sampled for palynological analysis. This report describes the outliers and one subsurface section for which palynological results are available.

The Tertiary exposures near Vancouver are also being re-examined. An outlier previously considered Tertiary is here demonstrated to contain a Cretaceous (Albian) palynomorph assemblage.

REGIONAL GEOLOGY

The Georgia Basin overlies three different basement entities: Wrangellia terrane on Vancouver Island; the Coast Belt on the mainland of British Columbia; and Cascade terranes in northwest Washington State (Fig. 1 and Monger, 1990). The

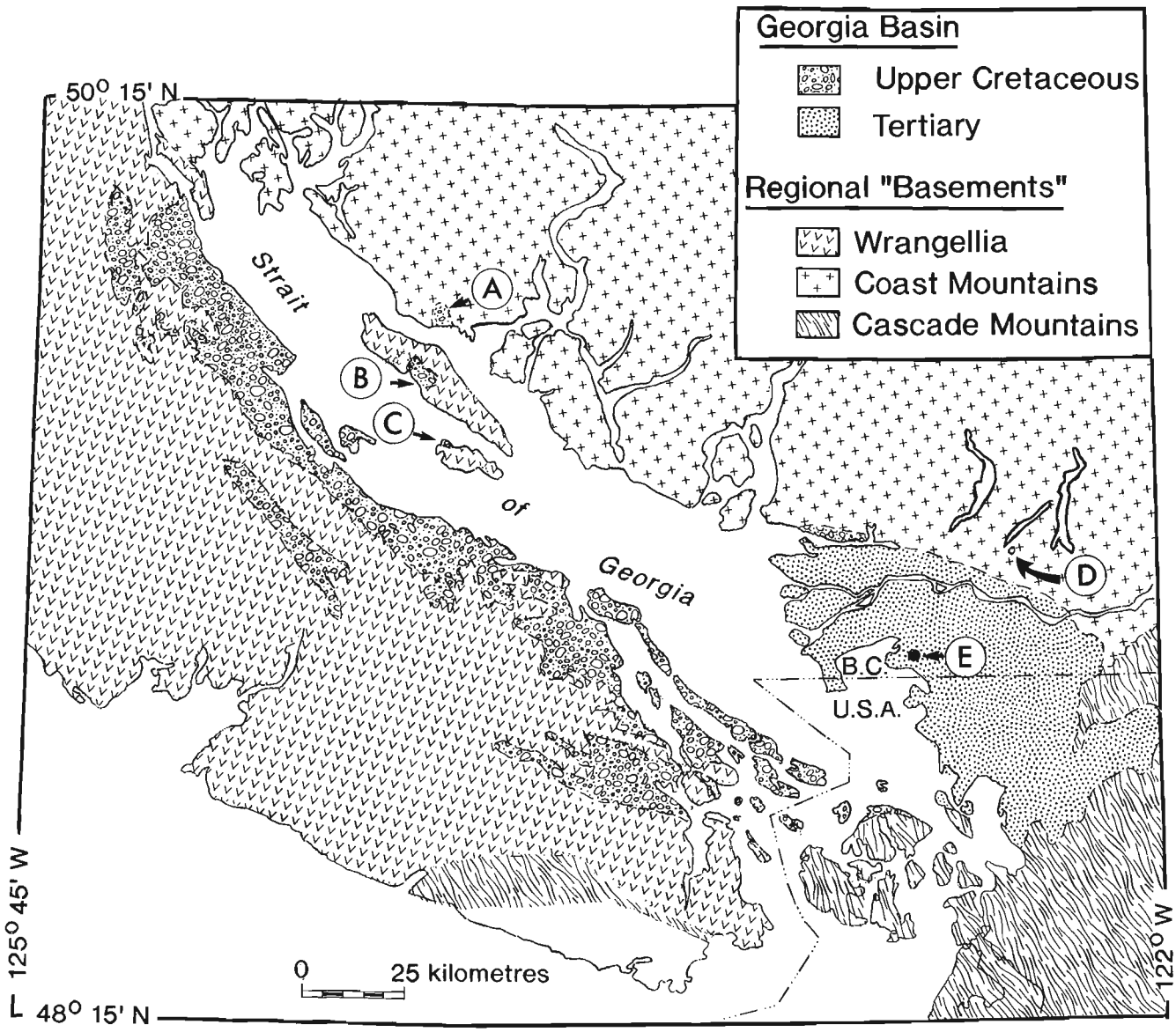

Figure 1. Regional setting of the Georgia Basin (modified from Monger, 1990). Letters indicate localities discussed in this study. **A.** Lang Bay outlier; **B.** Mouet Creek outlier; **C.** Lasqueti Island outlier; **D.** Blue Mountain outlier; **E.** Richfield-Pure Sunnyside exploration well.

main structural control on the sub-Georgia Basin rocks and Georgia Basin itself is underthrusting of the Farallon/Kula oceanic plates beneath the North American plate (Yorath et al., 1985). A mid- to late Cretaceous west-vergent thrust system is preserved at the southern margin of the Georgia Basin (Brandon et al., 1988) and in the eastern Coast Belt, mainly east of Harrison Lake (Journeay, 1990). Dextral strike-slip faults influenced both basin formation and depositional patterns during the Tertiary (Johnson, 1984). The basin has also been affected by early Tertiary compression, which resulted in southwest directed thrusting in the Nanaimo Group (England, 1989, 1990) and possibly caused northwest plunging folds in the Chuckanut Formation (Johnson, 1984). Younger (Miocene?) northeast trending faults and folds are evident on gravity and seismic profiles of the Fraser River lowlands. These are probably the subsurface expression of Tertiary structures preserved in the Coast and Cascade Mountains to the east and north (Monger, 1990).

The Nanaimo Group constitutes up to 4 km of Santonian (locally Turonian) to Maastrichtian age sedimentary rocks. The strata are commonly subdivided into nine formations comprising conglomerate, sandstone, and mudstone, with coal in lower units (Muller and Jeletzky, 1970). The basal, coal-bearing formations appear to have formed in coastal plain, deltaic and shallow marine environments (Muller and Jeletzky, 1970). Most recent interpretations of the other formations emphasize submarine fan models (eg. Ward and Stanley, 1982; England, 1990). Interpretations of the tectonic controls on basin sedimentation include forearc (Ward and Stanley, 1982; England, 1990), strike-slip (Pacht, 1984) and foreland (Brandon et al., 1988) models.

Except for an isolated occurrence of Paleocene rocks on Lasqueti Island (Rouse et al., 1990; this study), the Tertiary rocks of the Georgia Basin are only exposed in the lower Fraser Valley and northwestern Washington. The main stratigraphic components are nonmarine clastics of the Paleocene-Eocene Chuckanut Formation of Washington State, the partly equivalent upper Burrard and Kitsilano formations of the Vancouver area, the late Eocene to Oligocene age Huntingdon Formation, and younger (mostly Miocene) sedimentary rocks known from a few surface exposures and subsurface drilling. Bustin (1990) summarized the sedimentological history of these rocks. Upper Cretaceous rocks occur disconformably beneath the Tertiary strata at Burrard Inlet in Vancouver (Rouse et al., 1975) and in the western Fraser River delta subsurface (Hopkins, 1966). Gordy (1988) compiled available seismic and drillhole data and suggested that the upper Cretaceous and Tertiary strata continue to the west beneath Georgia Strait.

GEORGIA BASIN OUTLIERS

Lang Bay

A sedimentary outlier of about 35 km^2 is preserved at Lang Bay, about 13 km southeast of Powell River (Fig. 1, 2). Outcrop is limited to discontinuous exposures in Lang Creek (described in White, 1986). Conglomerate, sandstone and mudstone dip 10-15° to the southwest. The sequence unconformably overlies granodiorite and, in the northwest part of the outlier, mafic volcanics. Crickmay and Pocock (1963) and Bradley (1972) reported late Cretaceous palynomorphs from this outlier and suggested correlation with the lower Nanaimo Group (Comox or Extension formations). White (1986) reviewed the exploration history of the area, which most recently was evaluated for industrial kaolin. More than 50 drillholes were emplaced during 1987-89 by Fargo Resources Ltd. and Brenda Mines Ltd. to evaluate the kaolin deposits. The thickest drill intersection of Upper Cretaceous strata is about 70 m, with Quaternary alluvium directly overlying the Cretaceous strata. Drill cores from several of these holes were logged and sampled for this study, and the Lang Creek exposures were examined.

Two of the core logs are shown in Figure 2. Fining and thinning upward trends are apparent, both on the scale of the preserved sequence (tens of metres) and as smaller cycles (a few metres or less). Conglomerates are clast-supported and moderately sorted with subround pebbles and rare cobbles in an arkosic matrix. Conglomerate clasts are predominantly granitic or mafic volcanic in composition, compatible with local derivation. Sandstones are arkosic or lithic arenites. Mudstones are brown or grey-green and massive, rarely laminated. Normal grading is common in both conglomerate and sandstone beds. Many sandstones display planar or (less common) trough crossbedding. The few well-exposed crossbeds in Lang Creek indicate paleoflow towards the southwest. The small-scale fining upward cycles display gradational upward change from coarse, graded sandstone with abundant mudstone ripups to trough crossbedded medium-grained sandstone, to rippled or wavy bedded fine-grained sandstone and siltstone, to massive mudstone. Many mudstones are carbonaceous and contain abundant plant debris. Rare coal lenses are present in Lang Creek (White, 1986) and in one place, in situ root systems are preserved.

The metre-scale cycles display features of fluvial channel and point-bar deposits (cf. Walker and Cant, 1984). The isolated graded sandstone beds in mudstones are interpreted as crevasse-splay deposits. These features, plus the presence of coal lenses, and *in situ* rootlets support a fluvial-floodplain depositional model (also suggested by White, 1986).

Palynomorph assemblages have been obtained from about 6 surface samples along Lang Creek and 6 mudstone layers in drillcore (Table 1). Most palynomorphs range from the Santonian to Campanian, but a few range to Albian-Cenomanian, and others into the Maastrichtian. The Santonian-Campanian range agrees with the invertebrate-based range given for the Comox through Extension Formations by Muller and Jeletzky (1970), as modified by Ward (1978) and Haggart and Ward (1989).

At Lang Bay, several palynomorph species appear restricted to the upper beds, viz. *Proteacidites thalmanni, P. marginus, Tricolpopollenites divergens,* and *Tricolporopollenites punctatus*. These are also found in the Extension-Protection Formations of Vancouver Island, and the Lions Gate Formation at Vancouver (Rouse et al., 1975, p. 469, Table 1), but appear absent from Comox and older equivalents. Hence, preliminary results suggest that there is a contact between younger and older segments of the Santonian-Campanian series near the top of the Lang Bay sequence.

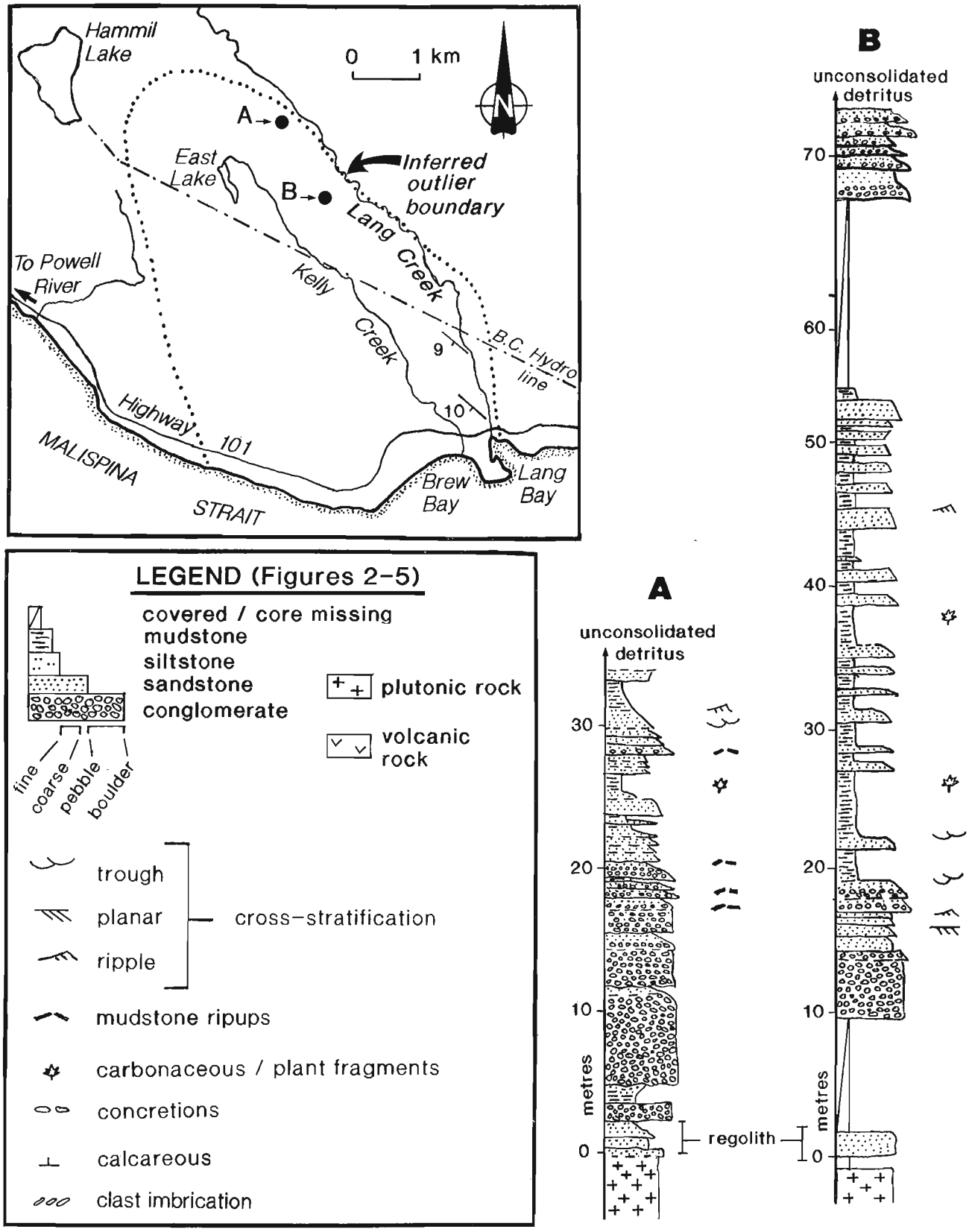

Figure 2. Lang Bay outlier with logs from two drillholes. Outlier boundary is modified from White (1986).

Table 1. Palynomorphs recovered from the Lang Bay outlier, listed according to main plant groups to facilitate paleoenvironmental translation.

Dinocysts	Fern Spores
Odochitina costata	*Gleicheniidites senonicus*
Isabelidinium arcuminatum	*Cyathidites minor*
I. cretaceum	*Ceratosporites cf. coulienisis*
Diconodinium glabrum	*Ornamentifera tuberculata*
D. multispinum	*Cicatricosisporites hughesi*
D. cf. inflatum	*C. cf. mohrioides*
Paleostomocystis laevigata	*C. sp.*
Astrocysta cretacea	*Laevigatosporites ovatus*
Deflandrea spectabilis	
D. cf. nucula	**Angiosperm pollen**
Lejeunia cf. schinoidea	*Tetraporites sp.-2*
Canningia colliveri	*Proteacidites thalmanni*
	P. marginus
Gymnosperm pollen	*Tricolpopollenites divergens*
Vitreisporites pallidus	*Tricolporopollenites punctatus*
Alisporites microformis	
Pinus haploxylon	**Fungal Spore**
	Pluricellaesporites psilatus

The predominance of dinocysts suggests a marine influence on deposition. A coastal plain setting for the fluvial-floodplain model suggested above seems probable, with dinocysts deposited during transgressive stages, mixing with small numbers of pollen and spores from ferns and trees surrounding the floodplain.

Mouat Creek, Texada Island

Several small sedimentary outliers were mapped on Texada Island by McConnell (1914), and correlated with the Nanaimo Group based on Upper Cretaceous megafossils. The largest outlier occurs at Gillies Bay (Fig. 3). The only significant outcrops are on Mouat Creek, which enters Mouat Bay 5 km southeast of the Gillies Bay townsite. The rocks are discontinuously exposed over about 3 km with the most westerly (stratigraphically highest) exposure about 1.5 km upstream of Mouat Bay.

Figure 3 shows a generalized section from Mouat Creek. The lowest sedimentary rocks unconformably overlie fractured mafic volcanic rock of the Triassic Texada Formation (Webster and Ray, 1990). The unexposed unconformity can be defined within 20 m. The lowest sedimentary rocks comprise a few metres of massive red-brown mudstone and sandstone with common cobbles and boulders of volcanic clasts extensively altered to clays and silts, leaving cores of remnant volcanic. This is interpreted as unconformity surface regolith (recognized by McConnell, 1914, p. 32).

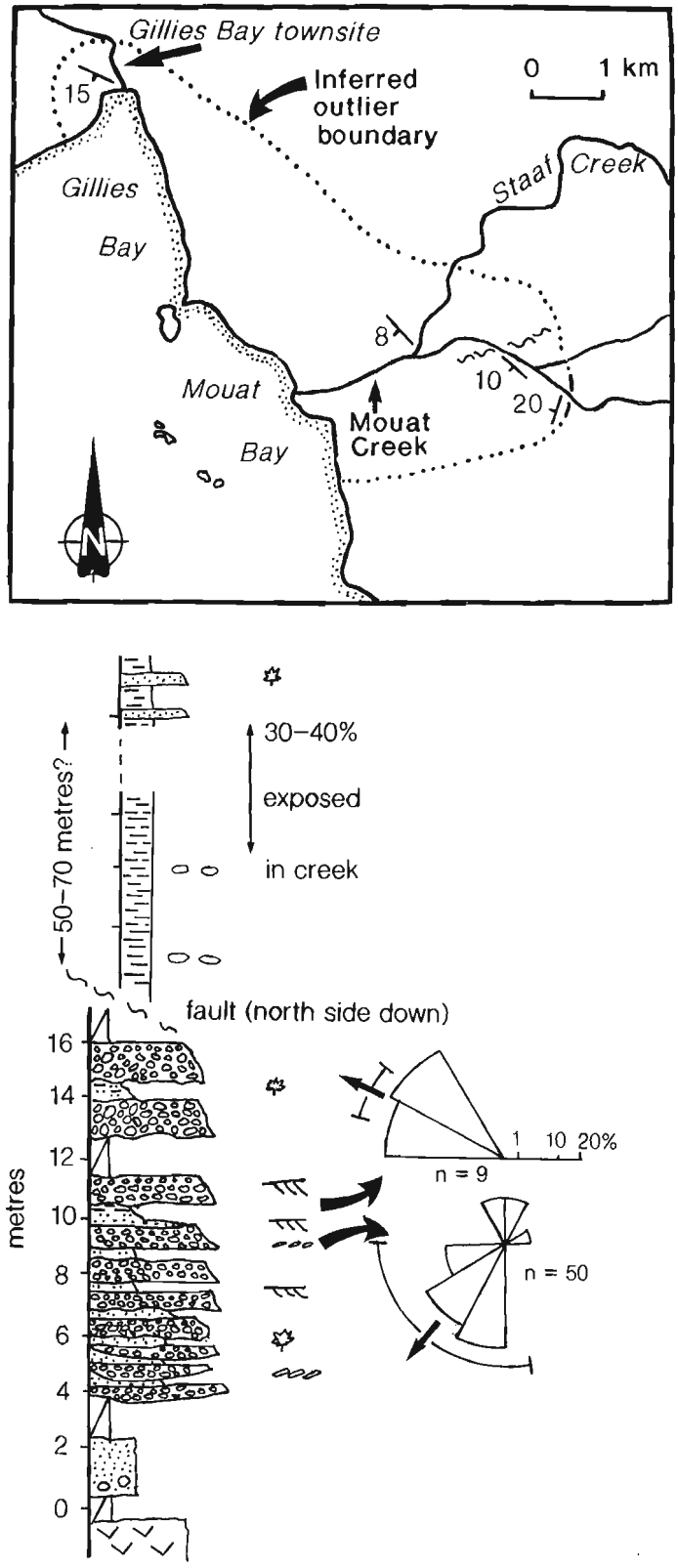

Figure 3. Mouat Creek outlier and generalized stratigraphic section. Outlier boundary is modified from McConnell (1914).

The regolith is overlain by about 15 m of pebble-cobble conglomerates with a few interbeds of sandstone and silt-rich mudstone. Beds dip at low angles (5-20°) and range in dip-direction between south and west. The conglomerates are clast-supported, moderately sorted and composed of > 90 % subround volcanic clasts similar to the basement volcanics. Most conglomerates are normally graded. Clast imbrication and planar crossbedding indicate paleoflow ranging from southwest- to northwest-directed. Conglomerate beds are generally < 1 m thick and discontinuous laterally over a few tens of metres. The sandstone and siltstone interbeds occur as discontinuous lenses cut out laterally by succeeding conglomerate channels. Sandstones are generally red-brown lithic arenites. Silt-rich mudstones are brown to dark grey. Some contain carbonaceous plant fragments, but insufficient well-preserved palynomorphs were recovered for meaningful analysis.

The lower unit is overlain by a thick mudstone succession. The contact is not exposed, but the outcrop pattern suggests a minor east-west oriented fault separates these units, with the mudstones downdropped on the north side. The mudstone is medium to dark grey, non-calcareous and massive, but rare sandstone interbeds near the west limit of exposure dip about 10° southwest. The discontinuous exposure and lack of lamina hinder measurement of a true thickness, estimated to be 50-70 m.

Invertebrate megafossils are preserved in the mudstone, many occurring within carbonate concretions (GSC Locality C-101519, Haggart, 1990). Most common are the bivalves *Inoceramus subundatus* Meek and *Inoceramus vancouverensis* Shumard. Also collected were several *Parallelodon (Nanonavis) vancouverensis* (Meek) bivalves, a single *Biplica obliqua* (Gabb) gastropod and two ammonites identified as *Canadoceres newberryanum* (Meek) and *Canadoceres* sp. transitional from *C. yokoyamei* (Jimbo) to *C. Newberryanum*. Ward (1978) collected *Baculites chicoensis* Trask from this unit and *Inoceramus schmidti* Michael from the underlying conglomerates. Ward correlated the conglomerates with the Extension Formation of the Nanaimo Group and the upper mudstone unit with the Pender Formation. The new fossil collection indicates an early Campanian age (Haggart, 1990), which supports the latter correlation.

The discontinuous outcrop on Mouat Creek does not contain sufficient features for a detailed interpretation of depositional environments. The overlapping conglomerate lenses with scoured bases, imbrication, and planar crossbedding suggest braided fluvial processes (cf. Rust and Koster, 1984). The local source of conglomerate clasts, presence of regolith and reworked regolith in lower beds, are all compatible with a subaerial fluvial interpretation. However, Ward (1978) collected one or more marine bivalves from this unit. Submarine braided channel conglomerates are well-documented (eg. Hein and Walker, 1982). Without strong evidence for subaerial deposition (desiccation cracks, *in situ* roots, etc.), a submarine braided channel model cannot be ruled out.

The upper mudstones generally lack sedimentary structures, implying sheltered deposition. The megafossil types and form of occurrence suggest a marine middle to outer shelf (Haggart, 1990).

Lasqueti Island

The northern end of Lasqueti Island contains an outlier of sedimentary rock well exposed on the main shoreline from Scottie Bay to Spring Bay, on the islands in Scottie Bay, and on Jelina Island to the east (Fig. 4). The rocks are shown on published maps as an unnamed Upper Cretaceous or Tertiary unit at the top of the Nanaimo Group (Muller and Jeletzky, 1970); part of the Gabriola Formation, the top unit of the Nanaimo Group (Muller, 1977); and as an undivided map unit correlative with the Upper Cretaceous lower Burrard and the Tertiary upper Burrard and Kitsilano formations of the Vancouver area (Roddick et al., 1976). Rouse et al. (1990) reported Paleocene palynomorphs in samples from this outlier, first reported as a personal communication to J.E. Muller in Muller and Jeletzky (1970, p. 33).

Three sedimentary units can be defined, dipping 10-25° northward (Fig. 4). The sedimentary rocks unconformably overlie mafic volcanics of the Triassic Karmutsen Formation. The unconformity is well exposed at Spring Bay and on Jelina Island. An irregular paleotopography with > 10 m of relief over about 40 m of lateral exposure is apparent. A breccia/conglomerate up to 3 m thick is preserved in a few places on the unconformity surface. Clasts are up to 2 m in diameter and all are of identical composition to the subjacent volcanics.

The basal breccia grades upward over a few decimetres to a sandstone unit about 30 m thick (Fig. 4, section A). The sandstone is a green-grey, medium- to very coarse-grained calcarenite. It is composed of broken fossil material and up to 30 % mafic volcanic sand grains in a sparry calcite cement. The carbonate grains include fragments of pelecypods, echinoderm plates, oolites, and micritic intraclasts and pellets. Thick walled, nearly complete oyster shells are common, but have not been identified to genus level. Several specimens of the pelecypod *Pterotrigonia evansana* (Meek) were recovered (Haggart, 1990; GSC localities C-101522 and C-101524). This fossil, indicative of an early Coniacian to Campanian age (Jones, 1960) also occurs in a small outlier of "coarse sedimentary breccias and greywacke" reported from southwest Lasqueti Island and from the basal Nanaimo Group Comox Formation at several places on Vancouver Island (Crickmay and Pocock, 1963). Correlation of the northern Lasqueti Island calcarenite with the Comox Formation is warranted.

The calcarenite occurs in slightly wavy beds up to 10 cm thick. Planar crossbedded sets occur as lenses up to 20 cm thick, but discontinuous laterally over a few tens of metres. Planar crossbeds demonstrate paleoflow was towards the northwest. Rare overlapping trough crossbedded lenses are also present. The association of these features with the reworked unconformity breccia, trigonids and thick-walled oysters, and abundant broken shell material indicates an open marine, inner shelf paleoenvironment, suggested by Haggart (1990) to be < 30 m paleodepth.

The calcarenite unit is overlain at Scottie Bay by > 80 m of pale yellow-orange lithic arenite with minor interbeds of siltstone and mudstone. The contact is sharp, but beds below and above are roughly parallel. However, the change from the underlying shelly carbonate clastic to the fossil-poor siliciclastic implies an unconformity.

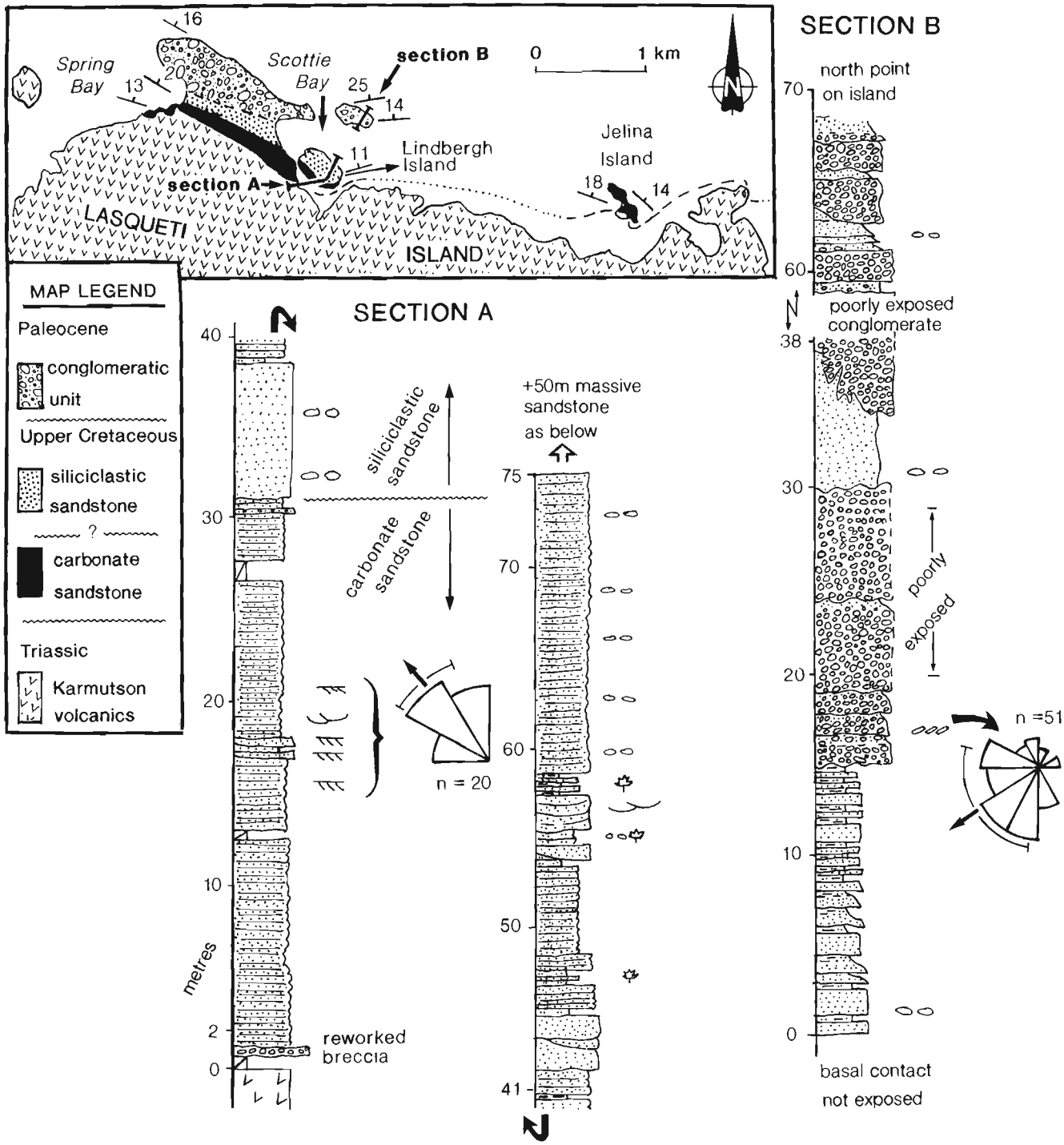

Figure 4. Lasqueti Island outlier and stratigraphic sections.

Most of the lithic arenite is medium- to coarse-grained, moderately sorted and composed of subangular to subround quartz (25-35 %), feldspar (15-20 %), and up to 50 % lithic grains, mostly mafic volcanic, chert and siltstone. Beds are generally slightly wavy, massive, structureless and occur as laterally continuous sheets up to 8 m thick. Ovoid carbonate concretions up to 2 m diameter are common. Interbeds include thin-bedded, fine-grained lithic arenites, siltstones with shell and detrital coal fragments, and grey carbonaceous mudstones, some with abundant plant fragments.

This sandstone-dominated unit is generally unfossiliferous. Simple horizontal trace fossils occur in some fine grained sandstone beds. Rare shell fragments include possible *Inoceramus* pelecypods. Two complete *Sphenoceramus elegans* (Sokolov) pelecypods were recovered (Haggart, 1990; GSC Locality C-101523). This is the index species of the lower, *S. elegans* subzone of the *Spenoceramus schmidti* zone of the Nanaimo Group (Muller and Jeletzky, 1970). The collection indicates a late Santonian or possibly

earliest Campanian age (Haggart, 1990) supporting correlation with the lower Nanaimo Group (possibly the Extension Formation).

No detailed interpretation of depositional environment is attempted for this unit. The thick, structureless sandstones with bases slightly erosive into finer sediments are somewhat similar to some submarine fan facies. However, a more thorough examination of this unit is needed before any depositional model is proposed.

The top unit is a > 70 m thick sequence exposed on the unnamed island at the northeast end of Scottie Bay and on the north-facing shoreline of Lasqueti Island. Beds dip 15-25° to the north. The contact with the underlying sandstone unit is within a covered interval 20-40 m thick. The lowest rocks comprise 15 m of interbedded greyish orange, fine- to medium-grained arkosic and micaceous arenite and dark grey mudstone (Fig. 4, section B). The sandstone occurs in sets of slightly wavy horizontal thin beds up to 3 m thick (most < 50 cm) with loaded contacts with the underlying mudstone interbeds. Ovoid carbonate concretions up to 1.5 m diameter occur in some sandstone beds. This sandstone-mudstone lithofacies is sharply overlain by > 55 m of pebble-cobble conglomerate and interbedded coarse-grained arkosic arenite. Conglomerate beds are generally clast-supported with a coarse-grained matrix. Bedding is commonly indistinct, but where definable beds are 0.5-2 m thick and occur as overlapping lenses. Conglomerate bases indicate several metres of erosion into underlying sandstone in some places. Loading of conglomerate into sandstone is also common and sandstone dykes cut some conglomerate beds. Clast imbrication indicate paleoflows ranging between west and southwest-directed. About half of the clasts are of mafic volcanic and dyke compositions. Granitic, felsic volcanic, grey chert and argillite make up remaining clast types, all compatible with the eastern provenance suggested by the paleocurrent data.

The top contact of many conglomerate beds is slightly irregular, with common projecting clasts. Rarely, a discontinuous, white, chalky carbonate layer a few centimetres thick is preserved at this contact, both draping and cementing pebbles. These layers are identical to subaerial caliche weathering horizons, common on alluvial fans (eg. Nilsen, 1982, Fig. 51). Most other features of this unit also suggest alluvial fan deposition, with the thick massive conglomerate deposited as debris flows and the thinner, better channelized conglomerate and pebbly sandstone deposited in braided channels. The immediately underlying interbedded sandstone and mudstone are probably lower fan fluvial and floodplain deposits.

Megafossils are absent from this unit, but a reasonably large and well preserved palynoassemblage was obtained from the finer facies and indicate a late Paleocene age (Table 2). This list is from samples collected in 1990, separate from that contained in Rouse et al. (1990, p. 110-11, #3).

The most diagnostic palynomorphs are the angiosperms *Subtriporopollenites* -A (pre-*Tilia*), and *Pistillipollenites mcgregorii*. These occur together only in zone P-4, late Paleocene, in the thick Eureka Sound section on Ellesmere Island and correlative sections on other Arctic islands, and in the Alberta foothills, Mackenzie Delta and Beaufort Sea regions (Rouse, 1977). This assemblage occurs just below

Table 2. Palynomorphs from the unnamed island in Scottie Bay, Lasqueti Island.

Fungal Spores	Angiosperm pollen
Multicellaesporites irregularis	*Quercoidites microheurici*
M. elongatus	*Q. explanata*
M. serratus	*Alnus vera*
M. conicus	*Momipites inaequalis*
M. Sp.-6	*Triporopollenites mullensis*
M. Sp.-10	*Paraalnipollenites alterniporus*
Tricellaesporonites semicirularis	*Subtriporopollenites* -A (= pre *Tilia*)
Dicellaesporites laevis	*Pistillipollenites mcgregorii*
Callimothallus pertusus	**Fern Spores**
Conifer Pollen	*Deltoidospora diaphana*
Cupressacites hiatipites	*Laevigatosporites ovatus*

early Eocene assemblages containing the earliest true *Tilia* pollen, eg. *T. crassipites* and *T. Vescipites*.

The mixture of fungal spores and angiosperm pollen suggests lowland conditions, compatible with a floodplain environment suggested above. The general lack of algal cysts also supports a terrestrial interpretation.

The late Paleocene palynoassemblage requires an unconformity in the unexposed interval separating this unit from the underlying Santonian-lower Campanian sandstone unit. There is no major change in bedding orientation and the sandstone in both units are similar, but the upper sandstones are much more micaceous, with up to 15 % muscovite visible in hand sample, and only traces visible in thin section in the lower.

Blue Mountain

An outlier of about 15 km^2 is preserved east of Blue Mountain, about 3 km east-southeast of the south end of Alouette Lake (Fig. 1, 5). Strata dip 5-25° to the south. This poorly exposed outlier unconformably overlies a diorite pluton and comprises up to 150 m of moderately to poorly indurated conglomerate, sandstone and mudstone, including a thick (15-30 m) mudstone intermittently evaluated as an industrial clay source since the early 1900s (eg. Ries and Keele, 1915). The outlier is shown on published maps as part of the Eocene-Oligocene Huntingdon Formation (Roddick et al., 1976) or part of an undivided Tertiary unit (Roddick, 1965). No fossils have been reported. The outlier has commonly been used to define the preserved north boundary of the Tertiary part of Georgia Basin (eg. Bustin, 1990, his Fig. 1).

Blue Mountain Explorations Inc. drilled nine diamond drillholes during the summer of 1990. Several drillcores were logged and sampled for this study. Outcrop were also examined and a stratigraphic section measured. Figure 5 displays the measured section and two drillcore logs.

The basal unconformity is exposed at the northwest end of the outlier, where diorite is overlain at a sharp irregular contact by a boulder-rich conglomerate. The conglomerate is > 60 m thick here, but only 5 m thick in the one drillhole

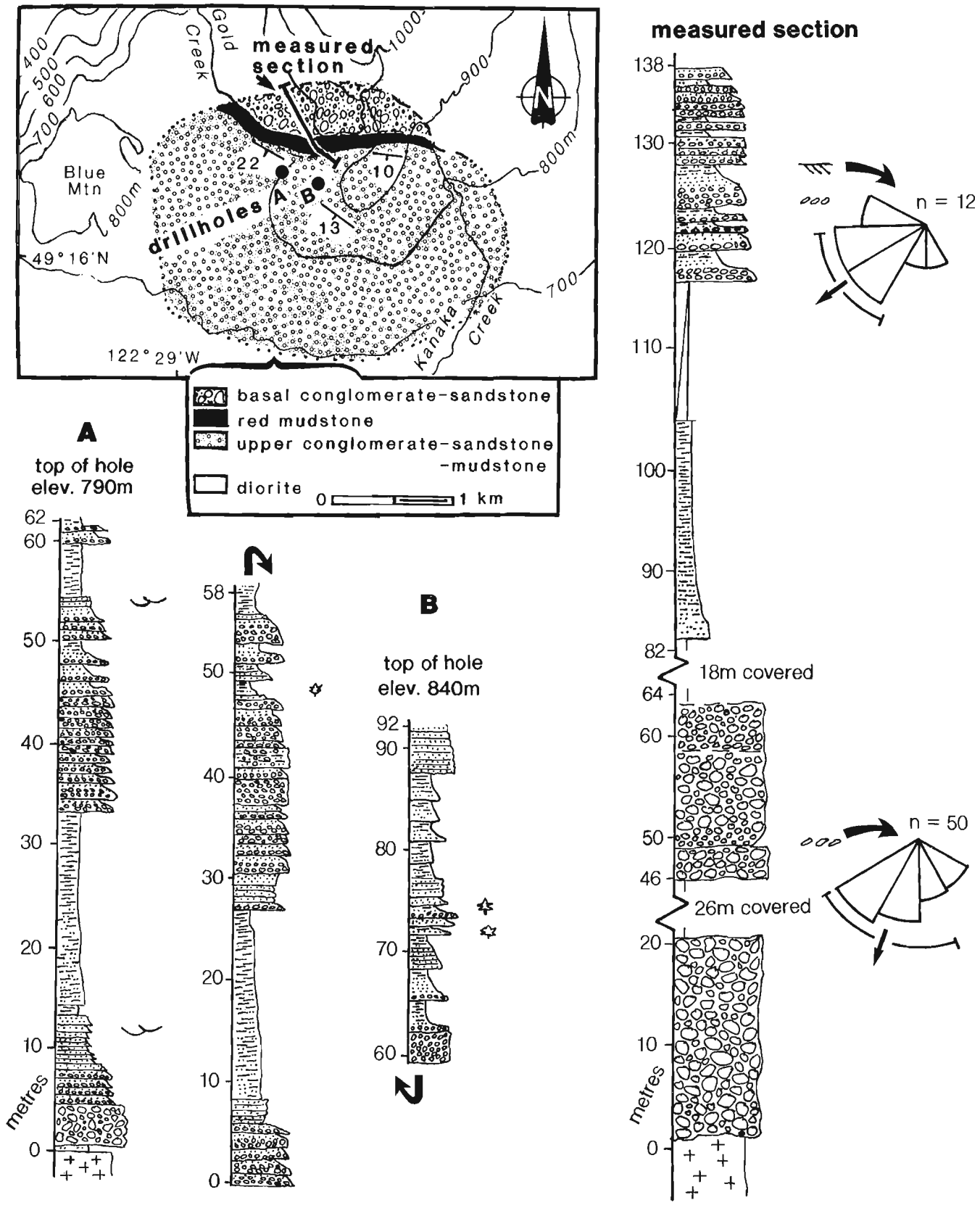

Figure 5. Blue Mountain outlier, two drillcore logs and measured stratigraphic section.

which reached the unconformity (Fig. 5, drillhole A). The conglomerate is clast-supported and poorly sorted with up to 40 % boulders in a coarse grained lithic wacke matrix. Clasts are subround to subangular and more than 70 % are dioritic, similar to the subjacent pluton. Massive, poorly defined beds generally > 2 m thick are typical. Rare reverse-graded beds contain imbrication indicating paleoflow towards the south.

The conglomerate is gradationally overlain by normal-graded pebbly lithic wacke, in turn overlain by the thick mudstone unit. The mudstone is red-brown, massive and slightly tuffaceous, with rare wispy lamina, and fines upward from a silt-rich base to claystone in the upper few metres. The mudstone is sharply overlain by up to 65 m of pebble-conglomerate, lithic arenite and mudstone organized in repeated fining-upward cycles generally 1-2 m thick. Planar and rarely trough crossbedding indicate paleoflow to the southwest. The mudstones which cap the cycles are dark brown or grey, both tuffaceous and carbonaceous and with abundant coalified plant debris and rare coaly lenses a few centimetres thick.

The poorly sorted boulder conglomerates are typical of debris flow alluvial fan deposits (cf. Rust and Koster, 1984). These change upward to pebbly sandstone, probably deposited in mid- or lower fan braided channels. The thick mudstone unit represents a subaqueous, probably marine incursion. The overlying cyclic pebbly sandstone-mudstone facies probably reflects a more meandering style of fluvial system, possibly in a floodplain environment.

Mudstone samples from this outlier yielded a reasonably diverse, well preserved, and unexpected palynoassemblage (Table 3). Samples were processed from surface exposures, and from the finer tuffaceous mudstones in the cores.

The assemblage contains a mixture of terrestrial and marine palynomorphs, including fern spores and a few dinocysts. The overall assemblage is directly correlative to those described in other areas from Albian suites, particularly from the Spences Bridge Group and correlatives of south-central British Columbia (Thorkelson and Rouse, 1989), and those from the Peace River region by Singh (1971). The most diagnostic palynomorphs are species of the fern spore genus *Distaltriangulisporites*, and the dinocyst *Pseudoceratium regium*, both restricted to the Albian (Singh, 1971).

This is the first report known to the writers of Albian palynomorphs on the British Columbia coast. However, comparison with other Albian units suggests an Albian age for this outlier is reasonable. Clastic sediments form much of the early Cretaceous (including Albian) Fire Lake Group and Gambier Group rocks preserved to the northwest (eg. Lynch, 1990; Roddick, 1965). Roddick (1965, p. 53) described a little disturbed, shallowly southeast dipping sequence of basal conglomerate from the Gambier Group at Mt. Seymour, about 30 km west of this outlier. We assume the Blue Mountain rock suite is part of the Gambier.

Table 3. Representative palynomorphs from the Blue Mountain outlier.

Fern spores	Conifer pollen
Distaltriangulisporites perplexus	*Cedripites cretaceus*
D. irregularis	*Parvisaccites radiatus*
Klukisporites pseudoreticulatus	Dinocysts
K. foveolatus	*Pseudoceratium regium*
Concavissimisporites variverrucatus	*P. sp.*
	Batioladinium jaegeri

RICHFIELD-PURE SUNNYSIDE WELL

A well cooperatively drilled by the Richfield and the Pure Oil Companies in 1962 penetrated > 3300 m into the subsurface of the Fraser Lowlands (Fig. 1). Hopkins (1966) conducted an early investigation of the palynology from this and other wells in the Fraser River lowlands. New samples from core breaks in the Sunnyside well have yielded a diverse assemblage of palynomorphs. The results are preliminary, but point to some interesting features if confirmed. The descriptions of drillcore depths follow the original well logging practise, using imperial units of measure.

The Tertiary-Upper Cretaceous contact occurs at about the 9000 ft. level. Below the contact are about 1000 feet of grey green silts and fine sands, many with coaly fragments. These are almost certainly equivalent to Nanaimo Group rocks preserved on the surface, and a few preliminary assemblages obtained suggest detailed palynoanalysis will be rewarding.

Samples from 10 863-10 865 feet and 10 868 feet are dark grey siltstone with a high ash content, and contain impressions of dicotyledon leaves. These have also yielded palynomorphs, including the following:

Spores:

Chomotriletes almegrensis, early Cretaceous to Cenomanian,
Cicatricosisporites hughesi, Aptian-Maastrichtian,
Cyathidites minor, later Mesozoic

Dinocysts:

Pareodinia minuta, mid-Mesozoic
Canningia colliveri, Aptian-Coniacian
Pseudoceratium cf. dettmannae, late Albian-early Cenomanian
Dingodinium cerviculum, Hauterivian-Turonian
Batioladinium jaegeri, Hauterivian-Cenomanian

This assemblage is interpreted to be Cenomanian.

A sample from 10 888 feet contains the fern spore *Distaltriangu-lisporites perplexus*, limited to the Albian, and the early angiosperm pollen *Psilatricolporites prolatus* of late Albian age. This sample is considered to be Late Albian. Finally, a sample near the base at 10 894 feet contains the fern spore species *Cicatricosisporites spiralis* and *C. cf. potomacensis*, both of Middle Albian age. This provides the first evidence that Albian age strata occur in the Georgia Basin subsurface.

THERMAL MATURATION

Measurements have been made on the TAI (Thermal Alteration Index) using the Chevron colour scale (0-4), which

predicts the likelihood of hydrocarbon generation. On this scale, values of about 2.0-2.5 indicate paleotemperatures conducive to gas generation, mainly diagenetic dry gases (methane, CO_2, N_2), values from 2.5 to about 3.2 denote the "oil window", and values about 3.0-3.3 represent the zone for optimum generation of wet gasses (condensate). The other important indicator of hydrocarbon generation is the kerogen type, with alginite and exinite favourable kerogens for oil generation, and vitrinites usually associated with gas generation.

The TAI from both surface and subsurface samples indicates at best only marginal maturation levels. This includes samples from the Albian sediments at Blue Mountain and at depths of over 10 000 feet in both the Sunnyside and Point Roberts exploration wells. Hence, the prognosis for substantial hydrocarbon generation in the eastern part of the Georgia Basin is not very favourable. This is corroborated by assessment of vitrinite reflectance values by R.M. Bustin (UBC, pers. comm., 1990).

DISCUSSION

This study provides new evidence that Nanaimo Group deposition occurred on the east side of Georgia Basin as early as late Santonian-early Campanian time. The west-directed paleoflow and subaerial paleoenvironment at Lang Bay and possibly Texada Island, and local provenance for many of the conglomerate clasts suggests these outliers were close to the then eastern margin of the basin. Most provenance studies of Nanaimo Group rocks have interpreted the lower coarse clastics to be derived from Wrangellia because of a large component of mafic volcanic detritus and small amount of plutonic detritus. (eg. Pacht, 1984; Muller and Jeletzky, 1970). However remnants of a several kilometre thick volcanic and clastic cover sequence to the Coast Mountain plutons is preserved on the British Columbia mainland as the lower Cretaceous Gambier Group and equivalents (Roddick, 1965; Lynch, 1990). Much of this volcanic arc has been eroded, with the Georgia Basin a possible depocentre. Late Cretaceous southwest directed thrusting in the eastern Coast Belt east of Georgia Basin (Journeay, 1990) could provide a tectonic mechanism both for uplifting the eastern margin of Georgia Basin and perhaps for initial formation of the basin itself. A zircon provenance study in progress may prove useful for discriminating clastic rocks derived from the generally early Cretaceous age Gambier Group from those derived from older (Jurassic to Paleozoic) volcanic rocks of Wrangellia.

The results from Lasqueti Island provide new evidence that there is no direct relationship between the Tertiary and late Cretaceous basin fills. The subtle disconformity at Lasqueti Island represents a time gap of perhaps 10 Ma (Campanian to late Paleocene). A similar and equally subtle disconformity was documented from the Vancouver area by Rouse et al. (1975) and from drillcore in the Fraser lowlands by Hopkins (1966).

The recognition of Albian age strata on Blue Mountain and in the Sunnyside well is significant. It indicates that the Georgia depression in the Vancouver area was receiving sediments as early as mid-Albian time, and raises the question of how much Albian and possibly older sedimentary rocks are preserved below the Upper Cretaceous strata generally considered the base of the Georgia Basin.

ACKNOWLEDGMENTS

Andy Shobridge provided cheerful and competent field assistance. Steve Phillips provided similar assistance for the Lasqueti Island study plus luxury accommodation on the good ship Galatea. Lauch Farris of Fargo Resources Ltd., permitted sampling of the Lang Bay drillcore and access to internal reports critical to understanding the setting of the Lang Bay deposit. Ted Belcher of Blue Mountain Explorations Inc., and Joe Chamberlain of Chamberlain Geological Associates Inc. provided access to the Blue Mountain drillcore and unpublished consultant reports. Jane Broatch provided very able lab processing and editorial assistance. David Johnson and co-workers from the Core Storage facilities of the BCDMPR at Charlie Lake gave first-rate assistance in obtaining sub-samples of wells.

REFERENCES

Bradley, R.K.
1972: Upper Cretaceous plant fossils from mainland coastal deposits north of Vancouver, British Columbia, Canada; Canadian Journal of Earth Sciences, v. 10, p. 1841-1843.

Brandon, M.T., Cowan, D.S., and Vance, J.A.
1988: The Late Cretaceous San Juan thrust system, San Juan Islands, Washington; Geological Society of America, Special Paper 221, 81 p.

Bustin, R.M.
1990: Stratigraphy, sedimentology, and petroleum source rock potential of the Georgia Basin, southwest British Columbia and northwest Washington State; in Current Research, Part F, Geological Survey of Canada, Paper 90-1F, p. 103-108.

Crickmay, C.E. and Pocock, S.A.J.
1963: Cretaceous at Vancouver, British Columbia, Canada; American Association of Petroleum Geologists Bulletin, v. 47, p. 1928-1942.

England, T.D.J.
1989: Lithostratigraphy of the Nanaimo Group, Georgia Basin, southwestern British Columbia; in Current Research, Part E, Geological Survey of Canada, Paper 89-1E, p. 103-108.
1990: Late Cretaceous to Paleogene evolution of the Georgia Basin, southwestern British Columbia; unpublished Ph.D. thesis, Memorial University of Newfoundland, St. John's, 481 p.

Gordy, P.L.
1988: Evaluation of the hydrocarbon potential of the Georgia depression; British Columbia Ministry of Energy, Mines and Petroleum Resources, Geological Report 88 03.

Haggart, J.W.
1990: Report on Cretaceous fossils submitted by Dr. Peter Mustard; unpublished Geological Survey of Canada internal paleontological report JWH-1990-03.

Haggart, J.W. and Ward, P.D.
1989: New Nanaimo Group ammonites (Cretaceous, Santonian-Campanian) from British Columbia and Washington State; Journal of Paleontology, v. 63, p. 218-227.

Hein, F.J. and Walker, R.G.
1982: The Cambro-Ordovician Cap Enragé Formation, Québec, Canada: conglomeratic deposits of a braided submarine channel with terraces; Sedimentology, v. 29, p. 309-329.

Hopkins, W.S.
1966: Palynology of Tertiary rocks of the Whatcom basin, southwestern British Columbia and northwestern Washington; Ph.D. thesis, University of British Columbia, Vancouver, 184 p.

Johnson, S.Y.
1984: Stratigraphy, age, and paleogeography of the Eocene Chuckanut formation, northwest Washington; Canadian Journal of Earth Sciences, v. 21, p. 92-106.

Jones, D.L.
1960: Pelecypods of the genus Pterotrigonia from the west coast of North America; Journal of Paleontology, v. 43, p. 433-439.
Journeay, J.M.
1990: A progress report on the structural and tectonic framework of the southern Coast Belt, British Columbia; in Current Research, Part E, Geological Survey of Canada, Paper 90-1E, p. 183-195.
Lynch, J.V.G.
1990: Geology of the Fire Lake Group, southwest Coast Mountains, British Columbia; in Current Research, Part E, Geological Survey of Canada, Paper 90-1E, p. 197-204.
McConnell, R.G.
1914: Texada Island, B.C.; Geological Survey of Canada, Memoir 58, 112 p.
Monger, J.W.H.
1990: Georgia Basin: regional setting and adjacent Coast Mountains geology, British Columbia; in Current Research, Part F, Geological Survey of Canada, Paper 90-1F, p. 95-107.
Muller, J.E.
1977: Geology of Vancouver Island (east half); Geological Survey of Canada, Open File 463.
Muller, J.E. and Jeletzky, J.A.
1970: Geology of the upper Cretaceous Nanaimo Group, Vancouver Island and Gulf Islands, British Columbia; Geological Survey of Canada, Paper 69-25, 77 p.
Nilsen, T.H.
1982: Alluvial fan deposits; in Sandstone Depositional Environments, P.A. Scholle and D. Spearing (ed.), American Association of Petroleum Geologists, Memoir 31, p. 49-86.
Pacht, J.A.
1984: Petrologic evolution and paleogeography of the Late Cretaceous Nanaimo Basin, Washington and British Columbia: implications for Cretaceous tectonics; Geological Society of America Bulletin, v. 95, p. 766-778.
Ries, H. and Keele, J.
1915: Clay and shale deposits of the western provinces (part IV); Geological Survey of Canada, Memoir 65.
Roddick, J.A.
1965: Vancouver North, Coquitlam, and Pitt Lake map-areas, British Columbia; Geological Survey of Canada, Memoir 335.
Roddick, J.A., Muller, J.E., and Okulitch, A.V.
1976: Fraser River, British Columbia-Washington, 1:1 000 000 Geological Atlas, Sheet 92; Geological Survey of Canada, Map 1386A.
Rouse, G.E.
1977: Paleogene palynomorph ranges in western and northern Canada; in Contributions of Stratigraphic Palynology, Vol. 1, Cenozoic Palynology; American Association of Stratigraphic Palynologists, Contribution Series 5A, p. 48-65.
Rouse, G.E., Mathews, W.H., and Blunden, R.H.
1975: The Lions Gate Member: a new late Cretaceous sedimentary subdivision in the Vancouver area of British Columbia; Canadian Journal of Earth Sciences, v. 12, p. 464-471.
Rouse, G.E., Lesack, K.A., and White, J.M.
1990: Palynology of Cretaceous and Tertiary strata of Georgia Basin, southwestern British Columbia; in Current Research, Part F, Geological Survey of Canada, Paper 90-1F, p. 109-113.
Rust, B.R. and Koster, E.H.
1984: Coarse alluvial deposits; in Facies Models, R.G. Walker (ed.), Geoscience Canada, Reprint Series 1, p. 53-70.
Singh, C.
1971: Cretaceous microfloras of the Peace River area, northwestern Alberta; Research Council of Alberta, Bulletin 28.
Thorkelson, D.J. and Rouse, G.E.
1989: Revised stratigraphic nomenclature and age determinations for mid-Cretaceous volcanic rocks in southwestern British Columbia; Canadian Journal of Earth Sciences, v. 26, p. 2016-2031.
Walker, R.G. and Cant, D.J.
1984: Sandy fluvial systems; in Facies Models, R.G. Walker (ed.), Geoscience Canada, Reprint Series 1, p. 71-90.
Ward, P.D.
1978: Revisions to the stratigraphy and biochronology of the Upper Cretaceous Nanaimo Group, British Columbia and Washington State; Canadian Journal of Earth Science, v. 15, p. 405-423.
Ward, P.D. and Stanley, K.O.
1982: The Haslam Formation: a Late Santonian-Early Campanian forearc basin deposit in the Insular Belt of southwestern British Columbia and adjacent Washington; Journal of Sedimentary Petrology, v. 52, p. 975-990.
Webster, I.C.L. and Ray, G.E.
1990: Geology and mineral deposits of northern Texada Island (92F/9, 10 and 15); in Geological Fieldwork 1989, British Columbia Ministry of Energy Mines and Petroleum Resources, Paper 1990-1, p. 257-265.
White, G.V.
1986: Preliminary report Lang Bay germanium prospect (92F/16W); in Geological Fieldwork 1985, British Columbia Ministry of Energy Mines and Petroleum Resources, Paper 1986-1, p. 261-264.
Yorath, C.J., Green, A.G., Clowes, R.M., Sutherland Brown, A., Brandon, M.T., Kanasewich, E.R., Hyndman, R.D., and Spencer, C.
1985: Lithoprobe, southern Vancouver Island: seismic reflection sees through Wrangellia to the Juan de Fuca plate; Geology, v. 13, p. 759-762.

Petrography and tectonics of the Scovil diorite, southwest Pine Pass map area, British Columbia

B.K. Northcote[1]
Cordilleran Division, Vancouver

Northcote, B.K., Petrography and tectonics of the Scovil diorite, southwest Pine Pass map area, British Columbia; in Current Research, Part A, Geological Survey of Canada, Paper 91-1A, p. 241-244, 1991.

Abstract

Scovil diorite forms a large sill-like body capping Mount Scovil ridge in Pine Pass map area. It may have been thrust on, or intruded into, sedimentary rocks of probable Devono-Mississippian age; the relationship is obscured by shearing along the contact. The dioritic appearance may be a consequence of extensive alteration of the plagioclase and replacement of the pyroxene of a former gabbro.

Résumé

La diorite de Scovil forme un grand corps apparenté à un filon-couche et coiffant la crête Mount Scovil dans la région cartographiée Pine Pass. Elle peut avoir été charriée sur, ou avoir pénétré, les roches sédimentaires datant probablement du Dévono-mississippien; la relation est obscurcie par le cisaillement le long du contact. L'aspect dioritique peut résulter d'une altération poussée des plagioclases et du remplacement du pyroxène d'un gabbro antérieur.

[1] Department of Geological Sciences, University of British Columbia, 6339 Stores Road, Vancouver, B.C. V6T 2B4

PROJECT SCOPE

Rocks underlying the Mount Scovil ridge system (Fig. 1) were mapped at 1:50 000 scale during reconnaissance 1:250 000 scale mapping of the southwestern part of the Pine Pass map area. The reconnaissance mapping supplements that of Muller (1961), and will complement recent work in adjacent map areas to the northwest, Manson Creek and Germansen Landing map areas (Ferri and Melville, 1988, 1989); to southwest, Tezzeron and Wittsichica creeks (J. Nelson, pers. comm., 1990); and to the south, McLeod Lake (Struik, 1989).

More detailed work on Mount Scovil was done to determine the petrology and contact relationships of a large foliated diorite body that caps the mountain tops. That diorite looked like dykes and sills within rocks of the Snowshoe and Black Stuart groups to the south in the Cariboo Lake map area (Struik, 1988). More detailed examination of the Scovil diorite was done to compare these two suites, and determine if they could be feeder dykes to upper Paleozoic basalt of the Slide Mountain Group. Some of the petrography and structural relationships of the Scovil diorite are reported here.

GENERAL GEOLOGY

Rocks of southwest Pine Pass map area consist of the high grade Wolverine Metamorphic Complex overlain in fault contact by Paleozoic(?) limestone, quartzite, phyllite, siliceous argillite, sandstone, grit and basalt tuff. These sedimentary and volcanic rocks are assumed, by comparison with rock sequences to the southeast to range from Cambrian through to Permian (Struik and Northcote, 1991). This Paleozoic sequence, previously mapped as part of the Slide Mountain Group (Muller, 1961), is separated by the McLeod Lake Fault from the Paleozoic carbonate platform sequence of the Rocky Mountains.

The Scovil diorite is part of a suite of diorite sills and dykes throughout Pine Pass map area that intrude the siliceous argillite, grit and tuff unit of presumed middle and upper Paleozoic age. Similar relationships are found to the northwest in Manson Creek map area where the Wolf Ridge Gabbro is bound by basalt and siliceous fine grained sedimentary rocks (Ferri and Melville, 1988).

GEOLOGY AT MOUNT SCOVIL

The highground near Mount Scovil is underlain by resistant medium grained diorite (here called Scovil diorite), and the surrounding valleys are underlain by various volcanic and clastic sedimentary rocks, and minor carbonate. Scovil diorite is a sill-like body, elongated roughly northwest. It is variably foliated, deformed, faulted and altered throughout. The foliation commonly strikes south or southeast and dips steeply. Lineations, typically elongated bands of crushed mafic minerals, generally plunge south or southeast up to 35°. Shear zones within the diorite often contain calcite having the appearance of marble. A smaller body of diorite to the southeast is indistinguishable from the Scovil diorite in hand specimen and thin section and is probably related (Fig. 2). The contact of this smaller body with surrounding rocks is covered with overburden.

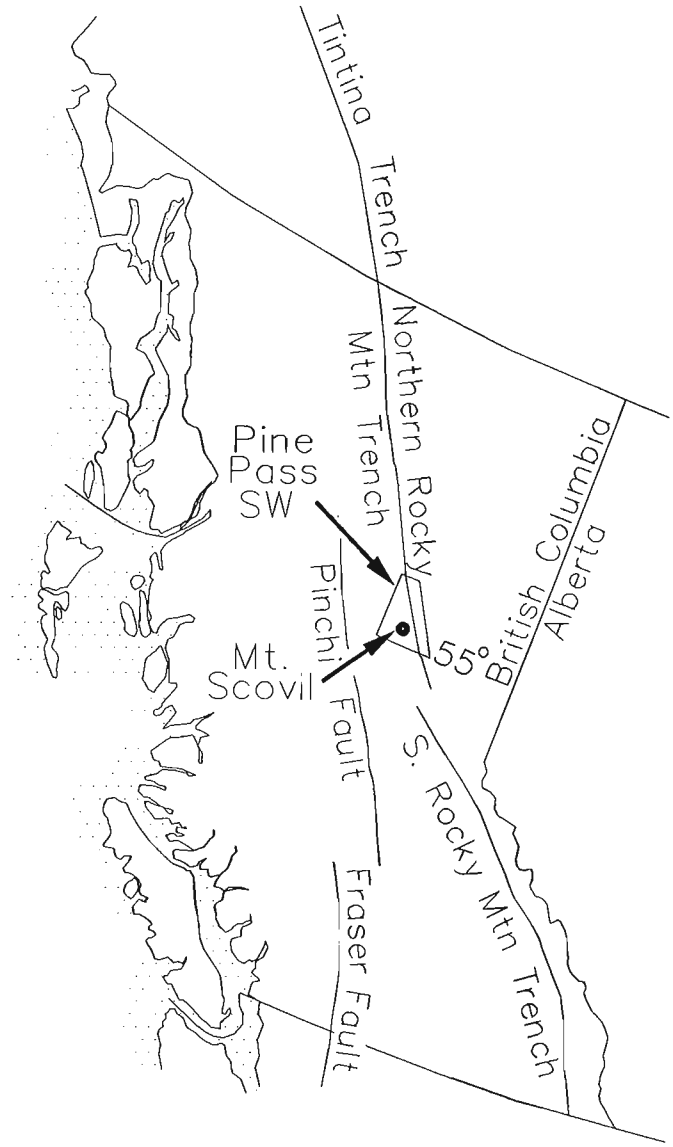

Figure 1. Location of Mount Scovil in British Columbia.

Hornblende porphyritic andesite dykes are found throughout the larger diorite body. The groundmass consists largely of sodic plagioclase, a few quartz grains, minor magnetite (samples are magnetic) and associated hematite. Quartz-epidote veins, generally thin and in many orientations, are scattered throughout the diorite.

The country rock to the diorite consists mainly of black siltite, argillite and phyllite, and lesser amounts of dolomite, micaceous quartzite, conglomerate and olive phyllitic tuff (Struik and Northcote, 1991). At the diorite contact the predominate rock type is olive phyllitic tuff, most of which has a penetrative shear fabric. Foliation in the country rock generally strikes southeast, and dips northeast; parallel to the foliation in the Scovil diorite. Outcrop-scale folds verge to the northeast and plunge mainly to the southeast.

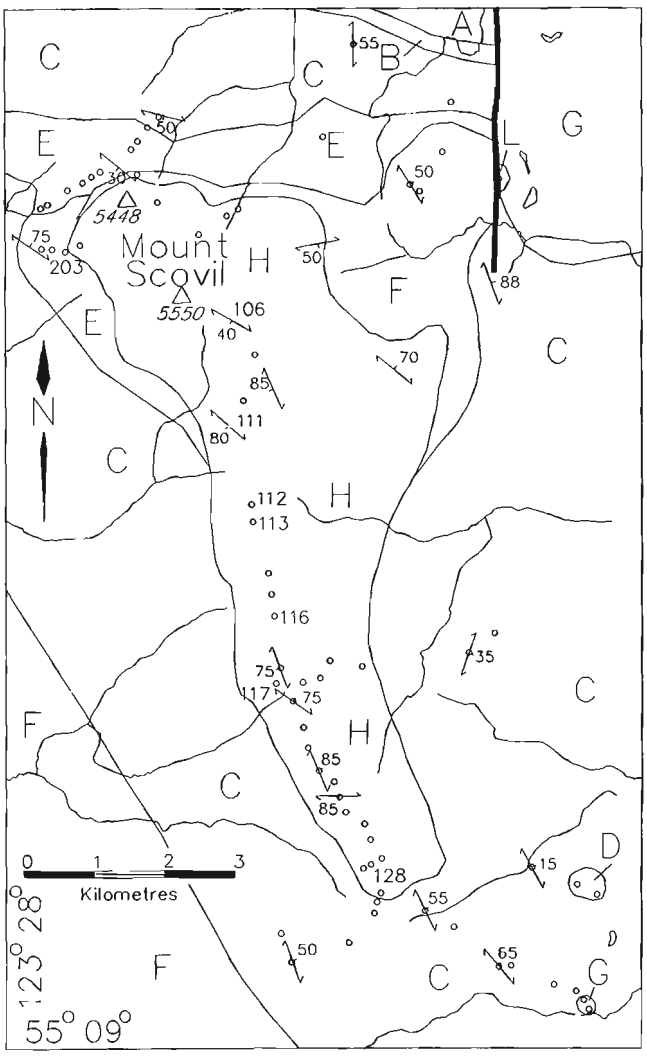

Figure 2. Geology at Mount Scovil.

Contacts of the Scovil diorite

Phyllite and metasandstone from areas near the Scovil diorite contact are sheared, but are not affected by contact metamorphism. In a transect through the western contact at locality 203 (Fig. 2) the diorite and country rock develop and intensify shear fabric toward each other. At the contact Scovil diorite is reduced to an augen mylonite and the country rock, basalt tuff, to a phyllonite.

Scovil diorite does not appear to have fine grained margins or distinct border phases. Crystal size is consistent throughout the diorite except at one locality to the southeast of Mount Scovil where it is finer (L. Struik, pers. comm., 1990). At some contact localities, fine grained altered rock resembles tuff in thin section, rather than an aphanitic border phase of the diorite; crystals do not appear to be interlocking and some are broken. The tuff may have been an extrusive phase of the intruding diorites. Diorite feeder dykes were not observed in the country rock immediately around the main pluton.

Scovil diorite may have originally intruded its host rock although its present contacts are tectonic. Similar diorite dykes several kilometres south intrude and are folded with the same country rocks as at Mount Scovil (Struik and Northcote, 1991). The small body of similar diorite to the southeast (Fig. 2) could be a separate intrusion related to the larger one, or a klippe if the diorite has been emplaced by thrusting.

PETROGRAPHY OF THE SCOVIL DIORITE

Primary minerals are plagioclase, now completely altered, and pyroxene, seen as rounded remnants. Secondary minerals include hornblende and fibrous tremolite-actinolite that surround pyroxene, or completely replace it. Alteration products of plagioclase comprise clay, chlorite and sericite. Quartz, albite, epidote, opaques and sphene are present.

Foliation observed in several specimens includes segregation of minerals into mafic and felsic layers. It seems unlikely that this could have arisen through the type of mechanical deformation observed, and it may represent original igneous or metamorphic layering.

Plagioclase

Original plagioclase has been completely altered to clay, chlorite and sericite. In most samples, patches of clay outline the former crystal, and these are often surrounded by chlorite and then by sericite at the outer edge. The minor amount of fresh plagioclase is albitic, and is interpreted to be a secondary phase. Albite commonly occupies small fractures together with minor quartz, for example. Altered plagioclase represents 40-60 % of the rock. Grain size is typically 2-3 mm.

Mafic minerals

Original unaltered pyroxene forms some rounded remnant cores and sieve texture, and is replaced by hornblende or more typically is surrounded by fibrous secondary tremolite-actinolite. Samples 111, 116, 117, 120 and 203 (Fig. 1) exhibit sheared mafic layers consisting of rounded pyroxene

grains surrounded by tremolite-actinolite (Fig. 3 photomicrograph). Pyroxene forms up to 40% of a specimen, depending on how much has been altered to amphibole. Crystals range up to 3 mm across.

Green or brown pleochroic hornblende occurs in several samples replacing pyroxene. Locally pyroxene has been completely replaced, but remnants are commonly left, surrounded by the hornblende. The hornblende appears very fresh and unaltered in several thin sections. Hornblende may form 20-50% of the rock, depending on the amount of pyroxene left unaltered. Grain size is typically 1-3 mm.

Fibrous amphibole (tremolite-actinolite) is found surrounding mafic grains. It grows parallel to foliation and across fractures. Minor epidote, carbonate and quartz are found in veins and interstices. Sphene is sometimes seen surrounding an opaque mineral.

DISCUSSION

It is suspected that the original plagioclase was a calcic high temperature form and thus was unstable and readily altered. None of the original plagioclase is left (it is only inferred from the reaction products that it was in fact plagioclase), whereas sodic plagioclase in veins is relatively fresh. Calcium released by the breakdown of the plagioclase may have gone into quartz-epidote veins and into calcium carbonate observed in shear zones throughout the area.

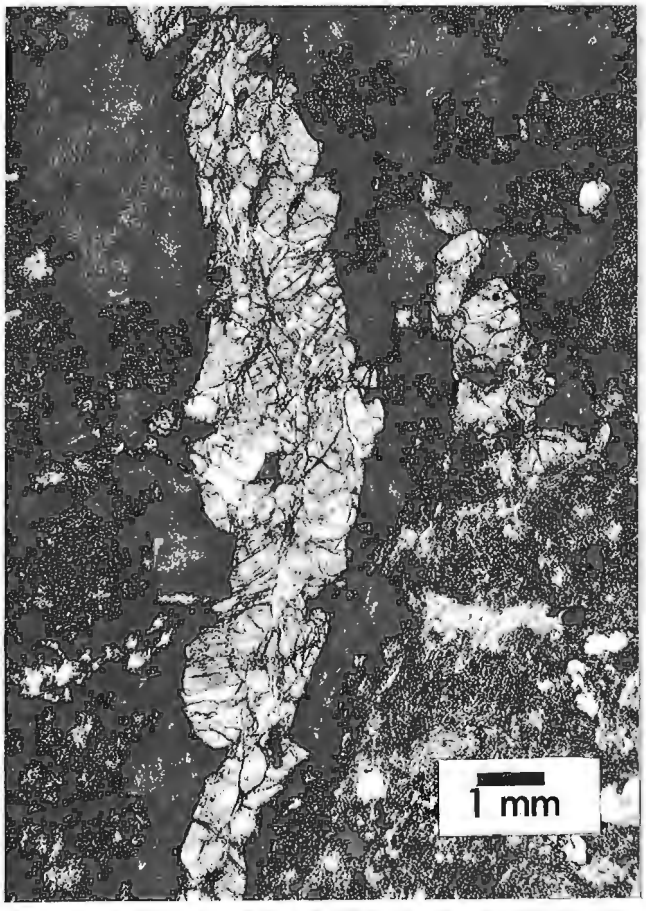

Figure 3. Photomicrograph of pyroxene deformation texture in the Scovil diorite.

Some hornblende replacing pyroxene appears to have formed before the plagioclase was completely altered, because in some places it outlines interstices between plagioclase crystals, which are now clay. The hornblende may have been a deuteric alteration product.

The pluton may have originated as a gabbro, with approximately 60% calcic plagioclase and 40% augite, possibly a mobilized part of the lower crust. Replacement of pyroxenes by amphiboles, and the addition of sodic plagioclase and very minor quartz make "diorite" a more appropriate rock name for this body.

CONCLUSIONS

Scovil diorite forms a large sill-like body that appears to be thrust(?) on undated argillite, quartzite, grit, tuff, and minor conglomerate within Pine Pass map area. The diorite probably originally crystallized as mainly plagioclase and pyroxene. The alteration history began with replacement of much of the pyroxene by hornblende. Later plagioclase was altered to clays, chlorite and sericite, and the remaining pyroxene was partly altered to fibrous secondary amphibole. Shear is recorded in the structural fabric of the diorite at many areas, and all observed contacts were sheared.

ACKNOWLEDGMENTS

Fieldwork was done under the supervision of L.C. Struik who also assisted in preparing this report. My thanks to J.K. Russel and J.V. Ross, who commented on several of the thin sections used for the report.

REFERENCES

Ferri, F. and Melville, D.M.
1988: Manson Creek mapping project (93N/09); in Geological Fieldwork 1987, British Columbia Ministry of Energy, Mines and Petroleum Resources, Paper 1988-1, p. 169-180.
1989: Geology of the Germansen Landing area, British Columbia (93N/10,15); in Geological Fieldwork 1988, British Columbia Ministry of Energy, Mines and Petroleum Resources, Paper 1989-1, p. 209-220.

Muller, J.E.
1961: Geology, Pine Pass, British Columbia; Geological Survey of Canada, Map 11-1961.

Struik, L.C.
1988: Structural geology of the Cariboo gold mining district, east-central British Columbia; Geological Survey of Canada, Memoir 421.
1989: Regional geology of the McLeod Lake map area, British Columbia; in Current Research, Part E, Geological Survey of Canada, Paper 89-1E, p. 109-114.

Struik, L.C. and Northcote, B.K.
1991: Pine Pass map area, southwest of the Northern Rocky Mountain Trench, British Columbia; in Current Research, Part A, Geological Survey of Canada, Paper 91-1A.

Geology of the Mesozoic volcanic and sedimentary rocks east of Pemberton, British Columbia

J.M. Riddell[1]
Cordilleran Division, Vancouver

Riddell, J.M., Geology of the Mesozoic volcanic and sedimentary rocks east of Pemberton, British Columbia; in Current Research, Part A, Geological Survey of Canada, Paper 91-1A, p. 245-254, 1991.

Abstract

The major east-side-up thrust fault that cuts the Mesozoic rocks west of Lillooet Lake, continues to the northwest through the Owl Creek valley. The results of mapping of the rocks east of this fault from Lillooet Lake north through the Tenquille Lake area, support correlation of these rocks with the Cadwallader Group.

South of Tenquille Creek a thin sequence of volcanic and sedimentary rocks lie unconformably upon the Triassic Cadwallader section. These rocks do not resemble rocks of the Cadwallader Group, and are probably Jurassic or Cretaceous.

Résumé

La principale faille chevauchante à compartiment est soulevé qui traverse les roches mésozoïques à l'ouest du lac Lillooet se poursuit vers le nord-ouest à travers la vallée du ruisseau Owl. La cartographie des roches à l'est de cette faille, à partir du lac Lillooet au nord jusqu'à travers la zone du lac Tenquille, a permis de recueillir des données qui corroborent la corrélation de ces roches avec le groupe de Cadwallader.

Au sud du ruisseau Tenquille, une mince séquence de roches volcaniques et sédimentaires repose en discordance sur la section triassique du groupe de Cadwallader. Ces roches ne ressemblent pas aux roches du groupe de Cadwallader et datent probablement du Jurassique ou du Crétacé.

[1] Department of Geology, University of Montana, Missoula, Montana 59812, U.S.A.

INTRODUCTION

East of Pemberton, B.C. (Fig. 1), Mesozoic volcanic and sedimentary rocks form a northwest-striking pendant about 70 km long and 10 to 30 km wide that is almost entirely surrounded by rocks of the Coast Plutonic Complex (Woodsworth, 1977). During the 1989 field season, mapping in the southernmost part of this Mesozoic band, adjacent to Lillooet Lake, confirmed that a major north-northwest-striking fault cuts the pendant. Triassic rocks, probably of the Cadwallader Group, lie to the east, Cretaceous Fire Lake Group rocks to the west (Riddell, 1990). The goals of this project for the 1990 field season were to trace the fault to the north through the pendant, to improve the map coverage east of the fault in the Triassic section, and to expand the map area to the north to compare the stratigraphy in the Lillooet Lake area to that of the Tenquille Lake area. In this report, the Mesozoic rocks within the map area (Fig. 2) are referred to as the "Pemberton belt". Field maps from this project will be released as an Open File by the British Columbia Geological Survey Branch in early 1991.

The major thrust fault can be traced through the Owl Creek valley (Fig. 2, 3), and probably extends through the topographic notch east of Mount Pauline. The Triassic rocks throughout the expanded map area generally compose a lower unit of massive basaltic and andesitic flows (Tr1) and unsorted lithic tuffs (Tr2), overlain by a section of well bedded tuffaceous and sedimentary rocks (Tr3). In some localities, a thin unit of predominantly sedimentary rocks (Tr4) conformably overlies Tr3.

In the Tenquille Lake area, a relatively thin sequence of volcanic and sedimentary rocks sits on top of the rocks of the Triassic sequence along an apparent unconformity. This section does not resemble rocks of the Cadwallader Group, and probably represents a younger overlap assemblage. If the age of this section can be determined, it will provide an upper constraint on the timing of accretion of this Triassic section.

TRIASSIC STRATIGRAPHY

Correlation with the Cadwallader Group

Triassic rocks in the Pemberton belt have been mapped as Cadwallader Group (Cairnes, 1925; Roddick and Hutchison, 1973; Woodsworth, 1977). The validity of this correlation is still a matter of discussion. The author's observations in the Pemberton belt, especially in the Mount Barbour area south of Tenquille Creek, support the correlation of these rocks with the Cadwallader section described by Rusmore (1985) in the Eldorado Creek area near Gold Bridge (Fig. 4). There are, however, some significant differences between the two sections.

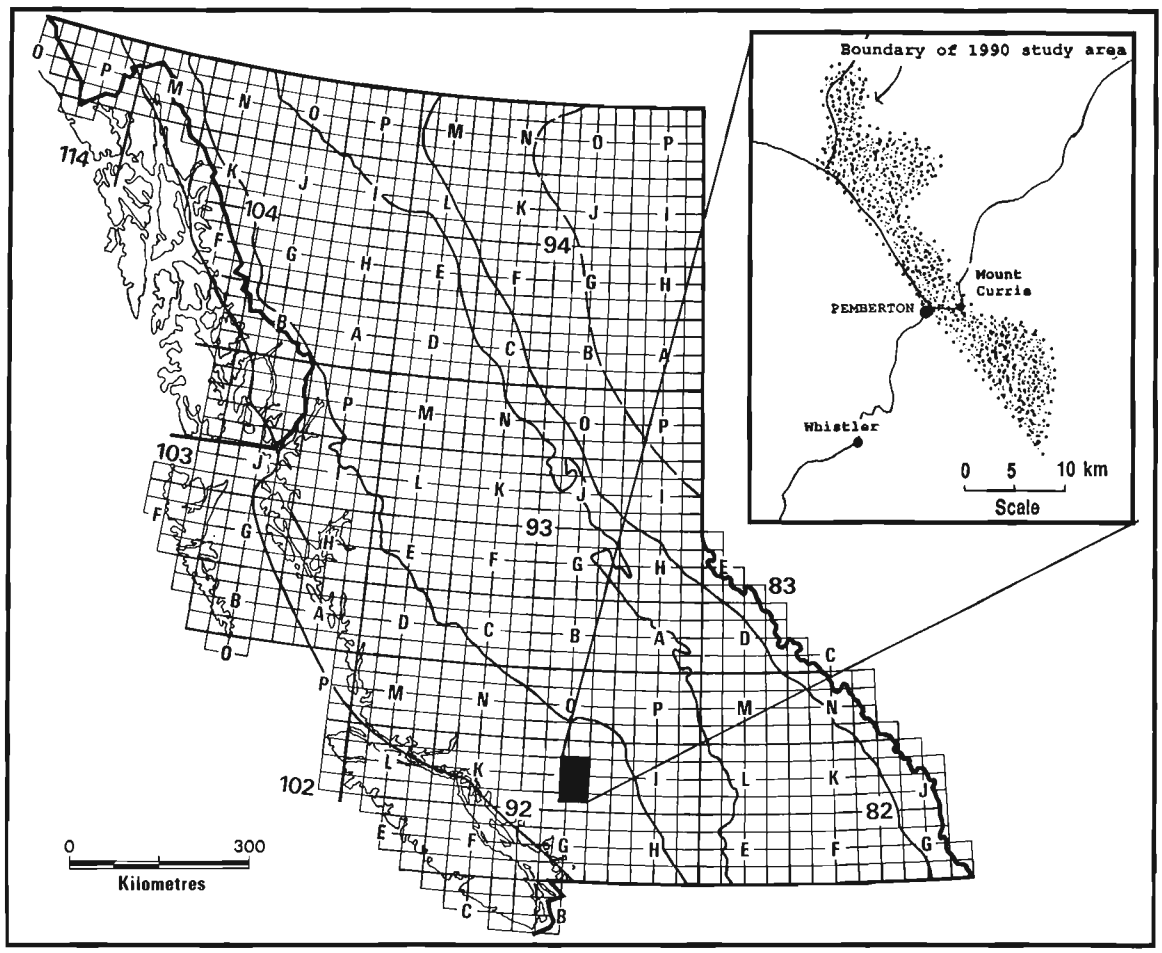

Figure 1. Location map of field area.

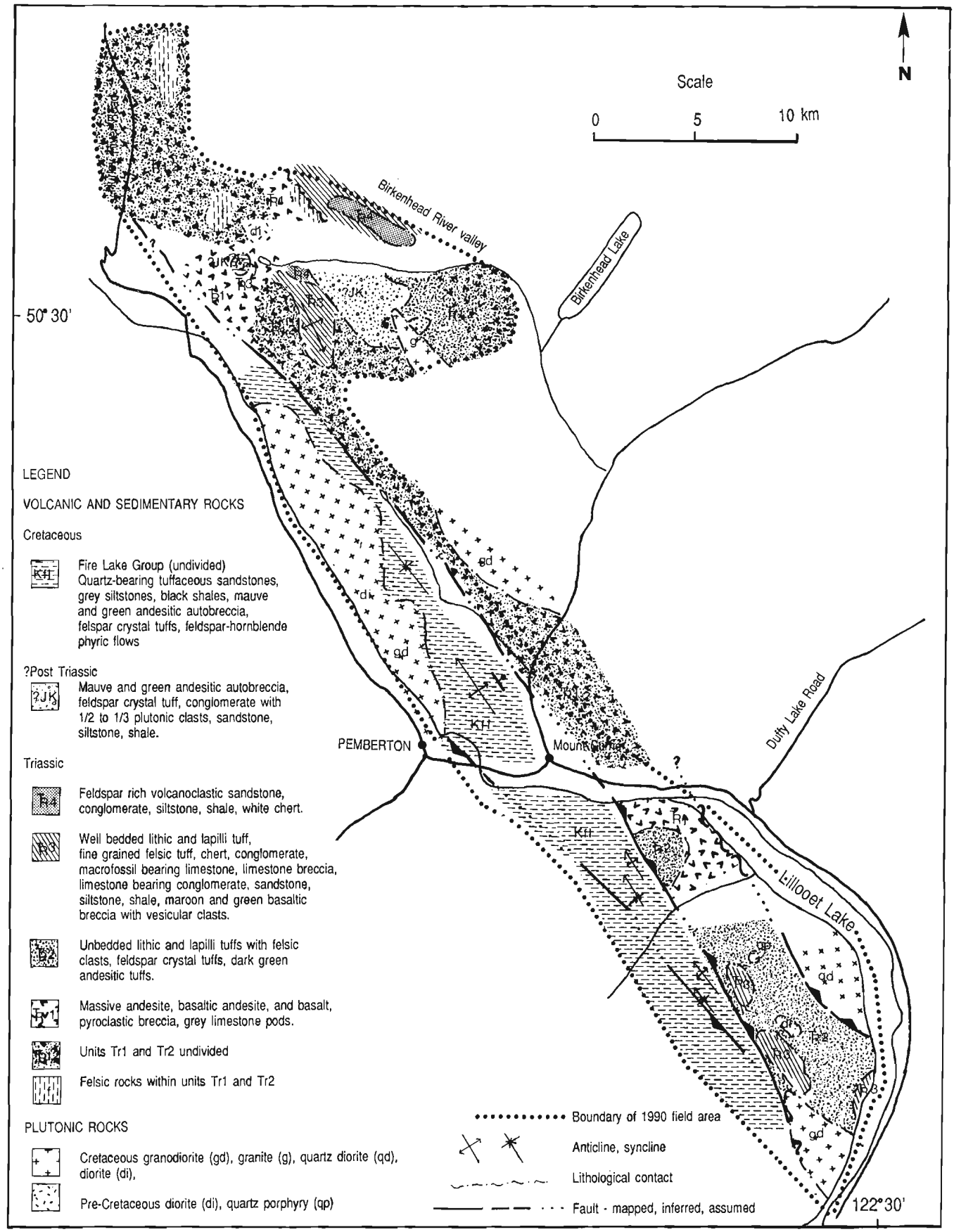

Figure 2. Geology map of the field area.

The Triassic rocks in the map area are referred to as the 'Pemberton Triassic section' in this report.

Figure 4 illustrates the major stratigraphic components of the two sections for comparison. The important similarities between the sections are:

1) a basal massive submarine mafic volcanic unit (the Pioneer Formation of the Cadwallader Group). Comparison of major and trace element analyses of mafic rocks from the Pemberton belt with those from Rusmore's (1985) study area show that their chemical signatures are similar, and they could have formed in the same arc (Schick, 1990);

2) a transitional unit of mixed volcanic, volcaniclastic, and sedimentary rocks. Distinctive features common to the two sections include limestone beds containing Triassic microfossils and bivalve macrofossils (Rusmore, 1985; Woodsworth, 1977; this study), felsic tuffs, a distinctive conglomerate with limestone clasts, and limestone breccias;

3) a predominantly sedimentary unit, consisting of conglomerates, sandstones, siltstones, and shales, at the top of the section (the Hurley Formation of the Cadwallader Group). The most convincing evidence that the two sections are correlative lies in the striking similarities between Rusmore's (1985) "transitional unit" and the mixed bedded sequence (Tr3) of the Pemberton Triassic section. Much of Cairnes' (1937) observations of the Pioneer formation in the Cadwallader valley near Bralorne accurately describe units Tr1 and Tr2 of the Pemberton Triassic section. The two sections differ most significantly in that the Pemberton section contains a much greater volume of volcaniclastic rock, and a much smaller volume of purely sedimentary material than the Gold Bridge section. Also, the basal volcanic unit near Gold Bridge is dominantly basaltic and amygdaloidal, and often pillowed, whereas in the basal unit of the Pemberton Triassic section andesite is dominant over basalt by volume, it is rarely amygdaloidal, and pillowed flows are absent. In the Pemberton section, isolated car-sized limestone pods are commonly found "floating" in the basal volcanic pile. Such pods are absent in the type Cadwallader section, and are more suggestive of stratigraphy in the Bridge River Complex than of the Cadwallader Group.

The Pemberton Triassic composite section

The Pemberton Triassic section comprises four distinct mappable units. The following idealized composite section is not preserved intact anywhere in the map area. Wide variation exists with respect to both the internal stratigraphy of the units, and spatial relationships between them. This variation is illustrated by Figure 5 and is further discussed in the section on Local variation in stratigraphy.

Massive basalt and andesite (Tr1)

The lowermost, mafic volcanic unit is well exposed on the Lill property at the north end of Lillooet Lake, on the east side of the Owl Creek valley, below the 2000 m level on Mount McLeod and Copper Mound, and in the bluffs of Finch Ridge west of the Grizzly Pass fault zone. This unit is characterized by massive, dark green basaltic andesite and lesser basalt flows, with common feldspar porphyritic phases and abundant epidote clots and veinlets. Pyroclastic breccias with clasts 3 cm and smaller are common. Limestone pods 2 to 30 m across are present in this unit, and they are especially abundant in the Mount McLeod area. Most of the mineral exploration that was done in the Pemberton area in the late 1800s and the 1930s concentrated on the mineralization in the magnetite-epidote-garnet skarns that are commonly associated with the limestone pods (Cairnes, 1925). The massive nature of this unit makes it difficult to estimate its thickness. At Copper Mound, where the section is flat-lying, it appears to be about 1000 m thick. The belt of felsic rocks in the Goat Peak and Grouty Peak areas sits within this massive unit, and will be discussed in more detail below.

Unbedded tuffaceous rocks (Tr2)

A thick deposit of unbedded lithic, lapilli, and feldspar-crystal tuffs and fine andesitic tuffs lies above unit Tr1. It is well exposed in the mountain above the Lill property, on the flank of the ridge west of Lillooet Lake, in the eastern Owl Creek valley, and on the eastern flank of Sungod Mountain. Rocks in this unit are all rich in feldspar crystal fragments in the matrix. The fine andesitic tuffs are dark green on the fresh surface; the crystal, lapilli, and lithic tuffs are pale green, and weather pale green or white. Clasts are subangular and are normally 3 to 4 cm or smaller, but locally clasts to 6 to 7 cm are present. Andesitic volcanic and felsic volcanic fragments are the most common clast types in the lithic tuffs. Locally, pale green chert, diorite, and basalt clasts were found. Textures are best displayed on the weathered surfaces. The lithic and lapilli tuffs tend to support a rusty coloured lichen that gives the rock a distinctive appearance in outcrop.

Well-bedded mixed volcanic and sedimentary rocks (Tr3)

The transition from massive lithic tuffs to well-bedded tuffs (without compositional change) marks the base of unit Tr3. This unit is best exposed on the Mount Barbour ridge, on Bastion Peak, and on Rampart Mountain. It comprises white and rusty-weathering lithic and lapilli tuffs, macrofossil-bearing grey limestone beds, conglomerate, calcareous feldspar-rich wackes, grey siltstone and black shale, fine grained felsic tuffs with cherty tops, limestone breccias, and mafic to intermediate flows. An outcrop of the distinctive limestone-clast-bearing "Cadwallader" conglomerate described by Cairnes (1937) and Rusmore (1985) has been noted northeast of Mount McLeod by M. Journeay (pers. comm., 1990). A deep maroon and green basaltic breccia with vesicular clasts is associated with this section at Mount Barbour and on Rampart Mountain.

Sedimentary rocks (Tr4)

Predominantly sedimentary sequences are quite rare in the Pemberton Triassic section. Shales, siltstones, sandstones, and conglomerates are present, but in almost all localities they are intermixed with tuffaceous sediments, tuffs, and flows, and are included in unit Tr3. Exceptions are at the top of the Mount Barbour Triassic section and on the eastern end of the ridge east of Grizzly Pass. These rocks are dominantly feldspar-rich, volcanic-derived sediments. Clasts of the underlying rock types are easily recognized. They

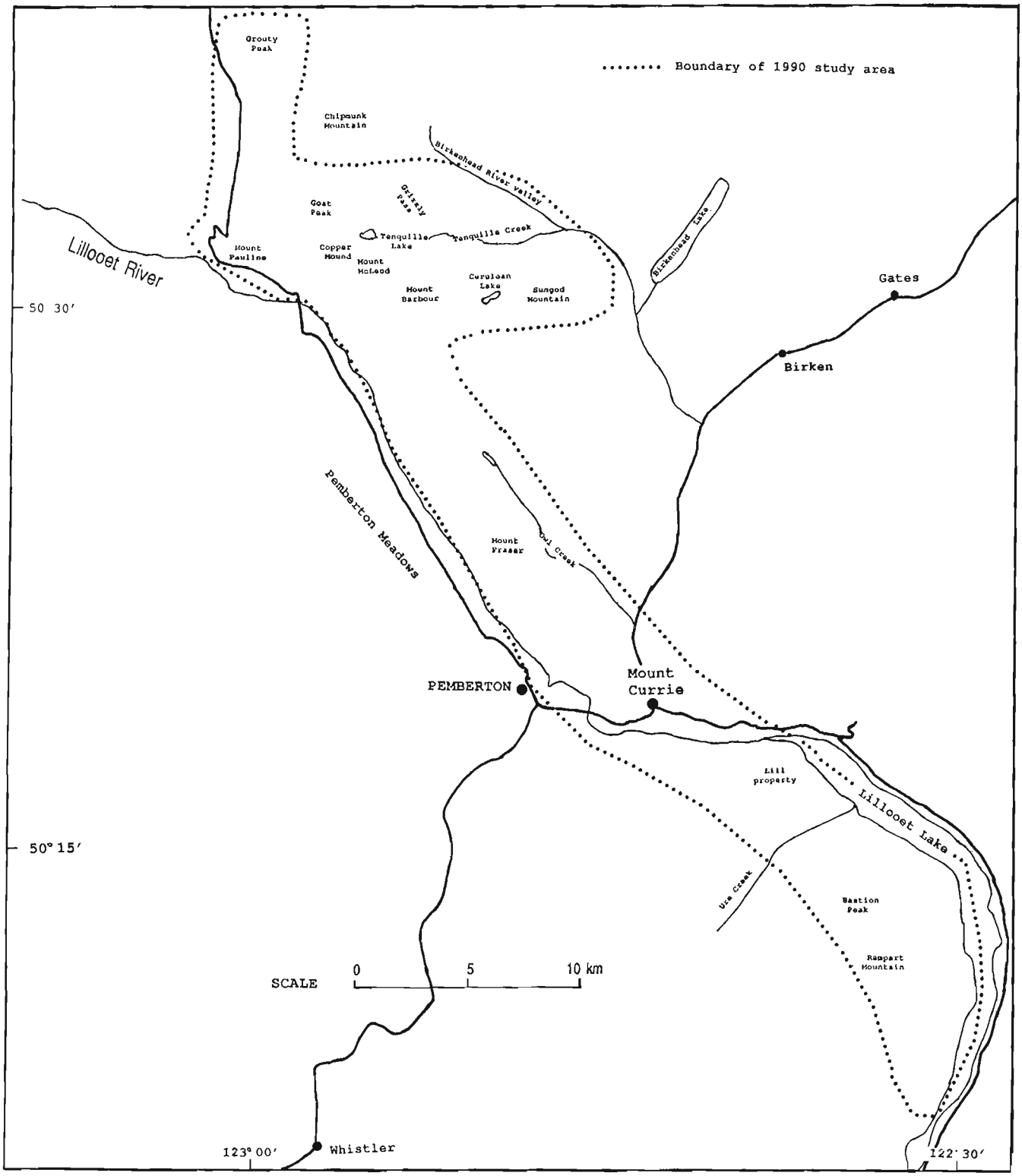

Figure 3. Place names in the Pemberton belt.

contain multiple, rapid fining-upward sequences from cobble conglomerate to black shale. White cherty beds are common.

?POST-TRIASSIC VOLCANIC AND SEDIMENTARY SECTION (?JK)

In the Tenquille Lake area, a relatively thin section of volcanic and sedimentary rocks sits apparently unconformably on the Triassic sequence. This section does not resemble any known Cadwallader stratigraphy. It is well exposed in the area surrounding Cerulean Lake, and small pockets are preserved at the very top of Copper Mound and on the northern flank of Goat Peak. The lowest exposed rocks in this section are mauve and green andesitic autobreccia, with beige feldspar and hornblende-phyric flows, and mauve and green lapilli and feldspar-crystal tuffs. These rocks are remarkably similar in appearance to the autobreccia unit of the Cretaceous Brokenback Hill Formation mapped in the Lillooet Lake pendant (Riddell, 1990), but the bounding stratigraphy is different. About 100 m of sedimentary rock overlies the volcanic pile. Its base is a boulder conglomerate, and it grades smoothly through cobble, pebble, and granule conglomerate, into quartz- and feldspar-rich calcareous sandstone, grey siltstone, and black shale. One third to one half of the clasts are fresh hornblende granodiorite, quartz diorite, and granite. It is similar to a Cretaceous conglomerate mapped by Arthur (1986) in the Chehalis valley. The source of these clasts is unknown. Remaining clasts tend to be representative of the local underlying rocks. Clasts of feldspar-phyric andesitic volcanics, argillite, green aphanitic volcanics, and mafic volcanics are common; chert pebbles, gneissic granitoids, and pyroxene granitoid clasts appear locally. Thin crossbedded magnetite-bearing sandstone beds are present within the conglomerate in a few places. North of Cerulean Lake these magnetite beds are several centimetres thick (P. Newman, pers. comm., 1990). A granodiorite boulder from the conglomerate has been sampled for radiometric dating.

CRETACEOUS STRATIGRAPHY (K)

Cretaceous stratigraphy west of the Owl Creek fault is not well exposed within the map area north of Pemberton; much of the area is underlain by quartz diorites and granodiorites of the Coast Plutonic Complex. The mauve and green volcanic breccia of the Brokenback Hill formation mapped in the Lillooet Lake pendant (Riddell, 1990) can be traced northwest to the Mount Fraser ridge system. Volcanic wackes, siltstones, and shale underlie the breccia.

TERTIARY VOLCANICS (T)

Chipmunk Mountain, just north of Tenquille Mountain, is a Tertiary volcanic centre. Dykes and small isolated outcrops of related basalt flows, volcanic breccias, and rhyolite are found throughout the map area. These rocks have distinctive drab brown and beige colours, and outcrops are often crumbly or flaggy. The basaltic rocks commonly contain euhedral biotite crystals up to 5 mm across. Basalt is the dominant clast type in the breccia, and they also contain biotite crystals and clear anhedral quartz eyes. The rhyolites and the basalt breccias contain 2 to 3 mm clear anhedral quartz eyes.

INTRUSIVE ROCKS

Diorites are associated with volcanic rocks of units Tr1 and Tr2 on Tenquille Mountain and southeast of Bastion Peak. These rocks show mutually crosscutting relationships with the volcanic rocks and so appear to be coeval. The diorites are characteristically altered or contaminated near the contacts with the Triassic rocks. Some appear to grade into tuffaceous rocks of unit Tr2, and in some places it is difficult to distinguish contaminated diorites from feldspar-crystal tuffs.

Large bodies of granodiorite and quartz diorite of the Cretaceous Coast Plutonic Complex intrude the map area.

LOCAL VARIATION IN STRATIGRAPHY

Figure 5 illustrates the observed lithological sequences in six areas where reasonable amounts of section are preserved, to show local variation in stratigraphy within the map area. Analyses of conodont and macrofossil samples collected during the 1990 field season will hopefully provide time control on these correlations.

Grouty Peak-Goat Peak-Tenquille Mountain

The northernmost part of the map area is underlain by massive andesites (Tr1) and unbedded tuffs (Tr2) with abundant coeval quartz-feldspar porphyry dykes and rhyolite flows. In much of the area the felsic rocks are the dominant lithology. Quartz eyes in the felsic rocks are often very coarse; they average 4 to 5 mm and locally form clusters up to a centimetre across. Mutually crosscutting relationships between quartz-feldspar porphyries, and dacitic and andesitic feldspar porphyry dykes are abundant, as are volcanic breccias with mixed intermediate and felsic clasts. Quartz-phyric felsic flows, tuffs, and breccias are exposed in the Grizzly Pass shear zone (Fig. 2, 3). Andesites near contacts with the rhyolitic rocks commonly display deep blue quartz eyes. At Grouty Peak, coarse quartz- and feldspar-rich epiclastic sandstone and grey siltstone directly overlie the flows. Intense silicification is apparent in most rocks in this area.

Felsic rocks are rare or absent within unit Tr1 throughout the rest of the map area.

Tertiary basalts and volcanic breccias are common, especially in areas adjacent to Chipmunk Mountain such as the Grizzly Pass shear zone, and on the northern flank of Goat Peak.

Mount McLeod

In the Mount McLeod area, the lowest rocks exposed are basaltic andesite flows mixed with pyroclastic breccias with 1 to 2 cm clasts that outcrop on the western flank of Copper Mound below the 700 m elevation level. At tree line and higher, basaltic andesite with large grey limestone pods are exposed. Unbedded tuffs of unit Tr2 overlie the mafic volcanics east of Mount McLeod, but they thin out and disappear to the west, and on Copper Mound, well bedded volcanic and sedimentary rocks of unit Tr3 sit directly on top of the mafic volcanic pile. A thin skiff of the mauve and green andesitic breccia of the post-Triassic ?JK section is preserved on the top of Copper Mound.

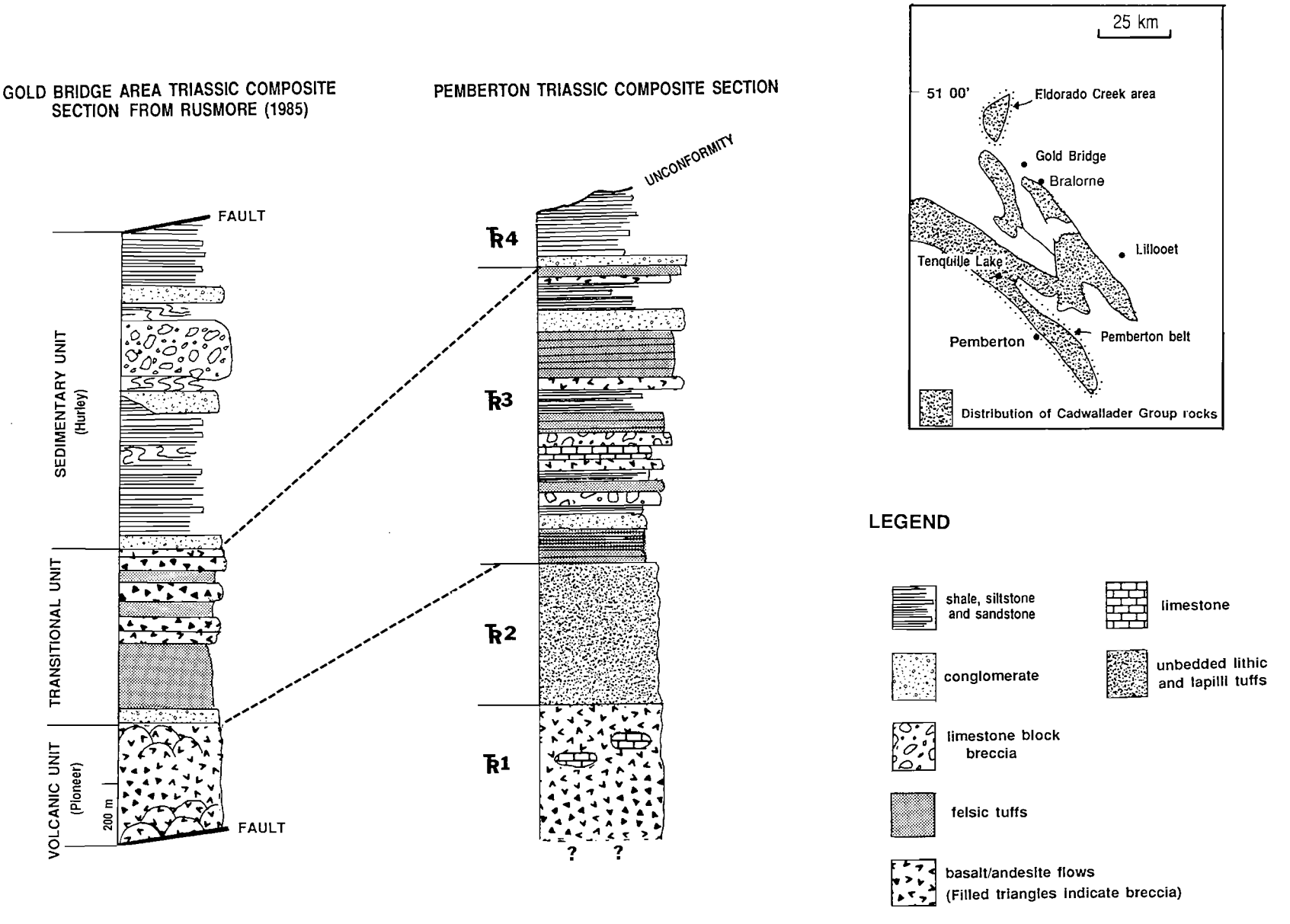

Figure 4. Composite Triassic sections from the Gold Bridge and Pemberton areas.

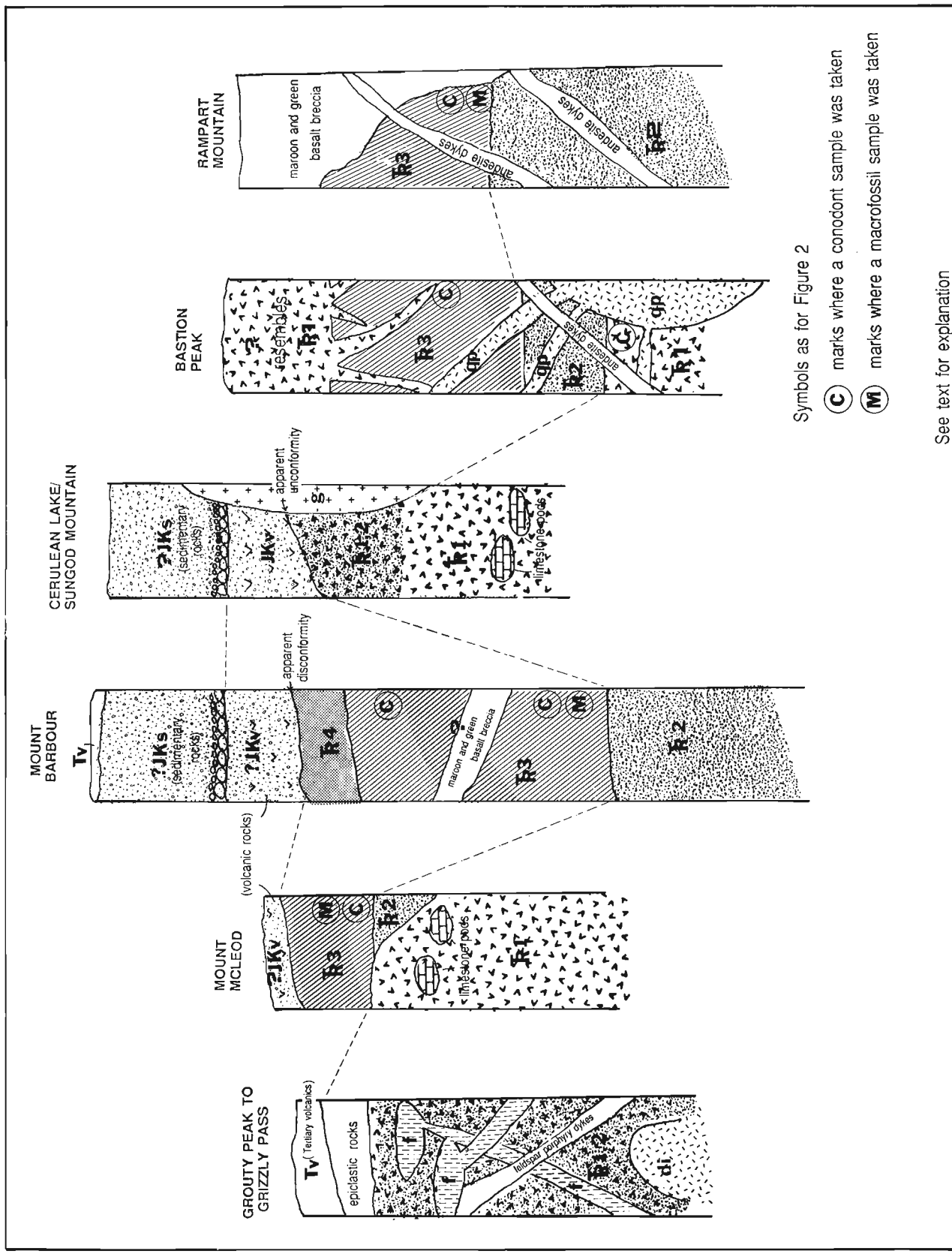

Figure 5. Local variation in stratigraphy.

Mount Barbour

Almost 2000 m of relatively intact section are preserved in the Mount Barbour ridge system; most of it is mixed volcanic and sedimentary rocks of unit Tr3. This section may be slightly thickened by repetition of stratigraphy on a fault just south of Mount Barbour peak. A maroon and green basaltic breccia with some vesicular basalt clasts outcrops on Mount Barbour north of this fault. The relationship of this breccia to the rest of the section is undetermined because the steepness of the cliffs on the peak prevented close inspection of the bounding contacts. However, the breccia appears to sit within the section, because clasts of it are present in the sandstones and conglomerate farther upsection.

The complete section of ?JK volcanic and sedimentary rocks are preserved north of the peak where they appear to sit disconformably on the Triassic rocks. Isolated outcrops of black Tertiary basalt are common around Mount Barbour at about the 2000 m elevation level.

Cerulean Lake-Sungod Mountain

Tr1 mafic flows and Tr2 unbedded tuffs underlie the Cerulean Lake and Sungod Mountain areas. Unit ?JK volcanic and sedimentary rocks sit unconformably on top of them.

Bastion Peak

On Bastion Peak units Tr1, Tr2, and the lower part of unit Tr3 are present in an intact section that strikes north-northwest and dips 45 to 50° to the west. Units Tr1 and Tr2 are intruded by abundant quartz porphyritic dykes and sills that emanate from a large body of pale grey quartz porphyry that forms a high knob just east of Bastion Peak. Toward the top of the section, cherty-topped felsic tuffs of unit Tr3 are crosscut by basalt and andesite dykes. The volume of dyke material increases upward until it overwhelms the bedded rocks. The needly peaks at the top of Bastion Peak ridge are composed of a second massive basaltic and andesitic flow unit with abundant pyroclastic breccia, similar in appearance to unit Tr1. This is puzzling because an upper massive flow unit has not been recognized anywhere else in the map area. The thickness of the material between the lower massive unit (Tr1) and the upper one is estimated at about 400 m, and contains abundant cherty material near its top.

All the rocks in the Bastion Peak area are crosscut by younger, medium green andesite dykes.

Rampart Mountain

The rocks in the Rampart Mountain area are the most severely deformed in the map area. Three separate north-northwest-striking faults are found, with an associated strong to intense shear foliation that is apparent in nearly all outcrops. Andesitic feldspar-crystal, lapilli, and lithic tuffs of unit Tr2 outcrop on the east and west flanks of the mountain. Bedded sedimentary rocks and tuffs of unit Tr3 are found at the base of the eastern flank on the shore of Lillooet Lake, and on the ridge top. The bedding strikes north-northwest with a near vertical dip, with younging to the west. The spatial relationship between units Tr2 and Tr3 here is unclear. Much of the area from just south of the top of Rampart Mountain to the bottom of the map area is overlain by a maroon and green basaltic breccia with some vesicular basalt clasts, which is identical in appearance to the breccia at the peak of Mount Barbour. The contact between this breccia and the bedded rocks of unit Tr3 is well exposed on the top of Rampart Mountain. The irregular east-west trending contact trace cuts off the north-northwest-striking, vertically dipping bedded rocks. At the contact the breccia is encrusted on to the bedded rocks; it is clearly an angular unconformity rather than a fault. The rocks at the top of Rampart Peak are cut by andesite dykes identical in appearance to the latest dykes cutting rocks in the Bastion Peak area.

STRUCTURE

The major fault that cuts the Lillooet Lake pendant continues to the northwest through the Owl Creek valley (Fig. 2, 3). In the Lillooet Lake area, Cretaceous rocks of the Fire Lake Group (equivalent to the Gambier Group; Roddick, 1965), are gently deformed, probably by the east-side-up movement on the fault (Riddell, 1990), into broad, open folds with gently plunging, north-northwest-trending fold axes that parallel the fault trace. East of the fault, the Triassic outcrops show a moderate to intense north-northwest-striking penetrative foliation. Bedding directions are parallel or near parallel to that foliation, indicating that the rocks have suffered high shear stress. This intense deformation is not apparent in the rocks east of the fault in the Tenquille Lake area. There, the Triassic rocks and the overlying ?post-Triassic rocks are gently folded into a broad anticline with a gentle southeast-plunging fold axis that lies just east of Mount McLeod (Fig. 2, 3). Axial planar cleavage is present. The Triassic rocks and the ?post-Triassic section were deformed together by one event some time after deposition of unit ?JK.

Part of a large shear zone is exposed in a new road on the Lill mining claims, along the shoreline at the mouth of the Lillooet River. The rocks show an intense north-northwest-striking shear foliation and gentle southeast-plunging lineations on the shear planes. Intensely gouged and powdered sections alternate with fairly competent, silicified blocks with the shear zone. This may be a continuation of an east-side-up thrust fault that lies along strike to the south on the western shore at the bend in Lillooet Lake. This structure continues across the lake farther to the south (Journeay, 1990) and appears to be an important regional feature. It may be the same fault that forms the Grizzly Pass shear zone, or alternatively, it may continue north through the Birkenhead River valley.

ACKNOWLEDGMENTS

Funding for the 1990 field season was provided by British Columbia Geoscience Grant 89-38. Teck Explorations Limited and the Geological Survey of Canada (Pemberton Project) provided logistical support. The author would like to thank Teck for allowing her to release information gathered while employed by the company. The author is grateful to Murray Journeay and Paul Schiarizza for providing good advice and encouragement. Jean Pautler of Teck provided helpful insight and was a most compatible field companion.

Scott Helm's voluntary mapping contribution is most gratefully acknowledged. Pemberton Helicopters provided another season of safe and dependable transportation.

REFERENCES

Arthur, A.J.
1986: Stratigraphy along the west side of Harrison Lake, southwestern British Columbia; in Current Research, Part B, Geological Survey of Canada, Paper 86-1B, p. 715-720.

Cairnes, C.E.
1925: Pemberton area, Lillooet District, British Columbia; in Summary Report 1924, Part A, Geological Survey of Canada, p. 76-99.
1937: Geology and mineral deposits of the Bridge River Mining Camp, British Columbia; Geological Survey of Canada, Memoir 213, 140 p.

Journeay, J.M.
1990: A progress report on the structural and tectonic framework of the southern Coast Belt, British Columbia; in Current Research, Part E, Geological Survey of Canada, Paper 90-1E, p. 183-195.

Riddell, J.M.
1990: Geology west of Lillooet Lake, near Pemberton, southwestern British Columbia; in Current Research, Part E, Geological Survey of Canada, Paper 90-1E, p. 219-225.

Roddick, J.A.
1965: Vancouver North, Coquitlam and Pitt Lake map area, British Columbia; Geological Survey of Canada, Memoir 335, 276 p.

Roddick, J.A. and Hutchison, W.W.
1973: Pemberton (east half) map area, British Columbia; Geological Survey of Canada, Paper 73-17, 21 p.

Rusmore, M.E.
1985: Geology and tectonic significance of the Upper Triassic Cadwallader Group and its bounding faults, southwest British Columbia; unpublished Ph.D. thesis, University of Washington, Seattle, 174 p.

Schick, J.D.
1990: Geochemistry and tectonic significance of greenstones from the Fire Lake pendant and Twin Islands Group, British Columbia; unpublished B.A. thesis, Middlebury College, Vermont, 58 p.

Woodsworth, G.J.
1977: Pemberton (92J) map area, British Columbia; Geological Survey of Canada, Open File 482.

A new bedrock mapping project near Mayo, Yukon

Charles F. Roots
Cordilleran Division, Vancouver

Roots, C.F., A new bedrock mapping project near Mayo, Yukon; in Current Research, Part A, Geological Survey of Canada, Paper 91-1A, p. 255-260, 1991.

Abstract

Mayo map area (105M) is the focus of field and laboratory investigations to update the geological map produced by H.S. Bostock fifty years ago.

Field work in 1990 explored the oldest known unit, the Hyland Group, which forms a wide band across the centre of the map area. It consists of metamorphosed sandstone and phyllitic siltstone, with rare beds of white quartzite and limestone. All outcrops are foliated and reveal tight recumbent fold hinges. Although small scale deformation is present, coherent stratigraphic units up to 400 m thick are exposed within the Hyland Group.

Cretaceous quartz monzonite plugs postdate deformation of the Hyland Group. The plugs with surrounding skarn and sericitized rock preferentially resist erosion. Indications of tungsten, minor tin and molybdenum are found where these rocks are well exposed.

Résumé

La région de la carte de Mayo (105M) fait l'objet de recherches sur le terrain et en laboratoire visant à mettre à jour la carte géologique dressée il y a cinquante ans par H.S. Bostock.

Dans le cadre de la campagne de 1990, on a exploré la plus ancienne unité connue, le groupe de Hyland, qui forme une large bande traversant le centre de la région cartographiée. Ce groupe consiste en grès et en siltstone phylliteux métamorphisés avec de rares couches de quartzite blanche et de calcaire. Tout les affleurements sont feuilletés et présentent des charnières de plis couchés serrés. Bien qu'il y ait déformation à petite échelle, des unités stratigraphiques cohérentes d'une épaisseur atteignant jusqu'à 400 m sont mises à nu à l'intérieur du groupe de Hyland.

Des bouchons de monzonite quartzique datant du Crétacé sont ultérieurs à la déformation du groupe de Hyland. Les bouchons et le skarn ainsi que la roche sériciteisée qui les entourent résistent de manière préférentielle à l'érosion. Il y a des indications de la présence de tungstène et de faibles quantités d'étain et de molybdène aux endroits où ces roches sont bien mises à nu.

INTRODUCTION

Mayo map area lies south of the Wernecke Mountains, northeast of the Tintina Trench (Fig. 1) and is bisected by the Stewart River. Mayo village is 400 km by road from Whitehorse. The map area includes the silver-lead-zinc veins of the Keno Hill mining camp (currently closed) near its northern edge, and the McArthur Game Sanctuary in its southwest corner.

Geological investigation followed discovery of placer gold (Keele, 1906) and galena-quartz veins (Cockfield, 1919). Reconnaissance mapping by Bostock (1948) led to 1:50 000 scale maps by Kindle (1962), Poole (1965), Green (1971) and Gordey (1990b) in the northern part of the map area. With the exception of two active placer mining operations and two dormant tungsten prospects, the central and southern parts of the map area have not been investigated since Bostock's traversed them with pack horses in 1938-1941.

In the past 50 years the rock units known to occur in Mayo map area have been studied in adjacent regions, and their age and depositional history are more precisely known. For example, conodonts found in the Keno Hill Quartzite near Dawson are Visean (Mississippian) age (M. Orchard, pers. comm., 1985). Previously this unit was considered Precambrian by Bostock (1948; his unit 3), then inferred to be Cretaceous (Tempelman-Kluit, 1970; Green, 1971). As a result of the more detailed mapping, and advances in the understanding of the tectonic framework of the region, Bostock's 1:250 000 scale map is in need of revision.

Mayo map area lies within the tectonic element known as Selwyn Basin (Fig. 1), a region of dominantly fine grained clastic strata deposited between latest Proterozoic and middle Paleozoic time. Beginning in the Middle Jurassic period, the Selwyn Basin rocks were telescoped and displaced northward as a result of arc-continent collision along the continental margin to the southwest (Tempelman-Kluit, 1979).

Most of Mayo map area forms part of two thrust sheets that juxtapose Selwyn Basin strata against similar-aged carbonate-dominated strata of the Mackenzie Platform, north of the area (Fig. 1). The Tombstone thrust sheet is exposed in the northern part of Mayo map area and contains the Keno Hill Quartzite. Overlying it and extending south as far as the Tintina Trench is the Robert Service thrust sheet.

Two major units comprise the Robert Service thrust sheet. The Hyland Group (Gordey, in press; see also the 'Grit Unit' of Green, 1971) includes sandstone, conglomerate, varicoloured silt-and mudstone with minor limestone. Along the southern and eastern edges of Mayo map area Hyland Group rocks are stratigraphically succeeded by Road River strata of middle Cambrian to Devonian age (Gordey, 1990a and pers. comm.).

In 1990 the lithology, structure and contacts of the Hyland Group were investigated in the central part of the map area (Fig. 2).

STRATIGRAPHY

The Hyland Group is sparsely exposed except on several ridge tops above about 1300 m elevation. It contains no marker units, but beds of distinctively weathering limestone and white quartzite could be traced several kilometres across areas of abundant exposure. Nevertheless the overall structure and thickness of the Hyland Group remain to be resolved. Linear valleys 2 km or more wide, veneered with glacial sediments and probably underlain by faults, separate the rounded ridges and undulating plateaus mapped in 1990.

Brown sandstone with pronounced foliation is the predominant rock type in all areas studied (Fig. 3). It consists of 0.5-1.0 mm grains of translucent quartz with silica cement and varying amounts of interstitial muscovite, with limonite and hematite stain. Distinctive blue-tinted quartz granules, diagnostic of Hyland Group successions, were noted north

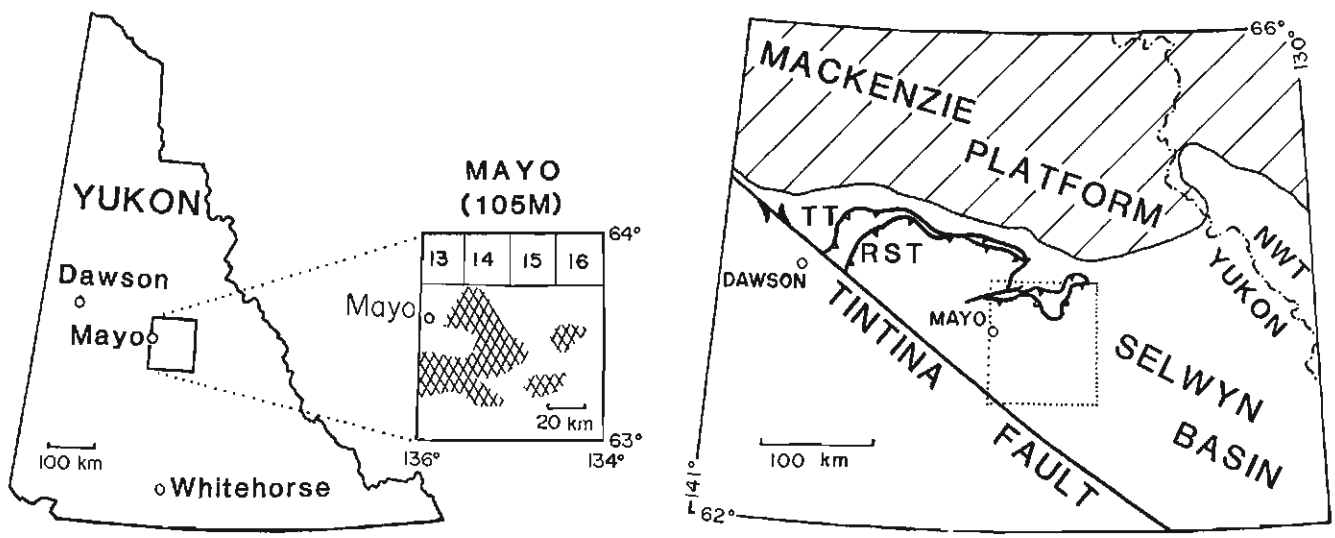

Figure 1. Location of the project area. Inset (centre) shows Mayo map area, with cross-hatched portion mapped in 1990. Numbered squares on inset indicate 1:50 000 maps by: 13 - Poole (1965); 14 - Kindle (1962); 15 - Green (1971) and 16 - Gordey (1990b). Geological setting is shown at right. Mayo map area is part of the Selwyn Basin between the Mackenzie Platform and Tintina Fault. The area between the Tombstone Trust (TT) and the Robert Service Thrust (RST) is the Tombstone thrust sheet. The larger area south of RST is the Robert Service thrust sheet.

of Janet Lake, east of Fraser Falls and on Kalzas Plateau. Beds of grit (consisting of angular grains 2-4 mm diameter) occur only on Nogold Plateau and Kalzas Plateau. On the latter, dark quartz grains and rip-up clasts of dark siltstone are common. In both these areas normal size grading is generally visible; crossbedding was not observed.

Interbedded with the sandstone are thinner beds of drab-coloured siltstone and mudstone. Most are schistose and primary sedimentary features are not preserved, except load-casts on the base of overlying sandstone beds. Along the south side of Nogold Plateau maroon argillite appears faulted against sandstone. The argillite contains 10-15 m thick lenses of mafic volcanic breccia. These rock types also occur together in the Dawson area to the northwest where trace fossils in similar argillite indicate an Early Cambrian age (Mustard et al., 1989).

Near Lonely Dome penetratively deformed chlorite-muscovite-quartz schist is similar to that described by Gordey (1990a) about 20 km to the north. Bostock's (1948) units 5 and 6 are distinguished by the proportion of quartz-mica schist to schistose quartzite. On ridges east and north of Lonely Dome the contact between units 5 and 6 could not be determined, and the north-trending fault indicated by Bostock is not evident (see also Gordey, 1990b).

Near Fraser Falls greenstone noted by Bostock (1948) is smaller than shown and its contacts are parallel to both foliation and bedding of the surrounding meta-sandstone. It is a dark coloured, medium grained and prominently banded rock (Fig. 4) consisting of alternating proportions of chlorite and amphibole. The body contains at least three lenses of sandstone greater than 50 cm thick; these contain some blue quartz grains. Although all primary sedimentary features have been obliterated by strain, this banded rock is probably a mafic tuffaceous sediment. Basaltic tuff is common in Hyland Group sections north of Dawson, and may contain enough zircon or baddelyite to isotopically date the unit.

At the west end of Nogold plateau 400 m high cliffs face northward and reveal three broad divisions of a thick bedded sandstone section. The relatively resistant lower member is light coloured and overlain by grey, friable strata with several limy horizons. The top member is blocky and grades upward to phyllitic sandstone. These members, or parts of them, are exposed at intervals for 15 km along the north side of Nogold Plateau, indicating that the Hyland Group in this area dips gently south.

In general the Hyland Group consists of compositionally uniform sediments distributed over a wide area. The source was a vast reservoir of quartz grains, perhaps underlain by highly weathered granitic or metamorphic rocks. The observed sedimentary structures are suggestive of deposition as sediment gravity flows. Although the Hyland Group lies on a thrust sheet that has travelled northward it is unlikely that the source area was to the north or east where carbonate shelf rocks predominate and terranes containing blue quartz are not exposed.

STRUCTURE AND METAMORPHISM

Where studied in Mayo map area the Hyland Group contains chlorite and sericite and is of greenschist metamorphic grade. Muscovite mica defines a foliation in sandstone. Where sediments were richer in clay, muscovite sheets now separate the framework grains. In fine grained rocks cleavage surfaces are smooth and phyllitic. The annealing of quartz grains and formation of muscovite have obliterated delicate sedimentary features, and folds in bedding are difficult to discern.

In some places the rocks are tightly folded on a minor scale, as revealed by the recumbent hinges of quartz veins and dark sediment layers preserved in outcrop faces (Fig. 5). Nevertheless thick sections can be traced laterally, suggesting that tight folding does not affect entire successions. In several places north of Nogold Plateau tightly folded graphitic rock is exposed on a topographic bench beneath the thick, undeformed succession. These rocks may lie in the footwall of a low angle fault, as shown in Figure 2.

The south-plunging Mayo Lake anticline interpreted by Bostock (1948) and Green (1971) is reflected by warping of the Tombstone and Robert Service thrust sheets. The rocks at Lonely Dome, near the hinge of the anticline are more strongly deformed than Hyland Group elsewhere and indicate a deeper structural level, arched upward during formation of the anticline. The plunge of minor fold lineations and dip of foliation is outward, to northeast and west, from the axis of the anticline.

Qualitative field observation suggests that deformation of Hyland Group rocks increases northward toward the Robert Service Thrust. Although the rock succession is apparently more continuous in the southern area of study, this does not preclude imbrication of the Hyland Group in this latter area by large, low-angle faults with considerable northward displacement.

MINERAL SHOWINGS

High peaks at the east end of Kalzas Plateau contain a tungsten deposit explored in the early 1980s. A 2 km diameter alteration halo in sandstone and siltstone of the Hyland Group was documented by Lynch (1989) and an intrusion is inferred to lie at shallow depth. Quartz veins contain tourmaline and prismatic wolframite (ferberite-heubnerite), a principal ore of tungsten.

Two Buttes is a high-standing area (Fig. 6) where fine grained sandstone has been metamorphosed adjacent to a porphyritic quartz monzonite plug. A limestone layer exposed across the north slope is altered to chloritic calc-silicate, possibly containing brown garnet. Minor scheelite-powellite is reported (DIAND, 1981) and molybdenite specks were observed. Northwest and south of Two Buttes are several pink to grey rhyolite dykes with up to 10% quartz phenocrysts. These intrusions typically have pyritic margins.

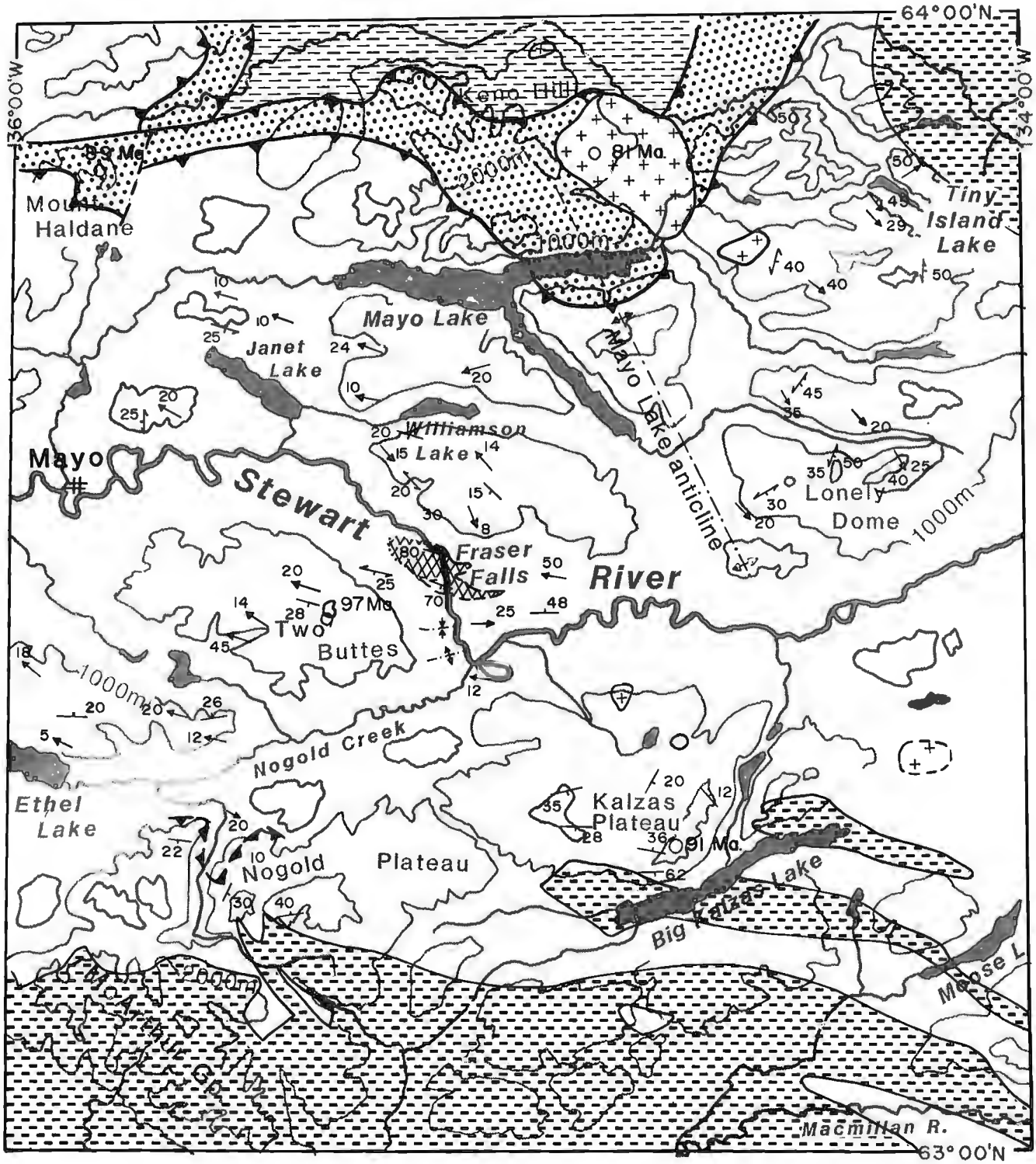

Figure 2. Simplified geology of Mayo map area. The regions where measurements are shown were traversed in 1990, except in the northeast near Tiny Island Lake, mapped by Gordey (1990b). Circles are locations of isotopic age determinations, noted in Table 1. General geological contacts are modified from Bostock (1948).

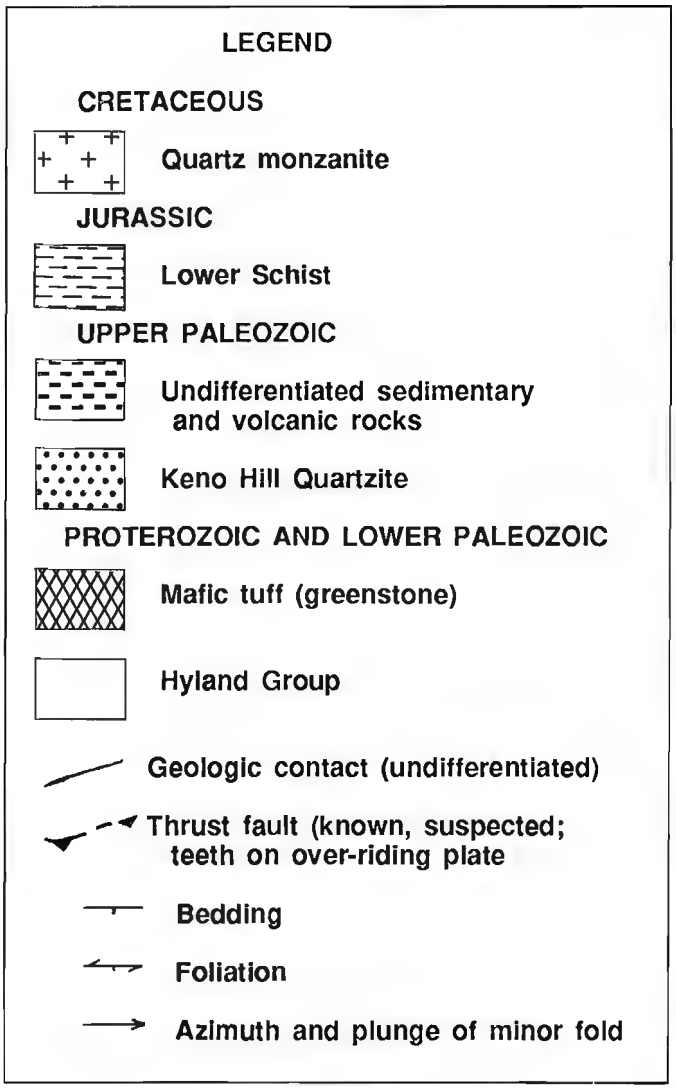

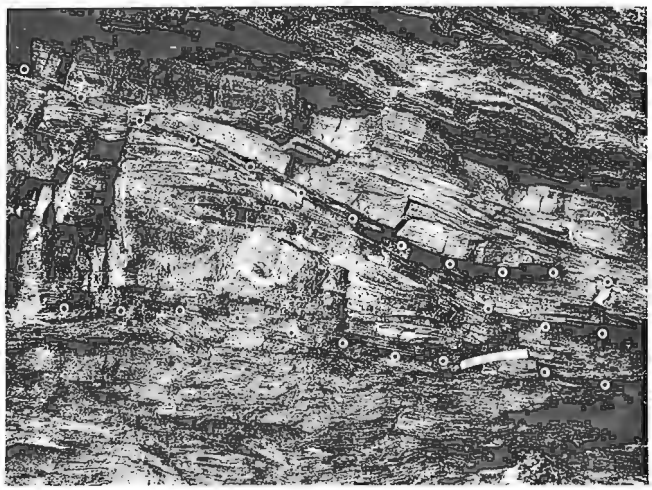

Figure 3. A band of metasandstone beds with schistose siltstone above and below is typical Hyland Group lithology about 4 km north of Ethel Lake. Bedding is cut by anastomosing shear planes (dots) so that primary features are preserved in lenticular zones. View is toward the west, with the scale bar in centimetres.

Figure 4. Dark chloritic mafic rock at Fraser Falls. It has a steep foliation and contacts are parallel with foliation within enclosing sedimentary rocks. The rock is interpreted as mafic tuff because quartz sandstone is intercalated with some bands. This view is eastward and the kink folds are consistent with northward contraction.

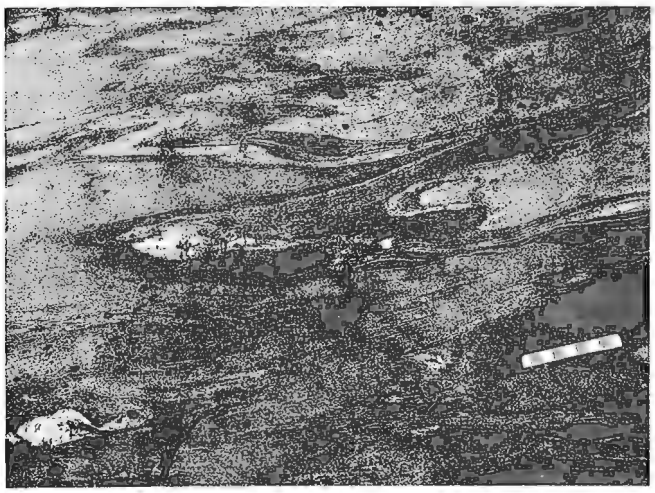

Figure 5. Recumbent folds outlined by a darker chloritic layer in metasandstone. The folds have been flattened into the plane of foliation indicated by muscovite growth. Note rootless folds of silica caught in hinge zones, and knots of quartz remaining from distended veins. View is downward with north at the top, 400 m southeast of Fraser Falls, and the scale bar indicates centimetres.

Table 1. K-Ar age determinations from biotite separates, Mayo map area.

Age	Intrusion	GSC #.	Reference
81.0	Roop pluton	62-81	Leech et al. 1963
89.0±2.6	Mt. Haldane porphyry	80-74	Stevens et al. 1982
90.7±1.4	Kalzas hornfels	87-165	Hunt et al. 1987
97.1±3.6	Two Buttes plug	81-38	Stevens et al. 1981

Figure 6 View southward across the meandering Stewart River toward Two Buttes. Only the angular summits, now mostly rock rubble, stood above the maximum height of Wisconsin Glaciation.

ACKNOWLEDGMENTS

I thank Peter Daubeny for cheerful assistance, pilots Will Tompson and Dave Reid of Trans North Air, Ltd. as well as Lise Tompson and Lasha Reid for their promptness and attention to detail. The sage advice of Doug Eaton and Rob Carne, as well as the hospitality of Archer Cathro and Associates, Ltd. contributed to a successful summer. The generosity of Randy and Pat Randolph and friends lifted spirits and extended our traverse range. The exploits described in Pack Horse Tracks (Bostock, 1979) provided constant inspiration.

REFERENCES

Bostock, H.S.
1948: Mayo, Yukon Territory; Geological Survey of Canada, Map 890A.
1957: Yukon Territory (selected field reports of the Geological Survey of Canada 1898-1933); Geological Survey of Canada, Memoir 284.
1979: Pack Horse Tracks - Recollections of a Geologist's Life in British Columbia and the Yukon, 1924-1954; Geological Survey of Canada, Open File 650.

Cockfield, W.E.
1919: Mayo area, Yukon; Geological Survey of Canada, Summary Report 1918, Part B, p. 1B-15B (reprinted in Bostock, 1957).

Department of Indian Affairs and Northern Development (DIAND)
1981: Yukon Geology and Exploration 1979-80; Annual Report of the Geology Section, Indian and Northern Affairs Canada, Whitehorse.

Gordey, S.P.
1990a: Geology and mineral potential, Tiny Island Lake map area, Yukon; in Current Research, Part E, Geological Survey of Canada, Paper 90-1E, p. 23-29.
1990b: Geology of the Tiny Island Lake map area (105M/16); Indian and Northern Affairs Canada, Exploration and Geological Services (Yukon), Open File 1990-2, scale 1:50 000.
in press: Evolution of the northern Cordilleran miogeocline, Nahanni map area (105I), Yukon Territory and District of Mackenzie; Geological Survey of Canada, Memoir 428.

Green, L.H.
1971: Geology of Mayo Lake, Scougale Creek and McQuesten Lake map areas, Yukon Territory; Geological Survey of Canada, Memoir 357.

Hunt, P.A. and Roddick, J.C.
1987: A compilation of K-Ar ages, Report 17, in Radiogenic and Isotopic Studies, Report 1; Geological Survey of Canada, Map 1987-2.

Keele, J.
1906: The Duncan Creek mining district; Geological Survey of Canada Annual Report vol. XVI, part A, p. 18A-42A (reprinted in Bostock, 1957).

Kindle, E.D.
1962: Geology, Keno Hill, Yukon Territory; Geological Survey of Canada, Map 1105A, scale 1:63 360.

Leech, G.B., Lowdon, J.A., Stockwell, C.H., and Wanless, R.K.
1963: Age determinations and geologic studies, including isotopic studies, Report 4; Geological Survey of Canada, Paper 63-17.

Lynch, J.V.G.
1989: Hydrothermal alteration, veining and fluid inclusion characteristics of the Kalzas wolframite deposit, Yukon; Canadian Journal of Earth Sciences, v. 26, p. 2106-2115.

Poole, W.H.
1965: Mount Haldane (105M/13) and Dublin Gulch (106D/4) map areas; in Report of Activities: Field 1964; Geological Survey of Canada, Paper 65-1, p. 32-35.

Stevens, R.D., DeLabio, R.N., and Lachance, G.R.
1981: Age determinations and geological studies: K-Ar isotopic ages, Report 15; Geological Survey of Canada, Paper 81-2.
1982: Age determinations and geological studies: K-Ar isotopic ages, Report 16; Geological Survey of Canada, Paper 82-2.

Tempelman-Kluit, D.J.
1970: Stratigraphy and structure of the 'Keno Hill Quartzite' in Tombstone River-Upper Klondike River map areas, Yukon Territory (116B/7, B/8); Geological Survey of Canada, Bulletin 180.
1979: Transported cataclasite, ophiolite and granodiorite in Yukon: evidence for arc-continent collision; Geological Survey of Canada, Paper 79-14.

Structure between Scrip Nappe and Monashee Terrane, southern Omineca Belt, British Columbia

Robert J. Scammell[1]
Cordilleran Division, Vancouver

Scammell, R.J., Structure between Scrip Nappe and Monashee Terrane, southern Omineca Belt, British Columbia; in Current Research, Part A, Geological Survey of Canada, Paper 91-1A, p. 261-269, 1991.

Abstract

In the immediate hanging wall of the Monashee Décollement, and south of Scrip Nappe, the Kootenay Terrane contains high-grade, polydeformed rocks inferred to be part of the Upper Proterozoic Horsethief Creek Group. A strong regional foliation records four phases of folding. The first-order macroscopic structure is an overall upright gentle synform which deforms the upright limb of an F_1 syncline inferred to underlie Scrip Nappe. The hinge zone of Scrip Nappe may outcrop in the study area, south of its previously inferred position. Later extensive F_2 and local F_3 folding, plus extensive emplacement of leucogranite complicate the macroscopic structure. Mesoscopic F_1 and F_2 folds are coaxial with an east-west trending sillimanite-grade mineral elongation lineation. Mesoscopic post-metamorphic F_3 and F_4 folds are rare. High-grade mylonitic fabrics record horizontal crustal shortening and possible thinning of the thrust sheet. Discrete shear zones, defined by low-grade unannealed mylonitic fabrics, record down-to-the-west normal motion and horizontal extension of the crust.

Résumé

Dans le toit immédiat du décollement de Monashee, et au sud de la nappe Scrip, le terrane de Kootenay renferme des roches ayant subi une orogenèse polyphasée et dont on suppose qu'elles font partie du groupe de Horsethief Creek du Protérozoïque supérieur. Une schistosité régionale marquée témoigne de quatre phases de plissement. La structure macroscopique de premier ordre est une synforme générale verticale de faible amplitude qui déforme le flanc vertical d'un synclinal F_1 que l'on suppose sous-jacent à la nappe Scrip. La zone charnière de la nappe Scrip peut affleurer dans la région d'étude au sud de la position qu'on lui avait antérieurement assignée. Un plissement F_2 généralisé et un plissement F_3 local, ainsi qu'une mise en place généralisée de leucogranite ont ultérieurement compliqué la structure macroscopique. Les plis à moyenne échelle F_1 et F_2 sont coaxiaux à une linéation d'étirement est-ouest matérialisée dans un minéral de la teneur de la sillimanite. Les plis à moyenne échelle post métamorphiques F_3 et F_4 sont rares. Les fabriques à teneur élevée en mylonite témoignent de raccourcissements crustaux horizontaux et d'un amincissement possible de la nappe de charriage. Des zones de cisaillement discrètes, définies par des fabriques mylonitiques à faible teneur non recuites, témoignent d'un déplacement normal vers le bas à l'ouest et d'une extension de la croûte dans le plan horizontal.

[1] Department of Geological Sciences, Queen's University, Kingston, Ontario K7L 3N6

INTRODUCTION

This paper summarizes structural data collected from multiply-deformed high-grade rocks in the southern Scrip and northern Seymour ranges (Fig. 1). Particular attention is directed towards the macroscopic geometry of these rocks. These data indicate: (i) deformed stratigraphic units are laterally continuous with rocks which outline Scrip Nappe to the north where they are inferred to be part of the Upper Proterozoic Horsethief Creek Group of North American affinity (Raeside and Simony, 1983; Raeside, 1982), (ii) the first-order macroscopic structure is an overall upright gentle synform which deforms the upright limb of a large recumbent syncline inferred to underlie Scrip Nappe (Fig. 2), and (iii) this first-order macroscopic structure is complicated by multiple folding at a smaller scale, and intrusion of leucogranite. Summary descriptions of lithology, stratigraphy, structure, metamorphism and granitoid rocks can be found in Scammell and Dixon (1989, 1990) and Scammell (1990).

REGIONAL GEOLOGY

Rocks in this region of the Omineca Belt (Fig. 1) can be broadly divided into three fault-bounded packages which record different but related thermal histories, and which represent zones of the crust that were positioned at different crustal levels immediately prior to Eocene extension (Carr and Brown, 1989; Johnson and Brown, 1989). The deepest exposed crustal level comprises polydeformed high-grade basement and cover gneisses of the Monashee Terrane (Brown et al., 1986; Journeay, 1986; Scammell and Brown, 1990).

The Monashee Décollement marks the upper boundary of the Monashee Terrane. This well-layered mylonitic shear zone is inferred to root to the west (Brown et al., 1986), and to have undergone episodic Mesozoic to Early Tertiary east-vergent thrusting (Brown et al., 1986; Lane et al., 1989; Journeay and Parrish, 1989).

The hanging wall of the Monashee Décollement is composed of rocks which were part of the "mid-crustal zone" immediately prior to Eocene extension. These rocks comprise a polydeformed sillimanite-grade sequence of sedimentary and igneous rocks which are part of the pericratonic Kootenay Terrane lying to the west and north of the Monashee Terrane (Wheeler and McFeely, 1987). They are believed to be Late Proterozoic in age (Scammell, 1990). The macroscopic structure of the Kootenay Terrane to the north of the study area is dominated by the southwest-verging Scrip Nappe (Raeside and Simony, 1983). Scrip Nappe is a fold nappe with a limb length of 50 km. It is refolded by tight northeast verging folds. Granitic rocks are ubiquitous and form a series of Paleozoic to Lower-Middle Eocene suites (Fig. 1; Carr, 1989; Sevigny et al., 1989; Parrish et al., 1988; Wheeler and McFeely, 1987; Okulitch, 1985). This "mid-crustal" package is characterized by Tertiary cooling, Eocene strain and extensive intrusion by Eocene leucogranitic rocks.

In the vicinity of the study area, the west-dipping Eagle River and North Thompson faults, and the east-dipping Columbia River fault form the upper boundaries of the package of pre-Eocene mid-crustal rocks (Journeay and Brown, 1986; Johnson and Brown, 1989). Displacements on these faults in the Eocene (Parrish et al., 1988; Sevigny and Simony, 1989) are inferred to have resulted in tectonic denudation of the Monashee Terrane and part of the Kootenay Terrane including the study area (Brown and Journeay, 1987; Parrish et al., 1988).

The "upper-crustal zone" is composed of rocks which lie in the hanging walls of the above normal-fault systems. They comprise polydeformed Upper Proterozoic to Lower Paleozoic sedimentary and mafic igneous rocks, and relatively undeformed Eocene volcanic and sedimentary rocks. Jurassic regional metamorphism and granitic intrusion of dominantly Jurassic and Cretaceous age are characteristics of this zone (e.g. Archibald et al., 1983; Leatherbarrow, 1981). The macroscopic structure of this zone is dominated by west-vergent nappes (Brown et al., 1986; Brown and Lane, 1988).

STRUCTURE

Mesoscopic Structures

Foliation

The most prominent mesoscopic structural element is a regionally penetrative metamorphic foliation defined by co-planar compositional layering, gneissic layering and schistosity marked by the dimensional preferred orientation of phyllosilicate, prismatic, and plastically deformed mineral grains, and concordant lenses of leucosome. It is co-planar with F_1 and F_2 fold limbs and primary compositional layering in metasedimentary rocks. It is designated S_{1+2} since this foliation is inferred to be a product of transposition or synkinematic recrystallization or static mimetic recrystallization or a combination of these processes, during or after folding of F_1 fabrics by F_2 folds which predate the quenching of metamorphic isograds (Raeside, 1982). It generally dips gently to moderately southwest to northwest, and its poles define a girdle pattern in stereographic projection (Fig. 3). This dispersion can be explained by superposed F_3 folding about an axis plunging gently to the west, and measurement of this fabric in the hinges of large-scale F_2 folds which do not crenulate the fabric.

Folds

The oldest identified folds (F_1) are commonly preserved in type-3 interference patterns (Thiessen and Means, 1980) generated by the co-axial superposition of F_2 folds on F_1 folds. They are also preserved as rare rootless isoclinal folds with centimetre to decimetre amplitudes. Both F_1 and F_2 folds appear to fold an earlier foliation defined by phyllosilicates, and except where overprinting relationships are observed, there are no diagnostic criteria separating the two.

F_2 folds are close to isoclinal, nonparallel, and display both angular and curved hinges. Their hinge zones commonly fold phyllosilicate foliations, but in some cases phyllosilicate-rich layers display a crenulation cleavage generated during folding and recrystallization of F_1 schistosity. Biotite is locally developed parallel to F_2 axial planes. These axial planes dip gently to moderately southwest to northwest (S_2, Fig. 3). Poles to S_2 plotted in stereographic projection display a girdle because of the superposition of F_3 folding. Fold axes of F_2 folds generally plunge gently to the west-northwest or to the east-southeast (L_2, Fig. 3). Some scatter

in L_2 orientations is a product of non-coaxial F_3 and F_4 folding. L_2 is invariably co-axial with a well-developed mineral elongation lineation.

F_3 folds are locally developed. They are non-cylindrical, generally upright structures with axes plunging gently to the west-northwest or southeast (see Fig. 3E of Scammell, 1990). They are commonly disharmonic in multilayers with gentle warps in quartzofeldspathic layers and open folds in phyllosilicate-rich layers. F_3 folds commonly fold the high-grade mineral elongation lineation (Ls), and typically display an upright crenulation in phyllosilicate-rich layers where phyllosilicates display undulose extinction and kink bands. This indicates that this crenulation has not experienced subsequent recrystallization. F_3 folds therefore postdate the metamorphic peak.

F_4 folds have been observed in two locations. They are non-cylindrical, east- and west-verging, late- to post-metamorphic folds, spatially associated with discrete brittle and late ductile shear zones.

Lineation

A mineral elongation lineation is marked by aligned sillimanite fibres, mica aggregates, hornblende prisms, and quartz rods, and is best developed in pelitic and quartzofeldspathic rocks. It plunges gently to moderately to the west or southeast (Ls, Fig. 3), and is co-linear with L_2.

Mylonitic fabrics

High-grade mylonitic fabrics are present in the south part of the map area. They record both upper-plate-to-the-east and -west ductile shearing, and may be related to thinning of the thrust sheet during east-vergent thrusting on the Monashee Décollement. Low-grade proto-to ultra-mylonite fabrics are present in metre-scale discrete shear zones localized in late leucogranite or marble horizons. They truncate S_{1+2} foliation and F_2 folds, and formed at low-grade in association with down-to-the-west normal faulting and tectonic denudation of the region.

Well-exposed shear-sense indicators consistently record upper-plate-to-the-east motion in the high strain zone associated with the Monashee Décollement. The population of shear-sense indicators includes C/S fabrics, asymmetric extension shears, back-rotated swells and foliation segments, shear-modified boudins, sheath folds, and winged porphyroclasts and inclusions.

Macroscopic structure

The geometry of map-scale structures in this region is difficult to determine due to the lack of unique marker horizons, the complexity of outcrop-scale folding, and stratigraphic discontinuities created by the emplacement of abundant granitoid rocks (Scammell, 1990). Co-axial folding coupled with the difficulty in determining the order of mesoscopic parasitic folds restrict the use of vergence of mesoscopic folds in determining the geometry of macroscopic structures. Identified macroscopic folds were delineated mostly by mapping marker horizons. Macroscopic F_1 and F_2 folds are present (Fig. 2). Macroscopic F_3 folds have not been documented, but they may be responsible for unresolved structural complexities at this scale in the northwest part of the map area. Three structural domains have been delineated at the macroscopic scale (Fig. 2 and 3). They are recognized primarily on the basis of gross orientation of the stratigraphic succession, co-planar with S_{1+2}.

Domain 1

The Monashee Décollement marks the south limit of Domain 1. It is composed of well-layered mylonitic rocks which mark a zone of high strain in excess of 1000 m in thickness. A distinctive stratigraphic sequence in cover gneisses of the Monashee Terrane is truncated by the décollement in its footwall (a footwall cutoff, Scammell, 1986), but its hanging wall counterpart has not been identified. A relatively high concentration of metre-thick sheets of sheared granitic rocks occurs locally at the base of this zone (Scammell, 1986). The Monashee Décollement is interpreted (Fig. 2) to lie along the locus of truncation of strata and structures in the footwall (Monashee Terrane). F_1 and F_2 folds in both foot and hanging walls are truncated by the high strain zone associated with the Monashee Décollement.

An upright stratigraphic sequence lies in the immediate hanging wall of the Monashee Décollement, and dips moderately west to northwest (Fig. 3). Structures generally plunge moderately to the west. At the headwaters of Ruddock Creek, Pb-Zn-bearing and calcareous horizons of unit 4 outline a kilometre-scale type-3 fold interference pattern (Fyles, 1970; Scammell, 1990). The F_1 structure at Ruddock Creek is inferred to have been originally southwesterly-verging based on long limb-short limb relationships. It is refolded by several reclined F_2 folds which can have kilometre-scale wavelengths and amplitudes, and plunge gently west-northwest.

Domain 2

Stratigraphic units in the central part of the map area have no consistent or dominant dip (Fig. 3). They have many orientations co-axial with the mineral elongation lineation which plunges moderately west (Fig. 3). Abundant leucogranite obscures the structure in the west part of this domain. Marbles of unit 2 delineate a large reclined F_2 structure in the east part of the domain. Marbles of unit 4 delineate a northeast-verging F_2 antiform in the northwest part of the domain.

Domain 3

In the north part of the study area the stratigraphic sequence generally dips moderately to the southwest, and structures plunge shallowly west-northwest or southeast (Fig. 3). In the northwest part of Domain 3 the stratigraphic sequence forms an upright panel that dips gently to moderately to the southwest, and has been structurally thickened by folding (F_1 or F_2?).

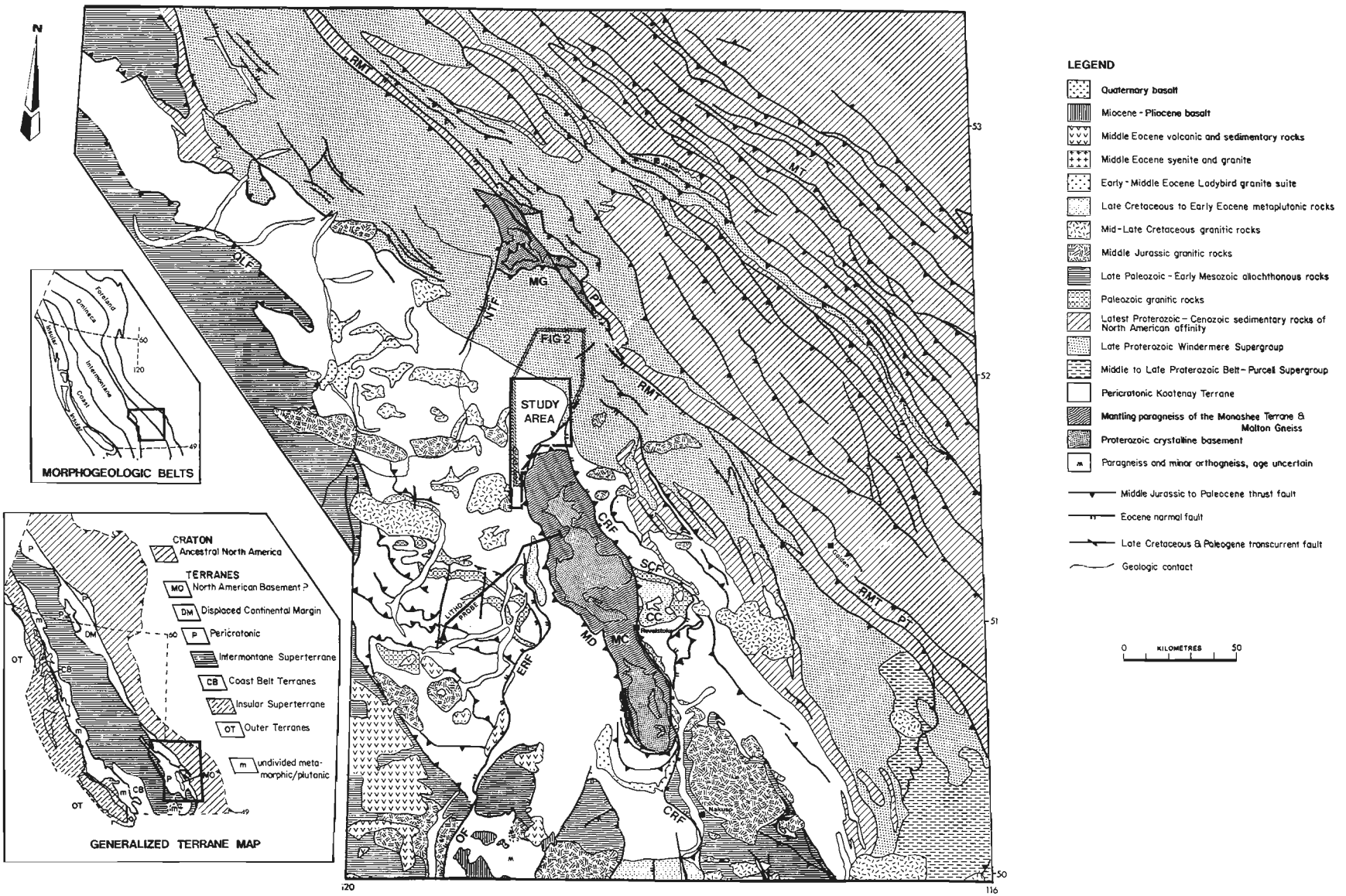

Figure 1. Location of the study area and regional geology (modified after Parrish et al., 1988, and Wheeler and McFeely, 1987). Faults: CRF = Columbia River fault, ERF = Eagle River fault, MD = Monashee Décollement, MT = McConnel Thrust fault, NTF = North Thompson fault, OF = Okanagan Fault, PT = Purcell Thrust fault, SCF = Standfast Creek fault, QLF = Quesnel Lake fault. Metamorphic complexes: MC = Monashee Terrane (or complex), CC = Clachnacudainn Complex, MG = Malton gneiss complex. RMT = Rocky Mountain Trench.

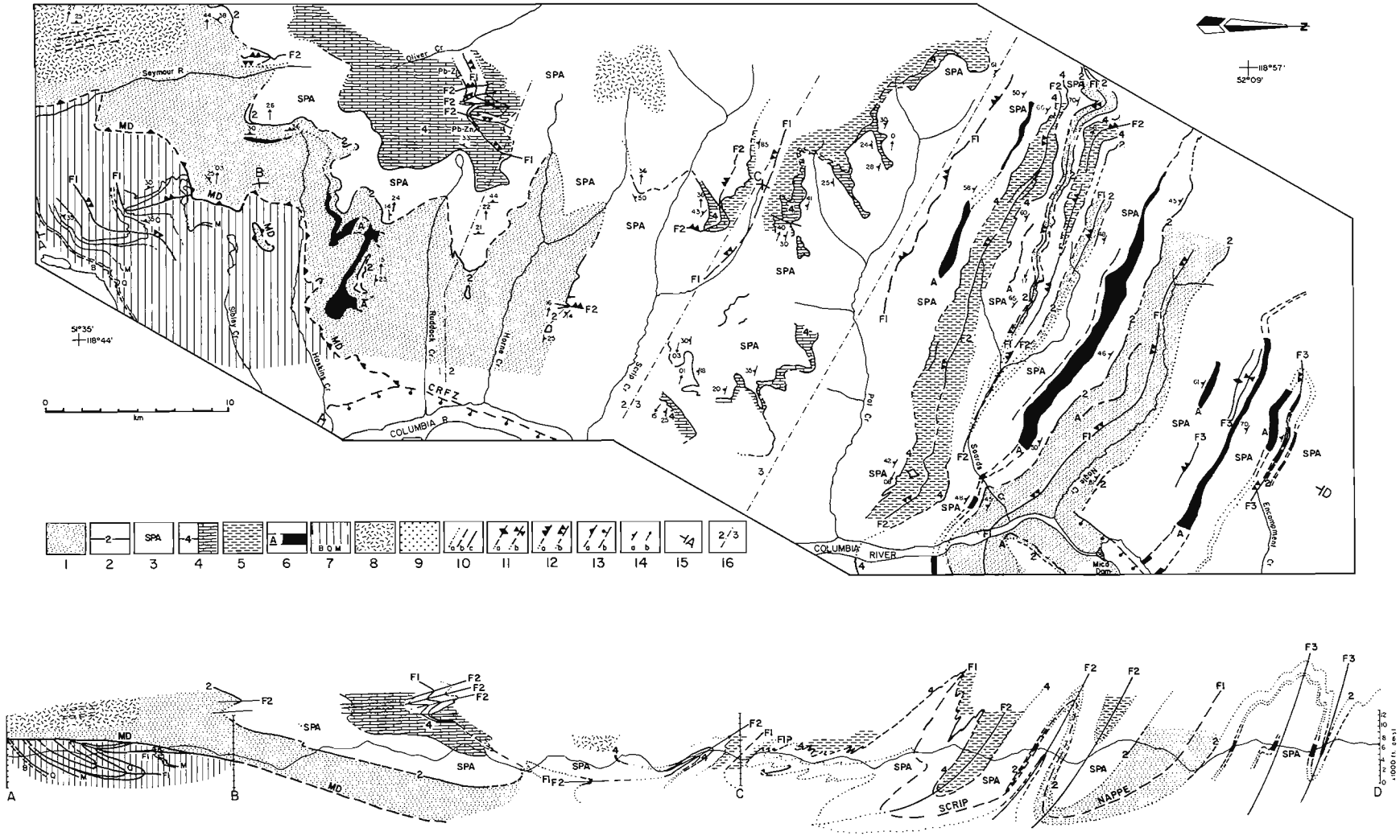

Figure 2. Simplified geological map of the study area. See Figure 1 for location. 1-5 are Horsethief Creek Group subdivisions; 1 = Lower Clastic; 2 = Lower Marble; 3 = Semipelite-Amphibolite; 4 = Middle Marble; 5 = Upper Clastic; 6 = Amphibolite or strata where amphibolite dominates; 7 = Monashee Terrane (B = basement gneisses, Q and M, are quartzite and marble horizons of the cover gneiss sequence); 8 = 50% or greater leucogranite; 9 = lineated hornblende granodiorite; 10 = geological contacts (a-assumed, b- approximate, c-defined); 11 = axial surface traces (a-anticline, b-syncline); 12 = axial surface traces of overturned folds (a-anticline, b-syncline, notation on downdip side); 13 = faults (a-thrust, b- normal); 14 = fabrics (a-strike and dip of S_{1+2}, b- trend and plunge of Ls); 15 = location of cross- section; 16 = boundary between structural domains (note the north boundary of Domain 3 is Pat Creek and the south boundary of Domain 1 is the Monashee Décollement); Pb-Zn = Ruddock Creek Pb-Zn horizon (Fyles, 1970), MD = Monashee Décollement, CRFZ = Columbia River Fault Zone. Data in the footwall of Monashee Décollement is from Scammell (1986), and north of Pat Creek from Raeside (1982). See text for discussion.

Discussion

The cross-section shown in Figure 2 is simplified and its interpretation is preliminary. Several features of the macroscopic geology and the construction of the cross-section are summarized in order to understand the limitations of the cross-section.

1. The line of section is perpendicular to the direction of thrust and extension movement assumed to be parallel to Ls.

2. Some structural data are projected from out of the plane of section. Location of contacts was performed by a modified method of plunge projection which accounts for both mesoscopic plunge variation and the non-cylindrical nature of the folds. Contacts above and below the topographic profile are therefore only rough estimates. For example, the hinge zone of Scrip Nappe (F_1) shown in the cross-section is projected from data presented in Sevigny and Simony (1989) approximately 20 km to the northwest, and is therefore very approximate.

3. Folds at all scales are not parallel. Therefore layer thicknesses are highly variable.

4. Granite is only shown in regions where it comprises 50% or more of the volume of the rock. In general leucogranite comprises 30-40% of the rocks in the study area (Scammell, 1990). It produces lateral discontinuities in the stratified rocks but in general does not offset or disrupt their trends significantly.

5. Widespread brittle deformation and narrow, discrete ductile shear zones play a minor role in the strain history at the macroscopic scale, and are ignored or their displacements were restored during construction of the cross-section.

Although the cross-section is highly interpretive, it serves to illustrate four inferences regarding the macroscopic structure. These are discussed below:

1. Two interpretations of the folded but upright panel of strata in the northwest part of Domain 3 are possible. The first is that it comprises a sequence of rocks that were part of the overturned limb of Scrip Nappe (F_1) in the vicinity of its hinge zone. This limb was then reoriented into an upright, gently to moderately southwest-dipping orientation by F_2 folding. This is the interpretation presented by Sevigny and Simony (1989) and by Raeside (1982). In this case the axial surface trace of Scrip Nappe, in the vicinity of its hinge, outcrops to the north of, or in the north part of Domain 3. The geometry presented by Sevigny and Simony (1989) is projected into the cross-section of Figure 2. Sevigny and Simony interpreted a down-faulted anticlinal structure outlined by Middle Marble as the "nose" of Scrip Nappe. The data they presented do not prove that this is an F_1 hinge or the hinge of Scrip Nappe.

The second interpretation is based on the observation that Middle Marble units that are laterally continuous with those that define the above "nose", dip more shallowly to the south over several kilometres into the north part of the study area, and they appear to form the upright limb to a refolded, reclined, southwest-closing antiform. Although the existing structural data are not diagnostic, they do leave open the possibility that this antiform is the hinge of Scrip Nappe (marked by a dotted line and F1? in Fig. 3). In which case the axial surface trace of Scrip Nappe, in the vicinity of its hinge, must outcrop in Domain 3, and the "nose" of Scrip Nappe discussed by Sevigny and Simony (1989) could be an antiformal F_2 hinge.

2. The cross-section in Figure 2 also illustrates an overall upright panel of inferred Horsethief Creek Group strata in the immediate hanging wall of the Monashee Décollement. Since Scrip Nappe is a fold nappe (Raeside and Simony, 1983), it must have an underlying north-closing synclinal mate composed of an inverted stratigraphic sequence overlying an upright sequence. The above upright panel is thought to be the upright limb of this synclinal mate. If this is correct, then the axial surface trace to this overturned syncline must outcrop in Domain 2 or 3. The cross-section shows this F_1 axial surface trace to lie in the vicinity of the boundary between domains 2 and 3. This placement is in part dependent on the chosen model. If the hinge zone of Scrip Nappe is refolded by an F_2 syncline to the north, as portrayed by Raeside (1982) and by Sevigny and Simony (1989; see cross-section in Fig. 2), then there should be an F_2 anticlinal mate to the south in the study area, possibly with the axial surface trace of the F_1 synclinal mate to Scrip Nappe between. The geometry and distribution of rock units in the vicinity of the anticline in the north part of Domain 2 fit this model. Identification of this feature is essential in order to delineate the extent of Scrip Nappe. Mapping to date places the possible F_1 synclinal axial surface trace in a valley. Tree cover does not provide adequate exposure of rock units to identify possible symmetry in the stratigraphic sequence or minor structures which would identify the F1 synclinal axial surface trace.

3. If the above geometry of an F_1 synclinal mate to Scrip Nappe is correct, and its axial surface trace lies in the Upper Clastic rocks of the Horsethief Creek Group, then there appears to be a room problem for younger Upper Proterozoic and Lower Paleozoic rocks of the miogeocline. That is, they are not involved in Scrip Nappe folding.

4. As one proceeds south from Scrip Nappe, F_2 axial planes have apparent dips which become more shallow to the south. This is likely a product of both heterogeneous simple shear of a thrust sheet with shear increasing towards the base (Sanderson, 1982; Ramsay and Huber, 1987), and arching of a thrust sheet during building of a domal structural culmination (Monashee Terrane) to the south.

FOLDING, AGES OF GRANITE AND REGIONAL METAMORPHISM

The age of Scrip Nappe and related F_1 structures is not known. West-vergent folds elsewhere in southern British Columbia are inferred to be Jurassic (Murphy, 1987) and possibly Paleozoic (Hoy, 1977). F_2 folds are thought to be ca. 100 Ma old peak-metamorphic folds. Evidence to support this is found to the northwest of the study area where F_2 folds are cut by 62.5 $\pm$ 0.2 Ma old leucogranite (Sevigny and Ghent, 1986; Sevigny et al., 1989); they fold 100 $\pm$ 1.0 Ma old granite which is inferred to have been emplaced in strata which was at amphibolite grade at this time (Sevigny et al., 1989; Sevigny and Simony, 1989); isograds are oblique to F_2 folds (Raeside, 1982); and Ls defined by inferred peak-metamorphic sillimanite is co-linear with F_2 fold axes (L_2). Since F_2 folds are truncated by the Monashee Décollement,

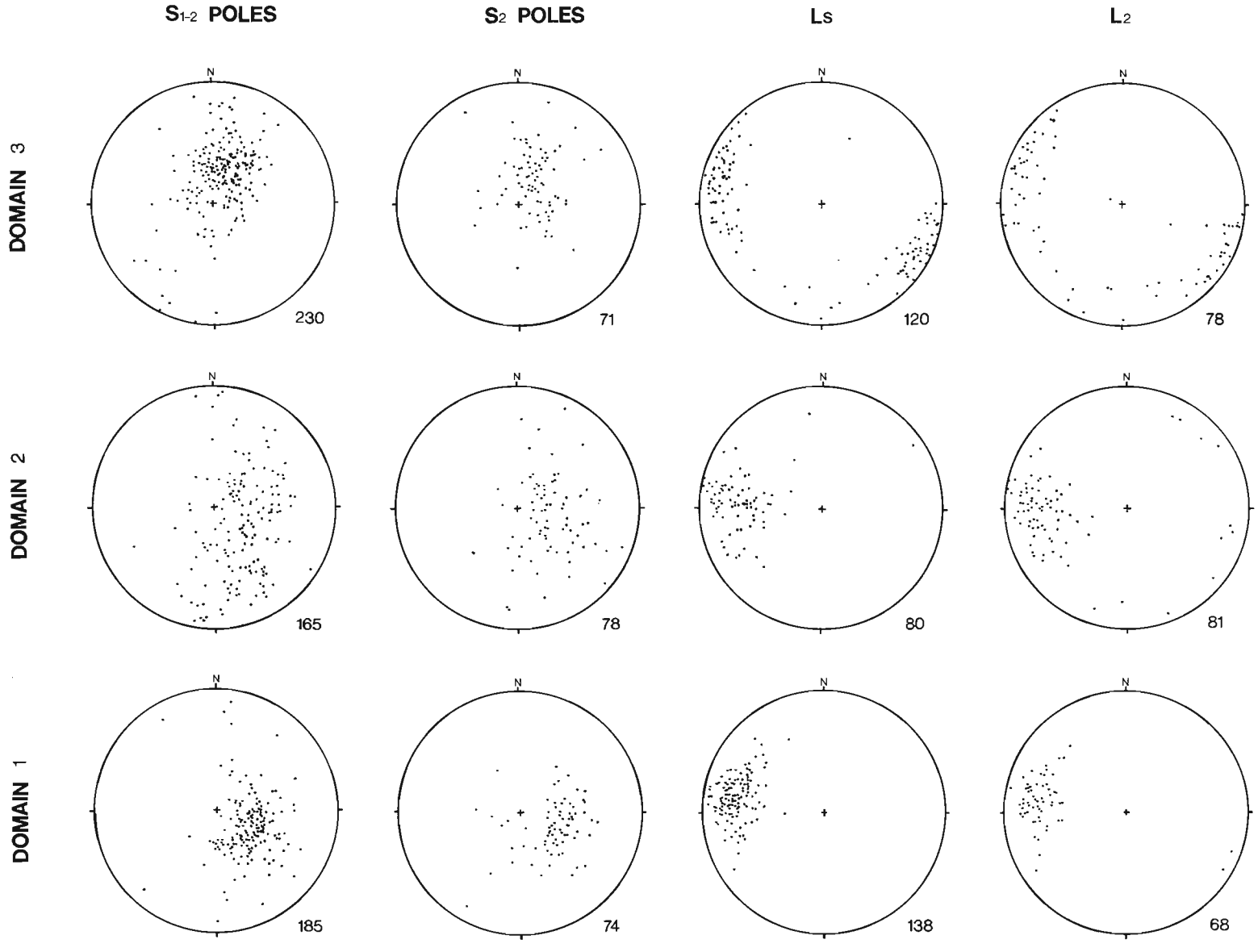

Figure 3. Lower hemisphere equal area stereonet compilation of planar and linear fabric element data. See Figure 2 for domain boundaries and the text for symbol definitions. Numbers in lower right corners are population sample sizes for each stereonet.

some motion on this structure must be younger than ca. 100 Ma. The age of F_3 folds is unknown, but they must postdate the metamorphic peak. Late down-to-the-west ductile faults cut the latest suite of granite in the study area. This granite may be correlative with the 62.5 $\pm$ 0.2 Ma suite to the northwest. U-Pb ages of 59 $\pm$ 1 Ma from metamorphic zircon in the Monashee Terrane (Parrish and Scammell, 1988) suggest that tectonic unroofing of this region occurred at this time.

CONCLUSIONS

Strata inferred to be part of the Horsethief Creek Group in the study area, comprise overall upright panels which dip west to northwest in the immediate hanging wall of the Monashee Décollement and southwest in the north part of the area. Strata in the south and central part of the map area are thought to form the upright limb of a large recumbent F_1 syncline inferred to underlie Scrip Nappe. The hinge zone of Scrip Nappe may lie in the north part of the study area, south of the location proposed by Sevigny and Simony (1989). The first-order macroscopic structure is complicated by later (ca. 100 Ma) northerly-verging F_2 folds. The structure in the central part of the study area is masked by intrusion of leucogranite. A strong, regionally-developed foliation (S_{1+2}), defined by co-planar primary layering, schistosity and gneissic layering records four phases of folding at the mesoscopic scale. F_1 and F_2 syn-metamorphic folds are penetrative and coaxial with a well-developed mineral elongation lineation. F_3 and F_4 folds are recognized only locally.

The Monashee Décollement is marked by a zone of highly strained mylonitic rocks in excess of 1000 m in thickness. Shear sense indicators indicate upper-plate-to-the-east thrusting. Truncation of F_2 folds indicates 100 Ma or younger thrusting. Mylonitic fabrics in the southern part of the region indicate deformation at high metamorphic grade, and both upper-plate-to-the-east and -west displacements. They may be related to east-vergent thrust motion on the Monashee Décollement and coeval thinning of the thrust sheet. Locally developed discrete metre-scale, low-grade, unannealed shear zones exhibit shear-sense indicators which document down-to-the-west normal motion, and are most likely associated with Tertiary tectonic unroofing of the region. Widespread brittle deformation and narrow, discrete ductile shear zones play a minor role in the strain history.

ACKNOWLEDGMENTS

Financial support for operation of this project during the 1990 field season was provided by an NSERC operating grant, a 1990/1991 EMR Research Agreement and NSERC Matching Funds, and a 1990 LITHOPROBE Supporting Geoscience grant to J.M. Dixon of Queen's University, and an NSERC post-graduate scholarship to the author. Thanks are extended to J.M. Dixon for his comments, J.R. Drobe for excellent assistance during the 1990 field season, D.A. MacKean for drafting Figure 3, and J.M. Journeay for critically reading the manuscript. LITHOPROBE Contribution No. 204.

REFERENCES

Archibald, D.A., Glover, J.K., Price, R.A., Farrar, E., and Carmichael, D.M.
1983: Geochronology and tectonic implications of magmatism and metamorphism, southern Kootenay Arc and neighbouring regions, southeastern British Columbia. Part I: Jurassic to mid-Cretaceous; Canadian Journal of Earth Sciences, v. 20, p. 1891-1913.

Brown, R.L. and Journeay, J.M.
1987: Tectonic denudation of the Shuswap metamorphic terrane of southeastern British Columbia; Geology, v. 15, p. 142-146.

Brown, R.L. and Lane, L.S.
1988: Tectonic interpretation of west-vergent folds in the Selkirk Allochthon of the southern Cordillera; Canadian Journal of Earth Sciences, v. 25, p. 292-300.

Brown, R.L., Journeay, J.M., Lane, L.S., Murphy, D.C., and Rees, C.J.
1986: Obduction, backfolding and piggyback thrusting in the metamorphic hinterland of the Southeastern Canadian Cordillera; Journal of Structural Geology, v. 8, nos. 3/4, p. 255-268.

Carr, S.D.
1989: Implications of Early Eocene Ladybird granite in Thor-Odin-Pinnacles area, southern British Columbia; in Current Research, Part E, Geological Survey of Canada, Paper 89-1E, p. 69-77.

Carr, S.D. and Brown, R.L.
1989: Crustal structure and tectonic chronology near the LITHOPROBE line in the Thor/Odin-Pinnacles-Cherryville-Vernon area, southeastern British Columbia: a progress report; in LITHOPROBE Cordilleran Workshop 1989, p. 27-36.

Fyles, J.T.
1970: Jordan River area; British Columbia Department of Mines and Petroleum Resources, Bulletin 57, 64 p.

Hoy, T.
1977: Stratigraphy and structure of the Kootenay Arc in the Riondel area, southeastern British Columbia; Canadian Journal of Earth Sciences, v. 14, p. 2301-2315.

Johnson, B.J. and Brown, R.L.
1989: Preliminary analysis of crustal structure of the southern Omineca Belt along the Trans-Canada Highway, southeastern British Columbia; in LITHOPROBE Cordilleran Workshop 1989, p. 37-44.

Journeay, J.M.
1986: Stratigraphy, internal strain and thermo-tectonic evolution of northern Frenchman Cap dome: an exhumed duplex structure, Omineca Hinterland, S.E. Canadian Cordillera; unpublished Ph.D. thesis, Queen's University, Kingston, Ontario.

Journeay, J.M. and Brown, R.L.
1986: Major tectonic boundaries of the Omineca Belt in southern British Columbia: a progress report; in Current Research, Part A, Geological Survey of Canada, Paper 86-1A, p. 81-88.

Journeay, J.M. and Parrish, R.R.
1989: The Shuswap thrust: sole fault to a metamorphic-plutonic complex of Late Cretaceous-Early Tertiary age, southern Omineca Belt, B.C.; Geological Society of America, Abstracts with Programs, v. 21, no. 5, p. 99.

Lane, L.S., Ghent, E.D., Stout, M.Z., and Brown, R.L.
1989: P-T history and kinematics of the Monashee Décollement near Revelstoke, British Columbia; Canadian Journal of Earth Sciences, v. 26, p. 231-243.

Leatherbarrow, R.W.
1981: Metamorphism of pelitic rocks from the northern Selkirk Mountains, southeastern British Columbia; unpublished Ph.D. thesis, Carleton University, Ottawa, Ontario.

Murphy, D.C.
1987: Suprastructure infrastructure transition, east-central Cariboo Mountains, British Columbia: geometry, kinematics and tectonic implications; Journal of Structural Geology, v. 9, p. 13-19.

Okulitch, A.V.
1985: Paleozoic plutonism in southeastern British Columbia; Canadian Journal of Earth Sciences, v. 22, p. 1409-1424.

Parrish, R.R. and Scammell, R.J.
1988: The age of the Mount Copeland syenite gneiss and its metamorphic zircons, Monashee Complex, southeastern British Columbia; in Radiogenic Age and Isotopic Studies: report 2, Geological Survey of Canada, Paper 88-2, p. 21-28.

Parrish, R.R., Carr, S.D., and Parkinson, D.L.
1988: Eocene extensional tectonics and geochronology of the southern Omineca Belt, British Columbia and Washington; Tectonics, v. 7, p. 181-212.

Raeside, R.P.
1982: Structure, metamorphism and migmatization of the Scrip Range, Mica Creek, British Columbia; unpublished Ph.D. thesis, University of Calgary, Alberta, 204 p.

Raeside, R.P. and Simony, P.
1983: Stratigraphy and deformational history of the Scrip Nappe, Monashee Mountains, British Columbia; Canadian Journal of Earth Sciences, v. 20, p. 639-650.

Ramsay, J.G. and Huber, M.I.
1987: The Techniques of Modern Structural Geology, Volume 2: Folds and Fractures; Academic Press, London, 700 p.

Sanderson, D.J.
1982: Models of strain variation in nappes and thrust sheets: a review; Tectonophysics, v. 88, p. 201-233.

Scammell, R.J.
1986: Stratigraphy, structure and metamorphism of the north flank of the Monashee Complex, southeastern British Columbia: a record of Proterozoic extension and Phanerozoic crustal thickening; unpublished M.Sc. thesis, Carleton University, Ottawa, Ontario, 205 p.
1990: Preliminary results of stratigraphy, structure, and metamorphism in the southern Scrip and northern Seymour ranges, southern Omineca Belt, British Columbia; in Current Research, Part E, Geological Survey of Canada, Paper 90-1E, p. 97-106.

Scammell, R.J. and Dixon, J.M.
1989: Stratigraphy along the north flank of Frenchman Cap dome, southern Omineca Belt, British Columbia (82M/10,15); in Geological Fieldwork 1988, British Columbia Ministry of Energy, Mines and Petroleum Resources, Paper 1989-1, p. 55-60.
1990: Preliminary results of geological mapping within the Kootenay Terrane north of LITHOPROBE Transect Line 19, southern Omineca Belt, British Columbia; in LITHOPROBE Cordilleran Workshop March 3-4, 1990, p. 30-37.

Scammell, R.J. and Brown, R.L.
1990: Cover gneisses of the Monashee Terrane: a record of synsedimentary rifting in the North American Cordillera; Canadian Journal of Earth Sciences, v. 27, p. 712-726.

Sevigny, J.H. and Ghent, E.D.
1986: Metamorphism an the northern Adams River area, Northeastern Shuswap Complex, Monashee Mountains, British Columbia; in Current Research, Part B, Geological Survey of Canada, Paper 86-1B, p. 693-698.

Sevigny, J.H. and Simony, P.S.
1989: Geometric relationship between the Scrip Nappe and metamorphic isograds in the northern Adams River area, Monashee Mountains, British Columbia; Canadian Journal of Earth Sciences, v. 26, p. 606-610.

Sevigny, J.H., Parrish, R.R., and Ghent, E.D.
1989: Petrogenesis of peraluminous granites, Monashee Mountains, southeastern Canadian Cordillera; Journal of Petrology, v. 30, p. 557-581.

Thiessen, R.L. and Means, W.D.
1980: Classification of fold interference patterns: a reexamination; Journal of Structural Geology, v. 2, no. 3, p. 311-316.

Wheeler, J.O. and McFeely, P.
1987: Tectonic assemblage map of the Canadian Cordillera and adjacent parts of the United States of America; Geological Survey of Canada, Open File 1565.

The Teslin suture zone in northwest Teslin map area, Yukon

R.A. Stevens[1]
Cordilleran Division, Vancouver

Stevens, R.A., The Teslin suture zone in northwest Teslin map area, Yukon; in Current Research, Part A, Geological Survey of Canada, Paper 91-1A, p. 271-277, 1991.

Abstract

The geology of the study area can be divided into two categories. The first is Teslin suture zone map units and consists of graphitic phyllite, siliceous schist and quartzite, an intermediate plutonic unit, marble, greenstone, hornblende tonalite to quartz diorite and diorite. Rocks in this category display mylonitic fabrics and thus are considered to be older than, or coeval with, deformation in the suture zone. Rocks of the second category, lack foliation and thus are considered to postdate deformation in the suture zone. Teslin suture zone map units can be further subdivided based on the penetrativeness of strain. The first four rock types display almost continuous ductile deformation, whereas the remaining two are ductilely deformed in zones bordered by massive to weakly deformed rock. All ductilely deformed rocks show a variety of planar and linear fabrics, folds and rare kinematic indicators.

Résumé

La géologie de la région à l'étude a été divisée en deux catégories. La première est constituée des unités cartographiques de la zone de suture de Teslin et est composée de phyllite graphitique, de schiste siliceux et de quartzite, d'une unité plutonique intermédiaire, de marbre, de roches vertes, de tonalite à hornblende se transformant en diorite quartzitique et de diorite. Les roches de cette catégorie présentent une fabrique mylonitique et sont donc considérées plus anciennes que la déformation de la zone de suture ou du moins contemporaine à celle-ci. Les roches de la seconde catégorie ne présentent pas de foliation et sont donc considérées postérieures à la déformation de la zone de suture. Les unités cartographiques de la carte de la zone de suture de Teslin peuvent être davantage subdivisées en fonction de la pénétration de la déformation. Les quatre premiers types de roches présentent une déformation ductile presque continue tandis que les deux autres types ont été déformés de façon ductile dans des zones bordées de roches dont le degré de déformation varie d'énorme à faible. Toutes les roches déformées de façon ductile sont caractérisées par diverses fabriques planaires et linéaires, des plis et de rares indicateurs cinématiques.

[1] Department of Geology, University of Alberta, Edmonton, Alberta T6G 2E3

INTRODUCTION

This report presents the results of field mapping in part of the Teslin suture zone located in the northwest quarter of the Teslin map area (NTS 105C). During June and July of 1990, mapping at 1:50 000 scale was accomplished northwest of the Canol Road, east of Johnsons Crossing, to Slate Mountain at the northern limit of the Teslin map area (Fig. 1). This mapping forms part of the author's Ph.D. project to investigate the geological evolution of the Teslin suture zone and to contribute towards understanding the tectonic history of the southern Yukon-Tanana Terrane.

REGIONAL SETTING AND PREVIOUS WORK

The Yukon-Tanana Terrane (Kootenay terrane of Wheeler et al., 1988) is a metamorphic-plutonic assemblage exposed in southern Yukon and east-central Alaska. It rests structurally above and adjacent to autochthonous North American rocks on the east and is in fault contact with accreted oceanic and island arc terranes of the Intermontane Belt to the west (Tempelman-Kluit, 1979; Hansen, 1989; Mortensen, in press). Over most of its length its characteristic fabrics are relatively flat-lying, however in southern Yukon they become steeply dipping within a mélange of ductilely deformed rocks of the Teslin suture zone (Erdmer, 1985; Hansen, 1989). The Teslin suture zone was named by Tempelman-Kluit (1979) and extends from north of the Laberge map area (NTS 105E), into the northwest part of the Teslin map area (Fig. 2). Hansen (1989) defined the Teslin suture zone to be "The package of rocks comprising the 15-20 km wide steeply-dipping portion of the Yukon-Tanana Terrane in southern Yukon."

In the Laberge map area the Teslin suture zone has been the locus of several studies (Tempelman-Kluit, 1979, 1984; Erdmer, 1985; Hansen, 1989; Hansen et al., 1989). These demonstrate that the suture zone consists of three assemblages of ductilely deformed metamorphic rocks with L-S tectonite fabrics. Individual assemblages outcrop as discrete, lensoid belts, 3-4 km wide and 20-30 km long. They include mylonitic siliceous and calcareous metasedimentary rocks (Nisutlin Allochthon or Assemblage), mafic metasedimentary and metavolcanic rocks (Anvil Allochthon or Assemblage) and orthogneiss (Simpson Allochthon in Erdmer, 1985 and Tempelman-Kluit, 1979 or peraluminous orthogneiss assemblage in Hansen et al., 1989). The Nisutlin and Anvil allochthons are metamorphosed to greenschist and albite-epidote amphibolite facies and preserve pre-Late Jurassic metamorphic cooling ages (Hansen, 1990). Orthogneiss of the Simpson Allochthon or peraluminous orthogneiss assemblage preserve Devono-Mississippian crystallization ages with Jurassic to Early Cretaceous metamorphic cooling ages (Hansen, 1990).

Hansen (1989) divided the Teslin suture zone into two structural domains, "Based on the distribution of two well-defined but differently oriented stretching lineations." These structures record a complex history of deformation that involved extensional shear, thrust shear and strike-slip shear and are interpreted to result from terrane accretion during oblique plate convergence.

Reconnaissance geology of the Teslin map area was described by Mulligan (1963). In addition, the geology of the northwest part of the map area is described by Lees (1936). The Teslin map area is presently being remapped at 1:50 000 and 1:250 000 scale by S.P. Gordey of the Geological Survey of Canada.

TESLIN SUTURE ZONE MAP UNITS

The geology of the study area is shown in Figure 1. On the basis of fabric development rock units can be divided into two categories. Rocks in the first, described under the heading Teslin Suture Zone Map Units, consist of three metasedimentary and four meta-igneous units which display mylonitic textures and are therefore considered to be older than, or coeval with, deformation in the suture zone. Rocks in the second category, described under the heading Other Map Units, consist of one sedimentary and three igneous units that lack foliation and are therefore considered to postdate development of the Teslin suture zone.

Graphitic Phyllite Unit (OD_N?)

This unit includes fissile, rusty red to black, fine grained (<1 mm), pyritic, graphitic phyllite, as well as calcareous graphitic phyllite, siliceous graphitic phyllite and marble. The rock types outcrop on ridges east and west of Red Mountain Creek, along a ridge northwest of the confluence of Sidney and Iron creeks, and near Muskrat Lake. Pyrite occurs as fine grained, variably oriented to layer parallel crystals or as coarse grained (>5 mm), cubic to subcubic crystals with quartz pressure shadows and tails. Chlorite and minor micas occur on foliation surfaces. Marble bands 10-30 m wide are locally interlayered with the graphitic phyllite and larger bands several hundred metres wide are also found. Minor greenstone and muscovite-biotite-graphite bearing impure quartzite are associated with the unit.

Contact relations indicate that rocks of units PMtqd, Kqm and K_{RM} (see descriptions below) intrude the Graphitic Phyllite unit. Sharp, fabric parallel contacts with diorite of unit PMd and in a few places with unit PMtqd are the result of strain along the contact.

North of the study area rocks similar to this assemblage have been described within the Teslin suture zone and are interpreted to be part of the autochthonous Nasina Formation (Tempelman-Kluit, 1977, 1984) or part of the Nisutlin Allochthon (Erdmer, 1985). Rocks of the Nasina Formation are primarily graphitic siltstones (Tempelman-Kluit, 1984), whereas rocks of the Nisutlin Allochthon are primarily muscovite-quartz schists and other siliceous rocks that are interfoliated with minor graphitic phyllites, slates and quartzites (Erdmer, 1985). At present it appears that the Graphitic Phyllite unit in the Teslin map area is not part of Nisutlin Allochthon, because although siliceous rocks (unit PMs) possibly correlative with the Nisutlin Allochthon are found in the map area, they are spatially and lithologically distinct from the graphitic phyllite rocks. The Graphitic Phyllite unit is interpreted to be part of the autochthonous Ordovician-Devonian Nasina Formation which has been caught up in the deformation of, and incorporated into the Teslin suture zone.

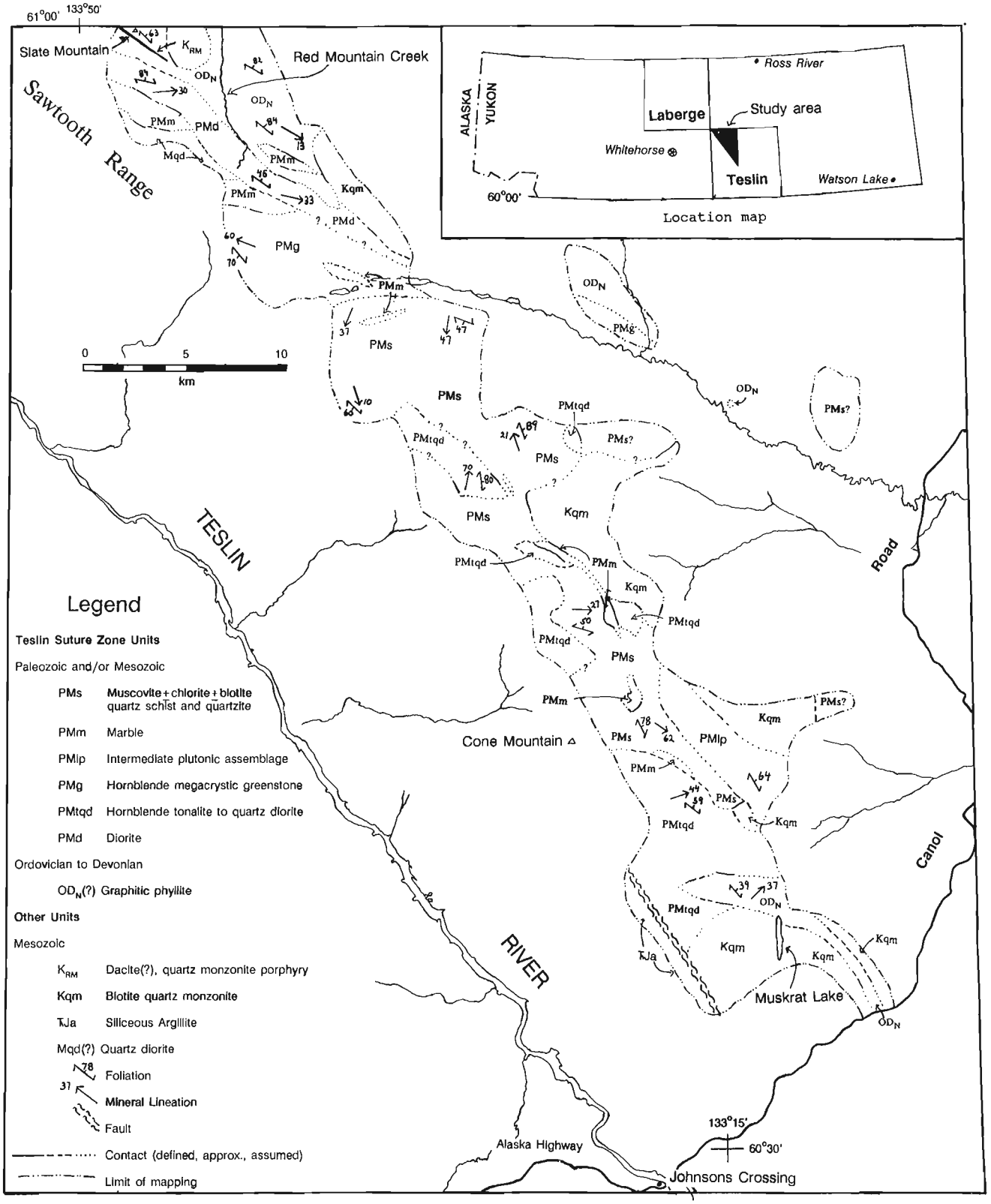

Figure 1. Location map and simplified geological map of the study area.

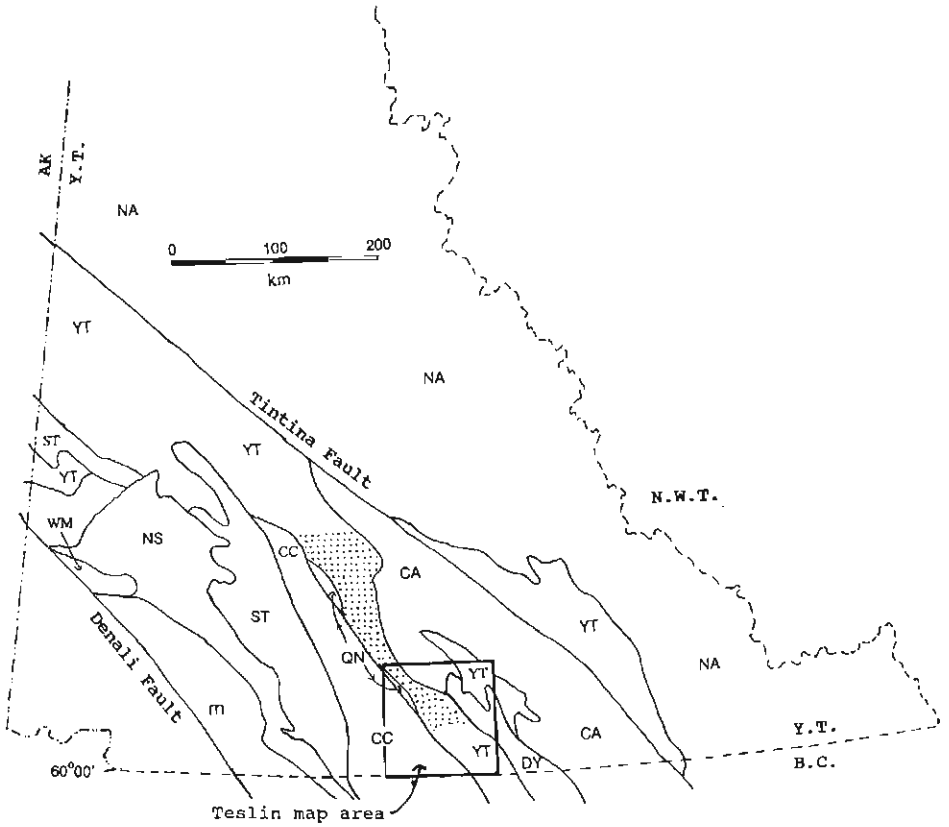

Figure 2. Generalized terrane map of Yukon between Tintina and Denali faults, including the part of the Yukon-Tanana Terrane east of Tintina Fault (modified from Wheeler and McFeely, 1987 and Hansen et al., 1989). The Teslin suture zone is shown in the stippled pattern. Terranes are: CA - Cassiar; CC - Cache Creek; DY - Dorsey; QN - Quesnellia; m - undivided metamorphics; NS - Nisling; ST - Stikinia; YT - Yukon Tanana; WM - Windy McKinley. NA represents ancestral North America.

Siliceous Schist and Quartzite Unit (PMs)

This unit outcrops as a broad band of mostly sheared siliceous schist and quartzite within the centre of the study area. The unit is lithologically heterogeneous, that is, even though end member rock types can be recognized each type shows considerable variability. In order of decreasing abundance, the prominent rock types are: mylonitic to blastomylonitic muscovite andor chlorite quartzite, muscovite-quartz schist to impure quartzite, muscovite-chlorite quartz schist to impure quartzite, chlorite schist, biotite-chlorite-pyrite-(muscovite?) schist to impure quartzite, marble, minor chloritic greenstone, possible felsic to mafic metaplutonic rocks and in one location a 5 m wide fragmental volcanic band. Schists and quartzites were seen to grade into each other commonly on the scale of metres to hundreds of metres. Slightly micaceous quartzite is the only consistently occurring rock type, although it is absent from the southern quarter of the study area. Quartz segregations are common in the schistose rocks. Marble is found both as small bands a few metres wide and as large units many hundred of metres wide. Greenstone and the possibly plutonic rocks occur as irregular bands and pods within the schist and quartzite. A band of manganese skarn 3 km northeast of Cone Mountain contains gem quality rhodonite (Marlin prospect; INAC, 1989 and references therein).

Colour and grain size vary considerably within the unit, the former ranges from medium grey-brown to silvery white to green. Grain size is primarily controlled by the intensity of shearing and ranges from microcrystalline in ultramylonites to medium grained (1-5 mm) in some schist and blastomylonite. After quartz, the major minerals are muscovite, chlorite, biotite, hornblende and pyrite. Minor feldspar is present in some rocks.

Plutonic rocks of units PMtqd and Kqm intrude the unit. Locally contacts of unit PMtqd with this unit show evidence of post-intrusive deformation and in other places, deformation has produced sharp fabric-parallel contacts and obscured any indication of an earlier intrusive contact. Rocks of units PMip grade into rocks of this unit over a diffuse, fabric parallel zone of high strain. Marble (PMm) is in conformable or possibly unconformable contact with the siliceous rocks in most places. One exception is the large marble band northeast of Cone Mountain which is at least partly in fault contact with siliceous schist. At the northern edge of this unit siliceous schist and quartzite grade into greenstones of unit PMg.

Rocks similar to those described above have been mapped in the Teslin suture zone north of the map area, and are included in Nisutlin Allochthon (Erdmer, 1985;

Tempelman-Kluit, 1984). Thus, this unit is interpreted to be part of Nisutlin Allochthon.

Marble (PMm)

Marble occurs as small 10-30 m wide bands within the stratigraphic succession of both the Graphitic Phyllite and Siliceous Schist and Quartzite units, and as mappable units several hundred metres thick located within the Graphitic Phyllite and Siliceous Schist and Quartzite units. The larger bands are mapped separately as unit PMm.

Most marble in unit PMm, consist of grey to buff and occasionally green, medium grained, sucrosic carbonate rock with 5-40 % interlayered white to colourless, 3-10 cm wide bands of fine grained quartz. In addition to carbonate and quartz, actinolite is a major component locally. Epidote, garnet and diopside were noted in a few locations. Marble south of the western edge of unit PMd has been intruded by fine grained mafic to intermediate dykes.

In the Teslin suture zone north of the map area marble was found in both the Nasina Formation and the Nisutlin Allochthon (Erdmer, 1985; Tempelman-Kluit, 1984). This correlates with marble found in the Graphitic Phyllite unit (interpreted to be part of Nasina Formation) and the Siliceous Schist and Quartzite unit (interpreted to be part of Nisutlin Allochthon).

Intermediate Plutonic Unit (PMip)

This unit outcrops east and south of the Siliceous Schist and Quartzite unit, and consists of rocks of plutonic parentage (possibly intermediate in composition), that are variably sheared and altered. Included in the unit are minor greenstone to amphibolite, fine grained rocks of unknown protolith and rare rocks of possible sedimentary origin. The typical rock type of the unit is grey to green and contains from 10-30 % medium grained megacrysts of quartz and feldspar (probably remnant igneous grains), surrounded by a fine grained matrix of chlorite, biotite, amphibole, quartz, and feldspar. Locally within small bands (<50 m thick) of weakly sheared rock, primary igneous textures can be seen. These bands are surrounded by generally fine grained, mylonitized rock of similar bulk composition, but lacking preservation of primary fabric.

The unit is in contact to the east with rocks of the Siliceous Schist and Quartzite unit. The two units appear to have undergone common deformation and the present contact is likely sheared.

It is unclear whether this unit correlates with plutonic rocks elsewhere in the Teslin suture zone or Yukon-Tanana Terrane. Its age is unknown, however it is older than or coeval with the deformation in the Teslin suture zone.

Greenstone (PMg)

A large band of greenstone outcrops to the southeast of the Sawtooth Range and is mapped as unit PMg. A number of smaller greenstone bodies (<100 m thick), most of which are included in the Graphitic Phyllite or Siliceous Schist and Quartzite units, occur in the northern half of the map area. The principal rock type is a massive, fine grained, medium to dark green mafic greenstone with 10-50 % megacrysts of medium- to coarse-grained hornblende. Other rock types in this unit include fine grained greenstone lacking hornblende megacrysts and medium grained hornblende amphibolite. Compositional layering is evident locally. In one location a 10-20 m wide band of coarse grained biotite and hornblende in a mafic matrix was found. Principal minerals of the mafic greenstone are hornblende, chlorite, epidote (as an alteration product), quartz and feldspar with accessory biotite and pyrite. Most of the unit has weak or no planar fabric; however, strong fabric is developed along the southwestern edge of the unit.

Along the northern edge of the unit carbonate rocks, similar to adjacent marble, were found as inclusions in the greenstone. This may indicate minimal dislocation along a possible original intrusive or flow contact.

In the Teslin suture zone north of the map area, greenstone, amphibolite, and other mafic and ultramafic rocks are included in the Anvil Allochthon (Erdmer, 1985; Tempelman-Kluit, 1984). It is unclear whether the rocks of this unit correlate directly with the Anvil Allochthon.

Hornblende Tonalite and Quartz Diorite (PMtqd)

This unit outcrops as a number of bodies scattered throughout the southern half of the study area. The principle rock type is blocky weathering, massive to mylonitic, grey-green medium grained hornblende tonalite to quartz diorite. In some places hornblendite and leucocratic quartz rich felsic plutonics are present. Rocks of this unit displays greater homogeneity and a lower degree of penetrative strain than rocks in unit PMip.

Several late mafic dykes cut the unit. The major minerals are feldspar, quartz (10-30 %), hornblende (10-40 %) and chlorite with accessory biotite and pyrite.

Contact metamorphism and inclusion of country rock indicates rocks of unit PMtqd intrude rocks of units OD_N and PMs. Locally intrusive relations are obscured or eliminated by deformation.

The age of this unit is unknown. However, hornblende-bearing metaplutonic rocks in the Yukon-Tanana Terrane are dominantly Devono-Mississippian or Late Triassic-Early Jurassic in age (Mortensen, in press).

In the Teslin suture zone north of the map area, hornblende-bearing plutonic rocks are included in the Simpson Allochthon (Erdmer, 1985). It is unclear if rocks of this unit are correlative with rocks of the Simpson Allochthon.

Diorite (PMd)

This unit outcrops as a northwest trending band located east of the Sawtooth Range. It comprises massive to mylonitic, green and white, coarse grained diorite cut by numerous mafic dykes. The diorite consists of 30-50 % hornblende, partly or wholly altered to chlorite and 50-70 % feldspar. The mafic dykes are dark green, fine grained and commonly well foliated. They constitute up to 5 % of the unit. At one location a small vein of serpentine asbestos was found.

Contacts relations are unclear at present but are likely structural and/or intrusive. Similarly, the age of the unit and its possible correlation with plutonic rocks elsewhere in the Teslin suture zone or Yukon-Tanana Terrane are uncertain.

OTHER MAP UNITS

Argillite (TRJa)

Along the southwestern edge of the map area, thinly laminated green to black fine grained siliceous argillite was found. The unit is bound on the east side by a brittle fault zone and on the west by the Teslin River valley. Rocks of this unit correlate with rocks of Mulligan's (1963) unit 9, which are shown to outcrop both east and west of the Teslin River valley and are thought to be Triassic and/or Jurassic in age.

Biotite Quartz Monzonite (Kqm)

A number of plutons of this unit are found in the map area. The rock is a blocky weathering, generally massive, leucocratic, medium grained equant to rarely porphyritic biotite quartz monzonite. This rock type occurs throughout the Teslin suture zone and Yukon-Tanana Terrane where it has been determined to be of mid-Cretaceous age (Tempelman-Kluit, 1984).

Red Mountain Complex (K_{RM})

Just east of Slate Mountain is a body of reddish-yellow to buff and brown, highly altered felsic rock. To the south and west of this body occurs a northwest trending, buff coloured, fine grained dyke. The protoliths of these rocks are unknown; however Brown and Kahlert (1986) called it the Red Mountain porphyry molybdenum deposit with the main body a quartz monzonite porphyry and the dyke a rhyolite porphyry. Mulligan (1963) refered to the main body as a dacite. Late Cretaceous K-Ar ages have been determined for the complex (Brown and Kahlert, 1986).

Quartz Diorite (Mqd?)

This unit outcrops near the northwestern part of the map area, in the Sawtooth Range. The unit is composed of fresh, massive, green and white, medium grained quartz diorite. Tonalite was found in one location, and coarse grained hornblendite to feldspar bearing hornblendite is present along the eastern contact. The rock is generally composed of 5-15 % quartz and 40-45 % each of feldspar and hornblende.

The rock may be part of unit PMtqd. However it appears to be fresher and more consistently massive than rocks of unit PMtqd and is thus separated here. It may also be a hornblendic phase of the Cretaceous rocks of unit Kqm.

STRUCTURAL GEOLOGY

Structurally, rock units of the Teslin suture zone (ie. those described under the heading Teslin Suture Zone Map Units), can be divided into two subsections based on the penetrativeness of strain. Rocks in the metasedimentary units OD_N and PMs and rocks of unit PMip show almost continuous ductile deformation. Marble (unit PMm) is included in this subsection although it has undergone extensive post-deformation recrystallization. The remaining units (PMg, PMtqd and PMd) show discontinuous ductile deformation. In these units massive to weakly deformed rock is bordered by zones of ductilely deformed rock 10 m to one or more kilometres in width. The structural fabrics described below are those found in the deformed rocks of all lithologies.

Planar fabrics

In the Graphitic Phyllite unit compositional layering, which likely represents transposed relict bedding, occurs in rocks east of Muskrat Lake, where marble and schistose rock interlayer with graphitic phyllite, and east of Red Mountain Creek, where graphitic rock grades into compositionally layered greenstone. In the Siliceous Schist and Quartzite unit, interlayering of quartzite and schist and compositional layering in some quartzites likely represent relict bedding. In marble, compositional variation and quartz interlayering may represent bedding. All apparent bedding planes are roughly parallel to the main orientation of metamorphic planar fabrics.

Metamorphic planar fabrics are prominent in the map area. They are: (1) strong schistosity defined by aligned chlorite and graphite in graphitic phyllite, micas and chlorite in schist and hornblende and chlorite in amphibolite and greenstone, (2) slaty cleavage in graphitic phyllite, (3) the parallel alignment of tabular quartz crystals and micas in quartzite, (4) a crenulation schistosity defined by micas in siliceous schist, (5) the parallel alignment of tabular quartz, feldspar, and hornblende crystals in plutonic rocks, and (6) the development of mylonitic fabric in all rock units, defined by elongate and/or stretched grains or aggregates of quartz, feldspar, hornblende and carbonate. Overall, planar fabrics strike northwest and dip steeply northeast. Local variations occur, particularly in the northern third of the siliceous schist and quartzite unit, where fabrics strike northwest but dip steeply to the southwest. In Laberge map area Teslin suture zone fabrics generally strike south to southeast and dip steeply west to northwest (Hansen, 1989).

Linear fabrics

Linear fabric elements are prominent in almost all the deformed rocks. They include: (1) crenulation hinges and fold axes, (2) mineral lineations defined by chlorite streaks in the graphitic rocks, alignment of quartz, mica, chlorite, hornblende, and carbonate minerals in siliceous metasedimentary rocks and of hornblende, feldspar, quartz, chlorite and biotite in plutonic rocks, (4) quartz pressure shadows around pyrite grains in graphitic rocks, and (5) boudinage structures.

Folds

Folding of compositional layering and metamorphic foliation are best developed in the graphitic phyllite and siliceous schist and quartzite units, and are rarer in marbles and plutonic rocks. Locally, folding is strongly developed in siliceous schists and calcareous graphitic phyllites. Crenulation folds, often located within larger folds, are the principal fold type. These folds are 1-10 mm in amplitude, rounded, symmetric and occur locally over wide areas of unit OD_N and PMs.

The majority of other folds are hand specimen to small outcrop scale, chevron to rounded folds with open to tight interlimb angles. Most are symmetric, but asymmetric folds were also found.

At present it appears that most of the folds observed are younger than or coeval with the deformation that produced the fabrics in schists and mylonites. This is evident by the general symmetric nature of the folds and the transposition of mylonitic and schistose fabrics into a crenulation schistosity. Folds transposed into the main planar fabric direction were found in a few locations.

Major faults

One brittle fault was found at the southwestern edge of the mapped area. It separates units Kqm and PMtqd from unit TRJa argillites. The fault is approximately 500 m wide and consists of cohesive and highly silicified bands and fragments of brittley and ductilely deformed rock derived from adjacent units and rock of unknown origin. Regional relationships indicate it is a major structural discontinuity, younger in age than Teslin suture zone deformation, that marks the boundary between the Yukon-Tanana Terrane to the east and poorly understood Mesozoic(?) volcanics and volcaniclastics to the west (see Gordey, 1991).

Kinematic indicators

Macroscopic kinematic indicators are rare in the study area. C-S fabric, asymmetric folds, tension fractures and rotated pyrite crystals occur locally. Future study will concentrate on delineating both macro- and microscopic movement indicators to understand the strain history within the suture zone.

ACKNOWLEDGMENTS

Field work was supported by a Natural Sciences and Engineering Research Council operating grant to P. Erdmer. Logistical support from the Department of Indian and Northern Development and helicopter support by the Geological Survey of Canada are gratefully acknowledged. P. Erdmer and S.P. Gordey are thanked for their visits in the field, for helpful and friendly discussions and for reviews of earlier versions of the manuscript. T. Harms is thanked for a careful review of the manuscript. Murray Rydman provided excellent assistance in the field.

REFERENCES

Brown, P. and Kahlert, B.
1986: Geology and mineralization of the Red Mountain porphyry molybdenum deposit south-central Yukon; in Mineral Deposits of the Northern Canadian Cordillera, J.A. Morin (ed.), Canadian Institute of Mining and Metallurgy, Special Volume 37, p. 288-297.

Erdmer, P.
1985: An examination of the cataclastic fabrics and structures of parts of Nisutlin, Anvil and Simpson allochthons, central Yukon: test of the arc-continent collision model; Journal of Structural Geology, v. 7, no. 1, p. 57-72.

Gordey, S.P.
1991: Teslin map area, a new geological mapping project in Southern Yukon; in Current Research, Part A, Geological Survey of Canada, Paper 91-1A.

Hansen, V.L.
1989: Structural and kinematic evolution of the Teslin suture zone, Yukon: record of an ancient transpressional margin; Journal of Structural Geology, v. 11, no. 6, p. 717-733.
1990: Yukon-Tanana Terrane: a partial acquittal; Geology, v. 18, p. 365-369.

Hansen, V.L., Mortensen, J.K., and Armstrong, R.L.
1989: U-Pb, Rb-Sr, and K-Ar isotopic constraints for ductile deformation and related metamorphism in the Teslin suture zone, Yukon-Tanana Terrane, south-central Yukon; Canadian Journal of Earth Science, v. 26, p. 2224-2235.

Indian and Northern Affairs Canada
1989: Yukon exploration 1988; Exploration and Geological Services Division, Yukon, Indian and Northern Affairs Canada, 304 p.

Lees, E.J.
1936: Geology of the Teslin-Quiet Lake area Yukon Territory; Geological Survey of Canada, Memoir 203.

Mortensen, J.K.
in press: Pre-Mid-Mesozoic tectonic evolution of the Yukon-Tanana Terrane, Yukon and Alaska; Tectonics.

Mulligan, R.
1963: Geology of the Teslin map area, Yukon Territory (105C); Geological Survey of Canada, Memoir 326.

Tempelman-Kluit, D.J.
1977: Quiet Lake (105F) and Finlayson Lake (105G) map areas, Yukon; Geological Survey of Canada, Open File 486.
1979: Transported cataclasite, ophiolite and granodiorite in Yukon: evidence of arc-continent collision; Geological Survey of Canada, Paper 79-14.
1984: Geology, Laberge (105E) and Carmacks (115I), Yukon Territory; Geological Survey of Canada, Open File 1101.

Wheeler, J.O. and McFeely, P.
1987: Tectonic assemblage map of the Canadian Cordillera and adjacent parts of the United States of America; Geological Survey of Canada, Open File 1565.

Wheeler, J.O., Brookfield, A.J., Gabrielse, H., Monger, J.W.H., Tipper, H.W., and Woodsworth, G.J.
1988: Terrane map of the Canadian Cordillera; Geological Survey of Canada, Open File 1894.

Handheld computer as a field notebook, and its integration with the Ontario Geological Survey's "FIELDLOG" program

L.C. Struik, A. Atrens[1], and A. Haynes
Cordilleran Division, Vancouver

Struik, L.C., Atrens, A., and Haynes, A., Hanheld computer as a field notebook, and its integration with the Ontario Geological Survey's "FIELDLOG" program; in Current Research, Part A, Geological Survey of Canada, Paper 91-1A, p. 279-284, 1991.

Abstract

The ASCII editor on the 0.5 kg Atari Portfolio handheld computer was used with some success as a field notebook. Drawings were made with pencil and paper. Systematized digital notes from the Atari Portfolio were loaded to database-readable files using several developmental-stage translation programs. Field data was then plotted using the Ontario Geological Survey FIELDLOG program that integrates its database with AutoCAD software. With this method digital data collected at the outcrop can be searched, plotted on maps, and statistically and graphically manipulated completely by computer on the same day it is collected.

Résumé

Le programme d'édition ASCII de l'ordinateur de poche Portfolio d'Atari de 0,5 kg a été utilisé avec un certain succès comme carnet de terrain. Des dessins ont été tracés sur papier avec un crayon. Les notes numériques systématisées ont été chargées sur fichiers exploitables sous forme de bases de données au moyen de plusieurs programmes expérimentaux de traduction. Les données de terrain ont ensuite été tracées à l'aide du programme FIELDLOG de la Commission géologique de l'Ontario qui intègre sa base de données au logiciel AutoCAD. Par cette méthode, les données numériques recueillies sur l'affleurement peuvent être explorées, tracées sur des cartes ainsi que statistiquement et graphiquement manipulées entièrement par ordinateur le jour même de leur collecte.

[1] Faculty of Education, Carleton University, Ottawa, Ontario K1S 5B6

INTRODUCTION

Geological maps can now be made on personal computers. Today's computers are fast enough, software programs are advanced enough, and plotters are detailed enough to take geological data from the researcher's office to the publication sales desk.

Geological data and reference searches can be made on personal computers. Computer aided database research gives more information in less time, and although it probably does not speed up research, it certainly assists with the use of an ever increasing amount of information.

Computer maps and databases can speed up and improve work once the data are in a computer; the trick is to get it there. Someone must type, digitize, or scan the data into the computer and that can take a lot of time. Here, we describe a method of taking geological notes on a computer, in the field, at the outcrop. Data entry on the computer while making the observations is the first and last time the data need be written and typed. Graphical data are still most efficiently collected manually. Hand drawings can be optically scanned in at base camp or at the office. This can be considered a temporary measure until the technology catches up.

We have made digital maps from the data typed in at the outcrop. Brodaric and Fyon (1988) have shown that digital maps can be made in the field. In this report, we describe in generalities the process of making such maps using compilation programs written by Atrens, and the Brodaric and Fyon (1988) FIELDLOG program.

Because we developed this process over the course of the summer and are still smoothing out the programs, the following description is a mixture of what we did this last summer and what we could do next summer.

OUTLINE OF THE DIGITAL NOTEBOOK METHOD

The Tools

To take computer notes at the outcrop we took with us a 0.5 kg XT palmtop computer (Atari Portfolio), one or two Atari Portfolio 128Kb RAM cards, a parallel interface for the Atari, an IBM compatible laptop, a portable printer (Kodak Diconex 150), power supplies for the laptop and printer, and a cable to connect the parallel interface and printer. To power these units we used AA batteries for the Atari, and the 12V power of the field pickup truck through a 12V to 110V converter. To complete the hardware system described here we would have also needed a small digitizing pad and its power supply. For software we used the built in features of the Atari, and the Atari file transfer program. The complete software system would also need the data compiler program of Atrens, a database program, an ASCII text editor, FIELDLOG, and AutoCAD. Other geological data manipulation programs could be used, such as a stereonet plotter.

The Atari Portfolio (Fig. 1) has 128Kb of internal memory (upto 80Kb of which can be used as a RAM drive) and removable RAM cards of up to 128Kb each. It runs on 3 "AA" batteries for 1 to 3 weeks depending on how its used, and has a 4 x 11 cm LCD screen. It's miniaturized keyboard layout resembles that of most laptop computers.

The Method

We set up an unambiguous note taking format, and used the Atari's ASCII editor to type in notes. On traverse, each station was entered as a file, named with the station number. The files were saved on the RAM drive and RAM card of the Atari. We carried the computer wrapped in a plastic zipper locking bag, stored in padded pouches in our back packs. The only field problem with the Atari computer was when we forgot to carry extra batteries. Loose leaf paper was used for outcrop sketches and backup in case the computer failed.

The Atari was used throughout the season, in good weather and bad. Care was taken to keep it away from dust, and out of the rain. On rainy days it was kept inside a large plastic zipper locking bag. The keys could be easily pressed through the plastic bag, and the screen was clearly visible. It was necessary to reach in the bag to open and close the computer. With the plastic bag the computer was more convenient in the rain than a paper notebook.

In the evening the station notes were edited visually, amalgamated into files of 10 stations and downloaded onto the hard and floppy disks of the basecamp laptop computer. Notes for the individual stations were printed on the same sheet paper used for that station's field sketches. In this way there was a complete set of written notes of a conventional format, both for safe keeping in case of electronic failure and for reference.

During the course of the summer Atrens wrote a compiler-editor program that reads the notes, and determines whether they are in the proper format. It interactively assists with the editing until the notes fit the prescribed format (using an ASCII text editor as a companion). Once the notes have the proper syntax the program compiles them into a table of database field labels and associated data. From there, several programs bring that table or parts of that table into a database program (in this case dBASE 4 and FIELDLOG). These subroutines are amalgamated into one program so that the database loading is done in one step.

Once in FIELDLOG the data can be plotted to AutoCAD drawings, this includes structural data, location of specific rock, mineral, fossil, or bedding types, or the location of sketches or photographs. For example you could locate all the sillimanite localities, or all the occurrences of finely crystalline granite, or plot all the mineral lineations. These plots can be made in the field, directly from the digital field notes.

DETAILS OF THE NOTE FORMAT

The style of the notes is meant to mimic the order and layout of handwritten notes (Fig. 1). It has some highly structured components, and some more freely structured ones. A simple text file on an ASCII editor was chosen because it was thought to have the most flexibility in organization.

In our case, the records (one for each station number) had a variable number of fields as opposed to a spreadsheet or database table which have a fixed number of fields. This facilitated data entry so that the fields could be written in a compact way with the minimum of typing. If a spreadsheet table had been used, there would have been a lot of null entries to be made or skipped over and recursive fields such as rocks

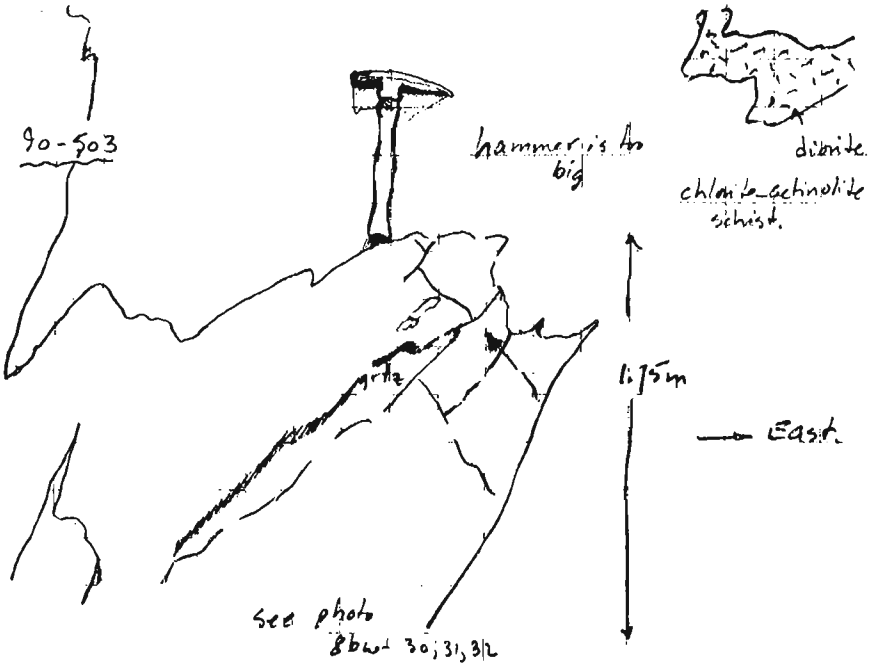


```
90+503
E473580
N6110675
1470
!to here have flattened diorite and
actinolite_schist;
o/c
!sos;
#
quartzite
white, lite_grey;
-qtz mm0.3-0.5;
...
BEDG cm40-80;
!thickness of the quartzite bed.  The
schist (metatuff?) is thicker on either
side, and is intruded by diorite;
..
@90-503 quartzite;
F1 340/09;
S1 162/50w;
diag;
PIC Bbw-30,31,32 !of anticline of
quartzite and schist.  Looking to the
northwest with hammer at the top, pick
point to the east.;
```

Figure 1. A sample set of field notes as typed onto the Atari Portfolio editor.

within rocks (conglomerate descriptions) would have been impossible to make. Also, all of the quantitative data are interpreted by the compilation programs as being in individual fields ready for analysis in the final data base. This quantitative data could be fixed character field data as well as numeric field data, eg. rock colour or mineral type. The rest of the qualitative (memo text) field data appears as comment fields.

Layout of the Field Notes on the Editor

The following is a sample station input. The order of the first five lines is fixed.

90-001	Station number.
E499800	Easting (UTM).
N6101900	Northing (UTM).
1200	Elevation in metres.
o/c	Nature of material. o/c = outcrop. Other examples; no/c = nearly outcrop, float, erratic, unconsolidated)
#	Denotes rock description.
limestone	Rock name.
grey, light_grey;	Fresh colour, weathered colour. The underline joins words to ease computer recognition.
-calcite mm0.05-1 %95-100;	Optional: mineral in the rock preceded by a dash and followed by its size and % range, if known. Units and % symbol precede the value. Any other characteristics of the mineral can follow immediately on that line with a comment. The line must end in a semicolon to end the mineral field.
!some breccia;	Optional: comment about the rock or anything else that does not fit in one of the defined categories begins with an ! and ends with a ; .
..	Two periods end the rock description, and other descriptions that have groups of items.
#	
vein	
white, white;	
!mm3-10 wide;	Veins are described as rocks.
-calcite mm5-20;	
..	
#	
lamprophyre	
dark, dark;	
!dyke cm50 wide;	
..	
#	
conglomerate	Here is a conglomerate description which consists of nested rock descriptions for the clasts. Each clast's description starts with a #.
grey, grey;	
-clasts cm0.4-2 %30 !matrix supported. subrounded, oblate.;	
#chert	This is the first clast of the conglomerate.
lite_grey, lite_grey;	
!laminated;	
..	
#qtz	This is the second clast of the conglomerate.
smokey, smokey;	
..	
!clasts form lenses in finer matrix.;	A comment on the conglomerate.
..	End of the conglomerate description.
S0 100/40s;	Bedding. Comments can follow the structural measurement, before the ; .
S0 100/45s !upright;	
S1 110/50s;	First cleavage, foliation, schistosity.
S2 100/20n crenulation !spaced mm1-2;	Subsequent cleavages follow in numeric order. Optional word descriptor used as a search variable comes before the comment.
L1 290/05 stretch;	Lineation measurement follows same scheme as S surfaces.
F1 290/05 !open folds, asymmetric to the west, see diagram;	Fold axes numbered in chronological order with comments like those of other structural measurements.
B1 010/20;	Boudin axis.
FT 190/40w extension;	Fault.
SLKS 190/00 sinistral;	Slickenside.
J1 040/40e;	Joints.
DYKE 100/89s lamprophyre;	Dyke orientation.
BEDG cm0.5-30;	Descriptions under the general tag BEDG are for all bedding characteristics. Description ends in double period.
-graded;	Bedding features are treated like minerals under the rock description.
-xbed_trough cm5 !height;	
-flames;	
-loads; !even and regular;	
..	
@90-001 limestone !for conodonts;	Samples are prefixed with @ and are followed by the rock type, and a comment on why the sample was taken. Ends with a ; .

FOSSIL -Archeocyathid mm10-20 %2 !poorly preserved and mostly dolomitized;	Tag for fossils. Fossil names and characteristics written like the mineral description under the rock tag.
-trilobite cm5 %3 !broken hash; ..	Ends in double period.
PIC 1bw-4,5,6 !of the archeocyathids;	A photograph is tagged with PIC, then the roll number, the type (either black and white -bw-, or colour -c-) then a dash followed by the frame numbers separated by commas. A standard comment for the description of the items photographed.

The format chosen reflects the reconnaissance nature of the mapping it was used for. It does not have fields for variables that other types of geological investigations would record. The note compilation program is structured to allow the construction of other note formats to fit the needs of individual projects and geologists.

In present form the notes are somewhat adaptable as the variables themselves are not understood by the compiler, they are just recorded. For example, the size range of the minerals could be substituted with the metreage along a drill core. It is the headings to the columns of the database file that assign meaning to the variables, not the variables themselves.

DISCUSSION

This system to record digital data at the outcrop and follow it through to a data management program can yield positive results in research, archiving and publication of geological information. However it also changes the style of geological investigation and the way your time is used. For the low budget geologist it is out of sight; not only because of the initial hardware and software costs, but also because of the higher field camp setup costs. For the academic geologist it may be too stifling. Yet for those who can work their way through some of the negatives, the positive aspects may well be sufficient reward.

Negatives

It is slow

It is slow enough to make you think you have missed the all important outcrop because of it. It is slow not only on the outcrop but also adds time at camp due to the editing and printing necessary for final copy.

By using the Atari Portfolio at the outcrop, to take advantage of its long battery life and lightness, we sacrificed some speed. The undersized keyboard forces people to hunt and peck with 2 to 4 digits. The keys have little depth response and only react on their upper side, so if they are not hit just right the character is missed. This adds outcrop and camp editing time.

It is slow because it requires two notebooks, the electronic one for the words and the paper one for the drawings. This means putting aside the computer in a safe place and getting out the pad of paper and pencil to draw a quartz vein, only to decide that you should write a quick note on the quartz crystal texture while still thinking of it, putting aside the paper, retrieving the computer, writing the note, and then returning to the paper and the sketch, on which you draw a few lines, and decide that you should make a note of the vein attitude before you forget, etc...

It is Geologically Degrading

The simple editor structure described here, like most computer routines, forced us to fit into a rigid to semirigid format. Formats in general appear to railroad thoughts into routine patterns. It takes an extra effort to break out of the routine, and to open the mind to new concepts. There is no longer a free flow of ideas from a free format.

It is a Thief

It steals time that could be better used looking at the map and thinking about the geological relationships. I hope that when the system, or one like it, is fully operational that the FIELDLOG generated maps will be an aid to the geological compilation and thought, but will there be enough time to benefit from it, unless it rains half the time in the field. It steals time because you have got to learn the Atari system, the dBASE integration system, FIELDLOG, dBASE, and AutoCAD. And this assumes familiarity with DOS as a computer operating system and all the other computer related techniques. The learning curve is at times ominous for someone who wants to make a geological map and not be a computer technician.

It is Intimidating

This is a real problem for summer assistants who like anyone else learned pencil and paper note taking techniques and now have to learn this new method with its rigid codes for maybe just one summer. Each summer the coding and related computer techniques have to be taught anew to a curious, but probably frustrated audience.

Positives

Research Power

With data on a computer in the field you can quickly plot locations of any variable. For people with perfect memories that is no advantage, but for the rest of us it is a powerful tool. If you would like to get a feeling for the trend of stretching lineations a map and a stereonet plot can be made in a few minutes. What is the distribution of epidote-quartz veins? The map could be made in the hour before your boss flies in.

Archival Power

Records of fossil locations and types can be retrieved almost instantly. All the sample sites can be plotted in minutes. Photographs files can be in personalized formats, with a map

of their locations. With a little adaption a complete drill log could be on file while you log the core. New data collected in the laboratory or from other workers can be added to the system database to give complete records of all the earth science data available for the area of interest.

Cartographic Power

The map you draw in the field is the map you could send to the publisher. You might want to think about the geology a bit longer, but then the map is there ready to be edited and replotted whenever a new concept or data come in. These maps can go directly to the professional computer cartographer for cleanup, embellishment, colour and publication. In theory they can be reformatted into different projections without redrafting.

Although the procedure we have described is designed for surface mapping, it could be adapted to cross-sections to aid the drafting of drill hole and ore body sections.

ACKNOWLEDGMENTS

This is the first report of a pilot program at the Cordilleran Division to enhance digital data manipulation from outcrop to published map. Other members of the division involved in this program include: Steve Gordey, Murray Journeay, Jim Roddick, Dirk Tempelman-Kluit and Glen Woodsworth. Bruce Northcote, as my field assistant in 1990, also used the Atari Portfolio as his notebook and his comments on the pros and cons of the system were useful in its evaluation. Don MacIntyre of the British Columbia Geological Survey Branch shared his field experience with the Atari Portfolio, and his techniques for data input and recovery.

REFERENCES

Brodaric, B. and Fyon, J.A.

1989: OGS FIELDLOG: A microcomputer-based methodology to store, process and display map-related data; Ontario Geological Survey, Open File Report 5709, 73 p. and 1 magnetic diskette.

Pine Pass map area, southwest of the Northern Rocky Mountain Trench, British Columbia

L.C. Struik and B.K. Northcote[1]
Cordilleran Division, Vancouver

Struik, L.C. and Northcote, B.K., Pine Pass map area, southwest of the Northern Rocky Mountain Trench, British Columbia; in Current Research, Part A, Geological Survey of Canada, Paper 91-1A, p. 285-291, 1991.

Abstract

The southwest part of the Pine Pass map area is underlain by mainly Mesozoic and Tertiary amphibolite facies metamorphic rocks of the Wolverine Complex; Precambrian(?) siltite, and quartzite; Cambrian(?) to upper Paleozoic(?) quartzite, limestone, siltite, argillite, grit, fragmental basalt, diorite and minor conglomerate and dacitic tuff, and their possible metamorphic equivalents; and Triassic and Jurassic fragmental basalt and greywacke of the Takla Group. Upper Paleozoic(?) fragmental basalt and diorite may represent an eastern equivalent of the Slide Mountain Group. Precambrian and lower Paleozoic siltstone, quartzite, limestone and dolostone like that in the Rocky Mountains northeast of the Trench underlies a strip west of Williston Lake and east of the McLeod Lake Fault. Southwest of the Trench rocks have been displaced along numerous strike-slip and extension faults and possibly along some thrust faults.

Résumé

La partie sud-ouest de la région de la carte Pine Pass repose principalement sur les roches métamorphiques mésozoïques et tertiaires du faciès des amphiboles du complexe de Wolverine; siltstone et quartzite du Précambrien (?); quartzite, calcaire, siltstone, argillite, grès grossiers, basalte détritique, diorite et quantités mineures de conglomérat et de tuf dacitique ainsi que leurs équivalents métamorphisés possibles du Cambrien (?) au Paléozoïque supérieur (?); et basalte détritique ainsi que grauwacke du Trias et du Jurassique du groupe de Takla. Le basalte détritique et la diorite du Paléozoïque supérieur (?) peuvent constituer un équivalent oriental du groupe de Slide Mountain. Le siltstone, la quartzite, le calcaire et la dolomie détritique du Précambrien et du Paléozoïque inférieur, tout comme ceux des montagnes Rocheuses au nord-est du sillon des Rocheuses, reposent sous une bande à l'ouest du lac Williston et à l'est de la faille Mcleod Lake. Au sud-ouest du sillon, les roches ont été déplacées le long de nombreux décrochements et de nombreuses failles d'extension ainsi que peut-être le long de certaines failles chevauchantes.

[1] Department of Geological Sciences, University of British Columbia, 6339 Stores Road, Vancouver, B.C. V6T 2B4

INTRODUCTION

The southwestern part of the Pine Pass map area borders the western side of the Northern Rocky Mountain Trench along southern Williston Lake (Fig. 1). Bedrock is poorly exposed except along a few high ridges. The broad low valley in the southwestern corner of the area is underlain by an extensive sheet of Pleistocene glaciofluvial gravel and glaciolacustrine silt. Much of the area can be accessed by forest service roads from Highway 97 at Parsnip River, from Mackenzie by barge, or from the Omineca highway north of Fort St. James.

Rocks in the southwest part of the Pine Pass map area are separated from the those in the Rocky Mountains by the dextral strike-slip McLeod Lake and Northern Rocky Mountain Trench faults, which approximately coincide with the position and orientation of the Rocky Mountain Trench. From the Rockies across the McLeod Lake Fault geological changes are extreme. In the Rockies the metamorphic grade is subgreenschist grade, whereas to the west metasedimentary rocks attain migmatitic sillimanite grade. The Paleozoic carbonate platform disappears and is replaced by basinal argillite, siltite, conglomerate, fragmental basalt, diorite plutons, and minor limestone. Of the dominant structures, fold and thrust geometry is replaced to the southwest by dextral strike-slip and extension faults. Absent from the Rockies are the Triassic-Jurassic island-arc basalts and extensive Cretaceous and Tertiary plutons.

This preliminary report covers the first summer of a reconnaissance program to re-evaluate the geology in Pine Pass map area southwest of the Trench. Large tracts of the area have yet to be mapped, leaving the following geological relationships and speculations somewhat tenuous.

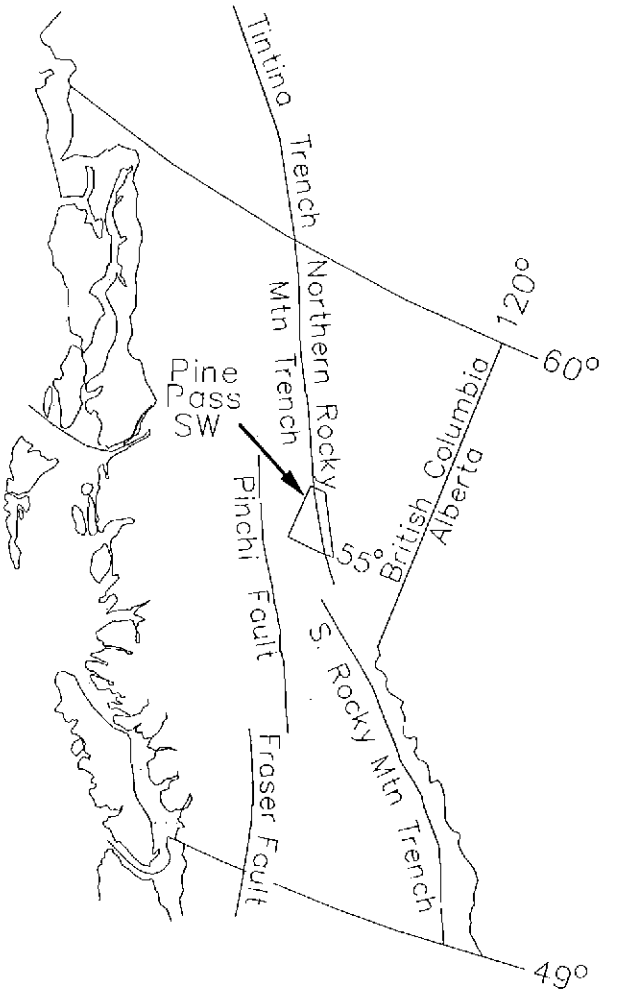

Figure 1. Location of Pine Pass southwest map area in British Columbia.

EAST OF MCLEOD LAKE FAULT

Precambrian and Paleozoic sedimentary and carbonate rocks underlie the area between the Rocky Mountain Trench and the McLeod Lake Fault (Fig. 2). They resemble rocks in the Rocky Mountains to the east and do not occur west of the McLeod Lake Fault. The sequence consists of Upper Precambrian or Lower Cambrian quartzite, siltite and slate; Lower Cambrian limestone, dolostone, quartzite, siltite, and slate; Cambrian limestone and phyllite; and Upper Cambrian or Ordovician limestone.

Upper Precambrian or Lower Cambrian

The lowest part of the sequence is exposed on the eastern slopes of Mount Chingee and forms the upright to overturned limb of a regional west verging fold. Lowest parts of the exposed sequence consist of several bundles of coarse grained, white and light grey quartzite (10-20 m) beds in mainly thin bedded, olive grey and grey slate and fine grained quartzite. The finest grained beds are graded, and some of the coarser grained quartzite is crossbedded. Toward the top of the sequence the finer grained rocks predominate, and within the top 150 m the siltite and slate are green and dark green. In contrast, southwest of Mount Chingee, the top of the sequence consists of coarse grained green and white quartzite (~40 m thick).

Lower Cambrian

Archeocyathid-bearing limestone and associated dolostone directly overlies the slate and siltite at Mount Chingee and coarse grained white and green quartzite southwest of Mount Chingee. The sequence consists of two carbonate bands separated and overlain by quartzite, siltite and slate units.

The limestone is mostly grey and weathers light grey, and has irregular patches and lenses (0.5-3 cm thick) of buff weathering dolomite. Oolitic sequences are found northwest and southwest of Mount Chingee. *Archeocyathid*-bearing limestone overlies the oolitic sequences at both places. *Archeocyathids* are most abundant and best preserved in the upper band of limestone.

The dolostone unit is confined to the Mount Chingee ridge. It is a buff and dull orange weathering, light grey rock of finely crystalline dolomite. It is featureless and massive, although it contains local sets of fracture cleavage. At one locality, along the logging road near Highway 97 it contains a possible, poorly preserved *Archeocyathid*. The dolostone unit is along strike to the northwest of *Archeocyathid*-bearing limestone in the McLeod Lake map area.

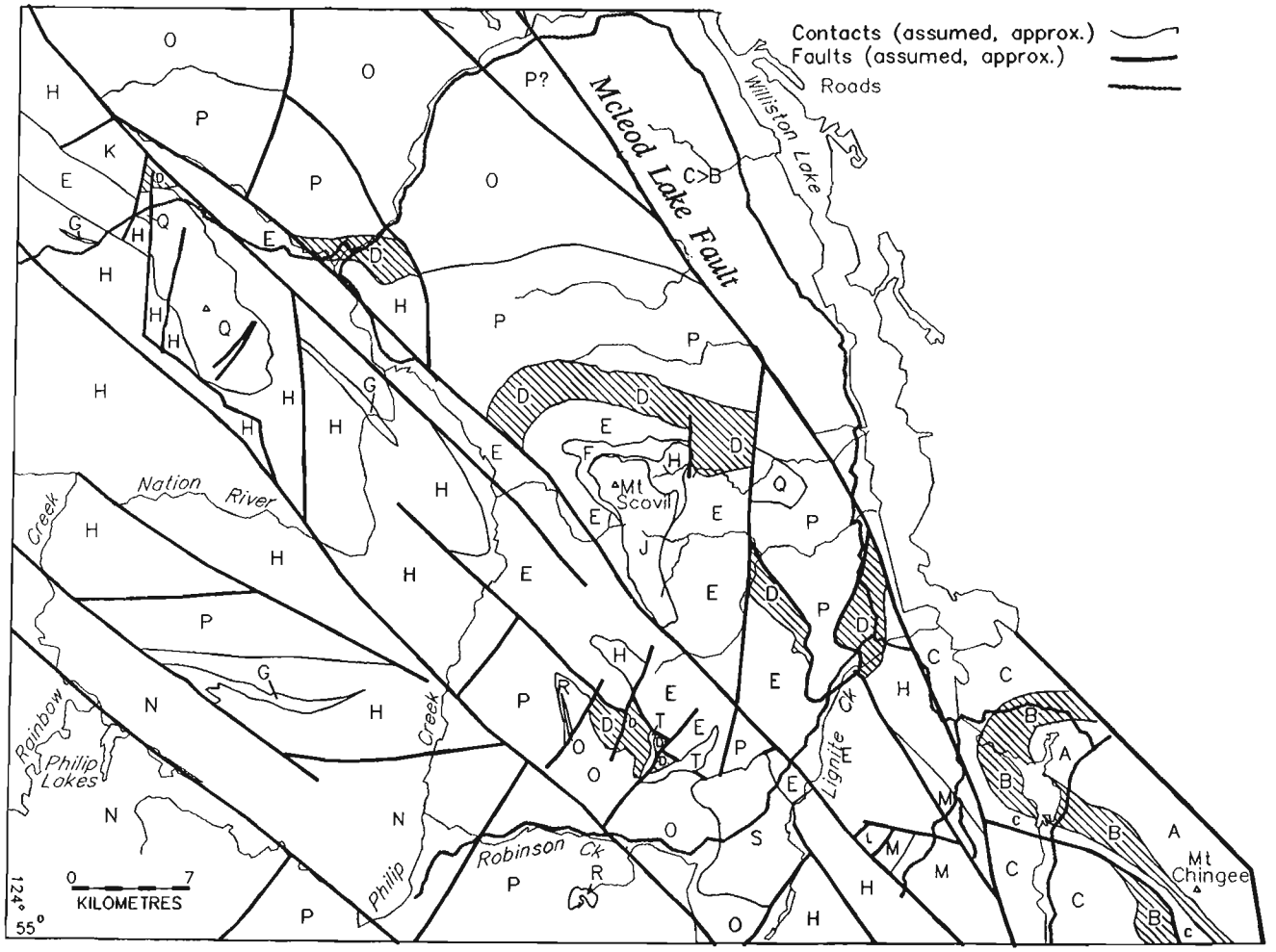

WEST OF MCLEOD LAKE FAULT

TERTIARY

T biotite granite

Lignite Granite

S biotite granite

CRETACEOUS AND TERTIARY

Wolverine Metamorphic Complex

R granite pegmatite

Q foliated granodiorite

P quartzofeldspathic gneiss, schist, granite pegmatite

O amphibolite, calcsilicate, marble, paragneiss, schist

TRIASSIC AND LOWER JURASSIC

Takla Gp

N fragmental augite porphyry basalt, limestone

M phyllite, greywacke, limestone

UPPER PALEOZOIC OR TRIASSIC

L pyroxenite

CARBONIFEROUS OR PERMIAN

K diorite

J Scovil Diorite

CARBONIFEROUS AND PERMIAN

Philip Ck succession

H diorite, fragmental basalt

G limestone

ORDOVICIAN(?) TO LOWER CARBONIFEROUS

Earn and (?) Road River Gps

F micaceous quartzite, tuff, phyllite, marble

E siltite, phyllite, conglomerate quartzite, limestone, basalt

LOWER CAMBRIAN

Atan Gp

D quartzite, limestone, marble

EAST OF MCLEOD LAKE FAULT

CAMBRIAN

Kechika Gp and Skoki Fm

C limestone, dolostone, phyllite

LOWER CAMBRIAN

Gog Gp

B quartzite, limestone, dolostone, slate, siltstone

PRECAMBRIAN

Misinchinka Gp

A quartzite, slate, siltstone conglomerate

Figure 2. Preliminary geology of Pine Pass southwest map area from this study and Muller (1961).

The clastic rocks consist of medium grained light grey quartzite interbedded with various grey and dark grey siltites and slates. The finer grained clastics are locally graded and the quartzite shows rare crossbeds.

Cambrian

Phyllite and limestone throughout the rest of the area are assumed to overlie the Lower Cambrian sequence and is similar to rocks that have yielded Late Cambrian fossils to the southeast in the McLeod Lake map area (Struik, 1989). The olive phyllite is calcareous and is found in one locality presumed to be in fault contact with the Lower Cambrian limestone. It is most like rocks of the Kechika Group to the northwest in the Cassiar Mountains (see descriptions by Gabrielse, 1963; and Cecile and Norford, 1979) and to the southeast in the McLeod Lake map area.

The phyllite is overlain by thinly interbedded grey limestone and buff-orange weathering dolostone, which in turn is gradational with overlying pisolitic limestone. To the southeast in the McLeod Lake map area the pisolitic limestone has yielded Ordovician conodonts. The thickness of these units is uncertain as there is no complete section exposed.

WEST OF THE MCLEOD LAKE FAULT

West of the McLeod Lake Fault the rocks consist of probable Cambrian limestone and quartzite; middle Paleozoic(?) fine grained, clastic rocks and minor basalt; upper Paleozoic(?) fragmental basalt, limestone and diorite, and Triassic and Lower Jurassic Takla Group all in structural contact with the Mesozoic and Tertiary granitic and metamorphic rocks of the Wolverine Complex.

Cambrian(?) limestone and quartzite (Atan Group?)

Limestone, limestone breccia, marble, quartzite and siltite underlie the area from Grayling Lake northwest along the McLeod Lake Fault to Tsedeka Creek, and at the Nation River. The quartzite and limestone resemble Lower Cambrian rocks to the northwest and southeast along the length of the Omineca Belt. These rocks may be the southward continuation of the Boya and Rosella formations of the Atan Group of the Cassiar Mountain assemblage to the northwest (Fritz, 1980; Ferri and Melville, 1990).

These rocks structurally overlie quartzofeldspathic gneiss and garnet-biotite schist of the Wolverine Metamorphic Complex, perhaps along a low angle extension fault. They are apparently overlain, perhaps structurally, by black clastics, fragmental basalt and minor limestone of middle and late Paleozoic(?) age.

Middle Paleozoic(?) clastic and volcanic rocks (Earn Group?)

Siliceous argillite, micaceous quartzite, tuff, conglomerate and minor basalt resemble rocks of the Devono-Mississippian Black Stuart and Snowshoe groups to the south in the Cariboo Lake region (Struik, 1988) and Earn Group rocks to the northwest (Ferri and Melville, 1990). They were mapped by Muller (1961) as Slide Mountain Group. To the northwest in the Manson Creek and Germansen Landing areas, Ferri and Melville (1988, 1989) included similar rocks in the Slide Mountain Group. This type of grouping follows the early definition of the Slide Mountain Group in the type area near Wells where the black clastic rocks of the Black Stuart Group were included with the structurally overlying basalt of the Antler Formation (Sutherland Brown, 1957; Struik, 1988).

The siliceous argillite and siltite are black to dark grey, thin to moderately bedded, and interbedded with lesser amounts of phyllite. They are fairly well exposed north of Mount Scovil where the ridge drops to the pass at the head of Tsedeka Creek. The interbedded phyllite is generally graphitic.

East of Mount Scovil calcareous basalt within the black clastic sequence resembles that of the Middle Devonian Waverly Formation near Cariboo Lake to the southeast (Struik, 1988).

Locally within the siltite-argillite succession are thin units of chert-pebble conglomerate. These conglomerates resemble those of the Earn Group to the northwest, and the Guyet Formation of the Black Stuart Group and the conglomerate of the Hardscrabble succession of the Snowshoe Group to the southeast (Struik, 1988).

The upper part of the siltite-argillite succession at Mount Scovil has a thin unit of olive micaceous quartzite of glassy grey quartz grains (50-80%) in a sericite-chlorite matrix. Quartz is poorly sorted ranging in size from silt to coarse sand. It is gradational to calcareous quartzite and locally includes beds of quartz pebble conglomerate. The quartzite occupies the upper part of the succession with the siltite and siliceous argillite. These rocks closely resemble some of the olive micaceous quartzite of the Ramos succession of the Snowshoe Group; particularly those rocks at Ramos Creek (Struik, 1988).

Upper Paleozoic rocks(?) (Philip Creek succession)

Included in this unit are basalt agglomerate and tuff, diorite, volcaniclastic rocks, limestone, and minor pyroxenite. The rocks were previously mapped as Slide Mountain Group within the Pine Pass map area (Muller, 1961), however the basalts do not resemble those of the type area near Wells, British Columbia. Neither the pillow basalt flows, ultramafic pods, nor radiolarian ribbon chert characteristic of the Slide Mountain Group to the south are found in the Pine Pass map area. Instead, basaltic rock, possibly of late Paleozoic age, is more like the agglomerate and tuff of the Takla Group. Although the fragmental texture of these two suites is similar the Paleozoic suite weathers dark grey and brown instead of the olive of the Takla Group, and it contains olivine whereas the Takla Group basalts do not. For discussion purposes these rocks will be called the Philip Creek succession, after Philip Creek which drains an area where the unit is best exposed. The Philip Creek succession is suspected to be of late Paleozoic age because its fragmental basalt and greywacke are interbedded with crinoidal limestone of possible Carboniferous age at two places along the Nation River and northeast of Philip Lakes.

The coarse grained basalt consists of augite porphyry breccia and agglomerate fragments in a pyroxene plagioclase sand. Generally the basalt is a tuff, locally in olive cherty sequences. Cherty tuff is common, can be either black or olive and forms units 1-15 m thick in lapilli tuff sequences. Beds of the cherty tuff are thin (0.5-4 cm) and mostly separated by films of phyllite or slate. The lapilli tuff beds can range from thin to thick with no particular relationship between the coarseness of the grain size and the thickness of the bedding. The fragmental basalt is intruded by diorite sills and dykes throughout the map area.

Volcaniclastic rocks consist of plagioclase-pyroxene greywacke and minor dark grey siltite, argillite, and conglomerate. They are gradational with rocks that have characteristics of pyroclastic debris flows. Bedding styles range from graded laminites to thick (1 m) beds stacked in bundles up to 10 m thick. Local synsedimentary slump features are rare.

Diorite, generally microporphyritic, intrudes both pyroclastic basalt and black siliceous argillite and micaceous quartzite. Locally, the rocks are foliated, such as parts of the Scovil diorite (Northcote, 1991), but mostly they appear undeformed. They consist of primary plagioclase (50-70 %), pyroxene and hornblende, and secondary hornblende, actinolite, epidote, chlorite and calcite.

The limestone is grey, weathers light grey and can have abundant poorly preserved macrofossils, most commonly large crinoid ossicles. North of Philip Lakes it is gradational with pyroxene-plagioclase sand and silt, where they are interbedded on a 2-5 cm scale. Generally the limestone is massive and featureless although this is probably due to later tectonism and recrystallization.

A small body of pyroxenite underlies a knoll west of McIntyre Lake. It has pods rich in magnetite and some of it has abundant pyrite.

Upper Paleozoic(?) diorite

Two large foliated diorite to gabbro sills, similar in composition and texture, intrude the Earn Group; one at Mount Scovil, the Scovil diorite (Fig. 2; Northcote, 1991) and the other to the northwest of Mount Scovil. The sills are interpreted to be of late Paleozoic age, because they intrude the Earn Group siltite-argillite sequence, and may be feeders to the Philip Creek succession basalt.

Takla Group

Rocks of the Takla Group are exposed in the southwest and possibly southeast parts of the map area and consist of olive weathering augite porphyry agglomerate, coarse lapilli tuff, and some greywacke and limestone. Augite porphyry fragmental basalts outcrop in the southwest.

Limestone and volcaniclastic greywacke southeast of Lignite Creek resembles the Takla Group sedimentary sequence directly to the south along the McLeod River in McLeod Lake map area. This greywacke and limestone is in a region where basalt of the Philip Creek succession is exposed and their unit assignment is uncertain.

Wolverine Metamorphic Complex

The metamorphic rocks of the Wolverine Complex generally are quartzofeldspathic gneiss, amphibolite, calcsilicate, granite pegmatite, and minor quartzite at sillimanite grade metamorphism. In some areas where the transition from low-grade to high grade may be transitional rather than a fault, amphibolite, grit, schist and marble have staurolite-kyanite assemblages. Foliated granodiorite and granite intrude and are deformed with the paragneisses.

Schist

Schist appears to be rare in the Wolverine Complex perhaps because it is recessive and the area is poorly exposed. Generally it consists of garnet, biotite, muscovite, feldspar and quartz. Locally, where it is decametres thick, it also contains sillimanite, and rarely, staurolite and kyanite.

Gneiss

Gneissic rocks of the Wolverine Complex generally are quartzofeldspathic leucocratic to somewhat biotitic. Garnet and sillimanite are locally present, and hornblende occurs in some places. Generally they are layered on the decametre scale and separated by leaves of biotite schist. They are commonly intruded by pegmatite and is granitized to pegmatite. Foliation is poorly expressed within the gneiss, however it commonly has an intense flattening and in many places a strong stretching fabric.

Amphibolite

Amphibolite units of the Wolverine Complex vary in composition and texture from finely crystalline to megablastic hornblendite to calcite marble. The various rocks have mixtures of garnet, quartz, biotite, calcite, hornblende and plagioclase. Where calcite forms a large part of the rock the hornblende forms knots of large felted crystals. In places the plagioclase, calcite, hornblende fabric is overprinted by porphyroblasts of hornblende. More finely crystalline hornblende generally defines a prominent lineation parallel with stretching and mullion fabrics. In places the amphibolite units contain interlayers of psammite, grit, gneiss and schist. Zoisite prisms are found in the amphibolite north of Robinson Creek.

Calcsilicate

Calcsilicate sequences consist of calcite, diopside, garnet, biotite, hornblende, and plagioclase in layers centimetres to decimetres thick. The thickest units are south of Mount Bisson and south of Robinson Creek.

TERTIARY INTRUSIONS

Biotite, potassium feldspar-megacrystic granite at Lignite Creek intrudes gneiss, schist and amphibolite of the Wolverine Metamorphic Complex, the Earn Group(?) siltite and phyllite, and the Philip Creek succession basalt. The granite is essentially undeformed although locally it has biotite segregations with aligned biotite, and along its eastern flank it has a finely spaced fracture cleavage where it is in contact with

Philip Creek succession basaltic tuff and argillite. To the south the contact between the granite and basalt is a brittle shear zone involving the granite.

Quartz feldspar porphyry dykes intrude Paleozoic black clastic rocks and the mylonitic shear zone between Paleozoic basalt and the Wolverine Complex amphibolite and orthogneiss at the head of Lignite Creek. Quartz and feldspar phenocrysts in the porphyry dykes are 2-5 mm across and occupy approximately 30% of the rock.

Diabase dykes of various textural maturity intrude the Wolverine Complex rocks throughout the area. Each of the dykes is undeformed and from 1-2 m thick. Where coarsest the diabase consists of hornblende, plagioclase and quartz phenocrysts. Locally it is amygdaloidal with zeolite fillings. Diabase dykes postdate regional shear as they cut mylonitic foliation of the gneiss and schist.

STRUCTURAL GEOLOGY

The region is transected by northwest and north-northwest trending dextral strike-slip faults and northeast and east-northeast trending extension faults. The geometry of the faults and their sense of motions appear to indicate the two fault sets are dynamically linked in an *en echelon* dextral strike-slip regime. The motion between the strike-slip faults is transferred through the extension faults as pull-aparts (Struik, 1989).

An example of this fault geometry is at upper Lignite Creek where Wolverine Complex orthogneiss and amphibolite are bound to the northeast by a dextral strike-slip fault and to the southeast by a shallowly southeast dipping extension fault, each against upper Paleozoic basalt. Displacement along the dextral strike-slip fault along upper Lignite Creek was determined from offset beds in cherty tuffs, and along the extension fault from pressure shadows around augen and porphyroblasts, and shear band geometry.

Isoclinal to open folds affect all the sedimentary, volcanic and metamorphic rocks and many of the plutonic rocks of the area. Some highlights from within the low-grade sequences include: tightly folded diorite sills in sedimentary rocks; weakly to unfoliated, thick basalt sequences that have ductile shear fabric along some fault zones; and recumbent, easterly verging, isoclinal folds in the Earn Group sequence. Some structural highlights from the high-grade rocks include: a regional, pervasive, generally layer parallel, low shear strain fabric folded by isoclinal to open semi-ductile folds with a weak crenulation cleavage; and a moderate- to high-shear-strain extension fabric synchronous with and postdating sillimanite metamorphism and localized in zones hundreds of metres thick along low-angle extension and high-angle strike-slip faults.

Stretching

Ductile extension as recorded by both growth and strain mineral lineations is common throughout much of the Wolverine Metamorphic Complex and its granodiorite and granite intrusions near their boundaries with overlying and adjacent low grade sedimentary rocks. Sillimanite, hornblende, biotite and in places kyanite show growth lineations. Elongations range from 2:1 to 10:1, and are commonly near 3 to 4:1.

Timing

Garnet grew helicitically with a muscovite-quartz fabric and records the earliest structural and tectonic events in the Wolverine Complex. Staurolite is poikioblastic, and grew around, and therefore after, the garnet and some biotite. Sillimanite, kyanite, and staurolite lie in the foliation planes, and generally are aligned in the regional stretching and fold axes directions. Garnet, muscovite, and biotite grew prior to a crenulation cleavage.

The Lignite granite intrudes the fault contact between the low-grade Philip Creek succession basalt and the amphibolite facies Wolverine Complex and is unfoliated. The granite therefore places an upper age limit on the local metamorphic fabric, and strike-slip and extension faults. Lignite granite is suspected to be of Eocene or Oligocene age because it resembles the late Eocene Eaglet pluton of the Mcleod Lake map area (Struik, 1989).

SPECULATION ON THE PHILIP CREEK SUCCESSION

The Philip Creek succession of fragmental basalt, diorite sills and dykes, and limestone may be an eastern continental margin rift facies equivalent to a western marginal basin rift floor facies of the Slide Mountain Group. If so, the Philip Creek succession would be an autochthonous (relatively) volcanic sequence.

Philip Creek succession may be autochthonous because it has diorite dykes and sills like those that intrude the Earn Group(?) clastic rocks and it rests on the Earn Group. Should these links be confirmed then the Philip Creek succession is tied to the Earn Group which is tied to the continental margin sequence of Paleozoic North America. One of the problems with the linkage is the tentative assignment of these rocks to the Earn Group.

Rocks equivalent to the Earn Group southeast at Cariboo Lake, the Black Stuart Group, are also intruded by diorite sills like those in Pine Pass map area. A similar diorite sill has intruded the Cambro-Hadrynian Midas Formation that underlies the Black Stuart Group (Struik, 1988). To the west of Cariboo Lake, Snowshoe Group continental clastics are also intruded by diorite sills (Struik, 1981, 1988) that closely resemble those of Pine Pass map area. All of these diorite intrusions are folded in regional structures. The sequence at Cariboo Lake is part of the Paleozoic western continental margin. So too probably is the one in the southwest part of the Pine Pass map area. The coincidence of sedimentary facies, diorite intrusions, fold history and overall stratigraphic context makes this correlation compelling. Perhaps the volcanic facies that may have been fed by the dioritic intrusions of the Cariboo Lake area is the one preserved in Pine Pass map area.

The Philip Creek succession fragmental basalt and diorite may be the Carboniferous rift edge facies of the breakup of North America (Struik, 1987). Another possibility is that they represent a Permian arc generated during the tectonism

implied by Permian thrust faults in the Slide Mountain Terrane (Klepacki, 1985; Harms, 1986) and Permo-Triassic eclogite and blueschist facies rocks in Yukon (Erdmer, 1987).

ACKNOWLEDGMENTS

Felippo Ferri kindly toured us through some of the geology of the Manson River map area.

REFERENCES

Cecile, M.P. and Norford, B.S.
1979: Basin to platform transition, lower Paleozoic strata of Ware and Trutch map area, northeastern British Columbia; in Current Research, Part A. Geological Survey of Canada, Paper 79-1A, p. 219-226.

Erdmer, P.
1987: Blueschist and eclogite in mylonitic allochthons, Ross River and Watson Lake area, southeastern Yukon; Canadian Journal of Earth Sciences, v. 24, p. 1439- 1449.

Ferri, F. and Melville, D.M.
1988: Manson Creek mapping project (93N/09); in Geological Fieldwork 1987, British Columbia Ministry of Energy, Mines and Petroleum Resources, Paper 1988-1, p. 169- 180.
1989: Geology of the Germansen Landing area, British Columbia (93N/10, 15); in Geological Fieldwork 1988, British Columbia Ministry of Energy, Mines and Petroleum Resources, Paper 1989-1, p. 209-220.
1990: Geology between Nina Lake and Osilinka River, north-central British Columbia (93N/15, north half and 94C/2 south half); in Geological Fieldwork 1989, British Columbia Ministry of Energy, Mines and Petroleum Resources, Paper 1990-1, p. 101-114.

Fritz, W.H.
1980: Two new formations in the Lower Cambrian Atan Group, Cassiar Mountains, north-central British Columbia; in Current Research, Part B, Geological Survey of Canada, Paper 80-1B, p. 217-225.

Gabrielse, H.
1963: McDame map-area, Cassiar District, British Columbia; Geological Survey of Canada, Memoir 319.

Harms, T.A.
1986: Structural and tectonic analysis of the Sylvester Allochthon, northern British Columbia: implications for paleogeography and accretion; Ph.D. thesis, University of Arizona, Tucson, 80 p.

Klepacki, D.W.
1985: Geology of Goat Range, Lardeau (82K) and Nelson (82F) map areas, southeastern British Columbia; Geological Survey of Canada, Open File 1148.

Muller, J.E.
1961: Geology, Pine Pass, British Columbia; Geological Survey of Canada, Map 11-1961.

Northcote, B.K.
1991: Petrography and tectonics of the Scovil Diorite, southwest Pine Pass map area, British Columbia; in Current Research, Part A, Geological Survey of Canada, Paper 91-1A.

Struik, L.C.
1981: Snowshoe Formation, central British Columbia; in Current Research, Part A, Geological Survey of Canada, Paper 81-1A, p. 213-216.
1987: The ancient western North American margin: an Alpine rift margin model for the east-central Canadian Cordillera; Geological Survey of Canada, Paper 87-15.
1988: Structural geology of the Cariboo gold mining district, east-central British Columbia; Geological Survey of Canada, Memoir 421.
1989: Regional geology of the McLeod Lake map area, British Columbia; in Current Research, Part E, Geological Survey of Canada, Paper 89-1E, p. 109-114.

Sutherland Brown, A.
1957: Geology of the Antler Creek Area, Cariboo District, British Columbia; British Columbia Department of Mines, Bulletin 38.

Preliminary results of fieldwork: Standfast Creek fault zone, southern British Columbia

James L. Crowley[1], Margaret E. Coleman[1], and Richard L. Brown[1]
Cordilleran Division, Vancouver

Crowley, J.L., Coleman, M.E., and Brown, R.L., Preliminary results of fieldwork: Standfast Creek fault zone, southern British Columbia; in Current Research, Part A, Geological Survey of Canada, Paper 91-1A, p. 293-301, 1991.

Abstract

The Standfast Creek fault zone (SCFZ) forms the upper boundary of the Clachnacudainn slice of the Selkirk allochthon. The fault zone is up to a kilometre wide and includes both penetrative ductile deformation and superimposed discrete brittle faulting. Ductile strain predates emplacement of the mid-Cretaceous Albert stock, but the age of discrete brittle faulting is unconstrained. Kinematic indicators within the fault zone point to a complex displacement history with evidence of both hanging-wall-to-the-west and hanging-wall-to-the-east sense of shear. Brittle normal faulting has occurred on moderate easterly dipping shears; the magnitude of displacement on these brittle shears is unknown but thought to be on the order of kilometres or less. Major displacement on the ductile Standfast Creek fault zone is not required by the data but cannot be ruled out.

Résumé

La zone de failles de Standfast Creek forme la limite supérieure du lambeau Clachnacudainn de l'allochtone de Selkirk. La zone de failles mesure jusqu'à un kilomètre de largeur et est caractérisée à la fois par une déformation ductile pénétrative et par des failles cassantes distinctes superposées. La déformation ductile a précédé la mise en place du stock d'Albert du Crétacé moyen mais l'âge des failles cassantes distinctes n'a pas été nettement établi. Les indicateurs cinématiques au sein de la zone de failles révèlent un déplacement complexe comme en témoigne le sens du cisaillement qui se caractérise à la fois par un compartiment supérieur incliné vers l'ouest et un compartiment supérieur vers l'est. Les failles normales cassantes se sont formées sur des zones de cisaillement à pendage modéré vers l'est, l'ampleur du déplacement sur ces zones de cisaillement cassantes n'a pas été déterminé mais pourrait être de l'ordre de quelques kilomètres au plus. Les données n'indiquent pas de déplacement important sur la zone de failles de Standfast Creek mais l'hypothèse d'un tel déplacement ne peut pas non plus être écartée.

[1] Department of Earth Sciences, Carleton University and Ottawa-Carleton Geoscience Centre, Ottawa, Ontario K1S 5B6

INTRODUCTION

The Standfast Creek fault zone (SCFZ) lies in an area of transition between two tectonic regimes (Thompson, 1972; Zwanzig, 1973; Sears, 1979) and separates two slices of the Selkirk allochthon (Brown and Lane, 1988) in the southeastern Canadian Cordillera (Fig. 1). The middle crustal regime with high grade metasediments, gneiss, and undeformed plutons in the Clachnacudainn slice underlies a higher crustal regime with lower grade metasediments and undeformed plutons in the Illecillewaet slice (Wheeler, 1965; Ross, 1968; Thompson, 1972; Zwanzig, 1973; Sears, 1979) (Fig. 2). The Selkirk allochthon metasediments include Upper Proterozoic and lower Paleozoic North American continental margin deposits and more distal, possibly marginal basin, sediments of a suspect terrane.

At the latitude of the Clachnacudainn slice, the Selkirk allochthon is separated from the underlying Monashee complex to the west by the east-dipping compressional Monashee décollement and the superposed brittle zone of the extensional Columbia River fault (Brown and Lane, 1988). The allochthon was displaced at least 80 km eastward onto the North American foreland on the mylonitic shear zone of the Monashee décollement initially during the Mesozoic (Read and Brown, 1981), with latest displacement occurring in Late Cretaceous and Paleocene (Journeay, 1986; Journeay and Brown, 1986; Parrish et al., 1988; Carr, 1990). East-directed displacement of the allochthon occurred on the Columbia River fault in the Eocene (Parrish et al., 1988). The Clachnacudainn slice is therefore entirely enclosed by faults; the Monashee décollement and Columbia River fault form the underlying faults and the Standfast Creek fault zone dips outward from the slice on all of the upper sides, isolating it from the rest of the Selkirk allochthon.

Evidence for the fault zone includes cutoff of footwall stratigraphy and attenuation of section (Thompson, 1972; Sears, 1979), duplication of section (Read and Thompson, 1980), a metamorphic discontinuity across the fault zone (Thompson, 1972; Sears, 1979), mylonitic footwall gneisses, fault breccia, and brittle faults. The timing, magnitude, and sense of displacement on the fault zone, however, remain largely conjectural. Fieldwork this past summer keyed on the following five elements in order to better interpret the significance of the Standfast Creek fault zone: fault zone geometry and kinematics, stratigraphic correlation, metamorphism, and structural style.

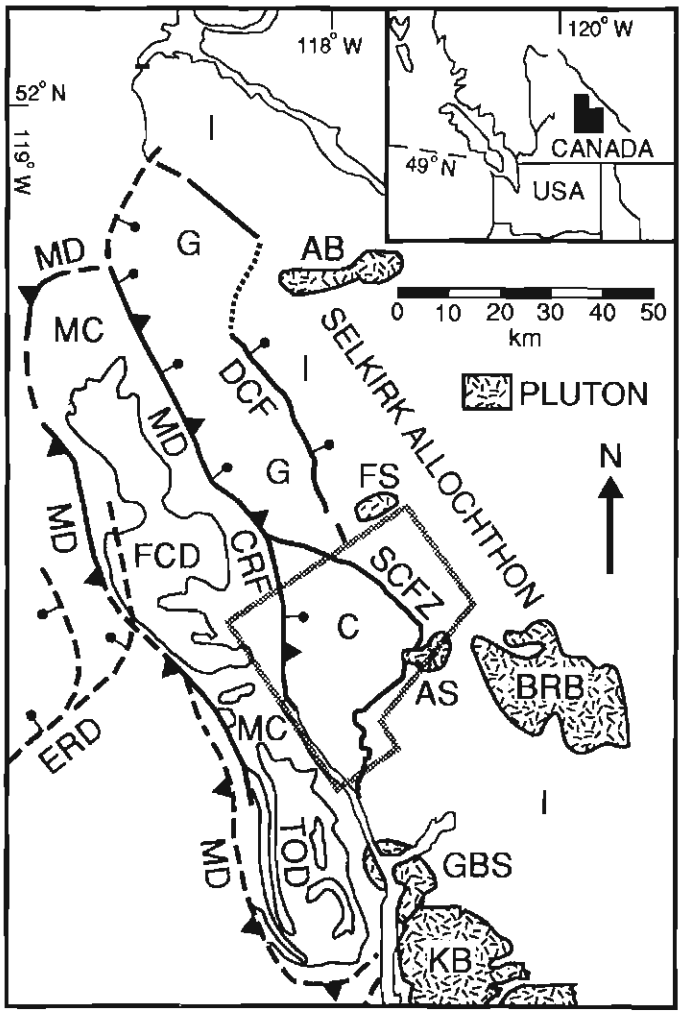

Figure 1. Major tectonic features of the northern Selkirk Mountains, modified from Brown and Lane (1988). Selkirk allochthon slices are Clachnacudainn (C), Goldstream (G), and Illecillewaet (I). Features in the Monashee complex (MC) are Frenchman Cap dome (FCD) and Thor-Odin dome (TOD). Faults are Columbia River fault (CRF), Downie Creek fault (DCF), Eagle River detachment (ERD), Monashee décollement (MD), and Standfast Creek fault zone (SCFZ). Plutons are Adamant batholith (AB), Albert stock (AS), Battle Range batholith (BRB), Fang stock (FS), Galena Bay stock (GBS), and Kushanax batholith (KB). Area outlined by the grey box is shown in more detail in Figure 2.

Previous work

Wheeler (1963) mapped a fault along the sheared-off underlimb of the tight southwest-verging Albert Canyon anticline. Wheeler (1965) suggested that this fault is related to the fault zone in the Columbia River valley north of LaForme Creek. The Standfast Creek fault zone was of interest to subsequent mappers because it was thought to be a possible discrete boundary between two different tectonic regimes. Ross (1968), working on the northwest-trending section of the fault zone between the Trans-Canada Highway and the Columbia River, found evidence for a fault but did not attribute it to displacement between tectonic regimes. Zwanzig (1973), working along the highway in the area of Albert Canyon, also found evidence of minor stratigraphic omission in the attenuated underlimb of the Albert Canyon anticline and suggested that it could be due either to a fault with minor displacement or instead to appressed isoclinal folds. Thompson (1972), mapping east of the Columbia River and south of the highway, found truncation of the footwall in two localities and used stratigraphy to imply extensional displacement. Sears (1979), mapping south of the highway, determined that the Albert stock intruded the Standfast Creek fault after an early period of extension that was followed by compression.

The previous workers have accepted the existence of the Standfast Creek fault zone based on the omission of stratigraphic units, but have found little concrete evidence

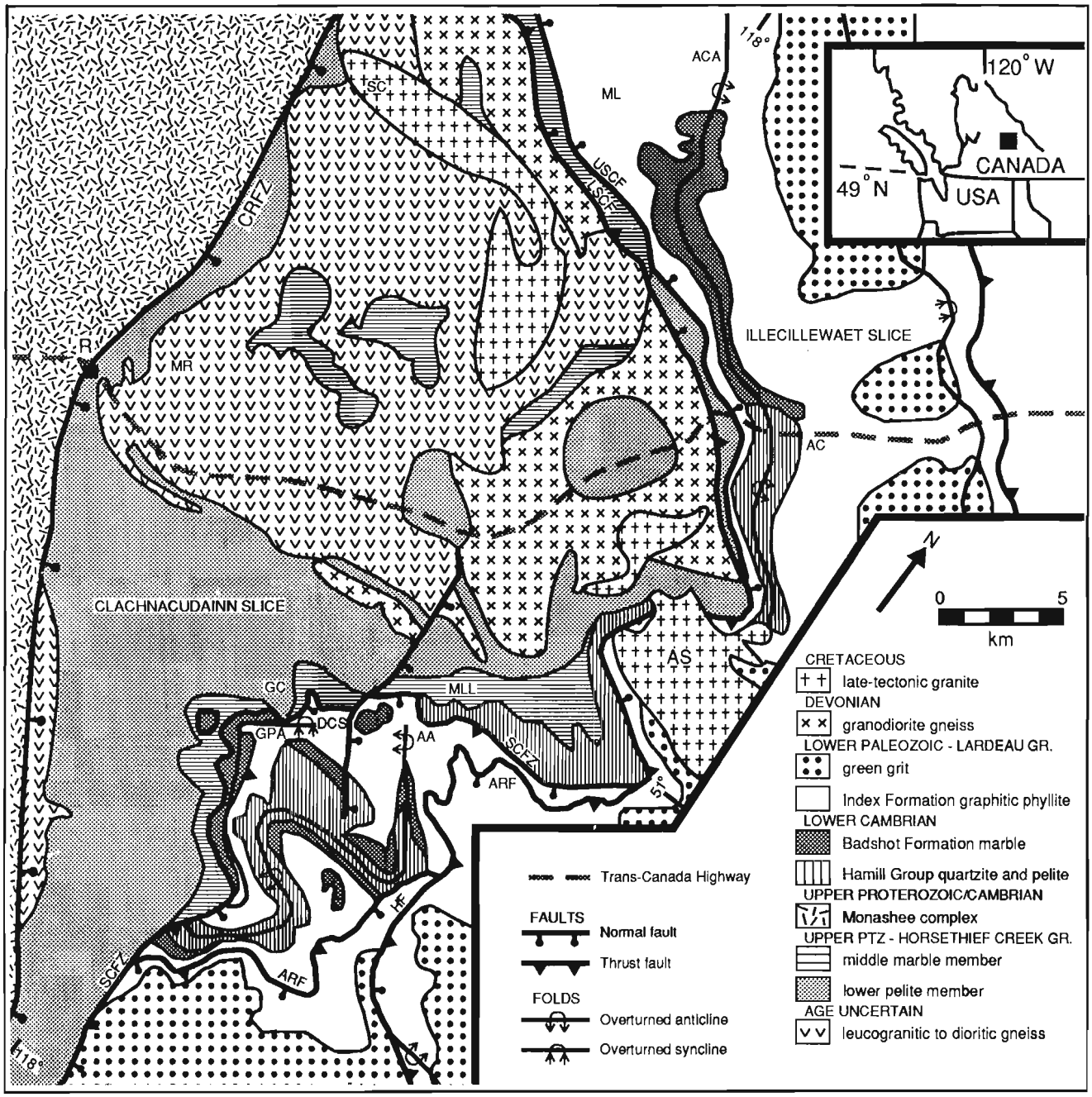

Figure 2. Map of the Standfast Creek fault zone (SCFZ) area. Correlation of Clachnacudainn slice metasedimentary stratigraphy is tentative. Unit contacts and fault locations are from Thompson (1972), Zwanzig (1973), Sears (1979), and Price (1986). Faults are Standfast Creek fault zone (SCFZ), lower Standfast Creek fault (LSCF), upper Standfast Creek fault (USCF), Akolkolex River fault (ARF), Holyk fault (HF), and Columbia River fault zone (CRFZ). Other geological features are Albert Canyon anticline (ACA), Albert stock (AS), and Akolkolex anticline (AA). Geographic features are Albert Canyon (AC), Ghost Peak area (GPA), Greeley Creek (GC), Mount LaForme (ML), Mount Llewelyn (MLL), Mount Revelstoke (MR), Revelstoke (R), and Sale Creek (SC).

for magnitude or direction of displacement. Gillett (1990), studying thin sections from a portion of the fault zone southwest of Revelstoke, found mainly hanging-wall-down-to-the-east sense of shear.

Recent models

Interest in the Standfast Creek fault zone has been renewed over the past 10 years due to the discovery that the Clachnacudainn slice and the fault zone are in the hanging wall of regional compressional (Monashee décollement) and extensional (Columbia River) faults that separate major tectonic elements. There are three current models concerning the timing, magnitude, and the direction of displacement on the Standfast Creek fault zone.

One model postulates that Late Jurassic and younger displacement of the Clachnacudainn slice occurred during eastward thrusting of the Selkirk allochthon on the Monashee décollement (Brown and Lane, 1988). In this scenario the Clachnacudainn slice is a structural horse that was accreted to the hanging wall of the Monashee décollement during initial stages of eastward development of a duplex of the Monashee complex. Evidence for early eastward displacement on the fault zone includes kinematic indicators in thin section (Gillett, 1990) and in the field (Brown and Lane, 1988), and mapping that shows the Monashee décollement truncating the fault zone (Brown and Lane, 1988).

A second model with a large magnitude of early west-directed thrust displacement on the Standfast Creek fault zone proposes that a tectonic wedge delaminated the crust (Price, 1986). In this model the Clachnacudainn slice and the Monashee complex have been inserted northeastward beneath the Illecillewaet slice by simultaneous displacement on the overlying Standfast Creek fault zone and an underlying sole thrust. Evidence for this model includes the southwest-verging folds in the Illecillewaet slice (such as the Albert Canyon anticline), which are attributed to synkinematic west-directed thrusting. Although these two models disagree on the major sense of displacement on the fault zone, they agree that minor brittle Eocene extensional (hanging-wall-to-the-east) reactivation occurred on the Standfast Creek fault zone in association with the Columbia River fault.

The third model concludes that major ductile Eocene extensional faulting associated elsewhere with the Columbia River fault is accommodated on the Standfast Creek fault zone (Parrish et al., 1988). In order to comply with the mid-Cretaceous age of the Albert stock (reported in Price et al., 1981), which intrudes the Standfast Creek fault zone (Sears, 1979), this model speculates that an extensional fault branch skirts its western edge. Evidence for this model includes mineral cooling data that imply both the Monashee complex and Clachnacudainn slice were at similar high temperatures in the Eocene (Parrish et al., 1988).

STANDFAST CREEK FAULT ZONE GEOMETRY AND KINEMATICS

Evidence presented in this section for multiple faults between the Clachnacudainn and Illecillewaet slices suggests there are numerous surfaces along which displacement has occurred. Therefore, the Standfast Creek fault studied by previous workers is termed the Standfast Creek fault zone (SCFZ) in this study. The fault zone bifurcates north of Albert stock; the inner and outer branches are termed the lower and upper Standfast Creek fault (SCF) respectively (Fig. 2). The two faults are 2.5 km apart where they are truncated by the Columbia River fault zone in the north, and generally about 1 km apart elsewhere. South of the Albert stock the Standfast Creek fault zone consists of one prominent fault trace with at least one minor splay. The fault zone dips outward from the Clachnacudainn slice on all sides at 30-45°.

The lower Standfast Creek fault in the vicinity of Mount LaForme lies within the uppermost part of the granodiorite gneiss, and places footwall gneiss against a hanging wall metasediment package consisting mainly of pelite and quartzite with minor marble and calc-silicate. The gneiss is mylonitic, and at the contact with the metasediments it is brecciated. Kinematic indicators were difficult to observe in the field because of extensive recrystallization of the mylonitic fabric. A stretching lineation defined by elongated splotches of biotite in the col 2 km south of Mount LaForme plunges shallowly to the southeast and northwest. At the Trans-Canada Highway the lower Standfast Creek fault lies 500 m within the granodiorite gneiss, in a 50 m wide cataclastic zone also observed by Zwanzig (1973). The lower Standfast Creek fault in the col south of Mount LaForme and at the highway appears to be a ductile fault.

In marked contrast, the upper Standfast Creek fault is a brittle fault. It places the pelite and quartzite package (the hanging wall of the lower SCF) in the footwall against a package of dark blue to black graphitic phyllite, marble, and quartzite that are in the underlimb of the southwest-verging Albert Canyon anticline. The upper Standfast Creek fault at the Trans-Canada Highway is composed of numerous brittle faults that are less than 2 m wide, contain fault gouge, and are enveloped by slickensided and striated surfaces (Fig. 3). Similar brittle faults occur within 2 km of the fault on both sides of the Standfast Creek fault zone (Fig. 4). Since there are no marker units offset across these brittle faults the amount of displacement on each is unknown, yet similar lithologies and metamorphic grade across the faults suggest that displacement is minor. Drag folds of bedding adjacent to the faults give hanging-wall-down-to-the-east sense of displacement on the brittle faults (Fig. 4).

The lower and upper Standfast Creek faults join together south of the highway along Albert Creek, and are truncated by the Albert stock (Sears, 1979). Even though the fault trace is covered by alluvium where it is truncated, the undeformed nature of the main pluton and crosscutting dykes lead to the conclusion that the stock plugs the fault (Fig. 5). South of the Albert stock the Standfast Creek fault zone consists mostly of one fault trace, except at the head of Greeley Creek. At this location, 150-200 m of footwall pelite overlies 200 m of hanging wall stratigraphy that is adjacent to the fault zone. This is evidence that a fault splay exists. South of the Albert stock the fault zone displays both brittle and ductile characteristics. Kinematic indicators observed in this section give opposite senses of movement on the Standfast Creek fault zone; S-C fabrics give mostly hanging-wall-to-the-west sense of shear, and younger shear bands give hanging-wall-to-the-east sense.

Figure 3. One of the numerous brittle faults of the upper SCF along the Trans-Canada Highway. Hammer in bottom centre of picture is the scale.

Figure 4. Brittle fault in the hanging wall of the SCFZ between the Mohican Formation (left) and Badshot marble, southwest of the north branch of Standfast Creek. Drag folds in the Mohican phyllites give hanging-wall- down-to-the-right (southeast).

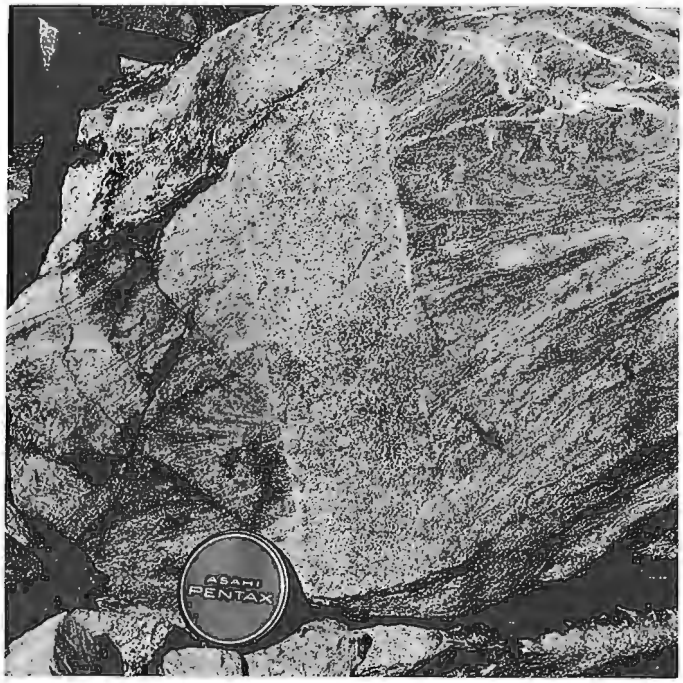

Figure 5. Dyke from the Albert stock cutting all structures north of Albert Peak.

Discussion of geometry and kinematics

The undeformed 100 Ma Albert stock (reported in Price et al., 1981) places a constraint on major post-Cretaceous displacement on the Standfast Creek fault zone. A possibility for younger displacement is that the lower and upper faults do not join 1 km north of the stock as mapped by Sears (1979), but instead one of the faults skirts the pluton to the west (Parrish et al., 1988). However, the apparently coherent and continuous stratigraphy outlined by marble layers exposed southwest of the stock in the cliff faces north of Mount Llewelyn makes this possibility unlikely, since a divergent fault trace must cut through this section to join the Standfast Creek fault zone south of Mount Llewelyn. Since the relationship of the Albert stock to the fault zone remains uncertain, further work in this area will hopefully delineate the exact trace of the fault and establish the ages of the various plutonic phases.

Kinematic indicators observed in the field fit the tentative hypothesis that the early ductile movement south of Albert stock was west-directed thrusting (this phase is still unclear in the north) and that the younger ductile and brittle movements were east-directed normal faulting (occurred in the north on the upper Standfast Creek fault only).

STRATIGRAPHIC CORRELATION

Correlation of the Clachnacudainn slice metasediments is difficult because they are surrounded on all sides by zones of tectonic or intrusive discordance (Fig. 2). Also, marker units are rare because the section is a heterogeneous assemblage of rock types that varies greatly due to facies changes. Hence, the following correlations of Clachnacudainn slice metasediments are tentative.

Gneissic and plutonic rock

Clachnacudainn slice metasediments are interlayered with sheets of leucogranitic to dioritic gneiss (Ross, 1968; Gilman, 1972) and by mostly undeformed granite to granodiorite plutons (Sears, 1979). The gneiss occurs only in the footwall and the plutons occur on both sides of the Standfast Creek fault zone. The absence of gneiss in the Illecillewaet slice may be significant in evaluating displacement on the fault zone. The strongly foliated and locally mylonitized granodiorite gneiss is dated by U-Pb zircon method as Devonian (R.R. Parrish, unpub. data; reported in Price et al., 1981). The age of the variably deformed leucogranitic to dioritic gneiss that comprises most of the igneous rock in the Clachnacudainn slice is not known. The granite and granodiorite plutons on both sides of the Standfast Creek fault zone are mid-Cretaceous from dating of the Albert stock (reported in Price et al., 1981) and the pluton near Sale Creek (R.L. Armstrong, unpub. data; R.R. Parrish, pers. comm., 1990). The mid-Cretaceous plutons are undeformed, except for the mylonitized western part of the latter pluton, where it is within 2 km of the Columbia River fault (Brown and Murphy, 1982). The presence of Tertiary plutonism, such as the Ladybird granite to the south (Parrish et al., 1988), in the compositionally and texturally diverse plutons is a possibility.

Lower metasedimentary section of the Clachnacudainn slice

The lower metasedimentary section of the Clachnacudainn slice is composed of (in decreasing abundance) thin-bedded micaceous quartzite, semipelite, thick-bedded tan to grey quartzite, ± staurolite garnet chlorite biotite schist, amphibolite, grey clean marble, coarse crystalline brown marble, calcareous phyllite, and calc-silicate schist.

Thompson (1972) distinguished informal units based on the amount of quartzite versus pelite, and stated that these rocks "appear to be part of the [lower Paleozoic] Hamill and possibly part of the [Upper Proterozoic] Horsethief Creek Group". Read and Thompson (1980) correlated these rocks with the lower Paleozoic Lardeau Group based on a 10-30 m thick amphibolite layer that resembles the Jowett Formation. Accordingly, rock units adjacent to the amphibolite comprise the upper part of the Index Formation and the overlying Broadview Formation. This correlation requires inversion of the sequence and a large west-verging syncline.

This study and Sears (1979) correlate the lower metasedimentary section with different members of the Horsethief Creek Group (Fig. 2). Sears (1979) placed it in the quartzofeldspathic grit member, whereas this study places it in the lower pelitic member described by Brown et al. (1978) to the north based on the assemblage of pelite, semipelite, and amphibolite. This section is probably not Lardeau Group because of the absence of dark blue to black graphitic phyllite that typifies the Index Formation in the hanging wall. Moreover, the multiple layers and lenses of amphibolite that are interbedded with the clastic rocks are characteristic of the lower pelitic member of the Horsethief Creek Group and are quite distinct from the basaltic flow nature of the Jowett Formation. The metasedimentary screens in the Devonian granodiorite gneiss along the Trans-Canada Highway described by Gilman (1972) and the amphibolitic mica schist in the valleys of Albert and Woolsey creeks (between the lower and upper faults) correlated by Zwanzig (1973) with the Lardeau Group also probably belong to this section.

Upper metasedimentary section of the Clachnacudainn slice

The upper metasedimentary section of the Clachnacudainn slice is marked at the base by 2 to 5 grey marble layers that drastically vary in width along strike (from 0-30 m), and at the top by thick clean quartzite intercalated with garnet biotite schist. The marble is interlayered with black phyllite, micaceous quartzite, green garnet biotite chlorite schist, hornblende garnet schist, and tan quartzite. In the Ghost Peak area two marble layers occur within 40 m of the Standfast Creek fault zone, whereas southwest of the Albert stock five marble layers occur within 1-6 km of the fault zone.

Read and Thompson (1980) correlated the thick clean quartzite-schist package with the Hamill Group, and the marble-pelite package with the lower Cambrian Badshot Formation and the Index Formation. Sears (1979) and this study correlate the thick clean quartzite-schist package with the Hamill Group and the marble-pelite package with the middle carbonate member of the Horsethief Creek Group (for description see Brown et al., 1978). The metasedimentary screens in the leucogranitic to dioritic gneiss are similar to these rocks according to descriptions by Ross (1968) and Gilman (1972). This section also includes the metasediments between the lower and upper Standfast Creek faults south of Mount LaForme. Therefore, the metasediments above the gneiss are nearly continuous from the confluence of the Columbia and Akolkolex rivers in the south around the eastern flank to LaForme Creek in the north.

Illecillewaet slice

The lithologies in the Illecillewaet slice are more readily correlated because marker horizons are continuous into areas of known stratigraphy (Thompson, 1972; Zwanzig, 1973; Sears, 1979). The Hamill quartzite in the core of the Akolkolex and Albert Canyon anticlines is overlain by the light green calcareous schist of the Mohican Formation, the bluish-grey Badshot marble, and the dark blue to black graphitic Index Formation phyllite.

Discussion of stratigraphic correlation

According to this tentative stratigraphic correlation, most of the Upper Proterozoic to lower Paleozoic stratigraphy is present in the vicinity of the Standfast Creek fault zone. Section is missing along the fault zone, but the presence of stratigraphy correlated with Hamill quartzite in the immediate footwall and only 200 m above the fault zone in the core of the Albert Canyon anticline along Albert Creek suggests that stratigraphic attenuation is not large. The juxtaposition of Horsethief Creek Group against the Index Formation in the underlimb of the Albert Canyon anticline north of the

highway suggests a larger amount of displacement. Sears (1979) used the thickness of nearby units to postulate that stratigraphic omission is between 2 and 3 km. The most significant lithological difference across the Standfast Creek fault zone may be the absence of large bodies of gneiss in the Illecillewaet slice.

One lithology that is entirely missing is the grit unit of the upper pelitic member of the Horsethief Creek Group. Brown et al. (1978) and Wheeler (1965), working to the north, suggested that faulting along the base of the Hamill Group has eliminated the grit unit over a widespread area.

METAMORPHISM

The apparent metamorphic break across the Standfast Creek fault zone is partly used in some models (Price, 1986; Parrish et al., 1988) to suggest major displacement.

As Thompson (1972) also observed, the high grade mineral assemblages are confined to a narrow zone directly above the leucogranitic to dioritic gneiss of uncertain age; sillimanite is restricted to the metasedimentary screens within the gneiss, kyanite is stable a few hundred metres above the gneiss, and the staurolite zone extends about 3 km into the overlying pelite. The only rocks farther up in the section that reached elevated conditions of metamorphism are those within the contact metamorphic aureole of the Albert stock (Sears, 1979). This aureole was observed to cross a fault at the head of the Akolkolex River. The screens of metasediment within the Devonian granodiorite gneiss do not contain sillimanite or kyanite (Gilman, 1972; Zwanzig, 1973), possibly because of retrogression during later thermal events, or because of a low-alumina content.

The garnet isograd crosses the lower Standfast Creek fault in at least two localities, whereas the upper fault and the fault zone south of the Albert stock appear to be coincident with the garnet isograd. This minor metamorphic break, however, may be a function of the composition of the two lithologies in the immediate hanging wall; the Badshot marble and the Index Formation black graphitic phyllite would probably retain the same assemblages at high grade conditions and therefore do not indicate metamorphic grade. The metamorphic grade in the hanging wall is at least biotite grade, and possibly higher; Zwanzig (1973) recorded staurolite pseudomorphs, garnet, and chloritoid in the only section where a pelitic lithology lies in the immediate hanging wall (Hamill quartzite in the core of the Albert Canyon anticline).

Discussion of metamorphic discontinuity

This simple, prograde variation of mineral assemblages outward from the leucogranitic to dioritic gneiss suggests the Standfast Creek fault zone does not disrupt regional metamorphic isograds. The minor break from garnet grade in the immediate footwall to biotite grade in the hanging wall may be accentuated by aluminous pelite in the footwall, and calcareous and graphitic lithologies in the hanging wall. Major displacement on the fault zone is restricted to early ductile displacement that occurred before or during formation of the regional isograds.

STRUCTURAL STYLE

The Standfast Creek fault zone lies in the transitional area between contrasting structural regimes, the Clachnacudainn slice and Monashee complex to the west and the remainder of the Selkirk allochthon to the east. A refolded west-verging recumbent nappe with an inverted limb length up to 25 km dominates the Selkirk allochthon to the north in the hanging wall of the fault zone (Brown and Lane, 1988). In contrast, the Monashee complex is dominated by northeasterly verging folds (see Brown et al., 1986 and references therein).

Phases of deformation

Lithological layering (S0) in the micaceous quartzite, pelite, and quartzite varies in scale from extremely thin laminations to metre-wide beds. Small-scale grey and blue colour banding is evident in the clean marbles, and dark grey and brown colours alternate in the micaceous marbles. The faintly present schistosity resulting from the first phase of deformation (S1) is parallel to S0 in the hinges of recumbent isoclinal phase 2 folds (F2). The recumbent southwest-verging Albert Canyon anticline (Zwanzig, 1973; Fig. 2) could be a first phase fold, similar to the Carnes nappe to the north (Brown and Lane, 1988). Thompson (1972) inferred a large recumbent fold in the footwall metasediments from stratigraphic and structural data. Sears (1979) disputed this inference because the lithological succession is non-repetitive and no major fold hinges are detected. The strong F2 axial-planar schistosity (S2) cuts across S0 and S1 in the thickened hinges and is parallel to both in the attenuated limbs. F2 axes generally plunge gently (10-25°) to the southeast and axial planes dip shallowly to the southeast. These observations apply to both the immediate footwall and hanging wall of the Standfast Creek fault zone. Isoclines in the hanging wall include the large-scale east-verging synformal Akolkolex anticline and antiformal Drimmie Creek syncline (Thompson, 1972) (Fig. 6).

Figure 6. Recumbent isoclinal folds of the Mohican Formation (dark colour) and Badshot marble (light colour) in the hinge zone of the Akolkolex anticline, east of upper West Twin Creek.

Figure 7. Isoclinal F2 refolded by open and upright F3 west of Ghost Peak.

Phase 3 folds (F3) are upright and open, and refold F2 isoclines (Fig. 7). F3 axes plunge gently to the southeast (same orientation as F2), and F3 axial planes are nearly vertical and strike southeast. F3 is equally pervasive on both sides of the fault zone. The axial-planar schistosity (S3) is especially prominent in the Index phyllite (Fig. 8). F3 crenulations are superposed on all earlier structures and are spatially related to larger open folds.

Discussion of structural style

The similarity of structures and the presence of three phases of deformation across the Standfast Creek fault zone leads this study to the same conclusion as Thompson (1972) and Sears (1979), namely that structural style is consistent across the fault zone. Hence, the Standfast Creek fault zone is probably not a boundary between structural domains. Sears (1979) placed a major structural boundary between recumbent isoclinal folds and upright folds to the east at the Akolkolex River fault (Fig. 2). Zwanzig (1973) placed a boundary between two contrasting tectonic regimes, the horizontally extended infrastructure and the horizontally compressed superstructure, in a 5 km wide transition zone in the centre of the Illecillewaet synclinorium, 11 km east of the fault zone.

SUMMARY

Opposing senses of displacement and the presence of both ductile and brittle faults require that there were multiple episodes of displacement on the Standfast Creek fault zone. Preliminary field observations suggest that across the fault zone the amount of stratigraphic attenuation can be accounted for by a few kilometres of displacement. The metamorphic break is not major, and the continuity of structural style across the fault zone also argue for limited displacement. However, major early ductile displacement could have occurred before quenching of the regional isograds, presumably coincident with F1 and F2 folding. Fieldwork in 1991 and continuing petrological and geochronological studies will further constrain the structural history of the Standfast Creek fault zone.

Figure 8. Southeast-trending, vertical S3 that is axial planar to F3 and cuts the horizontal S0, S1, and S2.

ACKNOWLEDGMENTS

This project is funded by NSERC Operating Grant A2693 and EMR Research Agreement 90/4/74 to R.L. Brown. We thank Randall R. Parrish for a discussion on the geochronology.

REFERENCES

Brown, R.L. and Lane, L.S.
1988: Tectonic interpretation of west-verging folds in the Selkirk allochthon of the southern Canadian Cordillera; Canadian Journal of Earth Sciences, v. 25, p. 292-300.

Brown, R.L. and Murphy, D.C.
1982: Kinematic interpretation of mylonitic rocks in part of the Columbia River fault zone, Shuswap Terrane, British Columbia; Canadian Journal of Earth Sciences, v. 19, p. 456-465.

Brown, R.L., Tippett, C.R., and Lane, L.S.
1978: Stratigraphy, facies changes, and correlations in the northern Selkirk Mountains, southern Canadian Cordillera; Canadian Journal of Earth Sciences, v. 15, p. 1129-1140.

Brown, R.L., Journeay, J.M., Lane, L.S., Murphy, D.C., and Rees, C.J.
1986: Obduction, backfolding and piggyback thrusting in the metamorphic hinterland of the southeastern Canadian Cordillera; Journal of Structural Geology, v. 8, p. 255-268.

Carr, S.D.
1990: Late Cretaceous-early Tertiary tectonic evolution of the southern Omineca Belt, Canadian Cordillera; unpublished Ph.D. thesis, Carleton University, Ottawa.

Gillett, J.
1990: A geologic and structural compilation of the Clachnacudainn Terrane with a metamorphic and kinematic study along the bordering Standfast Creek Fault; unpublished B.Sc. thesis, Carleton University, Ottawa, 48 p.

Gilman, R.A.
1972: Geology of the Clachnacudainn Salient near Albert Canyon, British Columbia; Canadian Journal of Earth Sciences, v. 9, p. 1447-1454.

Journeay, J.M.
1986: Stratigraphy, internal strain, and thermo-tectonic evolution of northern Frenchman Cap dome: an exhumed basement duplex structure, Omineca hinterland, southeastern Canadian Cordillera; unpublished Ph.D. thesis, Queen's University, Kingston.

Journeay, J.M. and Brown, R.L.
1986: Major tectonic boundaries of the Omineca Belt in southern British Columbia: a progress report; in Current Research, Part A, Geological Survey of Canada, Paper 86-1A, p. 81-88.

Parrish, R.R., Carr, S.D., and Parkinson, D.L.
1988: Eocene extensional tectonics and geochronology of the southern Omineca Belt, British Columbia and Washington; Tectonics, v. 7, p. 181-212.

Price, R.A.
1986: The southeastern Canadian Cordillera: thrust faulting, tectonic wedging and delamination of the lithosphere; Journal of Structural Geology, v. 8, p. 239-254.

Price, R.A., Monger, J.W.H., and Muller, J.E.
1981: Cordilleran cross-section - Calgary to Victoria; in Field Guides to Geology and Mineral Deposits, Calgary '81, Geological Association of Canada Mineralogical Association of Canada/Canadian Geophysical Union. p. 216-334.

Read, P.B. and Brown, R.L.
1981: Columbia River Fault zone: southeastern margin of the Shuswap and Monashee complexes, southern British Columbia; Canadian Journal of Earth Sciences, v. 18, p. 1127-1145.

Read, P.B. and Thompson, R.I.
1980: Bulletin 60-Geology of the Akolkolex River area-an addendum; in Geological Fieldwork, British Columbia Ministry of Energy, Mines, and Petroleum Resources, Paper 80-1, p. 183-187.

Ross, J.V.
1968: Structural relations at the eastern margin of the Shuswap Complex, near Revelstoke, southeastern British Columbia; Canadian Journal of Earth Sciences, v. 5, p. 831-849.

Sears, J.W.
1979: Tectonic contrasts between the infrastructure and superstructure of the Columbian orogen, Albert Peak area, western Selkirk Mountains, British Columbia; unpublished Ph.D. thesis, Queen's University, Kingston, 154 p.

Thompson, R.I.
1972: Geology of the Akolkolex River area near Revelstoke, British Columbia; unpublished Ph.D. thesis, Queen's University, Kingston, 125 p.

Wheeler, J.O.
1963: Rogers Pass map-area, British Columbia and Alberta; Geological Survey of Canada, Paper 62-32.
1965: Big Bend map-area, British Columbia; Geological Survey of Canada, Paper 64-32.

Zwanzig, H.V.
1973: Structural transition between the foreland zone and the core zone of the Columbian Orogen, Selkirk Mountains, British Columbia; unpublished Ph.D. thesis, Queen's University, Kingston, 158 p.

Blocky sediments in Bute and Knight inlets, British Columbia

T. J. Lewis and W. H. Bentkowski
Pacific Geoscience Division, Sidney, B.C.

Lewis, T.J. and Bentkowski, W.H., Blocky sediments in Bute and Knight inlets, British Columbia; in Current Research, Part A, Geological Survey of Canada, Paper 91-1A, p. 303-308, 1991.

Abstract

Studies of the blocky sediments in Bute and Knight inlets on PGC Cruise 89-11 included 3.5 kHz profiling, coring, marine heat-flow probing, pore pressure measurements, measurements of the sediment electrical resistivities and geochemical measurements on core samples. The 3.5 kHz sounding and geochemical data indicate the presence of free methane gas in stratified sediments but not in the blocky sediments. Temperature gradients in the sediments vary systematically with the sediment structure, probably controlled by biochemical processes. Although the blocky mounds may be formed by subsidence of gas-charged sediments, they are more likely sediment blocks broken off by turbidity currents. After travelling down the inlets and colliding with fjiord-mouth sills, the higher density fluids flow back into the basin, carrying with them low density blocks of sediment originally located on or near the sills.

Résumé

Les études des sédiments blocailleux dans les inlets Bute et Knight réalisées au cours de l'expédition 89-11 du CGP ont consisté notamment à établir des profils à 3,5 kHz, à prélever des carottes, à sonder l'écoulement thermique sous-marin, à mesurer les pressions interstitielles et la résistivité électrique des sédiments et à analyser la composition géochimique des échantillons carottés. Les données de sondage à la fréquence de 3,5 kHz et les données géochimiques indiquent la présence de gaz de méthane libre dans les sédiments stratifiés mais pas dans les sédiments blocailleux. Les gradients de température dans les sédiments varient systématiquement en fonction de la structure, probablement à cause de processus biochimiques. Même si les buttes blocailleuses ont pu avoir été formées par l'effondrement de sédiments chargés de gaz, il s'agirait davantage de blocs de sédiments fracturés par des courants de turbidité. Après avoir traversé les inlets et être entrés en collision avec les seuils des fjords, les fluides à forte densité retournent dans le bassin, transportant des blocs de sédiments de faible densité provenant des seuils ou de leur voisinage.

INTRODUCTION

The purpose of PGC Cruise 89-11 aboard CSS JOHN P TULLY in November, 1989, was to investigate the possible occurrences of gas hydrates in Bute and Knight Inlets (Fig. 1). Bornhold and Prior (1989) previously described unusual blocky mounds occurring in otherwise flat-lying sediments in these two fiords, and suggested two possible mechanisms for their formation: subsidence associated with earthquake-induced liquefaction, and uplift driven by the growth of localized gas hydrates. Previous water temperatures and a single heat-flow measurement showed that temperatures and pressures were near the stability field of gas hydrates and that heat was flowing downward into the top of the sediments from the water. Therefore another possible mechanism to be considered was subsidence associated with uneven melting of a relict gas hydrate layer.

This investigation included 3.5 kHz sounding, electromagnetic sounding to ascertain the electrical conductivity structure (Cheesman et al., in press), marine heat-flow measurements to determine the temperatures, temperature gradients in the sediments and thermal conductivity measured both in situ and on core samples, geochemical analyses of cores and pore fluids, including stable isotope analyses of core gases, and measurement of in situ pore pressures. This paper reports on gas distribution in the sediments as revealed by 3.5 kHz profiling and marine heat-flow measurements, which also show that gas hydrates do not occur in the sediments. The results and those from a companion paper describing initial geochemical results (Abercrombie and Gorham, 1991), support a different source for the mounds.

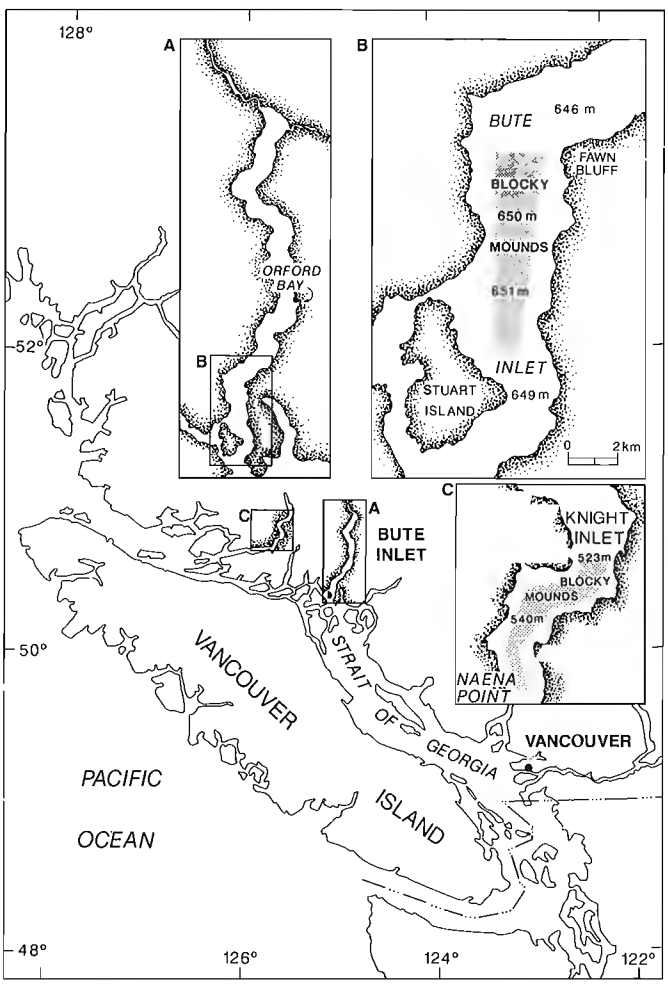

Figure 1. Locations of blocky mounds areas in Bute and Knight inlets, as shown by Bornhold and Prior (1989).

3.5 kHz PROFILING

Suitable sites for coring and deploying a marine heat-flow probe were selected on the basis of many mid-channel and cross-channel 3.5 kHz profiles. Each fiord has a deep, flat bottomed basin containing unstratified sediments, separated by a sill from down-channel, more shallow, undulating, stratified sediments. Soft, stratified sediments are found in many west coast fiords, whereas flat bottomed basins without stratified sediments are rare. Towards the sill, the flat bottom becomes progressively more irregular. Cross-channel profiles show a narrow, shallowing channel through each sill, with stratified sediments on the outward side of bends in the inlets.

A portion of the mid-channel profile from Knight Inlet (Fig. 2) is representative of the characteristics of the bottom sediments in these two inlets. In the stratified, shallow sediments, gas bubbles produce a structureless image, sometimes to within 2 or 3 m of the water-sediment interface. Larger amplitude reflectors appear at the top of apparently structureless sections near cross-channel profile 43 (Fig. 3). It is inferred that free gas is masking the sedimentary structure, and is flowing updip along horizons before eventually penetrating the overlying beds. Gas bubbles are concentrated at the highest point of seismic reflectors on cross-channel profile 43 (Fig. 3). The thick (more than 70 m on the mid-channel profile) section seen up-channel probably continues down-channel and underlies profile 43, but scattered reflections from the gas-charged upper sediments obliterate the record. Amplitudes of reflections in this sequence also increase updip.

The sill near Naena Point in Knight Inlet separates the stratified sediments, locally containing gas bubbles, from a flat, deeper sea floor. The area of blocky mounds (Fig. 2) is up-channel from this transition, the mounds all occurring within 4 km of the sill. One of the larger mounds appears to have a second reflector within it. Sampling revealed that some upstanding blocks are formed of low density material (Bornhold and Prior, 1989). Up-channel from the mounds, the sea floor at 525 m water depth is very flat with an irregular, somewhat diffuse seismic reflector which occurs beneath approximately 14 m of sediments. The reflector shoals towards the edges of the sediment prism, and its amplitude decreases up-channel. It does not occur beneath the most irregular areas, and may not exist beneath any mound, although it appears nearby.

In Bute Inlet a similar reflector was imaged (see Bornhold and Prior, 1989) 10 m beneath the 650 m deep sea floor, but only at the ends of most cross-channel profiles. In some places a second, similar reflector was imaged 20 m beneath the water-sediment interface. These reflectors appear to have a more irregular surface beneath the blocky area, and resemble some found 15 m beneath the seabed off Norway in approximately 200 m of water. Hovland (1990) attributes these to gas-charged sediments.

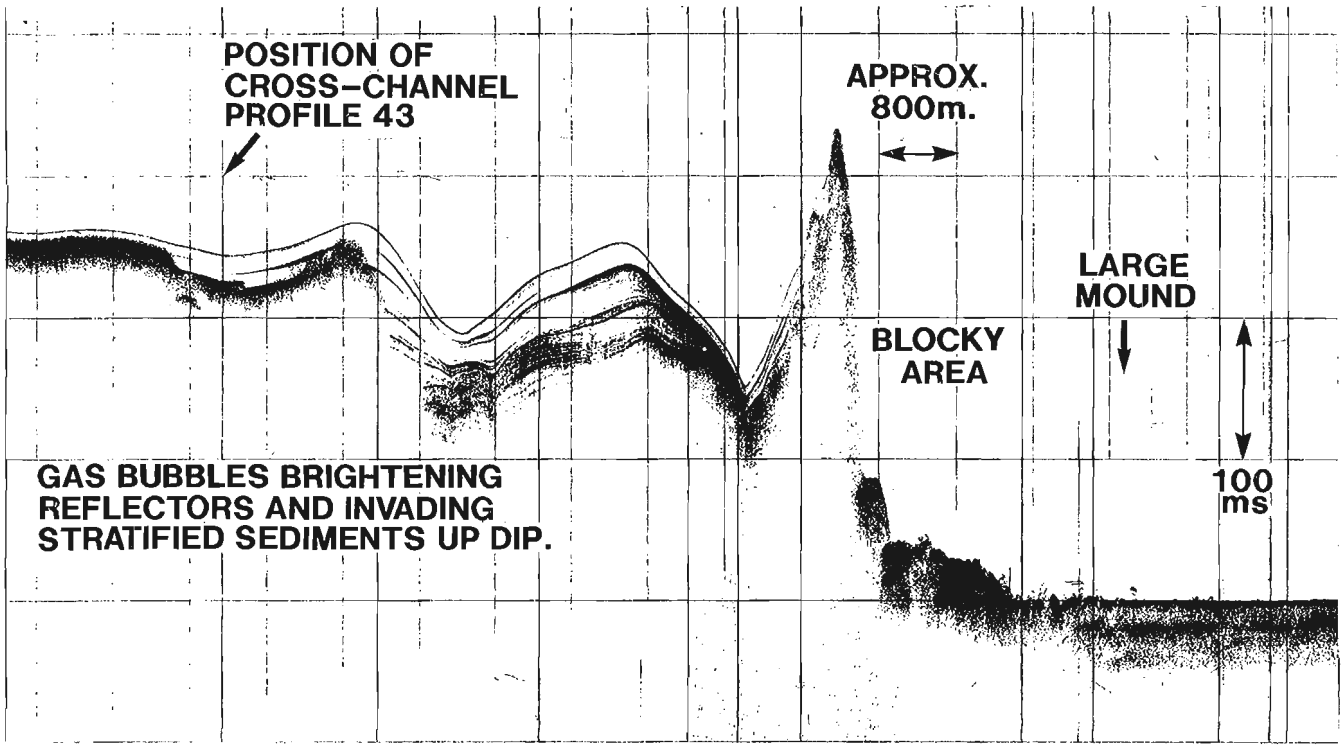

Figure 2. A portion of the mid-channel 3.5 kHz profile up Knight Inlet showing a blocky mounds area and stratified sediments partially invaded by gas bubbles.

CORE MEASUREMENTS

Eight piston cores ranging in length from 6 to 11 m were obtained, three in Knight Inlet (#5 to #7), and the remainder in Bute Inlet. Geochemical measurements including stable isotope analyses and head space gas analysis were made on core samples and/or extracted pore waters (Abercrombie and Gorham, 1991). A needle probe was used to measure the thermal conductivity of cored sediments (A.S. Judge, pers. comm., 1990).

Large variations in water and sand contents of the sediments are systematic (Table 1); the seven cores of basin sediments becoming progressively less sandy with a larger water content down-channel towards the sills. Core #7, representing stratified sediments located farther down-channel past the sills, has the least sand and the highest water content. Located on a cross-channel profile near and similar to profile 43 (Fig. 3), it was saturated with methane *in situ* (Abercrombie and Gorham, 1991). Core #8, positioned to sample a mound, had the next highest average water content. The lowest water contents and highest sand contents were in the four cores (#1,2,3 and 5) positioned farthest up-channel from each of the sills. In cores taken near the sills, some of the sands were distributed chaotically, as if deposited by turbulent flows.

GEOTHERMAL DATA

The bottom water temperature (BWT) was 7.92°C in Knight Inlet, and 8.69°C in Bute Inlet at the start of this cruise, higher than the gas hydrate stability field in sea water at the bottoms of these fiords. BWTs are found to be constant over long distances in the same basin of a fiord at the same depths (Lewis, 1983), and can be constant over periods of a few years, although they can change quickly, in periods of a few days (Lewis et al., 1988). The BWT had warmed by at least 0.21 K in Bute Inlet since a single station measured in 1988. Such a change in BWT before the 1989 cruise would explain why the upper few metres of sediments in Bute Inlet were two tenths of a degree warmer than the bottom water (Fig. 4). Since there was no transient detected in the sediments at a depth of 1 m and probably none at 0.5 m, the change happened less than 4 months before the cruise.

Thermal gradients and *in situ* thermal conductivities were measured in the sediments using an 11 m long, Lister type marine heat-flow probe (Hyndman et al., 1979). Penetration depths were usually 11 m even though there were sands present. Previously measured temperatures in stratified sediments of west coast fiords (Lewis et al., 1988; unpubl. data) increase with depth (a positive gradient), subject to variations due to past BWT changes. In these two fiords, the thermal gradients varied systematically from positive to negative values, according to the nature of the bottom: in stratified sediments down-channel from the sills, the gradient was positive, as in other inlets; in such sediments containing gas bubbles, the sediments were isothermal; also in the blocky mounds area of the basins near the sills, the sediments were isothermal; and in basin sediments up-channel from the blocky areas, the gradients were negative (see Fig. 4).

The *in situ* thermal conductivities varied with location and water content. Average values of stations ranged from 0.72 to 1.24 W/m K. Thermal conductivities were calculated using the water content of cores assuming a grain density

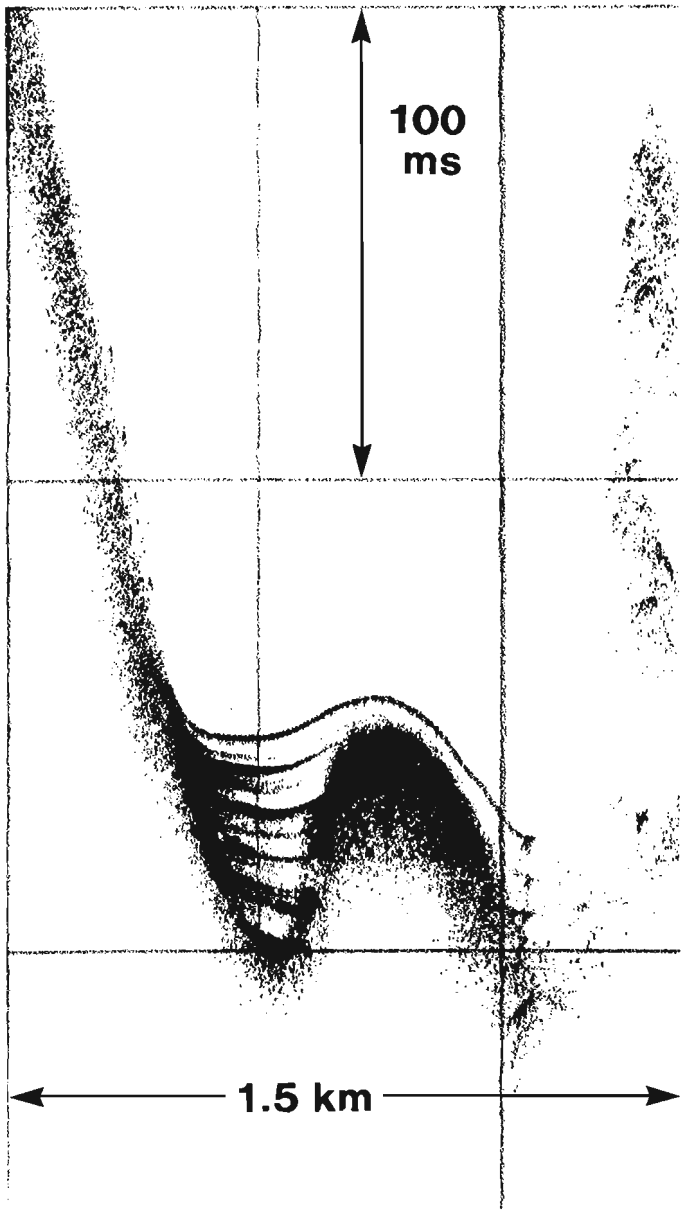

Figure 3. Cross-channel 3.5 kHz profile 43 in Knight Inlet, showing a structureless area within the sediments due to gas bubbles, and diffuse reflections at either end from the crystalline bedrock sides of the fiord.

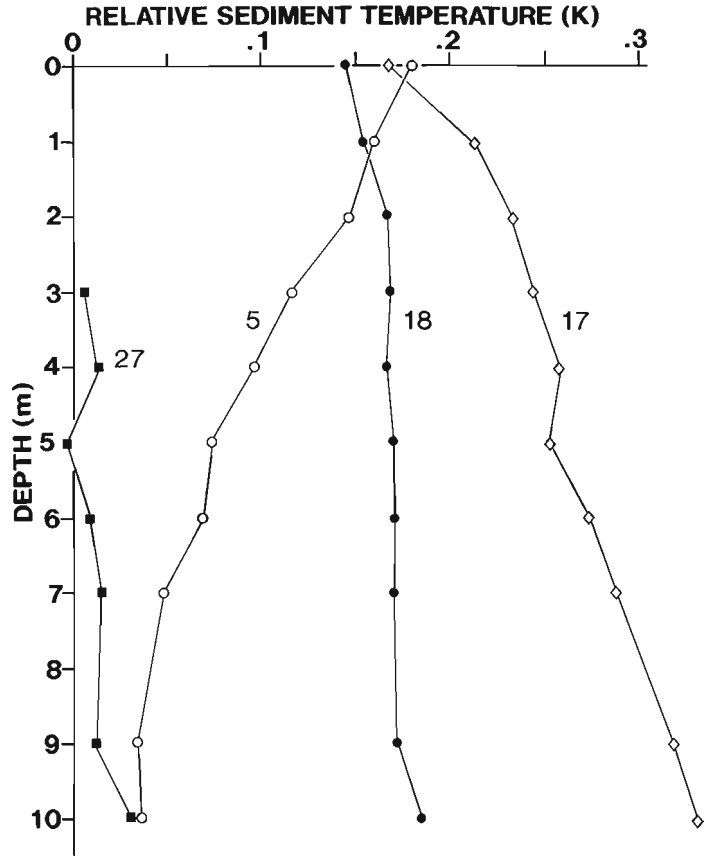

Figure 4. Representative sediment temperatures, measured with respect to BWT, as a function of depth below the water-sediment interface: Station 5, in the basin, up-channel from the blocky area, Bute Inlet; Station 17, non-gaseous, stratified sediments, Bute Inlet; Station 18, blocky area, Bute Inlet; Station 27, stratified sediments with gas bubbles, Knight Inlet.

of 2 600 kg/m^3 to obtain the porosity, and using a geometric conductivity model with an assumed grain thermal conductivity of 2.3 W/m K. Although the grain density does not significantly affect the calculated value, the value of grain conductivity does for sediments with low water contents. Average results from the one core of stratified sediments (without gas bubbles) were in good agreement with the *in situ* conductivity, but average results from the other seven cores containing more sand differed by 4 to 20% from the *in situ* conductivities (Table 1). If, as the sand content increases, the average thermal conductivity of grains increases to 2.8 W/m K, a likely value, then this discrepancy is greatly decreased. An upper limit on the amount of free gas *in situ* is 2%, given by restricting its effect on the thermal conductivity to 7%, the sum of the standard deviations of *in situ* conductivities measured in gas free sediments (0.746+/−0.020) and in and above gas charged sediments (0.724+/−0.031) at two nearby sites.

DISCUSSION

The 3.5 kHz profiles clearly show the distribution of gas bubbles in the stratified sediments down-channel from the sills by a characteristically structureless record. Methane-saturated pore fluids in core #7 support this conclusion. The increasing seismic reflectance of some horizons, particularly updip towards the sediments where bubbles are pervasive, indicate that gas is moving along these horizons. The high sand content (13 to 30%) measured farthest up-channel from the sills is expected to produce a diffuse, structureless seismic return similar to that caused by gas bubbles.

The diffuse, irregular reflectors occurring some places 10 to 15 m beneath the basin floors (and 20 m below) are probably caused by gas bubbles. Hovland (1990) attributed similar reflectors observed beneath 200 m of water off Norway to gas. The lower sand content (3.0 to 6.2%) of basin cores closer to the sill (#4, 6 and 8) is not much different from core #7 (2.4% sand) which was gas-charged, but

Table 1. Average core properties and *in situ* thermal conductivity, k.

Core Number	1	2	3	4	5	6	7	8
water content (%)	37.9	43.8	47.3	60.1	29.8	57.8	70.0	65.4
sand content (%)	29.7	14.9	13.3	6.2	26.5	3.6	2.4	3.0
calc. k (W/m K)	1.02	0.95	0.90	0.80	1.15	0.80	0.72	0.75
in situ k (W/m K)	0.93	1.05	0.99	0.90	1.24	1.06	0.72	0.78
depth range (m)	7	8	8	7	7	6	7	11

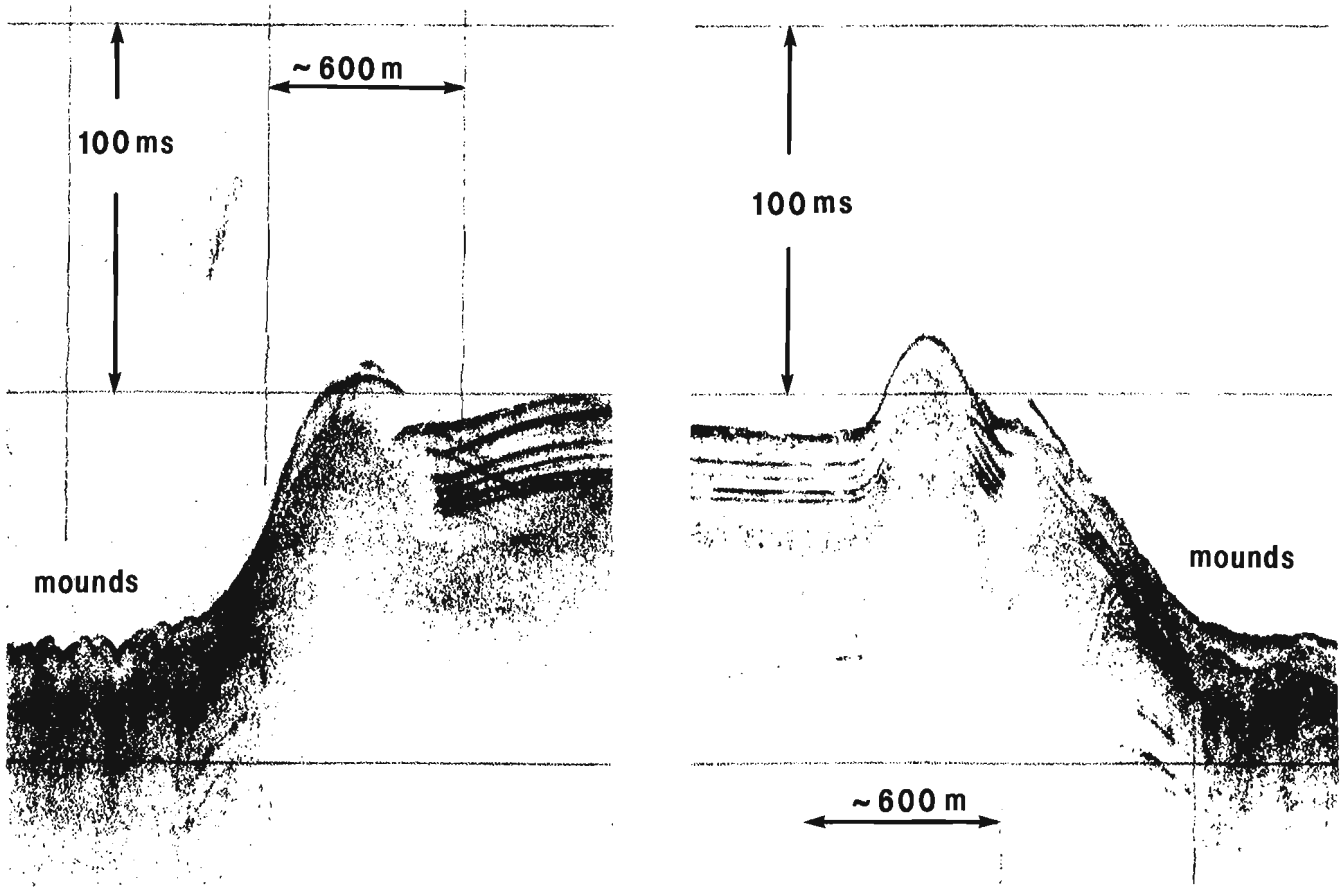

Figure 5. Profiles across the sill in Bute Inlet. Note the stratified sediments on the up-channel, basin side of the sill.

the sand in them appears as if deposited by turbulent flows, which would scatter acoustic energy, producing a structureless 3.5 kHz profile, as observed. Methane contents of pore waters in cores #2, 3, 4, 6 and 8 approach the limits of *in situ* solubility at only a very few depths (Abercrombie and Gorham, 1991), so free gas occurs pervasively only in the stratified sediments, represented by core #7.

Escaping gas or fluid (at very high rates) would tend to produce isothermal sediments at the temperature from which the deepest flow came. However, high sediment temperatures relative to BWT occurred at every station in Bute Inlet and not at all in Knight Inlet, in accordance with the observed decrease in BWT in Bute Inlet. Therefore the isothermal gradients are not caused by upward flows. The systematic variation in thermal gradient in the sediments, dependent upon the setting, is most likely related to the geochemical and biochemical processes occurring within the shallow sediments. The temperatures at the sea floor pressures in both fiords do not lie within the stability field of gas hydrates for pore waters with the measured salinities. The largest of the observed negative temperature gradients would have to continue over 100 m down into the sediments to approach this boundary.

Perhaps episodic escape of gas and/or fluid in the blocky mounds area produces structures similar to those studied by Hovland (1990) for the seabed off Norway. Possibly greater differences in permeability locally in the blocky areas have focussed the escape of gas, allowing subsidence of the surrounding sediments. However, both blocky areas occur just up-channel from a natural barrier to turbidity currents. A more likely mechanism for forming blocky mounds is a turbidity current with enough unspent energy to ascend a sill and break off sediment blocks (more like plates in shape) and then flow back chaotically into the basin. Figure 5 shows stratified sediments on the basin side of the sill in Bute inlet. Probably the returning remnants of the turbidity currents form much of the chaotic structure of the bottom, with upstanding blocks being lower density sediments from the sill.

ACKNOWLEDGMENTS

We thank V. Allen, M. Bone, G. Jewsbury, and J. Plaxton for technical assistance on the cruise, G. Ginsburg for sharing his knowledge of gas hydrates, and Capt. J. Anderson and officers and crew aboard CSS JOHN P TULLY for their willing assistance and able seamanship. We also thank E. Davis and C. Yorath for reviewing this paper and suggesting significant improvements.

REFERENCES

Abercrombie, H. and Gorham, B.
1991: Methane distribution and blocky mound formation in sediments of Bute and Knight inlets, British Columbia; in Current Research, Part A, Geological Survey of Canada, Paper 91-1A.

Bornhold, B.D. and Prior, D.B.
1989: Sediment Blocks on the Sea Floor in British Columbia Fjiords; Geo-Marine Letters, v. 9, p. 135-144.

Cheesman S.J., Law, L.K. and Edwards, R.N.
in press: Porosity Determinations of Sediments in Knight Inlet using a Transient Electromagnetic System; Geo-Marine Letters, submitted 1990.

Hovland, M.
1990: Suspected gas-associated clay diapirism on the seabed off Mid Norway; Marine and Petroleum Geology, v. 7, p. 267-276.

Hyndman, R.D., Davis, E.E. and Wright, J.A.
1979: The measurement of marine geothermal heat flow by a multi-penetration probe with digital acoustic telemetry and insitu thermal conductivity; Marine Geophysical Researches, v. 4, p. 181-205.

Lewis, T.J.
1983: Bottom water temperature variations as observed, and as recorded in the bottom sediments, Alice Arm and Douglas Channel, British Columbia; in Proceedings of a workshop on the Kitimat Marine Environment, Canadian Technical Report on Hydrography and Ocean Science, v. 18, p. 138-161.

Lewis, T.J., Bentkowski, W.H., Davis, E.E., Hyndman, R.D., Souther, J.G., and Wright, J.A.
1988: Subduction of the Juan de Fuca Plate: Thermal Consequences; Journal of Geophysical Research, v. 93, p. 15207-15225.

Methane distribution and blocky mound formation in sediments of Bute and Knight inlets, British Columbia

H.J. Abercrombie and B.L. Gorham
Institute of Sedimentary and Petroleum Geology, Calgary

Abercrombie, H.J. and Gorham, B.L., Methane distribution and blocky mound formation in sediments of Bute and Knight inlets, British Columbia; in Current Research, Part A, Geological Survey of Canada, Paper 91-1A, p. 309-316, 1991.

Abstract

Bottom sediments and associated pore waters were sampled in and near areas of blocky sediment mounds in Bute and Knight inlets, during PGC cruise 89-11. Elevated CH_4 concentrations were detected in four of five cores from Bute Inlet and two of three cores from Knight Inlet. The methane is biogenic and its abundance is related to sediment and organic matter types. Highest CH_4 concentrations approach saturation values and occur in stratified silts and muddy silts which contain organic material of marine origin with TOC values >0.25 %. The lowest CH_4 concentrations were found in sandy silts which contain <0.25 % oxidized or carbonized organic material. Abrupt discontinuities in several sediment properties were observed at 4 m in core TUL89E-08, which penetrated a blocky mound; these indicate that the mounds are coherent blocks of clayey, organic-rich silt, transported by submarine slides from elevated areas of the inlet floor to their present positions.

Résumé

Au cours de l'expédition 89-11 du CGP, on a prélevé dans les inlets Bute et Knight des échantillons de sédiments de fond et d'eau interstitielle associée dans des monticules de sédiments blocailleux et près de ceux-ci. Dans quatre des cinq carottes provenant de l'inlet Bute et dans deux des trois carottes provenant de l'inlet Knight, les concentrations de CH4 étaient élevées. Le méthane est biogénétique et son abondance est liée aux types de sédiments et de matières organiques. Les concentrations les plus élevées de CH4 dépassent les valeurs de saturation et s'observent dans les silts stratifiés et boueux qui contiennent des matières organiques d'origine marine titrant plus de 0,25 % de COT Les concentrations les plus basses de CH4 ont été enregistrées dans des silts sableux qui contiennent moins de 0,25 % de matières organiques oxydées ou carbonisées. On a relevé des discontinuités abruptes dans plusieurs propriétés des sédiments à 4 m dans la carotte TUL89E-08 prélevée dans un monticule blocailleux; ces discontinuités indiquent que les monticules sont des blocs cohérents de silt argileux riche en matières organiques, transportés par des glissements sous-marins depuis des zones élevées dans le fond de l'inlet jusqu'à leur position actuelle.

INTRODUCTION

Bornhold and Prior (1989) reported the discovery of fields of blocky sediment mounds in the deepest parts of Bute and Knight inlets. The blocky mounds are unusual and contrast sharply with the flat seafloor topography that characterizes the deep distal regions of both inlets (Bornhold and Prior, op. cit.; Lewis and Bentkowski, 1991). Three possible explanations for the blocky morphology have been advanced: i) differential subsidence due to sediment liquefaction, ii) differential subsidence due to gas hydrate decomposition, and iii) differential uplift due to gas hydrate formation.

To investigate the possible role of gas hydrates in the formation of the blocky mounds a series of eight piston cores were collected, in and adjacent to areas of irregular seafloor topography, during cruise PGC 89-11. Five cores (TUL89E-01 to -04, and -08) were collected from Bute Inlet, and three cores (TUL89E-05 to -07) were collected from Knight Inlet (Fig. 1). All sites were well characterized by 3.5 kHz profiling (Lewis and Bentkowski, 1991) to facilitate integration of geological, geochemical, and geophysical data.

Results of preliminary physical and chemical measurements of sediment samples and pore waters are presented here. Bulk density, water content, grain density, porosity, and grain size distributions were determined for selected sediment samples taken at one metre intervals through each core. The results of head space gas analysis, Rock-Eval analysis of organic material, and shipboard chloride analyses also are reported.

PHYSICAL PROPERTIES

Grain size distribution was determined by hydrometer analysis using procedures modified from Green (1981). Water contents were determined by weight loss on drying, and salt-corrected porosity was calculated using a density for seawater of 1.025 g/cm^3 and a grain density of 2.77 g/cm^3 (the mean value determined for samples from core TUL89E-01, standard deviation 0.16). Grain size distribution, water content, and porosity data are included in Table 1.

Silt is predominant in six of the eight cores collected from Bute and Knight inlets. Of these, three (TUL89E-01, -02, -05) show an increase in sand content with depth while the others (TUL89E-03, -04, -07) generally contain less than 5 per cent sand and essentially are silts to muddy silts. The remaining two cores, TUL89E-06 from Knight Inlet and TUL89E-08 from Bute Inlet, contain abundant clay with subequal amounts of silt and relatively little sand. These relationships are illustrated in Figure 2.

Sediment type is related to seafloor morphology and to sediment characteristics as determined by 3.5 kHz profiling (Lewis and Bentkowski, 1991). Areas with abundant sand, such as the sites of cores TUL89E-01, -02 and -05, are characterized by a flat seafloor and the presence of a single diffuse reflector at 10 to 12 m which is continuous, as in Knight Inlet, or present only at the sides of the inlet, as in Bute Inlet. Sediments uniformly rich in silt, such as TUL89E-07, are stratified and characteristically show smooth, undulating seafloor surfaces. In some areas the stratified silts pass laterally and downward into noisy, structureless, gas-charged sediments.

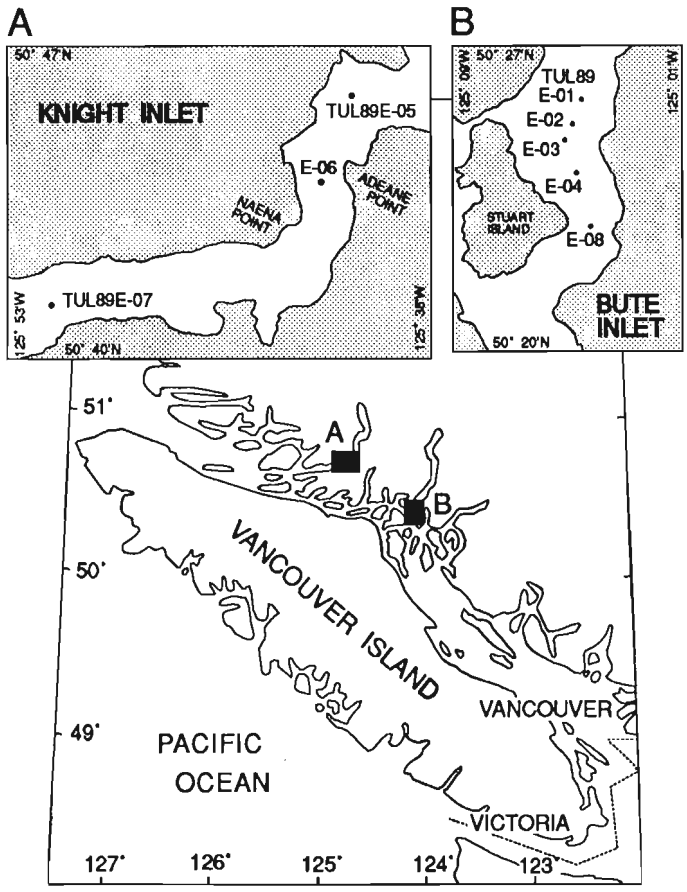

Figure 1. Location of cores in Knight and Bute inlets.

Cores, TUL89E-03, -04 and -08 from Bute Inlet and TUL89E-06 from Knight Inlet, are from the blocky sediment-mound fields. These areas are situated near and downslope from areas of undulating surface morphology and their surface expression varies from nearly flat with a few isolated mounds of low relief (TUL89E-03, -04), to isolated higher-relief mounds (TUL89E-06), to areas of ubiquitous high-relief blocky mounds with the characteristically hummocky seafloor surface (TUL89E-08).

Cores TUL89E-03 and -04 show continuous gradations in grain size from silt to muddy silt. Sediment characteristics obtained by 3.5 kHz profiling during lowering of the piston corer show the presence of a reflector in the upper 6 to 8 m of sediment (T.J. Lewis, pers. comm., 1990). Cross-channel profiles in this area also show diffuse to disrupted reflectors at 10 to 12 m and about 20 m. Core TUL89E-06 tends toward a bimodal grain size distribution and its sub-bottom profile is similar to those of cores TUL89E-03 and -04. Core TUL89E-08, however, exhibits a distinctly bimodal grain size distribution (Fig. 2). Subsurface reflections at this site are irregular with inclined to disrupted stratification occurring within metres of the sediment/water interface (Figure 5 in Lewis and Bentkowski, 1991).

It is significant that grain size distribution is related to seafloor morphology and sub-bottom sediment profiles. Flat seafloor surfaces and a single diffuse reflection occur at a depth of 10 to 12 m in areas with little clay and abundant sand. With increasing seafloor relief, sediments become

Table 1. Physical and geochemical properties of sediment samples recovered from Knight and Bute inlets.

Depth (cm)	Clay[1,2]	Silt[3]	Sand[4]	Water[1] Content	Porosity[5]	CH_4[6] (ppm)	CH_4[7] (ml/l)	Tmax[8] (°C)	TOC[1,8]	H[8] Index	O[8] Index	Cl[9] (mg/l)
TUL89E-01 Bute Inlet Lat. 50° 25.75' N, Long. 125° 04.53' W												
55	7	93	0	56	77	178	0.23	440	0.22	757	363	18400
155	24	73	3	48	71	2011	3.19	445	0.23	711	406	18700
255	29	54	17	45	69	1331	1.41	462	0.24	800	296	18300
355	29	60	11	46	69	592	0.52	386	0.27	793	348	18700
455	17	49	34	32	56	211	0.36	563	0.16	932	305	18100
555	13	47	40	28	51	143	0.17	566	0.14	804	179	18600
655	6	44	50	22	43	107	0.16	556	0.09	773	46	18100
TUL89E-02 Bute Inlet Lat. 50° 25.21' N, Long. 125° 04.84' W												
70	30	70	0	52	75	4071	4.38	500	0.23	798	336	18600
170	32	65	3	53	76	67953	31.53	387	0.39	724	321	18000
270	33	57	10	55	77	44961	33.05	394	0.53	780	308	18600
370	32	55	13	50	73	3099	3.12	377	0.41	808	357	18100
470	29	61	10	45	69	8905	8.84	388	0.29	764	421	18300
570	22	76	2	44	68	222	0.18	393	0.34	756	393	17800
670	30	51	19	41	65	3018	3.04	385	0.24	758	426	18300
770	21	68	11	31	56	37243	31.42	414	0.18	808	384	18000
TUL89E-03 Bute Inlet Lat. 50° 24.83' N, Long. 125° 05.09' W												
70	6	94	0	54	76	275	0.33	415	0.19	860	389	18300
170	27	72	1	46	70	13958	11.73	364	0.23	764	459	18800
270	30	61	9	46	70	3947	3.97	383	0.21	798	483	18100
370	42	56	2	49	73	4164	4.13	373	0.27	790	387	18100
470	22	71	7	66	84	61	0.05	387	1.22	439	363	17800
570	44	53	3	43	67	36850	36.13	386	0.28	618	401	18400
670	45	53	1	52	75	39087	31.70	386	0.72	448	260	17700
770	42	56	1	48	72	13111	11.19	384	0.48	599	292	18400
TUL89E-04 Bute Inlet Lat. 50° 24.08' N, Long. 125° 04.69' W												
70	19	80	1	74	89	461	0.31	381	1.31	622	291	18800
170	37	63	0	58	79	9555	8.48	386	0.88	418	221	18900
270	17	81	2	71	87	32496	25.13	406	1.47	419	409	18600
370	42	58	0	65	84	7880	5.97	377	0.63	792	435	18300
470	28	70	2	48	71	12399	11.65	395	0.77	395	392	18400
570	32	47	21	52	75	224	0.23	394	0.72	390	295	18200
670	38	61	1	62	82	44171	36.77	396	0.53	810	721	17600
770	31	67	2	59	80	257	0.17	383	0.95	585	336	17700
TUL89E-05 Knight Inlet Lat. 50° 45.86 'N, Long. 125° 40.07 'W												
70	23	77	0	50	73	120	0.12	420	0.18	932	657	18400
170	29	64	7	40	64	15808	17.13	412	0.14	947	776	18300
270	22	71	7	31	55	84	0.09	496	0.09	1055	656	18300
370	20	64	16	30	53	7	0.01	488	0.08	1056	681	18200
470	19	52	29	26	49	71	0.07	472	0.07	1143	657	18500
570	16	49	35	26	48	54	0.06	534	0.07	1079	543	18400
670	15	41	44	24	47	13	0.02	560	0.07	1085	521	18300
TUL89E-06 Knight Inlet Lat. 50° 43.95' N, Long. 125° 41.85' W												
70	53	35	12	54	76	384	0.31	373	0.22	859	903	18900
170	64	35	1	58	79	32179	29.03	373	0.32	844	469	18500
270	62	30	8	61	81	23456	27.79	371	0.37	760	565	18100
370	42	56	2	63	82	3860	4.41	370	0.37	804	639	18200
470	63	36	1	59	80	15572	15.46	374	0.32	818	575	18000
570	37	61	2	61	81	169	0.15	370	0.37	769	608	17400
TUL89E-07 Knight Inlet Lat. 50° 41.25' N, Long. 125° 51.43' W												
70	15	80	5	75	89	38919	39.52	374	0.87	783	414	17900
170	14	81	5	74	89	37027	54.32	381	1.53	507	204	17800
270	15	85	0	74	89	38351	50.91	375	1.36	544	260	17400
370	10	80	10	73	88	37677	47.94	380	1.51	492	248	17800
470	12	81	7	74	88	37747	49.29	375	1.07	604	309	17500
570	17	79	4	72	87	36923	47.71	374	1.13	602	318	17400
670	10	82	8	72	88	7741	9.38	379	1.09	540	310	17600
TUL89E-08 Knight Inlet Lat. 50° 22.85' N, Long. 125° 04.22' W												
70	46	40	14	77	90	39538	38.38	382	1.31	638	332	16600
170	50	35	15	73	88	46094	34.30	381	1.51	584	289	17400
270	48	40	12	73	88	43259	31.82	377	1.62	538	281	17300
370	50	39	11	73	88	46962	40.96	376	1.53	522	285	17100
470	19	67	14	71	87	223	0.13	379	1.34	600	325	17400
570	23	70	7	68	85	240	0.17	369	1.63	483	278	17200
670	18	70	12	70	86	1045	0.91	373	1.65	492	289	17800
770	21	75	4	67	85	61	0.05	374	1.4	573	315	17300
870	21	75	4	65	83	54	0.04	381	1.26	573	304	17500
970	37	63	0	52	74	141	0.12	381	0.42	810	507	17500
1070	24	67	9	69	86	358	0.29	383	1.52	493	328	17700

[1]Weight percent
[2]Clay: <2μm
[3]Silt: 2-62.5μm
[4]Sand: >62.5μm
[5]Volume percent
[6]Measured head space gas composition
[7]Calculated minimum in-situ CH_4 content
[8]Measured by Rock-Eval pyrolysis (Espitalié et al., 1977)
[9]Measured on porewater sample taken adjacent to head space gas sample.

muddier, sand is much less abundant and reflectors are disrupted. Sites with abundant blocky sediment mounds show irregular and disrupted sediments within metres of the seafloor. At the sites of cores TUL89E-06 and -08, attempts were made to penetrate elevated regions of the seafloor, although only core TUL89E-08 was confirmed, by 3.5 kHz imaging during lowering of the piston corer, to have penetrated a blocky mound. The high clay contents of these cores, their bimodal grain size distribution, and the observation that the greatest variation in the ratio of silt to clay occurs in the region of the blocky mounds, suggest that the mound areas may be sites of intermixing of sediments from two environments. The sands and sandy silts probably originate as distal turbidites (Bornhold and Prior, 1989) that are restricted to the inlet floors, while the finer grained silty muds observed within the blocky mound fields probably are typical of sediments deposited in elevated parts of the inlet floor, near the mouth of the inlet.

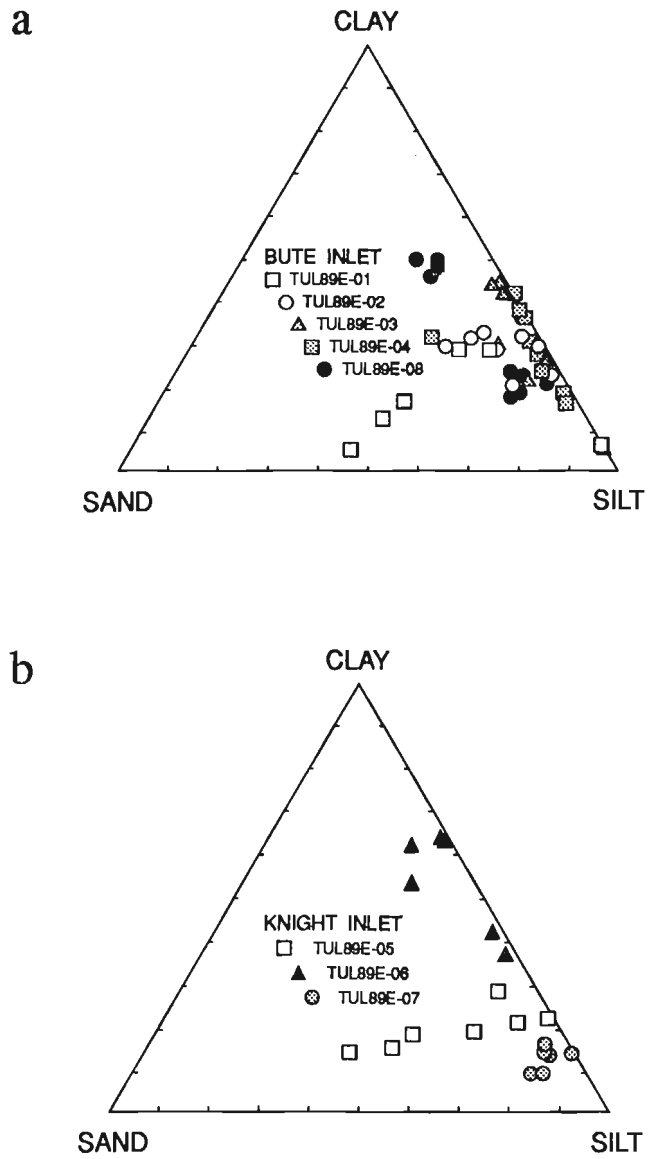

Figure 2. Grain size distribution for bottom sediments from Bute Inlet (a) and Knight Inlet (b).

ORGANIC MATERIAL

The composition of the organic material in the core sediment samples was determined by Rock-Eval pyrolysis (Espitalié et al., 1977; Snowdon, 1989). Results for all cores are presented in Table 1 and Figures 3a and b. Total organic carbon (TOC) measured in these sediments ranges from 0.07 to 1.83 weight per cent. The lowest TOC levels found are in sandy silts from cores TUL89E-01, and -05 (Table 1, Fig. 3a), which contain less than 0.25 % TOC. The higher TOC levels in cores TUL89E-02, -03 and -04 correspond with decreasing sand contents, and the highest TOC is found in core TUL89E-08, which has abundant clay. Core TUL89E-06 is an exception to this general trend. Samples from this core have the highest observed clay contents, but TOC only ranges from 0.22 to 0.37 %. Because clay is most abundant at the base of this core it may be glaciogenie, which would explain the low TOC values associated with these clayey sediments.

The nature of the organic material present in these samples can be deduced from Rock-Eval data. In Figure 3a, Tmax, which corresponds to the temperature of the maximum rate of hydrocarbon release during pyrolysis from 300 to 600°C, is plotted against TOC. Highest Tmax values were obtained for the organic material in cores with abundant sand, particularly cores TUL89E-01 and -05. Lower Tmax values, below 400°C, are restricted to cores with low sand contents. Organic material in the cores with abundant sand is characterized by Tmax values >400°C, which is consistent with the presence of oxidized and carbonized organic material (L.R. Snowdon, pers. comm., 1990). Samples with Tmax values less than about 400°C are from cores with abundant silt and clay; such values are typical of immature or unaltered organic material and probably reflect a local marine source for this type of organic carbon.

Further information concerning the origins of the various types of organic carbon are provided in Figure 3b, which shows the plot of Oxygen Index (OI) versus Hydrogen Index (HI). This is a pseudo-van Krevelen diagram (Snowdon, 1989) and may be used to differentiate organic matter type based on its chemical composition. The low TOC of the sand-rich sediments make interpretation of their OI-HI systematics unreliable. However, the high OI and HI values recorded for the silty and muddy sediments are consistent with a marine source for the organic material.

Organic carbon analysis supports the distinction made on the basis of grain size distribution between a coarser silty-sand facies and a finer silty-clay facies. The high Tmax values recorded for the coarser, turbiditic facies suggest that these sediments are oxidized and/or carbonized in the upper reaches of the inlet before being carried down its length by turbidity currents. The low Tmax values and high OI and HI values found for the organic carbon of the finer facies are consistent with a marine origin for this carbon and thereby support a local origin for this facies.

HEAD SPACE GAS ANALYSIS

Methods

Piston coring was done using a 10 cm diameter core tube and samples were taken at one metre intervals for head space gas analysis. Gas samples were collected soon after the core was cut. The sampling procedure involved inserting a 10 cm length of 6.7 cm diameter tubing into the centre of the larger core tube in an attempt to use a constant sampling volume. This proved to be unsuccessful. Instead, the mass of the sediment and the water were determined by weighing and the volume of head space gas was calculated using the known

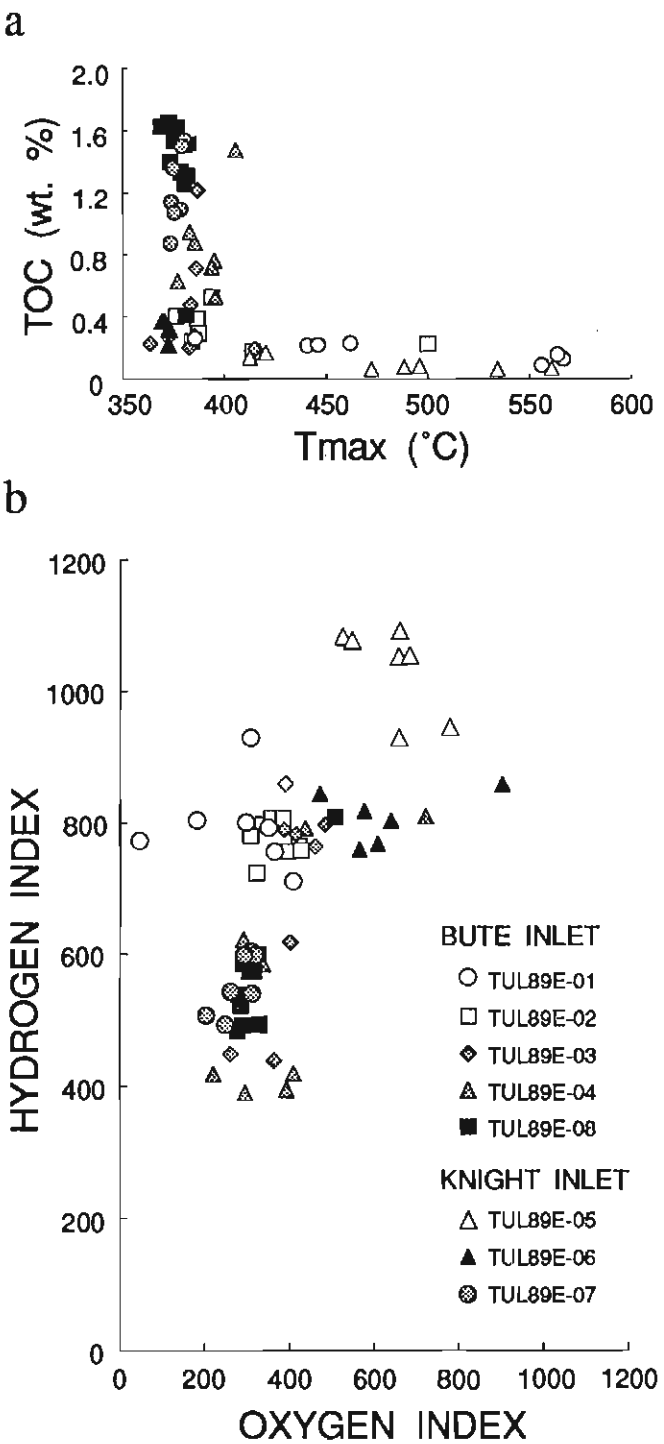

Figure 3. Results of organic carbon analyses by Rock-Eval pyrolysis for samples from Bute and Knight inlets.
a. Tmax versus TOC showing differences between sandy cores (open samples), silts (shaded) and clayey silts (black).
b. Oxygen Index versus Hydrogen Index.

masses of sediment and water, measured grain density, and tabulated values for seawater density.

Gas sample containers were refrigerated and shipped to Geochem Laboratories Ltd., Calgary, for analysis of head space hydrocarbon gases. Samples were analysed for C_1 to C_7 alkanes and alkenes by gas chromatography. In all but two samples, which contained approximately 1 ppm of propane and/or isobutane, the hydrocarbon gases comprised CH_4 exclusively. Additional gas samples that were collected in gas-tight syringes from holes drilled in the core prior to cutting the core tube, were analyzed by gas chromatography and found to contain greater than 1 ppm of all C_1 to C_4 and C_6 alkanes and alkenes, and up to 167 ppm butene (G. Ginsburg, pers. comm., 1990). The reason for the absence of hydrocarbon gases $>C_1$ in the head space gas samples is not known, although procedures followed elsewhere (Burke et al., 1981) include the addition of a sodium azide solution to stop all biological activity — this was not done here. It is not known whether biological activity during storage would have promoted the destruction of all hydrocarbon gases $>C_1$.

The concentrations of CH_4 in the head space gas samples are given in ppm in Table 1. Using these data, the concentrations of CH_4 in pore waters under in situ conditions were calculated by the following method. The volume of CH_4 in the head space was calculated from the measured CH_4 concentration and the head space volume. The partial pressure of CH_4 was then calculated assuming that N_2 and O_2, in atmospheric proportions, were the only significant gaseous species present in addition to CH_4. The volume of CH_4 remaining in the pore water was calculated for laboratory conditions of 100 kPa and 22°C assuming ideal gas behaviour and using the calculated partial pressure of CH_4, the Bunsen coefficient equation of Yamamoto et al. (1976) for methane solubility in seawater, and the equations of Wiesenburg and Guinasso (1979):

$$S(‰) = 1.80655(Cl‰), \quad (1)$$

where $S(‰)$ is salinity and $(Cl‰)$ is measured pore water Cl concentrations, and

$$C^* = (\beta P_G) \quad (2)$$

where C^* is the concentration of gas in solution, β is the Bunsen coefficient and P_G is the partial pressure of the specified gas. This calculation does not take into account the effect of pressure on the solubility of CH_4 in seawater. Data of Michels et al. (1936) reported by Onda et al. (1970) show, however, that pressures of up to 200 atmospheres do not significantly affect the solubility of methane in NaCl solutions, which tends to validate the approach used here.

The volumes of CH_4 in the head space and pore water were summed and, using the ideal gas law, the volume of CH_4 present in the pore water was calculated at the in situ temperatures reported by Lewis and Bentkowski (1991). The maximum dissolved methane concentration in pore waters under in situ (8°C) conditions, which is shown in Figures 4a and b, was calculated in a similar manner with the additional simplifying assumption that the in situ gas is composed entirely of CH_4.

Results

Concentrations of CH_4 are highest in pore waters from organic-rich silts and muds and are lowest in pore waters from organic-poor sandy silts (Figures 4a and b, respectively). The highest concentrations of CH_4 in pore waters exceed saturation values for in situ conditions of 8°C. This is supported by abundant evidence of the accumulation of gas in layers and diffuse zones in bottom sediments from Knight and Bute inlets (Lewis and Bentkowski, 1991). Gas bubbles can only exist if their associated pore waters are saturated with CH_4.

In Bute Inlet, CH_4 concentrations vary systematically with depth. In cores TUL89E-01 to -04, two zones of elevated CH_4 concentrations were observed. In the uppermost one metre of these cores CH_4 concentrations are low, but rise in the next 1 to 2 m below this depth. At 1.7 m in core TUL89E-02, CH_4 concentration is close to saturation values. The other cores (TUL89E-01, -03, -04) do not show evidence of CH_4 saturation in this upper zone. In all four cores CH_4 concentrations drop to lower values below this upper zone but, in three cores (TUL89E-02 to -04), the concentrations again rise to saturation values below 4 to 5 m. Isotopic data from this zone show $\delta^{13}C$ of CH_4 to be between -84 and -90‰, which confirms its biogenic origin (G. Ginsburg, pers. comm., 1990). No vertical permeability barriers to gas escape were observed at this depth and the origin of the second zone of elevated CH_4 concentration is not yet fully understood. These high methane concentrations, however, may explain the near-surface reflector observed at about 6 to 8 m during lowering of the piston corer at the site of core TUL89E-03. Elsewhere in Bute Inlet, core TUL89E-08 shows a different pattern of CH_4 enrichment. The upper 4 m of this core are saturated with CH_4, but below this depth CH_4 is virtually absent. The abrupt decline in CH_4 concentration in this core is correlated with an abrupt increase in grain size, as illustrated in Figure 5.

Methane concentration data from Knight Inlet (Fig. 4b), show similar patterns to those from Bute Inlet, with the exception of core TUL89E-07, which shows CH_4 saturation throughout the first 6 m of core. Cores TUL89E-05 and -06 do not reach saturation levels, and only core TUL89E-06 shows evidence of a second, weak, CH_4-enriched zone at about 5 m. The thick zone of elevated CH_4 concentrations in core TUL89E-07 corresponds to a noisy, structureless zone observed in 3.5 kHz profiles (Lewis and Bentkowski, 1991), which is consistent with the presence of gas bubbles and CH_4-saturated pore waters in this core.

DISCUSSION AND CONCLUSIONS

Origin of the blocky mounds

Sub-bottom 3.5 kHz profiling clearly documents that core TUL89E-08 was located within a blocky sediment mound. The vertical profile of grain size distribution and CH_4 concentrations in pore waters from core TUL89E-08 (Fig. 5) show a discontinuity in sediment properties at about 4 m, unlike the gradational changes in grain size observed in other cores. At this discontinuity, an abrupt 30 per cent decrease

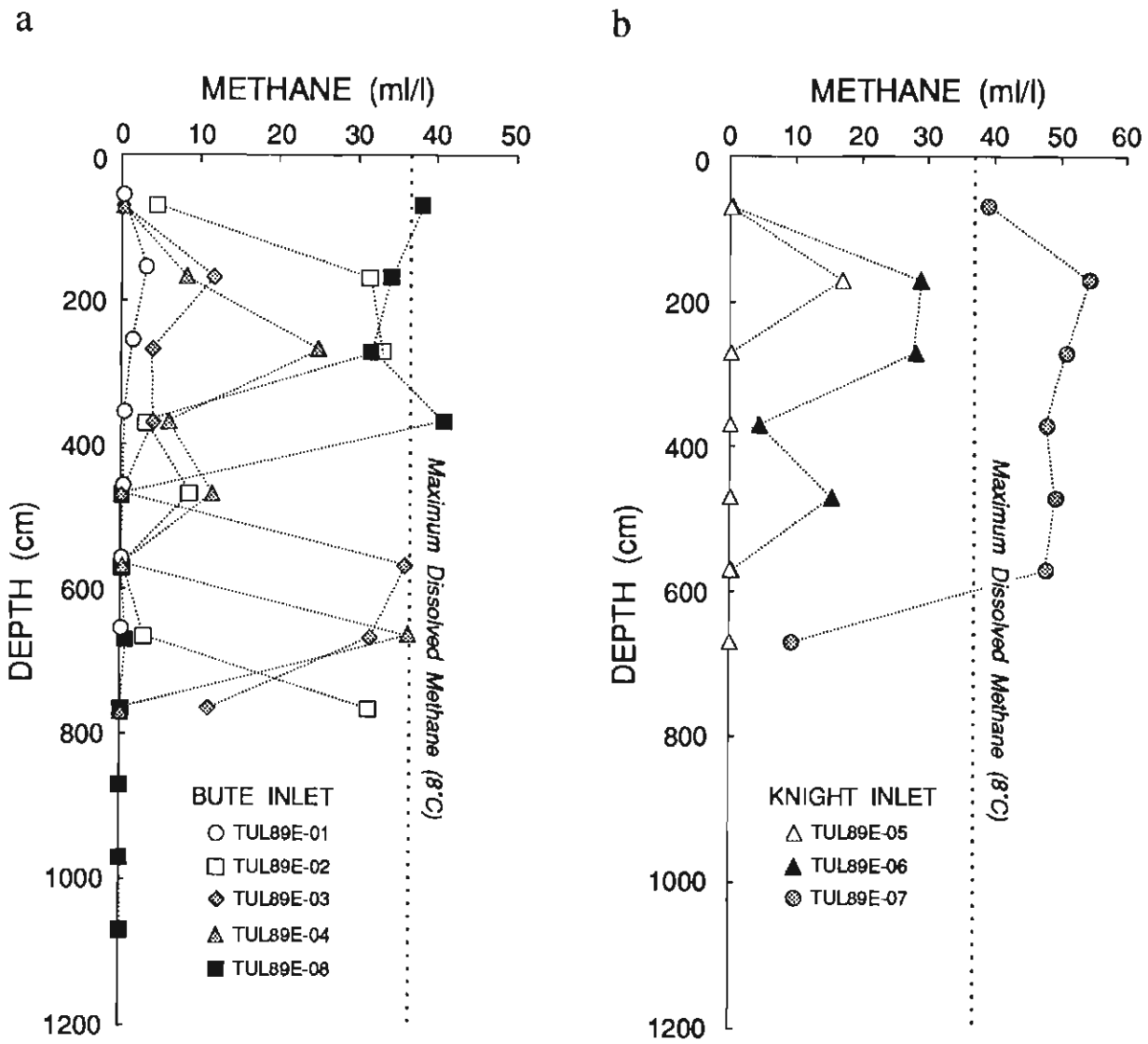

Figure 4. In situ CH_4 compositions of pore waters from Bute and Knight inlets. The vertical lines show maximum dissolved CH_4 values at 8°C for measured pore water compositions. The dashed lines joining data points are for reference purposes only.

in clay content and a reduction of CH_4 concentrations from saturation to near-zero values is observed over a one metre interval. However, porosity changes across the boundary are negligible and, with one exception, TOC values show similar ranges above and below the discontinuity.

No data consistent with either the sediment liquefaction or gas hydrate models of mound formation were discovered. The presence of gas hydrates would probably have been observed upon recovering the core, and would have been apparent on analysis of the pore waters. All pore waters have normal salinities. No freshening of the pore waters, which would be expected upon decomposition of gas hydrates, was observed. The data obtained do, however, show evidence of processes that cannot be explained by either model, such as the extreme variation in grain size distribution.

The favoured model for origin of the blocky mounds has been developed by integrating geological, geochemical, and geophysical data from the mound areas. The occurrence of the mounds in the deepest parts of the inlets and their proximity to elevated regions of the inlet floor suggest that the mounds are coherent blocks of sediment that had become detached from the elevated areas and were moved on submarine slides to their present positions in the deepest parts of the inlets. The sliding of large coherent blocks would undoubtedly be accompanied by the movement of abundant unconsolidated and comminuted sediments, which explains the wide variations in the ratio of silt to clay observed in the blocky mound areas. However, only where a slide block came to rest would bimodal grain size distributions be observed within any one particular core. This model also explains the presence of calcite concretions dated at 6420 ±130 BP (Bornhold and Prior, 1989) at the surface of a blocky mound. If the lower, slightly consolidated sediments of the block remained intact during sliding while the upper sediments were stripped off, it is possible that previously buried sediments would be exposed at the seafloor.

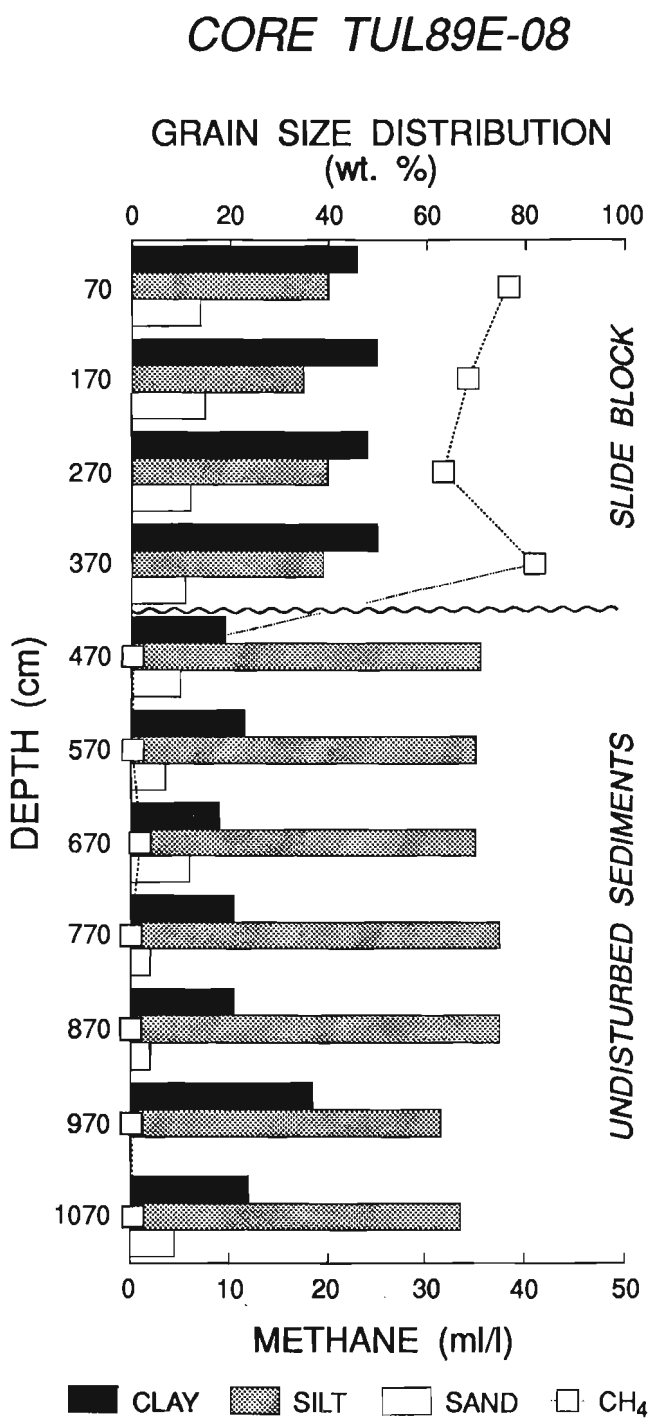

Figure 5. Vertical profile of grain size distribution and methane concentrations in pore waters from core TUL89E-08, Bute Inlet. The wavy horizontal line marks the boundary between the upper CH_4-saturated clayey silts and the lower gas-poor silts, and is interpreted as marking the boundary between autochthonous sediments and an allochthonous slide block.

Controls on methane distribution

The primary control on the distribution of CH_4 in sediments from Bute and Knight inlets is the type and abundance of organic matter. Coarser sandy silts, which are found in cores TUL89E-01 and TUL89E-05, contain less than 0.25 % TOC composed largely of oxidized and carbonized organic material. Methane concentrations in these cores show that this type of organic material is unfavourable for the generation of biogenic CH_4. Highest CH_4 concentrations occur in cores from the blocky sediment mound areas and in cores from gas-charged sediments that occur in elevated parts of the inlet floor. Sediments in these locations show a variety of grain sizes, but all contain organic material of marine origin, which is favourable for the production of biogenic CH_4.

Calculations of in situ CH_4 contents of bottom sediments from head space gas analysis data show that the maximum CH_4 contents of these samples exceed saturation values for in situ conditions. Core samples with CH_4 concentrations greater than saturation values are from regions where 3.5 kHz profiling indicates the presence of gas bubbles in the sediments. The close correspondence between geophysical evidence of saturation of pore waters with CH_4, and the documented saturation of CH_4 under in situ conditions, suggests that in situ CH_4 saturation of pore waters can be monitored reliably by determining the saturation state of CH_4 in head space gas samples.

ACKNOWLEDGMENTS

We gratefully acknowledge G. Jewsbury, W. Bentkowski, A. Judge, and G. Ginsburg for their assistance at sea and at PGC. We would also like to thank G. Ginsburg for analyses of gas compositions and isotopic ratios, Trevor Lewis for the invitation to participate in the cruise, and the captain and crew of C.S.S. Tully. Lloyd Snowdon is thanked for reviewing the paper and providing insights into the systematics and interpretation of Rock-Eval data.

REFERENCES

Bornhold, B.D. and Prior, D.B.
1989: Sediment blocks on the sea floor in British Columbia Fjords; Geo-Marine Letters, v. 9, p. 135-144.

Burke, R.A. Jr., Brooks, J.M., and Sackett, W.M.
1981: Light hydrocarbons in Red Sea brines and sediments; Geochimica et Cosmochimica Acta, v. 45, p. 627-634.

Espitalié, J., Laporte, J.L., Madec, M., Marquis, F., Leplat, P., Paulet, J., and Boutefeu, A.
1977: Méthode rapide de caractérisation des roches mères, de leur potentiel pétrolier et de leur degré d'évolution; Revue de L'Insitut Français du Pétrole, v. 32/1, p. 23-42.

Green, A.J.
1981: Particle-size analysis; in Manual on Soil Sampling and Methods of Analysis, J.A. McKeague (ed); Subcommittee on Methods of Analysis, Canadian Soil Survey Committee, p. 4-32.

Lewis, T.J. and Bentkowski, W.H.
1991: Blocky sediments in Bute and Knight inlets, British Columbia; in Current Research, Part A, Geological Survey of Canada, Paper 91-1A.

Michels, A., Gerver, J., and Bijl, A.
1936: Title unknown. Physica, v. 3, p. 797.

Onda, K., Sada, A., Kobayashi, T., Kito, S., and Ito, K.
1970: Salting-out parameters of gas solubility in aqueous salt solutions; Journal of Chemical Engineering of Japan, v. 3, p. 18-24.

Snowdon, L.R.
1989: Organic matter properties and thermal evolution; in Short Course on Burial Diagenesis, I.E. Hutcheon (ed.); Mineralogical Association of Canada, Short Course Handbook, v. 15, p. 39-60.

Wiesenburg, D.A. and Guinasso, N.L. Jr.
1979: Equilibrium solubilities of methane, carbon monoxide, and hydrogen in water and seawater; Journal of Chemical and Engineering Data, v. 24, p. 356-360.

Yamamoto, S., Alcauskas, J.B., and Crozier, T.E.
1976: Solubility of methane in distilled water and seawater; Journal of Chemical and Engineering Data, v. 21, p. 78-80.

Summary of 1990 studies of the Queen Charlotte Islands Frontier Geoscience Project, British Columbia

James W. Haggart
Cordilleran Division, Vancouver

Haggart, J.W., Summary of 1990 studies of the Queen Charlotte Islands Frontier Geoscience Project, British Columbia; in Current Research, Part A, Geological Survey of Canada, Paper 91-1A, p. 317-320, 1991.

INTRODUCTION

Reflecting on the large number of participants and the resultant geological advances made in the initial years (1987-1988) of the Queen Charlotte Islands Frontier Geoscience Project (QCI FGP), it is tempting to suggest that the basic geological and geophysical investigations of the islands and adjacent offshore region were completed at that time. However, as indicated by the papers that follow, such is most certainly not the case. Each year the islands offer new geological surprises. In fact, observations made during the 1990 field season fundamentally affect interpretations of the geological history of the islands and associated offshore region. Several of the important new geological advances detailed in the papers that follow are briefly summarized below.

Public involvement by members the QCI FGP was extensive in 1990. Staff of the Cordilleran Division of the Geological Survey of Canada worked with officers of the infant South Moresby Reserve to develop geology exhibits for the park's new information centres. It is hoped that this collaboration will grow into a continuing and fruitful association. Interviews and several public evenings held at a museum and town halls attracted great interest and substantial audiences, as the locals came down to find out "just what the geologists do." Many citizens initially expressed concern that the scientific studies undertaken by the Geological Survey would lead, ultimately, to environmental degradation in the region. In most instances such concern turned into appreciation, for the quality of scientific research that the Geological Survey is undertaking and the role that we play in providing the public with basic geological information.

Résumé des études de 1990 du projet géoscientifique des régions pionnières des îles de la Reine-Charlotte

James W. Haggart
Division de la Cordillière, Vancouver

Haggart, James W. Résumé des études de 1990 du projet géoscientifique des régions pionnières des îles de la Reine-Charlotte, Colombie Britannique, dans Recherches en cours, Partie A, Commission géologique du Canada, Étude 91-1A, p. 317-320, 1991.

INTRODUCTION

Si l'on considère le grand nombre de participants et les progrès géologiques accomplis au cours des premières années (1987-1988) de mise en oeuvre du Projet géoscientifique des régions pionnières dans les îles de la Reine-Charlotte (PGRP-IRC), on est tenté de conclure que les recherches géologiques et géophysiques de base dans les îles et la région extracôtière adjacente ont été complétées à cette époque. Cependant, comme l'indiquent les documents qui suivent, tel n'est certainement pas le cas. Chaque année, ces îles offrent de nouvelles surprises en ce qui a trait à leur géologie. De fait, les observations faites au cours de la saison 1990 modifient fondamentalement les interprétations de l'histoire géologique des îles et de la région extracôtière associée. Plusieurs des nouveaux faits géologiques importants présentés en détail dans les documents qui suivent sont résumés ci-dessous.

En 1990, les membres du PGRP-IRC ont joué un rôle public important. Le personnel de la Division de la Cordillère de la Commission géologique du Canada a collaboré avec les représentants de la nouvelle réserve de Moresby-Sud afin de préparer des expositions sur la géologie à l'intention des nouveaux centres d'information du parc. Il est à espérer que cette collaboration se transforme en une association continue et fructueuse. Des entrevues et plusieurs soirées d'information du public tenues à un musée et à différents hôtels de ville ont soulevé beaucoup d'intérêt et attiré des assistances nombreuses, les gens de la région étant désireux de s'informer du travail des géologues. De nombreux citoyens ont d'abord exprimé leurs préoccupations face aux études scientifiques entreprises par la Commission géologique qui, selon eux, finiraient par détruire l'environnement de la région. Dans la plupart des cas, ces préoccupations ont laissé place à une prise de conscience de la qualité de la recherche scientifique accomplie par la Commission géologique et du rôle qu'elle joue à renseigner le grand public sur la géologie de base.

An attempt by Survey staff to develop a recycling program with local communities was premature. However, the field party did manage to recycle a substantial quantity of its leftovers, including newspapers, aluminum and tin cans, paper, metal, glass, and plastic, thereby minimizing the impact on local refuse facilities. Hopefully, the interest generated by these efforts will lead to an enhancement of community participation in the future.

STRATIGRAPHY AND SEDIMENTOLOGY

New stratigraphic units were identified at several localities in the islands during 1990, including the first positive identification of Paleozoic strata in the Queen Charlotte Islands. Jonny Hesthammer, Jarand Indrelid, Peter Lewis and Mike Orchard describe a carbonate and chert succession of Permian and possible Carboniferous age which is lithologically similar to late Paleozoic Buttle Lake rocks of Vancouver Island. The identification of Permian rocks in the Queen Charlotte Islands expands the known distribution of Permian strata in the Insular Belt and attests to the integral nature of Permian strata within the Wrangellia Terrane.

Possibly related to the Permian sequence, new lithologies of volcanic rocks have also been identified from the islands' west coast, in geographic association with the Karmutsen Formation volcanic sequence. Indrelid and Hesthammer describe these rocks and suggest that they may be correlative with the Late Paleozoic Sicker Group volcanic succession of Vancouver Island.

Beautifully-preserved radiolarians from the lower Middle Jurassic Phantom Creek Formation are the subject of the paper by Beth Carter and Giselle Jakobs. The radiolarians were discovered in association with ammonites not previously identified from the Queen Charlotte Islands but which are very useful in limiting the age of the microfossil assemblage. The radiolarians are preliminarily described in the report and the implications of the fauna to the development of a radiolarian biostratigraphic zonation for the northeast Pacific region are assessed.

The stratigraphy and lithology of the Middle Jurassic Yakoun Group rocks are extensively discussed in two contributions. Hesthammer describes the diverse lithologies of volcanic strata and interstratified volcanic-rich sedimentary rocks which characterize the group in the central part of Graham Island, including several lithologies not previously recognized in the Yakoun Group. Jim Haggart describes sections correlated with the Yakoun Group from Lyell Island and the northwest coast of Graham Island, this latter locality significantly expanding the known geographic distribution of the Yakoun Group.

A new stratigraphic scheme for Cretaceous strata of the islands is informally proposed by Haggart, Susan Taite, Indrelid, Hesthammer and Lewis. The scheme was developed

Il était prématuré de la part du personnel de la Commission d'élaborer un programme de recyclage avec les agglomérations locales. Toutefois, le groupe de travail sur le terrain a réussi à recycler une grande quantité de ses déchets, notamment le papier journal, les canettes d'aluminium et de fer blanc, le papier, le métal, le verre et le plastique, minimisant ainsi les répercussions sur les installations locales d'entreposage des déchets. Espérons que l'intérêt soulevé par ces activités se traduira par une augmentation de la participation communautaire dans l'avenir.

STRATIGRAPHIE ET SÉDIMENTOLOGIE

En 1990, on a identifié de nouvelles unités stratigraphiques à plusieurs endroits dans les îles, notamment des couches paléozoïques que l'on n'avait pas encore découvertes dans les îles de la Reine-Charlotte. Jonny Hesthammer, Jarand Indrelid, Peter Lewis et Mike Orchard décrivent une succession de roches carbonatées et de chert d'âge permien et peut-être carbonifère dont la lithologie est semblable à celle des roches de Buttle Lake de la fin du Paléozoïque dans l'île de Vancouver. La présence de roches permiennes dans les îles de la Reine-Charlotte élargit la répartition connue des couches permiennes dans la zone insulaire et témoigne de la nature intégrale des couches permiennes au sein du terrane de Wrangellia.

De nouvelles lithologies de roches volcaniques, probablement liées à la séquence permienne, ont également été relevées dans le littoral occidental des îles, en association géographique avec la séquence volcanique de la formation de Karmutsen. Indrelid et Hesthammer décrivent ces roches et établissent une corrélation possible entre elles et la succession volcanique du groupe de Sicker du Paléozoïque tardif dans l'île de Vancouver.

Les radiolaires superbement conservés de la formation de Phantom Creek de la base du Jurassique moyen sont traités dans le document de Beth Carter et Giselle Jakobs. Ces radiolaires sont associés à des ammonites qui n'avaient pas encore été relevés dans les îles de la Reine-Charlotte mais qui s'avèrent très utiles lorsqu'il s'agit de définir l'âge de l'assemblage de microfossiles. Le rapport présente une description préliminaire des radiolaires et une évaluation des répercussions de la faune sur la formation d'une zonation biostratigraphique des radiolaires dans la région du nord-est du Pacifique.

Dans deux documents, il est abondamment question de la stratigraphie et de la lithologie des roches du groupe de Yakoun du Jurassique moyen. Hesthammer décrit les diverses lithologies des couches volcaniques et des roches sédimentaires interstratifiées riches en roches volcaniques qui caractérisent le groupe dans la partie centrale de l'île Graham, y compris plusieurs lithologies qui viennent d'être découvertes dans le groupe de Yakoun. Jim Haggart décrit des coupes corrélées au groupe de Yakoun dans l'île Lyell et le littoral nord-ouest de l'île Graham; les découvertes à ce dernier endroit permettent d'élargir considérablement la répartition géographique connue du groupe de Yakoun.

Un nouveau schéma stratigraphique des couches crétacées dans les îles est proposé de façon officieuse par Haggart, Susan Taite, Indrelid, Hesthammer et Lewis. Ce schéma

in response to the need for a more useful mapping stratigraphy and to reflect the new stratigraphic interpretations of the Cretaceous rocks as revealed by molluscan biostratigraphic studies. The proposed scheme is based solely on outcrop lithology and does not require fossil control to identify the stratigraphic unit. This stratigraphic scheme is utilized in Open-File reports detailing the mapping undertaken during the field season.

Aspects of the sedimentology of the Cretaceous rocks are addressed by Charle Gamba. Gamba has identified structures in the type section of the Honna Formation indicative of storm-event deposition, revitalizing the theory of a shallow-water origin for the Honna Formation which was popular in previous years.

GEOLOGICAL MAPPING

The geological mapping program moved into logistically-demanding areas in 1990. Most areas mapped were not accessible by logging road, as was much of the ground covered by earlier FGP mapping efforts. Jonny Hesthammer, Jarand Indrelid, Peter Lewis and Susan Taite deserve special commendation for their strong efforts in mapping the precipitous rainforest terrain of the west coast, and the mountain crest of the islands.

Mapping covered significant new areas and filled in gaps with other, previously-mapped regions (Fig. 1). Along the crest of the islands northeast of Rennell Sound, older Tertiary volcanic rocks were found to blanket a wide area. These rocks unconformably overlie an extensive and previously unrecognized belt of Cretaceous rocks, a continuation of the Cretaceous outcrop belt seen farther to the south, near Mount Stapleton.

The volcanic strata which form the massif of Mount Stapleton were also identified on central Louise Island and northern Graham Island, these rocks previously mapped as Cretaceous sedimentary rocks. The widespread and lithologically-diverse volcanic rocks suggest that the Tertiary magmatic history of the islands is exceedingly complex.

Regional mapping in other parts of the islands has identified structural styles not widely recognized previously. Working in the vicinity of Burnaby Island, Lewis has determined that Tertiary movement along the north-south trending Louscoone Inlet fault system has had a significant dextral strike-slip component. Strike-slip offsets of similar magnitudes have not previously been recognized in the more northerly parts of the islands. Lewis compares the geometries seen onshore with possible structural trends observed in the adjacent offshore region.

a été élaboré pour répondre aux besoins d'une stratigraphie mieux adaptée et plus utile à la cartographie et pour mieux traduire les nouvelles interprétations stratigraphiques des roches crétacées révélées par les études biostratigraphiques des mollusques. Le schéma proposé est fondé uniquement sur la lithologie des affleurements et ne requiert pas la présence de fossiles pour identifier les unités stratigraphiques. Ce schéma stratigraphique est utilisé dans des rapports de la série des Dossiers publics qui présentent en détail la cartographie entreprise au cours des travaux sur le terrain.

Certains aspects de la sédimentologie des roches crétacées sont abordés par Charle Gamba. Celui-ci a identifié des structures dans le stratotype de la formation de Honna, indicatrices d'une sédimentation dans des conditions de tempête ; cette découverte lui permet de reprendre une ancienne théorie selon laquelle la formation de Honna se serait accumulée en milieu épicontinental.

CARTOGRAPHIE GÉOLOGIQUE

En 1990, le programme de cartographie géologique a couvert des zones difficiles sur le plan logistique. La plupart des zones cartographiées n'étaient pas accessibles par les chemins forestiers tout comme une grande partie des terres qui avaient été cartographiées au cours de travaux précédents du PGRP. Les travaux importants de cartographie de la zone forestière ombrophile de la côte ouest et de la crête montagneuse des îles accomplis par Jonny Hesthammer, Jarand Indrelid, Peter Lewis et Susan Taite méritent d'être soulignés de façon spéciale.

Les travaux de cartographie ont couvert de nouvelles zones de grande étendue et ont permis de combler les vides au niveau d'autres régions précédemment cartographiées (Fig. 1). Le long de la crête des îles, au nord-est du détroit de Rennell, des roches volcaniques tertiaires plus anciennes s'étendent sur une vaste région. Elles reposent en discordance sur une grande zone de roches crétacées non identifiées jusqu'ici, qui est un prolongement de la zone d'affleurement crétacée aperçue plus loin au sud, près du mont Stapleton.

Les couches volcaniques qui forment le massif du mont Stapleton se retrouvent également dans le centre de l'île Louise et dans le nord de l'île Graham ; ces roches avaient auparavant été cartographiées comme des roches sédimentaires du Crétacé. Le fait que les roches volcaniques soient répandues et présentent une lithologie diversifiée porte à croire que l'évolution magmatique des îles au Tertiaire a été des plus complexes.

La cartographie régionale dans d'autres parties des îles a permis de relever des styles structuraux qui n'avaient pas été largement identifiés dans le passé. Alors qu'il travaillait dans les environs de l'île Burnaby, Lewis a déterminé que le déplacement tertiaire le long du système de failles de Louscoone Inlet, à direction nord-sud, comportait un important décrochement dextre. On n'avait pas auparavant relevé de décalages par décrochement aussi importants dans les parties les plus septentrionnales des îles. Lewis compare les géométries observées sur le littoral avec les directions structurales possibles de la région extracôtière adjacente.

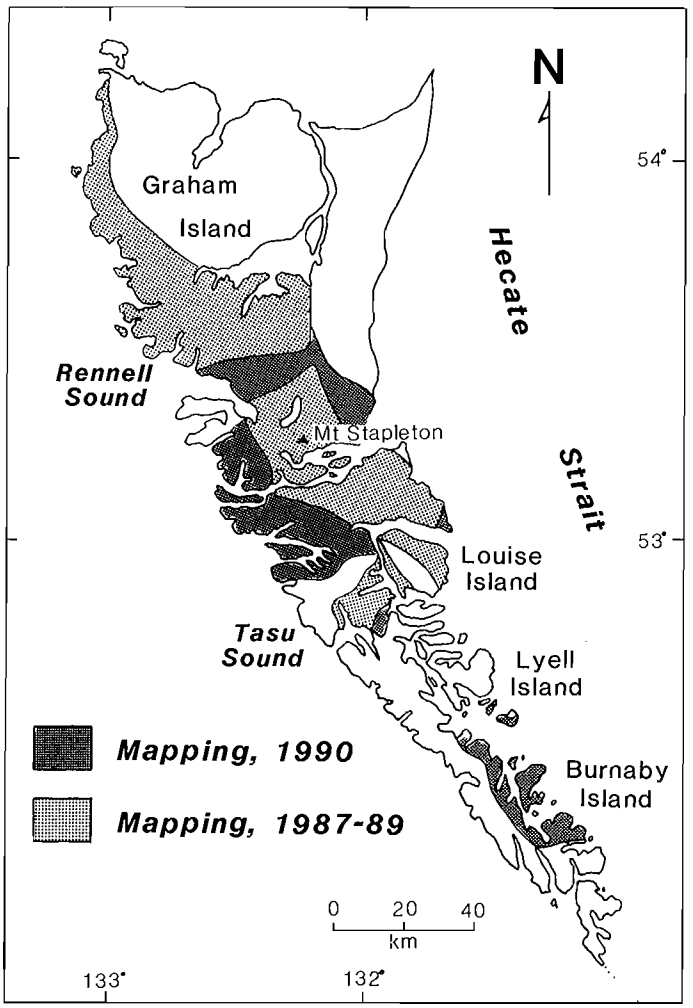

Figure 1. Geological mapping undertaken by the Geological Survey of Canada in the Queen Charlotte Islands, British Columbia, under the QCI FGP.

Figure 1. Cartographie géologique entreprise par la Commission géologique du Canada dans les îles de la Reine-Charlotte (Colombie-Britannique) dans le cadre du PGRP-IRC.

To the north, in the Sewell Inlet-Tasu Sound area, multiple fault trends have been identified. Taite interprets this complex structural pattern as reflecting an interaction, in this critical part of the islands, of the diverse structural styles which typically characterize other areas. Taite recognizes both the later Jurassic block faulting event identified previously in the central part of the islands, as well as trends likely associated with the Tertiary strike-slip regime observed to the south and east by Lewis.

Mapping has not been restricted to the onshore region. Henry Lyatsky has taken a fresh look at geophysical data from the offshore basin and concluded that modelling of the Tertiary basin fill is likely more complex than previously considered: the presence of numerous volcanic units within the succession mask the depth to acoustic basement of the Tertiary sequence. Lyatsky concludes that interpretation of the structural and stratigraphic history of the offshore basin will be facilitated by an integrated geophysical and geological program.

Au nord, dans la zone de l'inlet Sewell et du détroit de Tasu, on a identifié des directions de failles multiples. Taite interprète cette configuration structurale complexe comme étant le reflet, dans cette partie cruciale des îles, d'une interaction des divers styles structuraux caractérisant d'autres zones. Taite fait état non seulement du morcellement par failles plus récent du Jurassique, identifié précédemment dans la partie centrale des îles, mais également des directions vraisemblablement associées au régime de décrochement tertiaire observé au sud et à l'est par Lewis.

La région littorale n'a pas été la seule région cartographiée. Henry Lyatsky a examiné de nouveau les données géophysiques recueillies dans le bassin extracôtier et en a conclu que la modélisation du remplissage du bassin au Tertiaire est probablement plus complexe qu'on ne l'avait cru: la présence de nombreuses unités volcaniques au sein de la succession masque la profondeur du socle acoustique de la séquence tertiaire. Lyatsky conclut que l'interprétation de l'histoire structurale et stratigraphique du bassin extracôtier peut être facilitée par la mise en oeuvre d'un programme géophysique et géologique intégré.

Permian strata on the Queen Charlotte Islands, British Columbia[1]

J. Hesthammer[2], J. Indrelid[2], P.D. Lewis[2], and M.J. Orchard
Cordilleran Division, Vancouver

Hesthammer, J., Indrelid, J., Lewis, P.D., and Orchard, M.J., Permian strata on the Queen Charlotte Islands, British Columbia; in Current Research, Part A, Geological Survey of Canada, Paper 91-1A, p. 321-329, 1991.

Abstract

During the summer of 1990, several sedimentary successions underlying the Karmutsen Formation on northwestern Moresby Island, Queen Charlotte Islands, were located. Two of these locations have yielded Permian and possibly Carboniferous conodonts. These rocks comprise interlayered limestone, dolomite, and chert (the "carbonate-chert unit"), and are lithologically similar to parts of the Paleozoic Buttle Lake Group on Vancouver Island. At one locality an unconformity between the "carbonate-chert unit" and the Karmutsen Formation was observed. Occurrence of Permian strata in Wrangellian assemblages in Oregon, Vancouver Island, Alaska, and now the Queen Charlotte Islands, indicate that this succession is more extensive than documented earlier.

Résumé

Pendant l'été de 1990, plusieurs successions sédimentaires sous-jacentes à la formation de Karmutsen ont été localisées dans la partie nord-ouest de l'île Moresby de l'archipel de la Reine-Charlotte. En deux endroits de ces emplacements on a relevé des conodontes du Permien et peut-être du Carbonifère. Les roches qui les renferment consistent en calcaire, en dolomie et en chert interstratifiés («carbonate-chert unit») et sont lithologiquement similaires à celles de parties du groupe paléozoïque de Butte Lake sur l'île de Vancouver. À un endroit, une discordance a été observée entre la «carbonate-chert unit» et la formation de Karmutsen. La présence de couches du Permien dans des assemblages wrangelliens en Orégon, sur l'île de Vancouver, en Alaska et maintenant dans les îles de la Reine-Charlotte indique que cette succession est plus répandue que ne le laissait croire les connaissance antérieures.

[1] Contribution to the Frontier Geoscience Program
[2] Department of Geological Sciences, University of British Columbia, 6339 Stores Road, Vancouver, B.C. V6T 2B4

INTRODUCTION

Wrangellian strata on the Queen Charlotte Islands comprise a 5+ km thick sequence of volcanic and sedimentary rocks. Prior to the 1990 field season, the oldest known rocks in this sequence were Upper Triassic submarine volcanic rocks of the Karmutsen Formation, although several workers recognized hints of older underlying strata (Sutherland Brown, 1968; Barker et al., 1989; Anderson and Reichenbach, 1991). In more southerly parts of Wrangellia, on Vancouver Island, the Karmutsen Formation lies on Upper Paleozoic arc-related volcanic and sedimentary rocks (Muller, 1980); the equivalent pre-Triassic rocks may be exposed on the Queen Charlotte Islands.

As part of regional mapping exercises during the 1990 field season, we identified several locations on the Queen Charlotte Islands where sedimentary successions possibly underlie the Karmutsen Formation. Most of these outcrops were previously mapped as parts of the Mesozoic Kunga Group (Sutherland Brown, 1968), but the lithologies present are notably different from any known exposures of Mesozoic strata in the islands, and warrant definition of a new map unit. Two of these locations have yielded conodonts of Late Carboniferous and/or Permian age. On both faunal and lithological grounds, we correlate this succession with the Buttle Lake Group on Vancouver Island. This demonstrates further the regional extent of Wrangellian strata. In this paper, we present, stratigraphic and paleontological evidence for this correlation. The newly discovered sedimentary succession is composed largely of carbonates, cherts, and lesser schists and phyllites; for discussion purposes we informally designate it the "carbonate-chert unit".

FIELD OCCURRENCES AND DESCRIPTION

Most of the pre-Triassic rocks on the Queen Charlotte Islands occur in the Englefield Bay area on the west coast of Moresby Island (Fig. 1). A possible additional locality exists 75 km southeast at Hutton Point. All locations are in close proximity to the Karmutsen Formation, and at one locality (Kitgoro Inlet) an unconformity between the unit and the Karmutsen Formation was observed. In the Englefield Bay area, several greenish-grey mafic intrusions cut the "carbonate-chert unit". All known exposures occur in sea cliffs or steep shoreline outcrops, and the longest continuous sections are less than 60 m thick. Two stratigraphic sections were measured on the northwestern part of Hibben Island (Fig. 1, locations 1 and 2).

Overall lithology

In most exposures, the "carbonate-chert unit" comprises thinly- to thickly-bedded chert, limestone, and dolomite. The presence of chert and dolomite makes the sequence easily

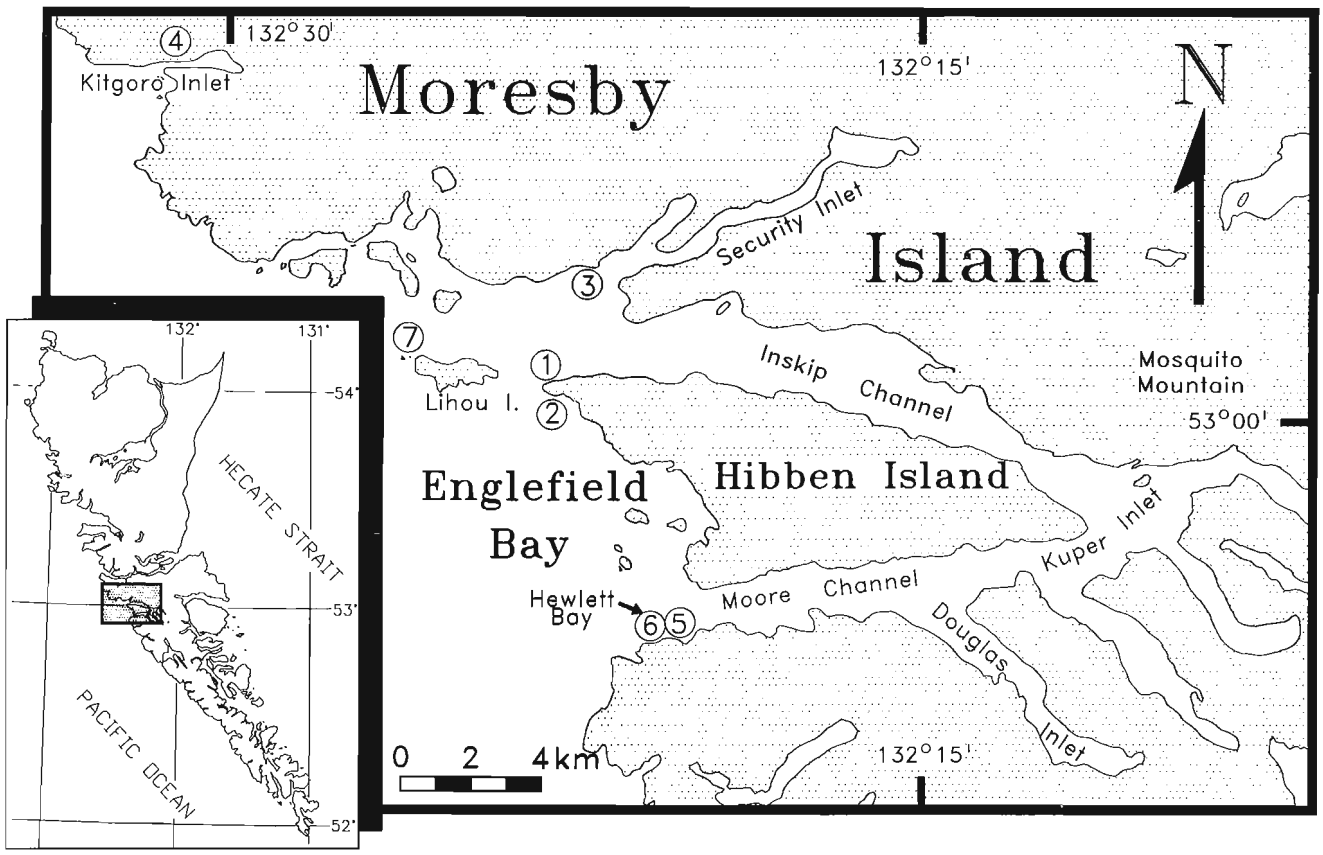

Figure 1. Location map for rocks of possible pre-Triassic age. One conodont sample from location 1, and two conodont samples collected at location 2, yielded Permian and possibly Carboniferous age. Locations 1 through 5 show outcrops of sedimentary rocks, whereas locations 6 and 7 indicate possible subaerially erupted pyroclastic rocks. Sections 1 and 2 where measured at locations 1 and 2, respectively.

distinguishable from other rock units in the Queen Charlotte Islands. Black lichen covers parts of the outcrops, giving the rocks a characteristic black and grey banded appearance.

Limestones occur as continuous layers, or as lenticular to diamond-shaped pods or pinch and swell layers. Discontinuous pods can be up to 30 cm long and 20 cm thick, and continuous limestone layers range in thickness from several centimetres to more than 1 m. These layers contain millimetre-scale banding defined by alternating dark grey and light grey colouration. Fresh surfaces are dark grey to light grey. The limestone is medium grained to microcrystalline and commonly contains abundant small (<2 mm) cubic pyrite crystals. Limestone/dolomite contacts are sharp and irregular. The limestone weathers recessive relative to chert and dolomite.

Chert layers range in thickness from a few centimetres to over a metre. They are internally bedded on centimetre-scale. Fresh surfaces are greenish and light grey, and weather to yellow or brownish-yellow. Layers are continuous and planar, and contacts with the limestone and dolomite are sharp. The resistant nature of chert causes layers to stand out like ridges. The chert also has a characteristic angular fracture.

Dolomite forms irregular and discontinuous layers, varying from a few millimetres to over 30 cm thick. Dolomite typically separates limestone layers from chert, leading to a characteristic chert-dolomite-limestone-dolomite-chert layering sequence. In these sequences, the dolomite layer below the limestone is often thicker than the layer above. Dolomite-chert contacts are sharp and planar, while dolomite-limestone contacts are sharp but irregular. Layers contain internal lamination and bedding ranging from 2 mm to 3 cm in thickness, easily recognized by differential weathering. Fresh surfaces are brown or beige, but can also be light grey. When weathered, the rocks are pinkish-brown or dark grey, commonly show honeycomb weathering, and are often covered with black lichen. Crystal size varies from very fine to very coarse. At some localities, thin laminae of medium grained (1-3 mm) subhedral periclase crystals occur within the dolomite. These grains are scattered in a dolomite and brucite matrix, and rarely form aggregate layers 0.5 cm thick. Periclase is replaced partially or completely by brucite.

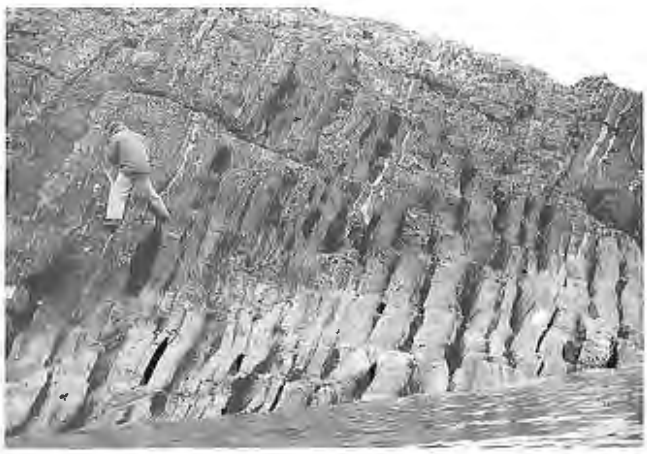

Figure 2. Lower part of section 1 (unit A). The rocks are cherts and dolomites interlayered with discontinuous limestone. Unit A measures more than 13 m, with the base not exposed.

DESCRIPTION OF STRATIGRAPHIC SECTIONS

Two sections of the "carbonate-chert unit" on Hibben Island were measured in detail (Fig. 1, locations 1 and 2). Within these two sections, we recognized 3 distinct lithological units which may be regionally mappable. Both sections have subtidal bases and covered tops. Section 1 (55 m) grades from alternating cherts and dolomites with rare limestones (unit A) into a sequence of interlayered limestones, cherts, and dolomites (unit B). Section 2 (57 m) is characterized by thinner layers and a general lack of dolomite higher in the section (unit C).

Section 1

Unit A

This unit forms the lowermost 13 m of outcrop in section 1, and is characterized by abundant chert, and minor dolomite and limestone (Fig. 2). Limestone, where present, occurs only as pods and pinch and swell layers. Chert layers vary in thickness from 15-30 cm with average thickness close to 30 cm. Dolomite layers are up to 30 cm thick, but average less than 10 cm. The ratio of limestone:chert:dolomite for unit A is roughly 5:80:15.

Unit B

Unit B is more than 40 m thick, and overlies unit A along a gradational contact. It is characterized by continuous layers of all three rock types, which form a pronounced chert-dolomite-limestone-dolomite-chert sequence (Fig. 3). The relative abundance of limestone increases towards the top of the section, at the expense of dolomite and chert. Two continuous marker-beds exist: a 1 m thick chert layer approximately 5 m from the base of the unit, and a 60 cm thick chert layer 12 m from the base.

The limestone layers range from 1-15 cm thick (pinch and swell layers) at the base to 5-35 cm thick (average = 20 cm) layers at the top. Dolomite layers decrease in thickness from 5-30 cm at base to 2-8 cm at the top. Chert layers at the base range from 20-45 cm thick (average = 40 cm), while they range from 15-50 cm (average = 20 cm) at the top. The limestone-chert-dolomite ratio was estimated to be 15:60:25 at the base of the unit, and 45:45:10 at the top.

Section 2 (unit C)

Unit C (57 m thick) was not observed in contact with units A and B, but the decreasing amount of dolomite upsection in unit B and the general lack of dolomite in unit C, suggest that this unit overlies the two previous ones. The lower part of the section comprises 5-60 cm thick limestone layers (average 20 cm) interlayered with 5-80 cm thick chert layers (average 20 cm). Bed thickness decreases towards the top of the section. The limestone layers here range in thickness from

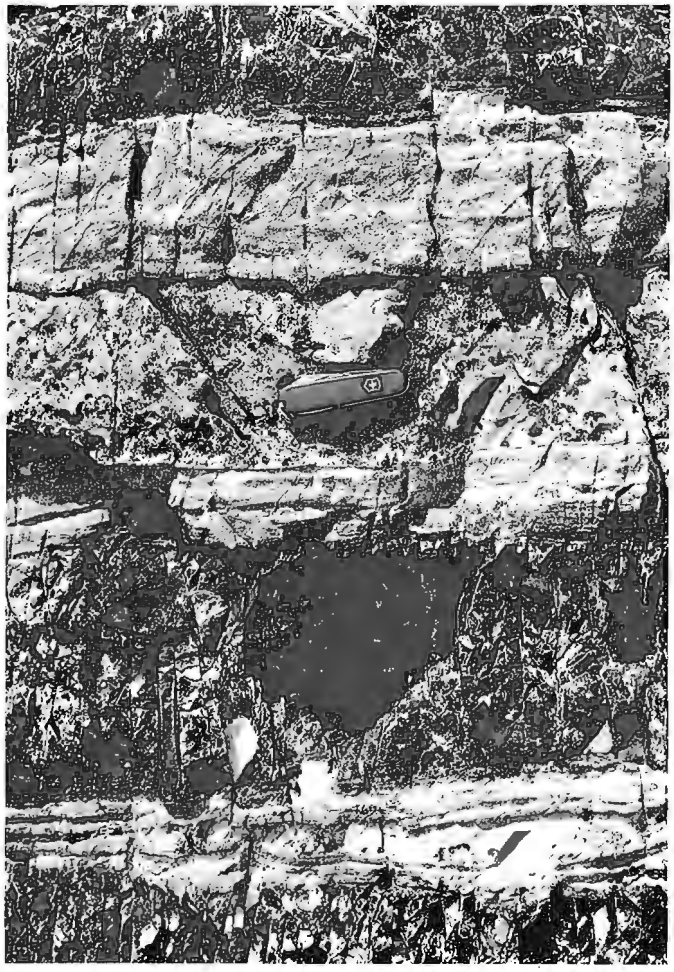

Figure 3. The "black-and-white" beds are chert layers, whereas the knife lies on limestone. Interlayered with these are yellowish-brown dolomite layers. The sequence with chert-dolomite-limestone- dolomite-chert is characteristic for unit B, and is easily recognizable.

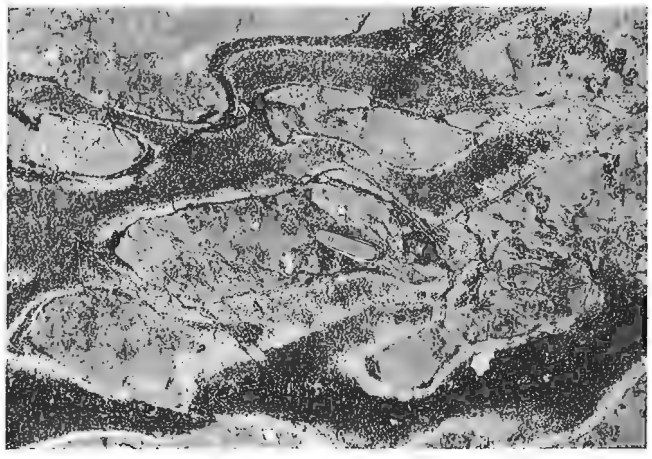

Figure 4. The lower part of unit C contains a 6-7 m thick sequence of irregularly bedded dolomite ("fish-net" dolomite). The knife lies on limestone, and the black layer in the lower part of the picture is a chert layer within the dolomite.

2-20 cm (average <10 cm), and chert layers range from as little as 1 cm to more than 60 cm (average 30 cm). The chert shows a more pronounced internal lamination than in the previous units. Dolomite layers are rare, and where present do not exceed 12 cm in thickness. Limestone-chert-dolomite ratios are approximately 47:47:6 at the base and 30:70:0 at the top.

A 7 m thick interval near the base of section 2 contains a much greater abundance of dolomite. Dolomite here forms 2-15 cm thick anastomosing layers within the limestone, giving it a very irregular appearance (Fig. 4). At a separate outcrop this lithology exceeds 20 m in thickness. The limestone-chert-dolomite-ratio is approximately 35:50:15 in this interval.

CONODONT FAUNAS

Four collections of conodonts have been recovered from the "carbonate-chert unit", all of them from sections 1 and 2 on northwest Hibben Island. In each case, the conodonts were fragmentary and distorted. The colour alteration index (CAI) is about 6 in all cases, implying post-depositional temperatures in the range of 360-550°C (Rejebian et al., 1987).

Two collections were recovered from reconnaissance samples of unspecified parts of sections 1 and 2. The first collection (section 1) (GSC No. C-185022) contains 1 specimen of *Neogondolella* sp. and 1 ramiform element. The collection from section 2 (GSC No. C-185023) contains 3 specimens of *Neogondolella* sp., 1 specimen of *Diplognathodus?* sp., and 1 ramiform element. The age of these collections is regarded as latest Carboniferous through Permian, based largely on the configuration of the neogondolellid. A more precise age is not possible due to poor preservation.

Two further collections were recovered from systematic recollection of section 2. One (GSC No. C-184992), from near the base of the section, contains 9 specimens of *Neogondolella* sp. and 35 parts of ramiform elements. This is the largest collection recovered and reveals a little more on the neogondolellid morphology, i.e. all have low anterior blades and prominent cusps. These are features of several species that may be as old as latest Carboniferous or earliest Permian (Gzhelian-Sakmarian), although a younger Permian age is also possible. A second faunule (GSC No. C-184993), from near the top of section 2, contains single fragments of *Merrillina?* sp. and *Sweetognathus?* sp. accompanied by 4 ramiform elements. Both these genera range within the Permian, the former only within the Upper Permian. Because the identifications are questionable, the age of this second collection is regarded only as Permian.

Other localities with possible Permian strata

Several of the outcrops in the Englefield Bay area have lithologies similar to sections 1 and 2, and may be correlative (Fig. 1, locations 3,4,5). These include a 25 m thick sequence on Lihou Island, a more than 15 m thick section in Hewlett Bay; a 27 m thick sequence in possible contact with the Karmutsen Formation in Kitgoro Inlet; and a 55 m thick sequence at Hutton Point (Juan Perez Sound, not shown

in Fig. 1). Most of the "carbonate-chert unit" is exposed discontinuously on Lihou Island and along the northwestern shoreline of Hibben Island. Possible subaerial pyroclastic rocks seen in the area (Fig. 1, locations 6 and 7), previously mapped as Karmutsen Formation (Sutherland Brown, 1968), may also be a part of the pre-Triassic package. The following section describes the lithologies found at these other localities.

Security Inlet

A beach exposure of a chert-carbonate unit was observed at the mouth of Security Inlet, approximately 4 km north of sections 1 and 2 (Fig. 1, location 3). The lower part of this unit comprises thinly-interlayered limestones and cherts and resembles the upper part of unit C. We therefore suggest that it conformably overlies unit C. The outcrop is cut by faults; the longest unbroken section is 25 m thick. The lower 16 m of this unbroken section consist of thinly-bedded (1-15 cm, average = 5 cm) chert layers. Overlying this interval, chert layers are thicker, and are interlayered with thin (<5 cm) chlorite schist and minor phyllitic layers. Chlorite schist layers increase in thickness to 60 cm in uppermost exposures, and form 40% of the rock.

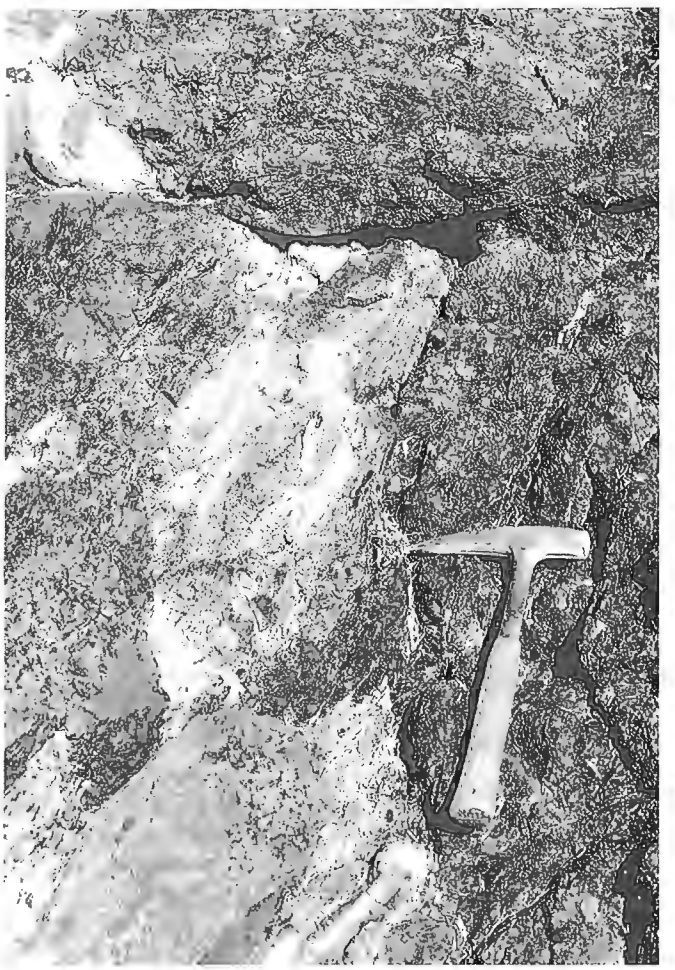

Figure 5. Contact between the Karmutsen Formation (right) and underlying pre-Triassic rocks (left). The contact is marked by an angular unconformity, and is partly obscured by some fault movement. The unit underlying the Karmutsen Formation here may be the equivalent to the St. Mary's Lake Formation on Vancouver Island.

Kitgoro Inlet

At one locality in Kitgoro Inlet (Fig. 1, location 4) Karmutsen Formation volcanic rocks unconformably overlie sedimentary strata (Fig. 5). Sedimentary strata directly below the contact comprise a 6 m thick sequence of interlayered pebble conglomerate and coarse, green feldspathic sandstone. Bed thickness varies from 5-60 cm. Conglomerate clasts (mainly chert) are subrounded and supported by a sand matrix similar in appearance to the interlayered sandstone. This sequence conformably overlies a 1 m thick succession of thinly-bedded cherts, which in turn conformably overlies a 20 m thick interval of thinly- to medium-bedded, interlayered limestones and cherts. This interval is lithologically similar to unit C, but is more thinly-bedded.

Hewlett Bay

A thick (<15 m) sedimentary sequence exposed at Hewlett Bay (Fig. 1, location 5) comprises laminated to thinly-bedded (0.1-10 cm) argillite, chert, and siliceous turbiditic siltstone. The sedimentary rocks have light grey and black banding on weathered surfaces. The sequence is bounded by intrusive rocks.

Hutton Point

At Hutton Point in Juan Perez Sound, a continuously-exposed section of interlayered carbonate, cherty carbonate, greenstone, sandstone, and volcanic conglomerate occurs structurally below a several kilometre thick section of Karmutsen Formation volcanic rocks. These different rock types alternate in layers 0.5-5 m thick; the total section is 55 m thick. The base is faulted against outcrops of the Karmutsen Formation, and the top is covered by beach gravels. Carbonate layers range from microcrystalline to coarse grained, bioclastic intervals containing abundant crinoid fragments. Chert occurs as scattered, discontinuous pods up to 20 cm long, or as continuous layers 15-20 cm thick, interbedded with carbonate. Greenstone and volcanic conglomerate layers have a strong tectonic foliation, and the former contains abundant euhedral feldspar phenocrysts. Conglomerate clasts are nearly all pebble- to cobble-sized scoriaceous volcanic fragments with a fine grained volcanic or carbonate interclast matrix.

Sutherland Brown (1968) suggested a Permian age for these rocks on the basis of poorly-preserved crinoid columns. The stratigraphic position of the section and similarities to strata at Englefield Bay are in accord with this interpretation.

Pyroclastic rocks at Lihou Island and Hewlett Bay

Possible subaerially erupted volcanic rocks occur close to the sedimentary rock assemblage (Fig. 1, locations 6 and 7). These may represent parts of the Karmutsen Formation, but they could also be a part of a Paleozoic sequence similar to the Sicker Group on Vancouver Island (*see* Indrelid and Hesthammer (1991) for further discussion). The rocks do

not resemble any previously described lithologies of the Karmutsen Formation on the Queen Charlotte Islands.

CORRELATIONS

Upper Paleozoic Wrangellian strata exposed in Oregon, on Vancouver Island, and in southern Alaska, bear lithological similarities to the "carbonate-chert unit" of the Queen Charlotte Islands, and are likely correlatives (Fig. 6).

Vancouver Island

On Vancouver Island the Buttle Lake Group comprises three formations (Fig. 6; adapted from Sutherland Brown and Yorath, in press; Massey and Friday, 1989). The Fourth Lake Formation is a thinly-bedded, cherty unit occurring at the base of the Buttle Lake Group. Muller (1980) described parts of the formation as thinly-bedded turbidite-like massive argillites, cherts, and siltstones that are highly silicified, with a characteristic dark-light banding on joint surfaces. Overlying and laterally interfingering with this unit are massive limestone layers, chert, and minor argillite interbeds, and rare shale beds and maroon tuffaceous shales of the Mount Mark Formation (Massey and Friday, 1989). The uppermost unit of the Buttle Lake Group is the St. Mary's Lake Formation, which conformably overlies the Mount Mark Formation limestones. This formation comprises sandstone and argillite graded beds, volcanic sandstones, and pebble conglomerates, as well as siliceous argillites, and cherts (Massey and Friday, 1989).

Interlayered limestone and chert of the Mount Mark Formation have lithological similarities to the "carbonate-chert unit" of the Queen Charlotte Islands. The sedimentary sequence found at Hewlett Bay has lithological similarities to parts of the Fourth Lake Formation. Sedimentary rocks at Kitgoro Inlet have lithological similarities to rocks of the St. Mary's Lake Formation. On Vancouver Island, the latter formation was cut out most places by the unconformity beneath the Karmutsen Formation. A similar distribution may be present in the Queen Charlotte Islands, where the unit has only been recognized in a 6 m thick exposure directly below the Karmutsen Formation. Subaerial pyroclastic rocks exposed in the Englefield Bay area, if they are older than the Triassic Karmutsen Formation, may be the equivalent of volcanic rocks of the Middle to Upper Devonian Sicker Group on Vancouver Island (*see* Indrelid and Hesthammer, 1991).

Alaska

In Alaska, volcanic, rift-fill tholeiitic basalts and pillow lavas of the Triassic Nikolai Greenstone overlie a 100 m thick sequence of Ladinian cherts, siltstones, and fissile shales (Jones et al., 1977; Plafker et al., 1989). This sequence unconformably overlies the Permian and Pennsylvanian Skolai Group, a 2500 m thick sequence of slightly metamorphosed volcanic rocks (Smith and MacKevett, 1970; MacKevett, 1978). The group is divided into two formations. The uppermost is the Lower Permian Hasen Creek Formation (Smith and MacKevett, 1970), comprising widely occurring argillite, shale, chert, limestone, sandstone, and minor conglomerate. The upper part of the unit contains an up to 250 m thick sequence of limestone. The Hasen Creek Formation conformably overlies the Lower Permian and Pennsylvanian Station Creek Formation, which consists of coarse volcanic breccia, volcanic greywacke, volcanic mudstone, and altered lavas (Smith and MacKevett, 1970).

Volcanic rocks of the Nikolai Greenstone are correlated with the Karmutsen Formation on Vancouver Island and on the Queen Charlotte Islands. The cherts and limestones of the Hasen Creek Formation may correlate with the pre-Triassic "carbonate-chert unit" on the Queen Charlotte Islands. The sandstone and minor conglomerate may be facies equivalents of the sandstone and conglomerate seen in Kitgoro Inlet (Fig. 1, location 4). Possible subaerially erupted volcanic rocks on the Queen Charlotte Islands may be correlative with the Station Creek Formation in Alaska.

Oregon

In the Hells Canyon and Wallowa Mountains in Oregon, Lower Permian sedimentary and volcanic strata unconformably underlie Triassic volcanic rocks of the Wild Sheep Creek Formation (Vallier, 1977). The Permian strata, which are part of the Seven Devils Group, form the Hunsaker Creek and the Windy Creek formations. The Hunsaker Creek Formation comprises conglomerate, breccia, argillite, rare limestone, sandstone, pyroclastic breccia, and tuff, whereas the Windy Creek Formation is made up of silicic volcanic flows and volcaniclastic rocks. The Permian and Triassic arc-assemblage is interpreted to have formed on ophiolitic basement rocks (Vallier, 1977).

The Permian rocks of the Hunsaker Creek Formation may be correlated to the pre-Triassic sediments exposed in the Englefield Bay area on the Queen Charlotte Islands. They are lithologically similar to sandstone and conglomerate found in Kitgoro Inlet, and argillite exposed in Hewlett Bay. There are, however, certain differences in the rock assemblages, and Sarewitz (1983) indicated that the rocks of the Seven Devils Group in Oregon may not be a part of Wrangellia at all. He pointed out differences in chemistry of the volcanic rocks, as well as stratigraphic and lithological differences, and suggested that the rocks may have formed close to each other without belonging to the same terrane.

Faunal comparisons

A summary of conodont faunules known from the Buttle Lake Group on Vancouver Island was given by Orchard in Brandon et al. (1986). Subsequent to that work, many more collections have been recovered, largely as a result of collecting by the British Columbia. Geological Survey (Massey and Friday, 1989). The collections range in age from late Carboniferous (mid-Pennsylvanian) through Early Permian. Those of Early Permian age are generally characterized by *Adetognathus, Hindeodus,* and *Neogondolella* species, along with fewer representatives of "*Gondolella*", *Streptognathodus*, and allied genera. Of these, only *Neogondolella* is common to the Queen Charlotte Islands collections. The differences may result from biofacies, with the typical Mount Mark Formation of Vancouver Island being of relatively more shallow water aspect. Alternatively, the faunas from the Queen

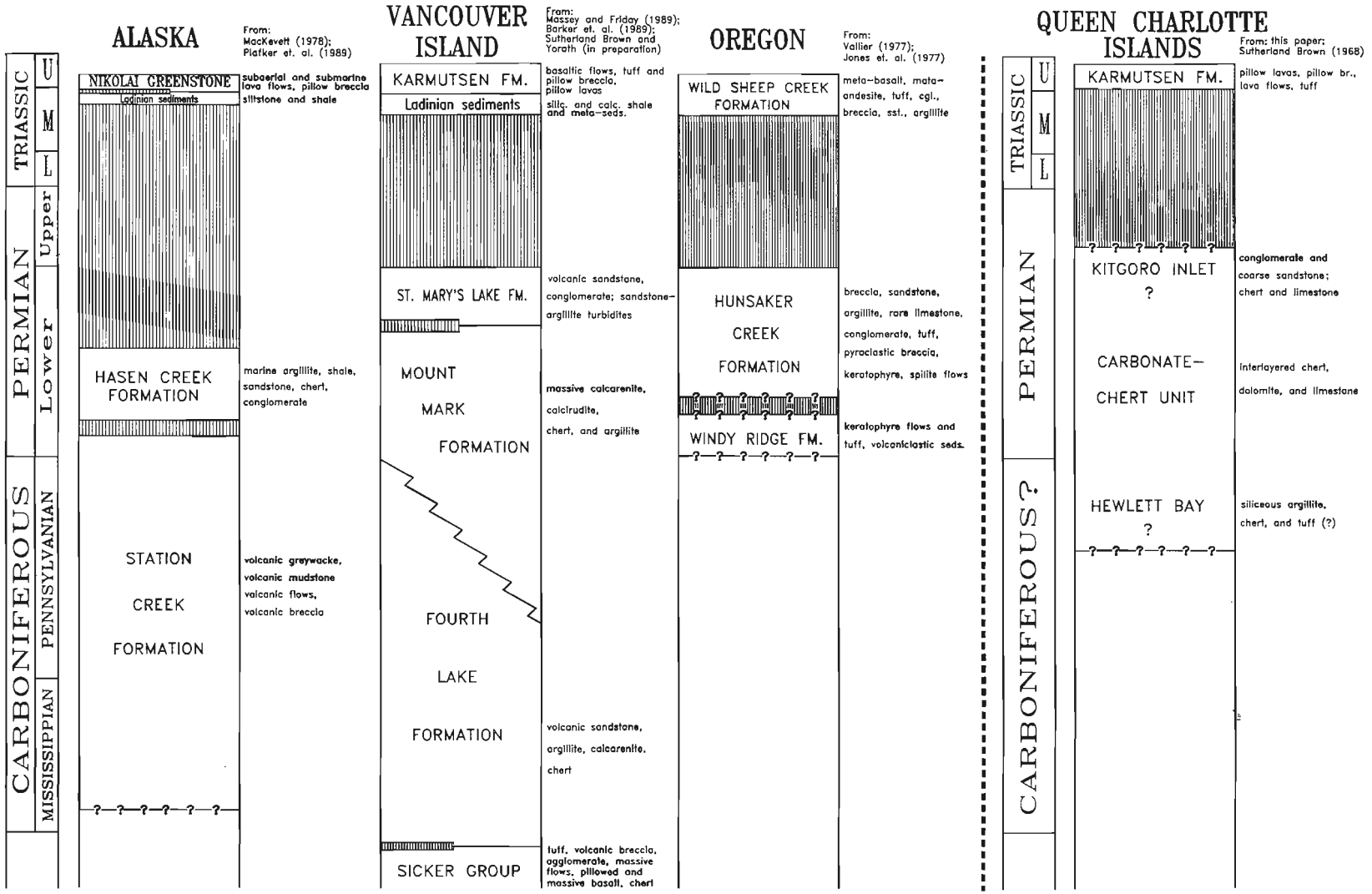

Figure 6. Columnar stratigraphic sections for the Wrangellia terrane, showing pre-Triassic rocks on the Queen Charlotte Islands with possibly correlative sections in Alaska, on Vancouver Islands, and in Oregon. Data sources as indicated.

Charlotte Islands may be mostly younger (post-Sakmarian), when many of the aforementioned genera from Vancouver Island were extinct. Suggested lithological correlation with the St. Mary's Lake Formation, the youngest unit of the Buttle Lake Group, is supported by the fact that the only known conodont fauna from that unit also consists of a mono-specific *Neogondolella* faunule, as do several others from the uppermost part of the Mount Mark Formation (author's collections).

DISCUSSION

Wrangellia extends from Oregon in the south to Alaska in the north. The presence of Permian rocks in Oregon, on Vancouver Island, in Alaska, and now also on the Queen Charlotte Islands, indicates that they are a characteristic component of Wrangellia. The presence of Buttle Lake Group equivalents, as well as possible Sicker Group volcanic equivalents (Indrelid and Hesthammer, 1991) on the Queen Charlotte Islands, supports the occurrence of a Paleozoic supracrustal assemblage similar to that on Vancouver Island.

The greenish-grey mafic to intermediate intrusions that surround and cut through the Permian rocks (Fig. 7), resemble the Karmutsen Formation both in weathering characteristics and mineralogy. These intrusions are possible feeders to the Karmutsen Formation volcanic rocks. Periclase within some of the dolomite layers, a common high-temperature alteration product of dolomite (Phillips and Griffen, 1981), may be related to the thermal affects of these intrusions.

The sequence of interlayered carbonates and cherts indicates an organic-rich deep-water environment. Deposition was probably close to the carbonate compensation depth (CCD), and changes in temperature and chemical composition of seawater may have resulted in the interlayering of carbonate and chert lithologies.

CONCLUSIONS

During the summer of 1990, several sedimentary successions were found possibly underlying the Karmutsen Formation.

Figure 7. Possible Permian rocks intruded by dark green intrusives. The intrusions are probably feeders to the Karmutsen volcanic rocks. It is likely that the high-temperature metamorphism of the sediments is caused by these intrusions.

Four collections of conodonts were recovered from two of the sections. The age of the collections is regarded as latest Carboniferous through Permian. Three lithological units are present in these two sections.

The lowermost (unit A) is a sequence of alternating cherts and dolomites with discontinuous limestone interbeds. Unit B conformably overlies unit A and comprises interlayered dolomite, chert, and limestone. This unit probably grades into unit C, which has thinner beds and less dolomite. The three units total more than 115 m, and based on these lithologies and lithologies observed elsewhere in the area, it is likely that the total thickness of pre-Triassic strata exceeds several hundred metres.

The rocks are lithologically similar to the Paleozoic Buttle Lake Group on Vancouver Island, specifically to the St. Mary's Lake and Mount Mark formations. Occurrence of Permian strata in Oregon, Vancouver Island, Alaska, and now also in the Queen Charlotte Islands, indicate that the succession is more extensive than believed earlier, and may underlie all of Wrangellia.

ACKNOWLEDGMENTS

We thank the Geological Survey of Canada and Jim Haggart for funding and logistical support. Mark Hamilton and Ian Foreman provided cheerful help in the field. Audrey Putterill is thanked for competent expediting. Quick processing of the samples by Peter Krauss enabled us to provide conodont identification shortly after returning from the field.

REFERENCES

Anderson, R.G. and Reichenbach, I.
1991: U-Pb and K-Ar framework for Middle to Late Jurassic (172-≥158 Ma) and Tertiary (46-27 Ma) plutons in Queen Charlotte Islands, British Columbia; in Evolution and Hydrocarbon Potential of the Queen Charlotte Basin, British Columbia, Geological Survey of Canada, Paper 90-10.

Barker, F., Sutherland Brown, A., Budahn, J.R., and Plafker, G.
1989: Back-arc with frontal arc component origin of the Triassic Karmutsen basalt, British Columbia, Canada; Chemical Geology, v. 75, p. 81-102.

Brandon, M.T., Orchard, M.J., Parrish, R.R., Sutherland Brown, A., and Yorath, C.J.
1986: Fossil ages and isotopic dates from the Paleozoic Sicker Group and associated intrusive rocks, Vancouver Island, British Columbia; in Current Research, Part A, Geological Survey of Canada, Paper 86-1A, p. 683-696.

Indrelid, J. and Hesthammer, J.
1991: Lithologies of a Paleozoic or lower Mesozoic volcanic rock assemblage on the Queen Charlotte Islands, British Columbia; in Current Research, Part A, Geological Survey of Canada, Paper 91-1A.

Jones, D.L., Silberling, N.J., and Hillhouse, J.
1977: Wrangellia - A displaced terrane in northwestern North America; Canadian Journal of Earth Sciences, v. 14, p. 2565-2577.

MacKevett, E.M., Jr.
1978: Geologic map of the McCarthy quadrangle, Alaska; United States Geological Survey Miscellaneous Investigative Series Map, I-1032.

Massey, N.W.D. and Friday, S.J.
1989: Geology of the Alberni-Nanaimo Lakes area, Vancouver Island (92F/1W, 92F/2E and part of 92F/7); in Geological Fieldwork, British Columbia Ministry of Energy, Mines and Petroleum Resources, Paper 1989-1, p. 61-74.

Muller, J.E.
1980: The Paleozoic Sicker Group of Vancouver Island, British Columbia; Geological Survey of Canada, Paper 79-30, 23 p.

Phillips, W.R. and Griffen, D.T.
1981: Optical mineralogy: the nonopaque minerals; in the collection A Series of Books in Geology, W.H. Freeman and Co., San Francisco, CA, United States, 665 p., illus. (incl. tables).

Plafker, G., Nokleberg, W.J., and Lull, J.S.
1989: Bedrock geology and tectonic evolution of the Wrangellia, Peninsular, and Chugach terranes along the trans-Alaska crustal transect in the Chugach Mountains and southern Copper River Basin, Alaska; Journal of Geophysical Research, v. 94, B4, p. 4255-4295.

Rejebian, V.A., Harris, A.G., and Huebner, J.S.
1987: Conodont colour and textural alteration: an index to regional metamorphism, contact-metamorphism, and hydrothermal alteration; Geological Society of America Bulletin, v. 99, p. 471-479.

Sarewitz, D.
1983: Seven Devils terrane: Is it really a piece of Wrangellia?; Geology, v. 11, p. 634-637.

Smith, J.G. and MacKevett, E.M., Jr.
1970: The Skolai Group in the McCarthy B-4, C-4, and C-5 quadrangles, Wrangell Mountains, Alaska; United States Geological Survey, Bulletin 1274-Q, p. Q1-Q26.

Sutherland Brown, A.
1968: Geology of the Queen Charlotte Islands, British Columbia; British Columbia Department of Mines and Petroleum Resources, Bulletin 54, 226 p.

Sutherland Brown, A. and Yorath, C.J.
in press: Stratigraphy, in LITHOPROBE, Phase 1, Southern Vancouver Island: Geology and Geophysics, C.J. Yorath (ed.), Geological Survey of Canada, Bulletin.

Vallier, T.L.
1977: The Permian and Triassic Seven Devils Group, western Idaho and northeastern Oregon; United States Geological Survey, Bulletin 1437, 58 p.

Lithologies of a Paleozoic or lower Mesozoic volcanic rock assemblage on the Queen Charlotte Islands, British Columbia[1]

J. Indrelid[2] and J. Hesthammer[2]
Cordilleran Division, Vancouver

Indrelid, J. and Hesthammer, J., Lithologies of a Paleozoic or lower Mesozoic volcanic rock assemblage on the Queen Charlotte Islands, British Columbia; in Current Research, Part A, Geological Survey of Canada, Paper 91-1A, p. 331-335, 1991.

Abstract

In the 1990 field season regional mapping was carried out in the area from Englefield Bay to Tana Bay on the west coast of the Queen Charlotte Islands. Several lithologies found in the area have not previously been described in the Queen Charlotte Islands. These rocks include a sequence of interlayered tuffs and lapilli tuffs, overlain by interlayered limestones and tuffs, and topped by a 6 m thick limestone. Two other localities consists of scoriaceous volcanic breccias or agglomerates. It is suggested that these rocks are either new lithologies within the Karmutsen Formation or part of a volcanic assemblage correlative to the Paleozoic Sicker Group on Vancouver Island.

Résumé

Pendant la campagne de cartographie régionale de 1990, des travaux ont été effectués dans la région comprise entre les baies Englefield et Tana sur la côte occidentale des îles de la Reine-Charlotte. Plusieurs des lithologies observées dans cette région n'avaient pas précédemment été décrites dans les îles de la Reine-Charlotte. Parmi ces roches mentionnons une séquence de tufs et de tufs à lapilli interstratifiés et recouverts de calcaires et de tufs interstratifiés puis par une épaisseur de calcaire de 6 m. En deux autres emplacements des brèches ou des agglomérats volcaniques scoriacés sont observés. Il est suggéré que ces roches constituent de nouvelles lithologies à l'intérieur de la formation de Karmutsen ou font partie d'un assemblage en corrélation au groupe paléozoïque de Sicker sur l'île de Vancouver.

[1] Contribution to Frontier Geoscience Program
[2] Department of Geological Sciences, University of British Columbia, 6339 Stores Road, Vancouver, B.C. V6T 2B4

INTRODUCTION

During the 1990 field season one and a half months were spent mapping the area from Moore Channel to Skidegate Channel on the northwest part of Moresby Island, and the southwestern part of Graham Island from Dawson Inlet to Tana Bay. Several lithologies found in the westernmost part of the area have not been described in the Queen Charlotte Islands previously. One of these lithologies, a carbonate-chert unit, is described by Hesthammer et al. (1991). Pyroclastic rocks are present in several localities and range from aquagene tuff and lapilli tuff to volcanic lapilli-block breccia. These rock types may be related to the upper Triassic Karmutsen Formation or to an older rock assemblage. Figure 1 shows the three locations where the pyroclastic rocks and breccias were found.

The three locations all contain different lithologies and will be described separately. A discussion on the depositional regime of each rock type follows the description. The discussion is based on outcrop and hand sample descriptions only. The stratigraphic relationship between the three outcrops is unclear, but some information may come from microfossils in the limestone layers that are currently being processed.

STRATIGRAPHY

Lihou Island

Lihou Island Volcanic rocks are located on the northwestern tip of Lihou Island (Fig. 1) and are in fault contact with a greenish-grey, mafic intrusion. The rocks are made up of monolithic, scoriaceous volcanic fragments which defines a poorly developed stratification. The fragments are situated in either a green tuffaceous matrix or a medium grey limestone cement (Fig. 2), the rocks are matrix supported. The unit has a rough and hard weathering surface with black vesicular fragments standing out from the matrix. Fresh surfaces are red to dark grey, and the fragments are rich in calcite amygdules that can make up about 50 volume per cent of the fragments and be up to 1 cm large. The fragments vary in size from a few centimetres up to 20 cm long and have prolate (cigar) shapes. The ratio of the longest axis to the intermediate and shortest axes is locally more than 4:1:1, but average is about 2:1:1. All long axes are aligned, and define a tectonic fabric (Fig. 2).

The large size and abundance of vesicles (up to 1 cm) in all fragments suggests that the eruption was in very shallow water, less than a few hundred metres, or even subaerial (Moore and Schilling, 1973; Moore, 1979). The rocks might have had a subaerial history prior to final deposition. The extensive amount of carbonate cement suggests that the source is not only from calcite present as amygdules, and indicates that at least parts of the deposition was subaqueous. The tuffaceous matrix present in parts of the outcrop may however, be either subaqueous or subaerial. The fragments are monolithological, indicating little mixing during transport from the eruptive centres. Deformation fabric obscure original fragment shapes.

Tana Bay

At the east end of Tana Bay (Fig. 1) is an isolated outcrop of volcanic rocks. Numerous faults made it impossible to work out a detailed stratigraphy, and fragments the outcrop into several zones. Most of the outcrop is made up of a massive, dark grey, aphanitic, and aphyric rock. Weathering is purple and brown.

Two smaller parts of the outcrop are made up of fragmental rocks with scoriaceous fragments. These rocks weathers to red and purple-red. On fresh surfaces the fragments appear more massive and dense, and have plagioclase phenocrysts (0.5-2 mm long) and greenish amygdules (0.1-1 mm large) in a red matrix. The fragments are generally subrounded with an average diameter of 3-5 cm. Other parts of the outcrop have scoriaceous, dark grey to black, subrounded fragments in a light grey matrix. The size and form of the fragments are similar to the red ones previously described from this outcrop. The volcanic rocks are cut by a light grey, feldspar-biotite phyric intrusion, along an uneven, sharp contact.

The similarities between the rocks of Tana Bay and those of Lihou Island suggests that the rocks of Tana Bay may have been deposited in a shallow subaqueous or subaerial environment as well.

Moore Channel

This outcrop is located on the southern shore of the westernmost part of Moore Channel (Fig. 1). The rocks here are intensely faulted and stratigraphic relationships are difficult to ascertain. The lowermost part of this section is in contact with a medium grained mafic intrusion of unknown size. The lowest part of the section comprises 2 m of interlayered tuffs and lapilli tuffs, and is overlain by a sequence of interlayered tuffs and limestones. The tuffs look very siliceous, and they may better be called cherty tuffs. The amount and thickness of limestone layers increase upward and the section is topped by a massive, (more than 6 m thick) light grey limestone.

The basal part is interlayered bright red tuffs and red and green lapilli tuffs (Fig. 3). The red tuff layers are 1-12 cm thick and display fine internal lamination in shades of red. Fresh surfaces have a more greyish red colour. It is impossible to tell if the oxidation leading to the bright red colour is primary or secondary. The layers are mainly massive, but some layers contain thin bands of small vesicles parallel to layering. The lapilli tuffs occur in layers 2-30 cm thick and their colour is a mixture of red and green. The main components in these layers are red volcanic fragments from 2 mm to more than 7 cm in diameter (averaging 1 cm). Some layers have a poorly defined fining-upward trend. The red colouration comes from fragments that looks similar to the tuff layers, but most of the fragments are more scoriaceous. Most fragments are fairly rounded and could be volcanic bombs. In some layers the red fragments make up over 80 % of the total number of fragments, and in other layers it is as low as 50 %. The green colour comes from aphanitic, massive, and scoriaceous fragments, as well as the matrix. A few fragments are black and aphanitic. The upper contacts of the tuff layers are very sharp and planar, in contrast to the lower contacts which are very rough and uneven.

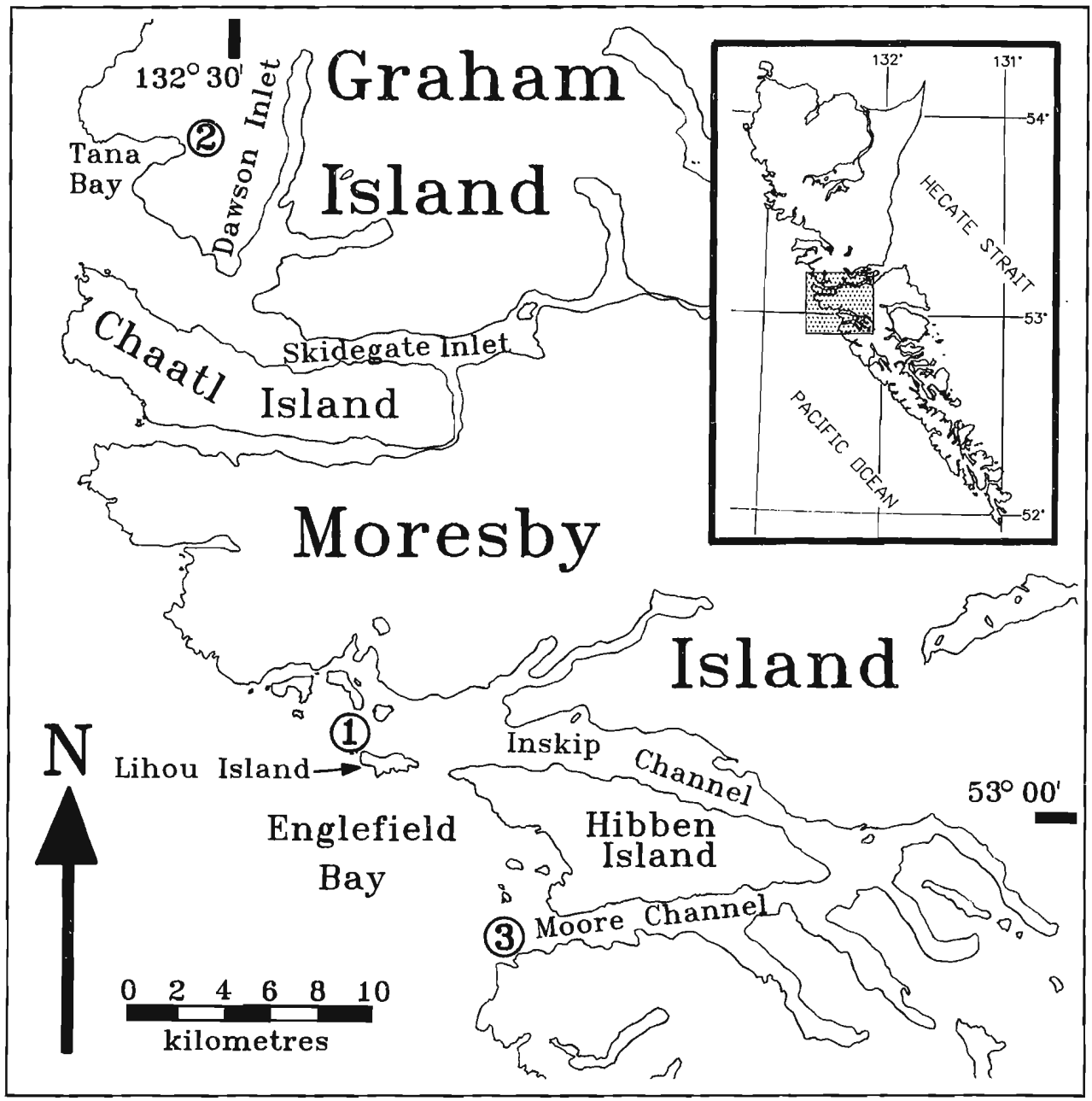

Figure 1. Location map showing the sites for the three outcrops discussed in this publication. 1 = Lihou Island, 2 = Tana Bay, 3 = Moore Channel.

A few thin limestone layers and lenses occur within the interlayered tuffs and lapilli tuffs. These are seldom thicker than 4 cm, except for one layer approximately 10 cm thick that was observed near the top of the section. The presence of limestone suggests that the deposition was at least in part subaqueous.

In fault contact with the tuffs and lapilli tuffs is a 7 m thick section of interlayered pale-grey limestones and cherty tuffs or cherts (Fig. 4). In the lower part of the sequence the limestone layers are 2-10 cm thick and the cherty layers thinner (1-7 cm thick). The limestones have a pale grey colour on fresh surfaces. Weathered surfaces are yellow to beige and have a typical "dog-tooth" (or "egg-carton") looking weathered appearance. The cherty layers have a dark brown to black colour, and are commonly covered with black lichen. On fresh surfaces the colour is more reddish. Outcrop surfaces of these cherty layers are banded due to resistant ridges. The cherty layers are more brittley deformed than the limestones.

Higher in the section the cherty layers become thinner and less regular, and eventually occur as discontinuous, isolated fragments scattered in the limestone. The fragments are 0.5-5 cm in diameter, subangular to subrounded, aphanitic, and dark red to black. Sorting is poor, but the total amount of fragments in different levels of the limestone varies and defines bedding. The volcanic fragments are cemented with carbonate, and on weathered surfaces the fragments stand out, creating a very rough surface. The abundance of fragments decreases upsection and the rock grades into a pure, light grey, more than 6 m thick limestone.

Figure 2. Volcanic agglomerate or breccias on Lihou Island. Note the alignment of fragments.

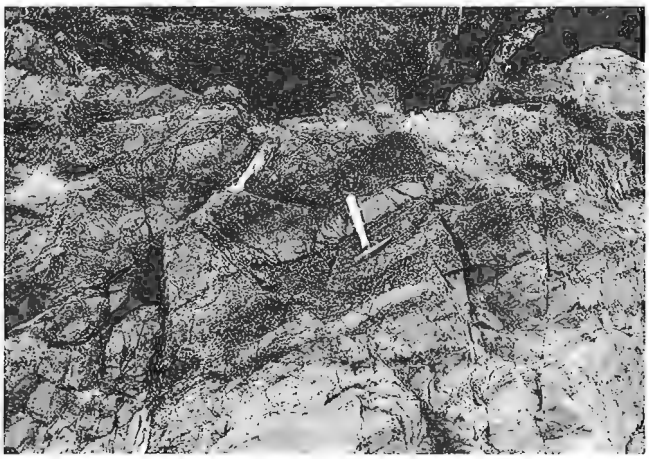

Figure 3. Interlayered tuffs and lapilli tuffs in Moore Channel. The massive layer passing behind the handle of the hammer is a tuff.

The deposition of the sequence in Moore Channel was probably entirely subaqueous, with the possible exception of the lowermost tuff and lapilli tuff unit. The limestones present in the rest of the sequence indicates that this part is subaqueous. The unit consisting of limestone with isolated volcanic fragments has a decreasing amount of fragments higher in section. This fact may indicate that the underlying continuous beds, that are also interlayered with limestones, are of volcanic origin. The volcanic activity seems to have decreased with time, and volcanic input becomes totally absent in the uppermost limestone layers.

CORRELATION

The lithologies described above are distinctly different from previously described units in the Queen Charlotte Islands. Field relationships show that they are all situated geographically close to volcanic rocks of the upper Triassic Karmutsen Formation, and also near rocks of Paleozoic age (Hesthammer et al., 1991).

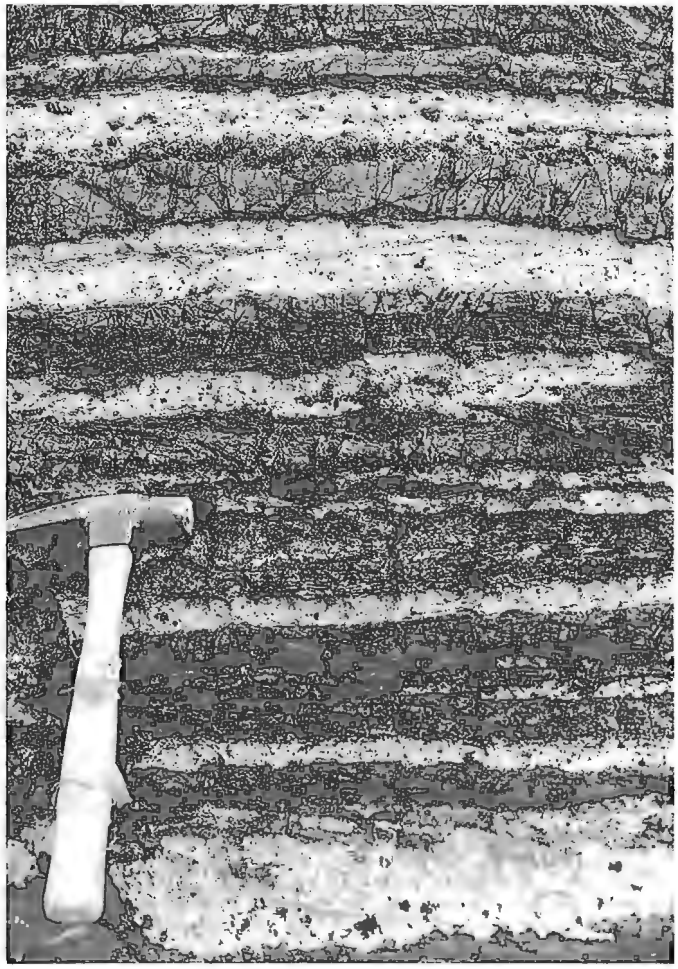

Figure 4. Interlayered limestones and cherty tuffs in Moore Channel. The lighter coloured layers are limestones. Isolated volcanic fragments can be seen within the limestone layers.

Sutherland Brown (1968) described the Karmutsen Formation as comprising primarily amygdaloidal chloritized basalt, basaltic pillow lavas, pillow breccia and related aquagene tuffs. The aquagene tuffs are described as being identical to the aquagene tuffs on Quadra Island east of Vancouver Island (Carlisle, 1963). The lithologies in Moore Channel may be aquagene tuffs, but they are not identical to the aquagene tuffs described earlier in the Queen Charlotte Islands by Sutherland Brown (1968).

On Vancouver Island several studies have focused on the Paleozoic Sicker Group. Muller (1980) presented a regional discussion of the Sicker Group. Later work includes that of Massey and Friday (1989). In the Cowichan uplift they noted volcanic rocks present in several formations within the Middle Devonian(?) to Lower Permian Sicker Group. Most volcanic rocks of this group are flows and breccias, though tuffs and lapilli tuffs are also present. The Nitinat Formation of the Sicker Group comprises a volcanic package of agglomerates, breccias, lapilli tuffs, and crystal tuff. Pyroxene-phyric, amygdaloidal flows are found in some areas. The amygdaloidal breccias of the Nitinat Formation may resemble the rocks on Lihou Island and Tana Bay. The rocks of the two outcrops on Queen Charlotte Islands are however tectonized, and it is difficult to tell if the depositional regime was similar to that of the Nitinat Formation. No direct correlation to the interlayered chert or cherty tuff and limestone in Moore Channel seems to exist on Vancouver Island. It is possible that the lithologies of this outcrop were developed locally and need not necessarily be of regional extent. The problem in defining a unifying stratigraphy for the Sicker Group on the Vancouver Island indicates that lithology correlations can be problematic over large distances.

CONCLUSION

The volcanic rocks of the three areas shown in Figure 1, belong to either the Sicker Group or the Karmutsen Formation. All outcrops are found on the westernmost part of the islands. Hesthammer et al. (1991) correlated Permian rocks found in this area with the Paleozoic Buttle Lake Group on Vancouver Island, where volcanic rocks are present in the underlying Sicker Group. These observations suggest that rocks on the Queen Charlotte Islands may be correlative to the Sicker Group. The rocks also occur close to the upper Triassic Karmutsen Formation, and this may indicate that the package belongs to this formation. If so, then they represents previously undescribed lithologies.

ACKNOWLEDGMENTS

The authors wish to thank the Geological Survey of Canada and J.W. Haggart for support in the field. C.J. Hickson of the Geological Survey of Canada and J.K. Russell of the University of British Columbia both provided invaluable information that greatly improved the quality of this publication. Peter Lewis supplied numerous ideas both in the field and in later discussions. Ian Foreman and Mark Hamilton provided skilful assistance in the field.

REFERENCES

Carlisle, D.
1963: Pillow breccias and their aquagene tuffs, Quadra Island, British Columbia; Journal of Geology, v. 71, p. 48-71.

Hesthammer, J., Indrelid, J., Lewis, P.D., and Orchard, M.J.
1991: Permian strata on the Queen Charlotte Islands, British Columbia; in Current Research, Part A, Geological Survey of Canada, Paper 91-1A.

Massey, N.W.D. and Friday, S.J.
1989: Geology of the Alberni-Nanaimo lakes area, Vancouver Island (92F/1W, 92F/2E and part of 92F/7); in Geological Fieldwork 1988, British Columbia Ministry of Energy, Mines and Petroleum Resources, Paper 1989-1, p. 61-74.

Moore, J.G.
1979: Vesicularity and CO_2 in mid-ocean ridge basalts; Nature, v. 282, p. 250-253.

Moore, J.G. and Schilling, J.G.
1973: Vesicles, water, and sulfur in Reykjanes Ridge basalts; Contribution to Mineralogy and Petrology, v. 41, p. 105-118.

Muller, J.E.
1980: The Paleozoic Sicker Group of Vancouver Island, British Columbia; Geological Survey of Canada, Paper 79-30, 23 p.

Sutherland Brown, A.
1968: Geology of the Queen Charlotte Islands, British Columbia; British Columbia Department of Mines and Petroleum Resources, Bulletin 54, 226 p.

New Aalenian Radiolaria from the Queen Charlotte Islands, British Columbia: implications for biostratigraphic correlation[1]

E.S. Carter[2] and G.K. Jakobs[3]
Cordilleran Division, Vancouver

Carter, E.S. and Jakobs, G.K., New Aalenian Radiolaria from the Queen Charlotte Islands, British Columbia: implications for biostratigraphic correlation; in Current Research, Part A, Geological Survey of Canada, Paper 91-1A, p. 337-351, 1991.

Abstract

This is a preliminary report on diverse, well preserved Aalenian radiolarians that have been found in a carbonate concretion from the belemnite sandstone member of the Phantom Creek Formation on the Yakoun River, Queen Charlotte Islands. The sample is associated with an Aalenian ammonite fauna that is previously unknown from this area and indicates a probable early late Aalenian age for the radiolarian sample. This faunal association extends the range of known Toarcian and Aalenian radiolarians, documents the presence of widely known taxa from other areas whose age may be equivalent to the Queen Charlotte Islands taxa, and illustrates some new forms. One ammonite and 37 radiolarian species are illustrated.

Résumé

Il s'agit d'un rapport préliminaire sur divers radiolaires aaléniens bien conservés qui ont été trouvés dans une concrétion carbonatée du membre de grès à belemnites de la formation de Phantom Creek sur la rivière Yakoun dans les îles de la Reine-Charlotte. L'échantillon est associé à une faune d'ammonites aaléniennes inconnue jusqu'ici dans cette région et un âge probable du début de la fin de l'Aalénien a été établi pour cet échantillon contenant des radiolaires. Cette association de faunes élargit la répartition des radiolaires toarciens et aaléniens connus, documente la présence de taxons généralement connus dans d'autres zones dont l'âge pourrait être équivalent à celui des taxons des îles de la Reine-Charlotte et illustre de nouvelles formes. Une espèce d'ammonites et 37 espèces de radiolaires sont illustrées.

[1] Contribution to the Frontier Geoscience Program
[2] 58335 Timber Road, Vernonia, Oregon 97064
[3] Department of Geological Sciences, University of British Columbia, 6339 Stores Road, Vancouver, B.C. V6T 2B4

INTRODUCTION

Recent field work on the Phantom Creek Formation of the Queen Charlotte Islands by G. Jakobs, has produced a more diverse Aalenian ammonite fauna than previously known (Poulton and Tipper, in press) and a well preserved and diverse radiolarian fauna. Based on closely associated ammonites, the radiolarians are probably early late Aalenian in age. Well dated Aalenian radiolarians are rare (Carter et al., 1988). The preliminary study of this fauna will contribute to understanding patterns of radiolarian faunal change from the Early to Middle Jurassic. The purpose of this report is to illustrate and briefly discuss the radiolarian assemblage, and to further document the occurrence of Aalenian ammonites in the Queen Charlotte Islands.

In their study of Aalenian ammonite faunas of the Canadian Cordillera, Poulton and Tipper (in press) described a small fauna of early Aalenian age from the Phantom Creek Formation of the Queen Charlotte Islands which includes *Tmetoceras scissum* (Benecke) and *Bredyia* cf. *manflasensis* Westermann. A single radiolarian sample found in association with these ammonites was studied by Carter, and the fauna included in a radiolarian zonation for the Queen Charlotte Islands that spanned late Pliensbachian to early Bajocian time (Carter et al., 1988). Comparable ammonite faunas occur in South America (Westermann and Riccardi, 1982; Hillebrandt and Westermann, 1985), Alaska (Westermann, 1964), and in western Canada (Poulton and Tipper, in press). Equivalent radiolarian faunas are found in western North America (east-central Oregon) (Pessagno and Whalen, 1982; Pessagno and Blome, 1982; Pessagno et al., 1986) and Japan (Takemura, 1986), and similarities are observed with younger Middle and Upper Jurassic faunas from the Mediterranean area (Baumgartner, 1984).

All ammonite collections and radiolarian sample C-156399 (see Locality Register) are from the type section of the Phantom Creek Formation (stratigraphic section 12 of Cameron and Tipper, 1985) on the Yakoun River (Fig. 1). Other Aalenian localities of the Phantom Creek Formation have yielded ammonites, but until now radiolarians have been found only at a waterfall locality on Branch Road 59 (stratigraphic section 13 of Cameron and Tipper, 1985), central Graham Island.

STRATIGRAPHY

The Phantom Creek Formation is a moderately resistant greenish grey sandstone with large (up to 1 m in diameter) buff-weathering concretions. It is best exposed along the Yakoun River and in stream cuts in Central Graham Island. It is late Toarcian to early late Aalenian in age and can be divided into two formal members.

The lower unit, informally designated the coquinoid sandstone member by Cameron and Tipper (1985), is separated from the upper unit, the belemnite sandstone member (Cameron and Tipper, 1985), by an erosional hiatus that varies in duration from locality to locality. The coquinoid sandstone member is late Toarcian in age and is composed

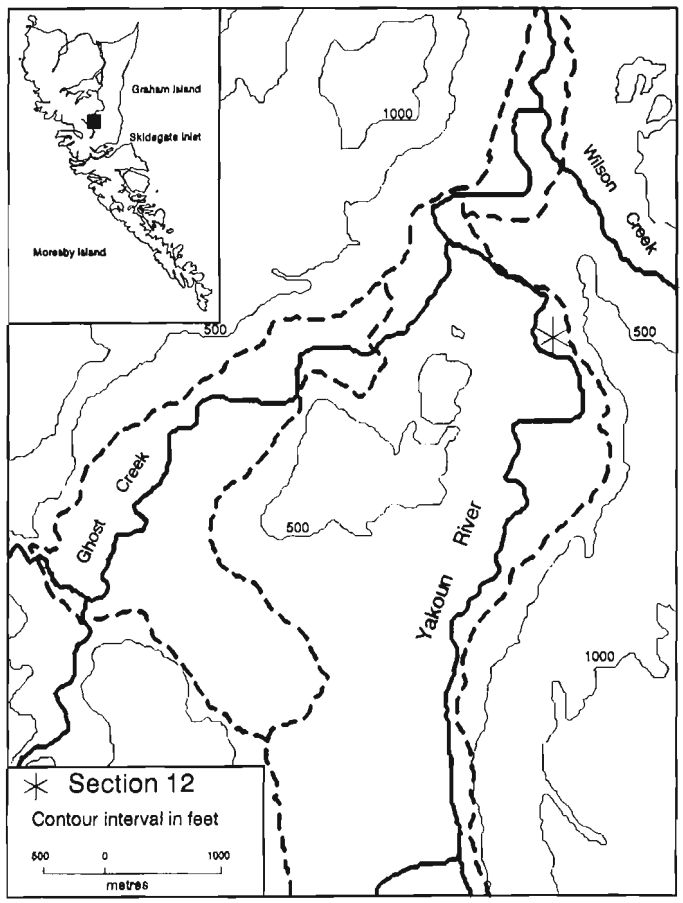

Figure 1. Locality map of Stratigraphic Section 12 on the east bank of the Yakoun River, Graham Island.

of a well bedded standstone with large fossiliferous concretions. The beds are approximately 60 cm thick and have an internal gradation from a coarse, friable, volcanic rich sand to a harder, finer sandstone with less volcanic detritus. The contact with the underlying shale of the Whiteaves Formation is conformable. The coquinoid sandstone member is approximately 5 m thick at the type section on the Yakoun River but thins southward towards Skidegate Inlet and Moresby Island, where it is absent and the belemnite sandstone member rests unconformably on the Whiteaves Formation. The belemnite sandstone member is a hard, massive sandstone with poorly defined bedding and spheroidal weathering. It contains large concretions some with Radiolaria, but none with ammonites. The contact with the overlying Bajocian Yakoun Group is unconformable but not exposed at the type section. The belemnite sandstone member is 15 m thick at the type section but thins towards the south. It is early to early late Aalenian in age. Both the coquinoid sandstone member and the belemnite sandstone member contain abundant belemnites, gastropods, and pectinoid bivalves.

AMMONITE BIOSTRATIGRAPHY

Poulton and Tipper (in press) summarized the Aalenian ammonite biostratigraphy of western Canada and outlined a zonation. Westermann has described Aalenian ammonites from Alaska (Westermann, 1964, 1969). Westermann and Riccardi (1982) and Hillebrandt and Westermann (1985) discussed the Aalenian zonation of South America. Recent field work in the Queen Charlotte Islands has yielded *Erycitoides howelli* (White) (Plate 1) (sample C-156871), *Bredyia* sp., and *Planammatoceras* sp. (Fig. 2). *Erycitoides howelli* is common elsewhere in the Cordillera but this is the first occurrence in the Queen Charlotte Islands. It ranges in age from beds equivalent to the middle of the *Murchisonae* Zone to the base of the *Concavum* Zone. *Bredyia* sp. occurs below and just above *Erycitoides. Bredyia* is not known in the Cordillera and its position in the Charlottes has been ambiguous in the past (Poulton and Tipper, in press). In Europe it occurs in the *Opalinum* Zone whereas in South America it occurs from the upper *Opalinum* Zone to the lower *Murchisonae* Zone. The earliest Aalenian, the *Opalinum* Zone may be absent in the Queen Charlotte Islands due to the erosional hiatus between the two members of the Phantom Creek Formation.

RADIOLARIAN BIOSTRATIGRAPHY

A rich, well preserved Aalenian fauna has recently been recovered from a carbonate concretion (sample C-156399) collected 5 m above the base of the belemnite sandstone member of the Phantom Creek Formation. This fauna is considerably more diverse than the one studied previously by Carter (1988) and contains representatives of over 50 genera. The most abundant and/or diverse are *Emiluvia* Foreman, *Hsuum* Pessagno, *Paronaella* Pessagno, and *Napora* Pessagno, followed by less frequent occurrences of *Parvicingula* Pessagno, *Higumastra* Baumgartner, *Parahsuum* Yao (= *Lupherium* Pessagno and Whalen), *Pseudocrucella* Baumgartmer, *Elodium* Carter, *Mesosaturnalis* Kozur and Mostler, *Tripocyclia* Haeckel, *Hagiastrum* Haeckel, *Protounuma* Ichikawa and Yao, *Tricolocapsa* Haeckel, and *Tympaneides* Carter. *Perispyridium* Dumitrica is quite diverse although individual specimens are not overly abundant. Pantanelliid abundance and diversity is low with only a few specimens of *Trillus* cf. *seidersi* Pessagno and Blome, and *Zartus* spp. observed. In the Queen Charlottes, pantanelliids are abundant and diverse in the upper Norian to Pliensbachian, nearly absent in the Toarcian and Aalenian (see Carter et al., 1988, p. 26) and the abundance/diversity increases again in the lower Bajocian. The reasons for this are not well understood but may be related to sea level change during this time (Carter, 1985) and/or variance in the many ecological factors that influence the distribution of radiolarians in the water column.

Almost all Aalenian taxa recorded earlier (Carter et al., 1988) are present in this sample. The upper range of other species such as *Homoeoparonaella hydensis* Yeh (=*H. reciproca* Carter), *Paronaella porosa* Carter, *P. variabilis* Carter, *Protounuma paulsmithi* Carter, *Pseudocrucella* sp. A of Carter (1988), *Rolumbus kiustaense* Carter, *Staurolonche ?* sp. B of Carter (1988), *Tympaneides charlottensis* Carter, *Caltrop nodosum* Carter, *Maudia yakounense* Carter, and the rarely occurring *Spongiostoma saccideon* Carter can now be extended to include the lower upper Aalenian. In addition, many new species are recognized; the majority figured here belong to *Emiluvia, Hsuum, Napora,* and *Perispyridium*. These and other taxa from this assemblage are illustrated in Plates 2 and 3; their relative abundance and ranges are given in Table 1.

Studies of Aalenian radiolarians from the Mesozoic clastic terrane of east-central Oregon include those on multicyrtid nassellarians (Pessagno and Whalen, 1982), bizarre nassellarians (Pessagno and Blome, 1982), the families Farcidae, Hilarisiregidae and Ultranaporidae (Pessagno et al., 1986), and the genus *Perispyridium* (MacLeod, 1988). In these reports, tentative Aalenian ages are frequently implied by comparison of the radiolarian fauna with others of older (late Toarcian) or younger (early Bajocian) age. Few samples can be directly tied to an association of Aalenian ammonites. Published ammonite data combined with comparison of radiolarian faunas suggest some samples may be closer to early Bajocian in age. Of the radiolarian taxa described from east-central Oregon, only the following are found in sample C-156399: *Parvicingula matura* Pessagno and Whalen, *Canoptum ?* sp. A of Pessagno and Whalen (1982), *Higumastra* cf. *transversa* Blome, *Napora bona Pessagno,* Whalen and Yeh, *Napora browni* Pessagno, Whalen and Yeh, *Napora* aff. *cosmica* of Pessagno et al. (1986), *Napora* aff. *fructuosa* Pessagno, Whalen and Yeh, *Hilarisirex* cf. *oregonense* Pessagno, Whalen and Yeh, and rare occurrences of *Droltus ? probosus* Pessagno and Whalen, and *Parahsuum officerense ?* (Pessagno and Whalen). None of the *Perispyridium* species described by MacLeod (1988) have been found.

Sample C-156399 also contains a number of species that commonly occur in the *Unuma echinatus* Assemblage (Yao et al., 1982) of Japan. Owing to the lack of independent dating of Japanese radiolarian assemblages, relative dating is generally achieved by comparison of these faunas with well dated faunas from North America and western Europe. Thus, the *Unuma echinatus* Assemblage is currently believed by most workers to be late Early Jurassic to early Middle Jurassic

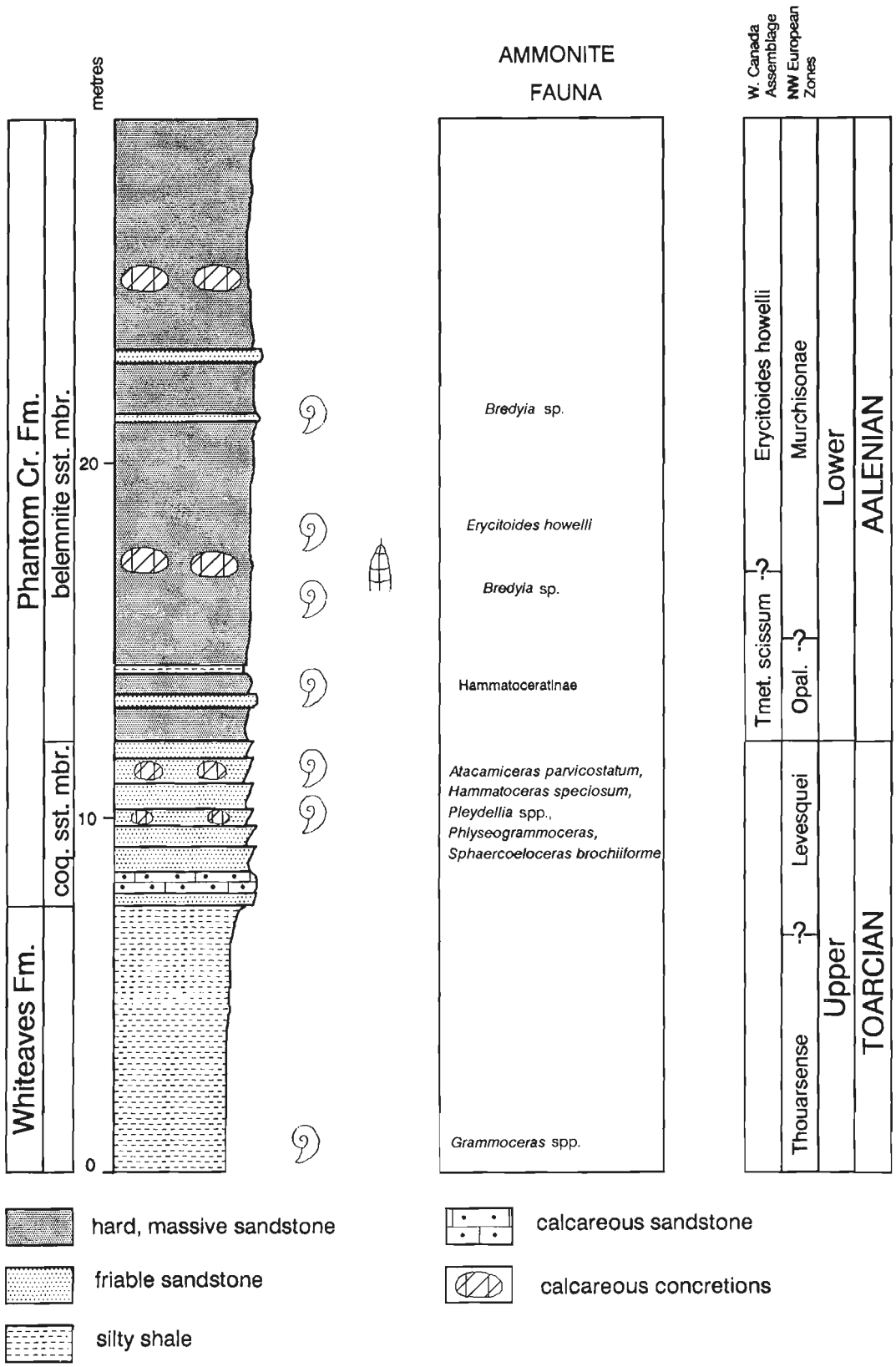

Figure 2. Stratigraphic Section 12 on the Yakoun River, central Graham Island.

Table 1. Range and relative abundance of radiolarian taxa illustrated in this report. Taxa ranges based chiefly on data from the Queen Charlotte Islands (Carter et al., 1988; this report) and east-central Oregon (Pessagno et al., 1986).

Abbreviations R = Rare, 1-2 specimens C = Common, 3-6 specimens A = Abundant, more than 6 specimens	Rel. Abd.	Lower Jurassic		Middle Jurassic			
		Toarcian		Aalenian		Bajocian	
		M	U	L	U	L	U
Acaeniotyle? sp. A, n. sp.	A			—	—		
Elodium cameroni Carter	A	—	—	—	—		
Emiluvia sp. A, n. sp.	A			—	—		
Emiluvia sp. B, n. sp.	C			—	—		
Emiluvia sp. C, n. sp.	A			—	—		
Gen. and sp. indet. A	C			—	—		
Gen. and sp. indet. B	A			—	—	—	?
Hagiastrum sp. cf. *H. egregium* Rust	A	—	—	—	—		
Higumastra sp. cf. *H. transversa* Blome	A			—	—	—	?
Hilarisirex sp. cf. *H. oregonensis* Pessagno et al.	C			—	— ?		
Hsuum sp. aff. *H. brevicostatum* (Ozvoldova)	R			—	—		
Hsuum sp. B, n. sp.	A	—	—	—	—		
Mesosaturnalis hexagonus (Yao)	A			—	— ?		
Mesosaturnalis tetraspinus (Yao)	A		—	—	—	—	?
Napora nipponica Takemura	C			—	— ?		
Napora sp. aff. *N. nipponica* Takemura	C			—	—		
Napora bona Pessagno et al.	C			—	—	— ?	
Napora sp. aff. *N. cosmica* Pessagno et al.	C		—	—	—	— ?	
Napora sp. aff. *N. fructuosa* Pessagno et al.	R			—	—		
Napora sp. A, n. sp.	A			—	—		
Paronaella porosa Carter	A	—	—	—	—		
Parvicingula sp. A, n. sp.	A			—	—		
Parvicingula sp. B, n. sp.	C			—	—		
Perispyridium sp. A, n. sp.	C			—	—		
Perispyridium sp. B, n. sp.	C			—	—		
Perispyridium sp. C, n. sp.	R			—	—		
Protounuma paulsmithi Carter	A	—	—	—	—		
Pseudocrucella sp. A, n. sp.	A		—	—	—		
Pseudopoulpus acutiopodium Takemura	C			—	— ?		
Staurolonche? sp. B, n. sp.	A		—	—	—		
?Staurosphaera amplissima Foreman	A	—	—	—	—		
Stichosapsa convexa Yao	A			—	— ?		
Tetraditryma sp. cf. *T. praeplena* Baumgartner	A			—	—		
Tetratrabs sp. aff. *T. zealis* (Ozvoldova)	A		—	—	—		
Tricolocapsa ruesti Tan	A	—	—	—	—	—	?
Turanta sp. A, n. sp.	C			—	—		
Tympaneides charlottensis Carter	A		—	—	—		

in age. Taxa common to the Queen Charlotte Aalenian fauna and to the *Unuma echinatus* Assemblage are *Mesosaturnalis hexagonus* (Yao), *M. tetraspinus* (Yao), *Napora nipponica* Takemura, *Pseudopoulpus* cf. *acutipodium* Takemura, *Tricolocapsa ruesti* Tan, and *Stichocapsa convexa* Yao.

The species used by Baumgartner (1984) in recognizing his Unitary Association zonation range in age from Middle Jurassic to Early Cretaceous. These forms are fairly cosmopolitan in low-latitude faunas from the Mediterranean Tethys, the Central Atlantic (DSDP), the California Coast Ranges, and Japan. Although Baumgartner's zonation extends no lower than the Bathonian (Zone AO), some zonal indicators (or closely related forms) are found in Aalenian strata of the Queen Charlotte Islands. These include *Pseudocrucella sanfilippoae* (Pessagno) and Eucyrtid gen. and sp. indet. of Baumgartner (1984). Other forms with affinities to *Homoeoparonaella argolidensis* Baumgartner, *Tetraditryma praeplena* Baumgartner, *Tetratrabs zealis* (Ozvoldova), *Hsuum brevicostatum* (Ozvoldova), and *Eucyrtidellium ptyctum* (Riedel and Sanfilippo) are rare to common in the assemblage. Two of these, *Homoeoparonaella argolidensis* Baumgartner, and *Tetratrabs zealis* (Ozvoldova) (=*T. gratiosa* Baumgartner) were recorded and figured previously in Carter et al. (1988).

Further evidence for the "patch-work quilt"

In their preliminary radiolarian zonation for the Jurassic of North America, Pessagno et al. (1987) likened it to a "patch-work quilt" in that the biostratigraphic data were derived from a variety of North American displaced terranes. Upper Toarican and Aalenian data originated largely from the Mesozoic clastic terrane (east-central Oregon) and the Wrangellian terrane (Queen Charlotte Islands). Further evidence in support of this zonal scheme follows together with comments on the new Aalenian fauna from the Queen Charlotte Islands:

1. The absence of *Canoptum s.s.* in the Aalenian of the Queen Charlotte Islands would appear to confirm the observation that *Canoptum s.s.* becomes extinct at the top of the Toarcian as suggested by Pessagno et al. (1987).

2. *Parvicingula matura* Pessagno and Whalen, and *Napora fructuosea* Pessagno, Whalen and Yeh have been used as supplementary marker taxa whose first appearance marks the base of the Aalenian (Subzone $1A_1$) (Pessagno et al., 1987). The former is common in sample C-156399 whereas the latter (presumably confined to the lower Aalenian) has not been found, although a form having affinities to this species (Plate 3, fig. 9) is present but very rare. *Parahsuum officerense* (Pessagno and Whalen) and *Droltus ? probosus* Pessagno and Whalen are rare; *Hsuum rosebudense* Pessagno and Whalen (with possibly more lower Bajocian affinities) is totally absent. Thus the evidence based on these latter forms is not sufficient at this time to prove an Aalenian age.

3. Subsequent to the above zonal scheme, an informally emended version has attempted to correlate North American and Japanese Jurassic biozones (Pessagno and Mizutani, internal report). As part of this emended scheme, the first occurrence of *Hilarisirex* is placed at the base of the Aalenian. At least one species of this genus is common in lower upper Aalenian strata of the Queen Charlotte Islands (see Plate 3, fig. 6) confirming that *Hilarisirex* is indeed a useful marker for the earliest Middle Jurassic.

In summary, this new fauna provides additional data on the distribution of Aalenian radiolarians on the Queen Charlotte Islands, extends the range of some Toarcian species to the lower upper Aalenian, and illustrates some of the more important species which include some new taxa. It also documents the presence of other widely known taxa described from east-central Oregon, the Mediterranean area, and Japan.

SYSTEMATIC PALEONTOLOGY

Alphabetical listing of species illustrated in this report with abbreviated synonymies and brief remarks.

Acaeniotyle ? sp. A, n. sp.

Plate 2, figure 8

Remarks. This form differs from *Acaeniotyle* s.s. in having rounded knob-like nodes that lack perforations. It also has very distinctive spines whose tips bear crown-like structures.

Elodium cameroni Carter

Plate 3, figure 18

Elodium cameroni Carter, *in* Carter et al. 1988, p. 56, Pl. 13, fig. 1, 2, 6, 9. Tipper et al. 1991, Pl. 9, fig. 12.

Emiluvia sp. A, n. sp.

Plate 2, figure 5

Remarks. This form with strongly concave sides has massive spines with deeply incised, strongly tapering grooves that terminate in crown-like structures. It is very abundant in sample C-156399 and has not been recognized previously in Aalenian strata of the Queen Charlotte Islands.

Emiluvia sp. B, n. sp.

Plate 2, figure 4

Remarks. Box-shaped form with large raised nodes on the upper and lower surfaces, and long tapering spines that are triradiate only on the proximal part.

Emiluvia sp. C, n. sp.

Plate 2, figure 6

Remarks. This form has deep, irregularly shaped pore frames, and robust, strongly-tapering spines of medium length.

Hagiastrum sp. cf. H *egregium Rüst*

Plate 2, figure 11

cf. *Hagiastrum egregium* Rüst 1885, p. 299, Pl. 34, fig. 5.
Tetratrabs sp. E, *in* Yeh 1987, p. 32, Pl. 11, fig. 12; Pl. 22, fig. 2.
Hagiastrum sp. cf. H. *egregium* Rüst, *in* Carter et al. 1988, p. 29, Pl. 7, fig. 11,12.

Higumastra sp. cf. H. *transversa* Blome

Plate 2, figure 3

cf. *Higumastra transversa* Blome 1984, p. 350, Pl. 1, fig. 3-5, 8-13, 16-19; Pl. 15, fig. 4.
cf. *Crucella* sp. A, *in* Carter et al. 1988, p. 43, Pl. 15, fig. 9, 12.

Remarks. Very similar to both *Higumastra transversa* Blome and *Crucella* sp. A (*in* Carter et al., 1988) but has very slightly tapering arms disposed in an X-shaped pattern (i.e. not at 90°). The latter feature may be only a minor variation of the true species as not all specimens in the assemblage are as extreme in shape as the one figured.

Hilarisirex sp. cf. H. *oregonensis* Pessagno, Whalen and Yeh

Plate 3, figure 6

cf. *Hilarisirex oregonensis* Pessagno et al. 1986, p. 31, Pl. 7, fig. 17, 18; Pl. 8, fig. 12, 18, 19.

Remarks. Illustrated specimen very similar to H. oregonensis but has a comparatively narrower, more elongate abdomen.

Hsuum sp. aff. *H. brevicostatum* (Ozvoldova)

Plate 3, figure 16

aff. *Lithostrobus brevicostatus* Ozvoldova 1975, p. 84, Pl. 102, fig. 1.

Remarks. This form has affinities to *H. brevicostatum* as defined by Baumgartner (1984, p. 769). It is a slender conical lobate form with discontinuous costae limited to one segment, and generally having two rows of pores between costae. However, it lacks strong irregular horizontal bars connecting the costae at their greatest bulge.

Hsuum sp. B, n. sp.

Plate 3, figure 15

Hsuum sp. B, *in* Carter et al. 1988, p. 52, pl. 5, fig. 7.

Mesosaturnalis hexagonus (Yao)

Plate 2, figure 15

Spongosaturnalis ? hexagonus Yao 1972, p. 31, Pl. 6, fig. 1-3, Pl. 11, fig. 3a-c.

Mesosaturnalis tetraspinus (Yao)

Plate 2, figure 16

Spongosaturnalis ? tetraspinus Yao 1972, p. 29, Pl. 4, fig. 1-6; Pl. 11, fig. 1-2.

Mesosaturnalis hexagonus (Yao), *in* Carter et al. 1988, p. 47, Pl. 9, fig. 11, 12. Tipper et al. 1991, Pl. 9, fig. 13.

Remarks. This form, illustrated previously by Carter as *M. Hexagonus* (Yao), is more probably *M. tetraspinus* (Yao) although peripheral spines on the ring developed perpendicular to the polar axis, are certainly stronger than on specimens figured by Yao (1979, see particularly Pl. 4, fig. 4). In this respect, there is little variation in Queen Charlotte Island specimens: they all have four well developed peripolar spines and two weak to moderately developed peripheral spines that are perpendicular to the polar axis.

Napora nipponica Takemura

Plate 3, figure 1

Napora nipponica Takemura 1986, p. 44, Pl. 2, fig. 16-21.

cf. *Napora baumgartneri* Pessagno et al. 1986, p. 35, Pl.6, fig. 11, 13, 15, 19, 22-24.

Remarks. Corresponds very closely to *N. nipponica*, and particularly to the paratype figured on Pl. 2, fig. 20. The form illustrated here is also similar to *N. baumgartneri* Pessagno et al. (1986), but the thorax is less hemispherical with less nodose pore frames, and the horn is longer with less prominent spines on each ridge.

Napora sp. aff. N. *nipponica* Takemura

Plate 3, figure 2

aff. *Napora nipponica* Takemura 1986, p. 44, Pl. 2, fig. 16-21.

Remarks. Differs from *N. nipponica* in having a more hemispherical cephalis and thorax, weakly developed (to absent) secondary spines on the horn ridges, and feet with a slightly lesser inward curve.

Napora bona Pessagno, Whalen and Yeh

Plate 3, figure 4

Napora bona Pessagno et al. 1986, p. 36, Pl. 6, fig. 4, 5.

Napora sp. aff. N. *cosmica* Pessagno, Whalen and Yeh

Plate 3, figure 3

Napora sp. aff. *N. cosmica* in Pessagno et al. 1986, p. 39, Pl. 6, fig. 8. Carter et al. 1988, p. 58, Pl. 14, fig. 2.

Napora sp. aff. *N. fructuosa* Pessagno, Whalen and Yeh

Plate 3, figure 5

aff. *Napora fructuosa* Pessagno et al. 1986, p. 39, Pl. 6, fig. 1-3; Pl. 11, fig. 6.

Remarks. Similar to *N. fructuosa* in possessing a large hemispherical thorax and narrow, incurved feet; differs in having a long straight horn, poorly defined cephalis, and much larger pores on the proximal part of the thorax.

Napora sp. A, n. sp.

Plate 3, figure 9

Remarks. This form has a long straight horn that lacks nodes or secondary spines. It has a hemispherical cephalis and thorax, and relatively straight triradiate feet. Forms of varying size and morphology but all with a straight horn are very common in Aalenian strata of the Queen Charlotte Islands.

Paronaella porosa Carter

Plate 2, figure 14

Paronaella porosa Carter, *in* Carter et al. 1988, p. 40, Pl. 4, fig. 6, 9.

Parvicingula sp. A, n. sp.

Plate 3, figure 19

Remarks. Large conical form with weakly developed horn and 12-14 post-abdominal chambers.

Parvicingula sp. B, n. sp.

Plate 3, figure 20

Remarks. This form, smaller in size than *Parvicingula* sp. A, n. sp., is conical in shape, has a moderately developed horn, approximately 8 post-abdominal chambers, and sharp circumferential ridges.

Perispyridium sp. A, n. sp.

Plate 3, figure 7

Remarks. Subcircular peripheral shell with large irregularly shaped nodose pore frames. Apical and primary lateral spines slim, triradiate and terminate in weakly developed crown structures.

Perispyridium sp. B, n. sp.

Plate 3, figure 8

Remarks. Subtriangular peripheral shell, with large nodose pore frames and relatively wide shell shoulders. Apical and primary lateral spines strong, triradiate and terminate in weakly developed crown structures.

Perispyridium sp. C, n. sp.

Plate 3, figure 11

Remarks. Large subcircular peripheral shell with highly raised nodes at pore frame vertices. Apical and primary lateral spines robust, triradiate and maintain their width throughout; spines terminate in weakly developed crown structures.

Protounuma paulsmithi Carter

Plate 3, figure 17

Protounuma paulsmithi Carter, *in* Carter et al. 1988, p. 54, Pl. 6, fig. 9, 12. Tipper et al. 1991, Pl. 9, fig. 8.

Remarks. In the original description of this species, Carter stated "apical horn lacking on all specimens examined". At that time this taxon had been found only in middle and upper Toarcian strata. The form figured in this report from Aalenian strata clearly illustrates *P. paulsmithi* has a small horn.

Pseudocrucella sp. A, n. sp.

Plate 2, figure 13

Pseudocrucella sp. A, *in* Carter et al. 1988, p. 29, Pl. 7, fig. 8, 9.

Pseudopoulpus acutipodium Takemura

Plate 3, figure 10

Pseudopoulpus acutipodium Takemura 1986, p. 40, Pl. 1, fig. 5-8.

Remarks. This form has slightly longer feet than *P. acutipodium* but otherwise is almost identical.

Staurolonche ? sp. B, n. sp.

Plate 2, figure 10

Staurolonche ? sp. B, *in* Carter et al. 1988, p. 34, Pl. 8, fig. 81, 9.

?Staurosphaera amplissima Foreman

Plate 2, figure 9

?Staurosphaera amplissima Foreman 1973, p. 259, Pl. 3, fig. 6. Carter et al. 1988, p. 27, Pl. 8, fig. 10-12.

Stichocapsa convexa Yao

Plate 3, figure 12

Stichocapsa convexa Yao 1979, p. 35, Pl. 5, fig. 14-16; Pl. 6, fig. 1-7. Takemura 1986, p. 55, Pl. 7, fig. 9, 10.

Tetraditryma sp. cf. *T. praeplena* Baumgartner

Plate 2, figure 1

cf. *Tetraditryma praeplena* Baumgartner 1984, p. 787, Pl. 9, fig. 8-9, 13-13a.

Remarks. Lacks slender triradiate lateral spines that extend from the ray tips at a 60-70° angle to the ray axis, but otherwise is very similar to P. *praeplena* and may be its immediate ancestor.

Tetratrabs sp. aff. *T. zealis* (Ozvoldova)

Plate 2, figure 7

aff. *Crucella zealis* Ozvoldova 1979, p. 34, Pl. 2, fig. 1.

Tetratrabs sp. aff. *T. gratiosa* Baumgartner, *in* Carter et al. 1988, p. 30, Pl. 7, fig. 10.

Tricolocapsa ruesti Tan

Plate 3, figure 14

Tricolocapsa ruesti Tan 1927, p. 50, Pl. 9, fig. 65. Takemura 1986, p. 54, Pl. 7, fig. 4.

Turanta sp. A, n. sp.

Plate 3, fig. 13

Remarks. This large monocyrtid form with robust A, D and V spines is the most common of numerous species of *Turanta* found in Aalenian strata of the Queen Charlotte Islands.

Tympaneides charlottensis Carter

Plate 2, figure 2

Tympaneides charlottensis Carter, *in* Carter et al. 1988, p. 37, Pl. 9, fig. 4, 5. Cordey 1988, p. 235-236, Pl. 19, fig. 10. Tipper et al. 1991, Pl. 9, fig. 10.

Remarks. Range for this species is extended to include the lower upper Aalenian of the Queen Charlotte Islands where it occurs in great abundance.

Gen. and sp. indet. A

Plate 2, fig. 12

Remarks. Distinctive spherical form with large triangular to pentagonal pore frames having raised rounded nodes at vertices. Eight to ten short tapering spines with terminal crown-like structures extend from surfaces of sphere. A morphologically like form with six spines disposed in hexagonal position has been observed previously in lower Bajocian strata of the Queen Charlotte Islands.

Gen. and sp. indet. B

Plate 2, figure 17

Remarks. Similar to *Acaeniotyle ?* sp. A, n. sp. (this report) but has a larger sphere, stronger nodes, and four morphologically alike spines that extend from the sphere in tetrahedral position.

REFERENCES

Baumgartner, P.O.
1984: A Middle Jurassic-Early Cretaceous low-latitude radiolarian zonation based on Unitary Associations and age of Tethyan radiolarites; Eclogae Geologicae Helvetiae, v. 77, no. 3, p. 729-837.

Blome, C.D.
1984: Middle Jurassic (Callovian) radiolarians from carbonate concretions, Alaska and Oregon; Micropaleontology, v. 30, no. 4, p. 343-389, pls. 1-16.

Cameron, B.E.B. and Tipper, H.W.
1985: Jurassic stratigraphy of the Queen Charlotte Islands, British Columbia; Geological Survey of Canada, Bulletin 365, 49 p.

Carter, E.S.
1985: Early and Middle Jurassic radiolarian biostratigraphy, Queen Charlotte Islands, British Columbia; unpublished M.Sc. thesis, University of British Columbia, Vancouver, 291 p.
1988: Part 2. Systematic Paleontology; in Lower and Middle Jurassic Radiolarian Biostratigraphy and Systematic Paleontology, Queen Charlotte Islands, British Columbia, E.S. Carter, B.E.B. Cameron, and P.L. Smith (ed.), Geological Survey of Canada, Bulletin 386, 110 p.

Carter, E.S., Cameron, B.E.B., and Smith, P.L.
1988: Lower and Middle Jurassic radiolarian biostratigraphy and systematic paleontology, Queen Charlotte Islands, British Columbia; Geological Survey of Canada, Bulletin 386, 110 p.

Cordey, F.
1988: Étude des Radiolaires permiens, triasiques et jurassiques des complexes ophiolitiques de Cache Creek, Bridge River et Hozameen (Colombie Britannique, Canada): implications paléogeographiques and structurales; Mémoires des Sciences de la Terre, Académie de Paris, Université Pierre et Marie Curie, no. 88-17, 374 p.

Foreman, H.P.
1973: Radiolaria from Deep Sea Drilling Project, Leg 20; in Initial Reports of the DSDP, B.C., Heezen et al. (ed.), U.S. Government Printing Office, Washington, D.C., v. 20, p. 249-305.

Hillebrandt, A. von and Westermann, G.E.G.
1985: Aalenian (Jurassic) ammonite faunas and zones of the southern Andes; Zitteliana, v. 12, p. 3-55, pls. 1-10.

MacLeod, N.
1988: Lower and Middle Jurassic *Perispyridium* (Radiolaria) from the Snowshoe Formation, east-central Oregon; Micropaleontology, v. 34, no. 4, p. 289-315, pls. 1-5.

Ozvoldova, L.
1975: Upper Jurassic radiolarians from the Jysuca Series in the Klippen Belt; Zepaone Karpaty, Ser. Paleontologia, v. 1, p. 73-86, 5 pls.
1979: Radiolarian assemblage of radiolarian cherts at Podbiel locality (Slovakia); Casopis pro Mineraloggi a Geologii, v. 24, no. 3, p. 249-266.

Pessagno, E.A. Jr. and Blome, C.D.
1982: Bizarre Nassellariina (Radiolaria) from the Middle and Upper Jurassic of North America; Micropaleontology, v. 28, no. 3, p. 289-318, Pl. 1-8.

Pessagno, E.A. Jr. and Mizutani, S.
— Correlation of radiolarian biozones of the eastern and western Pacific (North America and Japan); Internal Report, Programs in Geosciences, University of Texas at Dallas, Contribution No. 601, p. 1-9, 1 fig.

Pessagno, E.A. Jr. and Whalen, P.A.
1982: Lower and Middle Jurassic Radiolaria (multicyrtid Nassellariina) from California, east-central Oregon and the Queen Charlotte Islands, B.C.; Micropaleontology, v. 28, no. 2, p. 111-169.

Pessagno, E.A. Jr., Whalen, P.A., and Yeh, K.-Y.
1986: Jurassic Nassellariina (Radiolaria) from North American geologic terranes; Bulletins of American Paleontology, v. 91, no. 326, 68 p.

Pessagno, E.A. Jr., Blome, C.D., Carter, E.S., MacLeod, N., Whalen, P.A., and Yeh, K.-Y.
1987: Preliminary radiolarian zonation for the Jurassic of North America; in Studies of North American Jurassic Radiolaria; Part 2; Cushman Foundation for Foraminiferal Research, Special Publication no. 23, p. 1-18.

Poulton, T.P. and Tipper, H.W.
in press: Aalenian ammonites and strata of Western Canada; Geological Survey of Canada, Bulletin.

Rüst, H.
1885: Beiträge zur Kenntniss der fossilen Radiolarien aus Gesteinen des Jura; Palaeontographica, v. 31, p. 269-322, Pls. 26-45.

Takemura, A.
1986: Classification of Jurassic nassellarians (Radiolaria); Palaeontographica, Abteilung A, Band 195, p. 29-74, pls. 11-22.

Tan, S.H.
1927: Over di samenstelling en het ontstaan var krijt-en mergelgesteenten van de Molukken (On the composition and origin of chalks and marls in the Moluccas); Jaarboek van het Mijnwezen in Nederlandsch-Indie (1926), v. 55, no. 3, p. 2-165, Pls. 1-16.

Tipper, H.W., Smith, P.L., Cameron, B.E.B., Carter, E.S., Jakobs, G.K., and Johns, M.J.
1991: Biostratigraphy of the Lower Jurassic formations of the Queen Charlotte Islands, British Columbia; in Evolution and Hydrocarbon Potential of the Queen Charlotte Basin, British Columbia, Geological Survey of Canada, Paper 90-10.

Westermann, G.E.G.
1964: The ammonite fauna of the Kialagvik Formation at Wide Bay, Alaska Peninsula, Part I, Lower Bajocian (Aalenian); Bulletins of American Paleontology, v. 47, no. 216, p. 329-503, pls. 44-76.
1969: The ammonite fauna of the Kialagvik Formation at Wide Bay, Alaska Peninsula, Part II, *Sonninia Sowerbyi* Zone (Bajocian); Bulletins of American Paleontology, v. 57, no. 255, p. 1-226, pls. 1-47.

Westermann, G.E.G. and Riccardi, A.C.
1982: Ammonoid fauna from the Early Middle Jurassic of Mendoza Province, Argentina; Journal of Paleontology, v. 56, no. 1, p. 11-41, pls. 1-6.

Yao, A.
1972: Radiolarian fauna from the Mino Belt in the northern part of the Inuyama area, Central Japan, Part 1, Spongosaturnalids; Journal of Geosciences, Osaka City University, v. 15, no. 2, p. 21-64.
1979: Radiolarian fauna from the Mino Belt in the northern part of the Inuyama area, Central Japan, Part 2, Nassellaria 1; Journal of Geosciences, Osaka City University, v. 22, no. 2, p. 21-71.

Yao, A., Matsuoka, A., and Nakatani, T.
1982: Triassic and Jurassic radiolarian assemblages in Southwest Japan; News of Osaka Micropaleontologists 5, p. 27-43. (in Japanese, with English abstract).

Yeh, K-Y.
1987: Taxonomic studies of Lower Jurassic Radiolaria from east-central Oregon; National Museum of Sciences, Taichung, Taiwan, Republic of China, Special Publication no. 2, 169 p.

LOCALITY REGISTER

GSC C-156399: Lat. 53°25'20"N.; Long. 132°15'45"W. Stratigraphic section 12 of Cameron and Tipper (1985) located on the Yakoun River, Graham Island, approximately 2 km south of Ghost Creek; east side of river (Fig. 1). Sample from large ellipsoidal buff-weathering carbonate concretion (60 cm in diameter) collected 5 m above base of belemnite sandstone member of Phantom Creek Formation. Associated ammonites include *Erycitoides howelli* (White) which occurs 1 m above C-156399, and *Breydia* sp. which occurs both 0.7 m below and 4.3 m above C-156399. Sample is probably early late Aalenian in age (see section on Ammonite Biostratigraphy).

GSC C-156871: Lat. 53°25'20"N; Long. 132°15'45"W. Stratigraphic Section 12 of Cameron and Tipper (1985) located on the Yakoun River, Graham Island, approximately 2 km south of Ghost Creek; east side of river (Fig. 1). A body chamber fragment collected 6 m above the base of the belemnite sandstone member of the Phantom Creek Formation. It is early late Aalenian in age.

PLATE 1

Ammonite specimen from the Phantom Creek Formation, Queen Charlotte Islands, B.C. (GSC Loc. C-156871). All figures are natural size.

Figure 1a. *Erycitoides howelli* (White). GSC 99483, lateral view of body chamber.
Figure 1b. *Erycitoides howelli* (White). GSC 99483, ventral view.

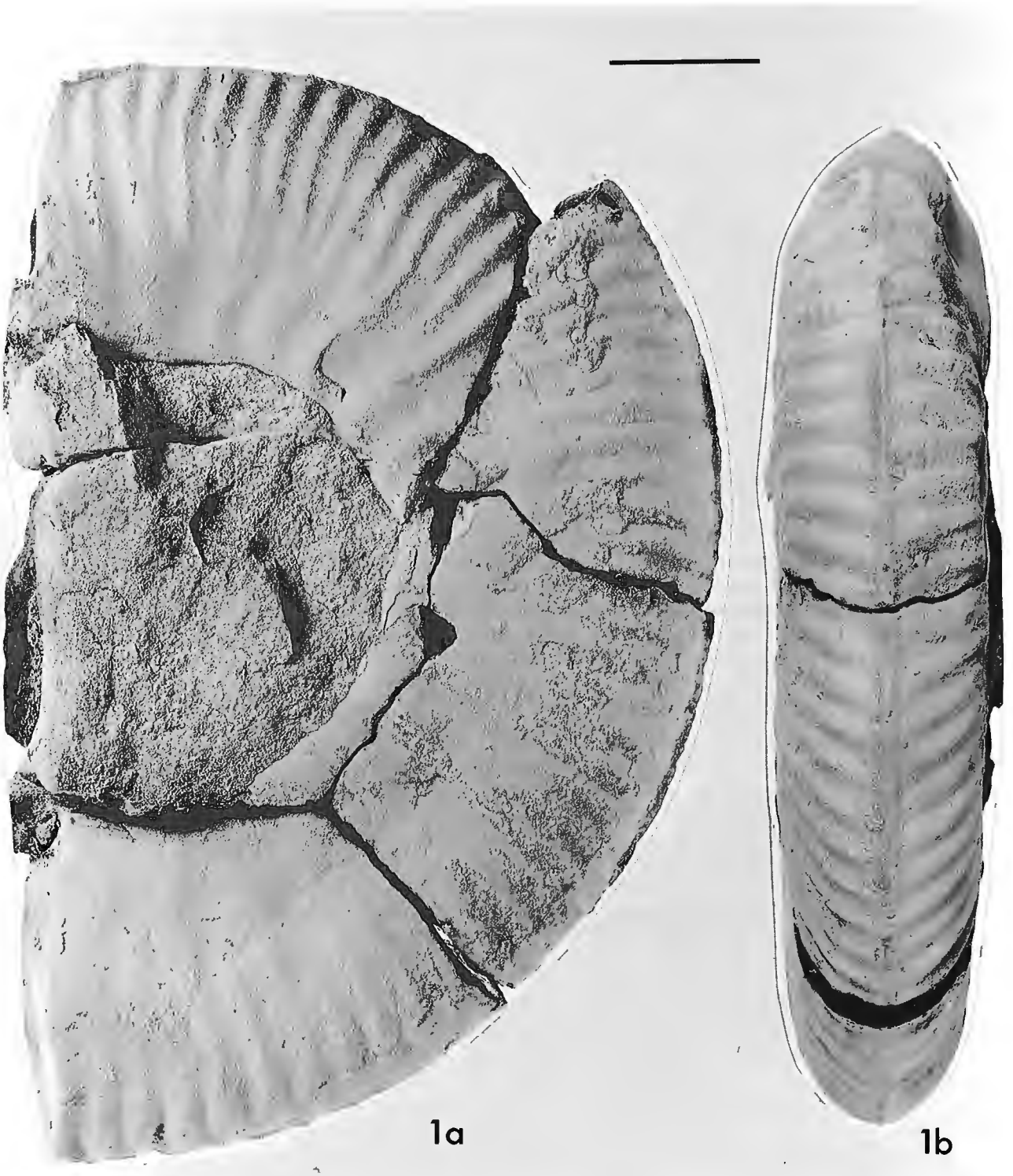
1a
1b

PLATE 2

Scanning electron micrographs of Aalenian Spumellariina (Radiolaria) from the Phantom Creek Formation, Queen Charlotte Islands, B.C. (GSC sample C-156399). Length of bar scale equals number of μm cited for each specimen illustrated.

Figure 1. *Tetraditryma* sp. cf. *T. praeplena* Baumgartner. GSC 85964, scale = 100 μm.
Figure 2. *Tympaneides charlottensis* Carter. GSC 85965, scale = 157 μm.
Figure 3. *Higumastra* sp. cf. *H. transversa* Blome. GSC 85966, scale = 100 μm.
Figure 4. *Emiluvia* sp. B, n. sp. GSC 85967, scale = 100 μm.
Figure 5. *Emiluvia* sp. A, n. sp. GSC 85968, scale = 100 μm.
Figure 6. *Emiluvia* sp. C, n. sp. GSC 85969, scale = 81 μm.
Figure 7. *Tetratrabs* sp. aff. *T. zealis* (Ozvoldova). GSC 85970, scale = 100 μm.
Figure 8. *?Staurosphaera amplissima* Foreman. GSC 85971, scale = 136 μm.
Figure 9. *Staurolonche?* sp. B, n. sp. GSC 85972, scale = 100 μ.
Figure 10. *Hagiastrum* sp. cf. *H. egregium* Rüst. GSC 85973, scale = 204 μm.
Figure 11. *Acaeniotyle?* sp. A, n. sp. GSC 85974, scale = 100 μm.
Figure 12. Gen. and sp. indet. A. GSC 99395, scale = 100 μm.
Figure 13. *Pseudocrucella* sp. A, n. sp. GSC 99396, scale = 100μm.
Figure 14. *Paronaella porosa* Carter. GSC 99397, scale = 100 μm.
Figure 15. *Mesosaturnalis hexagonus* (Yao). GSC 99398, scale = 133 μm.
Figure 16. *Mesosaturnalis tetraspinus* (Yao). GSC 99399, scale = 154 μm.
Figure 17. Gen. and sp. indet. B. GSC 99400, scale = 100 μm.

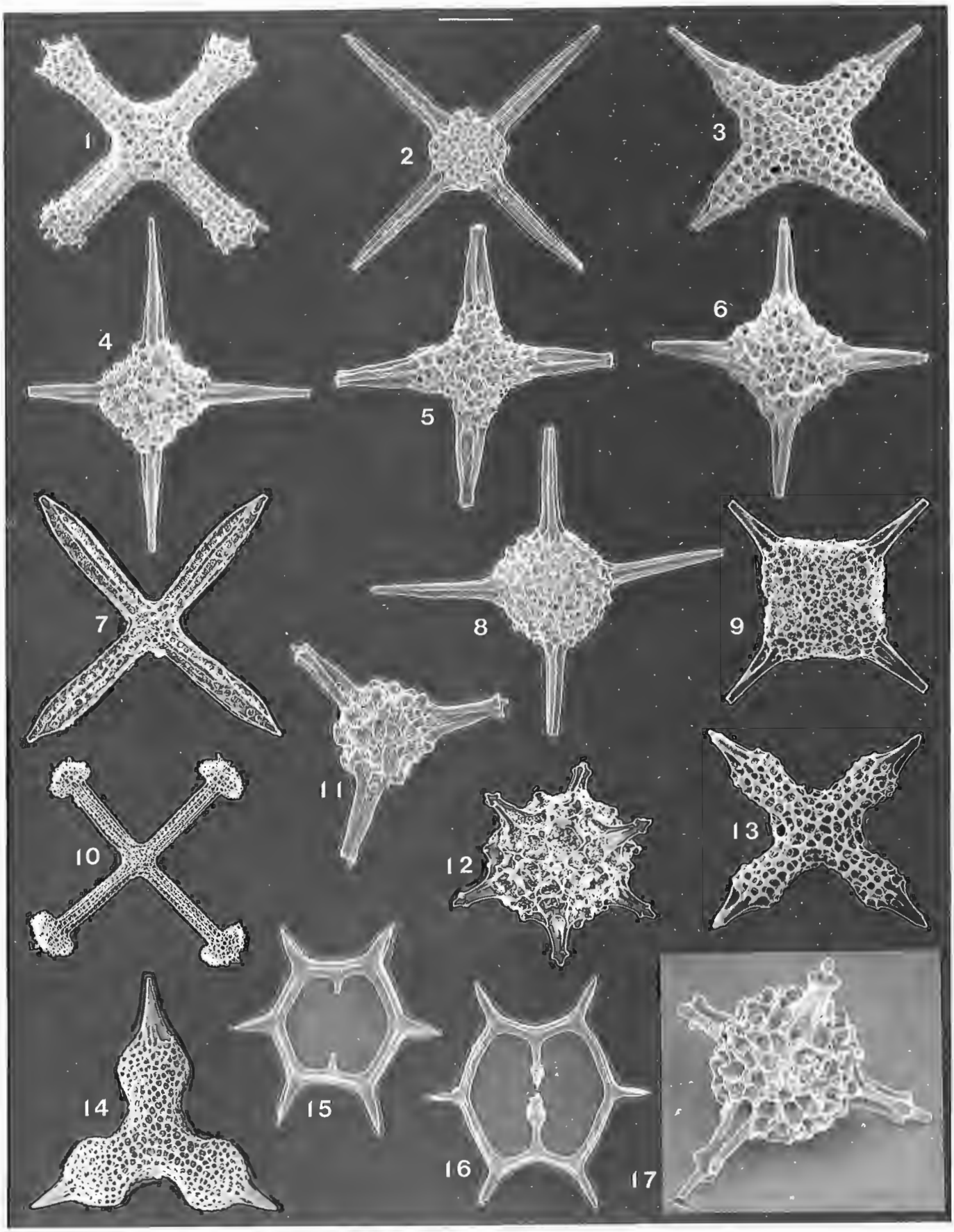
1
2
3
4
5
6
7
8
9
10
11
12
13
14
15
16
17

PLATE 3

Scanning electron micrographs of Aalenian Nassellariina (Radiolaria) from the Phantom Creek Formation, Queen Charlotte Islands, B. C. (GSC sample C-156399). Length of bar scale equals number of μm cited for each specimen illustrated.

Figure 1. *Napora nipponica* Takemura. GSC 99401, scale = 100 μm.
Figure 2. *Napora* sp. aff. *N. nipponica* Takemura. GSC 99402, scale = 100 μm.
Figure 3. *Napora* sp. aff. *cosmica* Pessagno, Whalen and Yeh. GSC 99403, scale = 100 μm.
Figure 4. *Napora bona* Pessagno, Whalen and Yeh. GSC 99404, scale = 81 μm.
Figure 5. *Napora* sp. aff. *fructuosa* Pessagno, Whalen and Yeh. GSC 99405, scale = 100 μm.
Figure 6. *Hilarisirex* sp. cf. *H. oregonensis* Pessagno, Whalen and Yeh. GSC 99406, scale = 100 μm.
Figure 7. *Perispyridium* sp. A, n. sp. GSC 99407, scale = 100 μm.
Figure 8. *Perispyridium* sp. B, n. sp. GSC 99408, scale = 100 μm.
Figure 9. *Napora* sp. A, n. sp. GSC 99409, scale = 100 μm.
Figure 10. *Pseudopoulpus acutipodium* Takemura. GSC 99410, scale = 100 μm.
Figure 11. *Perispyridium* sp. C, n. sp. GSC 99411, scale = 100 μm.
Figure 12. *Stichocapsa convexa* Yao. GSC 99412, scale = 69 μm.
Figure 13. *Turanta* sp. A, n. sp. GSC 99413, scale = 100 μm.
Figure 14. *Tricolocapsa ruesti* Tan. GSC 99414, scale = 67 μm.
Figure 15. *Hsuum* sp. B, n. sp. GSC 99415, scale = 100 μm.
Figure 16. *Hsuum* sp. aff. *H. brevicostatum* (Ozvoldova). GSC 99416, scale = 100 μm.
Figure 17. *Protounuma paulsmithi* Carter. GSC 99417, scale = 82 μm.
Figure 18. *Elodium cameroni* Carter. GSC 99418, scale = 100 μm.
Figure 19. *Parvicingula* sp. A, n. sp. GSC 99419, scale = 100 μm.
Figure 20. *Parvicingula* sp. B, n. sp. GSC 99420, scale = 100 μm.

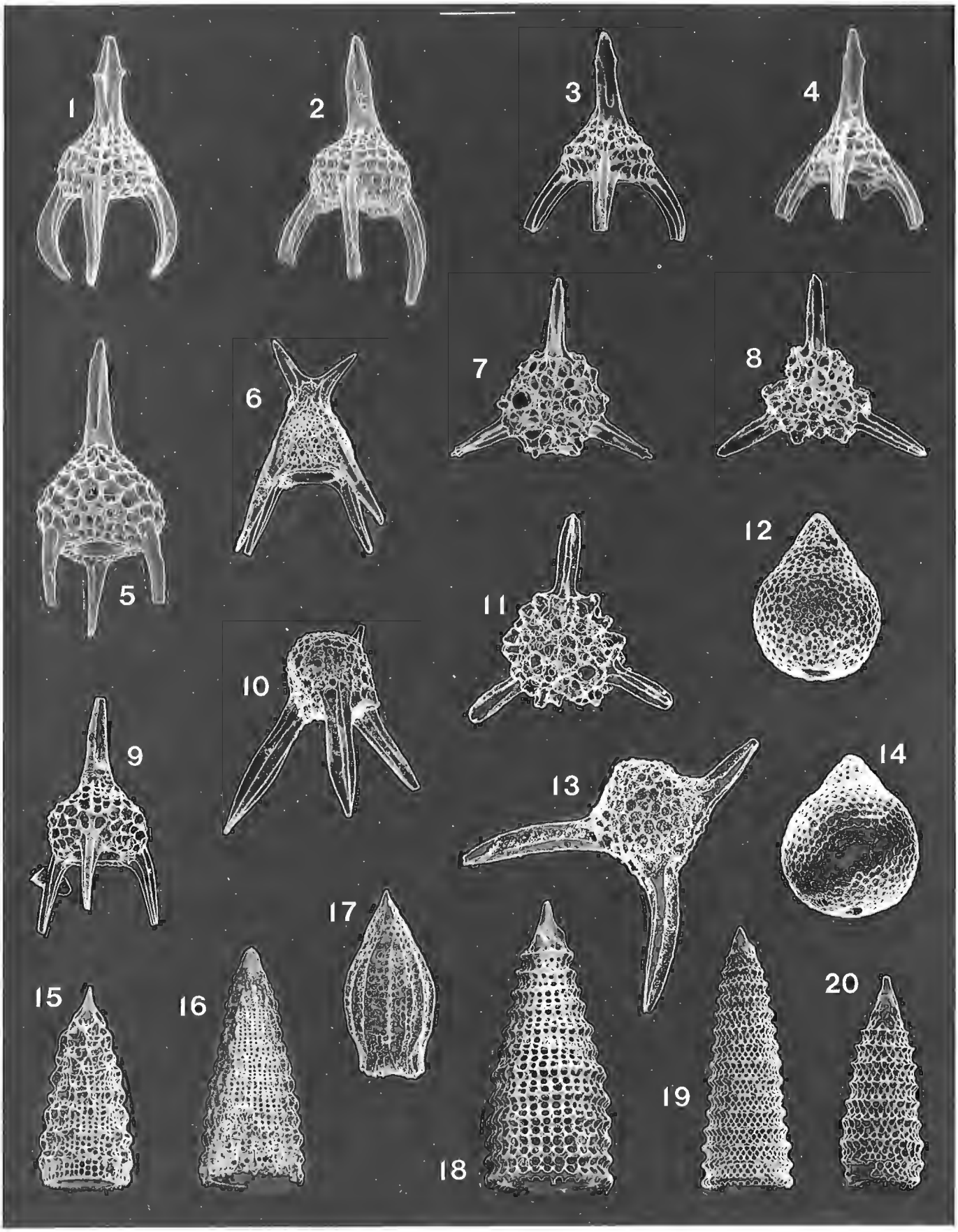
1
2
3
4
5
6
7
8
9
10
11
12
13
14
15
16
17
18
19
20

Lithologies of the Middle Jurassic Yakoun Group in the central Graham Island area, Queen Charlotte Islands, British Columbia[1]

Jonny Hesthammer[2]
Cordilleran Division, Vancouver

Hesthammer, J., Lithologies of the Middle Jurassic Yakoun Group in the central Graham Island area, Queen Charlotte Islands, British Columbia; in Current Research, Part A, Geological Survey of Canada, Paper 91-1A, p. 353-358, 1991.

Abstract

The Middle Jurassic Yakoun Group is one of the most extensive rock units on the Queen Charlotte Islands. The group is heterogeneous, laterally discontinuous, and comprises shale, siltstone, sandstone, conglomerate, lava flows, and pyroclastic rocks. In central Graham Island, four informal lithofacies were recognized. The shale and tuff lithofacies comprises interlayered shale, tuff, siltstone, and sandstone. The sandstone lithofacies consists of medium- to thickly-bedded sandstone interlayered with thinner bedded shale and tuff. The conglomerate lithofacies is a more than 60 m thick sequence of thickly-bedded pebble and cobble conglomerate layers interlayered with minor sandstone and shale. The volcanic lithofacies is a diverse unit of lava flows, air-fall tuff, pyroclastic flow deposits, and laharic rocks.

Résumé

Le groupe de Yakoun du Jurassique moyen est l'une des unités lithologiques les plus étendues des îles de la Reine-Charlotte. Il s'agit d'un groupe hétérogène, latéralement discontinu et composé de shale, de siltstone, de grès, de conglomérat, de coulées de lave et de roches pyroclastiques. Au centre de l'île Graham, on distingue quatre lithofaciès non-désignés. Le lithofaciès de shale et de tuf contient des interstratifications de shale, de tuf, de silstone et de grès. Le lithofaciès de grès est composé de grès à stratifications de puissance moyenne à épaisse au sein duquel s'intercalent des couches plus minces de shale et de tuf. Le lithofaciès de conglomérat est une séquence de plus de 60 m d'épaisseur comprenant des couches épaisses de conglomérat à petits et gros cailloux interstratifiées avec une faible quantité de grès et de shale. Le lithofaciès volcanique est une unité de nature variée caractérisée par la présence de coulées de lave, de tuf de retombée, d'ignimbrites et de roches de lahar.

[1] Contribution to Frontier Geoscience Program
[2] Department of Geological Sciences, University of British Columbia, 6339 Stores Road, Vancouver, B.C. V6T 2B4

INTRODUCTION

The Middle Jurassic Yakoun Group on the Queen Charlotte Islands is known for its extensive distribution and lithological variety. Shale, siltstone, sandstone, conglomerate, lava flows, and pyroclastic rock deposits make up the unit. The time of deposition is coeval to, or postdates one of the major compressional events recorded on the islands (Thompson et al., 1991; Lewis and Ross, 1991).

The volcanic rocks of the Yakoun Group were first described by Dawson (1880) and were originally named Yakoun Formation by MacKenzie (1916). Sutherland Brown (1968) divided the unit into five informal members. Biostratigraphic studies by Cameron and Tipper (1985) redefined the Yakoun Formation as the Yakoun Group comprising two formations and several members.

Lithologies of the Yakoun Group in the central Graham Island area (Fig. 1) are important in reconstruction of the Middle Jurassic paleogeography in the Queen Charlotte Islands. The results presented here are the product of three seasons of field mapping on the Queen Charlotte Islands as part of the Frontier Geoscience Program (FGP). They include outcrop and petrographic descriptions of several new lithologies.

PREVIOUS WORK

The Yakoun Group rocks overlie the Maude and Kunga groups along a moderate to sharp angular unconformity (Thompson and Thorkelson, 1989; Indrelid et al., 1991). At Skidegate Inlet and on central Graham Island, the Yakoun Group consists of two formations, the Graham Island Formation, and the overlying Richardson Bay Formation which make up more than 1000 m of strata (Cameron and Tipper, 1985). The Graham Island Formation was subdivided into four informal members. In ascending order, these are the shale-tuff member (found on central Graham Island); the mottled siltstone member (found around Skidegate Inlet); the volcanic sandstone member (central Graham Island); and the lapilli member (Skidegate Inlet). The lower two members are fossil poor, and are interpreted as deep to shallow marine deposits. The upper two members typically contain a greater amount of sandstone and volcanic material, and are interpreted as shallow marine and partly nonmarine.

The Richardson Bay Formation was subdivided into two informal members, the volcanic breccia member and the dark sandstone member (Cameron and Tipper, 1985). The volcanic breccia member comprises epiclastic breccia and conglomerate, tuff, and lahars. The dark sandstone member is typified by dark, greenish-grey, volcanic-derived sandstone containing bivalves, wood, and plant fragments, interlayered with siltstone and shale. The age of the unit is early Bajocian (Cameron and Tipper, 1985).

A NEW STRATIGRAPHIC SCHEME FOR THE YAKOUN GROUP

Because of the diverse lithology and abrupt facies change within the Yakoun Group, Cameron and Tipper's (1985) subdivisions cannot be mapped regionally without extensive fossil control. For example shale and tuff are most common in the

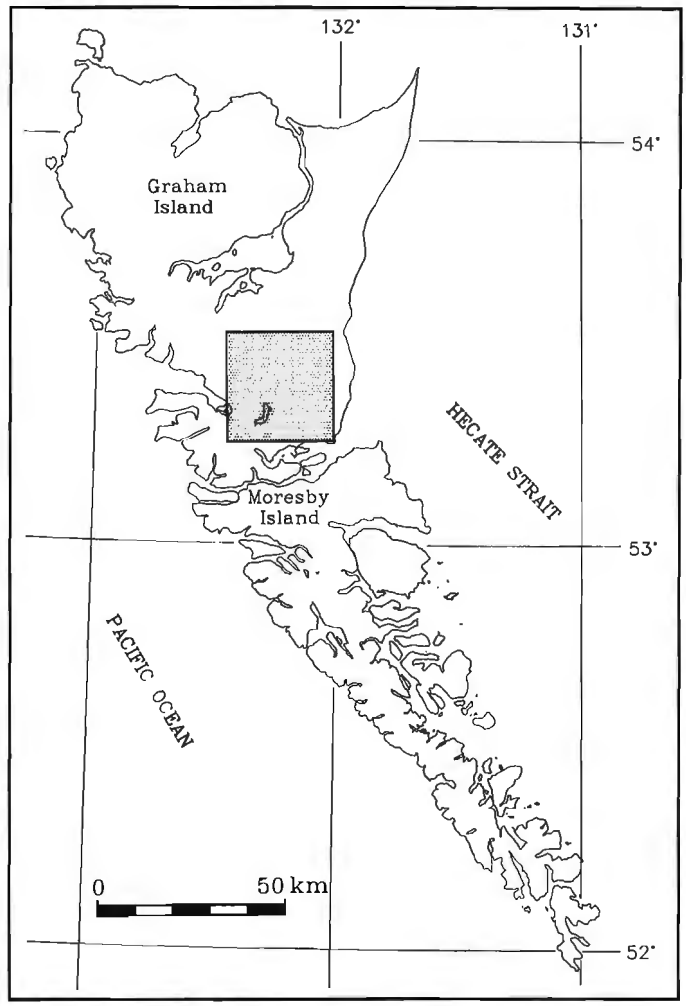

Figure 1. Location map showing study area on central Graham Island.

Graham Island Formation, but are also present several places within the Richardson Bay Formation. It is difficult to distinguish between the volcanic sandstone member of the Graham Island Formation and the dark sandstone member of the Richardson Bay Formation. A conglomerate lithofacies is mainly restricted to the Richardson Bay Formation, but likely interfingers with the upper part of the Graham Island Formation. The "volcanic breccia member" is not an adequate description of all volcanic lithologies now recognized in the Yakoun Group. Also, volcanic rocks of the Yakoun Group are not restricted to the Richardson Bay Formation, but interfinger with the Graham Island Formation. These new findings led me to map the Yakoun Group as several different lithological types rather than the formal formations. Four lithofacies are defined: the shale and tuff lithofacies; the sandstone lithofacies; the conglomerate lithofacies; and the volcanic lithofacies. The lithofacies are defined on the major lithology seen in each unit, and comprise several additional lithologies. The conglomerate lithofacies contains the only regionally extensive unit, a conglomerate layer up to 20 m thick (Hesthammer, 1990). The character of each lithofacies in central Graham Island is described below in the context of Cameron and Tipper's (1985) formal divisions.

Shale and tuff lithofacies

The shale and tuff lithofacies is more than 200 m thick and occurs mostly in northern and western parts of the map area (Fig. 1). The unit comprises interbedded shale, tuff, siltstone, and sandstone. Lithologically it resembles the Sandilands Formation (Kunga Group) or the Ghost Creek Formation (Maude Group), but can often be differentiated from these older units by its greater amount of terrestrial wood fragments. Medium- to thickly-bedded shale dominate over minor, intercalated crystal tuff, siltstone, and sandstone (Fig. 2). Bed thickness in places reaches 30-40 cm, and rare thicker (up to 50 cm), internally bedded sandstone layers occur. Potato-like concretions, 2-3 cm large, are common in the more calcareous parts of the lithofacies. Pyritic nodules and layers (1-3 cm thick) are also abundant. Black or dark grey to blue and bluish-grey fresh surfaces weather to brown, rusty, or green. The rocks are mostly loose and friable, and the shale component often has a well-developed bedding plane fissility.

Quartz in the sandstone and siltstone does not exceed 20 %, and mostly has a plutonic source, whereas volcanic quartz is rare. Some sandstone layers comprise up to 80 % volcanic rock fragments and feldspar laths up to 2 mm. Those rock fragments are intermediate to mafic in composition. The sandstone matrix commonly is iron-rich. Some of the shale units are rich in organic material, and may contain up to 60 % silicified radiolarians. Crystal tuff layers comprise up to 60 % unbroken, euhedral feldspar crystals, which are commonly partially altered to clay. Chlorite is the most common mica seen in all rock types.

Sorting and sphericity is poor and the grains are angular. Well preserved terrestrial wood fragments, minor coal seams, belemnites, and ammonite imprints are common. The abundance of wood fragments, may indicate near-shore environment. Pyrite and preserved coal suggest that the sediments were rapidly enclosed in a reducing environment. Angular grains indicate short transport distances. Deposition of the unit was coeval with nearby active volcanism, but it was distal enough so that only ash-size air-fall fragments reached the basins. The shale and tuff lithofacies is lithologically similar to the shale-tuff member of the Graham Island Formation, but some units are probably part of the Richardson Bay Formation.

Sandstone lithofacies

The sandstone lithofacies occurs in all parts of the study area except in the most easterly regions. It consists of spheroidal weathering, medium- to thickly-bedded lithic arenite, interlayered with thinly-bedded shale. Parts of the unit resemble the Fannin and the Haida formations, and it can be difficult to distinguish between them without fossil control. The sandstone lithofacies overlies the shale and tuff lithofacies with a gradational contact (Fig. 3). Light grey or bluish-grey fresh surfaces weather green, yellowish-green, brownish-grey, or rusty. Shale, crystal tuff, and pyrite beds, 2-10 cm thick, are commonly interbedded with the sandstone layers. Minor granule to pebble conglomerate beds (<1.5 m thick) occur throughout the sequence. A coal bed in the northeastern part of the map area, near Wilson Creek, measures more than 2 m in thickness. Load structures, mud drapes, crossbedding, and bioturbation are common.

Grain sizes within the sandstone layers vary from clay to pebble (average = 0.5 mm). Sorting is poor to medium and the grains are angular with poor to medium sphericity. The sandstone layers lack porosity. Fragments of ammonites, belemnites, bivalves, as well as coal and detrital wood are common in all parts of the lithofacies.

The sandstone matrix is chlorite and contains up to 30 % glauconite which likely gives the rocks the green colour. Angular feldspar crystals, partially altered to clay, are also common in some of the sandstone layers, and are probably associated with volcanic fall-out of crystal tuff. The rocks contain up to 30 % plutonic quartz grains with undulose extinction. Volcanic quartz exists occasionally, and may have been derived from dacite of the intercalated volcanic rocks. Less than 10 % chert and polycrystalline quartz are present. Biotite, microcline, plagioclase, and potassium feldspar are minor constituents. The sandstones have abundant lithic fragments, some weathered to clay. The organic-rich matrix is high in siderite. A few chamosite oolites occur in some of the coarser sandstone layers.

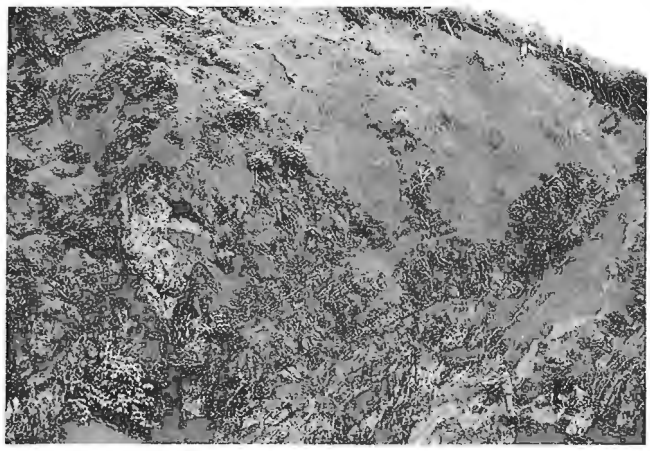

Figure 2. The shale and tuff lithofacies. The main components are shale and tuff, but the unit also comprises minor siltstone, sandstone, and pyrite layers.

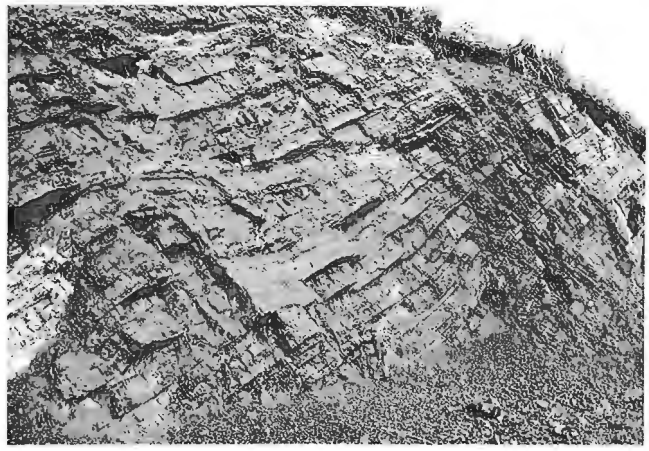

Figure 3. The lower part of the sandstone lithofacies. The unit overlies the shale and tuff lithofacies with a gradational contact.

The presence of coal, detrital wood, bivalves, and oolites suggest a shallow marine and possible partly nonmarine setting. Contemporaneous volcanism, suggested by crystal tuff members, probably was too far away to provide epiclastic fragments larger than ash-size. Angular lithic grains indicate a local source. This unit is mostly the equivalent of the volcanic sandstone member of the Graham Island Formation, but some parts are lithologically similar to the dark sandstone member of the Richardson Bay Formation.

Conglomerate lithofacies

This sequence comprises thickly-bedded pebble and cobble conglomerate interbedded with thinly-bedded sandstone, shale, siltstone, and rare tuff. The best exposure of the unit is 60 m thick and provides a minimum estimate of its thickness.

The conglomerate varies from 15 cm to 1.5 m thick and is massive. Dark fresh surfaces weather to brown or rust. Spheroidal weathering is rare and the matrix is soft and friable. The friable and brown weathering appearance as well as lack of granitic clasts distinguish the unit from the Honna Formation conglomerate. Clasts range from large pebbles to cobbles (1-40 cm, average = 4 cm), and are of plutonic, volcanic, and sedimentary origin. Volcanic clasts and sandstone clasts are apparently mostly derived from underlying parts of the Yakoun Group. Some volcanic clasts are brick red. Clasts are poorly to moderately sorted and exhibit medium rounding and sphericity. The most resistant clasts are angular, and breccia is a local component.

The rocks are matrix-supported with very little or absent porosity. The sandstone matrix contains quartz, quartzite, and plagioclase. The plagioclase is often altered to calcite. Other common matrix minerals are chlorite, biotite, and amphibole. Siderite dominates the cement, but carbonate may also occur in veins and as single crystals. Concretions contain well-preserved but rare ammonites. One specimen constrains the age of part of the conglomerate lithofacies to late Bajocian (H.W. Tipper, pers. comm., 1990), the age of the Richardson Bay Formation. Abundant wood may indicate a near-shore environment of deposition.

Volcanic lithofacies

Andesitic to basaltic lava flows, pyroclastic rocks, and lahars make up the volcanic lithofacies. Felsic rocks are rare. The unit is several hundred metres thick and overlies or partly interfingers with the other units. Individual flows vary from 10 cm to a few metres in thickness, but pyroclastic deposits and lahars are usually several metres thick.

Lava flows

Intermediate to mafic (rarely felsic) lava flows are commonly columnar jointed. Fresh surface-colour ranges from white to black, but is generally dark grey to bluish-grey. Weathered outcrops are quite soft and can be mistaken for a feldspar-rich sandstone. The unit is aphanitic with feldspar and pyroxene micro phenocrysts and commonly vesicular or amygdaloidal with calcite infillings. Plagioclase can comprise up to 80 % of the rock. Plagioclase phenocrysts are euhedral, 1-4 mm in diameter, and partially replaced by calcite. Pyroxene and biotite occur as rare phenocrysts. The groundmass comprises 30 % or less (but up to 70 % chlorite, and is also high in siderite. A few samples show a weak linear alignment of plagioclase laths and chlorite crystals. Columnar jointing suggests, but is not an evidence for, subaerial eruption (Spry, 1961).

Pyroclastic rocks

Pyroclastic rocks include both pyroclastic flow deposits and air-fall deposits. Pyroclastic flow deposits in the central Graham Island area include thickly-bedded and massive, monolithic to heterolithic, matrix-supported pyroclastic breccia (Fig. 4), ash-flow tuff (Fig. 5), and lapilli tuff. Columnar jointing and flow textures are scarce in all the pyroclastic deposits. Both weathered and fresh surfaces have a dark to intermediate colour, and the rocks are commonly very hard. In coarse pyroclastic breccia and the lapilli-flow tuff, cognate or accidental clasts dominate over juvenile clasts. Clast colours vary, and may be black, grey, blue, red, or green, ranging in composition from intermediate to felsic. Clast size is mostly less than 20 cm (average = 2-3 cm), but rare clasts

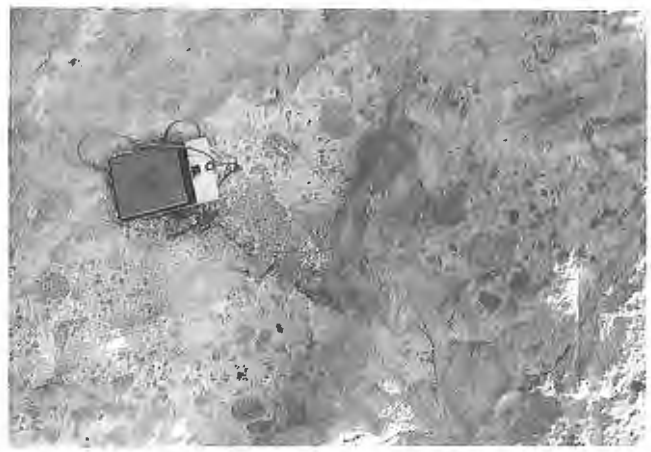

Figure 4. Coarse pyroclastic breccia of the volcanic lithofacies. Clasts are of cognate or accidental origin.

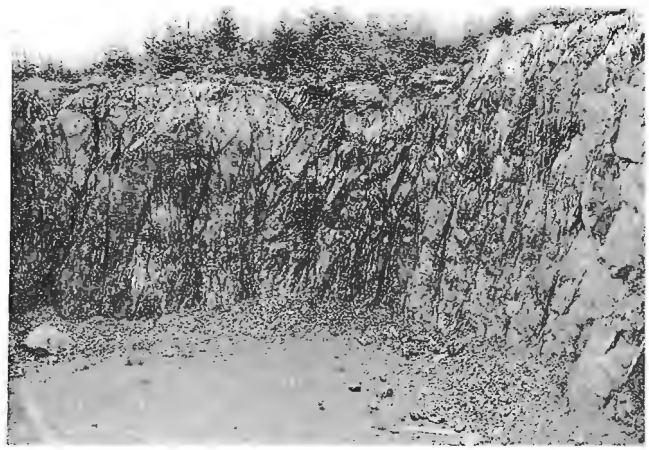

Figure 5. Ash-flow tuff of the volcanic lithofacies. The outcrop is very faulted, which is typical for the competent rocks of the Yakoun Group. No bedding is seen at this outcrop.

are up to 50 cm in diameter. Sorting is poor and fragments are commonly angular and free-floating in the matrix. Large clast sizes in some of the pyroclastic breccia suggest deposition close to the volcanic sources. Sedimentary accidental clasts indicate a basement of sedimentary origin (possibly from the lower part of the Yakoun Group).

Ash-flow tuff and the groundmass of the pyroclastic breccia and the lapilli-flow tuff are commonly intermediate in composition, aphanitic, and may resemble the lava flows. In addition to the dominant feldspar, amphibole, orthopyroxene, and clinopyroxene also occur as phenocrysts but none are aligned.

Air-fall deposits are generally moderate to well-sorted, graded beds of air-fall crystal-tuff of intermediate composition. Plagioclase phenocrysts are embedded in an ash-matrix. Agglomerate described by Cameron and Tipper (1985) are rare in the central Graham Island area. The volcanic rocks are commonly interbedded with sedimentary rocks of the Yakoun Group and this helps distinguishing this unit from the Tertiary Masset Formation.

Lahars

The lahars are poorly lithified and contain poorly sorted, angular, heterolithic clasts (0.5 cm to more than 2 m in size; Fig. 6). A granular greywacke and mud matrix contain reworked feldspar phenocrysts, pyroxene, potassium feldspar, chlorite, biotite, calcite, siderite, and pyrite. Epiclastic fragments can make up as much as 80 % of the clast-supported rocks. These fragments may contain up to 70 % lithic or crystal tuff, and lesser clasts of sedimentary or plutonic origin. No primary fabric occurs in the lahars. Fossil wood is abundant. The lithofacies is partly equivalent to Cameron and Tipper's (1985) volcanic breccia member of the Richardson Bay Formation.

SUMMARY

Four lithofacies of the heterogeneous Yakoun Group are distinguished on the basis of lithological differences rather than fossil fauna.

Figure 6. Lahar of the volcanic lithofacies. The rocks are poorly sorted with angular, heterolithic clasts. Clast sizes vary from 0.5 cm to more than 2 m.

The shale and tuff lithofacies comprises thin alternating beds of shale, tuff, siltstone, sandstone, and rare pyrite. The sandstone lithofacies consists of medium- to thickly-bedded lithic arenite interbedded with thin beds of shale, tuff, pyrite, and minor conglomerate. The conglomerate lithofacies is a more than 60 m thick sequence of thickly-bedded pebble and cobble conglomerate layers interlayered with thinner beds of sandstone, shale, and siltstone. Clasts are mostly volcanic with minor plutonic or sedimentary sources. The volcanic lithofacies is divided into several sub-units. The lava flows comprise thickly-layered feldspar-pyroxene-phyric, mostly aphanitic, and vesicular or amygdaloidal, medium dark rocks of mainly intermediate composition. Pyroclastic flow deposits consist of coarse pyroclastic breccia and lapilli-flow tuff, containing heterolithic, cognate and accidental clasts, and feldspar-phyric and amygdaloidal andesitic ash-flow tuff. Air-fall deposits are mainly crystal tuff. The lahars are poorly sorted debris-flows with angular to moderately rounded heterolithic clasts.

ACKNOWLEDGMENTS

The Geological Survey of Canada supported the program financially. Without the help of Howard Tipper, an understanding of the Yakoun Group would have been very difficult. Jarand Indrelid, Peter Lewis, Susan Taite, Jim Haggart, John Ross, and Bill Barnes are thanked for invaluable and useful discussion.

REFERENCES

Cameron, B.E.B. and Tipper, H.W.
1985: Jurassic stratigraphy of the Queen Charlotte Islands; Geological Survey of Canada, Bulletin 365.

Dawson, G.M.
1880: Queen Charlotte Islands; Geological Survey of Canada, Report of Progress, 1878-1879.

Hesthammer, J.
1990: Structural interpretation of Upper Triassic and Jurassic units exposed on central Graham Island, Queen Charlotte Islands, British Columbia; in Current Research, Part F, Geological Survey of Canada, Paper 90-1F, p. 11-18.

Indrelid, J., Hesthammer, J., and Ross, J.V.
1991: Structural geology and stratigraphy of Mesozoic rocks of central Graham Island, Queen Charlotte Islands, British Columbia; in Evolution and Hydrocarbon Potential of the Queen Charlotte Basin, British Columbia, Geological Survey of Canada, Paper 90-10.

Lewis, P.D. and Ross, J.V.
1991: Mesozoic and Cenozoic structural history of the central Queen Charlotte Islands, British Columbia; in Evolution and Hydrocarbon Potential of the Queen Charlotte Basin, British Columbia, Geological Survey of Canada, Paper 90-10.

MacKenzie, J.D.
1916: Geology of Graham Island, British Columbia; Geological Survey of Canada, Memoir 88.

Spry, A.
1961: The origin of columnar jointing, particularly in basalt flows; Geological Survey of Australia, Bulletin, v. 8, p. 191-216.

Sutherland Brown, A.
1968: Geology of the Queen Charlotte Islands, British Columbia; British Columbia Department of Mines and Petroleum Resources, Bulletin 54, 226 p.

Thompson, R.I. and Thorkelson, D.
1989: Regional mapping update, central Queen Charlotte Islands, British Columbia; in Current Research, Part H, Geological Survey of Canada, Paper 89-1H, p. 7-12.

Thompson, R.I., Haggart, J.W., and Lewis, P.D.
1991: Late Triassic through early Tertiary evolution of the Queen Charlotte Basin, British Columbia, with a perspective on hydrocarbon potential; in Evolution and Hydrocarbon Potential of the Queen Charlotte Basin, British Columbia, Geological Survey of Canada, Paper 90-10.

New sections of Yakoun Group (Middle Jurassic) strata, Queen Charlotte Islands, British Columbia

James W. Haggart
Cordilleran Division, Vancouver

Haggart, J.W., New sections of Yakoun Group (Middle Jurassic) strata, Queen Charlotte Islands, British Columbia; in Current Research, Part A, Geological Survey of Canada, Paper 91-1A, p. 359-366, 1991.

Abstract

New sections of Yakoun Group strata have been identified in the northern and southern parts of the Queen Charlotte Islands. The northern locality significantly expands the known distribution of Yakoun Group strata in the islands region. Lithologically, the strata at both localities resemble rocks at the type localities of the Graham Island and Richardson Bay formations of the Yakoun Group, although differences exist. The paleogeography of the Middle Jurassic volcanic arc complex in the Queen Charlotte Islands region was likely quite complex.

Résumé

De nouvelles sections de couches du groupe de Yakoun ont été identifiées dans les parties septentrionale et méridionale des îles de la Reine-Charlotte. L'emplacement septentrional permet d'étendre de manière importante la distribution connue des couches du groupe de Yakoun dans la région insulaire. Du point de vue lithologique, les couches aux deux emplacements ressemblent aux roches des localités types des formations de Graham Island et de Richardson Bay, bien qu'il y ait des différences. La paléogéographie du complexe d'arc volcanique du Jurassique moyen dans la région des îles de la Reine-Charlotte était vraisemblablement très complexe.

INTRODUCTION

Volcanic and sedimentary deposits of the Middle Jurassic (Bajocian) Yakoun Group form a significant part of the stratigraphic succession of the Queen Charlotte Islands. The stratigraphy of this unit has been described principally from exposures in the central islands region (Sutherland Brown, 1968; Cameron and Tipper, 1985) and little is known of the lithological and temporal variations of the unit outside of that area.

Field studies undertaken in 1989 and 1990 identified two new localities of Yakoun Group strata, one on extreme northern Lyell Island and the other on the northwest coast of Graham Island (Fig. 1). The stratigraphic successions at these two localities provide important new information on the nature and geographic extent of Middle Jurassic deposition in the islands region.

LYELL ISLAND

The Lyell Island exposures are on the island's north coast (Fig. 2). The outcrops are along the east side of the bay west of Dodge Point, from the back of the bay for about 0.75 km northwards towards the point. The strata are preserved in wide, wave-cut benches in the higher intertidal zone and were previously mapped as Lower Cretaceous Longarm Formation (Sutherland Brown, 1968). Cameron and Hamilton

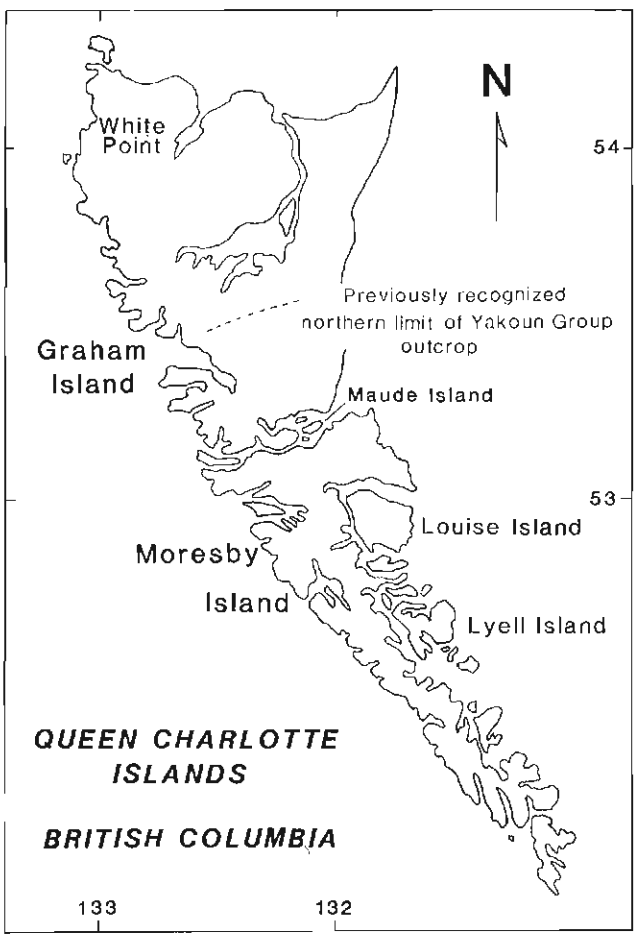

Figure 1. Location map showing principal study areas.

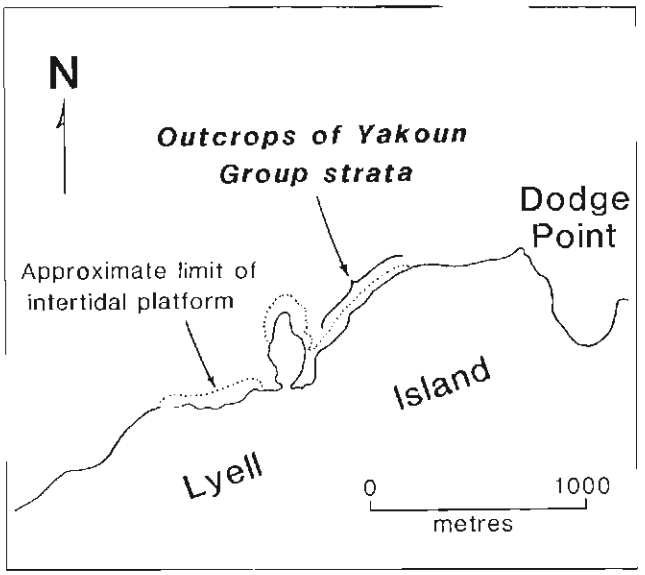

Figure 2. Location map of Lyell Island exposures.

(1988) briefly discussed outcrops on northern Lyell Island and suggested, on lithological grounds, that an assignment of some of the exposures to the Yakoun Group was preferable.

The outcrops form a wide syncline plunging to the southeast. Two stratigraphic sections are preserved, one on each limb of the fold. Strata in these two sections are relatively undeformed but the hinge zone is intensely faulted and intruded. Although similar lithologies are noted in each of the sections, continuity of bedding across the fold's axis can not be demonstrated.

The section on the south limb of the syncline is approximately 59 m thick. The lower and upper limits of the section are not exposed. Ammonites collected from this section (GSC loc. C-156698 and loc. C-156699) include stephanoceratids and sonniniids suggestive of an Early Bajocian age (unpub. GSC Fossil Report HWT-1990-J6). The following succession of lithofacies is found in the section, in ascending stratigraphic order: a basal mudstone and siltstone lithofacies; a sandstone and mudstone lithofacies; a conglomerate and sandstone lithofacies; and a massive sandstone lithofacies.

Approximately 38 m of strata were measured in the section on the north limb of the syncline. The lower and upper limits of this section are not exposed and no age-diagnostic fossils were collected. Strata in this section consist predominantly of interstratified conglomerate and sandstone, and are considered correlative to the conglomerate and sandstone lithofacies found on the syncline's southern limb. Neither the underlying mudstone and siltstone lithofacies nor the sandstone and mudstone lithofacies is preserved in the northern section.

Volcanic deposits which appear to be interstratified with the sedimentary strata at the top of the northern section are described as a separate, volcanic lithofacies.

Each of the five lithofacies found near Dodge Point is described in detail below.

Mudstone and Siltstone Lithofacies (30.6 m maximum thickness)

The base of the preserved southern section consists of a 30.6 m-thick, coarsening upward sequence of bioturbated mudstone and laminated siltstone (Fig. 3a). Several small-scale faults were noted within this lithological unit. The lower 6-8 m of the lithofacies is composed predominantly of mudstone (60 %) but the proportion of siltstone increases in the upper 20 m. Associated with the mudstone and siltstone are minor, thin (2-4 cm), silty fine grained sandstone interbeds. Pink calcareous concretions occur within the mudstone beds and some of the sandstone interbeds are cemented with calcite cement. No macrofossils were noted. These beds are conformably but sharply overlain by the sandstone and mudstone lithofacies.

Sandstone and Mudstone Lithofacies (5.6 m maximum thickness)

This lithofacies consists of 0.5-1.0 m-thick laminated, lithic-rich sandstone interstratified with minor, thinly-bedded mudstone. Bioturbation is minimal and restricted to the mudstone intervals. The basal part of the unit shows local trough cross-stratification where it is channelled into the underlying mudstone and siltstone unit (Fig. 3b). No macrofossils were found.

Conglomerate and Sandstone Lithofacies (15.9 m maximum thickness)

Expansive exposures of this lithofacies are found in the intertidal zone in both Lyell Island sections. The bulk of the strata found in this lithofacies consists of conglomerate and sandstone (Fig. 3c) although minor siltstone and even mudstone are found.

The thickly-bedded conglomerate is moderately- to poorly-sorted and composed of well-rounded to angular clasts, ranging in size from several centimetres to 0.4 m. Most clasts are of volcanic composition (80 %), although argillite and sandstone (10 %) and shale intraclasts (10 %) are also found. One plutonic clast was noted. The matrix of the conglomerate is a greenish lithic arenite, rich in poorly-sorted and angular, medium- to coarse-grained volcanic fragments. The conglomerates grade, both laterally and upsection, into sandstone of similar composition but lacking large clasts. Locally, they are internally graded, cross-stratified, and channelled into the underlying beds.

The conglomerate beds thicken upsection. At the base of the lithofacies unit the conglomerate beds are of decimetre thickness with a generally small clast size. Near the top, however, some beds, composed of generally larger clast sizes, are more than 2 m thick.

Beds of fine grained sandstone, siltstone, and minor silty mudstone are interstratified within the succession, the coarser of these exhibiting a composition similar to the matrix of the conglomerates. The sandstone beds and associated siltstones are commonly graded or laminated (Fig. 3d) and locally show abundant organic detritus and coalified plant fragments. The boundaries of these beds with the conglomerates are generally abrupt.

Marine molluscs are common within the conglomerate and sandstone lithofacies. They appear in places to be preserved in reworked shale intraclasts incorporated into the conglomerate deposits, although some were found in the conglomerate matrix. The shale clasts with fossils are all poorly lithified, and the shell material delicately preserved, suggesting that the clasts are intraclasts rather than reworked from older deposits.

Massive Sandstone Lithofacies (7.2 m maximum thickness)

This lithofacies consists of thickly-bedded, massive to graded sandstone, locally with shale rip-up clasts and minor conglomerate at the base of some fining-upward sequences. The sandstone is medium- to coarse-grained, poorly-sorted, and lithic-rich, similar in composition to the underlying conglomerate and sandstone lithofacies. Molluscs were commonly collected from these beds, principally abraded and poorly-preserved belemnites, fragments of oysters, and other bivalves.

Volcanic Lithofacies (estimated 30+ m maximum thickness)

The final lithofacies noted in the Lyell Island sections is a volcanic facies, including pyroclastic flows, breccias, and associated lahar deposits. Outcrops of this lithofacies are separated from the main part of the northern section by covered intervals and faults. Despite this limitation, the volcanic rocks are considered part of the Jurassic succession for two principal reasons: 1) conglomerate and sandstone similar to that seen in both the southern and northern sections is interstratified with the volcanic rocks, and the lithic component of these sedimentary strata is present in the volcanics; and 2) lithologies similar to the volcanic rocks are noted in the clasts within the conglomerates of both the northern and southern sections.

The volcanic rocks are principally intermediate pyroclastic flows and breccias, generally dark in colour; some basalt was noted. A feldspar porphyry texture is common in the flows, with euhedral phenocrysts to 2 mm in length. Individual flow units are generally thin, 1-2 m thick, with lateral variation. The pyroclastic breccia horizons are commonly thicker, up to 3 or 4 m, and also laterally variable. Volcanic rock fragments 1.5 m in diameter are common in the breccias (Fig. 3e). The pyroclastic breccias include volcanic fragments of similar composition to the flow rocks.

Beds of sandstone and conglomerate exhibiting chaotic soft-sediment deformation are interstratified with the volcanic rocks in this lithofacies. Lithologically, these sedimentary strata are of similar composition to the conglomerate and sandstone lithofacies of the adjacent stratigraphic sections. Locally, large blocks of pyroclastic-flow debris are noted in these sandstone and conglomerate beds. Some of these mixed sedimentary and volcanic deposits appear to be lahars, containing a clastic matrix rich in volcanic material, as if formed from a slurry of sand, gravel, and volcanic ejecta.

Depositional environment

A detailed analysis of the depositional environment of these deposits is beyond the scope of this paper. The presence of

ammonites, abraded belemnites, and oyster and trigoniid fragments suggests a shallow marine environment. A shallow water to subaerial interpretation is also supported by the presence of coalified plant debris in the conglomerate and sandstone lithofacies as well as the associated volcanic deposits.

The section is a regressive sequence, with deeper-water siltstone and mudstone at the base grading into shallow-marine sandstones and conglomerates, and finally, into volcanic flows and lahars.

NORTHWEST GRAHAM ISLAND

Exposures of volcanic rocks which outcrop south of White Point, on northwestern Graham Island (Fig. 1), were previously considered to belong to the Tertiary Masset Formation (Sutherland Brown, 1968; Haggart, 1989; Hickson, 1990). Study of additional exposures in this area in 1990 showed that the volcanic rocks underlie strata of Tithonian age (previously assigned to the Longarm Formation by Sutherland Brown [1968]; *see* discussions of Haggart [1989] and Gamba [1991]) and are thus likely correlative with the Yakoun Group.

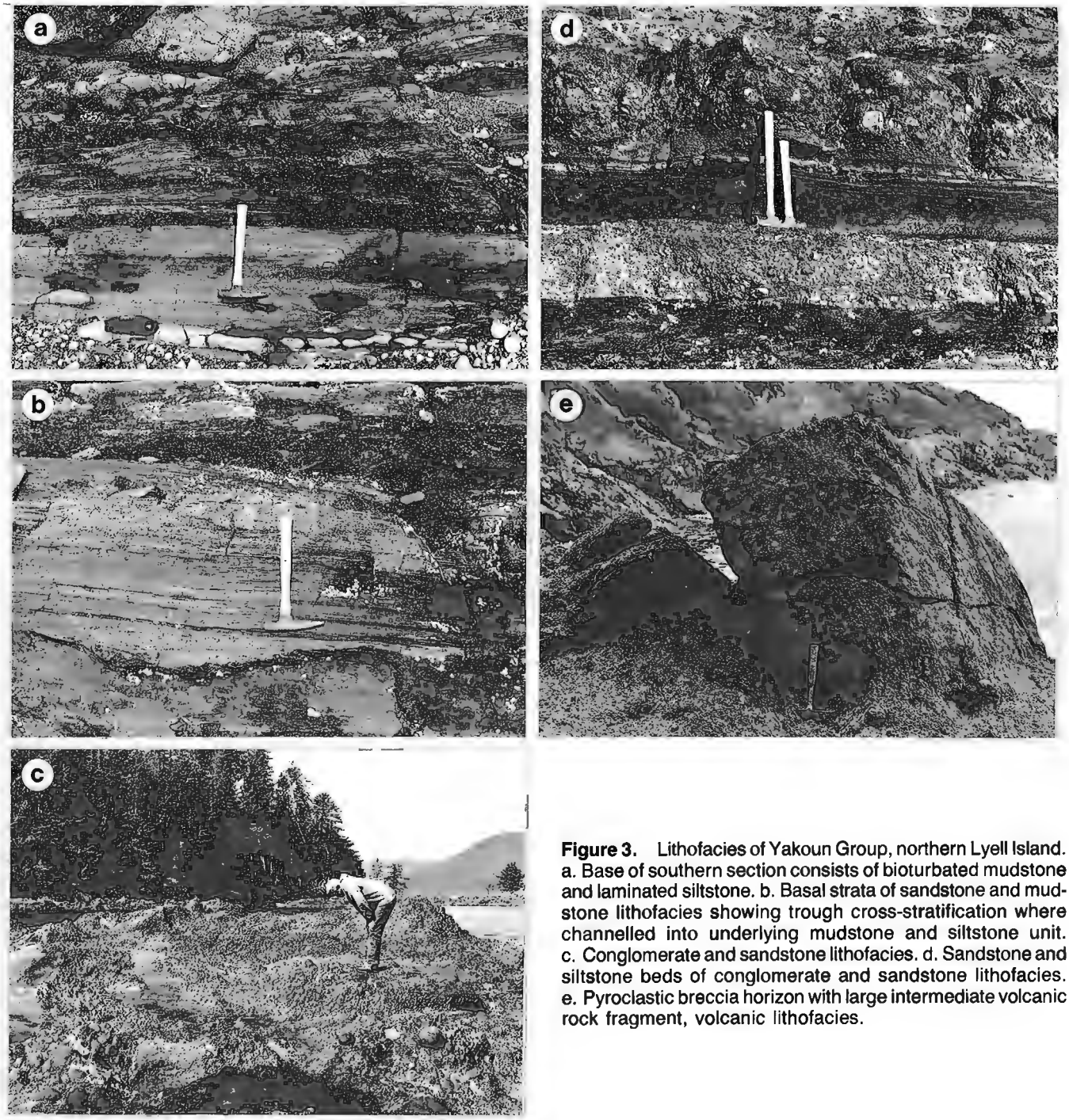

Figure 3. Lithofacies of Yakoun Group, northern Lyell Island. a. Base of southern section consists of bioturbated mudstone and laminated siltstone. b. Basal strata of sandstone and mudstone lithofacies showing trough cross-stratification where channelled into underlying mudstone and siltstone unit. c. Conglomerate and sandstone lithofacies. d. Sandstone and siltstone beds of conglomerate and sandstone lithofacies. e. Pyroclastic breccia horizon with large intermediate volcanic rock fragment, volcanic lithofacies.

The exposures are found at two different localities (Fig. 4). The first is on the shore of Graham Island about 1.1 km southwest of White Point. The second is at the western end of the small island complex offshore from the Graham Island exposures. Additional outcrops of similar volcanic strata, previously mapped as Cretaceous Longarm Formation (Hickson, 1990), are found along the coast for about 2 km to southward. These rocks are herein correlated with the Yakoun Group. Hickson (*in* Haggart, 1989; pers. comm., 1990) previously noted the lithological uniqueness of these volcanic rocks, compared to typical Masset Formation.

Graham Island exposures

The section of Jurassic volcanic rocks and associated sedimentary strata found on Graham Island is overlain by conglomerates of probable Tithonian age. The lower limit is not exposed. The upper contact is faulted or covered but is considered to be unconformable. About 0.5 km to the north, this block of Jurassic strata is faulted against pyroclastic rocks of the Tertiary Masset Formation (Hickson, 1990).

The section of volcanic strata is approximately 55 m in thickness. Two distinct lithofacies are noted in the section: a basal, dark-coloured volcanic flow lithofacies; and an overlying, mixed pyroclastic and minor volcanic flow lithofacies.

The volcanic rocks, as well as the overlying Tithonian conglomerates, commonly contain tar seeps. The seeps are typically associated with fractures, but also occur in the sedimentary strata in zones of greater porosity.

Volcanic Flow Lithofacies (10 m approximate thickness)

Several horizons of dark-coloured volcanic flows, intermediate to mafic in composition, are found at the base of the section. These flow rocks are deeply weathered to dark green to black; a fresh surface is typically dark green. Individual flows are between 1 and 2 m thick and contain common euhedral feldspar phenocrysts (1-2 mm size) and minor angular, fragmental debris. Small, millimetre-size spherules of a dark-green mineral, possibly pyroxene, are common and weather out to form a pitted surface. Jasper fragments are also noted.

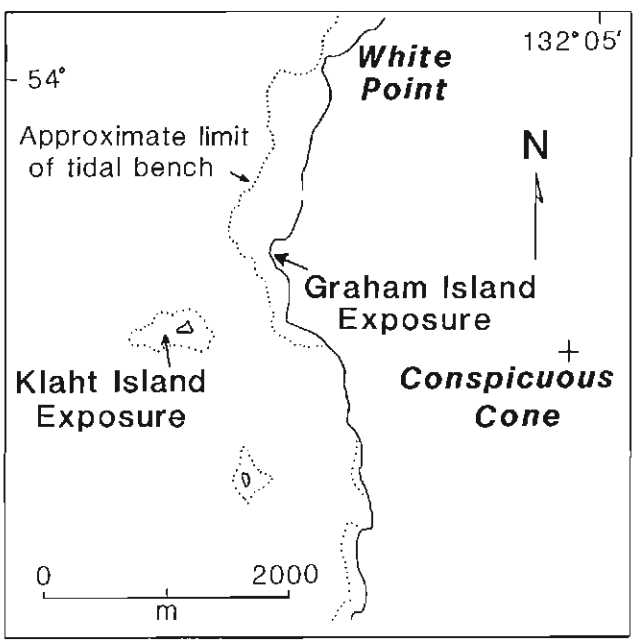

Figure 4. Location map of northwest Graham Island exposures.

Pyroclastic Breccia Lithofacies (45 m approximate thickness)

The upper part of the Graham Island section consists mainly of pyroclastic breccias, typically light green to pink or red. Minor flow rocks, similar to those seen lower in the section and commonly with a vesicular texture, are interstratified.

The pyroclastic breccias are characterized by a light green to pink, deeply-weathered and crumbly tuffaceous matrix showing millimetre-size feldspar crystals (Fig. 5a). Locally, the rocks are scoriaceous. Breccia blocks range from several centimetres to several metres in diameter (Fig. 5b) and also exhibit millimetre-size feldspar phenocrysts. Basalt blocks with small (2-4 mm), dark-green to black pyroxene? crystals as well as fist-sized jasper fragments are common within the pyroclastic rocks. The composition of the breccia component of these rocks is therefore quite similar to that of the underlying flow rocks.

Some of the pyroclastic rocks locally include cross-stratified, coarse grained clastic horizons with abundant volcanic debris, possibly lahar deposits. A block with this lithology was noted in the basal beds of the overlying conglomerate sequence and contained belemnites and bivalve shell fragments. Thus, the sequence was likely deposited in, or near, a shallow marine environment.

Klaht Island exposures

Outcrops of volcanic rocks and interstratified sedimentary rocks were also found on the complex of small islands lying several hundred metres west of the Graham Island exposures (Fig. 4). Volcanic rocks were not previously described from here but were mapped as Honna Formation (Sutherland Brown, 1968).

On the southwest part of the principal island mass, Klaht Island (Klaht = Haida for "Gull's Eyes"), the main exposures of volcanic rocks are found in small, fault-bounded blocks surrounded by water. The exposures are in fault contact with younger, Tithonian-age strata described previously by Haggart (1989) and more recently by Gamba (1991). More volcanic rocks are found in fault contact beneath probable Tithonian strata on the small islet just west of Klaht Island; these appear to be on-strike with the Klaht Island exposures. Although an exposure showing the overlap relationship of the Tithonian beds on the underlying volcanic/sedimentary package has not been found here, discordance between the two sequences is considered to be slight: the attitudes of the blocks bearing the Tithonian strata and the older Jurassic volcanic/sedimentary package are essentially the same.

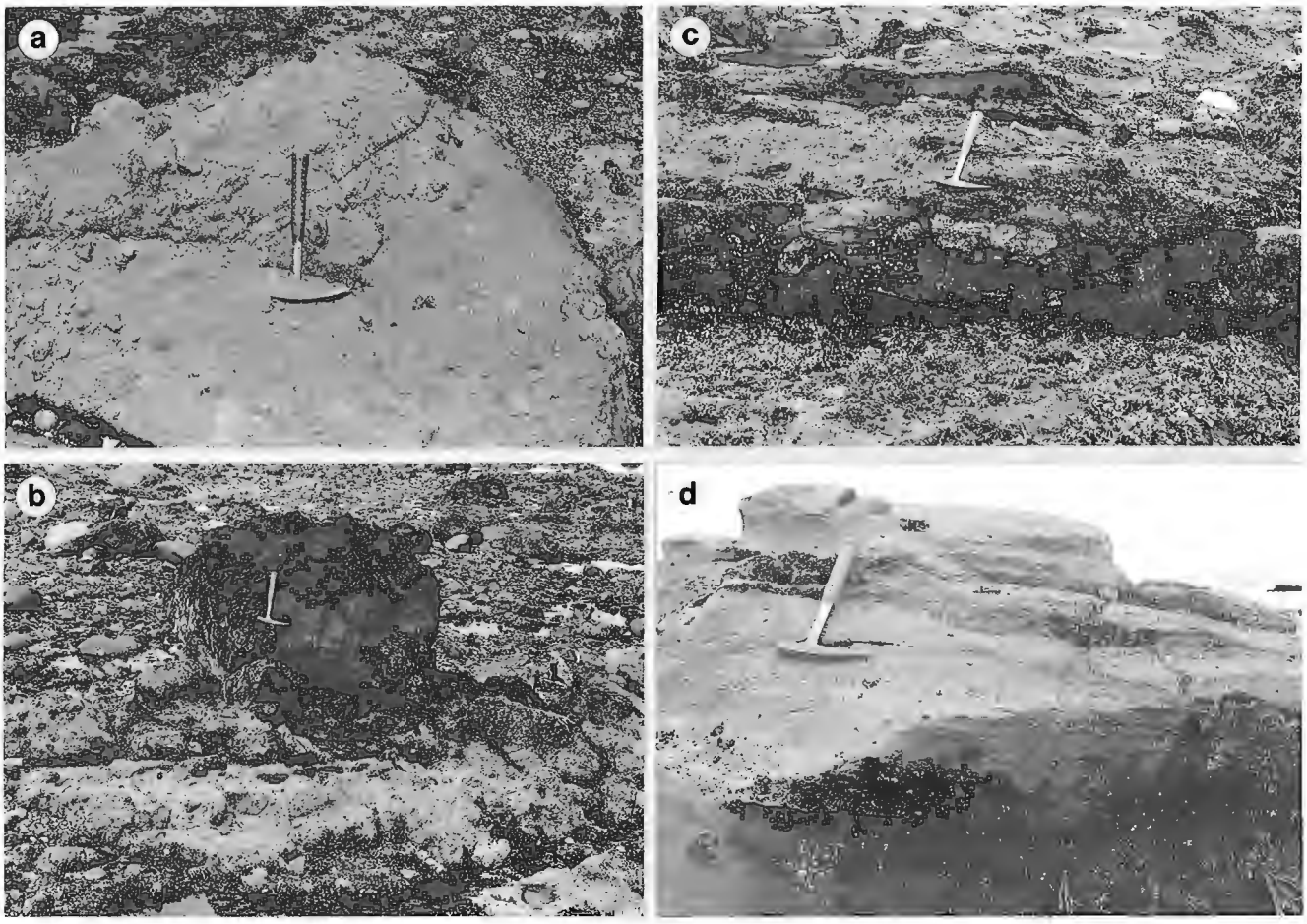

Figure 5. a. Pyroclastic breccia lithofacies, Graham Island section, showing deeply weathered and crumbly tuffaceous matrix. b. Large breccia blocks in tuffaceous matrix, pyroclastic breccia lithofacies, Graham Island section. c. Cross-stratified, volcanic-rich sandstone and pebble/cobble conglomerate lithofacies, Klaht Island. d. Cross-stratified, fine grained sandstone with shell beds, Klaht Island.

The isolated nature of the small blocks forming the Klaht Island exposures precludes measurement of a continuous stratigraphic section through the pre-Tithonian strata. Two distinct lithofacies are noted at this locality and these are described separately. Each lithofacies overlies the other on select structural blocks; the total succession preserved on the island includes several repetitions of both lithofacies.

Volcanic Lithofacies (11 m maximum observed thickness)

Altered volcanic flows and breccias, similar to those in the Graham Island section described above, are the most common lithologies noted on Klaht Island. Flow rock and breccia fragments typically contain millimetre-size feldspar crystals. Flows and breccias vary in thickness and can reach several metres. Additional breccia horizons, inaccessible due to water, overlie the major outcrop of this lithofacies.

Sedimentary Lithofacies (8 m maximum observed thickness)

The volcanic rocks are interstratified with volcanic-rich sandstone and pebble/cobble conglomerate (Fig. 5c). These sedimentary rocks locally exhibit cross-stratification and contain calcareous concretions. The strongly-indurated sandstones are coarse- to fine-grained, poorly-sorted lithic arenites. The coarser grained strata commonly contain volcanic fragments up to 0.75 m diameter, and appear to have an ash component. Sedimentary clasts in the conglomerate beds are rounded to subangular and range up to 4 cm in diameter. These beds are unfossiliferous and may be altered pyroclastic or lahar deposits.

Other sandstones (typically the finer grained facies) are cross-stratified and contain much shell debris, including abundant brachiopod and oyster fragments (Fig. 5d). These strata are seen to directly overlie the volcanic breccia at one locality, and are likely of shallow-marine origin.

DISCUSSION

The two new localities of Yakoun Group volcanic and sedimentary strata described above are important for two reasons: 1) the outcrops include new information on the range of rock types deposited during Yakoun Group-time; and 2) the new localities expand our understanding of the distribution of the Yakoun Group deposits and the volcanic arc which they likely represent (*see* Lewis et al., 1991).

The Yakoun Group was extensively described by Sutherland Brown (1968) who recognized that sedimentary rocks form a large part of the unit. Cameron and Tipper (1985) expanded this discussion and described lithologies of the group from outside the type locality on Maude Island. None of these workers included the deposits on Lyell Island or northwest Graham Island in the Yakoun Group.

Strata on Lyell Island appear to represent Cameron and Tipper's (1985) Graham Island and Richardson Bay formations of the Yakoun Group. The fossils collected from the southern section on Lyell Island suggest a correlation with the earliest Bajocian Graham Island Formation (H.W. Tipper, pers. comm., 1990). This suggests that the cross-stratified sandstone and conglomerate forming the bulk of the Lyell Island deposits is temporally correlative with the volcanic sandstone member of the Graham Island Formation. However, the extensive conglomerate seen in the Lyell Island sections was not recognized by Cameron and Tipper (1985) in the sections in the central part of the Queen Charlotte Islands; the regional significance of these deposits on Lyell Island remains to be assessed but similar thick conglomerate sequences have recently been recognized in the Yakoun Group in the central Graham Island area (Hesthammer, 1991).

The mudstone and siltstone underlying these beds may be equivalent to the lower part of the Graham Island Formation of central Graham Island, a sequence of shale-tuffs and mottled siltstones (Cameron and Tipper, 1985); alternatively, these strata may perhaps be of Aalenian age (H.W. Tipper, pers. comm., 1990).

Given the age equivalence of the clastic-dominated beds of the Lyell Island section, it is reasonable to correlate the overlying volcanic breccias in these sections with the volcanic breccia member of the Richardson Bay Formation of Cameron and Tipper (1985).

The previously unrecognized occurrence of Jurassic volcanic strata on extreme northern Lyell Island raises the possibility that some of the volcanic rocks on the northeastern part of the island, previously mapped as Tertiary Masset Formation (Sutherland Brown, 1968), may actually be of Jurassic age.

Strata found on the northwest coast of Graham Island also can be compared, on lithology, with the volcanic breccia member of the Richardson Bay Formation. However, these sections include a succession of volcanic and sedimentary rock types which is probably more complex than that described for the type locality of the formation by either Sutherland Brown (1968) or Cameron and Tipper (1985).

The occurrence of Yakoun Group deposits on northwestern Graham Island significantly extends the distribution of the group to the northern Queen Charlotte Islands. Lewis et al. (1991) have described the Yakoun Group deposits as representing a volcanic arc succession. Haggart (1991) showed that subsequent, Cretaceous, deposition in the islands region occurred during a period of tectonic and volcanic quiescence; the shallow-marine, latest Jurassic to Cretaceous succession resulted from marine transgression onto the remnant Jurassic volcanic arc deposits. The onlapping relationship of this latest Mesozoic sedimentary sequence on Yakoun Group deposits, is readily seen in the central part of the islands. The same relationship is duplicated on northwest Graham Island where latest Jurassic (Tithonian) sedimentary strata onlap the Yakoun volcanic rocks.

Overall, the Lyell Island section represents a regressive sequence, with deeper-water mudstone and siltstone at the base succeeded by shallow-marine and possibly subaerial deposits at the top. The thickness of sedimentary strata found in the Lyell Island section is substantially less than seen in typical sections in central Graham Island (*see* Cameron and Tipper, 1985). This southward-thinning of Yakoun Group deposits across the Queen Charlotte Islands may reflect increasing proximity to a highland in the south. In support of this interpretation, no Jurassic deposits younger in age than Aalenian are presently known from northern Vancouver Island (Jeletzky, 1976; H.W. Tipper, pers. comm., 1990). Instead, a major period of intrusion (Coast Intrusions) and erosion characterized that region at the time.

CONCLUSIONS

1. New outcrops of the Yakoun Group have been identified in the southern and northern parts of the Queen Charlotte Islands. Lithologically, these outcrops appear to represent the Graham Island and Richardson Bay formations of Cameron and Tipper (1985). Lithological differences between these outlying areas and the formations' type localities, however, indicate a paleogeographically-complex model of Yakoun Group deposition.
2. The occurrence of Yakoun Group deposits on northwestern Graham Island significantly extends the distribution of that unit to the northern Queen Charlotte Islands.
3. The Lyell Island section represents a regressive sequence. The southward-thinning of Yakoun Group sedimentary strata across the Queen Charlotte Islands may reflect onlap onto a highland associated with the Coast Intrusive complex of northern Vancouver Island.

ACKNOWLEDGMENTS

The author thanks J. Hesthammer and H.W. Tipper for illuminating discussion regarding the Yakoun Group, and their informative reviews of the manuscript.

REFERENCES

Cameron, B.E.B. and Tipper, H.
1985: Jurassic stratigraphy of the Queen Charlotte Islands, British Columbia; Geological Survey of Canada, Bulletin 365.

Cameron, B.E.B. and Hamilton, T.S.
1988: Contributions to the stratigraphy and tectonics of the Queen Charlotte Basin, British Columbia; in Current Research, Part E, Geological Survey of Canada, Paper 88-1E, p. 221-227.

Gamba, C.A.
1991: An update on the Cretaceous sedimentology of the Queen Charlotte Islands, British Columbia; in Current Research, Part A, Geological Survey of Canada, Paper 91-1A.

Haggart, J.W.
1989: Reconnaissance lithostratigraphy and biochronology of the Lower Cretaceous Longarm Formation, Queen Charlotte Islands, British Columbia; in Current Research, Part H, Geological Survey of Canada, Paper 89-1H, p. 39-46.
1991: A synthesis of Cretaceous stratigraphy, Queen Charlotte Islands, British Columbia; in Evolution and Hydrocarbon Potential of the Queen Charlotte Basin, British Columbia, Geological Survey of Canada, Paper 90-10.

Hesthammer, J.
1991: Lithologies of the Middle Jurassic Yakoun Group in the central Graham Island area, Queen Charlotte Islands, British Columbia; in Current Research, Part A, Geological Survey of Canada, Paper 91-1A.

Hickson, C.J.
1990: Geology, Frederick Island, British Columbia; Geological Survey of Canada, Map 8-1990, scale 1:50,000.

Jeletzky, J.A.
1976: Mesozoic and ?Tertiary rocks of Quatsino Sound, Vancouver Island, British Columbia; Geological Survey of Canada, Bulletin 242.

Lewis, P.D., Haggart, J.W., Anderson, R.G., Hickson, C.J., Thompson, R.I., Dietrich, J.R., and Rohr, K.M.M.
1991: Triassic to Neogene geological evolution of the Queen Charlotte Basin; Canadian Journal of Earth Sciences, v. 27 (in press).

Sutherland Brown, A.
1968: Geology of the Queen Charlotte Islands, British Columbia; British Columbia Department of Mines and Petroleum Resources, Bulletin 54.

A revision of stratigraphic nomenclature for the Cretaceous sedimentary rocks of the Queen Charlotte Islands, British Columbia

James W. Haggart, Susan Taite[1], Jarand Indrelid[1], Jonny Hesthammer[1], and Peter D. Lewis[1]
Cordilleran Division, Vancouver

Haggart, J.W., Taite, S., Indrelid, J., Hesthammer, J., and Lewis, P.D., A revision of stratigraphic nomenclature for the Cretaceous sedimentary rocks of the Queen Charlotte Islands, British Columbia; in Current Research, Part A, Geological Survey of Canada, Paper 91-1A, p. 367-371, 1991.

Abstract

Problems associated with the stratigraphic description and mapping of Cretaceous sedimentary rocks in the Queen Charlotte Islands are assessed. These include the similarity of lithological types encompassed by the present rock-stratigraphic units, and the necessity of paleontological control to confidently assign outcrops into the established stratigraphic nomenclature. A new stratigraphic scheme for the Cretaceous sedimentary rocks of the islands is proposed, based on lithology. This scheme reflects the underlying genetic processes which produced the rock section preserved in the islands.

Résumé

Des problèmes associés à la description et à la cartographie stratigraphiques des roches sédimentaires du Crétacé dans les îles de la Reine-Charlotte sont abordés. Mentionnons entre autres la similarité des types lithologiques que couvrent les actuelles unités lithostratigraphiques et la nécessité d'un contrôle paléontologique pour l'assignation en toute confiance des affleurements à la nomenclature stratigraphique établie. Une nouvelle organisation de la stratigraphie basée sur la lithologie est proposée pour les roches sédimentaires crétacées des îles. Cette réorganisation reflète les processus génétiques sous-jacents qui ont donné les profils lithologiques conservés dans les îles.

[1] Department of Geological Sciences, University of British Columbia, 6339 Stores Road, Vancouver, B.C. V6T 2B4

INTRODUCTION

Field studies of the Cretaceous rocks of the Queen Charlotte Islands have expanded dramatically over the past several years through the efforts of scientists involved in the Geological Survey of Canada's Queen Charlotte Islands Frontier Geoscience Program (QCI FGP). These multidisciplinary studies have focused on stratigraphy, paleontology, structural geology and sedimentology (summarized in Haggart, 1991), and new localities of Cretaceous rocks have also been identified in several areas of the islands as a result of the geological mapping program (e.g., Hesthammer et al., 1991). The Cretaceous rocks play an important role in constraining models of the stratigraphic and structural evolution of the Queen Charlotte Islands region (Thompson et al., 1991; Haggart, 1991; Lewis et al., 1991).

These studies have shown that several difficulties presently exist in the usage and application of current Cretaceous stratigraphic nomenclature. Central to these problems is the recognition, based on molluscan biostratigraphic studies, that the stratigraphic succession of the Queen Charlotte Islands does not consist of time-specific lithological units, as previously thought. Thus, earlier ideas of unconformity-bound lithological associations within the Cretaceous succession, each defining a discrete stratigraphic unit, are incorrect.

This paper presents a solution to these nomenclatural problems. This nomenclature is utilized in new Open File geological maps of the Queen Charlotte Islands that are being released by the Geological Survey of Canada concurrently with this volume (Hesthammer et al., 1991).

PRESENT STRATIGRAPHIC NOMENCLATURE

A detailed summary of the development of Cretaceous stratigraphic nomenclature for the islands is presented by Woodsworth and Tercier (1991) and is not repeated here. The multidisciplinary studies undertaken by the QCI FGP have utilized the basic stratigraphic scheme for the Cretaceous rocks proposed by Sutherland Brown (1968), with some modifications (*see* Haggart, 1991). This scheme is summarized in Figure 1.

Sutherland Brown (1968) recognized two major stratigraphic packages in the Cretaceous of the Queen Charlotte Islands, the Longarm Formation and the Queen Charlotte Group, separated by an unconformity. The younger of these, the Queen Charlotte Group, was defined by Clapp (1914; as Queen Charlotte Series) on the basis of his, and earlier (Richardson, 1873; Dawson, 1880), mapping. As presently used, the Queen Charlotte Group includes: basal marine sandstone and shale (Haida Formation); shales with turbidite sandstones (Skidegate Formation); a distinctive conglomerate and sandstone deposit (Honna Formation); and, at the top of the sequence, a further succession of shale (presently unnamed).

The age of the richly fossiliferous sandstone of the Haida Formation is well constrained at the type locality (Albian-Cenomanian), on the basis of its mollusc content (*see* McLearn, 1972) and new dating has significantly revised the age of the type section of the Skidegate Formation, from post-Turonian to Albian-early Turonian (Haggart, 1986, 1987, 1991). The youngest shales of the package are locally dated as Santonian, also on molluscs (Haggart and Higgs, 1989; Haggart, 1991). The age of the Honna Formation, however, is still relatively poorly understood, but appears to be post-Turonian to early Santonian at the type locality (Haggart, 1991). All these units are considered as a conformable, interstratified succession.

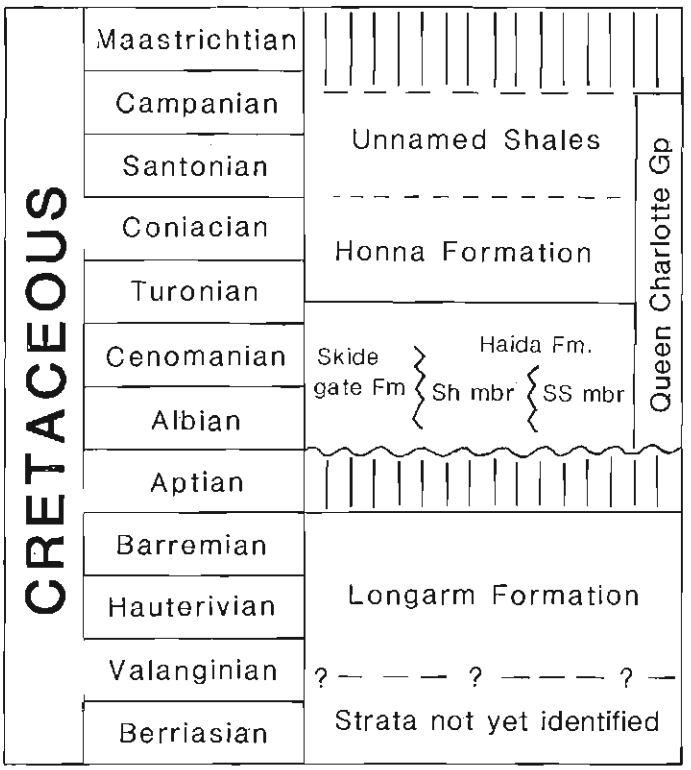

Figure 1. Stratigraphic nomenclature for Cretaceous sedimentary rocks of the Queen Charlotte Islands utilized in prior Frontier Geoscience Program mapping (based principally on Sutherland Brown, 1968; summarized in Haggart, 1991). Stage durations equilibrated.

Sutherland Brown's (1968) second major stratigraphic package, the Longarm Formation, was originally proposed by him for a poorly understood sequence of marine conglomerate, sandstone and shale found at many localities on the islands. This succession was considered to be significantly older than the Queen Charlotte Group and separated from it by an unconformity. Sutherland Brown (1968) did not designate a formal type section for the Longarm Formation, but indicated that exposures in Long Inlet were typical. The early geologists (Richardson, 1873; Dawson, 1880; Clapp, 1914) had noted the lithological similarity of these exposures with the sandstones and shales of the Queen Charlotte Group and Clapp (1914) consequently included them in his Queen Charlotte Group. Although all lithologies of Sutherland Brown's (1968) Longarm Formation were known in the Queen Charlotte Group as well, the interpretation of an unconformity between the two units provided the rationale that the Longarm Formation strata represented a discrete stratigraphic package. No section showing the actual contact relationship of the Longarm Formation with the younger Queen Charlotte Group was known, however (Sutherland Brown, 1968; Yorath and Chase, 1981).

THE PROBLEMS

Problems with the current stratigraphic nomenclature were initially encountered during studies of the molluscan biostratigraphic succession of the Cretaceous rocks. Field studies initiated in 1985 questioned some of the assumptions of the Cretaceous stratigraphic model of Sutherland Brown (1968); these are summarized in Haggart (1991). The crucial observation was that the supposed unconformity between the Longarm Formation and the Queen Charlotte Group, spanning the Aptian, was non-existent: stratigraphic sections were located which contained ammonite faunas indicative of Barremian through Albian time, including several faunas within the critical Aptian interval (Haggart, 1991). The sections were previously mapped as Haida Formation but are lithologically similar to Longarm sections nearby.

Analysis of Cretaceous lithostratigraphy, undertaken concurrently with the molluscan biostratigraphic studies (Haggart, 1986, 1989, 1991; Haggart and Gamba, 1990), has shown that the Longarm and Haida formations consist of similar lithological successions, deposited in similar depositional environments, but at different geological times. No unconformity separates the two units. Continuous marine deposition in the Queen Charlotte Islands is responsible for a continuous stratigraphic succession. The rocks presently called Haida Formation thus represent younger, lithological equivalents of the strata traditionally called Longarm Formation; any stratigraphic boundary between the two is artificial.

The inaccurate model of the Cretaceous stratigraphic succession presented by the current nomenclature is also reflected in problems encountered in geological mapping. As a result of the lithological similarity of many of the Cretaceous rocks, mappers have relied heavily on paleontological data, rather than outcrop lithology, to discriminate rock units. Unfortunately, paleontological control is usually forthcoming some time after the geologist visits the outcrop. Thus, what is often mapped in the Cretaceous of the islands are time-stratigraphic units, or age-belts based on fossil data, rather than units of distinctive lithology.

A GENETIC MODEL

A solution to the problems inherent in the present Cretaceous stratigraphic nomenclature for the Queen Charlotte Islands can be proposed, based on an understanding of the nature of Cretaceous sedimentation in the region. A genetic model reflecting marine transgression fully encompasses all lithological units presently recognized in the Cretaceous sequence of the islands.

Cretaceous deposition in the islands region has been interpreted as a result of eastward-directed transgression across a shelf, bounded to the east at some distance by a volcanic arc (Haggart, 1991; Lewis et al., 1991). Paleocurrent data suggest an easterly source for the sediments (Yagishita, 1985; Sutherland Brown et al., 1983; Higgs, 1990; Gamba, 1991; Gamba et al., 1990). The basin deepened to westward (Haggart, 1991) and is thus suggested to have occupied a fore-arc setting, open to the west. Oldest basal Cretaceous rocks are preserved on the western side of the outcrop belt and the younger deposits are preserved farther to the east (Fig. 2). Widespread Cretaceous deposition in the western islands region appears to have commenced in Late Valanginian time: shallow-water facies of this age onlap older strata at many localities in the central islands region (Sutherland Brown, 1968; Haggart, 1991). Tithonian strata present at one locality on the west coast (Jeletzky, 1984; Haggart, 1989) may reflect local basin infilling prior to subsequent, widespread Cretaceous deposition (Gamba, 1991).

The basal strata of the sedimentary cycle are sandstone and conglomerate, interpreted as a shoreline, or nearshore shallow-marine, facies. These rocks young eastward to Albian-Cenomanian age and define an eastward transgression in the islands region, with deeper-water shale deposits (shelf setting: Haggart, 1986) succeeding the shallow-water deposits at any location. By Early Turonian time virtually all of the islands region was the site of deeper-water shale deposition (Haggart, 1991).

This overall transgressive regime was interrupted by westerly progradation of coarse clastics of the Honna Formation in Late Cretaceous time. The Honna Formation is interstratified at many localities with shale and turbidite deposits, as well as with sandstone of the Haida Formation at one locality. Gamba et al. (1990) have suggested that the turbidite deposits are related to progradation of the Honna Formation depositional system.

THE SOLUTION

Three major lithological units - shallow-water sandstone, deeper-water shale, and the Honna Formation conglomerate - thus form the Cretaceous stratigraphic succession in the islands. All three units are easily recognized in outcrop, they are persistent across large regions and are readily mappable,

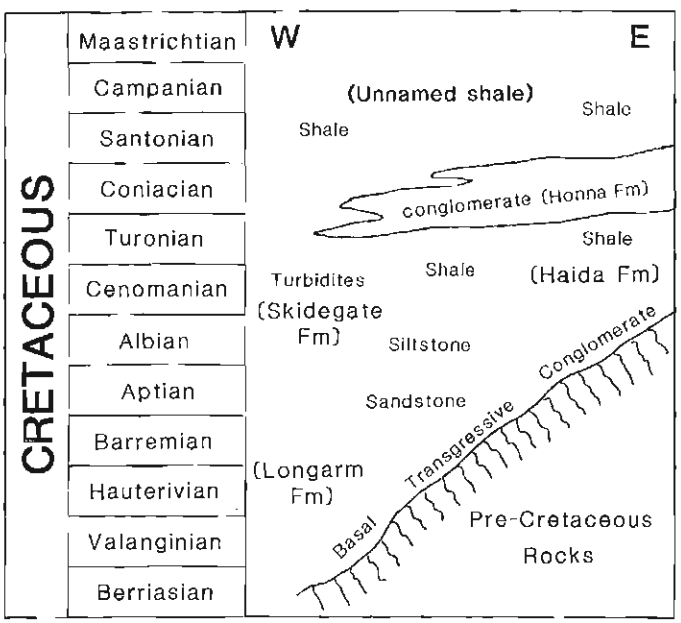

Figure 2. Genetic model of Cretaceous deposits in the Queen Charlotte Islands. Old formational nomenclature is indicated in parentheses (). The oldest deposits are preserved on the western side of the Cretaceous outcrop belt and strata progressively young to eastward.

and they can be integrated in a genetic model. They are therefore ideal as basic mapping units, or formations. Continued usage of the name 'Honna Formation' is justified but publication of new stratigraphic names for the other units is premature at this time; we thus refer to the other two units informally as 'Cretaceous sandstone' and 'Cretaceous shale'.

These major lithological units show considerable internal variation. For example, an early phase of marine onlap in the southern islands region is locally represented by a very coarse grained basal transgressive conglomerate lithofacies, well-developed in the Arichika Island and Poole Inlet sections (Sutherland Brown, 1968; Haggart and Gamba, 1990). Similar basal transgressive conglomerates are found in other areas of the islands, but they are often substantially thinner, better sorted, and of finer grain size than those in the south. In all areas, however, the conglomerate beds are quickly succeeded upsection by thick, interstratified accumulations of shallow-marine sandstone.

Similarly, extensive turbidite sandstone and shale deposits are often found interstratified with pure shale sequences in the central and southern islands and are thus an integral component of the deeper-water shale succession. The turbidite sandstone and shale lithofacies may be abruptly succeeded by conglomerate and sandstone locally (i.e., the Honna Formation), but development of this lithofacies is still related to the shale depositional regime.

Such locally-developed internal variations are recognizable in each of the three major, formational units. We refer to them informally as lithofacies, i.e., the 'basal transgressive conglomerate lithofacies' of the Cretaceous sandstone, the 'turbidite sandstone and shale lithofacies' of the Cretaceous shale, or the 'sandstone lithofacies' of the Honna Formation. Table 1 summarizes the major components of the stratigraphic scheme which we propose for the Cretaceous sedimentary rocks of the islands.

BENEFITS

The system of stratigraphic nomenclature proposed above is useful in several respects. First, all localities of similar lithology (i.e., Cretaceous sandstone) can be shown directly on the geological maps, the basic premise of mapping. The ages of particular localities can be shown as well. In this way the transgressive nature of the Cretaceous sequence is readily seen from examination of the geological maps.

Similarly, ambiguous map relations introduced by the present Cretaceous stratigraphic nomenclature for the islands may be avoided. For example, a map of the Skidegate Channel area (Thompson and Lewis, 1990) portrays the Honna Formation resting directly on the Longarm Formation. A thin shale interval is present beneath the Honna Formation conglomerates in this area, but it was previously mapped as part of the 'Longarm Formation'. The implication of this mapping, based on the stratigraphic nomenclature of Sutherland Brown (1968; Fig. 1), is that the Honna Formation unconformably overlies the older deposit in the Skidegate Channel area (*see* Thompson et al., 1991). At other localities in the islands, however, the Honna Formation conglomerate is conformable within the Cretaceous sequence (Haggart, 1986, 1991; Indrelid, 1990; Taite, 1990; Fogarassy and Barnes, 1991). It is thus more parsimonious to interpret the relationship in Skidegate Channel as one where the Honna Formation is conformable with the underlying shale strata.

This scheme of geological mapping for the Cretaceous also allows specific lithofacies, as well as specific time intervals, to be more easily targeted by specialists undertaking studies on Cretaceous sedimentation, geochemistry, and paleontology. Additional lithofacies may subsequently be defined within each of the major formational units.

Given the nature of exposure of the Cretaceous rocks of the Queen Charlotte Islands, problems will no doubt persist in assigning particular outcrops to specific stratigraphic units. However, the classification scheme proposed in this paper has been 'field-tested', and has proved very useful in geological mapping over a wide region of the islands. It is also flexible, allowing for further differentiation of lithofacies within the formational units. Finally, it more accurately reflects the current understanding of the Cretaceous geological evolution of the islands region.

Table 1. Informal stratigraphic nomenclature for Cretaceous sedimentary rocks of the Queen Charlotte Islands discussed in this report and utilized in recent geological mapping. Listing is not exhaustive.

Formational Unit	Cretaceous Sandstone	Cretaceous Shale	Honna Formation
Informal Lithofacies (No temporal or geographic ordering implied)	Siltstone lithofacies	Turbidite sandstone and shale lithofacies	Sandstone lithofacies
	Sandstone lithofacies	Shale lithofacies	Conglomerate lithofacies
	Basal transgressive cgl lithofacies		

ACKNOWLEDGMENTS

The authors thank Mike Orchard for suggestions that improved the text.

REFERENCES

Clapp, C.H.
1914: A geological reconnaissance on Graham Island, Queen Charlotte Group, B.C.; in Geological Survey of Canada, Summary Report, 1912, p. 12-40.

Dawson, G.M.
1880: Report on the Queen Charlotte Islands, 1878; Geological Survey of Canada, Report of Progress for 1878-79, Part B, p. 1-239.

Fogarassy, J.A.S. and Barnes, W.C.
1991: Stratigraphy and diagenesis of the middle to Upper Cretaceous Queen Charlotte Group, Queen Charlotte Islands, British Columbia; in Evolution and Hydrocarbon Potential of the Queen Charlotte Basin, British Columbia, Geological Survey of Canada, Paper 90-10.

Gamba, C.A.
1991: An update on the Cretaceous sedimentology of the Queen Charlotte Islands, British Columbia; in Current Research, Part A, Geological Survey of Canada, Paper 91-1A.

Gamba, C.A., Indrelid, J., and Taite, S.
1990: Sedimentology of the Upper Cretaceous Queen Charlotte Group, with special reference to the Honna Formation, Queen Charlotte Islands, British Columbia; in Current Research, Part F, Geological Survey of Canada, Paper 90-1F, p. 67-73.

Haggart, J.W.
1986: Stratigraphic investigations of the Cretaceous Queen Charlotte Group, Queen Charlotte Islands, British Columbia; Geological Survey of Canada, Paper 86-20.
1987: On the age of the Queen Charlotte Group of British Columbia; Canadian Journal of Earth Sciences, v. 24, p. 2470-2476.
1989: Reconnaissance lithostratigraphy and biochronology of the Lower Cretaceous Longarm Formation, Queen Charlotte Islands, British Columbia; in Current Research, Part H, Geological Survey of Canada, Paper 89-1H, p. 39-46.
1991: A synthesis of Cretaceous stratigraphy, Queen Charlotte Islands, British Columbia; in Evolution and Hydrocarbon Potential of the Queen Charlotte Basin, British Columbia, Geological Survey of Canada, Paper 90-10.

Haggart, J.W. and Gamba, C.A.
1990: Stratigraphy and sedimentology of the Longarm Formation, southern Queen Charlotte Islands, British Columbia; in Current Research, Part F, Geological Survey of Canada, Paper 90-1F, p. 61-66.

Haggart, J.W. and Higgs, R.
1989: A new Late Cretaceous mollusc fauna from the Queen Charlotte Islands, British Columbia; in Current Research, Part H, Geological Survey of Canada, Paper 89-1H, p. 59-64.

Hesthammer, J., Indrelid, J., Lewis, P.D., and Haggart, J.W.
1991: Geology of southern Graham Island (map sheets 103F/8 and 103G/5, and parts of map sheets 103F/7 and 103F/9), Queen Charlotte Islands, British Columbia; Geological Survey of Canada, Open File Report 2319, 2 sheets, scale 1:50 000.

Higgs, R.
1990: Sedimentology and tectonic implications of Cretaceous fan-delta conglomerates, Queen Charlotte Islands, Canada; Sedimentology, v. 37, p. 83-103.

Indrelid, J.
1990: Stratigraphy and structures of Cretaceous units, central Graham Island, Queen Charlotte Islands, British Columbia; in Current Research, Part F, Geological Survey of Canada, Paper 90-1F, p. 5-10.

Jeletzky, J.A.
1984: Jurassic-Cretaceous boundary beds of western and arctic Canada and the problem of the Tithonian-Berriasian stages in the Boreal Realm; in Jurassic-Cretaceous Biochronology and Paleogeography of North America, G.E.G. Westermann (ed.), Geological Association of Canada, Special Paper 27, p. 175- 255.

Lewis, P.D., Haggart, J.W., Anderson, R.G., Hickson, C.J., Thompson, R.I., Dietrich, J.R., and Rohr, K.M.M.
1991: Triassic to Neogene geological evolution of the Queen Charlotte Basin; Canadian Journal of Earth Sciences, v. 27 (in press).

McLearn, F.H.
1972: Ammonoids of the Lower Cretaceous Sandstone member of the Haida Formation, Skidegate Inlet, Queen Charlotte Islands, British Columbia; Geological Survey of Canada, Bulletin 188.

Richardson, J.
1873: Report on the coal-fields of Vancouver and Queen Charlotte islands, with a map of the distribution of the former; Geological Survey of Canada, Report of Progress for 1872-73, p. 32-65.

Sutherland Brown, A.
1968: Geology of the Queen Charlotte Islands, British Columbia; British Columbia Department of Mines and Petroleum Resources, Bulletin 54.

Sutherland Brown, A., Yorath, C.J., and Tipper, H.W.
1983: Geologic and tectonic history of the Queen Charlotte Islands; Geological Association of Canada/Mineralogical Association of Canada, Canadian Geophysical Union, Joint Annual Meeting, Victoria, Fieldtrip 8, Guidebook, 21 p.

Taite, S.
1990: Observations on structure and stratigraphy of the Sewell Inlet-Tasu Sound area, Queen Charlotte Islands, British Columbia; in Current Research, Part F, Geological Survey of Canada, Paper 90-1F, p. 19-22.

Thompson, R.I. and Lewis, P.D.
1990: Geology, Skidegate Channel, British Columbia; Geological Survey of Canada, Map 4-1990, scale 1:50 000.

Thompson, R.I., Haggart, J.W., and Lewis, P.D.
1991: Late Triassic through early Tertiary evolution of the Queen Charlotte Basin, British Columbia, with a perspective on hydrocarbon potential; in Evolution and Hydrocarbon Potential of the Queen Charlotte Basin, British Columbia, Geological Survey of Canada, Paper 90-10.

Woodsworth, G.J. and Tercier, P.E.
1991: Evolution of stratigraphic nomenclature of the Queen Charlotte Islands, British Columbia; in Evolution and Hydrocarbon Potential of the Queen Charlotte Basin, British Columbia, Geological Survey of Canada, Paper 90-10.

Yagishita, K.
1985: Evolution of a provenance as revealed by petrographic analyses of Cretaceous formations in the Queen Charlotte Islands, British Columbia, Canada; Sedimentology, v. 32, p. 671-684.

Yorath, C.J. and Chase, R.L.
1981: Tectonic history of the Queen Charlotte Islands and adjacent areas - a model; Canadian Journal of Earth Sciences, v. 18, p. 1717-1739.

An update on the Cretaceous sedimentology of the Queen Charlotte Islands, British Columbia[1]

Charle A. Gamba[2]
Cordilleran Division, Vancouver

Gamba, C.A., An update on the Cretaceous sedimentology of the Queen Charlotte Islands, British Columbia; in Current Research, Part A, Geological Survey of Canada, Paper 91-1A, p. 373-382, 1991.

Abstract

A coarse clastic Tithonian to Early Cretaceous succession exposed south of White Point on northwestern Graham Island is interpreted as a rapidly infilled fault-bounded precursor of the main Cretaceous Queen Charlotte Basin. The occurrence of pre-Longarm turbidites disconformably underlying shallow shelf deposits of the Longarm Formation on Ramsay Island suggests the existence of a similar, semi-restricted basin in the South Moresby area. The Valanginian to Hauterivian Longarm Formation consists entirely of shelf deposits exhibiting a pronounced west to southwestwards deepening trend. A similar trend is observed within the deposits of the Honna Formation. The occurrence of storm deposits within the conglomeratic fan delta deposits of the Honna to the east suggests a shallow shelf setting, while interbedded turbidites to the west indicate a deeper marine environment.

Résumé

Une succession de roches clastiques grossières datant du Tithonique au Crétacé précoce et affleurant au sud de la pointe White dans le nord-ouest de l'île Graham, est interprétée comme un précurseur, limité par des failles rapidement comblées de sédiments, du bassin principal de la Reine-Charlotte du Crétacé. La présence de turbidites antérieures à la formation de Longarm reposant en discordance sous les dépôts épicontinentaux de plate-forme de la formation de Longarm dans l'île Ramsay semble indiquer l'existence d'un bassin similaire semi-restreint dans la région de South Moresby. La formation de Longarm, dont la mise en place date du Valanginien à l'Hauterivien, est entièrement composée de sédiments de plate-forme continentale affichant une direction marquée ouest-sud-ouest de plus en plus profonde. On observe une direction semblable au sein des sédiments de la formation de Honna. La présence de sédiments de tempête au sein des sédiments de cône de déjection conglomératiques de la formation de Honna à l'est semble indiquer que la sédimentation s'est faite en milieu épicontinental tandis que les turbidites interstratifiées à l'ouest indiquent un milieu marin plus profond.

[1] Contribution to Frontier Geoscience Program

[2] Department of Geology, McMaster University, Hamilton, Ontario L8S 4M1

INTRODUCTION

An ongoing investigation of the Cretaceous sedimentology of the Queen Charlotte Islands continued during the 1990 field season. This paper concentrates on an examination of the Longarm Formation in the southern Moresby Island and the northwestern Graham Island areas. In addition, a detailed section through the Honna Formation was measured in the northwestern Graham Island area in order to better resolve its internal stratigraphy. Examination of the Honna in the Lina Narrows area of Skidegate Inlet revealed the occurrence of interbedded shallow marine deposits, whereas in the northwestern Graham Island area the Honna was observed to rest conformably upon shelf mudstones. This suggests that the deep marine fan delta setting proposed by Higgs (1990) is incorrect.

SEDIMENTOLOGY OF THE LONGARM FORMATION

Northwestern Graham Island

A spectacular and heavily faulted Tithonian to Hauterivian(?) coarse clastic succession is exposed south of White Point and on a small island located to the west (Fig. 1). This succession was interpreted as shallow marine and tentatively assigned to the Longarm Formation by Haggart (1989) on the basis of the lithological similarity with other Longarm exposures located in Cumshewa and Skidegate Inlets. Haggart (1989) suggested that the successions overall fining-upwards nature, from conglomerate to sandstone, justified this correlation. However a detailed sedimentological investigation of this succession reveals significant lithostratigraphical differences from typical Valanginian to Hauterivian Longarm successions exposed elsewhere on the archipelago. These differences have a profound affect upon the succession's relationship to much of the Longarm in general.

Stratigraphy

Three lithofacies assemblages may be recognized within the 542 m thick succession; a basal Tithonian conglomeratic assemblage, an overlying mudstone assemblages of slightly younger age, and an upper Hauterivian sandstone assemblage which is in fault contact with the underlying mudstone assemblage (Fig. 2). The conglomerate lithofacies assemblage rests with probable unconformity upon Jurassic volcanics of the Yakoun (?) Formation. Two sections measured upon a small island located to the west of the mainland localities (Fig. 2: GI1 and GI2) are, based upon lithological similarities, correlative to the conglomerate lithofacies assemblage exposed south of White Point.

Conglomerate lithofacies assemblage

This assemblage is composed primarily of framework, poorly sorted, massive and crossbedded polymictic cobble conglomerate forming strongly channelized units up to 3 m thick. Units are vertically stacked, with minor lenticular interbeds of trough crossbedded (TXB) pebbly sandstones. The conglomerate is composed primarily of rounded to well rounded volcanic clasts (Yakoun Formation) and lesser granitic, sedimentary (Sandilands, Kunga limestone) and

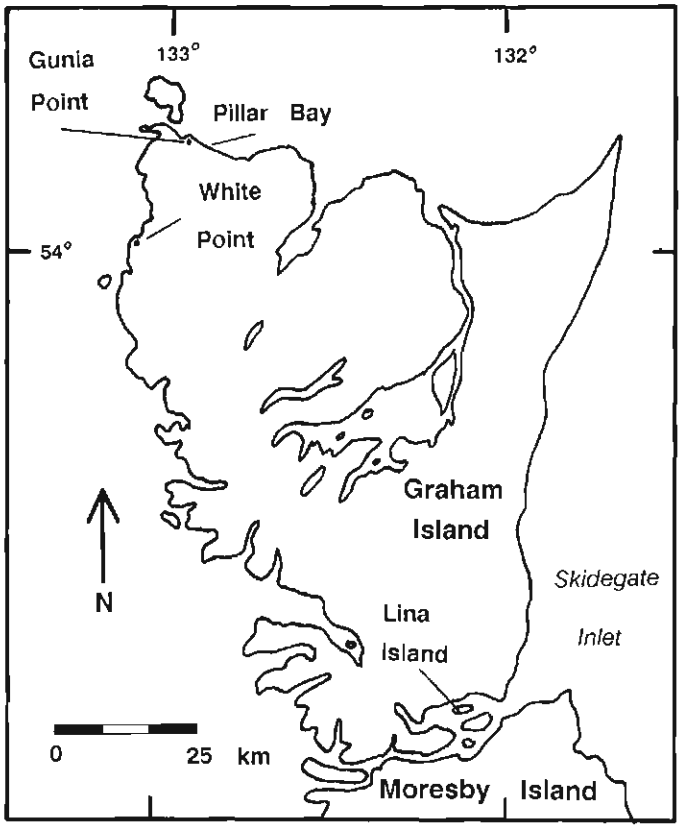

Figure 1. Map featuring location of study areas.

mudstone intraclasts. Clasts within the conglomerate exhibit a well developed a-b axis imbrication, which, coupled with their poorly sorted nature and the presence of bivalve fragments, indicate rapid deposition from strong unidirectional flow within a marine environment. Two sequences of swaley cross-stratified (SCS) fine- to medium-grained sandstone are interbedded with conglomerate units near the top of the assemblage. The massive to crossbedded, non-graded nature of the conglomerates, along with the absence of associated finer grained turbidites and the presence of interbedded SCS sandstone, indicate that they were deposited by traction currents operating in a shallow shelf setting, likely within a fan delta system. Paleocurrents derived from clast imbrication exhibit a variety of transport directions generally indicative of westward paleoflow (Fig. 2).

Mudstone lithofacies assemblage

The conglomerate lithofacies assemblage is abruptly and conformably capped by muddy fine grained deposits of the mudstone lithofacies assemblage (Fig. 2). This assemblage is composed primarily of sharp based, hummocky cross-stratified (HCS) sandstone overlain by variably bioturbated mudstone forming tabular, non-amalgamated units up to 40 cm thick. These units are interpreted as classical, offshore storm deposits. A single channelized unit of massive, poorly sorted cobble conglomerate interbedded with storm deposits occurs near the base. Muddy debris flow deposits up to 13 m thick composed of homogenized sandy mudstone and scattered extraformational cobbles are interbedded within the remainder of the assemblage. A 14 m thick debris flow deposit

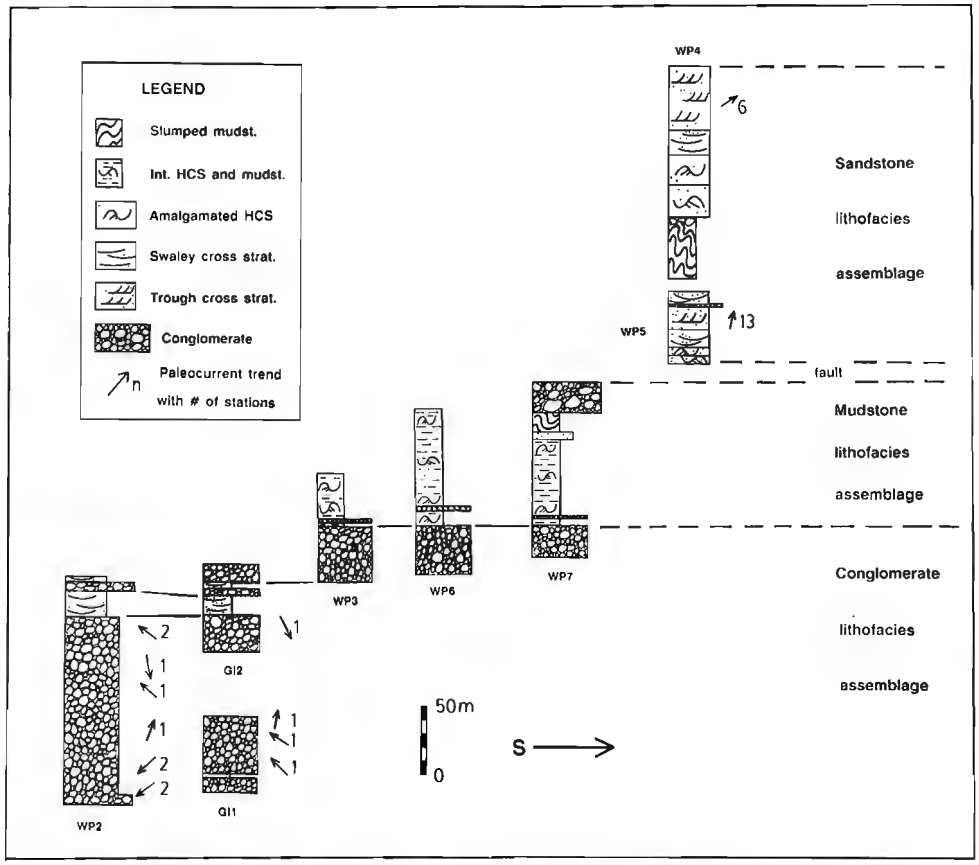

Figure 2. Stratigraphy of the succession exposed south of White Point. HCS — hummocky cross-stratification.

occurs near the top of the assemblage, heralding the onset of very coarse clastic deposition. The poorly sorted boulder conglomerates which cap the top of the assemblage (Fig. 3) mark the return and development of a second fan delta system to this location.

Sandstone lithofacies assemblage

This assemblage is separated from mudstone assemblage by a prominent fault. The assemblage is composed of two shallowing upwards (SU) regressive sequences separated by a single transgressive sequence (Fig. 4). Each shallowing upwards sequence exhibits a similar vertical sequence of facies: 1) a basal unit composed of interbedded hummocky cross-stratified sandstones and mudstones with abundant whole *Buchia* bivalves, 2) a unit of amalgamated hummocky cross-stratified sandstones, 3) a unit of swaley cross-stratified sandstone containing abundant *Inoceramus* bivalve fragments, and 4) a disconformably overlying unit of trough crossbedded sandstone.

This vertical arrangement of facies reflects a shallowing upwards trend with the *Buchia* beds representing relatively deeper water offshore deposits, the amalgamated hummocky cross-stratified sandstone representing shallower water lower shoreface to offshore deposits, and the *Inoceramus* beds representing lower shoreface deposits. The environmental significance of each of these storm deposits (tabular hummocky, amalgamated hummocky, and swaley

Figure 3. Poorly sorted fan delta conglomerates capping the mudstone lithofacies assemblage exposed south of White Point. Note the light coloured mudstone intraclasts.

cross-stratified) is well documented in the literature (eg. Dott and Bourgeois, 1982; Walker, 1985). The trough crossbedded sandstones are interpreted as middle shoreface deposits formed by the longshore or shorewards migration of sinuous crested megaripples during fairweather wave conditions (Hunter et al., 1979). The disconformity separating the *Inoceramus* beds from the trough crossbedded sandstones formed during the basinwards migration of the middle

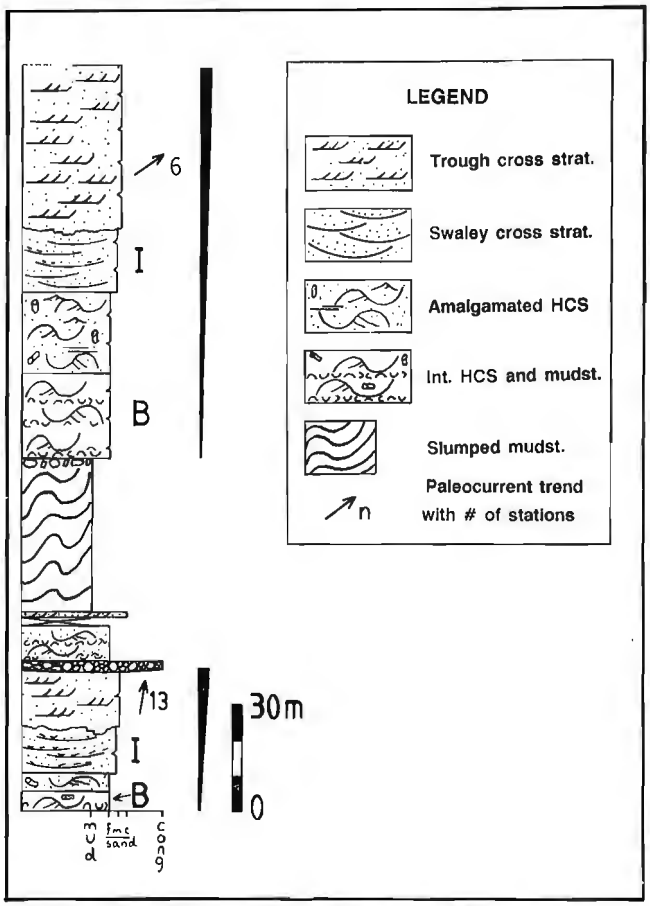

Figure 4. Detailed stratigraphic section of the sandstone lithofacies assemblage exposed south of White Point. Note the two regressive or shallowing upwards sequences. B-*Buchia* beds, I-*Inoceramus* beds, HCS — hummocky cross-stratification.

shoreface under conditions of falling relative sea level. Such disconformities located at the base of shoreface sandstones are common within many regressive shoreface sequences (Upper Cretaceous Milk River and Chungo formations, southern Alberta), and are attributed to eustatic sea level drops or forced regressions (McCrory and Walker, 1986; Rosenthal and Walker, 1986). In the case of the White Point succession however, these regressions may have been tectonically induced. The lower shallowing upwards sequence is overlain by a 44 m thick unit composed primarily of complexly deformed offshore mudstones with interbedded wave rippled very fine- to fine-grained sandstones. The slumped mudstones are capped by a layer of matrix- to clast-supported boulder conglomerate one or two clasts thick (Fig. 5). This conglomerate is composed predominantly of angular carbonate cemented silty mudstone intraclasts up to 2.4 m in diameter with lesser well rounded volcanic and granitic boulders up to 2 m diameter. The intraclastic boulders are clearly derived by the winnowing of carbonate cemented layers within the underlying slump unit, perhaps during a series of high energy storm events. The origin of the extraformational boulders, although more perplexing, may also be attributed to this process. Rapid emplacement of extraformational conglomerates on top of the originally undeformed offshore mudstones

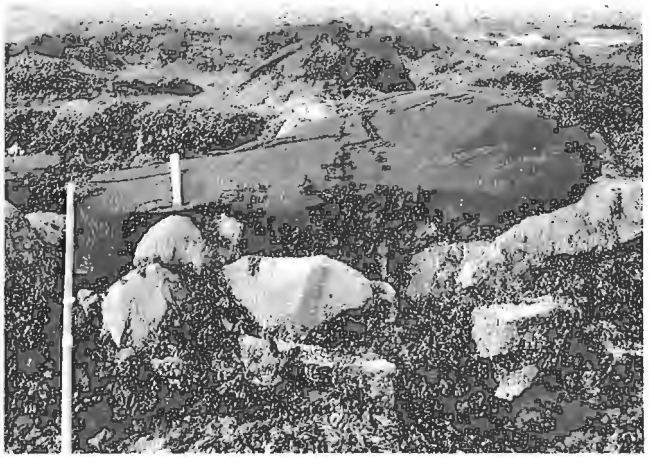

Figure 5. Boulder conglomerate capping the slumped offshore mudstones of the sandstone lithofacies assemblage exposed south of White Point. Note the abruptly overlying hummocky cross-stratified sandstone of the *Buchia* beds.

may have resulted in their liquification and failure. Subsequent storm activity winnowed the top of the slump removing all but the largest clasts. The boulder layer is abruptly overlain by fine grained hummocky cross-stratified sandstones of the *Buchia* beds.

A Late Jurassic to Early Cretaceous fault-bounded basin

The above succession comprises the deposits of two distinct depositional systems occupying different tectonic settings. The Tithonian conglomerate and mudstone lithofacies assemblages represent the deposits of a marine fan delta emplaced at shallow shelf depths within a rapidly subsiding fault-bounded basin. The abundance of shallow marine channelized conglomerates and associated muddy debris flows are two characteristics common of modern and ancient fan delta's deposited in shallow shelf settings (Ethridge and Wescott, 1984). One prominent northwest-southeast trending fault which may have controlled sedimentation is located to the north of White Point (Sutherland Brown, 1968). This parallels the regional northwest to southeast trend of Mesozoic and Cenozoic faults identified by Thompson et al. (1991). The locus of sedimentation shifted rapidly back and forth along the margin of the basin, resulting in an abrupt transition from the active fan delta deposits of the conglomerate assemblage to the outer shelf deposits of the mudstone assemblage. The appearance of poorly sorted boulder conglomerates at the top of the mudstone assemblage marks the return of active fan delta deposition to this locality. The overlying Hauterivian sandstone lithofacies assemblage represents the deposits of an attached storm-dominated strand plain subject to relative sea level fluctuations, induced either tectonically or by eustatic sea level fluctuations. The complete absence of conglomeratic fan delta deposits suggests a decrease of large-scale fault activity during the Hauterivian.

Rapid infilling of the basin by the deposits of the conglomeratic and mudstone lithofacies assemblages, along with a cessation of active faulting and a progressive eastwards marine transgression during the Hauterivian (Haggart, 1991), marked the onset of shallow shelf deposition within the Queen

Charlotte Basin, represented here by the deposits of the sandstone lithofacies assemblage and elsewhere on the archipelago by the Longarm Formation.

The succession exposed south of White Point differs in many respects from that of the typical Longarm to which it has been tentatively assigned (Haggart, 1989). As suggested by Haggart (1989), both the lithology and age of the fossiliferous sandstones of the sandstone lithofacies assemblage are typical of the lower portions of the Longarm exposed elsewhere on the Queen Charlotte Islands (Fig. 7). The lithology, age, sedimentology, and tectonic setting of the conglomeratic and mudstone lithofacies assemblages of the White Point succession however differ significantly from typical Longarm exposed elsewhere on the islands. These assemblages were deposited within an earlier fault-bounded precursor of the Queen Charlotte Basin, and are unique to the succession exposed south of White Point.

Moresby Island

All localities on Moresby Island described by Sutherland Brown (1968) as well as those visited by Haggart and Gamba (1990) were examined. In addition, a new section of Longarm was identified along the southeast shoreline of Bolkus Island. Detailed sections were measured at Carpenter Bay, Poole Inlet, Sea Pigeon Island, Huston Point, Arichika Island, Dawson Cove, and Ramsay Island (Fig. 6).

Stratigraphy

Haggart and Gamba (1990) identified six lithofacies within the Longarm of Moresby Island. Two of these facies, the laminated siltstone and mudstone, and the turbidite facies, occur in exposures on Murchison and Ramsay islands respectively. A subsequent visit to Ramsay Island by the author led to the observation that the turbidite facies disconformably underlie typical shallow shelf sandstones of definite Hauterivian (Longarm) age. The absence of megafossils and microfossils within this facies, as well as within the laminated mudstone and siltstone facies to the north on Murchison Island, casts doubt on their relationship with other facies of the Longarm. This, plus the discovery of similar turbidites of poorly constrained age in the western Burnaby Island area, indicates the occurrence of pre-Longarm (Late Jurassic-Early Cretaceous?) deposition within a turbidite basin located in this area. One Tithonian pre-Longarm fault-controlled precursor of the Queen Charlotte Basin has already been described in detail from the northwestern Graham Island area. The occurrence of another small precursor basin within the Lyell-Burnaby Island area therefore is a distinct possibility. Unfortunately, the paucity of macro and micro-fauna hampers interpretations concerning the relationship between the turbidites and the shelf deposits of the Longarm. One Late Jurassic age was obtained from a foraminiferal sample collected from the turbidites exposed on Boulder Island (unpublished Bujak Davies Group Report No. 890043, 1989).

Sedimentology

The Longarm exposed on Moresby Island is composed exclusively of shelf deposits exhibiting a prominent northeast to southwest deepening trend (Fig. 7). Thick sequences

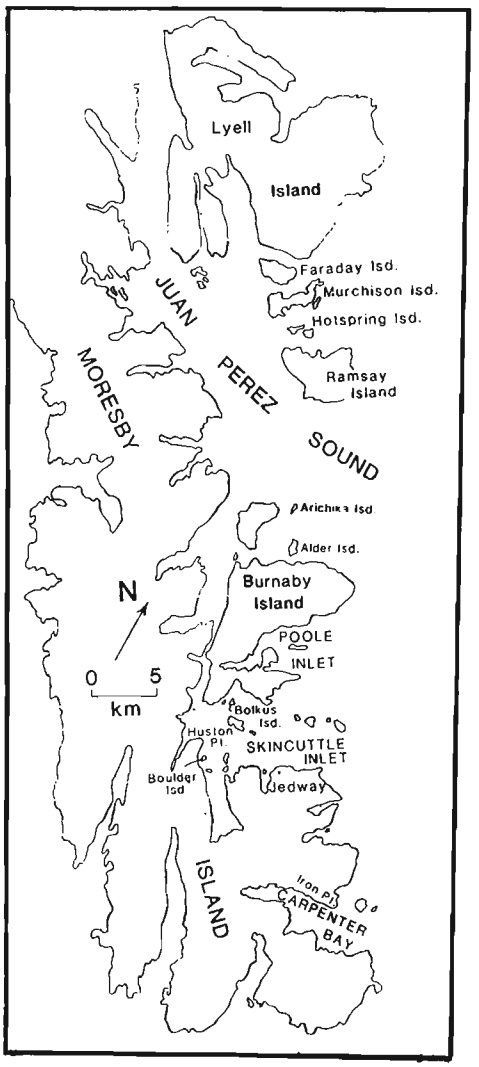

Figure 6. Location map of measured sections in the south Moresby Island area.

of crossbedded, middle shoreface sandstones and conglomerates (Fig. 8), exposed to the east on Arichika Island and in Poole Inlet, grade west and southwestwards into offshore sequences composed of interbedded hummocky cross-stratified sandstone and mudstone, exposed on Sea Pigeon Island and in Carpenter Bay (Fig. 9). Paleocurrent trends from the crossbedded sandstones on Arichika Island indicate a north-northwest direction of paleoflow, whereas those from a similar facies exposed in Poole Inlet are directed towards the southwest (Fig. 7). Paleoflow within the trough crossbedded sandstones reflects the direction of longshore transport during fairweather conditions, with currents oriented parallel or oblique to shoreline trends. The divergence of paleoflow trends between Arichika Island and Poole Inlet suggests an irregular shoreline configuration comprising headlands and embayments. Paleocurrent indicators obtained from sole marks and oriented belemnites within the storm deposits of Carpenter Bay indicate a predominantly westwards direction of transport into the basin.

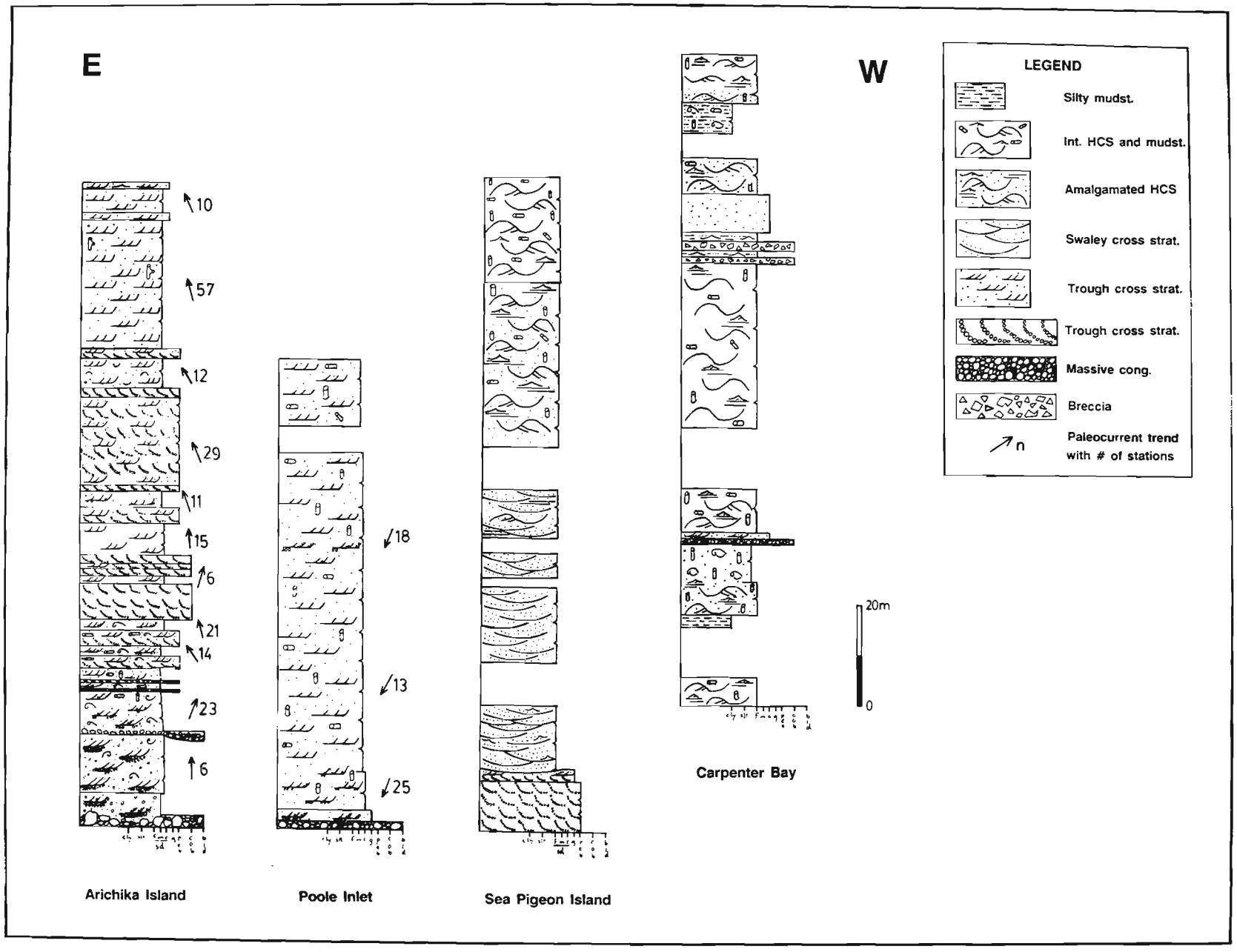

Figure 7. East to west deepening trend within the Longarm Formation of southern Moresby Island. Note thickness of crossbedded shoreface sands on Arichika Island, as well as the rapid westwards transition to storm deposits exposed on Sea Pigeon Island. Also note transgressive sequences within Longarm exposed at Carpenter Bay. Arrows denote paleocurrent trends, with number of observations.

Rocky shoreline deposits of Arichika Island

A spectacular sequence of middle shoreface sandstones and conglomerates is exposed on the southern tip and east coast of Arichika Island. The sequence is composed of tabular units of trough crossbedded pebble and cobble conglomerates interbedded with tabular units composed of grouped cosets of trough crossbedded medium grained sandstone (Fig. 8). The base of the sequence is composed of a transgressive polymictic boulder lag containing Yakoun volcanic boulders up to 17 m in diameter. This succession was deposited along volcanics located to the immediate east. This cliff may represent a relict Late Jurassic to Early Cretaceous fault scarp which became inactive during Hauterivian time, when the succession at Arichika Island was deposited. Weathering of the inactive fault scarp provided the gigantic boulder clasts incorporated into the basal transgressive lag. The transgressive lag therefore represents reworked beach boulders, which explains their generally well rounded form (Haggart and Gamba, 1990). The overlying interbedded sandstones and conglomerates represent alternating periods of storm and fairweather deposition. The conglomerates were deposited during storm events, when gravel was transported from nearshore zones by powerful storm surge ebb currents and deposited upon the middle shoreface as large, gravelly bedforms. The interbedded grouped cosets of crossbedded sandstones represent periods of fairweather wave conditions, when sand was transported towards the north-northwest by steady longshore currents. This indicates a northerly to north-northwesterly oriented shoreline, which is in keeping with the gross shoreline trends derived from molluscan biostratigraphy by Haggart (1991).

Early Cretaceous transgression

The thin middle shoreface gravels and sandstones observed near the basal contact to the west at Sea Pigeon Island and Huston Point suggest that eastwards transgression was initially rapid, leading quickly to the establishment of deeper water lower shoreface to offshore environments represented by the overlying swaley and hummocky cross-stratified storm deposits (Fig. 7). Sea level then stabilized for a relatively long period of time, as indicated by the great thickness of

Figure 8. Interbedded middle shoreface crossbedded sandstones and conglomerates exposed on Arichika Island.

Figure 9. Interbedded offshore hummocky cross-stratified sandstones and mudstones exposed in Carpenter Bay.

middle shoreface deposits on Arichika Island and within Poole Inlet to the east.

At a very large scale the deposits of the Longarm, as well as those of the overlying Haida Formation, record a gradual eastwards marine transgression (Haggart, 1991). Longarm successions at Carpenter Bay and along the northwestern coast of Graham Island however reveal that smaller scale fluctuations in sea level periodically affected sedimentation. Two transgressive sequences are recorded within the succession exposed at Carpenter Bay (Fig. 7). Alternatively, the sandstone lithofacies assemblage exposed on northwestern Graham Island records two regressive sequences separated by a thinner transgressive sequence (Fig. 4). These smaller scale cycles may reflect the effects of eustasy upon sedimentation. At least three similar scale transgressive sequences were identified within the informal Haida sandstone member exposed near Onwards Point in Skidegate Inlet and at Lauder Point, northwestern Graham Island.

The thickness of Hauterivian shoreface successions exposed at Arichika Island and Poole Inlet imply immense rates of sedimentation within the eastern part of the Queen Charlotte Basin. This must have been accompanied by a high rate of subsidence, induced both tectonically and by sediment loading, allowing for the relative stability of the Hauterivian shoreline near Arichika Island and Poole Inlet. It is therefore likely that the progressive eastwards onlap observed during the Early Cretaceous was the result of an overall rate of subsidence which exceeded (only slightly) the rate of sedimentation. The global eustatic sea level rise observed during the Early Cretaceous (Haq et al., 1987) only accentuated this trend. Global eustatic sea level trends like those of Haq et al. (1987) must be applied with extreme caution to tectonically active settings such as the Queen Charlotte Basin.

STRATIGRAPHY AND SEDIMENTOLOGY OF THE HONNA FORMATION

A 1600 m thick section through the Honna Formation was measured in the northwest Graham Island area in order to document the internal stratigraphy within the Honna

(Fig. 1, 10A). Honna exposed in the Lina Narrows area was also examined to document the occurrence of interbedded shallow marine deposits.

Westwards deepening trend

Exposures of the Honna in both the northwest Graham Island and Lina Narrows areas document a general westwards deepening trend, which is consistent with the trends observed in the underlying Haida and Longarm formations. To the east, particularly within the Lina Narrows area, interbedded finer grained successions exhibiting wave formed structures such as hummocky and swaley cross-stratification indicate shoreface to offshore depositional environments (Fig. 10B, 11). The occurrence of swaley cross-stratified sandstone erosively overlying wave-rippled offshore sandy mudstone is indicative of a forced regression. The association of these facies with typical resedimented Honna conglomerates suggests that the Honna depositional system was located within a shallow shelf setting in the eastern part of the Queen Charlotte Basin.

In the northwestern Graham Island area, thick sequences of resedimented Honna conglomerate are interbedded with relatively thin sequences composed of finer grained turbidites (Fig. 10A). Two primary types of finer grained turbidites were observed: sandy turbidites composed of amalgamated fine to coarse grained thick bedded (Ta) sandstones, and much finer grained turbidites exhibiting the classical Bouma Tabcde sequence or some variation thereof. This suggests that a deeper water depositional environment existed to the west during Honna time. The absence of storm deposits within the Honna in these areas suggests water depths greater than 200 m (ie. below storm wave base). It is interesting to note however that at both Gunia Point and along the east coast of Langara Island the conglomerates marking the base of the Honna rest conformably upon offshore mudstones of the informal mudstone member of the Haida Formation. These mudstones exhibit well developed tempestites as well as spectacular slump units indicative of a shelf setting. At Gunia Point, the base of the Honna conformably overlies a sandstone sequence exhibiting trough crossbedding and swaley cross-stratification, both features indicative of a shallow shoreface environment (Fig. 12). A detailed fabric analysis (40 stations) of conglomerates within the Honna exposed on northwestern Graham Island reveals a consistent westwards paleoflow (Fig. 10A). Divergence of paleoflow trends between stratigraphically adjacent stations in excess of 150° is noted, which is indicative of a point source feeding the Honna fans (Gamba et al., 1990). Westwards paleoflow in this region is consistent with the westward trends documented by Yagishita (1985) and Higgs (1990) from the Honna in the Skidegate Inlet area.

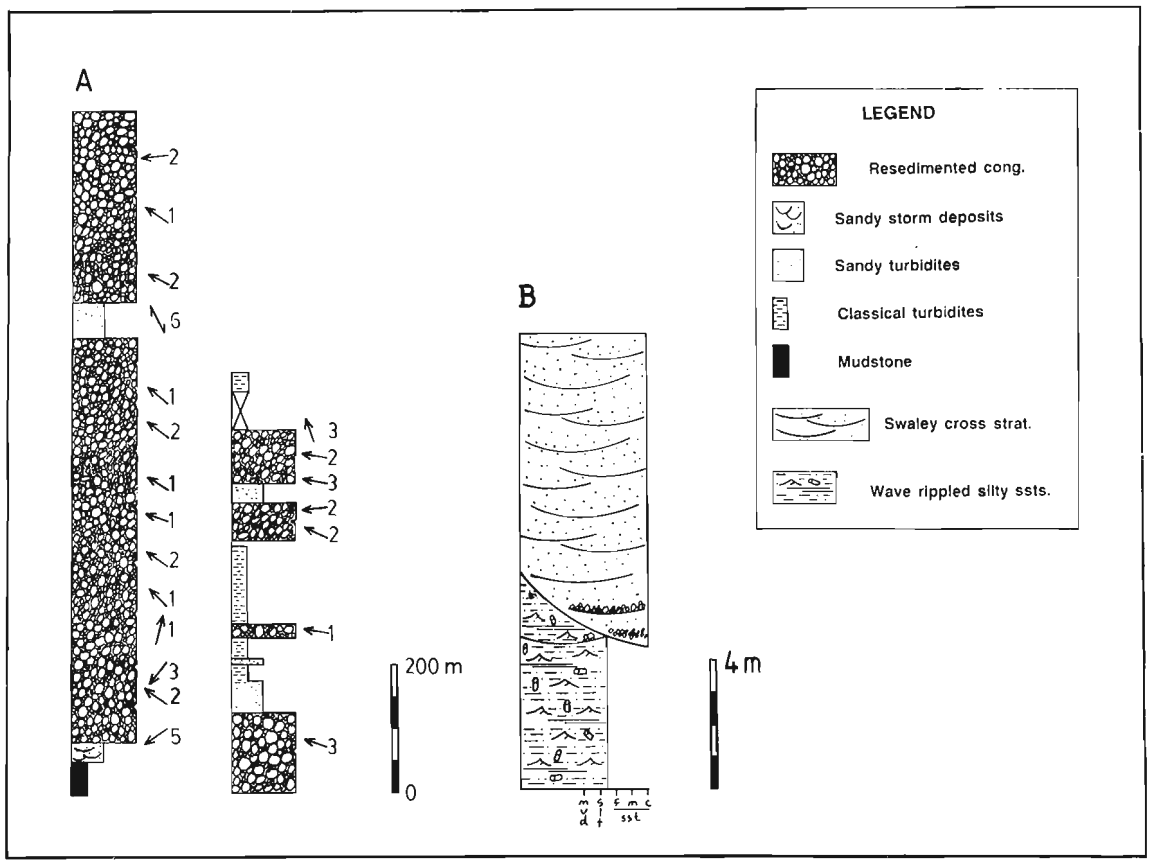

Figure 10. Stratigraphic sections of the Honna exposed A) between Gunia Point and Pillar Bay, and B) at western Lina Island, Skidegate Inlet. Arrows denote paleoflow directions and number of stations (each station representing 25 measured orientations). Note the general westwards paleoflow, as well as the interbedded finer grained turbidites within the Honna exposed on northwestern Graham Island.

Figure 11. Swaley cross-stratified shoreface sandstones interbedded within Honna conglomerates exposed on western Lina Island, Skidegate Inlet. Note the low- angle truncations of laminae.

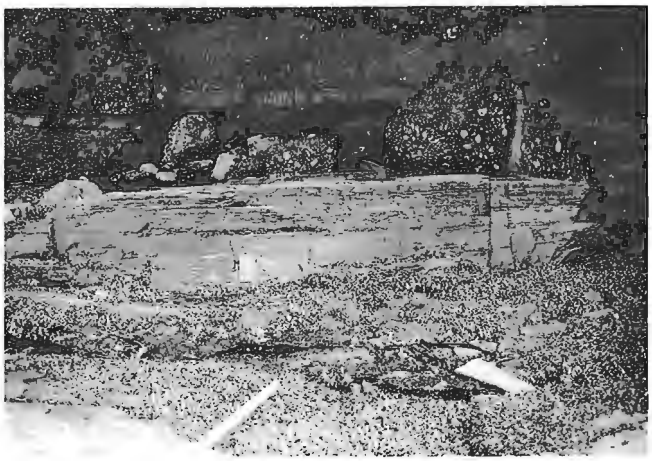

Figure 12. Swaley cross-stratified shoreface sandstones located directly beneath conglomerates marking the base of the Honna at Gunia Point, northwestern Graham Island.

DISCUSSION AND CONCLUSIONS

Cooling dates from the Burnaby Island and San Christoval plutonic suites (Anderson, 1988; Anderson and Greig, 1989) indicate a period of regional uplift and erosion during the Late Jurassic. According to Thompson et al. (1991), this uplift was associated with vertical block faulting resulting in offsets in the order of a kilometre or more. It is possible therefore that a small amount of extensional offset occurred, resulting in the creation of two small fault-bounded basins, one located within the northwestern Graham Island area, the other within the Lyell-Burnaby Island area. This period of Late Jurassic-Early Cretaceous block faulting was followed by a relatively quiescent period characterized by rapid subsidence and the initiation of the main phase of Cretaceous deposition within the Queen Charlotte Basin.

The southwestward to westward deepening trends reported from both the Longarm and Honna formations support those observed by Haggart (1986) from the Haida and Skidegate formations from the Skidegate and Cumshewa Inlet regions. The overall eastwards directed Early Cretaceous transgression observed by Haggart (1991) appears to have been initially quite rapid, with later stabilization during the Hauterivian. In addition, much smaller fluctuations in relative sea level are superimposed upon this trend.

The abrupt appearance of the Honna during Turonian to Coniacian time appears to signify a fundamental change in depositional environments within the Queen Charlotte Basin. Higgs (1990) interpreted the deposits of the Honna as those of a 'deep-water fan delta', due in large part to the absence of associated shelf deposits. The occurrence of interbedded shoreface sediments within the Honna in the Lina Narrows area however suggests that the eastern portion of the Honna system was deposited within a shallow shelf environment. Indeed, the depositional contact between Honna conglomerates and shelf deposits of the Haida mudstone within the northeastern Graham Island-Langara Island area strengthens the interpretation that much of the Honna was deposited at shelf depths. There is at present no direct sedimentological evidence suggesting that the western occurrences of the Honna, like those within the northwestern Graham Island and Langara Island areas, were deposited at lower bathyal to abyssal depths as suggested by Higgs (1990). The absence of wave formed structures within the Honna at these locations does however indicate deposition at depths greater than 200 m, which is the limit of wave influence upon the sea floor. It is therefore probable that much of the Honna system was deposited at shelf depths, making it a shelf-type fan in the classification of Ethridge and Wescott (1984).

The overall western paleoflow direction observed within the Honna from all parts of the Queen Charlotte Islands suggests deposition within a single westwards deepening basin open to the paleo-Pacific. Topography within the basin may have been modified by localized highs and lows related to episodic block faulting which is believed to have been active throughout the Cretaceous (Thompson et al., 1991). Uniform westward paleoflow on a regional scale suggests that these uplifted and down-dropped blocks did not form prominent sub-basins which acted as a locus for sedimentation, as implied by Thompson et al. (1991).

ACKNOWLEDGMENTS

Mark Hamilton is thanked for his excellent assistance and good humour in the field. Thanks to Jim Haggart and Peter Lewis for useful discussions, and to Audrey and Dave Putterhill for being so terrific. Brian Ricketts provided useful comments concerning an earlier draft of the manuscript. Thanks also to Jim Haggart and the Frontier Geoscience Program for logistical support during the 1990 field season.

REFERENCES

Anderson, R.G.
1988: Jurassic and Cretaceous-Tertiary plutonic rocks on the Queen Charlotte Islands, British Columbia; in Current Research, Part E, Geological Survey of Canada, Paper 88-1E, p. 213-216.

Anderson, R.G. and Greig, C.J.
1989: Jurassic and Tertiary plutonism in the Queen Charlotte Islands, British Columbia; in Current Research, Part H, Geological Survey of Canada, Paper 89-1H, p. 95-104.

Dott, R.H. Jr. and Bourgeois, J.
1982: Hummocky stratification: significance of its variable bedding sequences; Geological Society of America Bulletin, v. 93, p. 663-680.

Ethridge, F.G. and Wescott, W.A.
1984: Tectonic setting, recognition and hydrocarbon potential of fan delta deposits; in Sedimentology of Gravels and Conglomerates, E.H. Koster and R.J. Steel (ed.), Canadian Society of Petroleum Geologists, Memoir 10, p. 217-235.

Gamba, C.A., Indrelid, J., and Taite, S.
1990: Sedimentology of the Upper Cretaceous Queen Charlotte Group, with special reference to the Honna Formation, Queen Charlotte Islands, British Columbia; in Current Research, Part F, Geological Survey of Canada, Paper 90-1F, p. 67-73.

Haggart, J.W.
1986: Stratigraphic investigations of the Cretaceous Queen Charlotte Group, Queen Charlotte Islands, British Columbia; Geological Survey of Canada, Paper 86-20.
1989: Reconnaissance lithostratigraphy and biochronology of the Lower Cretaceous Longarm Formation, Queen Charlotte Islands, British Columbia; in Current Research, Part H, Geological Survey of Canada, Paper 89-1H, p. 39-46.
1991: A synthesis of Cretaceous stratigraphy, Queen Charlotte Islands, British Columbia; in Evolution and Hydrocarbon Potential of the Queen Charlotte Basin, British Columbia, Geological Survey of Canada, Paper 90-10.

Haggart, J.W. and Gamba, C.A.
1990: Stratigraphy and sedimentology of the Longarm Formation, southern Queen Charlotte Islands, British Columbia; in Current Research, Part H, Geological Survey of Canada, Paper 90-1H, p. 61-66.

Haq, B.U., Hardenbol, P., and Vail, P.R.
1987: Chronology and fluctuating sea levels since the Triassic; Science, v. 235, p. 1156-1167.

Higgs, R.
1990: Sedimentology and tectonic implications of Cretaceous fan-delta conglomerates, Queen Charlotte Islands, Canada; Sedimentology, v. 37, p. 83-104.

Hunter, R.E., Clifton, H.E., and Phillips, R.L.
1979: Depositional processes, sedimentary structures, and predicted vertical sequences in barred nearshore systems, southern Oregon coast; Journal of Sedimentary Petrology, v. 49, p. 711-726.

McCrory, V.L.C. and Walker, R.G.
1986: A storm and tidally-influenced prograding shoreline- Upper Cretaceous Milk River Formation of southern Alberta; Sedimentology, v. 33, p. 47-60.

Rosenthal, L.R.P. and Walker, R.G.
1986: Lateral and vertical facies sequences in the Upper Cretaceous Chungo Member, Wapiabi Formation, southern Alberta; Canadian Journal of Earth Science, v. 24, p. 771-783.

Sutherland Brown, A.
1968: Geology of the Queen Charlotte Islands, British Columbia; British Columbia Department of Mines and Petroleum Resources, Bulletin 54, 226 p.

Thompson, R.I., Haggart, J.W., and Lewis, P.D.
1991: Late Triassic through early Tertiary evolution of the Queen Charlotte Basin, British Columbia, with a perspective on hydrocarbon potential; in Evolution and Hydrocarbon Potential of the Queen Charlotte Basin, British Columbia, Geological Survey of Canada, Paper 90-10.

Walker, R.G.
1985: Geological evidence for storm transportation and deposition on ancient shelves; in Shelf Sands and Sandstone Reservoirs, R.W. Tillman, D.J.P. Swift, and R.G. Walker (ed.), Society of Economic Paleontologists and Mineralogists, Short Course Notes 13, p. 243-302.

Yagishita, K.
1985: Mid- to Late Cretaceous sedimentation in the Queen Charlotte Islands, British Columbia: lithofacies, paleocurrent and petrographic analyses of sediments; unpublished Ph.D. thesis, University of Toronto, Ontario.

Dextral strike-slip faulting and associated extension along the southern portion of the Louscoone Inlet fault system, southern Queen Charlotte Islands, British Columbia

Peter D. Lewis[1]
Cordilleran Division, Vancouver

Lewis, P.D., Dextral strike-slip faulting and associated extension along the southern part of the Louscoone Inlet fault system, southern Queen Charlotte Islands, British Columbia; in Current Research, Part A, Geological Survey of Canada, Paper 91-1A, p. 383-391, 1991.

Abstract

The Louscoone Inlet fault system extends north-northwesterly for 120 km through the southern Queen Charlotte Islands. In the vicinity of Burnaby Island, it is a 3 km wide anastomosing fault zone, that divides largely undeformed rocks with southwesterly dips on the west from rocks recording south-directed, Tertiary extension on the east. Structural fabrics in the fault zone indicate that major fault motion is dextral strike-slip. Displacement decreases to the north, so that at Cumshewa Inlet the fault system has zero offset. A structural model links the northward decrease in displacement with extension east of the fault system. This model indicates the southern portion of the fault system has undergone several tens of kilometres of offset since Oligocene time.

Résumé

Le réseau de failles du bras de mer Louscoone s'étend en direction du nord-nord-ouest sur 120 km dans la partie méridionale des îles de la Reine-Charlotte. Aux environs de l'île Burnaby il consiste en une zone faillée anastomosée d'une largeur de 3 km séparant les roches à l'ouest en grande partie non déformées et à pendages en direction du sud-ouest des roches à l'est indiquant une extension en direction du sud au Tertiaire. Les fabriques de la structure dans la zone faillée indiquent que le décrochement majeur est dextre. Le déplacement diminue en direction du nord jusqu'à devenir nul dans le réseau de failles du détroit de Cumshewa. Un modèle structural relie la diminution du déplacement en direction du nord à l'extension à l'est du réseau de failles. Ce modèle indique qu'il y a eu un déplacement de plusieurs disaines de kilomètres le long de la partie méridionale du réseau de failles depuis l'Oligocène.

[1] Department of Geological Sciences, University of British Columbia, 6339 Stores Road, Vancouver, B.C. V6T 2B4

INTRODUCTION

The Louscoone Inlet fault system (LIFS) comprises a group of subparallel, north-northwest-trending faults which extend over 120 km through the southern Queen Charlotte Islands (Fig. 1). It was originally described by Sutherland Brown (1968), who mapped it as the southern portion of his Rennell Sound/Louscoone Inlet fault system. Based on structural style, mesoscopic structural fabrics, and offset fold trends, he hypothesized late Mesozoic and Cenozoic dextral strike-slip displacements on the fault of between 20 km and 100 km. Yorath and Chase (1981) proposed a tectonic model involving Tertiary displacement along the fault system in response to Neogene rifting in the southern Queen Charlotte Basin offshore. They considered the Louscoone Inlet fault system and the Rennell Sound fault zone (RSFZ) to be separate entities, with the latter offsetting the former from its postulated northern extension, the Sandspit fault.

Recent regional mapping (Thompson et al., 1991; Lewis et al., in press) and detailed structural analyses (Lewis and Ross, 1991) have yielded new information regarding the structural evolution of these features in the central Queen Charlotte Islands. The Rennell Sound fault zone is now recognized as a zone of concentrated shortening active in the Middle Jurassic and Late Cretaceous/Early Tertiary, with little or no strike-slip faulting along it (Lewis and Ross, 1988, 1991; Thompson, 1988; Thompson and Thorkelson, 1989; Thompson and Lewis, 1990; Thompson et al., 1991). Recent mapping in the Louise Island area shows faults of the northern Louscoone Inlet fault system with little demonstrable lateral offset of Cretaceous/Tertiary stratigraphic and structural trends. However, reconnaissance examinations of rocks along the southern portions of the Louscoone Inlet fault system reveal well-developed subhorizontal mineral fabrics (Sutherland Brown, 1968; Anderson, 1988; Lewis and Ross, 1991) which could be indicative of strike-slip displacements.

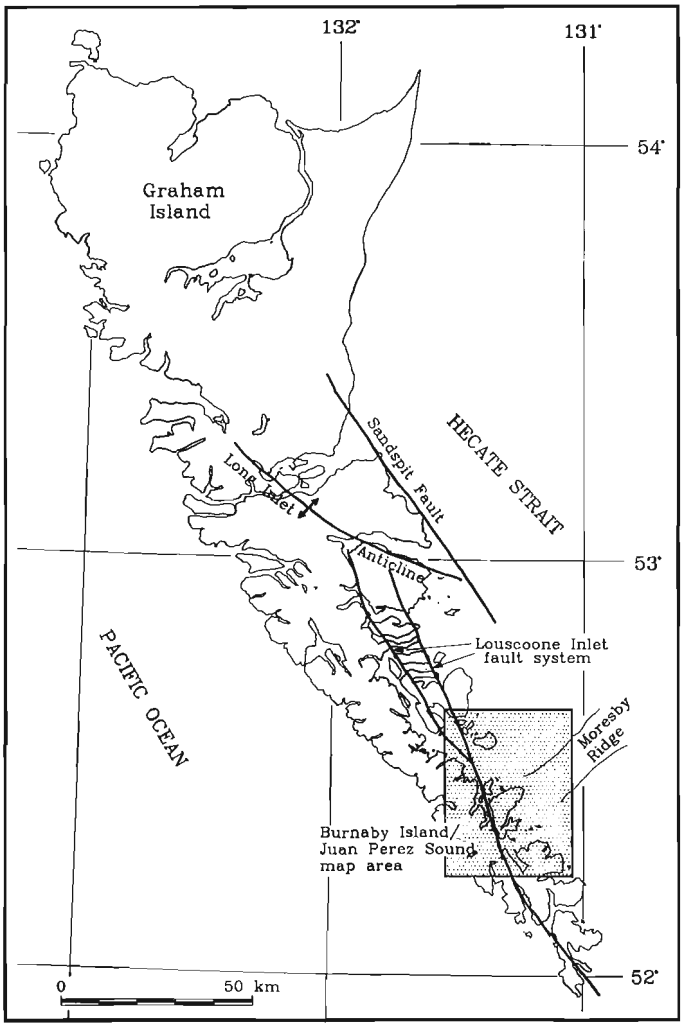

Figure 1. Location of the Burnaby Island/Juan Perez Sound map area, traces of Louscoone Inlet fault system as mapped by Sutherland Brown (1968), and geographic locations referred to in text. Long Inlet anticline follows trace of Sutherland Brown's Rennell Sound "fault zone".

Six weeks were spent conducting regional and detailed structural mapping along the Louscoone Inlet fault system in the southern Queen Charlotte Islands in an attempt to reconcile these apparently disparate observations. This effort concentrated on the Burnaby Island/Juan Perez Sound area, where shoreline exposures provide a good transect through the fault system (Fig. 1, 2). Clearly, the displacement history of such a major fault system could play a significant role in the development of the adjacent Tertiary Queen Charlotte Basin, and is vital to our understanding of the tectonic history of the region. The following paper presents new structural data which indicate that strike-slip offsets of several tens of kilometres occurred along the Louscoone Inlet fault system. It explores how these offsets relate to structures mapped elsewhere in the Queen Charlotte Islands, and presents a structural model showing that these offsets are compatible with mapping constraints outlined by Thompson et al. (1991) for the northern part of the fault system.

STRUCTURAL GEOLOGY OF THE BURNABY ISLAND/JUAN PEREZ SOUND REGION

This study included preparation of 1:50 000 scale geological maps for most of the Burnaby Island map sheet (103B/6) and the southern half of the Ramsay Island map sheet (103B11). Figure 2 shows the simplified geology of the map sheets. The geology of the map region is amenable to division into three structural domains (A,B, and C, Fig. 2) with north-northwest-trending boundaries. The westernmost domain (A) is defined by moderate southwest stratal dips in internally undeformed rocks. Domain B is a 3 km wide zone characterized by abundant north-northwest-trending faults and intrusive contacts, locally intensely folded and faulted rocks, and penetrative tectonic fabrics. The eastern domain (C) contains moderately north-dipping beds, cut by orthogonal east-west and north-south fault systems.

Domain A

Nearly all rocks in domain A belong to the Triassic Karmutsen Formation. Exceptions are at George Bay, where fault-bound Jurassic strata outcrop (Sandilands Formation and Yakoun Group); just west of the map area limits, where Sutherland Brown (1968) mapped Jurassic intrusive rocks; and Hutton Point, where possible Permian carbonate and clastic rocks underlie the Karmutsen Formation (Hesthammer et al., 1991).

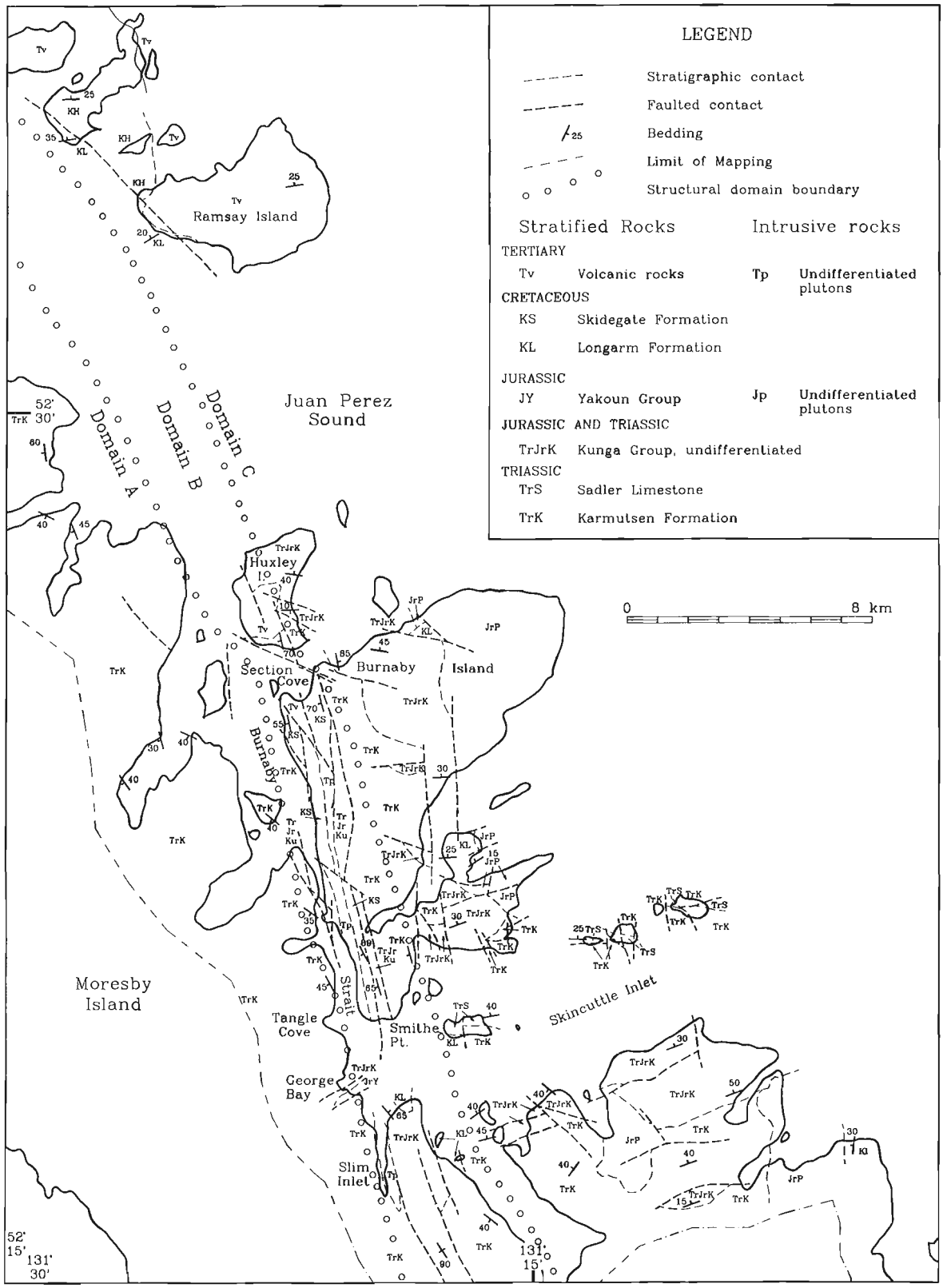

Figure 2. Simplified geological map of the Burnaby Island/Juan Perez Sound area.

The Karmutsen Formation in domain A consists entirely of basaltic submarine pillow flows, pillow breccias, volcanic breccias, and massive flows. Regional dips within the Karmutsen Formation are 30-50° to the southwest, except west of Tangle Cove, where dips in volcanic breccia are to the south-southeast. Primary igneous features are well preserved, and tectonic fabrics are absent except within narrow (<4 m wide) steeply-dipping brittle fault zones with variable trends. The fault zones commonly are filled with carbonate gouge and breccia, but are not traceable for more than a few hundred metres.

Domain B

The boundary between domains A and B is obscured by water in northern Burnaby Strait, and occurs within the Karmutsen Formation in southern Burnaby Strait and Skincuttle Inlet. Here, the boundary is a zone several hundred metres wide dividing rocks with well-preserved original textures (domain A) from those containing superimposed penetrative fabrics (domain B). Rocks ranging in age from Late Triassic (Karmutsen Formation) to Tertiary (unnamed volcanic rocks, and plutons which intrude Cretaceous and older strata) are present in domain B. All of these map units outline northerly-elongate belts bounded by faults and intrusive contacts. Map-scale faults dip steeply and occur in two main orientations: those trending 160-180°, and those trending 110-130°. Unequivocal fault-offset markers are lacking, but well-developed mesoscopic and microscopic fabrics allow kinematic histories to be inferred. These fabrics are present in all map units, but are best displayed in rocks of the Karmutsen Formation and Kunga Group at Slim Inlet, Smithe Point, and Section Cove (Fig. 2). The Slim Inlet and Smithe Point localities are located along north-northwest trending faults. Rocks in both locations contain steeply-dipping penetrative foliations with weakly to strongly developed subhorizontal elongation lineations. At Smithe Point, these foliations occur in fault slivers of the Karmutsen Formation and Sadler Limestone and strike 160-175°. Mesoscopic faults which cut the foliation trend 005-015°. Foliated limestone pods bounded by these faults have asymmetric sigmoidal shapes in plan view, and they indicate dextral slip along the bounding faults (Fig. 3a). At Slim Inlet, penetrative schistosity and mylonitic foliation in the Karmutsen Formation generally strikes northerly, but is locally re-oriented by mesoscopic Z-folds or overprinted by kink bands (Fig. 4). Both folds and kink bands have variably plunging axes contained in the regional foliation, and axial surfaces oriented roughly 100-110°/90°. Asymmetric boudins formed from pulled-apart calcite veins consistently indicate dextral shear.

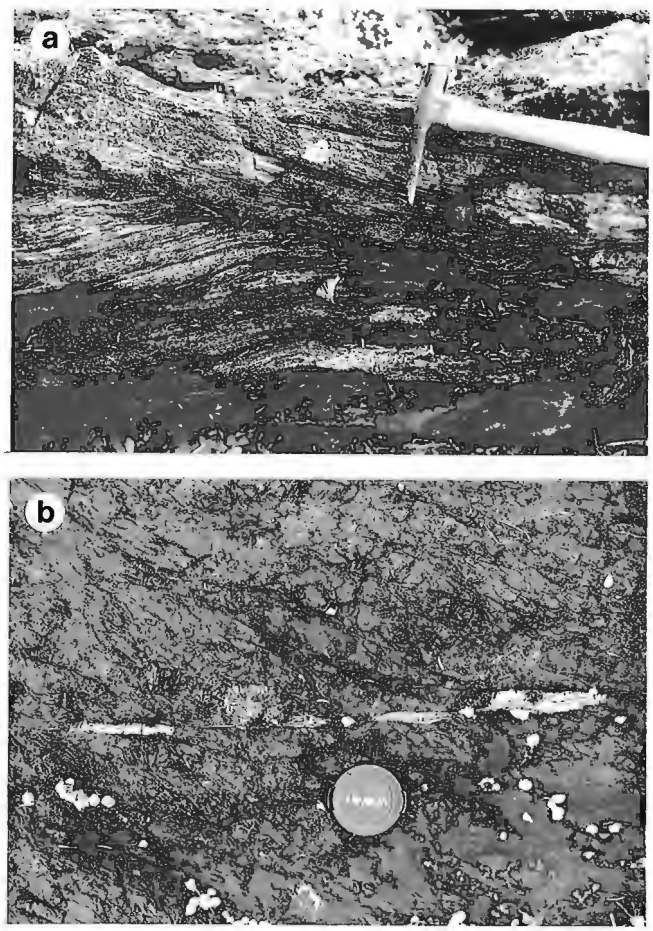

Figure 3. Mesoscopic kinematic indicators observed along the Louscoone Inlet fault system in domain B. a) Termination of asymmetric limestone boudin, Smithe Point, Burnaby Island; north is to right of photo. b) Calcite-filled sinistral pull-apart along mesoscopic fault in brittle shear zone at Section Cove; east is to right in photo.

At Section Cove on Burnaby Island, a west-northwest-trending brittle shear zone approximately 200 m wide separates strata of the Kunga Group and Karmutsen Formation from stratigraphically higher rocks of the Skidegate Formation. This shear zone is characterized by intense brecciation and abundant calcite veining. Throughgoing fractures strike 085-110° and dip steeply to both north and south. Most of these fractures contain calcite slickenfibre fills with subhorizontal fibres parallel to fracture walls. Asymmetric "steps" in the fracture walls consistently indicate sinistral slip (Fig. 3b). Subvertical planar extension veins with calcite fibres perpendicular to walls trend 020-040° in adjacent rocks; their orientation is consistent with late-stage formation in a sinistral shear zone.

Thin sections of fabrics from Smithe Point and Slim Inlet show a very fine grained matrix of calcite and chlorite, and fibrous chlorite+calcite growth in pressure shadows adjacent to euhedral plagioclase porphyroblasts. Pressure shadows have delta-shapes defining dextral shear; faulted porphyroblasts, shear bands, and recrystallized grain orientation also give the same sense of shear (Fig. 5a-b).

Thinly- to medium-bedded strata of the Triassic-Jurassic Peril and Sandilands formations, and of the Cretaceous Skidegate Formation in domain B commonly contain open to tight folds with penetrative axial planar cleavage (Fig. 6). Fold axes plunge shallowly to steeply to the northwest and southeast, and subvertical axial surfaces trend 130-160°. Analyses of deformed fossil prints from several locations confirm that the cleavage surfaces coincide with the plane of flattening.

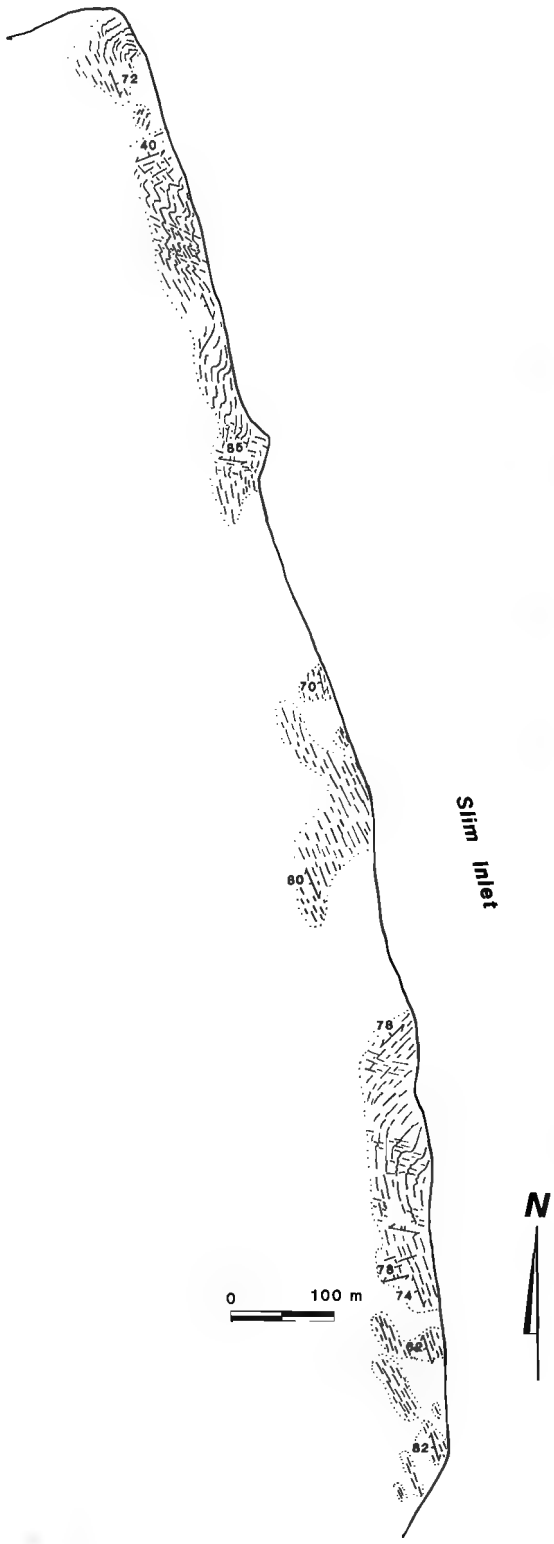

Figure 4. Field sketch showing geometry of folded mylonitic foliation at Slim Inlet. Dominant foliation orientation is north-northwest, parallel to faults and domain boundaries of Louscoone Inlet fault system. Younger mesoscopic folds and kink bands trend west-northwest.

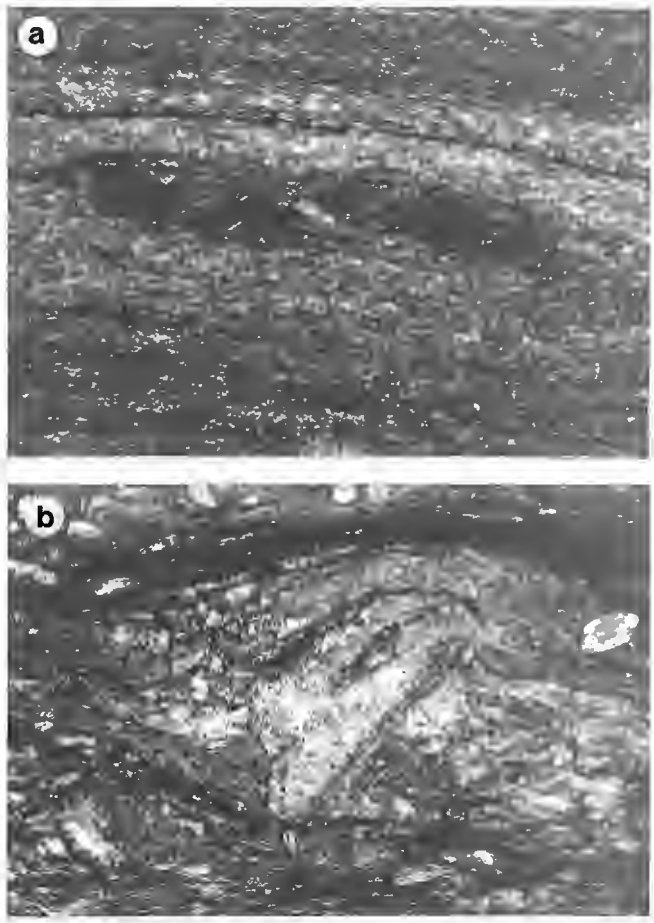

Figure 5. Thin section photomicrographs from shear zones at Smithe Point and Slim Inlet. North is to right in both photographs. a) Micro-faulted calcite porphyroblast with twinned internal structure. Both twin orientation and microfault offset indicate sinistral shear (photo shown in inverted position). b) Rotated feldspar porphyroblast with asymmetric pressure shadow indicating dextral shear.

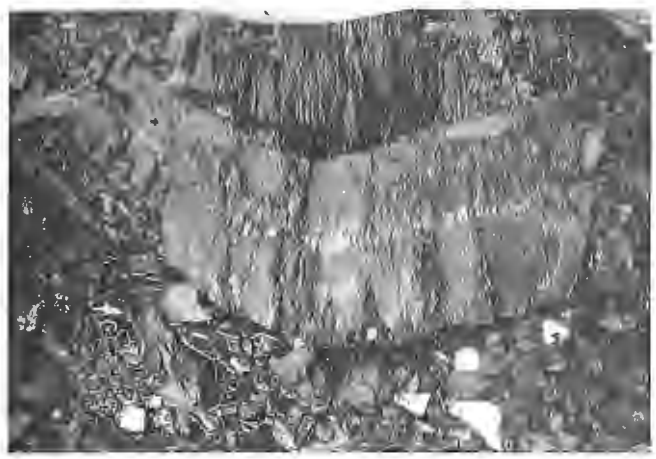

Figure 6. Open fold of Sandilands Formation siltstone, Huxley Island. Axial planar cleavage is subvertical and trends 140°, oblique to major faults and domain boundaries.

Domain C

The boundary between domains B and C occurs as a change from north-south structural trends to east-west trends, occurring over approximately 1 km. Strata ranging in age from Triassic to Tertiary outcrop in domain C. Two features are characteristic of this domain: all rocks lack penetrative fabrics, and nearly all strata dip gently to moderately to the north-northwest. Extensive Jurassic and Tertiary plutons intrude and locally metamorphose these rocks (Anderson and Greig, 1989).

Rocks within domain C are largely unfolded, even in locations where well-bedded strata (Sandilands and Peril formations) are exposed continuously for several kilometres. Two sets of major faults occur in domain C. Faults trending 070-100° dip gently to steeply southward, and usually have tens to hundreds of metres of dip-slip offset (south side down). These are cut and offset by subvertical to steeply east-dipping faults trending 150-180°. Faults of both sets occur as discrete surfaces or as narrow (<0.5 m) brecciated zones. Slickensides preserved on the north-northwest-trending faults are either subhorizontal or subvertical, and apparent slip directions are right-lateral or east-side-down.

Several dyke swarms associated with Tertiary and/or Jurassic magmatism (Souther, 1989) occur locally in domain C, and dykes can form up to 80 % of outcrop. In general, dykes are subvertical, tabular, and they trend approximately north-south; dyke orientation is independent of bedding orientation in country rocks.

INTERPRETATION

Fault history

The structural geometry of the Burnaby Island/Juan Perez Sound area indicates a history dominated by dextral strike-slip faulting. This faulting occurred on north-northwest-trending faults distributed across the width of domain B, and was coeval with and linked to south-directed extension in domain C. The most compelling evidence supporting strike-slip faulting comes from the dextral mesoscopic and microscopic kinematic indicators described above. In addition, steep, northwest-trending flattening fabrics and fold axial planes within domain B are consistent with northeast-directed shortening, the expected strain configuration inside a north-northwest-trending, dextral fault system. Northwest-trending folds of mylonitic fabrics at Slim Inlet show this same shortening direction, and likely record late stage flattening and folding of the older, more northerly-trending shear fabric. Microscopic fabrics show that shearing occurred at greenschist grades of metamorphism, accompanied by oriented calcite and chlorite growth in pressure shadows.

Map-scale fault orientations, although not conclusive in themselves, also support a strike-slip interpretation. The system of braided faults bounding structural blocks with strata of varying ages shown in the present mapping is a geometry typical of wrench fault systems (e.g. Moody and Hill, 1956). Sinistral, west-northwest-trending fabrics at Section Cove are antithetic to the dominant north-northwest-trending fault system, although timing constraints on movement are poor. The age of rocks affected (Triassic to Tertiary), variable crosscutting relationships, and similarities in structural style all suggest contemporaneous formation.

Structures in domain C support a structural history of south-directed, asymmetric extension, roughly coeval with transcurrent faulting along the Louscoone Inlet fault zone. Well-bedded strata of the Sandilands and Peril formations in domain C are virtually unfolded on the outcrop scale, and were not affected by the Mesozoic shortening documented in the central Queen Charlotte Islands (Thompson et al., 1991). The combination of gentle to moderate north-northwest dips and moderate to steeply-dipping, south-side-down normal faults is unambiguous evidence for asymmetric, south-directed extension. The present configuration of fault and bedding orientations is easily ascribed to domino-style extensional faulting and block rotations during extension.

Normal faults in domain C do not extend into domains A or B. This suggests that normal faulting was either antecedent to or synchronous with transcurrent faulting in domain B. If normal faulting preceded transcurrent faulting, structural styles similar to those in domain C should occur offset to the north on the west side of domain B; neither present map studies (Thompson et al., 1991; Taite, 1991) nor Sutherland Brown's (1968) original mapping recognize such structures, and deformation in the two domains is considered coeval.

Major faults were not observed in domain A, which behaved as a rigid block during deformation. The regional southwest tilts in this block may reflect a subsequent regional tilting, postdating the strike-slip faulting.

Relationships to mapping elsewhere in the Queen Charlotte Islands

The strike-slip faulting and associated extension described above represent a structural geometry that is confined to the southern Moresby Island region within the Queen Charlotte Islands. Sutherland Brown (1968) proposed a linkage between strike-slip faulting on the Rennell Sound fault zone and the Louscoone Inlet fault system; recent field mapping in the area where these two systems intersect shows that Cretaceous/Tertiary fold trends in the former are continuous across the most northerly extension of the latter, even though their formation predates movement on the Louscoone Inlet fault system (Thompson et al., 1991). Faults mapped by Sutherland Brown (1968) as elements of the northern Louscoone Inlet fault system are either not recognized in the recent detailed mapping, or have only minor offset. For example, the Carmichael Passage Fault, which has displacement of hundreds to a few thousand metres apparent dip-slip offset at Louise Narrows, does not offset contacts along the north shore of Cumshewa Inlet (Fig. 1).

Reconnaissance studies at several locations outside of the Burnaby Island/Juan Perez Sound map area where Sutherland Brown (1968) mapped the Louscoone Inlet fault system show structural styles similar to those in domain B. The most spectacular examples are at Shuttle Island in Darwin Sound (Fig. 1). Here, mylonitic fabrics are extensively developed over a 300 m wide zone in altered rocks of the Karmutsen Formation and a fine grained intrusion. The mylonitic foliation consistently strikes north-northwest (150-170°) and dips

moderately to steeply to the southwest and northeast. A well-developed subhorizontal mineral lineation is ubiquitous, and asymmetric fabrics and kinematic indicators consistently show dextral offset.

Sutherland Brown (1968), Anderson (1988), and Woodsworth (1988) described mylonitic fabrics in the Karmutsen Formation and Jurassic intrusive rocks on southern Kunghit Island at Luxana and Howe bays. These locations were not examined in the present study, but the fabrics described trend north-northwest, have subhorizontal mineral lineations, and are along trend with domain B at Skincuttle Inlet. East of the Luxana Bay and Howe Bay mylonite zones, Sutherland Brown's (1968) map shows subhorizontal dips in Triassic and Jurassic Kunga Group strata. This implies that the extension-related block tilting documented in domain C at Skincuttle Inlet may not extend that far south.

A STRUCTURAL MODEL FOR THE TERTIARY EVOLUTION OF THE SOUTHERN QUEEN CHARLOTTE ISLANDS

The structural history described above for the Burnaby Island/Juan Perez Sound area, when combined with constraints provided by previous mapping (Lewis and Ross, 1991; Thompson et al., 1991), defines a structural model for the southern Queen Charlotte Islands centred largely on offset along the Louscoone Inlet fault system. The Mesozoic structural history outlined by Lewis and Ross (1991) and Thompson et al. (1991) for the central and northern Queen Charlotte Islands involves three distinct structural events: Middle Jurassic southwest-directed contractional faulting and folding, Middle and Late Jurassic block faulting, and Late Cretaceous/Early Tertiary folding. The two shortening events are concentrated in the central islands, coextensive with the trace of the Rennell Sound fault zone outlined by Sutherland Brown (1968), and they led to structural thickening in this region. This Mesozoic structural history is not recognized in the Burnaby Island/Juan Perez Sound area, although recognition would be hindered by the paucity of Middle Jurassic strata in the area. However, beginning in Tertiary time, with transcurrent motion on the Louscoone Inlet fault system, structural links between the two areas are apparent. Transcurrent faulting did not extend into the central Queen Charlotte Islands, but it dies out at Cumshewa Inlet, where it intersects Mesozoic structures. Geometric constraints require that transcurrent displacement be transferred into one of the blocks bound by the fault. In this case, it is accommodated by extension in domain C, and the extension direction is parallel to displacement direction on the Louscoone Inlet fault system. This model, schematically illustrated in Figure 7, allows for several tens of kilometres of transcurrent faulting in the southern Queen Charlotte Islands, without offsetting structural trends in the central islands. The coincidence of transcurrent faulting with areas not significantly affected by Mesozoic deformation invites speculation that the two may be related; one possible connection is that the Louscoone Inlet fault system was mechanically restricted to crustal rocks not thickened during early regional shortening.

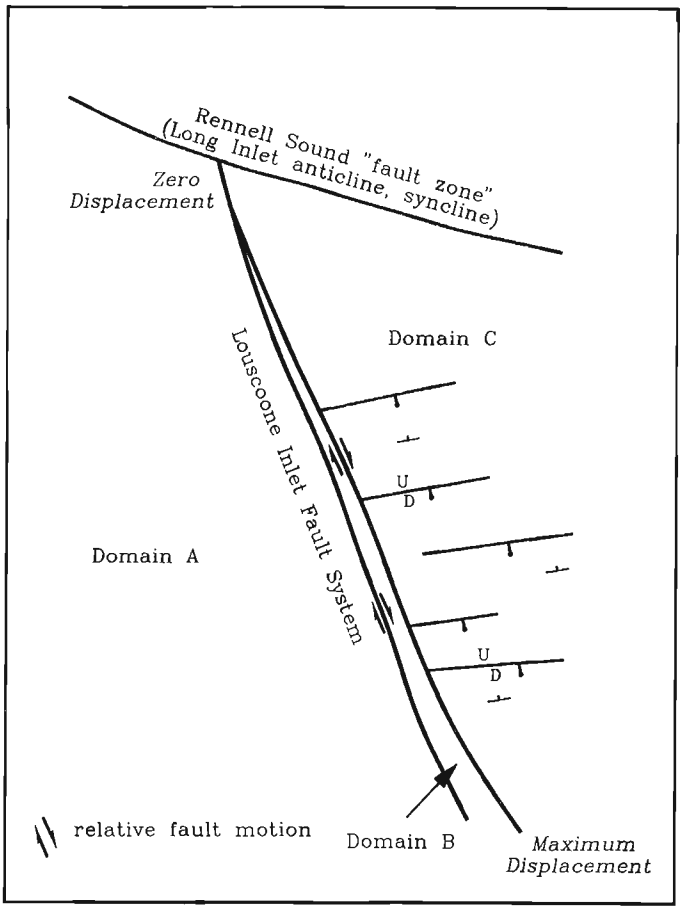

Figure 7. Schematic diagram showing linkage of transcurrent faulting in domain B and asymmetric extension in domain C.

Timing

The best constraints on timing of faulting are provided by crosscutting relationships in domains B and C. In domain B, Skidegate Formation strata yielding Early Cretaceous inoceramids are cut by north-northwest-trending faults and contain northwest-trending folds and flattening fabrics. Volcanic and intrusive rocks cut by these same faults are undated, but, on the basis of lithological character and contact relations, are interpreted to be Tertiary. For example, volcanic conglomerates with red-weathering, feldsparphyric clasts on Huxley Island are identical to strata on Ramsay Island which have yielded Oligocene radiometric ages. More conclusive timing relationships are provided in domain C on Ramsay Island. Here, moderately north-dipping volcanic strata have undergone extension and tilting similar to that in older strata to the south at Burnaby Island and Skincuttle Inlet. K-Ar whole rock dates of 41.1 $\pm$ 1.4 Ma and 35.9 $\pm$ 1.1 Ma from basalts (compiled by Hickson, 1988) here indicate that tilting and extension in domain C, and by inference, strike-slip faulting in domain B, were active since the Early Oligocene. No upper age limit for faulting is constrained.

Amounts of fault offset

No unambiguous markers exist with which to quantify strike-slip offsets in domain B. Sutherland Brown (1968) estimated up to 100 km of movement, but he based his estimates on offsets of poorly constrained structures and outcrop belts. Thompson et al. (1991), working near Louise Island, were unable to document any horizontally offset features along the northern extensions of the fault system.

The best estimate of fault offset in the Burnaby Island/Juan Perez Sound map area can be determined analytically by calculating the amount of extension in domain C, and assuming that all extension is transferred into dextral faulting in domain B. Values thus obtained represent the difference in offset between the north and south boundaries of the map area, and can be treated as minimum amounts of regional slip. Extension amount is best calculated from palinspastic restorations of cross-sections drawn in the plane of movement. However, structural geometry at depth, which will largely determine values for extension, is poorly constrained in domain C. Because extension is asymmetric and appears to be accompanied by domino-style block rotation, maximum and minimum values can be determined from a simple relationship relating extension to the angles describing amount of tilting (θ) and original fault dip ($\varnothing$) (Wernicke and Burchfiel, 1982):

$$\% \text{ extension} = 100\,\% \times \left[\frac{\sin \varnothing}{\sin (\varnothing - \theta)} - 1\right] \ldots (1)$$

This equation is valid for a single generation of planar normal faults and ignores contributions from internal deformation of fault blocks. With large amounts of extension, several generations of normal faults may be present, and equation (1) must be modified:

$$\% \text{ extension} = 100\,\% \times \left[\left(\frac{\sin \varnothing}{\sin (\varnothing - \theta/n)}\right)^n - 1\right] \ldots (2)$$

where n is the number of fault generations, each generation contributing equally to tilting of fault blocks.

(a) amount of tilting: if strata are flat-lying at the initiation of extension, bedding dips are the most reliable indicator of tilting due to block rotation. Rocks in domain C of the Burnaby Island/Juan Perez Sound area contain no significant structures older than the east-west-trending faults, and north-northwest-trending faults are interpreted as synchronous with or postdating extension. Average bedding dips for all ages of strata in domain C are 30-40° to the north and northwest.

(b) original fault dip: field studies in extended terranes show that normal faults commonly form with surface dips of 60-90°. In domain C, where rocks have undergone 30-40° of northward tilting, faults initiated at the onset of extension should have present-day dips of 20°-60°. However, fault surfaces measured in the field dip 40-90°, with most dipping around 60°. Several factors may be responsible. 1) Faults may be steeper at the present level of exposure than at depth. 2) Some of the observed faults may be antithetic, and have rotated to steeper dips during tilting. Several subvertical, north-side-down faults mapped in domain C are probably antithetic. 3) Faults may have formed continuously throughout extension, and steeper faults represent more recently formed structures. Two end member geometries illustrate minimum and maximum values for extension. In the first case, minimum possible extension amounts are considered. To accomplish this, faults are assumed to have formed perpendicular to bedding and have tilted 35° to present dips of 55°. Equation (1) yields an extension value of 22 % for this geometry. A second calculation treats maximum likely extensions: it assumes extension occurred on two generations of faults, each forming with a dip of 60° and accommodating 20° of tilting (more than two generations of faults would yield smaller amounts of extension, but are unlikely where total tilting is only 40°). For this geometry, equation (2) gives an extension of 82 %. In both cases, the calculated values represent minimums, as the assumptions inherent in equation (1) favour smaller values. However, localized extension of 80 % causes significant crustal thinning, unless linked along a low-angle detachment to more widely-distributed extension at lower crustal levels (Royden and Keen, 1980). Low-level and upward-continued gravity data (Lyatsky, 1991) contain no anomalies in offshore areas along trend to the northeast of domain C which might indicate crustal thinning (H.V. Lyatsky, pers. comm., 1990). For this reason, the actual amount of extension is probably closer to the smaller value.

Rocks in domain C affected by extension range from at least southern Lyell Island in the north to Carpenter Bay in the south, a cross-strike distance of 50 km. Extension estimates of 22 % and 82 % would yield elongations over this distance of 9 km and 22 km respectively. The model dictates that this extension is transformed into transcurrent faulting in domain B. These values therefore are the difference in strike-slip offset between the northern and southern ends of the map area, and should be considered a minimum amount of regional strike-slip offset on the Louscoone Inlet fault system. Recent mapping (Thompson and Lewis, 1990), reconnaissance studies, and Sutherland Brown's (1968) original mapping all show that the fault system extends north of the study area, probably as far as Cumshewa Inlet, and some strike-slip motion is likely north of the study area. Therefore, actual strike-slip offsets will be greater than that calculated above.

CONCLUSIONS

Dextral strike-slip offsets of at least 10-20 km have occurred along the southern portion of the Louscoone Inlet fault system since Oligocene time. Amounts of displacement gradually decrease to the north, and are transferred into extension in the eastern fault block. Strike-slip offsets of this magnitude are not documented elsewhere in the Queen Charlotte Islands, and structural styles for the northern and southern portions of the islands are fundamentally different.

Major extensional faults in domain C are along trend with the southern edge of the Moresby Ridge, a major offshore structural high northeast of the study area, which bounds Tertiary sedimentary depocentres to the south, north, and east (Fig. 1). Offshore seismic reflection data (Rohr and Dietrich, 1990) which cross the Moresby Ridge show that offshore sub-basins are half-grabens formed on north-tilted blocks bound by south-side-down normal faults, a geometry very similar to that in domain C. This invites speculation

that the structural evolution of the western margin of the offshore basin is tied to Tertiary faulting onshore. However, many intra-basinal potential-field anomaly trends offshore are north-south (Lyatsky, 1991), oblique to structures described in the southern Queen Charlotte Islands.

ACKNOWLEDGMENTS

Jim Haggart and the Geological Survey of Canada are thanked for generous logistical and technical support. M. Hamilton provided capable and untiring field assistance, and the competent, cheerful expediting services of A. Putterill brightened many damp days. Careful reviews by S. Taite, H. Lyatsky, and J. Monger substantially improved the manuscript.

REFERENCES

Anderson, R.G.
1988: Jurassic and Cretaceous Tertiary plutonic rocks on the Queen Charlotte Islands, British Columbia; in Current Research, Part E, Geological Survey of Canada, Paper 88-1E, p. 213-216.

Anderson, R.G. and Greig, C.J.
1989: Jurassic and Tertiary plutonism in the Queen Charlotte Islands, British Columbia; in Current Research, Part H, Geological Survey of Canada, Paper 89-1H, p. 95-104.

Hesthammer, J., Indrelid, J., Lewis, P.D., and Orchard, M.J.
1991: Permian strata on the Queen Charlotte Islands, British Columbia; in Current Research, Part A, Geological Survey of Canada, Paper 91-1A.

Hickson, C.J.
1988: Structure and stratigraphy of the Masset Formation, Queen Charlotte Islands, British Columbia; in Current Research, Part E, Geological Survey of Canada, Paper 88-1E, p. 269-274.

Lewis, P.D., Haggart, J.W., Anderson, R.G., Hickson, C.J., Thompson, R.I., Dietrich, J.R., and Rohr, K.M.M.
in press: Triassic to Neogene geologic evolution of the Queen Charlotte Basin; Canadian Journal of Earth Sciences.

Lewis, P.D. and Ross, J.V.
1988: Preliminary investigations of structural styles in Mesozoic strata of the Queen Charlotte Islands, British Columbia; in Current Research, Part E, Geological Survey of Canada, Paper 88-1E, p. 275-279.
1991: Mesozoic and Cenozoic structural history of the central Queen Charlotte Islands, British Columbia; in Evolution and Hydrocarbon Potential of the Queen Charlotte Basin, British Columbia, Geological Survey of Canada, Paper 90-10.

Lyatsky, H.V.
1991: Regional geophysical constraints on crustal structure and geologic evolution of the Insular Belt, British Columbia; in Evolution and Hydrocarbon Potential of the Queen Charlotte Basin, British Columbia, Geological Survey of Canada, Paper 90-10.

Moody, J.D. and Hill, M.J.
1956: Wrench fault tectonics; Geological Society of America Bulletin, v. 67. p. 1207-1247.

Rohr, K.M.M. and Dietrich, J.R.
1990: Deep seismic survey of Queen Charlotte Basin; Geological Survey of Canada, Open File 2258.

Royden, L. and Keen, C.E.
1980: Rifting process and thermal evolution of the continental margin of eastern Canada determined from subsidence curves; Earth and Planetary Science Letters, v. 51, p. 343-361.

Souther, J.G.
1989: Dyke swarms in the Queen Charlotte Islands, British Columbia; in Current Research, Part H, Geological Survey of Canada, Paper 89-1H, p. 117-120.

Sutherland Brown, A.
1968: Geology of the Queen Charlotte Islands, British Columbia; British Columbia Department of Mines and Petroleum Resources, Bulletin 54, 226 p.

Taite, S.P.
1991: Geology of the Sewell Inlet-Tasu Sound area, Queen Charlotte Islands, British Columbia; in Current Research, Part A, Geological Survey of Canada, Paper 91-1A.

Thompson, R.I.
1988: Late Triassic through Cretaceous geological evolution of the Queen Charlotte Islands, British Columbia; in Current Research, Part E, Geological Survey of Canada, Paper 88-1E, p. 217-219.

Thompson, R.I., Haggart, J.W., and Lewis, P.D.
1991: Late Triassic through Early Tertiary evolution of the Queen Charlotte Basin, British Columbia, with a perspective on hydrocarbon potential; in Evolution and Hydrocarbon Potential of the Queen Charlotte Basin, British Columbia, Geological Survey of Canada, Paper 90-10.

Thompson, R.I. and Lewis, P.D.
1990: Geology, Louise Island, British Columbia; Geological Survey of Canada, Map 2-1990, scale 1:50 000.

Thompson, R.I. and Thorkelson, D.J.
1989: Regional mapping update, central Queen Charlotte Islands, British Columbia; in Current Research, Part H, Geological Survey of Canada, Paper 89-1H, p. 7-11.

Wernicke, B. and Burchfiel, B.C.
1982: Modes of extensional tectonics; Journal of Structural Geology, v. 4, p. 105-115.

Woodsworth, G.
1988: Karmutsen Formation and the east boundary of Wrangellia, Queen Charlotte Basin, British Columbia; in Current Research, Part E, Geological Survey of Canada, Paper 88-1E, p. 209-212.

Yorath, C.J. and Chase, R.L.
1981: Tectonic history of the Queen Charlotte Islands and adjacent areas - a model; Canadian Journal of Earth Sciences, v. 18, p. 1717-1739.

Geology of the Sewell Inlet-Tasu Sound area, Queen Charlotte Islands, British Columbia

Susan Taite[1]
Cordilleran Division, Vancouver

Taite, S., Geology of the Sewell Inlet-Tasu Sound area, Queen Charlotte Islands, British Columbia; in Current Research, Part A, Geological Survey of Canada, Paper 91-1A, p. 393-399, 1991.

Abstract

The geological mapping project initiated in the Sewell Inlet-Tasu Sound area in 1989, continued in 1990. Stratigraphy is divided into four unconformity-bound packages: the Karmutsen Formation and Kunga Group, the Yakoun Group, the Cretaceous section, and Tertiary volcanic rocks. The map area is divided into three structural domains, with differing stratigraphic successions preserved in each. Domains A and C lack Cretaceous strata, and are structurally characterized by northwest-trending faults and folds. Domain B contains Cretaceous strata, and is characterized by open northeast-trending folds. These domains are analogous to structural blocks described by previous workers. North and northeast-trending faults dominate map patterns, a style unique within the Queen Charlotte Islands.

Résumé

Le projet de cartographie géologique qui a été entrepris en 1989 dans la région de l'inlet Sewell et du détroit de Tasu s'est poursuivi en 1990. La stratigraphie se divise en quatre ensembles limités par des discordances: la formation de Karmutsen et le groupe de Kunga, le groupe de Yakoon, la section crétacée et les roches volcaniques tertiaires. La zone cartographiée est divisée en trois domaines structuraux contenant chacun des successions stratigraphiques différentes. Les domaines A et C ne comprennent aucune couche du Crétacé et sont caractérisés structuralement par des failles et plis à direction nord-ouest. Le domaine B contient des couches crétacées et est caractérisé par des plis ouverts à direction nord-est. Ces domaines sont analogues aux blocs structuraux décrits dans des études antérieures. Les failles à direction nord et nord-est sont les principaux éléments structuraux figurés sur la carte; il s'agit-là d'un style unique dans les îles de la Reine-Charlotte.

[1] Department of Geological Sciences, University of British Columbia, 6339 Stores Road, Vancouver, B.C. V6T 2B4

INTRODUCTION

Geological mapping in the Sewell Inlet-Tasu Sound area (Fig. 1), initiated by the author in 1989 (Taite, 1990), continued during the 1990 field season. Map coverage was both refined and extended, and detailed structural and stratigraphic studies were engaged. This study forms the Master's thesis work of the author, to be completed in 1991. A generalized geological map is included in this report (Fig. 2); the complete detailed map will be published as a GSC Open File report in 1991.

The purposes of this study include mapping the regional geology of the Sewell Inlet-Tasu Sound area, examining anomalous structural trends found in the area, and testing the block faulting hypothesis outlined by Thompson et al. (1991). These questions are herein addressed within the context of recent regional and detailed mapping completed to the north (Thompson and Lewis, 1990; Thompson et al., 1991) and to the southeast of the study area (Lewis, 1991).

The dominant map scale features in the Sewell Inlet-Tasu Sound area are north- and northeast-trending faults. Within the Queen Charlotte Islands this style is only seen in the study area. Understanding its significance will be important in recreating the tectonic evolution of both the Queen Charlotte Islands and the Queen Charlotte Basin.

STRATIGRAPHY

The stratigraphy of the Sewell Inlet-Tasu Sound area is informally divided into four unconformity-bound sequences (Fig. 3). The basal package comprises Upper Triassic Karmutsen Formation volcanic rocks, and Upper Triassic and Lower Jurassic sedimentary rocks of the Kunga Group. Rocks of the Lower Jurassic Maude Group, which conformably overlie the Kunga Group elsewhere in the Queen Charlotte Islands, are absent in the study area.

The second sequence comprises pyroclastic and epiclastic rocks of the Middle Jurassic Yakoun Group. The third sequence encompasses Cretaceous sedimentary rocks, and Tertiary volcanic rocks comprise the fourth sequence. Extensive dykes and sills occur in all Mesozoic units. Major plutons described by Anderson and Greig (1989) occur west of the map limits, and do not outcrop in the study area.

Extensive descriptions of the stratigraphic units are available in numerous recent publications, but are based mainly on occurrences outside of the study area (general descriptions: Sutherland Brown, 1968; Jurassic stratigraphy: Cameron and Tipper, 1985; Cretaceous stratigraphy: Gamba et al., 1990; Haggart and Gamba, 1990; Haggart, 1991; Haggart et al., 1991; Tertiary stratigraphy: Hickson, 1988; 1989; dykes: Souther, 1989). The following section describes the lithological character of these units as they appear within the study area, with emphasis on unusual or anomalous occurrences.

Sequence 1: Karmutsen Formation and Kunga Group

The basal unit of the first stratigraphic package is the Upper Triassic Karmutsen Formation. Lithologies within the study area include massive volcanic flows, pillows, flow and pillow breccias, and the 'snowflake' feldspar porphyries described by Sutherland Brown (1968). Lenses of grey limestone less than a metre thick occur rarely within the volcanic rocks. This unit has been mapped as undifferentiated due to the limited areal extent of facies and sparse exposure.

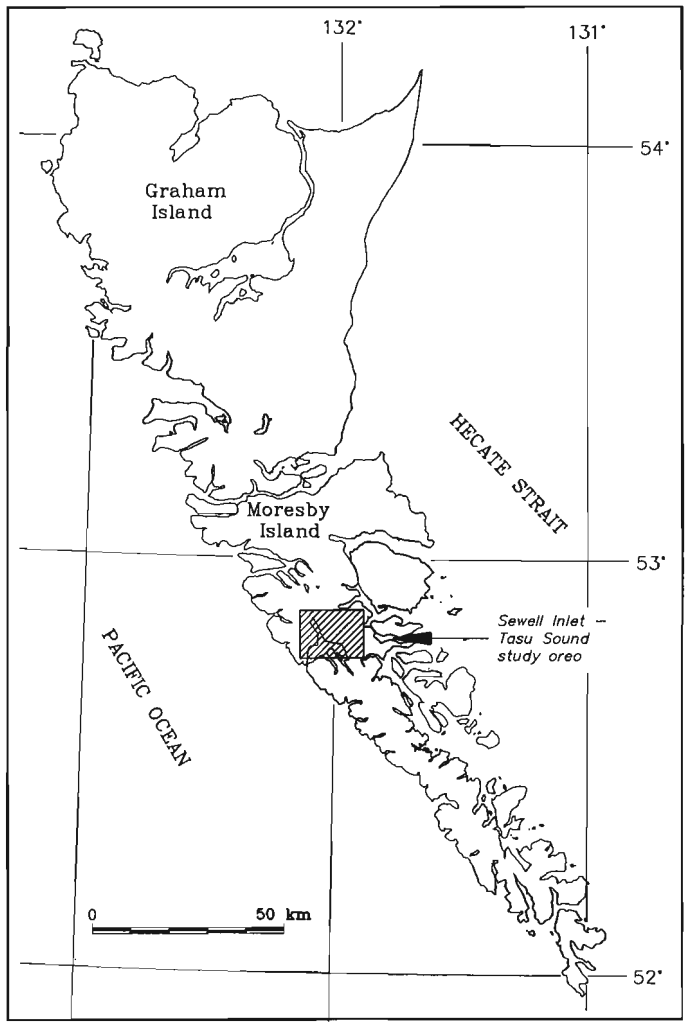

Figure 1. Location map of the Sewell Inlet Tasu Sound study area.

The basal member of the Kunga Group is the Upper Triassic Sadler Limestone, a lithologically distinctive unit which lies conformably on the Karmutsen Formation. It is typically a homogeneous, massive, light-grey limestone, and locally contains crinoid fragments and corals. Planar stratigraphic laminations occur near the top of the unit.

The Upper Triassic Peril Formation lies conformably on the Sadler Limestone. The contact is gradational over several metres and defined as a transition from massive grey limestone to bedded black argillaceous limestone (Fig. 4). In the study area, the Peril Formation contains rare coarse clastic layers up to a metre thick; these have not been described elsewhere in the Queen Charlotte Islands (Fig. 5).

The Peril Formation-Sandilands Formation contact is conformable, gradational and defined by the occurrence of thinly-bedded layers of clastic rocks. Sandilands Formation

rocks commonly comprise thinly-bedded argillaceous shales and siltstones, as described by Sutherland Brown (1968) and Cameron and Tipper (1985) elsewhere, but anomalous lithologies are unique to the Sewell Inlet-Tasu Sound area. At one location the rocks are thickly bedded (25-30 cm thick beds), coarsely clastic, non-fissile, and highly fossiliferous (Fig. 6). Complexly ornamented gastropods from these beds suggest a shallow marine depositional environment.

Sequence 2: The Yakoun Group

The Middle Jurassic Yakoun Group comprises andesitic pyroclastic and epiclastic volcanic and sedimentary rocks (Sutherland Brown, 1968). The base is commonly an angular unconformity, it is never observed overlying rocks older than the Sandilands Formation. Molluscs elsewhere in the Queen Charlotte Islands indicate a Bajocian age for the unit; faunal control is scarce in the study area.

Lapilli tuff, conglomerate, and interbedded sandstone, siltstone, and tuff are characteristic lithologies in this area (Fig. 7). Lapilli tuffs are poorly sorted to unsorted, and exhibit both reverse and normal grading. The unit's diagnostic olive green colour commonly weathers to a bright rust colour.

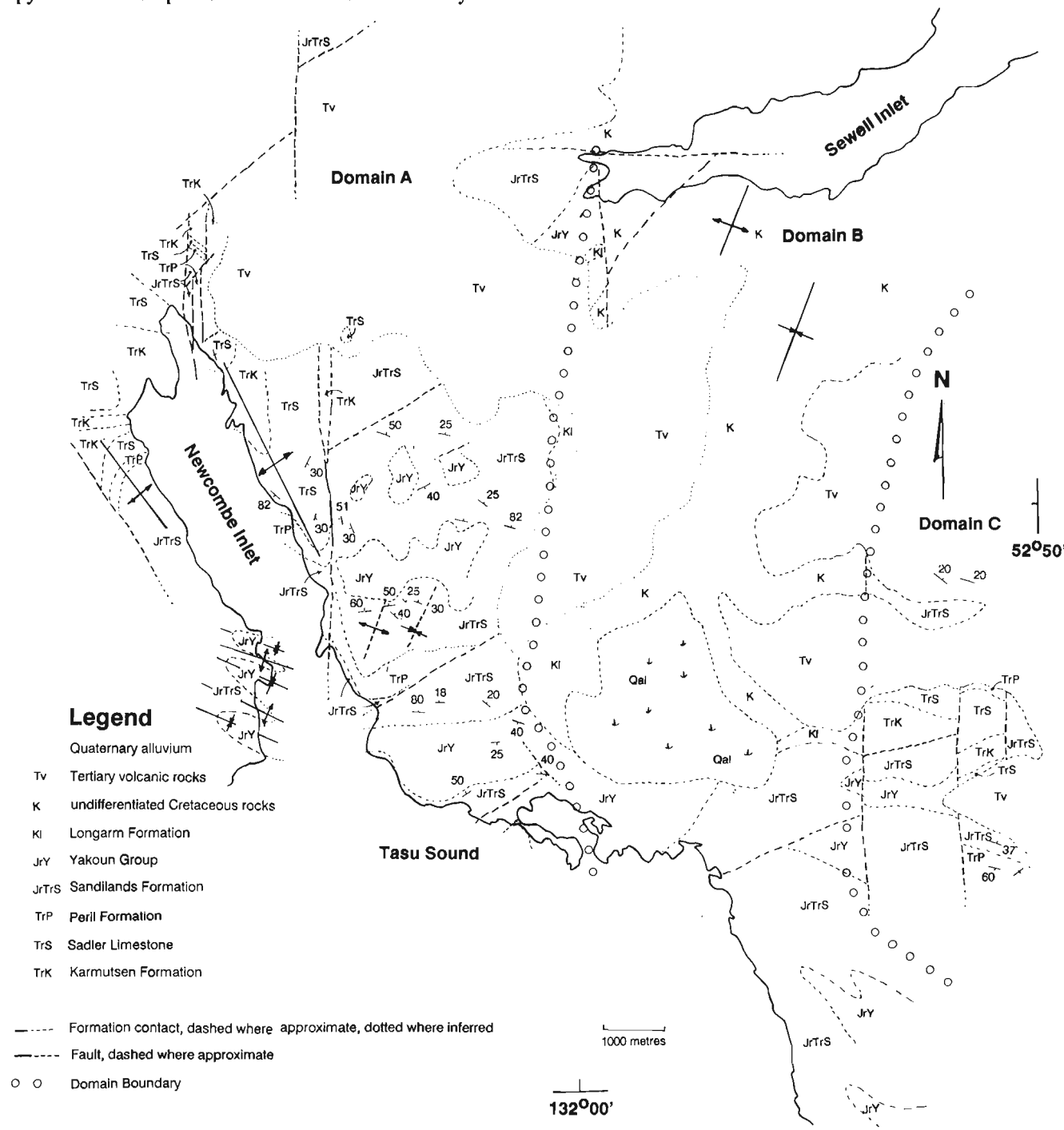

Figure 2. Schematic structural map of the study area.

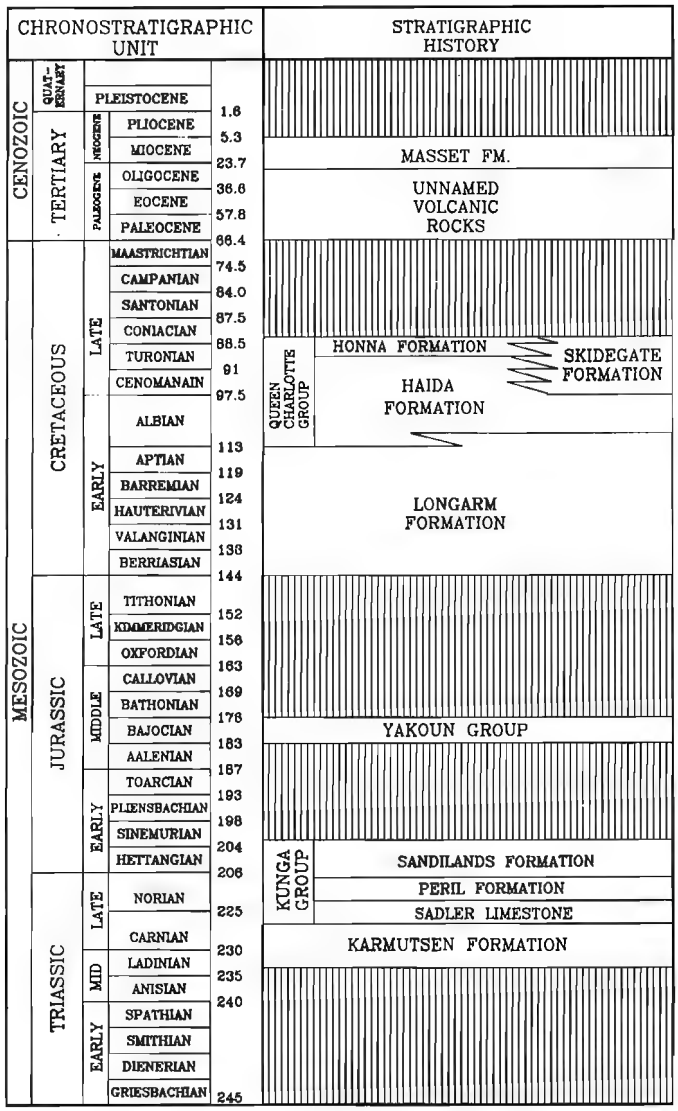

Figure 3. Stratigraphic column for strata within the Sewell Inlet-Tasu Sound area (adapted from Lewis and Ross, 1991).

Sequence 3: The Longarm Formation and Queen Charlotte Group

Nomenclature for Cretaceous rocks in the Queen Charlotte Islands has undergone extensive revisions as fieldwork elucidates chronostratigraphic and lithostratigraphic relationships. In this paper, the nomenclature of Gamba et al. (1990) is used, Haggart et al. (1991) provide a comprehensive discussion of current thought of Cretaceous lithostratigraphy. A basal transgressive sequence of Cretaceous rocks, identified during the 1990 field season, unconformably overlies rocks of both the Sandilands Formation and the Yakoun Group (Fig. 8), and consists of sandstone and siltstone, and clast and matrix-supported boulder, cobble, and granule conglomerate. Conglomerate clasts are derived from directly subjacent units. Recognition of this unit in the field can be difficult where it overlies rocks of the Yakoun Group, which it then resembles. Abundant inoceramid valves and shell fragments, common to this unit throughout the Queen Charlotte Islands, are distinctive. The basal Cretaceous section varies in thickness from only a couple of metres to several tens of metres.

Figure 4. Gradational contact between Sadler limestone (bedded on a metre scale) and the Peril Limestone.

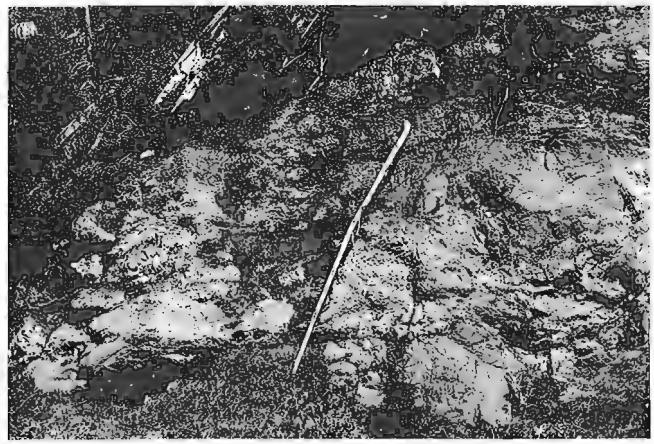

Figure 5. Coarse clastic, concretionary outcrop of the Peril Limestone.

Relationships between Cretaceous lithofacies of the Queen Charlotte Group in the Sewell Inlet-Tasu Sound area are poorly defined, due largely to poor biostratigraphic control. The most common lithologies exposed are shale and interbedded sandstone of the Haida and Skidegate formations.

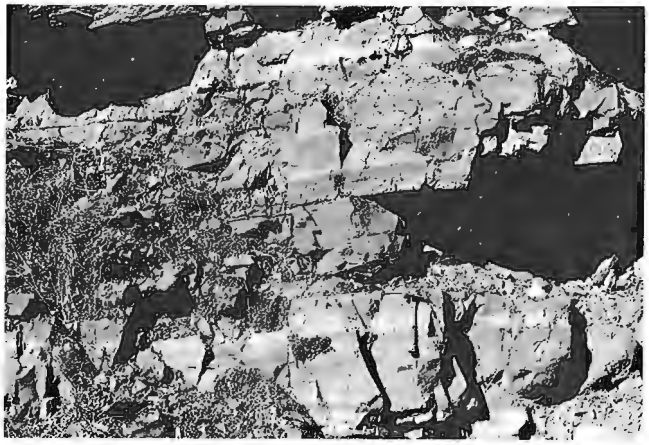

Figure 6. Coarse clastic, thickly bedded occurrence of the Sandilands Formation. Hammer for scale.

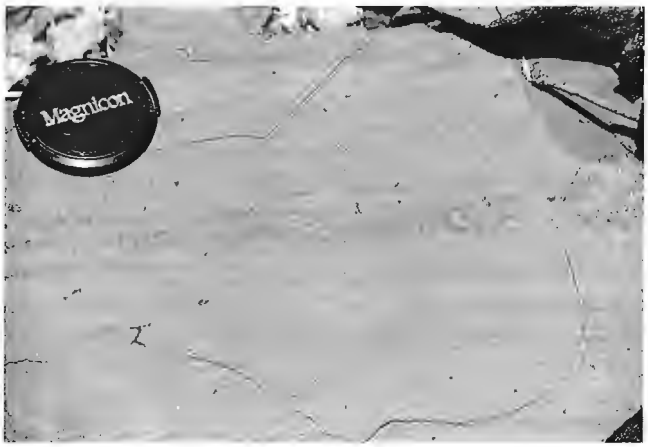

Figure 7. Interbedded siltstones and lapilli tuffs of the Yakoun Group.

The massive sandstone of the Haida Formation is frequently bioturbated, and is overlain by homogeneous, black shale. The thinly bedded turbiditic rocks of the Skidegate Formation (Fig. 9) interfinger with homogeneous black shale; division of these units at map scale is often impractical. The turbidites exhibit well developed, rare Bouma Tabcde sequences, and common Tbce and Tce sequences.

Honna Formation conglomerate exhibits different stratigraphic relations with the Haida and Skidegate formations throughout the Islands. On northern Moresby Island, the Honna Formation rocks unconformably overlie rocks of the Jurassic Yakoun Group and the Cretaceous Queen Charlotte Group. In the Sewell Inlet-Tasu Sound area, the Honna Formation conglomerate interfingers with Skidegate Formation turbiditic sandstone, and the two rock types are interpreted to represent submarine channel and overbank levee deposits respectively (Fig. 10; Gamba et al., 1990).

Sequence 4: Tertiary volcanic rocks

Igneous rocks of probable Tertiary age in the Sewell Inlet-Tasu Sound area include extrusive flows and pyroclastic deposits, and abundant intrusive dykes and sills. The flows

Figure 8. Conglomerate of the basal Cretaceous Longarm Formation unconformably overlying Sandilands Formation.

and pyroclastic rocks overlie the Cretaceous sedimentary strata and bear lithological similarities to the Neogene Masset Formation on Graham Island, however they are not dated, and may be Paleogene. These rocks are compositionally heterogeneous, ranging from massive intermediate or basaltic flows to flow-banded rhyolites. Debris flow deposits contain heterolithic clasts, including those derived from the underlying Cretaceous Queen Charlotte Group, the Yakoun Group, and the Kunga Group.

STRUCTURE

The map area has been divided into three structural domains (Fig. 2), on the basis of stratigraphy preserved within each domain, and unique internal structural characteristics.

Structures within domain A

Domain A includes rocks of the conformable sequence of the Karmutsen Formation and the Kunga Group, and the unconformably overlying Yakoun Group in the western part of the study area. To the east of Newcombe Inlet, Tertiary volcanic rocks unconformably overlie these strata. Cretaceous strata are notably absent from this domain. Strata in this domain have a regional southward tilt; the oldest rocks occur in the northwestern part of the domain. Northwest-trending folds and faults dominate structures in this domain. These may correlate with regional middle Jurassic deformation seen elsewhere in the Queen Charlotte Islands and described by Lewis and Ross (1991) and Thompson et al. (1991). East of Newcombe Inlet, a younger set of northeast-trending faults and folds are superimposed on northwest-trending structures.

Structures within domain B

Domain B, in the east-central part of the study area, is underlain by rocks of the Cretaceous Longarm Formation and Queen Charlotte Group. On the southern edge of the domain, the Sandilands Formation and thin erosional remnants of the Yakoun Group are unconformably overlain by the Cretaceous rocks. The western boundary of domain B occurs where rocks of the Longarm Formation onlap rocks

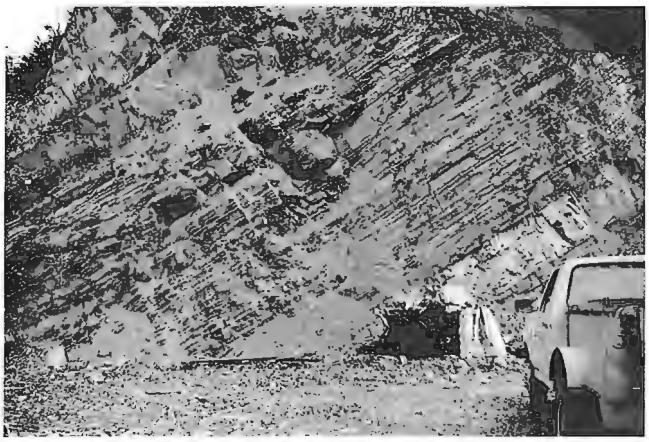

Figure 9. Thin, planar beds of the Cretaceous Skidegate Formation.

Figure 10. Interbedded Honna Formation conglomerates and turbidites of the Skidegate Formation.

of the Sandilands Formation and the Yakoun Group. The eastern boundary is an inferred fault contact between Cretaceous strata and rocks of the Karmutsen Formation. The northeast boundary is obscured by Tertiary volcanic rocks. Regional structural trends differ from those found in domain A; in domain B exposed strata are younger to the north. The basal Cretaceous section is exposed in the southwest and southeast corners of the domain, the Skidegate and Haida formations outcrop in the central and northeastern areas, and on the south shore of Sewell Inlet the Honna Formation is exposed. Structures within the Cretaceous strata are dominated by northeast-trending mesoscopic folds.

Structures in domain C

This domain contains the same stratigraphic sequence as that found in domain A: Triassic and Jurassic lithologies overlain by Tertiary volcanic rocks. North and northeast-trending faults dominate map patterns. Tertiary volcanic rocks exhibit a consistent shallow to moderate north to northeast dip. Oldest lithologies outcrop at the southern end of the domain.

DISCUSSION

The oldest structures recorded in the study area are northwest-trending folds and contractional faults involving strata of the Karmutsen Formation and the Kunga Group. This southwest-directed compressional event is observed throughout the Queen Charlotte Islands (Thompson and Thorkelson, 1989; Lewis and Ross, 1989; Thompson et al., 1991). These structures are observed in domains A and C, and likely underlie rocks in domain B. Rocks of the Yakoun Group are always observed overlying the Sandilands Formation with an angular unconformity. Structures within the Yakoun Group indicate later deformation was coaxial and possibly continuous with the earlier regional event.

Coarse clastic rocks which contain possible shallow marine fauna in the upper Kunga Group rocks, and the absence of Maude Group rocks, suggest the Early Jurassic sedimentary basin may have been areally restricted within the Queen Charlotte Islands. The sedimentary basin extant in the Queen Charlotte Islands during deposition of the Maude Group did not likely extend into the Sewell Inlet-Tasu Sound area.

Post-Bajocian and pre-Cretaceous tectonic activity in the Queen Charlotte Islands was dominated by block faulting (Thompson et al., 1991). This block faulting has resulted in northwest-trending belts of preserved Yakoun Group strata in the central Queen Charlotte Islands, and coincided with uplift and unroofing of Middle to Late Jurassic plutons (Anderson and Greig, 1989; Anderson and Reichenbach, 1989). Evidence for this tectonic event exists in the Sewell Inlet-Tasu Sound area. Domains A and C have Triassic and Jurassic strata overlain by Tertiary rocks; domain B contains Cretaceous strata overlying either rocks of the Kunga Group, or thin veneers of the Yakoun Group. This style is analogous to that described by Thompson et al. (1991). Direct evidence for tectonic activity coincident with Cretaceous sedimentation described by Thompson and Thorkelson (1989) does not exist in the study area. The presence of large angular, and likely fragile clasts of Kunga Group argillites in Honna Formation conglomerates indicates a nearby uplifted Kunga Group point source area which could be an artifact of renewed syndepositional tectonism.

Map scale north-trending faults crosscut all units. Varying amounts of offset of the different sequences suggest complex Mesozoic and Cenozoic histories for these features. The latest tectonic event recognized in the study area is the northerly regional tilting which produced consistent northerly dips of the Tertiary volcanic rocks. Lewis (1991) recognized similar orientations of structures to the southeast, and related them to strike-slip faulting along the Louscoone Inlet Fault Zone.

ACKNOWLEDGMENTS

I would again like to thank the employees of Western Forest Products in Sewell Inlet for many kindnesses and much assistance. In particular I thank Buzz Vidal, Tony Pineda, Bill Waugh and Paul Prestie. I thank Kevin Warwick for following me up creeks. Ian Foreman provided welcome assistance in the field. Discussions with J.V. Ross and P.D. Lewis, and thoughtful editing of R.G. Anderson greatly

improved the manuscript. Audrey Putterill provided cheerful assistance and expediting. The Collier family is especially thanked for providing much appreciated creature comforts.

REFERENCES

Anderson, R.G. and Greig, C.J.
1989: Jurassic and Tertiary plutonism in the Queen Charlotte Islands, British Columbia; in Current Research, Part H, Geological Survey of Canada, Paper 89-1H, p. 95-104.

Anderson, R.G. and Reichenbach, I.
1989: A note on the geochronometry of Late Jurassic and Tertiary plutonism in the Queen Charlotte Islands, British Columbia; in Current Research, Part H, Geological Survey of Canada, Paper 89-1H, p. 105-112.

Cameron, B.E.B. and Tipper, H.W.
1985: Jurassic stratigraphy of the Queen Charlotte Islands, British Columbia; Geological Survey of Canada, Bulletin 365, 49 p.

Gamba, C.A., Indrelid, J., and Taite, S.
1990: Sedimentology of the Upper Cretaceous Queen Charlotte Group, with special reference to the Honna Formation, Queen Charlotte Islands, British Columbia; in Current Research, Part F, Geological Survey of Canada, Paper 90-1F, p. 67-73.

Haggart, J.W.
1991: A synthesis of Cretaceous stratigraphy, Queen Charlotte Islands, British Columbia; in Evolution and Hydrocarbon Potential of the Queen Charlotte Basin, British Columbia, Geological Survey of Canada, Paper 90-10.

Haggart, J.W. and Gamba, C.A.
1990: Stratigraphy and sedimentology of the Longarm Formation, southern Queen Charlotte Islands, British Columbia; in Current Research, Part F, Geological Survey of Canada, Paper 90-1F, p. 61-66.

Haggart, J.W., Taite, S., Indrelid, J., Hesthammer, J., and Lewis, P.D.
1991: A revision of stratigraphic nomenclature for the Cretaceous sedimentary rocks of the Queen Charlotte Islands, British Columbia; in Current Research, Part A, Geological Survey of Canada, Paper 91-1A.

Hickson, C.J.
1988: Structure and stratigraphy of the Masset Formation, Queen Charlotte Islands, British Columbia; in Current Research, Part E, Geological Survey of Canada, Paper 88-1E, p. 269-274.
1989: An update on structure and stratigraphy of the Masset Formation, Queen Charlotte Islands, British Columbia; in Current Research, Part H, Geological Survey of Canada, Paper 89-1H, p. 73-79.

Lewis, P.D.
1991: Dextral strike-slip faulting and associated extension along the southern portion of the Louscoone Inlet Fault System, southern Queen Charlotte Islands, British Columbia; in Current Research, Part A, Geological Survey of Canada, Paper 91-1A.

Lewis, P.D. and Ross, J.V.
1989: Evidence for Late Triassic-Early Jurassic deformation in the Queen Charlotte Islands, British Columbia; in Current Research, Part H, Geological Survey of Canada, Paper 89-1H, p. 13-18.
1991: Mesozoic and Cenozoic structural history of the central Queen Charlotte Islands, British Columbia; in Evolution and Hydrocarbon Potential of the Queen Charlotte Basin, British Columbia, Geological Survey of Canada, Paper 90-10.

Souther, J.G.
1989: Dyke swarms in the Queen Charlotte Islands, British Columbia; in Current Research, Part H, Geological Survey of Canada, Paper 89-1H, p. 117-120.

Sutherland Brown, A.
1968: Geology of the Queen Charlotte Islands, British Columbia; British Columbia Department of Mines and Petroleum Resources, Bulletin 54, 226 p.

Taite, S.P.
1990: Observations on structure and stratigraphy of the Sewell Inlet-Tasu Sound area, Queen Charlotte Islands, British Columbia; in Current Research, Part F, Geological Survey of Canada, Paper 90-1F, p. 19-22.

Thompson, R.I. and Lewis, P.D.
1990: Geology, Louise Island, British Columbia; Geological Survey of Canada, Map 2-1990, scale 1:50 000, in press.

Thompson, R.I. and Thorkelson, D.
1989: Regional mapping update, central Queen Charlotte Islands, British Columbia; in Current Research, Part H, Geological Survey of Canada, Paper 89-1H, p. 7-11.

Thompson, R.I., Haggart, J.W., and Lewis, P.D.
1991: Late Triassic through Early Tertiary evolution of the Queen Charlotte Basin, British Columbia, with a perspective on hydrocarbon potential; in Evolution and Hydrocarbon Potential of the Queen Charlotte Basin, British Columbia, Geological Survey of Canada, Paper 90-10.

Diachronous acoustic basement in seismic reflection data from the Queen Charlotte Basin, British Columbia

Henry V. Lyatsky[1]
Cordilleran Division, Vancouver

Lyatsky, H.V., Diachronous acoustic basement in seismic reflection data from the Queen Charlotte Basin, British Columbia; in Current Research, Part A, Geological Survey of Canada, Paper 91-1A, p. 401-407, 1991.

Abstract

The position of acoustic basement in seismic reflection profiles from the Tertiary Queen Charlotte Basin is strongly influenced by transmission losses suffered by the seismic signal at igneous-sedimentary contacts and at other reflective surfaces in the basin fill. Transmission losses calculated for hypothetical layered earth models are large for sections containing numerous igneous layers. The resulting reduction in signal penetration may raise acoustic basement to shorter traveltimes and higher stratigraphic levels. Geological and geophysical evidence suggests regional variability in the number and age of igneous units within the Tertiary succession. The acoustic basement changes stratigraphic position correspondingly. Traveltime to the acoustic basement in the Queen Charlotte Basin does not necessarily represent thickness of Tertiary fill, and interpretations are improved by incorporating all available geological and geophysical data.

In the Harlequin D-86 well area, potential-field anomalies and seismic refraction data suggest that Tertiary sedimentary rocks in Mitchell's Trough may be underlain in part by an intrusive-extrusive igneous complex.

Résumé

La position du soubassement acoustique sur les profils de sismique réflexion du bassin du Tertiaire de la Reine-Charlotte est fortement influencée par des pertes de transmission subies par le signal sismique aux contacts entre roches ignées et sédimentaires ainsi qu'à d'autres surfaces réfléchissantes dans les matériaux de remplissage du bassin. Les pertes de transmission calculées pour des modèles hypothétiques de couches de terre sont importantes dans les modèles comportant de nombreuses couches de roches ignées. La réduction résultante de la pénétration du signal peut avoir comme conséquence de soulever le soubassement acoustique à cause des temps de parcours plus courts et par conséquent niveaux stratigraphiques plus élevés. Des indications géologiques et géophysiques suggèrent une variabilité régionale du nombre et de l'âge des unités ignées à l'intérieur de la succession tertiaire. La position stratigraphique du soubassement acoustique change ainsi de manière correspondante. Le temps de parcours au soubassement acoustique dans le bassin de la Reine-Charlotte ne représente pas nécessairement l'épaisseur des matériaux du Tertiaires de remplissage et les interprétations sont améliorées par l'incorporation de toutes les données géologiques et géophysiques disponibles.

Dans la région du puits Harlequin D-86, les anomalies du champ de potentiel et les données de simique réfraction suggèrent que les roches sédimentaires du Tertiaire de la dépression Mitchell peuvent reposer en partie sur un complexe igné de roches intrusives et effusives.

[1] Department of Geological Sciences, University of British Columbia, 6339 Stores Road, Vancouver, B.C. V6T 2B4

OBJECTIVES

The principal objective of this study is to investigate the relationship between Tertiary stratigraphy of the Queen Charlotte Basin and quality of reflection-seismic images of the basin fill. This was undertaken to evaluate the utility of seismic data for studies of geological evolution of the basin. The second objective is to integrate seismic reflection data with other geological and geophysical information in order to develop a practical methodology for future geoscience investigations in the Queen Charlotte Basin.

Data base

The Queen Charlotte Basin Frontier Geoscience Program acquired about 1000 km of multichannel seismic reflection data from Hecate Strait and Queen Charlotte Sound (Rohr et al., 1989; Rohr and Dietrich, 1990, 1991). These data and older petroleum-industry data were used to prepare an isopach map for strata above acoustic basement and to delineate structural trends in the basin (Rohr and Dietrich, 1991; P.D. Lewis, pers. comm., 1990). Geological interpretation of seismic reflection data is aided by information from eight oil-exploration wells in the Queen Charlotte Basin offshore (Shouldice, 1971, 1973), several marine seismic refraction profiles (Clowes and Gens-Lenartowicz, 1985; Pike, 1986), and gravity and magnetic maps (Currie et al., 1983a,b; Currie and Teskey, 1988; Lyatsky, 1991), and by projecting geological relationships observed onshore (Jeletzky, 1976; Muller, 1977; Thompson et al., 1991; P.D. Lewis, pers. comm., 1990).

QUEEN CHARLOTTE BASIN STRATIGRAPHY

Three stratigraphic units dominate the Tertiary sequence in the Queen Charlotte Islands (Sutherland Brown, 1968; Hickson, 1988, 1989; Thompson et al., 1991; Lewis, 1990; White, 1990; P.D. Lewis, pers. comm., 1990):

(1) the Neogene Skonun Formation, composed mainly of mudstone and sandstone;
(2) the Upper Oligocene-Miocene Masset Formation, composed mainly of volcanic rocks; and
(3) an unnamed succession of volcanic flows, mudstone, and sandstone of Early Neogene and Paleogene age.

Cumulative thickness of the Tertiary package may exceed 5 km. Drillhole penetrations indicate that the Skonun Formation beneath Hecate Strait and Queen Charlotte Sound contains interbeds of volcanic flows, sills and volcaniclastic rocks (Shouldice, 1971, 1973; Hopkins, 1981; Patterson, 1989; Higgs, 1991). In the Queen Charlotte Islands, geological investigations by Cameron and Hamilton (1988), Hickson (1988, 1989), and Haggart et al. (1990) revealed that Tertiary sedimentary and igneous rocks are commonly interstratified.

ACOUSTIC BASEMENT

One important aspect of seismic interpretation in the study area is the position and geological nature of the acoustic basement in seismic sections. Sheriff (1984) defined acoustic basement as "the deepest more-or-less continuous seismic reflector; often an unconformity below which seismic energy returns are poor or absent". Thus, acoustic basement is defined geophysically, and its position in a seismic section is influenced by power of the seismic energy source, surface or sea-floor conditions, signal attenuation, and recording, processing, and plotting parameters. The position of acoustic basement may also be affected by basin stratigraphy and interpreter's bias, and confusion between acoustic and geologic basement can be an interpretation pitfall.

Generally, acoustic basement may or may not represent a single geologic interface, and its correlation with specific unconformities or the crystalline basement is subjective. The present study suggests that acoustic basement in the Queen Charlotte Basin may occur at various stratigraphic levels within the basin fill, and it may not correspond to a single, isochronous geologic surface.

TRANSMISSION LOSSES

Knowledge of seismic velocities (Young, 1981; Clowes and Gens-Lenartowicz, 1985; Pike, 1986; Rohr and Dietrich, 1990, 1991) and rock densities (Sutherland Brown, 1968; Stacey and Stephens, 1969; Stacey, 1975; Anderson and Greig, 1989; Sweeney and Seemann, 1991) in the Queen Charlotte Basin is derived mainly from well and outcrop information and from parameters determined by processing and modelling reflection and refraction seismic data and gravity anomalies. Unfortunately, seismic reflection and refraction surveys generally do not reveal an identical or unique velocity structure of the subsurface (Berry and Mair, 1980). For example, apparent velocities derived from refraction data may be high due to acoustic anisotropy of the rock mass, as suggested by Davis (1982), Davis and Clowes (1986), and Pavlenkova (1989), especially where igneous sheets are interlayered with sedimentary rocks (Davis, 1982).

Available data indicate that normal-incidence amplitude reflection coefficients at sedimentary-igneous contacts in the Queen Charlotte Basin may exceed 0.2. The principal contributing factor is P-wave velocity variations across interfaces (commonly 3 ± 1 km/s for Tertiary sedimentary rocks versus 5 ± 1 km/s for igneous rocks), whereas density variations are relatively small (about 2.5 g/cm^3 for sedimentary rocks versus 2.7 g/cm^3 or more for igneous rocks). Because the seismic energy transmitted across an interface is less than the incident energy, an abundance of strongly reflective sedimentary-igneous contacts in the Tertiary section can produce significant transmission losses in the downgoing and upgoing seismic signal.

This problem was examined quantitatively. Transmission losses were calculated for one-dimensional layered earth models having only two lithologies with contrasting acoustic impedances.

In general, where N reflective interfaces occur above the target, the effective reflection-attenuation factor, F, is defined by the equation (Al-Sadi, 1980):

$$F = R_T \prod_{J=1}^{N} (1 - R_J^2) \qquad (1)$$

where R_T is the reflection coefficient at the target reflector, and R_J is the reflection coefficient at interface **J**. The term $(1-R_J^2)$ defines the two-way transmission coefficient at interface **J**. Normal incidence is assumed throughout the section, and all contacts are taken to be welded (*sensu* Krebes, 1987). All beds are assumed to be sufficiently thick for definitions of reflection and transmission at boundaries of semi-infinite media to apply. If the number of igneous layers above the target is **X** and if each layer contributes two reflective surfaces (top and base), then the number of interfaces where transmission losses would occur is **N=2X**. If reflection coefficients at all interfaces above the target have the same absolute value, **R**, formula (1) simplifies to

$$F = R_T(1-R^2)^{2X} = R_T P \qquad (2)$$

The parameter, **P**, which represents decay of the arrival from the target due to transmission losses, is

$$P = F/R_T = (1-R^2)^{2X} \qquad (3)$$

i.e. the product of two-way transmission coefficients at all interfaces above the target. With large transmission losses, **P** decreases, and the seismic image of the target degrades.

Formula (3) was used to compute signal decay for **R** ranging from 0.10 to 0.26 and for **X** ranging from 1 to 17, representing a wide range of the possible stratigraphic situations in the Queen Charlotte Basin. Roksandic (1985) relied on synthetic seismograms to illustrate transmission losses, but this approach was not used here because of the large number of earth models considered. Instead, results of the calculations were contoured on an **R-X** grid, and they are presented in Figure 1.

Examination of these results shows that transmission losses depend strongly on the layered earth model selected to represent basin stratigraphy. Transmission losses are small and **P** is large for low values of **R** and **X**, i.e. for situations with few strongly reflective interfaces. As **R** and **X** increase, transmission losses grow dramatically. In a seismic section, this would degrade the signal-to-noise ratio at large traveltimes, raising acoustic basement to higher stratigraphic levels.

Rohr and Dietrich (1991) have suggested that, in addition to igneous layers, coal seams within the Tertiary succession may cause high-amplitude reflections. This is expected as many coals have extremely low acoustic impedance (Lyatsky and Lawton, 1988; Lawton and Lyatsky, in press). Transmission losses occur also at mudstone-sandstone contacts. In Arctic sedimentary basins, severe signal-penetration problems are caused by permafrost (Poley et al., 1989), but this complication was not encountered in the study area.

The number of high-acoustic-impedance layers in the Tertiary Queen Charlotte Basin varies laterally. The number of igneous sheets, **X**, changes from drillhole to drillhole, ranging from none to more than 10. As a consequence, the quality of seismic images of deep strata varies: deep parts of the section are imaged better where the seismic signal suffers fewer transmission losses at shallow levels. The high reflection coefficients at sedimentary-igneous contacts, combined with constructive interference effects such as thin-bed tuning (Widess, 1973) of reflections from igneous layers, may produce seismic images with a stratified section at short

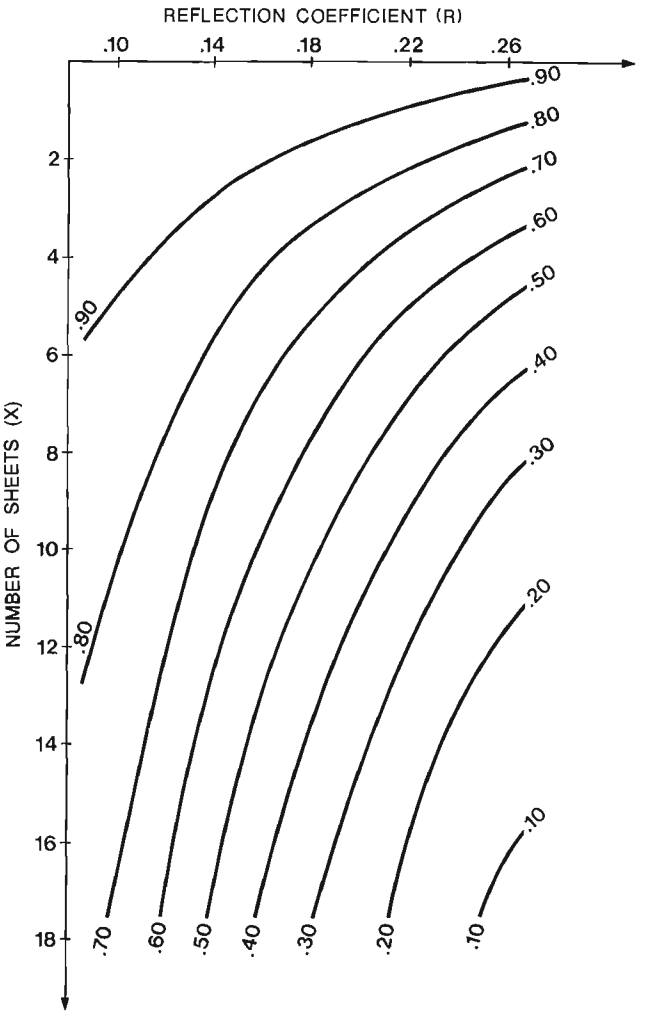

Figure 1. Attenuation of the seismic signal, **P**, as a function of the number of igneous sheets, **X**, and reflection coefficients at contacts, **R**, based on formula (3) in text.

traveltimes, separated by one or several high-amplitude events from a lower section containing few coherent reflections. Scattering of upgoing and downgoing seismic energy due to internal inhomogeneities and surface roughness of igneous horizons may further decay the signal-to-noise ratio at large traveltimes.

Acoustic basement may thus be confused with the true base of the Tertiary basin fill. This uncertainty complicates the interpretation of stratigraphy and structure in the basin. Because the age, abundance, and stratigraphic setting of Tertiary igneous layers varies, the acoustic basement in seismic reflection profiles can represent a diachronous set of geologic surfaces within the basin fill.

EXAMPLE

Figure 2a shows a segment of Line 1 of Rohr and Dietrich (1990). Acoustic basement, as defined by Sheriff (1984), occurs at about 700 ms in the southeastern part of the profile. This appearance of shallow basement is likely caused by an abundance of igneous rocks near the top of the

stratigraphic section in this area, as supported by the interpretation of seismic refraction data by Clowes and Gens-Lenartowicz (1985). These authors inferred massive volcanic rocks at a depth of about 1 km, but Davis (1982) cautioned that seismic refraction techniques do not always allow for unambiguous discrimination between massive volcanics and those interbedded with sedimentary rocks. Magnetic anomalies (Currie et al., 1983a,b; Lyatsky, 1991) in this part of the profile have an amplitude of some 500 nT and a substantial short-wavelength component, also consistent with a shallow igneous source.

In contrast with the southeastern part of the profile in Figure 2a, coherent seismic reflections are observable to the traveltime of 2 s or more near the Shell Anglo Harlequin D-86 well, where shallow igneous layers are lacking. Dominant lithologies in this well are interbedded sandstone and mudstone (Shouldice, 1971, 1973; Hopkins, 1981; Patterson, 1989), which presumably produce the observed reflections. Seismic refraction data of Clowes and Gens-Lenartowicz (1985) also show an increased thickness of low-velocity material in the area of the well.

A structural interpretation of the seismic profile is shown in Figure 2b. If the potential diachroneity of the acoustic basement in seismic data is ignored, northwest-side-down faults with a cumulative throw corresponding to as much as 1500 ms two-way traveltime may be required to explain the seismic reflection pattern observed between shot points (SP) B33000 and B33250. Although northwest-side-down faults undoubtedly occur in the area, a throw corresponding to 1500 ms is unlikely. Reflections at traveltimes of 1 s or less are minimally affected, and they do not exhibit the amount of drape that may be expected over faults with large dip-slip offset. Moreover, some of the faults in Figure 2, such as the one near SP B32890, seem to be associated with southeast-side-down deformation. Although the bathymetric depression between SP B32500 and B32950 (Mitchell's Trough of Luternauer and Murray, 1983) causes a velocity pull-down, its boundary at SP B32950 does not coincide with the location of the above-noted fault. Northwest-side-down displacement is thought to characterize faults at SP B33020 and B33160.

The high-amplitude seismic event which represents acoustic basement in the southeast loses amplitude toward the Harlequin D-86 well, where no igneous layers were intersected above 3135 m depth (Patterson, 1989). Dissipation of the igneous-related event coincides with strengthening of seismic reflections at traveltimes up to 2 s and with decay of magnetic anomalies (Currie et al., 1983a,b; Lyatsky, 1991), whose short-wavelength component is reduced and whose amplitudes drop to about 100 to 200 nT near the well. This suggests that the northwestward "thickening" of the Tertiary sequence in the seismic section in Figure 2 may be more apparent than real, caused partly by improvement in seismic-energy penetration due to disappearance of shallow reflective interfaces associated with igneous rocks. This implies that the acoustic basement in Figure 2 is not an isochronous geological surface or time line. Therefore, some of the large-traveltime reflections near the Harlequin D-86 well may be correlative with weak "sub-basement" events to the southeast.

The suspected volcanic rocks on the southeastern side of the profile in Figure 2a may be underlain by a large plutonic feeder system (Fig. 2b). This would help explain the high seismic velocities of rocks beneath the volcanics, detected by Clowes and Gens-Lenartowicz (1985) in an unreversed refraction profile and used by Rohr and Dietrich (1990) in the processing of seismic reflection data. It would also account for the persistence of the magnetic high in that area when the data are upward continued to 20 km (Lyatsky, 1991) and even 40 km (Teskey et al., 1989). A gravity high of 20 to 30 mGal (Stacey and Stephens, 1969; Currie et al., 1983a) occurs above the inferred igneous system, and it may reflect density contrasts with the surrounding sedimentary rocks.

The hypothetical igneous complex may be connected with plutons postulated in Queen Charlotte Sound by Lyatsky (1991), consistent with high vitrinite-reflectance values for Tertiary sedimentary rocks reported by Yorath and Hyndman (1983) from drillholes in that area. If the "sub-basement" seismic events under Mitchell's Trough (Fig. 2) are primary reflections, they can be interpreted as sills in the sediments housing a pluton or a neck, or as layers within the igneous complex.

Sagging of the igneous system could have caused structural inversion and southeast-side-down faulting, and this may have led to the formation of elements of Mitchell's Trough. The trough was later modified by Quaternary ice (Chase et al., 1975; Luternauer and Murray, 1983; Luternauer et al., 1989), and the coincidence of the trough with the postulated igneous system as imaged with magnetic, gravity and seismic data (Currie et al., 1983a,b; Lyatsky, 1991; P.D. Lewis, pers. comm., 1990) is lost south of the area examined, where the igneous complex and related structures are believed to acquire a north-south orientation. The northeast trend of Mitchell's Trough coincides with a regional fault pattern in the Insular Belt and with the orientation of other physiographic features (Peacock, 1935; Lyatsky, 1991). The interpretation proposed here (Fig. 2b) expands on the one presented by P.D. Lewis (pers. comm., 1990), where a structural ridge is shown southeast of the Harlequin D-86 well.

DISCUSSION

The author suspects that existence of igneous layers within the Tertiary stratigraphic succession influences the position of acoustic basement in seismic reflection profiles from the Queen Charlotte Basin. Even where shallow igneous rocks are lacking, as near the Harlequin D-86 well, substantial decay of the signal-to-noise ratio is observed at traveltimes of 2 s or more, and acoustic basement is not represented by a prominent seismic event (Fig. 2a). Thus, significant transmission losses seem to occur even in interbedded mudstone-sandstone sections. Thus, mapping of basin-fill thickness from seismic reflection data alone is not a reliable technique in the study area.

The geological basement of the Insular Belt is crystalline crustal rocks at the base of the entire supracrustal assemblage (Muller, 1977; Lyatsky, 1991), rather than rocks below just the Tertiary strata. Regional geological correlations (Jeletzky, 1976; Desrochers, 1989; Thompson et al., 1991; P.D. Lewis, pers. comm., 1990) and gravity (Stacey,

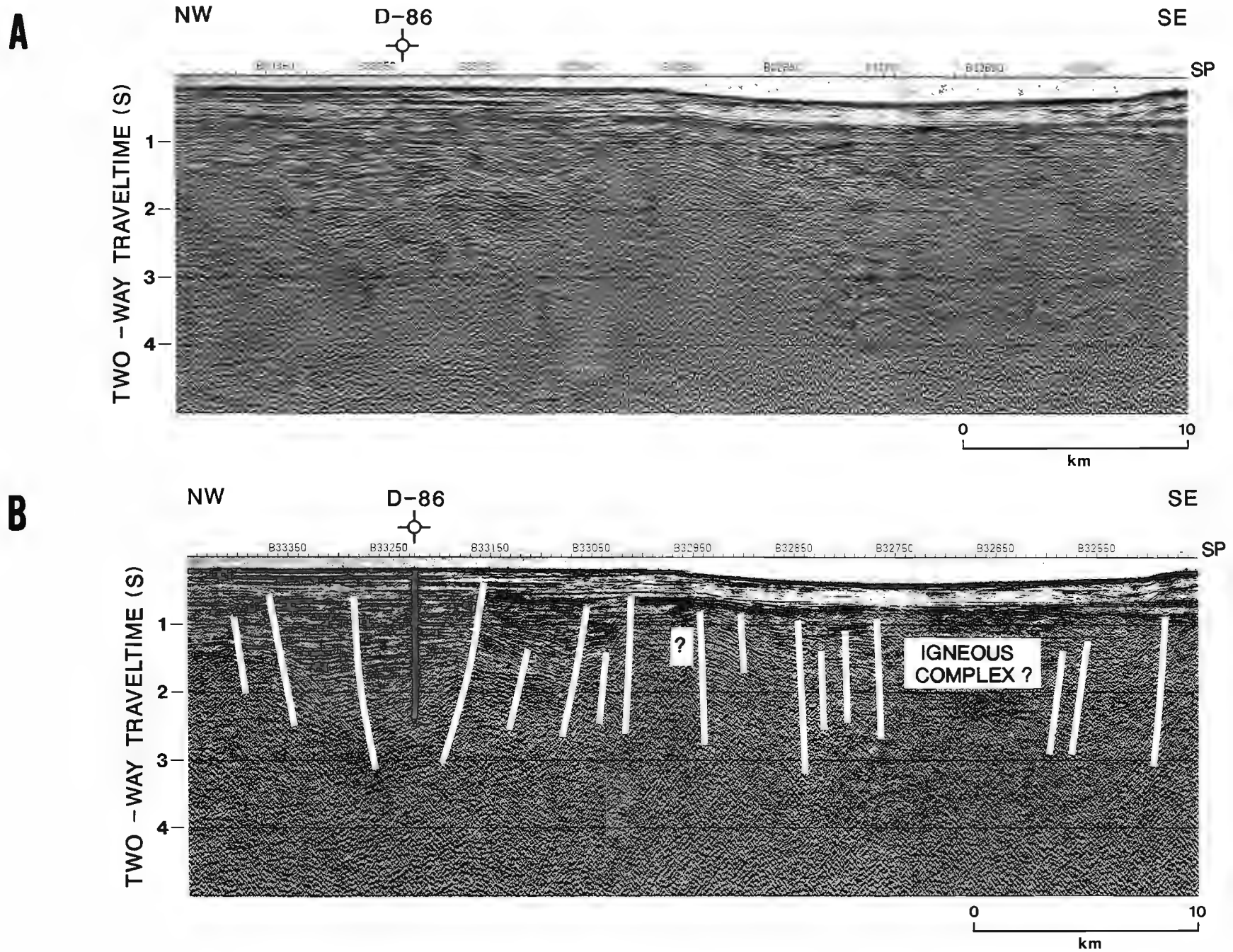

Figure 2. Segment of unmigrated seismic reflection Line 1 of Rohr and Dietrich (1990): **(a)** the data; **(b)** an interpretation (white lines represent inferred faults).

1975) and seismic refraction data (Clowes and Gens-Lenartowicz, 1985) suggest that a considerable and highly variable thickness of Mesozoic sedimentary rocks underlies the Tertiary rocks of the Queen Charlotte Basin. Geological mapping onshore (Thompson et al., 1991; P.D. Lewis, pers. comm., 1990) and geophysical studies offshore (Lyatsky, 1991) suggest that some of the Tertiary structures in the Insular Belt may be reactivated pre-existing faults. Thus, investigations of the Tertiary geological evolution of the Queen Charlotte Basin should consider such older deformation styles.

CONCLUSIONS

1. Abundance of strongly reflective surfaces in the Tertiary fill of the Queen Charlotte Basin degrades the quality of seismic images of deep strata in the basin. Many such surfaces are tops and bases of volcanic or volcaniclastic layers and sills; contacts between different sedimentary lithologies may also be highly reflective, contributing to signal degradation.
2. Lateral variations in the age, depth, and amount of volcanic rocks in the basin likely cause shifts in the stratigraphic position of acoustic basement in seismic reflection profiles. Therefore, traveltime to the acoustic basement is probably not a reliable representation of thickness of the Tertiary basin fill.
3. Elements of Mitchell's Trough in Queen Charlotte Sound may be underlain by a complex intrusive and extrusive igneous system, and mobility and structural deformation of this system may have influenced the evolution of the trough.

ACKNOWLEDGMENTS

The author thanks Dick Chase, Peter Lewis (University of British Columbia), Bob Thompson (GSC, Vancouver), Don Lawton (University of Calgary), and Jake Hudson (B.C. Ministry of Energy, Mines and Petroleum Resources) for their useful suggestions, criticism, and help with the early versions of the manuscript. Discussions with John Luternauer (GSC, Vancouver) helped improve understanding of bathymetric features in the study area. Thoughtful reviews were provided by Jim Haggart and Dirk Tempelman-Kluit (GSC, Vancouver). This work constitutes a component of the author's Ph.D. dissertation research at the University of British Columbia.

REFERENCES

Al-Sadi, H.N.
1980: Seismic Exploration Technique and Processing; Birkhäuser Verlag, 215 p.

Anderson, R.G. and Greig, C.J.
1989: Jurassic and Tertiary plutonism in the Queen Charlotte Islands, British Columbia; in Current Research, Part H, Geological Survey of Canada, Paper 89-1H, p. 95-104.

Berry, M.J. and Mair, J.A.
1980: Structure of the continental crust: a reconciliation of seismic reflection and refraction studies; in The Continental Crust and its Mineral Deposits, edited by D.W. Strangway, Geological Association of Canada, Special Paper 20, p. 195-213.

Cameron, B.E.B. and Hamilton, T.S.
1988: Contributions to the stratigraphy of the Queen Charlotte Basin, British Columbia; in Current Research, Part E, Geological Survey of Canada, Paper 88-1E, p. 221-227.

Chase, R.L., Tiffin, D.L., and Murray, J.W.
1975: The western Canadian continental margin; in Canada's Continental Margins and Offshore Petroleum Exploration, edited by C.J. Yorath, E.R. Parker, and D.J. Glass, Canadian Society of Petroleum Geologists, Memoir 4, p. 701-721.

Clowes, R.M. and Gens-Lenartowicz, E.
1985: Upper crustal structure of southern Queen Charlotte Basin from sonobuoy refraction studies; Canadian Journal of Earth Sciences, v. 22, p. 1696-1710.

Currie, R.G. and Teskey, D.J.
1988: Magnetics component of the Frontier Geoscience Program on the West Coast of Canada; in Current Research, Part E, Geological Survey of Canada, Paper 88-1E, p. 287.

Currie, R.G., Cooper, R.V., Riddihough, R.P., and Seemann, D.A.
1983a: Multiparameter geophysical surveys off the west coast of Canada; in Current Research, Part A, Geological Survey of Canada, Paper 83-1A, p. 207-212.

Currie, R.G., Seemann, D.A., and Riddihough, R.P.
1983b: Total field magnetic anomaly offshore British Columbia; Geological Survey of Canada, Open File 828, scale 1:1 000 000.

Davis, E.E.
1982: Evidence for extensive basalt flows on the sea floor; Bulletin of the Geological Society of America, v. 93, p. 1023-1029.

Davis, E.E. and Clowes, R.M.
1986: High velocities and seismic anisotropy in Pleistocene turbidites off Western Canada; Geophysical Journal of the Royal Astronomical Society, v. 84, p. 381-399.

Desrochers, A.
1989: Depositional history of Upper Triassic carbonate platforms on Wrangellia Terrane, western British Columbia, Canada; Bulletin of the American Association of Petroleum Geologists, v. 73, p. 349-350 (abstract).

Haggart, J.W., Indrelid, J., Hesthammer, J., Gamba, C.A., and White, J.M.
1990: A geological reconnaissance of the Mount Stapleton-Yakoun Lake region, central Queen Charlotte Islands, British Columbia; in Current Research, Part F, Geological Survey of Canada, Paper 90-1F, p. 29-36.

Hickson, C.J.
1988: Structure and stratigraphy of the Masset Formation, Queen Charlotte Islands, British Columbia; in Current Research, Part E, Geological Survey of Canada, Paper 88-1E, p. 269-274.
1989: An update on structure and stratigraphy of the Masset Formation, Queen Charlotte Islands, British Columbia; in Current Research, Part H, Geological Survey of Canada, Paper 89-1H, p. 73-79.

Higgs, R.
1991: Sedimentology, basin-fill architecture and petroleum geology of the Tertiary Queen Charlotte Basin; in Evolution and Hydrocarbon Potential of the Queen Charlotte Basin, British Columbia, Geological Survey of Canada, Paper 90-10.

Hopkins, Jr., W.S.
1981: Palynology of four offshore British Columbia wells; Geological Survey of Canada, Open File Report 808, 83 p.

Jeletzky, J.A.
1976: Mesozoic and ?Tertiary rocks of Quatsino Sound, Vancouver Island, British Columbia; Geological Survey of Canada, Bulletin 242, 243 p.

Krebes, E.S.
1987: Reflection and transmission at plane boundaries in nonwelded contacts; Journal of the Canadian Society of Exploration Geophysicists, v. 23, p. 66-72.

Lawton, D.C. and Lyatsky, H.V.
in press: Density-based reflectivity in seismic exploration for coal in Alberta, Canada; Geophysics, v. 56.

Lewis, P.D.
1990: New timing constraints on Cenozoic deformation in the Queen Charlotte Islands, British Columbia; in Current Research, Part F, Geological Survey of Canada, Paper 90-1F, p. 23-28.

Luternauer, J.L. and Murray, J.W.
1983: Late Quaternary morphologic development and sedimentation, central British Columbia continental shelf; Geological Survey of Canada, Paper 83-21, 38 p.

Luternauer, J.L., Conway, K.W., Clague, J.J., and Blaise, B.
1989: Late Quaternary geology and geochronology of the central continental shelf of western Canada; Marine Geology, v. 89, p. 57-68.

Lyatsky, H.V.
1991: Regional geophysical constraints on crustal structure and geologic evolution of the Insular Belt, British Columbia; in Evolution and Hydrocarbon Potential of the Queen Charlotte Basin, British Columbia, Geological Survey of Canada, Paper 90-10.

Lyatsky, H.V. and Lawton, D.C.
1988: Application of the surface reflection seismic method to shallow coal exploration in the Plains of Alberta; Canadian Journal of Exploration Geophysics, v. 24, p. 124-140.

Muller, J.E.
1977: Evolution of the Pacific margin, Vancouver Island, and adjacent regions; Canadian Journal of Earth Sciences, v. 14, p. 2062-2085.

Patterson, R.T.
1989: Neogene foraminiferal biostratigraphy of the southern Queen Charlotte Basin; in Contributions to Canadian Paleontology, Geological Survey of Canada, Bulletin 396, p. 229-265.

Pavlenkova, N.I.
1989: The Kola well and its significance for deep seismic sounding; Sovetskaya Geologiya (Soviet Geology), 1989, no. 6, p. 16-23 (in Russian).

Peacock, M.A.
1935: Fiord-land of British Columbia; Bulletin of the Geological Society of America, v. 46, p. 633-696.

Pike, C.J.
1986: A seismic refraction study of the Hecate Sub-basin, British Columbia; M.Sc. thesis, Department of Geophysics and Astronomy, University of British Columbia, Vancouver, 133 p.

Poley, D.F., Lawton, D.C., and Blasco, S.M.
1989: Amplitude-offset relationships over shallow velocity inversions; Geophysics, v. 54, p. 1114-1122.

Rohr, K. and Dietrich, J.
1990: Deep seismic survey of Queen Charlotte Basin; Geological Survey of Canada, Open File 2258.
1991: Deep seismic reflection survey of the Queen Charlotte Basin; in Evolution and Hydrocarbon Potential of the Queen Charlotte Basin, British Columbia, Geological Survey of Canada, Paper 90-10.

Rohr, K.M.M., Spence, G., Asudeh, I., Ellis, R., and Clowes, R.
1989: Seismic reflection and refraction experiment in the Queen Charlotte Basin, British Columbia; in Current Research, Part H, Geological Survey of Canada, Paper 89-1H, p. 3-5.

Roksandic, M.M.
1985: Stratification and reflections; First *Break*, v. 3, no. 9, p. 9-16.

Sheriff, R.E.
1984: Encyclopedic Dictionary of Exploration Geophysics, Second Edition; Society of Exploration Geophysicists, 323 p.

Shouldice, D.H.
1971: Geology of the Western Canadian continental shelf; Bulletin of Canadian Petroleum Geology, v. 19, p. 405-436.
1973: Western Canadian continental shelf; in The Future Petroleum Provinces of Canada - Their Geology and Potential, edited by R.G. McGrossan, Canadian Society of Petroleum Geologists, Memoir 1, p. 7-35.

Stacey, R.A.
1975: Structure of the Queen Charlotte Basin; in Canada's Continental Margins and Offshore Petroleum Exploration, edited by C.J. Yorath, E.R. Parker, and D.J. Glass, Canadian Society of Petroleum Geologists, Memoir 4, p. 723-741.

Stacey, R.A. and Stephens, L.E.
1969: An interpretation of gravity measurements on the west coast of Canada; Canadian Journal of Earth Sciences, v. 6, p. 463-474.

Sutherland Brown, A.
1968: Geology of the Queen Charlotte Islands, British Columbia; British Columbia Department of Mines and Mineral Resources, Bulletin 54, 226 p.

Sweeney, J.F. and Seemann, D.A.
1991: Crustal density structure of Queen Charlotte Islands and Hecate Strait, British Columbia; in Evolution and Hydrocarbon Potential of the Queen Charlotte Basin, British Columbia, Geological Survey of Canada, Paper 90-10.

Teskey, D.J., Hood, P.J., and Dods, S.D.
1989: Magnetic Anomaly Map of Canada - upward continued to 40 km; Geological Survey of Canada, Canadian Geophysical Atlas, Map 13, scale 1:10 000 000.

Thompson, R.I., Haggart, J.W., and Lewis, P.D.
1991: Late Triassic through early Tertiary evolution of the Queen Charlotte Basin, British Columbia, with a perspective on hydrocarbon potential; in Evolution and Hydrocarbon Potential of the Queen Charlotte Basin, British Columbia, Geological Survey of Canada, Paper 90-10.

White, J.M.
1990: Evidence of Paleogene sedimentation on Graham Island, Queen Charlotte Islands, west coast, Canada; Canadian Journal of Earth Sciences, v. 27, p. 533-538.

Widess, M.B.
1973: How thin is a thin bed?; Geophysics, v. 38, p. 1176-1180.

Yorath, C.J. and Hyndman, R.D.
1983: Subsidence and thermal history of Queen Charlotte Basin; Canadian Journal of Earth Sciences, v. 20, p. 135-159.

Young, I.F.
1981: Structure of the western margin of the Queen Charlotte Basin; M.Sc. thesis, Department of Geological Sciences, University of British Columbia, Vancouver, 380 p.

AUTHOR INDEX

NOTE TO CONTRIBUTORS

Submissions to the *Discussion* section of *Current Research* are welcome from both the staff of the Geological Survey of Canada and from the public. Discussions are limited to 6 double-spaced typewritten pages (about 1500 words) and are subject to review by the Chief Scientific Editor. Discussions are restricted to the scientific content of Geological Survey reports. General discussions concerning sector or government policy will not be accepted. All manuscripts must be computer word-processed on an IBM compatible system and must be submitted with a diskette using Word Perfect 5.0 or 5.1. Illustrations will be accepted only if, in the opinion of the editor, they are considered essential. In any case no redrafting will be undertaken and reproducible copy must accompany the original submissions. Discussion is limited to recent reports (not more than 2 years old) and may be in either English or French. Every effort is made to include both *Discussion* and *Reply* in the same issue. *Current Research* is published in January and July. Submissions should be sent to the Chief Scientific Editor, Geological Survey of Canada, 601 Booth Street, Ottawa, Canada, K1A 0E8.

AVIS AUX AUTEURS D'ARTICLES

Nous encourageons tant le personnel de la Commission géologique que le grand public à nous faire parvenir des articles destinés à la section *discussion* de la publication *Recherches en cours*. Le texte doit comprendre au plus six pages dactylographiées à double interligne (environ 1500 mots), texte qui peut faire l'objet d'un réexamen par le rédacteur en chef scientifique. Les discussions doivent se limiter au contenu scientifique des rapports de la Commission géologique. Les discussions générales sur le Secteur ou les politiques gouvernementales ne seront pas acceptées. Le texte doit-être soumis à un traitement de texte informatisé par un système IBM compatible et enrégistré sur disquette Word Perfect 5.0 ou 5.1. Les illustrations ne seront acceptées que dans la mesure où, selon l'opinion du rédacteur, elles seront considérées comme essentielles. Aucune retouche ne sera faite au texte et dans tous les cas, une copie qui puisse être reproduite doit accompagner le texte original. Les discussions en français ou en anglais doivent se limiter aux rapports récents (au plus de 2 ans). On s'efforcera de faire coïncider les articles destinés aux rubriques *discussions* et *réponses* dans le même numéro. La publication *Recherches en cours* paraît en janvier et en juillet. Les articles doivent être envoyés au rédacteur en chef scientifique: Commission géologique du Canada, 601 rue Booth, Ottawa, Canada, K1A 0E8.

Geological Survey of Canada Current Research, is now released twice a year, in January and in July. The four parts published in January 1991 (Paper 91-1, parts A to D) are listed below and can be purchased separately.

Recherches en cours, une publication de la Commission géologique du Canada, est publiée maintenant deux fois par année, en janvier et en juillet. Les quatre parties publiées en janvier 1991 (Étude 91-1, parties A à D) sont énumérées ci-dessous et vendues séparément.

Part A, Cordillera and Pacific Margin
Partie A, Cordillère et marge du Pacifique

Part B, Interior Plains and Arctic Canada
Partie B, Plaines intérieures et région arctique du Canada

Part C, Canadian Shield
Partie C, Bouclier canadien

Part D, Eastern Canada and national and general programs
Partie D, Est du Canada et programmes nationaux et généraux